Volume

1

NATIONAL
URANIUM
TAILINGS
PROGRAM

Energy, Mines and Resources Canada Énergie, Mines et Ressources Canada

Canada

URANIUM TAILINGS ASSESSMENT PROGRAM (UTAP.3): USER'S MANUAL

A Research Report Prepared under
DSS Contract No. 23317-6-1728/01-SQ

for the

The National Uranium Tailings Program
Canada Centre for Mineral and Energy Technology
Energy, Mines and Resources Canada
555 Booth Street
Ottawa, Ontario
K1A 0G1

by

SENES Consultants Limited
499 McNicoll Avenue
Willowdale, Ontario
M2H 2C9

MICROMEDIA

105 pp

April 1987

ABSTRACT

This report represents part of the ongoing efforts of the National Uranium Tailings Program (NUTP) to develop the capability to predict the long-term effects of Canadian Uranium mill tailings. In three previous studies a comprehensive Uranium Tailings Assessment Program (UTAP) was developed. The UTAP program incorporates a Monte Carlo procedure which permits the user to enter input parameters as probability density functions rather than as single numbers and to calculate frequency distributions for output variables. The output distributions can be interpreted as a subjective probability telling us quantitatively what we are entitled to believe about the output variables.

To date the approach has been to apply UTAP, in a generic fashion, to a hypothetical reference site. The focus of the present study has been to modify UTAP, where appropriate, for application to a real site (Lacnor) and to the extent practicable to calibrate the system model using site-specific measurements. Since the primary product of the NUTP modelling studies is the generic UTAP program, the UTAP Program has been thoroughly reviewed and modified along with the supporting documentation where appropriate. The current version of the updated generic code which reflects these revisions is referred to as UTAP.3. UTAP.3 also reflects revisions of a generic nature which were identified through the application of UTAP to the Lacnor site.

This volume is a user's manual for UTAP.3. It provides some background information regarding the structure of UTAP and describes its input and output characteristics. The information provided is sufficient to allow a user to run the program as it currently exists, modifying the inputs and obtaining a variety of outputs. Furthermore, sufficient details are provided to allow a more sophisticated user to modify existing modules of code and/or replace entire modules.

NOTICE

This report was prepared by SENES Consultants Limited (SENES) under contract to the National Uranium Tailings Program (NUTP). Neither NUTP nor SENES makes any warranty, expressed or implied, or assumes any liability with respect to any damage or loss incurred as a result of the use made of the information contained in this publication.

TABLE OF CONTENTS

Page

Abstract i
Notice i

1.0 INTRODUCTION 1-1
  1.1 Background 1-1
  1.2 How to Use the Manual 1-2
  1.3 Objectives of the Uranium Tailings Assessment Program 1-3
    1.3.1 Constituents 1-4
    1.3.2 Pathways 1-4

2.0 CONTROL MODULE FUNCTIONS 2-1
  2.1 Input 2-1
  2.2. Draw Random Samples 2-1
  2.3 Select Parameters for Output and Statistics 2-2
  2.4 Compute Statistics on Selected Variables 2-2
  2.5 Write Data to Output Files 2-2
    2.5.1 Statistics File 2-2
    2.5.2 Detailed Results File 2-3
  2.6 Step Through Time 2-3
  2.7 Confidence Bands 2-3

3.0 BUILDING INPUT FILES AND SELECTING OUTPUT 3-1
  3.1 First Input File 3-1
    3.1.1 Application to a Real Site 3-4
    3.1.2 Selecting Alternate Scenarios 3-4
  3.2 Second Input File 3-5
    3.2.1 Receptor Information 3-5
    3.2.2. Watershed Information 3-6
    3.2.3 Output Selection Information 3-7
  3.3 Air Dispersion Data 3-9

Table of Contents, Cont'd.

Page

4.0 COMPILING AND LINKING 4-1

5.0 RUNNING THE PROGRAM 5-1

6.0 ALTERING THE PROGRAM 6-1
  6.1 Changing COMEX 6-2
  6.2 Writing Component Modules 6-2
  6.3 Passing Variables 6-2
    6.3.1 Include File MODEL.INC 6-2
    6.3.2 Include File VAR.INC 6-6
  6.4 Obtaining Additional Outputs 6-7
  6.5 Modifying First Input File 6-8
  6.6 Modifying Second Input File 6-8
  6.7 Other Changes and Information 6-8

7.0 CONFIDENCE BANDS 7-1
  7.1 Running the Program 7-1

REFERENCES

APPENDIX A - ERROR AND WARNING MESSAGES
APPENDIX B - SAMPLE INPUT FILES
APPENDIX C - SAMPLE OUTPUT FILES
APPENDIX D - INPUT DISTRIBUTION DESCRIPTIONS
APPENDIX E - APPLICATION TO LACNOR SITE SAMPLE INPUT AND OUTPUT FILES

LIST OF FIGURES

		Follows Page
1.1	The System Model	1-4
1.2	Exposure Pathways	1-5
3.1	Input and Output Files	3-1
3.2	Forms of the Weibull Distribution Probability Density Function	3-2
3.3	Forms of the Beta Distribution Probability Density Function	3-2
3.4	An Arbitrary Probability Density Function	3-2
3.5.	Conceptual Diagram of Spatial Coordinate System	3-5
3.6	Reference Site: Tailings Area	3-6
6.1	Control Module Structure	6-1
6.2	Subroutine COMEX and the Component Modules	6-1
7.1	Plots of 95% Confidence Bands for a Normal Distribution	7-2

LIST OF TABLES

Follows Page

3.1. Sample of First Input File 3-1

3.2 Format of First Input File (INPUT1.DAT) 3-1

3.3 Distribution Descriptors 3-2

3.4 Tailings Closeout Options - Nominal UTAP Input Parameters 3-5

3.5 Sample of Second Input File (INPUT2.DAT) 3-5

3.6 Format of Second Input File (INPUT2.DAT) 3-5

3.7 Output Parameters 3-8

3.8 Substance Codes 3-8

3.9 Format of AES Wind Data File 3-10

5.1 Sample Session 5-1

7.1 Confidence Bands Program Sample Session 7-1

7.2 Confidence Bands Program Sample Output File 7-2

1.0 INTRODUCTION

1.1 Background

In 1982 Energy, Mines and Resources Canada established the National Uranium Tailings Program (NUTP) to pull together previous work on Canadian uranium mill tailings, to fund additional work where significant information on gaps were found and to develop the capability to predict the long-term effects of tailings with a known degree of confidence while incorporating variability and uncertainty in the input data. Such evaluations require the use of mathematical models to simulate the behaviour of the real system. Results of the previous phases of work have demonstrated that a probabilistic approach provides the framework necessary for incorporating uncertainty into a simulation (SENES, 1984; 1985; 1986).

An earlier study (Phase I) funded by the NUTP demonstrated how probabilistic techniques could be used to take account of the variability and uncertainty in model input parameters in such a simulation analysis (SENES, 1984). Subsequently, the NUTP sponsored a followup study (Phase II, SENES, 1985) to extend and refine the probabilistic tools developed in the Phase I study and to investigate various issues of technical interest involved in carrying out and interpreting a probabilistic analysis.

The Phase III study extended the capabilities of the Phase II system model and then applied the upgraded (Phase III) system model to a hypothetical reference site. The emphasis of the Phase IV work is to demonstrate the use of the Uranium Tailings Assessment Program (UTAP) in assessing a real (vs. hypothetical) uranium tailings site. The Lacnor tailings area in Elliot Lake, Ontario, for which the NUTP has recently carried out an extensive field study (Golder _et_ _al_., 1986), was chosen for this purpose. The primary objective is to learn what is entailed in such an application, e.g. what are the data requirements, what level of modelling detail is appropriate, and what are the difficulties and limitations of such an application.

1.2 How to Use the Manual

Three versions of UTAP are the products of the Phase III and Phase IV studies. These are:

- UTAP.1 the original Phase III code, "UTAP", now archived and inactive
- UTAP.2 the original Phase III code as revised based on a comparison of UTAP with AECL's SYVAC code (WNRE, 1987).
- UTAP.3 an updated generic code which reflects the revisions made on the basis of the WNRE/SENES intercomparison as well as revisions of a generic nature identified from the Lacnor study (Phase IV)

UTAP version 1 is documented in the Phase III report. Changes to UTAP made for version 2 are reflected in this report which also documents UTAP.3 The Phase III documentation (SENES, 1986) was divided into the following four volumes:

Volume 1: Probabilistic Model Development for the Assessment of Uranium Mill Tailings in Canada - Phase III, Volume 1: Summary Report.

Volume 2: Probabilistic Model Development for the Assessment of Uranium Mill Tailings in Canada - Phase III, Volume 2: System Description and Control Module Documentation.

Volume 3: Probabilistic Model Development for the Assessment of Uranium Mill Tailings in Canada - Phase III, Volume 3: Component Model Documentation.

Volume 4: Probabilistic Model Development for the Assessment of Uranium Mill Tailings in Canada - Phase III, Volume 4: Uranium Tailings Assessment Program (UTAP) User's Manual.

In documenting the Phase IV study, Volumes 3 and 4 of the Phase III study have been updated incorporating changes made in producing UTAP.3 and these volumes have been reissued in their entirety (SENES, 1987c and this report). An addendum to Volume 2 has also been issued, outlining changes which apply to the Phase IV study (SENES, 1987a). Volume 1 has been replaced by a report specific to the application of UTAP to the Lacnor site and the user interested in applying UTAP to a real site is referred to this report for further information.

This user's manual for the Uranium Tailings Assessment Program (UTAP.3) is geared toward two types of users. The first type is the Level I user who simply wishes to use the program. Such considerations as building and modifying input files and obtaining desired output are dealt with in the Level I user sections. The second type of user is the Level II user who actually wishes to change the program by adding new lines of code or new modules. The level of detail provided to the Level II user is, hence, considerably higher.

The first two sections of the manual provide both Level I and II users with necessary background on UTAP. The third and fourth sections called "Building Input Files and Obtaining Output" and "Running the Program" are for the Level I user but must also be understood by the Level II user. The fifth section titled "Altering the Program" is intended for the Level II user.

1.3 Objectives of the Uranium Tailings Assessment Program

The principal objective of the Uranium Tailings Assessment Program is to perform a probabilistic analysis of the behaviour and environmental effects of uranium mill tailings, following close-out of milling operations. The models in this Phase IV study have been designed to allow predictions to be made for distances up to 50 kilometres in all directions from the tailings area. In addition, the models provide many other features. These include the ability to incorporate different receptors and site characteristics and to deal with input parameters which vary with time.

To achieve its objectives, the Uranium Tailings Assessment Program is composed of a number of modules. These may be classified as either component or control modules. Component modules (or models) are the programs directly concerned with the simulation of a uranium tailings physical system; that is, the computer implementation of the mathematical models representing the uranium tailings pile and surrounding environment. Control modules provide the infrastructure for probabilistic analysis using the component modules. These functions include probabilistic sampling of input parameters, and many input, output and bookkeeping functions. The integrated control and component modules are referred to as the system model or UTAP as illustrated in Figure 1.1.

1.3.1 Constituents

The radionuclides modelled are natural uranium, total thorium, radium-226, radon-222 and lead-210. The pH of the reference uranium tailings site and the chained river-lake system discussed later are also modelled. As in Phases II and III, pH is modelled in UTAP.3 by an equilibrium relationship which explicitly accounts for the dissolved concentrations in the aqueous phase of calcium, iron and sulphate.

1.3.2 Pathways

The following pathways of dose to the receptors are modelled in UTAP.3 for the aforementioned radionuclides:

1) Water Consumption: dispersion of tailings effluent in the receiving water environment and consumption by humans.
2) Fish Consumption: the transfer of radionuclides from the receiving water environment to fish and consumption by humans.
3) Radon Inhalation: dispersion of radon exhaled from the reference tailings site through the air environment and inhalation by humans.
4) Dust Inhalation: dispersion of dust eroded from the surface of the reference tailings site in the air environment and inhalation by humans.

FIGURE 1.1

THE SYSTEM MODEL

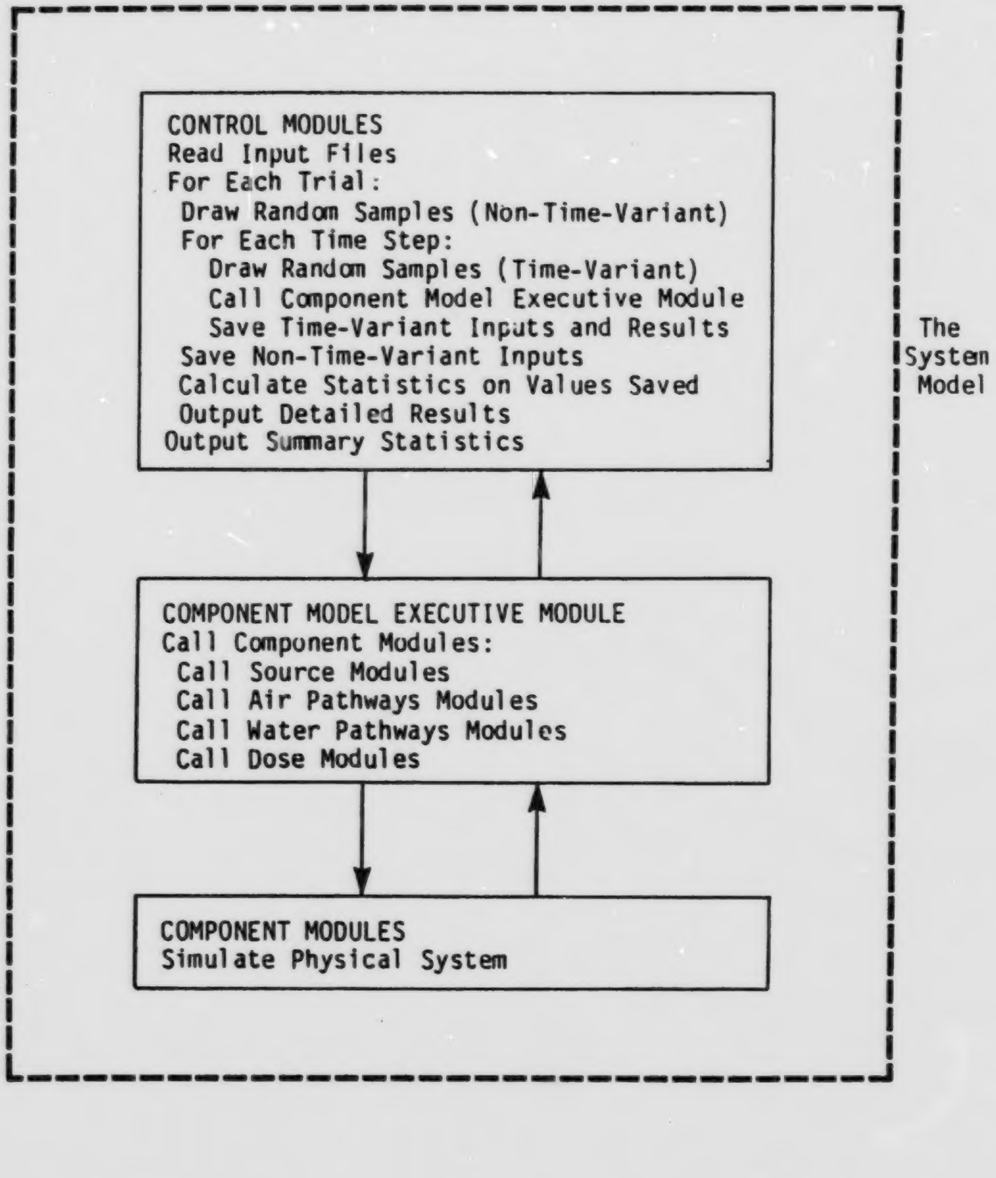
CONTROL MODULES
Read Input Files
For Each Trial:
Draw Random Samples (Non-Time-Variant)
For Each Time Step:
Draw Random Samples (Time-Variant)
Call Component Model Executive Module
Save Time-Variant Inputs and Results
Save Non-Time-Variant Inputs
Calculate Statistics on Values Saved
Output Detailed Results
Output Summary Statistics
COMPONENT MODEL EXECUTIVE MODULE
Call Component Modules:
Call Source Modules
Call Air Pathways Modules
Call Water Pathways Modules
Call Dose Modules
COMPONENT MODULES
Simulate Physical System
The System Model

5) Vegetable Consumption: the transfer of radionuclides to above and below ground vegetation and subsequent consumption by humans.

6a) Animal Produce Consumption: the uptake of radionuclides by forage vegetation and lichens, subsequent transfer to moose, caribou and deer and consumption of the animal meat by humans.

6b) Animal Produce Consumption: the uptake of radionuclides by aquatic vegetation, subsequent transfer to moose and deer and consumption of the animal meat by humans.

6c) Animal Produce Consumption: caribou, moose and deer consumption of lake and river water and subsequent consumption of the animal meat by humans.

7) Groundshine: direct radiation from deposited dust.

These pathways are illustrated in Figure 1.2.

Detailed descriptions of the mathematical models and assumptions used in the development of each component module are presented in Volume 3 of the Phase IV System Model Development documentation.

FIGURE 1.2

EXPOSURE PATHWAYS

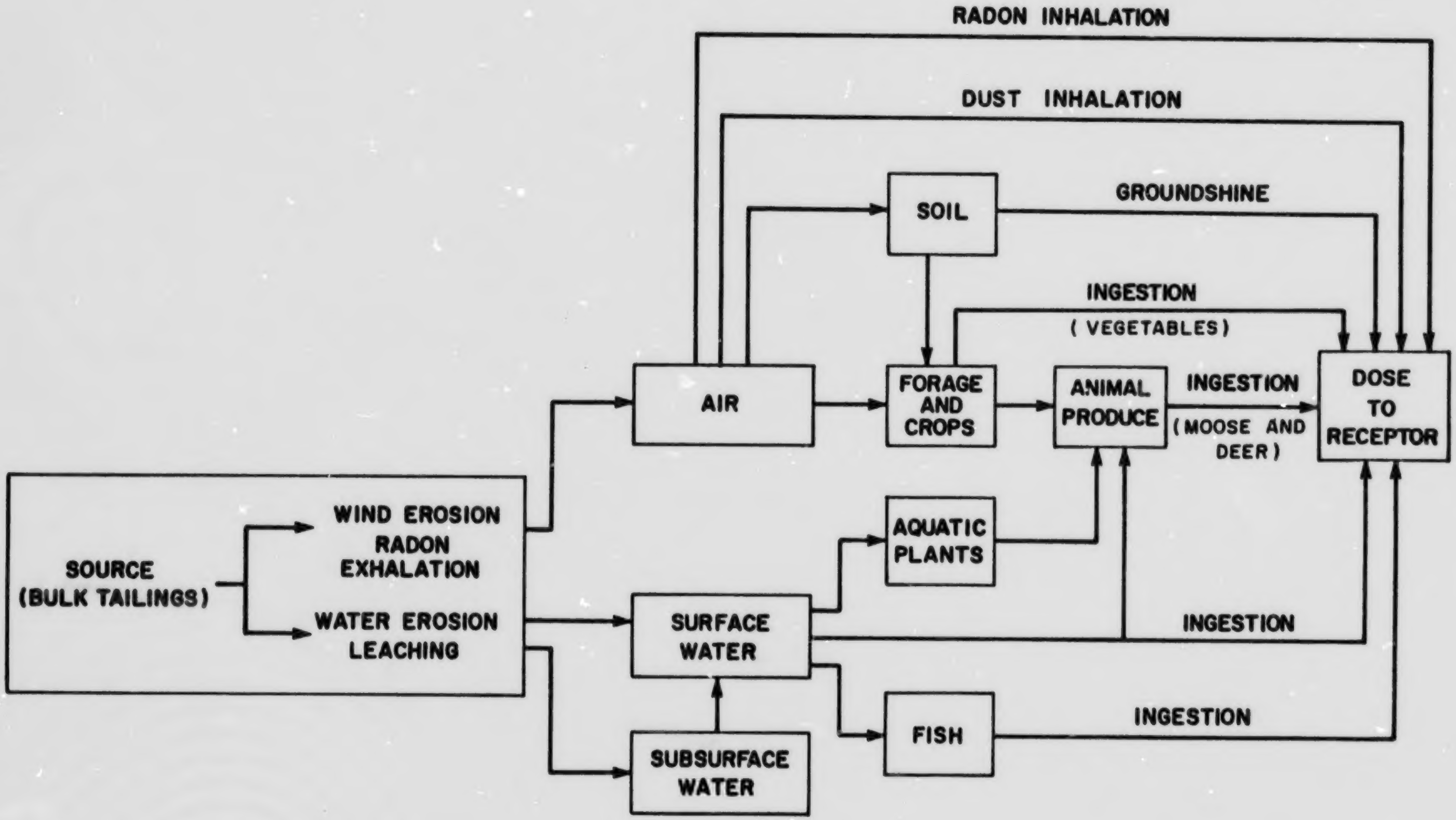

2.0 CONTROL MODULE FUNCTIONS

2.1 Input

The control modules open, access and read the three input files required for the probabilistic assessment of uranium tailings. These include the first input file, the second input file, and the air dispersion file. The first input file specifies output files and the distributions of input parameters. The second input file contains input variables specific to UTAP and output selections.

2.2 Draw Random Samples

The control modules draw random samples from the following user-specified probability distributions for the input model parameters:

1) Constant
2) Normal
3) Lognormal
4) Uniform
5) Log uniform
6) Triangular
7) Weibull
8) Beta
9) Arbitrary
10) Correlated

Variables are sampled once for each trial except for those specified as time-variant which are sampled each time step of each trial.

The selected random samples are routed to the appropriate component modules.

2.3 Select Parameters for Output and Statistics

The user may specify concentration and dose data as well as selected input parameters for output at selected time intervals without having to alter the program. These data reside in a series of arrays in the program. Parameter selection for output is achieved by specifying the time intervals desired and the positions in the concentration and dose arrays required for output.

Two output options are available: 1) summary statistics (key file), the default option and 2) writing selected outputs for all trials to a disk file (detailed results file) in addition to creating the key file of option 1.

2.4 Compute Statistics on Selected Variables

Summary statistics are computed for user-selected output parameters and input distributions. These statistics are updated at the end of each trial and printed to a disk file at the end of the simulation.

2.5 Write Data to Output Files

The two output files discussed below are available to the user. Sample output files are shown in Appendix C.

2.5.1 Key File

This file is the default and is created for every run. The following summary statistics computed by the statistics routines are output to a user-specified disk file, called the key file:

Mean
Standard deviation
Geometric mean
Geometric standard deviation
Minimum
Maximum

Skewness and kurtosis are also available as an output option.

The parameter names, specifications, and the time intervals selected are output, as appropriate.

Statistics not calculated will appear as blanks in the key file. For instance, if only one trial is performed, standard deviations, skewness and kurtosis will not be calculated and blanks will be written to the key file.

2.5.2 Detailed Results File

In addition to the key file described above, a detailed results file can be selected in the first input file.

The detailed results file contains the actual data from which the statistics written to the key file are calculated. The user-selected parameters are written to the detailed results file at the end of each trial.

The rows of the key file correspond to the columns of the detailed results file. For instance, the third row of the key file describes the data contained in the third column of the detailed results file. These two files also serve as input to the confidence bands program (CBAND).

2.6 Step Through Time

The total time to be modelled and the time increment are specified in the first input file. The maximum number of time steps allowed is 300.

2.7 Confidence Bands

The confidence band programs (BIN and CBAND) are post-processing programs that calculate confidence band estimates on user-selected data. The programs process the detailed results file and the key file to obtain these confidence band estimates.

3.0 BUILDING INPUT FILES AND SELECTING OUTPUT

The program reads input data from three files. Examples of the generic site input files are provided to the user on disk and are called INPUT1.DAT, INPUT2.DAT, and AVERAGE.DAT. Listings of these files are shown in Appendix B and the output files resulting from them are included in Appendix C. The third file of these contains the air dispersion data. The contents of the input files are illustrated in Figure 3.1. The user is prompted interactively for the names of the first two input files while the name of the third file is specified within the second input file.

3.1 First Input File (INPUT1.DAT)

This file is used to specify the output files desired and the distributions of input parameters. A sample file containing the different distribution types available is shown on Table 3.1. Descriptive labels not found in an actual input file have been added to Table 3.1. The file format is described on Table 3.2.

The first line of this file is the run title to be written to the key file. Next, two flags are specified. The first flag controls the opening of a detailed results file named on the next line and the second flag controls output of skewness and kurtosis to the key file, also named below this. The key file is always created.

The total number of distributions, as well as the numbers of arbitrary and correlated distributions are input. The specifics of the run are set up by reading the random number seed, the number of trials, the simulation length, and the time increment. The following random number seeds have been thoroughly tested:

824064364
913566091
2096730329
281629770

FIGURE 3.1

INPUT AND OUTPUT FILES

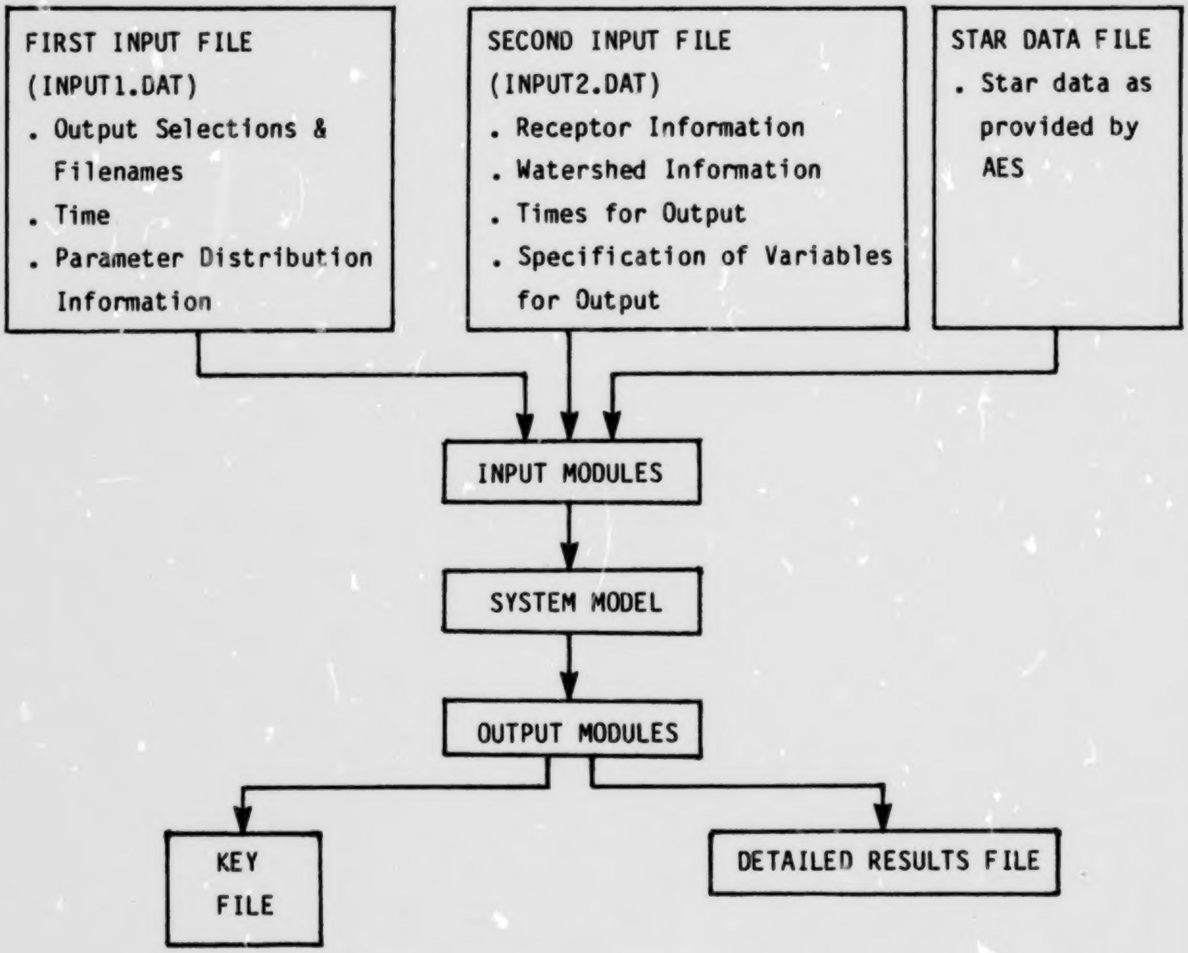

Table 3.1

SAMPLE OF FIRST INPUT FILE

```
     Title
PROBABILISTIC ANALYSIS: TEST CASE

┌────Detailed Results file indicator
│  ┌──────Skewness and kurtosis indicator
Y N
     Detailed Results file name
RES.OUT
     Key file name
KEY.OUT
   ┌─Number of input distributions
   │   ┌───Number of arbitrary distributions
   │   │   ┌────Number of correlated parameters
  10   1   1
  ┌──Random number seed
  │          ┌───Number of trials
0913566091  10
    ┌Years in simulation
    │     Time increment in years
   100.   10.
     Regular distributions:
   ┌──────Parameter name
   │   ┌───────Output flag
   │   │  ┌─────────Distribution type number
   │   │  │ ┌────────────Time-variant flag
   │   │  │ │                 Distribution descriptors
CONST  N  1 N        2.0
NORMAL N  2 V       10.0        2.0        0.0       20.0
LNORM  N  3 V     1.0E02        1.5        1.0      1.0E3
UNI    F  4 N        1.0        2.0
LOGUNI N  5 N       0.01        0.5
TRIANG N  6 N       0.01       0.03        0.1
WEIBUL F  7 V        0.0        1.5        0.9
BETA   N  8 N       10.0      100.0        2.0        2.0
     Arbitrary distributions:
 ┌────────Parameter name
 │     ┌───────Output flag
 │     │  ┌─────────Distribution type number
 │     │  │ ┌────────────Time-variant flag
 │     │  │ │ ┌───────────────Number of cells in distribution
 │     │  │ │ │                    Distribution descriptors
ARB    N  9 N 10    1.0   11.0  2.0  2.0  2.0  8.0  8.0  8.0 12.0 12.0  4.0  4.0

     Correlated distributions:
  ┌───────Parameter name
  │    ┌───────Output flag
  │    │  ┌─────────Distribution type number
  │    │  │ ┌────────────Time-variant flag
  │    │  │ │ ┌───────────────Name of independent distribution
  │    │  │ │ │                    Distribution descriptors
CORREL N 10 N NORMAL       50.0       10.0        0.7       10.0        2.0
```

Table 3.2

FORMAT OF FIRST INPUT FILE (INPUT1.DAT)

	Column	Format	Description
Line 1:			
	1-40	A40	Title
Line 2:			
	1	A1	Detailed results file desired (Y/N)
	3	A1	Skewness and Kurtosis desired in key file (Y/N)
Line 3:			
	1-12	A12	Detailed results file name
Line 4:			
	1-12	A12	Key file name
Line 5:			
	1-4	I4	Number of input distributions (max. 300)
	5-8	I4	Number of arbitrary distributions
	9-12	I4	Number of correlated parameters
Line 6:			
	1-10	I10	Random Number Seed
	11-14	I4	Number of trials
Line 7:			
	1-7	E7.2	Years in Simulation
	8-14	E7.2	Time increment in years (maximum of 10 years is recommended)

Distributions:

Constant, Normal, Lognormal, Uniform, Loguniform, Triangular, Weibull, and Beta distributions. One line for each distribution:

Column	Format	Description
1-6	A6	Parameter name
8	A1	Output flag (F/N)*
10-11	I2	Distribution Type Number (Table 3.3)
13	A1	Time-Variant Flag (Variant, Not => V/N**)
14-57	4E11.6	Distribution Descriptions (Table 3.3)

Arbitrary distributions. One line for each distribution:

Column	Format	Description
1-6	A6	Parameter name
8	A1	Output flag (F/N)*
10-11	I2	Distribution Type Number (Table 3.3)
13	A1	Time-Variant Flag (Variant, Not =>V/N**)
14-16	I3	Number of cells in distribution (max. 25)
17-38	2E11.6	Minimum and Maximum x-values
39-188	25F6.2	Function value for each cell

Table 3.2/cont'd.

Correlated distributions. One line for each distribution:

1-6	A6	Parameter name
8	A1	Output flag (F/N)*
10-11	I2	Distribution Type Number (Table 3.3)
13	A1	Time-Variant Flag (Variant, Not => V/N**)
15-20	A6	Name of independent variable
21-75	5E11.6	Distribution Descriptions

Notes

* F = detailed results files, N = no output of variable. Default is No output.

** Default is N, non-time-variant

The time increment must divide evenly into the simulation length and the maximum number of time steps allowed is 300. A maximum time step of ten years is recommended to preserve the accuracy of the model. The minimum time step is one year.

The input parameters are specified as distributions with their type numbers according to Table 3.3. Each type of distribution is specified using different descriptors as indicated on Table 3.3 The weibull, beta, and arbitrary distributions are illustrated in Figures 3.2, 3.3 and 3.4, respectively. The location parameter "a" for the weibull distribution, not shown on Figure 3.2, determines the position of the origin on the horizontal axis. For instance, if a = 2 the origin is shifted 2 places to the right.

The input distributions required are described in Appendix D. These must be entered in exactly the same order as they appear in the Appendix and in the example file, INPUT1.DAT, shown in Appendix B.

Included in the input distributions described in Appendix D are various print codes. These are used to turn on and off numerous write statements within the program that generate detailed output to the screen. In general, a zero value turns off this output and one turns it on. Other values available for use are listed on page D-1 of Appendix D. The detailed printouts can be used to check calculations performed by the program.

The distribution names specified are used by the program to identify correlated parameters. These names are also written to the key file.

The "output flag" indicated in Table 3.2 (column 8) allows the user to output sampled parameter values to the files selected, if desired. The default is no output.

Distributions can be either time-variant or non-time-variant as indicated by the time-variant flag. The default is non-time-variant. Time-variant parameters are sampled for each time step of each trial while non-time-variant

Table 3.3

DISTRIBUTION DESCRIPTORS

Distribution	Distribution Number	Distribution Descriptors	Column
Constant	1	Constant	14-24
Normal	2	Mean	14-24
		Standard Deviation	25-35
		Minimum	36-46
		Maximum	47-57
Lognormal	3	Geometric Mean	14-24
		Geometric Standard Deviation	25-35
		Minimum	36-46
		Maximum	47-57
Uniform	4	Minimum	14-24
		Maximum	25-35
Log-uniform	5	Minimum	14-24
		Maximum	25-35
Triangular	6	Minimum	14-24
		Mode	25-35
		Maximum	36-46
Weibull (Figure 3.2)	7	Location Parameter (Minimum)(a)	14-24
		Scale Parameter (b)	25-35
		Shape Parameter (c)	36-46
Beta (Figure 3.3)	8	Minimum	14-24
		Maximum	25-35
		a shape parameters	36-46
		b	47-57
Arbitrary (Figure 3.4)	9	Number of cells (max. 25)	14-16
		Minimum x-value	17-27
		Maximum x-value	28-38
		Ordinate Values	39-(188)
Correlated	10	Mean of dependent variable	21-31
		Standard Deviation of Dependent Variable	32-42
		Correlation Coefficient	43-53
		Mean of Independent Variable	54-64
		Standard Deviation of Independent Variable	65-75

FIGURE 3.2

FORMS OF THE WEIBULL DISTRIBUTION
PROBABILITY DENSITY FUNCTION

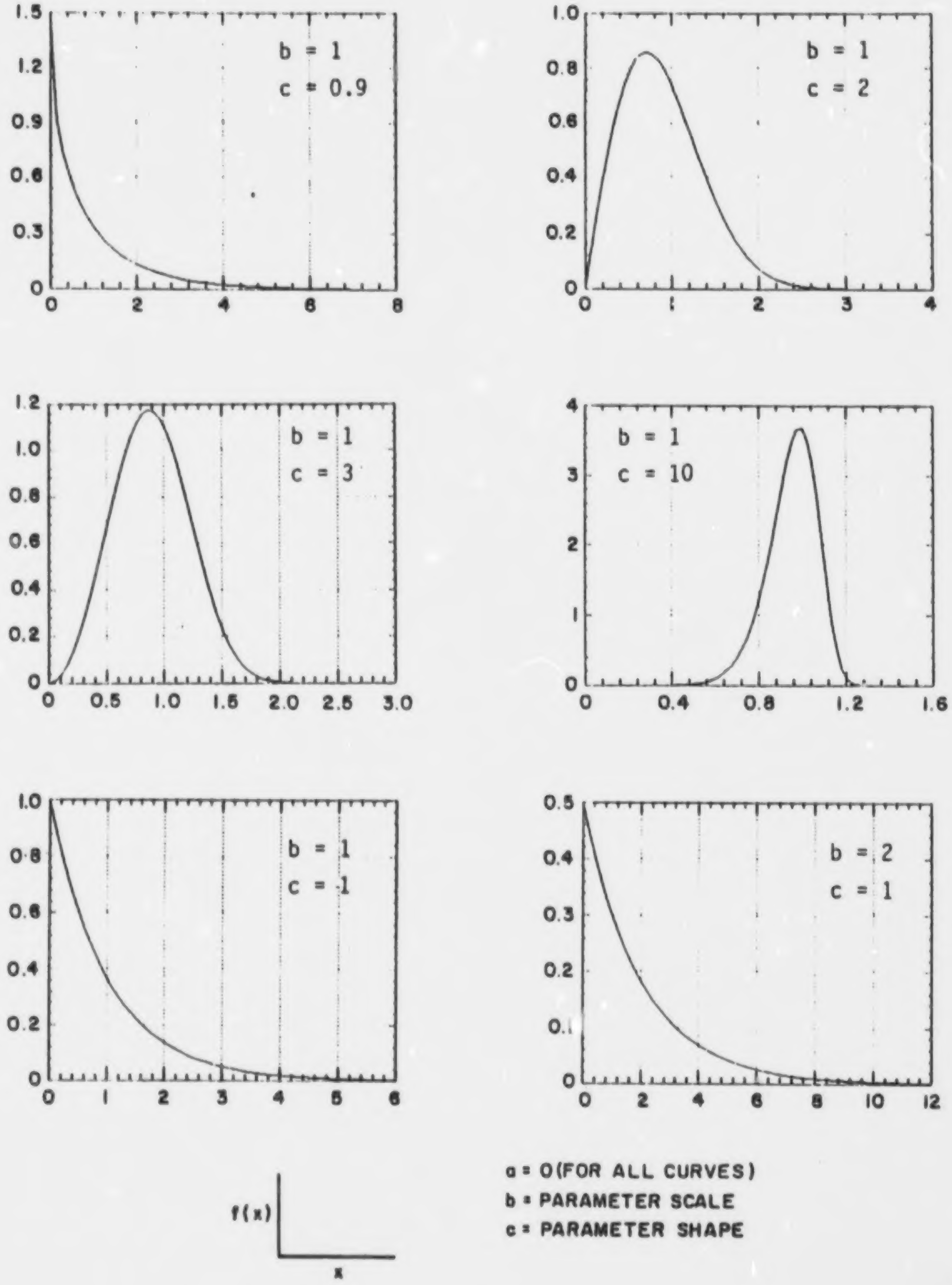

a = 0 (FOR ALL CURVES)
b = PARAMETER SCALE
c = PARAMETER SHAPE

FIGURE 3.3

FORMS OF THE BETA DISTRIBUTION PROBABILITY DENSITY FUNCTION

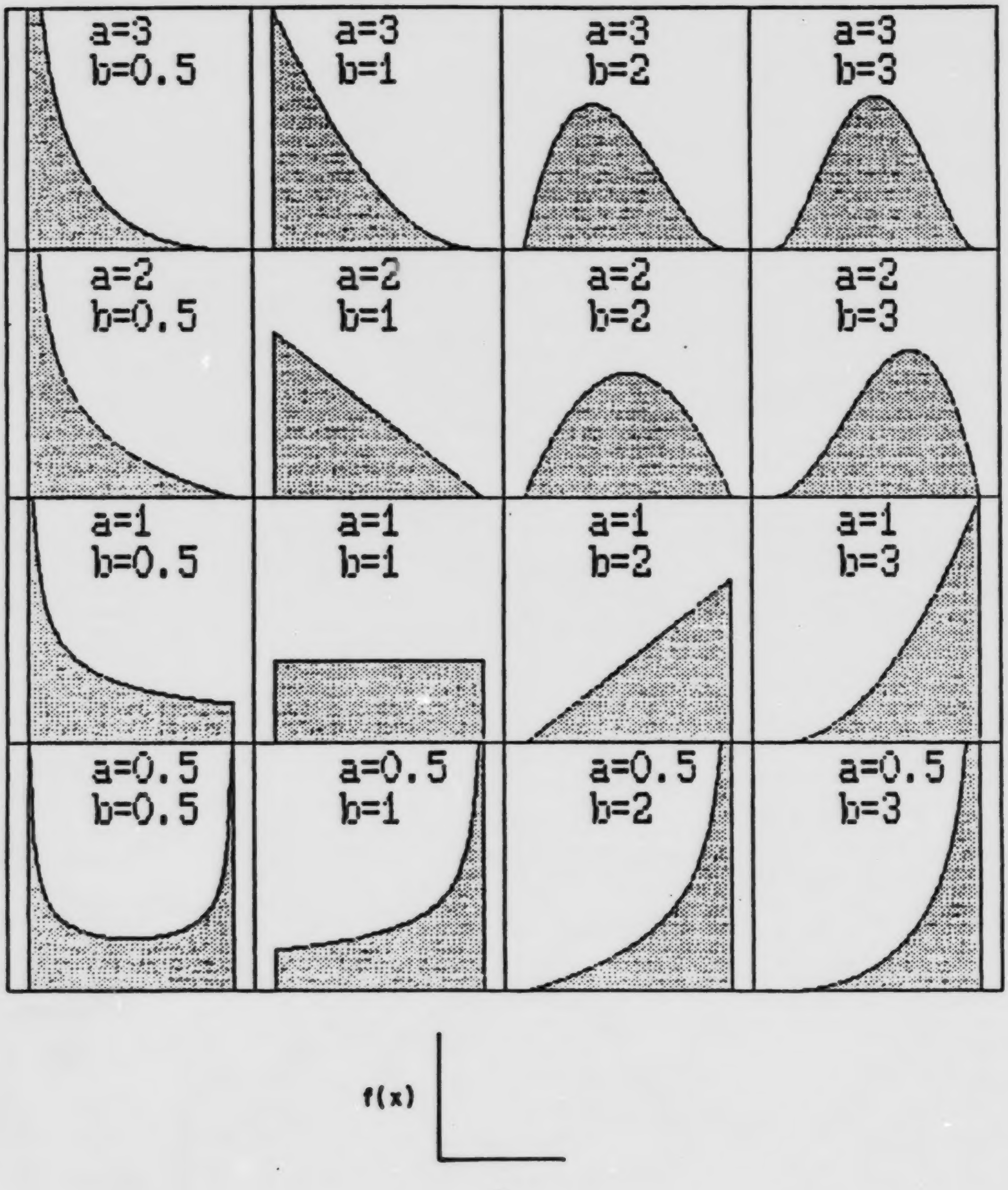

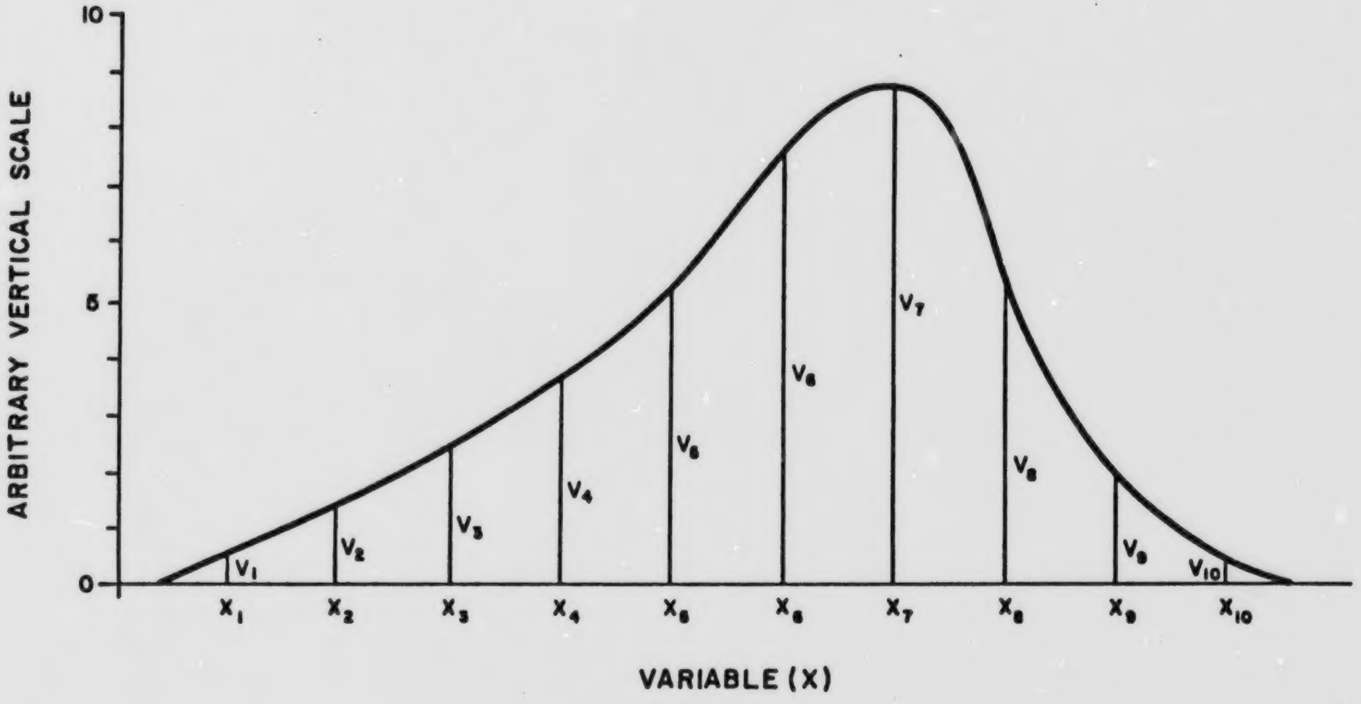

FIGURE 3·4
AN ARBITRARY
PROBABILITY DENSITY FUNCTION

parameters are sampled once for each trial.

Time variant parameters should be adjusted to correspond to the time step being used. The standard deviation should be set equal to that for annual data (one year time step) divided by the square root of the time step used. Thus, if the standard deviation of a normal distribution is .1 for a one year time step, it should be changed to $.1/\sqrt{10}$ or 0.03 for a ten year time step. The mean value is unaffected. A similar procedure should be used for lognormal distributions that are time variant. For instance, a geometric standard deviation of 1.2 for a one year time step should be converted to a ten year time step by computing the logarithm of the geometric standard deviation, dividing by the square root of the time step and then taking the anti-logarithm of this. The new geometric standard deviation becomes the anti-logarith of $\log (1.2)/\sqrt{10}$ or 1.06. Note that strictly this conversion applies to normally distributed time variant parameters or time-variant parameters whose logarithms are normally distributed.

In practice, however, this is not a restriction. Because they vary from one sample to the next, sample statistics such as the mean and variance are themselves random variables with the properties:

$$E(\overline{x}) = \mu$$

$$\mathrm{Var}(\overline{x}) = \sigma^2/n$$

$$E(s^2) = \sigma^2$$

That is, on repeated sampling, the long-term average values of the sample mean ($E(\overline{x})$) and variance ($\mathrm{Var}(\overline{x})$) are the pupulation mean (μ) and variance (σ^2), of which these are estimates. The distribution of the sample mean has a further very important property; namely, that as a consequence of the Central Limit Theorem, thus as the sample size becomes larger the form of the distribution of the sample mean (e.g. mean annual windspeed) approaches the normal distribution.

3.1.1 Application to a Real Site

The main purpose of the Phase IV study was to apply UTAP to the Lacnor site, calibrating input parameters based on the results of an extensive field study and evaluating different closeout options. Sample probabilistic input files and the corresponding results for the base case (no remedial work carried out) are shown in Appendix E. The input files used are available to the user on disk and are called LAC1.DAT and LAC2.DAT. The air dispersion data file used is called AVERAGE.DAT, the same file as used by the generic site as shown in Appendix B.

The user interested in applying UTAP to another site is referred to the Lacnor report (SENES, 1987d) which details the field data required and outlines the type of calibration procedures necessary, using the Lacnor study as an example.

3.1.2 Selecting Alternate Scenarios

UTAP has been developed to allow the examination of several distinct tailings management options, or scenarios. The default option (i.e. that specified by the data supplied with this program), also referred to as the base case option, represents a situation in which no extraordinary measures are taken in closing out the tailings area.

Five closeout options were made available for the Lacnor study. These are:

Option 1) Base Case Option: tailings surface vegetated; no other remedial work carried out.

Option 2) Waste Rock Cover: application of a 0.6 m cover of waste rock on the tailings area; no other remedial work carried out.

Option 3) Depyritized Tailings Cover: application of a 2 m cover of tailings from which the pyrite component has been substantially removed;

construction of new dams on the southeast rim to raise the water table in the tailings area; construction of a new spillway at the southwest corner; tailings surface vegetated.

Option 4) Earthen Cover: application of a 2 m cover of glacial till on the tailings area; construction of new dams on the south-east rim to raise the water table in the tailings area; construction of a new spillway at southwest corner.

Option 5) Water Cover: application of a water cover to the tailings: construction of new dams on the south-east rim to raise the water table; construction of a new spillway on the southwest side of the basin; construction of cells within the tailings basin using dykes.

Input parameters to the UTAP model which must be altered to simulate the various options are presented in Table 3.4 along with those values used for the Lacnor Study (SENES, 1987d).

3.2 Second Input File (INPUT2.DAT)

The second input file contains the name of the air dispersion data file, receptor information, watershed information and output selection information in that order. Table 3.5 illustrates a sample file, "INPUT2.DAT". This is formatted according to the description on Table 3.6. The choice of air dispersion data files is discussed further in Section 3.3.

Receptor position is defined by a windrose structure while the watershed is defined as a series of segments. Windrose and watershed concepts as well as the specification of output selection information are discussed in the next three sections.

3.2.1 Receptor Information

The windrose structure shown in Figure 3.5 defines a system of spatial

Table 3.4

TAILINGS CLOSEOUT OPTIONS - NOMINAL UTAP INPUT PARAMETERS

Tailings/Cover Material Properties	Closeout Options Opt.1 Base Case	 Opt.2 Waste Rock Cover	 Opt.3 Depyritized Tailings Cover	 Opt.4 Glacial Till Cover	 Opt.5 Water Cover
Pyrite as FeS_2 ($mol.m^{-3}$) "PYRITI"	700.	700.	54.	700.	700.
Initial Sulphate Production Rate ($mol.g_{tailings}^{-1}.yr^{-1}$) "SULPRD"	4.1×10^{-6}	4.1×10^{-6}	2.43×10^{-8}	3.15×10^{-6}	4.1×10^{-6}
% Moisture Content $g_{water}.g^{-1}_{tailings}$) in Layer One "MPCH2O"	13	13	13	28	28
Effective Oxygen Diffusivity ($m^2.yr^{-1}$) "O2DIFF"	37	37	37	6.2×10^{-3}*	6.2×10^{-3}*
Fraction of Direct Surface Runoff "XRUNOF"	0.60	0.30	0.60	0.60	0.85
Uranium as U_3O_8 (%) in ore "PCURAN"	0.1	0.1	0.08	0.1	0.1
Fraction of Uranium Dissolved as a Result of Pyrite Oxidation "FRACU"	0.6	0.6	0.058	0.6	0.6
Calcite as $CaCO_3$ ($g_{calcite}.g^{-1}_{tailings}$) "XLIME"	0.0005	0.0005	0.01	0.0005	0.0005
Hydraulic Conductivity ($m.yr^{-1}$) "HCGWAT"	69.4	69.4	6.9**	6.9**	6.9**
Fraction of Radon Attenuation by Cover "CAFR"	0.0	0.0	0.0	0.99	0.5

Table 3.4 continued

Tailings/Cover Material Properties	Closeout Options Opt.1 Base Case	 Opt.2 Waste Rock Cover	 Opt.3 Depyritized Tailings Cover	 Opt.4 Glacial Till Cover	 Opt.5 Water Cover
Fraction of Dust Attenuation by Cover "CAFD"	0.0	0.95	0.0	1.0	0.75
Minimum Fraction of Initial Ground Cover "MINVEG"	0.6	0.0	0.6	0.90	0.0
Depth of Layer 2 (m) "DUNSAT"	0.5	0.5	0.5	0.10	0.10
Depth of Layer 3(m) "DMIX"	11.5	11.5	11.5	11.9	11.9
Depth of Layer 4 (m) "DBOT"	0.75	0.75	2.75	0.75	0.75

NOTE
* have assumed layers 1 and 2 are saturated
** have made dams impermeable

Table 3.5

SAMPLE OF SECOND INPUT FILE (INPUT2.DAT)

```
     Flag to indicate if variable wind data is desired
  N
     File containing appropriate wind data
STARAV.DAT
     Number of receptor locations
  5
     Number of rings
  5
     Ring limits
   1    3    5   10   20   50
     Receptor information:
              Receptor number
                   Sector number
                        Ring number
                             Drinking water source segment number
                                  Fish source segment number
                                       Receptor type
                                            Population
  1 16  1  1  1 C    2
  2 16  3  2  2 A    5
  3 14  3  2  2 A    6
  4  1  1  1  1 C    1
  5  7  3  2  2 A    3
    Number of watershed segments
          Number of groundwater flow paths
  8  2
    End node numbers of watershed segments groundwater flows into
  1  1
     Layers for groundwater flow
  3  3
     Watershed information:
              End node or segment number
                  Segment type
                        Sector number of end node
                             Ring number of end node
                                  Lake depth
                                       Watershed area
                                            Lake surface area/River length
  1 R 11  1             1.5E07    3.0E3
  2 L 11  1   1.0E01    2.0E07    5.0E05
  3 R 10  2             3.2E07    3.5E3
  4 L 10  2   4.0       3.8E07    2.5E05
  5 R  9  3             7.0E07    7.0E3
  6 R  9  4             1.2E08    1.3E4
  7 L  9  4   5.0       1.4E08    4.0E06
  8 R  9  5             4.0E08    3.0E4
       Number of time steps to be saved
  4
     Time steps to be saved
  .1E2  .2E2  .3E2  .4E2
```

Table 3.5 cont'd

```
     Number of arrays to be checked for output
 36
 ┌──Array name
 │     ┌─Array size
WCONC   0
CONC    0
PH      0
WATC    2
  ┌──Substance code
  │   ┌── Location code
  2  3
  3  5
WATAVG  3
  1  1
  3  1
  4  1
WATPH   3
  1  7
  1  4
  1  2
GWATC   0
EMRATE  0
EROTOT  0
AIRC    0
SOILC   0
AVEGC   0
BVEGC   0
SUFOC   0
BRWSC   0
LICHC   0
AQVEGC  0
FISHC   0
ADERC   0
WDERC   0
AMOSC   0
WMOSC   0
ACARC   0
WCARC   0
WATD    0
SHINED  0
INHD    0
RADD    0
VEGD    0
FISHD   0
MEATD   0
DOSE    0
POPDT   0
BLANK1  0
BLANK2  0
```

Table 3.6

FORMAT OF SECOND INPUT FILE (INPUT2.DAT)

	Column	Format	Description
1 Line:			
	3	A1	Air dispersion variable data flag (Variable/ Not variable => V/N*)
* Default is N, not variable			
1 Line:			
	1-12	A12	Name of air dispersion input data file
RECEPTOR INFORMATION			
1 Line:			
	1-3	I3	Number of receptor locations (max 80)
1 Line:			
	1-3	I3	Number of rings (max5)
Ring Limits (in km's of Radius):* 1 Line:			
	1-5	I5	Distance to inside of 1st ring (min 1 km)
	6-10	I5	Distance to outside of 1st ring
	11-15	I5	Distance to outside of 2nd ring
	16-20	I5	Distance to outside of 3rd ring
	21-25	I5	Distance to outside of 4th ring
	26-30	I5	Distance to outside of 5th ring
* Specify Distances for number of rings desired			
Receptors. One line per receptor location:			
	1-3	I3	Receptor Identification Number
	4-6	I3	Sector Number (1 to 16)
	7-9	I3	Ring Number (1 to NRING)
	10-12	I3	Water Source Segment Number (0 is other source)
	13-15	I3	Fish Source Segment Number (0 if other source)
	17	A1	Receptor Type (Critical/Average=> C/A)
	18-22	I5	Population
WATERSHED INFORMATION:			
1 Line:			
	1-3	I3	Number of watershed segments (max 10)
	4-6	I3	Number of groundwater flow paths (max 5)
1 Line:			
	1-15	5I3	Node numbers where groundwater flow paths enter surface water system.
1 Line:			
	1-15	5I3	Layers for groundwater flow (specify for each flow path)

Table 3.6/cont'd

1 Line for each watershed segment:

1-3	I3	End node or watershed segment number
5	A1	Segment Type (Lake, River=>L/R)
6-8	I3	End node sector number
9-11	I3	End node ring
12-20	E9.3	River Depth (m)
21-29	E9.3	Cumulative watershed area (m^2)
30-38	E9.3	Surface areas of lake (m^2) or length of rivers (m)

SITE AND OUTPUT INFORMATION:

1 Line:

1-3	I3	Number of time steps to be saved

1 Line:

1-66	11(E6.2)	Time steps to be saved

1 Line:

1-3	I3	Number of variables to be checked for output

FOR EACH VARIABLE:

1 Line:

1-6	A6	Names of parameters in order specified on Table 3.7
7-9	I3	Number of location, substance combinations (0 if no output for parameter)

1 Line for each receptor, substance combination (if any):

1-3	I3	Substance Code (see Tables 3.7 and 3.8)
4-6	I3	Location Identification Number (see Table 3.7)

FIGURE 3.5

CONCEPTUAL DIAGRAM OF SPATIAL COORDINATE SYSTEM

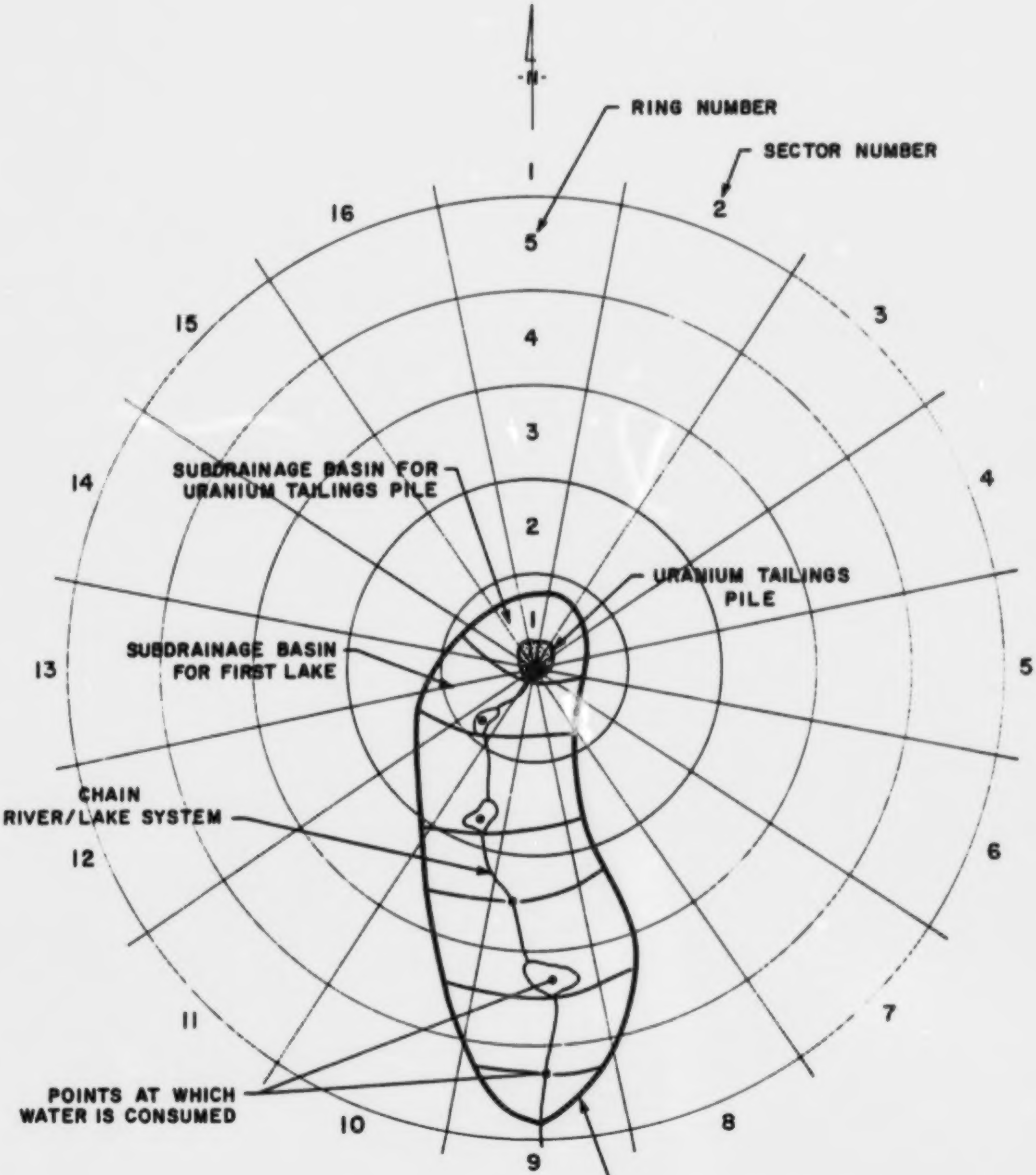

coordinates. There are 16 direction sectors to correspond to the traditional windrose structure. The number of rings, up to a maximum of 5, and the spacing of the rings, from a minimum distance of 1 km to a maximum of 50 km, are user-specified. The rings are continuous, with the outer limit of one ring forming the inner limit of the next. The receptors are placed within the windrose structure as follows:

First the number of receptor locations and the number of rings are specified (16 directions are always used). The number of receptor locations is the count of direction/ring combinations with receptors residing in them.

Next, the radii of the rings are specified in kilometres of radius. Since the outside of each ring is the inside of next ring, the only inside distance that need be specified is for the first ring. This distance must be at least 1 km and all distances must be rounded to the nearest kilometre.

Lastly, the details of each receptor location are specified. Location is input as sector and ring number. The sources of the receptors' drinking water and of fish consumed by the receptors are given by segment numbers which correspond to the segment reference numbers in the watershed information. If the receptor does not obtain drinking water or fish from the watershed downstream of the tailings area, these numbers are zero. The descriptions of critical and average receptors are to be input in the distributions in the first input file as indicated in Appendix D.

3.2.2 Watershed Information

The watershed downstream of the tailings pile handles up to 10 user-specified components (segments). Calculations are done at each river or lake outflow point known as end nodes. The node number, and the position of the river or lake outflow point by sector and ring number are specified. Figures 3.5 and 3.6 illustrate the generic site watershed corresponding to Table 3.5 and the sample input files in Appendix B.

FIGURE 3.6
REFERENCE SITE
TAILINGS AREA

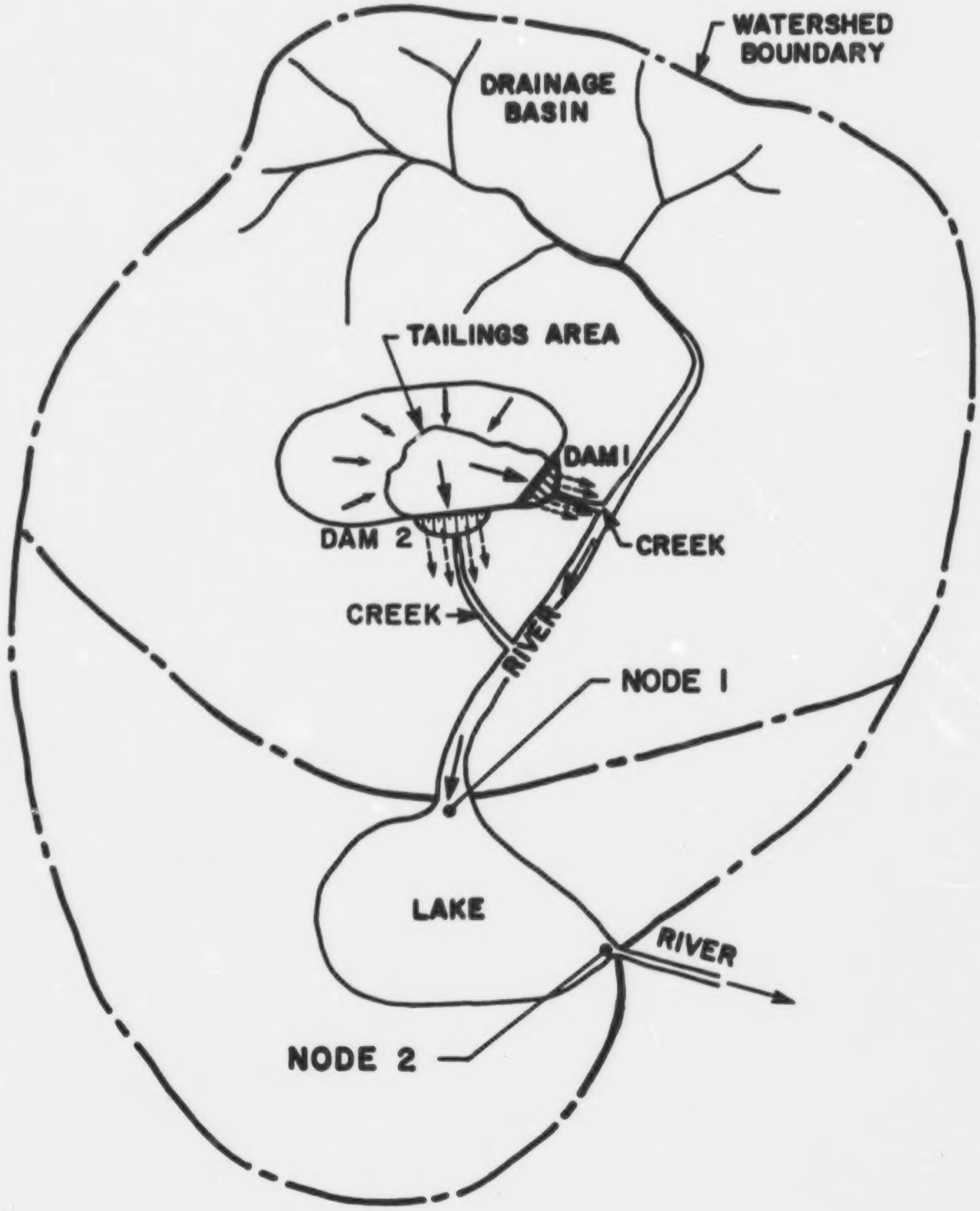

For each segment, the type (i.e. river or lake) and the cumulative watershed area are defined. The surface areas and depths of lakes and the lengths of rivers are specified.

The program performs an internal check to assure that segments are specified in order, starting with the upstream ones, with end node numbers and watershed areas increasing. When choosing the location of nodes for a watershed, nodes should be selected in as many sectors that the watershed passes through as possible.

Up to five groundwater flow pathways are available and are selected by specifying the numbers of the end nodes at which each flowpath enters the surface water system. For each flow path, the layer in the source through which the groundwater flows is specified. This is generally layer 3, the mixing zone.

There are two restrictions to the specifications of the watershed. The first segment must be specified as a river and the groundwater must be specified as flowing into a river. If source or groundwater input directly to a lake is desired, a river segment with a length and sub-basin area of zero (i.e. cumulative watershed area equal to the upstream segment) should be used immediately upstream of the lake. Computationally, this is exactly equivalent to input directly into the lake.

3.2.3 Output Selection Information

As was indicated earlier, UTAP offers the user the ability to select information for output. The following section describes how this is achieved.

The time steps to be saved are input. These must correspond to the time increment requested. For example, one cannot ask for output at 5 and 15 years with a 10 year time increment. A selection of the times computed may be saved, up to a maximum of 11.

The variables for which data can be obtained are a series of arrays. The first position in the array refers to the substance and the second position to the location. These locations can, as discussed below, refer to a variety of different physical locations. For each array, the number of substance/location combinations desired are specified followed by the list of these combinations. If no output from an array is desired, then zero is specified for the number of outputs and the next line then contains the name of the next array.

The variables available for output are shown in the sample input file and on Table 3.7 and must be specified in the order indicated. In addition, two variables, BLANK1 and BLANK2, are provided for future use if additional variables are desired for output (see Section 5.4). A counter of the number of variables to be checked for output is used and should count at least as high as the last variable in the list that output is desired for. Any variables past this in the list will be ignored by the program and do not need to be erased from the file.

For the different variables, different substances and locations are available as indicated also on Table 3.7. The substance codes are shown on Table 3.8. The location codes refer to layers in the tailings, watershed segment, ground water pathway, or receptor location as indicated on Table 3.7. The watershed segments and receptor locations correspond to the watershed segment end node numbers and the receptor numbers respectively.

For example, if the the air concentration of Ra-226 for receptor location 2 is desired the user would specify (4,2) in the array AIRC. The sector/ring location of receptor number 2 is defined using the technique described in Section 3.2.1.

For modelling purposes, a number of layers have been defined in the tailings. These are:

1 - Layer 1, surface layer (gypsum has been depleted)
2 - Layer 2, remainder of unsaturated zone (gypsum present)

Table 3.7
OUTPUT PARAMETERS

Variable	Definition	Units	Substances Available	Location Type**
WCONC	Tailings liquid phase concentration	(Bq or mol/m^3)***	1-10	Layer
CONC	Tailings solid phase concentration	(Bq or mol/m^3)***	1-10	Layer
PH	Tailing pH		1*	Layer
WATC	Water concentration	(Bq or mol/m^3)***	1-4,7,8	Watershed segment
WATAVG	Average watershed concentration	(Bq/m^3)	1-4	1
WATPH	pH in lakes and rivers		1*	Watershed segment
GWATC	Ground water concentration	(Bq or mol/m^3)***	1-4	1
EMRATE	Emission Rate from tailings	(Bq/s)	1-5	1
EROTOT	Erosion of tailings pile overtime step	(g)	1*	1
AIRC	Air concentration	(Bq/m^3)	1-5	Receptor Number****
SOILC	Soil concentration	(Bq/m^3)	1-4	Receptor Number****
AVEGC	Above ground vegetation concentration	(Bq/g)	1-4	Receptor Number
BVEGC	Below ground vegetation concentration	(Bq/g)	1-4	Receptor Number
SUFOC	Summer foliage concentration	(Bq/g)	1-4	Averaging Number
BRWSC	Browsing vegetation concentration	(Bq/g)	1-4	1 (Average for Watershed)
LICHC	Lichen concentration	(Bq/g)	1-4	1 (Average for Entire area)
AQVEGC	Aquatic vegetation concentration	(Bq/g)	1-4	1
FISHC	Fish concentration	(Bq/g)	1-4	Watershed segment
ADERC	Deer concentration from vegetation	(Bq/g)	1-4	1
WDERC	Deer concentration from water consumption	(Bq/g)	1-4	1
AMOSC	Moose concentration from vegetation	(Bq/g)	1-4	1
WMOSC	Moose concentration from water consumption	(Bq/g)	1-4	1
ACARC	Caribou concentration from vegetation	(Bq/g)	1-4	1
WCARC	Caribou concentration from water consumption	(Bq/g)	1-4	1
WATD	Drinking water dose	(µSv/a)	1-4,11	Receptor Number
SHINED	Groundshine dose	(µSv/a)	1-4,11	Receptor Number
INHD	Inhalation dose	(µSv/a)	1-4,11	Receptor Number
RADD	Radon dose	(µSv/a)	5	Receptor Number
VEGD	Vegetable consumption dose	(µSv/a)	1-4,11	Receptor Number
FISHD	Fish consumption dose	(µSv/a)	1-4,11	Receptor Number
MEATD	Meat consumption dose	(µSv/a)	1-4,11	Receptor Number
DOSE	Total Individual Dose	(µSv/a)	1-4,11	Receptor Number
POPDT	Total Dose for Entire Study Population	(µSv/a)	11	1

Notes

* Variables do not correspond to substances codes. Specify substance as 1.

** Variables with location types listed as 1 are not location dependent.

*** Radionuclide concentrations are measured in Bq/m^3. Concentrations of other substances are mol/m^3.

**** Specifying the total number of receptors (N) plus 1 produces average concentration over the entire study area and N+2 produces the average for the watershed area.

Table 3.8

SUBSTANCE CODES

Code	Compound
1	Natural Uranium
2	Total Thorium
3	Lead-210
4	Radium-226
5	Radon-222
6	Sulphate (SO_4^{2-}) from pyrite oxidation
7	Total Sulphate
8	Total Calcium (Ca^{2+})
9	Ferric Iron (Fe^{3+})
10	Ferrous Iron (Fe^{2+})
11	Total of Radionuclides

3 - Layer 3, mixing zone
4 - Layer 4, deep zone of tailings

Layers 1 and 2 comprise the unsaturated zone; that is, the tailings lying above the water table. A number of chemical species dissolve in a front-wise manner in the unsaturated zone. Thus, layer 1 represents that thickness of tailings from which a given substance has been depleted. Layer 1 acts as the source of windblown tailings dust. Layer 2 represents the remaining thickness of the unsaturated zone. Layers 3 and 4 comprise the saturated tailings zone, lying below the water table. Layer 3 (the mixing zone) represents the upper metre (or so) of the saturated zone. Most of the porewater from layer 3 ultimately enters the surface water regime, thus acting as a source of surface water contamination. Some of the layer 3 porewater flows downward into layer 4, and ultimately into the subsurface (i.e. groundwater) flow regime.

The location type labelled as averaging number on Table 3.7 can have two values. If it has the value 1, the concentration is an average for the entire area. If it has the value 2, the average is taken over the watershed (i.e. those sectors having watershed nodes situated in them).

3.3 Air Dispersion Data

The user must specify, in the second input file, the name of the file containing the air dispersion data. Two options are available. The first is to use one average set of data; that is, a long term average. The second option is to read twenty average sets of data corresponding to the time increment. One of the twenty sets of data is then randomly selected for each time step of each trial. This option must be selected by the flag in the second input file (see Table 3.6). The default is non-variance of the air dispersion data.

The program reads the one average set of the air dispersion data file as formatted by the Atmospheric Environment Service (AES) for the site under study. The twenty average sets of data are read from one file that is simply twenty files (one set of data per file) of data, combined, in the same format as received from AES, into one file. An example of the file (AVERAGE.DAT) containing one long-term average set of data is shown in Appendix B. Table 3.9 illustrates the format of this file. Note that in creating the file containing twenty sets of data, the first line (the file label) of each smaller file being combined is included in the new file. Examples of the two files, ONE.DAT and TEN.DAT containing twenty sets of one year and ten year averages, respectively, are provided to the user on disk.

Table 3.9

FORMAT OF AES WIND DATA FILE

AES File Title

```
P1397.TOTAL.
```

Direction

Stability Class

Frequencies of wind for velocity classes

AES Codes

```
  N A 0.000400.000290.0    0.0     0.0     0.0           62925 1A176584
NNE A 0.000370.000120.0    0.0     0.0     0.0           62925 2A176584
 NE A 0.000270.000150.0    0.0     0.0     0.0           62925 3A176584
ENE A 0.000110.000060.0    0.0     0.0     0.0           62925 4A176584
  E A 0.000050.000020.0    0.0     0.0     0.0           62925 5A176584
ESE A 0.000010.000010.0    0.0     0.0     0.0           62925 6A176584
 SE A 0.000030.000030.0    0.0     0.0     0.0           62925 7A176584
SSE A 0.000050.000030.0    0.0     0.0     0.0           62925 8A176584
  S A 0.000190.000150.0    0.0     0.0     0.0           62925 9A176584
SSW A 0.000300.000190.0    0.0     0.0     0.0           6292510A176584
 SW A 0.000270.000190.0    0.0     0.0     0.0           6292511A176584
WSW A 0.000270.000200.0    0.0     0.0     0.0           6292512A176584
  W A 0.000460.000260.0    0.0     0.0     0.0           6292513A176584
WNW A 0.000280.000180.0    0.0     0.0     0.0           6292514A176584
 NW A 0.000130.000080.0    0.0     0.0     0.0           6292515A176584
NNW A 0.000240.000100.0    0.0     0.0     0.0           6292516A176584
  N B 0.002130.001650.000930.0     0.0     0.0           62925 1B176584

                               .
                               .
                               .

WNW F 0.006990.005420.0    0.0     0.0     0.0           6292514F176584
 NW F 0.006690.005180.0    0.0     0.0     0.0           6292515F176584
NNW F 0.005770.004090.0    0.0     0.0     0.0           6292516F176584
```

4.0 COMPILING AND LINKING

For ease of compiling, the file "UTAP.FOR" is provided. This file contains a list of "INCLUDE" statements for all of the modules. The necessary FORTRAN files are as follows:

EXEC.FOR
INPUT.FOR
SAMPLE.FOR
SAVE.FOR
STATS.FOR
OUTPUT.FOR
SEXEC.FOR
INCONI.FOR
INCONN.FOR
IONS1.FOR
IONSIL.FOR
IONS3.FOR
IONS4.FOR
URANUM.FOR
THORUM.FOR
RADIUM.FOR
LEAD.FOR
EROS.FOR
RADON.FOR
DUST.FOR
COMEX.FOR
WIND.FOR
AIRDIS.FOR
SOIL.FOR
GSHINE.FOR
VEGCON.FOR
GWATER.FOR
WATEX.FOR
WATVEG.FOR
ANIMAL.FOR
FISH.FOR
DOSE.FOR

The above listed files contain "INCLUDE" statements for the following additional files:

IO.INC
CONC.INC
RECEP.INC
STATS.INC
COUNTS.INC
INFO.INC
OUT.INC
INPT.INC
INPT2.INC
UPDATE.INC
PARAM.INC
INTERM.INC
WIND.INC
MODEL.INC
VAR.INC

All of these files must be present in order to compile and link the program.

The compiler recommended for UTAP is the $F_{77}L$ compiler by Lahey (1986) version two or higher. If another compiler is used, problems may ensue. One potential source of problems in linking is the subroutine "FILER" which calls the $F_{77}L$ and DOS specific functions DATE and TIME and then writes the date and time to the output files. If these functions are not available simply remove this subroutine and the call statements for it in subroutines INPUT1, WRITE, and OUTPUT (four call statements). Instead, simply write a blank line to the output files so that the format of the file is not changed. This is important if the output files are to be used for input to the confidence bands program.

The format of the INCLUDE statements used in UTAP is also specific to the $F_{77}L$ compiler. While other compilers support INCLUDE statements, their format may not be the same. If errors are encountered while compiling, these statements should be changed to match the syntax of the compiler being used.

If the $F_{77}L$ compiler is used, the following options specified in the file "F77L. FIG" are recommended:

```
/a/nf/o/b/i/p/nw/l
```

Further explanation of these options can be found in the user's manual accompanying the compiler.

If the Lahey compiler is used or if a different compiler is used and the option to remember local variables is available, it should not be used.

5.0 RUNNING THE PROGRAM

UTAP should be run on a computer having at least 640 kilobytes of Random Access Memory (RAM) and a hard disk drive. A sample session is shown on Table 5.1. The program prompts the user for the names of the input files and indicates, to the screen, the input and output files that are opened.

If errors are encountered in reading these files, messages will be generated accordingly. In some cases, questionable input will result in warning messages, and the user will be asked if it is all right to continue execution of the program or if the program should be stopped. Typing "Y" for yes will cause execution to resume. All error and warning messages are described in Appendix A. If an error occurs in reading an input file, the line number of the last line read is also printed to the screen.

While the program is running, the current trial and time step are written to the screen so that the progress of the program can be checked.

When execution of the program is complete, the output files can be examined. Sample output files are shown in Appendix C.

Table 5.1

SAMPLE SESSION

```
C:UTAP

UTAP - Version 3.0

RUN STARTED 02/17/87 AT 13:14:42

First Input File Name? INPUT1.DAT

Opening File : INPUT1.DAT
Opening File : RES.OUT
Opening File : KEY.OUT

Second Input File Name? INPUT2.DAT

Opening File : INPUT2.DAT
Opening File : AVERAGE.DAT



TRIAL NUMBER :     1     TIME :     0
TRIAL NUMBER :     1     TIME :    10
TRIAL NUMBER :     1     TIME :    20
TRIAL NUMBER :     1     TIME :    30
TRIAL NUMBER :     1     TIME :    40
TRIAL NUMBER :     1     TIME :    50
TRIAL NUMBER :     2     TIME :     0
TRIAL NUMBER :     2     TIME :    10
TRIAL NUMBER :     2     TIME :    20
TRIAL NUMBER :     2     TIME :    30
TRIAL NUMBER :     2     TIME :    40
TRIAL NUMBER :     2     TIME :    50


RUN COMPLETED

C:
```

6.0 ALTERING THE PROGRAM

The Uranium Tailings Assessment Program is composed of a number of modules. These may be classified as either component or control modules. Component modules (or models) are the programs directly concerned with the simulation of a uranium tailings physical system; that is, the mathematical models representing the uranium tailings pile and surrounding environment. Control modules provide the infrastructure for probabilistic analysis of the component modules. These functions include probabilistic sampling of input parameters, and many input, output and bookkeeping functions. The integrated control and component modules are referred to as the system model or UTAP. The general function of the control and component modules are illustrated in Figure 1.1.

The control modules are called in logical order by a primary control module called EXEC. The calling sequence, the interactions between the program EXEC and the other control modules and the functions of the control modules are illustrated in flowchart form in Figure 6.1. The component module executive subroutine COMEX is called by EXEC for each trial and time step. The subroutine COMEX and the modules it calls are illustrated in Figure 6.2.

The control modules are fully documented, including code listings and variable dictionaries in Volume 2 of the Phase III report (SENES, 1986) and in the addendum to Volume 2 produced as part of this report (SENES, 1987a). The component modules 3 are also documented as a part of this report (SENES, 1987c). Changes to the control modules made by the user should never be required. This chapter is intended to give the user a general background necessary for making changes to the component modules; however, examination of the appropriate sections of the component modules report is recommended before code changes are made.

Component modules should be implemented by following the points outlined below.

FIGURE 6.1

THE CONTROL MODULE STRUCTURE

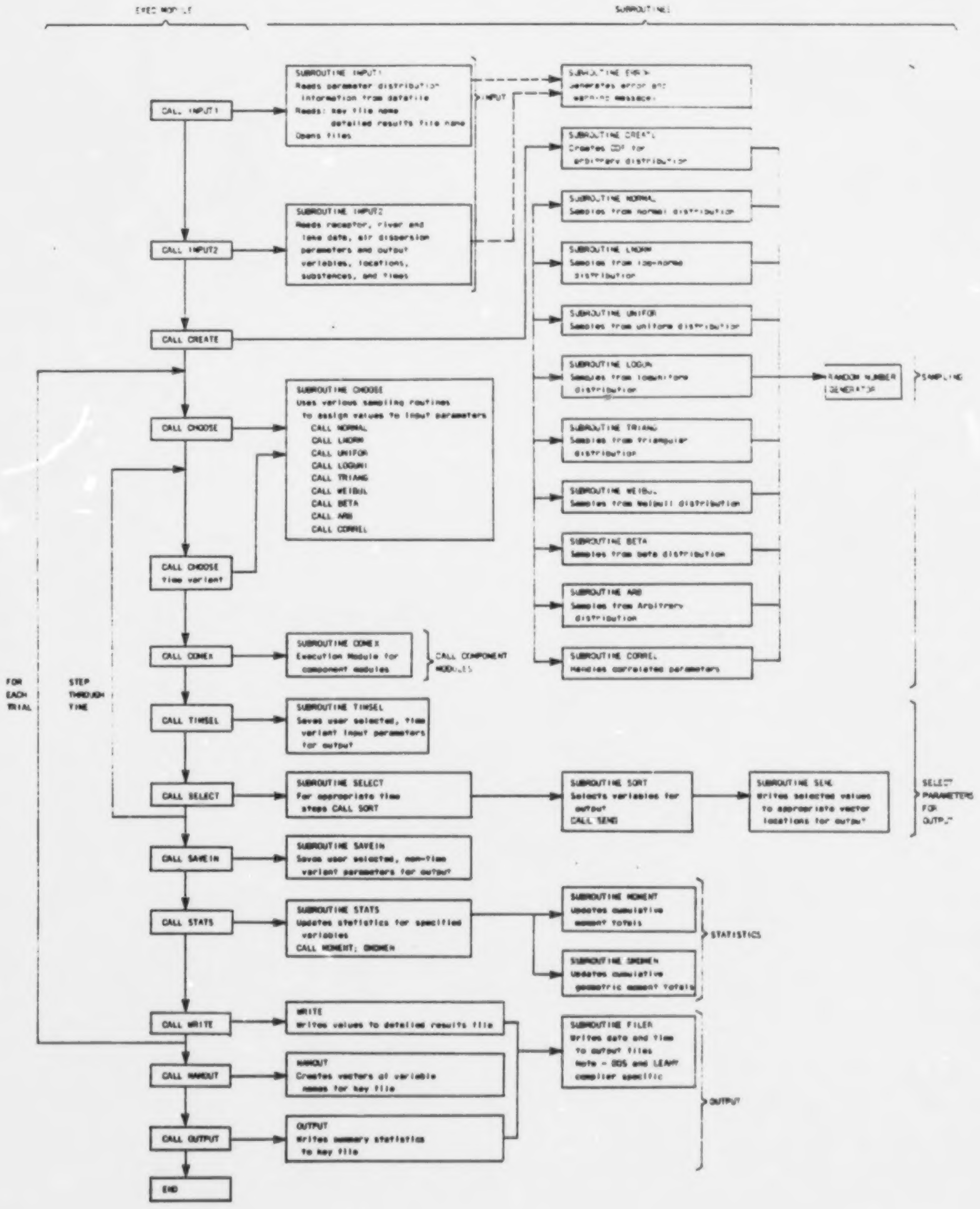
EXEC MODULE
SUBROUTINES
CALL INPUT1
SUBROUTINE INPUT1
Reads parameter distribution information from datafile
Reads: key file name
detailed results file name
Opens files
INPUT
SUBROUTINE ERROR
Generates error and warning messages
CALL INPUT2
SUBROUTINE INPUT2
Reads receptor, river and lake data, air dispersion parameters and output variables, locations, substances, and times
SUBROUTINE CREATE
Creates CDF for arbitrary distribution
SUBROUTINE NORMAL
Samples from normal distribution
SUBROUTINE LNORM
Samples from log-normal distribution
SUBROUTINE UNIFOR
Samples from uniform distribution
CALL CREATE
SUBROUTINE LOGUNI
Samples from log-uniform distribution
RANDOM NUMBER GENERATOR
SAMPLING
CALL CHOOSE
SUBROUTINE CHOOSE
Uses various sampling routines to assign values to input parameters
CALL NORMAL
CALL LNORM
CALL UNIFOR
CALL LOGUNI
CALL TRIANG
CALL WEIBUL
CALL BETA
CALL ARB
CALL CORREL
SUBROUTINE TRIANG
Samples from triangular distribution
SUBROUTINE WEIBUL
Samples from Weibull distribution
SUBROUTINE BETA
Samples from beta distribution
CALL CHOOSE
time variant
SUBROUTINE ARB
Samples from Arbitrary distribution
CALL COMEX
SUBROUTINE COMEX
Execution Module for component modules
CALL COMPONENT MODULES
SUBROUTINE CORREL
Handles correlated parameters
FOR EACH TRIAL
STEP THROUGH TIME
CALL TIMSEL
SUBROUTINE TIMSEL
Saves user selected, time variant input parameters for output
CALL SELECT
SUBROUTINE SELECT
For appropriate time steps CALL SORT
SUBROUTINE SORT
Selects variables for output
CALL SEND
SUBROUTINE SEND
Writes selected values to appropriate vector locations for output
SELECT PARAMETERS FOR OUTPUT
CALL SAVEIN
SUBROUTINE SAVEIN
Saves user selected, non-time variant parameters for output
CALL STATS
SUBROUTINE STATS
Updates statistics for specified variables
CALL MOMENT; GMOMEN
SUBROUTINE MOMENT
Updates cumulative moment totals
STATISTICS
SUBROUTINE GMOMEN
Updates cumulative geometric moment totals
CALL WRITE
WRITE
Writes values to detailed results file
SUBROUTINE FILER
Writes date and time to output files
Note - DOS and LEAHY compiler specific
CALL NAMOUT
NAMOUT
Creates vectors of variable names for key file
OUTPUT
CALL OUTPUT
OUTPUT
Writes summary statistics to key file
END

FIGURE 6.2

THE SUBROUTINE COMEX
AND COMPONENT MODULES

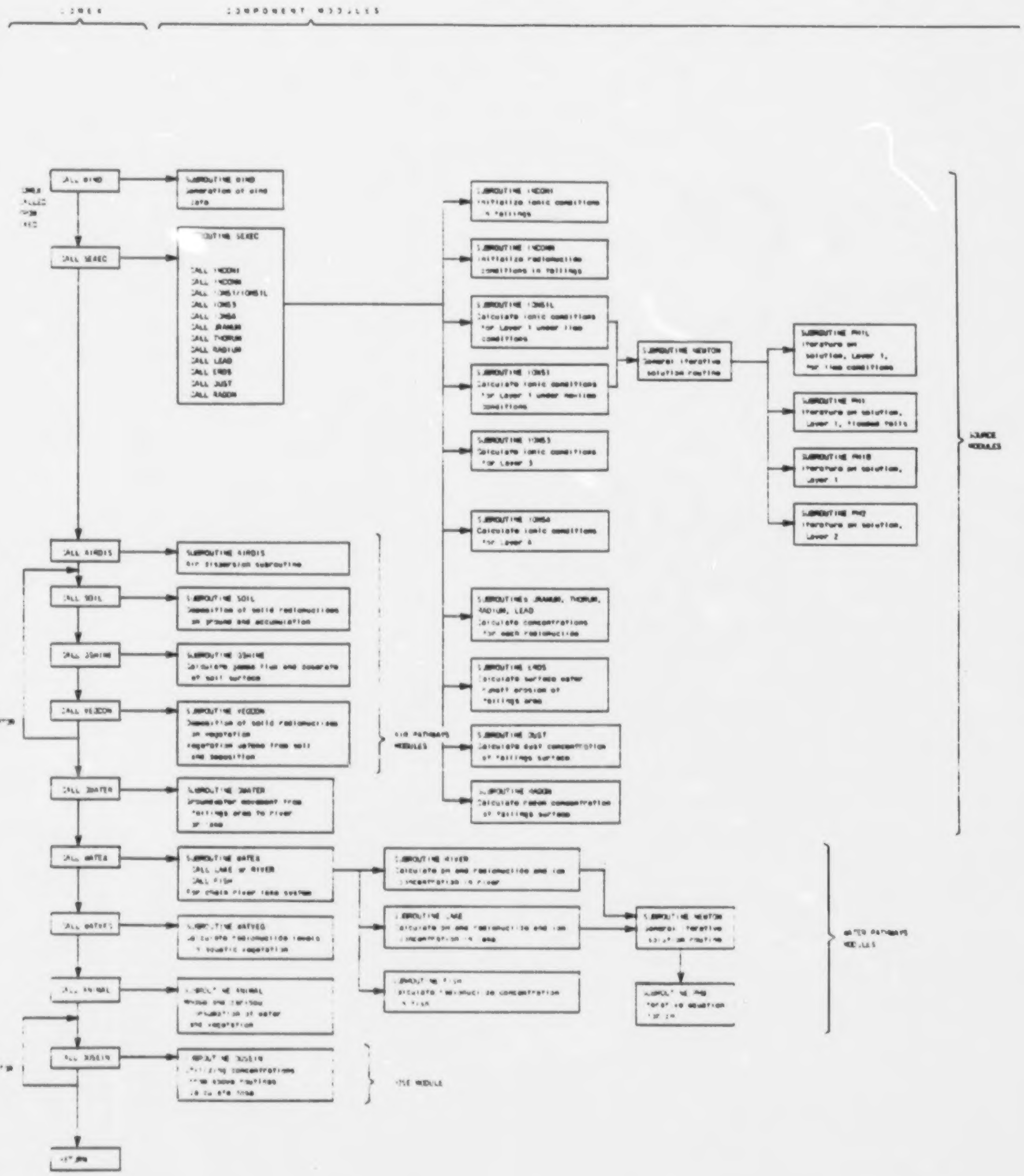
COMEX
COMPONENT MODULES
CALL WIND
ONLY CALLED
SUBROUTINE WIND
Generation of wind data
CALL SEXEC
SUBROUTINE SEXEC
CALL INCONI
CALL INCONR
CALL IONS1/IONS1L
CALL IONS3
CALL IONS4
CALL URANUM
CALL THORUM
CALL RADIUM
CALL LEAD
CALL EROS
CALL DUST
CALL RADON
SUBROUTINE INCONI
Initialize ionic conditions in tailings
SUBROUTINE INCONR
Initialize radionuclide conditions in tailings
SUBROUTINE IONS1L
Calculate ionic conditions for Layer 1 under lime conditions
SUBROUTINE IONS1
Calculate ionic conditions for Layer 1 under non-lime conditions
SUBROUTINE IONS3
Calculate ionic conditions for Layer 3
SUBROUTINE IONS4
Calculate ionic conditions for Layer 4
SUBROUTINES URANUM, THORUM, RADIUM, LEAD
Calculate concentrations for each radionuclide
SUBROUTINE EROS
Calculate surface water runoff erosion of tailings area
SUBROUTINE DUST
Calculate dust concentration of tailings surface
SUBROUTINE RADON
Calculate radon concentration of tailings surface
SUBROUTINE NEWTON
General iterative solution routine
SUBROUTINE PH1L
Iterature on solution, Layer 1, for lime conditions
SUBROUTINE PH1
Iterature on solution, Layer 1, flooded tails
SUBROUTINE PH1B
Iterature on solution, Layer 1
SUBROUTINE PH2
Iterature on solution, Layer 2
SOURCE MODULES
CALL AIRDIS
SUBROUTINE AIRDIS
Air dispersion subroutine
CALL SOIL
SUBROUTINE SOIL
Deposition of solid radionuclides on ground and accumulation
CALL GSHINE
SUBROUTINE GSHINE
Calculate gamma flux and doserate of soil surface
CALL VEGCON
SUBROUTINE VEGCON
Deposition of solid radionuclides on vegetation
Vegetation uptake from soil and deposition
FOR EACH RECEPTOR
AIR PATHWAYS MODULES
CALL GWATER
SUBROUTINE GWATER
Groundwater movement from tailings area to river or lake
CALL WATER
SUBROUTINE WATER
CALL LAKE or RIVER
CALL FISH
for chain river lake system
SUBROUTINE RIVER
Calculate pH and radionuclide and ion concentration in river
SUBROUTINE LAKE
Calculate pH and radionuclide and ion concentration in lake
SUBROUTINE FISH
Calculate radionuclide concentration in fish
SUBROUTINE NEWTON
General iterative solution routine
SUBROUTINE PHW
Iterative equation for pH
WATER PATHWAYS MODULES
CALL WATVEG
SUBROUTINE WATVEG
Calculate radionuclide levels in aquatic vegetation
CALL ANIMAL
SUBROUTINE ANIMAL
Moose and caribou consumption of water and vegetation
FOR EACH RECEPTOR
CALL DOSEIN
SUBROUTINE DOSEIN
Utilizing concentrations from above routines to calculate dose
USE MODULE
RETURN

6.1 Changing COMEX

Subroutine COMEX is the control module for the component modules. It is called for each time step of each iteration. It, in turn, calls the component modules. Call statements must be added to COMEX if any new component modules are added.

6.2 Writing Component Modules

All subroutines should be written in Fortran 77 and compiled on the Lahey compiler Version 2.0 or higher making certain not to use any compiler specific options so as to ensure portability of the program. Variables should be in units corresponding to the rest of the program; namely Becquerels, metres, grams, moles, and microsieverts.

6.3 Passing Variables

Two files containing input, output, and saved variables are available to the component modeller and should be included in all subroutines. These are MODEL.INC and VAR.INC.

6.3.1 Include File MODEL.INC

The following common statements and variables contained in the INCLUDE file "MODEL.INC" are necessary for implementing new component modules. This file should be added to component modules, using an include statement. **The user should never need to alter this file.**

a) TIME

This common statement contains the following variables:

T - The current time (Real)
NUMTRL - The trial number

NTRIAL - The total number of trials
NYEARS - Years in simulation (Integer)
NDT - Time increment (Integer)
RYEARS - Years in simulation (Real)
DT - Time increment (Real)
NT - The current time (Integer)

Both integer and real variables are made available to avoid frequent conversion from one to the other throughout the program.

b) CONCEN

The matrices of output concentrations and doses described on Table 3.6 are sent back from the component modules to the control modules through this common block. Note that this block is also contained in and should be identical to the include file, CONC.INC, used by the control modules. These are dimensioned as follows:

WCONC (10,4,3)
CONC (10,4,3)
PH (4)
WATC (8,10)
WATAVG (4)
WATPH (10)
GWATC (4,5)
EMRATE (5)
EROTOT
AIRC (5,82)
SOILC (4,82)
AVEGC (4,80)
BVEGC (4,80)
SUFOC (4,2)
BROWSC (4)
LICHC (4)

FISHC (4,10)
ADERC (4)
WDERC (4)
AMOSC (4)
WMOSC (4)
ACARC (4)
WCARC (4)
WATD (5,80)
SHINED (5,80)
RADD (80)
VEGD (5,80)
FISHD (5,80)
MEATD (5,80)
DOSE (5,80)
POPDT
BLANK1 (4,80)

AQVEGC (4)   BLANK2 (10,10)

The first position in the matrices is the substance identifier. The substance codes are shown on Table 3.8. The second dimension in the matrices is a location identifier as described in Section 3.2.3.

In the matrices with three dimensions, the third position is time and the codes are as follows:

1 - Initial time (T = 0)
2 - Previous time step
3 - Current time step

Note that only the current time can be obtained for output.

c) RECEPT

This common statement contains the receptor information. The variables are:

NRECEP - Number of receptor locations
NRING - Number of rings
RDIR(80) - Receptor sectors
RRING(80) - Receptor rings
RWSSEG(80) - Receptor drinking water source segment numbers
RFSEG(80) - Receptor fish source segment numbers
RPOP(80) - Receptor populations
RNGMID(5) - Radial distance to midpoint of ring (m)
RTYPE(80) - Receptor type (C=Critical, A=Average)
RAREA(5) - Sector areas for each ring (m^2)
NREC - Counter of Receptors
TAREA - Total area of all rings (m^2)
NDREC - Number of Receptor locations plus two

d) WATER

The variables pertaining to the watershed are transferred using this block. These variables are:

NSEG - Number of watershed segments
NODDIR(10) - End Node sector numbers
NODRNG(10) - End Node Ring Numbers
STYPE(10) - Segment Types (R=River, L=Lake)
SDEPTH(10) - Average Lake Depths (m)
LAREA(10) - Lake Areas (m^2) for lake segments and Lengths (m) for river segments
SHEDAR(10) - Cumulative watershed areas (m^2)
LAKVOL(10) - Lake Volumes (m^3) (Area x Average Depth)
PSDIR(10) - Receptor sectors by watershed wind rose locations
PSRING(10) - Receptor ring numbers by watershed wind rose locations
PSNUM - Number of wind rose locations in watershed
PSAREA - Total Area of wind rose locations in which the watershed lies
GSEG(5) - End node numbers at which groundwater flow paths enter the surface water model.

The vectors, PSDIR and PSRING, are provided to maximize program efficiency when calculations need to be performed only once for each wind rose location containing a watershed end node. These contain the same information as the vectors NODDIR and NODRNG but in a more compressed form. For instance, two or three segment end nodes could lie within the same wind rose location; however, some calculations need only be performed once for that location.

e) WIND

The wind data is contained within the following variables:

FWIND1(16) - Frequency of observations of windspeed over 5.4 m/s by direction
FWINDT - Sum of frequencies in FWIND1

UWIND(16,6) - Average windspeed (m/s) by direction and stability class

FWIND2(16,6) - Frequency of wind by direction and stability class

FWIND(16,6,6,20) - Vector containing wind speed (knots) by direction, stability class, speed, and year (1 or 20 years or sets of data)

The vector, FWIND, is used by subroutine WIND to create the wind data contained in the variables FWIND1, FWIND2, FWINDT, and UWIND. Note that the direction used for wind refers to the direction the wind blows to (i.e. direction of downwind receptor from the tailings).

6.3.2 Include file VAR.INC

This file contains two common blocks set up to facilitate easy additions or changes to component modules. It should be included in all new component modules and can be altered by the user.

The first block described below (INPT) contains sampled values from the input distributions while the other common block (INTERM) is used for saving values within subroutines or for passing values between different subroutines. Any variables used for these purposes should be added to the appropriate common block.

a) INPT

The variable contained within this common block as seen by the control modules is XIN(300). XIN is a vector containing the values sampled from the input distributions. To add new input distributions, the variables should be added to the list in this common block as well as to the first input file. The format of input distributions is described in Section 3.1. **The order of parameters listed in common (INPT) must correspond exactly to the order of the probabilistic inputs listed in the file INPUT1.DAT.**

Note that the size of the common block INPT is limited to 300 input variables.

Errors will result if the user attempts to exceed this number.

b) INTERM

This common block is used for transferring real numbers between subroutines. It corresponds to a common block within the file "INTERM.INC" included in the main program, EXEC. If this common block is not large enough, its size can be increased by changing it within INTERM.INC.

If additions to this block are made, the size of the altered block should be checked. A simple way to do this is to compile, with warning messages turned on, the file TEST.FOR, provided with UTAP, which contains include statements for the files INTERM.INC and VAR.INC. If a warning message results, it should indicate that the common block INTERM is smaller in the file VAR.INC than it is in the file INTERM.INC (i.e. smaller than a previous program unit declaration).

If this common block is not large enough, its size will have to be increased within the control modules. The size of INTERM can be increased by altering the size of the array in the file "INTERM.INC". Note that if this array is made too large, the potential exists for the executable code to become too large to run with 640 kilobytes of random access memory.

6.4 Obtaining Additional Outputs

The arrays BLANK1 and BLANK2, not used at present, are available for obtaining output for any parameter desired. To do this, the user should go to the end of subroutine COMEX and equate any positions desired in either BLANK1 or BLANK2 to the variable for which output is desired. The two positions in the array can then be requested for output from the second input file as substance and location, respectively. Note that only variables included in the common block INTERM can be obtained for output in this manner. Additional variables can, however, be added to this common block as described in Section 6.3.2.

As an option to setting BLANK1 and BLANK2 at the end of COMEX, a new subroutine to do this could be called from the end of COMEX.

6.5 Modifying First Input File

The input file, INPUT1.DAT, should be modified to include all of the input distributions (see Section 3.1) required by the component module. These must be listed in exactly the same order as they appear in the common block INPT. The output files desired should be opened and all counters set to match the numbers of input distributions.

6.6 Modifying Second Input File

The second input file, INPUT2.DAT, should be modified to obtain the desired output variables, substances, locations and time steps (see Section 3.2). The receptor and watershed information may also be changed. The list of arrays available for output should never be altered.

6.7 Other Changes and Information

If more complex changes are to be made to the program and a more detailed description of the modules or variables is required, refer to Volume 2 of the Phase III report (SENES, 1986), the addendum to Volume 2 (SENES, 1987a), and the component models report (SENES, 1987c).

7.0 CONFIDENCE BANDS

Confidence bands are generated by two post-execution programs, BIN and CBAND. The first of these programs reads the detailed results file and the key file produced by UTAP. The data are binned and output is written to a disk file called "BIN.DAT". A log transformation of the data may also be requested.

The second program fits a probability distribution function to the binned data and then fits 95% confidence bands to the cumulative distribution function and to the probability distribution function. Output is sent to a user-specified disk file in a formatted form with descriptive headings.

7.1 Running the Program

The two files, BIN.FOR and CBAND.FOR, containing the FORTRAN program code should each be compiled and linked. A sample session is shown on Table 7.1. After UTAP has been run, the detailed results file and the key file are utilized by BIN. Each variable name and the specifics such as location and substance codes and time if applicable are indicated within the file and the variables are assigned reference numbers (see example key file in Appendix C with reference numbers in first column). These reference numbers are used by the binning program to identify the desired variable.

The program, BIN, prompts the user for the names of the detailed results file and the key file. It also asks the reference number of the variable of interest, and whether or not a log transformation is desired. Output is sent to the file "BIN.DAT".

The second program, CBAND, reads the file "BIN.DAT" and prompts the user for the name of the output file. If the program is not successful, selecting the log transformation, (or not selecting it if it was previously used) may work.

A sample output file for a normal distribution and plots of these results done using STATGRAFICS, (STSC, 1985), a statistical graphics package, are shown on

Table 7.1

CONFIDENCE BANDS PROGRAM SAMPLE SESSION

```
C:BIN

DETAILED RESULTS FILE NAME? RES.OUT

Opening file: RES.OUT
KEY FILE NAME? KEY.OUT

Opening file: KEY.OUT
Opening file: BIN.DAT
ENTER ID. NO. OF VARIABLE TO BE ANALYZED: 1

DO YOU WANT LOG TRANSFORMATION (Y/N)? N

C:CBAND

Opening file: BIN.DAT
ENTER NAME OF OUTPUT FILE: BAND.OUT

Opening file: BAND.DAT

C:
```

Table 7.2 and Figure 7.1, respectively.

The program fits curves based on the variability of the data values and computes the 95% confidence bands. The interpretation is that one is entitled to feel 95% confident that the true probability density function or cumulative probability function of the output variable from a Monte Carlo calculation will fall within these bounds.

Table 7.2

CONFIDENCE BANDS PROGRAM SAMPLE OUTPUT FILE

```
    CDF      LOWERLIMIT   FITTEDCDF   UPPERLIMIT
0.9242E+02  0.5229E+02  0.6599E+02  0.8082E+02
0.1157E+03  0.1045E+03  0.1197E+03  0.1341E+03
0.1389E+03  0.1439E+03  0.1574E+03  0.1678E+03
0.1622E+03  0.1685E+03  0.1801E+03  0.1869E+03
0.1854E+03  0.1830E+03  0.1918E+03  0.1958E+03
0.2086E+03  0.1913E+03  0.1971E+03  0.1990E+03
0.2319E+03  0.1960E+03  0.1991E+03  0.1998E+03
0.2551E+03  0.1986E+03  0.1998E+03  0.2000E+03
0.2784E+03  0.2000E+03  0.2000E+03  0.2000E+03
    PDF      LOWERLIMIT   FITTEDPDF   UPPERLIMIT
0.9242E+02  0.5229E+02  0.6599E+02  0.8082E+02
0.1157E+03  0.4799E+02  0.5372E+02  0.5820E+02
0.1389E+03  0.3101E+02  0.3764E+02  0.4433E+02
0.1622E+03  0.1783E+02  0.2271E+02  0.2807E+02
0.1854E+03  0.8592E+01  0.1179E+02  0.1569E+02
0.2086E+03  0.3117E+01  0.5268E+01  0.8625E+01
0.2319E+03  0.8353E+00  0.2026E+01  0.4758E+01
0.2551E+03  0.1680E+00  0.6708E+00  0.2593E+01
0.2784E+03  0.2557E-01  0.1912E+00  0.1383E+01
```

FIGURE 7.1

PLOTS OF 95% CONFIDENCE BANDS FOR A NORMAL DISTRIBUTION (500 TRIALS)

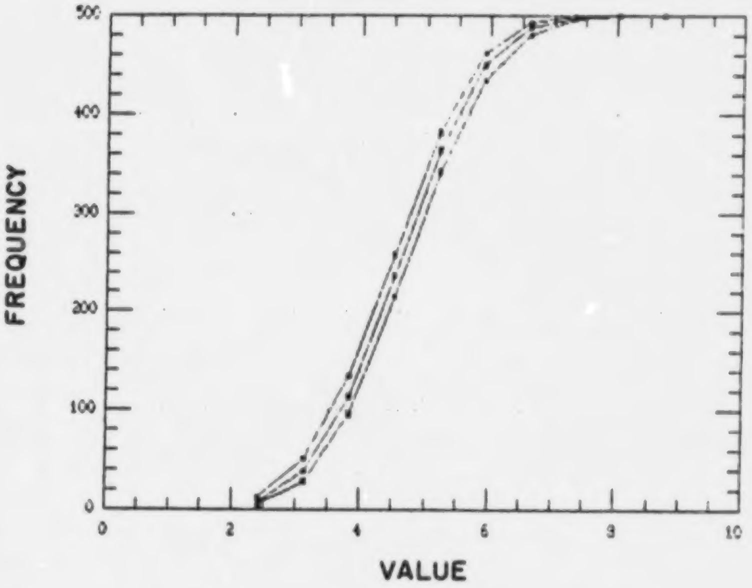

A) CUMULATIVE DISTRIBUTION FUNCTION

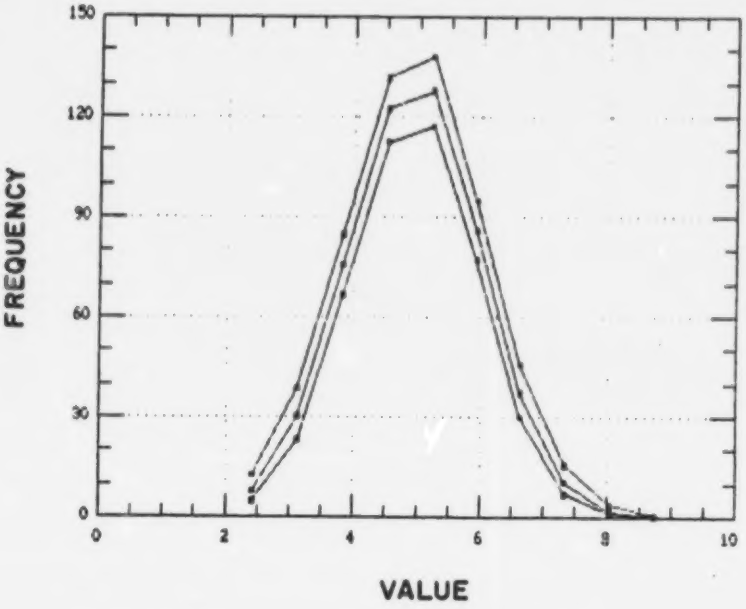

B) PROBABILITY DISTRIBUTION FUNCTION

REFERENCES

Golder Associates, Beak Consultants, SENES Consultants and Cumming, Cockburn and Associates, 1986. Lacnor Field Study, Elliot Lake, Ontario. Prepared for the National Uranium Tailings Program, CANMET, EMR.

Lahey Computer Systems, Inc., 1986. "$F_{77}L$ - FORTRAN 77 Language System for the Personal Computer." California, U.S.A.

SENES Consultants Limited, 1984. "A Study to Develop and Demonstrate Techniques for the Probabilistic Assessment of the Long-Term Effects of Uranium Mill Tailings in Canada - Phase I." Research Report Prepared for the National Uranium Tailings Program, CANMET, EMR, under Supply and Services Canada Contract No. OSQ83-00236.

SENES Consultants Limited, 1985. "A Study to Develop and Demonstrate Techniques for the Probabilistic Assessment of the Long-Term Effects of Uranium Mill Tailings in Canada - Phase II." Research Report prepared for the National Uranium Tailings Program, CANMET, EMR, under Supply and Services Canada Contract No. OSQ84-00207.

SENES Consultants Limited, 1986. "Probabilistic Model Development for the Assessment of the Long-Term effects of the Uranium Mill Tailings in Canada - Phase III." Research Report Prepared for the National Uranium Tailings Program, CANMET, EMR under Supply and Services Canada Contract No. OSQ85-00182.

SENES Consultants Limited, 1987a. "Uranium Tailings Assessment Program (UTAP.3) Addendum to Volume 2 - System Description and Control Module Documentation." Research Report Prepared for the National Uranium Tailings Program, CANMET, EMR under DSS Contract No. 23317-6-1728/01-SQ.

SENES Consultants Limited, 1987c. "Uranium Tailings Assessment Program (UTAP.3) Component Model Documentation." Research Report Prepared for the National Uranium Tailings Program, CANMET, EMR under DSS Contract No. 23317-6-1728/01-SQ.

SENES Consultants Limited, 1987d. "Uranium Tailings Assessment Program (UTAP.3) Application to the Lacnor Tailings Site." Research Report Prepared for the National Uranium Tailings Program, CANMET, EMR under DSS Contract No. 23317-6-1728/01-SQ.

Statistical Graphics Corporation (STSC), 1986. "STATGRAPHICS - Statistical Graphics System." U.S.A.

Whiteshell Nuclear Research Establishment (WNRE), 1987. "Comparison of UTAP.2 and SYVAC-UT3." Atomic Energy of Canada Limited. Report in preparation.

APPENDIX A

ERROR AND WARNING MESSAGES

APPENDIX A

ERROR AND WARNING MESSAGES

(001) WATER SOURCE SEGMENTS NOT IN ORDER

The watershed segment end nodes specified in the second input file must be consecutively increasing integers (i.e. numbered from upstream to downstream).

(002) WATERSHED AREAS MUST INCREASE

Watershed areas are cumulative and must increase for each downstream segment specified in the second input file.

(003) ERROR IN INPUT FILE

An error occured reading the indicated line of the input file. Check all counters and the format of inputs on the line of the error.

(004) CORRELATED NAME NOT FOUND

Name of independent variable for correlated distribution not found in input file. Distribution name must appear before correlated parameter.

(005) UNEXPECTED END OF DATA

Input file empty, doesn't exist, or too short.

(006) TYPE ERROR IN REGULAR DIST'ns

Distribution type number greater than 8. Numbers of parameters or arbitrary or correlated distributions incorrect.

(007) TYPE ERROR IN CORRELATED DIST'ns

Distribution type number not equal to 10. Numbers of parameters or arbitrary or correlated distributions incorrect.

(008) TYPE ERROR IN ARBITRARY DIST'ns

Distrubtion type number not equal to 9. Numbers of parameters or arbitrary or correlated distributions incorrect.

(009) NUMBER OF PARAMETERS INCORRECT

End of file reached before specified numbers of parameters read.

(010) RECEPTORS NOT LISTED IN ORDER

Receptor numbers must be consecutively increasing integers starting at one.

(011) TIME STEPS MUST INCREASE

Time steps to be saved for output must increase.

(012) DISTRIBUTION NUMBER NOT DEFINED

(013) MAXIMUM OF 8 WATERSHED SEGMENTS ALLOWED

An attempt was made to read information for more than 8 watershed segments.

(014) GROUNDWATER LAYERS NOT POSSIBLE

The groundwater layers must be equal to 1, 2, 3, or 4.

(015) CAN'T SAVE TIME STEPS SPECIFIED

The time steps requested to be saved to either the detailed results or the statistics file are not a multiple of the time increment.

(016) TIME FOR OUTPUT TOO BIG

Time step(s) requested for output are bigger than simulation time.

(017) RECEPTOR FISH SOURCE NUMBER TOO BIG

A receptor is obtaining fish from an unidentified segment.

(018) CANNOT CORRELATE PARAMETERS

The independent parameter cannot be time variant unless the dependent parameter is.

(019) TIME STEPS DON'T MATCH SIMULATION TIME

The simulation time must be divisible by the time increment with not remainder.

(020) MAXIMUM OF 80 RECEPTORS ALLOWED

Attempt was made to read in information for more than 80 receptors locations.

(021) MAXIMUM OF 5 RINGS ALLOWED

Attempt was made to read in ring limits for more than 5 rings.

(022) RING LIMITS MUST INCREASE

The ring limits must be specified beginning with the inner ring and moving outwards.

(023) RECEPTOR RING NUMBER TOO BIG

A receptor's ring number is larger than the number of rings dimensioned.

(024) FIRST WATERSHED SEGMENT MUST BE RIVER

The first watershed segment specified must always be a river, not a lake. Use a river of zero length and sub-basin area.

(025) GROUNDWATER MUST FLOW INTO RIVER

Groundwater cannot be specified as flowing directly into a lake. Use a river of zero length and sub-basin area.

(026) RECEPTOR WATER SOURCE NO. TOO BIG

A receptor is obtaining water from an undefined segment.

(027) CONVERGENCE FAILED IN FUNCTION n

UTAP was unable to solve the pH equation corresponding to n where n refers to: 1-4, Layer number; 6 Initial pH calculations; 7 River pH; 8 Lake pH

(028) TOO MANY OUTPUTS

A maximum of 300 variables can be output to the detailed results and key files. Reduce number of variables or number of time steps.

(029) FILE NOT FOUND

Input file named does not exist.

(030) ERROR IN LOGNORMAL SPECIFIERS

Lognormal distribution has equal, reversed, or undefined minimum and maximum values. Check input file.

(031) ERROR IN NORMAL SPECIFIERS

Normal distributions has equal, reversed, or undefined minimum and maximum values. Check input file.

(032) TIME MUST BE IN WHOLE NUMBERS

Only 1 and 10 year time steps are available.

(033) ERROR IN TRIAGULAR SPECIFIERS

Triangular distribution has equal, reversed, or undefined minimum and maximum values. Check input file.

(034) ERROR IN BETA SPECIFIERS

Either the minimum is greater than or equal to the maximum specified or A or B are not greater than zero.

(35) GROUNDWATER OUTFLOWS NOT POSSIBLE

The groundwater outflows must correspond to watershed segment end node numbers.

(102) ABOUT TO OVER WRITE EXISTING FILE

Continuing execution will cause the contents of the file named directly above the warning to be erased.

APPENDIX B

SAMPLE INPUT FILES

EXAMPLE OF FIRST INPUT FILE (INPUT1.DAT)

```
GENERIC SITE SAMPLE RUN
Y Y
RES.OUT
KEY.OUT
 278   0   0
0913566091  10
  100.0   10.0
CODION N  1 N         0.0
CODNUC N  1 N         0.0
CODPH  N  1 N         0.0
CODERO N  1 N         0.0
CODDUS N  1 N         0.0
CODRAD N  1 N         0.0
CODWIN N  1 N         0.0
CODAIR N  1 N         0.0
CODSOL N  1 N         0.0
CODGS  N  1 N         0.0
CODVEG N  1 N         0.0
CODGW  N  1 N         0.0
CODWAT N  1 N         0.0
CODFIS N  1 N         0.0
CODWVG N  1 N         0.0
CODANI N  1 N         0.0
CODDOS N  1 N         0.0
PYRITI N  6 N       600.0      700.0      800.0
RHOTAL N  2 N      1.4E+6     1.0E+5     1.1E+6     1.7E+6
FRACGP N  4 N        0.05       0.06
KPRIME N  4 N        0.01        0.1
SULPRD N  6 N      3.0E-6     4.1E-6     5.3E-6
O2CONC N  1 N        9.04
O2DIFF N  6 N         4.0       45.0      115.0
DUNSAT F  4 N        0.75       1.25
KSUBSO N  1 N        50.0
FACTCO N  6 N         0.4        0.5        0.6
NPRCP  F  2 V         0.4        0.1       0.15       0.65
DMIX   N  4 N         1.0        2.0
AVPRCP N  1 N         0.4
ATAIL  N  1 N      5.0E+5
XLIME  N  1 N      5.0E-4
PCURAN N  1 N         0.1
FURAN  N  4 N        0.90       0.94
FT230  N  6 N        0.65       0.80       0.95
FT232  N  6 N        0.55       0.65       0.75
FRAD   N  6 N        0.25       0.60       0.95
FLEAD  N  4 N        0.76       0.86
FRACU  N  4 N        0.30       0.90
KDUO2  N  3 N      2.0E-5        3.0     5.0E-6     5.0E-4
PCTHOR N  4 N        0.02       0.04
XRADI  N  6 N      6.0E-6     1.2E-5     1.8E-5
KSBAR  N  1 N     1.07E-4
KFBAR  N  1 N       0.501
KRAD   N  4 N         0.5       0.56
KDRAD  N  3 N      4.5E-5        1.5     1.3E-6    1.52E-4
```

```
CLEADI N  6 N         1.0         2.0         3.0
KSLEAD N  1 N       0.012
KFLEAD N  1 N       0.501
KDLEAD N  3 N      6.0E-5         1.5      2.0E-5      1.0E-4
XRATE  N  1 N        0.10
DBOT   N  4 N         5.0        10.0
WSTAIL N  1 N      5.0E+5
XRUNOF N  6 N        0.10        0.15        0.20
SLOPE  N  1 N         1.0
THALF  N  4 N        15.0        25.0
RRAIN  N  4 N        65.0        97.5
RSOIL  N  4 N      1.0E-8      1.0E-7
DM     N  4 N      0.0015       0.075
STORM  N  4 N        36.0        48.0
FLENGT N  1 N       710.0
MINVEG N  1 N         0.0
BEDTRP N  1 N         0.0
SUSTRP N  1 N         0.0
WYEAR  N  4 V         1.0  20.9999999
EMANAT N  6 N        0.05        0.20        0.50
WTSFLX N  3 N        0.02         2.0       0.002         0.2
MPCH2O N  6 N         7.0        15.0        25.0
NSUBW  N  1 N         5.0
CAFR   N  1 N         0.0
SILT   N  6 N        30.0        45.0        60.0
FPREC  N  2 V       149.0        17.0       115.0       183.0
CAFD   N  1 N         0.0
HSRC   N  4 N         1.0         3.0
DEPVEL N  4 N       0.003        0.03
DSOIL  N  1 N        0.05
DSOIL  N  1 N        0.15
FWAT   N  6 N        0.02        0.16        0.48
RHOS   N  3 N       129.0         1.3        20.0       450.0
RHOS   N  3 N      1342.0         1.1      1000.0      1800.0
SOILKD N  5 N    1.3E-04        790.0
SOILKD N  5 N      0.0033       150.0
SOILKD N  5 N        0.18        63.0
SOILKD N  5 N      0.0051       950.0
SOILKD N  5 N    1.3E-04        790.0
SOILKD N  5 N      0.0033       150.0
SOILKD N  5 N        0.18        63.0
SOILKD N  5 N      0.0051       950.0
WC     N  4 N        0.75         1.4
WC     N  3 N        0.13         1.4        0.05        0.36
EMFRAC N  1 N         0.2
XRGWA1 N  6 N        25.0        35.0       200.0
XRGWA2 N  6 N        50.0        70.0       200.0
XRGWA3 N  1 N         0.0
XRGWA4 N  1 N         0.0
XRGWA5 N  1 N         0.0
AXGWA1 N  1 N      2000.0
AXGWA2 N  1 N      1000.0
AXGWA3 N  1 N         0.0
```

```
AXGWA4 N  1 N       0.0
AXGWA5 N  1 N       0.0
POGWA1 N  4 N       0.30        0.36
POGWA2 N  4 N       0.30        0.36
POGWA3 N  1 N       0.0
POGWA4 N  1 N       0.0
POGWA5 N  1 N       0.0
DCGWA1 N  3 N       0.02        2.5       0.005         0.5
DCGWA2 N  3 N       0.5         2.15      0.05          5.0
DCGWA3 N  3 N       0.67        1.73      0.13          3.5
DCGWA4 N  3 N       0.07        1.9       0.01          0.5
SDGWA1 N  2 N    2650.0       110.0    2320.0        2980.0
SDGWA2 N  2 N    2650.0       110.0    2320.0        2980.0
SDGWA3 N  1 N       0.0
SDGWA4 N  1 N       0.0
SDGWA5 N  1 N       0.0
HCGWA1 N  3 N     420.0         1.95     60.0        3100.0
HCGWA2 N  3 N     300.0         1.95     40.0        2200.0
HCGWA3 N  1 N       0.0
HCGWA4 N  1 N       0.0
HCGWA5 N  1 N       0.0
HGGWA1 N  2 N       0.05        0.01      0.03          0.07
HGGWA2 N  2 N       0.03        0.01      0.01          0.05
HGGWA3 N  1 N       0.0
HGGWA4 N  1 N       0.0
HGGWA5 N  1 N       0.0
ACTCO  N  6 N       0.6         0.8       0.9
WATCAB N  1 N       0.1
WTSO4B N  1 N       0.071
WATNAB N  1 N       0.079
WATKB  N  1 N       0.016
WATMGB N  1 N       0.032
WATCLB N  1 N       0.02
WSIGS1 N  6 N      95.0       230.0     615.0
WSIGS2 N  6 N     105.0       260.0     765.0
WSIGS3 N  6 N      85.0       210.0     515.0
WSIGS4 N  1 N       0.0
WSIGS5 N  1 N       0.0
WTRHOS N  1 N    1.84E+6
WATEPS N  6 N       0.83        0.94      0.97
WTMIXD N  1 N       0.05
WKDU   N  3 N    0.0045         2.2     0.0004        0.048
WKDPB  N  3 N     0.015         2.5      0.001         0.23
WKDRA  N  3 N    0.0065         2.5     0.0004          0.1
KDPRIM N  3 N      0.02         2.5      0.002          0.3
BURYF  N  4 N       0.5         0.7
CURRNT N  4 N    3.15E+4    3.15E+5
DIFFC  N  1 N      0.02
FCONC  N  6 N       0.0        0.02        0.1
FCONC  N  6 N       0.0       0.005       0.02
FCONC  N  6 N       0.0        0.02        0.1
FCONC  N  6 N       0.0        0.02        0.1
BIOACF N  3 N   1.55E-6         6.1     1.0E-8       5.8E-5
BIOACF N  3 N   1.18E-5       2.6     1.1E-6     1.1E-4
BIOACF N  3 N   1.74E-5      3.25     1.7E-6     5.7E-4
BIOACF N  3 N   1.31E-5       3.3     1.2E-6     6.0E-4
WATVTC N  3 N    1.5E-5       5.5     1.0E-6     7.0E-4
WATVTC N  3 N    1.1E-5       6.8     1.0E-6     1.6E-4
WATVTC N  3 N    1.3E-4       2.0     4.0E-5     4.3E-4
WATVTC N  3 N    4.5E-5       2.9     1.0E-5     3.3E-4
FDEPSF N  4 N       0.1       0.3
FDEPSF N  4 N       0.1       0.3
FDEPSF N  2 N      0.47       0.3       0.01        1.0
FDEPSF N  2 N      0.47       0.3       0.01        1.0
FDEPSF N  4 N       0.8       1.0
FDEPED N  4 N       0.8       1.0
FDEPED N  4 N      0.05      0.15
FDEPED N  4 N       0.8       1.0
FDEPED N  4 N       0.8       1.0
FDEPED N  4 N       0.8       1.0
VEGLAM N  4 N    2.9E-7    1.2E-6
VEGLAM N  4 N    2.9E-7    1.2E-6
VEGLAM N  4 N    2.9E-7    1.2E-6
VEGLAM N  4 N    2.9E-7    1.2E-6
VEGLAM N  4 N    1.5E-9    4.4E-9
DUREXP N  6 N    2.6E+6    5.2E+6     7.8E+6
DUREXP N  6 N    2.6E+6    5.2E+6     7.8E+6
DUREXP N  4 N    1.3E+6    3.9E+6
DUREXP N  4 N    1.3E+6    3.9E+6
DUREXP N  1 N   1.0E+10
YDEN   N  4 N    1000.0    3000.0
YDEN   N  4 N    1000.0    3000.0
YDEN   N  4 N     500.0    1000.0
YDEN   N  4 N     500.0    1000.0
YDEN   N  4 N     400.0     600.0
SPTCAV N  3 N    6.1E-4       8.9     7.7E-6      0.007
SPTCAV N  3 N    0.0042       9.0     5.2E-5       0.34
SPTCAV N  3 N    0.0040       9.0     4.9E-5       0.32
SPTCAV N  3 N    0.0085      10.0     8.0E-5       0.89
SPTCBV N  3 N    3.2E-4       3.9     2.1E-5     0.0049
SPTCBV N  3 N    0.0042       4.0     2.6E-4      0.067
SPTCBV N  3 N    0.0040       4.0     2.5E-4      0.064
SPTCBV N  3 N    0.0027       4.5     1.3E-4      0.066
SPTCSF N  3 N    0.0066       8.9     8.3E-5       0.52
SPTCSF N  3 N     0.022       9.5     2.5E-4        2.0
SPTCSF N  3 N     0.022       3.6     0.0017       0.27
SPTCSF N  3 N      0.21       3.6     0.0019       0.24
SPTCB  N  3 N    0.0066       8.9     8.3E-5       0.52
SPTCB  N  3 N     0.022       9.5     2.5E-4        2.0
SPTCB  N  3 N     0.022       3.6     0.0017       0.27
SPTCB  N  3 N      0.21       3.6     0.0019       0.24
SPTCL  N  1 N       0.0
SPTCL  N  1 N       0.0
SPTCL  N  1 N       0.0
SPTCL  N  1 N       0.0
FIRC   N  6 N    5000.0    7000.0     9000.0
```

```
WIRC    N  6 N     0.0077     0.0115     0.0153
FAISFC  N  6 N       0.05        0.2        0.5
FAILC   N  6 N       0.05        0.2        0.5
FMTCC   N  6 N     1.1E-7     3.4E-7     1.0E-6
FMTCC   N  6 N     0.7E-7     2.0E-7     0.6E-6
FMTCC   N  6 N     1.3E-7     4.0E-7     1.2E-6
FMTCC   N  6 N     1.7E-7     5.1E-7     1.5E-6
FIRM    N  1 N     2.7E+4
WIRM    N  6 N      0.024      0.036      0.048
FAIBM   N  6 N        0.8        0.9       0.95
FMTCM   N  6 N     1.1E-7     3.4E-7     1.0E-6
FMTCM   N  6 N     0.7E-7     2.0E-7     0.6E-6
FMTCM   N  6 N     1.3E-7     4.0E-7     1.2E-6
FMTCM   N  6 N     1.7E-7     5.1E-7     1.5E-6
FIRD    N  6 N     1800.0     7500.0     1.0E+4
WIRD    N  4 N     0.0007     0.0014
FAISFD  N  6 N       0.25       0.33       0.40
FMTCD   N  6 N     1.1E-7     3.4E-7     1.0E-6
FMTCD   N  6 N     0.7E-7     2.0E-7     0.6E-6
FMTCD   N  6 N     1.3E-7     4.0E-7     1.2E-6
FMTCD   N  6 N     1.7E-7     5.1E-7     1.5E-6
EFR     N  6 N        0.2        0.5        0.8
SHLD    N  6 N       0.05        0.2        0.4
OF      N  6 N        0.8        0.9        1.0
OF      N  6 N        0.8        0.9        1.0
INOCC   N  6 N        0.6        0.9        1.0
INOCC   N  6 N        0.6        0.9        1.0
AIRIN   N  1 N     8400.0
AIRIN   N  1 N     8400.0
AFACT   N  4 N        0.5        1.0
AVEGIN  N  4 N    4.53E+4    5.08E+4
AVEGIN  N  4 N    4.53E+4    5.08E+4
AFLOC   N  6 N        0.0        0.1        0.2
AFLOC   N  6 N        0.1        0.3        0.6
BFACT   N  4 N        0.5        1.0
BVEGIN  N  4 N    7.38E+4    8.24E+4
BVEGIN  N  4 N    7.38E+4    8.24E+4
BFLOC   N  6 N        0.0        0.1        0.2
BFLOC   N  6 N        0.1        0.3        0.6
CARMIN  N  1 N     3800.0
CARMIN  N  1 N     2.6E+4
CFLOC   N  4 N        0.0        1.0
CFLOC   N  4 N        0.0        1.0
MOSMIN  N  1 N     3800.0
MOSMIN  N  1 N     2.6E+4
MFLOC   N  1 N        0.0
MFLOC   N  1 N        1.0
DERMIN  N  1 N     3800.0
DERMIN  N  1 N     2.6E+4
DFLOC   N  6 N        0.0       0.25        0.5
DFLOC   N  1 N        1.0
WATIN   N  1 N        0.6
WATIN   N  1 N        0.6
```

```
FISHIN N  1 N     8000.0
FISHIN N  1 N     8000.0
FFLOC  N  4 N        0.0          0.1
FFLOC  N  1 N        1.0
```

EXAMPLE OF SECOND INPUT FILE (INPUT2.DAT)

```
  N
AVERAGE.DAT
  5
  5
    1    3    5   10    20    50
  1 16   1  1  1 C     2
  2 16   3  2  2 A     5
  3 14   3  2  2 A     6
  4  1   1  1  1 C     1
  5  7   3  2  2 A     3
  8  2
  1  1   0  0  0
  4  4   0  0  0
  1 R 11  1                1.5E07    3.0E3
  2 L 11  1          10.0  2.0E07   5.0E05
  3 R 10  2                3.2E07    3.5E3
  4 L 10  2           4.0  3.8E07   2.5E05
  5 R  9  3                7.0E07    7.0E3
  6 R  9  4                1.2E08    1.3E4
  7 L  9  4           5.0  1.4E08   4.0E06
  8 R  9  5                4.0E08    3.0E4
  3
  10.0  30.0 100.0
 35
WCONC   0
CONC    0
PH      0
WATC    0
WATAVG  0
WATPH   0
GWATC   0
EMRATE  0
EROTOT  0
AIRC    0
SOILC   0
AVEGC   0
BVEGC   0
SUFOC   0
BRWSC   0
LICHC   0
AQVEGC  0
FISHC   0
ADERC   0
WDERC   0
AMOSC   0
WMOSC   0
ACARC   0
WCARC   0
WATD    2
  1  1
 11  1
SHINED  0
INHD    0
```

```
RADD    0
VEGD    0
FISHD   0
MEATD   0
DOSE    1
  2  2
POPDT   0
BLANK1  0
BLANK2  0
```

EXAMPLE FILE CONTAINING LONG TERM AVERAGE SET OF WIND DATA AS PROVIDED BY AES

```
P1397.TOTAL.
  N A 0.000400.000290.0    0.0    0.0    0.0            62925 1A176584
NNE A 0.000370.000120.0    0.0    0.0    0.0            62925 2A176584
 NE A 0.000270.000150.0    0.0    0.0    0.0            62925 3A176584
ENE A 0.000110.000060.0    0.0    0.0    0.0            62925 4A176584
  E A 0.000050.000020.0    0.0    0.0    0.0            62925 5A176584
ESE A 0.000010.000010.0    0.0    0.0    0.0            62925 6A176584
 SE A 0.000030.000030.0    0.0    0.0    0.0            62925 7A176584
SSE A 0.000050.000030.0    0.0    0.0    0.0            62925 8A176584
  S A 0.000190.000150.0    0.0    0.0    0.0            62925 9A176584
SSW A 0.000300.000190.0    0.0    0.0    0.0            6292510A176584
 SW A 0.000270.000190.0    0.0    0.0    0.0            6292511A176584
WSW A 0.000270.000200.0    0.0    0.0    0.0            6292512A176584
  W A 0.000460.000260.0    0.0    0.0    0.0            6292513A176584
WNW A 0.000280.000180.0    0.0    0.0    0.0            6292514A176584
 NW A 0.000130.000080.0    0.0    0.0    0.0            6292515A176584
NNW A 0.000240.000100.0    0.0    0.0    0.0            6292516A176584
  N B 0.002130.001650.000930.0    0.0    0.0            62925 1B176584
NNE B 0.001940.001580.000750.0    0.0    0.0            62925 2B176584
 NE B 0.001410.000770.000540.0    0.0    0.0            62925 3B176584
ENE B 0.000700.000280.000150.0    0.0    0.0            62925 4B176584
  E B 0.000830.000230.000150.0    0.0    0.0            62925 5B176584
ESE B 0.000410.000100.000050.0    0.0    0.0            62925 6B176584
 SE B 0.000430.000120.000070.0    0.0    0.0            62925 7B176584
SSE B 0.000600.000350.000250.0    0.0    0.0            62925 8B176584
  S B 0.001380.001270.001320.0    0.0    0.0            62925 9B176584
SSW B 0.001310.001310.000980.0    0.0    0.0            6292510B176584
 SW B 0.001550.001520.001220.0    0.0    0.0            6292511B176584
WSW B 0.001370.001520.000880.0    0.0    0.0            6292512B176584
  W B 0.002270.001800.001350.0    0.0    0.0            6292513B176584
WNW B 0.001160.001010.000740.0    0.0    0.0            6292514B176584
 NW B 0.001060.000800.000530.0    0.0    0.0            6292515B176584
NNW B 0.001050.000760.000310.0    0.0    0.0            6292516B176584
  N C 0.000980.002000.003640.000350.000020.00001        62925 1C176584
NNE C 0.001180.002030.002700.000110.0    0.0            62925 2C176584
 NE C 0.001120.001580.002160.000180.000010.0            62925 3C176584
ENE C 0.000640.000680.000990.000090.0    0.0            62925 4C176584
  E C 0.000700.000790.001460.000150.000010.0            62925 5C176584
ESE C 0.000670.000460.000700.000050.0    0.0            62925 6C176584
 SE C 0.000680.000520.000660.000070.0    0.0            62925 7C176584
SSE C 0.000690.000830.001790.000330.000030.00001        62925 8C176584
  S C 0.001140.001680.007320.001960.000150.00004        62925 9C176584
SSW C 0.000730.001340.004530.000940.000030.0            6292510C176584
 SW C 0.000670.001300.004820.001030.000020.0            6292511C176584
WSW C 0.000710.001280.003210.000510.000050.00002        6292512C176584
  W C 0.001110.002000.006260.001430.000210.00002        6292513C176584
WNW C 0.000810.001330.004510.001110.000200.00003        6292514C176584
 NW C 0.000770.001110.003090.000600.000100.00002        6292515C176584
NNW C 0.000640.000910.002090.000200.000020.00001        6292516C176584
  N D 0.002480.003680.009810.015030.002830.00043        62925 1D176584
NNE D 0.002520.003980.008840.010610.002150.00043        62925 2D176584
 NE D 0.002200.003630.009480.013360.003420.00099        62925 3D176584
```

```
ENE D 0.002310.003550.009970.012710.003840.00098      62925 4D176584
  E D 0.003540.005030.013370.013500.003680.00090      62925 5D176584
ESE D 0.002610.003540.008110.007960.002170.00047      62925 6D176584
 SE D 0.002480.003380.007630.005870.001310.00016      62925 7D176584
SSE D 0.002560.004090.011150.011480.002650.00057      62925 8D176584
  S D 0.003770.005830.017620.026690.008500.00265      62925 9D176584
SSW D 0.002080.003290.009840.017170.005910.00212      6292510D176584
 SW D 0.002080.003230.009620.014230.004700.00141      6292511D176584
WSW D 0.001880.003000.007440.010990.003730.00158      6292512D176584
  W D 0.003310.005700.015580.027570.009890.00325      6292513D176584
WNW D 0.002260.004610.014190.028500.010070.00334      6292514D176584
 NW D 0.002230.003740.010380.014560.003840.00144      6292515D176584
NNW D 0.002040.003450.008680.012640.002710.00074      6292516D176584
  N E 0.0    0.001770.005530.0    0.0    0.0          62925 1E176584
NNE E 0.0    0.001760.004000.0    0.0    0.0          62925 2E176584
 NE E 0.0    0.001910.004090.0    0.0    0.0          62925 3E176584
ENE E 0.0    0.002030.003600.0    0.0    0.0          62925 4E176584
  E E 0.0    0.002890.002640.0    0.0    0.0          62925 5E176584
ESE E 0.0    0.002220.001200.0    0.0    0.0          62925 6E176584
 SE E 0.0    0.001970.001200.0    0.0    0.0          62925 7E176584
SSE E 0.0    0.002380.002240.0    0.0    0.0          62925 8E176584
  S E 0.0    0.003050.003620.0    0.0    0.0          62925 9E176584
SSW E 0.0    0.001520.002750.0    0.0    0.0          6292510E176584
 SW E 0.0    0.001480.003100.0    0.0    0.0          6292511E176584
WSW E 0.0    0.001370.002600.0    0.0    0.0          6292512E176584
  W E 0.0    0.002880.007580.0    0.0    0.0          6292513E176584
WNW E 0.0    0.002410.007560.0    0.0    0.0          6292514E176584
 NW E 0.0    0.002470.005610.0    0.0    0.0          6292515E176584
NNW E 0.0    0.001660.004400.0    0.0    0.0          6292516E176584
  N F 0.005450.003780.0    0.0    0.0    0.0          62925 1F176584
NNE F 0.004790.003180.0    0.0    0.0    0.0          62925 2F176584
 NE F 0.005170.003130.0    0.0    0.0    0.0          62925 3F176584
ENE F 0.004720.002980.0    0.0    0.0    0.0          62925 4F176584
  E F 0.007800.003120.0    0.0    0.0    0.0          62925 5F176584
ESE F 0.005840.002810.0    0.0    0.0    0.0          62925 6F176584
 SE F 0.006000.002330.0    0.0    0.0    0.0          62925 7F176584
SSE F 0.005990.002890.0    0.0    0.0    0.0          62925 8F176584
  S F 0.007570.003590.0    0.0    0.0    0.0          62925 9F176584
SSW F 0.004210.002120.0    0.0    0.0    0.0          6292510F176584
 SW F 0.003920.002430.0    0.0    0.0    0.0          6292511F176584
WSW F 0.003990.002160.0    0.0    0.0    0.0          6292512F176584
  W F 0.009040.006220.0    0.0    0.0    0.0          6292513F176584
WNW F 0.006990.005420.0    0.0    0.0    0.0          6292514F176584
 NW F 0.006690.005180.0    0.0    0.0    0.0          6292515F176584
NNW F 0.005770.004090.0    0.0    0.0    0.0          6292516F176584
```

APPENDIX C

SAMPLE OUTPUT FILES

SAMPLE KEY FILE (KEY.OUT)

```
FILE CREATED 04/29/87 AT 09:37:26
 GENERIC SITE SAMPLE RUN
 NUMBER OF TRIALS:    10
     PARAMETER  SUBSTANCE  LOC       TIME      MEAN      STD DEV    GEOM MEAN   GEOM SD    MINIMUM    MAXIMUM    SKEWNESS   KURTOSIS
  1    DUNSAT                                0.109E+01  0.129E+00  0.108E+01  0.113E+01  0.812E+00  0.125E+01  -.906E+00  0.316E+01
  2    NPRCP                        .100E+02  0.358E+00  0.731E-01  0.351E+00  0.124E+01  0.236E+00  0.463E+00  -.259E+00  0.221E+01
  3    NPRCP                        .300E+02  0.391E+00  0.789E-01  0.384E+00  0.123E+01  0.262E+00  0.525E+00  0.221E-01  0.229E+01
  4    NPRCP                        .100E+03  0.406E+00  0.834E-01  0.397E+00  0.127E+01  0.224E+00  0.523E+00  -.773E+00  0.350E+01
  5    WATD          1          1   .100E+02  0.318E+01  0.212E+01  0.256E+01  0.209E+01  0.622E+00  0.713E+01  0.866E+00  0.265E+01
  6    WATD          1          1   .300E+02  0.195E+02  0.942E+01  0.165E+02  0.204E+01  0.313E+01  0.367E+02  -.808E-01  0.290E+01
  7    WATD          1          1   .100E+03  0.173E+02  0.100E+02  0.149E+02  0.180E+01  0.485E+01  0.400E+02  0.110E+01  0.370E+01
  8    WATD         11          1   .100E+02  0.896E+03  0.321E+03  0.855E+03  0.136E+01  0.619E+03  0.168E+04  0.156E+01  0.464E+01
  9    WATD         11          1   .300E+02  0.640E+03  0.117E+03  0.630E+03  0.121E+01  0.445E+03  0.794E+03  -.266E+00  0.191E+01
 10    WATD         11          1   .100E+03  0.217E+03  0.980E+02  0.204E+03  0.140E+01  0.151E+03  0.484E+03  0.226E+01  0.683E+01
 11    DOSE          2          2   .100E+02  0.750E+02  0.153E+02  0.735E+02  0.124E+01  0.474E+02  0.962E+02  -.231E+00  0.218E+01
 12    DOSE          2          2   .300E+02  0.129E+03  0.238E+02  0.127E+03  0.120E+01  0.915E+02  0.172E+03  0.535E+00  0.264E+01
 13    DOSE          2          2   .100E+03  0.554E+02  0.269E+02  0.509E+02  0.151E+01  0.320E+02  0.121E+03  0.154E+01  0.464E+01
```

SAMPLE DETAILED RESULTS FILE (RES.OUT)

```
FILE CREATED 04/29/87 AT 09:34:03
 0.812E+00 0.258E+00 0.303E+00 0.342E+00 0.652E+01 0.367E+02 0.164E+02 0.109E+04 0.752E+03 0.187E+03 0.764E+02 0.119E+03 0.353E+02
 0.114E+01 0.393E+00 0.336E+00 0.498E+00 0.317E+01 0.269E+02 0.112E+02 0.752E+03 0.700E+03 0.177E+03 0.651E+02 0.140E+03 0.553E+02
 0.125E+01 0.447E+00 0.380E+00 0.420E+00 0.110E+01 0.752E+01 0.968E+01 0.807E+03 0.794E+03 0.229E+03 0.912E+02 0.172E+03 0.543E+02
 0.105E+01 0.463E+00 0.447E+00 0.224E+00 0.258E+01 0.200E+02 0.400E+02 0.100E+04 0.765E+03 0.484E+03 0.910E+02 0.164E+03 0.121E+03
 0.111E+01 0.236E+00 0.526E+00 0.523E+00 0.713E+01 0.241E+02 0.116E+02 0.168E+04 0.589E+03 0.164E+03 0.962E+02 0.114E+03 0.407E+02
 0.120E+01 0.339E+00 0.262E+00 0.376E+00 0.228E+01 0.208E+02 0.125E+02 0.666E+03 0.668E+03 0.151E+03 0.647E+02 0.126E+03 0.320E+02
 0.995E+00 0.369E+00 0.423E+00 0.436E+00 0.345E+01 0.211E+02 0.203E+02 0.692E+03 0.494E+03 0.159E+03 0.782E+02 0.119E+03 0.438E+02
 0.101E+01 0.401E+00 0.374E+00 0.386E+00 0.200E+01 0.170E+02 0.220E+02 0.669E+03 0.572E+03 0.228E+03 0.629E+02 0.126E+03 0.736E+02
 0.119E+01 0.342E+00 0.468E+00 0.427E+00 0.299E+01 0.181E+02 0.242E+02 0.619E+03 0.445E+03 0.220E+03 0.771E+02 0.120E+03 0.639E+02
 0.116E+01 0.334E+00 0.393E+00 0.425E+00 0.622E+00 0.313E+01 0.485E+01 0.975E+03 0.619E+03 0.173E+03 0.474E+02 0.915E+02 0.337E+02
```

APPENDIX D

INPUT DISTRIBUTION DESCRIPTIONS

Variable	Definition	Units
CODION	Print code for Water source model ions (1)*	--
CODNUC	Print code for Water source model nuclides (1)	--
CODPH	Print code for Water source model pH (1)	--
CODERO	Print code for erosion model (1,2)	--
CODDUS	Print code for SUBROUTINE DUST (1,2,3)	--
CODRAD	Print code for SUBROUTINE RADON (1,2,3)	--
CODWIN	Print code for SUBROUTINE WIND (1,2,3)	--
CODAIR	Print code for SUBROUTINE AIRDIS (1,2,3)	--
CODSOL	Print code for soil model (1,2,3)	--
CODGS	Print code for groundshine routine (1,2,3)	--
CODVEG	Print code for SUBROUTINE VEGCON (1,2,3)	--
CODGW	Print code for groundwater (1,2,3)	--
CODWAT	Print code for water models (1,2,3,4,6)	--
CODFIS	Print code for fish model (1,2)	--
CODWVG	Print code for aquatic vegetation (1,2)	--
CODANI	Print code for SUBROUTINE ANIMAL (1,2,3)	--
CODDOS	Print code for SUBROUTINE DOSEIN (1,2,3)	--
PYRITI	Initial Pyrite content of tailings	$mol.m^{-3}$
RHOTAL	Tailings bulk density (dry)	$g.m^{-3}$
FRACGP	Initial mass fraction of gypsum in tailings	--
KPRIME	Ratio of O_2 half saturation constant to $[O_2]$	--
SULPRD	Sulphate production rate	$mol.g^{-1}.yr^{-1}$
O2CONC	O_2 concentration at the tailings surface	$mol.m^{-3}$
O2DIFF	O_2 diffusivity through the tailings	$m^2.yr^{-1}$
DUNSAT	Thickness of the unsaturated layer	m
KSUBSO	Solubility constant for $CaSO_4$	$mol^2.m^{-6}$
FACTCO	Activity coefficient for divalent ions	--
NPRCP	Annual net precipitation	$m.yr^{-1}$
DMIX	Thickness of the mixing zone	m
AVPRCP	Long term mean annual net precipitation	$m.yr^{-1}$
ATAIL	Tailings surface area	m^2
XLIME	Initial mass fraction of $CaCO_3$ in tailings	--
PCURAN	Mass % of uranium (as U_3O_8) in the ore	--
FURAN	Mass fraction of uranium recovered in the mill	--
FT230	Fraction of Th-230 assumed to be ultimately soluble	--
FT232	Fraction of Th-232 assumed to be ultimately soluble	--
FRAD	Fraction of Ra-226 assumed to be ultimately soluble	--
FLEAD	Fraction of Pb-210 assumed to be ultimately soluble	--
FRACU	Fraction of uranium associated with pyrite	--
KDUO2	Uranium solid-liquid distribution coefficient	$m^3.g^{-1}$
PCTHOR	Mass % of thorium (as ThO_2) in the ore	--
XRADI	Initial mol fraction of Ra-226 in $BaSO_4$	--
KSBAR	Solubility constant for $BaSO_4$	$mol^2.m^{-6}$
KFBAR	Formation constant for $BaSO_4(aq)$	$m^3.mol^{-1}$
KRAD	Radium distribution coefficient	--
KDRAD	Radium solid-liquid distribution coefficient	$m^3.g^{-1}$
CLEADI	Initial concentration of $PbSO_4$ in tailings	$mol.m^{-3}$
KSLEAD	Solubility constant for $PbSO_4$	$mol^2.m^{-6}$
KFLEAD	Formation constant for $PbSO_4(aq)$	$m^3.mol^{-1}$
KDLEAD	Lead solid-liquid distribution coefficient	$m^3.g^{-1}$

Note:

* Numbers in parentheses indicate values that yield detailed printouts.

Variable	Definition	Units
XRATE	Fraction of R_s which occurs when calcite is present	--
DBOT	Depth of the deep saturated zone	m
WSTAIL	Surface area of the watershed	m^2
XRUNOF	Fraction of net precipitation which is surface runoff	--
TYPE	Flag to indicate if restart option is required	--
SLOPE	Overall % slope of tailings pile	--
THALF	Revegetation half life	yr
RRAIN	Rainfall erosivity factor	--
RSOIL	Proportionality constant for bedload transport equation	--
DM	Silt particle diameter	mm
STORM	24 hour rainfall for a two year return period	mm
FLENGT	Flow length of tailings pile	m
MINVEG	Minimum fraction of vegetated cover	--
BEDTRP	Bedload % trapping efficiency for pond	--
SUSTRP	Suspended sediment % trapping efficiency for pond	--
WYEAR	Random variable for selection of wind data	--
EMANAT	Radon Emanation coefficient from tailings	--
WTSFLX	Winter/Summer radon flux ratio	--
MPCH2O	Percent moisture content by weight of tailings (wet)	%
NSUBW	Number of winter months (freezing conditions) per year	months
CAFR	Cover attenuation factor for radon	--
SILT	Silt content of tailings (% of particles < 75 μm)	--
FPREC	Number of days per year with more than .25 mm precipitation	--
CAFD	Cover attenuation factor for dust	--
HSRC	Height of source	m
DEPVEL	Deposition velocity	m.s^{-1}
DSOIL	Depth of soil layer 1	m
DSOIL	Depth of soil layer 2	m
FWAT	Fraction of net precipitation in runoff	--
RHOS	Soil bulk density for layer 1	kg(soil).m^{-3}
RHOS	Soil bulk density for layer 2	kg(soil).m^{-3}
SOILKD	Soil K_d for U in soil layer 1	m^3.kg^{-1}
SOILKD	Soil K_d for Th in soil layer 1	m^3.kg^{-1}
SOILKD	Soil K_d for Pb in soil layer 1	m^3.kg^{-1}
SOILKD	Soil K_d for Ra in soil layer 1	m^3.kg^{-1}
SOILKD	Soil K_d for U in soil layer 2	m^3.kg^{-1}
SOILKD	Soil K_d for Th in soil layer 2	m^3.kg^{-1}
SOILKD	Soil K_d for Pb in soil layer 2	m^3.kg^{-1}
SOILKD	Soil K_d for Ra in soil layer 2	m^3.kg^{-1}
WC	Water content of soil layer 1	kg(water).kg^{-1}(soil)
WC	Water content of soil layer 2	kg(water).kg^{-1}(soil)
EMFRAC	Fraction of radon emanated from soil at receptors	--
XRGWA1	Groundwater discharge distance for dam 1	m
XRGWA2	Groundwater discharge distance for dam 2	m
XRGWA3	Groundwater discharge distance for dam 3	m
XRGWA4	Groundwater discharge distance for dam 4	m

Variable	Definition	Units
XRGWA5	Groundwater discharge distance for dam 5	m
AXGWA1	Cross sectional area of aquifer one's window	m^2
AXGWA2	Cross sectional area of aquifer two's window	m^2
AXGWA3	Cross sectional area of aquifer three's window	m^2
AXGWA4	Cross sectional area of aquifer four's window	m^2
AXGWA5	Cross sectional area of aquifer five's window	m^2
POGWA1	Porosity of aquifer one	m^3(water).m^{-3}(solid)
POGWA2	Porosity of aquifer two	m^3(water).m^{-3}(solid)
POGWA3	Porosity of aquifer three	m^3(water).m^{-3}(solid)
POGWA4	Porosity of aquifer four	m^3(water).m^{-3}(solid)
POGWA5	Porosity of aquifer five	m^3(water).m^{-3}(solid)
DCGWA1	Distribution coefficient for uranium	$m^3.kg^{-1}$
DCGWA2	Distribution coefficient for thorium	$m^3.kg^{-1}$
DCGWA3	Distribution coefficient for lead	$m^3.kg^{-1}$
DCGWA4	Distribution coefficient for radium	$m^3.kg^{-1}$
SDGWA1	Bulk density of aquifer one	$kg.m^{-3}$
SDGWA2	Bulk density of aquifer two	$kg.m^{-3}$
SDGWA3	Bulk density of aquifer three	$kg.m^{-3}$
SDGWA4	Bulk density of aquifer four	$kg.m^{-3}$
SDGWA5	Bulk density of aquifer five	$kg.m^{-3}$
HCGWA1	Hydraulic conductivity of aquifer one	$m.yr^{-1}$
HCGWA2	Hydraulic conductivity of aquifer two	$m.yr^{-1}$
HCGWA3	Hydraulic conductivity of aquifer three	$m.yr^{-1}$
HCGWA4	Hydraulic conductivity of aquifer four	$m.yr^{-1}$
HCGWA5	Hydraulic conductivity of aquifer five	$m.yr^{-1}$
HGGWA1	Hydraulic gradient of aquifer one	$m.m^{-1}$
HGGWA2	Hydraulic gradient of aquifer two	$m.m^{-1}$
HGGWA3	Hydraulic gradient of aquifer three	$m.m^{-1}$
HGGWA4	Hydraulic gradient of aquifer four	$m.m^{-1}$
HGGWA5	Hydraulic gradient of aquifer five	$m.m^{-1}$
ACTCO	Water activity coefficient	--
WATCAB	Background water concentration of calcium	$mol.m^{-3}$
WTSO4B	Background water concentration of sulphate	$mol.m^{-3}$
WATNAB	Background water concentration of sodium	$mol.m^{-3}$
WATKB	Background water concentration of potassium	$mol.m^{-3}$
WATMGB	Background water concentration of of magnesium	$mol.m^{-3}$
WATCLB	Background water concentration of chlorine	$mol.m^{-3}$
WSIGS1	Sediment flux of total solids in first lake	$g.m^{-2}yr^{-1}$
WSIGS2	Sediment flux of total solids in second lake	$g.m^{-2}yr^{-1}$
WSIGS3	Sediment flux of total solids in third lake	$g.m^{-2}yr^{-1}$
WSIGS4	Sediment flux of total solids in fourth lake	$g.m^{-2}yr^{-1}$
WSIGS5	Sediment flux of total solids in fifth lake	$g.m^{-2}yr^{-1}$
WTRHOS	Density of stabilized sediment solids in lakes	$g.m^{-3}$
WATEPS	Volume fraction of solids in lake sediment	$cm^3.cm^{-3}$
WTMIXD	Thickness of sediment exchange zone in lakes	m
WKDU	Uranium distribution coefficient for lakes	$m^3.g^{-1}$
WKDPB	Lead distribution coefficient for lakes	$m^3.g^{-1}$
WKDRA	Radium distribution coefficient for lakes	$m^3.g^{-1}$
KDPRIM	Relation of thorium distribution coefficient to pH	--
BURYF	Fraction of sedimenting material buried in lake	--
CURRNT	Current velocity in lake	m/yr^{-1}

Variable	Definition	Units
DIFFC	Diffusivity coefficient for lakes	m^2/yr^{-1}
FCON	Soluble fraction of uranium in eroded solids	--
FCONC	Soluble fraction of thorium in eroded solids	--
FCONC	Soluble fraction of lead in eroded solids	--
FCONC	Soluble fraction of radium in eroded solids	--
BIOACF	Bioaccumulation factor of uranium in fish	$m^3.g^{-1}$
BIOACF	Bioaccumulation factor of thorium in fish	$m^3.g^{-1}$
BIOACF	Bioaccumulation factor of lead in fish	$m^3.g^{-1}$
BIOACF	Bioaccumulation factor of radium in fish	$m^3.g^{-1}$
WATVTC	Water vegetation transfer coefficient for uranium	$m^3.g^{-1}$
WATVTC	Water vegetation transfer coefficient for thorium	$m^3.g^{-1}$
WATVTC	Water vegetation transfer coefficient for lead	$m^3.g^{-1}$
WATVTC	Water vegetation transfer coefficient for radium	$m^3.g^{-1}$
FDEPSF	Fraction of total deposition retained on above ground vegetation	--
FDEPSF	Fraction of total deposition retained on below ground vegetation	--
FDEPSF	Fraction of total deposition retained on summer forage	--
FDEPSF	Fraction of total deposition retained on browse vegetation	--
FDEPSF	Fraction of total deposition retained on lichen	--
FDEPED	Fraction of plant deposition retained on edible portions of above ground vegetation	--
FDEPED	Fraction of plant deposition retained on edible below ground vegetation	--
FDEPED	Fraction of plant deposition retained on edible summer forage	--
FDEPED	Fraction of plant deposition retained on edible browse vegetation	--
FDEPED	Fraction of plant deposition retained on edible lichen	--
VEGLAM	Decay constant for weathering losses from above ground vegetation	s^{-1}
VEGLAM	Decay constant for weathering losses from below ground vegetation	s^{-1}
VEGLAM	Decay constant for weathering losses from summer forage	s^{-1}
VEGLAM	Decay constant for weathering losses from browse vegetation	s^{-1}
VEGLAM	Decay constant for weathering losses from lichen	s^{-1}
DUREXP	Duration of exposure to deposition for above ground vegetation	s
DUREXP	Duration of exposure to deposition for below ground vegetation	s
DUREXP	Duration of exposure to deposition for summer forage	s
DUREXP	Duration of exposure to deposition for browse vegetation	s
DUREXP	Duration of exposure to deposition for lichen	s
YDEN	Yield density (wet) for above ground vegetation	$g.m^{-2}$

Variable	Definition	Units
YDEN	Yield density (wet) for below ground vegetation	g.m^{-2}
YDEN	Yield density (wet) for summer forage	g.m^{-2}
YDEN	Yield density (wet) for browse vegetation	g.m^{-2}
YDEN	Yield density (wet) for lichen	g.m^{-2}
SPTCAV	Soil-to-plant transfer coefficient for above ground vegetation for uranium	Bq.g^{-1}(wet)/Bq.g^{-1}(dry)
SPTCAV	Soil-to-plant transfer coefficient for above ground vegetation for thorium	Bq.g^{-1}(wet)/Bq.g^{-1}(dry)
SPTCAV	Soil-to-plant transfer coefficient for above ground vegetation for lead	Bq.g^{-1}(wet)/Bq.g^{-1}(dry)
SPTCAV	Soil-to-plant transfer coefficient for above ground vegetation for radium	Bq.g^{-1}(wet)/Bq.g^{-1}(dry)
SPTCBV	Soil-to-plant transfer coefficient for below ground vegetation for uranium	Bq.g^{-1}(wet)/Bq.g^{-1}(dry)
SPTCBV	Soil-to-plant transfer coefficient for below ground vegetation for thorium	Bq.g^{-1}(wet)/Bq.g^{-1}(dry)
SPTCBV	Soil-to-plant transfer coefficient for below ground vegetation for lead	Bq.g^{-1}(wet)/Bq.g^{-1}(dry)
SPTCBV	Soil-to-plant transfer coefficient for below ground vegetation for radium	Bq.g^{-1}(wet)/Bq.g^{-1}(dry)
SPTCSF	Soil-to-plant transfer coefficient for summer forage for uranium	Bq.g^{-1}(wet)/Bq.g^{-1}(dry)
SPTCSF	Soil-to-plant transfer coefficient for summer forage for thorium	Bq.g^{-1}(wet)/Bq.g^{-1}(dry)
SPTCSF	Soil-to-plant transfer coefficient for summer forage for lead	Bq.g^{-1}(wet)/Bq.g^{-1}(dry)
SPTCSF	Soil-to-plant transfer coefficient for summer forage for radium	Bq.g^{-1}(wet)/Bq.g^{-1}(dry)
SPTCB	Soil-to-plant transfer coefficient for browse vegetation for uranium	Bq.g^{-1}(wet)/Bq.g^{-1})
SPTCB	Soil-to-plant transfer coefficient for browse vegetation for thorium	Bq.g^{-1}(wet)/Bq.g^{-1}(dry)
SPTCB	Soil-to-plant transfer coefficient for browse vegetation for lead	Bq.g^{-1}(wet)/Bq.g^{-1}(dry)
SPTCB	Soil-to-plant transfer coefficient for browse vegetation for radium	Bq.g^{-1}(wet)/Bq.g^{-1}(dry)
SPTCL	Soil-to-plant transfer coefficient for lichen for uranium	Bq.g^{-1}(wet)/Bq.g^{-1}(dry)
SPTCL	Soil-to-plant transfer coefficient for lichen for thorium	Bq.g^{-1}(wet)/Bq.g^{-1}(dry)
SPTCL	Soil-to-plant transfer coefficient for lichen for lead	Bq.g^{-1}(wet)/Bq.g^{-1}(dry)
SPTCL	Soil-to-plant transfer coefficient for lichen for radium	Bq.g^{-1}(wet)/Bq.g^{-1}(dry)
FIRC	Daily feed ingestion rate for caribou	g(wet).d^{-1}
WIRC	Daily water ingestion rate for caribou	m^{3}.d^{-1}
FAISFC	Fraction of caribou annual intake that is summer forage	--
FAILC	Fraction of caribou annual intake that is lichen	--
FMTCC	Feed-to-meat transfer coefficient for caribou for uranium	Bq.g^{-1}(wet)/Bq.d^{-1}

Variable	Definition	Units
FMTCC	Feed-to-meat transfer coefficient for caribou for thorium	$Bq.g^{-1}(wet)/Bq.d^{-1}$
FMTCC	Feed-to-meat transfer coefficient for caribou for lead	$Bq.g^{-1}(wet)/Bq.d^{-1}$
FMTCC	Feed-to-meat transfer coefficient for caribou for radium	$Bq.g^{-1}(wet)/Bq.d^{-1}$
FIRM	Daily feed ingestion rate for moose	$g(wet).d^{-1}$
WIRM	Daily water ingestion rate for moose	$m^3.d^{-1}$
FAIBM	Fraction of moose annual intake that is browse	--
FMTCM	Feed-to-meat transfer coefficient for moose for for uranium	$Bq.g^{-1}(wet)/Bq.d^{-1}$
FMTCM	Feed-to-meat transfer coefficient for moose for for thorium	$Bq.g^{-1}(wet)/Bq.d^{-1}$
FMTCM	Feed-to-meat transfer coefficient for moose for for lead	$Bq.g^{-1}(wet)/Bq.d^{-1}$
FMTCM	Feed-to-meat transfer coefficient for moose for for radium	$Bq.g^{-1}(wet)/Bq.d^{-1}$
FIRD	Daily feed ingestion rate for deer	$g(wet).d^{-1}$
WIRD	Daily water ingestion rate for deer	$m^3.d^{-1}$
FAISFD	Fraction of deer annual intake that is summer forage	--
FMTCD	Feed-to-meat transfer coefficient for deer for uranium	$Bq.g^{-1}(wet)/Bq.d^{-1}$
FMTCD	Feed-to-meat transfer coefficient for deer for thorium	$Bq.g^{-1}(wet)/Bq.d^{-1}$
FMTCD	Feed-to-meat transfer coefficient for deer for lead	$Bq.g^{-1}(wet)/Bq.d^{-1}$
FMTCD	Feed-to-meat transfer coefficient for deer for radium	$Bq.g^{-1}(wet)/Bq.d^{-1}$
EFR	Equilibrium fraction for radon daughter to radon	--
SHLD	Shielding factor for time spent indoors	--
OF	Fraction of year at receptor location (Average)	--
OF	Fraction of year at receptor location (Critical)	--
INOCC	Fraction of time spent indoors (Average)	--
INOCC	Fraction of time spent indoors (Critical)	--
AIRIN	Annual inhalation rate (Average)	m^3yr^{-1}
AIRIN	Annual inhalation rate (Critical)	m^3yr^{-1}
AFACT	Fraction of activity in above ground vegetation remaining after food preparation	--
AVEGIN	Annual intake of above ground vegetation (Average)	$g(wet).yr^{-1}$
AVEGIN	Annual intake of above ground vegetation (Critical)	$g(wet).yr^{-1}$
AFLOC	Fraction of above ground vegetation grown locally (Average)	--
AFLOC	Fraction of above ground vegetation grown locally (Critical)	--
BFACT	Fraction of activity in below ground vegetation remaining after food preparation	--
BVEGIN	Annual intake of below ground vegetation (Average)	$g(wet).yr^{-1}$

Variable	Definition	Units
BVEGIN	Annual intake of below ground vegetation (Critical)	g(wet).yr^{-1}
BFLOC	Fraction of below ground vegetation grown locally (Average)	
BFLOC	Fraction of below ground vegetation grown locally (Critical)	--
CARMIN	Annual intake of caribou meat (Average)	g.yr^{-1}
CARMIN	Annual intake of caribou meat (Critical)	g.yr^{-1}
CFLOC	Fraction of annual intake of caribou meat that is local (Average)	--
CFLOC	Fraction of annual intake of caribou meat that is local (Critical)	--
MOMIN	Annual intake of moose meat (Average)	g.yr^{-1}
MOMIN	Annual intake of moose meat (Critical)	g.yr^{-1}
MFLOC	Fraction of annual intake of moose meat that is local (Average)	--
MFLOC	Fraction of annual intake of moose meat that is local (Critical)	--
DERMIN	Annual intake of deer meat (Average)	g.yr^{-1}
DERMIN	Annual intake of deer meat (Critical)	g.yr^{-1}
DFLOC	Fraction of annual intake of deer meat that is local (Average)	--
DFLOC	Fraction of annual intake of deer meat that is local (Critical)	--
WATIN	Annual intake of water (Average)	m^3.yr^{-1}
WATIN	Annual intake of water (Critical)	m^3.yr^{-1}
FISHIN	Annual intake of fish (Average)	g.yr^{-1}
FISHIN	Annual intake of fish (Critical)	g.yr^{-1}
FFLOC	Fraction of annual intake of fish that is local (Average)	--
FFLOC	Fraction of annual intake of fish that is local (Critical)	--

APPENDIX E

APPLICATION TO
LACNOR SITE
SAMPLE INPUT AND OUTPUT FILES

FIRST INPUT FILE (LAC1.DAT)

```
LACNOR BASE CASE SAMPLE RUN (OPTION 1)
Y Y
LAC.RES
LAC.KEY
 278   0   0
0913566091  10
   50.0   10.0
CODION N  1 N        0.0
CODNUC N  1 N        0.0
CODPH  N  1 N        0.0
CODERO N  1 N        0.0
CODDUS N  1 N        0.0
CODRAD N  1 N        0.0
CODWIN N  1 N        0.0
CODAIR N  1 N        0.0
CODSOL N  1 N        0.0
CODGS  N  1 N        0.0
CODVEG N  1 N        0.0
CODGW  N  1 N        0.0
CODWAT N  1 N        0.0
CODFIS N  1 N        0.0
CODWVG N  1 N        0.0
CODANI N  1 N        0.0
CODDOS N  1 N        0.0
PYRITI N  6 N      600.0      700.0      800.0
RHOTAL N  6 N     1.1E+6     1.3E+6     1.5E+6
FRACGP F  2 N       0.06      0.005       0.05       0.07
KPRIME N  4 N       0.01        0.1
SULPRD N  6 N     3.0E-6     4.1E-6     5.3E-6
O2CONC N  1 N       9.04
O2DIFF N  6 N        5.0       37.0       70.0
DUNSAT N  6 N       0.25        0.5        2.0
KSUBSO N  1 N       50.0
FACTCO N  6 N        0.4        0.5        0.6
NPRCP  F  2 V       0.51        0.1       0.25       0.85
DMIX   N  4 N        8.0       14.0
AVPRCP N  1 N       0.51
ATAIL  N  1 N    2.41E+5
XLIME  N  1 N     5.0E-4
PCURAN N  1 N        0.1
FURAN  N  4 N       0.90       0.94
FT230  N  6 N       0.65       0.80       0.95
FT232  N  6 N       0.55       0.65       0.75
FRAD   N  6 N       0.25       0.60       0.95
FLEAD  N  6 N       0.25       0.60       0.95
FRACU  N  4 N       0.30       0.90
KDUO2  N  3 N     2.0E-5        3.0     5.0E-6     5.0E-4
PCTHOR N  4 N       0.02       0.04
```

```
XRADI  N  6 N    6.0E-6     1.2E-5     1.8E-5
KSBAR  N  1 N   1.07E-4
KFBAR  N  1 N    0.501
KRAD   N  4 N      0.5       0.56
KDRAD  N  3 N    4.5E-5       1.5     1.3E-6    1.52E-4
CLEADI N  6 N      1.0        2.0        3.0
KSLEAD N  1 N    0.012
KFLEAD N  1 N    0.501
KDLEAD N  3 N    6.0E-5       1.5      2.E-5      1.E-4
XRATE  N  1 N     0.10
DBOT   N  4 N      0.5        1.0
WSTAIL N  1 N    5.7E+5
XRUNOF N  6       0.55       0.60       0.65
SLOPE  N  1 N     0.92
THALF  N  4 N     15.0       25.0
RRAIN  N  4 N     65.0       97.5
RSOIL  N  4 N    1.0E-8     1.0E-7
DM     N  6 N   0.0015      0.017      0.075
STORM  N  4 N     36.0       48.0
FLENGT N  1 N    880.0
MINVEG N  1 N      0.6
BEDTRP N  1 N    100.0
SUSTRP N  6 N     85.0       98.0      100.0
WYEAR  N  4 V      1.0 20.9999999
EMANAT N  6 N     0.05       0.20       0.50
WTSFLX N  3 N     0.02        2.0      0.002        0.2
MPCH2O N  6 N      9.0       13.0       23.0
NSUBW  N  1 N      5.0
CAFR   N  1 N      0.0
SILT   N  6 N     30.0       45.0       60.0
FPREC  N  2 V    149.0       17.0      115.0      183.0
CAFD   N  1 N      0.0
HSRC   N  4 N      1.0        3.0
DEPVEL N  4 N    0.003       0.03
DSOIL  N  1 N     0.05
DSOIL  N  1 N     0.15
FWAT   N  6 N     0.02       0.16       0.48
RHOS   N  3 N    129.0        1.3       20.0      450.0
RHOS   N  3 N   1342.0        1.1     1000.0     1800.0
SOILKD N  5 N   1.3E-04     790.0
SOILKD N  5 N   0.0033      150.0
SOILKD N  5 N     0.18       63.0
SOILKD N  5 N   0.0051      950.0
SOILKD N  5 N   1.3E-04     790.0
SOILKD N  5 N   0.0033      150.0
SOILKD N  5 N     0.18       63.0
SOILKD N  5 N   0.0051      950.0
WC     N  4 N     0.75        1.4
WC     N  3 N     0.13        1.4       0.05       0.36
EMFRAC N  1 N      0.2
```

```
XRGWA1 N  6 N      0.1       2.0       4.0
XRGWA2 N  6 N      5.0       7.0       9.0
XRGWA3 N  1 N      0.0
XRGWA4 N  1 N      0.0
XRGWA5 N  1 N      0.0
AXGWA1 N  1 N   2005.0
AXGWA2 N  1 N   3590.0
AXGWA3 N  1 N      0.0
AXGWA4 N  1 N      0.0
AXGWA5 N  1 N      0.0
POGWA1 N  4 N     0.33      0.40
POGWA2 N  4 N     0.33      0.40
POGWA3 N  1 N      0.0
POGWA4 N  1 N      0.0
POGWA5 N  1 N      0.0
DCGWA1 N  3 N    0.012      1.50    0.0036      0.04
DCGWA2 N  3 N     0.05      1.50     0.015      0.17
DCGWA3 N  3 N     0.06      1.50     0.018       0.2
DCGWA4 N  3 N    0.045      1.50     0.013      0.15
SDGWA1 N  2 N   2650.0     100.0    2200.0    2980.0
SDGWA2 N  2 N   2650.0     100.0    2200.0    2980.0
SDGWA3 N  1 N      0.0
SDGWA4 N  1 N      0.0
SDGWA5 N  1 N      0.0
HCGWA1 N  3 N     69.4      2.40      12.0     400.0
HCGWA2 N  3 N     69.4      2.40      12.0     400.0
HCGWA3 N  1 N      0.0
HCGWA4 N  1 N      0.0
HCGWA5 N  1 N      0.0
HGGWA1 N  2 N    0.051      0.01     0.041     0.061
HGGWA2 N  2 N    0.176      0.03     0.146     0.206
HGGWA3 N  1 N      0.0
HGGWA4 N  1 N      0.0
HGGWA5 N  1 N      0.0
ACTCO  N  6 N      0.6       0.8       0.9
WATCAB N  1 N     0.19
WTSO4B N  1 N     0.14
WATNAB N  1 N     0.34
WATKB  N  1 N     0.02
WATMGB N  1 N     0.06
WATCLB N  1 N     0.38
WSIGS1 N  6 N     30.0      70.0     170.0
WSIGS2 N  6 N    125.0     255.0     635.0
WSIGS3 N  6 N    500.0    1000.0    2035.0
WSIGS4 N  6 N    140.0     300.0     740.0
WSIGS5 N  6 N     40.0      95.0     225.0
WTRHOS N  1 N 1.955E+6
WATEPS N  6 N     0.83      0.90      0.97
WTMIXD N  1 N     0.05
WKDU   N  3 N   0.0045       2.2    4.0E-4     0.048
```

```
WKDPB  N 3 N    0.015       2.5     0.001      0.23
WKDRA  N 3 N   0.0065       2.5    4.0E-4       0.1
KDPRIM N 3 N     0.02       2.5     0.002       0.3
BURYF  N 4 N     0.76      0.86
CURRNT N 4 N  3.15E+4   3.15E+5
DIFFC  N 1 N     0.02
FCONC  N 6 N      0.0      0.02       0.1
FCONC  N 6 N      0.0     0.005      0.02
FCONC  N 6 N      0.0      0.02       0.1
FCONC  N 6 N      0.0      0.02       0.1
BIOACF N 3 N  1.55E-6       6.1    1.0E-8    5.8E-5
BIOACF N 3 N  1.18E-5       2.6    1.1E-6    1.1E-4
BIOACF N 3 N  1.74E-5      3.25    1.7E-6    5.7E-4
BIOACF N 3 N  1.31E-5       3.3    1.2E-6    6.0E-4
WATVTC N 3 N   1.5E-5       5.5    1.0E-6    7.0E-4
WATVTC N 3 N   1.1E-5       6.8    1.0E-6    1.6E-4
WATVTC N 3 N   1.3E-4       2.0    4.0E-5    4.3E-4
WATVTC N 3 N   4.5E-5       2.9    1.0E-5    3.3E-4
FDEPSF N 4 N      0.1       0.3
FDEPSF N 4 N      0.1       0.3
FDEPSF N 2 N     0.47       0.3      0.01       1.0
FDEPSF N 2 N     0.47       0.3      0.01       1.0
FDEPSF N 4 N      0.8       1.0
FDEPED N 4 N      0.8       1.0
FDEPED N 4 N     0.05      0.15
FDEPED N 4 N      0.8       1.0
FDEPED N 4 N      0.8       1.0
FDEPED N 4 N      0.8       1.0
VEGLAM N 4 N   2.9E-7    1.2E-6
VEGLAM N 4 N   2.9E-7    1.2E-6
VEGLAM N 4 N   2.9E-7    1.2E-6
VEGLAM N 4 N   2.9E-7    1.2E-6
VEGLAM N 4 N   1.5E-9    4.4E-9
DUREXP N 6 N   2.6E+6    5.2E+6    7.8E+6
DUREXP N 6 N   2.6E+6    5.2E+6    7.8E+6
DUREXP N 4 N   1.3E+6    3.9E+6
DUREXP N 4 N   1.3E+6    3.9E+6
DUREXP N 1 N  1.0E+10
YDEN   N 4 N   1000.0    3000.0
YDEN   N 4 N   1000.0    3000.0
YDEN   N 4 N    500.0    1000.0
YDEN   N 4 N    500.0    1000.0
YDEN   N 4 N    400.0     600.0
SPTCAV N 3 N   6.1E-4       8.9    7.7E-6     0.007
SPTCAV N 3 N   0.0042       9.0    5.2E-5      0.34
SPTCAV N 3 N   0.0040       9.0    4.9E-5      0.32
SPTCAV N 3 N   0.0085      10.0    8.0E-5      0.89
SPTCBV N 3 N   3.2E-4       3.9    2.1E-5    0.0049
SPTCBV N 3 N   0.0042       4.0    2.6E-4     0.067
SPTCBV N 3 N   0.0040       4.0    2.5E-4     0.064
SPTCBV N  3 N   0.0027       4.5      1.3E-4      0.066
SPTCSF N  3 N   0.0066       8.9      8.3E-5      0.52
SPTCSF N  3 N    0.022       9.5      2.5E-4       2.0
SPTCSF N  3 N    0.022       3.6      0.0017      0.27
SPTCSF N  3 N     0.21       3.6      0.0019      0.24
SPTCB  N  3 N   0.0066       8.9      8.3E-5      0.52
SPTCB  N  3 N    0.022       9.5      2.5E-4       2.0
SPTCB  N  3 N    0.022       3.6      0.0017      0.27
SPTCB  N  3 N     0.21       3.6      0.0019      0.24
SPTCL  N  1 N      0.0
SPTCL  N  1 N      0.0
SPTCL  N  1 N      0.0
SPTCL  N  1 N      0.0
FIRC   N  6 N   5000.0    7000.0      9000.0
WIRC   N  6 N   0.0077    0.0115      0.0153
FAISFC N  6 N     0.05       0.2         0.5
FAILC  N  6 N     0.05       0.2         0.5
FMTCC  N  6 N   1.1E-7    3.4E-7      1.0E-6
FMTCC  N  6 N   0.7E-7    2.0E-7      0.6E-6
FMTCC  N  6 N   1.3E-7    4.0E-7      1.2E-6
FMTCC  N  6 N   1.7E-7    5.1E-7      1.5E-6
FIRM   N  1 N   2.7E+4
WIRM   N  6 N    0.024     0.036       0.048
FAIBM  N  6 N      0.8       0.9        0.95
FMTCM  N  6 N   1.1E-7    3.4E-7      1.0E-6
FMTCM  N  6 N   0.7E-7    2.0E-7      0.6E-6
FMTCM  N  6 N   1.3E-7    4.0E-7      1.2E-6
FMTCM  N  6 N   1.7E-7    5.1E-7      1.5E-6
FIRD   N  6 N   1800.0    7500.0      1.0E+4
WIRD   N  4 N   0.0007    0.0014
FAISFD N  6 N     0.25      0.33        0.40
FMTCD  N  6 N   1.1E-7    3.4E-7      1.0E-6
FMTCD  N  6 N   0.7E-7    2.0E-7      0.6E-6
FMTCD  N  6 N   1.3E-7    4.0E-7      1.2E-6
FMTCD  N  6 N   1.7E-7    5.1E-7      1.5E-6
EFR    N  6 N      0.2       0.5         0.8
SHLD   N  6 N     0.05       0.2         0.4
OF     N  6 N      0.5       0.9         1.0
OF     N  6 N      0.5       0.9         1.0
INOCC  N  6 N      0.6       0.9         1.0
INOCC  N  6 N      0.6       0.9         1.0
AIRIN  N  1 N   8400.0
AIRIN  N  1 N   8400.0
AFACT  N  4 N      0.5       1.0
AVEGIN N  1 N  4.53E+4
AVEGIN N  1 N  4.53E+4
AFLOC  N  6 N      0.0       0.1         0.2
AFLOC  N  6 N      0.1       0.3         0.6
BFACT  N  4 N      0.5       1.0
BVEGIN N  1 N   7.4E+4
BVEGIN N  1 N     7.4E+4
BFLOC  N  6 N        0.0          0.1         0.2
BFLOC  N  6 N        0.1          0.3         0.6
CARMIN N  1 N        0.0
CARMIN N  1 N        0.0
CFLOC  N  4 N        0.0          1.0
CFLOC  N  4 N        0.0          1.0
MOSMIN N  1 N     6000.0
MOSMIN N  1 N    3.95E+4
MFLOC  N  6 N        0.0         0.25         0.5
MFLOC  N  1 N        1.0
DERMIN N  1 N     6000.0
DERMIN N  1 N    3.95E+4
DFLOC  N  1 N        1.0
DFLOC  N  1 N        1.0
WATIN  N  1 N        0.6
WATIN  N  1 N        0.6
FISHIN N  1 N     8000.0
FISHIN N  1 N     8000.0
FFLOC  N  6 N        0.0         0.25         0.5
FFLOC  N  1 N        1.0
```

SECOND INPUT FILE (LAC2.DAT)

```
  N
 AVERAGE.DAT
  5
  4
    1    3    5    7   10
   1  8  1  0  6 C    0
   2 11  2  0  6 A    0
   3 12  3  0  0 A    0
   4  9  3  6  6 C    0
   5  8  3  6  6 A    0
   7  2
   1  1  0  0  0
   3  3  0  0  0
   1 R  7  1             4.2E5    200.0
   2 R 10  1           15.24E6   4300.0
   3 L 10  2       6.6  20.94E6  1.149E6
   4 L 10  3       7.5  22.22E6  1.396E5
   5 L  9  3       4.5  24.33E6   2.69E5
   6 L  8  4       7.8 235.77E6   2.06E6
   7 L  7  4       3.3 246.09E6   3.12E5
   2
   10.0  50.0
  35
 WCONC   0
 CONC    0
 PH      0
 WATC    2
   2  7
   7  1
 WATAVG  0
 WATPH   0
 GWATC   0
 EMRATE  0
 EROTOT  0
 AIRC    0
 SOILC   0
 AVEGC   0
 BVEGC   0
 SUFOC   0
 BRWSC   0
 LICHC   0
 AQVEGC  0
 FISHC   0
 ADERC   0
 WDERC   0
 AMOSC   0
 WMOSC   0
 ACARC   0
```

```
WCARC   0
WATD    0
SHINED  0
INHD    0
RADD    0
VEGD    0
FISHD   0
MEATD   0
DOSE    1
 11  1
POPDT   0
BLANK1  0
BLANK2  0
```

KEY FILE (LAC.KEY)

```
FILE CREATED 04/29/87 AT 09:44:21
 LACNOR BASE CASE SAMPLE RUN (OPTION 1)
 NUMBER OF TRIALS:    10
    PARAMETER  SUBSTANCE  LOC       TIME      MEAN       STD DEV    GEOM MEAN   GEOM SD    MINIMUM    MAXIMUM    SKEWNESS   KURTOSIS
  1   FRACGP                                0.569E-01  0.509E-02  0.567E-01  0.109E+01  0.501E-01  0.654E-01  0.143E+00  0.189E+01
  2   NPRCP                        .100E+02  0.517E+00  0.834E-01  0.511E+00  0.117E+01  0.410E+00  0.648E+00  0.230E+00  0.180E+01
  3   NPRCP                        .500E+02  0.503E+00  0.119E+00  0.492E+00  0.124E+01  0.364E+00  0.796E+00  0.150E+01  0.488E+01
  4   WATC          2        7     .100E+02  0.111E+00  0.748E-01  0.803E-01  0.276E+01  0.782E-02  0.217E+00  0.272E+00  0.173E+01
  5   WATC          2        7     .500E+02  0.649E+00  0.269E+00  0.601E+00  0.152E+01  0.330E+00  0.116E+01  0.582E+00  0.229E+01
  6   WATC          7        1     .100E+02  0.432E+01  0.449E+00  0.430E+01  0.111E+01  0.353E+01  0.501E+01  -.285E+00  0.227E+01
  7   WATC          7        1     .500E+02  0.845E+01  0.203E+01  0.825E+01  0.125E+01  0.618E+01  0.130E+02  0.105E+01  0.368E+01
  8   DOSE         11        1     .100E+02  0.884E+01  0.125E+02  0.483E+01  0.314E+01  0.777E+00  0.432E+02  0.237E+01  0.721E+01
  9   DOSE         11        1     .500E+02  0.447E+01  0.478E+01  0.328E+01  0.215E+01  0.896E+00  0.177E+02  0.239E+01  0.728E+01
```

DETAILED RESULTS FILE (LAC.RES)

```
FILE CREATED 04/29/87 AT 09:42:23
 0.596E-01 0.410E+00 0.481E+00 0.839E-01 0.552E+00 0.423E+01 0.618E+01 0.777E+00 0.896E+0p0
 0.535E-01 0.452E+00 0.508E+00 0.970E-01 0.927E+00 0.475E+01 0.886E+01 0.932E+01 0.333E+01
 0.506E-01 0.520E+00 0.426E+00 0.815E-01 0.353E+00 0.435E+01 0.667E+01 0.432E+02 0.177E+02
 0.531E-01 0.541E+00 0.364E+00 0.215E+00 0.682E+00 0.449E+01 0.647E+01 0.848E+01 0.441E+01
 0.624E-01 0.439E+00 0.555E+00 0.782E-02 0.330E+00 0.440E+01 0.130E+02 0.644E+01 0.289E+01
 0.654E-01 0.567E+00 0.480E+00 0.353E-01 0.430E+00 0.383E+01 0.765E+01 0.321E+01 0.311E+01
 0.603E-01 0.536E+00 0.796E+00 0.188E+00 0.116E+01 0.465E+01 0.918E+01 0.460E+01 0.457E+01
 0.576E-01 0.430E+00 0.547E+00 0.513E-01 0.605E+00 0.501E+01 0.981E+01 0.830E+01 0.366E+01
 0.501E-01 0.630E+00 0.459E+00 0.135E+00 0.568E+00 0.353E+01 0.785E+01 0.285E+01 0.247E+01
 0.567E-01 0.648E+00 0.411E+00 0.217E+00 0.889E+00 0.396E+01 0.875E+01 0.116E+01 0.165E+01
```

Volume

2

NATIONAL
URANIUM
TAILINGS
PROGRAM

Energy, Mines and Resources Canada
Energie, Mines et Ressources Canada

Canada

URANIUM TAILINGS ASSESSMENT PROGRAM (UTAP.3) APPLICATION TO THE LACNOR TAILINGS SITE

A Research Report Prepared Under
Contract No.23317-6-1728/01-SQ

for

The National Uranium Tailings Program
Canada Centre for Mineral and Energy Technology
Energy, Mines and Resources Canada
555 Booth Street
Ottawa, Ontario K1A 0G1

by

SENES Consultants Limited
499 McNicoll Avenue
Willowdale, Ontario
M2H 2C9

March 1987

MICROMEDIA

294 pp

ABSTRACT

This report represents part of the ongoing efforts of the National Uranium Tailings Program (NUTP) to develop the capability to predict the long-term effects of Canadian uranium mill tailings and to assess the long-term effects of alternative closeout technologies. In three previous studies a comprehensive Uranium Tailings Assessment Program (UTAP) was developed. The UTAP program incorporates a Monte Carlo procedure which permits the user to enter input parameters as probability density functions rather than as single numbers and to calculate frequency distributions for output variables. The output distributions can be interpreted as a subjective probability telling us quantitatively what we are entitled to believe about the output variables.

To date the approach has been to apply UTAP, in a generic fashion, to a hypothetical reference site. The focus of the present study has been to modify UTAP, where appropriate, for application to a real site (Lacnor) and, to the extent practicable, to calibrate the system model using site-specific measurements. Since the primary product of the NUTP modelling studies is the generic UTAP program, it has been thoroughly reviewed and modified along with the supporting documentation where appropriate.

This project report describes the application of the most current version of the code, UTAP.3, to the Lacnor uranium tailings site.

NOTICE

This report was prepared by SENES Consultants Limited (SENES) under contract to the National Uranium Tailings Program (NUTP). Neither the NUTP nor SENES makes any warranty, expressed or implied, or assumes any liability with respect to any damage or loss incurred as a result of the use made of the information contained in this publication.

TABLE OF CONTENTS

Page

Abstract i
Notice i

1.0 INTRODUCTION 1-1
- 1.1 Background 1-1
- 1.2 Scope of Lacnor Modelling Study 1-4
- 1.3 The Lacnor Modelling Report 1-5

2.0 SITE DESCRIPTION 2-1
- 2.1 Site History 2-1
  - 2.1.1 Mining and Milling 2-1
  - 2.1.2 Tailings Deposition 2-2
  - 2.1.3 Post Deposition Modifications to the Tailings Area 2-2
  - 2.1.4 Routine Field Monitoring 2-3
  - 2.1.5 Special Field Studies 2-4
- 2.2 Tailings Description 2-4
  - 2.2.1 Topography 2-4
  - 2.2.2 Regional Geology 2-5
  - 2.2.3 Geohydrology and Geochemistry 2-6
- 2.3 Watershed 2-9
  - 2.3.1 Surface Water 2-9
  - 2.3.2 Groundwater 2-11
- 2.4 Biology 2-12
  - 2.4.1 Bacteria 2-12
  - 2.4.2 Terrestrial 2-13
  - 2.4.3 Aquatic 2-16
- 2.5 Meteorology and Air Quality 2-17
  - 2.5.1 Meteorology 2-17
  - 2.5.2 Air Quality and Radioactivity 2-18

Table of Contents (continued)

Page

2.6 Adjacent Tailings 2-20
2.6.1 Description 2-20
2.6.2 Influence on Lacnor Tailings Monitoring/Modelling 2-21
2.7 Demographic Considerations 2-22

3.0 SITE-SPECIFIC UTAP MODEL 3-1
3.1 Conceptual Approach to Site-Specific Model Development 3-1
3.1.1 Lacnor Tailings Scenario 3-1
3.1.2 Environmental Pathways 3-2
3.1.3 Receptor Locations and Characteristics 3-3
3.1.4 Spatial Considerations 3-4
3.2 Model Calibration/Validation 3-4
3.2.1 Nature of Calibration/Validation Efforts 3-4
3.2.2 Description of Field Data 3-7
3.2.3 Comparison of UTAP Predictions With Lacnor Field Data 3-8

4.0 TAILINGS CLOSEOUT OPTIONS 4-1
4.1 Overview 4-1
4.2 Alternative Closeout Concepts 4-2
4.2.1 Base Case 4-2
4.2.2 Waste Rock Cover 4-3
4.2.3 Depyritized Tailings Cover 4-3
4.2.4 Earthen Cover 4-4
4.2.5 Water Cover 4-5
4.2.6 Limestone Incorporation 4-6
4.3 Options Selected for Modelling 4-7
4.4 Input Parameters 4-8
4.4.1 Pyrite Concentration as FeS_2 (PYRITI) 4-9
4.4.2 Initial Sulphate Production (SULPRD) 4-9
4.4.3 Percent Wet Weight Moisture Content (MPCH2O) 4-11

Table of Contents (continued)

Page

4.4.4 Effective Oxygen Diffusivity (O2DIFF) 4-11
4.4.5 Fraction of Direct Surface Runoff (XRUNOF) 4-12
4.4.6 Uranium as U_3O_8 (%) in Ore (PCURAN) 4-13
4.4.7 Fraction of U_3O_8 Dissolved (FRACU) 4-13
4.4.8 Dry Weight Fraction of Calcite as $CaCO_3$ (XLIME) 4-14
4.4.9 Hydraulic Conductivity (HCGWAT) 4-14
4.4.10 Fraction of Radon Attenuation by Cover (CAFR) 4-14
4.4.11 Fraction of Dust Attenuation by Cover (CAFD) 4-16
4.4.12 Minimum Fraction of Initial Vegetative Cover (MINVEG) 4-16
4.4.13 Depth of Layers 4-17

5.0 UTAP.3 PROBABILISTIC ASSESSMENT RESULTS FOR LACNOR 5-1
5.1 Introduction 5-1
5.2 Option 1: The Base Case 5-2
5.2.1 Total Dose by Receptor 5-2
5.2.2 Dose by Pathway 5-3
5.2.3 The Water Pathways 5-5
5.3 Option 2: Waste Rock Cover 5-8
5.3.1 Dose by Pathway 5-8
5.3.2 The Water Pathway 5-9
5.4 Option 3: Pyrite Removal 5-10
5.4.1 Dose by Pathway 5-10
5.4.2 The Water Pathways 5-11
5.5 Option 4: Glacial Till Cover 5-12
5.5.1 Dose by Pathway 5-12
5.5.2 The Water Pathways 5-12
5.6 Option 5: Water Cover 5-13
5.6.1 Dose by Pathway 5-13
5.6.2 The Water Pathways 5-14
5.7 Summary 5-15

Table of Contents (continued)

Page

6.0 SUMMARY AND RECOMMENDATIONS 6-1

REFERENCES R-1

APPENDIX A: WATER SOURCE MODEL A-1

A.1 Conceptual Approach A-1

A.2 Site-Specific Model Alterations A-2

A.3 Site-Specific Parameters A-2

A.3.2 Initial Mass Fractions A-2

A.3.3 Tailings Bulk Density A-4

A.3.4 Oxygen Diffusivity Through Tailings A-4

A.3.5 Thickness of the Unsaturated Zone A-5

A.3.6 Thickness of the Mixing Zone A-6

A.3.7 Thickness of Layer 4 A-6

A.3.8 Annual Net Precipitation A-6

A.3.9 Long-Term Mean Annual Precipitation A-7

A.3.10 Tailings Watershed Area A-7

A.3.11 Initial Sulphate Production Rate (FeS_2 Oxidation) A-7

A.3.12 Rate Fraction A-8

A.3.13 Mass Fraction of Uranium Recovered in the Mill A-9

A.3.14 Tailings Surface Area A-9

A.3.15 Fraction of Surface Runoff A-9

A.4 Model Calibration A-10

A.4.1 Introduction A-10

A.4.2 Description of Field Data A-11

A.4.3 Comparison of Field Data with Predicted Concentrations A-12

A.4.4 Comparison of Field Data with RATAP Predictions A-14

A.5 Model Validation A-15

A.5.1 Introduction A-15

A.5.2 Description of Field Data A-15

Table of Contents (continued)

Page

A.5.3 Comparison of Field Data with Predicted Concentrations A-16
A.6 Overall Summary of Validation A-18

APPENDIX B: EROSION MODEL B-1
B.1 Conceptual Approach B-1
B.2 Site-Specific Model Alterations B-1
B.3 Site-Specific Parameters B-1
B.3.1 Silt Particle Diameter B-1
B.3.2 Minimum Fraction of Tailings Covered by Vegetation B-2
B.3.3 Flow Length of Tailings Pile B-2
B.3.4 Bedload Pond Trapping Efficiency B-3
B.3.5 Suspended Sediment Pond Trapping Efficiency B-4
B.3.6 Slope of the Tailings Pile B-4
B.4 Model Validation/Calibration B-4

APPENDIX C: AIR SOURCE MODEL C-1
C.1 Conceptual Approach C-1
C.2 Site-Specific Model Alterations C-1
C.3 Site-Specific Parameters C-1
C.3.1 Silt Content C-1
C.3.2 Moisture Content C-2
C.3.3 Number of Days with Rain C-2
C.4 Model Validation C-2

APPENDIX D: AIR DISPERSION MODEL D-1
D.1 Conceptual Approach D-1
D.2 Site-Specific Model Alterations D-1
D.3 Site-Specific Parameters D-1
D.4 Model Validation/Calibration D-1

Table of Contents (continued)

Page

APPENDIX E: SOIL MODEL E-1
- E.1 Conceptual Approach E-1
- E.2 Site-Specific Model Alterations E-1
- E.3 Site-Specific Model Parameters E-1
- E.4 Model Validation/Calibration E-1

APPENDIX F: GROUNDSHINE MODEL F-1
- F.1 Conceptual Approach F-1
- F.2 Site-Specific Model Alterations F-1
- F.3 Site-Specific Model Parameters F-1
- F.4 Model Validation/Calibration F-1

APPENDIX G: TERRESTRIAL VEGETATION MODELS G-1
- G.1 Conceptual Apporach G-1
- G.2 Site-Specific Model Alterations G-1
- G.3 Site-Specific Model Parameters G-1
- G.4 Model Validation/Calibration G-2

APPENDIX H: SUBSURFACE TRANSPORT MODEL H-1
- H.1 Conceptual Approach H-1
- H.2 Site-Specific Model Alterations H-1
- H.3 Site-Specific Parameters H-2
  - H.3.1 Introduction H-2
  - H.3.2 Cross-Section Area of Flow H-2
  - H.3.3 Hydraulic Gradient H-2
  - H.3.4 Hydraulic Conductivity H-3
  - H.3.5 Distribution Co-efficients H-4
  - H.3.6 Porosity H-6
  - H.3.7 Average Net Precipitation H-6
  - H.3.8 Discharge Distance H-6
  - H.3.9 Particle Density H-7

Table of Contents (continued)

Page

H.3.10 Tailings Discharge layer H-7
H.4 Model Calibration/Validation H-8
H.4.1 Introduction H-8
H.4.2 Calculated Parameters H-8
H.4.3 Model Calibration H-10
H.5 Probabilistic Evaluation H-12

APPENDIX I: SURFACE WATER DISPERSION MODELS I-1
I.1 Conceptual Approach I-1
I.2 Site-Specific Model Alterations I-1
I.3 Site-Specific Parameters I-1
I.3.1 Watershed Characteristics I-2
I.3.2 Surface Runoff (Net Precipitation) I-4
I.3.3 Major Ions I-5
I.3.4 Lake Sediment Characteristics I-5
I.4 Model Validation/Calibration I-8

APPENDIX J: AQUATIC MODELS J-1
J.1 Conceptual Approach J-1
J.2 Site-Specific Model Alterations J-1
J.3 Site-Specific Parameters J-1
J.4 Model Validation/Calibration J-1

APPENDIX K: ANIMAL PRODUCE MODELS K-1
K.1 Conceptual Approach K-1
K.2 Site-Specific Model Alterations K-1
K.3 Site-Specific Parameters K-1
K.4 Model Validation/Calibration K-1

Table of Contents (continued)

Page

APPENDIX L: DOSE MODELS L-1
- L.1 Conceptual Approach L-1
- L.2 Site-Specific Alterations L-1
- L.3 Site-Specific Parameters L-2
  - L.3.1 Introduction L-2
  - L.3.2 Vegetation Ingestion Model L-2
  - L.3.3 Caribou Ingestion Model L-2
  - L.3.4 Moose Ingestion Model L-2
  - L.3.5 Deer Ingestion Model L-3
  - L.3.6 Drinking Water Model L-3
  - L.3.7 Fish Ingestion model L-3
- L.4 Model Validation/Calibration L-4

APPENDIX M: INPUT PARAMETERS M-1

LIST OF FIGURES

		Follows Page
2.1	Topography of Lacnor Tailings Basin	2-5
2.2	Elliot Lake Watershed: Serpent River System	2-11
3.1	Lacnor Site Drainage (Schematic)	3-1
3.2	Exposure Pathways Analysed	3-2
3.3	Spatial Considerations	3-4
3.4	Comparison of Predicted Pyrite Contents for UTAP and RATAP Models	3-9
4.1a	Base Case	4-17
4.1b	Waste Rock Cover	4-17
4.1c	Depyritized Tailings Cover	4-17
4.1d	Glacial Till Cover	4-17
4.1e	Water Cover	4-17
5.1	Total Dose vs. Time for Option 1 - All Receptors	5-2
5.2	Deterministic Simulation of Dose vs. Time by Pathway for Option 1 - Receptor 4	5-3
5.3	Dose vs. Time by Pathway for Option 1 - Receptor 4	5-4
5.4	Total Dose Histogram for Option 1 - Receptor 4	5-5
5.5	Water Concentration vs Time for Option 1 - Depot Lake	5-5
5.6	pH vs. Time for Option 1 - 3 Watershed Nodes	5-7
5.7	Dose vs. Time by Pathway for Option 2 - Receptor 4	5-8
5.8	Total Dose Histogram for Option 2 - Receptor 4	5-9
5.9	Water Concentration vs. Time for Option 2 - Depot Lake	5-9
5.10	pH vs. Time for Option 2 - 3 Watershed Nodes	5-10
5.11	Dose vs. Time by Pathway for Option 3 - Receptor 4	5-10
5.12	Total Dose Histogram for Option 3 - Receptor 4	5-11
5.13	Water Concentration vs. Time for Option 3 - Depot Lake	5-11
5.14	pH vs. Time for Option 3 - 3 Watershed Nodes	5-11
5.15	Dose vs. Time by Pathway for Option 4 - Receptor 4	5-12
5.16	Total Dose Histogram for Option 4 - Receptor 4	5-12

List of Figures (continued)

Follows Page

5.17 Water Concentration vs. Time for Option 4 - Depot lake 5-12
5.18 pH vs. Time for Option 4 - 3 Watershed Nodes 5-13
5.19 Dose vs. Time by Pathway for Option 5 - Receptor 4 5-13
5.20 Total Dose Histogram for Option 5 - Receptor 4 5-14
5.21 Water Concentration vs. Time for Option 5 - Depot Lake 5-14
5.22 pH vs. Time for Option 5 - 3 Watershed Nodes 5-15
5.23 Total Dose vs. Time by All Options 5-15
5.24 pH vs. Time at Nordic Lake Outlet for All Options 5-16
A.1 Plot of Log Uranium vs. Depth A-6
A.2 Plot of Log Ra-226 vs. Depth A-6
A.3 Plot of Log Th-228 vs. Depth A-6
A.4 Plot of Log Pb-210 vs. Depth A-6
C.1 Comparison of Predicted and Measured Radon Flux for Summertime Conditions C-3
H.1 Probabilistic Analysis of Uranium Concentration H-13
H.2 Probabilistic Analysis of Thorium Concentration H-13
H.3 Probabilistic Analysis of Lead Concentration H-13
H.4 Probabilistic Analysis of Radium Concentration H-13

LIST OF TABLES

		Follows Page
3.1	Lifestyle Assumptions Used in the Dose Calculations for the Elliot Lake (east and west) and Depot Lake (east) Receptors (receptor type 1)	3-4
3.2	Lifestyle Assumptions Used in the Dose Calculations for the Nordic Townsite and Depot Lake West Receptor (receptor type 2)	3-4
3.3	Water Source Model Calibration using Nordic Field Data	3-9
3.4	Water Source Model Validation against Nordic Field Data	3-9
3.5	Radon Model Validation with Lacnor Field Data	3-10
3.6	Comparison of Predicted Constituent Concentrations with Field Data	3-11
4.1	Tailings Closeout Options - Option Assumptions	4-8
4.2	Tailings Closeout Options - Nominal UTAP Input Parameters	4-8
A.1	Water Source Model Site-Specific Parameter Values	A-2
A.2	Uranium Concentration in Tailings Solids	A-9
A.3	Key Input Parameters Used in the Calibration to Nordic Field Data	A-10
A.4	Site-Specific Parameters Used in the Calibration to Nordic Field Data	A-11
A.5	Observed and Predicted pH Values	A-12
A.6	Observed and Predicted Aqueous Sulphate Concentrations	A-12
A.7	Observed and Predicted Aqueous Calcium Concentrations	A-13
A.8	Observed and Predicted Aqueous Iron Concentrations	A-13
A.9	Observed and Predicted Calcite Depletion Fronts	A-14
A.10	Observed and Predicted Gypsum Depletion Fronts	A-14
A.11	Observed and Predicted Pyrite Depletion Fronts	A-14
A.12	UTAP and RATAP Predicted Pyrite Contents	A-15
A.13	Predicted and Observed pH Values	A-16
A.14	Predicted and Observed Suphate Concentrations	A-16
A.15	Predicted and Observed Calcium Concentrations	A-17
A.16	Predicted and Observed Aqueous Iron Concentrations	A-17

List of Tables (continued)

Follows Page

A.17 Predicted and Observed Aqueous Uranium Concentrations A-17
A.18 Predicted and Observed Aqueous Thorium Concentrations A-17
A.19 Predicted and Observed Aqueous Lead Concentrations A-18
A.20 PRedicted and Observed Aqueous Radium-226 Concentrations A-18
B.1 Erosion Model Site-Specific Parameter Values B-1
C.1 Site-Specific Air Source Model Inputs C-1
H.1 Subsurface Transport Model Site-Specific Parameter Values H-2
H.2 Surface Water Flow at the Lacnor Tailings Site H-9
H.3 Hydraulic Gradient Calcualted for the Lacnor Tailings Site H-9
H.4 Comparison of Predicted Concentrations with Field Data H-10
I.1 Characteristics of Lacnor Study Area Watershed I-3
I.2 Lake Sedimentation Flux Values I-7
L.1 Lifestyle Assumptions Used in the Dose Calculations for the Elliot Lake (east and west) and Depot Lake (east) Receptors (receptor type 1) L-1
L.2 Lifestyle Assumptions Used in the Dose Calculations for the Nordic Townsite and Depot Lake West Receptor (receptor type 2) L-1
L.3 Dose Model - Site-Specific Parameter Values L-2
M.1 Lacnor Base Case (Option 1) M-1
M.2 Lacnor Waste Rock Tailings Cover (Option 2) M-1
M.3 Lacnor Depyritized Tailings Cover (Option 3) M-1
M.4 Lacnor Glacial Till Tailings Cover (Option 4) M-1
M.5 Lacnor Water Table Elevation (Option 5) M-1

1.0 INTRODUCTION

1.1 Background

Uranium mining and milling operations began in the Northwest Territories in 1943 and have been conducted in Ontario and northern Saskatchewan since the mid-1950's. Since that time, 19 uranium mining operations have produced more than 160 million tonnes of uranium tailings. Of this total, approximately 150 million tonnes have been deposited in a variety of surface impoundments covering a total of about 635 ha, with the remainder deposited underwater in lakes or used as mine backfill. The bulk of the uranium mine tailings, (about 135 million tonnes), are located in the Elliot Lake area of Ontario.

In 1982, Energy, Mines and Resources Canada established the National Uranium Tailings Program (NUTP) to pull together previous work on Canadian uranium mill tailings, to fund additional work where significant information gaps were found and to develop the capability to predict the long-term effects of tailings with a known degree of confidence while incorporating uncertainty and variability in the input data. The NUTP comprises three components: modelling, measurement and disposal technology.

An earlier study in the modelling component (Phase I) funded by the NUTP demonstrated how probabilistic techniques could be used to take account of the uncertainty and variability in model input parameters in such a simulation analysis (SENES, 1984). In Phase I quasi-steady-state models of a simplified, hypothetical, reference tailings site were used to demonstrate the feasibility and appropriateness of probabilistic analysis. Environmental pathways models were used to estimate human exposure from the release of radium-226 to the air and water and of radon-222 to the air. A number of related technical and philosophical matters were addressed in a series of review papers.

Subsequently, the NUTP sponsored a followup study (Phase II) to extend and to refine the probabilistic tools developed in the Phase I study and to investigate various issues of technical interest involved in carrying out and interpreting a probabilistic analysis (SENES, 1985). The Phase II work built upon Phase I results in order to demonstrate broader application of the probabilistic technique. In particular, the environmental component models and overall systems framework were modified and expanded to explicitly incorporate the time-varying behaviour of the natural system. As well, an additional radionuclide (thorium), several inorganic chemical species (calcium, sulphate and iron) and pH were modelled.

Sensitivity/uncertainty analysis techniques were investigated in detail in Phase II and were applied to probabilistic results, indicating pathways and parameters of importance to the hypothetical reference site. Order of magnitude estimates of the long-term effects (and associated uncertainties) of a number of different tailings management "scenarios" were also obtained.

As well, a number of special topics were investigated in Phase II including:

- interpretation of probabilistic results
- methods for estimating confidence regions on output distributions
- techniques for handling correlated parameters
- model response to time-variant input parameters
- implications of model aggregation for use in assessment models.

The underlying objective of the Phase III studies (SENES, 1986a) was to extend the capabilities of the Phase II system model and then to apply the Phase III system model to an expanded hypothetical reference site. Among the tasks addressed in Phase III were:

- expand the simulation models to include additional major radionuclides and water erosion of tailings cover materials
- expand the simulation models to include additional selected pathways of exposure
- modify the system model to permit air dispersion calculations to be carried out to greater distances in all directions
- modify the system model to permit water dispersion calculations to be performed on an entire watershed

- streamline the system code, update the documentation and prepare a users' manual.

As well, a number of special activities related to the development, use, or interpretation of probabilistic assessment codes were carried out, namely:

- an extensive program of software quality assurance including: testing of the random number generator; an intercomparison study with two other probabilistic assessment codes; testing of the system's control modules; and testing of the Phase III component modules, both on a stand-alone basis and integrated within the system model
- further investigation of the use of aggregate models in environmental assessment
- implementation of a technique for placing confidence bands on the output of probabilistic (i.e. Monte Carlo) calculations.

The present study, Phase IV of the Probabilistic Assessment of the Long-term Effects of Uranium Tailings in Canada, demonstrates the application of UTAP to the Lacnor tailings site. For sake of brevity, it is referred to herein as the Lacnor Modelling Study but should not be confused with the field studies carried out at Lacnor as part of a previous investigation as discussed below.

In December 1984, the NUTP, as part of its measurement program, awarded a contract to carry out a field study at the Lacnor uranium tailings area. The objective of the field program was to design and operate a sampling program to collect chemical, physical and biological data to characterize the Lacnor tailings area and its environs. The field study required the sampling of tailings solids, sub-tailings soil and rock, the surrounding soil and rock, tailings porewater and surface water, the measurement of surface water runoff, the gathering of meteorological and atmospheric data, and a biological assessment of the site.

The field program was intended to be a data gathering exercise and interpretation of the results was specifically excluded from the terms of reference for the study. Field investigations were carried out from December

1984 up to the end of October 1985 when monitoring was discontinued. An overview of the program and the data collected are provided in the summary report (Golder et al., 1986).

1.2 Scope of the Lacnor Modelling Study

One of the principal objectives of the National Uranium Tailings Program (NUTP) is the development of the capability to predict the long-term effects of uranium mill tailings for alternate closeout technologies with a known degree of confidence, while incorporating variability and uncertainty in the input data. Results of the previous phases of work have demonstrated that a probabilistic approach provides the framework necessary for incorporating uncertainty into a simulation (SENES, 1984; 1985; 1986a).

To date, the emphasis has been on the overall system modelling approach with application to a hypothetical reference site. The emphasis of this project is to demonstrate the use of the Uranium Tailings Assessment Program (UTAP) in assessing a real (vs hypothetical) uranium tailings site. The Lacnor tailings area in Elliot Lake, Ontario, was chosen for this purpose. The primary objective was to learn what is entailed in such an application, e.g. what are the data requirements, what level of modelling detail is appropriate, and what are the difficulties and limitations of such an application. Less emphasis was placed on the numbers being produced by the exercise, though, of course, they are as realistic as practicable. In this sense, then, this application of UTAP can be considered "preliminary", with the Lacnor tailings serving as a test site for the trial application of UTAP to a real site. Though the predictions made could be useful to an assessment of the effects of the various closeout options studied, this is not a primary objective of this project.

The goals set out for this project (as specified in the Request for a Proposal) were as follows:

Task 1: Review the system component models existing at the end of Phase III for applicability to the Lacnor site, and then modify them as necessary to describe the site characteristics. These characteristics include tailings constituents and natural processes occurring in the tailings, contaminant transfer along pathways to man, critical group receptors, and any other peculiarity of the site needed to describe its environmental impact.

Task 2: In conjunction with the Scientific Authority, determine the disposal options to be studied in order to demonstrate the system model's usefulness in distinguishing the impacts between various options. Incorporate the chosen options in the system computer code.

Task 3: Prepare the input data for the code. This will rely heavily on the data from the NUTP field program, but other sources of data may need to be sought. Many of the input parameters require the development of a probability density distribution for their input.

Task 4: Run the system model developed in Task 1 with the data from Task 3 for each disposal option selected in Task 2. Analyse the results.

Task 5: Prepare draft and final written reports describing the model and input data development and analysis. The report should describe any major difficulties encountered in application of the system model to a real site plus any recommendations as to future applications.

1.3 The Lacnor Modelling Report

The primary product of the NUTP modelling studies is the UTAP program. There are currently three versions of UTAP:

- UTAP.1 the original Phase III code (SENES, 1986a), "UTAP", now archived and inactive
- UTAP.2 the original Phase III code as revised based on a comparison of UTAP with AECL's SYVAC code (WNRE, 1987)
- UTAP.3 an updated generic code which reflects the revisions made on the basis of the UTAP/SYVAC intercomparison as well as

revisions of a generic nature identified from the Lacnor study (Phase IV).

The Phase III (SENES, 1986a) documentation was divided into the following four volumes:

Volume 1: Probabilistic Model Development for the Assessment of the Long-term Effects of Uranium Mill Tailings in Canada - Phase III, Volume 1: Summary Report.

Volume 2: Probabilistic Model Development for the Assessment of the Long-term Effects of Uranium Mill Tailings in Canada - Phase III, Volume 2: System Description and Control Module Documentation.

Volume 3: Probabilistic Model Development for the Assessment of the Long-term Effects of Uranium Mill Tailings in Canada - Phase III, Volume 3: Component Model Documentation.

Volume 4: Probabilistic Model Development for the Assessment of the Long-term Effects of Uranium Mill Tailings in Canada - Phase III, Volume 4: Uranium Tailings Assessment Program (UTAP) User's Manual.

In documenting the Phase IV study, Volumes 3 and 4 have been updated incorporating changes made in producing UTAP.3 and these volumes have been reissued in their entirety. An addendum which outlines changes to the control modules of UTAP.3 from those of UTAP.1 and UTAP.2, as described in Volume 2 of the Phase III report, has also been prepared.

This report discusses the application of UTAP.3 to the Lacnor site and includes the following sections.

2. Site Description in which the history of the Lacnor site is discussed and the data available to characterize the site and environs are stated.

3. Site-Specific UTAP Model in which the ways in which the generic UTAP model required modification for application to the Lacnor site are described. The efforts made to develop site specific parameter distributions and to calibrate component models are also described.

4. Tailings Close out Options in which the various tailings closeout options assessed using UTAP are discussed.

5. UTAP Assessment Results in which the results of the various computer simulations performed with UTAP are discussed.

6. Summary and Recommendations in which the principal findings are summarized, especially areas in which application of UTAP to Lacnor proved difficult. Recommendations as to future applications are also provided.

7. Appendices in which the input parameters required for the application of UTAP.3 to the Lacnor site are provided.

2.0 SITE DESCRIPTION

2.1 Site History

Much of the following text has been directly extracted from the Lacnor Field Study report (Golder et al., 1986) prepared by Golder Associates, SENES Consultants Limited, Beak Consultants Limited and Cumming-Cockburn and Associates Limited. During the course of the Lacnor field study, information on the mining, milling and deposition of tailings at Lacnor was provided by Rio Algom Limited. Supplementary data from other sources were limited in extent.

2.1.1 Mining and Milling

The Lacnor mine is located approximately 5 km east of Elliot Lake. Mining operations at Lacnor were carried out from January 1957 to December 1959. According to OWRC (1966), the Lacnor mine was formerly known as Lake Nordic Uranium Mines Limited. It was the first mine in Elliot Lake to close down.

Ore deposits in the Elliot lake area are large, relatively low-grade deposits with uranium and thorium occurring in brannerite, uraninite and monazite minerals. The principal accessory metallic mineral in the Elliot Lake ores is pyrite (iron sulfide). The average grade of ore at Lacnor during 1958 was 0.95 kg/tonne, but this increased to 1.0 kg/tonne during 1959.

The mill at the Lacnor complex was rated for 3,640 tonnes/day, but because the Lacnor mine only produced 3,450 tonnes/day, additional ore was received from Buckles Mine. The first drum of U_3O_8 was produced on 22 November 1957. Up to November 1959, Lacnor had shipped more than 17,000 drums of U_3O_8, each drum weighing about 125 kg. Milling operations ceased in July 1960 (OWRC, 1966).

No definitive information is available on the reagents used during processing.

2.1.2 Tailings Deposition

Very little information is available concerning the deposition of the Lacnor tailings. The basin, which is located about 600 m east of the mill, is approximately 1,200 m long along its major east-west axis and about 200 m wide in a north-south direction. The tailings area covers approximately 25 hectares.

Examination of the 1957 airphotos reveal that, prior to tailings deposition, the area of the tailings basin was a valley, which was primarily tree covered. Three small ponds connected by low or marshy areas were also located within the limits of the basin.

According to OWRC (1966), the valley was dammed at the easterly end to create the impoundment area. Information supplied by previous employees indicates that tailings were only discharged at the west end. The sole treatment during operation was pH adjustment with lime to pH 8 in the mill; there was no treatment plant of runoff water from the Lacnor tailings within the Lacnor basin. OWRC (1966) noted that the tailings overflow from Lacnor drained to the Nordic tailings area which was receiving barium chloride treatment before it entered the Serpent River watershed.

OWRC (1966) estimated that, based on production figures, the volume of tailings waste for the Lacnor mine was 1.8 million cubic metres containing 0.77 kg of radium-226. MacLaren (1977) estimated that the tailings area contained 2.7 million tonnes of waste.

2.1.3 Post Deposition Modifications to the Tailings Area

In May 1978, investigations were carried out on vegetation of approximately a 12 hectare test plot at the Lacnor tailings site. Based on these investigations and the results of the test plots at Nordic, a limestone application rate of 7 tonnes per hectare was inferred for the Lacnor tailings area.

Since 1978, remedial work has included surface stabilization and drainage modifications. Following grading and shaping, 5 to 10 tonnes per hectare of agricultural limestone was applied to the tailings surface to buffer the shallow root zone from acidity. A new spillway was constructed to improve flow control and reduce the water table in the tailings mass. From the iron staining of the bedrock surrounding the tailings pond, it may be inferred that the pond was lowered by some 1.5 to 2 m when the channel was cut through the bedrock for the pond effluent. With the exception of an area near the pond which was not trafficable by heavy equipment, efforts were made to vegetate the tailings area by hydroseeding with a blend of various grass seeds.

2.1.4 Routine Field Monitoring

No records have survived of any monitoring of the Lacnor tailings area for the period after the end of tailings deposition up to about 1977. However, in 1966 it was noted in a report by OWRC that "...at present, there is little overflow from the Lacnor tailings area except in periods of heavy and/or extended rainfall and during spring runoff."

A comprehensive data base and an analysis of chemical fluxes through the Serpent River watershed was developed by MacLaren (1978) as a part of the environmental assessment of mine expansion for Rio Algom Limited and Denison Mines Limited. A listing of data gathered in the Serpent River watershed is assembled in data publications such as Ontario Ministry of the Environment (1984). Data for the creek leaving the Lacnor tailings pond (called station L-03 by Rio Algom Limited) are not included. The closest water quality station to the Lacnor tailings management area which is monitored on a regular basis and reported in public documents is the Nordic discharge (called N-17 by Rio Algom Limited).

As a part of its monitoring program, Rio Algom has obtain samples from the outflow from the Lacnor pond on a monthly to bi-monthly basis. The data for 1979 to 1984 indicate the following ranges of values:

Parameter	Value
TDS (mg.L^{-1})	400 to 1500
Iron (mg.L^{-1})	10 to 110
Radium-226 (pCi.L^{-1})	5 to 60 (185 to 2220 mBq.L^{-1})
Acidity (mg.L^{-1}, $CaCO_3$)	100 to 1500
pH	2.5 to 3.7

A few samples have also been analyzed for trace metals. The values are of the following order: Pb (0.1 mg.L^{-1}), Zn (0.1 mg.L^{-1}), Ni (0.2 mg.L^{-1}), Co (0.2 mg.L^{-1}), Mn (2 mg.L^{-1}), Cr (0.1 mg.L^{-1}).

2.1.5 Special Field Studies

In December 1984, Golder Associates, SENES Consultants Limited, Beak Consultants Limited and Cumming-Cockburn and Associates Limited were awarded a contract by the National Uranium Tailings Program to carry out a field study at the Lacnor uranium tailings area. The objective of the field program was to design and operate a sampling program to collect chemical, physical and biological data to characterize the Lacnor tailings area and its immediate environs. The field study required the sampling of tailings solids, sub-tailings soil and rock, the surrounding soil and rock, tailings porewater, surface water, the measurement of surface water runoff, the gathering of meteorological and atmospheric data, and a biological assessment of the site.

Field investigations were carried out from December 1984 up to the end of October 1985 when monitoring was discontinued. An overview of the data collected is provided in the remainder of this chapter.

2.2 Tailings Description

2.2.1 Topography

The topography of the Lacnor basin prior to the deposition of tailings was briefly discussed in Section 2.1.2. There are no known available topographic maps prior to tailings deposition.

The topography of the Lacnor basin as it exists today is shown in Figure 2.1. It should be noted that between 24 April and 17 June, 1985, the outflow from the Lacnor pond was blocked by Rio Algom to reduce water flow to the downstream Nordic tailings area. For this reason, the Lacnor tailings pond was abnormally high when the mapping was performed.

2.2.2 Regional Geology

The ground surface within the Elliot Lake area is characteristic of Canadian Shield terrain. It is rugged but of relatively low relief with elevation differences being generally about 30 to 60 m or less. Topographic highs consist typically of rock knolls or ridges and intervening low areas generally contain swamps, lakes or streams (Davis et al., 1979). The topography is dominantly controlled by the structural orientations in the underlying bedrock.

The underlying bedrock is largely Lower Proterozoic age metasediments comprised or quartzite, arkose, conglomerate and minor argillaceous strata. These rocks have been folded into a broad, westward plunging syncline some 8 to 10 km in width known as the Quirke Syncline (Robertson, 1968). The Lacnor Mine is located on the south limb of the syncline. The folded metasedimentary strata are cross cut by intrusive diabase sills and dykes (Nipissing Diabase) and faults (Robertson, 1968).

Regional fault structures are oriented both northwest-southeast and east-west. These features tend to occur at 5 to 6 kilometre intervals. Smaller scale faulting tends to be more intense (1 to 2 features per square kilometre) and, while generally steeply dipping, exhibit variable strike and persistence. Intruded diabase dykes, specifically those oriented northwest-southeast, are commonly associated with regional faulting.

FIGURE 2.1

TOPOGRAPHY OF LACNOR TAILINGS BASIN

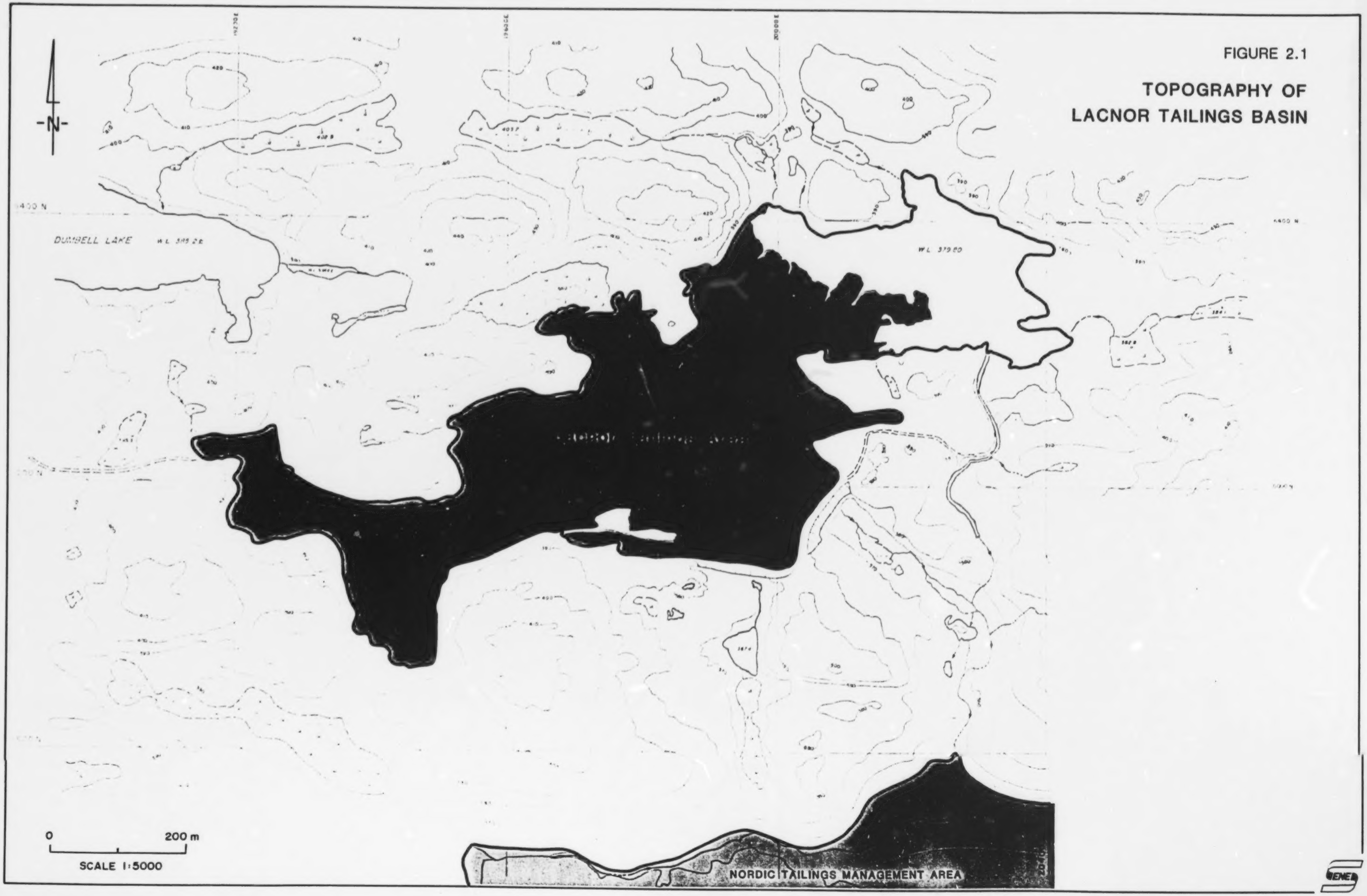

Overburden is largely restricted to topographic lows and, with the exception of recent bog or swamp deposits, consists predominantly of cohesionless silty to sandy till deposits and fluvial sands and gravels of glacial outwash origin. Till deposits also occur to a limited extent on the flanks of bedrock ridges.

2.2.3 Geohydrology and Geochemistry

The geochemical evolution of representative inactive pyrite tailings impoundments in the Elliot Lake uranium district has been summarized by Dubrovsky et al., (1985) and Feenstra et al., (1981) and others. Geochemical data obtained between 1979 and 1983 from networks of piezometer nests and cores from several inactive uranium tailings impoundments in the Elliot Lake district indicated that precipitation recharging the groundwater zone had been acidified at shallow depths in the tailings as a result of the oxidation of pyrite. This upper zone of low pH water, with high concentrations of sulphate, iron and heavy metals and higher concentrations of radionuclides, appeared to be expanding downwards. Mill process water with neutral pH and low concentrations of heavy metals that was initially present in the tailings was gradually displaced by the downward migration of the low pH water from the active zone of pyrite oxidation.

Further discussion of the details of the geochemistry of pyrite tailings is found in Dubrovsky et al., (1985) and Feenstra et al., (1981). In comparison with the detailed work at some other inactive uranium tailings sites in the Elliot Lake area, relatively little work had.been carried out at the Lacnor tailings site prior to the field study. The available information comprised the results of limited sampling programs of surficial tailings solids and of the tailings porewater.

A total of 12 surficial samples were collected in 1978 from the western end of the Lacnor tailings area. These samples showed pH values between 2.4 and 3.1. Three samples were also analysed to determine the grain size distribution of the tailings taken from the west end. These samples showed a variation of from 4.7 per cent to 27.3 per cent passing the 325 mesh for coarse tailings in the area of the existing stream bed. It was inferred that these values showed that the Lacnor tailings were slightly coarser than the Nordic tailings.

Dubrovsky et al., (1985) reported the results of analyses from a nest of piezometers in the Lacnor tailings area together with their more extensive work on the Nordic tailings area. Low pH waters were found to extend to a depth of approximately 6 m (with groundwater sampled from depths less than 4.6 m having pH values between 2 and 3.7) and high iron waters were found to occur through the entire thickness of tailings (approximately 8 m deep at the piezometer nest).

As part of the 1985 field program, gradation analyses of surficial tailings samples obtained during an initial site reconnaissance confirmed that the tailings varied from coarse sand tailings at the western end and northern half of the basin to finer predominantly silt sized tailings in the eastern and southeastern parts of the basin.

Boreholes were put down at five locations across the tailings area. Between 8 m and 15 m of tailings were encountered at the five borehole locations across the tailings, overlying variable deposits of till, peat and sands, silts and gravels. The results of in-situ hydraulic conductivity tests in the tailings varied between 2×10^{-6} $cm.s^{-1}$ and 5×10^{-4} $cm.s^{-1}$, but these were lower than those determined from constant head laboratory permeameter tests. The sand and gravel below the tailings was more pervious. The permeability of the bedrock ranged from low (3×10^{-7} $cm.s^{-1}$) to relatively high (3×10^{-3} $cm.s^{-1}$).

Soluble sulfur, which likely was present in the tailings as calcium sulphate, occurred at concentrations as high as 5 per cent. Measured concentrations of reduced sulfur, which was assumed to exist as pyrite, were less than 3 per cent. Uranium concentrations in the tailings solids ranged from 10 to 80 ppm. Radium-226 and thorium-230 concentrations ranged from 0.6 to approximately 12.5 $Bq.g^{-1}$.

Sampling of selected monitoring wells indicated that the chemical characteristics of the porewater existing in the Lacnor tailings basin in 1985 had been influenced by the initial composition of the process water and solids originally discharged to the basin and the low pH recharge water that had developed as a consequence of pyrite oxidation at shallow depths within the tailings since their deposition. The porewater was generally acidic at shallow depths and moderately acidic to neutral at depths of more than several metres within the tailings.

The pH increased and electrical conductance in the porewater decreased with depth in the coarse tailings in the western section of the basin. In the interlayered fine and coarse tailings in the east and southeastern portions of the tailings area, the profiles of pH and electrical conductance in the porewater were not depth dependent. However, these trends may have been influenced by the unusual occurrence of ponded surface water during the spring and early summer of 1985 when the discharge spillway for runoff from the Lacnor pond was temporarily dammed.

The concentrations of the primary dissolved constituents in the porewater such as sulfate, iron, major ions and the concentrations of metals were variable across the tailings. In many cases, peak concentrations were associated with low pH. With the exception of uranium, which exhibited a trend of increased concentrations with depth, the concentrations of radiological parameters in the porewater typically did not vary with depth in the tailings.

The monitoring program indicated that the chemistry of the groundwater in the sub-tailings overburden and, to a lesser extent, the sub-tailings bedrock, had been influenced by the tailings porewater.

Off-tailings boreholes were drilled in two valleys south of the tailings area. These valleys were considered to contain the major potential groundwater seepage pathways exiting from the tailings area.

Based on the geological mapping of the basin and previous experience in the Elliot Lake area, these valleys were considered to contain the major potential fault or fracture zones, and hence the major groundwater seepage pathways exiting from the tailings area.

A total of nine separate boreholes were drilled at the two off-tailings sites. The tailings porewater appeared to have had little or no impact on the groundwater chemistry at the off-tailings monitoring sites. The pH of the groundwater ranged from 5.5 to 7.5 and the electrical conductance ranged from 210 to 450 $\mu S.cm^{-1}$. The concentrations of the major ions and metals, including iron and sulphate, and the radiological parameters in the bedrock groundwater at the off-tailings monitoring stations were much lower than those encountered in the tailings porewater.

No solid samples were collected during these operations since all holes were drilled pneumatically. The cuttings were, however, examined to determine the rock types encountered.

2.3 Watershed

2.3.1 Surface Water

The Lacnor tailings area is located at the headwaters of a small valley which drains southward to the Nordic Tailings Basin. The watershed covers about 1.0 km^2 although the exposed tailings surface covers only about 0.24 km^2. Surface runoff reports to the Lacnor tailings pond before overflowing the decant structure at station SW-03 (see Golder et al.,1986 for station locations).

As part of this field study three weirs were constructed to monitor surface flow from the Lacnor tailings area. One was installed on Lacnor Creek to monitor outflow from the tailings pond (SW-03), while two were located on creeks to monitor seepage (SW-01 and SW-02). Continuous flow monitoring was carried out between 23 March and 3 November 1985. Flow from the Lacnor tailings pond was severely curtailed during the spring runoff when an earth-fill dam had to be constructed in Lacnor Creek to reduce flooding downstream on the Nordic tailings area where a decant tower had collapsed. Therefore, both monthly surface water and seepage flows were altered from those which would normally occur.

Mean monthly flows at the pond outlet varied significantly from 0.4 $L.s^{-1}$ in July to 124 $L.s^{-1}$ in April. Although mean monthly seepage rates ranged from 0.2 to 1.2 $L.s^{-1}$ and 1.2 to 12.3 $L.s^{-1}$ at the other two sites during the study period, the seepage rates were relatively constant during the period when the earth-fill dam was not in place. The total average discharge flow for the 8 month data collection program was approximately 14.7 $L.s^{-1}$ which compares well with an average expected unit runoff rate of about 16.2 $L.s^{-1}.km^{-2}$ (0.51 $m.yr^{-1}$ net precipitation) from the 1 km^2 basin.

Surface water samples were collected on a routine basis from the streams at the three weir locations during the period January through to October 1985. The surface waters were found to be acidic with iron, calcium, aluminum and manganese being the dominant cations, at concentrations of tens to hundreds of $mg.L^{-1}$. Sulphate was the most abundant anion, ranging from several hundred to several thousands of $mg.L^{-1}$. Redox reactions involving iron appear to be the dominant control on pH in the streams. The iron would appear to result from pyrite oxidation, the calcium and sulphate from gypsum dissolution, and the aluminum and manganese from acid attack of aluminosilicate minerals in the tailings. The other twenty or so anions and cations measured were present in concentrations less than 1 $mg.L^{-1}$.

The radionuclides in both the uranium and natural thorium decay series showed considerable variability in their surface water concentrations. Uranium levels varied from about 0.01 $mg.L^{-1}$ to 0.2 $mg.L^{-1}$ while thorium levels ranged from less than 0.05 $mg.L^{-1}$ to 0.29 $mg.L^{-1}$. The observed level of thorium-230 in the surface water are substantially greater than those observed for the other radioactive daughters of uranium-238. This is likely a consequence of the relatively higher sensitivity of thorium solubility to pH.

The data suggest that pH and acidity are the factors which have the most profound influence on the levels of radionuclides and trace elements in the streams draining the tailings. The pH, which was observed to range from 2.8 to 5.4, is sufficiently low to preclude the presence of any fish in the streams draining the site.

The overflow for the basin passes through the Nordic tailings area and is treated prior to release to Buckles Creek. From Buckles Creek the water flows to Nordic Lake, and then through a small, unnamed lake before entering the eastern end of Esten Lake. This section of Esten Lake was dammed in 1982 and the outlet flow was diverted to Depot Lake so that discharge from the the new Elliot Lake sewage plant would bypass several lakes in the western branch of the Serpent River Watershed (see Figure 2.2).

In Depot Lake the diverted flow from Esten Lake is reunited with the flow in the main western branch of the Serpent River and the combined flow continues eastward to the west arm of McCarthy Lake. The cumulative area of the watershed to the outlet of the west arm of McCarthy Lake is 246 km^2 as compared with the Lacnor watershed area of 1 km^2.

The biological productivity or trophic status of the lakes in the western branch of the Serpent River varies widely as determined in a 1981 study by the Ministry of Environment (Myslik, 1985). At that time, Esten Lake contained the highest total phosphorus levels and was classified as a eutrophic water body. The immediate downstream lakes, Marshland, Grandeur and Trout Lakes, were classified as eutrophic to mesotrophic while Depot Lake was classified as being mesotrophic. Nordic Lake, the unnamed lake just to the south of Nordic Lake and McCarthy Lake were found to be characteristic of oligotrophic lakes with low total phosphorus levels.

2.3.2 Groundwater

Groundwater flows in the Elliot Lake area tend to follow short pathways and be near surface. The groundwater flows concentrate in glacial deposits below the

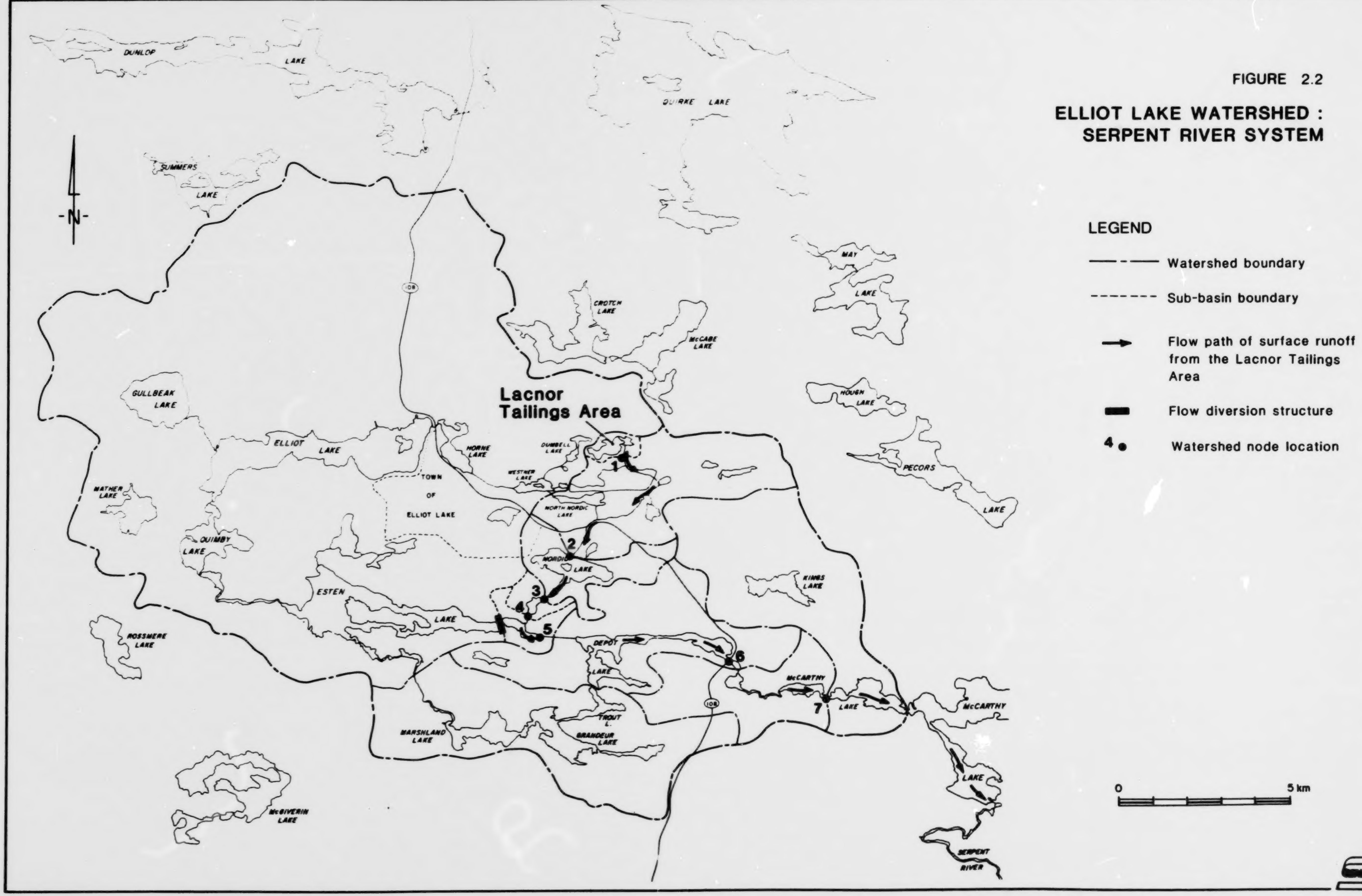
FIGURE 2.2

ELLIOT LAKE WATERSHED : SERPENT RIVER SYSTEM tailings areas or in geological features (faults) that pass through the basin. At Lacnor, the perimeter is well contained by bedrock and because there is a minimal depth of overburden, there is, in effect, no overburden groundwater aquifer below the tailings. Groundwater flow through subsurface faults and features in the rock is expected to be quite small relative to the tailings basin water balance. For example, the total, estimated groundwater discharge flows from the Stanleigh tailings basin has been estimated by Golder (1980) to be less than 2 per cent of the net precipitation into the basin.

2.4 Biology

There are very few historical data from the study region which can be directly related to the Lacnor site. The Lacnor tailings site was only operated for about three years (1957 to 1960), at a time when monitoring was less sophisticated than at present. Because drainage from the Lacnor tailings area flows directly into the much larger Nordic tailings area, the overall environmental influences from the Lacnor tailings are largely masked by the effects of this larger operation.

2.4.1 Bacteria

No historical data were found on bacteria relevant to the Lacnor tailings. The Lacnor tailings contain levels of pyritic minerals that generate acid through microbial iron oxidation. This process which generates sulfuric acid in turn results in the solubilization and mobilization of radionuclides and trace elements at low pH levels. Deeper in the tailings, in the absence of free oxygen, other bacteria may derive energy from the system through the reduction of sulfate back to sulfide. In order to quantify the level of microbial activity responsible for these processes at various depths in the tailings, a series of microbiological studies were undertaken during the 1985 field studies. These included:

- aerobic plate count
- anaerobic deep tube count
- sulfate-reducing bacteria count
- most probable number (MPN) sulfur oxidizers estimate, and
- MPN iron oxidizers estimate.

There were no apparent trends in the numbers of bacteria by either depth or type of tailings material. The variation in numbers of colonies between successive layers in the tailings was as great as 10^6 times.

2.4.2 Terrestrial

Vegetation

There are considerable data on vegetation for the Espanola District of Northern Ontario, of which the Elliot Lake region is a subset. The area is within the Great Lakes - St. Lawrence Forest Region. The Espanola District is 76 per cent productive forest (Corbett, pers. comm., 1985). MacLaren (1977) describe the forest composition in this region as mixed, consisting of hardwoods common to the Deciduous Forest Region and conifers common to the Boreal Forest Region. Characteristic species are red and white pine, eastern hemlock, and yellow birch. Sugar and red maple, white birch, trembling aspen, black and white spruce, white cedar, balsam fir and jack pine are widely distributed. Red oak, basswood, white elm, large-tooth aspen, beech, white oak, butternut, white ash, and balsam poplar are common but more restricted in their occurrence.

Corbett provided further data indicating there are 91 farms in Spanish River Township totalling 11,557 ha. With a 180-day growing season, oats, barley and beef are the main produce. The OWRC (1972) indicated there was little production or use of home produce in the area. The farms in the Spanish River district are much further away from the Lacnor tailings area than are the receptors used in the trial application of UTAP.3 to Lacnor. In view of this it was clear that the consumption of local game and home grown vegetables by the receptors used in the trial analysis would lead to higher dose than those envisaged for a Spanish River farmer, particularly since his water supply would not be affected.

Considerable vegetation and vegetation-herbivore food chain research has been in progress in the Elliot Lake area, with several studies on the Lacnor and Nordic tailings (Ontario Environmental Assessment Board, 1979; and personal communications with Ontario Ministry of Environment, Laurentian University, University of Toronto, CANMET Laboratories, 1985). Although some of the data go back as far as 1977, researchers contacted indicated most of these data were pending publication.

Specific to vegetation on and in the vicinity of uranium tailings, McIlveen (1977) reported lead-210 results for soils and vegetation in the Elliot Lake area concluding that levels were elevated in the most common tree, white birch, in tailings areas. Kalin (1983, 1984) studied several tailings areas in the Elliot Lake region, including Lacnor and Nordic. In general, the conclusions were that neither radionuclides nor heavy metals showed significant trends in bioconcentration by vegetation. Dave et al. (1984) also indicated no correlation between radionuclide concentrations in vegetation and their tailings substrate. Levels of Ra-226, Pb-210 and total Pb were detectable in vegetation sampled, while levels of Th-232, Th-230, Th-228, total Th and total U were not. In their opinion the radium and lead concentrations in vegetation were not great enough to result in significant bioaccumulation in higher trophic levels.

The following types of vegetation community types were identified on the surface of the tailings area during the 1985 Lacnor field study: birdsfoot trefoil; cattail; red fescue; reed canary grass; wild red raspberry; and bare unvegetated. No surveys away from the tailings area were reported.

Birds and Mammals

Historical data are available on the common species found in the vicinity of tailings areas in the Elliot Lake area (MacLaren, 1978), and hunting and trapping harvests of these (Ministry of Natural Resources, Blind River and Espanola Districts, pers. comm., 1985).

MacLaren (1977) provide the following descriptions of the moose, deer and game birds for the region. Moose is the prime big game species in the Elliot Lake area with a 1975 harvest of 302 animals.

White-tailed deer are at the northern extent of their range in this area and are found only in certain locations. A 9 km to 15 km strip north of the North Channel shore has the most dense deer population in the Blind River district with a major deer yard located near Iron Bridge. In the vicinity of the Elliot Lake mining area, a small deer yard is located between Slipper Lake and the northwest portion of Esten Lake with some 12 to 24 deer taken annually.

Ruffed grouse is the major game bird in the area with waterfowl being less abundant targets due to the lack of suitable wetland habitat. (This pathway was not considered in the trial applicaton of UTAP.3 to the Lacnor site. In view of the relatively high consumption of local game (deer and moose) and the relatively low importance of game pathways, this omission is not expected to be of any significance to the final dose. However, these assumptions could be reviewed and the "grouse" pathway added to UTAP in the future if considered desirable.)

Radionuclide levels in Elliot Lake area moose (Pb-210: 2.0 pCi.g^{-1} (74 mBq.g^{-1}); Ra-226: 0.09 pCi.g^{-1} (3 mBq.g^{-1})) and deer (Pb-210: 0.5 pCi.g^{-1} (20 mBq.g^{-1}); Ra-226: 0.15 pCi.g^{-1} (6 mBq.g^{-1})) are provided by MacLaren (1978). However, no paired vegetation or stomach content analyses are available.

A series of reports on small mammalian herbivores, which include studies at the Nordic and Lacnor tailings sites, have recently been published, are in press or are submitted for publication by researchers at Laurentian University and the CANMET, Elliot Lake Laboratories (Clulow, pers. comm., 1986).

2.4.3 Aquatic

Regional data are available on aquatic biota from the Elliot Lake sub-basin downstream of the Lacnor tailings area. However the presence of other larger tailings sites such as Nordic, which drain into the Serpent River proper, masks any effects of Lacnor on the aquatic biota of this basin.

Data on benthic invertebrates were assessed in the environmental assessment study reported by MacLaren (1977). The findings indicated that species diversity had been depressed in Nordic Lake which receives the main flow from the Nordic (and Lacnor) tailings. A Shannon-Weiner Index (a measure of total species diversity) of 0.6 was reported for Nordic Lake. Westner Lake which receives minor seepage flows from these tailings also had a depressed benthic diversity (Index 1.3), while Elliot Lake itself showed signs of moderately depressed benthic diversity (Index 3.2). Clams were generally absent from lakes in the area, which was attributed to their sensitivity to low pH. Zooplankton populations, benthic populations, and species diversity were noted to decrease in waterways affected by drainage from uranium properties (MacLaren, 1977). In a study in 1981 (Myslik, 1985) benthic invertebrate communities in six lakes in the western area, including Elliot, Esten, Nordic, Unnamed, Depot and McCarthy Lakes, were reported to be depauperate both in terms of species diversity and standing crop.

Most fisheries data relevant to this study were extracted from studies carried out on the Serpent River. All regional data indicate that this is a potentially important pathway leading to human exposure (Corbett, pers. comm., 1985). MacLaren (1978) reviewed available data at that time and concluded there were no correlations between radionuclide levels in fish and the waters in which they were caught. MacLaren (1978) further reported that the Elliot Lake sub-basin was generally not affected by tailings effluents, except for Nordic and Westner Lakes which were virtually fishless.

A two-phase study was carried out by SENES and SRC (1984, 1985) for the NUTP to assess the distribution of the uranium-series radionuclides in aquatic organisms in the vicinity of uranium mining properties. The study included collection of field samples in the Elliot Lake and Wollaston Lake areas of benthic organisms, sediments, water and a limited number of fish for analysis of radionuclide levels. The data were used to compute water-to-sediment transfer factors, water-to-benthos bioaccumulation factors and water-to-fish bioaccumulation factors. Values have been used previously in the Phase II and III probabilistic assessment studies (SENES, 1985; 1986a).

The 1985 Lacnor field study did not include an aquatic biota sampling program.

2.5 Meteorology and Air Quality

2.5.1 Meteorology

A limited amount of long-term meteorological data is available for the Elliot Lake area. Meteorological parameters of wind speed, wind direction, precipitation and temperature have been or continue to be measured at various locations in the Elliot Lake area; however, no data specific to the Lacnor site were found prior to the Lacnor field study.

Monthly temperature summaries (Dec. 1984 to Oct. 1985) from Lacnor indicate that the mean daily temperatures ranged from -12°C in January to 20°C in July over this time period. The daily minimum temperature ranged from -15.7°C in January to 15.6°C in July, while the daily maximum temperature ranged from -7.7°C in January to 24.6°C in July (Golder _et al_., 1986). Based on 13 years of data the extreme temperatures ranged from -42.8°C in February to 32.2°C during June and July (Golder _et al_., 1986).

Based on a 10 to 14 year period of record, the mean annual rainfall for Elliot Lake is 70.3 cm and the mean annual snowfall is 219.0 cm. The annual total precipitation is 92.6 cm with measurable precipitation occurring on 110 days (Golder _et al_., 1986).

Although wind data are available for the private aviation weather recording station at the Elliot Lake airport, the data have not been compiled to obtain any annual or seasonal trends (Golder et al., 1986).

During the Lacnor field study (Golder et al., 1986), meteorological conditions were monitored at three locations. The main meteorological station was located on the Lacnor tailings, where wind speed and direction (at a height of 10 m), temperature, solar radiation, precipitation and evaporation were monitored. Wind speed and direction were also monitored on the Nordic tailings area to the south, while temperature, relative humidity, barometric pressure and precipitation were monitored in the Town of Elliot lake. Details are provided in the Golder report.

2.5.2 Air Quality and Radioactivity

In the 10 years prior to the Lacnor field study, several measurement programs and brief surveys had been carried out in the Elliot Lake area. However, none of them gathered data specific to the Lacnor tailings area. The Nordic tailings area is the closest tailings area to Lacnor which has undergone air quality monitoring. Suspended particulate matter, dustfall and ambient radon, radon daughter and radon exhalation sampling were carried out as part of these programs. Suspended particulate matter samples were analysed for total particulate loading, total uranium and radium-226, and gross alpha and gross beta activity. The insoluble and soluble fractions of dustfall were determined along with gross alpha and gross beta levels for each fraction. The results of these measurement programs are presented in MacLaren (1978).

Prior to the 1985 field study, the only data collected which were directly relevant to Lacnor pertain to surface radiation measurements which were made during the 1977 field program for the environmental assessment of the proposed Elliot Lake uranium mines expansion. Gamma levels over the Lacnor tailings were found to be between 50 and 500 $\mu R.h^{-1}$ above background.

During the Lacnor field study, air quality was monitored at eight locations for dustfall and at two locations for suspended particulate matter (SPM).

Monthly dustfall samples were analysed to determine the organic/mineral and soluble/insoluble fractions. Three-month composites of the inorganic fractions were prepared and analysed for various radionuclides. Samples from four sites on the edge of the tailings were analysed for radium-226, thorium-228, 230, 232, lead-210 and uranium. The four off-tailings samples were analysed for only radium-226, thorium-230 and uranium.

The overall average dustfall level measured during the January to October period was 1.4 $g.m^{-2}$ per 30 days. Organic contents ranged from 39 to 95%. Lead-210 activity per gram was the highest of the five parameters for the four on-tailings sites and ranged from 0.05 to 1.10 $Bq.g^{-1}$. For the four off-tailings sites radium-226 activity per gram was equal to or higher than thorium-230, and ranged from 0.004 to 0.169 $Bq.g^{-1}$. Uranium levels at the eight sites averaged 0.32 $\mu g.g^{-1}$.

Ambient radon monitoring, radon exhalation testing and surface gamma radiation surveys were measured during the 1985 Lacnor field study. Ambient radon levels were measured at twelve locations in the vicinity of the tailings. Between the edge of the tailings and 100 m from the tailings the radon levels ranged from less than 0.002 to 0.040 $Bq.L^{-1}$. Radon exhalation rates from the surface of the tailings were determined for various tailings conditions. The exhalation rates ranged from a low of 0.0089 $Bq.m^{2}.s^{-1}$ in March on a dry, hard sandy non-vegetated tailings surface to 6.67 $Bq.m^{-2}.s^{-1}$ in June on a damp non-vegetated surface. A comprehensive surface gamma radiation survey of the tailings area was carried out on a 30 m x 30 m grid. The contact gamma levels ranged from a low of 30 $\mu R.h^{-1}$ to a high of 1100 $\mu R.h^{-1}$. The higher gamma levels (>500 $\mu R.h^{-1}$) were found on the eastern third of the site.

In addition to the Lacnor field study, the NUTP sponsored a one year program of monthly radon level measurements at locations in proximity to uranium mine tailings piles at Elliot Lake, Ontario (SENES, 1986b). An array of sixty-three specially designed electrostatically enhanced solid-state track detectors were used to make the measurements in the vicinity of five tailings areas and at several background sites. The electrostatic-enhancement system provided the capability to measure low ambient radon levels during the monthly periods. Radon levels were also measured at 4 heights (1 m, 2 m, 4 m, 8 m) above the surface of tailings at two sites.

While measurements were not taken at Lacnor for this study, these data provide an indication of the source strength of the other tailings sites. As well, some of the radon monitors that were placed far away from the tailings areas provide an indication of ambient background radon levels in the Elliot Lake region. For the three monitoring stations within the Town of Elliot Lake the mean radon concentration was 0.005 $Bq.L^{-1}$ and ranged from a minimum of 0.002 $Bq.L^{-1}$ to a maximum of 0.019 $Bq.L^{-1}$ during the one year monitoring period. For the three background monitoring stations located within a 25 to 35 km radius of Elliot Lake the mean and minimum levels were the same as the Town stations while the maximum was slightly lower at 0.018 $Bq.L^{-1}$.

2.6 Adjacent Tailings

2.6.1 Description

The Lacnor tailings area lies between two other tailings basins: the Stanleigh tailings area 3 km to the north and the Nordic tailings area 0.5 km to the south.

The Stanleigh mine was reopened in 1983 and operates at a rate of 4500 $t.d^{-1}$. The tailings basin currently contains an estimated 12 million tonnes of tailings and waste rock with an exposed surface area of approximately 50 ha. The mine has a planned production of an additional 60 million tonnes which would maintain operations well into the 21st century. At the completion of the operations, it is expected that the tailings area will contain about 72 million tonnes of tailings and waste rock and cover some 400 ha (MacLaren and Golder, 1981).

The Stanleigh mine orebody is typical of the low-grade pyritic Elliot Lake uranium ores with an average grade of approximately 0.1% U_3O_8. Runoff from the tailings area is treated with lime and barium chloride and filtered through dual media sand/anthracite filters. The discharge is released to McCabe Lake which flows into the Eastern Branch of the Serpent River.

The Nordic mine operated until 1968 producing an estimated 12 million tonnes of tailings which cover 107 ha (MacLaren, 1977). Since that time the surface has been vegetated and a treatment plant has been maintained to treat surface runoff and seepage from the Nordic and Lacnor tailings basins. In fact, both seepage and runoff from the Lacnor tailings area pass through the Nordic tailings basin before treatment and discharge to the west branch of the Serpent River system.

2.6.2 Influence on Lacnor Tailings Monitoring/Modelling

The Stanleigh tailings area has no impact on the water quality monitoring and modelling predictions for Lacnor as the basin drainage reports to a section of the Serpent River downstream of the modelling nodes (see Chapter 3). Because the basin is operating and the tailings are discharged over a long beach, the tailings surface will be very wet. This will reduce both dust and radon emissions from the Stanleigh tailings basin thus minimizing any potential influence on the Lacnor site. Nonetheless some dust and radon will be released from the Stanleigh tailings area and will contribute to the ambient measurements of these parameters made in proximity to the Lacnor site.

Nordic on the other hand is much closer and is in the same subwatershed as Lacnor. Water quality monitoring and modelling predictions upstream of Nordic are unaffected by its presence. However, because the Nordic tailings area is much larger than the Lacnor tailings area, downstream water quality will be dominated by the Nordic discharge.

The Nordic basin is vegetated and should not be a major source of suspended dust; however, the tailings area does have a low water table and could have correspondingly high radon emission rates. Therefore, as a consequence of its proximity and potentially relatively high radon release rates, there is a potential for radon emissions from Nordic to influence the ambient radon level measured in the area of the Lacnor tailings sites especially those located between the Nordic and Lacnor sites.

2.7 Demographic Considerations

The Lacnor tailings area is approximately 5 km east of the Town of Elliot Lake and 2 km north of the Nordic townsite. Highway 108, which is the main access road in the area, runs northwest from the east end of Depot Lake, passing north of Nordic Lake and into the Town of Elliot Lake. Most of the people are concentrated in the Town of Elliot Lake with a 1985 population of 18,332 (Powell, 1987), and the Nordic Townsite, approximately 64 persons (Diotte, 1987), with some people scattered in cottages on local lakes as access permits.

The area is characterized by abundant lakes and streams, with about 20 to 25% of the total area being covered by water. The region is sufficiently forested with mixed coniferous and deciduous species to support lumbering. The bulk of the population rely upon the two existing mining companies for employment. There is some tourism involving camping, fishing and hunting. There is little farming or farming potential in the area.

3.0 SITE-SPECIFIC UTAP MODEL

In previous studies the Uranium Tailings Assessment Program (UTAP) has been developed and applied to a hypothetical reference site (SENES, 1984; 1985; 1986a). The focus of the present study has been to apply UTAP (actually UTAP.3) to the Lacnor tailings site in Elliot Lake, Ontario. The primary objective was to learn what is involved in applying UTAP to a real site. Taking the Lacnor site as "more or less representative" of relatively low-grade acid-generating uranium tailings, application of the UTAP program was demonstrated for several closeout options, i.e. the purpose of the project was not to evaluate closeout options, but to demonstrate the use of UTAP.3 to a real site. This chapter discusses the basic features of the Lacnor site which are of interest to a radiological assessment study; eg. a short discussion of the Lacnor site itself, possible pathways of exposure, and the characteristics of the various receptors are discussed. This chapter also describes the efforts made to calibrate or validate the various component models with data specific to the Lacnor setting.

3.1 Conceptual Approach to Site-Specific Model Development

3.1.1 Lacnor Tailings Scenario

The Lacnor tailings basin is typical of valley impoundments encircled by a bedrock rim with small dams located at low points along the rim as described in more detail in Chapter 2. In the case of the Lacnor site there are two such dams, as shown on Figure 3.1. In general terms, precipitation falling within the Lacnor tailings watershed reports to a pond located at the eastern end of the tailings basin. Overflow from the pond flows south across the Nordic tailings area and eventually enters Depot Lake and the main flow of the Serpent River as illustrated on Figure 2.2. As discussed in Section 2.1.2 groundwater flow paths in the Elliot Lake area tend to follow short pathways near the surface. At Lacnor groundwater flow is assumed to occur in the proximity of the two small dams shown on Figure 3.1 emerging into small streams which flow to the Nordic tailings site.

FIGURE 3.1

LACNOR SITE DRAINAGE SCHEMATIC

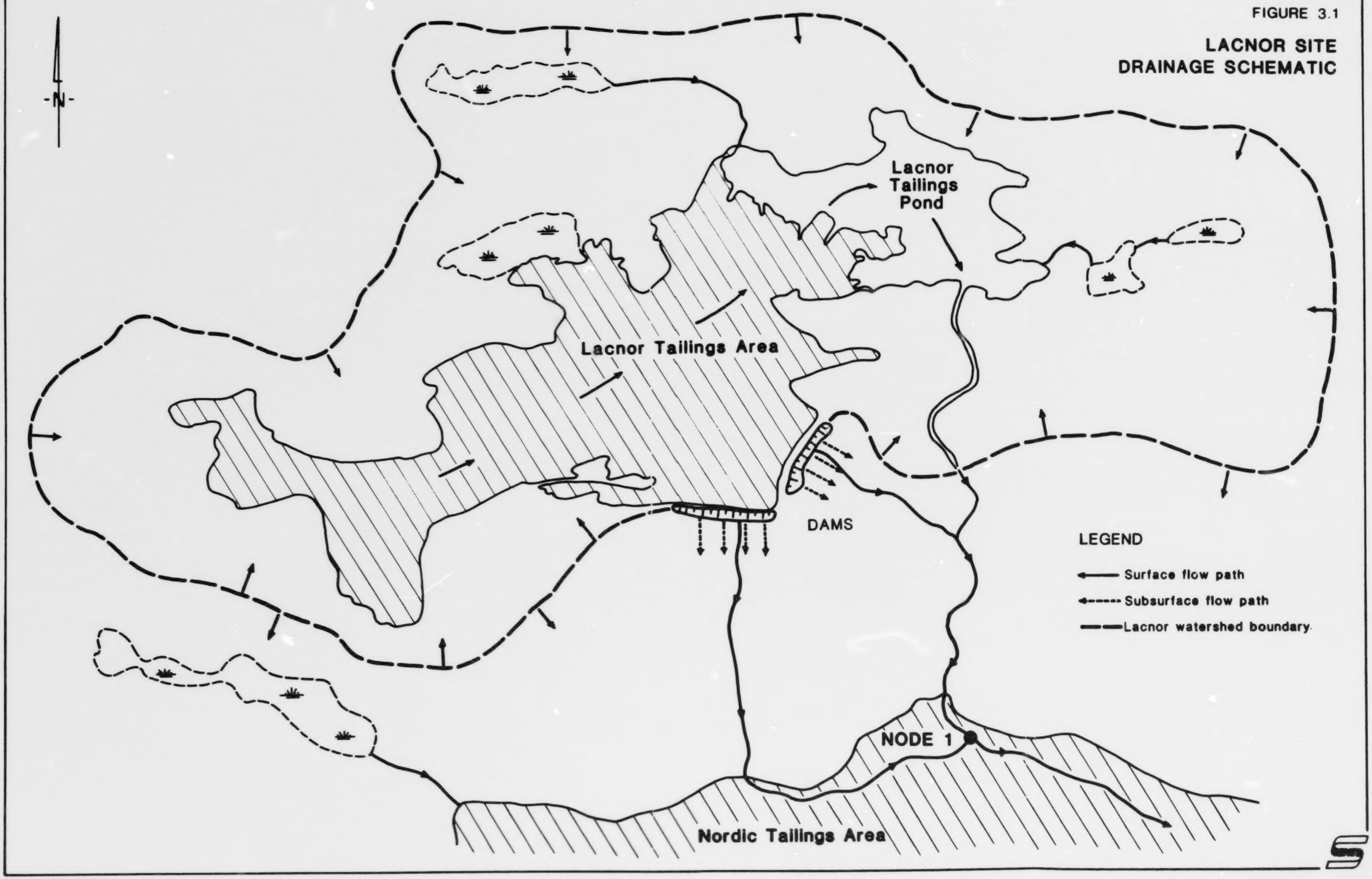

In total, the Lacnor tailings basin encompasses some 100 ha of which about 25 ha is covered with about 2.7 million tonnes of uranium tailings. Other than uranium which was removed during milling the radionuclide content of the tailings when deposited were indicative of an ore with an average grade of about 0.1% U_3O_8. The tailings also contain about 6% pyrite and, hence, are acid generating. Acid discharges occur through the surface outlet at the easterly end of the site as well as through two subsurface seepage streams at the southeast corner of the site.

Much of the surface of the tailings area has been effectively vegetated as the result of treating the surface of the tailings with a limestone fertilizer and a blend of various grass seeds.

The average depth of the Lacnor tailings is in the order of 10 m and the water table occurs at a depth of between 0.5 to 1.0 m below the surface. Overall, many of the characteristics of the Lacnor site resemble those of the generic tailings facilities examined in previous studies (SENES, 1984; 1985; 1986a).

A more detailed description of the Lacnor tailings is presented in Chapter 2.0.

3.1.2 Environmental Pathways

The assessment of the radiation dose to receptors from radionuclides released from the Lacnor tailings site involved the analysis of the exposure pathways illustrated in Figure 3.2 and included:

1) Lake Water Consumption: dispersion of tailings effluent in the receiving water environment and consumption by humans.
2) Fish Consumption: the transfer of radionuclides from the receiving water environment to fish and consumption by humans.
3) Radon Inhalation: dispersion of radon exhaled from the Lacnor tailings site through the air environment and inhalation by humans.

FIGURE 3.2

EXPOSURE PATHWAYS ANALYZED

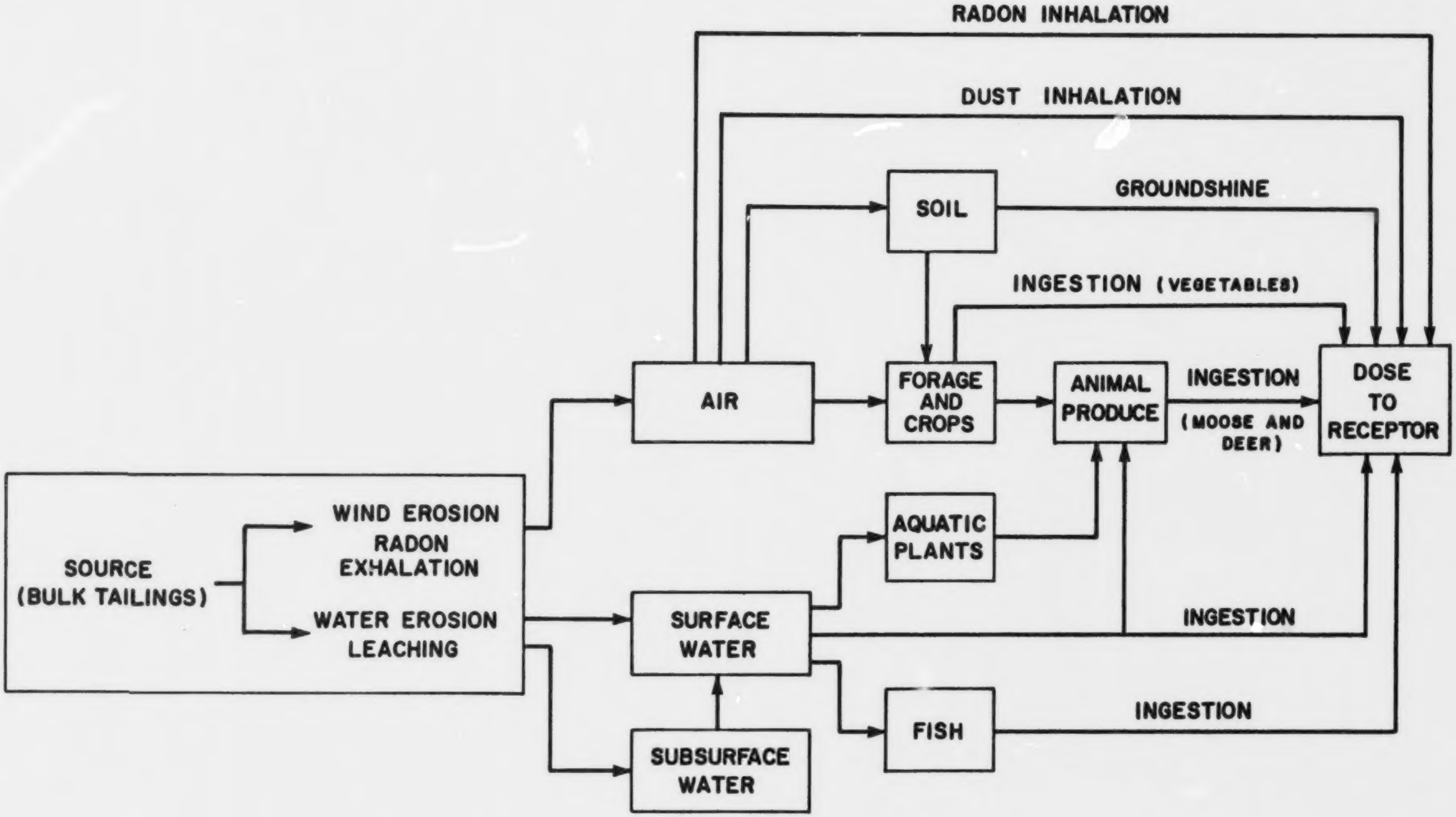

4) Dust Inhalation: dispersion of dust eroded from the surface of the Lacnor tailings site in the air environment and inhalation by humans.

5) Vegetable Consumption: the transfer of airborne radionuclides to above and below ground vegetation and subsequent consumption by humans.

6a) Animal Produce Consumption: the uptake of radionuclides by forage vegetation, subsequent transfer to moose and deer and consumption of the animal meat by humans.

6b) Animal Produce Consumption: the uptake of radionuclides by aquatic vegetation, subsequent transfer to moose and consumption of the animal meat by humans.

6c) Animal Produce Consumption: the uptake of water containing radionuclides by moose and deer and the subsequent consumption of animal meat by humans.

7) Groundshine: direct radiation from deposited dust.

The component models which simulate the behaviour of the tailings and of the environment over time can be used to predict the behaviour of various radioactive species in the environment and the resulting dose to man. The radionuclides which are included in the analysis are radium-226, radon-222, total thorium, natural uranium and lead-210. The release and behaviour of non-radioactive species (eg. sulphate, calcium and iron) is also simulated and used to calculate pH in the tailings porewater and in receiving waters.

The component models for UTAP.3 are described in an accompanying report (SENES, 1987c). The way in which these models were adapted to the Lacnor site and the model parameters used in the analysis of the Lacnor site are described in the Appendices to this report. Similarly, the way in which the models and the parameters were adopted to evaluate the closeout options are described in Chapter 4 of this report.

3.1.3 Receptor Locations and Characteristics

Five receptors were chosen for the pathways analysis: a resident at Nordic townsite (receptor 1); two residents of the Town of Elliot Lake (east and west, receptors 2 and 3, respectively); and two permanent residents on Depot Lake (east and west, receptors 4 and 5 respectively). Each of these receptors locations are shown on Figure 3.3.

In UTAP.3, lifestyle characteristics of two types of receptors may be specified. Tables 3.1 and 3.2 describe the receptor types chosen for this application to the Lacnor tailings site. In subsequent discussions each of the five receptors are designated as type 1 or type 2 as indicated on the tables. Details on the characteristics of the receptors are provided in Appendices L and M.

3.1.4 Spatial considerations

The spatial coordinates of the area modelled for the Lacnor assessment are shown on Figure 3.3. The structure of the windrose grid is the same as that used in previous studies (SENES, 1986a), namely wind data are resolved into 16 sectors, each with an angular width of 22.5°. The sector-averaged concentration was calculated for each of the angular rings. The appropriate sector concentrations were then used in calculating the air pathway doses shown on Figure 3.3 to the five selected receptors.

The watershed pathways encompass the Elliot Lake sub-basin (i.e. western arm of Serpent River Basin) to the point of discharge into McCarthy Lake. Figure 2.2 shows the locations of the various watershed nodes used in the analysis of surface water quality. The intake of contaminated water and fish by the receptors was achieved by linking them to the appropriate models.

3.2 Model Calibration/Validation

3.2.1 Nature of Calibration/Validation Efforts

The confidence that one can place in a model is often measured in terms of the success achieved in model verification, calibration, and validation. Verification of the generic UTAP.2 model was performed as part of the Phase

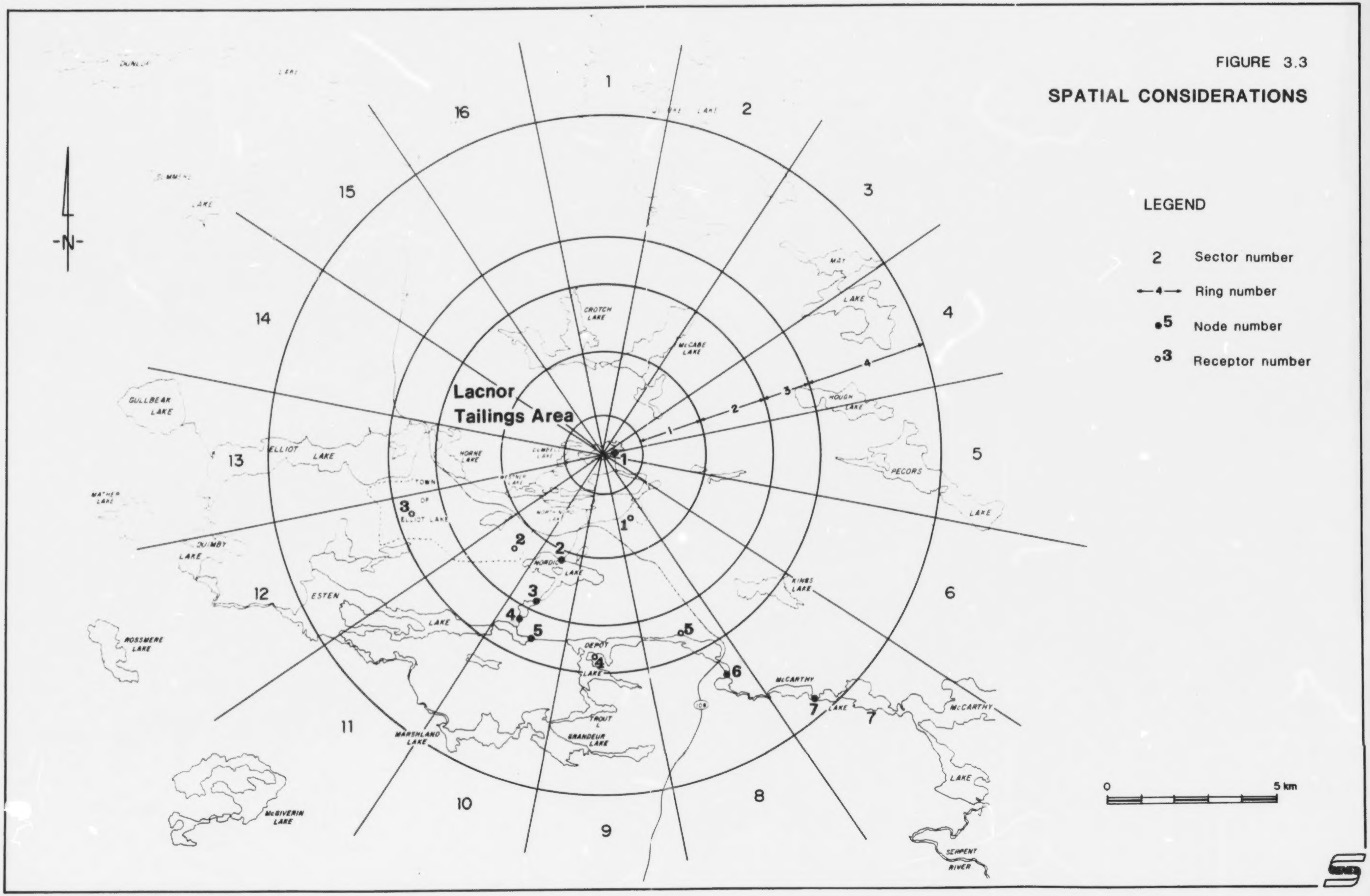

FIGURE 3.3

SPATIAL CONSIDERATIONS

Table 3.1

LIFESTYLE ASSUMPTIONS USED IN THE DOSE CALCULATIONS FOR THE ELLIOT LAKE (EAST AND WEST) AND DEPOT LAKE (EAST) RECEPTORS (RECEPTOR TYPE 1)

Inhalation and External Exposure	-	spends 80 to 100 percent of the year at that location	
	-	Vegetables	- from 0 to 20 percent are grown at the receptor location
	-	Meat	- eat wild game (deer and moose) once a week - eat deer and moose in equal proportions - 0 to 50 percent of the game meat is obtained from the watershed
	-	Water	- taken from closest lake (east and west Elliot Lake receptor - Elliot Lake; Depot Lake east receptor - Depot Lake) - percent of total consumed locally is equal to the percent of the year spent at that location
Ingestion Exposure	-	Fish	- 0 to 50 percent of annual intake is from Depot Lake for the Elliot Lake east and Depot Lake east receptors - the Elliot Lake west receptor eats no fish from the watershed
	-	Other Foodstuffs	- assumed to be store bought and grown outside the model area

Table 3.2

LIFESTYLE ASSUMPTIONS USED IN THE DOSE CALCULATIONS FOR THE NORDIC TOWNSITE AND DEPOT LAKE WEST RECEPTOR (RECEPTOR TYPE 2)

Inhalation and External Exposure
- spends 80 to 100 percent of the year at that location
- Vegetables - from 10 to 60 percent are grown at the receptor location
- Meat
  - eat deer and moose meat only year round, in equal proportions
  - 100 percent of the game meat is obtained from the watershed
- Water
  - taken from closest lake (Nordic Townsite receptor - Ryan Lake; Depot Lake west receptor - Depot Lake)
  - percent of total consumed locally is equal to the percent of the year spent at that location
- Fish - 100 percent of the annual intake is from Depot Lake
- Other Foodstuffs - assumed to be store bought and grown outside the model area

III study (SENES, 1987d). Verification procedures are presented throughout the Phase III report and were further expanded in the supplementary Quality Assurance (QA) report (SENES, 1987d).

Based upon the experience gained from model verification in the Phase III study, a detailed in-house review of UTAP.2 early in the present study, and second party review and implementation of UTAP.2, several modifications were suggested. These were implemented in the current UTAP.3 code which was used for the Lacnor assessment. Each of the changes proposed for UTAP.2 was tested prior to inclusion in the updated system model, UTAP.3 . The details of the UTAP.3 code are described in accompanying documentation (SENES, 1987a, 1987b and 1987c). The remainder of this chapter is devoted to the calibration and validation of the UTAP.3 model.

The terms calibration and validation are often used in the scientific literature without clearly defining their meaning. By calibration, we mean the selection of values for the parameters of a model to give the best fit of model results to field or laboratory data. By validation, we mean the application of the calibrated model to a new situation and comparison of the model results to the new set of field or laboratory data. This validation step gives an indication of how confident we can feel about the model predictions. This confidence is limited to applications under conditions similar to those for which validation has been done. If the natural system is to be perturbed far from conditions for which the model has been validated, the model may only yield, at best, the general trends of the perturbed system (Broissia, 1986).

In the Lacnor field study the tailings and area immediately adjacent (i.e. area within 100 m) were monitored. The surrounding airshed and watershed; however, were not monitored. Hence, the use of the measured field data for the Lacnor site in calibration/validation is restricted to the water source model, subsurface transport module and radon source model. The latter is contained within the air source model.

Because of the uncertainty associated with key site-specific parameters, e.g. radionuclide distribution coefficients and aquifer discharge distances and the lack of independent data sets, the subsurface transport model could only be calibrated. The key parameter selected for adjustment was the aquifer discharge distance.

The radon model's only site specific input is the soil water content which could be inferred from the Lacnor field study (Golder et al., 1986). The radon source model was "calibrated" in a similar previous study (Rogers et al., 1980). In the present study, the predicted radon fluxes were validated by comparison to the measured radon fluxes.

In order to calibrate the rate of pyrite oxidation employed in the water source model Nordic field data were used. The Nordic data allowed for the calibration since pyrite contents and sulphate levels in the unsaturated zone were measured. Nordic field data presented by Smyth (1981) and Dubrovsky et al. (1985), were employed in a previous study to validate model predictions of acid generation rates and limits in sulphidic uranium tailings for the the Reactive Acid Tailings Assessment Program (RATAP) (SENES and Beak, 1986). Calibration of the UTAP source model therefore introduced a comparison of predicted results against field data collected at two sampling locations on the Nordic tailings and against RATAP code predicitons over a 100 year simulation period.

The UTAP water source model was also validated against Lacnor field data. In the validation process, the rate of pyrite oxidation determined from the aforementioned calibration with Nordic field data was employed and found to yield good agreement between predicted and measured values of the residual pyrite content, sulphate levels and pH in the tailings porewater.

3.2.2 Description of Field Data

Lacnor Tailings

Because the Lacnor field study was not designed specifically to produce inputs to the UTAP model, certain inadequacies exist in the database. These include the absence of porewater samples for the unsaturated zones and measurement of tailings solids water erosion losses.

To perform a detailed calibration of the model one would also require off-site measurements of radionuclides resulting from the Lacnor tailings. Because of the presence of other tailings operations in the area, the influence of the Lacnor tailings on the receiving environment cannot be distinguished from the other facilities.

Porewater concentrations of radioactive and non-radioactive constituents measured during the Lacnor field study (Golder et al., 1986) were of use in validating the water source model. Porewater and groundwater samples were collected in the spring and in the summer of 1985. The spring set was collected between June 11 and 14 and the summer set of samples was collected between August 19 and 21. The June sampling program comprised of 32 tailings, sub-tailings, and off-tailings piezometers. The August sampling program was restricted to 16 of the tailings and sub-tailings piezometers.

The porewater analysis in the field included: temperature, pH, electrical conductivity, dissolved oxygen, Eh, acidity and ferrous iron. A suite of chemical and radiological species were analysed on the porewater and groundwater samples including major cations and metals (silver, aluminum, arsenic, boron, beryllium, cadmium, cobalt, chromium, copper, iron, potassium, magnesium, manganese, molybdenum, sodium, nickel, phosphorus, lead, selenium, silicon, strontium, thorium, titanium, vanadium, zinc, zirconium), major anions (fluoride, chloride, phosphate, nitrate, nitrite, bromide, sulphate), ammonia, reduced sulphur, and several radionuclides (total uranium, radium-226, radium-228, thorium-230, thorium-232, polonium-210, lead-210).

The subsurface model was calibrated using the surface water measurements at the toes of the dam, i.e. at the stations designated SW-01 and SW-02 in the Lacnor field study. Station SW-01 was situated just to the south (downstream) of the western most dam on the west branch of Lacnor Creek. The flow at this station comprised mainly of seepage from the tailings areas. Station SW-02 was located south (downstream) of the main dam on the southeast corner of the tailings area. The flow from this dam also comprised mainly of seepage and is carried in the east branch of Lacnor Creek.

Samples were collected from SW-01 and SW-02 on approximately a weekly to bi-weekly basis from late January to the end of October 1985. The samples were analysed for the same parameters as those described previously for the porewater samples. Concrete weirs with steel V-notch centre plates were constructed at the monitoring stations and water levels were recorded using continuous recording equipment housed in heated enclosures.

Nordic Tailings

Porewater data for the Nordic tailings was taken from Smyth (1981) and Dubrovsky et al. (1985). The data were obtained between 1979 and 1983 from a network of piezometer nests. Measurement of pH and dissolved oxygen was made in the field. The chemical analyses of the porewater included major cations and metals (aluminum, cobalt, copper, iron, potassium, sodium, nickel, lead, silicon), major anions (fluoride, chloride, phosphate, nitrate, sulphate) and radiological elements (total uranium, radium-226, thorium-228, thorium-230, thorium-232 and lead-210).

3.2.3 Comparison of UTAP Predictions With Lacnor Field Data

Water Source Model Calibration

The rate of pyrite oxidation employed in the water source model was calibrated using Nordic field data, Smyth (1981) and Dubrovsky et al. (1985). A detailed description of the data used in the calibration is presented in Appendix A.4.

Table 3.3 summarizes the predicted and observed levels of several parameters which were used to demonstrate the "best fit" (calibrated) of the model. The "best fit" at location T3 was achieved using an initial rate of pyrite oxidation (R_s) of 3.0 x 10^{-6} mol.g^{-1}.yr^{-1} and a rate fraction (X_{Rate}), of 0.10. The X_{rate} factor adjusts the rate of pyrite oxidation for the presence of calcite which buffers the porewater pH at about 6.5 and reduces the rate of bacteria-assisted pyrite oxidation. At location T5 the "best fit" was obtained for an R_s value of 1.4 x 10^{-5} mol.g^{-1}.yr^{-1} and a X_{Rate} value of 0.10. The higher initial rate of pyrite oxidation at T5 was attributed to a much higher initial pyrite content at this location in the Nordic tailings area. Overall, the predicted and observed levels of all porewaters included on Table 3.3 are seen to be quite comparable.

The UTAP model predictions were also compared to those obtained from the RATAP model which was previously calibrated against the Nordic data. This comparison was carried out to determine how the pyrite content changes with time over the long-term. Figure 3.4 presents the predicted pyrite contents for both models for a 100 year simulation. The best fit resulted when a R_s value of 3.0 x 10^{-6} mol.g^{-1}.$yr^{-1}$and an X_{Rate} value of 0.10 were used as before. The range of parameter values chosen was the same as those presented for location T3 in Appendix A, Table A.4. While the two codes predict slightly different trends in the rate of pyrite depletion, as expected since the RATAP code is a much more detailed code, the results overall are quite comparable.

Water Source Model Validation

Table 3.4 presents predicted and observed levels for several parameters in the saturated zone (layer 3) which were analyzed in the validation study. Only layer 3 is presented since the porewater of this layer governs the concentration of radionuclides in surface runoff and the groundwater (seepage) discharges from the tailings area. Detailed comparisons of the remaining layers are presented in Appendix A, Section A.5.

Table 3.3

WATER SOURCE MODEL CALIBRATION USING NORDIC FIELD DATA*

Location	pH		SO_4 ($mol.m^{-3}$)		Ca ($mol.m^{-3}$)		Fe_t ($mol.m^{-3}$)		Calcite Front (m)		Gypsum Front (m)		Pyrite Content ($mol.m^{-3}$)	
	Pre	Obs	Pre	Obs	Pre	Obs	Pre	Obs	Pre	Obs	Pre	Obs	Pre	Obs
Location T3														
Layer 1	2.2	3.5	-	-	-	-	-	-			0.23	0.4	-	22
Layer 2	3.1	5.5	90	78	5	11	43	54	6.25	3.25			562	430
Layer 3	4.8	5.5	53	94	4	-	37	-						
Layer 4	4.9	-	46	-	4	-	31	-						
Location T5														
Layer 1	2.2	2	-	-	-	-	-	-			0.22	-	-	540
Layer 2	3	3.5	129	198	4	12	63	86	4.0	4.0			1140	1080
Layer 3	4.4	5.3	124	313	2	-	92	179						
Layer 4	4.4	7.0	124	52	2	-	92	-						

Reference

* Smyth (1981) and Dubrovksy et al. (1986).

Note:

Obs Measured field value.
Pre Predicted level.

FIGURE 3.4

COMPARISON OF PREDICTED PYRITE CONTENTS FOR UTAP AND RATAP MODELS

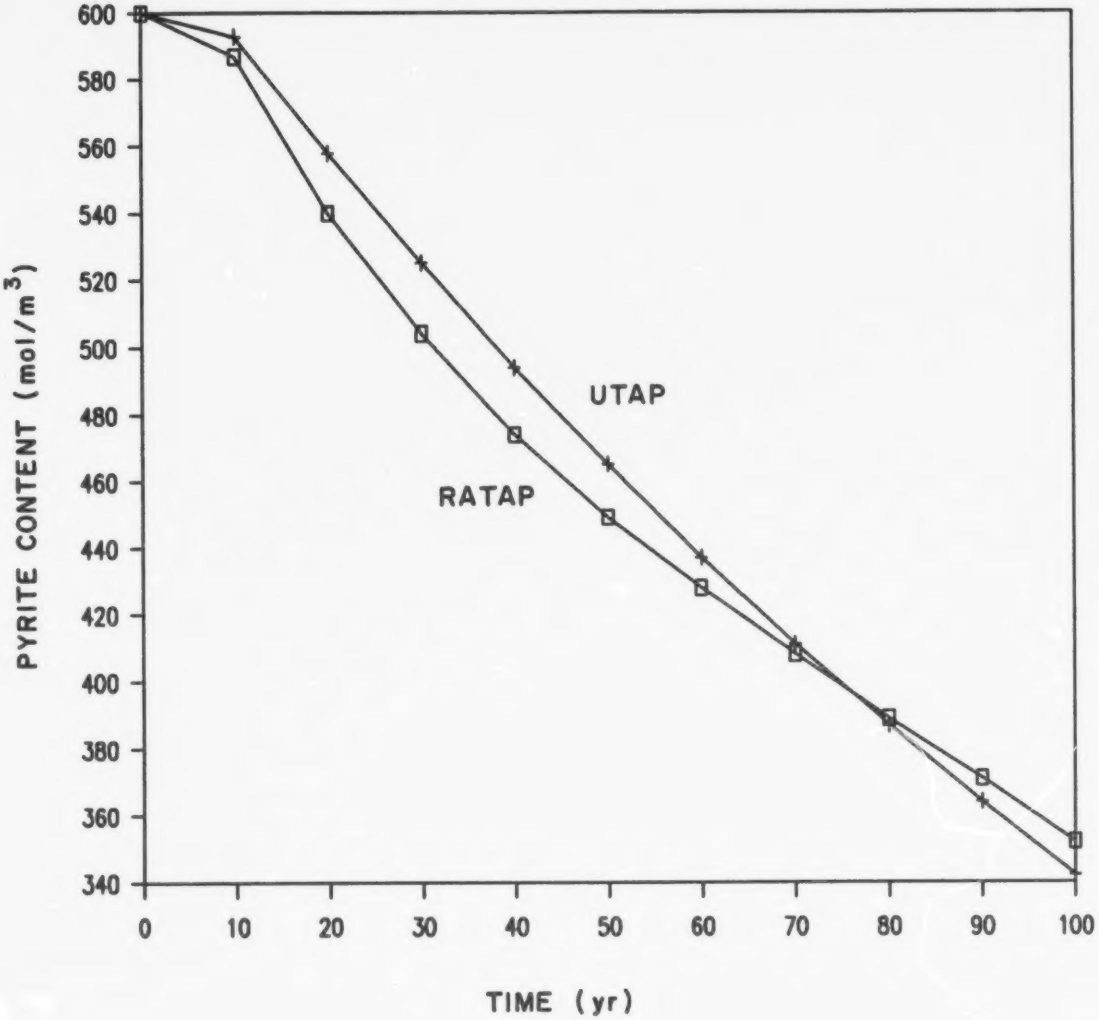

Table 3.4

WATER SOURCE MODEL VALIDATION AGAINST LACNOR FIELD DATA
(Layer 3 Discharge)

		Mean Value (95% Confidence Interval)	
Parameter	Units	Predicted*	Observed**
pH		4.9 (4.6,5.2)	5.2 (2.9,7.5)
SO_4	($mol.m^{-3}$)	44.6 (25.2,78.9)	63.8 (28.0,145)
Ca	($mol.m^{-3}$)	4.5 (2.4,8.3)	10.8 (8.9,13.1)
Fe_t	($mol.m^{-3}$)	29.0 (14.0,61.0)	41.1 (4.8,350)
U	($Bq.m^{-3}$)	1570 (240,1.0E4)	2830 (24.4,3.3E5)
Th	($Bq.m^{-3}$)	3330 (2.2E3,5.1E3)	1320 (87,2.0E4)
Pb-210	($Bq.m^{-3}$)	17400 (8.5E3,3.6E4)	2120
Ra-226	($Bq.m^{-3}$)	4300 (2.8E3,6.7E3)	4370 (660.,2.9E4)

Reference

** Golder et al., (1986)

Note

*50 trials of 25 years duration employed in probabilistic run.
- pH ; arithmetic mean
- other parameters; geometric mean
- (2.9,7.5) lower and upper 95% confidence interval of point estimates

Overall good agreement exists between the predicted and observed values for pH, sulphate, total iron, uranium and radium-226. For calcium, total thorium and lead-210, the observed geometric means lie outside of the predicted 95% confidence interval of the point estimates. However, even these differences are acceptable when one considers that UTAP predictions are mean annual values for a presumably homogeneous tailings mass while the observed results are representative of two sets of porewater samples taken from five piezometer nests with different tailings characteristic.

Radon Model Validation

For the Lacnor field study radon exhalation rates were monitored during spring, summer and winter conditions. Because the snow and ice cover was removed from the tailings for the winter monitoring program, only the spring and summer monitored exhalation rates were used in the validation. A detailed description of the validation exercise is presented in Appendic C, Section C.4.

Table 3.5 presents the predicted and observed exhalation rates. There exists very good agreement. The differences between the standard deviations (the monitored standard deviation being larger) is not unexpected since the monitored exhalation rates were for 2 to 6 hour averages whereas the model predictions were for annual averages.

Subsurface Transport Model Calibration

To calibrate the subsurface transport model, two sets of Lacnor field data were considered: field data representative of the mean aqueous source concentrations and field data representative of the subsurface discharge concentrations. The data were used to calibrate the parameter for discharge distance at each dam. A detailed description of the validation exercise is presented in Appendix H, Section H.4.

To estimate the source concentrations of the radionuclides, the tailings field

Table 3.5

RADON MODEL VALIDATION WITH LACNOR FIELD DATA

	Exhalation Rate ($Bq.m^{-2}.s^{-1}$)	
	Mean	Standard Deviation
Predicted**	1.05	0.55
Measured	1.12*	1.50

Reference

* Golder *et al*., (1986)
** arithmetic mean of 500 trials

data (Golder et al., 1986; Appendix 1.0, locations GW-1 to GW-5) were evaluated. Two assumptions were employed in using the data. The first was that the field data measured in 1985 were representative of the tailings porewater concentrations for the last twenty years since the tailings were deposited. The second assumption was that the porewater emerging as seepage at dams 1 and 2 is acidic, hence only field data representing acidic conditions, pH < 4.0, were evaluated in characterizing the quality of the seepage source feed to the subsurface transport model. This condition was imposed based upon the observation of low pH conditions in the subsurface discharge at the toes of the dams.

The field data assumed to be representative of the subsurface discharge concentrations at dam 1 and dam 2 were the surface water samples taken at locations SW-01 and SW-02 during the Lacnor field study.

Table 3.6 presents the predicted and observed values for total uranium, total thorium, lead-210, radium-226, sulphate and calcium when discharge distances of 2 m and 7 m are employed for dams 1 and 2, respectively. Considering that there is high uncertainty in the source concentrations in the areas adjacent to the dams, good agreement exists overall between predicted and observed values.

Table 3.6

COMPARISON OF PREDICTED CONSTITUENT CONCENTRATIONS WITH FIELD DATA

Dam	Constituent	Units	Predicted Discharge Concentration** ($Bq.m^{-3}$)	Mean Observed Discharge Concentration* ($Bq.m^{-3}$)
1	Tot. U	($Bq.m^{-3}$)	6480	(SW-01) 6650***
	Tot. Th	"	4490	10340
	Pb-210	"	1750	2565
	Ra-226	"	1380	762
	SO_4^{2-}	($mol.m^{-3}$)	61.6	16.8
	Ca^{2+}	"	11.5	6.5
2	Tot. U	($Bq.m^{-3}$)	3000	(SW-02) 3080***
	Tot. Th	"	4270	5260
	Pb-210	"	1640	980
	Ra-226	"	1330	570
	SO_4^{2-}	($mol.m^{-3}$)	61.6	25.1
	Ca^{2+}	"	11.5	7.0

Reference

* Golder et al., (1986); Appendix 3, Table 3.20 and 3.21.

Note

** The predicted concentrations are the results of a deterministic run obtained using the characteristics of acidic porewater as the source input to the subsurface transport model.

*** The mean observed discharge concentration was found to be higher than the mean observed source strength value. Hence, the former was used to estimate the mean source strength of the tailings porewater adjacent to the two dams on the southeast perimeter.

4.0 TAILINGS CLOSEOUT OPTIONS

4.1 Overview

The closeout options desribed in this section are all feasible options for uranium tailings in the Elliot Lake area. Consistent with the overall project objectives as discussed in Section 1.2, they were chosen for use in a demonstration of a trial application of UTAP.3 to a real site. Some options would not be feasible for Lacnor, but would be for other active tailings areas. In this sense, the UTAP results presented in Chapter 5 can be thought of as "generic" to the options under study.

The data collected from the NUTP field study on the Lacnor site (Golder *et al.*, 1986) were used to characterize the tailings mass as a whole. In general, values measured at Lacnor were found to closely parallel those predicted for a generic uranium tailings produced from a low grade (0.1 percent) uranium deposit. A summary of the nominal values for those parameters which are most important to the assessment of the effects of disposal options are given below:

bulk density = 1.3×10^3 kg.m^{-3}
specific activity (Th-230/Ra-226/Pb-210) = 10.0 Bq.g^{-1}
uranium concentration (as U_3O_8) = 0.008 %
pyrite content (as FeS_2) = 6.5 %
calcite content (as $CaCO_3$) = 0.05 % (estimated)
calcium sulphate content (as $CaSO_4$) = 6.0 %

To date, reclamation work at the Lacnor site has entailed reshaping and vegetation of the tailings. Under the existing conditions, the water table is generally within the upper 2 metres of the surface of the pile, exposing only this surface layer of tailings to active oxidation. This oxidation zone is, however, sufficient to cause a substantial level of acidity in the runoff and seepage from the area. Seepage flows continuously from the pervious dams on the south rim while the surface runoff discharges through a man-made rock spillway at the southeast corner. These flows are collected and treated at the Nordic treatment plant.

Closeout concepts for uranium tailings basins normally consider application of some type of cover material. The most commonly considered covers are: vegetation, waste rock, depyritized tailings, limestone modified tailings, earthen material or water. The primary objective in applying a cover to sulphidic tailings is to stabilize the surface and, where possible, reduce or eliminate the continuing production of acidic conditions in the tailings basin.

The following section is a generic review of the closeout options applicable to uranium tailings in the Elliot Lake area.

4.2 Alternative Closeout Concepts

4.2.1 Base Case

The base case includes grading, shaping and vegetation of the tailings surface, as well as, construction of drainage works where applicable. This management scheme has been adopted at the existing Lacnor site. The remedial work involved the application of 5 to 10 t. ha^{-1} of agricultural limestone to the tailings surface to buffer the shallow root zone from acidity. A new spillway was constructed to provide better flow control and reduce the water table in the tailings mass. With the exception of an area near the pond which was not trafficable by heavy equipment, the tailings area was vegetated by hydroseeding.

This program has been effective at reducing wind erosion as was demonstrated by the low particulate levels measured in the air monitoring program. Vegetation does not appear to have had a significant effect on acid generation.

4.2.2 Waste Rock Cover

The application of a waste rock cover is a viable and realistic waste management strategy at sites where waste rock is available. Waste rock is a durable cover, and provides excellent surface stabilization. A depth in the order of 0.5 to 1 m is normally considered sufficient to provide long-term control against tailings erosion.

Application of a waste rock cover at a site such as Lacnor where vegetation is currently in place would have minimal additional benefit in reducing contaminant losses via erosion of tailings solids except in areas where vegetation has not been established. The primary benefit would be the reduction in the surface gamma radiation level. Much of the waste from the Elliot Lake mines is acid generating but contains a low level of radiation. While the waste rock could contribute to the acidity level it is not likely to magnify the acidity problem. The overall reduction in the surface gamma level is dependent upon the specific activity of the waste applied.

Because a waste rock cover is very porous, the cover should not affect the water level in the tailings. In addition, the porous cover would not provide a physical barrier to oxygen diffusion, therefore, the rate of acid generation in the tailings would not likely be affected.

4.2.3 Depyritized Tailings Cover

The application of a pyrite-reduced cover has long been proposed as a viable strategy for controlling acid generation in pyritic tailings. While large scale testing of this technology has not been attempted, experience with a test plot in Elliot Lake suggests that acid conditions may not result (Barnes, 1986). Regardless of whether the depyritized tailings do or do not produce acid, limestone can be added to the depyritized tailings cover to mitigate any acid produced.

Pyrite removal will also marginally affect the specific activity of the depyritized tailings. It appears that some radionuclides (radium for instance) tend to be removed more so than others with the pyrite concentrate. Typically, the reduction in the radium level is reported to be between 10 to 20 percent. However, one sample of depyritized tailings produced at Denison Mines contained less than 50 percent of the radium content of untreated tailings produced at the mill.

The application of a pyrite-reduced cover at Lacnor is not readily achievable as the mill is no longer operational. However, setting this practicality aside, the effect of pyrite removal can be illustrated using Lacnor as an example case. To be totally effective, the pervious dams on the south rim would have to be replaced to permit the water table in the vicinity of these dams to be raised. Under these conditions, a 2 m cap of depyritized tailings would effectively eliminate further acid generation by flooding the pyritic tailings. The surface gamma level and radon emanation rate would also be marginally reduced (in proportion to the reduction in radionuclide content of depyritized tailings). The surface would be revegetated for stabilization.

Because of the large inventory of acid porewater contained in the Lacnor tailings, surface runoff and seepages would likely remain contaminated for many years.

4.2.4 Earthen Cover

The placement of earthen covers over uranium tailings is a commonly proposed method for closing out uranium tailings areas. The cover serves to reduce radon emissions, surface gamma radiation levels, wind and water erosion of tailings and acid generation rates. Two of the primary drawbacks to the placement of an earthen cover are the cost and the availability of suitable cover materials.

For earthen covers to be effective for controlling acid generation, they should be fine grained to maximize the resistance to oxygen diffusion and, hopefully, to cause the water table to rise above the pyritic tailings surface into the cover material.

In concept, the application of an earthen cover at Lacnor is a potentially viable option. The cost however, would be prohibitive. The cover would preferrably consist of 2 m of glacial till. As with the pyrite removal and limestone incorporation options, the surface would be vegetated and the pervious dams would be replaced. The benefits would include effective elimination of gamma radiation and radon emissions from the tailings area and prevention of further acid generation. The latter benefit is based on the assumption that the water table migrates into the earthen cover. However, even if the area was covered today, it would take tens of years to flush out the existing inventory of acidic porewater.

4.2.5 Water Cover

Flooding of the Panel tailings area in Elliot Lake was one of the original concepts considered for closeout of this facility. The objectives of this option were to prevent acid generation and to isolate the tailings from the environment. With time, tailings placed under a water cover can be expected to become covered with sediment and be effectively removed from active leaching. Alternatively, if the water table is raised to the surface of the tailings, the surface may eventually become overgrown with aquatic plants.

The use of a water cover as a management tool was not readily acceptable during the 1970's since the concept was contrary to the commonly accepted principle of keeping water out of tailings areas. With an elevated water level, the seepage rate through the tailings would be higher and concern over containment dam stability would be enhanced. Today the scientific community generally agrees that raising the water table to the surface of the tailings is an acceptable technology for controlling acid generation. The primary problem with this option is that few sites are readily adaptable to this technology.

Raising the water table at the Lacnor site is possible but not very practical.

A water retaining dam some 720 m long and 10 m high would be required to enclose the southeast corner of the tailings area. This dam would need about 200,000 m^3 of fill and is estimated to cost in the vicinity of $5,000,000 (at $25/$m^3$). Under this concept, a new spillway would be constructed in the natural valley on the southwest side of the basin.

With the water cover option, the surface gamma level and radon emissions would be effectively eliminated and further acid generation would be prevented. As with the other cover options it would take tens of years to flush the existing inventory of contaminated porewater from the site.

4.2.6 Limestone Incorporation

The incorporation of limestone in the upper zone of a pyritic tailings area has been suggested as a means of controlling the rate of acid generation and neutralizing the acid produced from pyrite oxidation. Experience has demonstrated that tailings with more buffering capacity than acid generation potential do not produce acid runoff. Therefore, if one incorporates sufficient buffering material (such as limestone) in tailings, the release of acid runoff should theoretically be prevented.

There is some concern about the long-term effectiveness of limestone as it is known to become less reactive when coated with reaction products from acid neutralization. Reaction products in tailings include gypsum and iron hydroxides. Given that the limestone is crushed to the same grain size as the tailings, loss of reactivity of the limestone particles is not likely to be a major factor as this phenomenon does not occur in other pyritic wastes with elevated levels of naturally occurring limestone.

For tailings with a 6.5 percent pyrite content, a limestone addition rate of about 10 percent of the tailing mass is required. This amount of limestone would neutralize all the acid which could potentially be produced if the entire sulphidic mineral inventory oxidized. With the addition of this large mass of limestone, the surface gamma activity would be marginally reduced (due to dilution).

The incorporation of limestone in the surface layer at Lacnor is not readily achievable. Ideally, the limestone would be added to the mill discharge during the last several years of operation. The mill at Lacnor however, is no longer operational. Even if it were operational the ability of achieving uniform placement of limestone throughout the surface zone is questionable. Limestone is known to concentrate in tailings slimes while pyrite tends to be more uniformly distributed throughout the tailings mass. Large scale testwork is necessary therefore to demonstrate that limestone can be distributed uniformly. This problem can potentially be alleviated if the tailings are thickened before discharge.

Barring the potential problems and the lack of a mill at Lacnor, limestone addition would be a viable management technology. This closeout option would include limestone addition to the upper 2 m of the tailings, revegetation of the tailings surface and replacement of the existing dams. Because acid generation is controlled and not prevented, sulphate and calcium levels in the tailings porewater would remain somewhat elevated for several hundred years as pyrite slowly oxidizes in the cover and the resultant acid is neutralized through calcite dissolution. Acid conditions would persist for tens of years until the existing acidic porewaters are flushed from the system.

4.3 Options Selected for Modelling

Six options for closeout of the Lacnor site were reviewed in Section 4.2. Of these options, five are appreciably different and were identified for inclusion in the comparison using UTAP. These are:

Option 1) Base Case Option: tailings surface vegetated; no other remedial work carried out.

Option 2) Waste Rock Cover: application of a 0.6 m cover of waste rock on the tailings area; no other remedial work carried out.

Option 3) Depyritized Tailings Cover: application of a 2 m cover of tailings from which the pyrite component has been substantially removed; construction of new dams on the southeast rim to raise the water table in the tailings area; construction of a new spillway at the southwest corner; tailings surface vegetated.

Option 4) Earthen Cover: application of a 2 m cover of glacial till on the tailings area; construction of new dams on the south-east rim to raise the water table in the tailings area; construction of a new spillway at southwest corner.

Option 5) Water Cover: application of a water cover to the tailings: construction of new dams on the south-east rim to raise the water table; construction of a new spillway on the southwest side of the basin; construction of cells within the tailings basin using dykes.

4.4 Input Parameters

The assumptions employed in the development of the input parameters for the closeout options are presented in Table 4.1. The input parameters which must be altered to simulate the options are summarized in Table 4.2. A total of 15 input parameters are affected. The basis for the input parameters are briefly reviewed below. A detailed listing of the probabilistic distributions and descriptions for all of the input parameters in each option is presented in Appendix M.

The assessment of nominal parameter values and parameter probability distributions involved several different approaches. In those cases where sufficient data were available, the data were processed using commercially available distribution fitting software. From this analysis, the distribution with the best fit as measured by the Chi-square statistic was selected. The statistical attributes of the distribution were also determined from the summary statistics derived from the distribution fitting. The limits of unbounded distributions (e.g. normal and lognormal distributions) were

Table 4.1

TAILINGS CLOSEOUT OPTIONS - OPTION ASSUMPTIONS

OPTIONS	ASSUMPTIONS
1: Base Case	- revegetation is 60% initially; ingrowth of vegetation to clean area will occur naturally* - subsurface flow from tailings area occurs through the dams on the southern rim
2: Waste Rock Cover	- the effect of the cover on the tailings temperature in the oxidizing zone is negligible therefore the effect on the initial rate of sulphate production with depth is negligible - subsurface flow from tailings area occurs through the dams on the southern rim - waste rock cover does not affect radon emanation - waste rock attenuates tailings dust emissions by 95%
3: Depyritized Tailings	- revegetation is 60% efficient initially; ingrowth of vegetation to clear areas will occur naturally - water table raised 2.0 m due to construction of more impervious dams - subsurface flow reduced several fold due to new dams - the initial sulphate production rate is reduced as a result of low pyrite content in the surface layer - the fraction of uranium dissolved is directly proportional to the rate constant for pyrite - the addition of 1.0% calcite to the tailings is made to neutralize acidity produced from oxidation of residual pyrite content of surface layer
4: Glacial Till	- water table raised 2.0 m due to construction of more impervious dams - subsurface flow reduced several fold due to new dams - revegetation is 90% efficient initially to reduce erosion of cover material - effective oxygen diffusivity is that for water, not air - glacial till cover attenuates the tailings dust emission by 100%

Table 4.1 continued

OPTIONS	ASSUMPTIONS
5: Water Cover	- tailings have been flooded following the construction of more impervious dams - layers 1 and 2 are saturated and hence the effective oxygen diffusivity is that for water, not air - increase in surface runoff due to the high water table which limits the downward movement of water through the tailings site - subsurface flow is reduced several fold due to the dams - the attenuation of the tailings dust is 90% effective

Note

* A topdressing of 5 to 10 $t.ha^{-1}$ of agricultural limestone is added to the tailings surface to buffer the shallow root zone from acidity. This small limestone addition is taken to have a negligible effect on the chemistry of the tailings system.

Table 4.2

TAILINGS CLOSEOUT OPTIONS - NOMINAL UTAP INPUT PARAMETERS

Tailings/Cover Material Properties	Closeout Options				
	Opt.1 Base Case	Opt.2 Waste Rock Cover	Opt.3 Depyritized Tailings Cover	Opt.4 Glacial Till Cover	Opt.5 Water Cover
Pyrite as FeS_2 ($mol.m^{-3}$) "PYRITI"	700.	700.	54.	700.	700.
Initial Sulphate Production Rate ($mol.g^{-1}$ $tailings \cdot yr^{-1}$) "SULPRD"	4.1×10^{-6}	4.1×10^{-6}	2.43×10^{-8}	3.15×10^{-6}	4.1×10^{-6}
% Moisture Content $g_{water} \cdot g^{-1}_{tailings}$) in Layer One "MPCH2O"	13	13	13	28	28
Effective Oxygen Diffusivity ($m^2.yr^{-1}$) "O2DIFF"	37	37	37	6.2×10^{-3}*	6.2×10^{-3}*
Fraction of Direct Surface Runoff "XRUNOF"	0.60	0.30	0.60	0.60	0.85
Uranium as U_3O_8 (%) in ore "PCURAN"	0.1	0.1	0.08	0.1	0.1
Fraction of Uranium Dissolved as a Result of Pyrite Oxidation "FRACU"	0.6	0.6	0.058	0.6	0.6
Calcite as $CaCO_3$ ($g_{calcite} \cdot g^{-1}_{tailings}$) "XLIME"	0.0005	0.0005	0.01	0.0005	0.0005
Hydraulic Conductivity ($m.yr^{-1}$) "HCGWAT"	69.4	69.4	6.9**	6.9**	6.9**
Fraction of Radon Attenuation by Cover "CAFR"	0.0	0.0	0.0	0.99	0.5

Table 4.2 continued

Tailings/Cover Material Properties	Closeout Options Opt.1 Base Case	Opt.2 Waste Rock Cover	Opt.3 Depyritized Tailings Cover	Opt.4 Glacial Till Cover	Opt.5 Water Cover
Fraction of Dust Attenuation by Cover "CAFD"	0.0	0.95	0.0	1.0	0.75
Minimum Fraction of Initial Ground Cover "MINVEG"	0.6	0.0	0.6	0.90	0.0
Depth of Layer 2 (m) "DUNSAT"	0.5	0.5	0.5	0.10	0.10
Depth of Layer 3(m) "DMIX"	11.5	11.5	11.5	11.9	11.9
Depth of Layer 4 (m) "DBOT"	0.75	0.75	2.75	0.75	0.75

NOTE

* have assumed layers 1 and 2 are saturated
** have made dams impermeable

truncated at three standard deviations from the mean values unless the extreme values of the data base suggested other truncation limits. For those parameters for which there were little or no data available, the distributions were assessed based on theoretical principles or simply on best judgement. Such parameters were generally described by triangular, uniform or loguniform distributions based on evaluations of the expected range and model characteristics of the parameters.

In either case the selection of input distributions always involves, to a greater or lesser degree, some subjective input from the modeller(s) and hence the input parameter probability distributions are always subjective in nature.

4.4.1 Pyrite Concentration as FeS_2 (PYRITI)

The initial pyrite concentration for the Lacnor tailings was estimated to be 6.5% by weight or 700 $mol.m^{-3}$. This initial pyrite content is only changed for the pyrite removal option. Pyrite removal reduces the pyrite content of tailings from 6.5% to 0.5% or from 700 $mol.m^{-3}$ to 54 $mol.m^{-3}$.

For this option, the pyrite content has a triangular distribution with a mode of 54 $mol.m^{-3}$, and minimum and maximum values of 39.0 $mol.m^{-3}$ and 69.0 $mol.m^{-3}$, respectively. The minimum and maximum values are calculated as three standard deviations away from the mean.

4.4.2 Initial Sulphate Production (SULPRD)

The initial sulphate production data for the base case is derived from experimental data on Elliot Lake tailings and computer simulations using the Reactive Acid Tailings Assessment Program (SENES and Beak, 1986). This rate applies to the annual average rate of pyrite oxidation in layers 1 and 2. Pyrite oxidation is modelled as a first order decay reaction where:

$$[FeS_2]_t = [FeS_2]^0 \; [\exp(-KCONST.t)] \qquad (4.1)$$

where:

$[FeS_2]_t$ = concentration of pyrite at time t ($mol.m^{-3}$)
$[FeS_2]^o$ = initial pyrite content ($mol.m^{-3}$)
KCONST = rate constant for pyrite oxidation (yr^{-1})
t = time (yr)

The rate constant in turn is determined from the following functional relationship:

$$\text{KCONST} \ \alpha \ \frac{(\text{SULPRD})^{.5}}{[FeS_2]^o} \qquad (4.2)$$

With the waste rock cover and water cover options, the initial pH, temperature and pyrite content are the same as for the base case option. Therefore the theoretical experimental sulphate production rate is the same for all three options. The amount of pyrite which oxidizes with the water cover option however, is considerably less due to limitations imposed by the high water table on oxygen transport into the tailings mass.
For the depyritized tailings option, the initial pyrite content is reduced from 700 to 54 $mol.m^{-3}$. Therefore in order to maintain the same rate constant, KCONST, the sulphate production must be reduced by the ratio $(54/700)^2$.

For this option, the initial sulphate production rate was assumed to have a triangular distribution with a minimum value of 1.27×10^{-8} $mol.g^{-1}.yr^{-1}$, a mode of 2.43×10^{-8} $mol.g^{-1}.yr^{-1}$, and a maximum value of 4.0×10^{-8} $mol.g^{-1}.yr^{-1}$.

The glacial till option reduces the average annual temperature in layer 2 and 3 which produces a small reduction in the sulphate production rate from 4.1×10^{-6} to 3.15×10^{-6} $mol.g^{-1}.yr^{-1}$.

A triangular distribution with a minimum value of 2.3×10^{-6} $mol.g^{-1}.yr^{-1}$, a mode of 3.15×10^{-6} $mol.g^{-1}.y^{-1}$, and a maximum value of 4.07×10^{-6} $mol.g^{-1}.yr^{-1}$ was assumed.

4.4.3 Percent Wet Weight Moisture Content (MPCH2O)

The percent moisture content is reported as % weight of water in the wet tailings or cover material. This factor affects diffusion of oxygen into the tailings and radon out of the tailings. The base case moisture content in the unsaturated zone is 13%. This is equivalent to 40% of the void space being filled with water. For the glacial till and water cover options, the tailings material is saturated hence, the % moisture level is increased to a constant value representing saturation (i.e. 28%).

4.4.4 Effective Oxygen Diffusivity (O2DIFF)

The diffusivity of oxygen through the unsaturated zone is primarily a function of moisture content. At a moisture content of 13% by weight of wet tailings, the effective diffusivity is calculated to be 37 $m^2.yr^{-1}$ using the following equation:

$$\mathrm{O2DIFF} = 630.7 \left(\frac{n_a - 0.05}{0.95}\right)^{1.7} \qquad (4.3)$$

where:

n_a = the volumetric air content of the tailings ($m^3.m^{-3}$)

and

$$n_a = \epsilon - n_w = (1 - \P_T/\P_s) - n_w \qquad (4.4)$$

where

ϵ = porosity ($m^3.m^{-3}$)

n_w = water content ($m^3.m^{-3}$)

$\P_T$ = tailings bulk density ($kg.m^{-3}$)

$\P_s$ = tailings particle density ($kg.m^{-3}$)

This level is maintained unless the moisture content is changed. The water cover and glacial till options both increase the moisture content in layer 2 to saturation. Equation (4.3) is only valid for air contents greater than

0.05 $m^3.m^{-3}$. At saturated conditions the diffusivity is reduced by approximately 3 orders of magnitude to 6.2 x 10^{-2} $m^2.yr^{-1}$ (Shumate and Brant, 1971).

A triangular distribution with a minimum value of $4x10^{-3}$ $m^2.yr^{-1}$ a mode of $6.2x10^{-2}$ $m^2.yr^{-1}$, and a maximum value of $8x10^{-2}$ $m^2.yr^{-1}$ was assumed.

4.4.5 Fraction of Direct Surface Runoff (XRUNOF)

Surface runoff plays a major role in the water balance at the Lacnor site. The tailings have a high natural water content with a shallow water table which causes in a large percentage of the precipitation to report as surface runoff. The fraction of the net precipitation that runs off from the watershed without entering the tailings pores has been estimated by mass balance calculations of sulphate levels in the tailings pond effluent and the tailings porewater. The calculations suggested that approximately 60% of the runoff flows directly to the tailings pond (i.e. XRUNOF = 0.6) while approximately 40% infiltrates through layers 1 and 2 and takes on the characteristics of the tailings porewater. This distribution of the net precipitation on the tailings area watershed was assumed to hold true for the base case, pyrite removal and glacial till options.

With the waste rock cover option, however, the infiltration rate increases. It is estimated that the fraction of runoff will be reduced by approximately one half to 30% of the net precipitation (i.e. XRUNOF = 0.3). A triangular distribution with a minimum value of 0.25, a mode of 0.3, and a maximum value of 0.35 was assumed.

The water cover option provides for saturated conditions over much of the tailings basin. Therefore, infiltration will be limited by the seepage rate and the small amount of water which travels horizontally through the mixing zone. Because only about 50% of the tailings area will have water ponded on the surface, lateral flow will occur through the mixing zone in the exposed tailings. The fraction of direct runoff is estimated to be 0.85. A triangular distribution with a minimum value of 0.80, a mode of 0.85, and a maximum value of 0.90 was assumed.

4.4.6 Uranium as U_3O_8 (%) in Ore (PCURAN)

The uranium content in the Lacnor ore averaged 0.1% U_3O_8. This parameter value remains constant unless the radionuclide content in the surface layer of the tailings is changed. All options except pyrite removal have a PCURAN content of 0.1 %. The pyrite removal option reduces the level of uranium, radium, lead and thorium in the tailings by 20%. This adjustment in the tailings activity is achieved by reducing the input value for PCURAN from 0.1 to 0.08%.

4.4.7 Fraction of U_3O_8 Dissolved (FRACU)

Uranium dissolution in the tailings is linked to pyrite oxidation. As pyrite is oxidized, ferric ions are available to oxidize uranium from the insoluble U^{+4} state to the soluble U^{+6} state. Experimental data indicates that the oxidation of 70 moles FeS_2 will dissolve 6% of the uranium at a concentration of .008% in the tailings. With complete oxidation of all 700 $mol.m^{-3}$ of FeS_2, 60 % of the uranium would be dissolved. Therefore the weight fraction of uranium associated with pyrite oxidation is 0.6.

The fraction only changes with the depyritized tailings cover option which has 54 $mol.m^{-3}$ of pyrite and a lower uranium concentration in the tailings. Therefore the fraction of uranium dissolved by pyrite oxidation for the pyrite removal option is:

$$\frac{\text{54 moles } FeS_2}{\text{700 moles } FeS_2} \times \text{.6 weight fraction } U_3O_8 \times \frac{\text{.1\% } U_3O_8 \text{ PCURAN Base Case}}{\text{.08\% } U_3O_8 \text{ PCURAN } FeS_2 \text{ removal}}$$

$$= 0.058$$

A uniform distribution with a minimum value of 0.028 and a maximum value of

0.088 was assumed.

4.4.8 Dry Weight Fraction of Calcite as $CaCO_3$ (XLIME)

The dry weight fraction of calcite was estimated to be .0005 $g.g^{-1}$ tailings. This weight fraction remains constant unless a buffering agent is added to the tailings. The depyritzed tailings cover removal option includes the addition of 1% $CaCO_3$ to the tailings raising the weight fraction to .01.

4.4.9 Hydraulic Conductivity (HCGWAT)

The hydraulic conductivity of the aquifer which transports subsurface seepage from the Lacnor site was determined to be 69.4 $m.yr^{-1}$ based on field measurements (Golder et al.,1986). The hydraulic conductivity remains constant unless the permeability of the aquifer is modified. With three of the options, the dams on the southern rim must be replaced. These new dams have low permeability cores which penetrate through the aquifer and reduce the effective hydraulic conductivity in the aquifer by approximately one order of magnitude to 6.9 $m.yr^{-1}$.

A lognormal distribution with a mean of 6.9 $m.yr^{-1}$, a standard deviation of 2.4 $m.yr^{-1}$, and minimum and maximum values of 1.2 $m.yr^{-1}$ and 40 $m.yr^{-1}$, respectively was assumed. The standard deviation was assumed to be the same as that employed in the base case. The minimum and maximum values are based upon two standard deviations.

4.4.10 Fraction of Radon Attenuation by Cover (CAFR)

Covers on the surface of a tailings area can reduce the radon emissions. The effectiveness of the cover depends on many factors including its depth and permeability. For the uncovered base case the attenuation factor is zero.

The waste rock cover is not likely to be an effective attenuation barrier for radon as it contains uranium and an equilibrium quantity of decay products at an activity of 1 $Bq.g^{-1}$. The waste rock cover is also very porous and a 0.6 m thick layer is therefore not likely to be very effective in reducing the radon release from the tailings surface. For example, a relaxation length of 1 to 2 m is of the proper order for a waste rock cover. Assuming a nominal relaxation length of 1.5 m for example, the radon flux from the surface of the waste rock would be about exp(-0.6/1.5) = 0.67 or 67% of the radon flux from the bare tailings surface. In view of this observation and noting that radon would be released from the cover itself, no credit is taken for radon attenuation by the waste rock cover.

The pyrite removal option has a reduced radium content which will result in a lower radon emission rate. The influence of the factor is taken into account by the parameter PCURAN which is used in the model to calculate the equilibrium level of the radionuclides. There is no other factor with this option which could attenuate radon. Therefore, the attenuation factor for pyrite-reduced tailings is zero.

Till cover will dramatically reduce the radon flux. The water table is raised into the cover material with this option effectively saturating the tailings. Any radon released from the submerged tailings must pass through 2 m of till before being released to the atmosphere. Assuming a nominal relaxation length of about 45 cm in till, a two metre thick till cover would reduce the radon flux from the surface of the till to about exp (-2/0.45) = 0.011 or 1% of the radon flux from the bare tailings surface.

Water cover will also reduce the radon flux. For those areas actually covered with standing water, the radon release will be approximately zero. By design, approximately 50% of the tailings surface would be water covered while the remaining surface would be a low lying saturated boggy area. This latter area would continue to release small quantities of radon. Therefore, the attenuation factor for water cover is conservatively taken to be 0.5.

4.4.11 Fraction of Dust Attenuation by Cover (CAFD)

Covers on the surface of a tailings areas can reduce dust emissions. The base case and pyrite removal option have no covers and therefore have an attenuation factor of zero.

With the waste rock cover option, dust releases should be greatly curtailed. However, radioactive dust will be released to the atmosphere from the waste rock cover itself. To allow for imperfect placement of the waste rock cover, some mixing of tailings and cover material during placement and the fact that the waste rock cover is radioactive, the cover is assumed to result in an overall reduction of 95% in the dust source strength. Therefore the waste rock cover attenuation factor is 0.95.

Glacial till cover at 2m depth on top of the tailings would effectively eliminate dust and therefore has a cover attenuation factor of 1.0.

The water cover option assumes that 50% of the tailings have free standing water while 50% are saturated. The portion of the tailings not covered with water can be expected to be subjected to dusting during the early spring and later fall when the surfaces are freeze dried and not covered with snow. For this noncovered area, it is expected that conditions would not be conducive to dusting more than 50% of the time; therefore, the overall attenuation factor for the water cover option is 0.75.

4.4.12 Minimum Fraction of Initial Vegetative Cover (MINVEG)

Cover options may or may not include vegetation as part of the reclamation plan, but it is expected that natural vegetation will eventually be restored for all options. The existing Lacnor site is 60% vegetated. Therefore, the base case option has an initial vegetation cover factor of 0.6. Pyrite removal followed by vegetation was assumed to have the same initial vegetation cover factor. Both the waste rock and water cover options would experience little revegetation and therefore the initial vegetation cover factor was set at zero. Glacial till is readily vegetated; therefore, a high initial vegetation cover factor of 0.9 was assigned for this option.

4.4.13 Depth of Layers

The nominal depth of each layer used in the UTAP.3 model runs for the five options are shown on Figures 4.1 a), b), c), d) and e). The input parameters for depth vary for layers 1 and 2, the unsaturated zone (DUNSAT), layer 3, the mixing zone (DMIX) and layer 4, the bottom zone (DBOT). The depths of layers 1 and 2 change with time. The depth for layer 2 is initially equal to the total depth of unsaturated zone while the depth of layer 1, the gypsum depleted portion of the unsaturated zone, has an initial value of zero.

Layer 2, called the unsaturated zone, is more appropriately called the zone of oxidation. For the base case, waste rock and depyritized tailings options this zone has a nominal depth of 0.5m and reflects the depth to the water table. With the till cover and water cover options, layer 2 is saturated but oxidation can still occur. Oxygen is supplied by diffusion through porewater and advection in the infiltrating water. Over the UTAP model period, oxygen inflow was estimated to be sufficient to oxidize a layer approximately 0.1 m deep. Therefore, layer 2 is assigned a depth of 0.1m for these options.

Layer 3 is the top layer of the saturated zone and is referred to here as the mixing zone. In this zone, the main flow path occurs laterally and is the primary source of flow into the tailings pond. At the Lacnor site this layer is also the source of seepage flow through and under the dams. The total depth of layers 2 and 3, based on assessment of porewater quality data, was found to equal about 12 m at Lacnor.

Layer 4 is the bottom layer of the tailings pile. For the generic case, layer 4 is the zone from which groundwater discharge occurs. At Lacnor, layer 4 is assumed to be a dead zone at the bottom of the tailings which serves no function. The depth of this layer is assumed to be 0.75 m for all options but the pyrite removal option. Because pyrite removal is assumed to add 2m of tailings to the top of the basin, the bottom zone was expanded by 2m to 2.75m.

UTAP Layer 2	0.5 m	Tailings
UTAP Layer 3	11.5 m	Tailings
UTAP Layer 4	0.75 m	Tailings

A) BASE CASE

Cover	0.6 m
UTAP Layer 2	0.5 m
UTAP Layer 3	11.5 m
UTAP Layer 4	0.75 m

B) WASTE ROCK COVER

Cover	2.0 m
UTAP Layer 2	0.1 m
UTAP Layer 3	11.9 m
UTAP Layer 4	0.75 m

D) GLACIAL TILL COVER

FIGURE 4.1

SCHEMATIC REPRESENTATION OF TAILINGS PROFILES FOR THE CLOSEOUT OPTIONS

Waste Rock
Tailings
Tailings
Tailings

UTAP Layer 2 (Cover Material)	0.5 m	Depyritized Tailings
UTAP Layer 3 (Mixture of Cover Material and Tailings)	1.5 m	Depyritized Tailings
	10.0 m	Tailings
UTAP Layer 4	2.75	Tailings

C) DEPYRITIZED TAILINGS COVER

Glacial Till
Tailings
Tailings
Tailings

Cover		Water
Layer 2	0.10 m	Tailings
Layer 3	11.9 m	Tailings
Layer 4	0.75 m	Tailings

E) WATER COVER

5.0 UTAP.3 PROBABILISTIC ASSESSMENT RESULTS FOR LACNOR

5.1 Introduction

This Chapter presents the results of a probabilistic assessment for the Lacnor tailings site. Environmental predictions are made as if Lacnor were the only tailings site in the area. Thus, air concentrations and watershed conditions downstream of the Nordic tailings do not represent actual conditions. Five generic closeout options are considered in this UTAP.3 demonstration. The approach to modelling the options is presented in Chapter 4. The exposure pathways considered in the Lacnor assessment are shown on Figure 3.2. The component models which were used to simulate the behaviour of the tailings and the environment over time are essentially those of UTAP.3 which are described in an accompanying document (SENES, 1987c). The ways in which these models were adopted for application to the Lacnor site and the input parameters used in the Lacnor assessment are discussed in the appendices of this report.

UTAP is a tool which permits the user to include uncertainty in the analysis of any chosen uranium tailings closeout scenario. By 'scenario' we mean a particular tailings disposal option and a particular environmental setting. In carrying out the probabilistic analysis we assume that the component models provide a 'true' (or at least reasonably true) representation of the uranium tailings scenario. Many of the input parameters are uncertain due to a lack of observational data and measurements and some may also be inherently variable in space and/or time.

In UTAP, uncertain parameters are assigned distribution(s) of values, as opposed to single values as in deterministic analyses. Uncertainty is propagated through the component models to produce distributions of output results. The output distribution(s) can be interpreted as a subjective probability distribution(s) telling us quantitatively what we are entitled to believe about the output variable(s). Standard statistical descriptors such as the arithmetic mean and standard deviation or geometric mean and geometric standard deviation can be calculated from the distribution of the output variables.

The number of trials required for a particular simulation depends on the information desired regarding the calculated variable(s). If only an estimate of the mean and its associated standard deviation are needed, a relatively small number of trials (say 50) is often sufficient. If estimation of the entire frequency distribution is desired many more trials are necessary. Except where stated otherwise, the basic statistics and histograms for the analyses described in this Chapter were generated from 200 trials.

5.2 Option 1: The Base Case

The basic features of the Lacnor tailings area and environment are described in Chapter 3. The Base Case scenario examines the effects of walking away from the tailings site at the cessation of the mill operating life. The only reclamation work assumed is the vegetation of the exposed surface as has been carried out at Lacnor.

5.2.1 Total Dose by Receptor

Figure 5.1 is a plot of the geometric mean total dose for all pathways versus time for all of the five receptors studied in the present analysis namely:

Receptor No. 1	a resident of the Nordic townsite
Receptors No. 2 and No. 3	two residents of Elliot Lake (east and west respectively)
Receptors No. 4 and No. 5	two permanent residents on Depot Lake (west and east respectively)

The actual physical locations of these receptors are shown on Figure 3.4.

From Figure 5.1 it can be seen that the permanent residents of Depot Lake

FIGURE 5.1

TOTAL DOSE vs TIME FOR OPTION 1 - ALL RECEPTORS

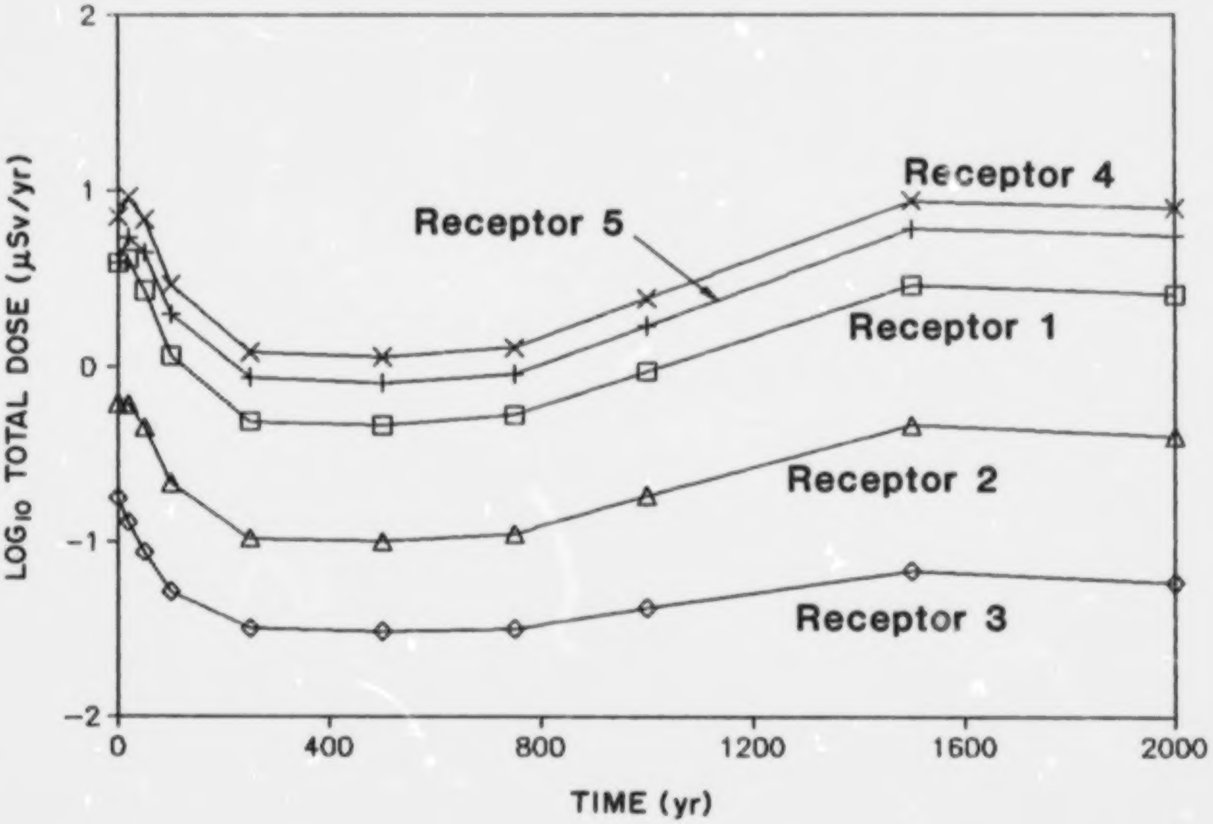

NOTE: GEOMETRIC MEAN VALUE OF 200 TRIALS

receive the highest exposures. The dose to the west Depot Lake resident (receptor 4) is slightly larger than that to the east Depot Lake receptor (receptor 5). This can be attributed to the assumed greater intakes of fish from Depot Lake and game (moose and deer) by the west Depot Lake receptor compared to that of the east Depot Lake receptor (see Tables 3.1 and 3.2).

Receptor No. 1, the resident of the Nordic townsite has the next highest dose. This is largely due to his consumption of fish from Depot Lake and local game (deer and moose). Also, since he is closer to the tailings area his dose via the air pathways is somewhat larger than that of the Depot Lake receptors.

The doses to the Elliot Lake residents (receptors 2 and 3) are substantially lower (note the logarithmic scale on the vertical dose axis) than those predicted for either of the Depot Lake residents or for the resident of the Nordic townsite.

In view of the observation that the dose to the west Depot Lake receptor (receptor No. 4) is larger at all times than the doses to the other receptors, the dose to receptor No. 4 is selected as the basis for comparison of the five closeout options. In subsequent sections "dose" means dose to receptor No. 4 (west Depot Lake resident) unless explicitly noted to be otherwise.

5.2.2 Dose by Pathway

Deterministic Simulations

Figure 5.2 is a plot of the dose versus time from a deterministic simulation carried out using nominal values of the input parameters. The figure shows the dose for the individual exposure pathways and for the total dose over a 5000 year simulation period. This particular plot was created to demonstrate how the dose curves behave over the long term. Similar deterministic simulations for the other closeout options showed that the dose curves peaked within the initial 2000 year period in four of the five options (i.e. for Options 1,2,3 and 4). Since the total dose curve for the other option (Option

FIGURE 5.2

DETERMINISTIC SIMULATION OF DOSE vs TIME BY PATHWAY FOR OPTION 1 - RECEPTOR 4

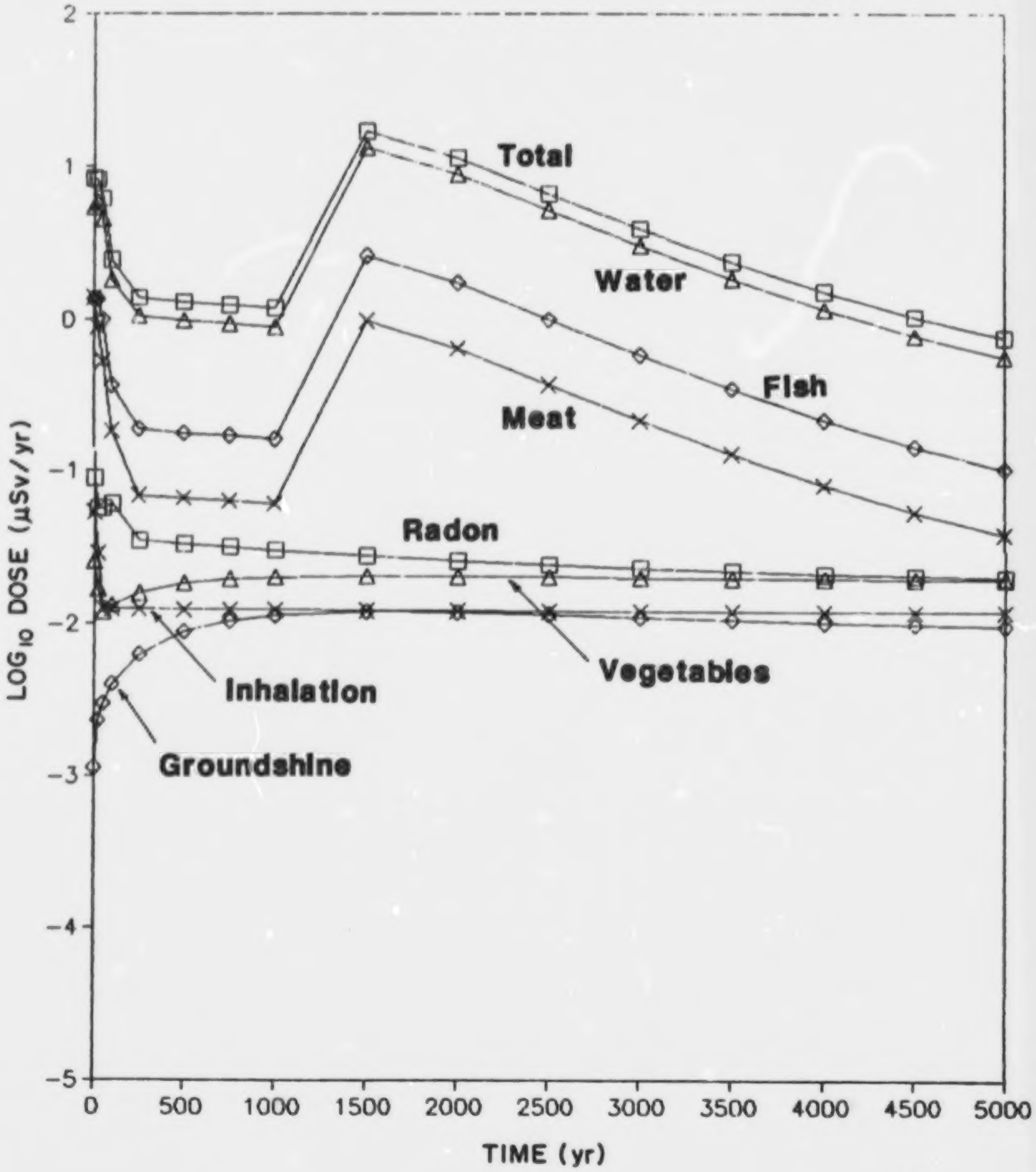

5) was found to be considerably less than the same curves for the other options and to remain relatively constant with time, the duration of the probabilistic simulations was limited to 2000 years to minimize computer time and to optimize the number of time intervals at which data could be saved for subsequent analyses.

Probabilistic Simulations

Figure 5.3 is a plot of the geometric mean dose versus time for all of the individual exposure pathways and for the total dose. The dose due to drinking water consumption dominates for the entire simulation period. The dose due to fish consumption is the second most important contributor to total dose except for the first two time steps. Consumption of meat (game) results in the third largest contribution to total dose over most of the simulation period. During the initial time steps, the dose from meat consumption is higher than that from fish consumption. The remaining pathways are more than an order of magnitude smaller contributors to total dose than those just noted.

The total dose shown on Figure 5.3 declines from approximately year 20 to year 400 and then increases to about year 1500 from which point it declines gradually. The temporal behaviour of the total dose is influenced by several factors, the most important of which relates to the water pathway which is discussed in the next section.

The radon and dust inhalation pathways decline with time as radionuclides are progressively leached from the upper unsaturated layer of tailings. In addition, as the pH of the tailings porewater increases above pH 4 vegetative cover on the tailings surface develops, also contributing to reduced dose via inhalation pathways. At early times the vegetable pathway is dominated by direct deposition of tailings dust; however, over time, radionuclides accumulate in the upper soil horizon leading to greater contributions via root uptake. Similarly, the groundshine dose increases as time passes due to an increase in the concentration of radionuclides in the upper soil horizon. In the long term, a steady state radionuclide soil level is attained at which

FIGURE 5.3

DOSE vs TIME BY PATHWAY FOR OPTION 1 - RECEPTOR 4

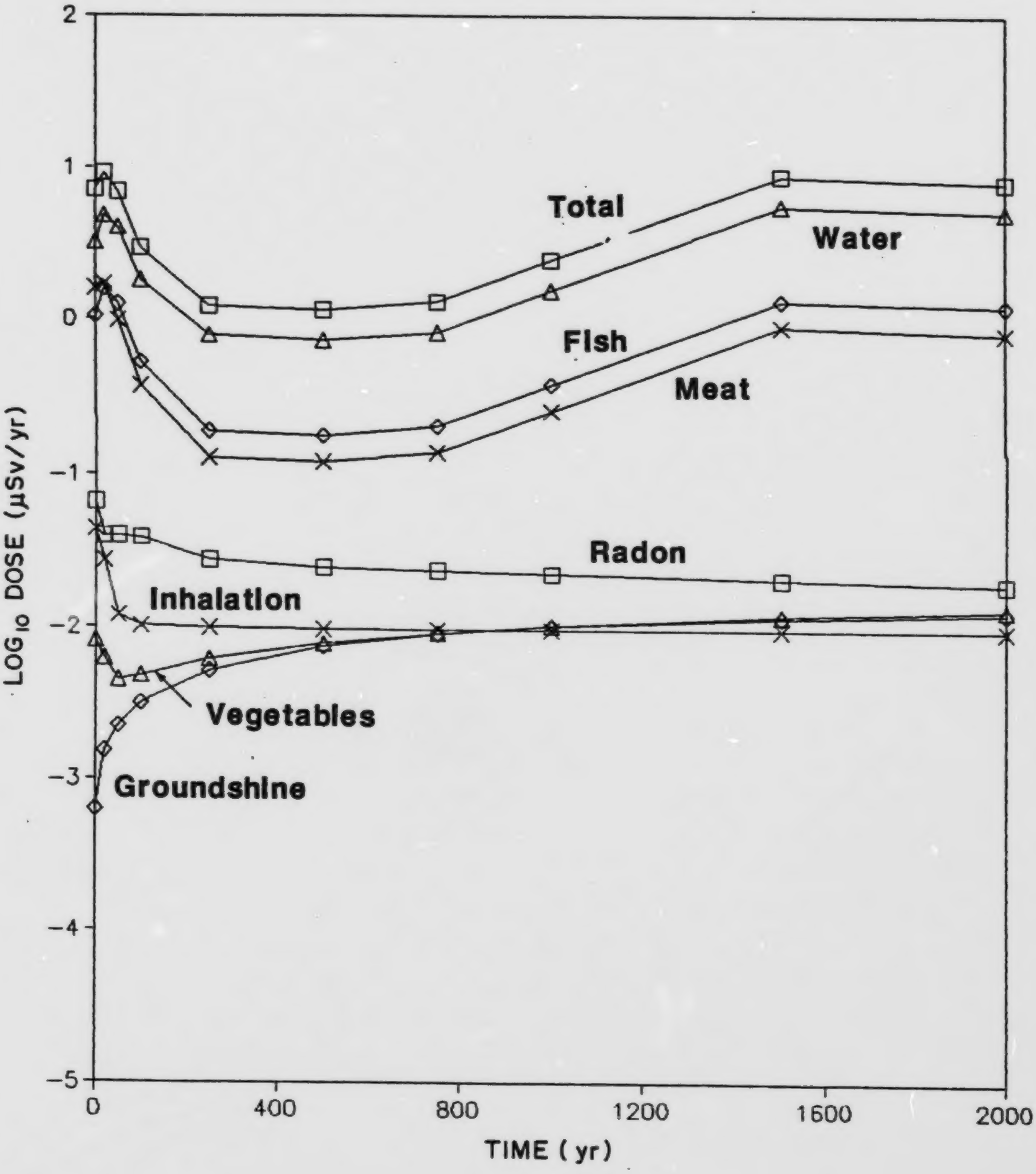

NOTE: GEOMETRIC MEAN VALUE OF 200 TRIALS

point radionuclide migration downward via leaching offsets the input from air deposition.

The mean dose from the meat (game) pathway closely parallels the water pathway indicating that radionuclide transfer to game from water (and aquatic vegetation) is more important than transfer via terrestrial vegetation.

Figure 5.4 shows histograms of total dose at t=20 and t=1500 years. Both histograms show a skewed shape suggestive of lognormal behaviour.

5.2.3 The Water Pathways

Radionuclide Concentrations

The concentrations of total uranium, total thorium, lead-210 and radium-226 in Depot Lake are shown on Figure 5.5. The concentration profiles are the geometric mean predicted values from 200 trials. The trends are similar at other locations in the watershed and in the tailings source. Hence, the observations and conclusions drawn from the curves for Depot Lake are applicable in the broader sense. Also, the dose contribution from each radionuclide would generally reflect the same trends with time as the water concentrations.

The profiles on Figure 5.5 indicate that all radionuclides increase in concentration over the initial two or three time steps. This behaviour is attributable, in part at least, to a higher overall flux of radionuclides from the water column to the sediment at time t=0 years than at time t=20 years, for example. As the radionuclide inventory builds up in the sediment, the flux from the water column to the sediments and the flux from the sediment back to the water column reduces. The behaviour of the curves once the sediments become enriched with radionuclides is dominated by other factors as discussed below.

Lead-210 concentrations are the highest of all radionuclides initially and

FIGURE 5.4

TOTAL DOSE HISTOGRAM FOR OPTION 1 - RECEPTOR 4

NOTE: HISTOGRAMS BASED ON 200 TRIALS

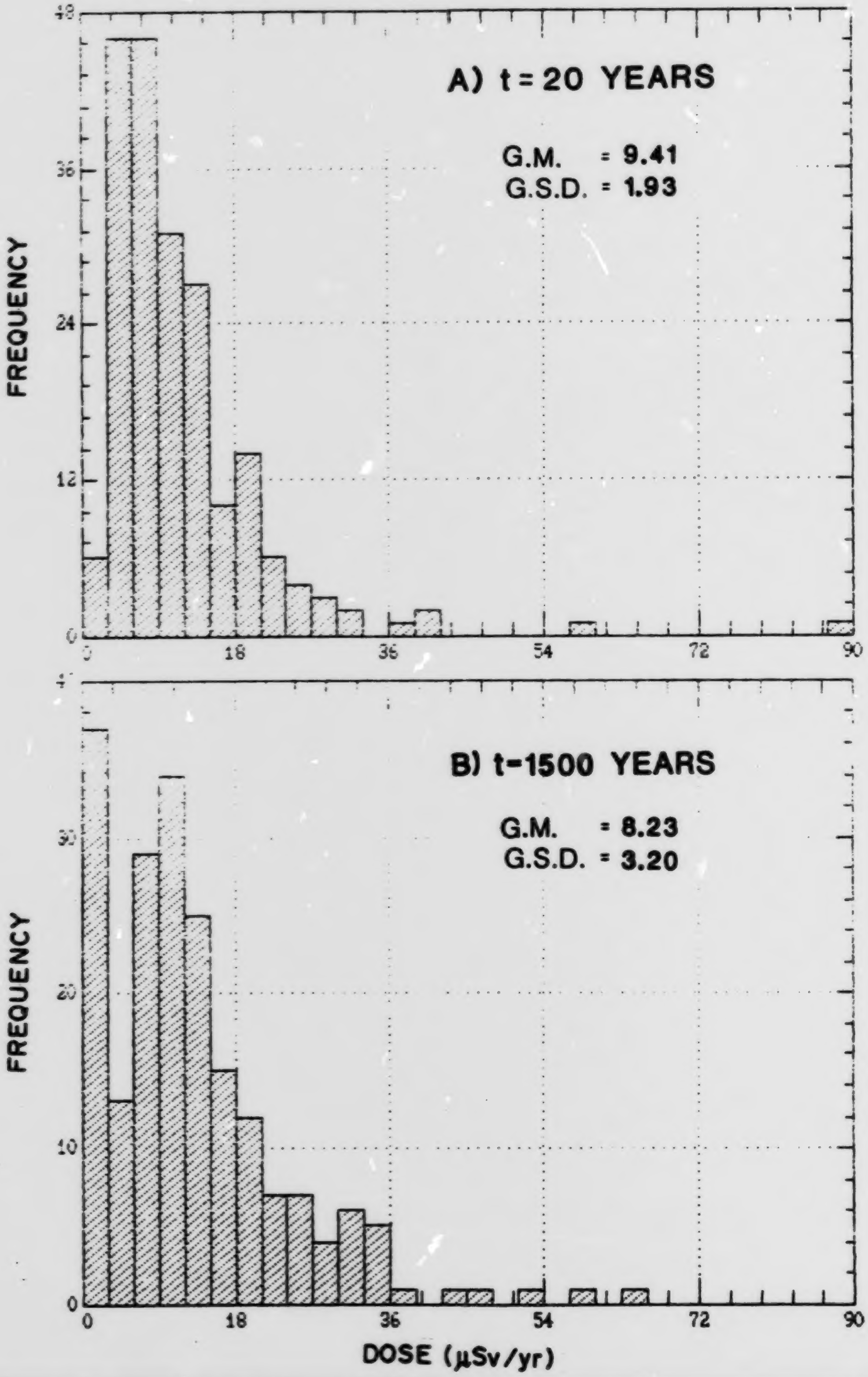

FIGURE 5.5

WATER CONCENTRATION vs TIME FOR OPTION 1 - DEPOT LAKE

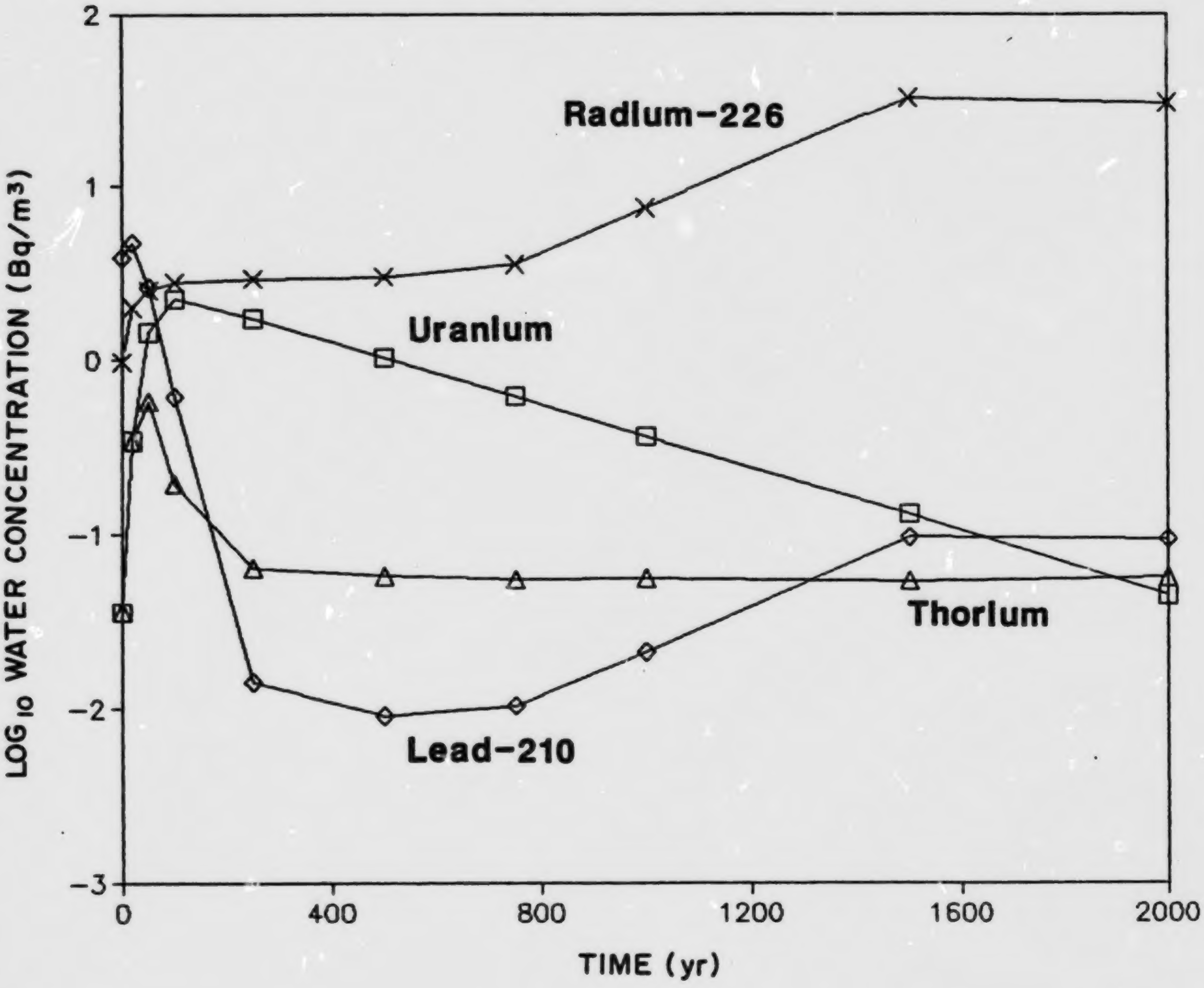

NOTE: GEOMETRIC MEAN VALUE OF 200 TRIALS

decline rapidly over the first two hundred years. Most of the lead-210 present in the tailings is assumed to exist in soluble form as a co-precipitate with lead sulphate ($PbSO_4$). This inventory of relatively soluble $PbSO_4$ results in the large initial concentration of lead-210. However, lead-210 has a relatively short radioactive half-life (21 years), which results in the sharp reduction in the lead-210 water concentration over the first 200 years. Lead-210 also ingrows from its radioactive parent, radium-226. This provides a long-term source of lead-210 and causes the concentration via lead-210 to mirror that of radium-226 in the long-term. Lead-210 does not track radium-226 in the short term because the inventory of potentially soluble radium is much less than that of lead-210 and because lead-210 has not ingrown to an equilibrium level in the radium precipitate. Hence, at early times there is insufficient input of lead-210 from radium coprecipitate dissolution to counter the radioactive decay of lead-210 in the lead sulphate precipitate.

Radium-226 levels increase slowly with time and radium-226 becomes the dominant radionuclide by year 100. The time pattern of radium-226 behaviour is explained by the gradual dissolution of barite (barium-radium sulphate) in the unsaturated tailings layer. Water infiltrating the tailings dissolves the barium-radium sulphate in the uppermost tailings layer. However, concurrent pyrite oxidation in the uppermost layer produces an abundance of sulphate ions causing the reprecipitation of some of the dissolved radium-226 as a barium-radium sulphate coprecipitate in lower layers.

Because radium forms a non-ideal solid solution with barium sulphate, the reprecipitated barium-radium sulphate contains a higher concentration of radium than the original coprecipitate. As pyrite is depleted from the unsaturated layer, more and more of the solid phase coprecipitate dissolves, resulting in a gradual increase in the amount of radium-226 released to the porewater.

Once pyrite oxidation is completed, at about year 150, the sulphate level is controlled by the dissolution of gypsum. The amount of barite which dissolves is then controlled by the sulphates from gypsum dissolution which maintains the radium concentration at a nearly constant level until year 800. Between year 800 and year 1500, the gypsum is depleted in the mixing zone and the radium level increases as more barite dissolves once the sulphate level drops. Beyond year 1500, the radium level slowly declines until such time as the soluble radium inventory in the tailings is exhausted. Because the radium level in the receiving waters is also influenced by feedback from deposited sediments, the level in the aqueous phase would not decline to background until such time as the sediments are buried. The time required to completely bury and isolate sediment is estimated to take a hundred or so years after input from the tailings ceases.

The uranium concentration is a function of pyrite oxidation and peaks during the initial 100 years. Once pyrite is depleted from the unsaturated layer, the uranium concentration declines in the source term discharge and in the receiving waters. The gradual decline in the uranium curve reflects the slow release of uranium, absorbed to particle surfaces in the mixing zone of the tailings which is modelled as a k_d-controlled phenomenum. The curve is also influenced by removal on sedimenting solids and release from decomposing sediment in lakes on the watershed as noted above in the discussion for radium.

Thorium-230 release from the tailings source is modelled as a direct function of pH and sulphate concentration and as such peaks between year 20 and year 50 when pyrite oxidation is at its maximum. As the pH in the system recovers, thorium level declines to a near constant level. The fact that the thorium level in Depot Lake remains relatively constant from about year 500 to year 2000 reflects a steady input to the watershed from the tailings once the pH of the porewater recovers and stabilizes at a constant level.

pH

The changes in pH with time at Nodes 1, 3 and 6 (see Figure 3.3) are shown on Figure 5.6. The pH level in the combined surface and seepage water flow from the Lacnor site declines to below 4.0 between years 20 and 50. This minimum

FIGURE 5.6

pH vs TIME FOR OPTION 1 - 3 WATERSHED NODES

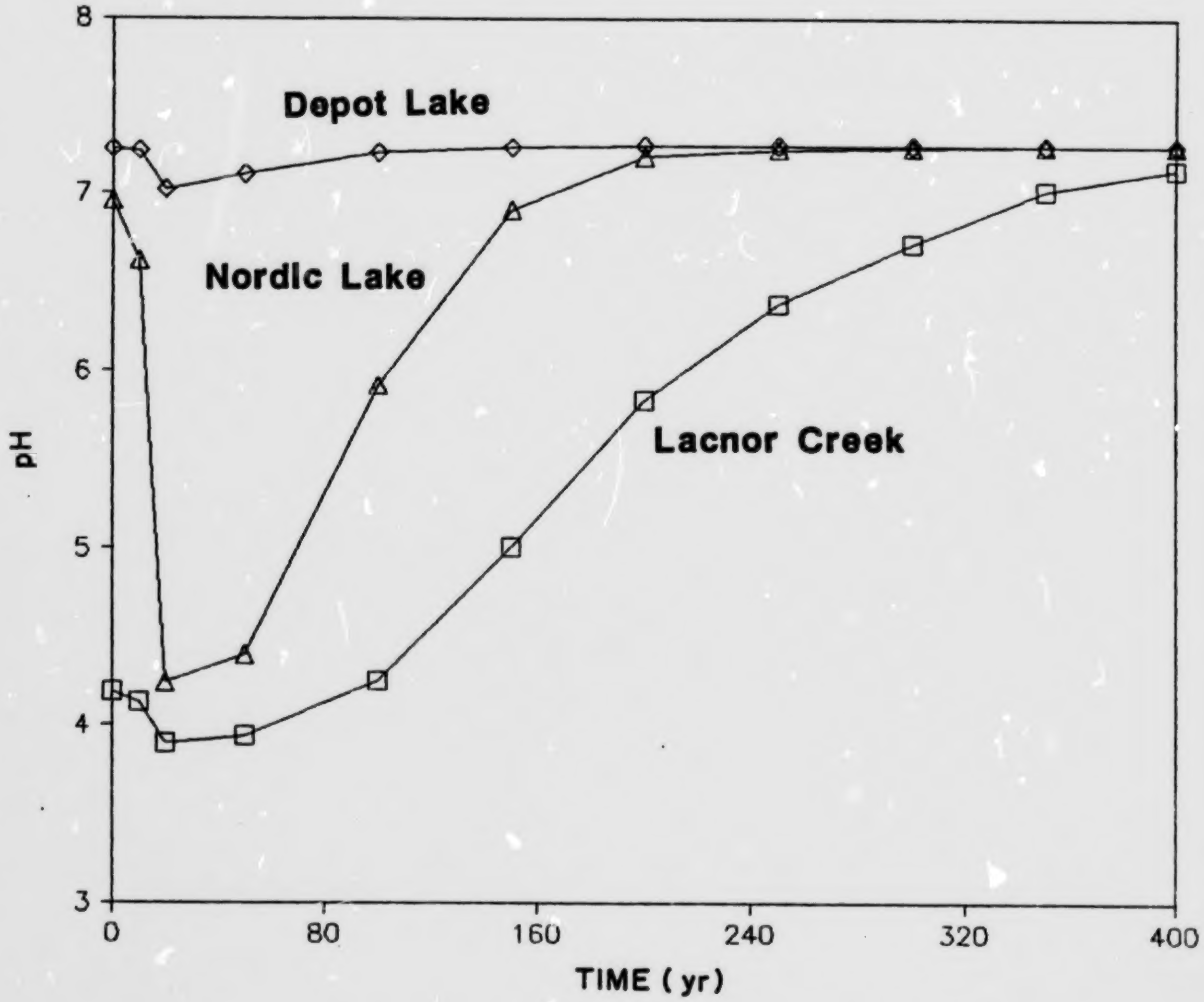

NOTE: GEOMETRIC MEAN VALUE OF 200 TRIALS

pH occurs once residual calcite is depleted from the tailings and acid conditions prevail throughout the tailings profile. Given that the pyrite oxidation rate declines continuously (i.e. it is expressed as a function of the residual pyrite content), pH recovery occurs progressively as the rate of acid generation slows down. The pH recovery is seen to start at about year 50 and the pH returns to near background conditions by year 400. Beyond year 400, pyrite oxidation in the unsaturated zone is essentially complete and the acid reaction products are flushed from the mixing zone.

Nordic Lake (Node 3) is the first downstream lake in the watershed. Runoff in the Nordic Lake sub-basin dilutes the discharge flow from Lacnor by a factor of 15:1. This buffers the downstream pH level but substantial pH depression still occurs. The pH level in Nordic Lake is predicted to decline to 4.2 or lower between years 20 and 50 and to recover thereafter as the acid input from Lacnor declines.

Surface runoff at Depot Lake (Node 6) is predicted to have sufficient buffering capacity to neutralize the acid drainage from the Lacnor site. The pH in Depot Lake is depressed by less than 0.3 pH units during the peak period of acid discharge.

5.3 Option 2: Waste Rock Cover

The waste Rock cover option is identical to the Base Case except that 0.6 m of crushed rock is applied to the exposed tailings surface. The rock cover is assumed to substantially reduce wind erosion losses but increase the amount of precipitation infiltrating the tailings.

5.3.1 Dose by Pathway

Figure 5.7 is a plot of the geometric mean dose versus time for Option 2 for each of the exposure pathways and for total dose. As for Option 1, the three largest dose contributors are, in descending order, water dose, fish dose and meat (game) dose. Meat dose is, as with Option 1, higher than fish dose over

FIGURE 5.7

DOSE vs TIME BY PATHWAY FOR OPTION 2 - RECEPTOR 4

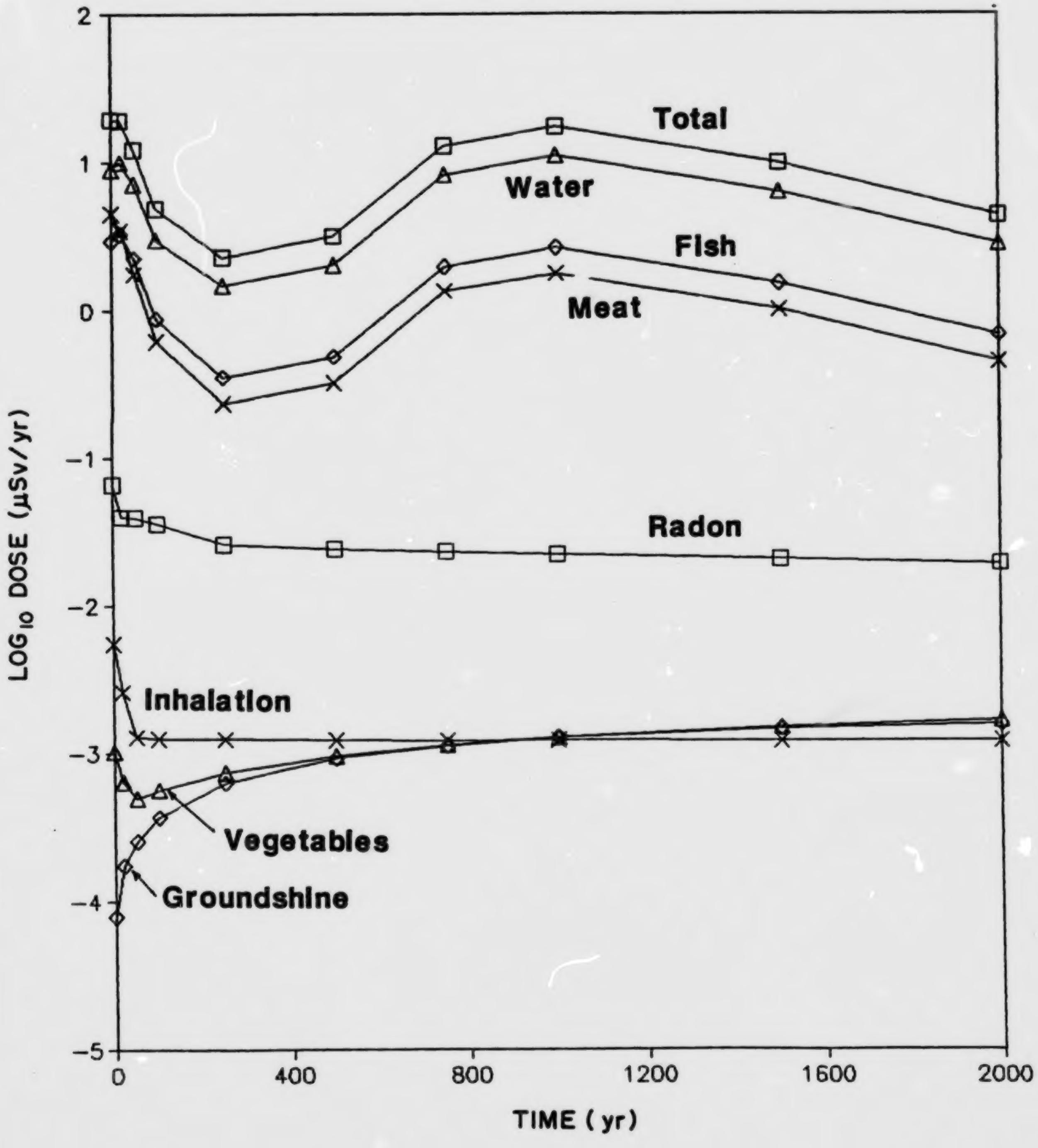

NOTE: GEOMETRIC MEAN VALUE OF 200 TRIALS

about the first twenty years of simulation. The contribution of radon to total dose is similar to Option 1 since it was assumed that the waste rock cover is porous and hence provides very little reduction in the radon release rate. However, the pathways related to wind erosion and transport of tailings dust are greatly reduced compared to Option 1 as the waste rock cover is assumed to be highly effective in limiting wind erosion of the tailings surface.

The general temporal pattern of the total dose curve is similar to that of Option 1 except that the changes occur sooner in time. This is a consequence of the way the water pathways respond to a waste rock cover as discussed in the next section.

Figure 5.8 shows frequency histograms for total dose for years 20 and 800. As for Option 1 these histograms are skewed which is suggestive of lognormal behaviour. The mean doses for this option are about twice as large as the mean doses at corresponding times for Option 1 (i.e. year 20 and a 'year' representative of future maximum dose). This is again a result of the water pathway as discussed in the next section.

5.3.2 The Water Pathway

Radionuclide Concentrations

The water concentrations at Depot Lake (Node 6 see Figure 3.3) for total uranium, total thorium, lead-210 and radium-226 are shown in Figure 5.9. The trends for all radionuclides are similar to the base case option, however, the changes occur much sooner in time. With the waste rock option, the infiltration rate into the mixing zone in the tailings pile is increased dramatically. Therefore the mixing zone flushes much more rapidly. As a consequence of the increased flow through the tailings mass, the uranium level in Depot Lake peaks at a higher level with Option 2 in the initial one hundred years, but declines more rapidly as the uranium inventory is flushed from the system. The thorium level remains essentially constant after about

FIGURE 5.8

TOTAL DOSE HISTOGRAM FOR OPTION 2 - RECEPTOR 4

NOTE: HISTOGRAMS BASED ON 200 TRIALS

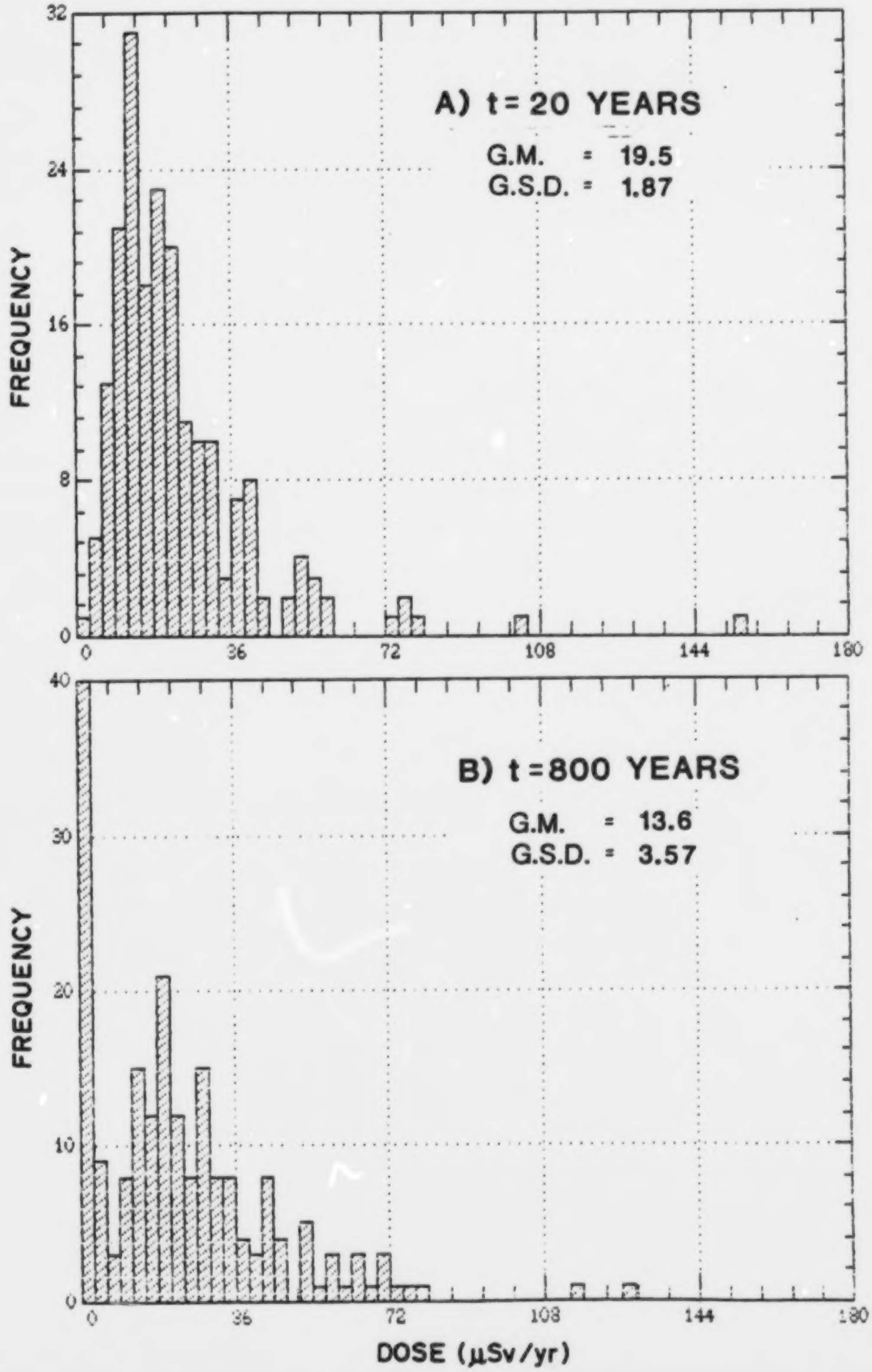

FIGURE 5.9

WATER CONCENTRATION vs TIME FOR OPTION 2 - DEPOT LAKE

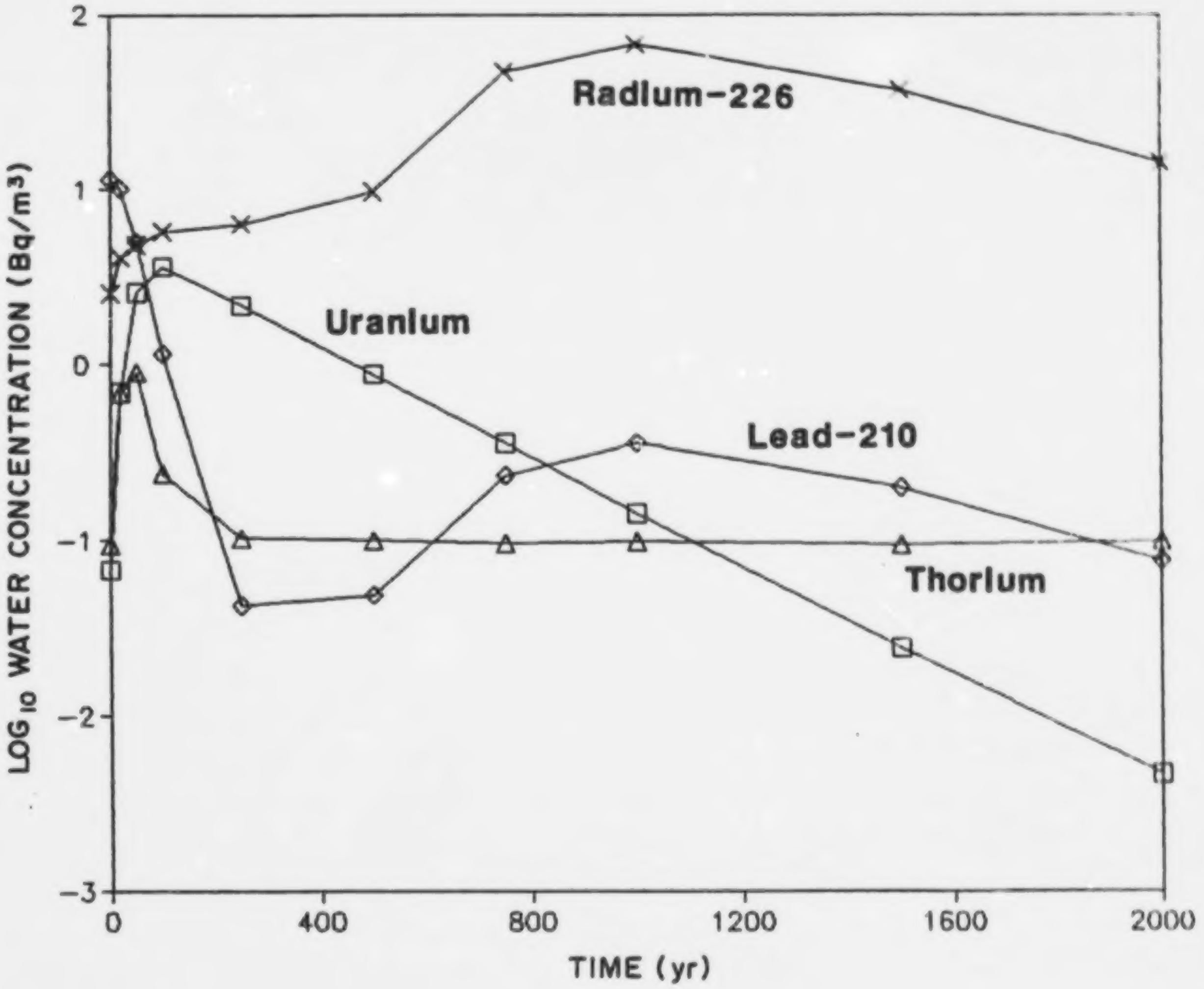

NOTE: GEOMETRIC MEAN VALUE OF 200 TRIALS

the first 250 years in Depot Lake as the input to the system is controlled strictly by the porewater pH.

Radium-226 and lead-210 levels are higher at all times during the first 1500 years because the porewater sulphate level is lower due to dilution. The reduced sulphate level increases the solubility of both the lead sulphate precipitate and barium/radium sulphate coprecipitate. The concentration of both nuclides peak much sooner as gypsum is depleted between year 500 and year 1000. The peak concentrations occur around year 1000 and decline as the radium and lead inventories are leached from the pile.

pH

The pH changes with time for Option 2 at nodes 1, 3 and 6 are shown on Figure 5.10. The pH curves for all nodes closely parallel those for the the base case. Because the rate of flushing of acidity from the tailings is higher with Option 2, the result is a slightly lower pH level at year 20.

5.4 Option 3: Pyrite Removal

This option adds 2.0 m of depyritized tailings to the exposed surface of the Lacnor tailings. Calcite is added to neutralize any acid produced from residual pyrite oxidation and the permeable dams on the south rim are replaced. This causes the water table in the tailings to rise into the depyritized tailings cover. As a consequence, less pyrite is available to be oxidized with this option.

5.4.1 Dose by Pathway

Figure 5.11 is a plot of geometric mean dose versus time for each of the pathways and total dose for Option 3. In effect the doses are very similar to those predicted for Option 1. The water pathways continue to dominate for all times at approximately the same dose level as for Option 1. The nominal (about 20 %) reduction in radionuclide concentrations is offset by the

FIGURE 5.10

pH vs TIME FOR OPTION 2 - 3 WATERSHED NODES

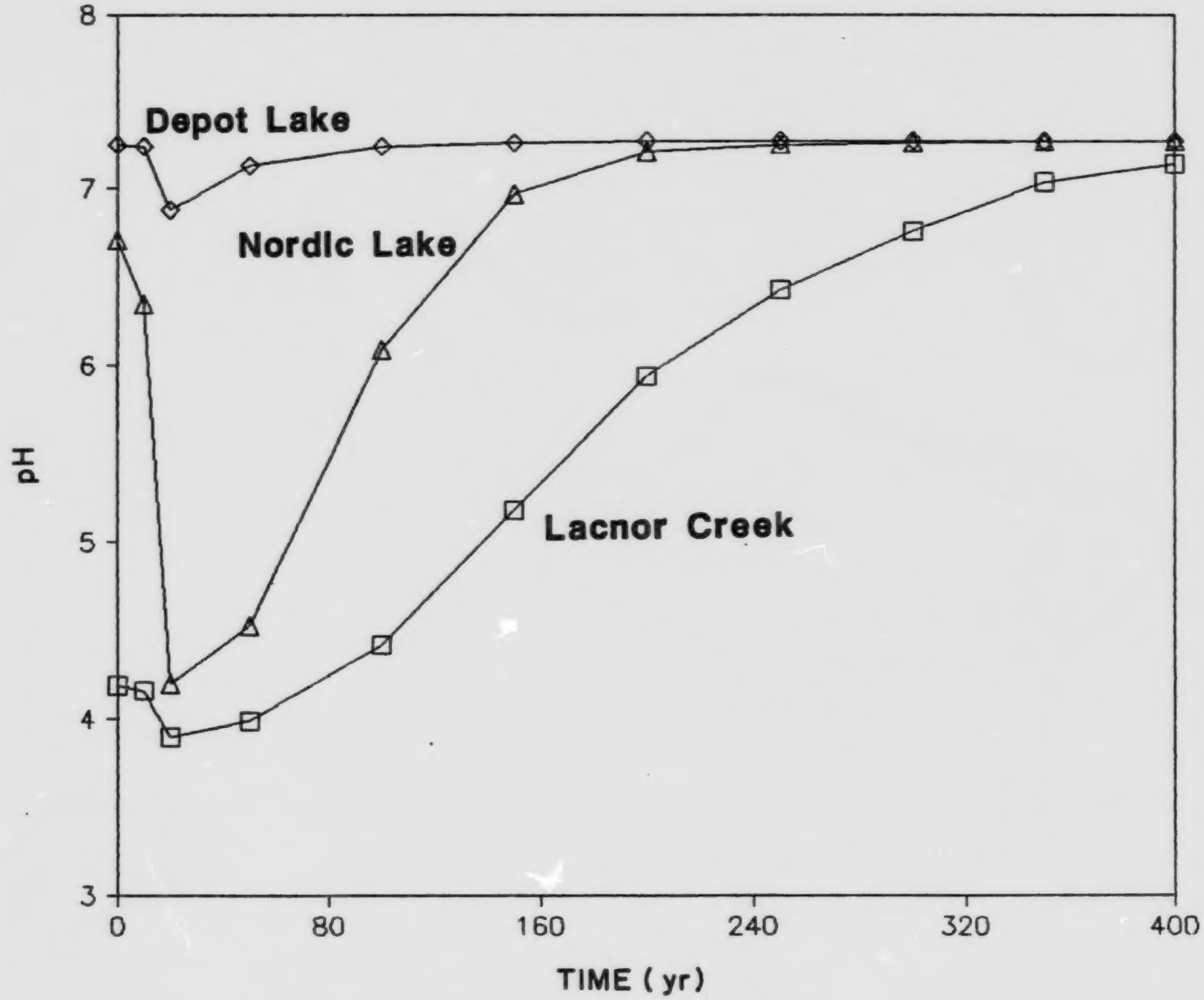

NOTE: GEOMETRIC MEAN VALUE OF 200 TRIALS

FIGURE 5.11

DOSE vs TIME BY PATHWAY FOR OPTION 3 - RECEPTOR 4

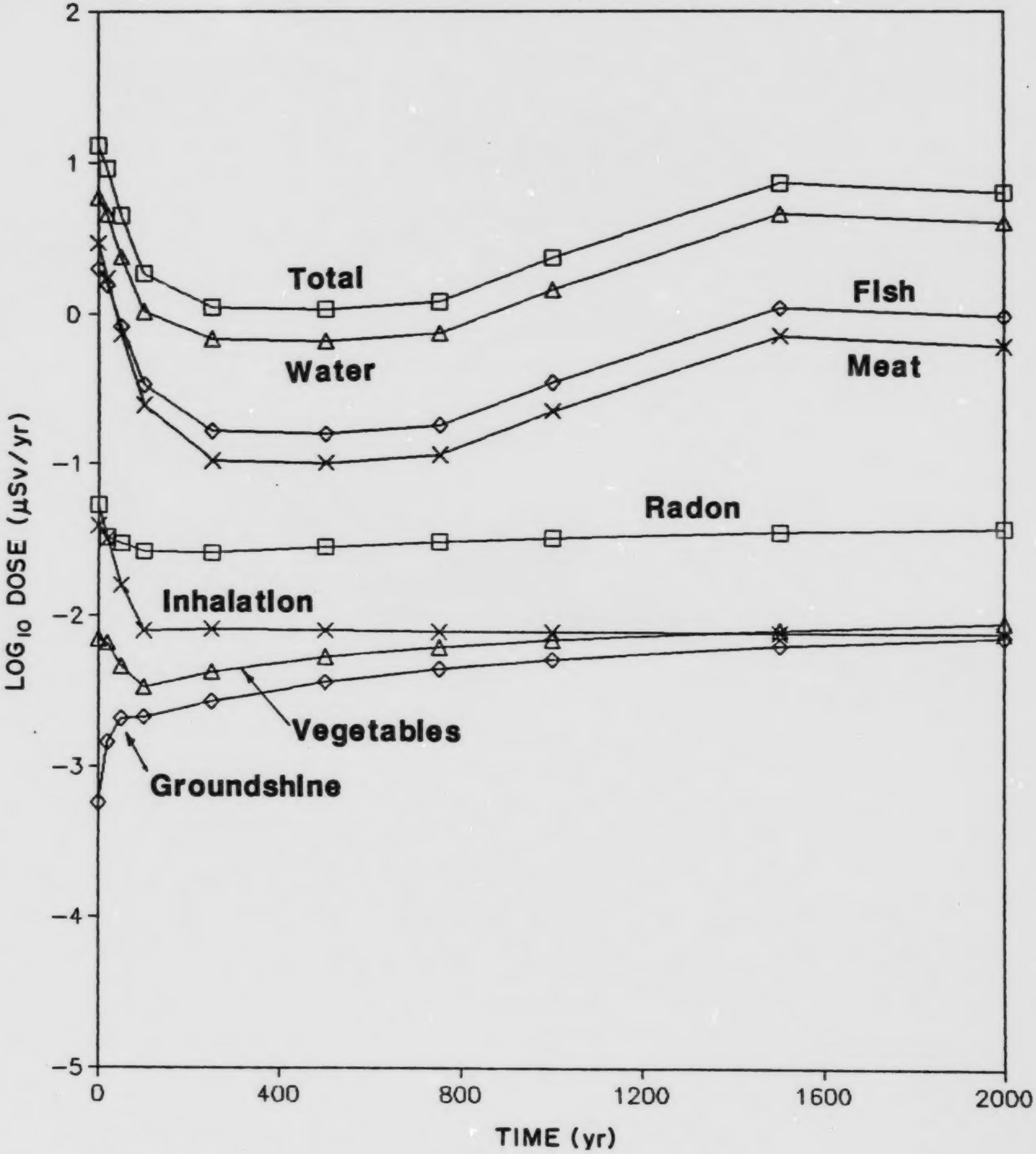

NOTE: GEOMETRIC MEAN VALUE OF 200 TRIALS

somewhat enhanced release of radium-226 and lead-210 which is attributable to a lower sulphate level in the porewater. The lower sulphate concentration is due to the addition of calcite to the depyritized tailings, which limits the rate of pyrite oxidation, and to the reduced pyrite content of the cover.

Figure 5.12 shows histograms of total dose at year 20 and at year 1500. The mean doses are similar to the mean doses for Option 1. Again the histograms have a skewed shape suggestive of lognormal behaviour.

5.4.2 The Water Pathways

Radionuclide Concentrations

The water concentration at Depot Lake (Node 6) for total uranium, total thorium, lead-210 and radium-226 are shown on Figure 5.13. The low uranium level may be attributed to the fact that there is little pyrite available to oxidize. Similarily, the thorium level, which is modelled as a function of pH, remains low as the pH does not drop below 4.5 in the mixing zone.

With the exception of the first 20 years, both lead-210 and radium-226 levels are essentially equivalent to the base case option. During the initial 20 years, these radionuclides are at higher concentrations because the sulphate level is lower than in the base case as a consequence of less pyrite being oxidized. However, once the sulphate level is controlled by gypsum solubility, the radium and lead levels are essentially the same as for the base case.

pH

The pH changes with time, at Nodes 1, 3 and 6 (see Figure 3.3) are shown on Figure 5.14. The pH at Node 1 is depressed to a much lesser extent than noted with Options 1 and 2 (i.e. pH of 5 versus 4) as a consequence of the slow oxidation of residual pyrite in the tailings cover. For the same reason, the discharge from the tailings area has little effect on the pH at downstream

FIGURE 5.12

TOTAL DOSE HISTOGRAM FOR OPTION 3 - RECEPTOR 4

NOTE: HISTOGRAMS BASED ON 200 TRIALS

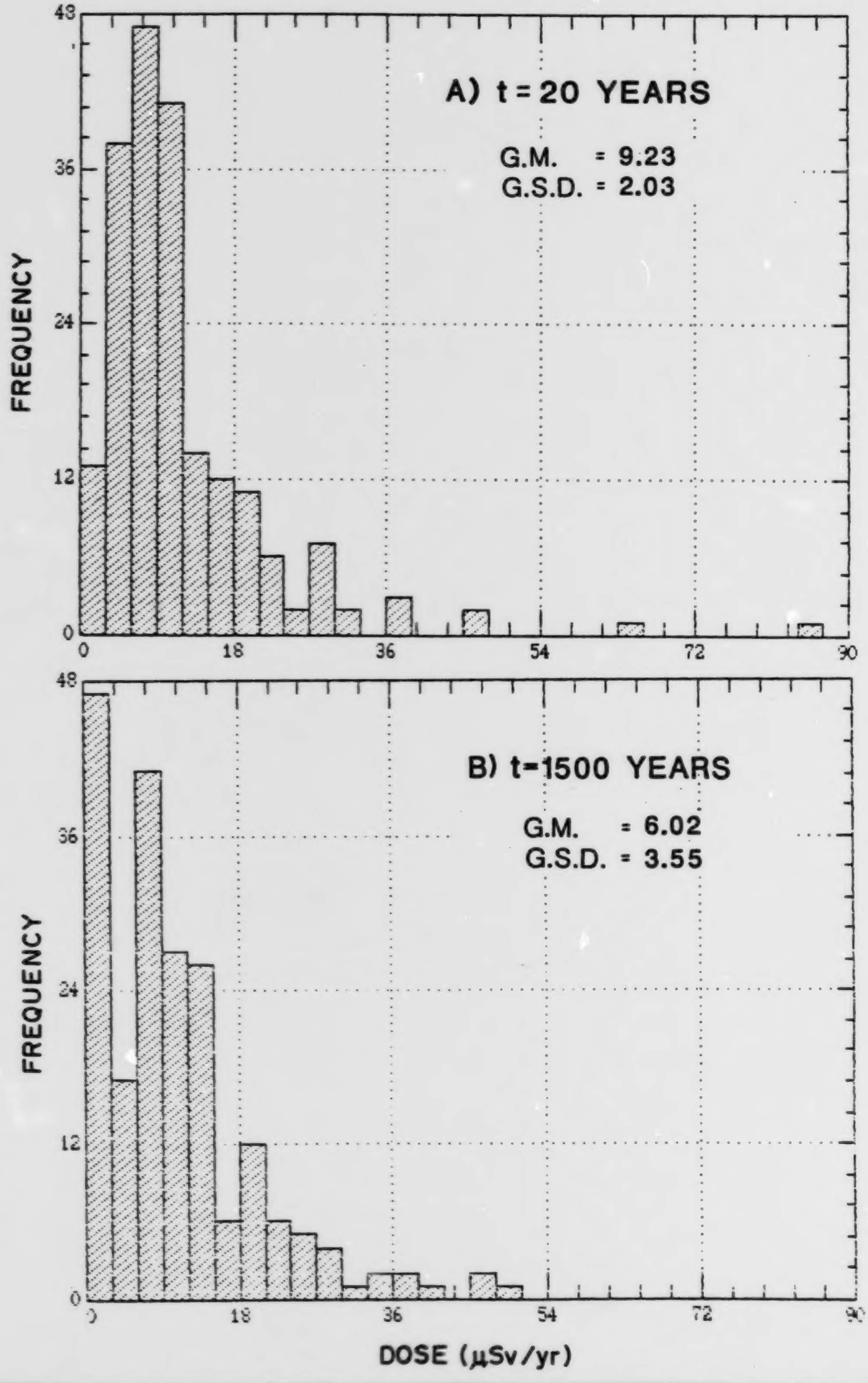

FIGURE 5.13

WATER CONCENTRATION vs TIME FOR OPTION 3 - DEPOT LAKE

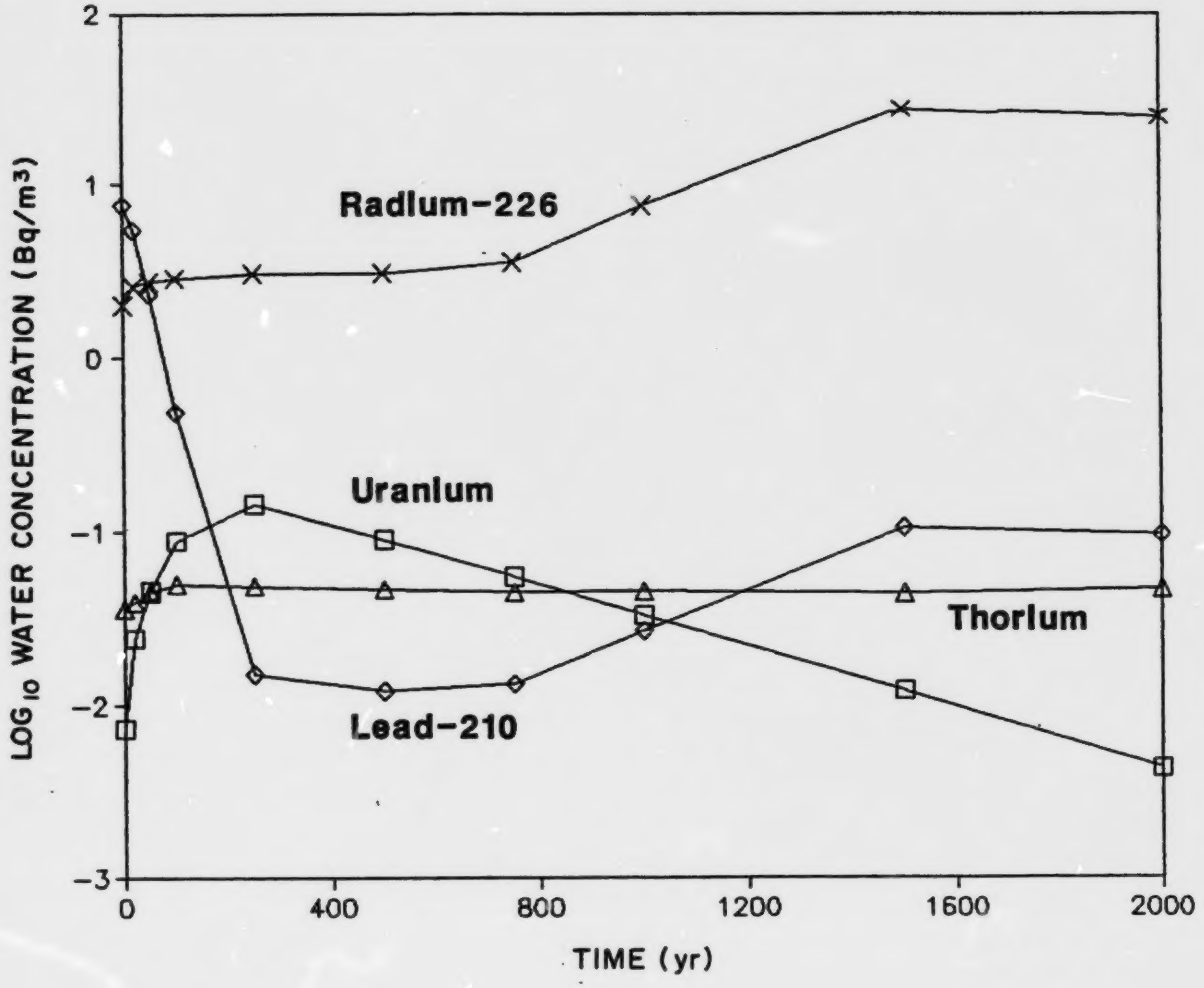

NOTE: GEOMETRIC MEAN VALUE OF 200 TRIALS

FIGURE 5.14

pH vs TIME FOR OPTION 3 - 3 WATERSHED NODES

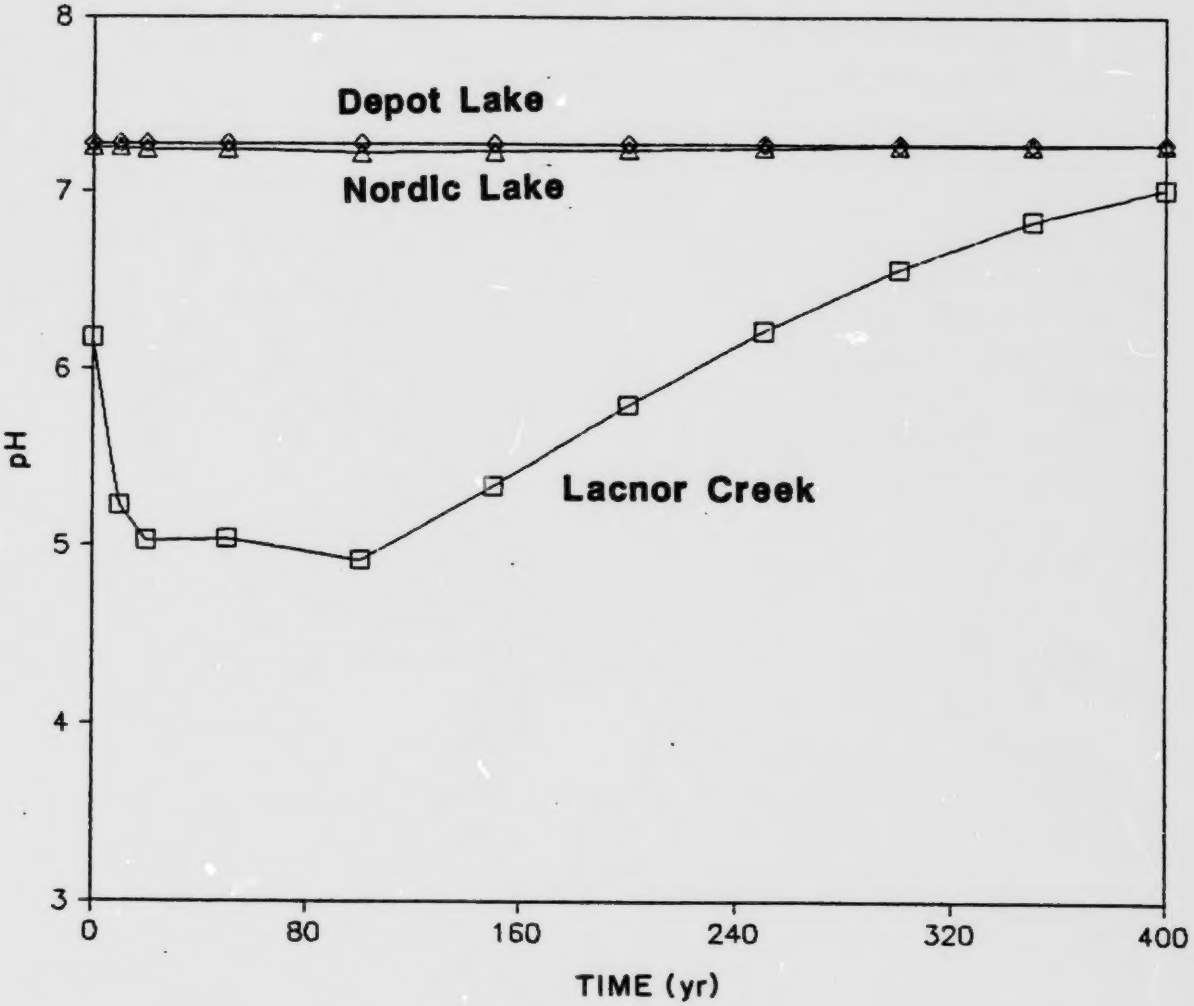

NOTE: GEOMETRIC MEAN VALUE OF 200 TRIALS

locations (i.e. Nodes 3 and 6). The pH at Node 1 takes a long time to recover due to the slow rate at which the pyrite is oxidized.

5.5 Option 4: Glacial Till Cover

This option adds 2.0 m of glacial till to the exposed surface of the Lacnor tailings. The permeable dams on the south rim are replaced and the water table rises into the till cover. The amount of pyrite which can potentially be oxidized in the submerged tailings is a function of the availability of oxygen which is limited to that carried downward with infiltrating water. Also, because the tailings are buried below 2.0 m of cover, the temperature is lower which reduces the rate of pyrite oxidation.

5.5.1 Dose by Pathway

Figure 5.15 shows a plot of the geometric mean dose by pathway and total dose versus time for Option 4. From Figure 5.15 it is readily seen that the air pathways have been eliminated as dose contributors. The dose via the water pathways is essentially the same as that for Option 1.

Figure 5.16 shows histograms of total dose for years 20 and 1500 for Option 4. The mean dose at t=20 years is marginally greater than that for the base case option, primarily due to more lead sulphate precipitate and radium sulphate coprecipitate being dissolved in Option 4. At t=1500 years, however, the mean dose for Option 4 is less than that for Option 1 primarily because the radium level is lower. As before, the histograms are suggestive of lognormal behaviour.

5.5.2 The Water Pathways

Radionuclide Concentrations

The water concentrations at Depot Lake (Node 6) for total uranium, total thorium, lead-210 and radium-226 are shown in Figure 5.17. The concentrations

FIGURE 5.15

DOSE vs TIME BY PATHWAY FOR OPTION 4 - RECEPTOR 4

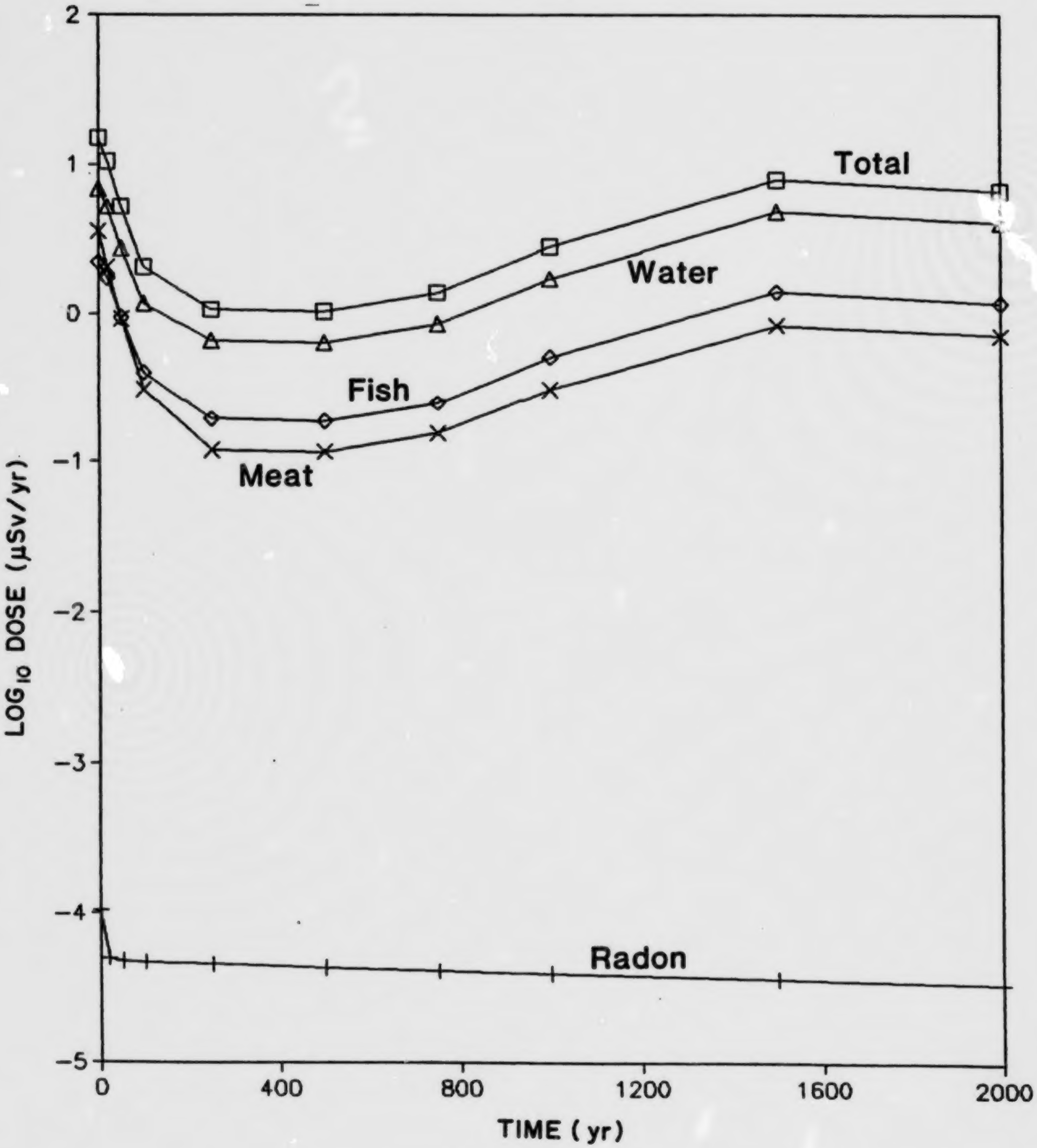

NOTE: GEOMETRIC MEAN VALUE OF 200 TRIALS

FIGURE 5.16

TOTAL DOSE HISTOGRAM FOR OPTION 4 - RECEPTOR 4

NOTE: HISTOGRAMS BASED ON 200 TRIALS

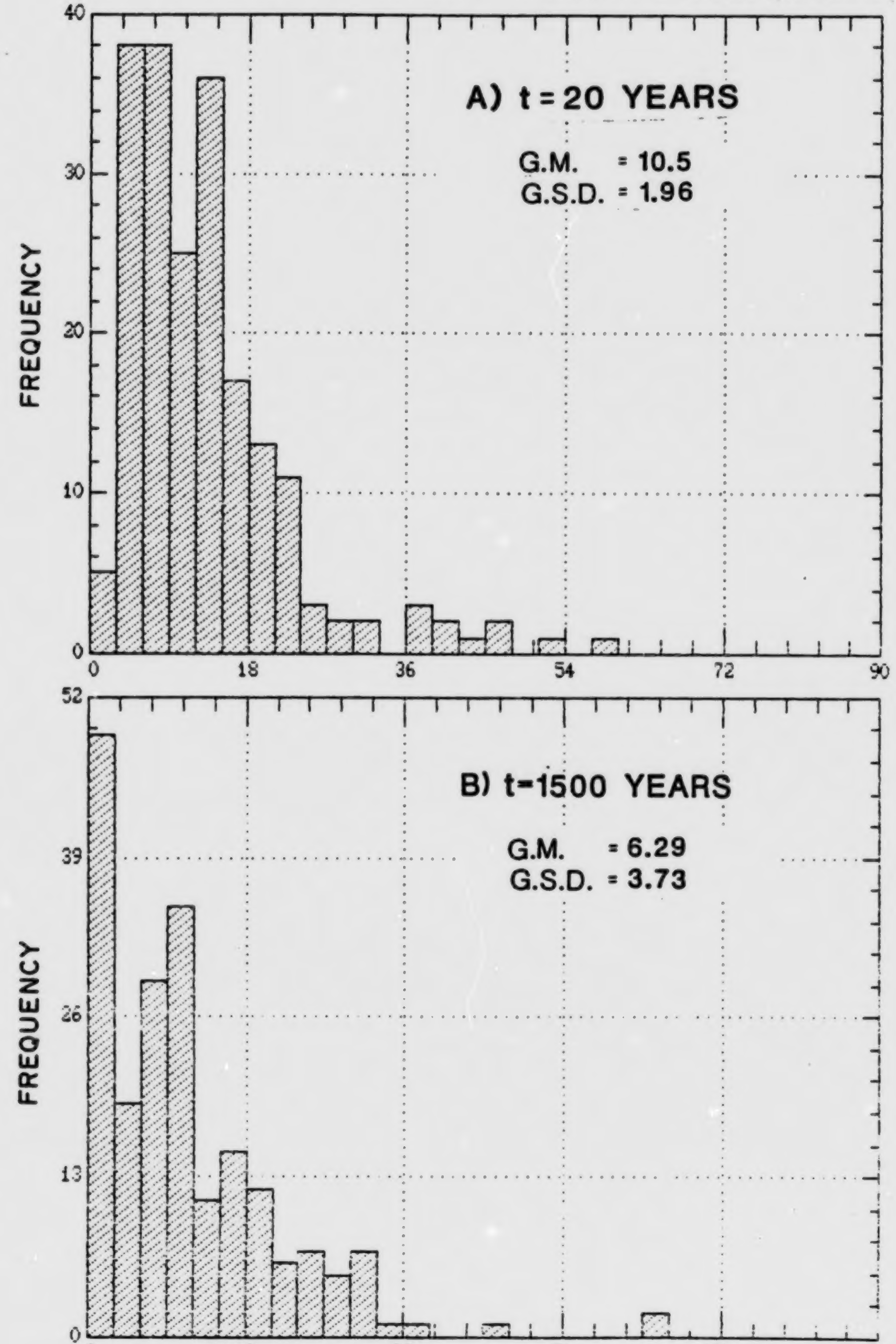

FIGURE 5.17

WATER CONCENTRATION vs TIME FOR OPTION 4 - DEPOT LAKE

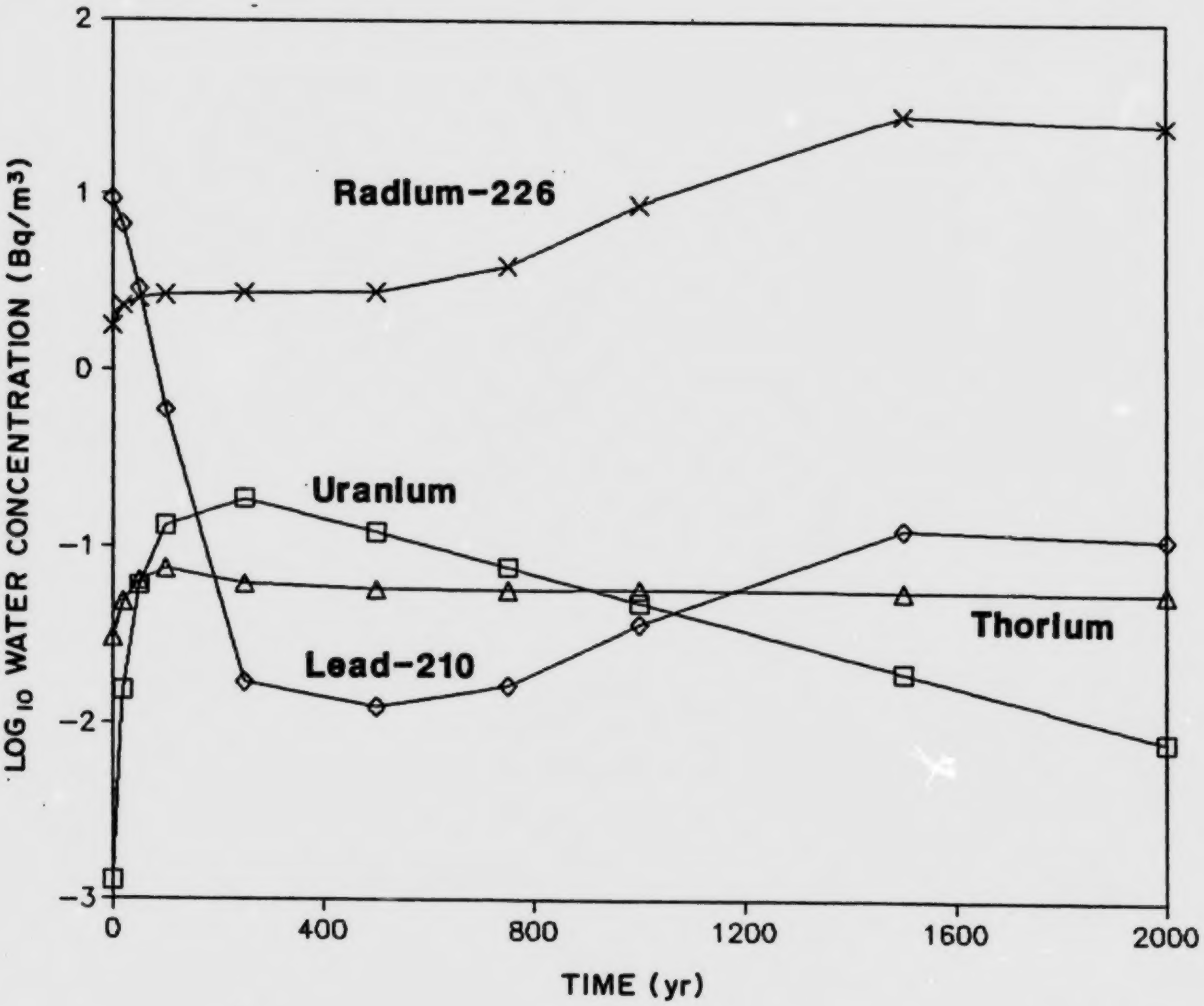

NOTE: GEOMETRIC MEAN VALUE OF 200 TRIALS

of all radionuclides are almost identical to those for Option 3, pyrite removal. Because there is minimal buffering in this system, the pH level is actually lower than the pyrite removal option. This results in a slightly higher thorium level.

pH

The pH changes with time at Nodes 1, 3 and 6 are shown on Figure 5.18. The trends in pH levels at the nodes are the same as for Option 3. The pH at Node 1 falls lower in Option 4 than in Option 3 as the system is not buffered with calcite. The pH at Node 3 is affected slightly more than in Option 3, however in neither case is there a significant pH shift. The pH at Depot Lake (Node 6) shows little change over the entire 400 years simulation period.

5.6 Option 5: Water Cover

With the water cover option, a new dam is constructed to submerge the tailings. The tailings are assumed to be saturated with one half the exposed surface covered with ponded water. Due to the high water table over the entire tailings area, the fraction of the net precipitation which infiltrates and moves through the tailings was assumed to be considerably less than with the other options. Consequently, the mass rate of flushing of radioactive and nonradioactive constituents from the tailings is expected to be less.

5.6.1 Dose by Pathway

Figure 5.19 is a plot of geometric mean dose versus time for each pathway and for total dose for Option 5. Again, the total dose is dominated by contributions from the water pathways as, for practical purposes, the dose via the air pathways is relatively insignificant. Total dose for Option 5 is lower at all times than for Option 1. This is partly due to the effective elimination of the air pathways but more importantly it is due to the rates at which radionuclides leach from the tailings and enter the water environment. The latter aspect is discussed in the next section.

FIGURE 5.18

pH vs TIME FOR OPTION 4 – 3 WATERSHED NODES

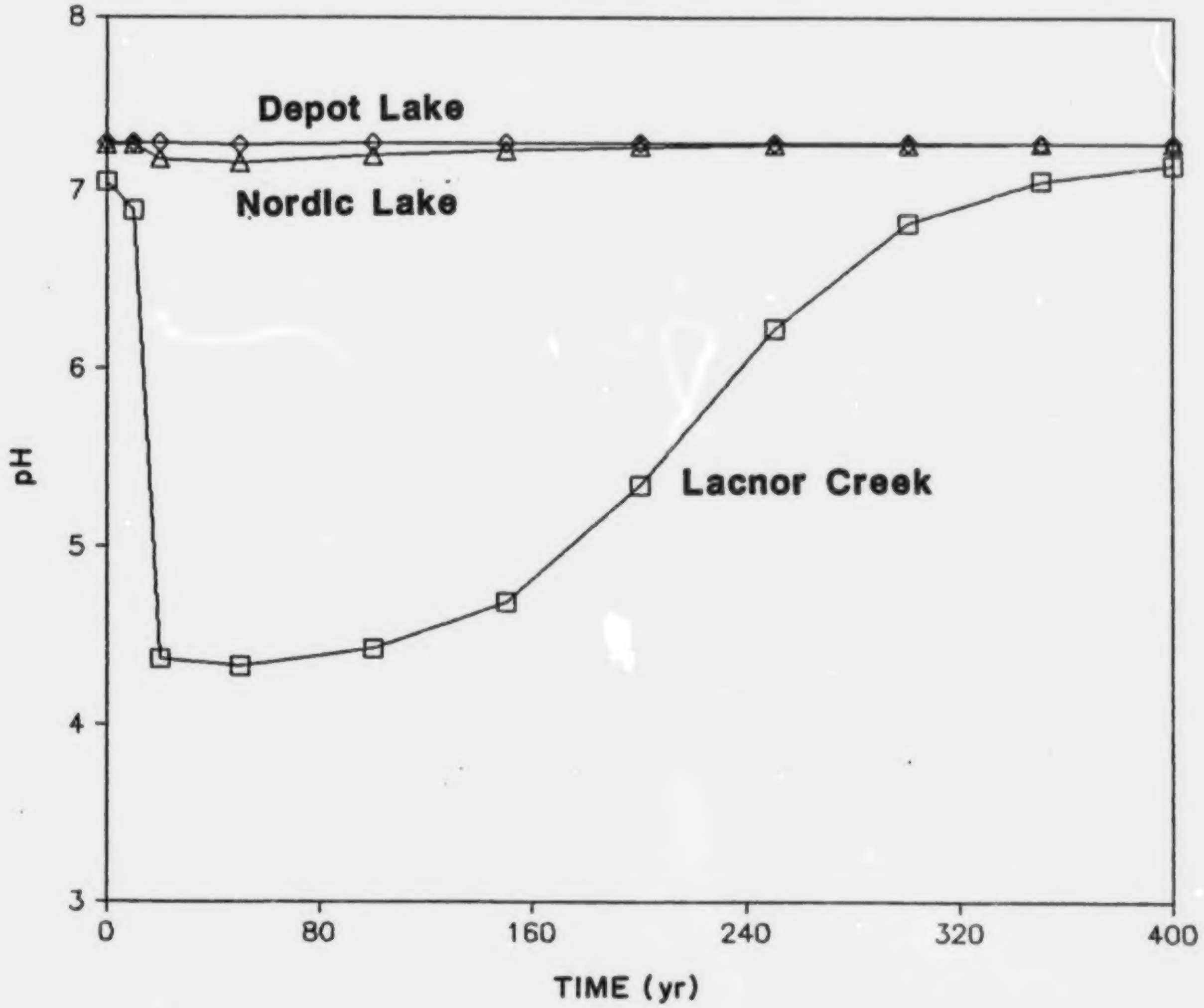

NOTE: GEOMETRIC MEAN VALUE OF 200 TRIALS

FIGURE 5.19

DOSE vs TIME BY PATHWAY FOR OPTION 5 - RECEPTOR 4

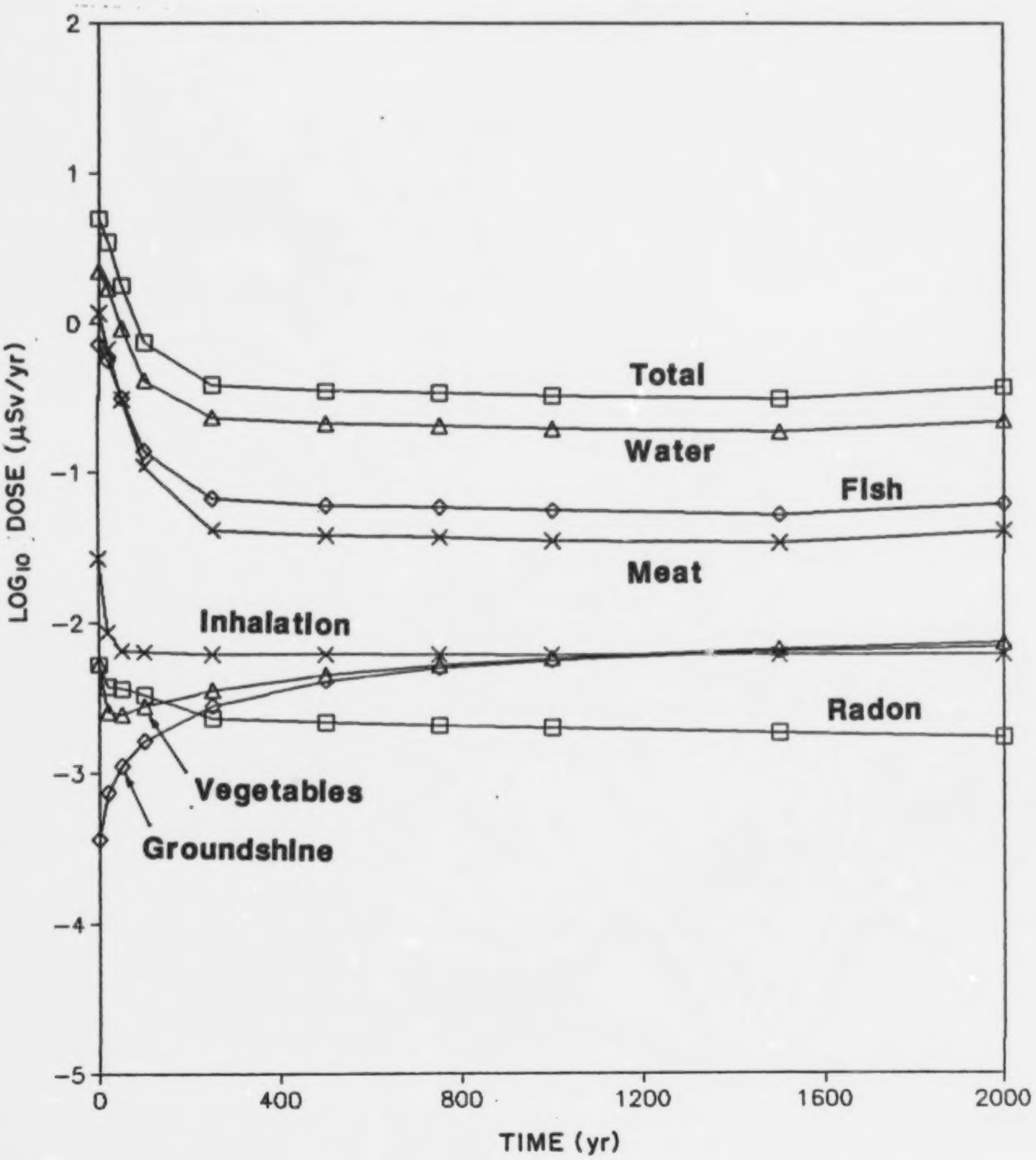

NOTE: GEOMETRIC MEAN VALUE OF 200 TRIALS

Figure 5.20 is a histogram of total dose for year 20 and year 1500. By comparison to Figure 5.4 it can be seen that at year 20 the mean dose due to Option 5 is about 37% of that due to Option 1 at the same time. The comparison of the two options at year 1500 is more dramatic with the mean dose for Option 5 being less than 1/25th of the mean dose for Option 1.

5.6.2 The Water Pathways

Radionuclide Concentration

The concentrations of total uranium, total thorium, lead-210 and radium-226 in Depot Lake are shown in Figure 5.21. In contrast to the other options, the water phase concentrations in Option 5 are dramatically different for several of the nuclides.

The concentration of uranium is substantially lower than predicted for Options 1 and 2 but similar to Options 3 and 4. The uranium level with Option 5 does not increase or decrease as rapidly as noted in Options 3 and 4. This is because the flushing rate from the tailings mixing zone is much lower for the water cover option therefore the downstream changes also occur more slowly.

The concentration of thorium in the mixing zone is the same as noted in Options 3 and 4 primarily because the pH of all three options are similar. The thorium level at Depot Lake is lower, however, than for Options 3 and 4 because the flushing rate of thorium from the mixing zone is much lower.

As with thorium, radium-226 and lead-210 levels in the receiving waters are much lower with the water cover option as compared with all other options. As noted above, this is because the flushing rate of porewater from the mixing zone is considerably lower than modelled for the other options.

pH

The changes in pH at Nodes 1, 3 and 6 (see Figure 3.2) are shown in Figure

FIGURE 5.20

TOTAL DOSE HISTOGRAM FOR OPTION 5 - RECEPTOR 4

NOTE : HISTOGRAMS BASED ON 200 TRIALS

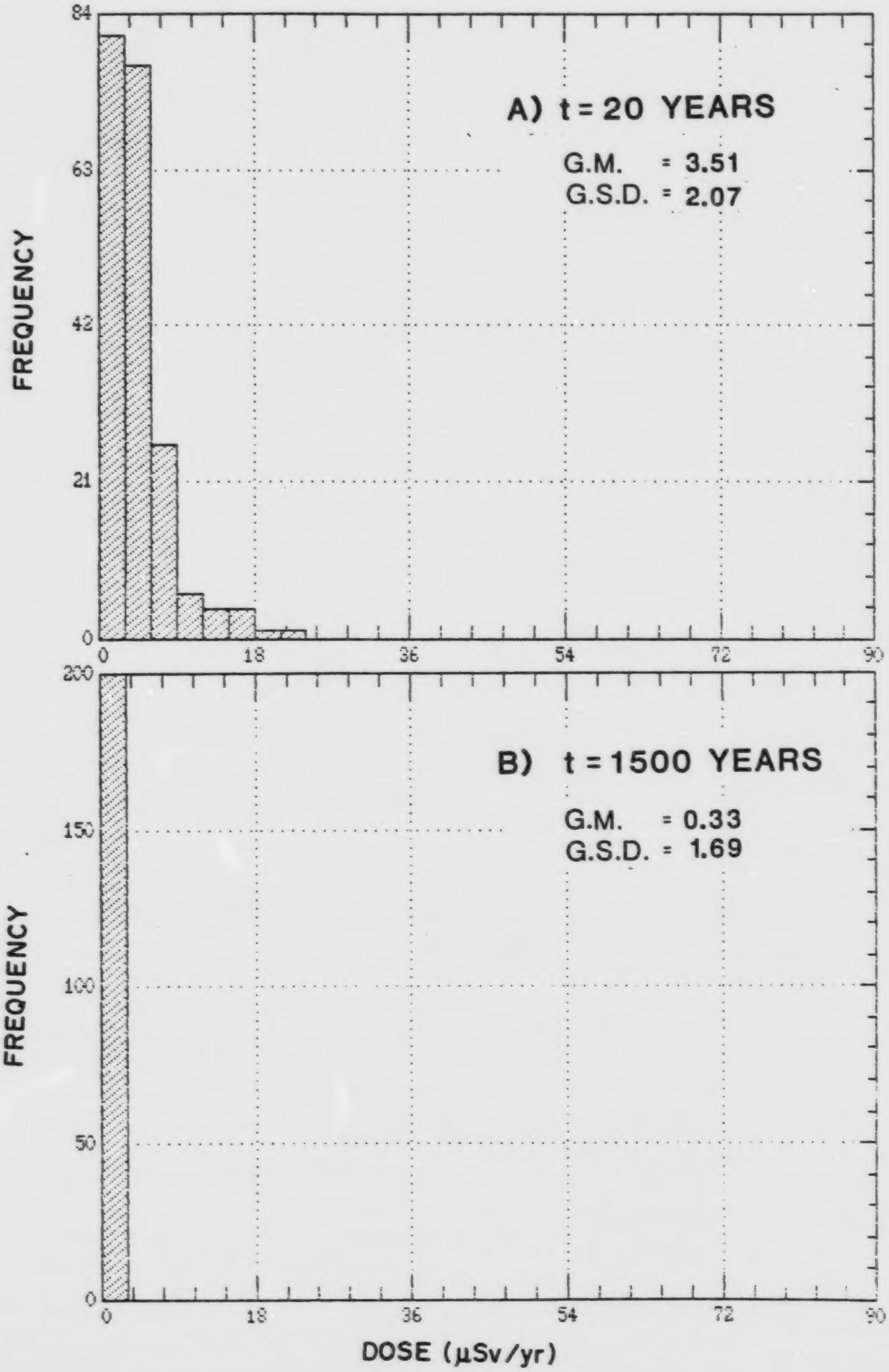

FIGURE 5.21

WATER CONCENTRATION vs TIME FOR OPTION 5 - DEPOT LAKE

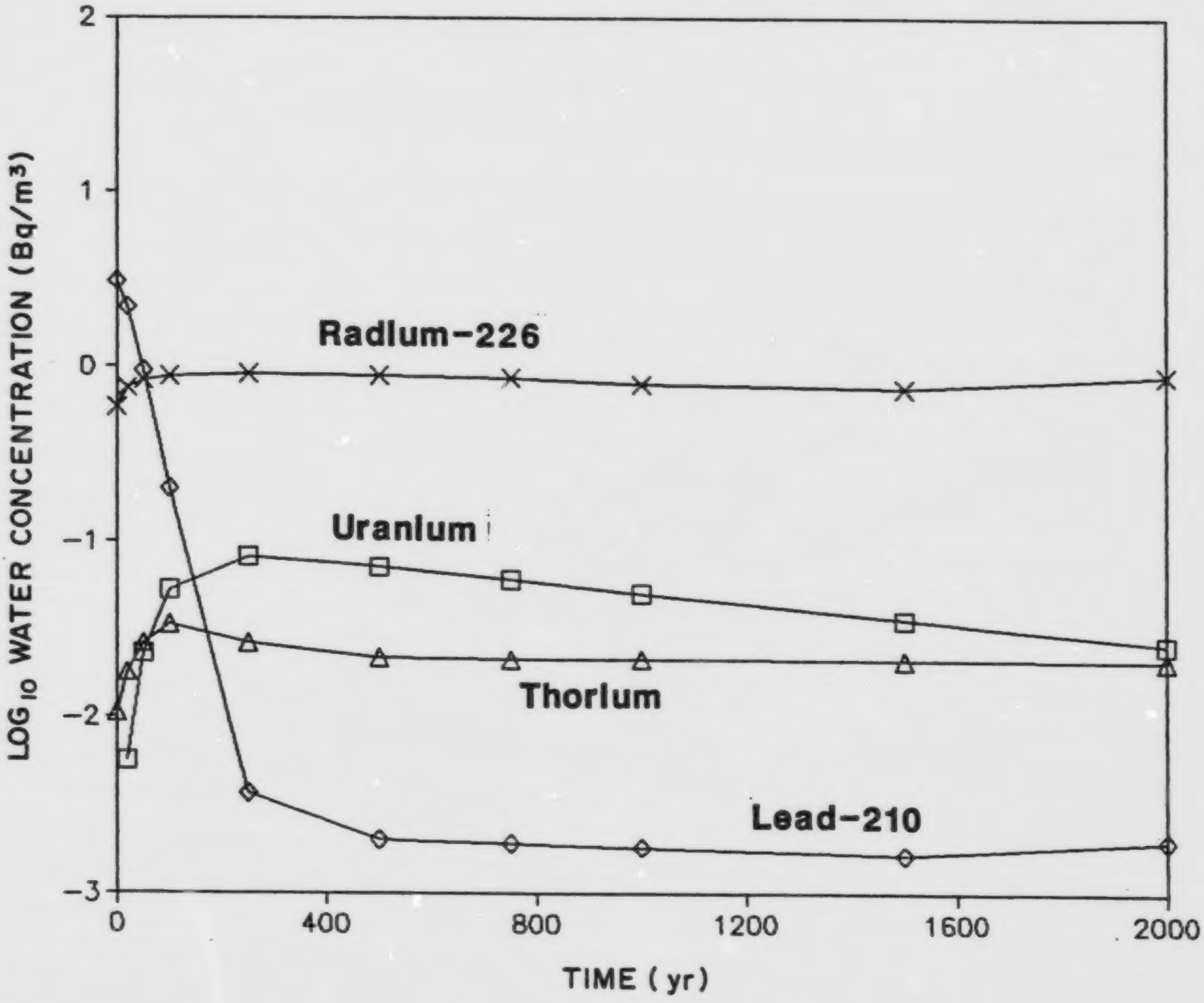

NOTE: GEOMETRIC MEAN VALUE OF 200 TRIALS

5.22. The pH trends with Option 5 are similar to the curves plotted for Option 4. This similarity was initially unexpected since the much lower flushing rate of porewater from the tailings with Option 5 should mean less acidity is added to the watershed. On further reflection, however, it was determined that the lower flushing rate with Option 5 was offset by a higher pyrite oxidation rate. The higher oxidation rate was determined from an independent evaluation of the effect of temperature on the rates of pyrite oxidation for the two options and included in the input parameter specifications.

5.7 Summary

Figure 5.23 is a plot of the geometric mean values of total dose versus time, for receptor 4, for each of the tailings closeout options included in the comparison to demonstrate the use of UTAP.3. The lowest mean dose at all times is that for Option 5 (water cover). The largest mean dose for all times less than about 1500 years is that for Option 2 (waste rock cover). The dose for Option 5 is lowest because it has the lowest rate of release of radionuclides to the water environment. The dose is higher in Option 2 because of the increased flushing of the tailings by precipitation. In the longer term, however, as leachable radium is depleted, the total dose for this pathway is predicted to decline. This is seen in Figure 5.23 as the dose for Option 2 becomes the second lowest by about year 1800.

The total dose associated with the other three options all exhibited essentially the same behaviour. The peak doses with Options 1, 3 and 4 occur around year 1500 and decline slowly thereafter.

The largest geometric mean dose calculated for Option 2, involving closeout with a waste rock cover, was in the order of 20 μSv.yr^{-1} (2 mrem.yr^{-1}). This dose is only about 1% of normal annual background dose (including that due to radon-222) and well within the normal variability of natural annual dose.

In terms of pH, Options 1 and 2 have the largest effect. The pH in Nordic

FIGURE 5.22

pH vs TIME FOR OPTION 5 - 3 WATERSHED NODES

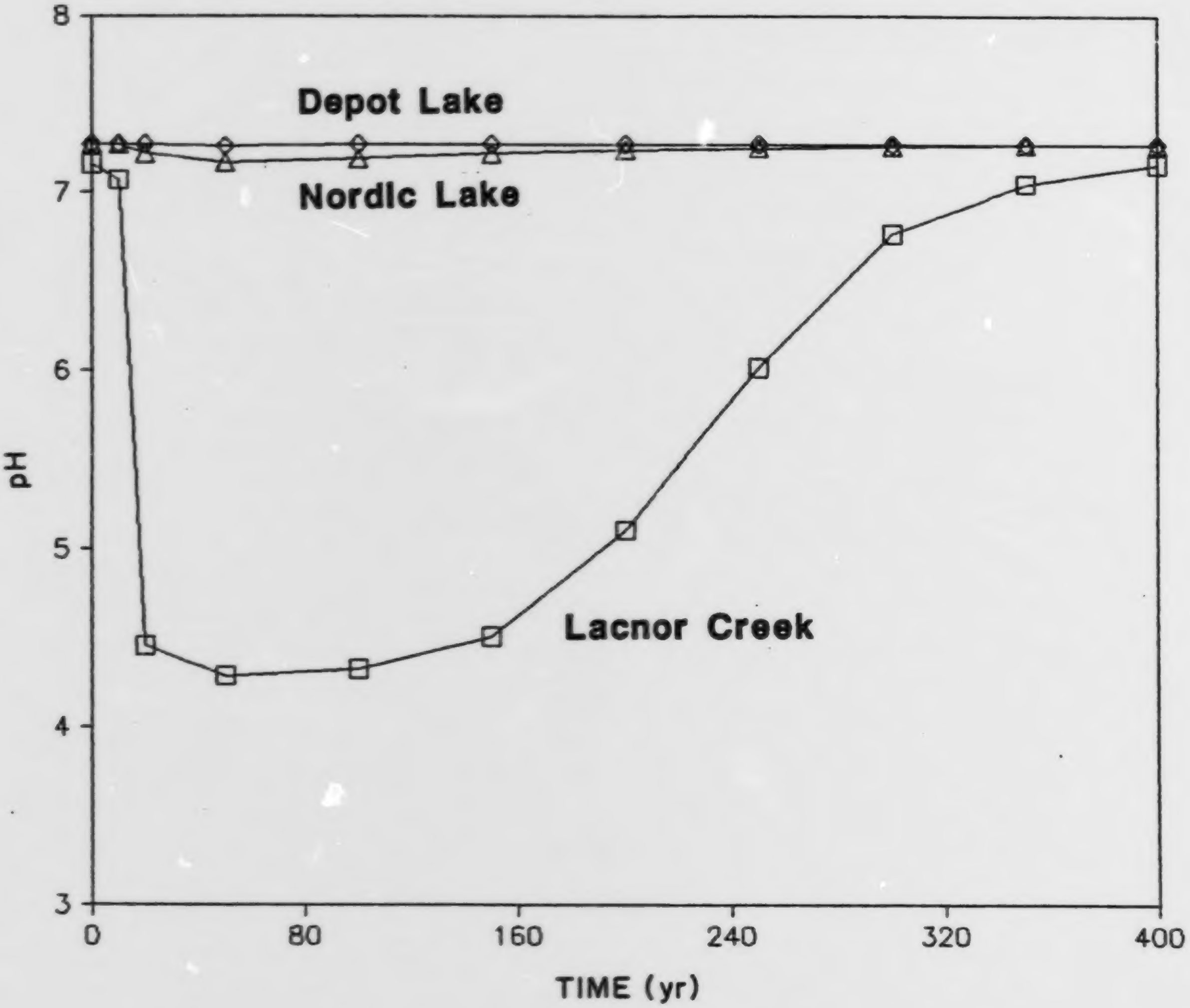

NOTE: GEOMETRIC MEAN VALUE OF 200 TRIALS

FIGURE 5.23

TOTAL DOSE vs TIME BY ALL OPTIONS

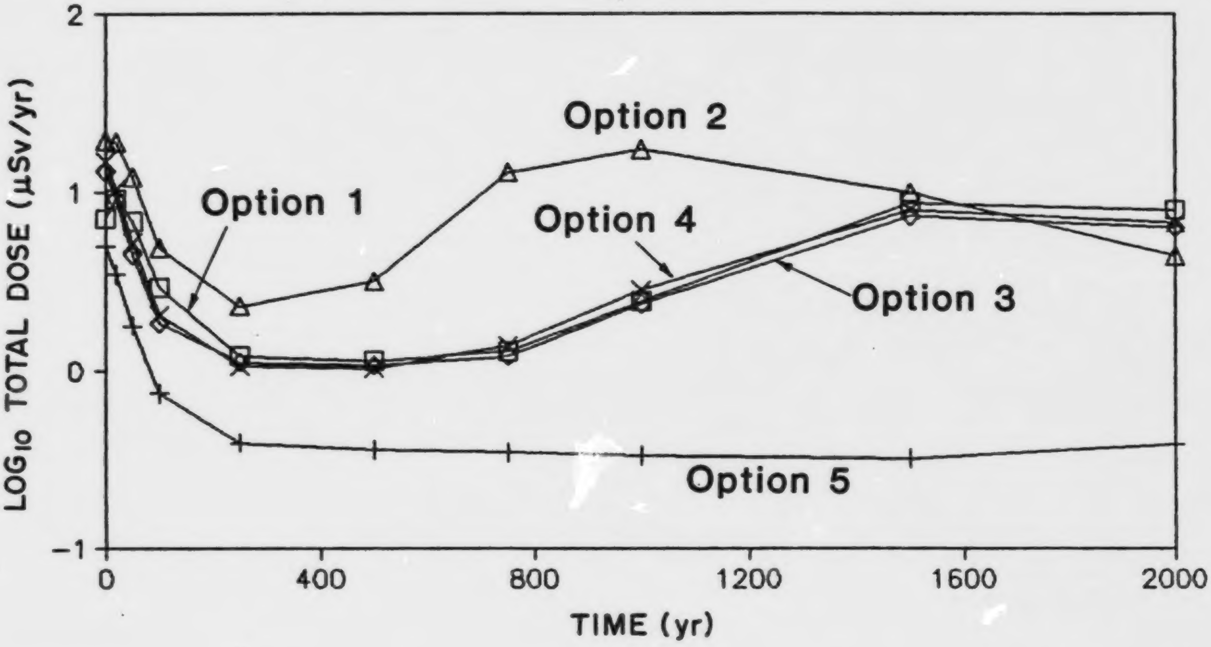

NOTE: GEOMETRIC MEAN VALUE OF 200 TRIALS

Lake is reduced to below 4.3 with both options (see Figure 5.24) although the effect lasts for only about 200 years. The effect on the pH level in Nordic Lake is minor with the three other options. Similarly, the effect on the pH level in Depot Lake is not appreciable with any of the options.

FIGURE 5.24

pH vs TIME AT NORDIC LAKE OUTLET FOR ALL OPTIONS

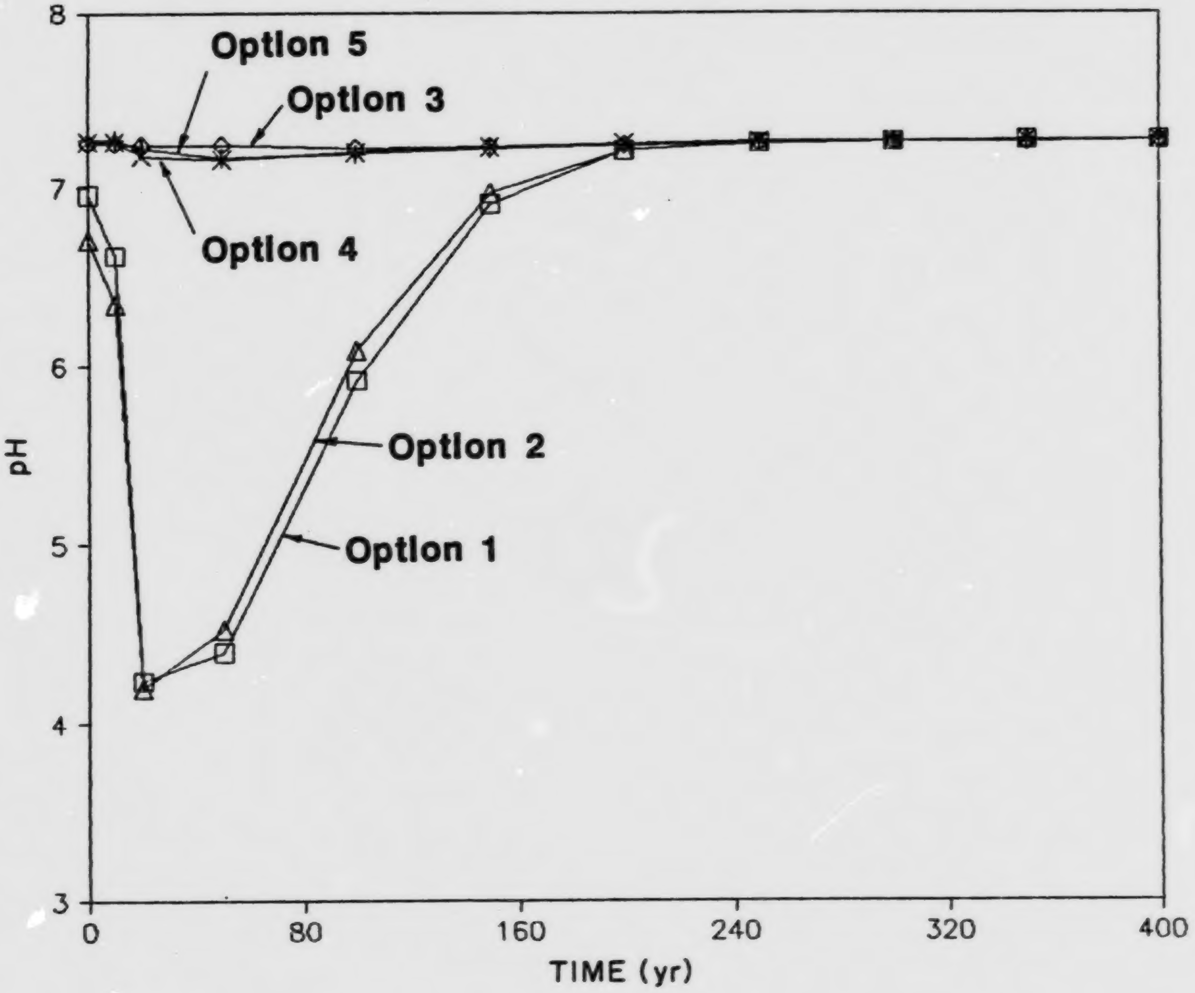

NOTE: GEOMETRIC MEAN VALUE OF 200 TIALS

6.0 SUMMARY AND CONCLUSIONS

The Lacnor Modelling Study

The primary objective of this project was to demonstrate the application of UTAP in assessing a real (versus hypothetical) uranium tailings site. The Lacnor tailings area in Elliot Lake, Ontario was selected for this purpose. The idea was to learn what is involved in such an application. For example, what are the data requirements for such an analysis, what modifications are required to the simulation models and what are the limitations of such an analysis. The UTAP model was also used to look at the relative effects of alternate closeout options assuming the Lacnor site to be representative of relatively low grade pyritic uranium tailings. In effect, this application of UTAP should be considered "preliminary" in the sense that the Lacnor tailings served as a test site for a trial application of UTAP to a real site. Thus, undue emphasis should not be given to the "numbers" produced in this modeling exercise.

UTAP Features

In this and previous studies (SENES, 1984; 1985; 1986a), the uranium mill tailings system is represented by a network of interconnected component models. At the present level of development the mathematical simulation models are a mix of quite complex component models (e.g. the tailings source term) and simpler aggregate models (e.g. transfer of radionuclides from water to fish flesh). This approach provides a flexible structure which can easily accommodate changes in component models and model input parameters. In the preceding studies the simulation models have been developed for a hypothetical, "reference" tailings facility. The computer implementation of these models (along with the probabilistic infrastructure) is known as the Uranium Tailings Assessment Program (UTAP). As noted earlier in this report there are several versions of the UTAP code, the most recent of which, namely UTAP.3, was used in the Lacnor study.

The current version of the Uranium Tailings Assessment Program, UTAP.3, simulates the behaviour of natural uranium, total thorium, radium-226, radon-222 and lead-210 and a number of inorganic chemical species as well as pH. The exposure pathways modelled are:

- water consumption
- fish consumption
- radon inhalation
- dust inhalation
- vegetable consumption
- meat consumption (caribou, moose and deer)
- external exposure (groundshine)

All of these pathways except for the consumption of caribou were used in the Lacnor analysis. Since UTAP was developed in a modular fashion it is possible for a modeller, who wishes to examine an exposure pathway other than one of those noted above, to add this pathway to the UTAP code. The way in which such changes could be implemented are discussed in the UTAP.3 User's Manual (SENES, 1987b).

UTAP Output

As with any predictive assessment, probabilistic analysis such as that performed with UTAP involves a mathematical expression (model) of some physical system, in this case a uranium mill tailings site. The model is a mathematical expression to which information is supplied, in the form of numerical values for one or more input variables, to produce the corresponding numerical values of one or more output variables.

Most of the input variables required by such a model are not known with certainty. The uncertainty arises because of normal experimental error in their measurement or because (sometimes) actual measurements are impossible and judgment must be used. Also, some input variables such as mean annual wind speed or mean annual precipitation inherently vary from year to year.

Consequently, it is impossible for most input variables to be adequately characterized by any single number. Fortunately, our full state of knowledge about any input variable can be described in the form of a (subjective) probability distribution. A distribution of calculated results is obtained by using a statistical sampling (or Monte Carlo) procedure which involves drawing many samples from each input parameter distribution.

The output variables from such an analysis can be considered as samples on objective random variables corresponding to the output variables. From the sample, the mean, variance, probability density function (pdf) or cumulative distribution function (cdf) may be estimated as desired. This information may be interpreted as describing the output variable in terms of subjective probability, telling us quantitatively what we are entitled to believe about the output variable.

UTAP is a tool which permits us to analyse the uncertainty about a particular tailings scenario. In doing the analysis we assume that the component models we are using provide a true (or at least reasonably true) representation of how a particular tailings site will evolve over time. As noted above, the input distributions involve some element of subjective probability in that they have been selected, by a modeller, in the belief that they best represent the data. Where the observational data base is large, the modeller may feel very confident in a data set and use it directly in the assessment; in other cases, where the modeller believes less strongly that the data base is appropriate, he may, perhaps in consultation with other experts, choose to modify the distribution before using it in his model. In any event, the relation which the mathematical model bears to the real world depends on the skill and judgement of the modeller and can be examined through model validation.

UTAP Application to Lacnor

In previous studies UTAP has been developed and applied to a hypothetical reference site. In this study, however, the focus was to apply UTAP to the

Lacnor tailings considering several closeout options. The Lacnor site was selected since it is more or less "representative" of relatively low grade, acid generating uranium tailings and , in comparison to other sites, an abundance of field data for the site was available.

The closeout options examined included the base case (Option 1 - essentially involving only the revegetation of the tailings surface), application of waste rock cover (Option 2), application of a cover of depyritized tailings (Option 3), application of glacial till cover (Option 4) and raising the water table to cover the tailings (Option 5). The period for which simulations were carried out for these options was from approximately 1960, the year in which the last tailings were deposited, to year 3960 (i.e. a two thousand year simulation period).

Several assumptions were necessary in order to apply UTAP for the assessment of the effects of the various closeout options. The principal parameters affected were the mixing zone depth, runoff rate, and the thickness of the oxidizing zone. The runoff rate plays a major role in determining the flushing rate of the tailings and the aqueous concentrations of those chemicals which are solubility controlled. The mixing zone depth is a major factor in determining the mass of chemicals and radionuclides which may potentially be transported out of the tailings pile. The thickness of the oxidizing zone is a determining factor in assessing the mass of pyrite which may oxidize and hence the amount of acid which may be produced. For the base case the oxidizing zone equals the depth of the unsaturated zone. For the options in which the tailings are submerged below the water table, the oxidizing zone was assumed to have a nominal thickness (i.e. 10 cm) as described previously in this report.

Another consideration in modelling the Lacnor tailings site pertained to surface runoff. Excess precipitation falling within the Lacnor tailings watershed reports to a pond located at the eastern end of the tailings basin (see Figure 3.1). Outflow from the tailings pond flows south from the Lacnor site onto the Nordic tailings area . In order to model the incremental effect of the Lacnor tailings on downstream water quality, it was assumed that the runoff from the Lacnor tailings passes straight across the Nordic tailings area to Buckles Creek. From Buckles Creek the flow moves southward through Nordic Lake, a small unnamed lake, and the east end of Esten Lake before flowing eastward to Depot Lake.

Five receptors were identified for inclusion in the assessment of dose to individuals (see Figure 3.3). The closest receptor to the Lacnor tailings area is situated in the Nordic townsite a distance of only 2 km to the south. Two receptors in the Town of Elliot Lake were included in the assessment; one located in the new subdivision development on the east side of town and the other in the older part of town on the west side. Because Depot Lake is the first large downstream lake on the western branch of the Serpent River Basin which receives runoff from the Lacnor site, two receptors were located at opposite ends of the lake in separate windrose directions. Both of these receptors were assumed to obtain their drinking water from Depot Lake in contrast to the other three receptors who obtain their drinking water from lakes which are not impacted by runoff from the Lacnor tailings area (i.e. Ryan Lake and Elliot Lake).

Limitations of the Model

The philosophy employed throughout the development of UTAP was to develop a reasonably accurate description of the tailings behaviour while still maintaining a relatively easy to use system model with a reasonable computation time and a manageable number of input parameters. To prevent the source term component of the UTAP code, in particular, from becoming too complex, the following limitations were imposed:

1) the tailings must be treated as a homogeneous mass in both the horizontal and vertical dimensions. This restriction means that the values specified for those parameters which characterize the chemical and radiological composition of the solid phase component are treated as

being homogeneous over the entire tailings depth at the start of the simulation.

2) pyrite oxidation is restricted to either the unsaturated zone or a specified depth into the saturated zone but not both. This restriction was imposed by the fact that the model was developed to apply to the usual situation where the water table is several hundred centimeters below the tailings surface and oxidation in the saturated zone is inconsequential or nonexistent. With some closeout options however, oxidation of the upper few centimeters in the saturated zone may be the only source of acid generation.

In Options 1, 2 and 3, pyrite oxidation occurs in the unsaturated zone. The high effective oxygen diffusivity, and hence, the high predicted sulphate production rate results in a high sulphate level for a short time duration. When pyrite is depleted from the unsaturated zone i.e. around year 70, the sulphate level drops.

With Options 4 and 5, it is assumed that pyrite oxidation occurs only in a very thin layer, i.e. 10 cm deep, of the saturated zone. Because the effective oxygen diffusivity through water is much less than air, the predicted sulphate production rate is significantly lower than with the other three options. The result is that it takes longer for the pyrite to oxidize, i.e. greater than year 150, although the sulphate level is considerably lower than with the other options.

Model Verification/Calibration/Validation

The degree of confidence that is assigned to a model depends upon the level of verification, calibration, and validation that has been achieved. Verification of the generic UTAP model was performed as part of the Phase III study and is presented throughout the Phase III report (SENES, 1986a). The verification procedures are detailed in a supplementary Quality Assurance (QA) report (SENES, 1987d).

Based upon the experience gained from model verification in the Phase III study, a detailed in-house review of the code early in the present study, and insight obtained through the application of UTAP.3 to the Lacnor site, a number of modifications were made to the generic UTAP code. In addition, the UTAP.2 code has been implemented by a second party, Whiteshell Nuclear Research Establishment (WNRE, 1987). Certain modifications to UTAP.2 were suggested by this exercise and have also been implemented in the current UTAP.3 code which was used for the Lacnor assessment. Each of the changes proposed for UTAP.2 was tested prior to inclusion in the updated system model, UTAP.3. The details of the UTAP.3 code are described in accompanying documentation (SENES 1987a, 1987b and 1987c).

In the Lacnor field study the tailings and the area immediately adjacent (i.e. the area within about 100 m) were monitored. The surrounding airshed and watershed however, were not monitored. Hence, the use of the measured field data for the Lacnor site in calibration/validation was restricted to the water source model, subsurface transport model and radon source model. The latter is contained within the air source model.

In the calibration of the models, key parameters were adjusted, while respecting some defined ranges, to give the "best fit" of the model results to either field or laboratory measurements.

In order to calibrate the rate of pyrite oxidation employed in the water source model, field data collected at two locations on the Nordic tailings area were used. The Nordic data presented by Smyth (1981) and Dubrovsky _et al_. (1985) was selected because it had proven to be useful in a prior study which included validation of a model which predicts the acid discharge from sulphidic tailings, namely the Reactive Acid Tailings Assessment Program (RATAP) (SENES and Beak, 1986). Calibration of the code was undertaken in two stages. The first stage involved a comparison of predicted results against the two sampling locations on the Nordic tailings. The second stage entailed a comparison of UTAP predictions with those of RATAP over a 100 year simulation period.

Calibration of the UTAP model was achieved by adjusting the initial values of the rate of pyrite oxidation for acidic and non-acidic conditions. The best fit of the model was achieved at one location with an initial pyrite content of 600 $mol.m^{-3}$ using a pyrite oxidation rate (R_s) of 3.0×10^{-6} $mol.g^{-1}.yr^{-1}$ and a rate fraction (X_{rate}) of 0.10. The rate fraction adjusts the rate of pyrite oxidation (R_s) to account for the effect of elevated pH when calcite is present. At the other location, which had an initial pyrite content of 1280 $mol.m^{-3}$, the best fit resulted for an R_s value of 1.4×10^{-5} $mol.g^{-1}.yr^{-1}$ and X_{rate} value of 0.10. This finding was found to be consistent with the previous finding since the rate of pyrite oxidation (R_s) is expressed as a function of the initial pyrite content. The two R_s values were found to be comparable when corrected for pyrite content.

The UTAP model was also calibrated by comparing predictions to those obtained using the RATAP model. For an initial pyrite content of 600 $mol.m^{-1}$, the comparison of results for a 100 year simulation period showed that the best fit was achieved for an R_s value of 3.0×10^{-6} $mol.g^{-1}.yr^{-1}$ and a X_{rate} value of 0.10 as before.

The water source model was then validated against Lacnor field data. In the validation the rate of pyrite oxidation, determined from the aforementioned calibration with Nordic field data, when adjusted for the pyrite content of the Lacnor tailings was confirmed to be applicable to the Lacnor site.

Overall, the agreement between observed and predicted values was found to be good. The observed geometric means of pH, sulphate, iron, natural uranium and radium-226 all fell well within the 95% confidence limits of the geometric mean values predicted by the water source module of UTAP. For calcium, total thorium and lead-210, however, the observed geometric means fell outside the 95% confidence interval of the predicted mean values. This observation is not surprising when one considers that the porewater samples were collected on only two dates within a single year whereas the UTAP model predicts long term average values. Moreover, the porewater samples were obtained from only five piezometer nests on the Lacnor tailings area. Due to the inhomogeneity of real (versus hypothetical) tailings, each of these measurement locations showed different values. On the other hand the UTAP model assumes the tailings to be homogeneously distributed.

The radon model's only site specific input is the soil water content which could be inferred from the Lacnor field study (Golder et al., 1986). The radon source model was "calibrated" in a previous study (Rogers et al., 1980). In the present study, the predicted radon fluxes were validated by comparison to the measured radon fluxes.

Radon exhalation rates were monitored during the Lacnor field study under spring, summer and winter conditions. Comparison of the data measured in the spring and summer against model predictions indicated good agreement between the mean predicted and observed exhalation rates. The predicted mean value equalled 1.05 $Bq.m^{-2}.s^{-1}$ (standard deviation 0.55) whereas the mean measured value was 1.12 $Bq.m^{-2}.s^{-1}$ (standard deviation 1.50). The difference in the standard deviations (the monitored standard deviation being larger) is not unexpected since the monitored exhalation rates were determined from measurements taken over 2 to 6 hour intervals whereas the model predictions represent annual average values.

With the subsurface transport model, there was uncertainty associated with key site-specific parameters, in particular the radionuclide distribution coefficients and the aquifer discharge distances at the two dams. The key parameter selected for adjustment was the aquifer discharge distance. The best fit of the data, in terms of the four radionuclides, sulphate and calcium concentrations was obtained for discharge distances of 2 m and 7 m at dams 1 and 2 respectively. These values were used in the Lacnor simulations.

Results

The base case closeout option involves walking away from the tailings site at the cessation of tailings deposition. The only reclamation work which was assumed to have been carried out was the revegetation of 60% of the tailings surface. From the discussion in Chapter 5 it can be seen that two receptors on Depot Lake (assumed to be permanent residents) are predicted to receive the highest exposures at all times throughout the simulation period. The major dose contributors are consumption of drinking water and fish from Depot Lake. The next largest dose contributor is that due to the consumption of locally caught moose and deer.

The temporal pattern of dose is related to the radionuclides leached from the tailings and distributed through the surface water environment. In the short term the water pathways are dominated by lead-210 concentrations which decline with time as soluble lead is leached from the tailings. In the longer term radium-226 levels increase, as pyrite and then gypsum are exhausted, and dominate the water related pathways. In the very long term the inventory of soluble radium is exhausted and the radium inventory declines.

The affect of the alternative closeout options on dose can be explained in terms of how the alternative closeout options affect the release of radionuclides. The principal considerations in this regard are the way the options affect the amount of water passing through the tailings, and way the options affect the rate and time of occurrence of pyrite oxidation. The lowest (geometric mean) dose at all times was predicted for the water cover option (Option 5). The largest geometric mean dose for all times less than about 1500 years is that for Option 2 (waste rock cover). The dose for Option 5 is lowest because it has the lowest rate of flushing of radionuclides from the tailings to the water environment. The dose is highest in Option 2 (waste rock) because of the increased rate of flushing of soluble chemical and radiological precipitates from the tailings. In the longer term, however, as leachable radium is depleted, the total dose for this pathway is predicted to decline. The largest geometric mean dose calculated for Option 2 was estimated to be in the order of 20 $\mu Sv.yr^{-1}$ (2 mrem $.yr^{-1}$). This dose is only about 1% of the normal annual background dose (including that due to radon-222) and well within the normal variability of natural annual dose.

The total dose associated with the other three options all exhibited essentially the same behaviour, namely the peak dose occurs around year 1500 and declines slowly thereafter.

In terms of pH, the base case and the waste rock cover options (Options 1 and 2) have the largest effect. The pH in Nordic Lake is reduced to below 4.3 with both options although the pH recovers to near the background level within 400 years. The effect on the pH level in Nordic Lake is less severe with the three other options. The effect on the pH level in Depot Lake is not appreciable with any of the options.

Conclusions

Based on this UTAP application to the Lacnor tailings, conclusions can be drawn about modelling and data requirements, and about future development of the generic code.

UTAP is a powerful and flexible tool for the analysis of uranium mill tailings. Previous studies have shown how UTAP can be applied to a hypothetical reference site. The present study has demonstrated that UTAP can be applied to a real site and as well that UTAP can be used to assess the environmental effects of alternative uranium tailings closeout options. It is worth pointing out in this regard that the updated generic code UTAP.3 was directly applied to the Lacnor site and no code changes unique to Lacnor were required. However, the application of the generic code to the alternate closeout options, while not requiring a change to the computer code, did require a redefinition of model concepts. UTAP application to other tailings having similar characteristics to Lacnor would not require significant modelling effort.

As noted earlier in this report an extensive year long study of the Lacnor site and its immediate environs was carried out and much data was collected.

However, the Lacnor field study was largely independent of the UTAP development and, as a consequence, much of the field data were not directly useful for the modelling exercise. Nonetheless, some field data were very useful in calibrating and validating aspects of the source models which are so fundamental to UTAP. Experience in applying UTAP.3 in a preliminary fashion to the Lacnor site suggests that in future applications:

> **...it would be beneficial to carry out a screening or preliminary level analysis of the tailing site using existing data and the existing UTAP code prior to launching on a campaign of field studies and/or further site specific model developments.**
>
> **The results of such a UTAP analysis could be used to identify the principal release mechanisms and exposure pathways, or deficiencies in same, and hence serve as the basis for designing a program of field or laboratory studies, if indeed any are required. Furthermore, the results of such an investigation can be used to decide which component modules need to be revised if any, or if new component models need to be developed for this particular application. Such a procedure would, at least in our view, be optimal in the utilization of resources and the protection of the environment.**

Notwithstanding the utility and flexibility of UTAP.3 it is recommended that in the event that future development of UTAP were to occur the most useful areas of development would be:

> **...expand the layer concept applied to the tailings and make the specification of the initial solid phase composition of each layer independent of the others. This modification would increase the flexibility of the UTAP code in evaluating tailings closeout options.**
>
> **...carry out field investigations of radionuclide transfer through the receiving environment to confirm and/or improve the models or**

parameter value estimates. In particular, because of the importance of the water pathways in most Canadian applications, the modelled removal of radionuclides on sedimenting solids and the feed back to the water column from decomposing sediment solids warrants special attention.

...add additional pathways (eg. irrigation of vegetable crops) to the dose models. This would provide a more complete picture of the pathways contributions to total dose and allow questions to be answered about the significance, or insignificance, of pathways which are not included in the current UTAP.3 code. It is noted however, that the primary pathways have been included in the code for most applications in the Canadian setting and that any new pathways which could be added would likely add very little to the total dose estimate in most circumstances.

...add additional radionuclides to the code. Again, this would provide a more complete picture of the total dose estimate although the principal radionuclides have been taken into account and the addition of radionuclides unaccounted for, would likely add only marginally to the total dose estimate in most circumstances.

...work with regulatory agencies and potential users to develop further agreement as to how the modelling should be performed and how the results should be interpreted in a regulatory setting.

REFERENCES

AES. "Precipitation Data from AES Computer Centre." AES Computer Centre, Downsview.

Barnes, E., 1986. Personal Communication, Rio Algom, Elliot Lake, Ontario.

Beak Consultants Limited, 1985. "Descriptive Algorithm Development for Physical, Chemical and Biological Processes Operational in Uranium Mill Tailings", Research report prepared for the National Uranium Tailings Program, CANMET, EMR.

Beak Consultants Limited, 1982. "An Approach to Long Term Aquatic Modelling of a Generic Uranium Tailings Site." Draft Report to the Atomic Energy Control Board, Ottawa.

Beals, D.I., 1985. "Soil and Climate Parameters for Post-Closure Biosphere Assessment." Atomic Energy of Canada Limited, Technical Record TR-285.

Broissia, M., 1986. "Selected Mathematical Models in Environmental Impact Assessment in Canada." Chemical Engineering Department, University of Sherbrooke, prepared for Canadian Environment Assessment Research Council.

Canmet Laboratories, 1985. Personal Communication with Staff at the Canmet Laboratories, Energy Mines and Resources, Elliot Lake, Ontario.

Chen, C.C., 1975. "Design of Sediment Retention Basins." National Symposium on Urban Hydrology and Sediment Control, University of Kentucky, BU109.

Clulow, 1986. Personal Communications.

Corbett, 1985. Personal Communications.

Dave, N.K., Cluthier, N.R., and Lim, T.P., 1984. "Radionuclide Levels in Vegetation Growing on Uranium Tailings, Elliot Lake, Ontario." CANMET Rept. MRP/MRL 84-104.

Davis, J.B., Knapp, R.A., and Sinclair, K.W., 1979. "The Control of Seepage from Uranium Mill Tailings Ponds in the Elliot Lake Mining Area." Proc. First Int. Mine Drainage Symposium, Denver.

Diotte, Mr., 1987. Personal Communication, Rio Algom Ltd., Elliot Lake, Ontario.

Dubrovsky, N.M., Cherry, J.A., Reardon, E.J., and Vivyurka, A.J., 1985. "Geochemical Evolution of Inactive Pyritic Tailings in the Elliot Lake Uranium District." Can. Geotech. Int. Vol. 22, No. 1, pp. 110-128.

Energy Mines and Resources Canada (EMR), 1975. "National Topographic Map 41 J/7, Edition 2."

Feenstra, S., Blair, R.D., Cherry, J.A., Chakravatti, J.L., and La Rocque, E., 1981. "Hydrogeochemical Investigations of Two Inactive Tailings Areas in the Elliot Lake Uranium District Ontario, Canada." Proceedings of the 4th Symposium on Uranium Mill Tailings Management, Fort Collins, Colarado.

Golder Associates, Beak Consultants Limited, SENES Consultants Limited, and Cumming-Cockburn and Associates Limited, 1986. "Lacnor Field Study." Research Report Prepared for National Uranium Tailings Program.

Golder Associates, 1980. "Stanleigh Mine Tailings Impoundment. Volume 3. Hydrogeological Assessment of the Tailings Impoundment Basin." Prepared for Rio Algom Limited.

Hvorslev, M.J., 1951. "Time Lag and Soil Permeability in Groundwater Observations." U.S. Army Corps of Engineers, Waterways Experiment Station, Vicksburg, Mississippi.

Kalin, M., 1983. "Long-Term Ecological Behaviour of Abandoned Uranium Mill Tailings. 1: Synoptic Survey and Identification of Invading Biota." Environ. Can. EPS-4-ES-83-1.

Kalin, M., 1984. "Long-Term Ecological Behaviour of Abandoned Uranium Mill Tailings. 2: Growth Patterns of Indigenous Vegetation on Terrestrial and Semi-Aquatic Areas." Environ. Can. EPS-3-HA-2.

MacLaren Limited, James F., 1977. "Environmental Assessment of the Proposed Elliot Lake Uranium Mines Expansion. Volume 1: Background Information." Prepared for Denison Mines Limited and Rio Algom Limited.

MacLaren Limited, James F., 1978. "Environmental Assessment of the Proposed Elliot Lake Uranium Mines Expansion. Volume 2: Background Information Update; Volume 3: Community Assessment; Volume 4: Environmental Assessment; and Addendum 1." Prepared for Denison Mines Limited and Rio Algom Limited.

MacLaren Limited, James F., and Golder Associates, 1981. "Stanleigh Mine Tailings Impoundment. Volume 5. Design Brief." Prepared for Rio Algom Limited.

McIlveen, W.D., 1977. "Survey for Lead-210 Accumulation in Vegetation and Soil in the Elliot Lake Area." Ontario Ministry of the Environment.

Ministry of Natural Resources, 1986. Personal Communications with Staff at the Blind River and Espanola District Office.

Morin, K.A., Cherry, J.A., Lim, T.P. and Vivyurka, A.J., 1982. "Contaminant Migration in a Sand Aquifer Near an Inactive Uranium Tailings Impoundment," Elliot Lake, Ontario, Can. Geotechn. Jour. Vol. 19, pp. 49-62.

Myslik, G., 1985. "The Eutrophication Potential of Nitrates in the Serpent River System of Northeastern Ontario." Ontario Ministry of the Environment.

National Research Council of Canada (NRC), 1983. "Radioactivity in the Canadian Aquatic Environment." Pub. No. NRCC 19250.

Nutrition Canada, not dated. "Food Consumption Patterns Report." Prepared by the Department of National Health and Welfare.

Ontario Environmental Assessment Board, 1979. "Public Hearing by the Environmental Assessment Board into the Expansion of the Uranium Mines in the Elliot Lake Area."

Ontario Ministry of the Environment, 1984. "Serpent River Basin Water Quality Data, 1982."

Ontario Water Resources Commission (OWRC), 1966. "Interim Report on Radiological Water Pollution in the Elliot Lake and Bancroft Areas."

Ontario Water Resources Commission (OWRC), 1972. "Water Pollution from the Uranium Mining Industry in the Elliot Lake and Bancroft Areas, Volume 2: Detailed Findings."

Powell, Mrs., 1987. Personal Communication, Elliot Lake City Hall, Elliot Lake, Ontario.

Rancon, D., 1973. "The Behaviour in Underground Environments of Uranium and Thorium Discharged by the Nuclear Industry." in Environmental Behaviour of Radionuclides Released in the Nuclear Industry, International Atomic Energy Agency Report, IAEA-SM-172/55.

Reardon, E.J., Moddle, P.M., 1985. "Gas Diffusion Coefficient Measurements in Uranium Mill Tailings: Implications to Cover Layer Design." Preprint to Reclamation and Revegetation Research.

Robertson, J.A., 1968. "Geology of Townships 149 and 150." Ontario Department of Mines, Geological Report No. 57.

Rogers, V.C. Overmyer, R.F., Putzig, K.M., Jensen, C.M., Nielson, K.K., and Sermon, B.W., 1980. "Characterization of Uranium Tailings Cover Materials for Radon-Flux Reduction." U.S. Nuclear Regulatory Commission NUREG/CR-1081, March.

SENES Consultants Limited, 1983. "Acid Generation Tests on Pyritic and Depyritized Tailings With and Without Limestone Addition." Draft Report Prepared for Denison Mines Limited, Elliot Lake.

SENES Consultants Limited and Saskatchewan Research Council (SRC), 1984. "A Study of the Distribution of Naturally Occurring Radionuclides in Freshwater Benthos and Their Environment - Phase I." Research Report Prepared for the National Uranium Tailings Program, CANMET, EMR, Ottawa.

SENES Consultants Limited, 1984. "A Study to Develop and Demonstrate Techniques for the Probabilistic Assessment of the Long-Term Effects of Uranium Mill Tailings in Canada - Phase I." Research Report Prepared for the National Uranium Tailings Program, CANMET, EMR, under Supply and Services Canada Contract No. OSQ83--00236.

SENES Consultants Limited, 1985. "A Study to Develop and Demonstrate Techniques for the Probabilistic Assessment of the Long-Term Effects of Uranium Mill Tailings in Canada - Phase II." Research Report Prepared for the National Uranium Tailings Program, CANMET, EMR, under Supply and Services Canada Contract No. 0SQ84-00207.

SENES Consultants Limited and Saskatchewan Research Council (SRC), 1985. "A Study of the Distribution of Naturally Occurring Radionuclides in Freshwater Benthos and Their Environment - Phase II." Research Report Prepared for the National Uranium Tailings Program, CANMET, EMR, Ottawa.

SENES Consultants Limited, 1986a. "Probabilistic Model Development for the Assessment of the Long-Term Effects of Uranium Mill Tailings in Canada - Phase III." Research Report Prepared for the National Uranium Tailings Program, CANMET, EMR, under Supply and Services Canada Contract No. 0SQ85-00182.

SENES Consultants Limited, 1986b. "Data on the Abundance and Distribution of Radon Around Uranium Tailings Piles in the Vicinity of Elliot Lake, Ontario." Research Report Prepared for the National Uranium Tailings Program, CANMET, EMR, Ottawa.

SENES Consultants Limited and Beak Consultants Limited, 1986. "Estimation of the Limits of Acid Generation by Bacteria-Assisted Oxidation in Uranium Mill Tailings." Research Report Prepared for the National Uranium Tailings Program, CANMET, EMR, under Supply and Services Canada Contract No. 0SQ85-00237.

SENES Consultants Limited, 1987a, "Uranium Tailings Assessment Program (UTAP.3): Addendum to Volume 2 - System Description and Control Module Documentation." Research Report Prepared for the National Uranium Tailings Program, CANMET, EMR, under Supply and Services Contract No. 23317-6-1728/01 SQ.

SENES Consultants Limited, 1987b, "Uranium Tailings Assessment Program (UTAP.3): Users Manual." Reserach Report Prepared for the National Uranium Tailings Program, CANMET, EMR, under Supply and Services Contract No. 23317-6-1728/01 SQ.

SENES Consultants Limited, 1987c, "Uranium Tailings Assessment Program (UTAP.3): Component Model Documentation." Research Report Prepared for the National Uranium Tailings Program, CANMET, EMR, under Supply and Services Contract No. 23317-6-1728/01 SQ.

SENES Consultants Limited, 1987d, "Probabilistic Model Development for the Assessment of the Long-Term Effects of Uranium Mill Tailings in Canada - Phase III. Software Development and Quality Assurance Supplementary Report." Research Report Prepared for the National Uranium Tailings Program, CANMET, EMR, under Supply and Services Contract No. 0SQ85-00182.

Sheppard, M.I., Beals, D.I., Thibault, D.H., and O'Connor, P., 1984. "Soil Nuclide Distribution Coefficients and Their Statistical Distributions." Atomic Energy of Canada Limited, Whiteshell Nuclear Research Establishment, December.

Smyth, D.J., 1981. "Hydrogeological and Geochemical Studies Above the Water Table in an Inactive Uranium Tailings Impoundment near Elliot Lake, Ontario." Unpublished M.Sc. Project, University of Waterloo, Waterloo, Ontario.

Veska, E., 1983. "Origin and Subsurface Migration of Radionuclides from Waste Rock at an Abandoned Uranium Mine Near Bancroft, Ontario." Unpublished Ph.D. Thesis, University of Waterloo.

Wetzel, R.G., 1975. "Limnology." Saunders College Publishing, Philadelphia.

Whiteshell Nuclear Research Establishment (WNRE), 1987. Comparison of the UTAP and SYVAC Codes, Phase II, Work in Progress.

APPENDIX A

WATER SOURCE MODEL

UTAP APPLICATION TO THE LACNOR TAILINGS

APPENDIX A: WATER SOURCE MODEL

A.1 Conceptual Approach

The Lacnor tailings basin is a typical valley impoundment with a bedrock rim and dams at two low points on the perimeter. The water table is located, on average, 0.5 to 1.0 m below the surface. Acid discharges are released through a surface drainage outlet at the south easterly side of the tailings area, as well as through seepage streams under the dams on the southern perimeter.

During the operation of the mill, the sole treatment of the tailings effluent was pH adjustment to a pH of about 8.0 with lime. It is noted, however, that the runoff from the Lacnor tailings area, which flows onto the Nordic tailings area received barium chloride treatment for radium removal prior to entering the Serpent River watershed (OWRC, 1966). Beginning in 1971, runoff from the Nordic tailings area was redirected to a new treatment plant at North Nordic Lake where facilities were provided for both lime and barium chloride addition for pH adjustment and radium removal, respectively.

The approach employed to model the physical and chemical behaviour of the tailings is conceptually similar to that employed in the generic model (SENES, 1987c). The main difference stems from the presence of permeable dams at the Lacnor tailings site. Conceptually these dams are perceived to be "pseudo aquifers" in the subsurface transport model.

In the generic model, the upper layer of the saturated zone (termed the mixing layer), which is the primary source of flow to the surface water component, is conceived to have a finite thickness. The source of flow to the subsurface transport component is conceived to be derived from a deep layer in the saturated zone (i.e. Layer 4). Porewater quality data at Lacnor suggests that the mixing layer (Layer 3) extends to near the bottom of the tailings area and is the source of porewater input to both the surface water and subsurface transport components. Hence, the subsurface transport model was connected to Layer 3 in the Lacnor application as discussed in Appendix H, Section H.1.

A.2 Site-Specific Model Alterations

No changes were required to the code of the generic water source module in order to simulate the conditions at the Lacnor tailings site.

A.3 Site-Specific Parameters

In the following section, short descriptions of the site-specific parameters are presented. Justifications for the selection of parameter values are also included. Table A.1 presents the site-specific parameters and their probability distributions and descriptions. The probability distributions reflect the uncertainties in the parameter values due to the heterogenic nature of the tailings and variability in the measurement techniques.

The non-site specific parameters are presented in SENES (1987c); Chapter 3.12.

A.3.2 Initial Mass Fractions

Pyrite Content

Little data was available on the initial pyrite content, $[FeS_2]^\circ$, of the Lacnor tailings; one sample of partially oxidized tailings contained approximately 350 $mol.m^{-3}$ of pyrite. Data were available, however, on the pyrite content of low grade, 0.1% U_3O_8, Elliot Lake tailings in general. Typical levels reported range from 600 to 800 $mol.m^{-3}$ (SENES, 1983).

For modelling purposes the initial pyrite content was assumed to have a triangular distribution with a minimum value of 600 $mol.m^{-3}$, a mode of 700 $mol.m^{-3}$, and a maximum value of 800 $mol.m^{-3}$.

Table A.1

WATER SOURCE MODEL

Site-Specific Parameter Values

Model Symbol	Description	Units	Nominal Value	Probability Distribution
A_{ws}	tailings watershed area	m^2	5.7×10^5	$C(5.7 \times 10^5)$
A_T	tailings surface area	m^2	2.4×10^5	$C(2.4 \times 10^5)$
D_{O2}	effective oxygen diffusivity	$m^2.yr^{-1}$	37	T(5,37,70)
$[FeS_2]^\circ$	initial pyrite content in tailings	$mol.m^{-3}$	700	T (600,700,800)
f_u	mass fraction of uranium recovered in the mill	$kg.kg^{-1}$	0.92	U(0.90,0.94)
P	annual net precipitation	$m.yr^{-1}$	0.51	N(0.51,0.1,0.25,0.85)
P_a	average annual net precipitation	$m.yr^{-1}$	0.51	C(0.51)
$[PbSO_4]^\circ$	initial lead sulphate concentration in tailings	$mol.m^{-3}$	2.0	T(1.0,2.0,3.0)
R_s	initial rate sulphate production (no calcite)	$mol.g^{-1}.yr^{-1}$	4.1×10^{-6}	$T(3 \times 10^{-6}, 4.1 \times 10^{-6}, 5.3 \times 10^{-6})$
X_{gyp}	initial mass fraction of gypsum in tailings	$kg.kg^{-1}$	0.06	N(0.06,0.005,0.05,0.07)
X_{rate}	fraction of R_s when calcite is present	unitless	0.10	C(0.10)
X_{Lime}	initial mass fraction of calcite in tailings	$kg.kg^{-1}$	0.0005	C(0.0005)
X_{run}	fraction of surface runoff from tailings	unitless	0.60	T(0.55,0.60, 0.65)
λ_w	thickness of the unsaturated zone	m	0.5	T(0.25,0.5,2.0)
λ_{mix}	thickness of mixing zone	m	11.5	U(8,14)
λ_4	thickness of layer 4	m	0.75	U(0.5,1.0)
ρ_t	tailings bulk density	$g.m^{-3}$	1.3×10^6	$T(1.1 \times 10^6, 1.3 \times 10^6, 1.5 \times 10^6)$

Notes

C - Constant (single value)

T - Triangular (min., mode, max)

U - Uniform (min, max)

N - Normal (mean, std. dev., min., max)

Gypsum Content

As with the pyrite content of the Lacnor tailings, no site specific information on the gypsum content, X_{gyp}, was available. Based upon the Lacnor Field Study (Golder *et al.*, 1986), 40% of the total sulphur content was estimated to be gypsum. The mean total sulphur content in the non-oxidized tailings was 3.56%, giving approximately 1.42% as gypsum sulphur. Therefore, the gypsum content was approximately 6% as $CaSO_4$. Based upon this Lacnor value and published data (SENES, 1983; MacLaren, 1977), a normal distribution with an arithmetic mean of 0.06, a standard deviation of 0.005, and lower and upper limits of 0.05 and 0.07 $kg.kg^{-1}$ were selected for the gypsum content.

Lead Sulphate

The initial lead sulphate concentration has been estimated from laboratory digestion experiments of tailings solids (Beak, 1985). The digestion of 1:3 (solids:liquid) ratio with 3M HNO_3 produced an average concentration of 98 mg/L of Pb in the liquid phase. Since $PbSO_4$ is soluble in HNO_3, the corresponding $PbSO_4$ concentration would be:

$$\left(\frac{98\text{ mg Pb}}{\text{L}}\right)\left(\frac{3\text{ L}}{1\text{ kg tailings}}\right)\left(\frac{1\text{ g}}{1{,}000\text{ mg}}\right)\left(\frac{1\text{ mole PbSO}_4}{207.19\text{ g Pb}}\right)\left(\frac{1{,}400\text{ kg tailing}}{\text{m}^3\text{ tailings}}\right)$$

$$= 1.99\ \frac{\text{moles PbSO}_4}{\text{m}^3\text{ tailings}} \qquad \text{(A.1)}$$

A range of concentrations from 68 to 136 mg/L of Pb in the liquid phase was observed in the study. Based on this information, a triangular distribution was assumed for the $PbSO_4$ concentration, with a mode of 2 $mol.m^{-3}$; ranging from 1 to 3 $mol.m^{-3}$.

Calcium Carbonate

The initial mass fraction of calcite present is an important parameter in the determination of the pH of the tailings porewater. It has been noted previously that pH adjustment of the tailings in the mill was the only treatment practical during tailings deposition. No calcite was specifically added to tailings during this period, although some would be present in the lime added for neutralization purposes. In 1978, limestone was added to the tailings surface for revegetation purposes, however, the limestone application rate was only 7 tonnes per hectare (Golder et al., 1986; chapter 2.0).

The initial mass fraction of limestone was assumed to equal 0.0005 g $CaCO_3$ per g tailings (0.05%).

A.3.3 Tailings Bulk Density

A discussion of the selection of the probability distribution type for tailings bulk density, ρ_t, is presented in Section 4.3, Radon Module. A triangular distribution with a mode of $1.3\text{x}10^6$ g.m^{-3} and a range of $1.1\text{x}10^6$ to $1.5\text{x}10^6$ g.m^{-3} was selected.

A.3.4 Oxygen Diffusivity Through Tailings

An equation for the effective oxygen diffusivity, D_{O2}, through tailings has been developed by Reardon and Moddle (1985).

$$D_{O2} = 630.7 \left(\frac{n_a - 0.05}{0.95} \right)^{1.7} \qquad \text{(A.2)}$$

where:

D_{O2} = effective oxygen diffusivity of the tailings ($\text{m}^2.\text{yr}^{-1}$)

n_a = measured air content of the tailings ($\text{m}^3_{air}.\text{m}^{-3}_{tailings}$)

The average measured volumetric water content and porosity of Lacnor tailings were 0.27 $\text{m}^3.\text{m}^{-3}$ and 0.5 $\text{m}^3.\text{m}^{-3}$, respectively (Golder et al., 1986; Appendix 1.0, Table 1.2).

The average air content therefore can be calculated from:

$$n_a = n_t - n_w^* \qquad (A.3)$$

where:

n_t = porosity of the tailings ($m^3_{void} \cdot m^{-3}_{tailings}$)

n_w^* = measured water content of the tailings ($m^3_{water} \cdot m^{-3}_{tailings}$)

The calculated effective diffusivity for the aformentioned average air content of 0.23 $m^3.m^{-3}$ is 37.3 $m^2.yr^{-1}$. The field data, however, were measured during "wet" summer months and hence may underpredict the actual effective diffusivity.

A triangular distribution has been assumed with a mode of 37 $m^2.yr^{-1}$ and minimum and maximum values of 5 and 70 $m^2.yr^{-1}$. The latter values are based upon a range in the volumetric water content of 0.19 $m^3.m^{-3}$ to 0.40 $m^3.m^{-3}$.

A.3.5 Thickness of the Unsaturated Zone

The unsaturated zone at the Lacnor tailings is shallow and in some locations is nonexistent as water is ponded on the tailings surface.

In the Golder et al. (1986) study the water table depth was not directly determined. The water levels in five piezometer nests, were determined over the summer months, however, the water levels were affected by a temporary dam placed at the eastern end of the tailings basin between late April and mid June. Consequently, the variation in the water level was much more pronounced than would normally be expected. In general, the highest water levels were recorded in March or April.

Using the field data reported by Golder et al. (1986; Appendix 1.0, Record of Boreholes) the thickness of the unsaturated zone, λ_w, was estimated to equal about 0.5 m on average. This parameter was assumed to be triangularly distributed with a mode of 0.5 m and minimum and maximum values of 0.25 and 2.0 m, respectively.

A.3.6 Thickness of the Mixing Zone

The mixing zone as defined herein has higher radionuclide concentrations than those in the deep, saturated zone, layer 4. Radionuclide concentrations measured during July and August in the Lacnor tailings (top 15 m) and the sub-tailings soils (from 15 to 28 m) are presented in Figures A.1 to A.4. The data indicates that a reduction in the radionuclide porewater concentrations occurs at a depth of approximately 11 m for total uranium, 15 m for radium-226, 15 m for total thorium and 10 m for lead-210. Hence, it is assumed that the depth of the bottom of the mixing zone is approximately 10 to 15 m.

As described in Section A.3.5, the thickness of the unsaturated zone, i.e. the depth at which the mixing zone starts, varies from 0.25 m to 2.0 m. Employing this information and the aforementioned range for the depth of the mixing zone, 10 to 15 m, results in the mixing zone having an approximate thickness, λ_{mix}, of 8 to 14 m. A uniform distribution was assumed for this parameter.

A.3.7 Thickness of Layer 4

Layer 4 is located between the mixing zone and the bottom of the tailings. Given the values previously stated for the thicknesses of the unsaturated zone, 0.25 to 2.0 m (Section A.3.5), and the mixing zone, 8 to 14 m (Section A.3.6) it follows that the thickness of layer 4 at the Lacnor site is quite shallow. This parameter was estimated to vary from 0.5 to 1.0 m and is described as a uniformly distributed input variable.

A.3.8 Annual Net Precipitation

Monthly precipitation data was available from the Lacnor tailings site during the year 1985. The data indicated that the annual precipitation, was 0.8 $m.yr^{-1}$ (Golder et al., 1986; Appendix 2.0, Table 2.2.6). This compares with a long-term annual mean of 0.926 $m.yr^{-1}$ for the Elliot Lake region (Canadian Climate Normals, 1983). Data on the net precipitation, P, (total

FIGURE A.1

MEASURED URANIUM CONCENTRATION

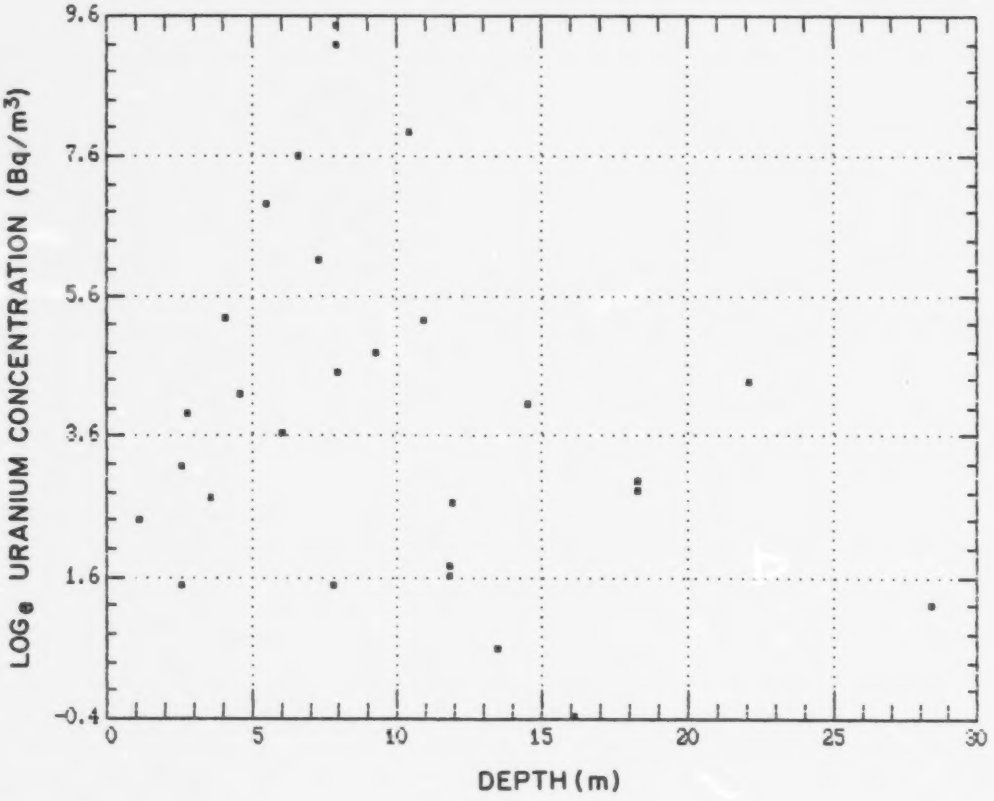

FIGURE A.2

MEASURED RADIUM-226 CONCENTRATION

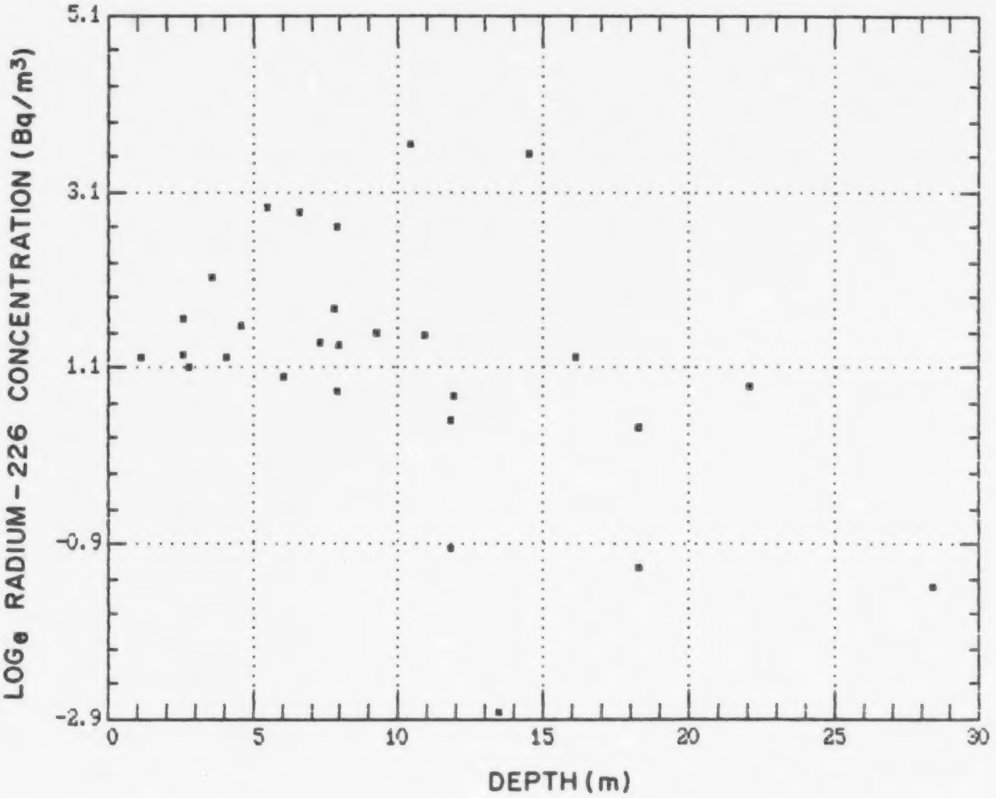

FIGURE A.3

MEASURED TOTAL THORIUM CONCENTRATION

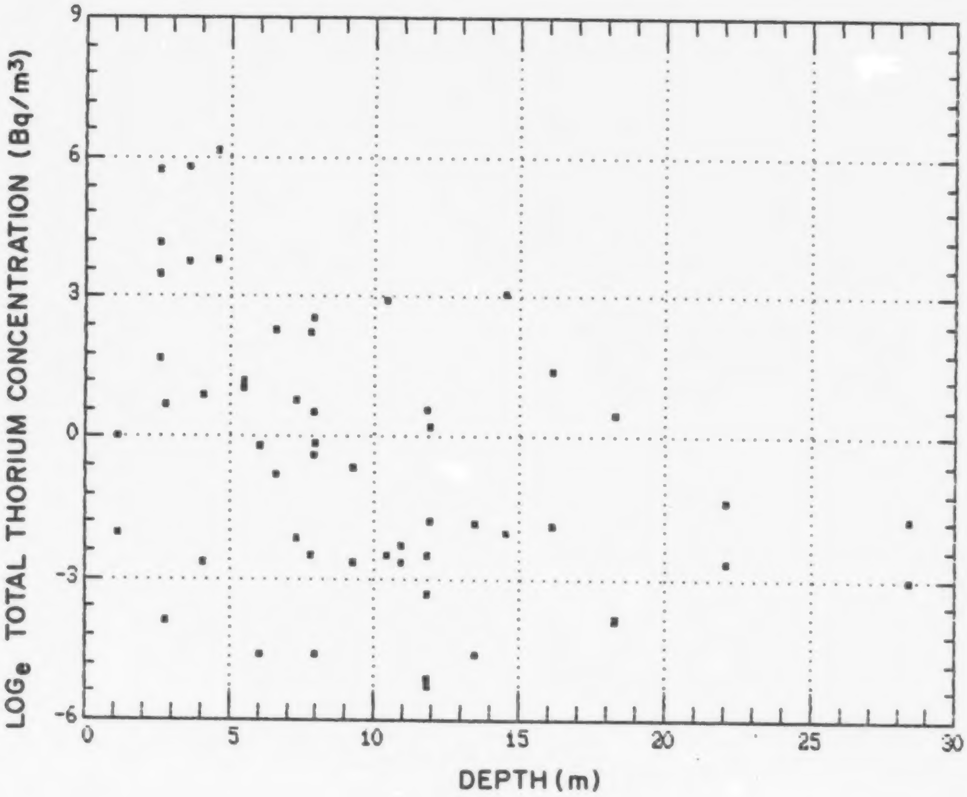

FIGURE A.4

MEASURED LEAD-210 CONCENTRATION

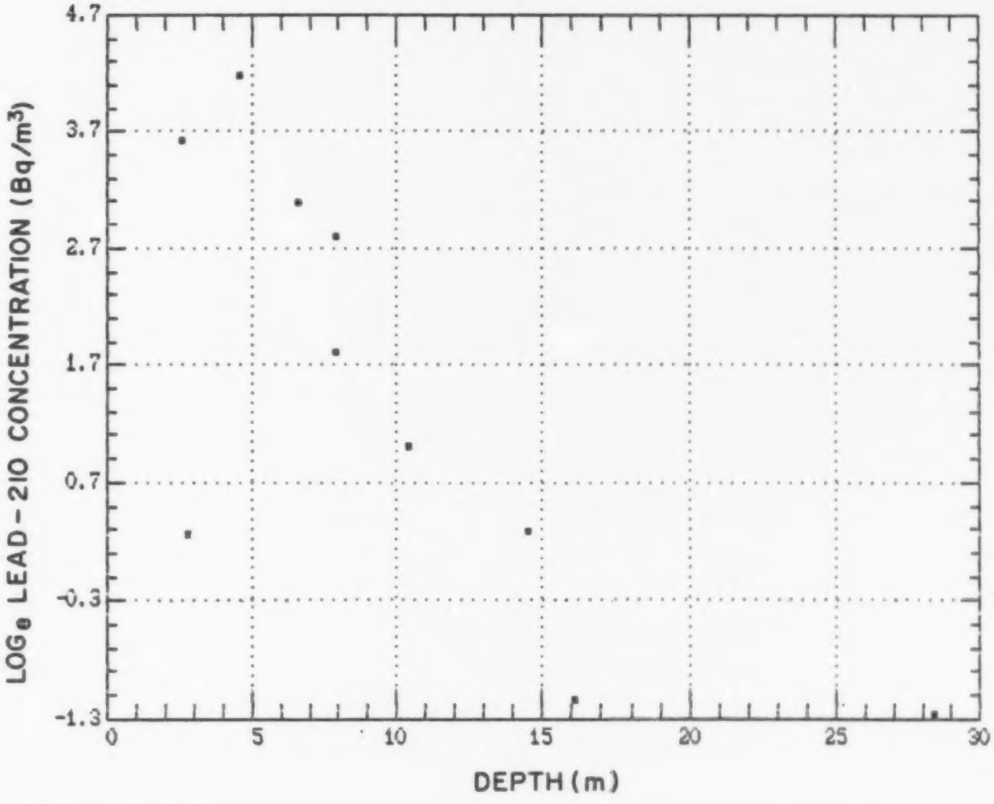

precipitation-evaporation losses) were not measured.

Surface runoff data (ie. watershed flows and surface water data) for the Serpent River Watershed were analyzed and found to be normally distributed with a mean of 0.51 $m.yr^{-1}$ and a standard deviation of 0.1 $m.yr^{-1}$. The lower and upper limits were estimated to be 0.25 and 0.85 $m.yr^{-1}$, respectively as discussed in Appendix I.

A.3.9 Long-Term Mean Annual Precipitation

The long-term, average annual net precipitation, P_a, was assumed to be constant at a value equal to the mean of the annual net precipitation (Section A.3.8), i.e. 0.51 $m.yr^{-1}$.

A.3.10 Tailings Watershed Area

The tailings watershed area, A_{ws}, was measured from a topographic map of the Lacnor tailings (Golder et al., 1986; Appendix 1.0, Figure 1.1) using a planimeter. The area measured 5.7×10^5 m^2.

A.3.11 Initial Sulphate Production Rate (FeS_2 Oxidation)

When calcite is present initially in pyritic tailings, the rate of pyrite oxidation may be characterized in three stages. During the first stage, the presence of calcite buffers the pH near neutrality, i.e., approximately 6.5, and the rate of sulphate production is chemically controlled.

In the second stage which begins when the calcite has been depleted, the pH drops to approximately 3.0, and the rate of sulphate production is biologically controlled. Depending upon the mass fraction of aluminum hydroxide present, this period may last from one to three years. It is during this period that high rates of sulphate production have been observed.

In the third stage, both the calcite and aluminum hydroxide have been depleted. In this stage the pH drops to approximately 2.0 and the overall rate of sulphate production is influenced by both chemical and biological processes. Ferric hydroxide or jarosite dissolution may provide some buffering. This period may last for decades.

The average sulphate production rates (averaged by month and depth) for a typical tailings, 600 $mol.m^{-3}$ pyrite content, are approximately $4x10^{-7}$ $mol.g^{-1}.yr^{-1}$ for stage 1 (calcite present), $1.8x10^{-6}$ $mol.g^{-1}.yr^{-1}$ for stage 2 (calcite absent) and $7x10^{-7}$ $mol.g^{-1}.yr^{-1}$ for stage 3 (calcite and aluminum hydroxide absent) (SENES and Beak, 1986).

The initial rate of sulphate production was one of the "key parameters" selected from adjustment in the calibration of the model (see Section A.4). For initial pyrite contents of 600 $mol.m^{-3}$ and 1280 $mol.m^{-3}$, R_s values of $3.0x10^{-6}$ $mol.g^{-1}.yr^{-1}$ and $1.4x10^{-5}$ $mol.g^{-1}.yr^{-1}$ were selected, respectively.

The probability distribution for the initial rate of sulphate production, R_s, when there is no $CaCO_3$ present has been assumed to be triangular. Based upon the calibration work and a pyrite content range of 600 to 800 $mol.m^{-3}$ a minimum value of $3x10^{-6}$ $mol.g^{-1}.yr^{-1}$, a mode of $4.1x10^{-6}$ $mol.g^{-1}.yr^{-1}$, and a maximum value of $5.3x10^{-6}$ $mol.g^{-1}.yr^{-1}$ were selected.

The aforementioned range for initial sulphate production rates is for an initial pyrite content of approximately 700 $mol.m^{-3}$. As indicated in the calibration of the model, Section A.4, the rate can be higher when higher pyrite contents are present.

A.3.12 Rate Fraction

When $CaCO_3$ is present, a rate fraction term, X_{rate}, is used to adjust the rate of sulphate production to account for the effect of pH on the biologically-mediated oxidation rate. During the calibration of the model an X_{rate} value of 0.10 resulted in the best overall agreement between predicted values and field data. Hence a value of 0.10 was employed for X_{rate} in the Lacnor simulations.

A.3.13 Mass Fraction of Uranium Recovered in the Mill

The initial mass fraction of U_3O_8 in the Lacnor ore was approximately 0.1% (Golder et al., 1986; Chapter 2.0). Table A.2 presents the uranium concentrations in the tailings measured during the Lacnor field study (Golder et al., 1986). The average content of U_3O_8 in the tailings is 0.0079%. Hence, the approximate mean mass fraction recovered was 92% which agrees with the operating experience at other mills in the Elliot Lake area.

A uniform distribution was assumed for the mass fraction of uranium recovered in the mill with a range of 0.90 to 0.94.

A.3.14 Tailings Surface Area

The tailings surface area, A_t, was measured from a topographic map of the Lacnor tailings (Golder et al., 1986; Appendix 1.0, Figure 1.1) using a planimeter. The measured value was 2.4×10^5 m^2.

A.3.15 Fraction of Surface Runoff

Hydrological and chemical data presented in the Lacnor Field Study (Golder et al., 1986) suggested that a substantial fraction of the surface runoff from the Lacnor site drainage basin passes directly to the tailings pond and hence to the outlet drainage channel. From a mass balance analysis of cations and anions in the tailings pond effluent and tailings porewater, it was estimated that about 60% of the runoff was comprised of freshwater flow. The surface runoff fraction, X_{run}, was determined from the analysis to have approximate lower and upper limits of 0.55 and 0.65.

For modelling purposes, the surface runoff fraction was assumed to be triangularly distributed with a minimum of 0.55, a mode of 0.60, and a maximum

Table A.2

URANIUM CONCENTRATION IN TAILINGS SOLIDS

Borehole Number*	Uranium Concentration (1) ppm	U_3O_8 Concentration ppm (%)
SO-04-b	58.4	68.9 (0.0069)
	62.3	73.5 (0.0073)
	65.9	77.7 (0.0077)
SO-04-g	79.1	93.3 (0.0093)
	69.9	82.4 (0.0082)
Average	67.1	79.1 (0.0079)

NOTE

* Only those borehole samples considered to be respresentative of unweathered tailings were included in this analysis. The selection was based in part on those samples with a Ra-226 content of 10 $Bq.g^{-1}$ which is considered to represent the average specific activity of the tailings mass as a whole (Golder et al., 1986)

REFERENCE

1. Golder et al., 1986; Appendix 1.0, Table 1.4.

of 0.65.

A.4 Model Calibration

A.4.1 Introduction

The calibration was performed by adjusting key input parameters of the model, while respecting some defined ranges, to give the best fit of model results to field data and another model, RATAP, that had been previously calibrated/ validated (SENES and Beak, 1986). The defined ranges of the input parameters were derived from published data. The field data employed were those collected at the Nordic tailings site in Elliot Lake, Ontario. Those data were found to be more extensive, in terms of the number of parameters and depths measured than the field data collected at the Lacnor tailings site.

The criteria for "best fit" was based on obtaining good agreement between predicted model values and measured field data or predicted model values using UTAP versus RATAP. The parameters selected for comparison include: pH, aqueous sulphate, calcium and iron concentrations, and solid phase calcite, gypsum, and pyrite levels. Layer 4 parameter values were not included in the calibration since not enough information was available on the vertical infiltration to this layer at the Nordic tailings.

In the first comparison, values predicted for the 20th year of a deterministic simulation of the tailings behaviour (the approximate age of the Nordic tailings area) were compared with field data. In the second comparison, pyrite contents calculated deterministically using UTAP.3 were compared with outputs generated by RATAP for a 100 year time period.

Two key input parameters, initial sulphate production rate and rate fraction, were chosen for calibration since little information is available on them in the literature. The range of values employed in the deterministic simulations are those values listed in Table A.3. Also presented are the selected values of the key variables, in brackets, which gave the "best fit" as described

Table A.3

KEY INPUT PARAMETERS USED IN THE CALIBRATION TO NORDIC FIELD DATA

PARAMETER	RANGE OF VALUES (BEST FIT VALUE) LOCATION T3	 LOCATION T5
R_s (mol.g^{-1}.yr^{-1})	1×10^{-8} to 1×10^{-4} (3.0×10^{-6})	1×10^{-8} to 1×10^{-4} (1.4×10^{-5})
X_{rate} (unitless)	0.05 to 0.46 (0.10)	0.05 to 0.46 (0.10)

Note: bracketed values are "best fit"

above.

The site specific parameters employed in the simulation are presented in Table A.4. The non-site specific parameters are those presented in SENES (1987c; Appendix A, Table A.1).

A.4.2 Description of Field Data

The field data of Smyth (1981) and Dubrovsky et al. (1985), were obtained between 1979 and 1983 at the Nordic tailings impoundment located approximately 4 km east of Elliot Lake, Ontario. The Nordic tailings were deposited from 1957 to 1968 during the operation of the mine.

The data selected for comparison with model predictions are from sampling sites located about 0.75 km apart on the tailings, designated as T3 and T5 by Smyth (1981). Water table elevations are quite different at these locations. Location T5 consists predominantly of coarse grained tailings adjacent to the tailings discharge pipe. The depth of the water table at this location varies between 4 and 4.5 m. At T3 the tailings are predominantly slime materials. At this location the water table depth varies between 6.0 and 6.5 m.

The field data include information on the tailings solids and on the porewater. Core samples were collected in the zone above the water table. Information on the solid phase includes a description of grain-size characteristics, bulk density, pyrite content and carbonate content. Liquid phase data include water content, pH and other chemical data.

Porewater data were obtained by Smyth (1981) and Dubrovsky et al., (1985). These data are variable with temporal trends not always consistent with expected temporal trends. In addition, porewater chemistry was inconsistent; electroneutrality was not always obtained for each sample. Some samples, especially those with high iron and sulphate concentrations had ion imbalances of greater than 30%. This implies that a disagreement between model

Table A.4

SITE SPECIFIC PARAMETERS USED IN THE CALIBRATION TO NORDIC FIELD DATA

Parameter	Selected Value		Reference
	Location T3	Location T5	
λ_w (m)*	6.25	4.0	(1)
λ_{mix} (m)	11.25	9.0	(1)
D_{O2} ($m^2.yr^{-1}$)**	65	65	(2)
$[F_eS_2]^\circ$ ($mol.m^{-3}$)	600	1280	(1)
P ($m.yr^{-1}$)	0.51	0.51	(see Section A.3.8)
A_{ws} (m^2)	$5x10^{-4}$	$5x10^{-4}$	
A_t (m^2)	$5x10^{-4}$	$5x10^{-4}$	
X_{run}	0.15	0.15	

Reference

1) Smyth, 1981
2) Reardon and Moddle, 1985

Note

* Measured site-specific value

** Based on porosities of 0.55 and 0.40 $m^3_{void} \cdot m^{-3}_{tailings}$ and mean volumetric water contents of 0.25, and 0.15 $m^3_{water} \cdot m^{-3}_{tailings}$ respectively (SENES and Beak, 1986).

calculations and observations in the range of 30% can be expected due to sampling and analytical variability.

A.4.3 Comparison of Nordic Field Data With Predicted Concentrations

In this section the field data for Nordic described in the previous section are compared to the results of the 20th year of a deterministic simulation using UTAP.

pH

The pH is very dependent upon the absence or presence of calcite and hence the initial calcite content. Table A.5 presents the observed and predicted pH values for locations T3 and T5. Model predictions generally agree with the observed values. In all but one case the predicted values are lower than the measured values. It is suspected that the model does not fully take into account the buffering capacity of mineral species (particularly the aluminum minerals) in the tailings which is suggested by the divergence of predicted and observed values at the deeper depths.

The prediction of low pH in layer 1, a layer which has been depleted of gypsum and calcite, is based upon the assumption that the aluminum hydroxide will have also been depleted at this point.

Sulphate

Aqueous sulphate concentrations in pyrite tailings are very dependent upon the sulphate flux from pyrite oxidation. The sulphate flux in turn is a function of several input parameters: the sulphate production rate, R_s, the effective oxygen diffusivity through the tailings, D_{O2}, and the initial pyrite content, $[FeS_2]^\circ$.

Table A.6 presents the aqueous sulphate concentrations predicted at locations T3 and T5 using R_s values of 3.0×10^{-6} mol.g^{-1}.yr^{-1} and 1.4×10^{-5} mol.g^{-1}.yr^{-1},

Table A.5

OBSERVED AND PREDICTED
pH VALUES

(Calibration Study)

Location	Layer (Depth)	Predicted pH	Observed pH
T3	L_1 (0.23 m)	2.2	3.5 (1)
	L_2 (6.25 m)	3.1	5.5 (1)
	L_3 (11.25 m)	4.7	5.5 (2)
T5	L_1 (0.22 m)	2.2	2.0 (1)
	L_2 (4.0 m)	3.1	3.5 (1)
	L_3 (9.0)	4.3	5.3 (1)

References

1) Smyth, 1981
2) Dubrovsky et al., 1985

Table A.6

OBSERVED AND PREDICTED AQUEOUS SULPHATE CONCENTRATIONS

(Calibration Study)

Location	Layer (Depth)	Aqueous Sulphate Concentration ($mol.m^{-3}$) Predicted	Observed
T3	L_2 (6.25 m)	102	78 (1)
	L_3 (11.25 m)	63	94 (2)
T5	L_2 (4.0 m)	196	198 (1)
	L_3 (9.0)	167	313 (2)

Reference

1) Smyth, 1981

2) Dubrovsky et al., 1985

respectively. At both locations the predicted sulphate concentrations in the unsaturated zone, layer 2, are in good agreement with the observed values. For the saturated zone, layer 3, however, the model underpredicted the sulphate levels at both locations.

Calcium

The aqueous calcium concentration is a function of the amount of gypsum dissolved which is limited by the solubility product of gypsum and the sulphate contribution from pyrite oxidation. Table A.7 presents the predicted and observed aqueous concentrations of calcium for the slime and coarse tailings. The field data representative of layer 2 indicate that the predicted calcium levels are two to four times lower than those observed. No field data were available for the deeper layers.

Iron

The aqueous iron concentration in the unsaturated zone, layer 2, is very dependent upon the rate of sulphate production and the porewater pH. Table A.8 presents the predicted and observed aqueous iron concentrations. The model's predictions are in good agreement with the observed values in the unsaturated zone.

In the saturated zone the aqueous iron concentrations are a function of the porewater pH and infiltration rate. In this layer the model slightly underpredicts the total iron concentration.

Calcite

The movement of the calcite depletion front is dependent upon the initial calcite content X_{CaCO3}, and the rate of sulphate production. Since the model only predicts the presence or absence of calcite within a layer, a comparison with field data can only be approximate.

Table A.7

OBSERVED AND PREDICTED
AQUEOUS CALCIUM CONCENTRATIONS

(Calibration Study)

Location	Layer (Depth)	Aqueous Calcium Concentration ($mol.m^{-3}$) Predicted	Aqueous Calcium Concentration ($mol.m^{-3}$) Observed
T3	L_2 (6.25 m)	4.4	11 (1)
	L_3 (11.25 m)	3.2	-
T5	L_2 (4.0 m)	2.6	12 (1)
	L_3 (9.0)	1.2	-

Reference

1) Smyth, 1981

Table A.8

OBSERVED AND PREDICTED TOTAL AQUEOUS IRON CONCENTRATIONS

(Calibration Study)

Location	Layer (Depth)	Aqueous Iron Concentration $(mol.m^{-3})$		
		Predicted		Observed
		Fe^{3+}	Fe^{2+}	Total
T3	L_2 (6.25 m)	49	-	54 (1)
	L_3 (11.25 m)	-	45	-
T5	L_2 (4.0 m)	97	-	86 (1)
	L_3 (9.0 m)	-	124	179 (2)

Reference

1) Smyth, 1981

2) Dubrovsky et al., 1985

At T3 the field data indicates that calcite has been depleted in approximately 50% of the unsaturated zone, i.e. to a depth of 3.25 m (Table A.9). The model predicts that the calcite has been depleted in all of the unsaturated zone, i.e. to a depth of 6.25 m.

At T5 both the model and field data indicate that the calcite has been depleted from the unsaturated zone, i.e. to a depth of 4. m.

Gypsum

The observed and predicted gypsum depletion fronts are presented in Table A.10. At both sites the field data and predicted values indicate a shallow gypsum depletion front.

Pyrite

The pyrite content of tailings at any point in time is very dependent upon the sulphate production rate. The pyrite content as a function of depth is presented in Table A.11. Employing the parameter values presented previously for sulphate production rate and rate fraction and initial pyrite contents of 600 and 1280 $mol.m^{-3}$ for locations T3 and T5, respectively, resulted in good agreement between predicted and field data.

A.4.4 Comparison of UTAP and RATAP Predictions

The RATAP model was developed to estimate the rate and quantity of acid generated by the bacterially-assisted oxidation of sulfide minerals in uranium tailings. The individual modules were calibrated using data reported in the literature. The integrated model was then validated against field data from two sampling stations on the Nordic tailings area in Elliot Lake, Ontario. Both the RATAP and UTAP models were run deterministically over a 100 year time period in order to predict the conditions at the Nordic tailings. The input data set used in the UTAP model is that presented in Table A.4 for location T3. The data set used in the RATAP model is not presented here because of its

Table A.9

OBSERVED AND PREDICTED CALCITE DEPLETION FRONTS

(Calibration Study)

Location	Depth of Depleted Front Predicted*	 Observed
T3	6.25 m	3.25 m (1)
T5	4.0 m	4.0 m (1)

Reference

1) Smyth, 1981

Note

* Model does not predict the calcite depletion front within a layer.

Table A.10

OBSERVED AND PREDICTED GYPSUM DEPLETION FRONTS

(Calibration Study)

	Depth of Depleted Front	
Location	Predicted*	Observed
T3	0.19	approx. 0.4 (1)
T5	0.15	surface (1)

Reference

1) Smyth, 1981

Note

* Predicted values represent the thickness of layer 1 in the model.

Table A.11

OBSERVED AND PREDICTED PYRITE DEPLETION FRONTS

(Calibration Study)

Location	Layer (Depth)	Pyrite Content ($mol . m^{-3}$) Predicted	Observed*
T3	L_1 (0.23 m)	-	approx. 22 (1)
	L_2 (6.25 m)	558	approx. 430 (1)
T5	L_1 (0.22 m)	-	approx. 540 (1)
	L_2 (4.0 m)	1084	approx. 1080 (1)

Note

* Pyrite content at depth equal to the midpoint of the layer

Reference

1) Smyth, 1981

size but is that found in a report to the NUTP by SENES and Beak (1986; Section 3.0).

The predicted pryite contents as a function of time in the unsaturated zone are presented in Table A.12 for the two computer codes. The values predicted by each model are in very good agreement. UTAP and RATAP predict an approximate 40% reduction in the overall pyrite content of the unsaturated zone.

A.5 Model Validation

A.5.1 Introduction

To validate the model, field data collected during the Lacnor field study (Golder et al., 1986) were compared with the outputs of the UTAP model. The predicted values were from a deterministic simulation of the Lacnor tailings behaviour over a 25 year time period, the approximate age of the Lacnor tailings area. The parameters compared included: pH, aqueous sulphate, calcium, iron, uranium, thorium, lead and radium concentrations.

For the model validation study the following values were used for the key input parameters: R_s, 4.1×10^{-6} mol.g^{-1}.yr^{-1} and X_{rate}, 0.10. These values were determined from the calibration study described in the previous section for location T3 at the Nordic tailings area. The R_s value from location T5 was not used because the pyrite content at this location was much higher than the Lacnor tailings.

A.5.2 Description of Field Data

During the Lacnor Field Study (Golder et al., 1986) five porewater sampling locations were monitored at sites on the tailings: GW-01, GW-02, GW-03, GW-04 and GW-05. Monitoring stations GW-01 and GW-02 were located in the western section of the basin and represent predominantly sandy, coarse tailings. Stations GW-03, GW-04 and GW-05 were located in the eastern end of the

Table A.12

UTAP AND RATAP
PREDICTED PYRITE CONTENTS

Time (year)	Tailings Pyrite Content ($mol.m^{-3}$) RATAP	UTAP
10	587	593
20	540	558
30	504	525
40	474	494
50	449	465
60	428	437
70	408	411
80	389	387
90	371	364
100	352	342

tailings and represent interlayered fine and coarse tailings. A detailed description of the field data is presented in Section 2.1.5, entitled Special Field Studies, of this report.

A.5.3 Comparison of Field Data With Predicted Concentrations

pH

The observed pH values are compared with model predictions in Table A.13. The observed values show considerable spacial variability. This reflects the extent of depletion of the buffering agents (aluminum minerals, calcite) in the reactive layer (Layer 2) and the mixing zone (Layer 3). Low pH values (pH <2.5) indicate local depletion. The predicted pH values are observed to be within the range of measured values.

Sulphate

The sulphate concentration, along with the pH, is a key water quality parameter for judging the appropriateness and the robustness of the model. The oxidation of pyrite to sulphate is undoubtedly the "pacemaker" reaction. In Table A.14, the predicted sulphate concentrations are compared with those observed during the Lacnor field study. Considering the uncertainty of the initial pyrite content and the uncertainty about the extent of pyrite and gypsum depletion after 25 years, the agreement is quite good.

In layer 4, the model underestimates the sulphate concentration. Only one field measurement of sulphate concentration was taken at the depth of layer 4, however. The high sulphate value, 102 $mol.m^{-3}$, at GW-02 indicates that considerable mixing is still occurring at this depth. In the model layer 4 is assumed to be quite stagnant and to receive only a nominal inflow from the mixing zone. Hence, the model predicts low sulphate levels.

Table A.13

PREDICTED AND OBSERVED
pH VALUES

(Validation Study)

Layers (Depth)	Predicted pH	Observed pH*				
		GW-1	GW-2	GW-3	GW-4	GW-5
L_2 (0.5m)	3.3	2.1	<2.0	-	-	4.8
L_3 (12m)	5.0	4.9-5.6	2.9-5.8	6.9	5.0-5.8	3.6 6.0
L_4 (12.75m)	5.3	-	5.2	-	-	-

Reference

Golder _et al_., 1986; Tables 1.10 and 1.11

Note

* Depth below the tailings surface: L_2 ranges from 0.25 to 2m, L_3 ranges from 8 to 12.5 m, and L_4 ranges from 12.6 to 15 m.

Table A.14

PREDICTED AND OBSERVED SULPHATE CONCENTRATIONS

(Validation Study)

Aqueous Sulphate Concentration (mol.m^{-3})

Layers (Depth)	Predicted	Observed*				
		GW-1	GW-2	GW-3	GW-4	GW-5
L_2 (0.5m)	31	24	-	-	-	7-31
L_3 (12m)	37	82-83	40-69	30	43-45	72-108
L_4 (12.75m)	24	-	102	-	-	-

Reference

Golder *et al*., 1986; Tables 1.10 and 1.11

Note

* Depth below the tailings surface: L_2 ranges from 0.25 to 2m; L_3 ranges from 8 to 12.5 m; and L_4 ranges from 12.6 to 15 m.

Calcium

The predicted and observed aqueous calcium concentrations are presented in Table A.15. Good agreement exists for layers 2 and 4. The predicted value in layer 3 is approximately 2 times lower than those observed. This indicates that other sources of calcium which were not accounted for in the model may have been present or that calcite may not have been acidified in some locations.

Iron

The predicted and observed aqueous concentrations of iron, Fe^{3+} and Fe^{2+}, are presented in Table A.16. The model's predictions for layers 2 and 3 are in good agreement with the field data, which exhibit a large range. As with the sulphate concentrations in layer 4, the model underpredicts the high iron level observed at GW-02.

Uranium

The predicted and observed aqueous uranium concentrations are presented in Table A.17. In general, the predicted values fall within the observed range of field data.

Once again, the difference in the depth of the mixing zone at GW-02 and the depth of the mixing zone employed in the model accounts for the large difference between predicted and observed uranium concentrations in layer 4.

Thorium

Table A.18 presents the predicted and observed aqueous thorium concentrations. The model predicts that the thorium will have been depleted in layer 2 by year 23 and hence predicts no aqueous thorium. Prior to depletion the thorium level was 6.1×10^5 $Bq.m^{-3}$. According to the field data, however, some thorium is still present in Layer 2. In Layers 3 and 4 the model predictions are

Table A.15

PREDICTED AND OBSERVED CALCIUM CONCENTRATIONS

(Validation Study)

Aqueous Calcium Concentration (mol.m^{-3})

Layers (Depth)	Predicted	Observed GW-1	GW-2	GW-3	GW-4	GW-5
L_2 (0.5m)	9.9	12.9	12.2-14.0	-	-	12.1
L_3 (12m)	5.5	10.4-12.0	11.3-12.1	10.5-11.5	-	8.5-10.9
L_4 (12.75m)	8.5	-	11.1	-	-	-

Reference

Golder _et_ _al_., 1986; Tables 1.10 and 1.11

Note

* Depth below the tailings surface: L_2 ranges from 0.25 to 2m, L_3 ranges from 8 to 12.5 m, and L_4 ranges from 12.6 to 15 m.

Table A.16

PREDICTED AND OBSERVED AQUEOUS IRON CONCENTRATIONS

(Validation Study)

Aqueous Iron Concentration (mol.m^{-3})

Layer (Depth)	Predicted Fe^{3+}	Predicted Fe^{2+}	Observed* Total Iron GW-1	GW-2	GW-3	GW-4	GW-5
L_2 (0.5m)	10.7	-	-	6.2- 21.6	-	-	5.0
L_3 (12m)	-	23.3	61.4- 68.4	29.8- 34.1	1.8	24.3- 27.7	70.4- 119.0
L_4 (12.75m)	-	11.2	-	83.9	-	-	-

Reference

Golder *et al*., 1986; Tables 1.10 and 1.11

Note

* Depth below the tailings surface: L_2 ranges from 0.25 to 2 m, L_3 ranges from 8 to 12.5 m, and L_4 ranges from 12.6 to 15 m.

Table A.17

PREDICTED AND OBSERVED AQUEOUS URANIUM CONCENTRATIONS

(Validation Study)

Aqueous Uranium Concentration* (Bq.m^{-3})

Layers (Depth)	Predicted	Observed* GW-1	GW-2	GW-3	GW-4	GW-5
L_2 (0.5m)	2.0×10^4	2.7×10^3	-	-	-	275.
L_3 (12m)	1.6×10^3	110- 148	7.4×10^4- 6.6×10^5	1×10^4	350- 1×10^3	2.6×10^3- 2.3×10^5
L_4 (12.75m)	13	-	1.5×10^3	-	-	-

Reference

Golder *et al*., 1986; Tables 1.10 and 1.11

Note

*Conversion factor is 1 Bq.m^{-3} = 25 ppb

** Depth below the tailings surface: L_2 ranges from 0.25 to 2 m, L_3 ranges from 8 to 12.5 m, and L_4 range from 12.6 to 15 m.

Table A.18

PREDICTED AND OBSERVED AQUEOUS THORIUM CONCENTRATIONS

(Validation Study)

Aqueous Thorium Concentration * (Bq.m^{-3})

Layers (Depth)	Predicted	Observed**				
		GW-1	GW-2	GW-3	GW-4	GW-5
L_2 (0.5m)	0.0	7.0×10^3	-	-	-	1.3×10^3
L_3 (12m)	3.1×10^3	350-2×10^3	1.5×10^3 1.8×10^4	1.6×10^4	1.0×10^3 1.6×10^3	240-1.7×10^3
L_4 (12.75m)	2.5×10^3	-	2.2×10^4	-	-	240

Reference

Golder *et al*., 1986; Tables 1.10 and 1.11

Note

* Th-228, Th-230, and Th-232

** Depth below the tailings surface: L_2 ranges from 0.25 to 2 m, L_3 ranges from 8 to 12.5 m, and L_4 range from 12.6 to 15 m.

comparable with observations.

Lead-210

Table A.19 presents the predicted and observed aqueous lead-210 concentrations. Because of the lack of field data on lead-210 concentrations only a limited comparison can be made. The data suggest that the lead-210 levels in layers 3 and 4 may be overestimated by the model.

Radium-226

The aqueous radium-226 concentrations, predicted and observed, are presented in Table A.20. Good agreement between predicted and observed values is evident.

A.6 Overall Summary of Validation

The validation study of the Water Source Model attempted to quantify the level of confidence that can be placed on the model predictions. The model predicts annual mean parameter values assuming an homogeneous tailings mass. In general, good agreement was found with the observed values, which are representative of instantaneous conditions at five piezometer nests with varying properties. It was concluded therefore that the UTAP.3 Water Source Model is suitable for use in predicting the behaviour of the Lacnor tailings.

Table A.19

PREDICTED AND OBSERVED
AQUEOUS LEAD CONCENTRATIONS

(Validation Study)

Aqueous Lead Concentration ($Bq.m^{-3}$)

Layers (Depth)	Predicted	Observed GW-1	GW-2	GW-3	GW-4	GW-5
L_2 (0.5m)	$1.5x10^4$	-	-	-	-	-
L_3 (12.0m)	$1.6x10^4$	-	$2.8x10^3$	-	-	-
L_4 (12.75m)	$1.6x10^4$	-	$1.3x10^3$	-	-	-

Reference

Golder *et al*., 1986; Tables 1.10 and 1.11

Note

** Depth below the tailings surface: L_2 ranges from 0.25 to 2 m, L_3 ranges from 8 to 12.5 m, and L_4 range from 12.6 to 15 m.

Table A.20

PREDICTED AND OBSERVED AQUEOUS RADIUM CONCENTRATIONS

(Validation Study)

Layers (Depth)	Predicted	Aqueous Radium-226 Concentration ($Bq.m^{-3}$) Observed GW-1	GW-2	GW-3	GW-4	GW-5
L_2 (0.5m)	$4.5x10^3$	$2.7x10^3$	-	-	-	$3.4x10^3$
L_3 (12m)	$4.3x10^3$	$1.5x10^3$-	$3.8x10^{-4}$ $2.4x10^5$	$3.7x10^3$	$2.2x10^{-3}$ $2.6x10^3$	$3.9x10^3$- $4.6x10^3$
L_4 (12.75m)	$4.4x10^{-3}$		$3.4x10^4$	-	-	-

Reference

Golder _et_ _al_., 1986; Tables 1.10 and 1.11

Note

** Depth below the tailings surface: L_2 ranges from 0.25 to 2 m, L_3 ranges from 8 to 12.5 m, and L_4 range from 12.6 to 15 m.

APPENDIX B

EROSION MODEL

APPENDIX B: EROSION MODEL

B.1 Conceptual Approach

The flow of water over the tailings surface occurs in a northeasterly direction, following the general slope of the tailings pile. The movement of the tailings surface layer is assumed to follow this direction of flow, with all of the eroded material being deposited in the pond at the east end of the tailings area. The pond traps a high percentage of the suspended sediment and bedload as suggested by low suspended solids levels measured in the pond effluent during the Lacnor field study (Golder et al., 1986).

B.2 Site-Specific Model Alterations

No site-specific alterations have been made to the generic erosion model in order to simulate the conditions at the Lacnor tailings.

B.3 Site-Specific Parameters

The following section outlines the parameters considered to be specific to the Lacnor site. Table B.1 lists the site-specific erosion parameters, including their nominal and probabilistic values.

The non site-specific input parameters are presented in SENES (1987c).

B.3.1 Silt Particle Diameter

The median diameter of the silt particles (d_m) at the tailings surface was determined using the results of ten surficial grab samples taken across the tailings area (Golder et al., 1986; Appendix 1.0, Figures 1.2 and 1.3).

For each of the ten samples, the median diameter of the silt particles (less than 0.075 mm) was determined, with the average of these median values being calculated as 0.017 mm. The diameter for which 95% of the particles were

Table B.1

EROSION MODEL
SITE-SPECIFIC PARAMETER VALUES

Symbol	Description	Units	Nominal	Probabilistic
d_m	median silt diameter*	mm	0.017	T(0.0015,0.017,0.075)
F_m	minimum fraction of tailings covered by vegetation	--	0.6	C(0.6)
L_f	flow length of tailings pile	m	880	C(880)
P_B	bedload pond trapping efficiency	%	100	C(100)
P_s	suspended sediment pond trapping efficiency	%	98	T(85,98,100)
S_o	slope of tailings pile	%	0.92	C(0.92)

Notes

C - Constant (single value)
T - Triangular (min., mode, max.)
* metric units

greater than was chosen to represent the minimum value in the distribution. The maximum value is the maximum silt particle diameter (by definition). The silt particle diameter was assumed to be triangularly distributed, with a minimum value of 0.0015 mm, a mode of 0.017 mm and a maximum of 0.075 mm.

B.3.2 Minimum Fraction of Tailings Covered by Vegetation

Currently, the Lacnor tailings area is partially covered with vegetation. It was assumed that the fraction of the surface covered would not fall below this initial level. To determine the initial fraction of surface vegetated, photographs of the site were used. An aerial photograph taken in 1985 showed that the entire tailings surface was vegetated except for an area near the pond that was flooded and two strips (approximately 10 m wide) along the two drainage channels running across the area.

Using a planimeter and a topographic map of the Lacnor tailings (Golder _et al_., 1986; Appendix 1.0, Figure 1.1), the total area with vegetation cover was determined to be 1.81×10^5 m^2. This area was further assumed to be 80% covered with vegetation, with the overall fraction of tailings covered calculated as:

$$\text{Overall Minimum Fraction Covered } (F_m) = 0.8 \, \frac{(\text{Vegetated Area})}{(\text{Total Area})} \qquad \text{(B.1)}$$

$$= (0.8)\, \frac{(1.81 \times 10^5 \text{ m}^2)}{(2.41 \times 10^5 \text{ m}^2)}$$

$$= 0.6$$

B.3.3 Flow Length of Tailings Pile

The erosion model treats the tailings pile as a rectangular area, and thus the length of the pile along the direction of flow must be specified. For the Lacnor site, the direction of flow is northeast, with the base of the pile located at the pond. Based upon a topographic map of the tailings (Golder _et_ al., 1986; Appendix 1.0, Figure 1.1), the width of the tailings pile at the pond was calculated to be 275 m (perpendicular to the direction of flow). Given a total tailings area of 2.41 x 10^5 m^2, the flow length (L_f) is then:

$$L_f = \frac{2.41 \times 10^5 \ m^2}{275 \ m} = 880 \ m \qquad (B.2)$$

B.3.4 Bedload Pond Trapping Efficiency

The bedload trapping efficiency of the pond (P_B) can be determined from the pond area, its outflow rate and the diameter of the bedload particles (Chen, 1975). Bedload, by definition, consists of all particles with a diameter greater than 0.075 mm. The bedload particles at the tailings surface range in diameter from 0.075 mm to 0.4 mm, with a mean value of 0.24 mm (Golder et al., 1986; Appendix 1.0, Figure 1.3). Using a planimeter and a topographic map (Golder et al., 1986; Appendix 1.0, Figure 1.1), the pond area was calculated to be 6.3 x 10^4 m^2. Finally, the outflow rate of the pond was determined using the results of surface water monitoring station SW-03, located 100 m downstream from the pond (Golder et al., 1986; Appendix 3.0, Table 3.4). The average flow rate for the study period was 28.7 $L.s^{-1}$.

The ratio of pond area to outflow rate is then calculated as:

$$\frac{\text{Pond Area } (m^2)}{\text{Outflow Rate } (m^3.s^{-1})} = \frac{6.3 \times 10^4 \ m^2}{0.028 \ m^3.s^{-1}} \qquad (B.3)$$

$$= 2.25 \times 10^6 \ s.m^{-1} \ (6.86 \times 10^5 \ s.ft^{-1})$$

For a 6.86x10^5 $s.ft^{-1}$ ratio of pond area to outflow, the pond trapping efficiency is 100% for bedload particles (SENES, 19876a; Volume 3.0, Figure 3.14).

B.3.5 Suspended Sediment Pond Trapping Efficiency

The suspended sediment trapping efficiency (P_s) is determined in the same manner as the bedload trapping efficiency. The particle diameter of the suspended sediment ranges from 0.0015 mm to 0.075 mm, with an average value of 0.04 mm (Golder _et al_., 1986; Appendix 1.0, Figure 1.3). For this range of particle diameters, the trapping efficiency (P_s) will range from 85% to 100%, with a mode of 98% (SENES, 1986a; Volume 3.0, Figure 3.14). This has been represented using a triangular distribution for P_s with a minimum of 85, a mode of 98, and a maximum of 100.

B.3.6 Slope of the Tailings Pile

The slope of the tailings pile is represented by the change in elevation that occurs along the direction of flow. Based on elevations at Lacnor (Golder _et al_., 1986; Appendix 1.0, Table 1.6), the slope (S_0) was calculated as:

$$S_0 = \frac{(\text{elev. at site WL-01}) - (\text{elev. at site WL-03})}{(\text{distance between WL-01 and WL-03})} \times 100\% \qquad (B.4)$$

$$= \frac{385.06\text{ m} - 379.54\text{ m}}{600\text{ m}} \times 100\%$$

$$= 0.92\%$$

B.4 Model Validation/Calibration

The erosion model could not be validated or calibrated since no field data were available on the loss of tailings material, i.e. no suspended sediment or bedload field measurements were taken.

Due to the large size of the pond at the east end of the tailings area, 100% of the bedload and a minimum of 85% of the suspended sediment that enter the pond are trapped. As a result, the total sediment mass leaving the pond and entering the river/lake system is small.

If the pond was removed (i.e. set the trapping efficiencies to zero), then the results of erosion would be more significant. A test run for Lacnor with no pond gave a total sediment mass of 9.8×10^3 $kg.yr^{-1}$ leaving the tailings area.

Erosion of 9.8×10^3 $kg.yr^{-1}$ tailings material translates into an approximate loss of 2.3×10^7 $Bq.yr^{-1}$ of total thorium (based on solids concentrations of 3×10^6 $Bq.m^{-3}$ at year 200). Employing the base case values for the total thorium desorption fraction (0.02), the total drainage area at node 1 (9.9×10^5 m^2), and the net precipitation rate (0.51 $m.yr^{-1}$) results in a total thorium aqueous concentration of 0.9 $Bq.m^{-3}$ at node 1. This value represents the contribution of erosion to total thorium concentration at node 1.

At year 200, the discharge of total thorium from the mixing zone has reached a steady state value of 8.22×10^2 $Bq.m^{-3}$, the result of which is a total thorium concentration at node 1 of 1.73×10^2 $Bq.m^{-3}$. Hence, the contribution of the maximum erosion to this value would be less than 1%.

APPENDIX C

AIR SOURCE MODEL

APPENDIX C: AIR SOURCE MODEL

C.1 Conceptual Approach

The dust and radon models included in UTAP.3 were used without change for modelling the dust and radon sources from the Lacnor tailings.

C.2 Site-Specific Model Alterations

No model alterations were required.

C.3 Site-Specific Parameters

In the following section, short descriptions of the site-specific parameters are presented. Justifications for the selection of parameter values are also included. Table C.1 presents the site-specific parameters and their probability distributions and descriptions.

Three of the site-specific parameters, tailings surface area (A_t), thickness of the unsaturated layer (λ_w) and tailings bulk density ($^{\rho}t$), are described in Appendix A, Section A.3.

The non-site specific parameters are presented in SENES (1987c), Chapter 4.0.

C.3.1 Silt Content

Based upon field data (Golder et al., 1986; Appendix 1.0, Figure 1.2 and 1.3) the silt content(s) of the tailings (% of particles < 75 μm) was approximately 45%, with a range of 30% to 60%.

For modelling purposes a triangular distribution was assumed with a minimum of 30, a mode of 45 and a maximum of 60. This data was also used for the generic model inputs (SENES, 1987c).

Table C.1

SITE-SPECIFIC AIR SOURCE MODEL INPUTS

Model Symbol	Description	Units	Nominal Value	Probability Distribution*	Computer Symbol
A_o	surface area of the tailings	m^2	$2.41x10^5$	$C(2.41x10^5)$	ATAIL
X_s	thickness of unsaturated layer	m	0.50	T(0.25,0.50,2.00)	DUNSAT
M	moisture content by weight of (wet) tailings	%	13.0	T(9.0,13.0,23.0)	MPCH20
ρ	tailings bulk density (dry)	$g.m^{-3}$	$1.3x10^6$	$T(1.1x10^6,1.3x10^6,1.5x10^6)$	RHOTAL

C.3.2 Moisture Content

Based on data from the Lacnor Field Study (Golder et al., 1986; Appendix 1, Table 1.2) the moisture content, M, in the unsaturated zone, depths of 0.3-0.9 m, had a mean of 13% and minimum and maximum values of 9% and 23%, respectively.

A triangular distribution was assumed for the moisture content with a minimum of 9%, a mode of 13% and a maximum of 23%.

C.3.3 Number of Days with Rain

The annual number of days with more than 0.25 mm of precipitation, P_n, was obtained from Atmospheric Environment Services (AES) precipitation data from the Gore Bay Weather Station, on Manitoulin Island (AES, not dated).

Precipitation data was collected during the Lacnor Field Study (Golder et al., 1986). However, samples were only collected for a one year period. Because of Lacnor study's short duration, Gore Bay data were considered to be more indicative of the Lacnor tailings climate.

The Gore Bay data has a normal distribution with a mean of 149, a standard deviation of 17 and minimum and maximum values of 115 and 183, respectively. This data was also used for the generic model inputs (SENES, 1987c).

C.4 Model Validation

One phase of the Lacnor Field Study was the monitoring of radon exhalation rates from various locations on the surface of the Lacnor tailings. For the spring and summer sampling, the radon exhalation rates were measured for a variety of tailings conditions including dry, damp, saturated, water-covered, vegetated and non-vegetated. For the winter sampling, the radon exhalation rates were measured on the surface of the frozen tailings, which had 35 to 70 cm of snow and 2 to 8 cm of ice removed to expose the tailings surface. The radon exhalation rates were monitored for a 2 to 6 hour period.

Because the snow and ice cover was removed from the tailings for the winter monitoring program, it was felt that the flux measurement made during the winter would not be representive of actual winter conditions; hence, it was decided to compare only the spring and summer exhalation rates with those predicted by the model under non-frozen conditions. The results are:

	Monitored	Modelled
Number of Readings	25	500 (Trials)
Mean ($Bq.m^{-2}s^{-1}$)	1.12	1.05
Standard Deviation ($Bq.m^{-2}s^{1}$)	1.50	0.55

The comparison between the means is extremely good. The difference between the standard deviations (the monitored standard deviation being larger) was expected since the monitored exhalation rates were 2 to 6 hour averages where the model predicts annual averages. These results are illustrated in Figure C.1. The relative frequency of the modelled radon exhalation rate is displayed with the averages of the monitored and modelled exhalation rates superimposed on the figure. Thus, Figure C.1 illustrates the capability of the radon model to predict realistic radon exhalation rates.

Data on suspended dust and dustfall are available for the study area, but sufficient data are not available to permit either direct or indirect validation of the dust source model for the Lacnor site. However, as discussed in SENES (1987c) Section 4.2, the dust source model is based on published empirical data and with appropriate input parameters can produce reasonable estimates of dust emission rates. Input parameters specific to Lacnor tailings and local meteorology were used in the analysis and hence the estimate of dust source strength is considered reasonable.

FIGURE C.1

COMPARISON OF PREDICTED AND MEASURED RADON FLUX FOR SUMMERTIME CONDITIONS

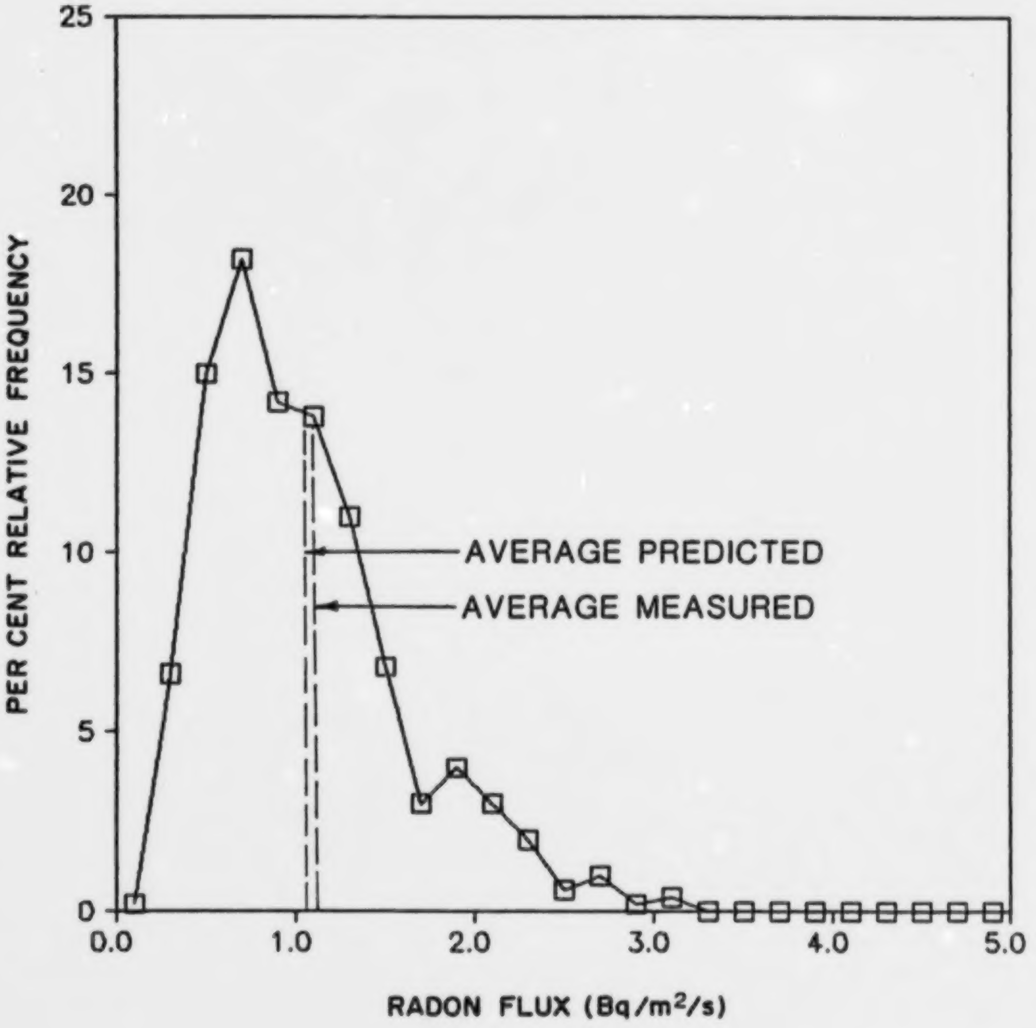

APPENDIX D

AIR DISPERSION MODEL

APPENDIX D: AIR DISPERSION MODEL

D.1 Conceptual Approach

The wind and air dispersion modules included in the UTAP.3 model (SENES, 1987c; Chapter 5) are suitable for modelling the atmospheric dispersion of dust and radon from the Lacnor tailings. The area-weighted average air concentration over the watershed area is calculated for the following directions and ring numbers respectively; (7,1), (10,2), (10,3), (8,4), and (7,4) which are the locations which contain the water nodes. Figure 3.4, Chapter 3.0 of SENES (1987c), presents the angular rings.

D.2 Site-Specific Model Alterations

No model alterations were required.

D.3 Site-Specific Parameters

No site-specific data were identified.

D.4 Model Validation/Calibration

The validation or calibration of the air dispersion model was not possible since "background noise", i.e. radon and dust loading, from an immediately adjacent tailings area, Nordic, was present as are other confounding influences.

APPENDIX E

SOIL MODEL

APPENDIX E: SOIL MODEL

E.1 Conceptual Approach

The soil module included in the UTAP.3 model (SENES, 1987c; Chapter 6) is suitable for modelling the concentration of radionuclides in the soil which have been deposited as particulate matter from the air to the surface of the soil in the surrounding district of the Lacnor tailings.

E.2 Site-Specific Model Alterations

No model alterations were required.

E.3 Site-Specific Model Parameters

The only Lacnor site-specific soil model parameter is the annual net precipitation (P) which is described in Section A.3.8 of Appendix A.

E.4 Model Validation/Calibration

No data were available to permit the validation or calibration of the soil model, i.e. no radionuclide concentrations were measured in off tailings soil.

APPENDIX F

GROUNDSHINE MODEL

APPENDIX F: GROUNDSHINE MODEL

F.1 Conceptual Approach

The generic UTAP.3 groundshine model (SENES, 1987c; Chapter 7) is suitable for modelling the external gamma radiation dose at the Lacnor receptors without modification. The model calculates the surface gamma flux and receptor dose resulting from the accumulation over time in the soil of radionuclides deposited from the air. The radionuclides included in this model are natural uranium (U238 and U234), radium-226 (plus radon daughters), Pb-210 and total thorium (Th232 plus daughters to Pb208 and Th230 from the uranium-238 chain).

The model uses radionuclide concentrations in two soil layers calculated by the soil model. The groundshine model approximates the self-shielding within each soil layer and the shielding provided by the top layer for gamma rays from the second layer. Also, radon emanation and subsequent exhalation to the atmosphere is modelled to account for the reduced concentration of radon daughters remaining in the soil.

F.2 Site-Specific Model Alterations

No site-specific alterations have been made to the generic groundshine model for the purposes of making Lacnor calculations.

F.3 Site-Specific Parameters

No site-specific parameters have been used to represent the Lacnor receptors.

F.4 Model Validation/Calibration

The validation and/or calibration of the groundshine model was not possible since no site-specific measurements of gamma dose rate from deposited radionuclides were made. Also, the natural background radiation in the area is much greater than the expected dose rate from wind-deposited radionuclides.

APPENDIX G

TERRESTRIAL VEGETATION MODELS

APPENDIX G: TERRESTRIAL VEGETATION MODELS

G.1 Conceptual Approach

The models included in UTAP.3 (SENES, 1987c; Chapter 8) are suitable for modelling the terrestrial vegetation at the Lacnor tailings site and surrounding areas. No changes in model application or interpretation are required.

G.2 Site-Specific Model Alterations

No model alterations are required.

G.3 Site-Specific Parameters

Some limited vegetation sampling was done during the Lacnor field study (Golder *et al.*, 1986). However, percentage moisture data were not recorded and paired soil samples were collected at only two of the six communities studied. Examination of the borehole soil sampling program (Golder *et al.*, 1986; Appendix 1, Borehole logs) indicated that only one additional soil sample was taken at a depth of less than one metre.

In addition to the limitations discussed above, the data was entirely for vegetation grown on tailings themselves, a drastically different chemical and physical environment as compared to the native surficial soils. It was therefore decided that the Lacnor vegetation data was unsuitable to use as replacement for that used in the derivation of soil-to-plant transfer coefficients ($B_{v,i}$'s) in UTAP.3.

No other site-specific data were identified for any of the input parameters for the terrestrial vegetation models.

G.4 Model Validation/Calibration

The terrestrial vegetation model was not validated or calibrated for the Lacnor site since no field data were available, i.e. the radionuclide concentrations in vegetation around the Lacnor site were not measured.

APPENDIX H

SUBSURFACE TRANSPORT MODEL

UTAP APPLICATION TO THE LACNOR TAILINGS; SUBSURFACE TRANSPORT MODEL

APPENDIX H: SUBSURFACE TRANSPORT MODULE

H.1 Conceptual Approach

The Lacnor tailings basin is situated within a bedrock valley formerly occupied by a swamp. In the generic model, the groundwater flowpaths were conceptualized as glaciofluvial sandy aquifers underlying the dam structures at outlet valleys. The dam structures were considered to be relatively impermeable. At the Lacnor tailings however, the majority of the subsurface discharge is through two permeable dams located on the southeast side of the basin. The field data indicate that the dams allow the discharge of water, but retard radionuclide movements.

For the aforementioned reasons, the dams are considered to be "pseudo aquifers" and are the transport paths in the subsurface transport model. These pseudo aquifers are considered to be a mixture of crushed rock, sand and tailings material, the latter having been incorporated in the dams during construction or having migrated into the dams over the past thirty years.

In the generic model all of the horizontal flow through layer 3 is assumed to be near surface runoff. In the Lacnor application only a fraction of this flow emerges as near surface runoff. The remaining fraction is assumed to be the source of the pseudo aquifers, while layer 4 is assumed to be stagnant.

The selection of layer 3 as the source of the pseudo aquifers was based upon the high radionuclide concentrations measured at the toes of the dams (Golder et al., 1986; Appendix 3.0, Tables 3.20 and 3.21).

H.2 Site-Specific Model Alterations

No changes were required to the code of the generic subsurface transport module in order to simulate the conditions at the Lacnor tailings.

H.3 Site-Specific Parameters

H.3.1 Introduction

The following is a short description of the parameters which are considered to be representative of the Lacnor tailings basin. Table H.1 presents the site-specific parameters and their probability distribution types and descriptors. The probability distributions reflect the uncertainties in the parameter values due to inhomogeneities in the geological formation and variability in the data measurement techniques.

The non-site specific parameters employed in the model are presented in SENES (1987c), Chapter 9.0.

H.3.2 Cross-Section Area of Flow

The cross-sectional area (A_x) is the area of the window through which the groundwater flow passes. For the Lacnor tailings site, these cross-sectional areas were calculated using field data (see Section H.4, Model Calibration/Validation).

The calculated cross sectional areas are 2005 m^2 and 3590 m^2 for dams 1 and 2, respectively.

H.3.3 Hydraulic Gradient

The hydraulic gradient (I) within sandy aquifers is generally considered to range from 0.005 $m.m^{-1}$ to 0.01 $m.m^{-1}$. Due to inhomogeneities, the hydraulic gradient varies not only from site to site on a macroscale level, but also within a site at the microscale level. High hydraulic gradients (0.05 $m.m^{-1}$) have been reported near some dam structures (Morin *et al*., 1982).

For the Lacnor tailings, the hydraulic gradients were calculated using field

Table H.1

SUBSURFACE TRANSPORT MODEL

SITE-SPECIFIC PARAMETER VALUES

Symbol	Description	Units	Dams	Nominal	Probabilistic
$A_{x,j}$	cross-sectional area of jth aquifer window	m^2	1	2005	C(2005)
			2	3590	C(3590)
I_j	hydraulic gradient	$m.m^{-1}$	1	0.051	N(0.051,0.01,0.03, 0.07)
			2	0.176	N(0.176,0.03,0.12, 0.24)
K_j	hydraulic conductivity	$m.yr^{-1}$	1 and 2	69.4	LN(69.4,2.4,12,400)
$K_{d,i}$	distribution coefficient	$m^3.kg^{-1}$	1 and 2		
	- total uranium			$1.2X10^{-2}$	LN($1.2X10^{-2}$,1.5, $3.6X10^{-3}$, $4X10^{-2}$)
	- total thorium			$5.0 X 10^{-2}$	LN($5X10^{-2}$, 1.5,$1.5X10^{-2}$ $1.7X10^{-1}$)
	- lead-210			$6.0X 10^{-2}$	LN($6X10^{-2}$, 1.5, $1.8X10^{-2}$, $2.0X10^{-1}$)
	- radium-226			$4.5 X 10^{-2}$	LN($4.5X10^{-2}$, 1.5, $1.3X10^{-2}$ $1.5X10^{-1}$)
n_j	porosity	$m^3.m^{-3}$	1 and 2	0.365	U(0.33, 0.40)
P_a	average net precipitation	$m.yr^{-1}$	1 and 2	0.51	C(0.51)
X_j	discharge distance	m	1	2	T(0.1,2,4)
			2	5	T(5,7,9)
$\rho_{s,j}$	particle density	$kg.m^{-3}$	1 and 2	2650	N(2650,100,2200,2980)
$\lambda_{d,j}$	tailings discharge layer	unitless	1 and 2	3	C(3)

Notes

i - ith radionuclide
j - jth subsurface flowpath
C - Constant (single value)
T - Triangular (min., mode, max.)
U - Uniform (min., max.)
LN -Lognormal (geo. mean, geo. std. dev., min., max.)
N - Normal (mean, std. dev., min., max.)

measurements of water table elevations (see Section H.4, Model Calibration/Validation).

The hydraulic gradients were assumed to be normally distributed. At dam 1, the calculated mean value was 0.051 $m.m^{-1}$, with an assumed standard deviation, lower limit and upper limit of 0.01, 0.03 and 0.07 $m.m^{-1}$, respectively. At dam 2, the calculated mean value was 0.176 $m.m^{-1}$, with an assumed standard deviation, lower limit and upper limit of 0.03, 0.12 and 0.24, respectively.

H.3.4 Hydraulic Conductivity

At the Lacnor tailings site, rising head hydraulic conductivity tests were carried out in various piezometers subsequent to their installation. In addition, falling head tests, using mechanical packers, were conducted within the borehole at two depths in the bedrock during the drilling of Borehole SO-05b (Golder et al., 1986).

The data from these tests were used to calculate hydraulic conductivities using the Hvorslev method (1951). The results are listed in Table 1.8 and 1.9 of the Golder et al. (1986) report.

The in situ hydraulic conductivity tests for the various tailings, sub-tailings and off-tailings geological materials are summarized below:

Fine Tailings, Slimes, Very Fine Silts	6.3×10^{-1} to 6.3 $m.yr^{-1}$
Coarse Tailings, Sands, and Silts	3.15 to 3.15×10^{1} $m.yr^{-1}$
Sands and Gravel	2.5×10^{2} to 3.15×10^{2} $m.yr^{-1}$
Diabase Bedrock	9.46×10^{-2} to 0.46×10^{2} $m.yr^{-1}$

Good agreement was obtained between the results of falling head hydraulic conductivity tests with packers in Borehole SO-05b and subsequent rising head tests on the piezometer installed in rock in the same borehole (Golder et al., 1986).

The in situ hydraulic conductivity tests in the tailings yielded hydraulic conductivity values which were generally lower than those determined from laboratory constant head permeameter tests on samples of coarse and fine tailings.

It was assumed that the hydraulic conductivity data for coarse tailings, sand and silts were representative of the hydraulic conductivity in the pseudo aquifers within and beneath the dams. The geometric mean and geometric standard deviation for the aforementioned hydraulic conductivity values (K) were calculated to be 69.4 $m.yr^{-1}$ and 2.4 $m.yr^{-1}$, respectively. The lower and upper limits were estimated to be 12 and 400 $m.yr^{-1}$, respectively.

H.3.5 Distribution Coefficients

Distribution coefficients (K_d) vary with the contaminant, soil type and groundwater pH; generally the K_d value is found to decrease as the pH decreases. They are also a function of the contaminant concentration in the liquid phase; at high concentrations saturation of available exchange sites can occur (Rancon, 1973). In most cases the K_d values are found to be lognormally distributed (Sheppard et al., 1984).

For the Lacnor site, the movement of radionuclide fronts through the aquifer is assumed to lag behind the movement of the acid plume front, such that K_d values representing low pH conditions (i.e. pH 3.0 to 5.0) are considered to apply.

In the generic model, the groundwater flowpaths were conceptualized as glaciofluvial sandy aquifers. For the Lacnor tailings the aquifer material is considered to be a mixture of coarse tailings, sands and silts. Hence, the K_d

values employed in the Lacnor simulation are different than those used in the generic model.

In the generic model geometric standard deviations ranging from 1.73 (for lead-210, to 2.5 and for total uranium), were employed. For the Lacnor study, a geometric standard deviation of 1.5 was employed for the distributions of the four radionuclides. This value was chosen to reflect the reduction in parameter uncertainty that is anticipated to occur when dealing with a specific site.

The uranium K_d values considered to be representative of the Lacnor site are those determined by Veska (1983) using solutions representative of waste-rock-influenced groundwater. At pH values of 3 and 4, the experiment K_d values were 7.8×10^{-3} and 1.6×10^{-2}, respectively. A geometric mean K_d value of 1.2×10^{-2} $m^3.kg^{-1}$ was used for this study. This value agrees well with the mean uranium K_d value of 2×10^{-2} $m^3.kg^{-1}$ presented by the NRC (1983). Assuming a geometric standard deviation of 1.5, the lower and upper limits were estimated to be 3.6×10^{-3} and 4×10^{-2} $m^3.kg^{-1}$, respectively.

Thorium K_d values are very dependent upon the groundwater pH. At pH conditions of 3.0 to 4.0, K_d values of 8.6×10^{-2} $m^3.kg^{-1}$ (Veska, 1983) and 5×10^{-2} $m^3.kg^{-1}$ (Rancon, 1973) have been reported. For this study, a geometric mean value of 5.0×10^{-2} $m^3.kg^{-1}$ was used with an assumed geometric standard deviation of 1.5. The lower and upper limits were estimated to be 1.5×10^{-2} and 1.7×10^{-1} $m^3.kg^{-1}$, respectively.

Little information exists on lead-210 K_d values. Veska (1983) reported a value of 1×10^{-1} $m^3.kg^{-1}$ for acidic conditions (i.e., pH = 3.5). Based on the premise that the lead-210 in tailings is associated with soil phase lead sulphate and assuming a soil $PbSO_4$ concentration of 5×10^{-4} $mol.dm^{-3}$ a K_d value of 2×10^{-2} $m^3.kg^{-1}$ was calculated using the Water Source Model (see SENES, 1987c; Section 3.0). Consequently, the K_d value for lead-210 was assumed to have a geometric mean value of 6×10^{-2} $m^3.kg^{-1}$ (i.e. the average of the aforementioned two K_d values). Assuming a geometric standard deviation of 1.5, the estimated lower and upper limits are 1.8×10^{-2} and 2.0×10^{-1} $m^3.kg^{-1}$, respectively.

Radium-226 K_d values of 2×10^{-2} $m^3.kg^{-1}$ (Veska, 1983) and 7×10^{-2} $m^3.kg^{-1}$ (Morin et al., 1982) have been reported for pH conditions of 3.5 to 4.5. A geometric mean K_d value of 4.5×10^{-2} $m^3.kg^{-1}$ was used with an assumed geometric standard deviation of 1.5. The estimated upper and lower limits are 1.3×10^{-2} and 1.5×10^{-1} $m^3.kg^{-1}$, respectively.

H.3.6 Porosity

The estimated range of porosity of the Lacnor tailings site is 0.29 to 0.64 $m^3.m^{-3}$; these estimates are based upon the field data for water contents (Golder et al., 1986; Appendix 1, Table 1.2) and the assumptions that the water contents are at saturation and that the tailings particle density is 2650 $kg.m^{-3}$.

For "sandy" and "silt" tailings the porosity range was approximately 0.33 to 0.40 (Golder et al., 1986; Appendix 1, Table 1.2). For this study, it was assumed that the aquifers (coarse tailings, sands and silts) at both dams have porosities with uniform distributions ranging from 0.33 to 0.40 $m^3.m^{-3}$.

H.3.7 Average Annual Net Precipitation

The average annual net precipitation (P_a) for the Lacnor tailings site is discussed in detail in Section A.3.8, Water Source Model. An average net precipitation value of 0.51 $m.yr^{-1}$ was derived from data on the Serpent River Watershed.

H.3.8 Discharge Distance

The discharge distance for the Lacnor tailings site was initially considered to be the width of the dams (approximately 18m). This was assumed since it has been observed that the majority of the subsurface flow discharges at the toe of each dam. However, it has been observed at Lacnor that tailings exist outside of the tailings basin, down-gradient of the dams, a result of historical containment failures (Golder et al., 1986; Figure 1.1, Appendix 1). The dams therefore must consist of tailings material, the source of contamination. During the model calibration (see Section H.4.2, Model Calibration/Validation) the discharge distances which produced the best fit were 2 m and 7 m for dams 1 and 2, respectively.

The discharge distances for both dams are assumed to be triangularly distributed. At dam 1, a minimum of 0.1 m, a mode of 2 m and a maximum of 4 m were selected. At dam 2, a minimum of 5 m, a mode of 7 m and a maximum of 9 m were selected. The selection of ±2m for the predicted minimum and maximum values was based upon a comparison of simulation outputs with the range of observed values.

H.3.9 Particle Density

The particle density (ρ_s) of sandy soils in the Canadian shield ranges from 2000 to 2700 kg.m^{-3} (Beals, 1985) with an average value for sand being 2650 kg.m^{-3}. For the sandy aquifer near the Nordic tailings, a particle density of 2980 kg.m^{-3} was reported (Morin et al., 1982). The density of the Lacnor tailings has been reported to be 2600 kg.m^{-3} (Golder et al., 1986; Appendix 1, Table 1.2).

For the Lacnor site, the soil particle density is considered to be normally distributed with a mean of 2650 kg.m^{-3}, a standard deviation of 100 kg.m^{-3}, and lower and upper limits of 2200 and 2980 kg.m^{-3}, respectively.

H.3.10 Tailings Discharge Layer

The majority of the subsurface discharge at the Lacnor tailings is through two permeable dams located on the southeast side of the basin. The dams are considered to be "pseudo aquifers" and are the transport paths in the subsurface transport model. The source of these pseudo aquifers is layer 3 of the tailings, the mixing zone. Hence layer 3 (ie. $\lambda_d = 3$) was used as the tailings discharge layer.

H.4 Model Calibration/Validation

H.4.1 Introduction

The calibration was performed in two stages. In the first stage input parameters which could be calculated directly from field data were determined. These parameters included the hydraulic gradient and the cross sectional areas of flow. In the second stage a key input parameter, the discharge distance, was adjusted to give the best fit of the model results to the field data. This parameter was selected since there existed a lack of site-specific information on its range of values.

H.4.2 Calculated Parameters

Cross-Sectional Areas of Flow

The cross-sectional areas were calculated using the following expression:

$$A_{x,j} = \frac{Q_{s,j}}{K_j^* I_j^*} \qquad \text{(H.1)}$$

where:

$A_{x,j}$ = cross-sectional area of the jth aquifer (m^2)
$Q_{s,j}$ = subsurface transport flow of jth aquifer ($m^3.yr^{-1}$)
K_j^* = measured mean hydraulic conductivity of the jth aquifer ($m.yr^{-1}$)
I_j^* = hydraulic gradient calculated from measured elevation changes of the jth aquifer ($m.m^{-1}$)

The measured field values for hydraulic conductivity and the calculated hydraulic gradient are presented in Section H.3.3 and H.3.4, respectively.

The subsurface transport flow is assumed to be equal to the surface water flows measured at the toe of each dam (sample locations SW-1 and SW-2) during the Lacnor field study (Golder et al., 1986).

$$Q_{s,j} = Q_j^* \qquad (H.2)$$

where:

Q_j^* = the mean surface water flow measured at the toe of dam j ($m^3.yr^{-1}$)

Table H.2 presents a summary of the surface water flow data. Only the field data from July to October were used to determine the mean surface water flow rates. The March, April, May and June data were not included, as the surface water discharge channel at the west end of the tailings site was temporarily blocked resulting in increased flows at dam 1 and dam 2 during this period. Substituting the aforementioned data into equation (H.1) gives cross-sectional areas of 2005 m^2 and 3590 m^2 for dams 1 and 2, respectively.

Hydraulic Gradients

For the Lacnor tailings, the hydraulic gradients were calculated using the following expression:

$$I_j = \frac{\Delta H_j^*}{\Delta L_j^*} \qquad (H.3)$$

ΔH_j^* = the measured elevation change at dam j (m)
ΔL_j^* = the measured distance for which ΔH_j is applicable (m)

Table H.3 presents the measured water table elevations and distances for dams 1 and 2. The change in elevation for dam 1 and its corresponding distance was that observed between sample location BH-85-5, located at the southeast corner of the tailings, and BH-85-6, located at the toe of dam 1. At BH-85-5, the water is ponded and hence the water table elevation is simply the surface elevation.

Table H.2

SURFACE WATER FLOW
AT THE LACNOR TAILINGS SITE

Month	Flow ($m^3.yr^{-1}$) Site SW-1	SW-2
July	5680	44,150
August	6310	41,310
September	7570	37,840
October	8830	52,030
Average	7100	43 800

Reference

Golder et al. (1986); Section 3.0, Tables 3.2 and 3.3

Table H.3

HYDRAULIC GRADIENT
CALCULATED FOR THE LACNOR TAILINGS SITE

Dam	Elevation change ΔH_j* (m)	Distance ΔL_j* (m)	Hydraulic Gradient I_j ($m.m^{-1}$)
1	11.29 (ref 1)	220 (ref 3)	0.051[i]
2	6 (ref 2)	34 (ref 3)	0.176[ii]

Note

* measured parameter

i) hydraulic gradient between sample locations BH-85-5 and BH-85-6

ii) hydraulic gradient existing at dam 2

Reference

(1) Golder *et al*. (1986); Appendix 1, Table 1.9

(2) Golder *et al*. (1986); Section 3.0, Figure 3.1

(3) Golder *et al*. (1986); Appendix 1, Figure 1.1

Employing the elevation change between sample lcoations BH-85-5 and BH-85-6, located at the toe of dam 2, results in a hydraulic gradient of 0.067 m.m^{-1}. However, at dam 2, water is ponded on the tailings surface adjacent to the dam. Because of this, the change in elevation and its corresponding distance were assumed to be the height of the dam and its thickness, respectively.

The calculated hydraulic gradients for dams 1 and 2 were 0.051 m.m^{-1} and 0.176 m.m^{-1}, respectively.

H.4.3 Model Calibration

Field Data

To determine the optimal discharge distance for each of the dams, two sets of field data were considered: field data for the radionuclide source concentrations (i.e. tailings porewater concentrations) and field data for the subsurface discharge concentrations. Field data were available only for the months of June and August, at seven locations.

Source Concentration

To estimate the source concentrations of the radionuclides, the tailings field data (Golder et al., 1986; Appendix 1.0, locations GW-1 to GW-5) were used. Two assumptions were employed in using the data. The first was that the field data measured in 1985 is representative of the tailings porewater concentrations for the last twenty five years. This assumption is required since the model is being tested independently of the water source model. The second assumption was that the source for dams 1 and 2 is acidic; hence, only field data representing acidic conditions, pH < 4.0, were evaluated. This assumption is based upon the observation of low pH conditions in the subsurface discharge at the toes of the dams.

Table H.4 presents the mean source concentrations used in the calibration

Table H.4

COMPARISON OF PREDICTED POREWATER CONCENTRATIONS WITH FIELD DATA

Dam	Radionuclide	Mean Source Strength** (Bq.m^{-3})	Predicted Discharge Concentration (Bq.m^{-3})	Mean Observed Discharge Concentration* (Bq.m^{-3})
1	U (Bq.m^{-3})	6650**	6480	(SW-1) 6650***
	Th	31200	4490	10340
	Pb	49200	1750	2565
	Ra	6910	1380	762
	SO_4^{2-} (mol.m^{-3})	67	61.6	16.8
	Ca^{2+}	10.5	11.5	6.5
2	U (Bq.m^{-3})	3080	3000	(SW-2) 3080***
	Th	31200	4270	5260
	Pb	49200	1640	980
	Ra	6910	1330	570
	SO_4^{2-} (mol.m^{-3})	67	61.5	25.1
	Ca^{2+}	10.5	11.5	7.0

Reference

* Golder et al., (1986); Apendix 3, Table 3.20 and 3.21.

Note

** The mean source strengths (i.e. tailings porewater concentration) represent acidic conditions, i.e. pH < 4.0, at depths less than 15.

*** The mean observed discharge concentration was found to be higher than the mean observed source strength value. Hence, the former was used to estimate the mean source strength of the adjacent tailings.

process to calculate the subsurface discharge concentrations. It must be emphasized that the true mean source concentrations are not known and that the measured source concentrations exhibited a wide range of values and represent very "localized" conditions.

Subsurface Discharge Concentration

The majority of the subsurface discharge occurs at the toes of both dams. Hence the surface water samples taken in these locations (Golder et al., 1986; Appendix 1.0, SW-1 and SW-2) were considered to be representative of the discharge concentrations. Table H.4 shows the mean measured radionuclide concentrations at the two sampling locations.

Comparison of Field Data with Predicted Concentrations

A 25 year simulation of the subsurface discharge was performed. The nominal values of the parameters presented in Section H.3 were used in the simulation along with the source strengths, assumed to be constant with time, shown in Table H.4. A number of variables could have been changed in the calibration. The most important of which, in terms of influencing the discharge concentrations, were the discharge distances, X, and partition coefficients, K_d. Literature values were available for K_d's. Even though these values had a wide range, it was believed that the literature values were sound. Considering the uncertainties associated with the field measurements and assumptions employed in selecting the mean source strengths, the literature values were believed to be the most appropriate data.

For the discharge distance, however, no information was available. Hence, it was decided to isolate and adjust only one key parameter, the discharge distance. Because of the uncertainty in the distance of the discharge flowpath, several values were tested in order to find an optiminal value. Based on these tests, nominal discharge distances of 2 m and 7 m for dams 1 and 2 were selected, respectively.

Aqueous Radionuclide

The predicted radionuclide concentrations in the subsurface discharge at dam 1 and dam 2 for year 25 are in good agreement with the observed values (Table H.4). The predicted and observed uranium concentrations indicate that complete breakthrough will have almost occured by year 25. This results from uranium having a K_d value approximately 5 times lower than the remaining radionuclides. The other radionuclides will have reached complete breakthrough by approximately year 125.

At dams 1 and 2, the predicted radium concentrations are slightly higher than those observed, indicating that the distribution coefficient may be too low and/or the mean source strengths are inappropriate. For thorium, the reverse occurs, i.e. the model under-predicts the concentrations at dams 1 and 2. This may result from the distribution coefficient for thorium being too high. The model slightly overpredicts the lead concentration at dam 1 while underpredicting the concentration at dam 2.

Aqueous Sulphate and Calcium

The predicted concentrations of calcium at both dams are in agreement with the observed values. The predicted sulphate concentrations, however, are higher than those observed at both dams. The difference may be attributed to (1) the dilution of the aquifer discharge by surface runoff from the tailings and surrounding area, (2) inappropriateness of the assumptions employed in the selection of the mean source strength and/or (3) the occurrence of gypsum reprecipitation.

H.5 Probabilistic Evaluation

In order to assess the upper and lower limits of the radionuclide concentrations, a probabilistic simulation comprising of 1000 trials was performed using the subsurface transport module. The simulation was performed for a 25 year period.

Figures H.1 to H.4 present the predicted arithmetic mean and lower and upper 95% confidence levels of point estimates for the radionuclide concentrations at dam 1. At year 25 the observed minimum, mean and maximum concentrations of the radionuclides are also presented. The mean observed concentrations for all four radionuclides fall within the 95% confidence bands predicted at year 25.

FIGURE H.1

PROBABILISTIC ANALYSIS OF URANIUM CONCENTRATION (DAM 1)

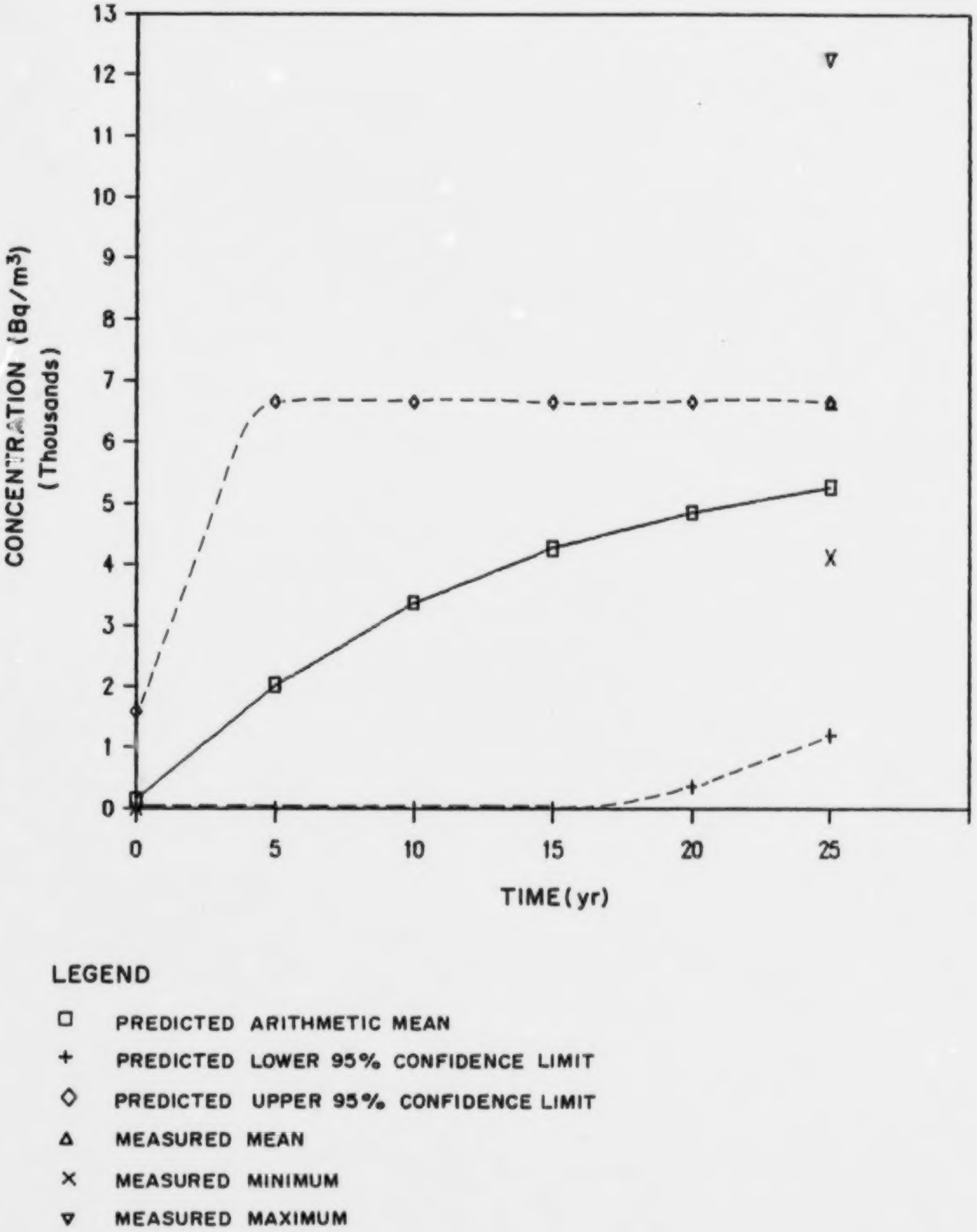

FIGURE H.2

PROBABILISTIC ANALYSIS OF THORIUM CONCENTRATION (DAM 1)

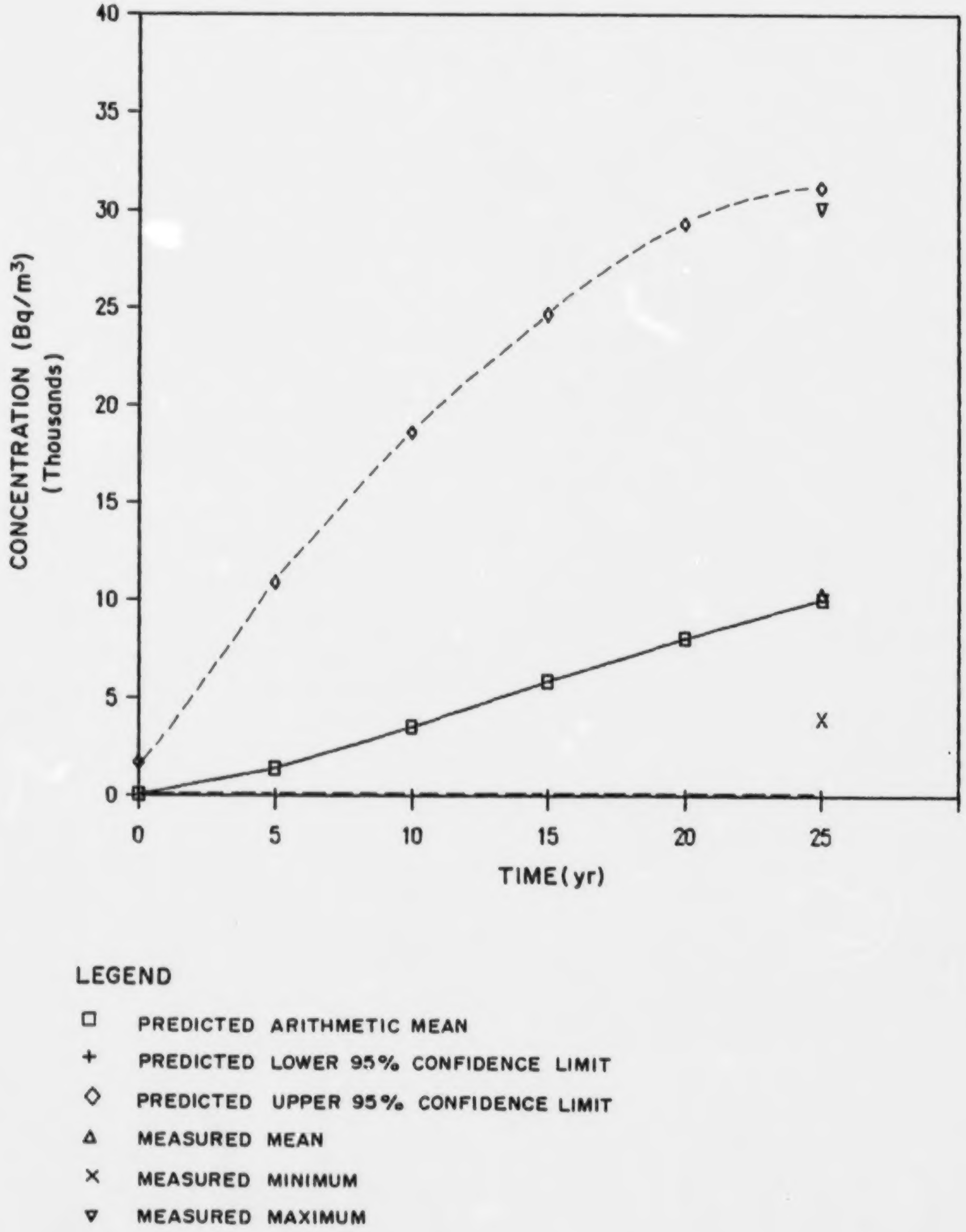

FIGURE H.3

PROBABILISTIC ANALYSIS OF LEAD-210 CONCENTRATION (DAM 1)

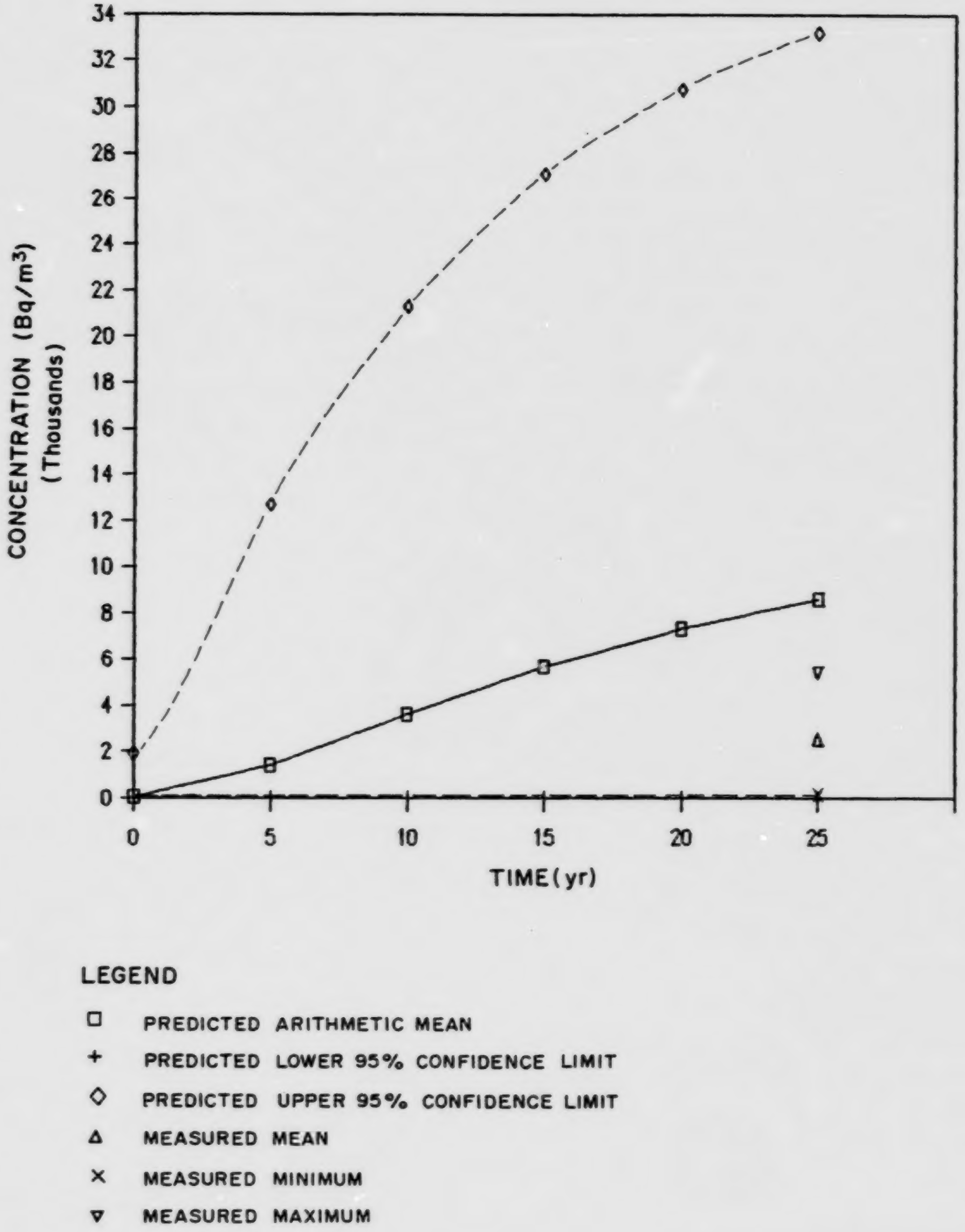

FIGURE H.4

PROBABILISTIC ANALYSIS OF RADIUM-226 CONCENTRATION (DAM 1)

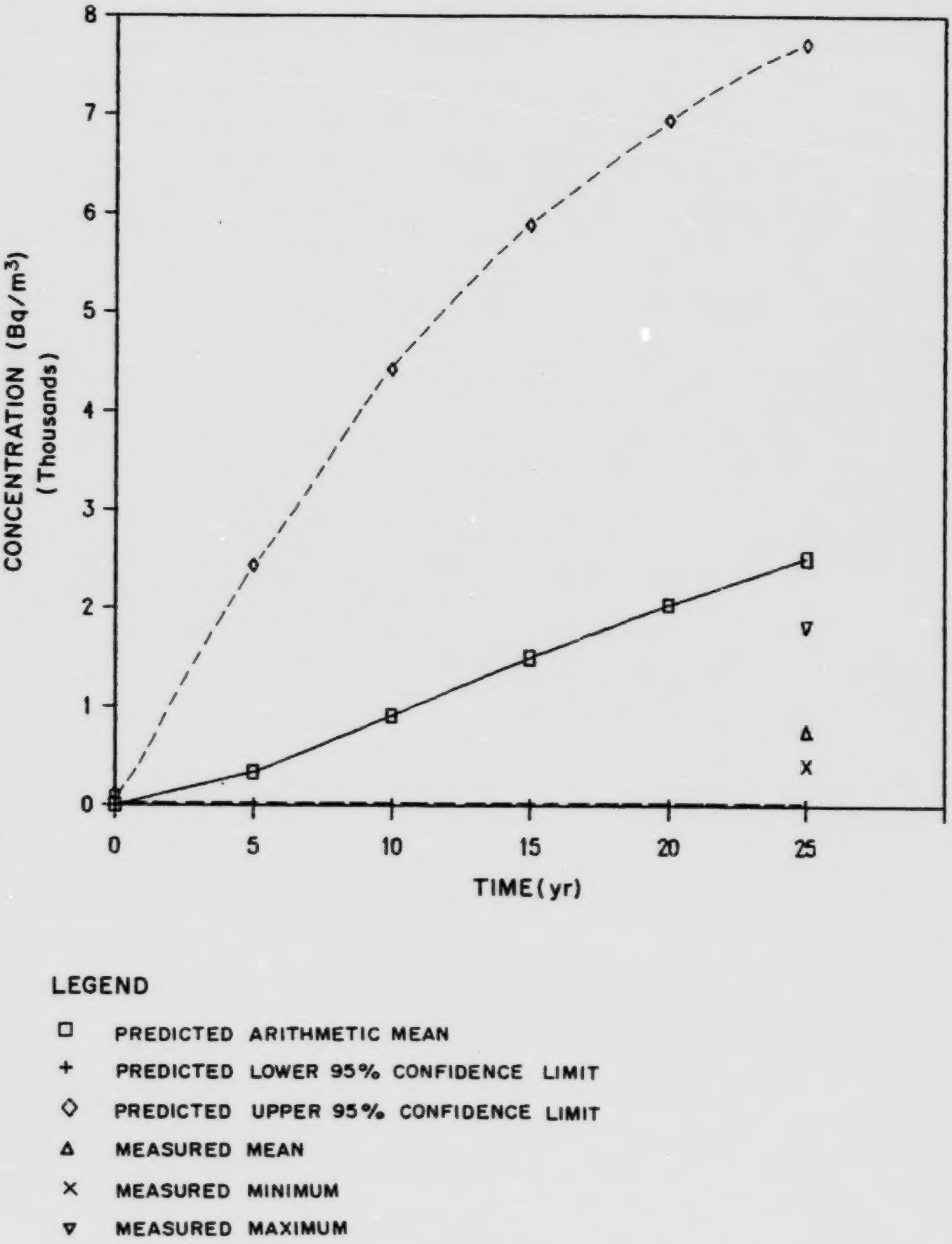

APPENDIX I

SURFACE WATER DISPERSION MODELS

APPENDIX I: SURFACE WATER DISPERSION MODEL

I.1 Conceptual Approach

As discussed in Chapter 2 of this report, surface and subsurface flows from the Lacnor tailings area discharge onto the Nordic tailings area a short distance (0.5 km) to the south. At this point, the drainage from Lacnor combines with that from the Nordic site. Runoff from the Nordic tailings area is currently collected and treated for pH adjustment and radium removal before being released to Buckles Creek. The flow in Buckles Creek passes through Nordic Lake and a small unnamed lake before entering Esten Lake on the western arm of the Serpent River (see Figure 2.2).

Prior to 1982, the flow from the eastern basin of Esten Lake passed through the main body of the lake and hence through Marshland, Grandeur, Trout and Depot Lakes before combining with flow in the main branch of the Serpent River at McCarthy Lake. During 1981, a dam was constructed across the narrows at the east end of Esten Lake to isolate the eastern basin from the rest of the lake. A diversion channel was also constructed at that time to carry flow from the eastern basin of Esten Lake directly to Depot Lake. The diversion works were built as part of a more comprehensive plan to reduce the nutrient input to Esten Lake, in particular, and the rest of the lakes on the upper reaches of the western arm of the Serpent River. The overall plan included the replacement of two sewage treatment plants at the Town of Elliot Lake with a new tertiary treatment plant and rerouting of the plant effluent through the eastern end of Esten Lake.

In order to model the incremental effects of the Lacnor tailings area on receiving water quality, it was necessary to make a number of simplifying assumptions. The most significant simplication involved ignoring the presence of the Nordic tailings area and the Nordic treatment plant. Surface and subsurface drainage from the Lacnor site was conceptualized to collect in Lacnor Creek, flow across the Nordic tailings area and join the flow in Buckles Creek on the south side of the Nordic tailings area. From there, the flow in Buckles Creek passes through Nordic Lake, a small unnamed Lake, the eastern basin of Esten Lake and Depot Lake before combining with the flow in the main stream of the Serpent River at McCarthy Lake. Because the runoff from Lacnor is diluted by a factor of over 400:1 at Depot Lake, the limits of the watershed were restricted to the western arm of the Serpent River Basin as shown on Figure 2.2. The incremental changes in water quality due to Lacnor downstream of Depot Lake were assessed to be too small to warrant inclusion in the watershed area to be modelled.

As previously noted, the presence of the Nordic treatment plant was ignored in all simulations as it was assumed that the plant would not be operated for more than a few years as compared to a simulation time of hundreds of years. Similarly, the effects of runoff and seepage from the Nordic tailings area were disregarded as the simulations were specifically designed to assess only the incremental effects of the Lacnor tailings area on downstream water quality.

I.2 Site-Specific Model Alterations

The watershed modelling concept incorporated in the UTAP.3 code (SENES, 1987c; Chapter 10) was determined to be fully applicable to the Lacnor demonstration and no site specific code changes were required.

I.3 Site-Specific Parameter

The surface water dispersion model includes several parameters which require site-specific input data. The parameters include physical, chemical and biological attributes of the system and are discussed in turn below.

I.3.1 Watershed Characteristics

The Elliot Lake sub-basin covers a drainage area of approximately 246 km^2 to the point where flow from the western arm of McCarthy Lake joins the main branch of the Serpent River. The boundary of the watershed and the location of the nodes selected for modelling in the study are shown on Figure 2.2 (see Chapter 2.0). Seven node points were identified as follows:

Node 1: Lacnor Creek which carries the combined surface and subsurface flow from the Lacnor tailings area (For convenience the drainage system carrying flow from the Lacnor tailings area southwest across the Nordic tailings area to the point of entry into Buckles Creek is referred to here as Lacnor Creek).

Node 2: on Buckles Creek at the inlet to Nordic Lake

Node 3: the outlet of Nordic Lake

Node 4: the outlet of the unnamed lake immediately to the south of Nordic Lake

Node 5: the outlet of the diversion ditch from the eastern basin on Esten Lake

Node 6: the outlet of Depot Lake

Node 7: the outlet of the western arm of McCarthy Lake

The physical attributes of the river and lake segments of the watershed are summarized on Table I.1 and include the length of the river reaches, the mean depth and surface area of the lakes and the watershed area of the drainage basins to each node. The lake morphometric data were taken largely from a report by the Ontario Ministry of Environment (Myslik, 1985) and verified against lake bathymetric maps obtained from the Blind River office of the Ontario Ministry of Natural Resources (1986). The river reaches and watershed areas were measured from 1:50,000 national topographic mapping of the Algoma District, Elliot Lake (EMR, 1975).

Table I.1

CHARACTERISTICS OF LACNOR STUDY AREA WATERSHED

End Node No.	Segment Type	River Reach Length (m)	Lake Mean Depth (m)	Lake Surface Area (m**2)	Sub-basin Area (km**2)	Cumulative Area (km**2)
1	River	200	---	---	0.42	0.42
2	River	4,300	---	---	14.82	15.24
3	Lake	---	6.6	1.15×10^6	5.70	20.94
4	Lake	---	7.5	1.40×10^5	1.28	22.22
5	Lake	---	4.5	2.69×10^5	2.11	24.33
6	Lake	---	7.8	2.06×10^6	211.44	235.77
7	Lake	---	3.3	3.12×10^5	10.32	246.09

Node Designation

1. Lacnor Creek at Outlet from Lacnor Tailings Area.
2. Buckles Creek at Inlet to Nordic Lake.
3. Nordic Lake Outlet.
4. Unnamed Lake Outlet.
5. Esten Lake (eastern bay) Outlet.
6. Depot Lake Outlet.
7. McCarthy Lake (west arm).

I.3.2 Surface Runoff (Net Precipitation)

The surface runoff factor (i.e. m^3(runoff).m^{-2}(surface area).yr^{-1}) for the Serpent River watershed was assessed using hydrologic data recorded at Highway #17 (Water Survey of Canada, Station No. 02CD001) for the period from 1967 to 1984. Distribution fitting using the normal, lognormal and Weibull distributions showed that the annual flow data were best described by the normal distribution. The calculated statistics of the surface runoff factor for the 18 years of data were an arithmetic mean of 0.51 $m.yr^{-1}$ and arithmetic standard deviation of 0.10. The range of values spanned from 0.34 to 0.77 $m.yr^{-1}$.

In addition to the Serpent River flow data, flow records on the Aux Sables River at Massey (Water Survey of Canada Station No. 02CE002) were also examined to extend the data base. The Aux Sables River was selected because it has a much longer period of discharge record (i.e. continuously from 1921 to date), has an identical size drainage area (i.e. 1350 km^2) and is located adjacent to the Serpent River basin. A statistical analysis of the 66 years of annual flow data gave an arithmetic mean value of 0.43 $m.yr^{-1}$, a standard deviation of 0.10 $m.yr^{-1}$, a minimum value of 0.24 $m.yr^{-1}$, and a maximum value of 0.73 $m.yr^{-1}$. While the runoff factor on the Aux Sables River was less (0.43 $m.yr^{-1}$) than that calculated for the Serpent River (0.51 $m.yr^{-1}$), the distributions for the two data bases showed essentially identical dispersion about the means as measured by the variances or standard deviations. The Aux Sables River data showed a greater spread to the data as would be expected considering the large size of the data base. This factor was taken into account therefore, in selecting the attributes to assign to the distribution for the net annual runoff (or net annual precipitation) parameter for the Serpent River. The attributes for the selected distribution are:

$$P = N\ (0.51,\ 0.10,\ 0.25,\ 0.85)$$

I.3.3 Major Ions

The concentrations of major ions in surface runoff from the watershed are modelled explicitly as they are used in the calculation of pH. The ions include calcium, chloride, magnesium, potassium, sodium and sulphate. Background levels of these constituents in runoff from the western arm of the Serpent River Watershed were determined using water quality data gathered by the Ontario Ministry of the Environment during 1984 and 1985 on Esten Lake. This lake was selected since it is downstream of the town of Elliot Lake but upstream of the main influence of the municipal sewage treatment discharge and the mining area runoffs in the watershed. The water quality in Esten Lake is characteristic of the main inflow to Depot lake where surface runoff from the Lacnor tailings area mixes with flow in the western branch of the Serpent River.

The mean concentrations measured for the six major ions noted above were:

calcium - $10^{-3.73}$ mol.L^{-1} (10^{-073} mol.m^{-3})
chloride - $10^{-3.42}$ mol.L^{-1} ($10^{-0.42}$ mol.m^{-3})
magnesium - $10^{-4.21}$ mol.L^{-1} ($10^{-1.21}$ mol.m^{-3})
potassium - $10^{-4.71}$ mol.L^{-1} ($10^{-1.71}$ mol.m^{-3})
sodium - $10^{-3.46}$ mol.L^{-1} ($10^{-0.46}$ mol.m^{-3})
sulphate - $10^{-3.86}$ mol.L^{-1} ($10^{-0.86}$ mol.m^{-3})

These parameters are treated as constant inputs in the UTAP.3 code.

I.3.4 Lake Sediment Characteristics

Radionuclide removal in the watershed occurs through transfer to sedimenting solids in the lakes of the system and by direct transfer to bottom sediments. As a consequence of sediment oxidation at the lake bottom, radionuclides are released from the decomposing sediment to the sediment interstitial water from which they may diffuse back into the water column. Radionuclides which remain bound to the residual solids eventually become buried in the sediment and thus are unavailable for exchange with the water column. Characterization of the productivity of the lakes therefore, is an important aspect of the surface water dispersion model.

Trophic Status

An investigation of the eutrophication status of lakes in the western arm of the Serpent River was carried out in 1981 by the Ontario Ministry of the Environment (Myslik, 1985). The study included the measurement of several chemical, biological and physical parameters during field surveys carried out in the spring, summer and fall. The trophic status of each lake was determined from and examination of several common indicators: Secchi disc visibility, chlorophyll a, phytoplankton and zooplankton biomass and total phosphorus. The designation of trophic status was based on classification of the lakes as either oligotrophic (low productivity), mesotrophic (medium productivity) or eutrophic (high productivity). Lakes following in the oligotrophic classification included Nordic Lake and McCarthy Lake. Mesotrophic categorizations were assigned to Depot Lake and the unnamed lake just to the south of Nordic Lake. The only lake classified as eutrophic was Esten Lake which had the highest total phosphorus content (47 $ug.L^{-1}$) of all the lakes.

Productivity Values

The productivity values for the lakes in the Elliot Lake watershed were assigned based on the trophic status classifications designated above and data published by Wetzel (1975). The range in the lake productivity values reported by Wetzel are:

oligotrophic lakes - 18 to 90 g(carbon).$m^{-2}.yr^{-1}$
mestotrophic lakes - 90 to 365 g(carbon).$m^{-2}.yr^{-1}$
eutrophic lakes - 365 to 1825 g(carbon).$m^{-2}.yr^{-1}$

Sedimentation Flux Values

Sedimentation rates for the watershed lakes were calculated using the above productivity values, a biomass organic content of 55%, degradation of 50% of the biomass solids during sedimentation in the water column and an inorganic solids input to the lakes of 1 to 7 $mg.L^{-1}$ in surface runoff. The sedimentation flux values calculated based on these assumptions are presented in Table I.2. This parameter is specified as being triangularly distributed with the minimum and maximum values emcompassing the expected extreme values.

Sediment Burial

As previously noted, sedimenting solids continue to biodegrade after deposition on the lake bottom, releasing radionuclides and other organic and inorganic constituents to the interstitial waters. The organic content of stabilized lake sediments in the Elliot Lake area was reported by SENES and SRC (1985) to be in the order of 13 to 24%. A mean value of 18.5% was measured on lakes in the western arm of the Serpent River. Based on this organic content, the rate of sediment burial, f_s, was calculated to range from 0.76 to 0.86. This parameter is specified to be uniformly distributed with the following attributes:

$$U\ (0.76,\ 0.86)$$

Sediment Density

The density of the stabilized sediment, $\P_s$, was caluclated to be 1.955 x 10^6 $g.m^{-3}$ based on an average organic content of 18.5%, a density of 1.05 x 10^6 $g.m^{-3}$ for the organic component and 2.45 x 10^6 $g.m^{-3}$ for the inorganic component.

Solids Void Fraction

The sediment samples analyzed by Swanson (1985) had an average moisture

Table I.2

LAKE SEDIMENTATION FLUX VALUES

Lake Node Number	Lake Surface Area (m^2)	Contributing Drainage Area (m^2)	Sedimentation Flux ($g.m^{-2}.a^{-1}$)				
			Runoff Solids	Biomass Solids	Total Solids Values		
					Nominal	Minimum	Maximum
1	1.15E6	20.94E6	20	50	70	30	170
2	1.40E5	1.28E6	15	240	255	125	635
3	2.69E6	2.11E6	40	960	1000	500	2035
4	2.06E6	211.44E6	60	240	300	140	740
5	3.12E5	10.32E6	45	50	95	40	225

content of 82% by weight. Based on this parameter value and the sediment density value given above, the nominal sediment volume occupied by solid matter was estimated to be 0.10 m^3(solids).m^{-3}(total). Conversely, the nominal void fraction was calculated to equal 0.90 m^3(voids).m^{-3}(total). This calculated porosity compares favourably with literature data for Canadian Shield Lakes of 0.83 to 0.97 m^3(voids).m^{-3}(total) (Beak, 1982). The probabilistic specifications for this parameter are:

T (0.83, 0.90, 0.97)

I.4 Model Calibration/Validation

Neither calibration or validation of the surface water dispersion model was possible. While there are several water quality monitoring stations in the immediate area, the quality at these stations is affected by runoff from both the Nordic and Lacnor tailings area. The quality at several stations is also impacted by storm runoff and the treatment plant discharge from the Town of Elliot Lake. Therefore, to calibrate the surface water dispersion model, it would be necessary to model all these sources. The scope of the Lacnor study precluded this level of detail. It was also felt that the level of effort which would be required to model multiple sources could not be justified as it was unlikely that full calibration or validation of the surface water dispersion model would be achieved given the data which are available.

APPENDIX J

AQUATIC MODELS

APPENDIX J: AQUATIC MODELS

J.1 Conceptual Approach

The aquatic models include subroutines for modelling the effect of pH on fish populations, the transfer of radionuclides from water to fish and the transfer of radionuclides from water to aquatic macrophytes which are in turn consumed by moose. The approach taken in developing the aquatic models permitted easy application to the Lacnor study. The only input specifications required were the physical characteristics of the watershed (presented in Appendix I).

J.2 Site-Specific Model Alterations

No model alterations were required.

J.3 Site-Specific Model Parameters

Data collected in the aquatic transfer study carried out for the NUTP by SENES and SRC (1984 and 1985) were used in the characterization of the transfer factors incorporated in the generic models (SENES, 1987c; Chapter 11). These data were also used in the Lacnor study. Because the site-specific data comprise a limited set of values, the data collected in other outlines were also used.

J.4 Model Calibration/Validation

No data were available to permit either calibration or validation of the aquatic models. The limited data base obtained in the aquatic transfer study pertaining to radionuclide levels in fish flesh and in their habitat was incorporated in much larger bases of data covering several sites across Canada. These large data bases were used to derive the probability density functions described in the Phase III study and have been used again here in the Lacnor study.

APPENDIX K

ANIMAL PRODUCE MODELS

APPENDIX K: ANIMAL PRODUCE MODEL

K.1 Conceptual Approach

The UTAP.3 models (SENES, 1987c; Chapter 12) were found to be suitable for modelling animal produce in the area surrounding the Lacnor tailings and no changes in model application or interpretation were required.

K.2 Site-Specific Model Alterations

No model alterations were required.

K.3 Site-Specific Parameters

No site-specific data were identified.

K.4 Model Validation/Calibration

No data were available to permit the validation or calibration of the animal produce model, i.e. no radionuclide concentrations were measured in deer or moose from the surrounding area.

APPENDIX L

DOSE MODELS

APPENDIX L: DOSE MODEL

L.1 Conceptual Approach

The Lacnor tailings area is approximately 5 km east of the Town of Elliot Lake and 2 km north of the Nordic townsite. Highway 108, which is the main access road in the area, runs northwest from the east end of Depot Lake, passing north of Nordic Lake and into the Town of Elliot Lake. Most of the people in the area live in the two towns, with scattered cottages on local lakes as access permits.

The area is characterized by abundant lakes and streams, with about 20 to 25% of the total area being covered by water. The region is sufficiently forested with mixed coniferous and deciduous species to support lumbering. The bulk of the population rely upon the two existing mining companies for employment. There is some tourism involving camping, fishing and hunting. There is little farming or farming potential in the area. Hardy crops can be grown in home gardens.

Based on the above, five receptors were chosen: a resident at the Nordic townsite; two residents of the Town of Elliot Lake (east and west); and two permanent residents on Depot Lake.

In UTAP.3, up to two receptor types may be specified. Tables L.1 and L.2 describe the receptor types chosen for this application to Lacnor tailings. The five receptors were then designated as type 1 or type 2, as detailed on Tables L.1 and L.2. Details on specific input parameters are provided below.

L.2 Site-Specific Model Alterations

No site-specific model alterations were required for this application. The input parameters required for the dose model are presented in SENES (1987c), Chapter 13.

Table L.1

LIFESTYLE ASSUMPTIONS USED IN THE DOSE CALCULATIONS FOR THE ELLIOT LAKE (EAST AND WEST) AND DEPOT LAKE (EAST) RECEPTORS (RECEPTOR TYPE 1)

Inhalation and External Exposure	- spends 80 to 100 percent of the year at that location - spends 60 to 100 percent of that time indoors
Ingestion Exposure	- Vegetables - from 0 to 20 percent from that location - Meat - eats wild game (deer or moose) once a week - eats deer and moose in equal proportions - 0 to 50 percent of this is from the watershed - Water - taken from closest lake (East and West Elliot Lake - Elliot Lake; Depot Lake East - Depot Lake) - fraction of total is equal to the percent of the year spent at that location - Fish - 0 to 50 percent, of annual intake is from Depot Lake for the Elliot Lake East and Depot Lake East receptors - the Elliot Lake West receptor eats no fish from the watershed - Other Foodstuffs - assumed to be store bought from outside the model area

Table L.2

LIFESTYLE ASSUMPTIONS USED IN THE DOSE CALCULATIONS FOR THE NORDIC TOWNSITE AND DEPOT LAKE WEST RECEPTOR (RECEPTOR TYPE 2)

Inhalation and External Exposure		- spends 80 to 100 percent of the year at that location - spends 60 to 100 percent of that time indoors
Ingestion Exposure	Vegetables	- from 10 to 60 percent from that location
	Meat	- eats deer and moose meat only year round, in equal proportions - 100 percent of this is from the watershed
	Water	- taken from closest lake (Nordic Townsite - Ryan Lake; Depot Lake West - Depot Lake) - fraction of total is equal to the percent of the year spent at that location
	Fish	- 100 percent of the annual intake is from Depot Lake
	Other Foodstuffs	- assumed to be store bought from outside the model area

L.3 Site-Specific Parameters

L.3.1 Introduction

Several lifestyle assumptions were employed in the dose calculations. Tables L.1 and L.2 present these assumptions for receptor types 1 and 2, respectively.

In the following section, short descriptions of the site-specific parameters are presented for six of the eight dose sub-models: vegetation ingestion, caribou ingestion, moose ingestion, deer ingestion, drinking water and fish ingestion. No site-specific parameters were required for the radon inhalation, dust inhalation and groundshine sub-models. Justifications for the selection of parameter values are also included. Table L.3 sumarizes the site-specific parameters for the two receptor types (N=1 and N=2) and their probabilistic distributions and descriptions. Note that no site-specific parameters were required for the inhalation and groundshine models.

L.3.2 Vegetation Ingestion Model

In the vegetation model the "site-specific" variables are the annual intake of above ground vegetables and below ground vegetables, $U_{v,r}$. The values of 4.53×10^4 g.yr^{-1}, above ground, and 7.4×10^4 g.yr^{-1}, below ground, are derived from Ontario averages for males (20 - 39 yrs) versus a range from Ontario to Prairie males (20-39 yrs) for UTAP.3 (Nutrition Canada, not dated).

L.3.3 Caribou Ingestion Model

The annual intake of caribou, $U_{c,r}$, was set to zero, as there are no caribou in the Lacnor area.

L.3.4 Moose Ingestion Model

For the moose ingestion model two site-specific parameters were required: the

Table L.3

DOSE MODEL SITE-SPECIFIC PARAMETER VALUES

			Receptor Type 1		Receptor Type 2	
Model Symbol	Computer Symbol	Units	Nominal	Probability Distribution	Nominal	Probability Distribution
Vegetation Model						
$U_{v,r}$	AVEGIN(N)	g(wet wt).yr^{-1}	4.53×10^4	$C(4.53 \times 10^4)$	4.53×10^4	$C(4.53 \times 10^4)$
	BVEGIN(N)	g(wet wt).yr^{-1}	7.4×10^4	$C(7.4 \times 10^4)$	7.4×10^4	$C(7.4 \times 10^4)$
Caribou Ingestion Model						
$U_{c,r}$	CARMIN(N)	g.yr^{-1}	0	0	0	0
Moose Ingestion Model						
$U_{m,r}$	MOSMIN(N)	g.yr^{-1}	6×10^3	$C(6 \times 10^3)$	39.5×10^3	$C(39.5 \times 10^3)$
$L_{m,r}$	MFLOC(N)	---	.25	T(0,.25,.5)	1.0	C(1.0)
Deer Ingestion Model						
$U_{d,r}$	DERMIN(N)	g.yr^{-1}	6×10^3	$C(6 \times 10^3)$	39.5×10^3	$C(39.5 \times 10^3)$
$L_{d,r}$	DFLOC(N)	---	.25	T(0,.25,.5)	1.0	C(1.0)
Drinking Water Model						
$U_{w,r}$	WATIN(N)	$m^3.yr^{-1}$	0.6	0.6	0.6	0.6
Fish Ingestion Model						
$U_{f,r}$	FISHIN(N)	g.yr^{-1}	8.0×10^3	$C(8.0 \times 10^3)$	8.0×10^3	$C(8.0 \times 10^3)$
$L_{f,r}$	FFLOC(N)	---	0.25	T(0,.25,.5)	1.0	C(1.0)

Notes:

C - Constant (single value)

T - Triangular (min., mode, max)

annual intake of moose meat, $U_{m,r}$, and the fraction of moose meat that is from the watershed downstream of the tailings site, $L_{m,r}$.

The annual intake of moose meat is based on the assumption that an adult Ontario male eats 79 kg of meat per year (Nutrition Canada, not dated). For receptor type 1 it was further assumed that one-seventh of this was game, and one-half of the game was moose meat (the other half is assumed to be deer). For receptor type 2, all meat was assumed to be game, one-half of which is moose (the other half is assumed to be deer).

Hence, the values for the annual intake of moose meat, $U_{m,r}$, for receptors 1 and 2 are $6x10^3$ $g.yr^{-1}$ and $39.5x10^3$ $g.yr^{-1}$, respectively.

In terms of the fraction of moose meat that is from the downstream watershed, Receptor 1 was assumed to obtain only part, 25%, of his game from this area, whereas receptor type 2 was assumed to eat 100% from the watershed. These values were chosen to give a range of local consumption in the receptor types available.

L.3.5 Deer Ingestion Model

The annual intake of deer meat, $U_{d,r}$, and the fraction of deer meat that is local, $L_{d,r}$, are the same as for moose, Section L.3.4.

L.3.6 Drinking Water Model

Water is obtained from the lakes specified in Tables L.1 and L.2. Note that the drinking water source is specified for each receptor, not each receptor type. The volume of drinking water consumed, $U_{u,r}$, is 0.6 $m^3.yr^{-3}$ (Nutrition Canada, not dated).

L.3.7 Fish Ingestion Model

The annual fish ingestion rate, $U_{f,r}$, for an adult Ontario male aged 20-39 is

$8x10^3$ $g.yr^{-1}$ (Nutrition Canada, not dated).

The fraction of the annual intake, $L_{f,r}$, that is from the lakes listed in Tables L.1 and L.2, was set equal to $L_{m,r}$ and $L_{d,r}$ to be consistent. Note that, as for drinking water,the source of fish is specified for each receptor, not by receptor type.

L.4 Model Validation/Calibration

No data were available to permit the validation or calibration of the dose model discussed in this section.

APPENDIX M

INPUT PARAMETERS

APPENDIX M - INPUT PARAMETERS

Tables M.1 to M.5 present the probabilistic input files for the various closeout options which were employed in the UTAP.3 application to the Lacnor tailings.

Table M.1

LACNOR BASE CASE (OPTION 1)

```
LACNOR BASE CASE PROBABILISTIC INPUTS (OPTION 1)
Y Y
OPT1.PR
OPT1.PK
 262   0   0
0913566091 200
 3000.0   10.0
CODION N  1 N        0.0
CODNUC N  1 N        0.0
CODPH  N  1 N        0.0
CODERO N  1 N        0.0
CODDUS N  1 N        0.0
CODRAD N  1 N        0.0
CODWIN N  1 N        0.0
CODAIR N  1 N        0.0
CODSOL N  1 N        0.0
CODGS  N  1 N        0.0
CODVEG N  1 N        0.0
CODGW  N  1 N        0.0
CODWAT N  1 N        0.0
CODFIS N  1 N        0.0
CODWVG N  1 N        0.0
CODANI N  1 N        0.0
CODDOS N  1 N        0.0
PYRITI N  6 N      600.0      700.0      800.0
RHOTAL N  6 N     1.1E+6     1.3E+6     1.5E+6
FRACGP N  2 N       0.06      0.005       0.05       0.07
KPRIME N  4 N       0.01        0.1
SULPRD N  6 N     3.0E-6     4.1E-6     5.3E-6
O2CONC N  1 N       9.04
O2DIFF N  6 N        5.0       37.0       70.0
DUNSAT N  6 N       0.25        0.5        2.0
KSUBSO N  1 N       50.0
FACTCO N  6 N        0.4        0.5        0.6
NPRCP  N  2 V       0.51        0.1       0.25       0.85
DMIX   N  4 N        8.0       14.0
AVPRCP N  1 N       0.51
ATAIL  N  1 N    2.41E+5
XLIME  N  1 N     5.0E-4
PCURAN N  1 N        0.1
FURAN  N  4 N       0.90       0.94
FT230  N  6 N       0.65       0.80       0.95
FT232  N  6 N       0.55       0.65       0.75
FRAD   N  6 N       0.25       0.60       0.95
FLEAD  N  6 N       0.25       0.60       0.95
FRACU  N  4 N       0.30       0.90
KDUO2  N  3 N     2.0E-5        3.0     5.0E-6     5.0E-4
PCTHOR N  4 N       0.02       0.04
XRADI  N  6 N     6.0E-6     1.2E-5     1.8E-5
KSBAR  N  1 N    1.07E-4
```

Table M.1 continued

KFBAR	N	1	N	0.501			
KRAD	N	4	N	0.5	0.56		
KDRAD	N	3	N	4.5E-5	1.5	1.3E-6	1.52E-4
CLEADI	N	6	N	1.0	2.0	3.0	
KSLEAD	N	1	N	0.012			
KFLEAD	N	1	N	0.501			
KDLEAD	N	3	N	6.0E-5	1.5	2.E-5	1.E-4
XRATE	N	1	N	0.10			
DBOT	N	4	N	0.5	1.0		
WSTAIL	N	1	N	5.7E+5			
XRUNOF	N	6	N	0.55	0.60	0.65	
SLOPE	N	1	N	0.92			
THALF	N	4	N	15.0	25.0		
RRAIN	N	4	N	65.0	97.5		
RSOIL	N	4	N	1.0E-8	1.0E-7		
DM	N	6	N	0.0015	0.017	0.075	
STORM	N	4	N	36.0	48.0		
FLENGT	N	1	N	880.0			
MINVEG	N	1	N	0.6			
BEDTRP	N	1	N	100.0			
SUSTRP	N	6	N	85.0	98.0	100.0	
WYEAR	N	4	V	1.0	20.9999999		
EMANAT	N	6	N	0.05	0.20	0.50	
WTSFLX	N	3	N	0.02	2.0	0.002	0.2
MPCH2O	N	6	N	9.0	13.0	23.0	
NSUBW	N	1	N	5.0			
CAFR	N	1	N	0.0			
SILT	N	6	N	30.0	45.0	60.0	
FPREC	N	2	V	149.0	17.0	115.0	183.0
CAFD	N	1	N	0.0			
HSRC	N	4	N	1.0	3.0		
DEPVEL	N	4	N	0.003	0.03		
DSOIL	N	1	N	0.05			
DSOIL	N	1	N	0.15			
FWAT	N	6	N	0.02	0.16	0.48	
RHOS	N	3	N	129.0	1.3	20.0	450.0
RHOS	N	3	N	1342.0	1.1	1000.0	1800.0
SOILKD	N	5	N	1.3E-04	790.0		
SOILKD	N	5	N	0.0033	150.0		
SOILKD	N	5	N	0.18	63.0		
SOILKD	N	5	N	0.0051	950.0		
SOILKD	N	5	N	1.3E-04	790.0		
SOILKD	N	5	N	0.0033	150.0		
SOILKD	N	5	N	0.18	63.0		
SOILKD	N	5	N	0.0051	950.0		
WC	N	4	N	0.75	1.4		
WC	N	3	N	0.13	1.4	0.05	0.36
EMFRAC	N	1	N	0.2			
XRGWA1	N	6	N	0.1	2.0	4.0	
XRGWA2	N	6	N	5.0	7.0	9.0	
XRGWA3	N	1	N	0.0			
XRGWA4	N	1	N	0.0			
XRGWA5	N	1	N	0.0			

Table M.1 continued

AXGWA1	N	1	N	2005.0			
AXGWA2	N	1	N	3590.0			
AXGWA3	N	1	N	0.0			
AXGWA4	N	1	N	0.0			
AXGWA5	N	1	N	0.0			
POGWA1	N	4	N	0.33	0.40		
POGWA2	N	4	N	0.33	0.40		
POGWA3	N	1	N	0.0			
POGWA4	N	1	N	0.0			
POGWA5	N	1	N	0.0			
DCGWA1	N	3	N	0.012	1.50	0.0036	0.04
DCGWA2	N	3	N	0.05	1.50	0.015	0.17
DCGWA3	N	3	N	0.06	1.50	0.018	0.2
DCGWA4	N	3	N	0.045	1.50	0.013	0.15
SDGWA1	N	2	N	2650.0	100.0	2200.0	2980.0
SDGWA2	N	2	N	2650.0	100.0	2200.0	2980.0
SDGWA3	N	1	N	0.0			
SDGWA4	N	1	N	0.0			
SDGWA5	N	1	N	0.0			
HCGWA1	N	3	N	69.4	2.40	12.0	400.0
HCGWA2	N	3	N	69.4	2.40	12.0	400.0
HCGWA3	N	1	N	0.0			
HCGWA4	N	1	N	0.0			
HCGWA5	N	1	N	0.0			
HGGWA1	N	2	N	0.051	0.01	0.041	0.061
HGGWA2	N	2	N	0.176	0.03	0.146	0.206
HGGWA3	N	1	N	0.0			
HGGWA4	N	1	N	0.0			
HGGWA5	N	1	N	0.0			
ACTCO	N	6	N	0.6	0.8	0.9	
WATCAB	N	1	N	0.19			
WTSO4B	N	1	N	0.14			
WATNAB	N	1	N	0.34			
WATKB	N	1	N	0.02			
WATMGB	N	1	N	0.06			
WATCLB	N	1	N	0.38			
WSIGS1	N	6	N	30.0	70.0	170.0	
WSIGS2	N	6	N	125.0	255.0	635.0	
WSIGS3	N	6	N	500.0	1000.0	2035.0	
WSIGS4	N	6	N	140.0	300.0	740.0	
WSIGS5	N	6	N	40.0	95.0	225.0	
WTRHOS	N	1	N	1.955E+6			
WATEPS	N	6	N	0.83	0.90	0.97	
WTMIXD	N	1	N	0.05			
WKDU	N	3	N	0.0045	2.2	4.0E-4	0.048
WKDPB	N	3	N	0.015	2.5	0.001	0.23
WKDRA	N	3	N	0.0065	2.5	4.0E-4	0.1
KDPRIM	N	3	N	0.02	2.5	0.002	0.3
BURYF	N	4	N	0.76	0.86		
CURRNT	N	4	N	3.15E+4	3.15E+5		
DIFFC	N	1	N	0.02			
FCONC	N	6	N	0.0	0.02	0.1	
FCONC	N	6	N	0.0	0.005	0.02	

Table M.1 continued

FCONC	N	6	N	0.0	0.02	0.1	
FCONC	N	6	N	0.0	0.02	0.1	
BIOACF	N	3	N	1.55E-6	6.1	1.0E-8	5.8E-5
BIOACF	N	3	N	1.18E-5	2.6	1.1E-6	1.1E-4
BIOACF	N	3	N	1.74E-5	3.25	1.7E-6	5.7E-4
BIOACF	N	3	N	1.31E-5	3.3	1.2E-6	6.0E-4
WATVTC	N	3	N	1.5E-5	5.5	1.0E-6	7.0E-4
WATVTC	N	3	N	1.1E-5	6.8	1.0E-6	1.6E-4
WATVTC	N	3	N	1.3E-4	2.0	4.0E-5	4.3E-4
WATVTC	N	3	N	4.5E-5	2.9	1.0E-5	3.3E-4
FDEPSF	N	4	N	0.1	0.3		
FDEPSF	N	4	N	0.1	0.3		
FDEPSF	N	2	N	0.47	0.3	0.01	1.0
FDEPSF	N	2	N	0.47	0.3	0.01	1.0
FDEPSF	N	4	N	0.8	1.0		
FDEPED	N	4	N	0.8	1.0		
FDEPED	N	4	N	0.05	0.15		
FDEPED	N	4	N	0.8	1.0		
FDEPED	N	4	N	0.8	1.0		
FDEPED	N	4	N	0.8	1.0		
VEGLAM	N	4	N	2.9E-7	1.2E-6		
VEGLAM	N	4	N	2.9E-7	1.2E-6		
VEGLAM	N	4	N	2.9E-7	1.2E-6		
VEGLAM	N	4	N	2.9E-7	1.2E-6		
VEGLAM	N	4	N	1.5E-9	4.4E-9		
DUREXP	N	6	N	2.6E+6	5.2E+6	7.8E+6	
DUREXP	N	6	N	2.6E+6	5.2E+6	7.8E+6	
DUREXP	N	4	N	1.3E+6	3.9E+6		
DUREXP	N	4	N	1.3E+6	3.9E+6		
DUREXP	N	1	N	1.0E+10			
YDEN	N	4	N	1000.0	3000.0		
YDEN	N	4	N	1000.0	3000.0		
YDEN	N	4	N	500.0	1000.0		
YDEN	N	4	N	500.0	1000.0		
YDEN	N	4	N	400.0	600.0		
SPTCAV	N	3	N	6.1E-4	8.9	7.7E-6	0.007
SPTCAV	N	3	N	0.0042	9.0	5.2E-5	0.34
SPTCAV	N	3	N	0.0040	9.0	4.9E-5	0.32
SPTCAV	N	3	N	0.0085	10.0	8.0E-5	0.89
SPTCBV	N	3	N	3.2E-4	3.9	2.1E-5	0.0049
SPTCBV	N	3	N	0.0042	4.0	2.6E-4	0.067
SPTCBV	N	3	N	0.0040	4.0	2.5E-4	0.064
SPTCBV	N	3	N	0.0027	4.5	1.3E-4	0.066
SPTCSF	N	3	N	0.0066	8.9	8.3E-5	0.52
SPTCSF	N	3	N	0.022	9.5	2.5E-4	2.0
SPTCSF	N	3	N	0.022	3.6	0.0017	0.27
SPTCSF	N	3	N	0.21	3.6	0.0019	0.24
SPTCB	N	3	N	0.0066	8.9	8.3E-5	0.52
SPTCB	N	3	N	0.022	9.5	2.5E-4	2.0
SPTCB	N	3	N	0.022	3.6	0.0017	0.27
SPTCB	N	3	N	0.21	3.6	0.0019	0.24
SPTCL	N	1	N	0.0			
SPTCL	N	1	N	0.0			

Table M.1 continued

SPTCL	N	1	N	0.0		
SPTCL	N	1	N	0.0		
FIRC	N	6	N	5000.0	7000.0	9000.0
WIRC	N	6	N	0.0077	0.0115	0.0153
FAISFC	N	6	N	0.05	0.2	0.5
FAILC	N	6	N	0.05	0.2	0.5
FMTCC	N	6	N	1.1E-7	3.4E-7	1.0E-6
FMTCC	N	6	N	0.7E-7	2.0E-7	0.6E-6
FMTCC	N	6	N	1.3E-7	4.0E-7	1.2E-6
FMTCC	N	6	N	1.7E-7	5.1E-7	1.5E-6
FIRM	N	1	N	2.7E+4		
WIRM	N	6	N	0.024	0.036	0.048
FAIBM	N	6	N	0.8	0.9	0.95
FMTCM	N	6	N	1.1E-7	3.4E-7	1.0E-6
FMTCM	N	6	N	0.7E-7	2.0E-7	0.6E-6
FMTCM	N	6	N	1.3E-7	4.0E-7	1.2E-6
FMTCM	N	6	N	1.7E-7	5.1E-7	1.5E-6
FIRD	N	6	N	1800.0	7500.0	1.0E+4
WIRD	N	4	N	0.0007	0.0014	
FAISFD	N	6	N	0.25	0.33	0.40
FMTCD	N	6	N	1.1E-7	3.4E-7	1.0E-6
FMTCD	N	6	N	0.7E-7	2.0E-7	0.6E-6
FMTCD	N	6	N	1.3E-7	4.0E-7	1.2E-6
FMTCD	N	6	N	1.7E-7	5.1E-7	1.5E-6
EFR	N	6	N	0.2	0.5	0.8
SHLD	N	6	N	0.05	0.2	0.4
OF	N	6	N	0.5	0.9	1.0
OF	N	6	N	0.5	0.9	1.0
INOCC	N	6	N	0.6	0.9	1.0
INOCC	N	6	N	0.6	0.9	1.0
AIRIN	N	1	N	8400.0		
AIRIN	N	1	N	8400.0		
AFACT	N	4	N	0.5	1.0	
AVEGIN	N	1	N	4.53E+4		
AVEGIN	N	1	N	4.53E+4		
AFLOC	N	6	N	0.0	0.1	0.2
AFLOC	N	6	N	0.1	0.3	0.6
BFACT	N	4	N	0.5	1.0	
BVEGIN	N	1	N	7.4E+4		
BVEGIN	N	1	N	7.4E+4		
BFLOC	N	6	N	0.0	0.1	0.2
BFLOC	N	6	N	0.1	0.3	0.6
CARMIN	N	1	N	0.0		
CARMIN	N	1	N	0.0		
CFLOC	N	4	N	0.0	1.0	
CFLOC	N	4	N	0.0	1.0	
MOSMIN	N	1	N	6000.0		
MOSMIN	N	1	N	3.95E+4		
MFLOC	N	6	N	0.0	0.25	0.5
MFLOC	N	1	N	1.0		
DERMIN	N	1	N	6000.0		
DERMIN	N	1	N	3.95E+4		
DFLOC	N	1	N	1.0		

Table M.1 continued

```
DFLOC  N  1 N        1.0
WATIN  N  1 N        0.6
WATIN  N  1 N        0.6
FISHIN N  1 N     8000.0
FISHIN N  1 N     8000.0
FFLOC  N  6 N        0.0       0.25        0.5
FFLOC  N  1 N        1.0
```

Table M.2

LACNOR WASTE ROCK TAILINGS COVER (OPTION 2)

```
LACNOR WASTE ROCK TAILING COVER PROBALILISTIC INPUTS (OPTION 2)
Y Y
OPT2.PR
OPT2.PK
 262   0   0
0913566091 200
 3000.0   10.0
CODION N  1 N         0.0
CODNUC N  1 N         0.0
CODPH  N  1 N         0.0
CODERO N  1 N         0.0
CODDUS N  1 N         0.0
CODRAD N  1 N         0.0
CODWIN N  1 N         0.0
CODAIR N  1 N         0.0
CODSOL N  1 N         0.0
CODGS  N  1 N         0.0
CODVEG N  1 N         0.0
CODGW  N  1 N         0.0
CODWAT N  1 N         0.0
CODFIS N  1 N         0.0
CODWVG N  1 N         0.0
CODANI N  1 N         0.0
CODDOS N  1 N         0.0
PYRITI N  6 N       600.0      700.0      800.0
RHOTAL N  6 N      1.1E+6     1.3E+6     1.5E+6
FRACGP N  2 N        0.06      0.005       0.05       0.07
KPRIME N  4 N        0.01        0.1
SULPRD N  6 N      3.0E-6     4.1E-6     5.3E-6
O2CONC N  1 N        9.04
O2DIFF N  6 N         5.0       37.0       70.0
DUNSAT N  6 N        0.25        0.5        2.0
KSUBSO N  1 N        50.0
FACTCO N  6 N         0.4        0.5        0.6
NPRCP  N  2 V        0.51        0.1       0.25       0.85
DMIX   N  4 N         8.0       14.0
AVPRCP N  1 N        0.51
ATAIL  N  1 N     2.41E+5
XLIME  N  1 N      5.0E-4
PCURAN N  1 N         0.1
FURAN  N  4 N        0.90       0.94
FT230  N  6 N        0.65       0.80       0.95
FT232  N  6 N        0.55       0.65       0.75
FRAD   N  6 N        0.25       0.60       0.95
FLEAD  N  6 N        0.25       0.60       0.95
FRACU  N  4 N        0.30       0.90
KDUO2  N  3 N      2.0E-5        3.0     5.0E-6     5.0E-4
PCTHOR N  4 N        0.02       0.04
XRADI  N  6 N      6.0E-6     1.2E-5     1.8E-5
KSBAR  N  1 N     1.07E-4
```

Table M.2 continued

KFBAR	N	1	N	0.501			
KRAD	N	4	N	0.5	0.56		
KDRAD	N	3	N	4.5E-5	1.5	1.3E-6	1.52E-4
CLEADI	N	6	N	1.0	2.0	3.0	
KSLEAD	N	1	N	0.012			
KFLEAD	N	1	N	0.501			
KDLEAD	N	3	N	6.0E-5	1.5	2.E-5	1.E-4
XRATE	N	1	N	0.10			
DBOT	N	4	N	0.5	1.0		
WSTAIL	N	1	N	5.7E+5			
XRUNOF	N	6	N	0.25	0.30	0.35	
SLOPE	N	1	N	0.92			
THALF	N	4	N	15.0	25.0		
RRAIN	N	4	N	65.0	97.5		
RSOIL	N	4	N	1.0E-8	1.0E-7		
DM	N	6	N	0.0015	0.017	0.075	
STORM	N	4	N	36.0	48.0		
FLENGT	N	1	N	880.0			
MINVEG	N	1	N	0.0			
BEDTRP	N	1	N	100.0			
SUSTRP	N	6	N	85.0	98.0	100.0	
WYEAR	N	4	V	1.0	20.9999999		
EMANAT	N	6	N	0.05	0.20	0.50	
WTSFLX	N	3	N	0.02	2.0	0.002	0.2
MPCH20	N	6	N	9.0	13.0	23.0	
NSUBW	N	1	N	5.0			
CAFR	N	1	N	0.0			
SILT	N	6	N	30.0	45.0	60.0	
FPREC	N	2	V	149.0	17.0	115.0	183.0
CAFD	N	1	N	0.95			
HSRC	N	4	N	1.0	3.0		
DEPVEL	N	4	N	0.003	0.03		
DSOIL	N	1	N	0.05			
DSOIL	N	1	N	0.15			
FWAT	N	6	N	0.02	0.16	0.48	
RHOS	N	3	N	129.0	1.3	20.0	450.0
RHOS	N	3	N	1342.0	1.1	1000.0	1800.0
SOILKD	N	5	N	1.3E-04	790.0		
SOILKD	N	5	N	0.0033	150.0		
SOILKD	N	5	N	0.18	63.0		
SOILKD	N	5	N	0.0051	950.0		
SOILKD	N	5	N	1.3E-04	790.0		
SOILKD	N	5	N	0.0033	150.0		
SOILKD	N	5	N	0.18	63.0		
SOILKD	N	5	N	0.0051	950.0		
WC	N	4	N	0.75	1.4		
WC	N	3	N	0.13	1.4	0.05	0.36
EMFRAC	N	1	N	0.2			
XRGWA1	N	6	N	0.1	2.0	4.0	
XRGWA2	N	6	N	5.0	7.0	9.0	
XRGWA3	N	1	N	0.0			
XRGWA4	N	1	N	0.0			
XRGWA5	N	1	N	0.0			

Table M.2 continued

AXGWA1	N	1	N	2005.0			
AXGWA2	N	1	N	3590.0			
AXGWA3	N	1	N	0.0			
AXGWA4	N	1	N	0.0			
AXGWA5	N	1	N	0.0			
POGWA1	N	4	N	0.33	0.40		
POGWA2	N	4	N	0.33	0.40		
POGWA3	N	1	N	0.0			
POGWA4	N	1	N	0.0			
POGWA5	N	1	N	0.0			
DCGWA1	N	3	N	0.012	1.50	0.0036	0.04
DCGWA2	N	3	N	0.05	1.50	0.015	0.17
DCGWA3	N	3	N	0.06	1.50	0.018	0.2
DCGWA4	N	3	N	0.045	1.50	0.013	0.15
SDGWA1	N	2	N	2650.0	100.0	2200.0	2980.0
SDGWA2	N	2	N	2650.0	100.0	2200.0	2980.0
SDGWA3	N	1	N	0.0			
SDGWA4	N	1	N	0.0			
SDGWA5	N	1	N	0.0			
HCGWA1	N	3	N	69.4	2.40	12.0	400.0
HCGWA2	N	3	N	69.4	2.40	12.0	400.0
HCGWA3	N	1	N	0.0			
HCGWA4	N	1	N	0.0			
HCGWA5	N	1	N	0.0			
HGGWA1	N	2	N	0.051	0.01	0.041	0.061
HGGWA2	N	2	N	0.176	0.03	0.146	0.206
HGGWA3	N	1	N	0.0			
HGGWA4	N	1	N	0.0			
HGGWA5	N	1	N	0.0			
ACTCO	N	6	N	0.6	0.8	0.9	
WATCAB	N	1	N	0.19			
WTSO4B	N	1	N	0.14			
WATNAB	N	1	N	0.34			
WATKB	N	1	N	0.02			
WATMGB	N	1	N	0.06			
WATCLB	N	1	N	0.38			
WSIGS1	N	6	N	30.0	70.0	170.0	
WSIGS2	N	6	N	125.0	255.0	635.0	
WSIGS3	N	6	N	500.0	1000.0	2035.0	
WSIGS4	N	6	N	140.0	300.0	740.0	
WSIGS5	N	6	N	40.0	95.0	225.0	
WTRHOS	N	1	N	1.955E+6			
WATEPS	N	6	N	0.83	0.90	0.97	
WTMIXD	N	1	N	0.05			
WKDU	N	3	N	0.0045	2.2	4.0E-4	0.048
WKDPB	N	3	N	0.015	2.5	0.001	0.23
WKDRA	N	3	N	0.0065	2.5	4.0E-4	0.1
KDPRIM	N	3	N	0.02	2.5	0.002	0.3
BURYF	N	4	N	0.76	0.86		
CURRNT	N	4	N	3.15E+4	3.15E+5		
DIFFC	N	1	N	0.02			
FCONC	N	6	N	0.0	0.02	0.1	
FCONC	N	6	N	0.0	0.005	0.02	

Table M.2 continued

FCONC	N	6	N	0.0	0.02	0.1	
FCONC	N	6	N	0.0	0.02	0.1	
BIOACF	N	3	N	1.55E-6	6.1	1.0E-8	5.8E-5
BIOACF	N	3	N	1.18E-5	2.6	1.1E-6	1.1E-4
BIOACF	N	3	N	1.74E-5	3.25	1.7E-6	5.7E-4
BIOACF	N	3	N	1.31E-5	3.3	1.2E-6	6.0E-4
WATVTC	N	3	N	1.5E-5	5.5	1.0E-6	7.0E-4
WATVTC	N	3	N	1.1E-5	6.8	1.0E-6	1.6E-4
WATVTC	N	3	N	1.3E-4	2.0	4.0E-5	4.3E-4
WATVTC	N	3	N	4.5E-5	2.9	1.0E-5	3.3E-4
FDEPSF	N	4	N	0.1	0.3		
FDEPSF	N	4	N	0.1	0.3		
FDEPSF	N	2	N	0.47	0.3	0.01	1.0
FDEPSF	N	2	N	0.47	0.3	0.01	1.0
FDEPSF	N	4	N	0.8	1.0		
FDEPED	N	4	N	0.8	1.0		
FDEPED	N	4	N	0.05	0.15		
FDEPED	N	4	N	0.8	1.0		
FDEPED	N	4	N	0.8	1.0		
FDEPED	N	4	N	0.8	1.0		
VEGLAM	N	4	N	2.9E-7	1.2E-6		
VEGLAM	N	4	N	2.9E-7	1.2E-6		
VEGLAM	N	4	N	2.9E-7	1.2E-6		
VEGLAM	N	4	N	2.9E-7	1.2E-6		
VEGLAM	N	4	N	1.5E-9	4.4E-9		
DUREXP	N	6	N	2.6E+6	5.2E+6	7.8E+6	
DUREXP	N	6	N	2.6E+6	5.2E+6	7.8E+6	
DUREXP	N	4	N	1.3E+6	3.9E+6		
DUREXP	N	4	N	1.3E+6	3.9E+6		
DUREXP	N	1	N	1.0E+10			
YDEN	N	4	N	1000.0	3000.0		
YDEN	N	4	N	1000.0	3000.0		
YDEN	N	4	N	500.0	1000.0		
YDEN	N	4	N	500.0	1000.0		
YDEN	N	4	N	400.0	600.0		
SPTCAV	N	3	N	6.1E-4	8.9	7.7E-6	0.007
SPTCAV	N	3	N	0.0042	9.0	5.2E-5	0.34
SPTCAV	N	3	N	0.0040	9.0	4.9E-5	0.32
SPTCAV	N	3	N	0.0085	10.0	8.0E-5	0.89
SPTCBV	N	3	N	3.2E-4	3.9	2.1E-5	0.0049
SPTCBV	N	3	N	0.0042	4.0	2.6E-4	0.067
SPTCBV	N	3	N	0.0040	4.0	2.5E-4	0.064
SPTCBV	N	3	N	0.0027	4.5	1.3E-4	0.066
SPTCSF	N	3	N	0.0066	8.9	8.3E-5	0.52
SPTCSF	N	3	N	0.022	9.5	2.5E-4	2.0
SPTCSF	N	3	N	0.022	3.6	0.0017	0.27
SPTCSF	N	3	N	0.21	3.6	0.0019	0.24
SPTCB	N	3	N	0.0066	8.9	8.3E-5	0.52
SPTCB	N	3	N	0.022	9.5	2.5E-4	2.0
SPTCB	N	3	N	0.022	3.6	0.0017	0.27
SPTCB	N	3	N	0.21	3.6	0.0019	0.24
SPTCL	N	1	N	0.0			
SPTCL	N	1	N	0.0			

Table M.2 continued

SPTCL	N	1	N	0.0		
SPTCL	N	1	N	0.0		
FIRC	N	6	N	5000.0	7000.0	9000.0
WIRC	N	6	N	0.0077	0.0115	0.0153
FAISFC	N	6	N	0.05	0.2	0.5
FAILC	N	6	N	0.05	0.2	0.5
FMTCC	N	6	N	1.1E-7	3.4E-7	1.0E-6
FMTCC	N	6	N	0.7E-7	2.0E-7	0.6E-6
FMTCC	N	6	N	1.3E-7	4.0E-7	1.2E-6
FMTCC	N	6	N	1.7E-7	5.1E-7	1.5E-6
FIRM	N	1	N	2.7E+4		
WIRM	N	6	N	0.024	0.036	0.048
FAIBM	N	6	N	0.8	0.9	0.95
FMTCM	N	6	N	1.1E-7	3.4E-7	1.0E-6
FMTCM	N	6	N	0.7E-7	2.0E-7	0.6E-6
FMTCM	N	6	N	1.3E-7	4.0E-7	1.2E-6
FMTCM	N	6	N	1.7E-7	5.1E-7	1.5E-6
FIRD	N	6	N	1800.0	7500.0	1.0E+4
WIRD	N	4	N	0.0007	0.0014	
FAISFD	N	6	N	0.25	0.33	0.40
FMTCD	N	6	N	1.1E-7	3.4E-7	1.0E-6
FMTCD	N	6	N	0.7E-7	2.0E-7	0.6E-6
FMTCD	N	6	N	1.3E-7	4.0E-7	1.2E-6
FMTCD	N	6	N	1.7E-7	5.1E-7	1.5E-6
EFR	N	6	N	0.2	0.5	0.8
SHLD	N	6	N	0.05	0.2	0.4
OF	N	6	N	0.5	0.9	1.0
OF	N	6	N	0.5	0.9	1.0
INOCC	N	6	N	0.6	0.9	1.0
INOCC	N	6	N	0.6	0.9	1.0
AIRIN	N	1	N	8400.0		
AIRIN	N	1	N	8400.0		
AFACT	N	4	N	0.5	1.0	
AVEGIN	N	1	N	4.53E+4		
AVEGIN	N	1	N	4.53E+4		
AFLOC	N	6	N	0.0	0.1	0.2
AFLOC	N	6	N	0.1	0.3	0.6
BFACT	N	4	N	0.5	1.0	
BVEGIN	N	1	N	7.4E+4		
BVEGIN	N	1	N	7.4E+4		
BFLOC	N	6	N	0.0	0.1	0.2
BFLOC	N	6	N	0.1	0.3	0.6
CARMIN	N	1	N	0.0		
CARMIN	N	1	N	0.0		
CFLOC	N	4	N	0.0	1.0	
CFLOC	N	4	N	0.0	1.0	
MOSMIN	N	1	N	6000.0		
MOSMIN	N	1	N	3.95E+4		
MFLOC	N	6	N	0.0	0.25	0.5
MFLOC	N	1	N	1.0		
DERMIN	N	1	N	6000.0		
DERMIN	N	1	N	3.95E+4		
DFLOC	N	1	N	1.0		

Table M.2 continued

```
DFLOC  N  1 N       1.0
WATIN  N  1 N       0.6
WATIN  N  1 N       0.6
FISHIN N  1 N    8000.0
FISHIN N  1 N    8000.0
FFLOC  N  6 N       0.0        0.25        0.5
FFLOC  N  1 N       1.0
```

Table M.3

LACNOR DEPYRITIZED TAILINGS COVER (OPTION 3)

```
LACNOR DEPYRITIZED TAILING COVER PROBABILISTIC INPUTS (OPTION 3)
Y Y
OPT3.PR
OPT3.PK
 262   0   0
0913566091 200
 3000.0   10.0
CODION N  1 N         0.0
CODNUC N  1 N         0.0
CODPH  N  1 N         0.0
CODERO N  1 N         0.0
CODDUS N  1 N         0.0
CODRAD N  1 N         0.0
CODWIN N  1 N         0.0
CODAIR N  1 N         0.0
CODSOL N  1 N         0.0
CODGS  N  1 N         0.0
CODVEG N  1 N         0.0
CODGW  N  1 N         0.0
CODWAT N  1 N         0.0
CODFIS N  1 N         0.0
CODWVG N  1 N         0.0
CODANI N  1 N         0.0
CODDOS N  1 N         0.0
PYRITI N  6 N        39.0       54.0       69.0
RHOTAL N  6 N      1.1E+6     1.3E+6     1.5E+6
FRACGP N  2 N        0.06      0.005       0.05       0.07
KPRIME N  4 N        0.01        0.1
SULPRD N  6 N     1.27E-8    2.43E-8    3.97E-8
O2CONC N  1 N        9.04
O2DIFF N  6 N         5.0       37.0       70.0
DUNSAT N  6 N        0.25        0.5        2.0
KSUBSO N  1 N        50.0
FACTCO N  6 N         0.4        0.5        0.6
NPRCP  N  2 V        0.51        0.1       0.25       0.85
DMIX   N  4 N         8.0       14.0
AVPRCP N  1 N        0.51
ATAIL  N  1 N     2.41E+5
XLIME  N  1 N        0.01
PCURAN N  1 N        0.08
FURAN  N  4 N        0.90       0.94
FT230  N  6 N        0.65       0.80       0.95
FT232  N  6 N        0.55       0.65       0.75
FRAD   N  6 N        0.25       0.60       0.95
FLEAD  N  6 N        0.25       0.60       0.95
FRACU  N  4 N       0.028      0.088
KDUO2  N  3 N      2.0E-5        3.0     5.0E-6     5.0E-4
PCTHOR N  4 N        0.02       0.04
XRADI  N  6 N      6.0E-6     1.2E-5     1.8E-5
KSBAR  N  1 N     1.07E-4
```

Table M.3 continued

KFBAR	N	1	N	0.501			
KRAD	N	4	N	0.5	0.56		
KDRAD	N	3	N	4.5E-5	1.5	1.3E-6	1.52E-4
CLEADI	N	6	N	1.0	2.0	3.0	
KSLEAD	N	1	N	0.012			
KFLEAD	N	1	N	0.501			
KDLEAD	N	3	N	6.0E-5	1.5	2.E-5	1.E-4
XRATE	N	1	N	0.10			
DBOT	N	4	N	2.5	3.0		
WSTAIL	N	1	N	5.7E+5			
XRUNOF	N	6	N	0.55	0.60	0.65	
SLOPE	N	1	N	0.92			
THALF	N	4	N	15.0	25.0		
RRAIN	N	4	N	65.0	97.5		
RSOIL	N	4	N	1.0E-8	1.0E-7		
DM	N	6	N	0.0015	0.017	0.075	
STORM	N	4	N	36.0	48.0		
FLENGT	N	1	N	880.0			
MINVEG	N	1	N	0.6			
BEDTRP	N	1	N	100.0			
SUSTRP	N	6	N	85.0	98.0	100.0	
WYEAR	N	4	V	1.0	20.9999999		
EMANAT	N	6	N	0.05	0.20	0.50	
WTSFLX	N	3	N	0.02	2.0	0.002	0.2
MPCH2O	N	6	N	9.0	13.0	23.0	
NSUBW	N	1	N	5.0			
CAFR	N	1	N	0.0			
SILT	N	6	N	30.0	45.0	60.0	
FPREC	N	2	V	149.0	17.0	115.0	183.0
CAFD	N	1	N	0.0			
HSRC	N	4	N	1.0	3.0		
DEPVEL	N	4	N	0.003	0.03		
DSOIL	N	1	N	0.05			
DSOIL	N	1	N	0.15			
FWAT	N	6	N	0.02	0.16	0.48	
RHOS	N	3	N	129.0	1.3	20.0	450.0
RHOS	N	3	N	1342.0	1.1	1000.0	1800.0
SOILKD	N	5	N	1.3E-04	790.0		
SOILKD	N	5	N	0.0033	150.0		
SOILKD	N	5	N	0.18	63.0		
SOILKD	N	5	N	0.0051	950.0		
SOILKD	N	5	N	1.3E-04	790.0		
SOILKD	N	5	N	0.0033	150.0		
SOILKD	N	5	N	0.18	63.0		
SOILKD	N	5	N	0.0051	950.0		
WC	N	4	N	0.75	1.4		
WC	N	3	N	0.13	1.4	0.05	0.36
EMFRAC	N	1	N	0.2			
XRGWA1	N	6	N	0.1	2.0	4.0	
XRGWA2	N	6	N	5.0	7.0	9.0	
XRGWA3	N	1	N	0.0			
XRGWA4	N	1	N	0.0			
XRGWA5	N	1	N	0.0			

Table M.3 continued

AXGWA1	N	1	N	2005.0			
AXGWA2	N	1	N	3590.0			
AXGWA3	N	1	N	0.0			
AXGWA4	N	1	N	0.0			
AXGWA5	N	1	N	0.0			
POGWA1	N	4	N	0.33	0.40		
POGWA2	N	4	N	0.33	0.40		
POGWA3	N	1	N	0.0			
POGWA4	N	1	N	0.0			
POGWA5	N	1	N	0.0			
DCGWA1	N	3	N	0.012	1.50	0.0036	0.04
DCGWA2	N	3	N	0.05	1.50	0.015	0.17
DCGWA3	N	3	N	0.06	1.50	0.018	0.2
DCGWA4	N	3	N	0.045	1.50	0.013	0.15
SDGWA1	N	2	N	2650.0	100.0	2200.0	2980.0
SDGWA2	N	2	N	2650.0	100.0	2200.0	2980.0
SDGWA3	N	1	N	0.0			
SDGWA4	N	1	N	0.0			
SDGWA5	N	1	N	0.0			
HCGWA1	N	3	N	6.9	2.4	1.2	40.0
HCGWA2	N	3	N	6.9	2.4	1.2	40.0
HCGWA3	N	1	N	0.0			
HCGWA4	N	1	N	0.0			
HCGWA5	N	1	N	0.0			
HGGWA1	N	2	N	0.051	0.01	0.041	0.061
HGGWA2	N	2	N	0.176	0.03	0.146	0.206
HGGWA3	N	1	N	0.0			
HGGWA4	N	1	N	0.0			
HGGWA5	N	1	N	0.0			
ACTCO	N	6	N	0.6	0.8	0.9	
WATCAB	N	1	N	0.19			
WTSO4B	N	1	N	0.14			
WATNAB	N	1	N	0.34			
WATKB	N	1	N	0.02			
WATMGB	N	1	N	0.06			
WATCLB	N	1	N	0.38			
WSIGS1	N	6	N	30.0	70.0	170.0	
WSIGS2	N	6	N	125.0	255.0	635.0	
WSIGS3	N	6	N	500.0	1000.0	2035.0	
WSIGS4	N	6	N	140.0	300.0	740.0	
WSIGS5	N	6	N	40.0	95.0	225.0	
WTRHOS	N	1	N	1.955E+6			
WATEPS	N	6	N	0.83	0.90	0.97	
WTMIXD	N	1	N	0.05			
WKDU	N	3	N	0.0045	2.2	4.0E-4	0.048
WKDPB	N	3	N	0.015	2.5	0.001	0.23
WKDRA	N	3	N	0.0065	2.5	4.0E-4	0.1
KDPRIM	N	3	N	0.02	2.5	0.002	0.3
BURYF	N	4	N	0.76	0.86		
CURRNT	N	4	N	3.15E+4	3.15E+5		
DIFFC	N	1	N	0.02			
FCONC	N	6	N	0.0	0.02	0.1	
FCONC	N	6	N	0.0	0.005	0.02	

Table M.3 continued

FCONC	N	6	N	0.0	0.02	0.1	
FCONC	N	6	N	0.0	0.02	0.1	
BIOACF	N	3	N	1.55E-6	6.1	1.0E-8	5.8E-5
BIOACF	N	3	N	1.18E-5	2.6	1.1E-6	1.1E-4
BIOACF	N	3	N	1.74E-5	3.25	1.7E-6	5.7E-4
BIOACF	N	3	N	1.31E-5	3.3	1.2E-6	6.0E-4
WATVTC	N	3	N	1.5E-5	5.5	1.0E-6	7.0E-4
WATVTC	N	3	N	1.1E-5	6.8	1.0E-6	1.6E-4
WATVTC	N	3	N	1.3E-4	2.0	4.0E-5	4.3E-4
WATVTC	N	3	N	4.5E-5	2.9	1.0E-5	3.3E-4
FDEPSF	N	4	N	0.1	0.3		
FDEPSF	N	4	N	0.1	0.3		
FDEPSF	N	2	N	0.47	0.3	0.01	1.0
FDEPSF	N	2	N	0.47	0.3	0.01	1.0
FDEPSF	N	4	N	0.8	1.0		
FDEPED	N	4	N	0.8	1.0		
FDEPED	N	4	N	0.05	0.15		
FDEPED	N	4	N	0.8	1.0		
FDEPED	N	4	N	0.8	1.0		
FDEPED	N	4	N	0.8	1.0		
VEGLAM	N	4	N	2.9E-7	1.2E-6		
VEGLAM	N	4	N	2.9E-7	1.2E-6		
VEGLAM	N	4	N	2.9E-7	1.2E-6		
VEGLAM	N	4	N	2.9E-7	1.2E-6		
VEGLAM	N	4	N	1.5E-9	4.4E-9		
DUREXP	N	6	N	2.6E+6	5.2E+6	7.8E+6	
DUREXP	N	6	N	2.6E+6	5.2E+6	7.8E+6	
DUREXP	N	4	N	1.3E+6	3.9E+6		
DUREXP	N	4	N	1.3E+6	3.9E+6		
DUREXP	N	1	N	1.0E+10			
YDEN	N	4	N	1000.0	3000.0		
YDEN	N	4	N	1000.0	3000.0		
YDEN	N	4	N	500.0	1000.0		
YDEN	N	4	N	500.0	1000.0		
YDEN	N	4	N	400.0	600.0		
SPTCAV	N	3	N	6.1E-4	8.9	7.7E-6	0.007
SPTCAV	N	3	N	0.0042	9.0	5.2E-5	0.34
SPTCAV	N	3	N	0.0040	9.0	4.9E-5	0.32
SPTCAV	N	3	N	0.0085	10.0	8.0E-5	0.89
SPTCBV	N	3	N	3.2E-4	3.9	2.1E-5	0.0049
SPTCBV	N	3	N	0.0042	4.0	2.6E-4	0.067
SPTCBV	N	3	N	0.0040	4.0	2.5E-4	0.064
SPTCBV	N	3	N	0.0027	4.5	1.3E-4	0.066
SPTCSF	N	3	N	0.0066	8.9	8.3E-5	0.52
SPTCSF	N	3	N	0.022	9.5	2.5E-4	2.0
SPTCSF	N	3	N	0.022	3.6	0.0017	0.27
SPTCSF	N	3	N	0.21	3.6	0.0019	0.24
SPTCB	N	3	N	0.0066	8.9	8.3E-5	0.52
SPTCB	N	3	N	0.022	9.5	2.5E-4	2.0
SPTCB	N	3	N	0.022	3.6	0.0017	0.27
SPTCB	N	3	N	0.21	3.6	0.0019	0.24
SPTCL	N	1	N	0.0			
SPTCL	N	1	N	0.0			

Table M.3 continued

SPTCL	N	1	N	0.0		
SPTCL	N	1	N	0.0		
FIRC	N	6	N	5000.0	7000.0	9000.0
WIRC	N	6	N	0.0077	0.0115	0.0153
FAISFC	N	6	N	0.05	0.2	0.5
FAILC	N	6	N	0.05	0.2	0.5
FMTCC	N	6	N	1.1E-7	3.4E-7	1.0E-6
FMTCC	N	6	N	0.7E-7	2.0E-7	0.6E-6
FMTCC	N	6	N	1.3E-7	4.0E-7	1.2E-6
FMTCC	N	6	N	1.7E-7	5.1E-7	1.5E-6
FIRM	N	1	N	2.7E+4		
WIRM	N	6	N	0.024	0.036	0.048
FAIBM	N	6	N	0.8	0.9	0.95
FMTCM	N	6	N	1.1E-7	3.4E-7	1.0E-6
FMTCM	N	6	N	0.7E-7	2.0E-7	0.6E-6
FMTCM	N	6	N	1.3E-7	4.0E-7	1.2E-6
FMTCM	N	6	N	1.7E-7	5.1E-7	1.5E-6
FIRD	N	6	N	1800.0	7500.0	1.0E+4
WIRD	N	4	N	0.0007	0.0014	
FAISFD	N	6	N	0.25	0.33	0.40
FMTCD	N	6	N	1.1E-7	3.4E-7	1.0E-6
FMTCD	N	6	N	0.7E-7	2.0E-7	0.6E-6
FMTCD	N	6	N	1.3E-7	4.0E-7	1.2E-6
FMTCD	N	6	N	1.7E-7	5.1E-7	1.5E-6
EFR	N	6	N	0.2	0.5	0.8
SHLD	N	6	N	0.05	0.2	0.4
OF	N	6	N	0.5	0.9	1.0
OF	N	6	N	0.5	0.9	1.0
INOCC	N	6	N	0.6	0.9	1.0
INOCC	N	6	N	0.6	0.9	1.0
AIRIN	N	1	N	8400.0		
AIRIN	N	1	N	8400.0		
AFACT	N	4	N	0.5	1.0	
AVEGIN	N	1	N	4.53E+4		
AVEGIN	N	1	N	4.53E+4		
AFLOC	N	6	N	0.0	0.1	0.2
AFLOC	N	6	N	0.1	0.3	0.6
BFACT	N	4	N	0.5	1.0	
BVEGIN	N	1	N	7.4E+4		
BVEGIN	N	1	N	7.4E+4		
BFLOC	N	6	N	0.0	0.1	0.2
BFLOC	N	6	N	0.1	0.3	0.6
CARMIN	N	1	N	0.0		
CARMIN	N	1	N	0.0		
CFLOC	N	4	N	0.0	1.0	
CFLOC	N	4	N	0.0	1.0	
MOSMIN	N	1	N	6000.0		
MOSMIN	N	1	N	3.95E+4		
MFLOC	N	6	N	0.0	0.25	0.5
MFLOC	N	1	N	1.0		
DERMIN	N	1	N	6000.0		
DERMIN	N	1	N	3.95E+4		
DFLOC	N	1	N	1.0		

Table M.3 continued

DFLOC	N	1	N	1.0		
WATIN	N	1	N	0.6		
WATIN	N	1	N	0.6		
FISHIN	N	1	N	8000.0		
FISHIN	N	1	N	8000.0		
FFLOC	N	6	N	0.0	0.25	0.5
FFLOC	N	1	N	1.0		

Table M.4

LACNOR GLACIAL TILL TAILINGS COVER (OPTION 4)

```
LACNOR GLACIAL TILL TAILING COVER PROBABILISTIC INPUTS (OPTION 4)
Y Y
OPT4.PR
OPT4.PK
 262   0   0
0913566091 200
 3000.0   10.0
CODION N  1 N       0.0
CODNUC N  1 N       0.0
CODPH  N  1 N       0.0
CODERO N  1 N       0.0
CODDUS N  1 N       0.0
CODRAD N  1 N       0.0
CODWIN N  1 N       0.0
CODAIR N  1 N       0.0
CODSOL N  1 N       0.0
CODGS  N  1 N       0.0
CODVEG N  1 N       0.0
CODGW  N  1 N       0.0
CODWAT N  1 N       0.0
CODFIS N  1 N       0.0
CODWVG N  1 N       0.0
CODANI N  1 N       0.0
CODDOS N  1 N       0.0
PYRITI N  6 N     600.0       700.0       800.0
RHOTAL N  6 N     1.1E+6      1.3E+6      1.5E+6
FRACGP N  2 N      0.06       0.005        0.05        0.07
KPRIME N  4 N      0.01         0.1
SULPRD N  6 N     2.3E-6     3.15E-6     4.07E-6
O2CONC N  1 N      9.04
O2DIFF N  6 N      0.04       0.062        0.08
DUNSAT N  6 N      0.05        0.10        0.15
KSUBSO N  1 N      50.0
FACTCO N  6 N       0.4         0.5         0.6
NPRCP  N  2 V      0.51         0.1        0.25        0.85
DMIX   N  4 N       8.4        14.0
AVPRCP N  1 N      0.51
ATAIL  N  1 N    2.41E+5
XLIME  N  1 N     5.0E-4
PCURAN N  1 N       0.1
FURAN  N  4 N      0.90        0.94
FT230  N  6 N      0.65        0.80        0.95
FT232  N  6 N      0.55        0.65        0.75
FRAD   N  6 N      0.25        0.60        0.95
FLEAD  N  6 N      0.25        0.60        0.95
FRACU  N  4 N      0.30        0.90
KDUO2  N  3 N     2.0E-5        3.0      5.0E-6      5.0E-4
PCTHOR N  4 N      0.02        0.04
XRADI  N  6 N     6.0E-6      1.2E-5      1.8E-5
KSBAR  N  1 N    1.07E-4
```

Table M.4 continued

KFBAR	N	1	N	0.501			
KRAD	N	4	N	0.5	0.56		
KDRAD	N	3	N	4.5E-5	1.5	1.3E-6	1.52E-4
CLEADI	N	6	N	1.0	2.0	3.0	
KSLEAD	N	1	N	0.012			
KFLEAD	N	1	N	0.501			
KDLEAD	N	3	N	6.0E-5	1.5	2.E-5	1.E-4
XRATE	N	1	N	0.10			
DBOT	N	4	N	0.5	1.0		
WSTAIL	N	1	N	5.7E+5			
XRUNOF	N	6	N	0.55	0.60	0.65	
SLOPE	N	1	N	0.92			
THALF	N	4	N	15.0	25.0		
RRAIN	N	4	N	65.0	97.5		
RSOIL	N	4	N	1.0E-8	1.0E-7		
DM	N	6	N	0.0015	0.017	0.075	
STORM	N	4	N	36.0	48.0		
FLENGT	N	1	N	880.0			
MINVEG	N	1	N	0.9			
BEDTRP	N	1	N	100.0			
SUSTRP	N	6	N	85.0	98.0	100.0	
WYEAR	N	4	V	1.0	20.9999999		
EMANAT	N	6	N	0.05	0.20	0.50	
WTSFLX	N	3	N	0.02	2.0	0.002	0.2
MPCH2O	N	1	N	28.0			
NSUBW	N	1	N	5.0			
CAFR	N	1	N	0.99			
SILT	N	6	N	30.0	45.0	60.0	
FPREC	N	2	V	149.0	17.0	115.0	183.0
CAFD	N	1	N	1.0			
HSRC	N	4	N	1.0	3.0		
DEPVEL	N	4	N	0.003	0.03		
DSOIL	N	1	N	0.05			
DSOIL	N	1	N	0.15			
FWAT	N	6	N	0.02	0.16	0.48	
RHOS	N	3	N	129.0	1.3	20.0	450.0
RHOS	N	3	N	1342.0	1.1	1000.0	1800.0
SOILKD	N	5	N	1.3E-04	790.0		
SOILKD	N	5	N	0.0033	150.0		
SOILKD	N	5	N	0.18	63.0		
SOILKD	N	5	N	0.0051	950.0		
SOILKD	N	5	N	1.3E-04	790.0		
SOILKD	N	5	N	0.0033	150.0		
SOILKD	N	5	N	0.18	63.0		
SOILKD	N	5	N	0.0051	950.0		
WC	N	4	N	0.75	1.4		
WC	N	3	N	0.13	1.4	0.05	0.36
EMFRAC	N	1	N	0.2			
XRGWA1	N	6	N	0.1	2.0	4.0	
XRGWA2	N	6	N	5.0	7.0	9.0	
XRGWA3	N	1	N	0.0			
XRGWA4	N	1	N	0.0			
XRGWA5	N	1	N	0.0			

Table M.4 continued

AXGWA1	N	1	N	2005.0			
AXGWA2	N	1	N	3590.0			
AXGWA3	N	1	N	0.0			
AXGWA4	N	1	N	0.0			
AXGWA5	N	1	N	0.0			
POGWA1	N	4	N	0.33	0.40		
POGWA2	N	4	N	0.33	0.40		
POGWA3	N	1	N	0.0			
POGWA4	N	1	N	0.0			
POGWA5	N	1	N	0.0			
DCGWA1	N	3	N	0.012	1.50	0.0036	0.04
DCGWA2	N	3	N	0.05	1.50	0.015	0.17
DCGWA3	N	3	N	0.06	1.50	0.018	0.2
DCGWA4	N	3	N	0.045	1.50	0.013	0.15
SDGWA1	N	2	N	2650.0	100.0	2200.0	2980.0
SDGWA2	N	2	N	2650.0	100.0	2200.0	2980.0
SDGWA3	N	1	N	0.0			
SDGWA4	N	1	N	0.0			
SDGWA5	N	1	N	0.0			
HCGWA1	N	3	N	6.9	2.4	1.2	40.0
HCGWA2	N	3	N	6.9	2.4	1.2	40.0
HCGWA3	N	1	N	0.0			
HCGWA4	N	1	N	0.0			
HCGWA5	N	1	N	0.0			
HGGWA1	N	2	N	0.051	0.01	0.041	0.061
HGGWA2	N	2	N	0.176	0.03	0.146	0.206
HGGWA3	N	1	N	0.0			
HGGWA4	N	1	N	0.0			
HGGWA5	N	1	N	0.0			
ACTCO	N	6	N	0.6	0.8	0.9	
WATCAB	N	1	N	0.19			
WTSO4B	N	1	N	0.14			
WATNAB	N	1	N	0.34			
WATKB	N	1	N	0.02			
WATMGB	N	1	N	0.06			
WATCLB	N	1	N	0.38			
WSIGS1	N	6	N	30.0	70.0	170.0	
WSIGS2	N	6	N	125.0	255.0	635.0	
WSIGS3	N	6	N	500.0	1000.0	2035.0	
WSIGS4	N	6	N	140.0	300.0	740.0	
WSIGS5	N	6	N	40.0	95.0	225.0	
WTRHOS	N	1	N	1.955E+6			
WATEPS	N	6	N	0.83	0.90	0.97	
WTMIXD	N	1	N	0.05			
WKDU	N	3	N	0.0045	2.2	4.0E-4	0.048
WKDPB	N	3	N	0.015	2.5	0.001	0.23
WKDRA	N	3	N	0.0065	2.5	4.0E-4	0.1
KDPRIM	N	3	N	0.02	2.5	0.002	0.3
BURYF	N	4	N	0.76	0.86		
CURRNT	N	4	N	3.15E+4	3.15E+5		
DIFFC	N	1	N	0.02			
FCONC	N	6	N	0.0	0.02	0.1	
FCONC	N	6	N	0.0	0.005	0.02	

Table M.4 continued

FCONC	N	6	N	0.0	0.02	0.1	
FCONC	N	6	N	0.0	0.02	0.1	
BIOACF	N	3	N	1.55E-6	6.1	1.0E-8	5.8E-5
BIOACF	N	3	N	1.18E-5	2.6	1.1E-6	1.1E-4
BIOACF	N	3	N	1.74E-5	3.25	1.7E-6	5.7E-4
BIOACF	N	3	N	1.31E-5	3.3	1.2E-6	6.0E-4
WATVTC	N	3	N	1.5E-5	5.5	1.0E-6	7.0E-4
WATVTC	N	3	N	1.1E-5	6.8	1.0E-6	1.6E-4
WATVTC	N	3	N	1.3E-4	2.0	4.0E-5	4.3E-4
WATVTC	N	3	N	4.5E-5	2.9	1.0E-5	3.3E-4
FDEPSF	N	4	N	0.1	0.3		
FDEPSF	N	4	N	0.1	0.3		
FDEPSF	N	2	N	0.47	0.3	0.01	1.0
FDEPSF	N	2	N	0.47	0.3	0.01	1.0
FDEPSF	N	4	N	0.8	1.0		
FDEPED	N	4	N	0.8	1.0		
FDEPED	N	4	N	0.05	0.15		
FDEPED	N	4	N	0.8	1.0		
FDEPED	N	4	N	0.8	1.0		
FDEPED	N	4	N	0.8	1.0		
VEGLAM	N	4	N	2.9E-7	1.2E-6		
VEGLAM	N	4	N	2.9E-7	1.2E-6		
VEGLAM	N	4	N	2.9E-7	1.2E-6		
VEGLAM	N	4	N	2.9E-7	1.2E-6		
VEGLAM	N	4	N	1.5E-9	4.4E-9		
DUREXP	N	6	N	2.6E+6	5.2E+6	7.8E+6	
DUREXP	N	6	N	2.6E+6	5.2E+6	7.8E+6	
DUREXP	N	4	N	1.3E+6	3.9E+6		
DUREXP	N	4	N	1.3E+6	3.9E+6		
DUREXP	N	1	N	1.0E+10			
YDEN	N	4	N	1000.0	3000.0		
YDEN	N	4	N	1000.0	3000.0		
YDEN	N	4	N	500.0	1000.0		
YDEN	N	4	N	500.0	1000.0		
YDEN	N	4	N	400.0	600.0		
SPTCAV	N	3	N	6.1E-4	8.9	7.7E-6	0.007
SPTCAV	N	3	N	0.0042	9.0	5.2E-5	0.34
SPTCAV	N	3	N	0.0040	9.0	4.9E-5	0.32
SPTCAV	N	3	N	0.0085	10.0	8.0E-5	0.89
SPTCBV	N	3	N	3.2E-4	3.9	2.1E-5	0.0049
SPTCBV	N	3	N	0.0042	4.0	2.6E-4	0.067
SPTCBV	N	3	N	0.0040	4.0	2.5E-4	0.064
SPTCBV	N	3	N	0.0027	4.5	1.3E-4	0.066
SPTCSF	N	3	N	0.0066	8.9	8.3E-5	0.52
SPTCSF	N	3	N	0.022	9.5	2.5E-4	2.0
SPTCSF	N	3	N	0.022	3.6	0.0017	0.27
SPTCSF	N	3	N	0.21	3.6	0.0019	0.24
SPTCB	N	3	N	0.0066	8.9	8.3E-5	0.52
SPTCB	N	3	N	0.022	9.5	2.5E-4	2.0
SPTCB	N	3	N	0.022	3.6	0.0017	0.27
SPTCB	N	3	N	0.21	3.6	0.0019	0.24
SPTCL	N	1	N	0.0			
SPTCL	N	1	N	0.0			

Table M.4 continued

```
SPTCL  N 1 N      0.0
SPTCL  N 1 N      0.0
FIRC   N 6 N   5000.0      7000.0     9000.0
WIRC   N 6 N   0.0077      0.0115     0.0153
FAISFC N 6 N     0.05         0.2        0.5
FAILC  N 6 N     0.05         0.2        0.5
FMTCC  N 6 N   1.1E-7      3.4E-7     1.0E-6
FMTCC  N 6 N   0.7E-7      2.0E-7     0.6E-6
FMTCC  N 6 N   1.3E-7      4.0E-7     1.2E-6
FMTCC  N 6 N   1.7E-7      5.1E-7     1.5E-6
FIRM   N 1 N   2.7E+4
WIRM   N 6 N    0.024       0.036      0.048
FAIBM  N 6 N      0.8         0.9       0.95
FMTCM  N 6 N   1.1E-7      3.4E-7     1.0E-6
FMTCM  N 6 N   0.7E-7      2.0E-7     0.6E-6
FMTCM  N 6 N   1.3E-7      4.0E-7     1.2E-6
FMTCM  N 6 N   1.7E-7      5.1E-7     1.5E-6
FIRD   N 6 N   1800.0      7500.0     1.0E+4
WIRD   N 4 N   0.0007      0.0014
FAISFD N 6 N     0.25        0.33       0.40
FMTCD  N 6 N   1.1E-7      3.4E-7     1.0E-6
FMTCD  N 6 N   0.7E-7      2.0E-7     0.6E-6
FMTCD  N 6 N   1.3E-7      4.0E-7     1.2E-6
FMTCD  N 6 N   1.7E-7      5.1E-7     1.5E-6
EFR    N 6 N      0.2         0.5        0.8
SHLD   N 6 N     0.05         0.2        0.4
OF     N 6 N      0.5         0.9        1.0
OF     N 6 N      0.5         0.9        1.0
INOCC  N 6 N      0.6         0.9        1.0
INOCC  N 6 N      0.6         0.9        1.0
AIRIN  N 1 N   8400.0
AIRIN  N 1 N   8400.0
AFACT  N 4 N      0.5         1.0
AVEGIN N 1 N  4.53E+4
AVEGIN N 1 N  4.53E+4
AFLOC  N 6 N      0.0         0.1        0.2
AFLOC  N 6 N      0.1         0.3        0.6
BFACT  N 4 N      0.5         1.0
BVEGIN N 1 N   7.4E+4
BVEGIN N 1 N   7.4E+4
BFLOC  N 6 N      0.0         0.1        0.2
BFLOC  N 6 N      0.1         0.3        0.6
CARMIN N 1 N      0.0
CARMIN N 1 N      0.0
CFLOC  N 4 N      0.0         1.0
CFLOC  N 4 N      0.0         1.0
MOSMIN N 1 N   6000.0
MOSMIN N 1 N  3.95E+4
MFLOC  N 6 N      0.0        0.25        0.5
MFLOC  N 1 N      1.0
DERMIN N 1 N   6000.0
DERMIN N 1 N  3.95E+4
DFLOC  N 1 N      1.0
```

Table M.4 continued

```
DFLOC  N  1 N      1.0
WATIN  N  1 N      0.6
WATIN  N  1 N      0.6
FISHIN N  1 N   8000.0
FISHIN N  1 N   8000.0
FFLOC  N  6 N      0.0      0.25      0.5
FFLOC  N  1 N      1.0
```

Table M.5

LACNOR WATER TABLE ELEVATION (OPTION 5)

```
LACNOR WATER TABLE ELEVATION PROBABILISTIC INPUTS (OPTION 5)
Y Y
OPT5.PR
OPT5.PK
 262   0   0
0913566091 200
 3000.0   10.0
CODION N  1 N       0.0
CODNUC N  1 N       0.0
CODPH  N  1 N       0.0
CODERO N  1 N       0.0
CODDUS N  1 N       0.0
CODRAD N  1 N       0.0
CODWIN N  1 N       0.0
CODAIR N  1 N       0.0
CODSOL N  1 N       0.0
CODGS  N  1 N       0.0
CODVEG N  1 N       0.0
CODGW  N  1 N       0.0
CODWAT N  1 N       0.0
CODFIS N  1 N       0.0
CODWVG N  1 N       0.0
CODANI N  1 N       0.0
CODDOS N  1 N       0.0
PYRITI N  6 N     600.0      700.0      800.0
RHOTAL N  6 N    1.1E+6     1.3E+6     1.5E+6
FRACGP N  2 N      0.06      0.005       0.05        0.07
KPRIME N  4 N      0.01        0.1
SULPRD N  6 N    3.0E-6     4.1E-6     5.3E-6
O2CONC N  1 N      9.04
O2DIFF N  6 N      0.04      0.062       0.08
DUNSAT N  6 N      0.05       0.10       0.15
KSUBSO N  1 N      50.0
FACTCO N  6 N       0.4        0.5        0.6
NPRCP  N  2 V      0.51        0.1       0.25        0.85
DMIX   N  4 N       8.4       14.0
AVPRCP N  1 N      0.51
ATAIL  N  1 N   2.41E+5
XLIME  N  1 N    0.0005
PCURAN N  1 N       0.1
FURAN  N  4 N      0.90       0.94
FT230  N  6 N      0.65       0.80       0.95
FT232  N  6 N      0.55       0.65       0.75
FRAD   N  6 N      0.25       0.60       0.95
FLEAD  N  6 N      0.25       0.60       0.95
FRACU  N  4 N      0.30       0.90
KDUO2  N  3 N    2.0E-5        3.0     5.0E-6      5.0E-4
PCTHOR N  4 N      0.02       0.04
XRADI  N  6 N    6.0E-6     1.2E-5     1.8E-5
KSBAR  N  1 N   1.07E-4
```

Table M.5 continued

KFBAR	N	1	N	0.501			
KRAD	N	4	N	0.5	0.56		
KDRAD	N	3	N	4.5E-5	1.5	1.3E-6	1.52E-4
CLEADI	N	6	N	1.0	2.0	3.0	
KSLEAD	N	1	N	0.012			
KFLEAD	N	1	N	0.501			
KDLEAD	N	3	N	6.0E-5	1.5	2.0E-5	1.0E-4
XRATE	N	1	N	0.10			
DBOT	N	4	N	0.5	1.0		
WSTAIL	N	1	N	5.7E+5			
XRUNOF	N	6	N	0.80	0.85	0.90	
SLOPE	N	1	N	0.92			
THALF	N	4	N	15.0	25.0		
RRAIN	N	4	N	65.0	97.5		
RSOIL	N	4	N	1.0E-8	1.0E-7		
DM	N	6	N	0.0015	0.017	0.075	
STORM	N	4	N	36.0	48.0		
FLENGT	N	1	N	880.0			
MINVEG	N	1	N	0.0			
BEDTRP	N	1	N	100.0			
SUSTRP	N	6	N	85.0	98.0	100.0	
WYEAR	N	4	V	1.0	20.9999999		
EMANAT	N	6	N	0.05	0.20	0.50	
WTSFLX	N	3	N	0.02	2.0	0.002	0.2
MPCH2O	N	1	N	28.0			
NSUBW	N	1	N	5.0			
CAFR	N	1	N	0.50			
SILT	N	6	N	30.0	45.0	60.0	
FPREC	N	2	V	149.0	17.0	115.0	183.0
CAFD	N	1	N	0.75			
HSRC	N	4	N	1.0	3.0		
DEPVEL	N	4	N	0.003	0.03		
DSOIL	N	1	N	0.05			
DSOIL	N	1	N	0.15			
FWAT	N	6	N	0.02	0.16	0.48	
RHOS	N	3	N	129.0	1.3	20.0	450.0
RHOS	N	3	N	1342.0	1.1	1000.0	1800.0
SOILKD	N	5	N	1.3E-04	790.0		
SOILKD	N	5	N	0.0033	150.0		
SOILKD	N	5	N	0.18	63.0		
SOILKD	N	5	N	0.0051	950.0		
SOILKD	N	5	N	1.3E-04	790.0		
SOILKD	N	5	N	0.0033	150.0		
SOILKD	N	5	N	0.18	63.0		
SOILKD	N	5	N	0.0051	950.0		
WC	N	4	N	0.75	1.4		
WC	N	3	N	0.13	1.4	0.05	0.36
EMFRAC	N	1	N	0.2			
XRGWA1	N	6	N	0.1	2.0	4.0	
XRGWA2	N	6	N	5.0	7.0	9.0	
XRGWA3	N	1	N	0.0			
XRGWA4	N	1	N	0.0			
XRGWA5	N	1	N	0.0			

Table M.5 continued

AXGWA1	N	1	N	2005.0			
AXGWA2	N	1	N	3590.0			
AXGWA3	N	1	N	0.0			
AXGWA4	N	1	N	0.0			
AXGWA5	N	1	N	0.0			
POGWA1	N	4	N	0.33	0.40		
POGWA2	N	4	N	0.33	0.40		
POGWA3	N	1	N	0.0			
POGWA4	N	1	N	0.0			
POGWA5	N	1	N	0.0			
DCGWA1	N	3	N	0.012	1.50	0.0036	0.04
DCGWA2	N	3	N	0.05	1.50	0.015	0.17
DCGWA3	N	3	N	0.06	1.50	0.018	0.2
DCGWA4	N	3	N	0.045	1.50	0.013	0.15
SDGWA1	N	2	N	2650.0	100.0	2200.0	2980.0
SDGWA2	N	2	N	2650.0	100.0	2200.0	2980.0
SDGWA3	N	1	N	0.0			
SDGWA4	N	1	N	0.0			
SDGWA5	N	1	N	0.0			
HCGWA1	N	3	N	6.9	2.4	1.2	40.0
HCGWA2	N	3	N	6.9	2.4	1.2	40.0
HCGWA3	N	1	N	0.0			
HCGWA4	N	1	N	0.0			
HCGWA5	N	1	N	0.0			
HGGWA1	N	2	N	0.051	0.01	0.041	0.061
HGGWA2	N	2	N	0.176	0.03	0.146	0.206
HGGWA3	N	1	N	0.0			
HGGWA4	N	1	N	0.0			
HGGWA5	N	1	N	0.0			
ACTCO	N	6	N	0.6	0.8	0.9	
WATCAB	N	1	N	0.19			
WTSO4B	N	1	N	0.14			
WATNAB	N	1	N	0.34			
WATKB	N	1	N	0.02			
WATMGB	N	1	N	0.06			
WATCLB	N	1	N	0.38			
WSIGS1	N	6	N	30.0	70.0	170.0	
WSIGS2	N	6	N	125.0	255.0	635.0	
WSIGS3	N	6	N	500.0	1000.0	2035.0	
WSIGS4	N	6	N	140.0	300.0	740.0	
WSIGS5	N	6	N	40.0	95.0	225.0	
WTRHOS	N	1	N	1.955E+6			
WATEPS	N	6	N	0.83	0.90	0.97	
WTMIXD	N	1	N	0.05			
WKDU	N	3	N	0.0045	2.2	4.0E-4	0.048
WKDPB	N	3	N	0.015	2.5	0.001	0.23
WKDRA	N	3	N	0.0065	2.5	4.0E-4	0.1
KDPRIM	N	3	N	0.02	2.5	0.002	0.3
BURYF	N	4	N	0.76	0.86		
CURRNT	N	4	N	3.15E+4	3.15E+5		
DIFFC	N	1	N	0.02			
FCONC	N	6	N	0.0	0.02	0.1	
FCONC	N	6	N	0.0	0.005	0.02	

Table M.5 continued

FCONC	N	6	N	0.0	0.02	0.1	
FCONC	N	6	N	0.0	0.02	0.1	
BIOACF	N	3	N	1.55E-6	6.1	1.0E-8	5.8E-5
BIOACF	N	3	N	1.18E-5	2.6	1.1E-6	1.1E-4
BIOACF	N	3	N	1.74E-5	3.25	1.7E-6	5.7E-4
BIOACF	N	3	N	1.31E-5	3.3	1.2E-6	6.0E-4
WATVTC	N	3	N	1.5E-5	5.5	1.0E-6	7.0E-4
WATVTC	N	3	N	1.1E-5	6.8	1.0E-6	1.6E-4
WATVTC	N	3	N	1.3E-4	2.0	4.0E-5	4.3E-4
WATVTC	N	3	N	4.5E-5	2.9	1.0E-5	3.3E-4
FDEPSF	N	4	N	0.1	0.3		
FDEPSF	N	4	N	0.1	0.3		
FDEPSF	N	2	N	0.47	0.3	0.01	1.0
FDEPSF	N	2	N	0.47	0.3	0.01	1.0
FDEPSF	N	4	N	0.8	1.0		
FDEPED	N	4	N	0.8	1.0		
FDEPED	N	4	N	0.05	0.15		
FDEPED	N	4	N	0.8	1.0		
FDEPED	N	4	N	0.8	1.0		
FDEPED	N	4	N	0.8	1.0		
VEGLAM	N	4	N	2.9E-7	1.2E-6		
VEGLAM	N	4	N	2.9E-7	1.2E-6		
VEGLAM	N	4	N	2.9E-7	1.2E-6		
VEGLAM	N	4	N	2.9E-7	1.2E-6		
VEGLAM	N	4	N	1.5E-9	4.4E-9		
DUREXP	N	6	N	2.6E+6	5.2E+6	7.8E+6	
DUREXP	N	6	N	2.6E+6	5.2E+6	7.8E+6	
DUREXP	N	4	N	1.3E+6	3.9E+6		
DUREXP	N	4	N	1.3E+6	3.9E+6		
DUREXP	N	1	N	1.0E+10			
YDEN	N	4	N	1000.0	3000.0		
YDEN	N	4	N	1000.0	3000.0		
YDEN	N	4	N	500.0	1000.0		
YDEN	N	4	N	500.0	1000.0		
YDEN	N	4	N	400.0	600.0		
SPTCAV	N	3	N	6.1E-4	8.9	7.7E-6	0.007
SPTCAV	N	3	N	0.0042	9.0	5.2E-5	0.34
SPTCAV	N	3	N	0.0040	9.0	4.9E-5	0.32
SPTCAV	N	3	N	0.0085	10.0	8.0E-5	0.89
SPTCBV	N	3	N	3.2E-4	3.9	2.1E-5	0.0049
SPTCBV	N	3	N	0.0042	4.0	2.6E-4	0.067
SPTCBV	N	3	N	0.0040	4.0	2.5E-4	0.064
SPTCBV	N	3	N	0.0027	4.5	1.3E-4	0.066
SPTCSF	N	3	N	0.0066	8.9	8.3E-5	0.52
SPTCSF	N	3	N	0.022	9.5	2.5E-4	2.0
SPTCSF	N	3	N	0.022	3.6	0.0017	0.27
SPTCSF	N	3	N	0.21	3.6	0.0019	0.24
SPTCB	N	3	N	0.0066	8.9	8.3E-5	0.52
SPTCB	N	3	N	0.022	9.5	2.5E-4	2.0
SPTCB	N	3	N	0.022	3.6	0.0017	0.27
SPTCB	N	3	N	0.21	3.6	0.0019	0.24
SPTCL	N	1	N	0.0			
SPTCL	N	1	N	0.0			

Table M.5 continued

SPTCL	N	1	N	0.0		
SPTCL	N	1	N	0.0		
FIRC	N	6	N	5000.0	7000.0	9000.0
WIRC	N	6	N	0.0077	0.0115	0.0153
FAISFC	N	6	N	0.05	0.2	0.5
FAILC	N	6	N	0.05	0.2	0.5
FMTCC	N	6	N	1.1E-7	3.4E-7	1.0E-6
FMTCC	N	6	N	0.7E-7	2.0E-7	0.6E-6
FMTCC	N	6	N	1.3E-7	4.0E-7	1.2E-6
FMTCC	N	6	N	1.7E-7	5.1E-7	1.5E-6
FIRM	N	1	N	2.7E+4		
WIRM	N	6	N	0.024	0.036	0.048
FAIBM	N	6	N	0.8	0.9	0.95
FMTCM	N	6	N	1.1E-7	3.4E-7	1.0E-6
FMTCM	N	6	N	0.7E-7	2.0E-7	0.6E-6
FMTCM	N	6	N	1.3E-7	4.0E-7	1.2E-6
FMTCM	N	6	N	1.7E-7	5.1E-7	1.5E-6
FIRD	N	6	N	1800.0	7500.0	1.0E+4
WIRD	N	4	N	0.0007	0.0014	
FAISFD	N	6	N	0.25	0.33	0.40
FMTCD	N	6	N	1.1E-7	3.4E-7	1.0E-6
FMTCD	N	6	N	0.7E-7	2.0E-7	0.6E-6
FMTCD	N	6	N	1.3E-7	4.0E-7	1.2E-6
FMTCD	N	6	N	1.7E-7	5.1E-7	1.5E-6
EFR	N	6	N	0.2	0.5	0.8
SHLD	N	6	N	0.05	0.2	0.4
OF	N	6	N	0.5	0.9	1.0
OF	N	6	N	0.5	0.9	1.0
INOCC	N	6	N	0.6	0.9	1.0
INOCC	N	6	N	0.6	0.9	1.0
AIRIN	N	1	N	8400.0		
AIRIN	N	1	N	8400.0		
AFACT	N	4	N	0.5	1.0	
AVEGIN	N	1	N	4.53E+4		
AVEGIN	N	1	N	4.53E+4		
AFLOC	N	6	N	0.0	0.1	0.2
AFLOC	N	6	N	0.1	0.3	0.6
BFACT	N	4	N	0.5	1.0	
BVEGIN	N	1	N	7.4E+4		
BVEGIN	N	1	N	7.4E+4		
BFLOC	N	6	N	0.0	0.1	0.2
BFLOC	N	6	N	0.1	0.3	0.6
CARMIN	N	1	N	0.0		
CARMIN	N	1	N	0.0		
CFLOC	N	4	N	0.0	1.0	
CFLOC	N	4	N	0.0	1.0	
MOSMIN	N	1	N	6000.0		
MOSMIN	N	1	N	3.95E+4		
MFLOC	N	6	N	0.0	0.25	0.5
MFLOC	N	1	N	1.0		
DERMIN	N	1	N	6000.0		
DERMIN	N	1	N	3.95E+4		
DFLOC	N	1	N	1.0		

Table M.5 continued

```
DFLOC  N  1 N      1.0
WATIN  N  1 N      0.6
WATIN  N  1 N      0.6
FISHIN N  1 N   8000.0
FISHIN N  1 N   8000.0
FFLOC  N  6 N      0.0        0.25        0.5
FFLOC  N  1 N      1.0
```

Volume

3

NATIONAL URANIUM TAILINGS PROGRAM

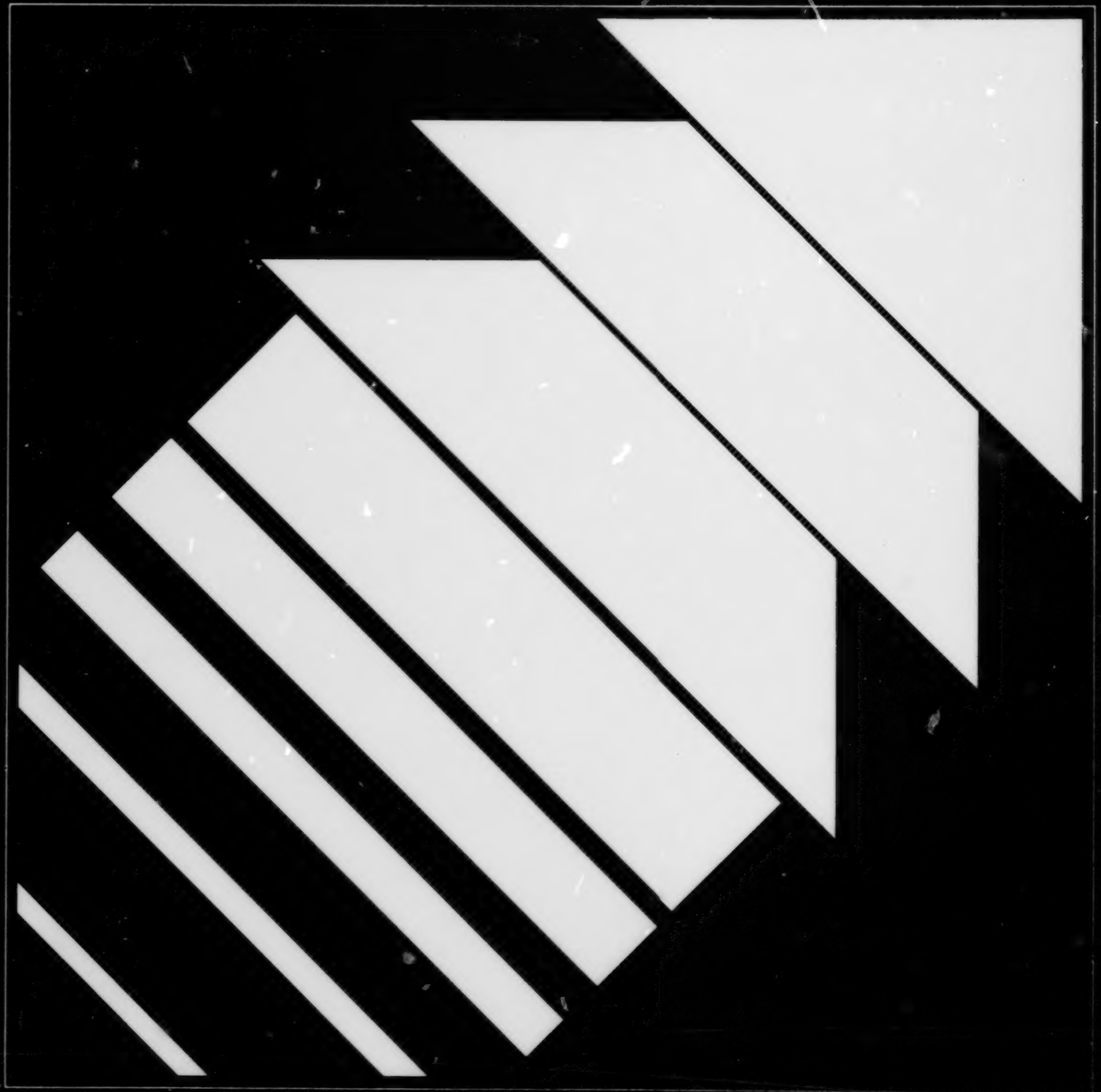

Energy, Mines and Resources Canada
Énergie, Mines et Ressources Canada

Canada

URANIUM TAILINGS ASSESSMENT PROGRAM (UTAP.3)

ADDENDUM TO VOLUME 2 - SYSTEM DESCRIPTION AND CONTROL MODULE DOCUMENTATION

A Research Report prepared under
DSS Contract No. 23317-6-1728/01-SQ

for

The National Uranium Tailings Program
Canada Centre for Mineral and Energy Technology
Energy, Mines and Resources Canada
555 Booth Street
Ottawa, Ontario
K1A 0G1

by

SENES Consultants Limited
499 McNicoll Avenue
Willowdale, Ontario
M2H 2C9

147 pp

March 1987

MICROMEDIA

ABSTRACT

This report represents part of the ongoing efforts of the National Uranium Tailings Program (NUTP) to develop the capability to predict the long-term effects of Canadian Uranium mill tailings. In three previous studies a comprehensive Uranium Tailings Assessment Program (UTAP) was developed. The UTAP program incorporates a Monte Carlo procedure which permits the user to enter input parameters as probability density functions rather than as single numbers and to calculate frequency distributions for output variables.

To date the approach has been to apply UTAP, in a generic fashion, to a hypothetical reference site. The focus of the present study has been to modify UTAP, where appropriate, for application to a real site (Lacnor) and to the extent practicable to calibrate the system model using site-specific measurements. Since the primary product of the NUTP modelling studies is the generic UTAP program, the UTAP Program has been throughly reviewed and modified along with the supporting documentation where appropriate.

This project report is an addendum to Volume 2 of the Phase III report which provides an overview of the system model structure and documentation for the "control module" aspects of UTAP. The "control modules" provide the infrastructure for probabilistic analyses; including sampling input parameters and many input, output and bookkeeping functions. This addendum encompases changes made to the control modules of UTAP with respect to this phase of the study and should be read in conjunction with the original Volume 2 report for a complete understanding.

NOTICE

This report was prepared by SENES Consultants Limited (SENES) under contract to the National Uranium Tailings Program (NUTP). Neither NUTP nor SENES makes any warranty, expressed or implied, or assumes any liability with respect to any damage or loss incurred as a result of the use made of the information contained in this publication.

TABLE OF CONTENTS

	Page
Abstract	i
Notice	i
1.0 INTRODUCTION	1-1
1.1 Background	1-1
1.2 Scope of Volume 2	1-2
1.3 Overview of Addendum to Volume 2	1-3
2.0 CONTROL MODULE OBJECTIVES AND CONCEPTUAL SPECIFICATIONS	2-1
2.1 Control Module Features	2-1
2.2 Input Modules	2-1
2.3 Random Sampling Modules	2-1
2.4 Output Selection Modules	2-1
2.4.1 Compute Summary Statistics	2-1
2.4.2 Write Detailed Results to Output File	2-1
2.5 Stepping Through Time	2-2
2.6 Confidence Bands	2-2
3.0 CONTROL MODULE DESCRIPTIONS	3-1
3.1 Main Program (EXEC)	3-1
3.2 Input Modules	3-1
3.2.1 First Input Routine (SUBROUTINE INPUT1)	3-1
3.2.2 Second Input Routine (SUBROUTINE INPUT2)	3-1
3.2.3 Generation of Error and Warning Messages (SUBROUTINE ERROR)	3-2
3.3 Sampling Routines	3-3
3.3.1 Objective	3-3
3.3.2 General Concepts	3-3
3.3.3 The Random Number Generator (FUNCTION RANDOM)	3-3

Table of Contents (continued)

Page

3.3.4 Creation of a Cumulative Distribution Function (SUBROUTINE CREATE) 3-3

3.3.5 Choice of Sampling Routine (SUBROUTINE CHOOSE) 3-3

3.3.6 Normal Distribution (SUBROUTINE NORMAL) 3-3

3.3.7 Lognormal Distribution (SUBROUTINE LNORM) 3-5

3.3.8 Uniform Distribution (SUBROUTINE UNIFOR) 3-5

3.3.9 Loguniform Distribution (SUBROUTINE LOGUNI) 3-5

3.3.10 Triangular Distribution (SUBROUTINE TRIANG) 3-5

3.3.11 Weibull Distribution (SUBROUTINE WEIBUL) 3-5

3.3.12 Arbitrary Distribution (SUBROUTINE ARB) 3-5

3.3.13 Correlated Parameters (SUBROUTINE CORREL) 3-6

3.3.14 Beta Distribution (SUBROUTINE BETA) 3-6

3.4 Output Selection Routines 3-8

3.4.1 Saving Time-Variant Sampled Parameters (SUBROUTINE TIMSEL) 3-8

3.4.2 Selection of Output Time Steps (SUBROUTINE SELECT) 3-8

3.4.3 Sorting of Output Variables (SUBROUTINE SORT) 3-8

3.4.4 Saving Output Variables (SUBROUTINE SEND) 3-9

Table of Contents (continued)

Page

3.4.5 Saving Non-Time-Variant Sampled Parameters (SUBROUTINE SAVEIN) 3-9
3.5 Statistics Routines 3-9
3.5.1 Computing Summary Statistics (SUBROUTINE STATS) 3-9
3.5.2 Computing Moment Values (SUBROUTINES MOMENT and GMOMEN) 3-10
3.6 Output Routines 3-10
3.6.1 Output of Detailed Results (SUBROUTINE WRITE) 3-10
3.6.2 Creation of Output Labels (SUBROUTINE NAMOUT) 3-10
3.6.3 Output of Summary Statistics (SUBROUTINE OUTPUT) 3-10
3.6.4 Dating of Output Files (SUBROUTINE FILER) 3-11

4.0 CONFIDENCE BANDS PROGRAM DESCRIPTION 4-1
4.1 Introduction and Background 4-1
4.2 The General Nature of the Confidence Bands Programs 4-2
4.2.1 The Binning Program (BIN) 4-2
4.2.2 The Confidence Band Program (CBAND) 4-3
4.3 Examples 4-5

REFERENCES
APPENDIX B Control Modules Code Listing and Variable Dictionary
APPENDIX F Development and Implementation of a Procedure for Establishing Confidence Regions for Output from Monte Carlo Calculations
APPENDIX G Confidence Bands Programs Code Listing and Variable Dictionary

LIST OF FIGURES

Follows Page

1.2 Control Module Structure 1-2

1.3 Subroutine COMEX and the Component Modules 1-2

3.5 Forms of the Beta Distribution Probability Density Function 3-6

3.6 Plot of Frequency Histogram (500 Samples) and Probability Distribution for Normal Distribution 3-5

3.15 Plot of Frequency Histogram (500 Samples) and Probability Distribution for Beta Distribution 3-8

4.1 Relation of Confidence Band Programs to UTAP 4-2

4.2 Binning Program (BIN) Structure 4-2

4.3 Confidence Bands Program (CBAND) Structure 4-3

4.4 Plots of 95% Confidence Bands for a Normal Distribution (500 Trials) 4-5

4.5 Plots of 95% Confidence Bands for a Log-Transformed Lognormal Distribution (500 Trials) 4-5

4.6 Plots of 95% Confidence Bands for the Logarithm of Radium in Fish at 100 Years (200 Trials) 4-5

LIST OF TABLES

Follows Page

3.2 Sample of First Input File 3-1

3.6 Sample of Second Input File 3-1

3.7 Output Parameters 3-2

1.0 INTRODUCTION

1.1 Background

In 1982 Energy, Mines and Resources Canada established the National Uranium Tailings Program (NUTP) to pull together previous work on Canadian uranium mill tailings, to fund additional work where significant information on gaps were found and to develop the capability to predict the long-term effects of tailings with a known degree of confidence while incorporating variability and uncertainty in the input data. Such evaluations require the use of mathematical models to simulate the behaviour of the real system. Results of the previous phases of work have demonstrated that a probabilistic approach provides the framework necessary for incorporating uncertainty into a simulation (SENES, 1984; 1985; 1986).

An earlier study (Phase I) funded by the NUTP demonstrated how probabilistic techniques could be used to take account of the variability and uncertainty in model input parameters in such a simulation analysis (SENES, 1984). Subsequently, the NUTP sponsored a followup study (Phase II, SENES, 1985) to extend and refine the probabilistic tools developed in the Phase I study and to investigate various issues of technical interest involved in carrying out and interpreting a probabilistic analysis.

The Phase III study extended the capabilities of the Phase II system model and then applied the upgraded (Phase III) system model to a hypothetical reference site. The emphasis of the Phase IV work is to demonstrate the use of the Uranium Tailings Assessment Program (UTAP) in assessing a real (vs. hypothetical) uranium tailings site. The Lacnor tailings area in Elliot Lake, Ontario, for which the NUTP has recently carried out an extensive field study (Golder *et al.*, 1986), was chosen for this purpose. The primary objective is to learn what is entailed in such an application, e.g. what are the data requirements, what level of modelling detail is appropriate, and what are the difficulties and limitations of such an application.

1.2 Scope of Volume 2

Three versions of UTAP are the products of the Phase III and Phase IV studies. These are:

. UTAP.1	the original Phase III code, "UTAP", now archived and inactive
. UTAP.2	the original Phase III code as revised based on a comparison of UTAP with AECL's SYVAC code (WNRE, 1987)
. UTAP.3	an updated generic code which reflects the revisions made on the basis of the UTAP/SYVAC intercomparison as well as revisions of a generic nature identified from the Lacnor study (Phase IV)

UTAP is composed of a number of modules. These may be classified as either component or control modules. The control modules are composed of a number of subprograms that provide the infrastructure for probabilistic analysis of the component modules. Their functions include sampling of input parameters, statistics, and many other input, output, and bookkeeping functions. The control modules (UTAP.3) and their functions are illustrated in flowchart form in Figure 1.2. The computer subprograms directly concerned with the simulation of a uranium tailings physical system (i.e. the computer implementation of the mathematical models representing the uranium tailings pile and surrounding environment) are referred to as the component modules (or models).

Figure 1.3 illustrates, in flowchart form, the functions of the component modules in UTAP.3. The integrated control and component modules are known as the system model.

The Phase III documentation was divided into the following four volumes:

FIGURE 1.2

THE CONTROL MODULE STRUCTURE

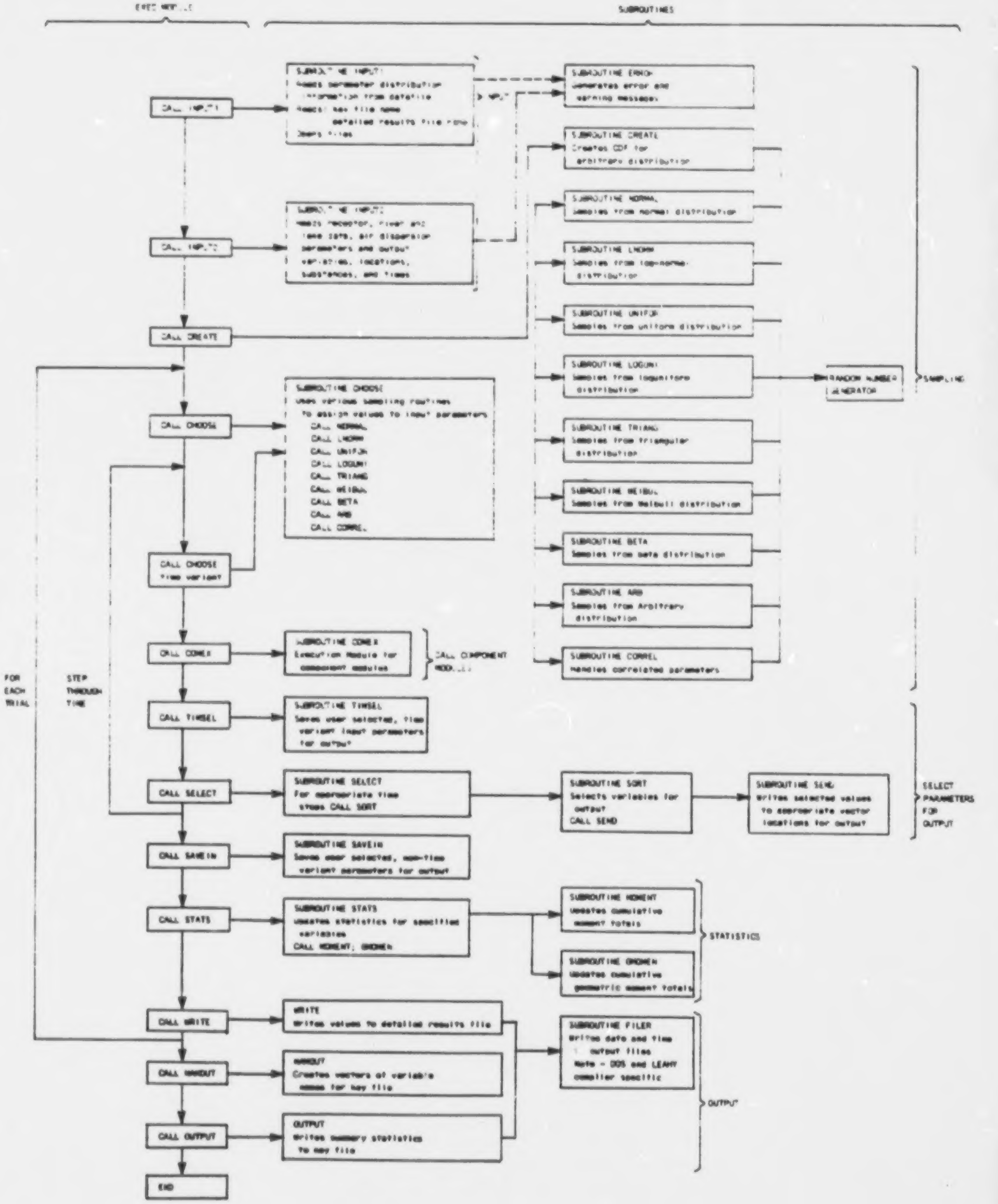

FIGURE 1.3

THE SUBROUTINE COMEX AND COMPONENT MODULES

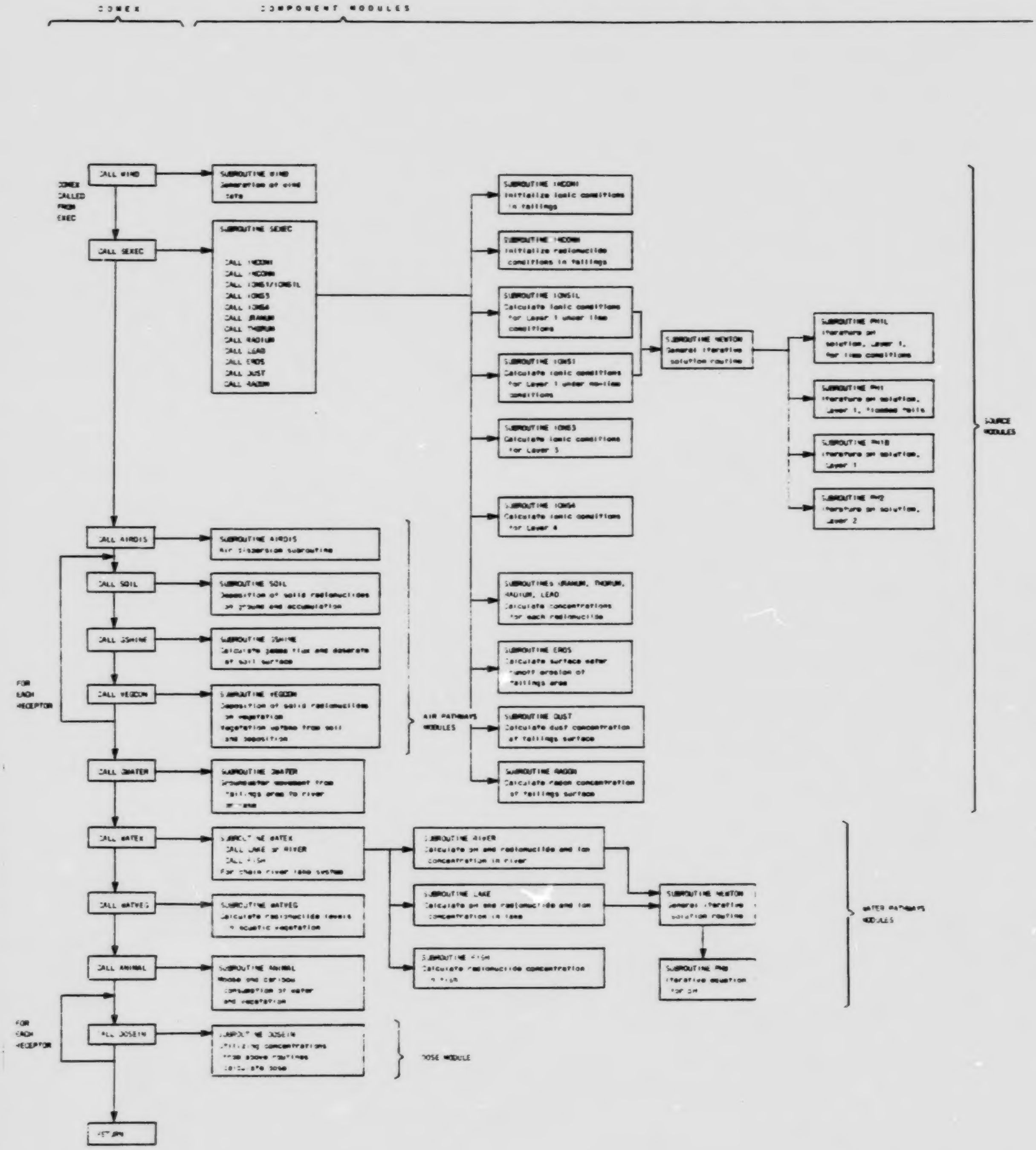
COMEX
COMPONENT MODULES
CALL WIND
COMEX CALLED FROM EXEC
SUBROUTINE WIND Generation of wind data
CALL SEXEC
SUBROUTINE SEXEC
CALL INCONI
CALL INCONR
CALL IONS1/IONS1L
CALL IONS3
CALL IONS4
CALL URANUM
CALL THORUM
CALL RADIUM
CALL LEAD
CALL EROS
CALL DUST
CALL RADON
SUBROUTINE INCONI Initialize ionic conditions in tailings
SUBROUTINE INCONR Initialize radionuclide conditions in tailings
SUBROUTINE IONS1L Calculate ionic conditions for Layer 1 under lime conditions
SUBROUTINE IONS1 Calculate ionic conditions for Layer 1 under non-lime conditions
SUBROUTINE IONS3 Calculate ionic conditions for Layer 3
SUBROUTINE IONS4 Calculate ionic conditions for Layer 4
SUBROUTINES URANUM, THORUM, RADIUM, LEAD Calculate concentrations for each radionuclide
SUBROUTINE EROS Calculate surface water runoff erosion of tailings area
SUBROUTINE DUST Calculate dust concentration of tailings surface
SUBROUTINE RADON Calculate radon concentration of tailings surface
SUBROUTINE NEWTON General iterative solution routine
SUBROUTINE PH1L Iteration on solution, Layer 1, for lime conditions
SUBROUTINE PH1 Iteration on solution, Layer 1, flooded tails
SUBROUTINE PH1B Iteration on solution, Layer 1
SUBROUTINE PH2 Iteration on solution, Layer 2
SOURCE MODULES
CALL AIRDIS
SUBROUTINE AIRDIS Air dispersion subroutine
CALL SOIL
SUBROUTINE SOIL Deposition of solid radionuclides on ground and accumulation
CALL GSHINE
SUBROUTINE GSHINE Calculate gamma flux and doserate of soil surface
CALL VEGCON
SUBROUTINE VEGCON Deposition of solid radionuclides on vegetation Vegetation uptake from soil and deposition
FOR EACH RECEPTOR
AIR PATHWAYS MODULES
CALL GWATER
SUBROUTINE GWATER Groundwater movement from tailings area to river or lake
CALL WATEX
SUBROUTINE WATEX CALL LAKE or RIVER CALL FISH For chain river lake system
SUBROUTINE RIVER Calculate pH and radionuclide and ion concentration in river
SUBROUTINE LAKE Calculate pH and radionuclide and ion concentration in lake
SUBROUTINE FISH Calculate radionuclide concentration in fish
SUBROUTINE NEWTON General iterative solution routine
SUBROUTINE PHB Iterative equation for pH
WATER PATHWAYS MODULES
CALL WATVEG
SUBROUTINE WATVEG Calculate radionuclide levels in aquatic vegetation
CALL ANIMAL
SUBROUTINE ANIMAL Moose and caribou consumption of water and vegetation
CALL DOSEIN
FOR EACH RECEPTOR
SUBROUTINE DOSEIN Utilizing concentrations from above routines calculate dose
DOSE MODULE
RETURN

Volume 1: Probabilistic Model Development for the Assessment of Uranium Mill Tailings in Canada - Phase III, Volume 1: Summary Report.

Volume 2: Probabilistic Model Development for the Assessment of Uranium Mill Tailings in Canada - Phase III, Volume 2: System Description and Control Module Documentation.

Volume 3: Probabilistic Model Development for the Assessment of Uranium Mill Tailings in Canada - Phase III, Volume 3: Component Model Documentation.

Volume 4: Probabilistic Model Development for the Assessment of Uranium Mill Tailings in Canada - Phase III, Volume 4: Uranium Tailings Assessment Program (UTAP) User's Manual.

In documenting the Phase IV study, Volumes 3 and 4 have been updated incorporating changes made in producing UTAP.3 and these volumes have been reissued in their entirety. Volume 1 has been replaced by a report specific to the application of UTAP to the Lacnor site. This addendum outlines changes to the control modules of UTAP.3 from those of UTAP.1 and UTAP.2 as described in Volume 2 of the Phase III report. It should be read in conjunction with the original Volume 2 report. Note that the control modules for UTAP.1 and UTAP.2 are the same.

1.3 Overview of Addendum to Volume 2

This addendum describes the changes made to the UTAP.1 and UTAP.2 control modules, implemented in UTAP.3. All of the chapters and subsection numbers have been preserved from the original Phase III Volume 2 report to enable the reader to easily identify portions of the Volume 2 report to which changes apply.

Some sections, namely Chapter 4 and Appendices B, F and G, have been reproduced in their entirety while Chapters 1 through 3 refer only to specific changes (or lack thereof) made to the computer coding. Since numerous changes were made throughout the confidence bands programs, these sections, namely Chapter 4 and Appendices F and G have been reproduced in full. Note that the numerous tables printed in Chapter 3 of Volume 2 showing code listings of the various control modules have not been reprinted but rather that the changed code has been reproduced in its entirety in Appendix B. Appendices A, C, D, E, H and I remain unchanged from the original Volume 2 report and have not been reproduced here in any form.

Three major changes were made to the general functions of the control modules. The first of these was the removal of one output file referred to, in Volume 2 as the statistics file. The main considerations in removing this file were reducing the amount of memory used by the program and the fact that another output file with essentially the same structure was also available.

The second major change involved replacing the routines for computing the beta and normal distributions in order to produce smoother distributions and reduce execution time, respectively.

The third change applies to the output. Statistics which cannot be computed due to insufficient values are now printed as blanks in the output file rather than as zeroes in order to avoid confusion.

These and other minor changes are outlined in more detail in the following pages.

2.0 CONTROL MODULE OBJECTIVES AND CONCEPTUAL SPECIFICATIONS

2.1 Control Module Features

The user can no longer save either summary statistics or detailed results but rather summary statistics are always saved on all variables selected and detailed results may be saved in addition to this, if desired.

2.2 Input Modules

No change.

2.3 Random Sampling Modules

No change.

2.4 Output Selection Modules

No change.

2.4.1 Compute Summary Statistics

The file created by this option, formerly known as the statistics file has been replaced by the key file which is always created. Skewness and kurtosis may be optionally written to this file. This output file is now known as the key file rather than the statistics file it was previously referred to as. In earlier versions, the key file was created only as part of the other output option, described below.

2.4.2 Write Detailed Results to Output File

This option, as before, writes all values of the user-selected parameters to a disk file on each trial. The function of the other file (the key file) formerly created by this is still filled by the key file but it is now created by the previously described output option rather than as part of this option. Namely, the row order of the key file corresponds to the column order of the detailed results file. Both the key and the detailed results file still serve as input to the confidence bands program.

2.5 Stepping Through Time

Where previously the time steps that could be used by UTAP.1 and UTAP.2 were restricted to either 1 or 10 years, there is no longer any such restriction. Any time step dividing evenly into the total simulation time may be used. However, the total number of time steps is limited to a maximum of 200 in UTAP.2 and UTAP.3 and a maximum of 199 in UTAP.1.

2.6 Confidence Bands

The confidence bands program now processes the key and detailed results files described in Section 2.4, rather than Section 2.4.2.

3.0 CONTROL MODULE DESCRIPTIONS

No change.

3.1 Main Program (EXEC)

No change.

3.2 Input Modules

No change.

3.2.1 First Input Routine (SUBROUTINE INPUT1)

A revised example of the first input data file is shown in Table 3.2. A statistics file is no longer opened by INPUT1; however, an additional flag for printing skewness and kurtosis to the key file is read in. The number of cells for beta distributions are no longer specified. Inputs controlling time (i.e. length of simulation and time increment) are now input as real numbers rather than as integers. The output flags "S" for summary statistics and "B" for both files are no longer used. "F" saves results to whichever output files are opened. The default is still "N" for no output.

3.2.2 Second Input Routine (SUBROUTINE INPUT2)

The modified second input file for UTAP.3 is shown on Table 3.6. There is no longer any restriction as to time steps for which air dispersion information may be time-variant. In addition to information previously assigned to each receptor, the watershed segment from which the receptor gets fish is also specified.

In UTAP.3 some additional variables are input regarding the groundwater flow paths. These are the number of flow paths, the nodes where the flow paths enter the surface water and the layers in the source through which the

Table 3.2

SAMPLE OF FIRST INPUT FILE

```
     Title
PROBABILISTIC ANALYSIS: TEST CASE

┌─── Detailed Results file indicator
│ ┌──────── Skewness and kurtosis indicator
Y N
     Detailed Results file name
RES.OUT
     Key file name
KEY.OUT
  ┌─ Number of input distributions
  │    ┌── Number of arbitrary distributions
  │    │   ┌──── Number of correlated parameters
 10    1   1
  ┌─Random number seed
  │          ┌─── Number of trials
0913566091  10
   ┌─Years in simulation
   │     Time increment in years
  100.   10.
     Regular distributions:
   ┌───────── Parameter name
   │     ┌──────── Output flag
   │     │   ┌──────────── Distribution type number
   │     │   │ ┌──────────────── Time-variant flag
   │     │   │ │                  Distribution descriptors
CONST    N   1 N        2.0
NORMAL   N   2 V       10.0          2.0         0.0        20.0
LNORM    N   3 V       1.0E02        1.5         1.0        1.0E3
UNI      F   4 N        1.0          2.0
LOGUNI   N   5 N        0.01         0.5
TRIANG   N   6 N        0.01         0.03        0.1
WEIBUL   F   7 V        0.0          1.5         0.9
BETA     N   8 N       10.0        100.0         2.0         2.0
     Arbitrary distributions:
 ┌──────────── Parameter name
 │      ┌──────── Output flag
 │      │  ┌──────────── Distribution type number
 │      │  │ ┌─────────────── Time-variant flag
 │      │  │ │  ┌──────────────── Number of cells in distribution
 │      │  │ │  │                      Distribution descriptors
ARB     N  9 N 10     1.0   11.0  2.0  2.0  2.0  8.0  8.0  8.0 12.0 12.0  4.0  4.0

     Correlated distributions:
  ┌──────────Parameter name
  │     ┌────────Output flag
  │     │  ┌──────────── Distribution type number
  │     │  │  ┌────────────── Time-variant flag
  │     │  │  │  ┌─────────────────── Name of independent distribution
  │     │  │  │  │                      Distribution descriptors
CORREL  N 10  N NORMAL        50.0       10.0        0.7        10.0        2.0
```

Table 3.6

SAMPLE OF SECOND INPUT FILE (INPUT2.DAT)

```
     Flag to indicate if variable wind data is desired
  N
     File containing appropriate wind data
STARAV.DAT
     Number of receptor locations
  5
     Number of rings
  5
     Ring limits
   1    3    5   10   20   50
     Receptor information:
 ┌───────── Receptor number
 │  ┌───────────── Sector number
 │  │  ┌──────────────── Ring number
 │  │  │  ┌──────────────── Drinking water source segment number
 │  │  │  │  ┌──────────────── Fish source segment number
 │  │  │  │  │  ┌──────────────── Receptor type
 │  │  │  │  │  │    ┌──────────────── Population
  1 16  1  1  1 C    2
  2 16  3  2  2 A    5
  3 14  3  2  2 A    6
  4  1  1  1  1 C    1
  5  7  3  2  2 A    3
 ┌Number of watershed segments
 │  ┌──── Number of groundwater flow paths
  8  2
   End node numbers of watershed segments groundwater flows into
  1  1
     Layers for groundwater flow
  3  3
     Watershed information:
 ┌──────── End node or segment number
 │ ┌──────────── Segment type
 │ │  ┌──────────── Sector number of end node
 │ │  │   ┌──────────── Ring number of end node
 │ │  │   │      ┌──────────── Lake depth
 │ │  │   │      │        ┌──────────── Watershed area
 │ │  │   │      │        │        ┌──── Lake surface area/River length
  1 R 11  1      │        1.5E07   3.0E3
  2 L 11  1   1.0E01   2.0E07   5.0E05
  3 R 10  2            3.2E07   3.5E3
  4 L 10  2   4.0      3.8E07   2.5E05
  5 R  9  3            7.0E07   7.0E3
  6 R  9  4            1.2E08   1.3E4
  7 L  9  4   5.0      1.4E08   4.0E06
  8 R  9  5            4.0E08   3.0E4
       Number of times at which output is saved
  4
     Times at which output is to be saved
 .1E2  .2E2  .3E2  .4E2  .5E2  .6E2  .7E2  .8E2  .9E2  .1E3
```

Table 3.6 cont'd

```
        Number of arrays to be checked for output
  36
  ┌──Array name
  │       ┌─Array size
WCONC   0
CONC    0
PH      0
WATC    2
   ┌──Substance code
   │  ┌─── Location code
   2  3
   3  5
WATAVG  3
   1  1
   3  1
   4  1
WATPH   3
   1  7
   1  4
   1  2
GWATC   0
EMRATE  0
EROTOT  0
AIRC    0
SOILC   0
AVEGC   0
BVEGC   0
SUFOC   0
BRWSC   0
LICHC   0
AQVEGC  0
FISHC   0
ADERC   0
WDERC   0
AMOSC   0
WMOSC   0
ACARC   0
WCARC   0
WATD    0
SHINED  0
INHD    0
RADD    0
VEGD    0
FISHD   0
MEATD   0
DOSE    0
POPDT   0
BLANK1  0
BLANK2  0
```

groundwater flows (usually layer 3 - the mixing zone).

In the watershed information, depths do not need to be specified for rivers, as previously stated, only for lakes. This applies to all versions of UTAP.

Output for only one set of times (up to 11) are sent to whichever files are opened rather than before when a different set of times could be selected for each of the two output options. These times are now input as real numbers rather than as integers. They must be multiples of the time increment.

The revised list of arrays available for output is shown on Table 3.7. The arrays ADERC and WDERC, described on Table 3.7 are new while AMOSC and WMOSC are the same as AMOC and WMOC, respectively, in the earlier versions. The variable DTAIL, cumulative erosion of the tailings pile, is no longer available. Previously, the user had to specify which output file each substance/location combination for each array was to be printed to. The flag to do this has been removed and all outputs selected are automatically sent to whichever file(s) have been opened.

The air dispersion data read by INPUT2 is not, as previously indicated, dependent on the time increment used but rather it is dependent on the air dispersion file named at the top of the second input file and **it is up to the user to ensure that this file corresponds to the chosen time increment.** This is the case for all versions of UTAP.

3.2.3 Generation of Error and Warning Messages (SUBROUTINE ERROR (I,ILINE)

An additional argument, ILINE, has been added to this subroutine. ILINE has the value of the line number of the last line read from an input file. When execution of the program is terminated by this subroutine, the number corresponding to ILINE is printed to the screen so that the user knows where in the input file to look for the error.

Table 3.7

OUTPUT PARAMETERS

Variable	Definition
WCONC	Tailings liquid phase concentration
CONC	Tailings solid phase concentration
PH	Tailings pH
WATC	Water concentration
WATAVG	Average watershed concentration
WATPH	pH in lakes and rivers
GWATC	Ground water concentration
EMRATE	Emission Rate from tailings
EROTOT	Erosion of tailings pile overtime step
AIRC	Air concentration
SOILC	Soil concentration
AVEGC	Above ground vegetation concentration
BVEGC	Below ground vegetation concentration
SUFOC	Summer folliage concentration
BRWSC	Browsing vegetation concentration
LICHC	Lichen concentration
AQVEGC	Aquatic vegetation concentration
FISHC	Fish concentration
ADERC	Deer concentration from vegetation
WDERC	Deer concentration from water consumption
AMOSC	Moose concentration from vegetation
WMOSC	Moose concentration from water consumption
ACARC	Caribou concentration from vegetation
WCARC	Caribou concentration from water consumption
WATD	Drinking water dose
SHINED	Groundshine dose
INHD	Inhalation dose
RADD	Radon dose
VEGD	Vegetable consumption dose
FISHD	Fish consumption dose
MEATD	Meat consumption dose
DOSE	Total Individual Dose
POPDT	Total Dose for Entire Study Population

3.3 Sampling Routines

3.3.1 Objective

No change.

3.3.2 General Concepts

No change.

3.3.3 The Random Number Generator (FUNCTION RANDOM)

No change.

3.3.4 Creation of a Cumulative Distribution Function (SUBROUTINE CREATE)

Subroutine CREATE, which previously created cumulative probability functions for both arbitrary and beta distributions, now is called only for arbitrary distributions. Thus, all references to beta distributions within this section are not applicable to UTAP.3.

3.3.5 Choice of Sampling Routine (SUBROUTINE CHOOSE)

The subroutine BETA, previously called for both arbitrary and beta distributions, has been renamed subroutine ARB and is now called only for arbitrary distributions. Otherwise, this subrountine remains unchanged.

An entirely new routine, subroutine BETA, has been created and is now called for beta distributions.

3.3.6 Normal Distribution (SUBROUTINE NORMAL)

A new algorithm for the normal distribution was implemented in UTAP.3 in order to improve execution time. The accuracy is comparable to the algorithm used previously.

The standard normal cumulative probability function (cpf) is defined as:

$$p = \Pr (X \leq x) = \frac{1}{\sqrt{2\pi}} \int^{x} \exp \frac{-u^2}{2} \, du \qquad (3.7)$$

where X is distributed as N(0,1).

The inverse cpf may be approximated by a rational function (Arbramowitz and Stegun, 1964). That is, given p, the probability level in equation 3.7 the normal deviate x may be found from:

$$\phi (p) = t - \frac{\sum_{i=0}^{n-1} a_i t^i}{1 + \sum_{i=1}^{n} b_i t^i} + \epsilon \qquad (3.8)$$

where $t = \sqrt{-2 \ln p}$ and $0 < p \leq 1/2$

The numerical coefficients for the degree of accuracy used is given by:

Upper Bound on $\lvert\epsilon\rvert$	n	i	a_i	b_i
.003	2	0	2.30753	---
		1	.27061	.99229
		2	--	.04421

where

$x = - \phi (p), \; 0 < p \leq 1/2$

$x = \phi (1-p), \; 1/2 < p < 1$

This function of p, which is the inverse of equation 3.7 is used along with the probability integral transformation to generate a standard normal random number X.

A typically normally distributed random variable sampled by subroutine NORMAL is shown in Figure 3.6. Summary statistics are presented on the bottom of Figure 3.6 and include the specified mean and standard deviation as well as the mean and standard deviation calculated from the sampled data. The chi-square goodness of fit statistic is also shown.

3.3.7 Lognormal Distribution (SUBROUTINE LNORM)

No change.

3.3.8 Uniform Distribution (SUBROUTINE UNIFOR)

No change.

3.3.9 Loguniform Distribution (SUBROUTINE LOGUNI)

No change.

3.3.10 Triangular Distribution (SUBROUTINE TRIANG)

No change.

3.3.11 Weibull Distribution (SUBROUTINE WEIBUL)

No change.

3.3.12 Arbritary Distribution (SUBROUTINE ARB)

This subroutine, formerly call subroutine BETA, was renamed and is now called only for arbitrary distributions, not beta. It remains otherwise unchanged.

FIGURE 3.6

PLOT OF FREQUENCY HISTOGRAM (500 SAMPLES) AND PROBABILITY DISTRIBUTION (SMOOTH CURVE) FOR NORMAL DISTRIBUTION

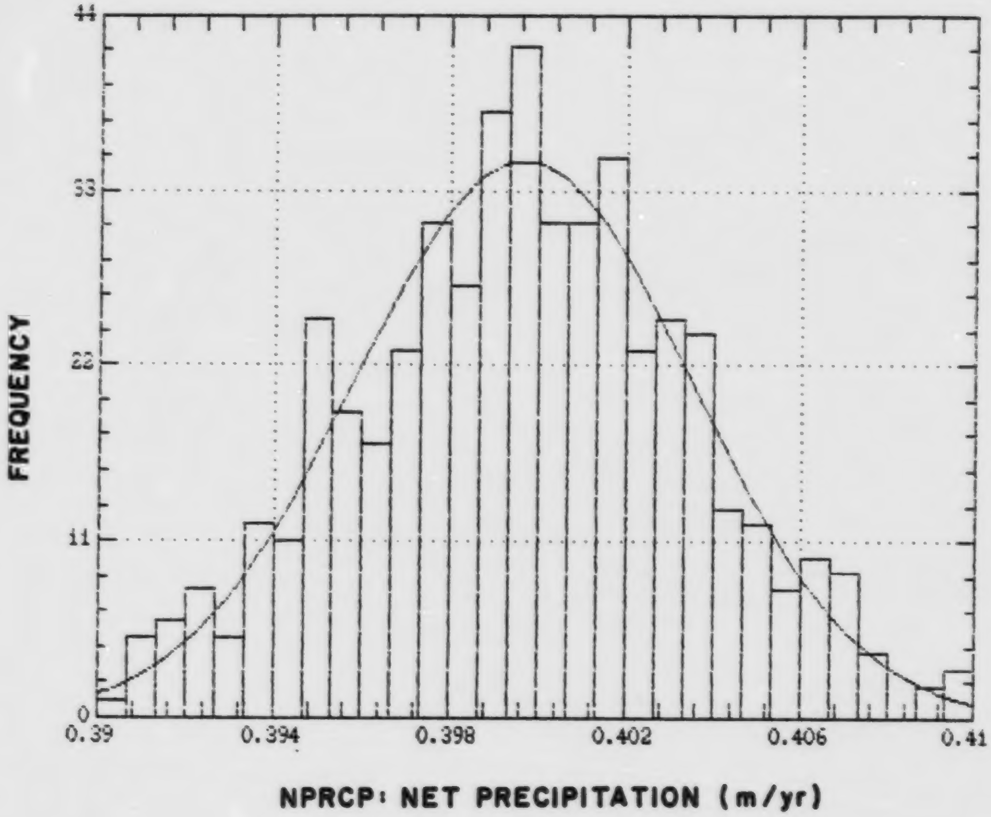

SUMMARY STATISTICS:

	SPECIFIED INPUT VALUES	CALCULATED SAMPLE VALUES
MEAN	0·400	0·400
STANDARD DEVIATION	4×10^{-3}	$3{\cdot}8 \times 10^{-3}$

CHI^2 GOODNESS-OF-FIT = 21.106 WITH 22 DEGREES OF FREEDOM

Beta distributions are now calculated by an entirely new subroutine BETA described in Section 3.3.14.

3.3.13 Correlated Parameters (SUBROUTINE CORREL)

No change.

3.3.14 Beta Distribution (SUBROUTINE BETA)

This subroutine is entirely new to UTAP.3 and should not be confused with subroutine BETA found in earlier versions of UTAP. The earlier version of subroutine BETA is now called subroutine ARB as discussed in Section 3.3.12.

Two methods called Acceptance - Rejection Methods A and B are used by this new subroutine BETA depending on the values of the shape parameters a and b (see Figure 3.5). If both a and b are greater than 1, method B is used, otherwise method A is used.

Method A

The following method is used to generate a beta-distributed random number X for any a, b > 0 (Kennedy and Gentle, 1980):

1. Generate a pair R_1, R_2 of independent uniformly distributed random numbers on the interval (0, 1).

2. Set $V_1 = R_1{}^{1/a}$, $V_2 = R_2{}^{1/b}$ and $W = V_1 + V_2$ (3.16)

3. If W > 1 go to step 1, otherwise go on to 4.

4. Set $X = V_1/W$

The expected number of pairs of uniformly distributed numbers which is required is $\frac{\Gamma(a+b+1)}{\Gamma(a+1)\,\Gamma(b+1)}$. This is quite good for a and b less than 1. For

FIGURE 3.5

FORMS OF THE BETA DISTRIBUTION PROBABILITY DENSITY FUNCTION

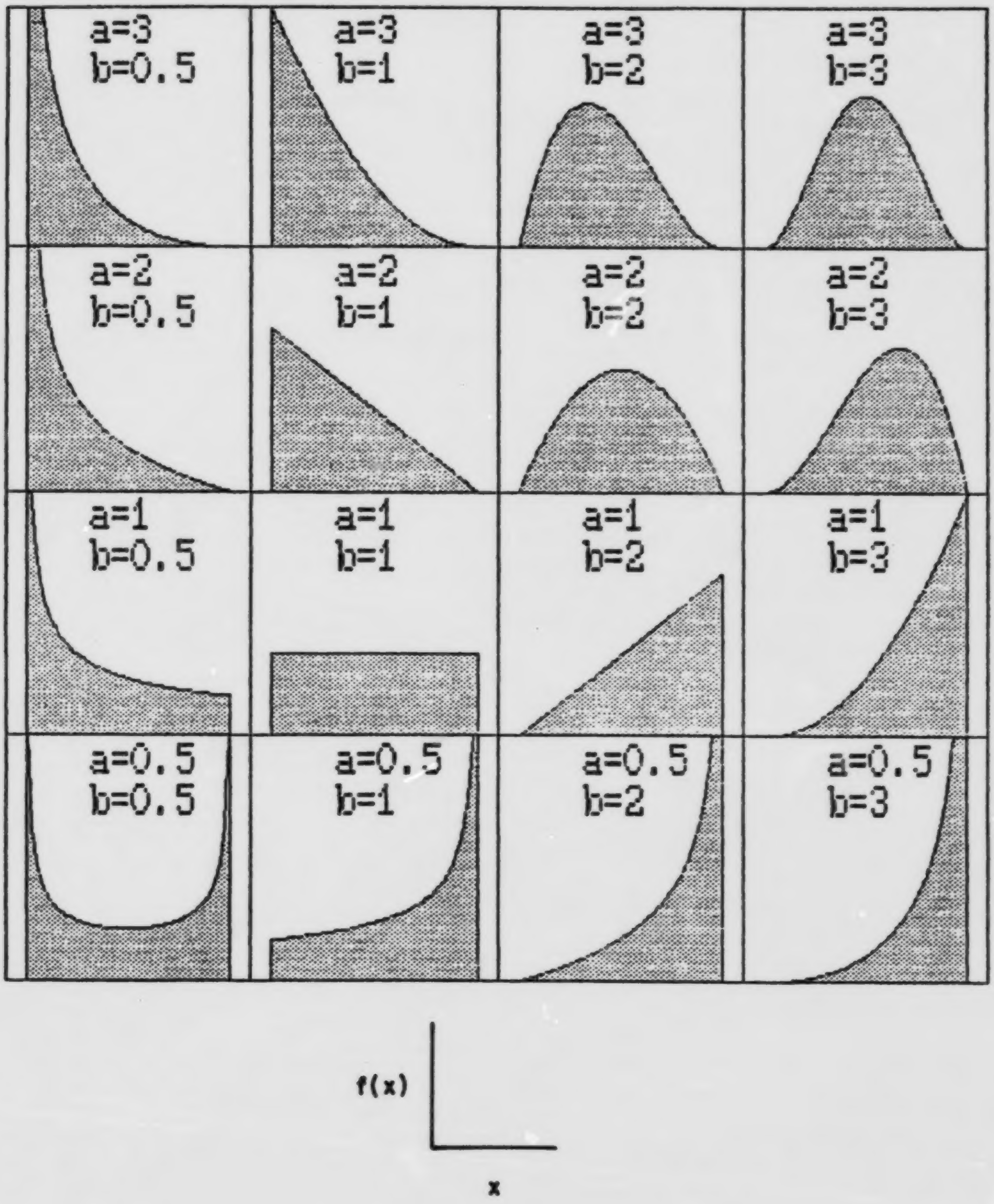

example, if $a = b = .5$, it is 1.273. However, for larger a and b it is not so good. For $a = b = 3$ it is 20 pairs. If only one of a and b is less than 1 it is still fairly good; for $a = 5$, $b = 0.5$, it is 2.71. For this reason, method B is used only for a and b both greater than one.

Method B

The following rule is applicable and is used if neither a nor b is less than or equal to one:

1. Generate a pair R_1, R_2 of independent uniformly distributed random numbers on the interval (0,1).
2. Set $X = R_1$. (3.17)
3. If $R_2 \geq X^{a-1}(1 - X)^{b-1} \left[\dfrac{(a + b - 2)^{a+b-2}}{(a - 1)^{a-1}(b - 1)^{b-1}},\right]$ go to 1, otherwise finish.

Step 3 shows that the method accepts R_1 as X with probability proportional to the probability density. The square-bracketted constant makes the process as efficient as possible by accepting the mode with probability 1.

The expected number of pairs of uniformly distributed random numbers required for each beta-distribution number is:

$$\frac{\Gamma(a + b)}{\Gamma(a)\,\Gamma(b)} \times \frac{(a - 1)^{a-1}(b - 1)^{b-1}}{(a + b - 2)^{a+b-2}} \qquad (3.18)$$

This, by mathematical coincidence is numerically equal to the probability density at the mode.

The method is fairly efficient. For $a = b = 2$ the expected number of pairs of uniformly distributed random numbers is 1.5. As a and b increase and the distribution consequently becomes narrower, the efficiency decreases but even at a = b = 10, only an average of 3.524 pairs of uniformly distributed random numbers is required.

Figure 3.15 shows two sampled beta distributions, one for each of the two methods A and B. Summary statistics and the chi-square goodness of fit statistics are also given in Figure 3.15.

3.4 Output Selection Routines

Formerly, two vectors of output values were created. One of these (the one for the statistics file) is no longer used.

3.4.1 Saving Time-Variant Sampled Parameters (SUBROUTINE TIMSEL)

Previously, the output flags for time-variant parameters indicated if the variables were to be printed to one, both, or neither of the ouput file options while now the flags indicate only if the variables are to be printed or not and all the values are saved in one vector.

3.4.2 Selection of Output Time Steps (SUBROUTINE SELECT)

Previously, two checks were made to determine if output for the current time step was to be saved. Now, the first check (namely for output to the no longer existent statistics file) has been removed. Only one check is now made.

3.4.3 Sorting of Output Variables (SUBROUTINE SORT)

The argument VECTOR has been removed from subroutine SORT since there are no longer two vectors possible for output to go to. Each output variable selected is automatically routed to the output vector.

FIGURE 3.15

PLOT OF FREQUENCY HISTOGRAM (500 SAMPLES) AND PROBABILITY DISTRIBUTION (SMOOTH CURVE) FOR BETA DISTRIBUTION

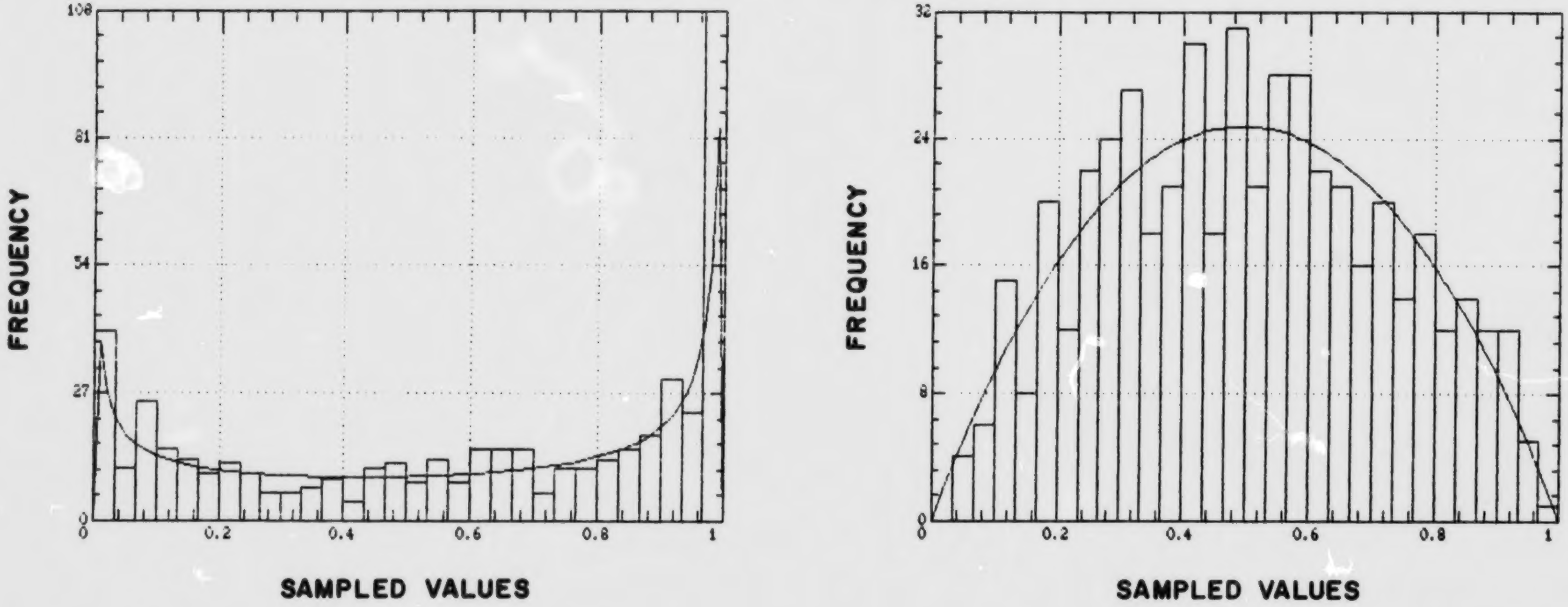

A) METHOD 'A'

B) METHOD 'B'

SUMMARY STATISTICS:

	SPECIFIED INPUT VALUES	CALCULATED SAMPLE VALUES
a	0.6	0.531
b	0.4	0.361

CHI^2 GOODNESS-OF-FIT = 38.016 WITH 27 DEGREES OF FREEDOM

SUMMARY STATISTICS:

	SPECIFIED INPUT VALUES	CALCULATED SAMPLE VALUES
a	1.90	1.96
b	2.10	1.98

CHI^2 GOODNESS-OF-FIT = 24.807 WITH 25 DEGREES OF FREEDOM

3.4.4 Saving Output Variables (SUBROUTINE SEND (XDUM))

As is the case with subroutine SORT, the subroutine argument VECTOR has been removed in this version of UTAP since there is only one vector for output.

3.4.5 Saving Non-Time Variant Sampled Parameters (SUBROUTINE SAVEIN)

Each non-time-variant parameter, previously checked to determine if it was to be saved to either, both, or neither output files is now, since only one output choice is possible, checked only to see if it is to be output or not. Those that are to be output are saved in the output vector.

3.5 Statistics Routines

The two vectors of outputs, XOUTS and XOUTF, described in Volume 2 are not used in UTAP.3. Instead, one output vector named XOUT is used and it is equivalent to the former vector XOUTF.

3.5.1 Computing Summary Statistics (SUBROUTINE STATS)

This subroutine now receives only one vector of values instead of the two vectors it received in earlier versions. The statistics are calculated on the contents of this one vector.

The results of some of the statistics may not be "defined" numbers. For instance, standard deviations cannot be computed on less than two numbers, skewness on less than three, or kurtosis on less than four. Also, geometric means and standard deviations cannot be computed on values equal to zero.

Where previously calculations that would produce "undefined" results were not computed and the parameters were subsequently set to zero, now all parameters that could potentially be undefined are initialized to -999 (a number that should never naturally occur since the outputs are all positive numbers) and retain this value if proper values cannot be calculated.

3.5.2 Computing Moment Values (SUBROUTINE MOMENT and GMOMEN)

No change.

3.6 Output Routines

No change.

3.6.1 Output of Detailed Results (SUBROUTINE WRITE)

In addition to its previous functions, SUBROUTINE WRITE now checks if output of detailed results is desired. The vector of output data is now called XOUT instead of XOUTF as it was previously named.

3.6.2 Creation of Output Labels (SUBROUTINE NAMOUT)

Subroutine NAMOUT which previously created labels for both the statistics and key files now creates only one vector of labels for the key file corresponding to the elements of the vector XOUT of outputs saved by subroutine SAVEIN.

3.6.3 Output of Summary Statistics (SUBROUTINE OUTPUT)

This subroutine writes statistics to the key file only, as opposed to the two files that it previously wrote statistics to.

The five statistical parameters for which results may not be defined, namely geometric mean, arithmetic and geometric standard deviation, skewness, and kurtosis, are no longer output directly. Instead, the program creates a character variable called VECTOR with a dimension of five (corresponding to the five parameters) and sets this variable equal to blanks. The statistical parameters are then checked for the -999 assigned to undefined values by subroutine STATS and if a -999 is not found, the calculated value is written to the variable VECTOR. The resulting contents of VECTOR, both values and blanks, are written to the key file along with the other statistical parameters, names and other information.

3.6.4 Dating of Output Files (SUBROUTINE FILER (UNIT))

This small subroutine is not new to this version of UTAP but was not previously described in the Volume 2 report. It remains unchanged from earlier versions.

The subroutine argument UNIT refers to the unit number of an open file (or the unit number corresponding to any device such as the screen). FILER uses DOS and compiler specific functions to obtain the current date and time and writes these to the device or file corresponding to the value of UNIT.

4.0 CONFIDENCE BANDS PROGRAM DESCRIPTION

4.1 Introduction and Background

The most important output from a Monte Carlo calculation is often the probability density function for one or more output variables. Each probability density function is obtained in approximate form as a set of counts in cells which correspond to discrete values of the variable. The observed relative frequencies in the cells provide an approximation to the probability density function of the variable.

If the number of Monte Carlo trials were extremely large (say 10^9) and the number of cells moderate (say 20), it would be expected that the graph of the relative frequency values versus the values of the variable corresponding to different cells would be a smooth curve which would agree very closely with the true probability density function. It would also vary little from one Monte Carlo run with the same number of trials to the next.

If, however, only 100 Monte Carlo trials are made with 20 cells, the relative frequency diagram can be expected to be "ragged", and to vary a good deal from one run of 100 trials to the next. Furthermore, the smooth curve drawn through the relative frequency points may not agree closely with the true probability density function.

There are various techniques for estimating the confidence in the output of a finite Monte Carlo calculation. Two were examined in this Phase III study. In Appendix E, Kaplan develops the theoretical basis for a Bayesian approach. In Appendix F, Reilly and Duever provide the theoretical basis for an alternative approach for estimating bounds from the output of a Monte Carlo simulation, within which the true probability density function (pdf) or cumulative density function (cdf) can be expected to lie with a given level of confidence. The Reilly and Duever approach has been implemented as a post-processing option to UTAP. The computer code for the current microcomputer implementation of this confidence band technique is provided in full in

Appendix G of this volume along with variable dictionaries for the confidence band program. This chapter outlines the computer implementation of the confidence band programs.

4.2 The General Nature of the Confidence Bands Programs

The confidence bands programs are provided as a post-processing option to UTAP. The general nature of the confidence bands programs and their relation to UTAP are indicated on Figure 4.1.

Prior to executing the confidence bands program, the desired variables must have been saved to the detailed results file generated by UTAP. The first activity within the confidence bands post-processor is then to read the required data from the UTAP output files. The information required by the confidence bands programs consists of the names of the variable(s) to be analysed, the minimum and maximum values, and, of course, the data itself. The user is asked, by the program, for the variable's identification number and whether a log transformation of the data is to be performed.

There are actually two confidence bands programs. The first, BIN, reads the data from UTAP and assigns this data into bins or cells. The second program, CBAND, uses the binned data to calculate the confidence bands. BIN and CBAND are described below. The program output is a file containing the cell midpoints, the cell counts, and the counts corresponding to the 95% confidence limits for both the probability density function and the cumulative distribution function.

4.2.1. The Binning Program (BIN)

Figure 4.2 shows the flowsheet of the binning program, which bins Monte Carlo realizations of a given variable. The data are read, using subroutine READ, from two output files created by the Monte Carlo sampling program. One file contains the actual Monte Carlo realizations which are read into a vector. The second statistics file supplies the binning program with the variable

FIGURE 4.1

RELATION OF CONFIDENCE BAND PROGRAMS TO UTAP

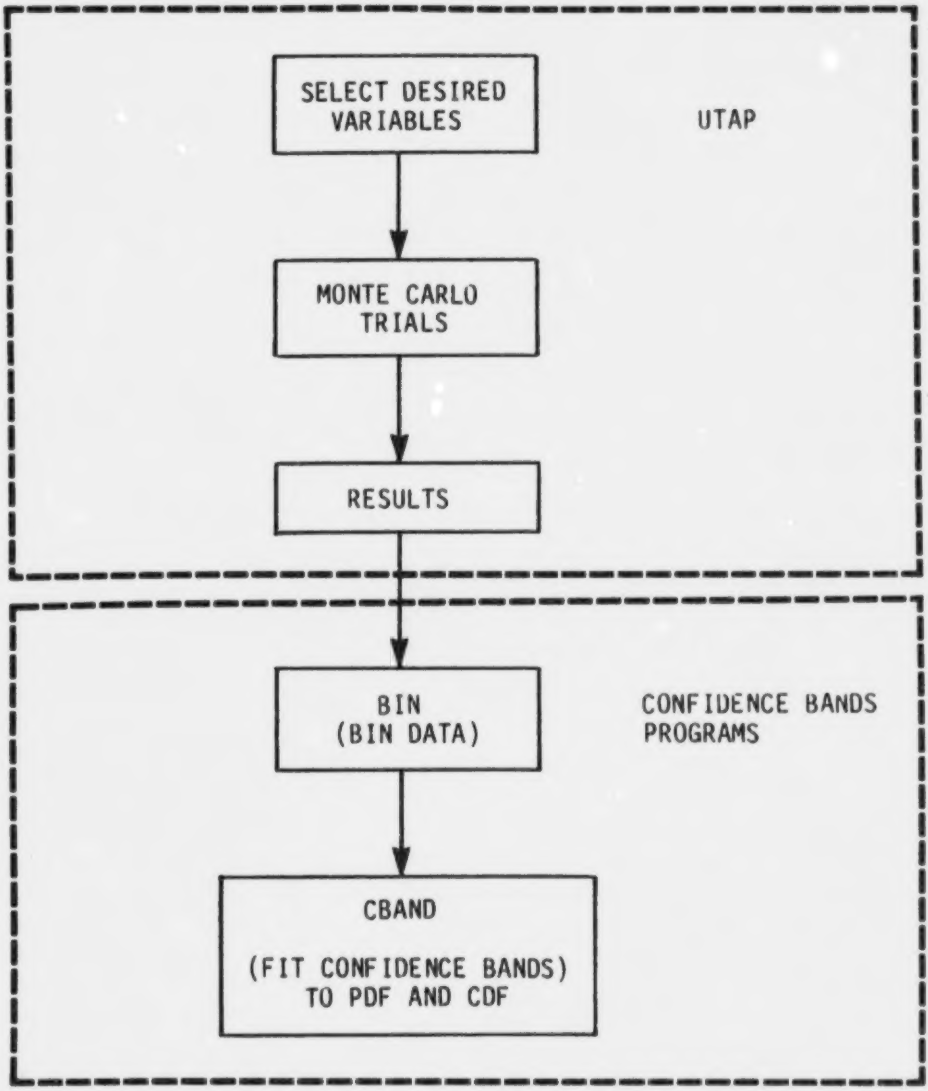

FIGURE 4.2

BINNING PROGRAM (BIN) STRUCTURE

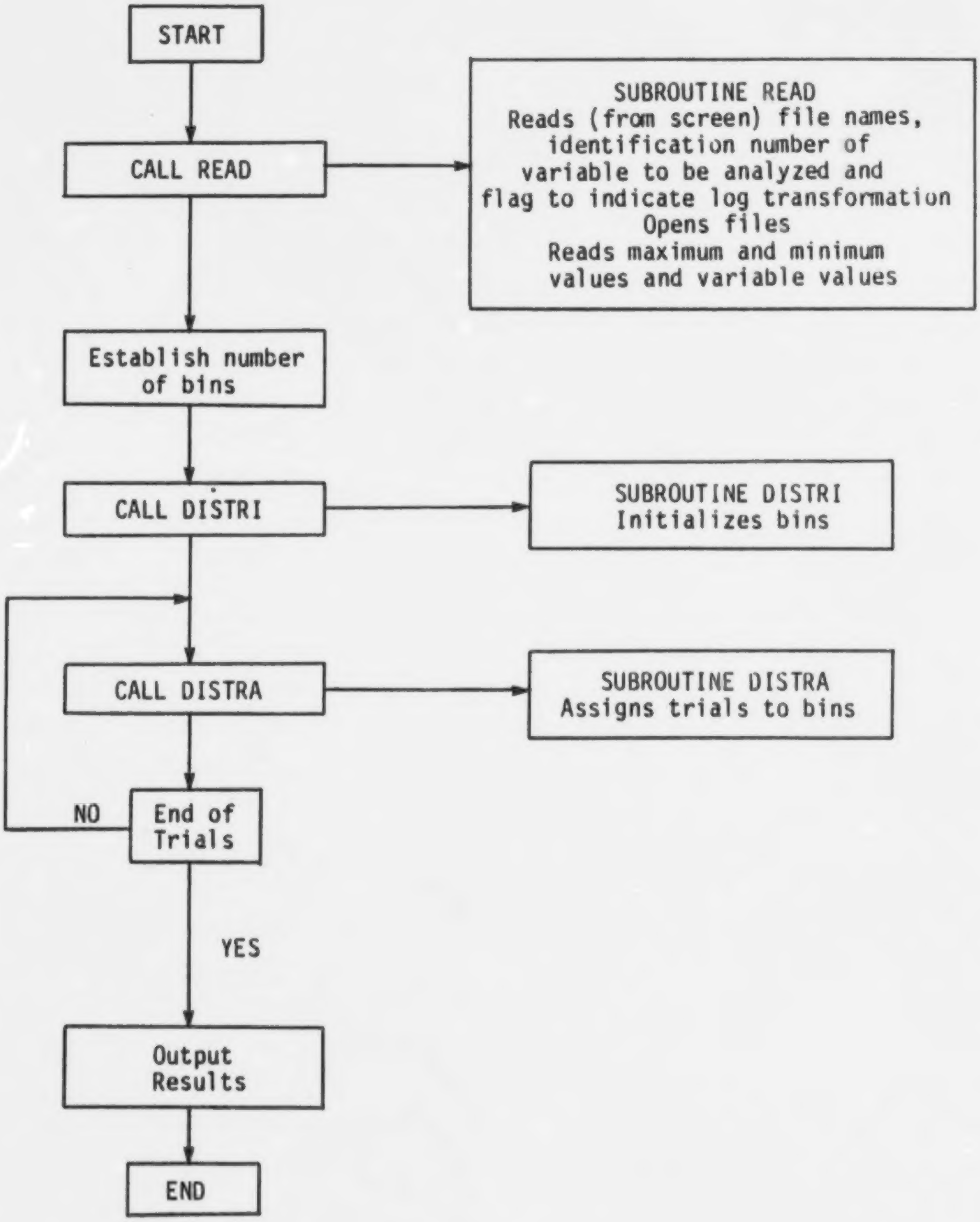

name, and the minimum and maximum values of the variable.

Based on a paper by Sturges (1926) the number of bins used in the program is the nearest integer to the value given by the expression:

$$[\log_{10} (\Delta\text{of Monte Carlo trials})/\log_{10} (2.0)] + 1.0 \tag{4.1}$$

The program allows for a logarithmic transformation of the data, which may be required for some highly skewed distributions. If a highly skewed distribution such as a lognormal is expected, it may be necessary to do more Monte Carlo trials to ensure that a broad enough range is established. If any suitable prior knowledge about the maximum or mimimum values of a variable is available, then this should be incorporated into the binning procedure, providing this information is supported by the observed data.

The binning process is initiated by a call to subroutine DISTRI. The observations are then binned by making a call to subroutine DISTRA for each observation.

Finally, the cell counts and the cell midpoints are stored in a file for use in the confidence bands program, CBAND.

4.2.2. The Confidence Band Program (CBAND)

Figure 4.3 is the logic flow sheet for the confidence bands program, CBAND The program CBAND first reads in the data file generated by the binning program. The information required by CBAND consists of the name of the variable being analysed, the number of cells or bins used, the number of Monte Carlo trials made, a flag indicating whether or not a logarithmic transformation of the data has been made, the cell midpoints and the cell counts.

A Newton-Raphson fitting procedure (implemented as subroutine NEWRAP) is used to fit a probability density function to observed cell counts. This subroutine

FIGURE 4.3
CONFIDENCE BANDS PROGRAM (CBAND) STRUCTURE

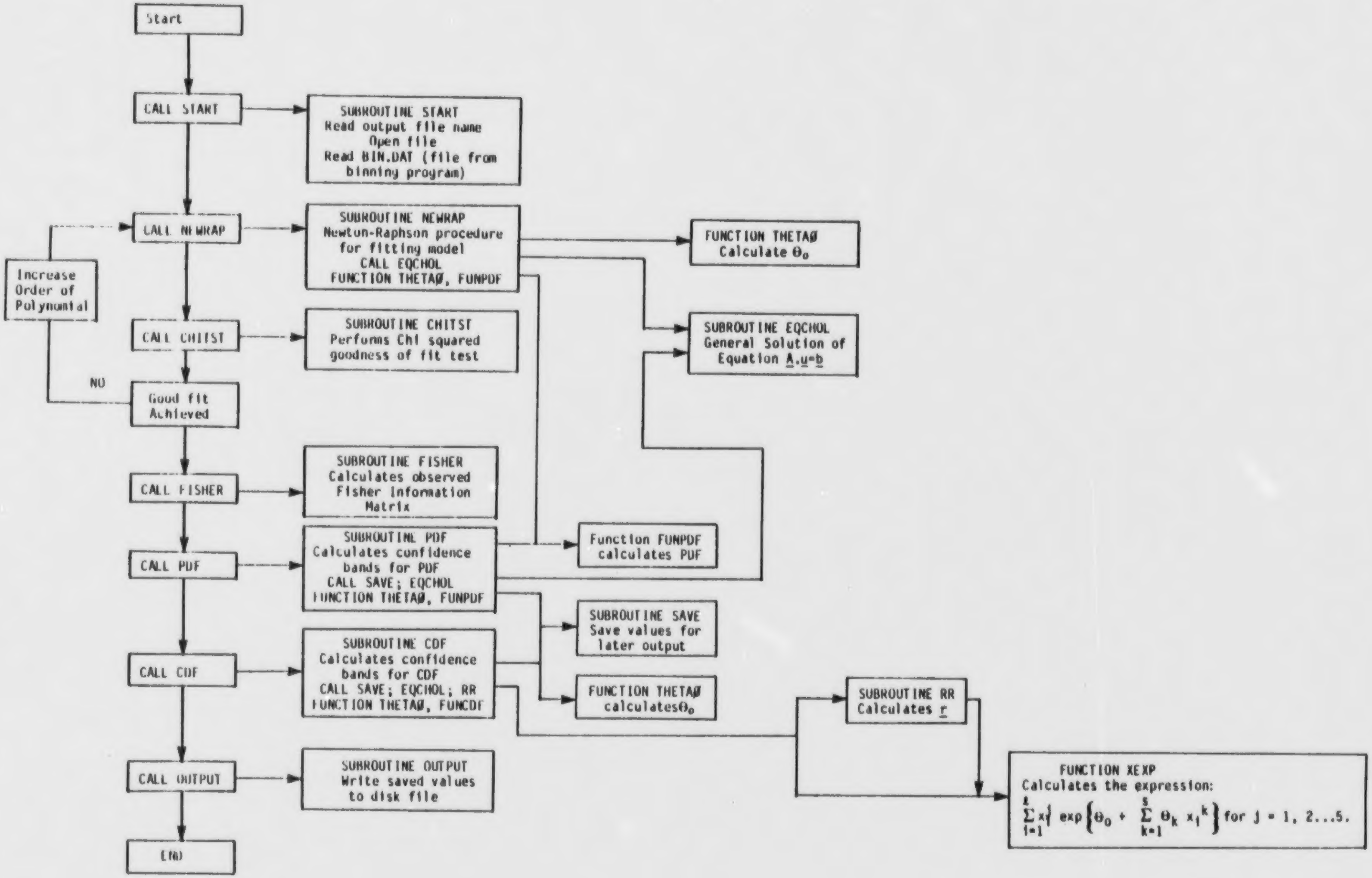
Start
CALL START
SUBROUTINE START
Read output file name
Open file
Read BIN.DAT (file from binning program)
CALL NEWRAP
SUBROUTINE NEWRAP
Newton-Raphson procedure for fitting model
CALL EQCHOL
FUNCTION THETAØ, FUNPDF
FUNCTION THETAØ
Calculate θ_0
SUBROUTINE EQCHOL
General Solution of Equation $\underline{A}.\underline{u}=\underline{b}$
Increase Order of Polynomial
CALL CHITST
SUBROUTINE CHITST
Performs Chi squared goodness of fit test
NO
Good fit Achieved
CALL FISHER
SUBROUTINE FISHER
Calculates observed Fisher Information Matrix
CALL PDF
SUBROUTINE PDF
Calculates confidence bands for PDF
CALL SAVE; EQCHOL
FUNCTION THETAØ, FUNPDF
Function FUNPDF
calculates PDF
SUBROUTINE SAVE
Save values for later output
CALL CDF
SUBROUTINE CDF
Calculates confidence bands for CDF
CALL SAVE; EQCHOL; RR
FUNCTION THETAØ, FUNCDF
FUNCTION THETAØ
calculatesθ_0
SUBROUTINE RR
Calculates $\underline{r}$
FUNCTION XEXP
Calculates the expression:
$\sum_{i=1}^{\ell} x_i^j \exp\left\{\theta_0 + \sum_{k=1}^{s} \theta_k x_i^k\right\}$ for j = 1, 2...5.
CALL OUTPUT
SUBROUTINE OUTPUT
Write saved values to disk file
END

requires two additional subroutines. The first function subroutine calculates the values of the probability density function at any value of x. The second subroutine provides a general solution to the matrix equation:

$$\underset{\mathrm{nxn}}{\underline{A}}\ \underset{\mathrm{nx1}}{\underline{u}} = \underset{\mathrm{nx1}}{\underline{b}} \qquad (4.2)$$

(See Appendix F1) Upon convergence of the fitting procedures a χ^2 goodness of fit test is performed to check whether or not the fitted form of the probability density function adequately describes the binned data. Notice that the degrees of freedom for this test are given by

$$\text{D.F.} = k - s - 1 \qquad (4.3)$$

where

k = no. of cells with fitted numbers of observations greater than 6
s = degree of approximating polynomial

If the fitted number of cell counts for a particular cell are less than 6, then it is collapsed into the next cell. The value of k may therefore be equal to the number of cells but this is not necessarily true. The program iterates, increasing the degree of the polynomial by 1 each iteration until a satisfactory fit is achieved. The goodness of fit is examined using the χ^2 test at the 25% significance level. If the degrees of freedom of the observed χ^2 is zero, a warning will be printed to this effect, however the confidence band calculation will be carried out using the last model calculated. Caution is advised when using results obtained this way.

Once a model passes the goodness of fit test the program enters the next phase in which confidence bands are evaluated. The first step is to evaluate the observed Fisher information matrix. The 95% confidence bands for the cumulative distribution function are calculated in subroutine CDF and finally the 95% confidence bands for the probability density functions are calculated in subroutine PDF.

Further discussion of the computer implementation of the confidence bands program is provided in Appendix F of this report, as is a discussion of the theoretical basis for the technique. A full listing of the two computer programs used for confidence band estimation (BIN and CBAND) is provided in Appendix G along with variable dictionaries for these two programs.

4.3 Examples

Three examples of 95% confidence bands calculated by the programs BIN and CBAND are included in this section.

The first two examples are of known distributions, randomly sampled using 500 trials. Figure 4.4 illustrates confidence bands fitted to the cumulative distribution function and the probability density function of a normal distribution. The confidence bands illustrated in Figure 4.5 are fitted to log transformed random samples drawn from a lognormal distribution.

The third example, shown in Figure 4.6, presents confidence bands fitted to actual output from UTAP. Radium concentration in fish at t=100 years is used in this example. The figure actually represents confidence bands on the log-transformed values obtained from 200 random trials.

FIGURE 4.4

PLOTS OF 95% CONFIDENCE BANDS FOR A NORMAL DISTRIBUTION (500 TRIALS)

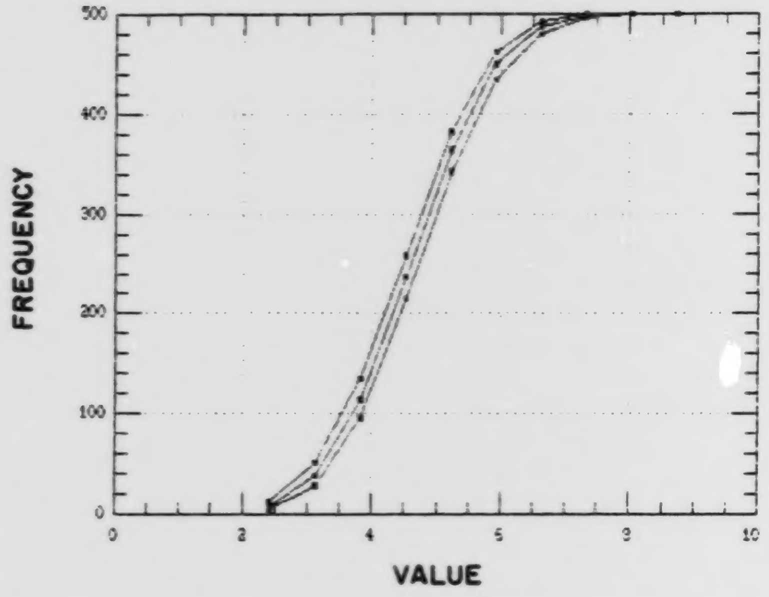

A) CUMULATIVE DISTRIBUTION FUNCTION

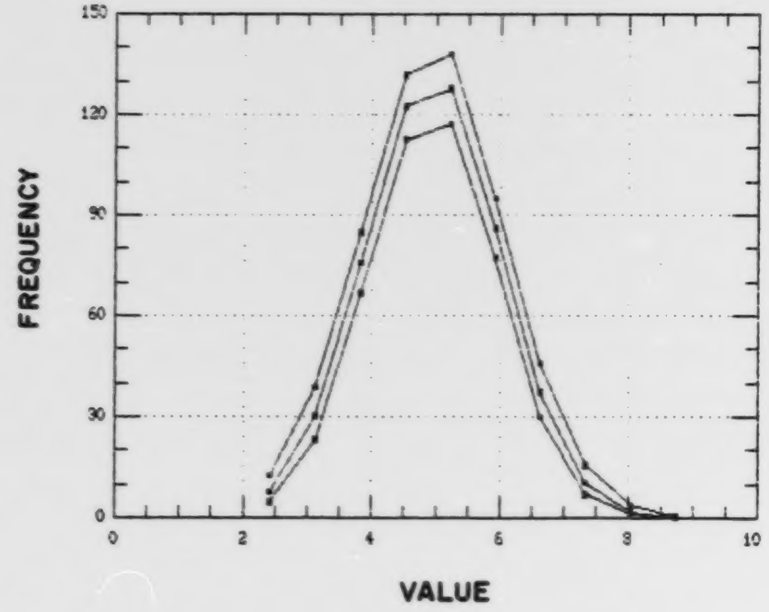

B) PROBABILITY DISTRIBUTION FUNCTION

FIGURE 4.5

PLOTS OF 95% CONFIDENCE BANDS
FOR A LOG - TRANSFORMED LOGNORMAL DISTRIBUTION
(500 TRIALS)

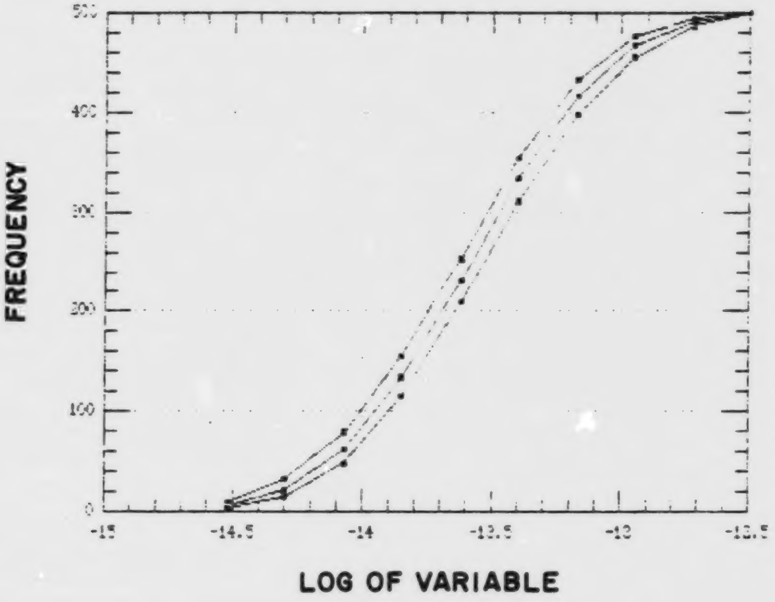

A) CUMULATIVE DISTRIBUTION FUNCTION

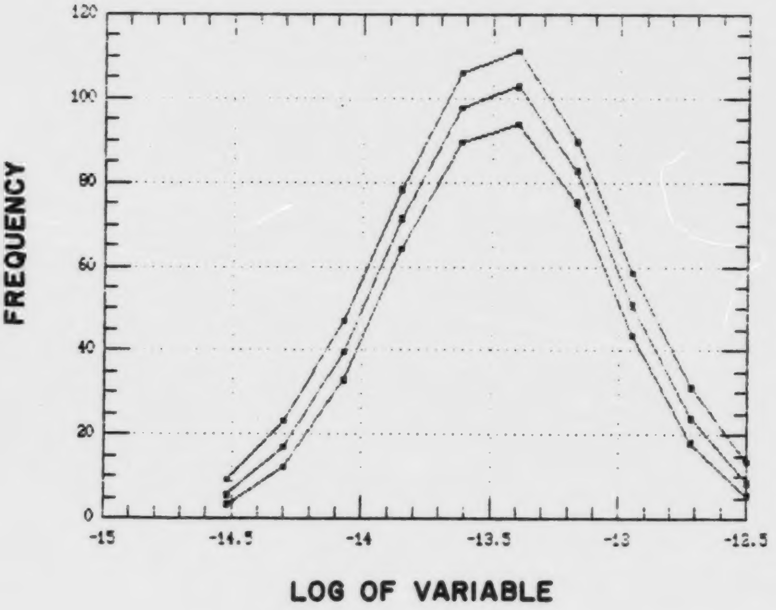

B) PROBABILITY DENSITY FUNCTION

FIGURE 4.6

PLOTS OF 95% CONFIDENCE BANDS FOR THE LOGARITHM OF RADIUM IN FISH AT 100 YEARS (200 TRIALS)

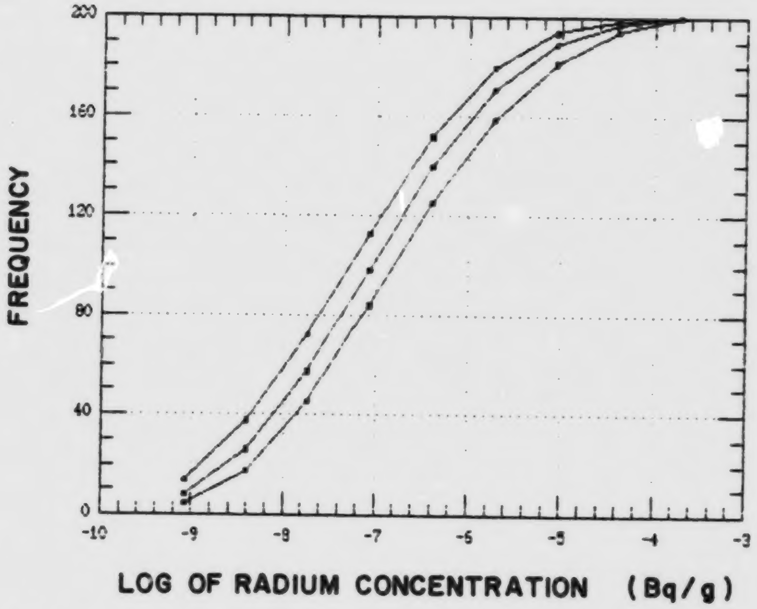

A) CUMULATIVE DISTRIBUTION FUNCTION

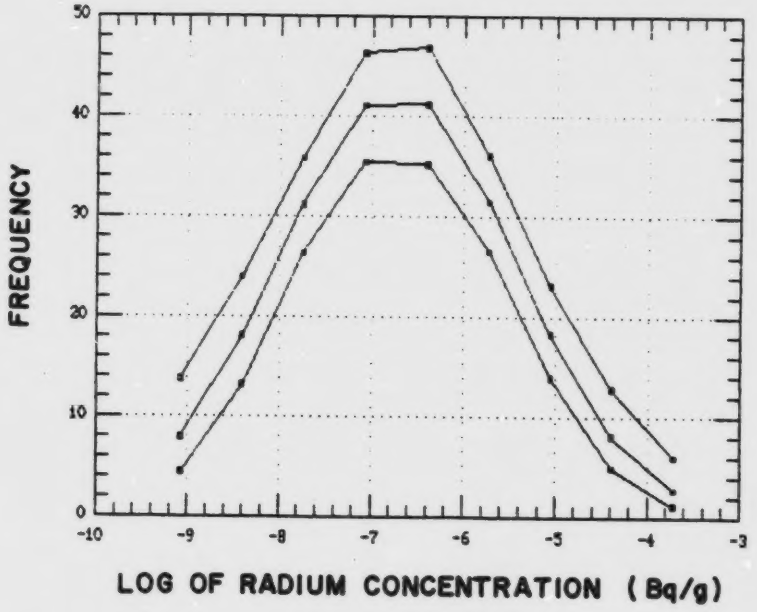

B) PROBABILITY DENSITY FUNCTION

REFERENCES

Abromowitz and Stegun, 1964. "Handbook of Mathematical Functions." U.S. Department of Commerce.

Andres, T., and Goodwin, B., 1985. "Techniques for Handlings Correlated Parameters."

Fishman, G.S., 1978. "Principles of Discrete Event Simulation, Wiley, N.Y."

Fishman, G.S., and Moore, L.R., 1980. "A Statistical Evaluation of Multiplicative Congruential Generators with Modulus 2^{31}-1." Technical Report, 78-11, University of North Carolina at Chapel Hill.

Golder Associates, Beak Consultants, SENES Consultants and Cumming, Cockburn and Associates, 1986. Lacnor Field Study, Ellot Lake, Ontario. Prepared for the National Uranium Tailings Program, CANMET, EMR, under Supply and Services Contract No. 0SQ84-00196.

Kennedy, W.J. and Gentle, J.E., 1980. "Statistical Computing." Marcel Dekker.

Kleijnen, J.P.C., 1974. "Statistical Techniques in Simulation - Part 1." Marcel Dekker Inc., New York.

Marse, K., and Roberts, D.S., 1983. "Implementing a Portable FORTRAN Uniform (0, 1) Generator, Simulation."

Schrage, L., 1979. "A More Portable FORTRAN Random Number Generator ACM Transactions on Mathematical Software 5."

SENES Consultants Limited, 1984. "A Study to Develop and Demonstrate Techniques for the Probabilistic Assessment of the Long-Term Effects of Uranium Mill Tailings in Canada - Phase 1." Research Report prepared for the National Uranium Tailings Program, CANMET, EMR, under Supply and Services Canada Contract No. 0SQ83-00236.

SENES Consultants Limited, 1985. "A Study to Develop and Demonstrate Techniques for the Probabilistic Assessment of the Long-Term Effects of Uranium Mill Tailings in Canada - Phase II." Research Report prepared for the National Uranium Tailings Program, CANMET, EMR, under Supply and Services Canada contract No. 0SQ84-00207.

SENES Consultants Limited, 1986. "Probabilistic Model Development for the Assessment of Long-Term Effects of Uranium Mill Tailings in Canada - Phase III." Research Report prepared for the National Uranium Tailings Program, CANMET, EMR, under Supply and Services Canada Contract No. 0SQ85-00182.

Spicer, C.C., 1972. "Algorithm AS52: Calculation of Power Sums of Deviations about the Mean." Applied Statistics 21, pp. 226-227.

Sturges, H.A., 1926. "The Choice of a Class Interval." Journal of the American Statistical Association. March.

Whiteshell Nuclear Research Establishment (WNRE), 1987. Comparison of UTAP.2 and SYVAC-UT3. Atomic Energy of Canada Limited. Report in preparation.

APPENDIX B

CONTROL MODULES

CODE LISTING

AND

VARIABLE DICTIONARY

Table B.1

Variable Dictionary for Control Modules

Variable	Type	Description	Units	Values
A	R	LOCATION PARAMETER FOR WEIBULL DISTRIBUTION		INPUT - WEIBUL
A	R	SHAPE PARAMETER FOR BETA DISTRIBUTION		INPUT - BETA
ACARC	R (4)	CARIBOU CONCENTRATION FROM VEGETATION CONSUMPTION	BQ/G	CALCULATED - ANIMAL
ADERC	R (4)	DEER CONCENTRATION FROM VEGETATION CONSUMPTION	BQ/G	CALCULATED - ANIMAL
AIRC	R (5,82)	AIR CONCENTRATION	BQ/M**3	CALCULATED - AIRDIS
AMOSC	R (4)	MOOSE CONCENTRATION FROM VEGETATION	BQ/G	CALCULATED - ANIMAL
AQVEGC	R (4)	CONCENTRATION IN AQUATIC VEGETATION	BQ/G	CALCULATED - WATVEG
ARB	I	NUMBER OF REGULAR AND ARBITRARY DISTRIBUTIONS		CALCULATED - INPUT1
AVEGC	R (4,80)	ABOVE GROUND VEGETABLES CONCENTRATION	BQ/G	CALCULATED - VEGCON
B	R	SCALE PARAMETER FOR WEIBULL DISTRIBUTION		INPUT - WEIBUL
B	R	SHAPE PARAMETER FOR BETA DISTRIBUTION		INPUT - BETA
BLANK1	R (4,80)	UNUSED VARIABLE FOR FUTURE OUTPUT		
BLANK2	R (10,10)	UNUSED VARIABLE FOR FUTURE OUTPUT		
BRWSC	R (4)	AVERAGE WATERSHED BROWSE CONCENTRATION	BQ/G	CALCULATED - VEGCON
BVEGC	R (4,80)	BELOW GROUND VEGETABLES CONCENTRATION	BQ/G	CALCULATED - VEGCON
C	R	SHAPE PARAMETER FOR WEIBULL DISTRIBUTION		INPUT - WEIBUL
CCOEFF	R	CORRELATION COEFFICIENT FOR CORRELATED DISTRIBUTION		INPUT - CORREL
CONC	R (10,4,3)	TAILINGS SOLID PHASE CONCENTRATION	(BQ OR MOL)/M**3	CALCULATED - SEXEC
CORNAM	C*6	CORRELATED PARAMETER INDEPENDANT VARIABLE NAME		INPUT
CORNUM	I (300)	CORRELATED PARAMETER INDEPENDENT PARAMETER REFERENCE NUMBER		CALCULATED - INPUT1
CPF	R (300,25)	ARBITRARY CUMULATIVE DISTRIBUTION FUNCTION		CALCULATED - CREATE
DAM	I	NUMBER OF GROUNDWATER FLOWPATHS		INPUT
DOSE	R (5,80)	TOTAL INDIVIDUAL DOSE	uSV/YEAR	CALCULATED - DOSEIN
DT	R	TIME INCREMENT	YEARS	INPUT
EFLAG	C*1 (300)	FLAG INDICATING IF SAMPLED VALUES ARE TO BE SAVED		INPUT - F/N =>FILE/NO
EMRATE	R (5)	EMISSION RATE FROM TAILINGS	BQ/S	CALCULATED - DUST, RADON
EROTOT	R	EROSION OF TAILINGS PILE OVER TIME STEP	KG	CALCULATED - EROS
EXPECT	R	EXPECTED VALUE OF NORMAL DISTRIBUTION		INPUT - NORMAL
FISHC	R (4,10)	CONCENTRATION OF RADIONUCLIDE IN FISH	BQ/G	CALCULATED - FISH
FISHD	R (5,80)	DOSE FROM FISH CONSUMPTION	uSV/YEAR	CALCULATED - DOSEIN
FNAME	C*12	FILE NAME		INPUT
FSAVE	C*1	DETAILED RESULTS FILE INDICATOR		INPUT - Y/N =>YES/NO
FUNIT	I	INPUT FILE UNIT NUMBER		4
FUNIT1	I	DETAILED RESULTS FILE UNIT NUMBER		1
FUNIT2	I	KEY FILE UNIT NUMBER		2
FWIND	R(16,6,6,20)	A.E.S. STAR DATA	KNOTS	INPUT

Table B.1 (continued)

Variable	Type	Description	Units	Values
GM	R	GEOMETRIC MEAN OF LOGNORMAL DISTRIBUTION		INPUT - LNORM
GMEAN	DP (300)	GEOMETRIC MEAN		CALCULATED - STATS
GN	I (300)	COUNTER USED FOR CALCULATING GEOMETRIC MOMENTS		CALCULATED - GMOMEN
GS1	DP (300)	VECTOR FOR UPDATING FIRST GEOMETRIC MOMENT		CALCULATED - GMOMEN
GS2	DP (300)	VECTOR FOR UPDATING SECOND GEOMETRIC MOMENT		CALCULATED - GMOMEN
GSD	DP (300)	NATURAL LOGARITHM OF GEOMETRIC STANDARD DEVIATION		CALCULATED - STATS
GSD	R	GEOMETRIC STANDARD DEVIATION OF LOGNORMAL DISTRIBUTION		INPUT - LNORM
GSDEV	DP (300)	GEOMETRIC STANDARD DEVIATION		CALCULATED - STATS
GSEG	I (5)	WATERSHED SEGMENT NUMBERS THAT GROUNDWATER FLOWS INTO		INPUT
GWATC	R (8,5)	GROUNDWATER CONCENTRATION	(BQ OR MOL)/M**3	CALCULATED - GWATER
GWLAYR	I (5)	GROUNDWATER FLOWPATH LAYERS		INPUT
I	I	ERROR NUMBER		INPUT - ERROR
I	I	COUNTER OF INPUT DISTRIBUTIONS		CALCULATED - CHOOSE
IERR	I	ERROR CODE FROM OPENING DISK FILES		CALCULATED - INPUT1, INPUT2
ILINE	I	INPUT FILE LINE NUMBER		CALCULATED - INPUT1, INPUT2
INHD	R (5,80)	DOSE FROM INHALATION	uSV/YEAR	CALCULATED
KURT	DP (300)	KURTOSIS		CALCULATED - STATS
LAKVOL	R (10)	LAKE VOLUMES	M**3	CALCULATED - INPUT2
LAREA	R (10)	LAKE AREAS OR RIVER LENGTHS AS APPROPRIATE	M**2 OR M	INPUT
LGM	R	LOGARITHM OF GEOMETRIC MEAN OF LOGNORMAL DISTRIBUTION		CALCULATED - LNORM
LGSD	R	LOGARITHM OF GEOMETRIC STANDARD DEVIATION OF LOGNORMAL DISTRIBUTION		CALCULATED - LNORM
LICHC	R (4)	AVERAGE LICHEN CONCENTRATION	BQ/G	CALCULATED - VEGCON
LMAX	R	MAXIMUM VALUE OF LOGUNIFORM DISTRIBUTION		INPUT - LOGUNI
LMIN	R	MINIMUM VALUE OF LOGUNIFORM DISTRIBUTION		INPUT - LOGUNI
LOC	I (300)	OUTPUT PARAMETER LOCATION CODES		INPUT
MAX	R	MAXIMUM VALUE OF NORMAL, LOGNORMAL, BETA, AND ARBITRARY DISTRIBUTIONS		INPUT - CREATE,NORMAL,LNORM
MAXSEG	I	MAXIMUM RECEPTOR WATER SOURCE SEGMENT NUMBER		CALCULATED - INPUT2
MEANX	R	MEAN OF INDEPENDENT VARIABLE FOR CORRELATED DISTRIBUTION		INPUT - CORREL
MEANY	R	MEAN OF DEPENDENT VARIABLE FOR CORRELATED DISTRIBUTION		INPUT - CORREL
MEATD	R (5,80)	DOSE FROM MEAT CONSUMPTION	uSV/YEAR	CALCULATED - DOSEIN
MIN	R	MINIMUM VALUE OF NORMAL, LOGNORMAL, BETA, AND ARBITRARY DISTRIBUTIONS		INPUT - CREATE,NORMAL,LNORM
N	I (300)	COUNTER USED FOR CALCULATING STATISTICAL MOMENTS		CALCULATED - MOMENT
NACELL	I (300)	NUMBER OF CELLS IN ARBITRARY DISTRIBUTIONS		INPUT - MAXIMUM 25
NAMEF	C*36 (300)	LABELS FOR OUTPUT TO KEY FILE		INPUT - NAMOUT
NARB	I	NUMBER OF ARBITRARY DISTRIBUTIONS		INPUT
NARRAY	I	NUMBER OF ARRAYS TO BE CHECKED FOR POSSIBLE OUTPUT		INPUT
NCORR	I	NUMBER OF CORRELATED PARAMETERS		INPUT
NDT	I	TIME INCREMENT	YEARS	INPUT
NFILE	I	NUMBER OF NON-TIME-VARIANT DISTRIBUTIONS FOR OUTPUT		CALCULATED - INPUT1

NODDIR I (10) WATERSHED SEGMENT END NODE DIRECTIONS INPUT

Table B.1 (continued)

Variable	Type	Description	Units	Values
NODRNG	I (10)	WATERSHED SEGMENT END NODE RINGS		INPUT
NOUT	I	TOTAL NUMBER OF OUTPUT PARAMETERS		CALCULATED - STATS
NPARM	I	NUMBER OF INPUT DISTRIBUTIONS		INPUT - MAXIMUM 300
NRECEP	I	NUMBER OF RECEPTOR LOCATIONS		INPUT - MAXIMUM 80
NRING	I	NUMBER OF RINGS		INPUT - MAXIMUM 5
NSEG	I	NUMBER OF WATERSHED SEGMENTS		INPUT - MAXIMUM 10
NSTART	I	RANDOM NUMBER SEED		INPUT/CALCULATED - RANDOM
NSTEPF	I	NUMBER OF TIME STEPS TO BE SAVED		INPUT - MAXIMUM 11
NSUB	I (300)	OUTPUT PARAMETER SUBSTANCE CODES		INPUT
NT	I	CURRENT SIMULATION TIME	YEARS	CALCULATED - EXEC
NTRIAL	I	TOTAL NUMBER OF TRIALS TO BE PERFORMED		INPUT
NTYPE	I (300)	DISTRIBUTION TYPE NUMBERS		INPUT
NUMF	I	COUNTER FOR VARIABLES TO BE SAVED		CALCULATED - TIMSEL, SELECT
NUMTRL	I	CURRENT TRIAL COUNT		CALCULATED - EXEC
NVAR	I (100)	NUMBER OF OUTPUTS FOR EACH VARIABLE		INPUT
NVARYF	I	NUMBER OF OUTPUT VARIABLES TO BE SAVED		CALCULATED - INPUT2
NYEARS	I	TOTAL TIME IN SIMULATION	YEARS	INPUT
OLDDIR	I	DIRECTION OF LAST WATERSHED SEGMENT READ IN		CALCULATED - INPUT2
OLDRNG	I	RING NUMBER OF LAST WATERSHED SEGMENT READ IN		CALCULATED - INPUT2
ORIGIN	R (300)	LOWER END OF FIRST CELL OF ARBITARY DISTRIBUTION		CALCULATED - CREATE
P1	R (300)	INPUT DISTRIBUTION DESCRIPTORS		INPUT
P2	R (300)	INPUT DISTRIBUTION DESCRIPTORS		INPUT
P3	R (300)	INPUT DISTRIBUTION DESCRIPTORS		INPUT
P4	R (300)	INPUT DISTRIBUTION DESCRIPTORS		INPUT
P5	R (300)	INPUT DISTRIBUTION DESCRIPTORS		INPUT
PH	R (4)	TAILINGS PH		CALCULATED - SEXEC
PI	R	THE VALUE PI		INPUT
POPDT	R	TOTAL DOSE FOR ENTIRE STUDY POPULATION	uSV/YEAR	CALCULATED - DOSEIN
PSAREA	R	AREA OCCUPIED BY WATERSHED SECTORS	M**2	CALCULATED - INPUT2
PSDIR	I (10)	DIRECTIONS BY WATERSHED SECTORS		INPUT
PSNUM	I	NUMBER OF SECTORS WATERSHED OCCUPIES		CALCULATED - INPUT2
PSRING	I (10)	RINGS BY WATERSHED SECTORS		INPUT
Q	C*1	RESPONSE TO WARNING MESSAGE		INPUT - Y/N =>YES/NO
R	R (6)	RING LIMITS	M	INPUT
R	R	RANDOM NUMBER RETURNED BY FUNCTION SUBROUTINE RANDOM		CALCULATED - SAMPLING ROUTINES
RADD	R (80)	DOSE FROM RADON	uSV/YEAR	CALCULATED - DOSEIN
RAREA	R (5)	SECTOR AREAS BY RING	M**2	CALCULATED - INPUT2
RCPNUM	I	RECEPTOR NUMBER		INPUT
RDIR	I (80)	RECEPTOR DIRECTIONS		INPUT - MAXIMUM 16
REG	I	NUMBER OF REGULAR DISTRIBUTIONS		CALCULATED - INPUT1
RFSEG	I (80)	RECEPTOR FISH SOURCE SEGMENT NUMBERS		INPUT
RNGMID	R (5)	RADIAL DISTANCES TO MIDPOINTS OF RINGS	M	CALCULATED - INPUT2
RPOP	I (80)	RECEPTOR POPULATION		INPUT
RRING	I (80)	RECEPTOR RING NUMBERS		INPUT
RTYPE	C*1 (80)	RECEPTOR TYPE		INPUT - C/A =>CRITICAL/AVERAGE
RWSSEG	I (80)	RECEPTOR WATER SOURCE SEGMENT NUMBERS		INPUT

RYEARS	R	TOTAL TIME IN SIMULATION	YEARS	INPUT

Table B.1 (continued)

Variable	Type	Description	Units	Values
S1	DP (300)	MEAN VALUES		CALCULATED - MOMENT
S2	DP (300)	SECOND MOMENT FOR UPDATING STATISTICS		CALCULATED - MOMENT
S3	DP (300)	THIRD MOMENT FOR UPDATING STATISTICS		CALCULATED - MOMENT
S4	DP (300)	FOURTH MOMENT FOR UPDATING STATISTICS		CALCULATED - MOMENT
SCRUNT	I	SCREEN UNIT NUMBER		
SDEPTH	R (10)	LAKE DEPTHS	M	INPUT
SDEV	DP (300)	STANDARD DEVIATION		CALCULATED - STATS
SDEVX	R	STANDARD DEVIATION OF CORRELATED DISTRIBUTION INDEPENDENT VARIABLE		INPUT - CORREL
SDEVY	R	STANDARD DEVIATION OF CORRELATED DISTRIBUTION DEPENDENT VARIABLE		INPUT - CORREL
SHEDAR	R (10)	CUMMULATIVE WATERSHED AREAS	M**2	INPUT
SHINED	R (5,80)	DOSE FROM GROUNDSHINE	uSV/YEAR	CALCULATED - DOSEIN
SKEW	DP (300)	SKEWNESS		CALCULATED - STATS
SKEWFG	C*1	SKEWNESS AND KURTOSIS INDICATOR		INPUT - Y/N =>YES/NO
SOILC	R (4,82)	SOIL CONCENTRATION	BQ/M**3	CALCULATED - SOIL
STDEV	R	STANDARD DEVIATION OF NORMAL DISTRIBUTION		INPUT - NORMAL
STYPE	C*1 (10)	WATERSHED SEGMENT TYPE		INPUT - R/L =>RIVER/LAKE
SUFOC	R (4,2)	SUMMER FOLLIAGE CONCENTRATION	BQ/G	CALCULATED - VEGCON
SUM	R	SUM OF CELL VALUES IN ARBITRARY DISTRIBUTION		CALCULATED - CREATE
T	R	CURRENT SIMULATION TIME	YEARS	CALCULATED - EXEC
TAREA	R	TOTAL AREA BETWEEN OUTER AND INNER RING LIMITS	M**2	CALCULATED - INPUT2
TFILE	R (12)	VECTOR CONTAINING TIME STEPS TO BE SAVED		INPUT
TITLE	C*40	RUN TITLE		INPUT
TMAX	R	LOGARITHM OF MAXIMUM VALUE OF LOGNORMAL DISTRIBUTION		CALCULATED - LNORM
TMIN	R	LOGARITHM OF MINIMUM VALUE OF LOGNORMAL DISTRIBUTION		CALCULATED - LNORM
TNUMBF	I	COUNT OF TIME STEPS SAVED		CALCULATED - TIMSEL
TNUMF	I	COUNT OF TIME STEPS SAVED		CALCULATED - SELECT
TVARY	C*1 (300)	TIME-VARIANT FLAG		INPUT - V/N =>VARIANT/NOT
UMAX	R	MAXIMUM VALUE OF UNIFORM DISTRIBUTION		INPUT - UNIFOR
UMIN	R	MINIMUM VALUE OF UNIFORM DISTRIBUTION		INPUT - UNIFOR
UNIT	I	DEVICE OR FILE UNIT NUMBER		INPUT - FILER
UNIT	R (300)	ARBITRARY DISTRIBUTION UNIT WIDTH		CALCULATED - CREATE
V	R (300,25)	ARBITRARY PROBABILITY DISTRIBUTION FUNCTION		CALCULATED - CREATE
VARIED	I (300)	TIME-VARIANT DISTRIBUTION NUMBERS FOR DIRECT ACCESS		CALCULATED - INPUT1
VARN	I	NUMBER OF NON-TIME-VARIANT DISTRIBUTIONS		CALCULATED - INPUT1
VARNAM	C*6 (300)	NAMES OF OUTPUT PARAMETERS		INPUT
VARNOT	I (300)	NON-TIME-VARIANT DISTRIBUTION NUMBERS FOR DIRECT ACCESS		CALCULATED - INPUT1
VARTIT	C*6 (300)	VECTOR OF NAMES OF INPUT PARAMETERS		INPUT
VARY	I	NUMBER OF TIME-VARIANT DISRIBUTIONS		CALCULATED - INPUT1
VARYF	I	NUMBER OF TIME-VARIANT DISTRIBUTIONS FOR OUTPUT		CALCULATED - INPUT1
VECTOR	C*9 (5)	VARIABLE USED FOR OUTPUTING STATISTICS		CALCULATED - OUTPUT
VEGD	R (5,80)	DOSE FROM VEGETABLE CONSUMPTION	uSV/YEAR	CALCULATED - DOSEIN
VMAX	R	MAXIMUM VALUE OF TRIANGULAR DISTRIBUTION		INPUT - TRIANG

Table B.1 (continued)

Variable	Type	Description	Units	Values
VMIN	R	MINIMUM VALUE OF TRIANGULAR DISTRIBUTION		INPUT - TRIANG
VMODE	R	PEAK VALUE OF TRIANGULAR DISTRIBUTION		INPUT - TRIANG
WATAVG	R (4)	AVERAGE WATER CONCENTRATION BY SUBSTANCE	BQ/M**3	CALCULATED - RIVER, LAKE
WATC	R (8,10)	WATER CONCENTRATION	(BQ OR MOL)/M**3	CALCULATED - LAKE, RIVER
WATD	R (5,80)	DOSE FROM DRINKING WATER CONSUMPTION	uSV/YEAR	CALCULATED - DOSEIN
WATPH	R (10)	PH IN LAKES AND RIVERS		CALCULATED - LAKE, RIVER
WCARC	R (4)	CARIBOU CONCENTRATION FROM WATER CONSUMPTION	BQ/G	CALCULATED - ANIMAL
WCONC	R (10,4,3)	TAILINGS LIQUID PHASE CONCENTRATION	(BQ OR MOL)/M**3	CALCULATED - SEXEC
WDERC	R (4)	DEER CONCENTRATION FROM WATER CONSUMPTION	BQ/G	CALCULATED - ANIMAL
WINDFG	C*1	FLAG INDICATING IF WIND IS TIME-VARIANT		INPUT - Y/N =>YES/NO
WMOSC	R (4)	MOOSE CONCENTRATION FROM WATER PATHWAYS	BQ/G	CALCULATED - ANIMAL
X	DP	VALUE ON WHICH STATISTICS ARE CALCULATED (SAME AS Z1)		INPUT - MOMENT, GMOMEN
XDUM	R	VALUE TO BE SAVED FOR OUTPUT		CALCULATED - SORT
XIN	R (300)	RANDOM VALUES SAMPLED FROM DISTRIBUTIONS		CALCULATED - CHOOSE
XMAX	R (300)	MAXIMUM VALUES FOR STATISTICS		CALCULATED - STATS
XMIN	R (300)	MINIMUM VALUES FOR STATISTICS		CALCULATED - STATS
XN	DP	NUMBER OF TRIALS STATISTICS CALCULATED ON		CALCULATED - STATS
XOUT	R (300)	VECTOR OF OUTPUT VALUES		CALCULATED - SEND
XVALUE	R (300)	SAMPLED DISTRIBUTION VALUES (SAME AS XIN)		CALCULATED - CORREL
Z1	DP	VALUE ON WHICH STATISTICS ARE CALCULATED		CALCULATED - STATS

B.2 Code Listing for Control Modules

B.2.1 Main Program

```
C FILE 'EXEC.FOR'
C
C     EXECUTIVE MODULE CALLS CONTROL MODULES AND COMPONENT
C     MODULES' CONTROL MODULE, STEPPING THROUGH TIME FOR EACH
C     TRIAL
C
      PROGRAM UTAP
C
      INCLUDE 'IO.INC'
      INCLUDE 'CONC.INC'
      INCLUDE 'RECEP.INC'
      INCLUDE 'STATS.INC'
      INCLUDE 'COUNTS.INC'
      INCLUDE 'INFO.INC'
      INCLUDE 'OUT.INC'
      INCLUDE 'INPT.INC'
      INCLUDE 'UPDATE.INC'
      INCLUDE 'PARAM.INC'
      INCLUDE 'INTERM.INC'
      INCLUDE 'WIND.INC'
C
C     CALL INPUT MODULES
C
      CALL INPUT1
      CALL INPUT2
C
C     CALL SAMPLING MODULES
C
      CALL CREATE
      WRITE(SCRUNT,300)
      DO 10 NUMTRL=1,NTRIAL
C
C        SAVE RANDOM NUMBER SEED
C
         OPEN(3,'SEED')
         WRITE(3,'(I10)')NSTART
         CLOSE(3)
C
C        SAMPLE NON-TIME-VARIANT INPUT DISTRIBUTIONS
C
         DO 20 I=1,VARN
            CALL CHOOSE(VARNOT(I))
20       CONTINUE
         NTIME=NYEARS/NDT+1
         DO 30 IYR = 1,NTIME
C
C           SAMPLE TIME-VARIANT DISTRIBUTIONS
C
            IF(VARY.GE.1)THEN
               DO 40 I=1,VARY
                  CALL CHOOSE(VARIED(I))
40             CONTINUE
```

```
               ENDIF
               NT=(IYR-1)*NDT
               T=FLOAT(NT)
               WRITE(SCRUNT,100)NUMTRL,NT
C
C              CALL COMPONENT MODULES
C
               CALL COMEX
C
C              CALL OUTPUT SELECTION ROUTINES
C
               CALL TIMSEL
               CALL SELECT
 30         CONTINUE
            CALL SAVEIN
C
C           CALL STATISTICS MODULES
C
            CALL STATS
C
C           CALL OUTPUT MODULES
C
            CALL WRITE
 10      CONTINUE
         CALL NAMOUT
         CALL OUTPUT
         WRITE(SCRUNT,300)
         WRITE(SCRUNT,200)
         STOP
 100     FORMAT(' TRIAL NUMBER : ',I4,4X,'TIME : ',I5)
 200     FORMAT(' RUN COMPLETED')
 300     FORMAT(///)
         END
```

B.2.2 Input Routines

```
C FILE 'INPUT.FOR'
C
      SUBROUTINE INPUT1
C
C      THE FOLLOWING SUBROUTINE INPUTS THE FILE CONTAINING THE
C      PROBABILISTIC PARAMATER DESCRIPTIONS AND ALLOWS THE USER
C      TO SAVE INPUTS TO KEY AND DETAILED RESULTS FILES
C
      INCLUDE 'IO.INC'
      INCLUDE 'COUNTS.INC'
      INCLUDE 'PARAM.INC'
      CHARACTER*12 FNAME
      CHARACTER*6 CORNAM
      CHARACTER*1 TVARY(300)
      INTEGER*2 REG,ARB,NCORR
      SCRUNT=0
      FUNIT1=1
      FUNIT2=2
      FUNIT=4
      WRITE(SCRUNT,1000) 3
      CALL FILER(SCRUNT)
C
C     OPEN FIRST INPUT FILE
C
      WRITE (SCRUNT,1250)
      READ (SCRUNT,1400) FNAME
      WRITE (SCRUNT,1350) FNAME
      OPEN (FUNIT,FILE=FNAME,STATUS='OLD',IOSTAT=IERR)
      IF (IERR.NE.0) CALL ERROR (29,0)
      ILINE=1
      READ (FUNIT,1400,END=998,ERR=996) TITLE
C
C     OPEN OUTPUT FILE(S)
C
      ILINE=ILINE+1
      READ (FUNIT,1410,END=998,ERR=996) FSAVE,SKEWFG
      ILINE=ILINE+1
      READ (FUNIT,1400,END=998,ERR=996) FNAME
      IF (FSAVE.EQ.'Y') THEN
C
C        OPEN DETAILED RESULTS FILE
C
         WRITE (SCRUNT,1350) FNAME
         OPEN (FUNIT1,FILE=FNAME,STATUS='NEW',IOSTAT=IERR)
         IF (IERR.NE.0) THEN
            CALL ERROR (102,0)
            OPEN (FUNIT1,FILE=FNAME)
         ENDIF
      ENDIF
      ILINE=ILINE+1
      READ (FUNIT,1400,END=998,ERR=996) FNAME
C
C     OPEN KEY FILE
C
```

```
      WRITE (SCRUNT,1350) FNAME
      OPEN (FUNIT2,FILE=FNAME,STATUS='NEW',IOSTAT=IERR)
      IF (IERR.NE.0) THEN
         CALL ERROR (102,0)
         OPEN (FUNIT2,FILE=FNAME)
      ENDIF
C
C     READ COUNTERS AND CHECK TIME
C
      ILINE=ILINE+1
      READ (FUNIT,1450,END=998,ERR=996) NPARM,NARB,NCORR
      ILINE=ILINE+1
      READ (FUNIT,1550,END=998,ERR=996) NSTART,NTRIAL
      ILINE=ILINE+1
      READ (FUNIT,1460,END=998,ERR=996) RYEARS,DT
      NYEARS=INT(RYEARS)
      NDT=INT(DT)
      IF (MOD(RYEARS,DT).NE.0) CALL ERROR (19,ILINE)
      IF (FLOAT(NDT).NE.DT.OR.FLOAT(NYEARS).NE.RYEARS) CALL ERROR (32,
     &   ILINE)
      NFILE=0
      VARY=0
      VARN=0
      VARYF=0
      REG=NPARM-(NCORR+NARB)
      ARB=NPARM-NCORR
      DO 1050 I=1,NPARM
         IF (I.LE.REG) THEN
C
C           READ REGULAR DISTRIBUTIONS
C
            ILINE=ILINE+1
            READ(FUNIT,1500,END=999,ERR=996)VARTIT(I),EFLAG(I),NTYPE(I),
     &         TVARY(I),P1(I),P2(I),P3(I),P4(I)
            IF (NTYPE(I).EQ.2) THEN
               IF (P4(I).LE.P3(I)) CALL ERROR (31,ILINE)
            ELSEIF (NTYPE(I).EQ.3) THEN
               IF(P4(I).LE.P3(I)) CALL ERROR (30,ILINE)
            ELSEIF (NTYPE(I).EQ.6) THEN
               IF(P3(I).LE.P1(I)) CALL ERROR (33,ILINE)
            ELSEIF (NTYPE(I).EQ.8) THEN
               IF(P2(I).LE.P1(I).OR.P3(I).LE.0.0.OR.P4(I).LE.0.0) CALL
     &            ERROR (34,ILINE)
            ELSEIF (NTYPE(I).EQ.9.OR.NTYPE(I).EQ.10) THEN
               CALL ERROR (6,ILINE)
            ELSEIF (NTYPE(I).NE.1.AND.NTYPE(I).NE.4.AND.NTYPE(I).NE.5
     &         .AND.NTYPE(I).NE.7) THEN
               CALL ERROR (12,ILINE)
            ENDIF
         ELSEIF (I.LE.ARB) THEN
C
C           READ ARBITRARY DISTRIBUTIONS
C
            ILINE=ILINE+1
            READ(FUNIT,1610,END=999,ERR=996)VARTIT(I),EFLAG(I),NTYPE(I),
     &         TVARY(I),NACELL(I),P1(I),P2(I),(V(I,I2),I2=1,NACELL(I))
```

```
            IF (NTYPE(I).NE.9) CALL ERROR (8,ILINE)
         ELSE
C
C           READ CORRELATED DISTRIBUTIONS
C
            ILINE=ILINE+1
            READ(FUNIT,1600,END=999,ERR=996)VARTIT(I),EFLAG(I),NTYPE(I),
     &         TVARY(I),CORNAM,P1(I),P2(I),P3(I),P4(I),P5(I)
            IF (NTYPE(I).NE.10) CALL ERROR (7,ILINE)
            K=1
10          IF (VARTIT(K).EQ.CORNAM) THEN
               IF (TVARY(K).NE.'V'.OR.(TVARY(K).EQ.'V'.AND.TVARY(I).EQ.
     &            'V')) THEN
                  CORNUM(I)=K
               ELSE
                  CALL ERROR (18,ILINE)
               ENDIF
            ELSEIF (K.LT.I) THEN
               K=K+1
               GOTO 10
            ELSE
               CALL ERROR (4,ILINE)
            ENDIF
         ENDIF
         IF (TVARY(I).EQ.'V') THEN
            VARY=VARY+1
            VARIED(VARY)=I
            IF (EFLAG(I).EQ.'F') VARYF=VARYF+1
         ELSE
            VARN=VARN+1
            VARNOT(VARN)=I
            IF (EFLAG(I).EQ.'F') NFILE=NFILE+1
         ENDIF
1050  CONTINUE
      CLOSE (FUNIT)
      RETURN
996   CALL ERROR (3,ILINE)
998   CALL ERROR (5,ILINE)
999   CALL ERROR (9,ILINE)
1000  FORMAT (' UTAP - Version ',F3.1,/)
1250  FORMAT (/,' First Input File Name? ')
1350  FORMAT (' Opening File : ',A12)
1400  FORMAT (A)
1410  FORMAT (A1,1X,A1)
1450  FORMAT (3I4)
1460  FORMAT (2E7.2)
1500  FORMAT (A6,1X,A1,1X,I2,1X,A1,4E11.6)
1550  FORMAT (I10,I4)
1600  FORMAT (A6,1X,A1,1X,I2,1X,A1,1X,A6,5E11.6)
1610  FORMAT (A6,1X,A1,1X,I2,1X,A1,I3,2E11.6,25(F6.2))
      END
C
C
C
      SUBROUTINE INPUT2
C
```

```
C     SUBROUTINE PROMPTS FOR INPUT FILE AND READS INPUT INFORMATION
C     SPECIFIC TO UTAP INCLUDING:
C        - NAME OF AIR DISPERSION DATA FILE
C        - RECEPTOR DATA
C        - WATERSHED DATA
C        - OUTPUT DATA CONTAINING INFO ON OUTPUT VARIABLES,
C          RECEPTOR NUMBERS, TIMES, ETC. OF VARIABLES TO BE SENT TO
C          DETAILED RESULTS AND KEY FILES
C     AIR DISPERSION FILE IS OPENNED AND DATA READ
C
      INCLUDE 'IO.INC'
      INCLUDE 'RECEP.INC'
      INCLUDE 'COUNTS.INC'
      INCLUDE 'INFO.INC'
      INCLUDE 'WIND.INC'
      INTEGER*2 OLDDIR,OLDRNG,MAXSEG,RCPNUM
      INTEGER*4 R(6)
      CHARACTER*12 FNAME
      REAL*4 PI
      DATA PI /3.1415927/
C
C     OPEN SECOND INPUT FILE
C
      WRITE (SCRUNT,700)
      READ (SCRUNT,810) FNAME
      WRITE (SCRUNT,820) FNAME
      OPEN (FUNIT,FILE=FNAME,STATUS='OLD',IOSTAT=IERR)
      IF (IERR.NE.0) CALL ERROR(29,0)
C
C     READ FLAG FOR TIME VARIANCE OF STAR DATA AND FILE NAME
C
      ILINE=1
      READ (FUNIT,960,END=999,ERR=996) WINDFG
      ILINE=ILINE+1
      READ (FUNIT,810,END=999,ERR=996) FNAME
C
C     READ RECEPTOR INFORMATION
C
      ILINE=ILINE+1
      READ (FUNIT,730,END=999,ERR=996) NRECEP
      IF (NRECEP.GT.80) CALL ERROR (20,ILINE)
      NDREC=NREC+2
      ILINE=ILINE+1
      READ (FUNIT,730,END=999,ERR=996) NRING
      IF (NRING.GT.5) CALL ERROR (21,ILINE)
      I=NRING+1
      ILINE=ILINE+1
      READ (FUNIT,710,END=999,ERR=996) (R(J),J=1,I)
      DO 35 J=1,I
         R(J)=1000*R(J)
35    CONTINUE
      DO 30 J=1,NRING
         IF (R(J).GE.R(J+1)) CALL ERROR (22,ILINE)
         RNGMID(J)=FLOAT(R(J)+R(J+1))/2.0
         RAREA(J)=PI*(R(J+1)**2-R(J)**2)/16.
30    CONTINUE
```

```
      TAREA=PI*(R(NRING+1)**2-R(1)**2)
      MAXSEG=0
      MFISH=0
      DO 40 I=1,NRECEP
      ILINE=ILINE+1
         READ(FUNIT,720,END=999,ERR=996)RCPNUM,RDIR(I),RRING(I),
     &      RWSSEG(I),RFSEG(I),RTYPE(I),RPOP(I)
         IF (RCPNUM.NE.I) CALL ERROR (10,ILINE)
         IF (RRING(I).GT.NRING) CALL ERROR (23,ILINE)
         IF (RWSSEG(I).GT.MAXSEG) MAXSEG=RWSSEG(I)
         IF (RFSEG(I).GT.MFISH) MFISH=RFSEG(I)
         IF (RTYPE(I).NE.'C') RTYPE(I)='A'
40    CONTINUE
C
C     READ & CHECK WATERSHED INFORMATION
C
      OLDDIR=0
      OLDRNG=0
      PSNUM=0
      AREA=0.
      PSAREA=0.
      ILINE=ILINE+1
      READ (FUNIT,725,END=999,ERR=996) NSEG,DAM
      ILINE=ILINE+1
      READ (FUNIT,725,END=999,ERR=996) (GSEG(I),I=1,DAM)
      ILINE=ILINE+1
      READ (FUNIT,725,END=999,ERR=996) (GWLAYR(I),I=1,DAM)
      IF (MAXSEG.GT.NSEG) CALL ERROR (26,ILINE)
      IF (MFISH.GT.NSEG) CALL ERROR (17,ILINE)
      IF (NSEG.GT.8) CALL ERROR (13,ILINE)
      DO 50 I=1,NSEG
         ILINE=ILINE+1
         READ (FUNIT,730,END=999,ERR=996) NODE,STYPE(I),NODDIR(I),
     &      NODRNG(I),SDEPTH(I),SHEDAR(I),LAREA(I)
         IF (STYPE(I).EQ.'L') LAKVOL(I)=SDEPTH(I)*LAREA(I)
         IF (NODE.NE.I) CALL ERROR (1,ILINE)
         IF (AREA.GT.SHEDAR(I)) CALL ERROR(2,ILINE)
         AREA=SHEDAR(I)
         IF (OLDDIR.NE.NODDIR(I).OR.OLDRNG.NE.NODRNG(I)) THEN
            PSNUM=PSNUM+1
            PSDIR(PSNUM)=NODDIR(I)
            PSRING(PSNUM)=NODRNG(I)
            PSAREA=PSAREA+RAREA(NODRNG(I))
         ENDIF
         OLDDIR=NODDIR(I)
         OLDRNG=NODRNG(I)
50    CONTINUE
      IF (STYPE(1).EQ.'L') CALL ERROR (24,ILINE)
      DO 51 I=1,DAM
         IF (STYPE(GSEG(I)).EQ.'L')CALL ERROR(25,ILINE)
         IF (GWLAYR(I).GT.4.OR.GWLAYR(I).LT.1)CALL ERROR(14,ILINE)
         IF (GSEG(I).LT.1.OR.GSEG(I).GT.NSEG)CALL ERROR(35,ILINE)
51    CONTINUE
C
C     READ OUTPUT PARAMETER SPECIFICATIONS
C
```

```
      NVARYF=0
C
C     READ TIME STEPS TO BE SAVED
C
      ILINE=ILINE+1
      READ (FUNIT,900,END=999,ERR=996) NSTEPF
      IF (NSTEPF.GT.0) THEN
         ILINE=ILINE+1
         READ (FUNIT,920,END=999,ERR=996) (TFILE(I),I=1,NSTEPF)
         NTEST=-1
         DO 52 I=1,NSTEPF
            IFILE=INT(TFILE(I))
            IF (MOD(IFILE,NDT).NE.0) CALL ERROR (15,ILINE)
            IF (NTEST.GE.IFILE) CALL ERROR (11,ILINE)
            NTEST=IFILE
52       CONTINUE
         IF (NTEST.GT.NYEARS) CALL ERROR (16,ILINE)
      ELSE
         ILINE=ILINE+1
         READ (FUNIT,810,END=999,ERR=996)
      ENDIF
      TFILE(NSTEPF+1)=-1.
C
C     READ OUTPUT PARAMETERS
C
      ILINE=ILINE+1
      READ (FUNIT,730,ERR=996) NARRAY
      J=1
      DO 10 I=1,NARRAY
         ILINE=ILINE+1
         READ (FUNIT,940,END=999,ERR=996) VARNAM(I),NVAR(I)
         IF (NVAR(I).GT.0) THEN
            NVARYF=NVARYF+NVAR(I)
            KK=NVAR(I)
            DO 20 K=1,KK
               ILINE=ILINE+1
               READ (FUNIT,950,END=999,ERR=996) NSUB(J),LOC(J)
               J=J+1
20          CONTINUE
         ENDIF
10    CONTINUE
      NARRAY=I-1
      IFILE=(NVARYF+VARYF)*NSTEPF+NFILE
      IF (IFILE.GT.300) CALL ERROR (28,ILINE)
C
C     READ AIR DISPERSION DATA
C
      IF (WINDFG.EQ.'Y') THEN
         NYEAR=20
      ELSE
         WINDFG='N'
         NYEAR=1
      ENDIF
      WRITE (SCRUNT,820) FNAME
      OPEN (FUNIT,FILE=FNAME,STATUS='OLD',IOSTAT=IERR)
      IF (IERR.NE.0) CALL ERROR (29,0)
      ILINE=0
      DO 60 IY=1,NYEAR
         ILINE=ILINE+1
         READ (FUNIT,400,END=999,ERR=996)
         DO 70 J=1,6
            DO 80 I=1,16
               L=I+8
               IF (L.GT.16) L=L-16
               ILINE=ILINE+1
               READ (FUNIT,500,END=999,ERR=996) (FWIND(L,J,K,IY),K=1,6)
80          CONTINUE
70       CONTINUE
60    CONTINUE
      CLOSE (FUNIT)
      RETURN
996   CALL ERROR (3,ILINE)
999   CALL ERROR (5,ILINE)
400   FORMAT (1X)
500   FORMAT (7X,6(F7.5))
700   FORMAT (/,' Second Input File Name? ')
710   FORMAT (6I5)
720   FORMAT (5I3,1X,A1,I5)
725   FORMAT (5I3)
730   FORMAT (I3,1X,A1,2I3,3E9.3)
810   FORMAT (A)
820   FORMAT (' Opening File : ',A12)
900   FORMAT (I3)
920   FORMAT (11(E6.2))
940   FORMAT (A6,I3)
950   FORMAT (2I3)
960   FORMAT (2X,A1)
      END
C
C
C
      SUBROUTINE ERROR (I,ILINE)
C
C     SUBROUTINE GENERATES ERROR AND WARNING MESSAGES.  ALL ERRORS
C     TERMINATE THE PROGRAM.  WARNINGS ASK IF EXECUTION IS TO BE STOPPED
C     OR CONTINUED.
C
      INCLUDE 'IO.INC'
      CHARACTER*1 Q
      WRITE (SCRUNT,300)
      IF (I.LE.100) THEN
C
C        GENERATE ERROR MESSAGES
C
         WRITE (SCRUNT,300) ' ***************  ERROR  ***************'
         IF (I.EQ.1) THEN
            WRITE (SCRUNT,300) ' (001) WATER SOURCE SEGMENTS NOT IN ORDE
     &R'
         ELSEIF (I.EQ.2) THEN
            WRITE (SCRUNT,300) ' (002) WATERSHED AREAS MUST INCREASE'
         ELSEIF (I.EQ.3) THEN
            WRITE (SCRUNT,300) ' (003) ERROR IN INPUT FILE'
         ELSEIF (I.EQ.4) THEN
            WRITE (SCRUNT,300) ' (004) CORRELATED NAME NOT FOUND'
         ELSEIF (I.EQ.5) THEN
            WRITE (SCRUNT,300) ' (005) UNEXPECTED END OF DATA'
         ELSEIF (I.EQ.6) THEN
            WRITE (SCRUNT,300) ' (006) TYPE ERROR IN REGULAR DIST''ns'
         ELSEIF (I.EQ.7) THEN
            WRITE (SCRUNT,300) ' (007) TYPE ERROR IN CORRELATED DIST''ns
     &'
         ELSEIF (I.EQ.8) THEN
            WRITE (SCRUNT,300) ' (008) TYPE ERROR IN ARBITRARY DIST''ns'
         ELSEIF (I.EQ.9) THEN
            WRITE (SCRUNT,300) ' (009) NUMBER OF PARAMETERS INCORRECT'
         ELSEIF (I.EQ.10) THEN
            WRITE (SCRUNT,300) ' (010) RECEPTORS NOT LISTED IN ORDER'
         ELSEIF (I.EQ.11) THEN
            WRITE (SCRUNT,300) ' (011) TIME STEPS MUST INCREASE'
         ELSEIF (I.EQ.12) THEN
            WRITE (SCRUNT,300) ' (012) DISTRIBUTION NUMBER NOT DEFINED'
         ELSEIF (I.EQ.13) THEN
            WRITE (SCRUNT,300) ' (013) MAXIMUM OF 8 WATERSHED SEGMENTS A
     &LLOWED'
         ELSEIF (I.EQ.14) THEN
            WRITE (SCRUNT,300) ' (014) GROUNDWATER LAYERS NOT POSSIBLE'
         ELSEIF (I.EQ.15) THEN
            WRITE (SCRUNT,300) ' (015) CAN''T SAVE TIME STEPS SPECIFIED'
         ELSEIF (I.EQ.16) THEN
            WRITE (SCRUNT,300) ' (016) TIME FOR OUTPUT TOO BIG'
         ELSEIF (I.EQ.17) THEN
            WRITE (SCRUNT,300) ' (017) RECEPTOR FISH SOURCE NUMBER TOO B
     &IG'
         ELSEIF (I.EQ.18) THEN
            WRITE (SCRUNT,300) ' (018) CANNOT CORRELATE PARAMETERS'
         ELSEIF (I.EQ.19) THEN
            WRITE (SCRUNT,300) ' (019) TIME STEPS DON''T MATCH SIMULATIO
     &N TIME'
         ELSEIF (I.EQ.20) THEN
            WRITE (SCRUNT,300) ' (020) MAXIMUM OF 80 RECEPTORS ALLOWED'
         ELSEIF (I.EQ.21) THEN
            WRITE (SCRUNT,300) ' (021) MAXIMUM OF 5 RINGS ALLOWED'
         ELSEIF (I.EQ.22) THEN
            WRITE (SCRUNT,300) ' (022) RING LIMITS MUST INCREASE'
         ELSEIF (I.EQ.23) THEN
            WRITE (SCRUNT,300) ' (023) RECEPTOR RING NUMBER TOO BIG'
         ELSEIF (I.EQ.24) THEN
            WRITE (SCRUNT,300) ' (024) FIRST WATERSHED SEGMENT MUST BE R
     &IVER'
         ELSEIF (I.EQ.25) THEN
            WRITE (SCRUNT,300) ' (025) GROUNDWATER MUST FLOW INTO RIVER'
         ELSEIF (I.EQ.26) THEN
            WRITE (SCRUNT,300) ' (026) RECEPTOR WATER SOURCE NO. TOO BIG
     &'
         ELSEIF (I.EQ.27) THEN
            WRITE (SCRUNT,310) ' (027) CONVERGENCE FAILED IN FUNCTION',
     &         ILINE
            ILINE=0
         ELSEIF (I.EQ.28) THEN
            WRITE (SCRUNT,300) ' (028) TOO MANY OUTPUTS'
         ELSEIF (I.EQ.29) THEN
            WRITE (SCRUNT,300) ' (029) FILE NOT FOUND'
         ELSEIF (I.EQ.30) THEN
            WRITE (SCRUNT,300) ' (030) ERROR IN LOGNORMAL SPECIFIERS'
         ELSEIF (I.EQ.31) THEN
            WRITE (SCRUNT,300) ' (031) ERROR IN NORMAL SPECIFIERS'
         ELSEIF (I.EQ.32) THEN
            WRITE (SCRUNT,300) ' (032) TIME MUST BE IN WHOLE NUMBERS'
         ELSEIF (I.EQ.33) THEN
            WRITE (SCRUNT,300) ' (033) ERROR IN TRIANGULAR SPECIFIERS'
         ELSEIF (I.EQ.34) THEN
            WRITE (SCRUNT,300) ' (034) ERROR IN BETA SPECIFIERS'
         ELSEIF (I.EQ.35) THEN
            WRITE (SCRUNT,300) ' (035) GROUNDWATER OUTFLOWS NOT POSSIBLE
     &'
         ENDIF
      ELSE
C
C        GENERATE WARNING MESSAGES
C
         WRITE (SCRUNT,300) ' ***************  WARNING  ***************'
         IF (I.EQ.101) THEN
            WRITE (SCRUNT,300) ' (101)'
         ELSEIF (I.EQ.102) THEN
            WRITE (SCRUNT,300) ' (102) ABOUT TO OVER WRITE EXISTING FILE
     &'
         ENDIF
         WRITE (SCRUNT,300) '  - OK TO CONTINUE (Y/N)? '
         READ (SCRUNT,300) Q
         IF (Q.EQ.'Y'.OR.Q.EQ.'y') THEN
C
C           RESUME EXECTION
C
            WRITE (SCRUNT,300) ' RESUMING EXECUTION'
            RETURN
         ENDIF
      ENDIF
C
C     STOP PROGRAM
C
      WRITE (SCRUNT,300) ' PROGRAM TERMINATED'
      WRITE (SCRUNT,320) ILINE
      WRITE (SCRUNT,300) ' SEE USERS MANUAL APPENDIX A'
      STOP
300   FORMAT (A)
310   FORMAT (A37,I3)
320   FORMAT (' LAST LINE READ =',I4)
      END
```

B.2.3 Sampling Routines

```
C FILE 'SAMPLE.FOR'
C
      SUBROUTINE CREATE
C
C     THIS ROUTINE GENERATES COMPLEMENTARY CUMULATIVE PROB-
C     ABILITY FUNCTIONS (CPF) FOR INPUT ARBITRARY
C     DISTRIBUTIONS.
C
      INCLUDE 'PARAM.INC'
      INCLUDE 'COUNTS.INC'
      REAL*4 MAX,MIN,SUM
C
C     CHECK IF THERE ARE ANY ARBITRARY DISTRIBUTIONS
C
      IF (NARB.NE.0) THEN
         DO 10 I=1, NPARM
            IF (NTYPE(I).EQ.8.OR.NTYPE(I).EQ.9) THEN
               MIN=P1(I)
               MAX=P2(I)
C
C                 INITIALIZE ARBITRARY DISTRIBUTIONS
C
                  UNIT(I)=(MAX-MIN)/(FLOAT(NACELL(I))-1.)
                  ORIGIN(I)=MIN-UNIT(I)
C
C              CALCULATE CUMULATIVE PROBABILITY FUNCTIONS
C
               SUM=0.0
               DO 1800 J=1,NACELL(I)
                  SUM=SUM+V(I,J)
                  CPF(I,J)=SUM
1800           CONTINUE
               DO 1900 J=1,NACELL(I)
                  CPF(I,J)=CPF(I,J)/SUM
1900           CONTINUE
            ENDIF
 10      CONTINUE
      ENDIF
      RETURN
      END
C
C
C
      SUBROUTINE CHOOSE (I)
C
C     THIS ROUTINE WILL RETURN A VALUE FOR EACH PARAMETER.
C     IT CALLS THE APPROPRIATE SUBROUTINE DEPENDING ON THE
C     TYPE OF DISTRIBUTION SPECIFIED:
C                                         1 = CONSTANT
C                                         2 = NORMAL
C                                         3 = LOG NORMAL
C                                         4 = UNIFORM
C                                         5 = LOG UNIFORM
C                                         6 = TRIANGULAR
```

```
C                                            7 = WEIBULL
C                                            8 = BETA
C                                            9 = ARBITRARY
C                                           10 = CORRELATED
C
      INCLUDE 'INPT.INC'
      INCLUDE 'PARAM.INC'
      INCLUDE 'COUNTS.INC'
      IF (NTYPE(I).EQ.1) THEN
         XIN(I) = P1(I)
      ELSEIF (NTYPE(I).EQ.2) THEN
         CALL NORMAL (NSTART,P1(I),P2(I),P3(I),P4(I),XIN(I))
      ELSEIF (NTYPE(I).EQ.3) THEN
         CALL LNORM (NSTART,P1(I),P2(I),P3(I),P4(I),XIN(I))
      ELSEIF (NTYPE(I).EQ.4) THEN
         CALL UNIFOR (NSTART,P1(I),P2(I),XIN(I))
      ELSEIF (NTYPE(I).EQ.5) THEN
         CALL LOGUNI (NSTART,P1(I),P2(I),XIN(I))
      ELSEIF (NTYPE(I).EQ.6) THEN
         CALL TRIANG (NSTART,P1(I),P2(I),P3(I),XIN(I))
      ELSEIF (NTYPE(I).EQ.7) THEN
         CALL WEIBUL (NSTART,P1(I),P2(I),P3(I),XIN(I))
      ELSEIF (NTYPE(I).EQ.8) THEN
         CALL BETA (NSTART,P1(I),P2(I),P3(I),P4(I),XIN(I))
      ELSEIF (NTYPE(I).EQ.9) THEN
         CALL ARB (NSTART,I,XIN(I))
      ELSEIF (NTYPE(I).EQ.10) THEN
         CALL CORREL (NSTART,P1(I),P2(I),P3(I),P4(I),P5(I),CORNUM(I),
     &         XIN(I))
      ENDIF
      RETURN
      END
C
C
C
      SUBROUTINE NORMAL (NSTART,EXPECT,STDEV,MIN,MAX,XIN)
C
C     THIS ROUTINE GENERATES NORMALLY DISTRIBUTED VARIATES USING
C     THE INVERSE NORMAL CUMULATIVE PROBABILTY FUNCTION WITH n=2
C
      REAL*4 XIN,MIN,MAX,EXPECT,STDEV,R,V,T,Z,X
1000  CONTINUE
         R=RANDOM(NSTART)
         V=R-0.5
         T=SQRT(-ALOG(V*V))
         X=T-(2.30753+T*0.27061)/(1.+T*(0.99229+T*0.04481))
         Z=SIGN(X,V)
         XIN=Z*STDEV+EXPECT
      IF (XIN.LT.MIN.OR.XIN.GT.MAX) GOTO 1000
      RETURN
      END
C
C
C
      SUBROUTINE LNORM (NSTART,GM,GSD,MIN,MAX,XIN)
C
```

```
C     THIS ROUTINE GENERATES LOG-NORMALLY DISTRIBUTED VARIATES
C
      REAL*4 GM, GSD, LGM, LGSD, TMIN, TMAX, TEMP, MIN, MAX, XIN
      LGM=ALOG10(GM)
      LGSD=ALOG10(GSD)
      IF (MIN.LE.0.0) THEN
         TMIN=-1.0E37
      ELSE
         TMIN=ALOG10(MIN)
      ENDIF
      TMAX=ALOG10(MAX)
      IF (TMIN.GT.TMAX) THEN
         TEMP=TMIN
         TMIN=TMAX
         TMAX=TEMP
      ENDIF
      CALL NORMAL (NSTART,LGM,LGSD,TMIN,TMAX,TEMP)
      XIN=10.**TEMP
      RETURN
      END
C
C
C
      SUBROUTINE UNIFOR (NSTART,UMIN,UMAX,XIN)
C
C    THIS ROUTINE GENERATES UNIFORMLY DISTRIBUTED RANDOM NUMBERS
C    BETWEEN UMIN AND UMAX
C
      REAL*4 RANDOM,R,XIN,UMIN,UMAX
1000  R=RANDOM(NSTART)
      IF (UMIN.LE.UMAX) THEN
         XIN=UMIN+R*(UMAX-UMIN)
      ELSE
         XIN=UMAX+R*(UMIN-UMAX)
      ENDIF
      RETURN
      END
C
C
C
      SUBROUTINE LOGUNI (NSTART,LMIN,LMAX,XIN)
C
C    THIS ROUTINE GENERATES LOG-UNIFORMLY DISTRIBUTED RANDOM NUMBERS
C    BETWEEN LMIN AND LMAX
C
      REAL*4 RANDOM,R,XIN,LMIN,TEMP,LMAX
1000  R=RANDOM(NSTART)
      TEMP=ALOG10(LMIN)+R*(ALOG10(LMAX)-ALOG10(LMIN))
      XIN=10**TEMP
      RETURN
      END
C
C
C
      SUBROUTINE TRIANG (NSTART,VMIN,VMODE,VMAX,XIN)
C
```

```
C      THIS ROUTINE GENERATES TRIANGULARLY DISTRIBUTED VARIATES
C
      REAL*4 XIN,R,VMAX,VMIN,VMODE,Z1,Z2
1000  R=RANDOM(NSTART)
      Z1=VMAX-VMIN
      Z2=VMODE-VMIN
      IF (R.LE.Z2/Z1) THEN
         XIN=VMIN+SQRT(R*Z1*Z2)
      ELSE
         XIN=VMAX-SQRT((1.-R)*(VMAX-VMODE)*Z1)
      ENDIF
      RETURN
      END
C
C
C
      SUBROUTINE WEIBUL (NSTART,A,B,C,XIN)
C
C     THIS SUBROUTINE GENERATES RANDOM SAMPLES FROM WEIBULL
C     DISTRIBUTIONS BY TRANSFORMING UNIFORMLY DISTRIBUTED SAMPLES
C     TO A SPECIFIED WEIBULL DISTRIBUTION
C
      REAL*4 A,B,C,XIN,R
      INTEGER*4 NSTART
1000  R=RANDOM(NSTART)
      XIN=A+B*((-ALOG(R))**(1.0/C))
      RETURN
      END
C
C
C
      SUBROUTINE BETA (NSTART,MIN,MAX,A,B,XIN)
C
C     THIS SUBROUTINE GENERATES BETA DISTRIBUTED RANDOM NUMBERS USING
C     THE ACCEPTANCE-REJECTION METHOD A IF a OR b < or = 1 AND
C     METHOD B IF a OR b >1.
C
      REAL*4 MIN,MAX,A,B,XIN,R1,R2,V1,V2,W,AM1,BM1,ABM2,TEMP
      IF (A.LE.1.0.OR.B.LE.1.0) THEN
C
C        USE ACCEPTANCE-REJECTION METHOD A
C
10       CONTINUE
11          CONTINUE
               R1=RANDOM(NSTART)
               R2=RANDOM(NSTART)
               V1=R1**(1/A)
               V2=R2**(1/B)
               W=V1+V2
               IF (W-1.0) 20,20,11
20          CONTINUE
            XIN=V1/W
         IF (XIN.LT.MIN.OR.XIN.GT.MAX) GOTO 10
      ELSE
C
C     USE ACCEPTANCE-REJECTION METHOD B
```

```
C
          AM1=A-1.
          BM1=B-1.
          ABM2=AM1+BM1
          F=(ABM2**ABM2)/((AM1**AM1)*(BM1**BM1))
110       CONTINUE
111          CONTINUE
                R1=RANDOM(NSTART)
                R2=RANDOM(NSTART)
                XIN=R1
                TEMP=(XIN**AM1)*((1.-XIN)**BM1)*F
                IF (R2-TEMP) 120,111,111
120          CONTINUE
          IF (XIN.LT.MIN.OR.XIN.GT.MAX) GOTO 110
       ENDIF
       RETURN
       END
C
C
C
       SUBROUTINE ARB (NSTART,I,XIN)
C
C       THIS ROUTINE SAMPLES VALUES OF ARBITRARY VARIATES.
C
       INCLUDE 'PARAM.INC'
       INTEGER*2 ICELL,I
       REAL*4 XIN,R
       R=RANDOM(NSTART)
       DO 1100 ICELL=1,NACELL(I)
          IF (CPF(I,ICELL).GE.R) GOTO 1000
1100   CONTINUE
       ICELL=NACELL(I)
1000   XIN=ORIGIN(I)+ICELL*UNIT(I)
       RETURN
       END
C
C
C
       SUBROUTINE CORREL(NSTART,MEANY,SDEVY,CCOEFF,MEANX,SDEVX,CORNUM,XIN
      &)
C
C      THIS SUBROUTINE CALCULATES THE VALUE OF AN INPUT PARAMETER WHICH
C      IS CORRELATED WITH SOME PREVIOUS INPUT PARAMETER.  IT EMPLOYS
C      KLEIJNEN'S CORRELATED GENERATION TECHNIQUE (KLEIJNEN, J.P.C.
C      (1974) STATISTICAL TECHNIQUES IN SIMULATION - PART 1, MARCEL
C      DEKKER,N.Y.) AS PRESENTED BY ANDRES AND GOODWIN (1984).
C
       INCLUDE 'INPT2.INC'
       INTEGER*2 CORNUM
       REAL*4 MEANY,SDEVY,CCOEFF,MEANX,SDEVX,XIN,A,B,U,Z,X,Y
       A=CCOEFF*SDEVY/SDEVX
       B=MEANY-CCOEFF*MEANX*SDEVY/SDEVX
       CALL NORMAL (NSTART,0.0,1.0,-1.0E37,1.0E37,Z)
       U=SDEVY*Z*SQRT(1.0-CCOEFF**2)
       X=XVALUE(CORNUM)
       Y=A*X+B+U
      XIN=Y
      RETURN
      END
C
C
C
      FUNCTION RANDOM (NSTART)
C
C     THIS PORTABLE FORTRAN RANDOM NUMBER GENERATOR WAS
C     ADAPTED FROM THAT DESCRIBED BY K. MARSE AND S.D. ROBERTS
C     ('SIMULATION', OCTOBER, 1983; PP 135-139)
C
      INTEGER*4 B2E15,B2E16,H115,H131,LOW15,LOWPRD,MODLUS,
     &          MULT1,MULT2,OVFLOW
      MULT1=24112
      MULT2=26143
      B2E15=32768
      B2E16=65536
      MODLUS=2147483647
      H115=NSTART/B2E16
      LOWPRD=(NSTART-H115*B2E16)*MULT1
      LOW15=LOWPRD/B2E16
      H131=H115*MULT1+LOW15
      OVFLOW=H131/B2E15
      NSTART=(((LOWPRD-LOW15*B2E16)-MODLUS)+
     &   (H131-OVFLOW*B2E15)*B2E16)+OVFLOW
      IF (NSTART.LT.0) NSTART=NSTART+MODLUS
      H115=NSTART/B2E16
      LOWPRD=(NSTART-H115*B2E16)*MULT2
      LOW15=LOWPRD/B2E16
      H131=H115*MULT2+LOW15
      OVFLOW=H131/B2E15
      NSTART=(((LOWPRD-LOW15*B2E16)-MODLUS)+(H131-OVFLOW*B2E15)*B2E16)
     &   +OVFLOW
      IF (NSTART.LT.0) NSTART=NSTART+MODLUS
      RANDOM=(2*(NSTART/256)+1)/16777216.0
      RETURN
      END
```

B.2.4 Results Saving Routines

```
C FILE 'SAVE.FOR'
C
      SUBROUTINE TIMSEL
C
C     THIS SUBROUTINE SAVES TIME-VARIANT INPUT VARIABLES
C     FLAGGED FOR OUTPUT
C
      INCLUDE 'COUNTS.INC'
      INCLUDE 'INPT.INC'
      INCLUDE 'OUT.INC'
      NUMF=1
C
C     CHECK IF ANY DISTRIBUTIONS ARE TIME-VARIANT
C
      IF (VARYF.NE.0) THEN
C
C        INITIALIZE OR INCREMENT TIME COUNTERS
C
         IF (NT.EQ.0) TNUMBF=1
C
C        CHECK IF THIS TIME TO BE SAVED
C
         IF (TFILE(TNUMBF).EQ.T) THEN
            DO 40 I=1,VARY
               J=VARIED(I)
C
C              CHECK IF VALUE TO BE OUTPUT
C
               IF (EFLAG(J).EQ.'F'.AND.NSTEPF.GE.TNUMBF) THEN
C
C                 SORT VALUES AND SAVE
C
                  JF=NSTEPF*(NUMF-1)+NFILE+TNUMBF
                  NUMF=NUMF+1
                  XOUT(JF)=XIN(J)
               ENDIF
40          CONTINUE
            TNUMBF=TNUMBF+1
         ENDIF
      ENDIF
      RETURN
      END
C
C
C
      SUBROUTINE SELECT
C
C     THIS SUBROUTINE CHECKS WHETHER PARAMETER VALUES ARE TO
C     BE SAVED AT EACH TIME, T. IT INDICATES WHETHER VALUES ARE
C     TO BE WRITTEN TO STATISTICS FILE OR DETAILED RESULTS FILE
C     VECTORS
C
      INCLUDE 'COUNTS.INC'
      NUMF=1
      IF (NT.EQ.0) TNUMF=1
C
C     CHECK IF THIS TIME STEP IS TO BE SAVED
C
         IF (TFILE(TNUMF).EQ.T) THEN
            CALL SORT
            TNUMF=TNUMF+1
         ENDIF
      RETURN
      END
C
C
C
      SUBROUTINE SORT
C
C     THIS SUBROUTINE CHECKS ALL OUTPUT ARRAYS.  FOR ANY ARRAYS
C     CONTAINING PARAMETERS TO BE SAVED, THE CURRENT PARAMETER
C     VALUE IS WRITTEN TO A DUMMY VARIABLE FOR TRANSFER TO
C     SUBROUTINE 'SEND'.
C
      INCLUDE 'COUNTS.INC'
      INCLUDE 'INFO.INC'
      INCLUDE 'CONC.INC'
      REAL*4 XDUM
      K=1
      DO 1000 I=1,NARRAY
         IF (NVAR(I).NE.0) THEN
            DO 2000 J=1,NVAR(I)
C
C              REROUTE TOTALS FOR DOSE TO LAST ARRAY LOCATION
C
               IF (NUMTRL.EQ.1.AND.NSUB(K).EQ.11) NSUB(K)=5
C
C              FIND CORRECT OUTPUT VALUE
C
               IF (I.EQ.1) THEN
                  XDUM=WCONC(NSUB(K),LOC(K),3)
               ELSEIF (I.EQ.2) THEN
                  XDUM=CONC(NSUB(K),LOC(K),3)
               ELSEIF (I.EQ.3) THEN
                  XDUM=PH(LOC(K))
               ELSEIF (I.EQ.4) THEN
                  XDUM=WATC(NSUB(K),LOC(K))
               ELSEIF (I.EQ.5) THEN
                  XDUM=WATAVG(NSUB(K))
               ELSEIF (I.EQ.6) THEN
                  XDUM=WATPH(LOC(K))
               ELSEIF (I.EQ.7) THEN
                  XDUM=GWATC(NSUB(K),LOC(K))
               ELSEIF (I.EQ.8) THEN
                  XDUM=EMRATE(NSUB(K))
               ELSEIF (I.EQ.9) THEN
                  XDUM=EROTOT
               ELSEIF (I.EQ.10) THEN
                  XDUM=AIRC(NSUB(K),LOC(K))
               ELSEIF (I.EQ.11) THEN
```

```
                   XDUM=SOILC(NSUB(K),LOC(K))
                 ELSEIF (I.EQ.12) THEN
                   XDUM=AVEGC(NSUB(K),LOC(K))
                 ELSEIF (I.EQ.13) THEN
                   XDUM=BVEGC(NSUB(K),LOC(K))
                 ELSEIF (I.EQ.14) THEN
                   XDUM=SUFOC(NSUB(K),LOC(K))
                 ELSEIF (I.EQ.15) THEN
                   XDUM=BRWSC(NSUB(K))
                 ELSEIF (I.EQ.16) THEN
                   XDUM=LICHC(NSUB(K))
                 ELSEIF (I.EQ.17) THEN
                   XDUM=AQVEGC(NSUB(K))
                 ELSEIF (I.EQ.18) THEN
                   XDUM=FISHC(NSUB(K),LOC(K))
                 ELSEIF (I.EQ.19) THEN
                   XDUM=ADERC(NSUB(K))
                 ELSEIF (I.EQ.20) THEN
                   XDUM=WDERC(NSUB(K))
                 ELSEIF (I.EQ.21) THEN
                   XDUM=AMOSC(NSUB(K))
                 ELSEIF (I.EQ.22) THEN
                   XDUM=WMOSC(NSUB(K))
                 ELSEIF (I.EQ.23) THEN
                   XDUM=ACARC(NSUB(K))
                 ELSEIF (I.EQ.24) THEN
                   XDUM=WCARC(NSUB(K))
                 ELSEIF (I.EQ.25) THEN
                   XDUM=WATD(NSUB(K),LOC(K))
                 ELSEIF (I.EQ.26) THEN
                   XDUM=SHINED(NSUB(K),LOC(K))
                 ELSEIF (I.EQ.27) THEN
                   XDUM=INHD(NSUB(K),LOC(K))
                 ELSEIF (I.EQ.28) THEN
                   XDUM=RADD(LOC(K))
                 ELSEIF (I.EQ.29) THEN
                   XDUM=VEGD(NSUB(K),LOC(K))
                 ELSEIF (I.EQ.30) THEN
                   XDUM=FISHD(NSUB(K),LOC(K))
                 ELSEIF (I.EQ.31) THEN
                   XDUM=MEATD(NSUB(K),LOC(K))
                 ELSEIF (I.EQ.32) THEN
                   XDUM=DOSE(NSUB(K),LOC(K))
                 ELSEIF (I.EQ.33) THEN
                   XDUM=POPDT
                 ELSEIF (I.EQ.34) THEN
                   XDUM=BLANK1(NSUB(K),LOC(K))
                 ELSEIF (I.EQ.35) THEN
                   XDUM=BLANK2(NSUB(K),LOC(K))
                 ENDIF
                 CALL SEND (XDUM)
                 K=K+1
 2000          CONTINUE
            ENDIF
 1000 CONTINUE
      RETURN
      END
C
C
C
      SUBROUTINE SEND (XDUM)
C
C     SUBROUTINE ACCEPTS THE CURRENT VALUE OF A VARIABLE AND ALLOCATES
C     IF TO AN APPROPRIATE POSITION IN THE OUTPUT VECTOR.
C
      INCLUDE 'COUNTS.INC'
      INCLUDE 'OUT.INC'
      REAL*4 XDUM
C
C     SORT OUTPUTS AND SEND THE VARIABLES TO OUTPUT VECTOR
C
      JF=(NUMF-1+VARYF)*NSTEPF+TNUMF+NFILE
      XOUT(JF)=XDUM
      NUMF=NUMF+1
      RETURN
      END
C
C
C
      SUBROUTINE SAVEIN
C
C     THIS SUBROUTINE SAVES ALL VALUES OF SELECTED NON-TIME-VARIANT
C     INPUT PARAMETERS TO VECTOR XOUT.
C
      INCLUDE 'OUT.INC'
      INCLUDE 'INPT.INC'
      INCLUDE 'COUNTS.INC'
C
C     CHECK IF ANY INPUT VALUES TO BE SAVED
C
      IF (NFILE.NE.0) THEN
         NFIL=0
         DO 10 J=1,VARN
            I=VARNOT(J)
            IF (EFLAG(I).EQ.'F') THEN
C
C              SAVE VALUE TO OUTPUT VECTOR
C
               NFIL=NFIL+1
               XOUT(NFIL)=XIN(I)
            ENDIF
10       CONTINUE
      ENDIF
      RETURN
      END
```

B.2.5 Statistics Routines

```
C FILE 'STATS.FOR'
C
      SUBROUTINE STATS
C
C     SUBROUTINE STATS CALCULATES SUMMARY STATISTICS FOR VARIABLES
C     CONTAINED IN THE VECTOR XOUT. THE ANALYSIS INVOLVES UPDATING
C     CALCULATIONS WHICH ARE PERFORMED IN SUBROUTINES MOMENT AND
C     GMOMENT.
C
      INCLUDE 'STATS.INC'
      INCLUDE 'OUT.INC'
      INCLUDE 'COUNTS.INC'
      INCLUDE 'UPDATE.INC'
      DOUBLE PRECISION XN,GSD(300),Z1
C
C     INITIALIZE STATISTICS ON FIRST TRIAL
C
      IF (NUMTRL.EQ.1) THEN
         NOUT=NSTEPF*(VARYF+NVARYF)+NFILE
         DO 1100 IDIST1=1,NOUT
            XMAX(IDIST1)=-1.0E+37
            XMIN(IDIST1)=+1.0E+37
            GN(IDIST1)=0
            N(IDIST1)=0
1100     CONTINUE
      ENDIF
C
C     ON EACH TRIAL, MAXIMUM,MINIMUM AND VARIOUS MOMENTS ARE UPDATED
C     FOR EACH PARAMETER.
C
      DO 1360 ID=1,NOUT
         Z1=XOUT(ID)
         IF (Z1.GT.XMAX(ID)) XMAX(ID)=SNGL(Z1)
         IF (Z1.LT.XMIN(ID)) XMIN(ID)=SNGL(Z1)
         CALL MOMENT (Z1,N(ID),S1(ID),S2(ID),S3(ID),S4(ID))
         CALL GMOMEN (Z1,GN(ID),GS1(ID),GS2(ID))
1360  CONTINUE
C
C     FOLLOWING THE FINAL TRIAL, THE CUMULATIVE MOMENT RESULTS ARE
C     USED TO CALCULATE SUMMARY STATISTICS.
C
      IF (NUMTRL.EQ.NTRIAL) THEN
         DO 1400 I=1,NOUT
            XN=DBLE(N(I))
            SDEV(I)=-999.
            SKEW(I)=-999.
            KURT(I)=-999.
            IF(N(I).GT.1)THEN
               SDEV(I)=DSQRT(S2(I)/(XN-1.0))
               IF(N(I).GT.2.AND.S2(I).GT.0.0)THEN
                  SKEW(I)=(S3(I)/XN)/((S2(I)/XN)**1.5)
                  IF(N(I).GT.3)KURT(I)=(S4(I)/XN)/((S2(I)/XN)**2.0)
               ENDIF
            ENDIF
         GMEAN(I)=-999.
         GSDEV(I)=-999.
         IF(GN(I).GE.1)THEN
            GMEAN(I)=DEXP(GS1(I))
            IF(GN(I).GE.2)THEN
               GSD(I)=DSQRT(GS2(I)/DBLE(GN(I)-1))
               GSDEV(I)=DEXP(GSD(I))
            ENDIF
         ENDIF
1400     CONTINUE
      ENDIF
      RETURN
      END
C
C
C
      SUBROUTINE MOMENT (X,N,S1,S2,S3,S4)
C
C     THIS SUBROUTINE CALCULATES THE FIRST FOUR MOMENTS
C     OF A RANDOM VARIABLE USING AN ALGORITHM BY C.C. SPICER
C     (APPLIED STATISTICS 21,226-227 (1972)).
C
      DOUBLE PRECISION X,S1,S2,S3,S4,AN,AN1,DX,DX2
      INTEGER*2 N
      N=N+1
      IF (N.EQ.1) THEN
         S1=X
         S2=0.0
         S3=0.0
         S4=0.0
      ELSE
         AN=N
         AN1=AN-1.0
         DX=(X-S1)/AN
         DX2=DX*DX
         S4=S4-DX*(4.0*S3-DX*(6.0*S2+AN1*(1.0+AN1**3)*DX2))
         S3=S3-DX*(3.0*S2-AN*AN1*(AN-2.0)*DX2)
         S2=S2+AN*AN1*DX2
         S1=S1+DX
      ENDIF
      RETURN
      END
C
C
C
      SUBROUTINE GMOMEN (X,N,GS1,GS2)
C
C     THIS SUBROUTINE CALCULATES THE GEOMETRIC MEAN AND
C     STANDARD DEVIATION USING THE METHOD OUTLINED IN
C     SUBROUTINE 'MOMENTS'.
C
      DOUBLE PRECISION X,GX,GS1,GS2,DX,DX2,AN,AN1
      INTEGER*2 N
      IF (X.GT.0.0) THEN
         GX=DLOG(X)
         N=N+1
```

```
          IF (N.EQ.1) THEN
             GS1=GX
             GS2=0.0
          ENDIF
          AN=FLOAT(N)
          AN1=FLOAT(N)-1.0
          DX=(GX-GS1)/AN
          DX2=DX*DX
          GS2=GS2+AN*AN1*DX2
          GS1=GS1+DX
       ENDIF
       RETURN
       END
```

B.2.6 Output Routines

```
C FILE 'OUTPUT.FOR'
C
       SUBROUTINE WRITE
C
C      WRITES VALUES CONTAINED IN 'XOUT' (SAMPLED INPUTS AND
C      CALCULATED PARAMETERS) TO DETAILED RESULTS FILE (UNIT 1)
C
       INCLUDE 'OUT.INC'
       INCLUDE 'IO.INC'
       INCLUDE 'COUNTS.INC'
       IF (FSAVE.EQ.'Y'.AND.NOUT.GT.0) THEN
          IF (NUMTRL.EQ.1) CALL FILER (FUNIT1)
          WRITE (FUNIT1,900) (XOUT(I),I=1,NOUT)
       ENDIF
       RETURN
900    FORMAT (2(150(1X,E9.3)))
       END
C
C
C
       SUBROUTINE NAMOUT
C
C      ASSIGNS VARIABLE NAMES AND LOCATION AND SUBSTANCE CODES TO
C      CHARACTER VARIABLES FOR OUTPUT IN KEY FILE
C
       INCLUDE 'IO.INC'
       INCLUDE 'INFO.INC'
       INCLUDE 'COUNTS.INC'
       KF=1
C
C      WRITE SAMPLED INPUT VARIABLE NAMES FOR KEY
C      FILE FOR NON-TIME-VARIANT DISTRIBUTIONS
C
       DO 10 I=1,VARN
          IF (EFLAG(VARNOT(I)).EQ.'F') THEN
             WRITE (NAMEF(KF),100) VARTIT(VARNOT(I))
             KF=KF+1
          ENDIF
 10    CONTINUE
```

```
      JJ=1
C
C     WRITE SAMPLED INPUT VARIABLE NAMES FOR KEY
C     FILE FOR TIME-VARIANT DISTRIBUTIONS
C
      IF (VARY.GE.1) THEN
         DO 60 I=1,VARY
            IF (EFLAG(VARIED(I)).EQ.'F') THEN
               DO 80 J=1,NSTEPF
                  WRITE (NAMEF(KF),150) VARTIT(VARIED(I)),TFILE(J)
                  KF=KF+1
80             CONTINUE
            ENDIF
60       CONTINUE
      ENDIF
C
C     WRITE OUTPUT VARIABLE NAMES FOR KEY FILE.
C     NAMES INCLUDE VARIABLE NAME, SUBSTANCE, LOCATION, AND TIME.
C
      DO 20 I=1,NARRAY
         IF (NVAR(I).GT.0) THEN
            DO 30 J=1,NVAR(I)
               IF (I.GE.25.AND.NSUB(JJ).EQ.5.AND.I.NE.28)NSUB(JJ)=11
                  DO 50 K=1,NSTEPF
                     WRITE (NAMEF(KF),200) VARNAM(I),NSUB(JJ),LOC(JJ),
     &                  TFILE(K)
                     KF=KF+1
 50               CONTINUE
               JJ=JJ+1
 30         CONTINUE
         ENDIF
 20   CONTINUE
 100  FORMAT (2X,A6)
 150  FORMAT (2X,A6,20X,E8.3)
 200  FORMAT (2X,A6,6X,I2,7X,I2,3X,E8.3)
      RETURN
      END
C
C
C
      SUBROUTINE OUTPUT
C
C     SUBROUTINE WRITES SUMMARY STATISTISTICS AND VARIABLE NAMES TO
C     A 'KEY' FILE (UNIT2)
C
      INCLUDE 'IO.INC'
      INCLUDE 'STATS.INC'
      INCLUDE 'COUNTS.INC'
      CHARACTER*9 VECTOR(5)
C
C     WRITE TO KEY FILE
C
      IF (NOUT.GT.0) THEN
         CALL FILER (FUNIT2)
         WRITE (FUNIT2,900) TITLE
         WRITE (FUNIT2,930) NTRIAL
         IF(SKEWFG.EQ.'Y')THEN
            WRITE(FUNIT2,910)
         ELSE
            WRITE(FUNIT2,915)
         ENDIF
         DO 20 I=1,NOUT
            DO 30 J=1,5
               VECTOR(J)='         '
30          CONTINUE
            IF(SDEV(I).NE.-999.)THEN
               WRITE(VECTOR(1),800)SDEV(I)
               IF(SKEWFG.EQ.'Y'.AND.SKEW(I).NE.-999.)THEN
                  WRITE(VECTOR(4),800)SKEW(I)
                  IF(KURT(I).NE.-999.)
     &                WRITE(VECTOR(5),800)KURT(I)
               ENDIF
            ENDIF
            IF(GMEAN(I).NE.-999.)THEN
               WRITE(VECTOR(2),800)GMEAN(I)
               IF(GSDEV(I).NE.-999.)THEN
                  WRITE(VECTOR(3),800)GSDEV(I)
               ENDIF
            ENDIF
            WRITE(FUNIT2,850)I,NAMEF(I),S1(I),(VECTOR(J),J=1,3),XMIN(I),
     &         XMAX(I),(VECTOR(J),J=4,5)
20       CONTINUE
      ENDIF
      CLOSE (FUNIT1)
      CLOSE (FUNIT2)
850   FORMAT(I3,2X,A36,3X,E9.3,3(2X,A9),2(2X,E9.3),2(2X,A9))
800   FORMAT(E9.3)
900   FORMAT (1X,A40)
910   FORMAT (5X,'PARAMETER',2X,'SUBSTANCE',2X,'LOC',7X,'TIME',5X,
     &   'MEAN',6X,'STD DEV',3X,'GEOM MEAN',3X,'GEOM SD',
     &   4X,'MINIMUM',4X,'MAXIMUM',4X,'SKEWNESS',3X,'KURTOSIS')
915   FORMAT (5X,'PARAMETER',2X,'SUBSTANCE',2X,'LOC',7X,'TIME',5X,
     &   'MEAN',6X,'STD DEV',3X,'GEOM MEAN',3X,'GEOM SD',
     &   4X,'MINIMUM',4X,'MAXIMUM')
930   FORMAT (1X,'NUMBER OF TRIALS: ',I5)
      RETURN
      END
C
C
C
      SUBROUTINE FILER(UNIT)
C
C     WRITES DATE AND TIME TO TOP OF OUTPUT FILES
C
      INTEGER*2 UNIT
      CHARACTER*8 DAY, HOUR
      CALL DATE(DAY)
      CALL TIME(HOUR)
      IF(UNIT.NE.0)THEN
         WRITE(UNIT,100)DAY,HOUR
      ELSE
         WRITE(UNIT,200)DAY,HOUR
      ENDIF
      RETURN
100   FORMAT('FILE CREATED ',A8,' AT ',A8)
200   FORMAT(' RUN STARTED ',A8,' AT ',A8)
      END
```

B.2.7 Include Files

```
C FILE 'IO.INC'
C
      INTEGER*2 SCRUNT,FUNIT,FUNIT1,FUNIT2
      COMMON /FILES/ SCRUNT,FUNIT,FUNIT1,FUNIT2
C
      CHARACTER*40 TITLE
      CHARACTER*6 VARTIT(300), VARNAM(100)
      CHARACTER*1 FSAVE,SKEWFG
      CHARACTER*36 NAMEF(300)
      COMMON /ID/ TITLE, VARTIT, FSAVE, NAMEF, VARNAM,SKEWFG


C FILE 'CONC.INC'
C
      REAL*4 WCONC(10,4,3),CONC(10,4,3),PH(4),WATC(8,10),WATAVG(4),
     &   WATPH(10),GWATC(8,5),
     &   EMRATE(5),EROTOT,AIRC(5,82),
     &   SOILC(4,82),AVEGC(4,80),BVEGC(4,80),SUFOC(4,2),
     &   BRWSC(4),LICHC(4),AQVEGC(4),FISHC(4,10),
     &   ADERC(4),WDERC(4),AMOSC(4),WMOSC(4),ACARC(4),WCARC(4),
     &   WATD(5,80),SHINED(5,80),INHD(5,80),RADD(80),
     &   VEGD(5,80),FISHD(5,80),MEATD(5,80),DOSE(5,80),
     &   POPDT,BLANK1(4,80),BLANK2(10,10)
      COMMON /CONCEN/ WCONC,CONC,PH,WATC,WATAVG,WATPH,GWATC,EMRATE,
     &   EROTOT,
     &   AIRC,SOILC,AVEGC,BVEGC,SUFOC,BRWSC,LICHC,AQVEGC,FISHC,
     &   ADERC,WDERC,AMOSC,WMOSC,ACARC,WCARC,WATD,SHINED,INHD,RADD,VEGD,
     &   FISHD,MEATD,DOSE,POPDT,
     &   BLANK1,BLANK2


C FILE 'RECEP.INC'
C
      INTEGER*2 NRECEP,NRING,RDIR(80),RRING(80),RWSSEG(80),RFSEG(80),
     &   RPOP(80),NREC,NDREC
      REAL*4 RNGMID(5),RAREA(5),TAREA
      CHARACTER*1 RTYPE(80)
      COMMON /RECEPT/ NRECEP,NRING,RDIR,RRING,RWSSEG,RFSEG,RPOP,RNGMID,
     &   RTYPE,RAREA,NREC,TAREA,NDREC
C
      INTEGER*2 NSEG,NODDIR(10),NODRNG(10),PSDIR(10),
     &   PSRING(10),PSNUM,GSEG(5),GWLAYR(5),DAM
      CHARACTER*1 STYPE (10)
      REAL*4 SDEPTH(10), LAREA(10), SHEDAR(10),LAKVOL(10),PSAREA
      COMMON /WATER/ NSEG,NODDIR,NODRNG,STYPE,SDEPTH,LAREA,
     &   SHEDAR,LAKVOL,PSDIR,PSRING,PSNUM,PSAREA,GSEG,GWLAYR,DAM
```

```
C FILE 'STATS.INC'
C
      DOUBLE PRECISION KURT(300),GMEAN(300),GSDEV(300),
     &   SDEV(300),SKEW(300),S1(300)
      REAL*4 XMIN(300),XMAX(300)
      COMMON /STATS/ KURT,GMEAN,GSDEV,XMAX,XMIN,SDEV,SKEW,S1


C FILE 'COUNTS.INC'
C
      REAL*4 TFILE(12)
      INTEGER*2 NSTEPF,NUMF,TNUMF,TNUMBF
      COMMON /TSTEP/ TFILE,NSTEPF,NUMF,TNUMF,TNUMBF
C
      INTEGER*4 NSTART
      INTEGER*2 NPARM,NARB
      COMMON /DISNUM/ NSTART, NPARM,NARB
C
      INTEGER*4 NYEARS,NT
      INTEGER*2 NUMTRL, NTRIAL, NDT
      REAL*4 T,RYEARS,DT
      COMMON /TIME/ T, NUMTRL, NTRIAL, NYEARS, NDT,RYEARS,DT,NT
C
      CHARACTER*1 EFLAG(300)
      COMMON /FLAGE/ EFLAG
C
      INTEGER*2 VARY, VARN, VARIED(300), VARNOT(300)
      COMMON /TIMEV/ VARY, VARN, VARIED, VARNOT
C
      INTEGER*2 NFILE,NVARYF,VARYF,NOUT
      COMMON /NUMSAV/ NFILE,NVARYF,VARYF,NOUT


C FILE 'INFO.INC'
C
      INTEGER*2 NVAR(100), NSUB(300), LOC(300), NARRAY
      COMMON /INFO/ NVAR, NSUB, LOC, NARRAY


C FILE 'OUT.INC'
C
      REAL*4 XOUT(300)
      COMMON /OUT/ XOUT


C FILE 'INPT.INC'
C
      REAL*4 XIN(300)
      COMMON /INPT/ XIN


C FILE 'INPT2.INC'
C
      REAL*4 XVALUE(300)
      COMMON /INPT/ XVALUE
```

```
C FILE 'UPDATE.INC'
C
      DOUBLE PRECISION S2(300),S3(300),S4(300),GS1(300),GS2(300)
      INTEGER*2 N(300), GN(300)
      COMMON /TEST/ S2,S3,S4,GS1,GS2,N,GN


C FILE 'PARAM.INC'
C
      INTEGER*2 NTYPE(300), NACELL(300), CORNUM(300)
      REAL*4 P1(300), P2(300), P3(300), P4(300), P5(300)
      COMMON /PARAM/ NTYPE, NACELL, P1, P2, P3, P4, P5, CORNUM
C
      REAL*4 UNIT(300), CPF(300,25), ORIGIN(300), V(300,25)
      COMMON /VAL/ UNIT, CPF, ORIGIN, V


C FILE 'INTERM.INC'
C
      CHARACTER*1 CHR(70000)
      COMMON /INTERM/ CHR


C FILE 'WIND.INC'
C
      CHARACTER*1 WINDFG
      REAL*4 FWINDT,FWIND1(16),FWIND2(16,6),UWIND(16,6),FWIND(16,6,6,20)
      COMMON /WIND/ FWINDT,FWIND1,UWIND,FWIND2,FWIND,WINDFG
```

APPENDIX F

DEVELOPMENT AND IMPLEMENTATION OF A PROCEDURE FOR ESTABLISHING CONFIDENCE REGIONS FOR OUTPUT DISTRIBUTIONS FROM MONTE CARLO CALCULATIONS

by

P. M. Reilly and T. Duever
University of Waterloo

for

SENES Consultants Limited
Willowdale, Ontario

January 1986

ABSTRACT

This paper describes a method of stating bounds within which the true probability density function or cumulative probability function of the output variable of a Monte Carlo calculation may be expected to lie, at a given confidence level. The method is an extension of work by Cheng and Iles and by Scheffe in which a probability density function of known mathematical form is fitted to observed relative frequency values and, using conventional statistical methods, a joint confidence region for the parameter values is found. The applicability of the method to output results of environmental assessment models is demonstrated. The confidence bands calculated for the cumulative probability function using this method were found to be narrower than the bands derived using a procedure developed by Kolmogorov and Smirnov, which was used in the Phase I study.

TABLE OF CONTENTS

Page

F.1 INTRODUCTION AND BACKGROUND F-1

F.2 GENERAL FORMS FOR OUTPUT PROBABILITY DENSITY FUNCTIONS F-3

F.3 FITTING THE PROBABILITY DENSITY FUNCTION TO THE DATA F-4

F.4 ESTABLISHING CONFIDENCE BOUNDS FOR THE FITTED PROBABILITY FUNCTION F-7

F.5 ESTABLISHING CONFIDENCE BOUNDS FOR THE CUMULATIVE PROBABILITY FUNCTION F-8

F.6 APPROACH TO COMPUTER IMPLEMENTATION F-10

F.7 ILLUSTRATION OF CONFIDENCE BOUNDS ESTIMATION F-12
- F.7.1 Introduction F-12
- F.7.2 Original Example F-12
- F.7.3 Additional Examples F-14

F.8 CONCLUSIONS F-15

REFERENCES

APPENDIX F1: NEWTON-RAPHSON ITERATIVE SOLUTION

APPENDIX F2: KOLMOGOROV CONFIDENCE BANDS

LIST OF FIGURES

		Follows Page
Figure F1	Relation of Confidence Band Programs to UTAP	F-10
Figure F2	Schematic Flowsheet for Confidence Band Program	F-10
Figure F3	Fitted Probability Density Functions For s=2, s=4 and s=6	F-13
Figure F4	95% Confidence Limits for Probability Density Function, Classroom Economic Study (s=4)	F-13
Figure F5	95% Confidence Limits for Probability Density Function, DOSRN 100 Trials - 2 Parameter Model	F-14
Figure F6	95% Confidence Limits for Cumulative Distribution Function, DOSRN 500 Trials - 2 Parameter Model	F-14
Figure F7	95% Confidence Limits for Cumulative Distribution Function, DOSRN 100 Trials - 2 Parameter Model	F-14
Figure F8	95% Confidence Limits for Probability Density Function, DOSRN 500 Trials - 2 Parameter Model	F-14
Figure F9	Plots of 95% Confidence Bands for a Normal Distribution (500 Trials)	F-14
Figure F10	Plots of 95% Confidence Bands for a Log Transformed Lognormal Distribution (500 Trials)	F-14
Figure F11	Plots of 95% Confidence Bands for Logarithm of Radium in Fish (200 Trials)	F-14

LIST OF TABLES

Follows Page

Table F1 Illustration of Cheng and Iles Technique F-12

Table F2 Variable DOSRN (100 Trials) F-14

Table F3 Variable DOSRN (500 Trials) F-14

APPENDIX F

DEVELOPMENT AND IMPLEMENTATION OF A PROCEDURE FOR ESTABLISHING CONFIDENCE REGIONS FOR OUTPUT DISTRIBUTIONS FROM MONTE CARLO CALCULATIONS

F.1 INTRODUCTION AND BACKGROUND

The most important output from a Monte Carlo calculation is often the probability density function for one or more output variables. Each probability density function is obtained in approximate form as a set of counts in cells which correspond to different discrete values of the variable. The observed relative frequencies at the discrete values provide an approximation to the probability density function of the variable.

If the number of Monte Carlo trials were extremely large (say 10^9) and the number of cells moderate (say 20), it would be expected that the graph of the relative frequency values versus the values of the variable corresponding to different cells would be a smooth curve which would agree very closely with the true probability density function. It would also vary little from one Monte Carlo run with the same number of trials to the next.

If however only 200 Monte Carlo trials are made with 20 cells, the relative frequency diagram can be expected to be "ragged", to vary a good deal from one run of 200 trials to the next, and the smooth curve drawn through the relative frequency points cannot be expected to agree closely with the true probability density function. It is the object of this exposition to describe a method of stating bounds within which the true probability density function may be expected to lie, at a given confidence level.

In the Phase I SENES study (SENES 1984) a distribution-free technique based on an extension of the Kolmogorov-Smirnov goodness of fit test (Kolmogorov 1941), as described for example in Kendall and Stuart (1961), was used to develop confidence bands for the cumulative distribution function. The test is based on the maximum absolute deviation between the empirical (i.e. observed) cumulative distribution function, and the underlying true cumulative distribution. Unfortunately, while the method is attractive because of its simplicity, it does have the disadvantage of being too conservative, particularly in the tails of the distribution. For example, ordinate values of less than zero for the left tail and greater than one for the right tail are obtained. In practice the confidence bands are truncated at zero or one respectively. This consideration prompted the further investigation of techniques for establishing confidence bands which led to the present paper.

The method discussed in this paper is an extension of the approach of Cheng and Iles (1983) and of Scheffe (1959), in which a probability density function of known mathematical form is fitted to the observed relative frequency values by estimating the values of the parameters in the probability density function. At the same time, by conventional statistical methods, a joint confidence region for the parameter values is found. Then the set of mathematical functions which might, at the confidence level being used, include the true probability density function is the set of mathematical functions obtained by substituting into the known mathematical form of the probability density function all values of the parameters within their joint confidence region. The envelope of this set of functional relations is the confidence region, at the confidence level being used, for the probability density function of the variable.

The theoretical investigations described in this Appendix were carried out originally by Park M. Reilly and T.A. Duever and have been described in a previous report (see the discussion paper on confidence regions by Reilly and Duever in Volume 2 of SENES 1985). Subsequently, Reilly and Duever were asked to develop a procedure to permit computer implementation of their technique for establishing confidence regions for output distributions from Monte Carlo calculations. For completeness and ease of reference it was decided to reproduce the original discussion of Reilly and Duever in this appendix. However, it should be noted that the original discussions by Reilly and Duever (in SENES 1985) have been modified or augmented in several areas. These areas include a discussion of an approach to overcoming ill-conditioned matrices, a revised examples section and a new section outlining the approach to computer implementation.

All theoretical investigations were carried out by Reilly and Duever as was the development of the initial computer routine. SENES in turn adapted the work of Reilly and Duever for inclusion in the Uranium Tailings Assessment Program (UTAP) a post-processing option. The principal SENES contributor in this regard was Cecile E. Hallam. Technical overview and coordination between Reilly and Duever and SENES staff was provided by Douglas B. Chambers of SENES.

F.2 GENERAL FORMS FOR OUTPUT PROBABILITY DENSITY FUNCTIONS

The first requirement in calculating the confidence interval for the probability density function is a method of establishing flexible mathematical forms for the probability density functions to which the observed data may be fitted. Occasionally the output probability density function is of known form because of known forms for the input variables and a simple function relating them to the output variable. In the more interesting cases however, the probability density functions for the output variables are not of simple form.

The following form is proposed for the output probability density function of a random variable represented, possibly in transformed form, by x. The possible set of discrete values of the random variable are presented by x_1, x_2, ...,x_m.

$$p(x) = \exp\,(\theta_0 + \theta_1 x + \theta_2 x^2 + ...+ \theta_s x^s) \qquad \text{(F1)}$$

$$\sum_{i=1}^{m} p(x_i) = 1$$

where p is the probability density function, s is an integer representing the degree of the approximating polynomial, θ_i are the constant coefficients of the approximating polynomial, and m is the number of cells.

The variable θ_0 is an auxiliary variable which can be interpreted as a normalizing constant. It can be eliminated if desired by writing (F1) in the following form:

$$p(x) = \frac{\exp(\theta_1 x + \theta_2 x^2 + \dots \theta_s x^s)}{\sum_{i=1}^{m} [\exp(\theta_1 x + \theta_2 x^2 + \dots + \theta_s x^s)]} \tag{F2}$$

which obviously sum to unity over all x_i

In actual practice the data are given as cell counts at a number, usually 10 to 20, of cells (bins), each cell usually representing a small range of values of x. After the binning procedure is complete, the assumption is applied that the possible values of the random variable are limited to the set of values corresponding to what were formerly called cell mid-points. Consequently the random variable is henceforth treated as a discrete one.

In that case, p(x) in equation (F1) can be interpreted as the probability of a count entering the cell which corresponds to the value of x at the mid-point of the cell. It will be only approximately true that if the p(x), interpreted as cell probabilities, sum to 1, then p(x) interpreted as a probability density as was done above, will integrate to 1. If necessary this deficiency can be corrected by adjusting the value of the normalizing constant.

F.3 FITTING THE PROBABILITY DENSITY FUNCTION TO THE DATA

Suppose that cell counts have been observed in m cells and the ith cell, the mid-point of which corresponds to the value x_i of the random variable, has recorded n_i counts. It is desired to estimate θ_j, j= 1, ..., s so as to fit equation (F1). At this time $p(x_i)$ in equation (F1) will be interpreted as the probability of a count entering the ith cell.

Such a situation is described by the multinomial likelihood function:

$$L(\theta_1,\ldots\theta_s) = \prod_{i=1}^{m} [p(x_i)]^{n_i} \qquad \text{(F3)}$$

A very good estimate of $\underline{\theta}$, the maximum likelihood estimate, is obtained by maximizing L, or more conveniently by minimizing its negative logarithm:

$$S(\underline{\theta}) = -\ln L(\underline{\theta}) = -\sum_{i=1}^{m} n_i \ln(p_i) \qquad \text{(F4)}$$

where

$$\ln(p_i) = \theta_0 + \sum_{k=1}^{s} \theta_k x_i^k \qquad \text{(F5)}$$

$$\sum_{i=1}^{m} p_i = 1 \qquad \text{(F6)}$$

and $p_i = p\ (x_i)$

This system can be solved by first differentiating both sides of equation F6 with respect to $_j$ (F6):

$$\frac{\partial}{\partial\theta_j} \sum_{i=1}^{m} \exp\left\{\theta_0 + \sum_{k=1}^{s} \theta_k x_i^k\right\} = 0 \quad : j = 1, 2, \ldots S$$

then

$$\sum_{i=1}^{m} p_i \left(\frac{\partial\theta_0}{\partial\theta_j} + x_i^j\right) = 0 \quad : j = 1, 2, \ldots S$$

Therefore

$$\frac{\partial\theta_0}{\partial\theta_j} = -\frac{\sum_{i=1}^{m} p_i x_i^j}{\sum_{i=1}^{m} p_i} = -\sum_{i=1}^{m} p_i x_i^j; \quad j = 1, \ldots, s \qquad \text{(F7)}$$

To find the minimum of equation (F4) differentiate with respect to $\theta_j; j=1,2,\ldots,s$:

$$\frac{\partial S}{\partial\theta_j} = -\sum_{i=1}^{m} n_i \left[\frac{\partial\theta_0}{\partial\theta_j} + x_i^j\right]$$

$$= -N\frac{\partial\theta_0}{\partial\theta_j} - \sum_{i=1}^{m} n_i x_i^j \qquad \text{(F8)}$$

where

$$N = \sum_{i=1}^{m} n_i$$

Substituting equation (F7) into equation (F8) and setting $\frac{\partial S}{\partial\theta_j}$ in equation (F8) to zero:

$$N\sum_{i=1}^{m} p_i x_i^j = \sum_{i=1}^{m} n_i x_i^j \qquad j = 1,2,\ldots,s \qquad \text{(F9)}$$

Note that for j=0 equation (F9) reduces to (F6) the constraint from which θ_0 is calculated.

Equation (F9) can be solved by the Newton-Raphson method as described in Appendix F1.

F.4 ESTABLISHING CONFIDENCE BOUNDS FOR THE FITTED PROBABILITY FUNCTION

The probability function having been fitted to each observed cell frequency, the approach of Cheng and Iles permits confidence bounds on it to be established as outlined previously (SENES, 1985). The first step in this is to establish a joint confidence region for the parameters $\underline{\theta}$. This region is:

$$(\underline{\theta} - \hat{\underline{\theta}})'\underline{M}(\underline{\theta} - \hat{\underline{\theta}}) \leq \gamma \qquad \text{(F11)}$$

where $\underline{\theta}$ is the sx1 vector of possible parameter values, $\hat{\underline{\theta}}$ is the sx1 vector of maximum likelihood parameter estimates and $\underline{M}$ is the sxs Fisher information matrix for the parameters. Also γ is a number which has approximately the value of a χ^2- distributed random variable with s degrees of freedom which is exceeded with probability (1-a), where a is the desired confidence level. The (j,k)th element (m_{jk}) of the sxs Fisher information matrix is given by:

$$\underline{M} = m_{jk} = \left[N \sum_{i=1}^{m} p_i x_i^{j+k} - N\left(\sum_{i=1}^{m} p_i x_i^{j}\right)\left(\sum_{i=1}^{m} p_i x_i^{k}\right) \right] \qquad \text{(F12)}$$

The next step in the Cheng and Iles procedure is to choose values of $\underline{\theta}$, so as to maximize and minimize p(x) in equation (F1) subject to equation (F11). Since exponentiation is a monotone function it will be sufficient to maximize and minimize lnp(x). With λ as the Lagrange multiplier the required Lagrangian is:

$$L(\underline{\theta}) = \theta_0 + \sum_{k=1}^{s} \theta_k x^k - \frac{1}{2}\lambda(\underline{\theta}-\hat{\underline{\theta}})'\,\underline{M}\,(\underline{\theta}-\hat{\underline{\theta}}) \qquad \text{(F13)}$$

Solving this leads to the following equation for calculating values of $\underline{\theta}$ which maximize and minimize p:

$$\underline{\theta} = \hat{\underline{\theta}} \pm \sqrt{\frac{\gamma}{(\underline{c}-\underline{b})\ \underline{M}^{-1}(\underline{c}-\underline{b})}}\ \underline{M}^{-1}\ (\underline{c}-\underline{b}) \qquad \text{(F14)}$$

where

$\underline{b} = [\sum_{i=1}^{m} p_i x_i^j]$ jth element of the sx1 vector $\underline{b}$

$\underline{c} = [x^j]$ jth element of the sx1 vector $\underline{c}$

Note that equation (F14) requires an iterative solution since $\underline{b}$ is a function of $\underline{\theta}$. A scheme based on simple iteration was found to give rapid convergence.

Having found the limiting values of $\underline{\theta}$, the limits on p are found by substituting these in equation (F1).

F.5 ESTABLISHING CONFIDENCE BOUNDS FOR THE CUMULATIVE PROBABILITY FUNCTION

If equation (F1) is interpreted as describing the probability density function for X, the cumulative probability function is defined by:

$$F(x) = \Pr(X \leq x) = \int_{-\infty}^{x} p(u)du = \int_{-\infty}^{x} \exp\left\{\theta_0 + \sum_{k=1}^{s} \theta_k\ u^{k}\right\} du \qquad \text{(F15)}$$

Confidence limits for F(x) for a fixed x may be found as in the last section by maximizing and minimizing F(x) by varying $\underline{\theta}$ within the limits given by equation (F11). They are found in terms of the vectors $\underline{\theta}$ which produce the maximum and minimum for F(x). The limiting $\underline{\theta}$ are found from the following equation, applied iteratively:

$$\underline{\theta} = \hat{\underline{\theta}} \pm \sqrt{\frac{\gamma}{\underline{r}'\ \underline{M}^{-1}\ \underline{r}}}\ \underline{M}^{-1}\ \underline{r} \qquad \text{(F16)}$$

where $\underline{\theta}$, $\hat{\underline{\theta}}$, γ and $\underline{M}$ are as defined previously and $\underline{r}$ is the sx1 vector:

$$\underline{r} = \int_{-\infty}^{x} [\underline{d}+\underline{e}] \exp\left\{\theta_0 + \sum_{k=1}^{s} \theta_k u^k\right\} du \qquad \text{(F17)}$$

where

$$d_j = \frac{\partial\theta_0}{\partial\theta_j} = -\int_{-\infty}^{+\infty} u^j \exp\left\{\theta_0 + \sum_{k=1}^{s} \theta_k u^k\right\} du$$

is the jth element of the sx1 vector $\underline{d}$

$e_j = [u^j]$ is the jth element of the sx1 vector $\underline{e}$.

Note that θ_0 is now given by:

$$\theta_0 = -\ln\left[\int_{-\infty}^{\infty} \exp\left\{\sum_{k=1}^{s} \theta_k u^k\right\} du\right] \qquad \text{(F18)}$$

In principle, numerical integration would be required to calculate the above integrals. In this paper we have chosen to work with the probability distribution in discrete form. This has the advantage of eliminating the need for numerical integration. Therefore in equations (F15), (F17) and (F18) summation over the appropriate range of x's replaces integration:

$$F(x_\ell) = P_r(x \leq x_\ell) = \sum_{i=1}^{\ell} \exp\left\{\theta_0 + \sum_{k=1}^{s} \theta_k x_i^k\right\} \qquad \text{(F19)}$$

$$r = \sum_{i=1}^{\ell} [\underline{d} + \underline{e}] \exp\left\{\theta_0 + \sum_{k=1}^{s} \theta_k x_i^k\right\} \qquad \text{(F20)}$$

where

$$d_j = \frac{\partial\theta_0}{\partial\theta_j} = \sum_{i=1}^{m} x_i^j \exp\left\{\theta_0 + \sum_{k=1}^{s} \theta_k x_i^k\right\}$$

$$e_j = x^j$$

$$\theta_0 = -\ln \sum_{i=1}^{m} \exp \sum_{k=1}^{s} \theta_k \, x_i^k \qquad \text{(F21)}$$

When the limit producing values of $\underline{\theta}$ have been found, the bounds on F(x) are found by substitution into equation (F19).

Note that as with the pdf, the limits on the cdf are only given at the discrete set of coordinates previously established.

F.6 APPROACH TO COMPUTER IMPLEMENTATION

For their original investigations, Reilly and Duever used various programs available in WATFIV and FORTRAN on the IBM 4341 mainframe computer at the University of Waterloo. The initial set of examples discussed in the next section were developed using the technique on the Waterloo mainframe computer. For the present investigations, Reilly and Duever were asked to develop an integrated micro-computer based approach for their confidence band technique. The way in which the confidence bands programs reside in UTAP is described below.

The general structure of the confidence bands programs and their relation to UTAP is shown on Figure F1. Figure F2 is a general logic flowsheet which outlines the way in which the confidence bands programs have been implemented.

The confidence bands programs are designed as a post-processing option to UTAP. The user identifies variables which are first read and then subdivided into an optimal number of bins or cells in a program named BIN using the expression:

$$[\log_{10} (\Delta \text{ of Monte Carlo trials})/\log_{10} (2.0)] + 1.0 \qquad \text{(F22)}$$

which is based on a paper by Sturges (1926).

The binned data are then transferred to another program (CBAND) which has been

FIGURE F.1

RELATION OF CONFIDENCE BAND PROGRAMS TO UTAP

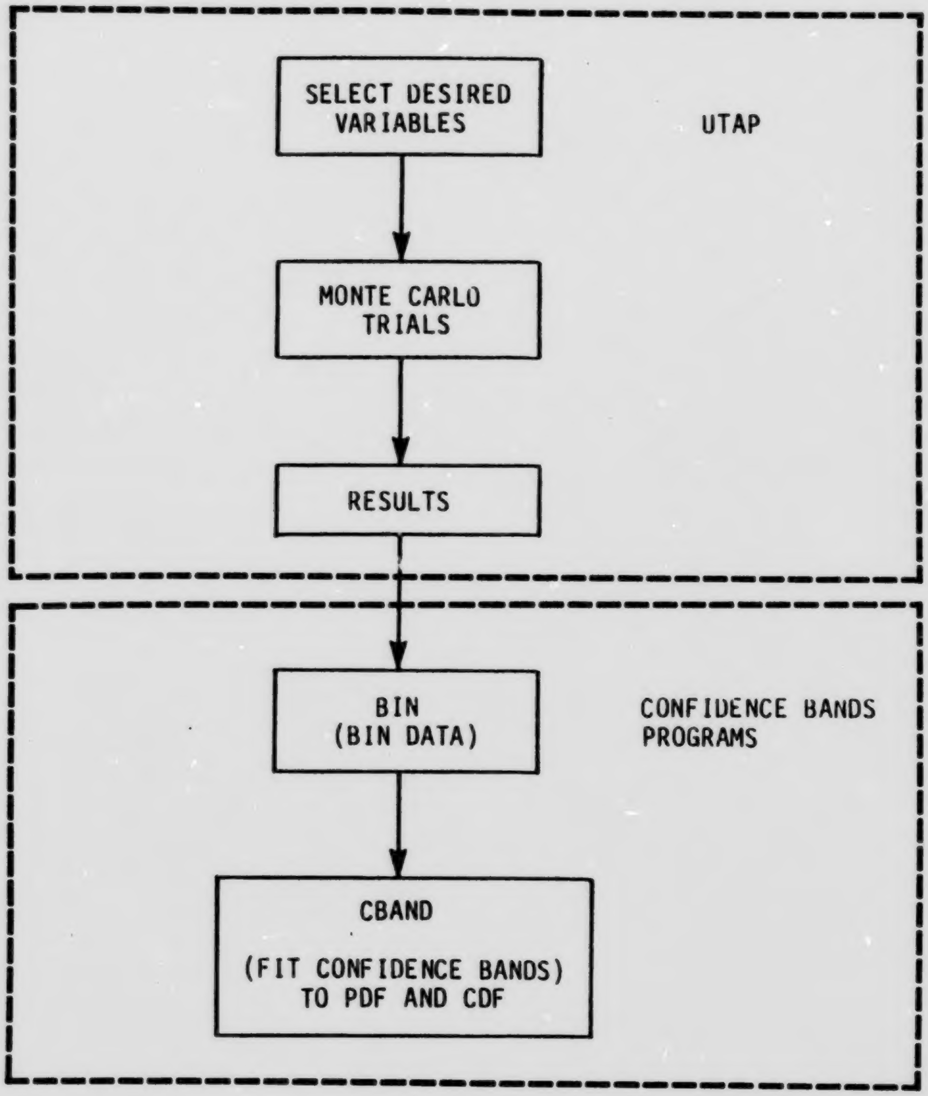

FIGURE F.2

SCHEMATIC FLOWSHEET
FOR CONFIDENCE BAND PROGRAM

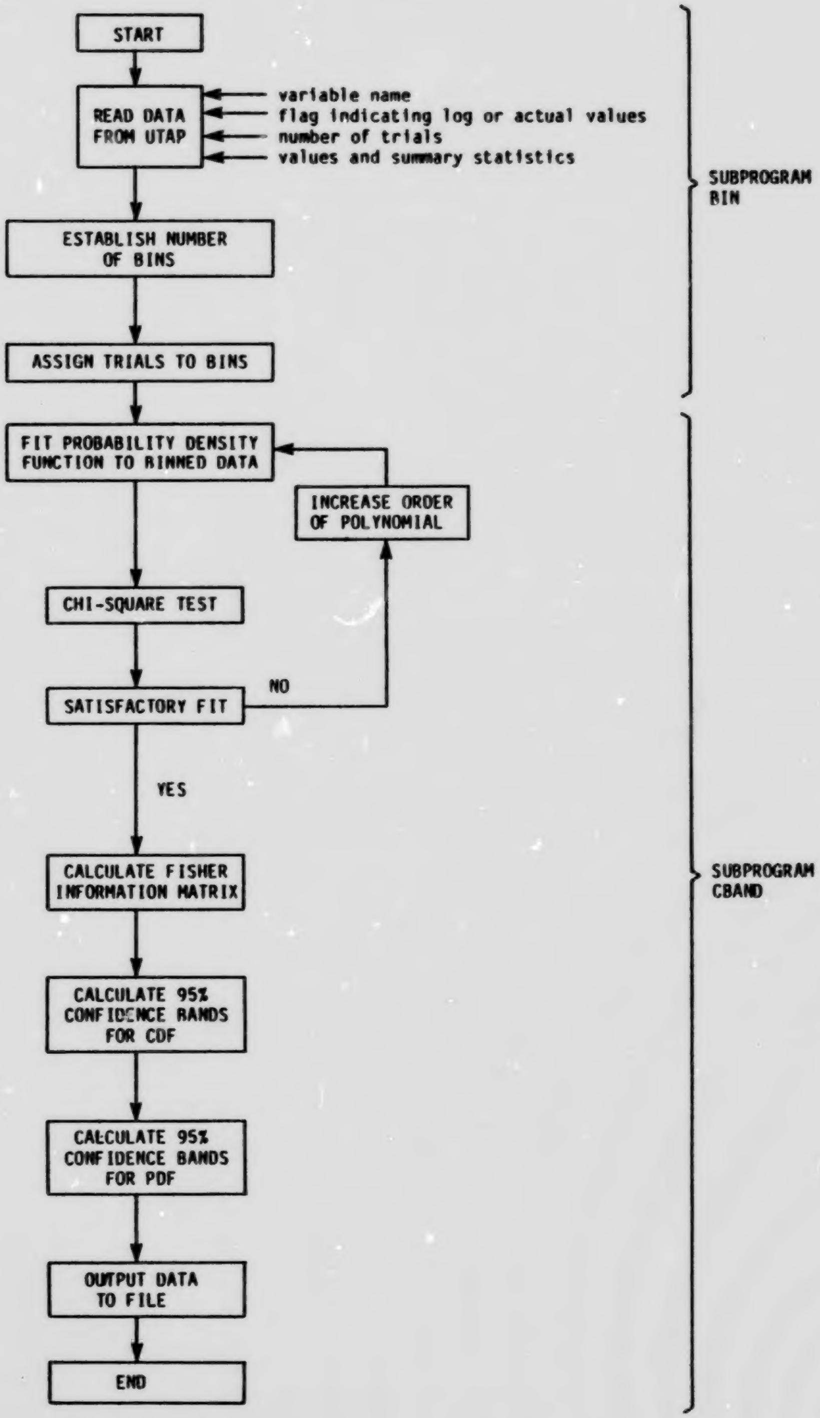
START
READ DATA FROM UTAP
variable name
flag indicating log or actual values
number of trials
values and summary statistics
ESTABLISH NUMBER OF BINS
ASSIGN TRIALS TO BINS
SUBPROGRAM BIN
FIT PROBABILITY DENSITY FUNCTION TO BINNED DATA
INCREASE ORDER OF POLYNOMIAL
CHI-SQUARE TEST
SATISFACTORY FIT
NO
YES
CALCULATE FISHER INFORMATION MATRIX
CALCULATE 95% CONFIDENCE BANDS FOR CDF
CALCULATE 95% CONFIDENCE BANDS FOR PDF
OUTPUT DATA TO FILE
END
SUBPROGRAM CBAND

written to perform all of the calculations described in sections F.3, F.4 and F.5. The program CBAND first reads in the data file generated by the binning program. The required information consists of the name of the variable being analysed, the number of cells or bins used, the number of Monte Carlo trials made, a flag indicating whether or not a logarithmic transformation of the data has been made and finally the cell midpoints and cell counts.

The Newton-Raphson fitting procedure described in section F.3 is accomplished within subroutine NEWRAP. This subroutine requires two additional subroutines. The first one calculates the values of the probability density function at any value of x. The second subroutine provides a general solution to the matrix equation.

$$\underset{n\times n}{\underline{A}}\ \underset{n\times 1}{\underline{u}} = \underset{n\times 1}{\underline{b}} \qquad \text{(F23)}$$

by Cholesky decomposition (see Appendix F1). Upon convergence of the fitting procedure, a χ^2 goodness of fit test at the 25% significance level is performed to see whether or not the fitted form of the probability density function adequately describes the binned data. Notice that the degrees of freedom for this test are given by

$$\text{D.F.} = k - s - 1$$

where

k = number of cells with fitted numbers of observations greater than 6
s = degree of approximating polynomial

If the fitted number of cell counts for a particular cell are less than 6, then that cell is combined with the next cell. The value of k may therefore be equal to or less than the number of cells. The program iterates, increasing the degree of the polynomial by 1 each iteration until a satisfactory fit is achieved. If the degrees of freedom of the observed χ^2 is zero, a warning will be printed to this effect; however, the confidence calculation will be carried out using the last model calculated. Caution is advised when using results obtained in this way.

Once a model passes the goodness of fit test the program enters the next phase in which confidence bands are evaluated. The first step is to evaluate the observed Fisher information matrix. The 95% confidence bands for the cumulative distribution function are calculated in subroutine CDF and finally the 95% confidence bands for the probability density functions are calculated in subroutine PDF. In both CDF and PDF, when the approximating polynomial is of degree one a very simple closed form solution is available.

Further discussion of the computer implementation of the confidence bands program is provided in Chapter 4 of this report. A full listing of the two computer programs used for confidence band estimation (BIN and CBAND) is provided in Appendix G of this report. Variable dictionaries for the two programs are also provided in Appendix G.

F.7 ILLUSTRATION OF CONFIDENCE BOUNDS ESTIMATION

F.7.1 Introduction

Two examples of confidence bands estimation were provided by Reilly and Duever in their original paper (see Volume 2 SENES, 1985). These orginal examples are included in this section. In addition, two examples utilizing the current microcomputer based version of the confidence program are also included as further demonstration of the technique.

F.7.2 Original Example

Table F.1 shows cell counts obtained in N=500 trials in a classroom example which used a random sampling program (OPANAL) in an economic study. The data were fitted using s=2, s=4 and s=6. Using the standard χ^2 test for goodness-of-fit the χ^2 values are respectively 26.54, 7.97 and 2.29 with 9, 7 and 5 degrees of freedom. The null hypothesis in each case is that the

Table F.1

ILLUSTRATION OF CHENG AND ILES TECHNIQUE

Cell number	1	2	3	4	5	6	7	8	9	10	11	12
Actual counts (n_i)	1	7	40	68	77	74	62	69	53	26	15	8
Fitted (s=2)	8.2	17.9	33.6	53.3	72.1	82.8	80.9	67.2	47.4	28.5	14.5	6.3
Fitted (s=4)	1.0	10.0	35.8	65.7	79.9	78.0	69.2	59.0	47.7	33.8	18.1	5.9
Fitted (s=6)	.8	8.5	37.6	69.9	77.0	71.4	67.7	64.7	52.3	29.8	12.9	8.5
Upper 95% Confidence Boundary (s=4)	5.8	19.3	47.8	80.8	92.4	90.2	81.0	69.1	59.1	45.0	27.0	16.2
Lower 95% Confidence Boundary (s=4)	0.2	4.8	25.9	52.3	67.7	65.8	57.3	48.4	36.8	24.0	11.2	1.9

corresponding s is correct and that the discrepancies between observed and expected number of counts occur by chance alone. On this basis, the probability of obtaining a set of cell counts which fits the form of the model used more poorly by chance is 0.2% for s=2. Simply put, this indicates that the polynomial of order S=2 provides a very poor fit to the observed cell counts. For s=4 the probability of obtaining a poorer fit by chance is 33.3%, which is considered acceptable. Because of the high probability of a poorer fit for s=6 of 80.8%, it may be considered overfitted; i.e. the use of too many parameters has probably caused the probability density function to be fitted to random fluctuations in the data. The value of s should be chosen to give a probability of a poorer fit roughly in the region of 25% so as to provide a reasonably good fit using as few parameters as possible and at the same time avoiding the fitting of chance fluctuations in the data.

Figure F.3 shows the plotted comparisons between the observed counts and fitted probability density functions for each of the three different degrees of the polynomial. In each case the smooth line is fitted while the heavy dots are observed values. The appearance of the curve for s=6 is consistent with its being overfitted. The curve for s=2 is the same as the normal probability density function with mean and variance estimated from the data. Figure F.4 shows the original data and the fitted curve for s=4 as in Figure F.2 and also shows 95% confidence limits for the probability density function. Note that fitted values, upper and lower 95% confidence limits were only calculated at the discrete values of x at which the random variable is defined. The smooth curves were obtained by using a smoothing procedure based on cubic spline functions. Smooth curves could have also been obtained by using a higher level of discretization along the axis and then evaluating the fitted function and the limits at a larger number of x-values. Cubic splines were used for numerical convenience only and it is expected that both procedures would produce practically the same curve.

A second example related to uranium mill tailings was also used to illustrate application of the technique. Specifically, two data sets, one of 100 trials and one of 500 trials, of the variable DOSRN were provided by SENES

FIGURE F.3

FITTED PROBABILITY DENSITY FUNCTIONS
FOR S=2, S=4 AND S=6

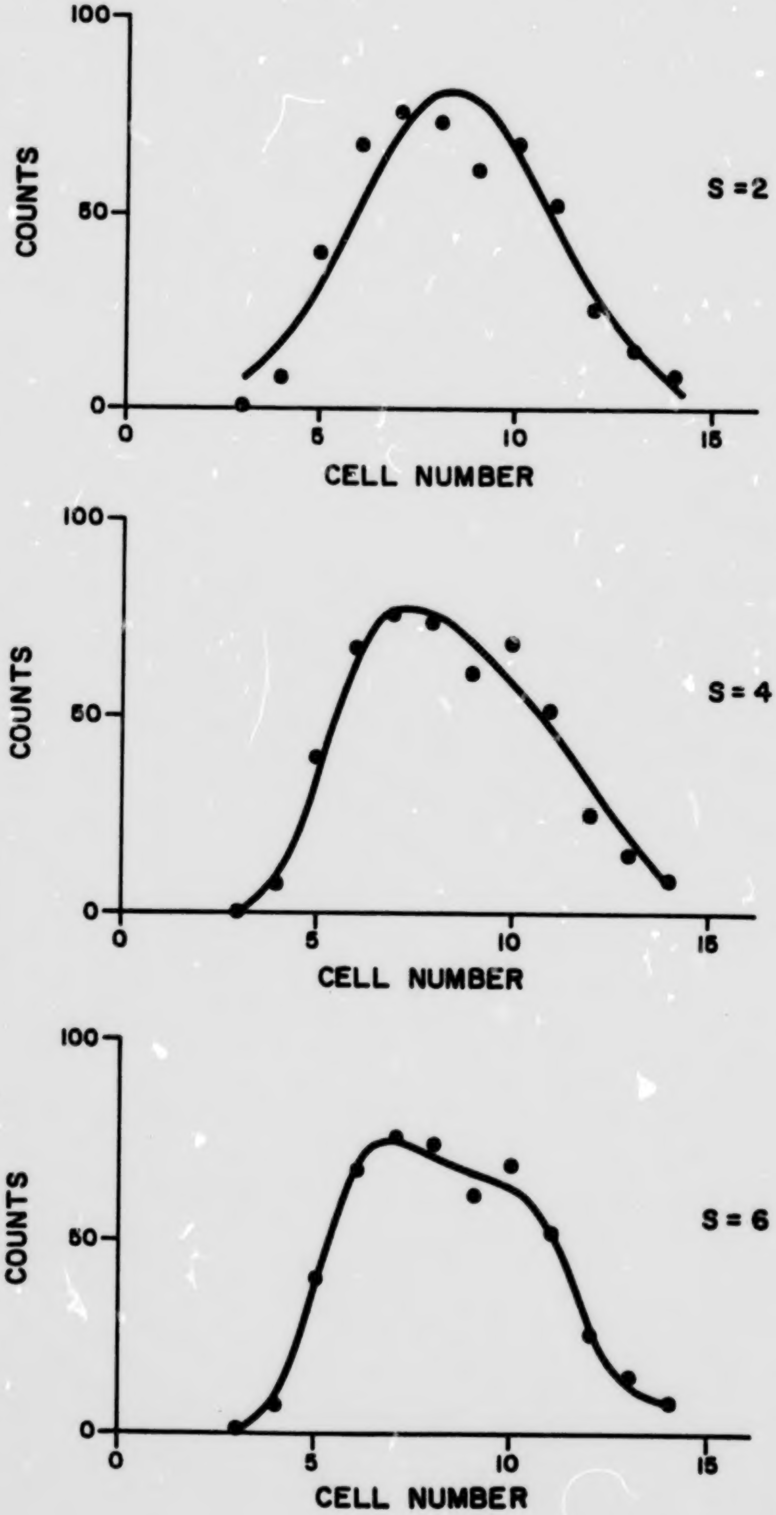

FIGURE F.4

95% CONFIDENCE LIMITS
FOR PROBABILITY DENSITY FUNCTION
CLASSROOM ECONOMIC STUDY (S=4)

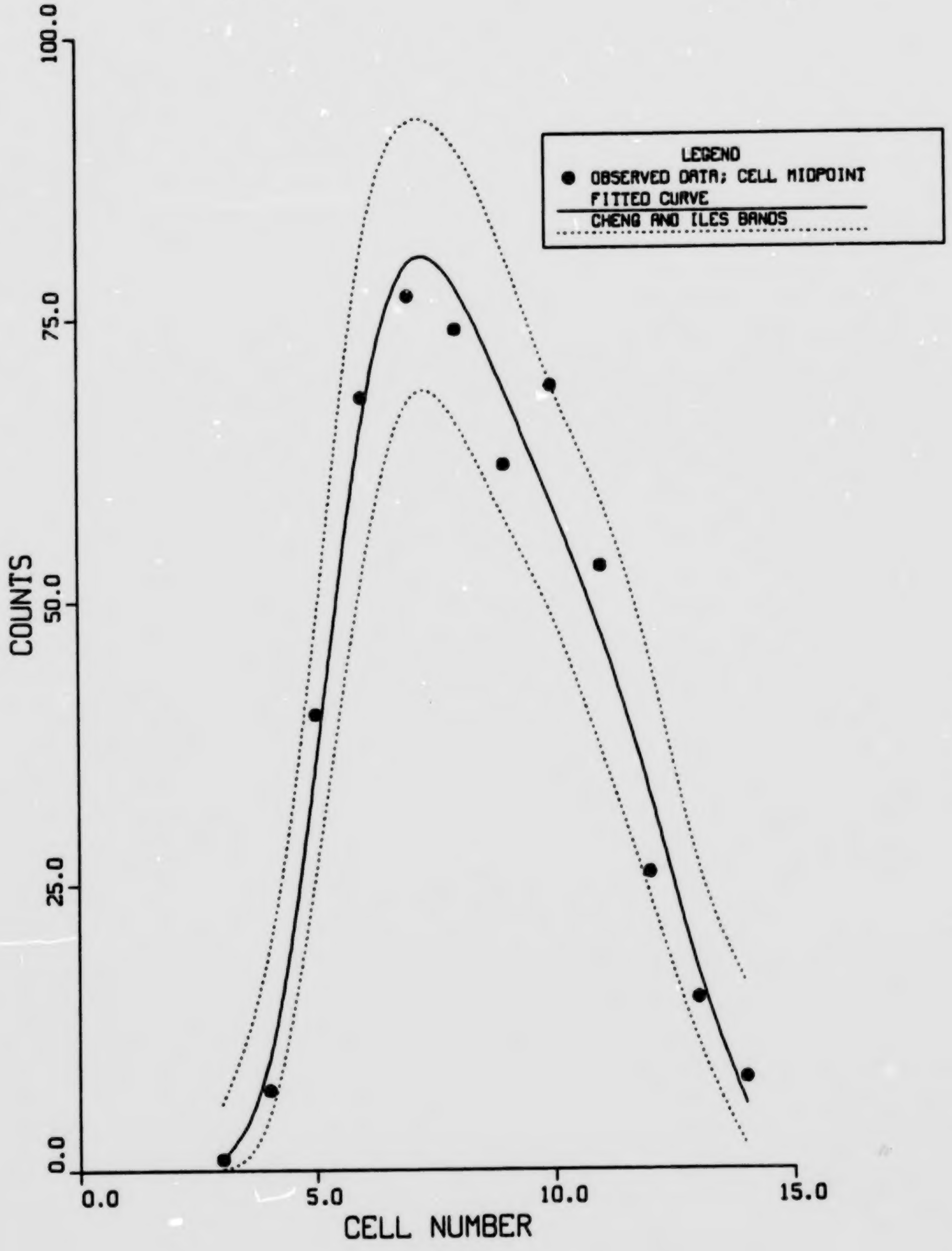

Consultants Limited. The values of the variable DOSRN are estimates of the annual dose to an adult male living year round about 2 km downwind of the reference uranium tailings area described in SENES (1984) and which arises from radon gas released from the tailings area.

Tables F.2 and F.3 show cell counts for the output variable DOSRN for 100 and 500 trials respectively. As shown the χ^2 goodness-of-fit test indicates that in both cases a model with s=2 is suitable. Figures F.5 and F.6 show the observed cell counts, the fitted probability density functions and the 95% confidence limits for these. As expected, the bands obtained at 500 trials are narrower than those at 100 trials.

Figures F.7 and F.8 show the corresponding cumulative distribution functions, including the 95% confidence bounds produced by this method as well as Kolmogorov bands. The procedure for obtaining the Kolmogorov bands is outlined in Appendix F.2.

In all of Figures F.5 to F.8, the cubic spline smoothing procedure described earlier was used.

F.7.3 Additional Examples

Two additional examples, calculated using the current microcomputer implementation (the actual computer code is given in Appendix G of this volume) are provided as additional demonstration of the technique.

The first example is a simple application of the technique to two known distributions, one of which uses the raw data and the second the log-transformed data. Figure F.9 illustrates the 95% confidence bands calculated from 500 random samples of a normal distribution. Figure F.10 illustrates the confidence bands calculated from 500 random samples of a lognormal distribution, log transformed by the confidence bands program.

The second example, illustrated in Figure F.11, is confidence bands fitted to

Table F.2

VARIABLE DOSRN (100 TRIALS)

Cell Number	Observed Counts	Fitted (s=2)	Upper 95% Conf. Limits	Lower 95% Conf. Limits
1	52	54.7	64.6	43.6
2	28	23.0	25.7	19.1
3	9	10.4	14.1	7.2
4	3	5.1	7.8	3.1
5	4	2.7	4.5	1.5
6	2	1.5	2.8	0.8
7	1	0.9	2.0	0.4
8	0	0.6	1.7	0.2
9	0	0.4	1.9	0.1
10	0	0.3	2.5	0.0
11	1	0.3	4.0	0.0

Goodness-of-Fit Test

s	χ^2	d.f.*	Pr.**
1	3.607	3	30.7%
2	2.47	2	30.4%

* d.f. = degrees of freedom
** Pr. = probability of obtaining a poorer fit

Table F.3

VARIABLE DOSRN (500 TRIALS)

Cell Number	Observed Counts	Fitted (s=2)	Upper 95% Conf. Limits	Lower 95% Conf. Limits
1	290	280.9	301.7	258.4
2	106	115.6	119.2	110.7
3	47	50.6	56.8	44.6
4	25	23.6	28.5	19.3
5	14	11.7	15.0	9.0
6	4	6.1	8.3	4.5
7	4	3.4	4.9	2.4
8	3	2.0	3.0	1.4
9	2	1.3	2.0	0.8
10	1	0.9	1.4	0.5
11	1	0.6	1.1	0.4
12	1	0.4	0.9	0.2
13	1	0.4	0.8	0.2
14	0	0.3	0.8	0.1
15	0	0.3	0.8	0.1
16	0	0.3	0.9	0.1
17	0	0.3	1.1	0.1
18	0	0.3	1.5	0.1
19	0	0.4	2.2	0.1
20	1	0.5	3.5	0.1

Goodness of Fit Test

s	χ^2	d.f.*	Pr.**
1	20.8	5	0.1%
2	3.24	4	53.0%

* d.f. = degrees of freedom
** Pr. = probability of obtaining a poorer fit

FIGURE F.5

95% CONFIDENCE LIMITS
FOR PROBABILITY DENSITY FUNCTION
DOSRN 100 RUNS - 2 PARAMETER MODEL

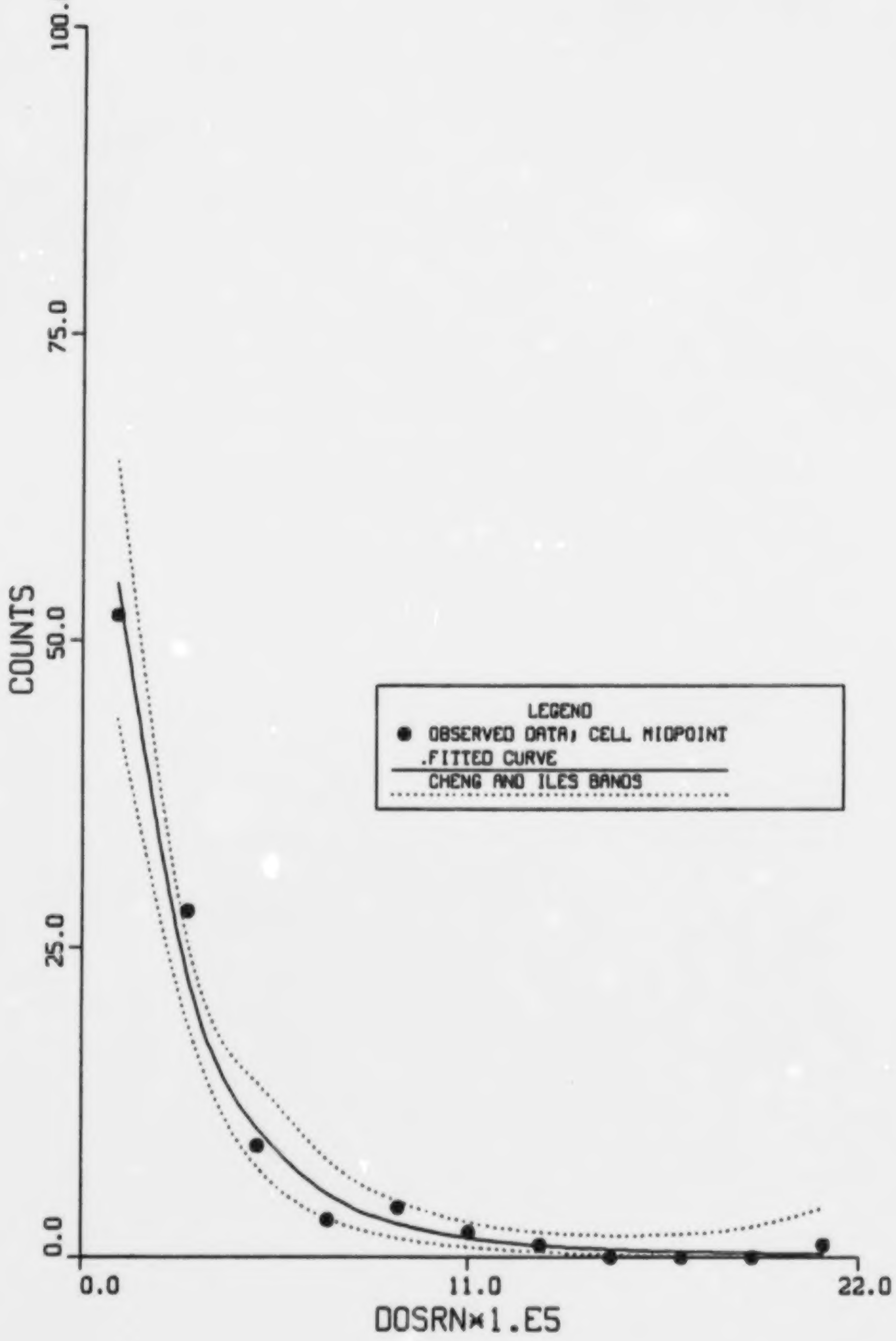

FIGURE F.6

95% CONFIDENCE LIMITS FOR PROBABILITY DENSITY FUNCTION DOSRN 500 RUNS - 2 PARAMETER MODEL

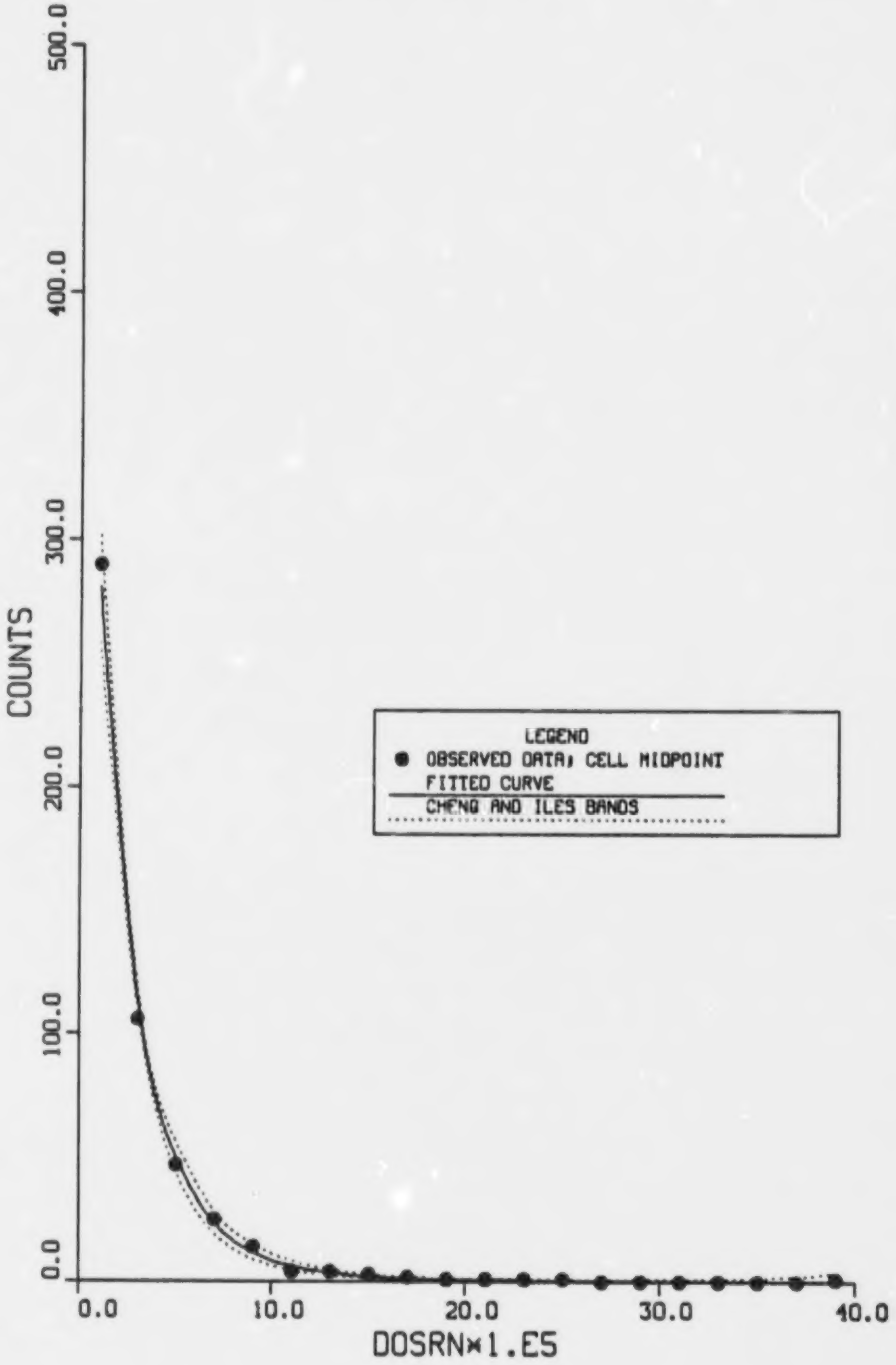

FIGURE F.7

95% CONFIDENCE LIMITS
FOR CUMULATIVE DISTRIBUTION FUNCTION
DOSRN 100 RUNS - 2 PARAMETER MODEL

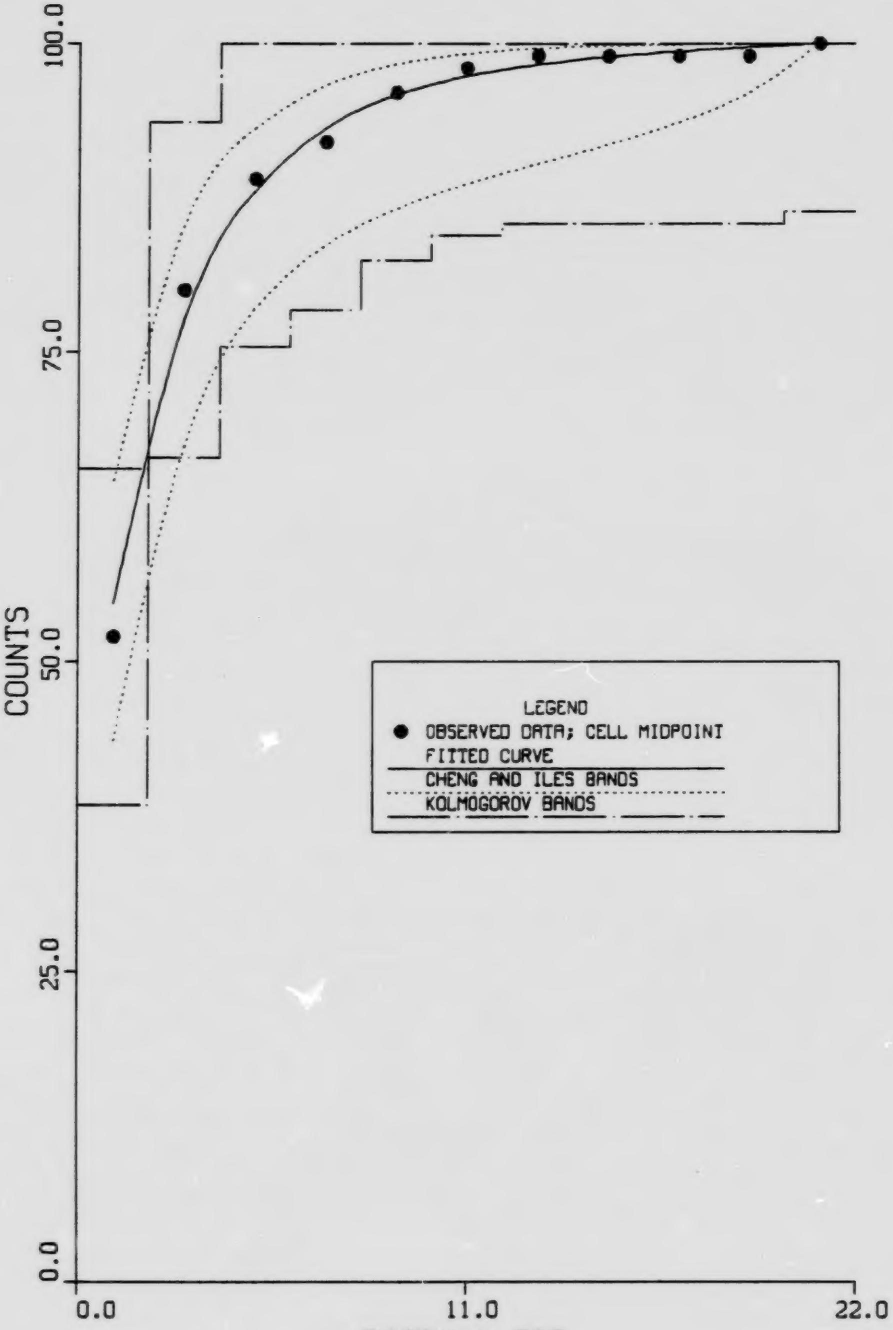

FIGURE F.8

95% CONFIDENCE LIMITS
FOR CUMULATIVE DISTRIBUTION FUNCTION
DOSRN 500 RUNS - 2 PARAMETER MODEL

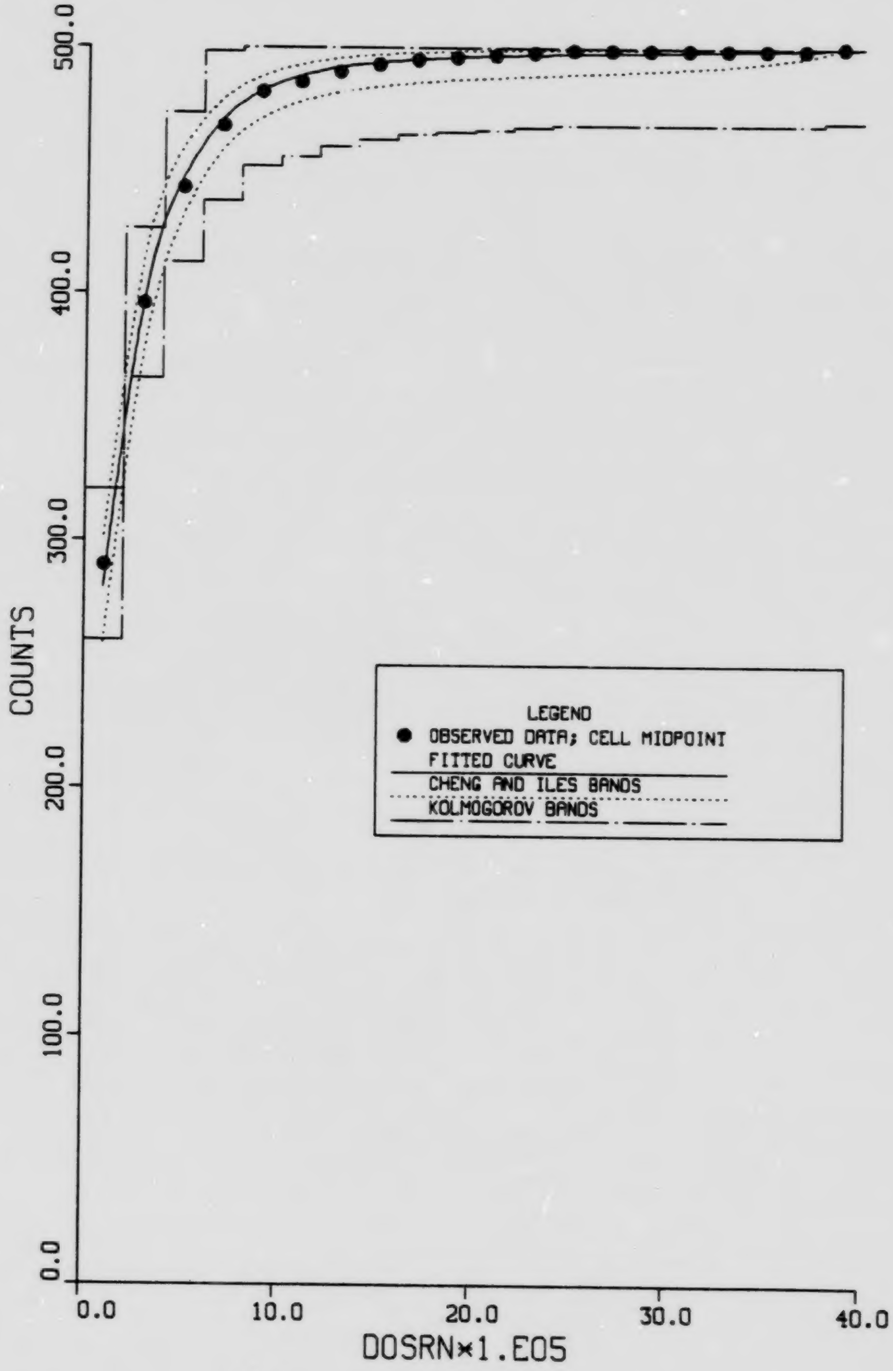

FIGURE F.9

PLOTS OF 95% CONFIDENCE BANDS
FOR A NORMAL DISTRIBUTION
(500 TRIALS)

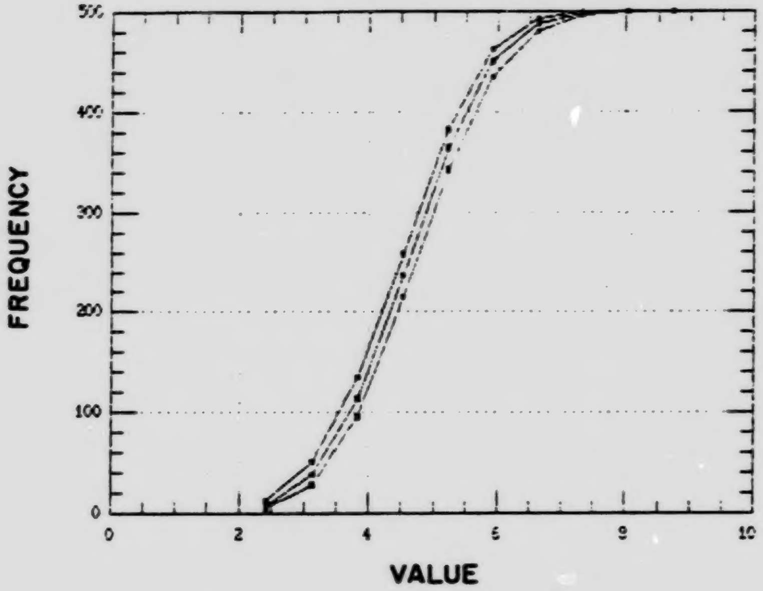

A) CUMULATIVE DISTRIBUTION FUNCTION

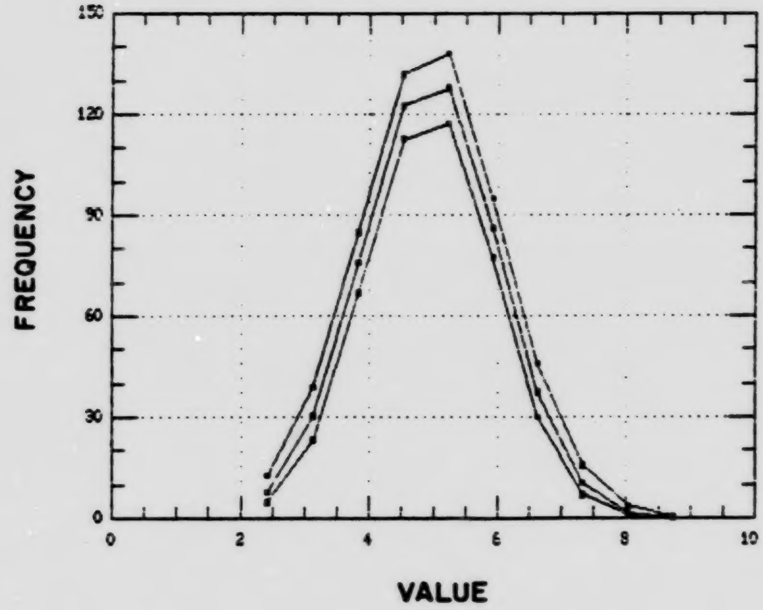

B) PROBABILITY DISTRIBUTION FUNCTION

FIGURE F.10

PLOTS OF 95% CONFIDENCE BANDS
FOR A LOG-TRANSFORMED LOGNORMAL DISTRIBUTION
(500 TRIALS)

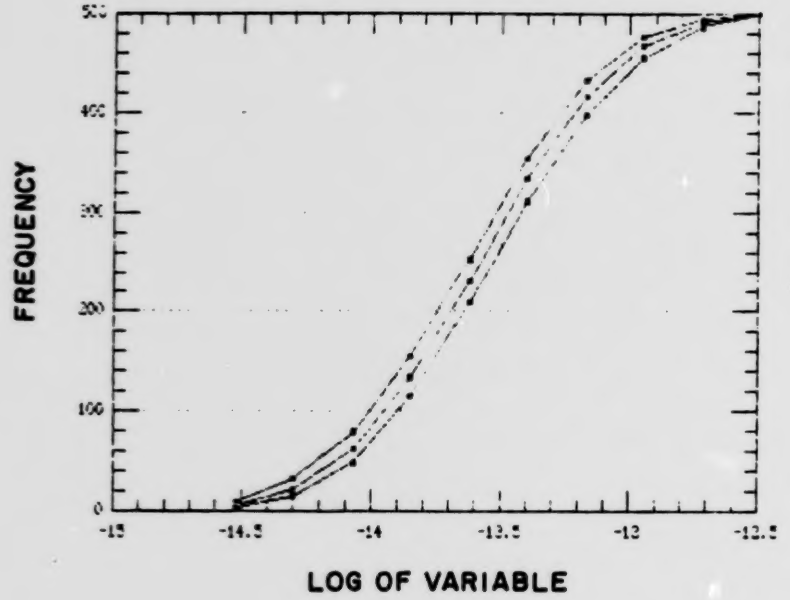

A) CUMULATIVE DISTRIBUTION FUNCTION

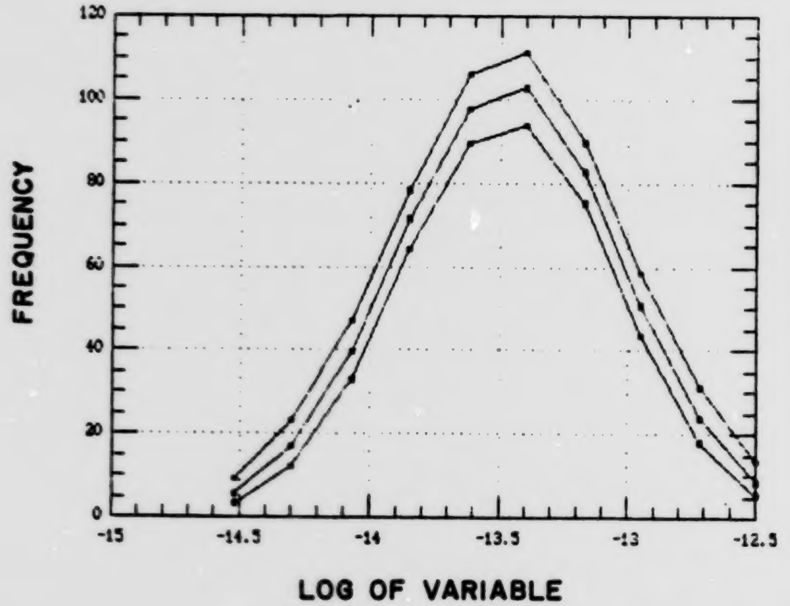

B) PROBABILITY DENSITY FUNCTION

FIGURE F.11

PLOTS OF 95% CONFIDENCE BANDS FOR THE LOGARITHM OF RADIUM IN FISH AT 100 YEARS (200 TRIALS)

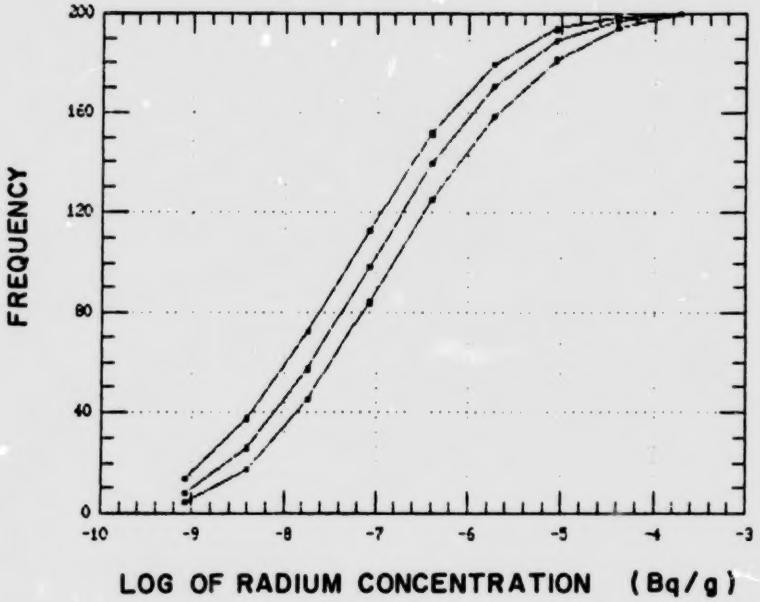

A) CUMULATIVE DISTRIBUTION FUNCTION

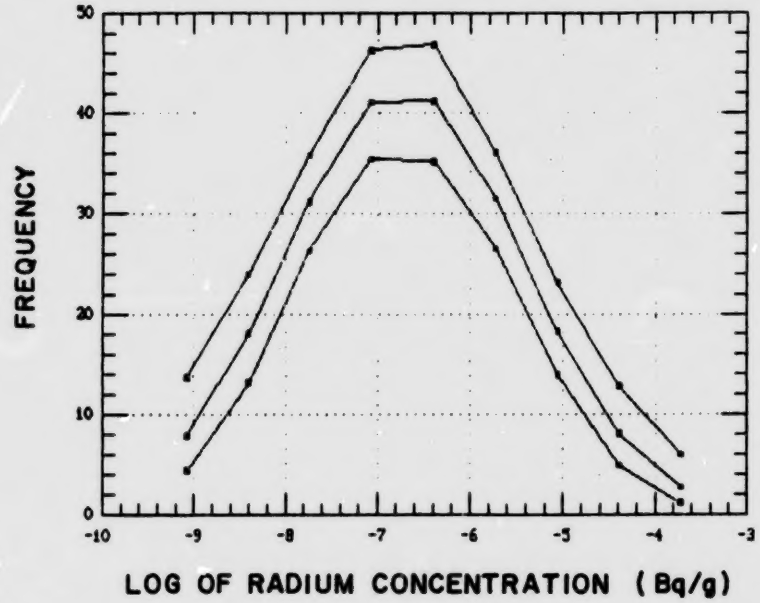

B) PROBABILITY DENSITY FUNCTION

actual output from the model UTAP. Two hundred probabilistic trials were used with the confidence bands being fitted to radium concentration in fish, after 100 years, using a log transformation of the data.

The following interpretation applies to Figure F.7. The bands show the 95% confidence region for the true cdf in the sense that upon repeated sampling, 95 out of 100 confidence bands generated in this way would contain the unknown true cdf. In other words there is a 95% probability that the bands shown in Figure F.7 enclose the true cdf. However,this must be accompanied by the statement "providing the assumed model is correct". The assumed model in this case refers to the fitted function and the assumption that no value larger than or smaller than the ones shown will be observed. This means that the value of the random variable corresponding to the last point shown (22×10^{-5}) is the largest possible value and cannot be exceeded with any probability. The value corresponding to the first cell represents the smallest possible value of the random variable. This value has a probability of 0.436 to 0.646 while any value smaller than this has a probability of zero.

This implies that the binning program must ensure that no value beyond the range shown can be observed. This does not mean that the probabilities in the first and last cells would be zero but only that the probability of any value occuring to the left of the first cell and to the right of the last cell be zero.

F.8 CONCLUSIONS

Reilly and Duever have developed a method for fitting a flexible generalized model to the output distribution from Monte Carlo type calculations.

The procedure for calculating confidence bands for probability density functions and cumulative distribution functions of Monte Carlo type output is an extension of the approach formulated by Cheng and Iles and by Scheffe.

The model and confidence band procedure has been successfully applied to environmental assessment model outputs.

The bands for the cdf based on this method compare well with the Kolmogorov bands. They give narrower confidence bands which are however rigorously correct.

REFERENCES

Bard, Y., 1974. "Nonlinear Parameter Estimation." Academic Press.

Cheng, R.C.H., and Iles, T.C., 1983. "Confidence Bands for Cumulative Distribution Functions of Continuous Random Variables." Technometrics, Vol. 25, pp. 77-86.

Davies, O.L., and Goldsmith, P.L., 1977. "Statistical Methods in Research and Production." Longman Group Ltd., London.

Kendall, M., and Stuart, A., 1961. "The Advanced Theory of Statistics, Vol. 2: Inference and Relationship." 1st Edition, Hafner Publishing Co.

Kolmogorov, A.N., 1941. "Confidence Limits for an Unknown Distribution Function." Ann. Math. Statist., Vol. 12, pp. 461-463.

SENES Consultants Limited, 1984. "A Study to Develop and Demonstrate Techniques for the Probabilistic Assessment of the Long-Term Effects of Uranium Mill Tailings in Canada - Phase I." Prepared for the National Uranium Tailings Program, Energy, Mines and Resources Canada, Ottawa, Ontario.

SENES Consultants Limited, 1985. "A Study to Develop and Demonstrate Techniques for the Probabilistic Assessment of the Long-Term Effects of Uranium Mill Tailings in Canada - Phase II." Prepared for the National Uranium Tailings Program, Energy, Mines and Resources Canada, Ottawa, Ontario.

Scheffe, H., 1959. "The Analysis of Variance." John Wiley and Sons, New York.

Sturges, H.A., 1926. "The Choice of a Class Interval." Journal of the American Statistical Association, March.

APPENDIX F1: NEWTON-RAPHSON ITERATIVE SOLUTION

An iterative procedure for solving equation (F10) by the Newton-Raphson method is as follows.

Define the (q+1)x1 vector function $\underline{F}(\underline{\theta})$ as:

$$\underline{F}(\underline{\theta}) = \sum_{i=1}^{m} x_i^{u-1} \left[\frac{n_i}{N} - p_i \right] \quad \text{uth element}$$

where all notation is as used previously and $p_i = p(x_i)$ is defined by equation (F.1). Define the (q+1)x(q+1) Jacobian matrix $\underline{Q}(\underline{\theta})$ as:

$$\underline{Q}(\underline{\theta}) = \frac{\underline{F}}{\partial \underline{\theta}} = \left[- \sum_{i=1}^{m} N p_i x_i^{\ u+v-2} \right] \quad \text{u,v element}$$

Then the iterative scheme consists of choosing a starting vector $\underline{\theta}^{(1)}$ and calculating successive vectors from:

$$\underline{\theta}^{(k+1)} = \underline{\theta}^{(k)} - \underline{\partial}^{(k)}$$

where $\underline{\theta}^{(k)}$ is found by solving the following set of linear equations for $\underline{\partial}^{(k)}$

$$\underline{Q}(\underline{\theta}^{(k)})\ \underline{\partial}^{(k)} = \underline{F}(\underline{\theta}^{(k)})$$

If q is large, say greater than 4, steps may be necessary to deal with the fact that $\underline{Q}$ will likely be badly conditioned.

The vector is calculated using the subroutine EQCHOL which was the Cusbesley decomposition method described by Plachett (1978). To use EQCHOL, $\underline{Q}$ must be positive definite. This condition is not always fullfilled. Multiplying $\underline{Q}$ by its transpose will result at least in a symmetric positive semi-definite matrix.

$$(\underline{Q}'\underline{Q})\ \underline{\partial}-\ (\underline{Q}'\underline{F})$$

In addition the matrix (Q'Q) will be better conditioned than $\underline{Q}$.

APPENDIX F2: KOLMOGOROV CONFIDENCE BANDS

For 95% confidence bands and for a number of trials larger than 50,

$d_{.95} = 1.3581\ n^{-1/2}$; n = number of trials

For DOSRN 100: $d_{.95} = .13581$

For DOSRN 500: $d_{.95} = .06076$

To plot the bands on graphs, multiply d by the sample size.

DOSRN 100: $d_{.95} = 13.6$

DOSRN 500: $d_{.95} = 30.4$

Kolmogorov bands are then obtained by plotting a band $\pm\ d_{.95}$ about the observed cumulative frequency function.

APPENDIX G

CONFIDENCE BANDS PROGRAMS
CODE LISTING
AND
VARIABLE DICTIONARY

G.1.1 Variable Dictionary for BIN

The following list defines the major variables used in BIN.FOR. In some cases, different variables are used for the same purpose in different segments of the program.

VARIABLE	DEFINITION
ABCISA = A	vector of abscissa values for bins; both right hand cell endpoints and cell midpoints.
EVNT	particular Monte Carlo outcome of variable being analyzed
HALF	one half width of bin interval; needed to calculate abscissa value at cell midpoint
HTS = H	vector of cell or bin counts
IFLAG	if IFLAG = 0, logarithmic transformation is made.
INTVLS	number of bins used given by $[\log_{10}(NTRIAL)/\log_{10}(2.0)] + 1.0$ rounded up to the nearest integer
IPL2	INTVLS + 2
MAX	maximum value of variable from statistics file

MIN	minimum value of variable from statistics file
N	integer identifying the variable to be analyzed
NAME	character variable specifying the name of the variable under consideration
NTRIAL	total number of Monte Carlo trials
VAR	vector of Monte Carlo outcomes for variables being considered
VARMAX = AMAX	maximum value of variable for purpose of binning
VARMIN = AMIN	minimum value of variable for purpose of binning
X	$= [\log_{10}(\text{NTRIAL})/\log_{10}(2.0)] + 1.0$

G.1.2 Variable Dictionary for CBAND

This list defines the major variables used in CBAND.FOR. Some variables have different meanings depending on the subroutine or function in which they are used. When this is the case, the meaning in each subroutine is given. References made are to sections, equations and appendices of the discussion paper by Reilly and Duever found in Appendix F.

VARIABLE		DEFINITION
A		"a" used in Appendix F2
ADJUST		$\sqrt{\frac{\gamma}{M}}$, s=1 equation F14 and F16
CHI25		vector containing $\chi^2_{.25}$ quantities with degrees of freedom 1 to 20
CHI05		vector of $\chi^2_{.05}$ quantities with degrees of freedom 1 to 20
CHIS2		calculated χ^2 value
CRIT		convergence criterion for various interactive procedures
CSUM	in CDF	$=\sqrt{\frac{\gamma}{\underline{r}'\underline{M}^{-1}\underline{r}}}$
	in PDF	$=\sqrt{\frac{\gamma}{(\underline{c}-\underline{b})'\underline{M}^{-1}(\underline{c}-\underline{b})}}$

F		$= \sum_{i=1}^{m} n_i x_i^{j-1} - N \sum_{i=1}^{m} p_i x_i^{j-1}$ where $j=1,2,\ldots,s+1$ (see equation F10)
FIT	in PDF	fitted cell count for pdf
	in CHITST	fitted cell counts for pdf such that $FIT \geq 6$
	in CDF	fitted cumulative cell count
FUNPDF		value of pdf at a given value of x
FUN		value of cumulative distribution at a given value of x
GAMMA		$= \chi^2_{.05,s}$; s = degree of polynomial
G		$= \frac{r}{M}$ in CDF for s = 1
		$= \sum_{i=1}^{n} p_i x_i$ in PDF = b for s = 1
ILOG		flag; if ILOG = 0 then logarithmic transformation has been used
IFLAG		flag; if IFLAG $\neq$1 then model passes goodness of fit test
IDF		number of counts for which FIT > 6 in CHITST
IDEF		degrees of freedom for χ^2 goodness of fit test

LOW		lower confidence band value
MAXIT		maximum number of iterations for iterative procedures
NAME		name of variable being analyzed
NCELLS		number of cells used
NI		vector of observed cell counts
NTOTAL		total number of Monte Carlo trials
OBS		observed cell counts corresponding to FIT in CHITST
ONE		= - 1 when k = 1, = + 1 when k = 2 in subroutines CDF and PDF
OUT		vector used to save values for output
P		vector of fitted probability density values
POSDEF		logical variable which has the value .FALSE. if the matrix supplied to EQCHOL is not positive definite
Q	in NEWRAP	- Jacobian matrix of Newton-Raphson procedure; $\frac{\partial F_j}{\partial \theta_k}$ j,k th element. - observed Fisher Information matrix otherwise

QEQ	in CDF and PDF	equal to Q when supplied to EQCHOL. Used to preserve Q since EQCHOL changes the matrix
QPQ	in NEWRAP	$\underline{Q}'\underline{Q}$
R	in CDF	equal to $\underline{r}$ shown in equation F16
	in PDF	it is the vector ($\underline{c} - \underline{b}$) shown in euqation F14
RMSD		root-mean-squared difference; used to determine convergence in iterative procedures
RPM	in CDF	corresponds to $\underline{M}^{-1}\underline{r}$
	in PDF	corresponds to $\underline{M}^{-1}(\underline{c} - \underline{b})$
S		degree of approximating polynomial
S2		= S x 2
SUMPX		vector the jth element of which is $\sum_{i=1}^{m} P_i x_i^j$ $j = 1,2,3... 2s$
T0		value of normalizing constant θ_0
T0NEW		maximum likelihood estimate $\hat{\theta}_0$
THETA		vector of upper and lower values of $\underline{\theta}$ given by equations F14 and F16

TNEW	maximum likelihood estimate $\hat{\underline{\theta}}$
TOLD	vector used to store (n-1)th value of $\underline{\theta}$ during nth iteration
U	= ∂ in Newton-Raphson procedure
UPP	upper confidence band limits
XEXP	$= \sum_{i=1}^{m} x^{j}_{i} P_i$ for a given value of j
XI	vector of indicator variables used in Newton-Raphson procedure. This is used instead of actual x - values for mathematical convenience and since the problem is well conditioned, resulting in easier convergence
XCMPT	cell midpoints in actual units of variable

G.2.1 Code Listings of Confidence Bands Binning Program - BIN.FOR

```
C             CONFIDENCE BANDS BINNING PROGRAM - BIN.FOR
C     UPDATED 10/02/87  TAD.
C
C     THE PROGRAM, BIN, READS DETAILED RESULTS AND DETAILED RESULTS
C     KEY FILES AS CREATED BY THE PROGRAM, UTAP.  IT ASSIGNS
C     OBSERVATIONS FROM MONTE CARLO TRIALS TO BINS, APPLYING A
C     LOG TRANSFORMATION IF DESIRED.  THE FILE BIN.DAT IS CREATED
C     FOR USE BY THE CONFIDENCE BANDS PROGRAM, OPAN.FOR.
C
      REAL HTS(22)
      DIMENSION ABCISA(22)
      INTEGER*4 SCRUNT,FUNIT1,FUNIT2,FUNIT3,DEBUG
      COMMON /UNITS/ SCRUNT,FUNIT1,FUNIT2,FUNIT3,DEBUG
      REAL*4 VAR(1000),MIN,MAX
      INTEGER*4 NTRIAL,N,IFLAG
      CHARACTER*6 NAME
      COMMON /IN/ VAR,NTRIAL,N,NAME,MIN,MAX,IFLAG
C
      CALL READ
      X=ALOG10(FLOAT(NTRIAL))/ALOG10(2.0)+1.0
C
      INTVLS = INT(X)
      IF(ABS(X-INTVLS).GT.0.50) INTVLS = INTVLS+1
      IPL2 = INTVLS+2
      IF(IFLAG.EQ.0) THEN
         DO 12 I=1,NTRIAL
            VAR(I) = ALOG(VAR(I))
12       CONTINUE
         IF(MIN.GE.1)THEN
            VARMIN = ALOG(MIN)
            VARMAX = ALOG(MAX)
         ELSE
            VARMIN=ALOG(MIN)
            VARMAX=ALOG(MAX)
         ENDIF
      ELSE
         VARMIN = MIN
         VARMAX = MAX
      ENDIF
      CALL DISTRI(ABCISA,HTS,INTVLS,VARMIN,VARMAX,IPL2)
      DO 20 I=1,NTRIAL
         CALL DISTRA(ABCISA,HTS,VAR(I),IPL2)
20    CONTINUE
      IF(HTS(2).GT.0)  HTS(3) = HTS(3)+1.0
      HTS(2) = 0.0
      WRITE(FUNIT3,1200) N,NAME,INTVLS,NTRIAL,IFLAG
      HALF = (ABCISA(4)-ABCISA(3))/2.0
      DO 40 I=3,IPL2
         ABCISA(I) = ABCISA(I)-HALF
         WRITE(FUNIT3,1300) HTS(I),ABCISA(I)
40    CONTINUE
      STOP
1200  FORMAT (1X,I3,1X,A6,5X,I5,2X,I5,2X,I5)
```

```
1300  FORMAT (2X,E10.4,2X,E10.4)
      END
C
C ***********************************************************************
C
      SUBROUTINE DISTRI (A,H,INTVLS,AMIN,AMAX,IPL2)
C
C     SUBROUTINE INITIALIZES BINS
C
      REAL A(IPL2),H(IPL2)
      INTEGER*4 SCRUNT,FUNIT1,FUNIT2,FUNIT3,DEBUG
      COMMON /UNITS/ SCRUNT,FUNIT1,FUNIT2,FUNIT3,DEBUG
C
      IF(DEBUG.EQ.1)WRITE(SCRUNT,*)' SUBROUTINE DISTRI'
      FINC=ABS((AMAX-AMIN)/INTVLS)
      A(1)=INTVLS+2
      M=A(1)
      A(2)=AMIN
      H(1)=0.0
      H(2)=0.0
      DO 100 I=3,M
         A(I)=A(I-1)+FINC
         H(I)=0.0
100   CONTINUE
      RETURN
      END
C
C ***********************************************************************
C
      SUBROUTINE DISTRA (A,H,EVNT,IPL2)
C
C     SUBROUTINE ASSIGNES TRIALS TO BINS
C
      REAL A(IPL2),H(IPL2)
      INTEGER*4 SCRUNT,FUNIT1,FUNIT2,FUNIT3,DEBUG
      COMMON /UNITS/ SCRUNT,FUNIT1,FUNIT2,FUNIT3,DEBUG

      IF(DEBUG.EQ.1)WRITE(SCRUNT,*)' SUBROUTINE DISTRA'
      M=ABS(A(1))
      DO 210 I=2,M
         IF (EVNT.LE.A(I))THEN
            H(I) = H(I)+1.0
            GO TO 225
         ENDIF
  210 CONTINUE
  225 H(1)=H(1)+1.0
      RETURN
      END
C
C ***********************************************************************
C
      SUBROUTINE READ
C
C     SUBROUTINE READS INPUT FILES AND OPENS OUTPUT FILE
C
```

```
      INTEGER*4 SCRUNT,FUNIT1,FUNIT2,FUNIT3,DEBUG
      COMMON /UNITS/ SCRUNT,FUNIT1,FUNIT2,FUNIT3,DEBUG
      REAL*4 VAR(1000),MIN,MAX
      INTEGER*4 NTRIAL,N,IFLAG
      CHARACTER*6 NAME
      COMMON /IN/ VAR,NTRIAL,N,NAME,MIN,MAX,IFLAG
      CHARACTER*1 Q
      CHARACTER*12 FNAME
      CHARACTER*18 COLUMN
C
      DEBUG=0
      SCRUNT=5
      IF(DEBUG.EQ.1)WRITE(SCRUNT,*)' SUBROUTINE READ'
      FUNIT1=1
      FUNIT2=2
      FUNIT3=3
      WRITE(SCRUNT,900)' DETAILED RESULTS FILE NAME? '
      READ(SCRUNT,900)FNAME
      WRITE(SCRUNT,800)FNAME
      OPEN(UNIT=FUNIT1,FILE=FNAME)
      WRITE(SCRUNT,900)' KEY FILE NAME? '
      READ(SCRUNT,900)FNAME
      WRITE(SCRUNT,800)FNAME
      OPEN(UNIT=FUNIT2,FILE=FNAME)
      FNAME='BIN.DAT'
      WRITE(SCRUNT,800)FNAME
      OPEN(UNIT=FUNIT3,FILE=FNAME)
      WRITE(SCRUNT,900) ' ENTER ID. NO. OF VARIABLE TO BE ANALYZED: '
      READ(SCRUNT,901) N
      WRITE(SCRUNT,900) ' DO YOU WANT LOG TRANSFORMATION (Y/N)? '
      READ(SCRUNT,900) Q
      IF(Q.EQ.'Y'.OR.Q.EQ.'y')THEN
         IFLAG=0
      ELSE
         IFLAG=1
      ENDIF
      READ(FUNIT2,100)
      READ(FUNIT2,100)
      READ(FUNIT2,200)NTRIAL
      DO 10 I=1,N
         READ(FUNIT2,100)
10    CONTINUE
      READ(FUNIT2,300)NAME,MIN,MAX
      READ(FUNIT1,100)
      IF(N.GT.1)THEN
         WRITE(COLUMN,102)'(',N-1,'(10X),1X,E9.3)'
         DO 15 I=1,NTRIAL
            READ(FUNIT1,COLUMN)VAR(I)
15       CONTINUE
      ELSE
         DO 20 I=1,NTRIAL
            READ(FUNIT1,400)VAR(I)
20       CONTINUE
      ENDIF
      CLOSE(FUNIT1)
      CLOSE(FUNIT2)
      RETURN
100   FORMAT (1X)
102   FORMAT (A1,I3,A14)
200   FORMAT (19X,I5)
300   FORMAT (7X,A6,73X,2E11.3)
400   FORMAT (1X,E9.3)
800   FORMAT (' Opening file: ',A12)
900   FORMAT (A)
901   FORMAT (I3)
      END
```

G.2.2 Code Listing of Confidence Bands Program - CBAND.FOR

```
C                   CONFIDENCE BANDS PROGRAM - CBAND.FOR
C
C     UPDATED 10/02/87 TAD.  DISCRETE VARIABLE ASSUMPTION.
C
C     PROGRAM, OPAN.FOR, READS THE FILE, BIN.DAT, CREATED BY THE
C     BINNING PROGRAM, BIN.FOR, AND FITS CONFIDENCE BANDS TO THE
C     CUMULATIVE AND PROBABILITY DENSITY FUNCTIONS.
C
      IMPLICIT REAL*8(A-H,O-Z)
      INTEGER*4 FUNIT1,FUNIT2,FUNIT3,SCRUNT,DEBUG
      COMMON /FILES/ FUNIT1,FUNIT2,FUNIT3,SCRUNT,DEBUG
      INTEGER*4 NCELLS,ILOG,S,MAXIT,S2
      CHARACTER*6 NAME
      COMMON /INIT/ NCELLS,ILOG,S,MAXIT,CRIT,NAME
      REAL*8 OUT(20,8)
      COMMON /OUTS/ OUT
      REAL*8 NI,CHI25(20),CHI05(20),NTOTAL,
     &   Q(20,20),QEQ(20,20),QPQ(20,20),F(20),P(20),RPM(20),
     &   SUMPX(20),TNEW(20),TOLD(20),THETA(20),U(20),R(20)
      COMMON/AREA1/XI(20),NI(20),NTOTAL
      COMMON/AREA2/CHI25
      COMMON/AREA3/CHI05
      COMMON/AREA4/XCMPT(20)
C
      CALL START
50    CONTINUE
C
C        START WITH DEGREE OF POLYNOMIAL EQUAL 1 AND INCREASE UNTIL FIT
C        FOUND
C
         S=S+1
         IF(DEBUG.EQ.2)WRITE(FUNIT1,1600) S
         S2 = 2*S
         TONEW = -1.0
         DO 60 I=1,S
            TNEW(I) = 0.001
60       CONTINUE
         CALL NEWRAP(TONEW,TNEW,SUMPX,S2,F,P,Q,QPQ,U,TOLD)
         DO 70 I = 1,NCELLS
            P(I) = FUNPDF(TONEW,TNEW,XI(I))
70       CONTINUE
         CALL CHITST(IFLAG,P)
C
C        CHECK IF DEGREE OF POLYNOMIAL EQUALS NUMBER OF BINS
C
         IF (S.GT.NCELLS-1) THEN
            WRITE(SCRUNT,1700)
            STOP
         ENDIF
      IF(IFLAG.EQ.1) GOTO 50
      IF(IFLAG.EQ.0) THEN
         WRITE(FUNIT2,1750)
         WRITE(SCRUNT,1750)
      ENDIF
      IF(DEBUG.EQ.2)THEN
         IF(IFLAG.EQ.0) WRITE(FUNIT1,1750)
         WRITE(FUNIT1,1800)
         WRITE(FUNIT1,1900)
      ENDIF
      DO 90 I=1,NCELLS
         IF(DEBUG.EQ.2)WRITE(FUNIT1,2000) NTOTAL*P(I),NI(I)
90    CONTINUE
      CALL FISHER(Q,P,SUMPX,S2)
      CRIT = 1.E-5
      GAMMA = CHI05(S)
      IF(ILOG.NE.1) THEN
         WRITE(SCRUNT,900) ' LOGARITHM OF VARIABLE IS USED'
         WRITE(FUNIT2,900) ' LOGARITHM OF VARIABLE IS USED'
      ENDIF
      CALL CDF(TONEW,TNEW,Q,GAMMA,QEQ,TOLD,THETA,RPM,R)
      CALL PDF(TONEW,TNEW,Q,GAMMA,QEQ,TOLD,THETA,RPM,R)
      CALL OUTPUT
      STOP
900   FORMAT (A)
1600  FORMAT (/,72('*'),/,5X,'FIT POLYNOMIAL OF DEGREE S = ', I5,//)
1700  FORMAT (/,5X,'PROCEDURE UNSUCCESSFUL, CHECK DATA')
1750  FORMAT (/,5X,'DEGREES OF FREEDOM FOR CHI-SQUARED TEST EQUAL ZERO',
     &        /,5X,'MODEL TO BE USED WITH CAUTION',/)
1800  FORMAT (/,5X,'PROBABILITY OF POORER FIT IS GREATER THAN 25%')
1900  FORMAT (/,5X,'FITTED VALUES',5X,'MEASUREMENTS',/)
2000  FORMAT (5X,E13.6,5X,E13.6,/)
2100  FORMAT (1X,A6)
      END
C
C **********************************************************************
C
      SUBROUTINE START
C
C     SUBROUTINE OPENS FILES AND READS INPUT FILE FROM BINNING
C     PROGRAM
C
      IMPLICIT REAL*8(A-H,O-Z)
      INTEGER*4 FUNIT1,FUNIT2,FUNIT3,SCRUNT,DEBUG
      COMMON /FILES/ FUNIT1,FUNIT2,FUNIT3,SCRUNT,DEBUG
      INTEGER*4 NCELLS,ILOG,S,MAXIT
      CHARACTER*6 NAME
      COMMON /INIT/ NCELLS,ILOG,S,MAXIT,CRIT,NAME
      REAL*8 NTOTAL,NI
      COMMON /AREA1 /XI(20), NI(20), NTOTAL
      COMMON /AREA4 /XCMPT(20)
      CHARACTER*12 FNAME
C
      DEBUG=0
      SCRUNT=5
      IF(DEBUG.GE.1)WRITE(SCRUNT,*)' SUBROUTINE START'
      FUNIT1=1
      FUNIT2=2
      FUNIT3=3
      IF(DEBUG.EQ.2)THEN
         FNAME='FIT.OUT'
         WRITE(SCRUNT,800)FNAME
         OPEN(UNIT=FUNIT1,FILE=FNAME)
      ENDIF
      FNAME='BIN.DAT'
      WRITE(SCRUNT,800)FNAME
      OPEN(UNIT=FUNIT3,FILE=FNAME)
      READ(FUNIT3,1000) NAME,NCELLS,NTRIAL,ILOG
      NTOTAL = FLOAT(NTRIAL)
      WRITE(SCRUNT,900)
      READ(SCRUNT,700)FNAME
      WRITE(SCRUNT,800)FNAME
      OPEN(UNIT=FUNIT2,FILE=FNAME)
      S = 0
      MAXIT = 50
      CRIT = 1.E-8
      IF(DEBUG.EQ.2)THEN
         WRITE(FUNIT1,1200) NAME, NTOTAL
         WRITE(FUNIT1,1300) MAXIT,CRIT,NCELLS,S
      ENDIF
      XM = NCELLS
      IF(DMOD(XM,2.0D0).GT.0.0) XM = NCELLS - 1.0
      XM = XM + 1.0
      IF(DEBUG.EQ.2)WRITE(FUNIT1,1400)
      DO 20 I=1,NCELLS
         READ(FUNIT3,1100) NI(I),XCMPT(I)
          XI(I)=I-XM/2.
         IF(DEBUG.EQ.2)WRITE(FUNIT1,1500) I,XI(I),I,NI(I)
20    CONTINUE
      RETURN
700   FORMAT(A)
800   FORMAT(' Opening file: ',A12)
900   FORMAT(' ENTER NAME OF OUTPUT FILE: ')
1000  FORMAT(5X,A6,5X,I5,2X,I5,2X,I5)
1050  FORMAT(2X,E10.4)
1100  FORMAT(2X,E10.4,2X,E10.4)
1200  FORMAT(/,2X,'VARIABLE: ',A6,/,5X,'NTOTAL = ',E13.6)
1300  FORMAT(/,5X,'MAXIT = ',I5, 2X, 'CRIT = ',E13.6,2X,'NCELLS = ',I5,
     &   2X,'S = ',I5)
1400  FORMAT(/,5X,'RANDOM VARIABLE',12X,'CELL COUNTS')
1500  FORMAT(/,5X,'XI(',I2,') = ',E13.6,5X,'NI(',I2,') = ',E13.6)
      END
C
C***********************************************************************
C
      BLOCK DATA
      REAL*8 CHI25(20)
      REAL*8 CHI05(20)
      COMMON/AREA2/CHI25
      COMMON/AREA3/CHI05
      DATA CHI25/1.32,2.77,4.11,5.39,6.63,7.84,9.04,10.22,11.39,12.55,
     &           13.70,14.85,15.98,17.12,18.25,19.37,20.49,21.60,
     &           22.72,23.83/
       DATA CHI05/3.84,5.99,7.81,9.49,11.07,12.59,14.07,15.51,16.92,
     &           18.31,19.68,21.03,22.36,23.68,25.00,26.30,27.59,
     &           28.87,30.14,31.41/
      END
C
C ***********************************************************************
C
      SUBROUTINE NEWRAP(TONEW,TNEW,SUMPX,S2,F,P,Q,QPQ,U,
     &                  TOLD)
C
C     NEWTON-RAPHSON PROCEDURE FOR FITTING MODEL
C
      IMPLICIT REAL*8(A-H,O-Z)
      INTEGER*4 FUNIT1,FUNIT2,FUNIT3,SCRUNT,DEBUG
      COMMON /FILES/ FUNIT1,FUNIT2,FUNIT3,SCRUNT,DEBUG
      INTEGER*4 NCELLS,ILOG,S,MAXIT,S2
      CHARACTER*6 NAME
      COMMON /INIT/ NCELLS,ILOG,S,MAXIT,CRIT,NAME
      REAL*8 NI, NTOTAL
      LOGICAL POSDEF
      DIMENSION F(S),P(NCELLS),Q(S,S),U(S),TOLD(S),TNEW(S),
     &          SUMPX(S2),QPQ(S,S)
      COMMON/AREA1/XI(20), NI(20), NTOTAL
C
      IF(DEBUG.GE.1)WRITE(SCRUNT,*)' SUBROUTINE NEWRAP'
      DO 170 I=1,MAXIT
         DO 20 K=1,S
            F(K) = 0.0
            DO 10 J = 1,S
               Q(K,J) = 0.0
10          CONTINUE
20       CONTINUE
         DO 30 I2=1,S
            TOLD(I2) = TNEW(I2)
30       CONTINUE
         TOOLD = THETAO(TOLD)
         DO 50 I1=1,NCELLS
            P(I1)=FUNPDF(TOOLD,TOLD,XI(I1))
            DO 40 I2=1,S
               X = XI(I1)**I2
               F(I2) = F(I2) + NI(I1)*X - NTOTAL*P(I1)*X
40          CONTINUE
50       CONTINUE
         DO 60 I2 = 1,S2
            SUMPX(I2) = 0.0
60       CONTINUE
         DO 80 I2 = 1,S2
            DO 70 I3 = 1,NCELLS
               SUMPX(I2) = SUMPX(I2) + P(I3)*XI(I3)**I2
70          CONTINUE
80       CONTINUE
         DO 90 I2 = 1,S
            DO 90 I3 = 1,S
               Q(I2,I3) = NTOTAL*(SUMPX(I2)*SUMPX(I3)-SUMPX(I2+I3))
90       CONTINUE
         DO 120 J = 1,S
```

```
            DO 110 L = 1,S
               SUM = 0.0
               DO 100 K = 1,S
                  SUM = SUM + Q(K,J)*Q(K,L)
100            CONTINUE
               QPQ(J,L) = SUM
110         CONTINUE
120      CONTINUE
         DO 140 J=1,S
            SUM = 0.0
            DO 130 K=1,S
               SUM = SUM + Q(K,J)*F(K)
130         CONTINUE
            U(J) = SUM
140      CONTINUE
         CALL EQCHOL(S,QPQ,U,POSDEF)
C
C        CHECK IF EQCHOL SUCCESSFUL
C
         IF(.NOT.POSDEF)THEN
            WRITE(SCRUNT,1500)
            STOP
         ENDIF
         DO 150 I1=1,S
            TNEW(I1) = TOLD(I1) - U(I1)
150      CONTINUE
         TONEW = THETAO(TNEW)
         RMSD = 0.0
         DO 160 I1=1,S
            RMSD = RMSD + DSQRT(U(I1)**2)
160      CONTINUE
         IF(DEBUG.EQ.2)THEN
            WRITE(FUNIT1,1000) I,RMSD
            WRITE(FUNIT1,1100) TONEW, TNEW
         ENDIF
         IF(RMSD.LT.CRIT)GOTO180
170   CONTINUE
180   CONTINUE
      IF(DEBUG.EQ.2)THEN
         WRITE(FUNIT1,1200)
         WRITE(FUNIT1,1300)
         WRITE(FUNIT1,1400) (F(J),J=1,S)
      ENDIF
      RETURN
1000  FORMAT (/,5X,'*****ITERATION : ',I5,2X,'*****',5X,'RMSD = ',E13.6)
1100  FORMAT (/,5X,'PARAMETER VALUES: ','TO = ',E13.6,/,5X,'THETA:',
     &   2(2X,E13.6))
1200  FORMAT (/,5X,'CONVERGENCE REACHED !')
1300  FORMAT (/,5X,'FUNCTION AT CONVERGENCE:')
1400  FORMAT (/,5X,E13.6)
1500  FORMAT (/,5X,'POSDEF IS FALSE - CANNOT SOLVE')
      END
C
C***********************************************************************
C
```

```
      SUBROUTINE CHITST(IFLAG,P)
C
C     SUBROUTINE PERFORMS CHI SQUARED GOODNESS OF FIT TEST
C
      IMPLICIT REAL*8 (A-H,O-Z)
      INTEGER*4 FUNIT1,FUNIT2,FUNIT3,SCRUNT,DEBUG
      COMMON /FILES/ FUNIT1,FUNIT2,FUNIT3,SCRUNT,DEBUG
      INTEGER*4 NCELLS,ILOG,S,MAXIT
      CHARACTER*6 NAME
      COMMON /INIT/ NCELLS,ILOG,S,MAXIT,CRIT,NAME
      REAL*8 CHI25(20),NI,NTOTAL
      DIMENSION P(NCELLS)
      COMMON/AREA1/XI(20), NI(20), NTOTAL
      COMMON/AREA2/CHI25
C
      IF(DEBUG.GE.1)WRITE(SCRUNT,*)' SUBROUTINE CHITST'
      IFLAG = 1
      CHISQ = 0.0
      IDF = 0
      I = 1
      IF(I.LT.NCELLS)THEN
10       CONTINUE
            FIT = 0.0
            OBS = 0.0
30          CONTINUE
               FIT = FIT + NTOTAL*P(I)
               OBS = OBS + NI(I)
               I = I+1
            IF(I.LE.NCELLS.AND.FIT.LT.6.0)GOTO 30
            CHISQ = CHISQ + ((OBS-FIT)**2)/FIT
            IDF = IDF + 1
         IF(I.LT.NCELLS)GOTO 10
      ENDIF
      IDEG = IDF - S - 1
C
C     CHECK DEGREES OF FREEDOM
C
      IF(IDEG.GT.20)THEN
         WRITE(SCRUNT,2000)' DEGREES OF FREEDOM GREATER THAN 20'
         STOP
      ENDIF
      IF(DEBUG.EQ.2)WRITE(FUNIT1,1000) CHISQ, IDEG
      IF(IDEG.LT.1) THEN
        IFLAG=0
        RETURN
      ENDIF
      IF(CHISQ.LT.CHI25(IDEG)) IFLAG = -1
      RETURN
1000  FORMAT (//,5X,'CHISQ GOODNESS OF FIT TEST RESULT: ',/,5X,'CALCULAT
     &ED CHISQ = ',E13.6,'  WITH ',I5,'  DEGREES OF FREEDOM')
2000  FORMAT (A)
      END
C
C***********************************************************************
C
```

```
      SUBROUTINE FISHER(Q,P,SUMPX,S2)
C
C     SUBROUTINE CALCULATES OBSERVED FISHER INFORMATION MATRIX
C
      IMPLICIT REAL*8 (A-H,O-Z)
      INTEGER*4 FUNIT1,FUNIT2,FUNIT3,SCRUNT,DEBUG
      COMMON /FILES/ FUNIT1,FUNIT2,FUNIT3,SCRUNT,DEBUG
      INTEGER*4 NCELLS,ILOG,S,MAXIT
      CHARACTER*6 NAME
      COMMON /INIT/ NCELLS,ILOG,S,MAXIT,CRIT,NAME
      REAL*8 NI,NTOTAL
      INTEGER*4 S2
      DIMENSION Q(S,S),SUMPX(S2),P(NCELLS)
      COMMON/AREA1/XI(20), NI(20), NTOTAL
C
      IF(DEBUG.GE.1)WRITE(SCRUNT,*)' SUBROUTINE FISHER'
      K = 2.*S
      DO 10 I=1,K
         SUMPX(I) = 0.0
10    CONTINUE
      DO 20 J=1,K
         DO 21 I=1,NCELLS
            SUMPX(J) = SUMPX(J) + P(I)*XI(I)**J
21       CONTINUE
20    CONTINUE
      DO 30 J=1,S
         DO 31 K=1,S
            Q(J,K) = NTOTAL*(SUMPX(J+K) - SUMPX(J)*SUMPX(K))
31       CONTINUE
30    CONTINUE
      IF(DEBUG.EQ.2)THEN
         WRITE(FUNIT1,1000)
         DO 40 I=1,S
            WRITE(FUNIT1,1200) (Q(I,K), K=1,S,1)
40       CONTINUE
      ENDIF
      RETURN
1000  FORMAT (/,5X,'OBSERVED FISHER INFORMATION MATRIX',/)
1200  FORMAT (/,5X,5(E11.4,1X))
      END
C
C***********************************************************************
C
      SUBROUTINE CDF(TONEW,TNEW,Q,GAMMA,QEQ,TOLD,THETA,RPM,R)
C
C     SUBROUTINE CALCULATES 95% CONFIDENCE BANDS FOR CDF
C
      IMPLICIT REAL*8 (A-H,O-Z)
      INTEGER*4 FUNIT1,FUNIT2,FUNIT3,SCRUNT,DEBUG
      COMMON /FILES/ FUNIT1,FUNIT2,FUNIT3,SCRUNT,DEBUG
      INTEGER*4 NCELLS,ILOG,S,MAXIT
      CHARACTER*6 NAME
      COMMON /INIT/ NCELLS,ILOG,S,MAXIT,CRIT,NAME
      LOGICAL POSDEF
      REAL*8 NI,NTOTAL,FUNCDF,LOW,FIT,UPP,
     &   TOLD(S),THETA(S),TNEW(S),Q(S,S),QEQ(S,S),
     &   RPM(S),R(S)
      COMMON/AREA1/XI(20), NI(20), NTOTAL
      COMMON/AREA4/XCMPT(20)
C
      IF(DEBUG.GE.1)WRITE(SCRUNT,*)' SUBROUTINE CDF'
      IF(S.LE.1)THEN
         ADJUST = DSQRT(GAMMA/Q(1,1))
         NCM1 = NCELLS -1
         DO 10 ICOUNT=1,NCM1
            ONE = -1.0
            CALL RR(TONEW,TNEW,ICOUNT,R)
            G = R(1)/Q(1,1)
            IF(G.LT.0.0) ONE = 1.0
            THETA(1) = TNEW(1) + ONE*ADJUST
            TO = THETAO(THETA)
            LOW = NTOTAL*FUNCDF(TO,THETA,ICOUNT)
            THETA(1)=TNEW(1) - ONE*ADJUST
            TO = THETAO(THETA)
            UPP = NTOTAL*FUNCDF(TO,THETA,ICOUNT)
            FIT = NTOTAL*FUNCDF(TONEW,TNEW,ICOUNT)
            CALL SAVE(1,ICOUNT,XCMPT(ICOUNT),LOW,FIT,UPP)
10       CONTINUE
         CALL SAVE(1,NCELLS,XCMPT(NCELLS),NTOTAL,NTOTAL,NTOTAL)
      ELSE
20       CONTINUE
         NCM1 = NCELLS - 1
         DO 150 ICOUNT=1,NCM1
            ONE = -1.0
            DO 140 K=1,2,1
               ONE = ONE**K
               DO 30 I=1,S,1
                  THETA(I) = TNEW(I)
30             CONTINUE
               TO = TONEW
                  DO 100 L=1,MAXIT,1
                     DO 40 I=1,S,1
                        TOLD(I) = THETA(I)
40                   CONTINUE
                     CALL RR(TO,THETA,ICOUNT,R)
                     DO 50 I=1,S,1
                        RPM(I) = R(I)
50                   CONTINUE
                     DO 60 I=1,S,1
                        DO 61 J=1,S,1
                           QEQ(I,J) = Q(I,J)
61                      CONTINUE
60                   CONTINUE
                     CALL EQCHOL(S,QEQ,RPM,POSDEF)
C
C                    CHECK IF EQCHOL SUCCESSFUL
C
                     IF(.NOT.POSDEF)THEN
                        WRITE(SCRUNT,1200)
                        STOP
                     ENDIF
                     CSUM = 0.0
                     DO 70 I=1,S,1
                        CSUM = CSUM + R(I)*RPM(I)
70                   CONTINUE
                     CSUM = DSQRT(GAMMA/CSUM)
                     DO 80 I=1,S,1
                        THETA(I) = TNEW(I) + ONE*CSUM*RPM(I)
80                   CONTINUE
                     TO = THETAO(THETA)
                     RMSD = 0.0
                     DO 90 I=1,S,1
                        RMSD = RMSD + DSQRT((TOLD(I) - THETA(I))**2)
90                   CONTINUE
                     IF(RMSD.LT.CRIT)GOTO 111
100               CONTINUE
C
C                 CHECK IF TOLERANCE REACHED
C
                  IF(RMSD.GE.CRIT)THEN
                     WRITE(SCRUNT,1100) ICOUNT,K
                     STOP
                  ENDIF
111            CONTINUE
               IF(K.NE.1)THEN
                  UPP = NTOTAL*FUNCDF(TO,THETA,ICOUNT)
               ELSE
                  LOW = NTOTAL*FUNCDF(TO,THETA,ICOUNT)
               ENDIF
               FIT = NTOTAL*FUNCDF(TONEW,TNEW,ICOUNT)
140         CONTINUE
            CALL SAVE(1,ICOUNT,XCMPT(ICOUNT),LOW,FIT,UPP)
150      CONTINUE
      CALL SAVE(1,NCELLS,XCMPT(NCELLS),NTOTAL,NTOTAL,NTOTAL)
      ENDIF
999   RETURN
1100  FORMAT (/,5X,'CONVERGENCE NOT REACHED FOR ICOUNT =',I5,
     &       2X,'AND K = ',I5)
1200  FORMAT (/,5X,'POSDEF IS FALSE - CANNOT SOLVE')
       END
C
C **********************************************************************
C
      SUBROUTINE PDF(TONEW,TNEW,Q,GAMMA,QEQ,TOLD,
C
C     SUBROUTINE CALCULATES 95% CONFIDENCE BANDS FOR PDF
C
     &   THETA,RPM,R)
      IMPLICIT REAL*8 (A-H,O-Z)
      INTEGER*4 FUNIT1,FUNIT2,FUNIT3,SCRUNT,DEBUG
      COMMON /FILES/ FUNIT1,FUNIT2,FUNIT3,SCRUNT,DEBUG
      INTEGER*4 NCELLS,ILOG,S,MAXIT
      CHARACTER*6 NAME
      COMMON /INIT/ NCELLS,ILOG,S,MAXIT,CRIT,NAME
      LOGICAL POSDEF
      REAL*8 CHI05(20),NI,NTOTAL,FUNPDF,LOW,FIT,UPP
      DIMENSION TOLD(S),THETA(S),TNEW(S),Q(S,S),QEQ(S,S),
     &   RPM(S),R(S)
      COMMON/AREA1/XI(20), NI(20), NTOTAL
      COMMON/AREA3/CHI05
      COMMON/AREA4/XCMPT(20)
C
      IF(DEBUG.GE.1)WRITE(SCRUNT,*)' SUBROUTINE PDF'
      IF(S.LE.1)THEN
         G=0.0
         DO 180 I=1,NCELLS
            G=G+XI(I)*FUNPDF(TONEW,TNEW,XI(I))
180      CONTINUE
         ADJUST = DSQRT(GAMMA/Q(1,1))
         DO 190 ICOUNT = 1,NCELLS
            ONE = -1.0
            IF(G.GT.XI(ICOUNT)) ONE = 1.0
            THETA(1) = TNEW(1) + ONE*ADJUST
            TO=THETAO(THETA)
            LOW = FUNPDF(TO,THETA,XI(ICOUNT))*NTOTAL
            THETA(1) = TNEW(1) - ONE*ADJUST
            TO=THETAO(THETA)
            UPP = FUNPDF(TO,THETA,XI(ICOUNT))*NTOTAL
            FIT = FUNPDF(TONEW,TNEW,XI(ICOUNT))*NTOTAL
            CALL SAVE(2,ICOUNT,XCMPT(ICOUNT),LOW,FIT,UPP)
190      CONTINUE
      ELSE
         DO 330 ICOUNT=1,NCELLS
            ONE = -1.0
            DO 320 K=1,2,1
               ONE = ONE**K
               DO 210 I=1,S,1
                  THETA(I) = TNEW(I)
210            CONTINUE
               TO=TONEW
               DO 290 L=1,MAXIT,1
                  DO 220 I=1,S,1
                     TOLD(I) = THETA(I)
220               CONTINUE
                  DO 230 I=1,S,1
                     R(I) = 0.0
                     DO 231 J=1,NCELLS
                        R(I) = R(I) + FUNPDF(TO,THETA,XI(J))*XI(J)**I
231                  CONTINUE
230               CONTINUE
                  DO 240 I=1,S,1
                     R(I) = XI(ICOUNT)**I - R(I)
                     RPM(I) = R(I)
240               CONTINUE
                  DO 250 I=1,S,1
                     DO 251 J=1,S,1
                        QEQ(I,J) = Q(I,J)
251                  CONTINUE
250               CONTINUE
                  CALL EQCHOL(S,QEQ,RPM,POSDEF)
```

```
C
C                 CHECK IF EQCHOL SUCCESSFUL
C
                  IF(.NOT.POSDEF)THEN
                     WRITE(SCRUNT,1200)
                     STOP
                  ENDIF
                  CSUM = 0.0
                  DO 260 I=1,S,1
                     CSUM = CSUM + R(I)*RPM(I)
260               CONTINUE
                  CSUM = DSQRT(GAMMA/CSUM)
                  DO 270 I=1,S,1
                     THETA(I) = TNEW(I) + ONE*CSUM*RPM(I)
270               CONTINUE
                  RMSD = 0.0
                  DO 280 I=1,S,1
                     RMSD = RMSD + DSQRT((TOLD(I) - THETA(I))**2)
280               CONTINUE
                  TO=THETAO(THETA)
C
C                 CHECK IF TOLERANCE REACHED
C
                  IF(RMSD.LT.CRIT)GOTO 300
290            CONTINUE
               WRITE(SCRUNT,1500)ICOUNT,K
               STOP
300            IF(K.NE.1)THEN
                  UPP = FUNPDF(TO,THETA,XI(ICOUNT))*NTOTAL
               ELSE
                  LOW = FUNPDF(TO,THETA,XI(ICOUNT))*NTOTAL
               ENDIF
320         CONTINUE
            FIT = FUNPDF(TONEW,TNEW,XI(ICOUNT))*NTOTAL
            CALL SAVE(2,ICOUNT,XCMPT(ICOUNT),LOW,FIT,UPP)
330      CONTINUE
      ENDIF
340   RETURN
1200  FORMAT (/,5X,'POSDEF IS FALSE - CANNOT SOLVE')
1500  FORMAT (/,5X,'CONVERGENCE NOT REACHED FOR ICOUNT =',I5,
     &       2X,'AND K = ',I5)
      END
C
C***********************************************************************
C
      FUNCTION FUNPDF(B,T,X)
C
C     FUNCTION CALCULATES VALUE OF PDF AT ANY VALUE OF X
C
      IMPLICIT REAL*8(A-H,O-Z)
      INTEGER*4 NCELLS,ILOG,S,MAXIT
      CHARACTER*6 NAME
      COMMON /INIT/ NCELLS,ILOG,S,MAXIT,CRIT,NAME
      REAL*8 FUNPDF
      DIMENSION T(S)
      INTEGER*4 FUNIT1,FUNIT2,FUNIT3,SCRUNT,DEBUG
      COMMON /FILES/ FUNIT1,FUNIT2,FUNIT3,SCRUNT,DEBUG
C
      IF(DEBUG.EQ.2)WRITE(SCRUNT,*)'      FUNCTION FUNDF'
      SUM = B
      DO 10 I=1,S
         SUM = SUM + T(I)*X**I
10    CONTINUE
      FUNPDF = DEXP(SUM)
      RETURN
      END
C
C***********************************************************************
C
      SUBROUTINE RR(TO,T,L,R)
C
C     SUBROUTINE CALCULATES R
C
      IMPLICIT REAL*8 (A-H,O-Z)
      INTEGER*4 FUNIT1,FUNIT2,FUNIT3,SCRUNT,DEBUG
      COMMON /FILES/ FUNIT1,FUNIT2,FUNIT3,SCRUNT,DEBUG
      INTEGER*4 NCELLS,ILOG,S,MAXIT
      CHARACTER*6 NAME
      COMMON /INIT/ NCELLS,ILOG,S,MAXIT,CRIT,NAME
      REAL*8 NI,NTOTAL,FUNCDF
      INTEGER*4 I,L
      DIMENSION T(S),R(S)
      COMMON/AREA1/XI(20),NI(20),NTOTAL
C
      IF(DEBUG.GE.1)WRITE(SCRUNT,*)' SUBROUTINE RR2'
      DO 20 I=1,S
         A=FUNCDF(TO,T,L)
         B=XEXP(TO,T,NCELLS,I)
         C=XEXP(TO,T,L,I)
         R(I)=A*B-C
20    CONTINUE
      RETURN
      END
C
C***********************************************************************
C
      FUNCTION FUNCDF(TO,T,L)
C
C     FUNCTION CALCULATES CDF
C
      IMPLICIT REAL*8 (A-H,O-Z)
      INTEGER*4 FUNIT1,FUNIT2,FUNIT3,SCRUNT,DEBUG
      COMMON /FILES/ FUNIT1,FUNIT2,FUNIT3,SCRUNT,DEBUG
      INTEGER*4 NCELLS,ILOG,S,MAXIT
      CHARACTER*6 NAME
      COMMON /INIT/ NCELLS,ILOG,S,MAXIT,CRIT,NAME
      REAL*8 FUNCDF,NI,NTOTAL
      INTEGER*4 L
      DIMENSION T(S)
      COMMON/AREA1/XI(20),NI(20),NTOTAL
```

```
C
      IF(DEBUG.EQ.2)WRITE(SCRUNT,*)'      FUNCTION FUNCDF'
      FUNCDF = 0.0
      DO 20 I = 1,L
         SUMJ = 0.0
         DO 10 J = 1,S
            SUMJ = SUMJ + T(J)*XI(I)**J
10       CONTINUE
         FUNCDF = FUNCDF + DEXP(T0 + SUMJ)
20    CONTINUE
      RETURN
      END
C
C************************************************************************
C
      FUNCTION XEXP(T0,T,L,J)
C
C     FUNCTION CALCULATES EXPRESSION IN THE FORMULA FOR R
C
      IMPLICIT REAL*8(A-H,O-Z)
      INTEGER*4 FUNIT1,FUNIT2,FUNIT3,SCRUNT,DEBUG
      COMMON /FILES/ FUNIT1,FUNIT2,FUNIT3,SCRUNT,DEBUG
      INTEGER*4 NCELLS,ILOG,S,MAXIT
      CHARACTER*6 NAME
      COMMON /INIT/ NCELLS,ILOG,S,MAXIT,CRIT,NAME
      REAL*8 NI,NTOTAL
      INTEGER*4 L,J
      DIMENSION T(S)
      COMMON/AREA1/XI(20),NI(20), NTOTAL
C
      IF(DEBUG.EQ.2)WRITE(SCRUNT,*)'      FUNCTION XEXP'
      XEXP = 0.0
      DO 20 I  = 1,L
         SUMK = 0.0
         DO 10 K = 1,S
            SUMK = SUMK + T(K)*XI(I)**K
10       CONTINUE
         XEXP = XEXP - DEXP(T0+SUMK)*(XI(I)**J)
20    CONTINUE
      RETURN
      END
C
C************************************************************************
C
      FUNCTION THETA0(T)
C
C     FUNCTION CALCULATES VALUE OF NORMALIZING CONSTANT THETA0,
C     APPROXIMATING INTEGRATION BY SUMMATION
C
      IMPLICIT REAL*8 (A-H,O-Z)
      INTEGER*4 FUNIT1,FUNIT2,FUNIT3,SCRUNT,DEBUG
      COMMON /FILES/ FUNIT1,FUNIT2,FUNIT3,SCRUNT,DEBUG
      INTEGER*4 NCELLS,ILOG,S,MAXIT
      CHARACTER*6 NAME
      COMMON /INIT/ NCELLS,ILOG,S,MAXIT,CRIT,NAME
      REAL*8 NI,NTOTAL
      DIMENSION T(S)
      COMMON/AREA1/XI(20),NI(20),NTOTAL
C
      IF(DEBUG.EQ.2)WRITE(SCRUNT,*)'      FUNCTION THETAO'
      SUM = 0.0
      DO 20 I = 1,NCELLS
         SUMJ = 0.0
         DO 10 J = 1,S
            SUMJ = SUMJ + T(J)*XI(I)**J
10       CONTINUE
         IF(SUMJ.GT.300)THEN
            WRITE(SCRUNT,1700)
            STOP
         ENDIF
         IF(SUMJ.GT.-300)SUM=SUM+DEXP(SUMJ)
20    CONTINUE
      IF (SUM.GT.0)THEN
         THETAO = -DLOG(SUM)
      ELSE
         WRITE(SCRUNT,1700)
         STOP
      ENDIF
      RETURN
1700  FORMAT (/,5X,'PROCEDURE UNSUCCESSFUL, CHECK DATA')
      END
C
C***********************************************************************
C
      SUBROUTINE EQCHOL(S,C,B,POSDEF)
C
C     SUBROUTINE SOLVES THE EQUATION A*u=b BY CHOLESKY DECOMPOSITION
C
      IMPLICIT REAL*8(A-H,O-Z)
      INTEGER*4 FUNIT1,FUNIT2,FUNIT3,SCRUNT,DEBUG
      COMMON /FILES/ FUNIT1,FUNIT2,FUNIT3,SCRUNT,DEBUG
      LOGICAL POSDEF
      INTEGER*4 S
      DIMENSION C(S,S),B(S)
C
      IF(DEBUG.GE.1)WRITE(SCRUNT,*)' SUBROUTINE EQCHOL'
      POSDEF=.TRUE.
      DO 70 I=1,S
         IF(I.NE.1)THEN
            IM1=I-1
            DO 20 J=1,IM1
               Z=C(J,I)
               C(I,J)=0.0
               DO 10 K=I,S
                  C(I,K)=C(I,K)-Z*C(J,K)
10             CONTINUE
               B(I)=B(I)-Z*B(J)
20          CONTINUE
         ENDIF
         Z=C(I,I)
```

```
            IF(Z.LE.0.0)THEN
               POSDEF=.FALSE.
               GOTO 999
            ENDIF
            Z=DSQRT(Z)
            C(I,I)=Z
            Z=1./Z
            IP1=I+1
            IF(I.NE.S)THEN
               DO 60 K=IP1,S
                  C(I,K)=C(I,K)*Z
60             CONTINUE
            ENDIF
            B(I)=B(I)*Z
70       CONTINUE
         DO 90 K=1,S
            I=S-K+1
            Z=B(I)
            IF(I.NE.S)THEN
               IP1=I+1
               DO 80 J=IP1,S
                  Z=Z-C(I,J)*B(J)
80             CONTINUE
            ENDIF
            B(I)=Z/C(I,I)
90       CONTINUE
999      RETURN
         END
C
C ************************************************************************
C
         SUBROUTINE SAVE(N,M,A1,A2,A3,A4)
C
C        SUBROUTINE X-ORDINATES, FITTED CURVE, AND CONFIDENCE BANDS
C        FOR LATER OUTPUT
C
         IMPLICIT REAL*8 (A-H,O-Z)
         REAL*8 OUT(20,8)
         COMMON /OUTS/ OUT
         INTEGER*4 N,M
C
         IF(N.EQ.1)THEN
            OUT(M,1)=A1
            OUT(M,2)=A2
            OUT(M,3)=A3
            OUT(M,4)=A4
         ELSE
            OUT(M,5)=A1
            OUT(M,6)=A2
            OUT(M,7)=A3
            OUT(M,8)=A4
         ENDIF
         RETURN
         END
C
```

```
C *********************************************************************
C
      SUBROUTINE OUTPUT
C
C     SUBROUTINE OUTPUTS SAVED VALUES OF X-ORDINATES, FITTED CURVE,
C     AND CONFIDENCE BANDS
C
      IMPLICIT REAL*8 (A-H,O-Z)
      INTEGER*4 FUNIT1,FUNIT2,FUNIT3,SCRUNT,DEBUG
      COMMON /FILES/ FUNIT1,FUNIT2,FUNIT3,SCRUNT,DEBUG
      INTEGER*4 NCELLS,ILOG,S,MAXIT
      CHARACTER*6 NAME
      COMMON /INIT/ NCELLS,ILOG,S,MAXIT,CRIT,NAME
      REAL*8 OUT(20,8)
      COMMON /OUTS/ OUT
C
      WRITE(FUNIT2,1000)
      DO 10 I=1,NCELLS
         WRITE(FUNIT2,1300) (OUT(I,K),K=1,4)
10    CONTINUE
      WRITE(FUNIT2,1100)
      DO 20 I=1,NCELLS
         WRITE(FUNIT2,1300) (OUT(I,K),K=5,8)
20    CONTINUE
      RETURN
1000  FORMAT (5X,'CDF',6X,'LOWERLIMIT',3X,'FITTEDCDF',2X,'UPPERLIMIT')
1100  FORMAT (5X,'PDF',6X,'LOWERLIMIT',3X,'FITTEDPDF',2X,'UPPERLIMIT')
1300  FORMAT (8(2X,E10.4))
      END
```

Volume

4

NATIONAL URANIUM TAILINGS PROGRAM

Energy, Mines and Resources Canada
Energie, Mines et Ressources Canada

Canada

URANIUM TAILINGS ASSESSMENT PROGRAM (UTAP.3): COMPONENT MODEL DOCUMENTATION

A Research Report Prepared Under
Contract No.23317-6-1728/01-SQ

for

The National Uranium Tailings Program
Canada Centre for Mineral and Energy Technology
Energy, Mines and Resources Canada
555 Booth Street
Ottawa, Ontario K1A 0G1

by

SENES Consultants Limited
499 McNicoll Avenue
Willowdale, Ontario
M2H 2C9

572 pp

March 1987

MICROMEDIA

ABSTRACT

This report represents part of the ongoing efforts of the National Uranium Tailings Program (NUTP) to develop the capability to predict the long-term effects of Canadian uranium mill tailings. In three previous studies, a comprehensive Uranium Tailings Assessment Program (UTAP) was developed. The UTAP program incorporates a Monte Carlo procedure which permits the user to enter input parameters as probability density functions rather than as single numbers and to calculate frequency distributions for output variables. The output distributions can be interpreted as a subjective probability telling us quantitatively what we are entitled to believe about the output variables.

To date, the approach has been to apply UTAP, in a generic fashion, to a hypothetical reference site. The focus of the present study has been to modify UTAP, where appropriate, for application to a real site (Lacnor) and to the extent practicable to calibrate the system model using site-specific measurements. Since the primary product of the NUTP modelling studies is the generic UTAP program, it has been thoroughly reviewed and modified along with the supporting documentation where appropriate. The current version of the updated generic code which reflects these revisions is referred to as UTAP.3. UTAP.3 also reflects revisions of a generic nature which were identified through the application of UTAP to the Lacnor site.

This volume presents the documentation of the mathematical models used in UTAP.3 to simulate the behaviour of the uranium tailings and the surrounding environment. The documentation consists of model derivations and descriptions, computer code listings and, in many instances, flow charts outlining model implementation and illustrative model results.

NOTICE

This report was prepared by SENES Consultants Limited (SENES) under contract to the National Uranium Tailings Program (NUTP). Neither NUTP nor SENES makes any warranty, expressed or implied, or assumes any liability with respect to any damage or loss incurred as a result of the use made of the information contained in this publication.

TABLE OF CONTENTS

Page

Abstract i

Notice i

1.0 INTRODUCTION 1-1
- 1.1 Background 1-1
- 1.2 Scope of This Study 1-3
- 1.3 Report Structure 1-5
- 1.4 References 1-6

2.0 COMPONENT MODULE OBJECTIVES AND CONCEPTUAL SPECIFICATIONS 2-1
- 2.1 Constituents 2-1
- 2.2 Pathways 2-1
- 2.3 Spatial Considerations 2-2
- 2.4 Receptor Locations, Characteristics and Population Dose 2-3
- 2.5 Temporal Considerations 2-4
- 2.6 Natural Physical Changes 2-5
- 2.7 Disposal Option(s) 2-6
- 2.8 Input Parameters 2-6
- 2.9 Outputs 2-6
- 2.10 References 2-7

3.0 WATER SOURCE MODELS 3-1
- 3.1 Modelling Concepts 3-1
- 3.2 Initial Conditions - Ions and pH 3-2
  - 3.2.1 Initial Inventories 3-3
  - 3.2.2 Calcium and Sulphate Concentrations 3-4
  - 3.2.3 Initial pH Levels 3-6
  - 3.2.4 Iron Concentrations 3-7
- 3.3 Ions - Layers 1 and 2 3-7
  - 3.3.1 Sulphates Derived from Pyrite Oxidation 3-8
  - 3.3.2 Gypsum Dissolution and Reprecipitation 3-12
  - 3.3.3 Calcium and Sulphate Concentrations 3-17

Table of Contents, cont'd. Page

3.3.4 Iron Concentration 3-19
3.3.5 Modifications for Limestone Addition 3-20
3.4 Ions - Layer 3 3-26
3.4.1 Calcium and Sulphate Concentrations Prior to Gypsum Depletion 3-26
3.4.2 Gypsum Depletion 3-28
3.4.3 Calcium and Sulphate Concentrations Following Gypsum Depletion 3-29
3.4.4 Iron Concentration 3-30
3.5 Ions - Layer 4 3-30
3.6 pH Calculations 3-33
3.6.1 Layer 1 3-33
3.6.2 Layer 2 3-44
3.6.3 Layer 3 3-46
3.6.4 Layer 4 3-51
3.6.5 Implementation/Solution of pH Expressions 3-51
3.7 Initial Conditions - Radionuclides 3-57
3.7.1 Uranium 3-57
3.7.2 Thorium 3-60
3.7.3 Radium 3-65
3.7.4 Lead 3-69
3.8 Uranium 3-72
3.9 Thorium 3-75
3.9.1 Unsaturated Zone 3-75
3.9.2 Layers 3 and 4 3-79
3.10 Radium 3-81
3.10.1 Radioactive Ingrowth and Decay 3-81
3.10.2 Unsaturated Zone 3-82
3.10.3 Layers 3 and 4 3-91
3.11 Lead 3-95
3.11.1 Unsaturated Zone 3-95
3.11.2 Layers 3 and 4 3-99

Table of Contents, cont'd.

Page

3.12 Input Parameter Values 3-102

3.12.1 Concentration of O_2 at the Tailings Surface 3-103

3.12.2 D_{O2}-O_2 Diffusivity Through the Tailings 3-103

3.12.3 f - Activity Coefficient for Divalent Ions 3-104

3.12.4 P - Annual Net Precipitation 3-105

3.12.5 Gypsum Solubility Constant 3-105

3.12.6 f_{Th-230} - Fraction of Th-230 Assumed to be Ultimately Soluble 3-106

3.12.7 f_{Th-232} - Fraction of Th-232 Assumed to be Ultimately Soluble 3-106

3.12.8 f_{Ra} - Fraction of Radium-226 Assumed to be Ultimately Soluble 3-106

3.12.9 f_{Pb} - Fraction of Lead-210 Assumed to be Ultimately Soluble 3-107

3.12.10 $X^{o}_{Ra/BaSO_4}$ - Initial Mole Fraction of Ra-226 in $BaSO_4$ 3-107

3.12.11 $[PbSO_4]^o$ - Initial Concentration of $PbSO_4$ in the Tailings 3-108

3.12.12 Initial Sulphate Production Rate (FeS_2 Oxidation) 3-108

3.12.13 Rate Fraction 3-110

3.12.14 Surface Runoff Fraction 3-111

3.12.15 K_d - Solid-Liquid Distribution Coefficient 3-111

3.12.16 Half-Lives 3-118

3.13 Water Source Model Demonstration 3-118

3.14 Tailings Erosion Model 3-125

3.14.1 Introduction 3-126

3.14.2 The Universal Soil Loss Equation 3-127

3.14.3 Tailings Vegetation 3-130

3.14.4 Tailings Geometry 3-132

3.14.5 Deposition and Transport 3-133

3.14.6 River/Lake System Loading 3-138

Table of Contents, cont'd. Page

3.14.7 Review of Input Parameters 3-140
3.14.8 Erosion Model Demonstration 3-142
3.15 References 3-143

4.0 AIR SOURCE MODELS 4-1
4.1 Introduction 4-1
4.2 Radon Source Model 4-1
4.2.1 Radon Source Model Development 4-2
4.2.2 Parameter Values 4-6
4.2.3 Description of the Computer Model 4-7
4.3 Dust Source Model 4-8
4.3.1 Dust Source Model Development 4-8
4.3.2 Parameter Values 4-10
4.3.3 Description of the Computer Model 4-11
4.4 Air Source Models Test Program 4-11
4.5 References 4-12

5.0 AIR DISPERSION AND WIND MODELS 5-1
5.1 Introduction 5-1
5.2 Air Dispersion Model 5-1
5.2.1 Air Dispersion Model Development 5-1
5.2.2 Parameter Values 5-4
5.2.3 Description of the Computer Model 5-5
5.3 Wind Model 5-5
5.3.1 Wind Model Development 5-5
5.3.2 Parameter Values 5-6
5.3.3 Description of the Computer Model 5-6
5.4 Air Dispersion and Wind Models Test Program 5-7
5.5 References 5-7

6.0 SOIL MODEL 6-1
6.1 Introduction 6-1

Table of Contents, cont'd. Page

6.2 Soil Model Development 6-1
6.3 Parameter Values 6-6
6.4 Description of the Computer Model 6-8
6.5 Soil Model Test Program 6-8
6.6 References 6-8

7.0 GROUNDSHINE MODEL 7-1
7.1 Introduction 7-1
7.2 The Basic Model 7-2
7.3 Two Soil Layers 7-3
7.4 Attenuation Coefficient 7-4
7.5 Radionuclide Groups 7-6
7.6 Exhalation of Radon 7-9
7.7 Energy Flux Density to Dose Rate Conversion 7-10
7.8 Calibration 7-11
7.9 References 7-12

8.0 TERRESTRIAL VEGETATION MODEL 8-1
8.1 Introduction 8-1
8.2 Above-Ground and Below-Ground Vegetables (AVEGC and BVEGC) 8-5
8.3 Summer Forage (SUFOC) 8-5
8.4 Browse (BRWSC) 8-6
8.5 Lichens (LICHC) 8-7
8.6 Description of Computer Model 8-9
8.7 Terrestrial Vegetation Model Test Program 8-9
8.8 References 8-9

9.0 SUBSURFACE CONTAMINANT TRANSPORT MODEL 9-1
9.1 Introduction 9-1
9.2 Aquifer Characteristics 9-2
9.3 Theoretical Approach 9-4

Table of Contents, cont'd. Page

9.3.1 Auxiliary Equations 9-4
9.3.2 Mass Balance 9-9
9.3.3 Assumptions 9-11
9.4 Solution to Mass Balance 9-13
9.4.1 Constant Source 9-13
9.4.2 Time-Variant Source 9-14
9.5 Review of Parameters and Constants 9-15
9.5.1 Discharge Distance 9-15
9.5.2 Porosity 9-16
9.5.3 Hydraulic Conductivity 9-16
9.5.4 Hydraulic Gradient 9-17
9.5.5 Soil Density 9-18
9.5.6 Distribution Coefficient 9-18
9.5.7 Mean Net Annual Precipitation 9-22
9.5.8 Cross-Sectional Area 9-23
9.5.9 Discharge Layer 9-23
9.6 Model Demonstration 9-23
9.7 Description of the Computer Model 9-25
9.8 References 9-26

10.0 SURFACE WATER DISPERSION MODELS 10-1
10.1 Approach to Watershed Modelling 10-1
10.2 The Reference Watershed 10-1
10.3 The Hydrologic Component 10-2
10.4 Major Ions Component 10-4
10.4.1 Baseline Levels 10-4
10.4.2 River Segments 10-4
10.4.3 Lake Segments 10-6
10.5 pH Component 10-7
10.6 Radionuclide Component 10-12
10.6.1 River Segments 10-14
10.6.2 Lake Segments 10-15

Table of Contents, cont'd.

Page

10.7 Parameter Values and Code Listing 10-31
10.8 Surface Water Dispersion Models Test Program 10-31
10.9 References 10-32

11.0 AQUATIC MODELS 11-1
11.1 Components Considered 11-1
11.2 Effect of pH on Fish Populations 11-1
11.3 Radionuclide Transfer to Aquatic Biota 11-6
11.3.1 Modelling Approach 11-6
11.3.2 Bioaccumulation in Fish 11-8
11.3.3 Bioaccumulation in Aquatic Macrophytes 11-10
11.4 Parameter Values and Code Listing 11-12
11.5 Aquatic Biota Models Test Program 11-12
11.6 References 11-13

12.0 ANIMAL PRODUCE MODEL 12-1
12.1 Introduction 12-1
12.2 Radionuclides in Caribou Flesh 12-3
12.2.1 Air Pathway to Caribou Flesh (ACARC) 12-3
12.2.2 Water Pathway to Caribou Flesh (WCARC) 12-5
12.3 Radionuclides in Moose Flesh 12-7
12.3.1 Air Pathway to Moose Flesh (AMOSC) 12-8
12.3.2 Water Pathway to Moose Flesh (WMOSC) 12-9
12.4 Radionuclides in Deer Flesh 12-10
12.4.1 Air Pathway to Deer Flesh (ADERC) 12-11
12.4.2 Water Pathway to Deer Flesh (WDERC) 12-12
12.5 Description of Computer Model 12-13
12.6 Animal Produce Model Test Program 12-13
12.7 References 12-14

13.0 DOSE MODEL 13-1
13.1 Introduction 13-1

Table of Contents, cont'd. Page

13.1.1 Background 13-1
13.1.2 Dose Conversion Factors 13-2
13.2 Ingestion Dose 13-6
13.2.1 Annual Dose Due to the Ingestion of Vegetables 13-6
13.2.2 Annual Dose Due to the Ingestion of Caribou 13-8
13.2.3 Annual Dose Due to the Ingestion of Moose 13-10
13.2.4 Annual Dose Due to the Ingestion of Deer 13-12
13.2.5 Annual Dose Due to the Ingestion of Drinking Water 13-14
13.2.6 Annual Dose Due to the Ingestion of Fish 13-15
13.3 Inhalation Dose 13-17
13.3.1 Annual Dose to the Inhalation of Suspended Particulates 13-17
13.3.2 Annual Dose to the Inhalation of Radon and its Daughters 13-18
13.4 External Dose 13-21
13.5 Receptor Specification 13-22
13.5.1 Receptor Identification Number 13-22
13.5.2 Sector Number 13-22
13.5.3 Ring Number 13-22
13.5.4 Water Source Segment Number 13-22
13.5.5 Fish Source Segment Number 13-23
13.5.6 Receptor Type 13-23
13.5.7 Population 13-23
13.6 Population Dose 13-23
13.7 Description of Computer Model 13-24
13.8 Dose Model Test Program 13-24
13.9 References 13-24

APPENDIX A Water Source Models:
Code Listing and Variable Dictionary

LIST OF FIGURES

Follows Page

2.1 The Subroutine COMEX and Component Modules 2-2
2.2 Exposure Pathways Analyzed 2-2
2.3 Conceptual Diagram of Spatial Coordinate System 2-2
3.1 Concept Adopted for Modelling the Tailings Source Term 3-2
3.2 Structure of the Tailings Source Model 3-2
3.3 Sulphate Ion Concentrations 3-120
3.4 Calcium Ion Concentrations 3-120
3.5 Iron Ion Concentrations 3-122
3.6 Porewater pH 3-122
3.7 Solid Phase Radionuclide Concentrations in Surface Layer 3-122
3.8 Dissolved Uranium Concentrations 3-124
3.9 Dissolved Thorium Concentrations 3-124
3.10 Dissolved Radium-226 Concentrations 3-124
3.11 Dissolved Lead-210 Concentrations 3-126
3.12 Typical Range of Grain Size Distribution for Acid Generating Tailings 3-134
3.13 Flowsheet of Computational Approach 3-140
3.14 Trapping Efficiency bs Ratio of Pond Area to Outflow Rate 3-142
3.15 Cumulative Tailings Depletion and pH vs Time 3-142
4.1 Predicted Radionuclide Release Rate to the Air vs Time 4-12
5.1 Predicted Radionuclide Air Concentration vs Distance 5-8
5.2 Predicted Radionuclide Air Concentration vs Time 5-8
6.1 Schematic Representation of Soil Deposition/Leaching Concepts 6-2
6.2 Predicted Radionuclide Concentration in Soil Layer 2 vs Time 6-8
7.1 Uranium-238 Decay Series 7-6
7.2 Thorium-232 Decay Series 7-6
7.3 Flowsheet for Groundshine Model 7-12
7.4 Predicted Radionuclide Groundshine Dose Rate vs Time 7-12
8.1 Predicted Radionuclide Concentration in Above- and Below-Ground Vegetation vs Time 8-10

List of Figures, cont'd.

Follows Page

8.2 Predicted Radionuclide Concentration in Lichen and Summer Forage vs Time 8-10
9.1 Structure of Subsurface Transport Model 9-2
9.2 Concept of Reference Tailings Groundwater Flowpath at Each Dam on the Reference Tailings Site 9-2
9.3 Time-Variant Source 9-14
9.4 Constant Source Concentration of Each Radionuclide (Model Demonstration) 9-24
9.5 Groundwater Concentration of Uranium (Constant Source, Dam 1) 9-24
9.6 Groundwater Concentration of Total Thorium (Constant Source, Dam 1) 9-24
9.7 Groundwater Concentration for Lead-210 (Constant Source, Dam 1) 9-24
9.8 Groundwater Concentration for Radium-226 (Constant Source, Dam 1) 9-24
9.9 Time Variant Source Concentration of Each Radionuclide (Model Demonstration) 9-26
9.10 Groundwater Concentration for Uranium (Variant Source-Time) 9-26
9.11 Groundwater Concentration of Total Thorium (Variant Source-Time) 9-26
9.12 Groundwater Concentration for Lead-210 (Variant Source-Time) 9-26
9.13 Groundwater Concentration for Radium-226 (Variant Source-Time) 9-26
10.1 Reference Watershed Schematic 10-2
10.2 Conceptual Schematic of Reference Lake 10-16
11.1 Aggregate Aquatic Transfer Model 11-8
11.2 Frequency Histogram of Uranium Bioaccumulation Factor Values 11-10
11.3 Frequency Histogram of Thorium Bioaccumulation Factor Values 11-10
11.4 Frequency Histogram of Radium-226 Bioaccumulation Factor Values 11-10
11.5 Frequency Histogram of Lead-210 Bioaccumulation Factor Values 11-10
12.1 Predicted Radionuclide Concentration in Caribou Flesh vs Time 12-14
12.2 Predicted Radionuclide Concentration in Moose Flesh vs Time 12-14
12.3 Predicted Radionuclide Concentration in Deer Flesh vs Time 12-14
13.1 Predicted Dose vs Time by Pathway 13-24
13.2 Frequency Histogram of Total Dose at t=0 Years 13-24
13.3 Frequency Histogram of Total Dose at t=500 Years 13-24

LIST OF TABLES

Follows Page

2.1 Summary of UTAP.3 Component Module Objectives 2-2
2.2 COMEX Model Code Listing 2-2
2.3 Input Parameter Distribution Specifications 2-6
3.1 Relative Activities of Aluminum Hydroxo Complexes 3-36
3.2 Relative Activities of Iron (III) Hydroxo Complexes 3-38
3.3 Ionic Equilibrium for Electroneutrality 3-40
3.4 Water Source Model Input Parameters 3-102
3.5 Rates of Sulphate Production 3-110
3.6 Radioactive Half-Life 3-118
3.7 Erosion Model Variables 3-140
4.1 Radon Source Model Variables 4-8
4.2 Radon Model Code Listing 4-8
4.3 Dust Model Variables 4-10
4.4 Dust Source Model Code Listing 4-12
5.1 Power Law Exponents and Coefficients for $\sigma_{z,x}$, 5-4
5.2 Air Dispersion Model Variables 5-4
5.3 Air Dispersion Model Code Listing 5-6
5.4 Wind Model Variables 5-6
5.5 Wind Model Code Listing 5-6
6.1 Soil Model Parameters 6-6
6.2 Soil Model Code Listing 6-8
7.1a Average Radionuclide Parameters for Groundshine Calculations 7-8
7.1b Groundshine Model Parameters 7-12
7.2 Groundshine Model Code Listing 7-12
8.1 Above-Ground Vegetables Model Variables 8-6
8.2 Below-Ground Vegetables Model Variables 8-6
8.3 Summer Forage Model Variables 8-6
8.4 Browse Model Variables 8-6
8.5 Lichen Model Variables 8-8
8.6 Terrestrial Vegetation Model Code Listing 8-10

List of Tables, cont'd.

Follows Page

9.1 Assumptions Employed in Subsurface Transport Model 9-12
9.2 Subsurface Transport Model Parameters 9-16
9.3 Comparison of K_d Values for U-238 (IV) and U-238 (VI) as a Function of pH 9-20
9.4 Subsurface Contaminant Transport Model Code Listing 9-26
10.1 Characteristics of the Reference Watershed 10-2
10.2 Lake Sedimentation Flux Values 10-18
10.3 Sediment to Water k_d Values 10-22
10.4 Assessed Mass Transfer Coefficient Values 10-24
10.5 Watershed Model Variables 10-32
10.6 Watershed Model Code Listing 10-32
11.1 Large (Game) Fish Flesh Uranium Bioaccumulation Factors 11-10
11.2 Large (Game) Fish Flesh Thorium Bioaccumulation Factors 11-10
11.3 Large (Game) Fish Flesh Radium-226 Bioaccumulation Factors 11-10
11.4 Large (Game) Fish Flesh Lead-210 Bioaccumulation Factors 11-10
11.5 Aquatic Model Variables 11-12
11.6 Fish Model Code Listing 11-12
11.7 Aquatic Macrophyte Model Code Listing 11-12
12.1 Caribou Flesh Model Variables 12-4
12.2 Moose Flesh Model Variables 12-10
12.3 Deer Flesh Model Variables 12-12
12.4 Animal Produce Model Code Listing 12-14
13.1 Dose Conversion Factors 13-4
13.2 Dose Conversion Factors for this Study 13-4
13.3 Variables Used in the Calculation of Annual Dose to the Critical Receptor 13-24
13.4 Variables Used in the Calculation of Annual Dose to the Average Receptor 13-24
13.5 Dose Model Code Listing 13-24

1.0 INTRODUCTION

1.1 Background

Uranium mining and milling operations began in the Northwest Territories in 1943 and have been conducted in Ontario and northern Saskatchewan since the mid-1950's. Since that time, 19 uranium mining operations have produced more than 160 million tonnes of uranium tailings. Of this total, approximately 150 million tonnes have been deposited in a variety of surface impoundments covering a total of about 635 ha, with the remainder deposited underwater in lakes or used as mine backfill. The bulk of the uranium mine tailings, (about 135 million tonnes), is located in the Elliot Lake area of Ontario.

In 1982 Energy, Mines and Resources Canada established the National Uranium Tailings Program (NUTP) to pull together previous work on Canadian uranium mill tailings, to fund additional work where significant information gaps were found and to develop the capability to predict the long-term effects of tailings with a known degree of confidence while incorporating uncertainty and variability in the input data. The NUTP comprises three components: modelling, measurement and disposal technology.

An earlier study in the modelling component (Phase I) funded by the NUTP demonstrated how probabilistic techniques could be used to take account of the variability and uncertainty in model input parameters in a simulation analysis (SENES, 1984). In Phase I quasi-steady-state models of a simplified, hypothetical, reference tailings site were used to demonstrate the feasibility and appropriateness of probabilistic analysis. Environmental pathways models were used to estimate human exposure from the release of radium-226 to the air and water and of radon-222 to the air. A number of related technical and philosophical matters were addressed in a series of review papers.

Subsequently, the NUTP sponsored a followup study (Phase II) to extend and refine the probabilistic tools developed in the Phase I study and to investigate various issues of technical interest involved in carrying out and interpreting a probabilistic analysis (SENES, 1985). The Phase II work built upon Phase I results in order to demonstrate broader application of the probabilistic technique. In particular, the environmental component models and overall systems framework were modified and expanded to explicitly incorporate the time-varying behaviour of the natural system. As well, an additional radionuclide (thorium), several inorganic chemical species (calcium, sulphate and iron) and pH were modelled.

Sensitivity/uncertainty analysis techniques were investigated in detail in Phase II and were applied to probabilistic results, indicating pathways and parameters of importance to the hypothetical reference site. Order of magnitude estimates of the long-term effects (and associated uncertainties) of a number of different tailings management "scenarios" were also obtained.

As well, a number of special topics were investigated in Phase II including:

- interpretation of probabilistic results
- methods for estimating confidence regions on output distributions
- techniques for handling correlated parameters
- model response to time-variant input parameters
- implications of model aggregation for use in assessment models.

The underlying objective of the Phase III studies (SENES, 1986) was to extend the capabilities of the Phase II system model and then to apply the Phase III system model to an expanded hypothetical reference site. Among the tasks addressed in Phase III were:

- expand the simulation models to include additional major radionuclides and water erosion of tailings cover materials
- expand the simulation models to include additional selected pathways of exposure
- modify the system model to permit air dispersion calculations to be carried out to greater distances in all directions
- modify the system model to permit water dispersion calculations to be performed on an entire watershed
- streamline the system code, update the documentation and prepare a user's

manual.

As well, a number of special activities related to the development, use, or interpretation of probabilistic assessment codes were carried out, including:

- an extensive program of software quality assurance including: testing of the random number generator; an intercomparison study with two other probabilistic assessment codes; testing of the system's control modules; and testing of the Phase III component modules, both on a stand-alone basis and integrated within the system model
- further investigation of the use of aggregate models in environmental assessment
- implementation of a technique for placing confidence bands on the output of probabilistic (i.e. Monte Carlo) calculations.

In December 1984, the NUTP, as part of its measurement program, awarded a contract to carry out a field study at the Lacnor uranium tailings area. The objective of the field program was to design and operate a sampling program to collect chemical, physical and biological data to characterize the Lacnor tailings area and its environs. The field study required the sampling of tailings solids, sub-tailings soil and rock, the surrounding soil and rock, tailings porewater, surface water, the measurement of surface water runoff, the gathering of meteorological and atmospheric data, and a biological assessment of the site.

The field program was intended to be a data gathering exercise and interpretation of the results was specifically excluded from the terms of reference for the study. Field investigations were carried out from December 1984 up to the end of October 1985 when monitoring was discontinued. An overview of the program and the data collected are provided in the summary report (Golder _et al_., 1986).

1.2 Scope of This Study

One of the principal objectives of the National Uranium Tailings Program

(NUTP) is the development of the capability to predict the long-term effects of uranium mill tailings and alternate closeout technologies with a known degree of confidence, while incorporating variability and uncertainty in the input data. Results of the previous phases of work have demonstrated that a probabilistic approach provides the framework necessary for incorporating uncertainty into a simulation (SENES, 1984; 1985; 1986).

To date, the emphasis has been on the overall system modelling approach with application to a hypothetical reference site. The emphasis of this project is to demonstrate the use of the Uranium Tailings Assessment Program (UTAP) in assessing a real (vs hypothetical) uranium tailings site. The Lacnor tailings area in Elliot Lake, Ontario, was chosen for this purpose. The primary objective is to learn what is entailed in such an application. Less emphasis is being placed on the numbers being produced by the exercise, though, of course, they are as realistic as practicable. In this sense, then, this application of UTAP can be considered "preliminary". Though the predictions made could be useful to an assessment of the final closeout of the site, this is not a primary objective of this project.

The goals set out for this project (as specified in the Request for a Proposal) were as follows:

Task 1: Review the system component models existing at the end of Phase III for applicability to the Lacnor site, and then modify them as necessary to describe the site characteristics. These characteristics include tailings constituents, natural processes occurring in the tailings, contaminant transfer along pathways to man, critical group receptors, and any other peculiarity of the site needed to describe its environmental impact.

Task 2: In conjunction with the Scientific Authority, determine the disposal options to be studied in order to demonstrate the system model's usefulness in distinguishing the impacts between various options. Incorporate the chosen options in the system computer code.

Task 3: Prepare the input data for the code. This will rely heavily on the data from the NUTP field program, but other sources of data may need to be sought. Many of the input parameters require the development of a probability density distribution for their input.

Task 4: Run the system model developed in Task 1 with the data from Task 3 for each disposal option selected in Task 2. Analyse the results.

Task 5: Prepare draft and final written reports describing the model input data development and analysis. The report should describe any major difficulties encountered in application of the system model to a real site plus any recommendations as to future applications.

1.3 Report Structure

The primary product of the NUTP modelling studies is the UTAP program. There are currently three versions of UTAP:

. UTAP.1	the original Phase III code (SENES, 1986), "UTAP", now archived and inactive
. UTAP.2	the original Phase III code with minor revisions
. UTAP.3	an upgraded and expanded version of the Phase III code

The Phase III (SENES, 1986) documentation was divided into the following four volumes:

Volume 1: Probabilistic Model Development for the Assessment of Uranium Mill Tailings in Canada - Phase III, Summary Report

Volume 2: Probabilistic Model Development for the Assessment of Uranium Mill Tailings in Canada - Phase III, System Description and Control Module Documentation

Volume 3: Probabilistic Model Development for the Assessment of Uranium Mill Tailings in Canada - Phase III, Component Model Documentation

Volume 4: Probabilistic Model Development for the Assessment of Uranium Mill Tailings in Canada - Phase III, Uranium Tailings Assessment Program (UTAP) User's Manual.

In documenting this study Volume 1 of the Phase III study has been replaced by a new volume which describes the application of UTAP.3 to the Lacnor site. Volumes 3 and 4 of the Phase III study have been updated to reflect changes incorporated in UTAP.3 and have been reissued in their entirety. Also, an addendum to Volume 2 of the Phase III report, which outlines changes made to the control modules of UTAP.3 from those of UTAP.1 and UTAP.2, has been prepared.

This volume, which replaces Volume 3 of the Phase III study, documents the component models incorporated in UTAP.3.

1.4 References

Golder Associates, SENES Consultants Limited, BEAK Consultants Limited and Cumming-Cockburn Associates Limited, 1986. "Lacnor Field Study." Research report prepared for the National Uranium Tailings Program, CANMET, EMR.

SENES Consultants Limited, 1984. "A Study to Develop and Demonstrate Techniques for the Probabilistic Assessment of the Long-Term Effects of Uranium Mill Tailings in Canada - Phase I." Research report prepared for the National Uranium Tailings Program, CANMET, EMR, under Supply and Services Canada Contract No. 0SQ83-00236.

SENES Consultants Limited, 1985. "Probabilistic Model Development for the Assessment of the Long-Term Effects of Uranium Mill Tailings in Canada - Phase II. Volume 1: Main Report. Volume 2: Workshop Notes and Topical Discussion Papers. Volume 3: Probabilistic Analysis User's Manual and Documentation for the Uranium Tailings Assessment Program (UTAP)." Research report prepared for the National Uranium Tailings Program, CANMET, EMR, under Supply and Services Canada Contract No. 0SQ84-00207.

SENES Consultants Limited, 1986. "Probabilistic Model Development for the Assessment of the Long-Term Effects of Uranium Mill Tailings in Canada - Phase III. Volume 1: Summary Report. Volume 2: Uranium Tailings Assessment Program (UTAP): System Description and Control Module Documentation. Volume 3: Uranium Tailings Assessment Program (UTAP) Component Model Documentation. Volume 4: Uranium Tailings Assessment Program (UTAP) User's Manual." Research report prepared for the National Uranium Tailings Program, CANMET, EMR, under Supply and Services Canada Contract No. 0SQ85-00182.

2.0 COMPONENT MODULE OBJECTIVES AND CONCEPTUAL SPECIFICATIONS

The UTAP.3 system model was designed to probabilistically assess the behaviour and environmental effects of uranium mill tailings following closeout. The component modules (or models) are the computer subprograms of the UTAP.3 model which are directly concerned with the simulation of a uranium tailings physical system; i.e. the computer implementation of the mathematical models representing the uranium tailings and surrounding environment. The control modules provide the infrastructure for the probabilistic analysis of the component models and are discussed in Volume 2 of Phase III (SENES, 1986) and its addendum (SENES, 1987c).

The objectives specified at the outset for use in the development of the UTAP.3 component modules are summarized in Table 2.1, and are discussed in more detail in the following sections of this chapter. Figure 2.1 illustrates, in flowchart form, the functions of the component modules. The computer code listing for the subroutine COMEX which calls the individual component modules is provided in Table 2.2. The remainder of the chapters in this volume discuss the development and modelling concepts, and provide code listings for each of the individual component modules.

2.1 Constituents

The radionuclides modelled are natural uranium, total thorium, radium-226, radon-222 and lead-210. The pH of the reference uranium tailings site and the chained river-lake system discussed later are also modelled. The pH is modelled by an equilibrium relationship which explicitly accounts for the dissolved concentrations in the aqueous phase of calcium, iron and sulphate.

2.2 Pathways

The following pathways of dose to the receptors are modelled in UTAP.3 for the aforementioned radionuclides:

1) Water Consumption: dispersion of tailings effluent in the receiving water environment and subsequent consumption by humans.

2) Fish Consumption: the transfer of radionuclides from the receiving water environment to fish and subsequent consumption by humans.

3) Radon Inhalation: dispersion of radon exhaled from the reference tailings site in the air environment and subsequent inhalation by humans.

4) Dust Inhalation: dispersion of dust eroded from the surface of the reference tailings site in the air environment and subsequent inhalation by humans.

5) Vegetable Consumption: the transfer of radionuclides to above- and below-ground vegetation and subsequent consumption by humans.

6a) Animal Produce Consumption: the uptake of radionuclides by forage vegetation and lichens, subsequent transfer to caribou, moose and deer and consumption of the animal meat by humans.

6b) Animal Produce Consumption: the uptake of radionuclides by aquatic vegetation, subsequent transfer to moose and consumption of the animal meat by humans.

6c) Animal Produce Consumption: caribou, moose and deer consumption of lake and river water and subsequent consumption of the animal meat by humans.

7) Groundshine: direct radiation from deposited dust.

These pathways are illustrated in Figure 2.2.

2.3 Spatial Considerations

The windrose structure shown in Figure 2.3 defines the system of spatial coordinates used in UTAP.3. As indicated, there are 16 direction sectors to correspond to the traditional windrose structure. The number of rings, up to a maximum of 5, and the spacing of the rings, from a minimum distance of 1 km to a maximum of 50 km, are user-specified. The rings are continuous, with the outer limit of one ring forming the inner limit of the next. Distance-related concentration calculations in the air dispersion model utilize the distance to the centre of the specified rings. This concentration is assumed to represent the average value over the windrose location defined by the sector and ring

FIGURE 2.1

THE SUBROUTINE COMEX AND COMPONENT MODULES

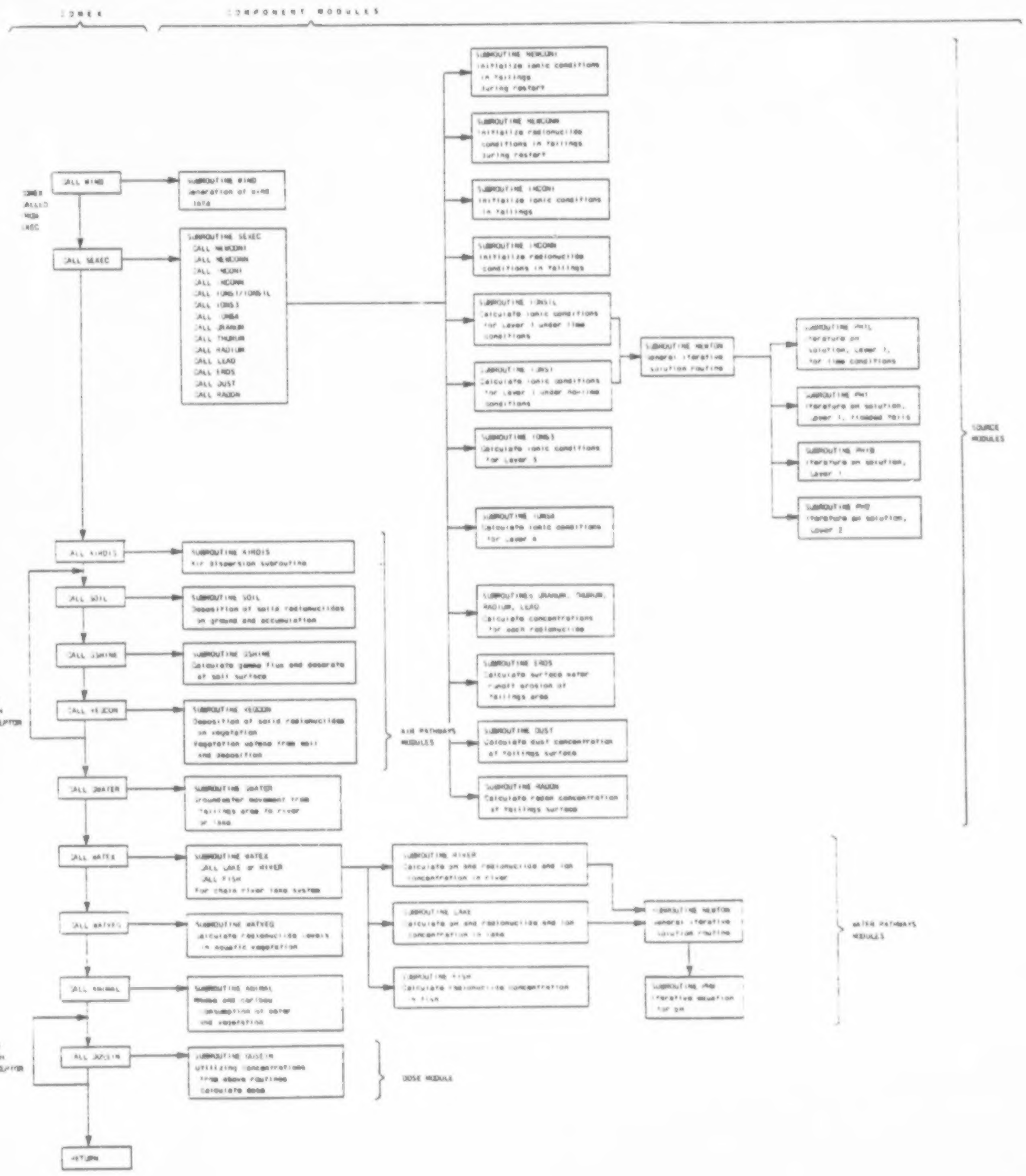
COMEX
COMPONENT MODULES
COMEX CALLED FROM EXEC
CALL WIND
SUBROUTINE WIND
Generation of wind data
CALL SEXEC
SUBROUTINE SEXEC
CALL NEWCONI
CALL NEWCONN
CALL INCONI
CALL INCONN
CALL IONS1/IONS1L
CALL IONS3
CALL IONS4
CALL URANUM
CALL THORUM
CALL RADIUM
CALL LEAD
CALL EROS
CALL DUST
CALL RADON
SUBROUTINE NEWCONI
Initialize ionic conditions in tailings during restart
SUBROUTINE NEWCONN
Initialize radionuclide conditions in tailings during restart
SUBROUTINE INCONI
Initialize ionic conditions in tailings
SUBROUTINE INCONN
Initialize radionuclide conditions in tailings
SUBROUTINE IONS1L
Calculate ionic conditions for Layer 1 under lime conditions
SUBROUTINE IONS1
Calculate ionic conditions for Layer 1 under no-lime conditions
SUBROUTINE NEWTON
General iterative solution routine
SUBROUTINE PH1L
Iterature pH solution, Layer 1, for lime conditions
SUBROUTINE PH1
Iterature pH solution, Layer 1, flooded tails
SUBROUTINE PH1B
Iterature pH solution, Layer 1
SUBROUTINE PH2
Iterature pH solution, Layer 2
SUBROUTINE IONS3
Calculate ionic conditions for Layer 3
SUBROUTINE IONS4
Calculate ionic conditions for Layer 4
SUBROUTINES URANUM, THORUM, RADIUM, LEAD
Calculate concentrations for each radionuclide
SUBROUTINE EROS
Calculate surface water runoff erosion of tailings area
SUBROUTINE DUST
Calculate dust concentration at tailings surface
SUBROUTINE RADON
Calculate radon concentration at tailings surface
SOURCE MODULES
CALL AIRDIS
SUBROUTINE AIRDIS
Air dispersion subroutine
CALL SOIL
SUBROUTINE SOIL
Deposition of solid radionuclides on ground and accumulation
CALL GSHINE
SUBROUTINE GSHINE
Calculate gamma flux and doserate at soil surface
CALL VEGCON
SUBROUTINE VEGCON
Deposition of solid radionuclides on vegetation
Vegetation uptake from soil and deposition
FOR EACH RECEPTOR
AIR PATHWAYS MODULES
CALL GWATER
SUBROUTINE GWATER
Groundwater movement from tailings area to river or lake
CALL WATEX
SUBROUTINE WATEX
CALL LAKE or RIVER
CALL FISH
For chain river lake system
SUBROUTINE RIVER
Calculate pH and radionuclide and ion concentration in river
SUBROUTINE LAKE
Calculate pH and radionuclide and ion concentration in lake
SUBROUTINE FISH
Calculate radionuclide concentration in fish
SUBROUTINE NEWTON
General iterative solution routine
SUBROUTINE PH0
Iterative equation for pH
WATER PATHWAYS MODULES
CALL WATVEG
SUBROUTINE WATVEG
Calculate radionuclide levels in aquatic vegetation
CALL ANIMAL
SUBROUTINE ANIMAL
Moose and caribou consumption of water and vegetation
CALL DOSEIN
SUBROUTINE DOSEIN
Utilizing concentrations from above routines calculate dose
FOR EACH RECEPTOR
DOSE MODULE
RETURN

FIGURE 2.2

EXPOSURE PATHWAYS ANALYZED

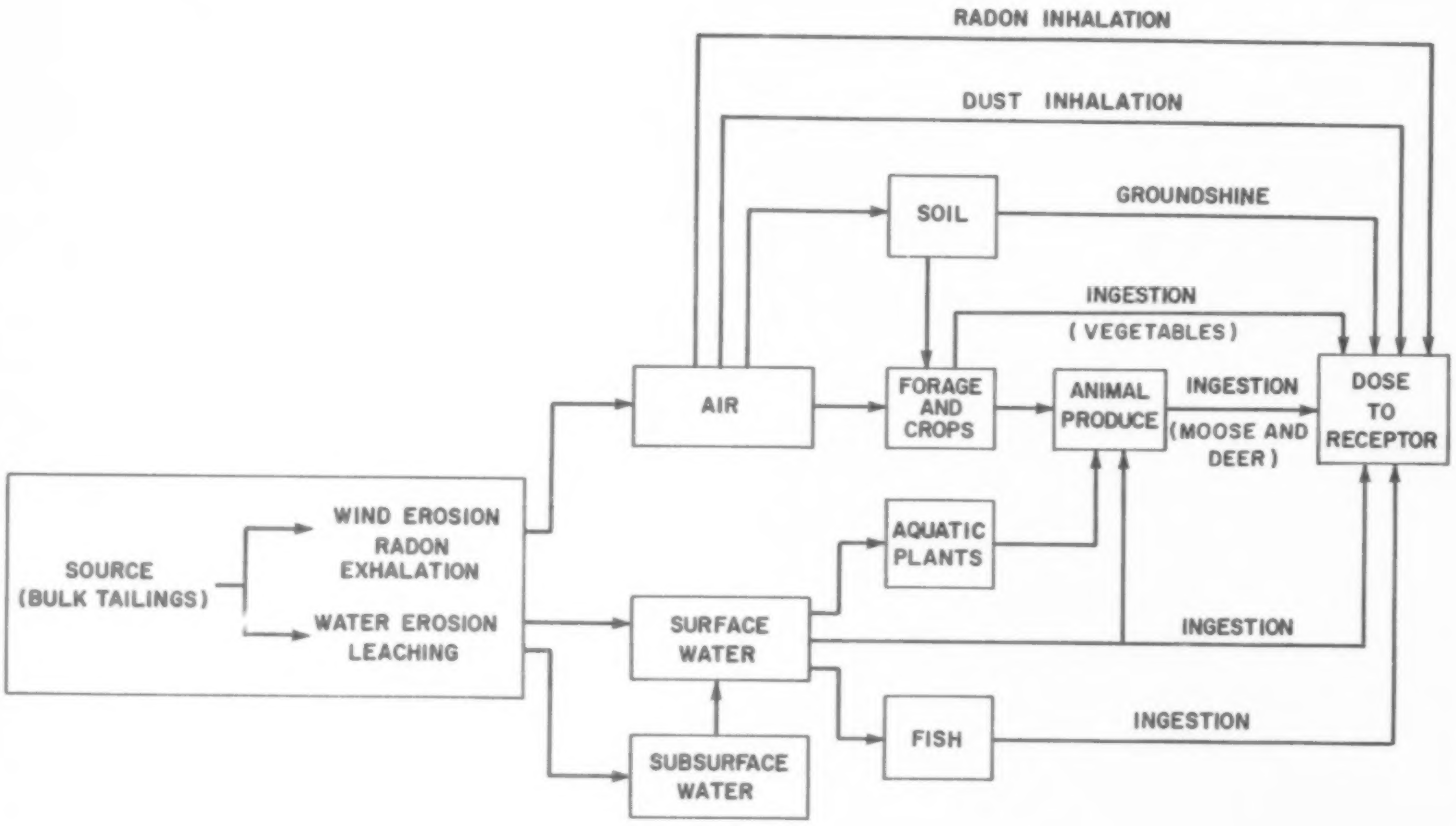

FIGURE 2.3
CONCEPTUAL DIAGRAM
OF SPATIAL COORDINATE SYSTEM

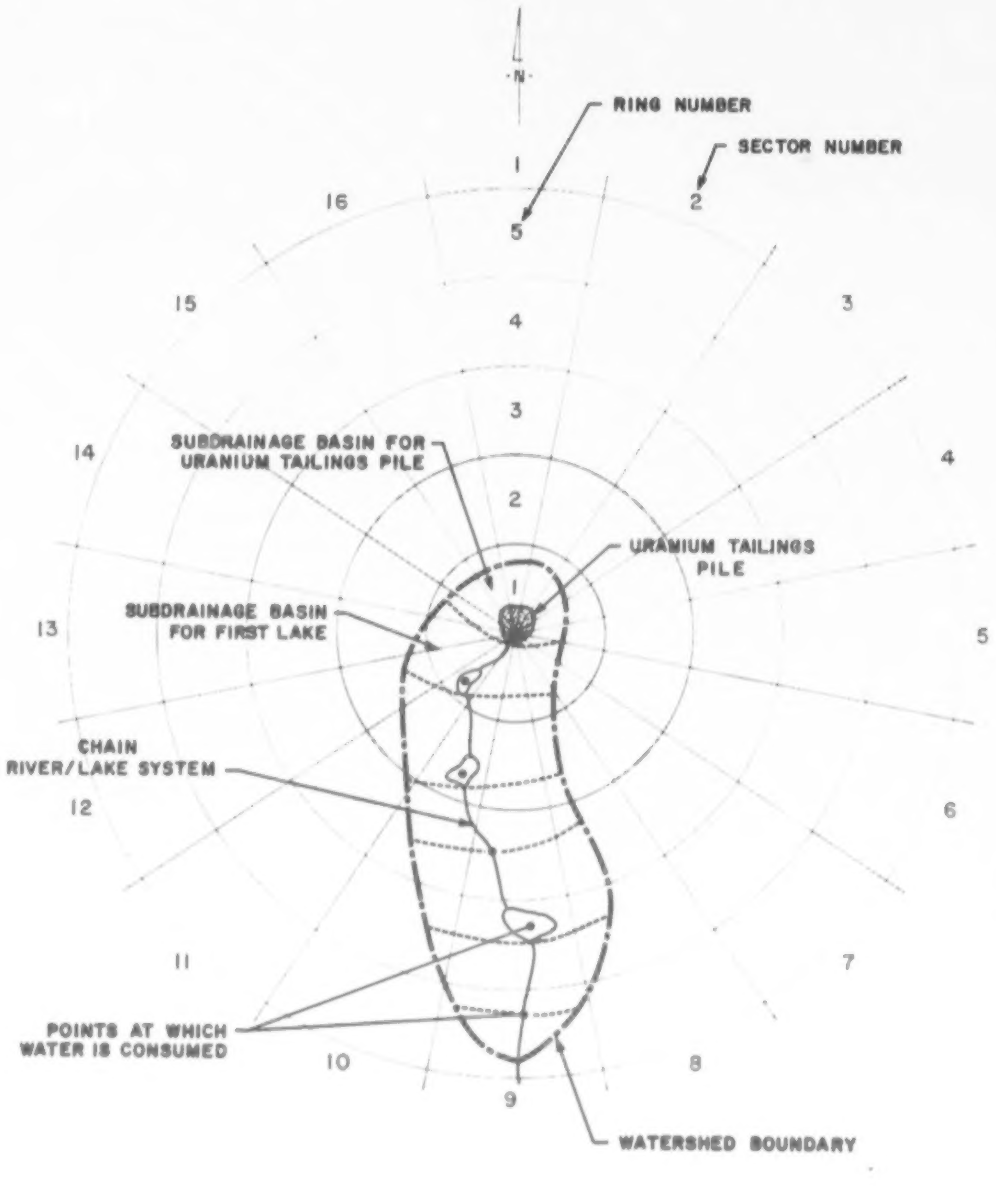

Table 2.1

SUMMARY OF UTAP.3 COMPONENT MODULE OBJECTIVES

CONSTITUENTS	PATHWAYS	SPATIAL AND RECEPTOR LOCATIONS	TEMPORAL CONSIDERATIONS	NATURAL PHYSICAL CHANGES	CLOSEOUT OPTIONS
Natural Uranium Total Thorium Radium-226 Radon-222 Lead-210 Calcium Iron Sulphate pH	Lake Water Consumption Fish Consumption Radon Inhalation Dust Inhalation Vegetable Consumption Animal Produce Consumption (from animals feeding on land and aquatic vegetation and drinking water) Groundshine	Air Pathways: 16 Directions and up to 5 Radial Distances From 1 To 50 km Water Pathways: Up To 10 Chained River/Lake Segments Up To 80 Receptor Locations Up To 2 Receptor Types	Time-Variant Parameters Can Be Sampled Every Step Time Increments of 1 to 10 Years Up To 300 Time Steps	Sheet Erosion of Tailings Surface As A Function of Vegetation Cover Revegetation of Tailings Surface with Time As A Function of pH Recovery of Fish Population Following pH Recovery	Base Case: Pyritic Tailings, Tailings Surface Revegetated, No Other Remedial Work Carried Out Alternative Closeout Options Are Site Specific. See Lacnor Report (SENES, 1987a) For Application of UTAP.3 to Alternative Closeout Options

Table 2.2

COMEX MODEL CODE LISTING

```
      SUBROUTINE COMEX
      INCLUDE 'MODEL.INC'
      INCLUDE 'VAR.INC'
      IF(WINDFG.EQ.'Y'.OR.(NT.EQ.0.AND.NUMTRL.EQ.1))CALL WIND
      CALL SEXEC
      CALL AIRDIS
      DO 10 NREC=1,NRECEP
         CALL SOIL
         CALL GSHINE
         CALL VEGCON
10    CONTINUE
      CALL GWATER
      CALL WATEX
      CALL WATVEG
      CALL ANIMAL
      DO 11 NREC=1,NRECEP
         CALL DOSEIN
11    CONTINUE
      RETURN
      END
```

boundaries.

The watershed model handles up to 10 user-specified components (segments) in the river-lake system. The user specifies the appropriate river and lake characteristics (i.e. lake area, lake depth, drainage area, etc.). Calculations are done at each river or lake outflow point. The user specifies the relationship between rivers and lakes (i.e. the order of linkage of the river and lake segments). The program provides a validation step to ensure that a physically feasible watershed has been specified.

Dilution is the only mechanism accounted for in the river model. That is, adsorption and desorption are not considered. The lake model accounts for adsorption, desorption and dilution. The user specifies different biological and/or chemical characteristics for the lakes in addition to physical characteristics. Data for two lake types with distinct biological and chemical characteristics are specified in the probabilistic input file accompanying the UTAP.3. The user has the option however of specifying biological and/or chemical data appropriate for each lake in the system being modelled.

2.4 Receptor Locations, Characteristics and Population Dose

The system model permits the calculation of contaminant concentrations and receptor dose in all 80 windrose locations (i.e. 5 radial distances and 16 directions). The user thus possesses great power to perform a comprehensive analysis of the system. The code allows the user to model up to 80 receptors with user-defined characteristics. To minimize computer set-up and run time we recommend the use of the minimum number of receptors consistent with the objectives of a particular study.

Two receptor types are available for analysis, for example, an average receptor and a critical receptor. The characteristics of the two receptors are fixed for a given run, but may be changed from one run to the next. Both receptors are assumed to breathe the air, be exposed to groundshine and consume vegetables grown in the sector in which they are located. However, their water and fish intake comes from a user-specified river or lake.

Population dose is computed for each populated sector as the dose to a receptor (either type 1, type 2 or both) multiplied by a user-specified population. The dose for sectors with populations are summed to obtain the total population dose.

2.5 Temporal Considerations

In the deterministic evaluation of a time-dependent simulation model, input parameters are entered into the mathematical model and values of the time-dependent output variable(s) are calculated as the system evolves in time from a specified initial state. This approach also holds in a probabilistic evaluation of the model. In this case, however, the input parameter values are not uniquely specified, but rather for each trial (i.e. each individual simulation) a set of parameter values are selected by randomly sampling from a probability distribution of possible values for each parameter. The system is then allowed to evolve through time with the parameter values fixed at the initially-selected values. In the next trial, new parameter values are selected by randomly sampling again from the specified input parameter distributions, and the system is allowed to evolve once more in time. The process is repeated until the desired number of trials have been carried out.

However, some input parameters, such as the "mean annual precipitation" may vary from year to year. The value of this parameter in any past year is known (in the sense that it can be estimated from observational data) and is a single constant value (except for observational uncertainty). However, the mean annual precipitation varies from year to year and hence even if there was no observational uncertainty, the amount of precipitation in any future year would be inherently uncertain, in the sense that it would vary from year to year. Variability from year to year in input parameters also gives rise to uncertainty in the output variable.

In UTAP.3 the modeller can identify each parameter as either time-variant or non-time-variant. The default is non-time-variant. Time-variant parameters are sampled for each time step of each trial while non-time-variant parameters are sampled once, at the start of each trial.

Interval time steps of between 1 and 10 years are permitted in UTAP.3. The component models are not designed for shorter than annual time steps. When time steps are much greater than 10 years interesting temporal dependencies may be bypassed. For most applications a time step of 10 years is recommended.

The maximum number of time steps permitted in UTAP.3 is 300. Thus, with a 10 year time increment and 300 time steps, simulation can be extended to 3000 years in the future. The user is cautioned that, clearly, the further in the future we extend our modelling the less confident we can feel about the model predictions. In effect, the presumption is that the (reference) scenario which has been defined at the start of the simulation will continue throughout the simulation period. The UTAP.3 code was modified from earlier versions of UTAP in this regard is to permit the modeller to examine the temporal dynamics of the defined scenario at times sufficiently far in the future to ensure that the system is behaving in a well defined fashion (e.g. dose due to the water pathway is decreasing monotonically etc.)

2.6 Natural Physical Changes

This involves consideration of natural processes which have the potential to affect contaminant release rates from the tailings in a gradual way over many years. It does not include episodic events, such as floods or forest fires. Sheet erosion by water action is modelled using the Universal Soil Loss Equation. This approach provides a direct source of solids loading to the watershed element nearest the tailings. We have also included a factor which accounts for natural vegetation of the tailings when the pH of the tailings porewater exceeds 4.0. The revegetation term has the effect of reducing water erosion and dust suspension. Finally, UTAP.3 includes a factor to account for the effect of pH on the availability of game fish in local lakes.

2.7 Disposal Option(s)

UTAP.3 has been used to examine several distinct uranium tailings closeout options. The generic models described in this report focus on the base case, namely that of low-grade pyritic uranium tailings for which the tailings surface has been revegetated but for which no other remedial work has been carried out. The assessment of alternative tailings closeout options involves the use of different input parameters specific to the option and in some instances a different conceptualization of model predictions. Tailings closeout options and parameter sets are very site specific. The reader interested in the details of how to apply UTAP.3 to an actual tailings site and alternative tailings closeout options is referred to the report on UTAP Application to the Lacnor Tailings Site (SENES, 1987a.)

2.8 Input Parameters

Each component model requires values for a number of independent variables or "input parameters". In a probabilistic analysis, these inputs are specified as probability distributions. The input parameter distributions available in UTAP.3 include: constant, uniform, loguniform, normal, lognormal, triangular, Weibull, beta , arbitrary and pairwise correlated.

Each distribution is defined by its own attributes as indicated in Table 2.3. For instance, a normal distribution is specified by its mean, standard deviation, minimum value and maximum value, while a uniform distribution is completely specified by its minimum and maximum values. The distributions given in Table 2.3 are referenced frequently in tables of parameter definitions included in the following chapters.

2.9 Outputs

The user may specify concentration and dose data as well as selected input

Table 2.3

INPUT PARAMETER DISTRIBUTION SPECIFICATIONS

Distribution Type		Distribution Specifications
C	Constant	single numerical value
U	Uniform	minimum, maximum
LU	Loguniform	minimum, maximum
N	Normal	arithmetic mean, arithmetic standard deviation, minimum, maximum
LN	Lognormal	geometric mean, geometric standard deviation, minimum, maximum
T	Triangular	minimum, mode (peak), maximum
W	Weibull	location parameter (minimum) (a), scale parameter (b), shape parameter (c)
B	Beta	minimum, maximum, shape parameters (a and b)
CR	Correlated	name of independent variable, mean of dependent variable, standard deviation of dependent variable, correlation coefficient, mean of independent variable, standard deviation of independent variable
A	Arbitrary	number of cells, minimum value, maximum value, ordinate values

parameters for output at selected time intervals without having to alter the program. The following summary statistics are routinely computed:

Mean
Standard deviation
Geometric mean
Geometric standard deviation
Minimum
Maximum

Skewness and kurtosis are also available as an output option.

The parameter names, specifications, and the time intervals selected are output as appropriate.

Statistics not calculated appear as blanks in the output file. For instance, if only one trial is performed, standard deviations, skewness and kurtosis will not be calculated and blanks will be written to the output file.

In addition to the summary statistics the user has the option to access a detailed results file which contains the actual data from which the summary statistics are calculated. Finally, UTAP.3 also contains a post-processing program which calculates confidence bands for user-selected data.

Full details of how to use the UTAP.3 program are provided in the User's Manual (SENES, 1987b).

2.10 References

SENES Consultants Limited, 1986. "Probabilistic Model Development for the Assessment of the Long-Term Effects of Uranium Mill Tailings in Canada - Phase III. Volume 2: Uranium Tailings Assessment Program (UTAP): System Description and Control Module Documentation." Research report prepared for the National Uranium Tailings Program, CANMET, EMR under Supply and Services Canada Contract No. OSQ85-00182.

SENES Consultants Limited, 1987a. "Uranium Tailings Assessment Program (UTAP.3): Application to the Lacnor Tailings Site." Research report prepared for the National Uranium Tailings Program, CANMET, EMR, under Supply and Services Canada Contract No. 23317-6-1728/01-SQ.

SENES Consultants Limited, 1987b. "Uranium Tailings Assessment Program (UTAP.3): User's Manual." Research report prepared for the National Uranium Tailings Program, CANMET, EMR, under Supply and Services Canada Contract No. 23317-6-1728/01-SQ.

SENES Consultants Limited, 1987c. "Uranium Tailings Assessment Program (UTAP.3): Addendum to Volume 2 - System Description and Control Modules Documentation." Research report prepared for the National Uranium Tailings Program, CANMET, EMR, under Supply and Services Canada Contract No. 23317-6-1728/01-SQ.

3.0 WATER SOURCE MODELS

3.1 Modelling Concepts

The approach to modelling the physical and chemical behaviour of the tailings is very similar to that adopted in a previous study (SENES, 1986). Specifically, the tailings are modelled as a multi-layered system, as indicated on Figure 3.1. The features shown on the figure are explained in more detail in subsequent sections. Briefly, the tailings consist of an upper, unsaturated (oxidizing) zone, and a much thicker saturated (reducing) zone.

The tailings contain significant quantities of gypsum and other sulphate minerals. Over time, these sulphate compounds dissolve, and are gradually depleted. The depletion is hypothesized to proceed as a series of fronts moving downward through the tailings. Since the different sulphate compounds have different solubilities, the fronts may move at different rates. The tailings above each front are thus depleted of the solid sulphate, while the layer below the front is enriched in the same compound.

The upper layer of the saturated zone has been specified for modelling purposes as a 'mixing layer' in which adsorption of several species may occur. This feature is built into the model to account for the natural retardation processes which occur in large tailings areas.

The aqueous phase concentrations of a number of chemical species are explicitly modelled. These include calcium (Ca^{2+}), sulphate (SO_4^{2-}), ferric and ferrous iron (Fe^{3+} and Fe^{2+}). The pH of the aqueous phase is modelled as a function of several of these ions. As well, both the solid and liquid phase concentrations of a number of radionuclides (natural uranium, total thorium, radium-226 and lead-210) are included in the model.

The physical and chemical processes modelled include:

- pyrite oxidation
- gypsum dissolution and reprecipitation
- dissolution of uranium and thorium
- Ra-226 dissolution and coprecipitation with $BaSO_4$
- Pb-210 dissolution and coprecipitation with $PbSO_4$
- radioactive decay and ingrowth (as required)
- sheet erosion as a direct source of radionuclide loading
- tailings vegetation over time, resulting in reduced erosion

The necessary calculations are performed in a number of modules, as outlined on Figure 3.2. The modular structure has facilitated model development, review and implementation. Model structures and derivations are presented in the following sections, corresponding roughly to the modules indicated on Figure 3.2. A complete listing of the source model code is provided in Appendix A. Also included in the appendix is a variable dictionary which summarizes all the variables used in the models, and indicates symbols used in the computer implementation.

The tailings erosion and vegetation model is included as Section 3.14. It was developed separately from the remainder of the water source model and is included here since it acts as an additional source of radionuclide loading to the receiving environment. Section 3.14 contains a complete description and illustration of this model including the computer code listing and variable dictionary.

The dust and radon models indicated on Figure 3.2 are described in Chapter 4.

3.2 Initial Conditions - Ions and pH

As indicated on Figure 3.2, the initial condition calculations are performed in the first simulation time step, which is representative of the period from $-\Delta t$ years to zero years. The values calculated in this time step are considered representative of $t=0$ years. Thus the $t=0$ values do not represent

FIGURE 3.1

CONCEPT ADOPTED FOR MODELLING THE TAILINGS SOURCE TERM

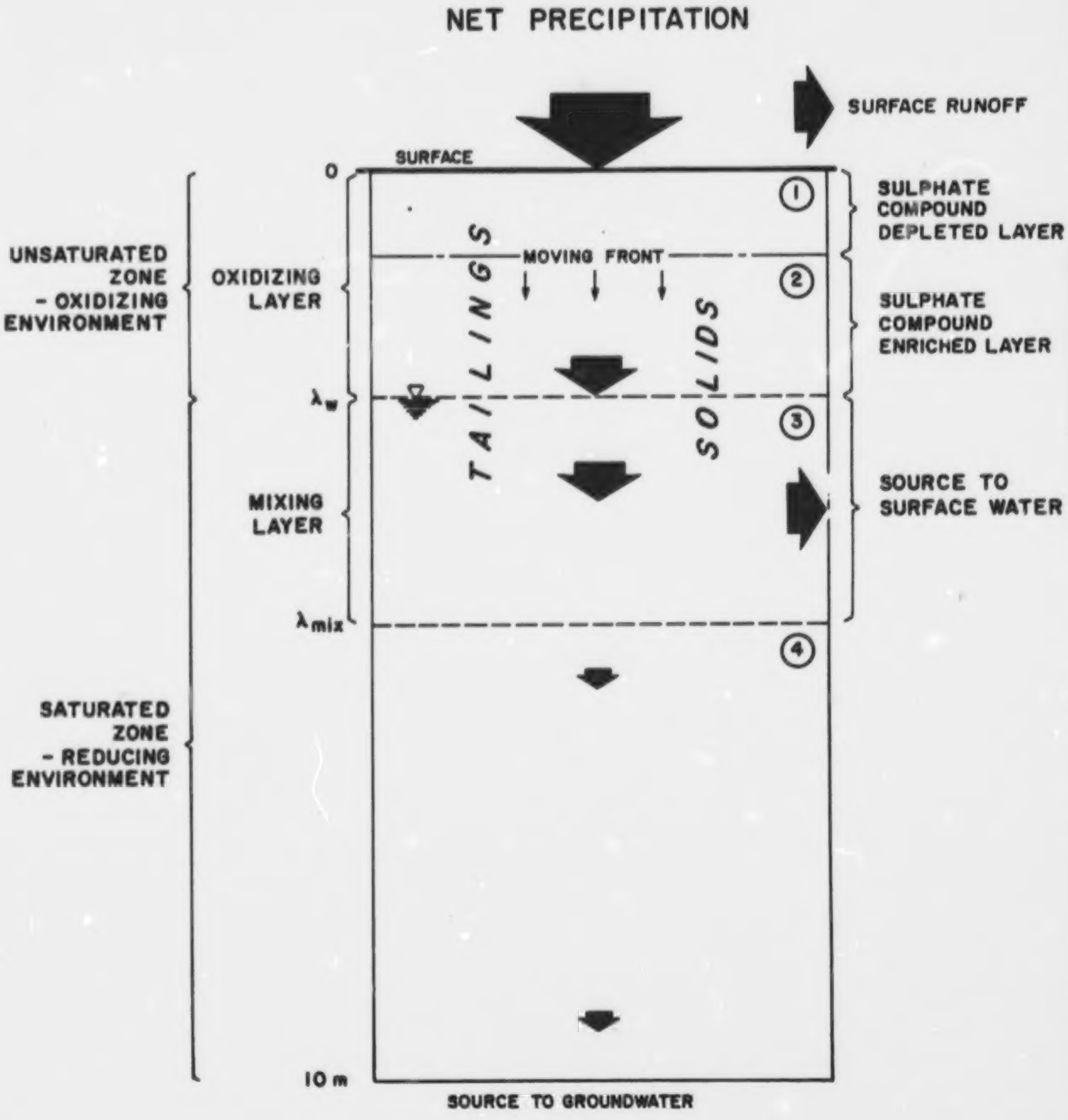

FIGURE 3.2

STRUCTURE OF THE TAILINGS SOURCE MODEL

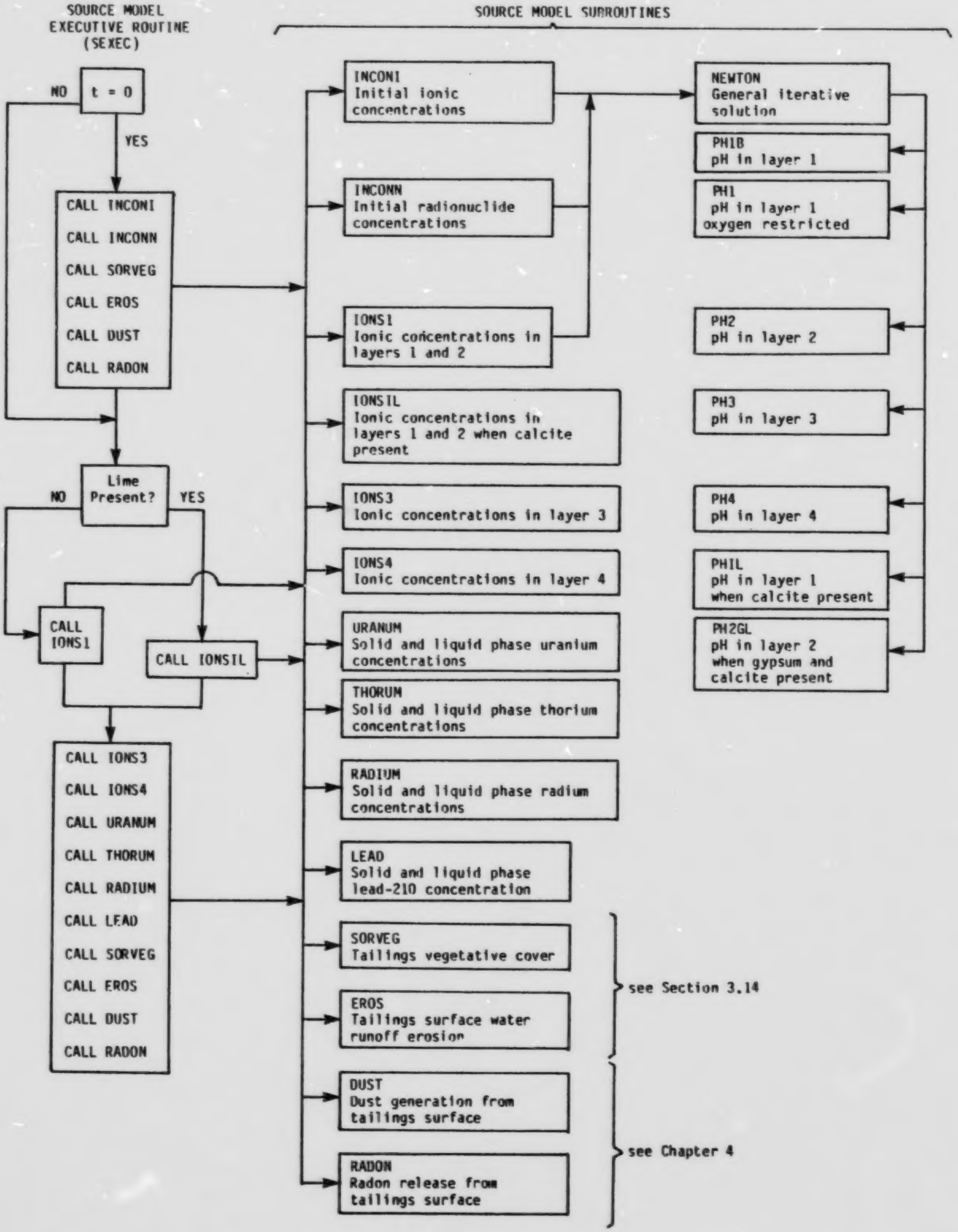
SOURCE MODEL
EXECUTIVE ROUTINE
(SEXEC)
SOURCE MODEL SUBROUTINES
t = 0
NO
YES
CALL INCONI
CALL INCONN
CALL SORVEG
CALL EROS
CALL DUST
CALL RADON
Lime Present?
NO
YES
CALL IONS1
CALL IONSIL
CALL IONS3
CALL IONS4
CALL URANUM
CALL THORUM
CALL RADIUM
CALL LEAD
CALL SORVEG
CALL EROS
CALL DUST
CALL RADON
INCONI
Initial ionic concentrations
INCONN
Initial radionuclide concentrations
IONS1
Ionic concentrations in layers 1 and 2
IONSIL
Ionic concentrations in layers 1 and 2 when calcite present
IONS3
Ionic concentrations in layer 3
IONS4
Ionic concentrations in layer 4
URANUM
Solid and liquid phase uranium concentrations
THORUM
Solid and liquid phase thorium concentrations
RADIUM
Solid and liquid phase radium concentrations
LEAD
Solid and liquid phase lead-210 concentration
SORVEG
Tailings vegetative cover
EROS
Tailings surface water runoff erosion
DUST
Dust generation from tailings surface
RADON
Radon release from tailings surface
see Section 3.14
see Chapter 4
NEWTON
General iterative solution
PH1B
pH in layer 1
PH1
pH in layer 1 oxygen restricted
PH2
pH in layer 2
PH3
pH in layer 3
PH4
pH in layer 4
PHIL
pH in layer 1 when calcite present
PH2GL
pH in layer 2 when gypsum and calcite present

the initial, or background conditions of the environment in the absence of the tailings. Rather, they represent the initial or background conditions, affected for Δt years by the presence of the tailings. Performing the calculations in this way builds one time step of "memory" into the system. It also eliminates many of the unrealistically sudden increases or decreases in calculated values which would otherwise be apparent.

The calculations described in this section therefore serve two purposes. First, a number of quantities (such as initial mass inventories, background concentrations, etc.) are initialized. Secondly, appropriate calculations, representative of the period $-\Delta t$ to 0 years, are performed.

Many of the calculations relevant in the first time period are also applicable to all other time steps. In these instances, no detailed derivations are provided in this section. Rather, reference is made to the appropriate derivation in a subsequent section. It may be most useful for the reader to skim this section quickly, and proceed to the subsequent, more detailed sections; returning to this section, as required, to determine initial conditions and calculations.

3.2.1 Initial Inventories

The initial inventory of pyrite (FeS_2) in the tailings is specified as an input parameter. That is:

$$[FeS_2]_{t=0} = [FeS_2]^o \qquad (3.2.1)$$

where
$[FeS_2]^o$ = initial concentration of pyrite in tailings ($mol.m^{-3}$).

The initial inventory of anhydrous gypsum ($CaSO_4$), which is referred to throughout this report simply as gypsum, is calculated as a function of two input parameters:

$$g_0 = \rho_T \, x_{gyp}/136 \qquad (3.2.2)$$

where

g_o = initial concentration of gypsum in tailings ($mol.m^{-3}$)

ρ_T = tailings bulk density ($g.m^{-3}$)

x_{gyp} = mass fraction of gypsum in tailings

136 = molecular weight of anhydrous gypsum ($g.mol^{-1}$).

3.2.2 Calcium and Sulphate Concentrations

Sulphates are formed as a result of pyrite oxidation in the unsaturated layer during the initial time step (i.e. $-\Delta t$ to $t=0$). The details of this process are presented in Section 3.3.1. In summary, it can be shown that:

$$[SO_4^{2-}]^{o}_{p,\lambda w} = \frac{2\, \lambda_w\, [FeS_2]^o\, [1-e^{-k\Delta t}]}{I_n\, \Delta t} \tag{3.2.3}$$

where

$[SO_4^{2-}]^{o}_{p,\lambda w}$ = initial sulphate concentration at λ_w resulting from pyrite oxidation ($mol.m^{-3}$)

λ_w = thickness of the unsaturated zone (m)

k = rate constant for pyrite oxidation (yr^{-1}) (see Section 3.3.1)

I_n = net infiltration rate ($m.yr^{-1}$).

and

$$I_n = P\,(1 - X_{run})\,\frac{W_s}{A_t}$$

where

P = annual net precipitation (i.e. total precipitation less evapotranspiration) ($m.yr^{-1}$)

X_{run} = fraction of surface runoff from tailings

W_s = watershed surface area (m^2)

A_t = surface area of tailings (m^2).

Although little or no pyrite oxidation occurs in the mixing zone, the sulphates formed by this process in the unsaturated zone are transported downwards via infiltrating rainwater, resulting in an increased sulphate concentration in the mixing zone. This is expressed by (see Section 3.6.1):

$$[SO_4^{2-}]^{o}_{p,mix} = [SO_4^{2-}]_{p,\lambda w} - [SO_4^{2-}]_{p,\lambda w} \exp[-I_n \Delta t/\epsilon\lambda_{mix}] \qquad (3.2.4)$$

where

$[SO_4^{2-}]^{o}_{p,mix}$ = initial sulphate concentration in the mixing zone resulting from pyrite oxidation in the unsaturated zone ($mol.m^{-3}$)

ϵ = porosity

λ_{mix} = thickness of the mixing zone (m).

The porosity is determined from:

$$\epsilon = 1 - \rho_T/\rho_S$$

where

ρ_S = the particle density of the tailings; 2.6×10^6 ($kg.m^{-3}$)

ρ_T = soil bulk density ($kg.m^{-3}$).

We assume that sulphate concentration resulting from pyrite oxidation in the bottom layer (layer 4) is zero in the first time step. That is:

$$[SO_4^{2-}]^{o}_{p,4} = 0 \quad \text{at } t=0 \qquad (3.2.5)$$

where

$[SO_4^{2-}]^{o}_{p,4}$ = initial sulphate concentration in the bottom layer (layer 4) resulting from pyrite oxidation in the unsaturated zone ($mol.m^{-3}$).

This indicates that the sulphates formed in the upper layer have not yet had an impact on the lower layer.

The total concentrations of calcium and sulphate can be calculated as functions of the concentrations of sulphates resulting from pyrite oxidation. In the unsaturated layer, the relationships are:

$$[Ca^{2+}]_{\lambda w} = \sqrt{\frac{K_s^o d}{f^2} + 0.25\, [SO_4^{2-}]^2_{p,\lambda w}} - 0.5\, [SO_4^{2-}]_{p,\lambda w} \qquad (3.2.6)$$

and

$$[SO_4^{2-}]_{\lambda w} = \sqrt{\frac{K_s^o\, d}{f^2} + 0.25\, [SO_4^{2-}]_{p,\lambda w}^2} + 0.5\, [SO_4^{2-}]_{p,\lambda w} \qquad (3.2.7)$$

where

$[Ca^{2+}]_{\lambda w}$ = concentration of Ca^{2+} at λ_w ($mol.m^{-3}$)
$[SO_4^{2-}]_{\lambda w}$ = concentration of SO_4^{2-} at λ_w ($mol.m^{-3}$)
K_s^o = solubility equilibrium constant for $CaSO_4$ ($mol^2.m^{-6}$)
f = activity coefficient for divalent ions
d = correction factor accounting for sulphate complexation.

The details regarding these relationships are provided in Section 3.3.3.

In the mixing zone, the concentrations are given by:

$$[Ca^{2+}]_{mix} = \sqrt{\frac{K_s^o}{f^2} + 0.25\, [SO_4^{2-}]_{p,mix}^2} - 0.5\, [SO_4^{2-}]_{p,mix} \qquad (3.2.8)$$

$$[SO_4^{2-}]_{mix} = \sqrt{\frac{K_s^o}{f^2} + 0.25\, [SO_4^{2-}]_{p,mix}^2} + 0.5\, [SO_4^{2-}]_{p,mix} \qquad (3.2.9)$$

Again, the details are provided elsewhere (Section 3.4.1).

In the bottom layer (layer 4), no sulphates resulting from pyrite oxidation are present in the first time step. Hence, gypsum represents the only source of dissolved calcium and sulphate ions, and the original concentrations can be calculated from equilibrium considerations. Namely:

$$[SO_4^{2-}]_4 = [Ca^{2+}]_4 = \sqrt{\frac{K_s^o}{f^2}} \qquad (3.2.10)$$

3.2.3 Initial pH Levels

The derivations of the pH equations are provided elsewhere, and will not be repeated here. At t=0 years, a gypsum-depleted layer does not really exist. Hence the pH for the unsaturated zone (layers 1 and 2) is calculated using the relationship for layer 2 (equation (3.6.27), as described in Section 3.6.2).

The pH of layers 3 and 4 is calculated using equation (3.6.39) (Section 3.6.3) with variables appropriate for the different layers.

3.2.4 Iron Concentrations

Iron exists in solution in the unsaturated zone in its oxidized state (Fe^{3+}). The $[Fe^{3+}]$ in the unsaturated zone is calculated as a function of the initial pH and $[SO_4^{2-}]$ in the same layer. The functional relationship is given by equation (3.3.44) in Section 3.3.4.

In the mixing zone, iron exists in its reduced state (Fe^{2+}). From the stoichiometric relationship between Fe^{3+} and Fe^{2+} we can state:

$$[Fe^{2+}]_{mix} = 1.5\ [Fe^{3+}]_{\lambda w} \qquad (3.2.11)$$

where

$[Fe^{3+}]_{\lambda w}$ = concentration of Fe^{3+} in unsaturated zone ($mol.m^{-3}$)
$[Fe^{2+}]_{mix}$ = concentration of Fe^{2+} in saturated zone (layer 3) ($mol.m^{-3}$).

Again, further information can be found in Section 3.4.4.

In keeping with our previous assumptions regarding the effects of pyrite oxidation in the bottom layer in the first time step, we assume that $[Fe^{2+}]$ in layer 4 is zero in the first time step. That is:

$$[Fe^{2+}]_4 = 0 \quad \text{at } t=0 \qquad (3.2.12)$$

3.3 Ions - Layers 1 and 2

The concentrations of dissolved calcium $[Ca^{+2}]$ and sulphate $[SO_4^{2-}]$ ions in layers 1 and 2 are primarily dependent on two phenomena. First, gypsum ($CaSO_4$) formed during the neutralization of tailings in the mill, dissolves to yield Ca^{2+} and SO_4^{2-}. Secondly, pyrite (FeS_2) in the tailings undergoes oxidation resulting in SO_4^{2-} production. These phenomena and their effects are discussed in more detail in the following sections.

3.3.1 Sulphates Derived From Pyrite Oxidation

The oxidation of pyrite is initiated by the action of ferric ion on the pyrite surface (Nordstrom, 1982):

$$FeS_2 + 2\ Fe^{3+} \longrightarrow 3\ Fe^{2+} + 2\ S_o \qquad (3.3.1)$$

The reduced iron (Fe^{2+}) in solution is rapidly oxidized to the ferric state by bacteria:

$$2\ Fe^{2+} + 2\ H^+ + \frac{1}{2}\ O_2 \longrightarrow 2\ Fe^{3+} + H_2O \qquad (3.3.2)$$

The rate determining step is the bacterial oxidation of the sulphur layer on the pyritic surface leading to the overall stoichiometry:

$$2\ FeS_2 + 7.5\ O_2 + H_2O \longrightarrow 2\ Fe^{3+} + 2\ H^+ + 4\ SO_4^{2-} \qquad (3.3.3)$$

From the above relationship, it is apparent that the rate of pyrite oxidation is stoichiometrically related to the rate of sulphate formation as follows:

$$-\frac{d\,[FeS_2]}{dt} = \frac{1}{2}\,\frac{d[SO_4^{2-}]}{dt} \qquad (3.3.4)$$

The rate of pyrite oxidation is assumed to be first order with respect to pyrite content, i.e.:

$$-\frac{d\,[FeS_2]}{dt} = k[FeS_2] \qquad (3.3.5),$$

It follows, that the initial rate of oxidation is given by:

$$-\left.\frac{d\,[FeS_2]}{dt}\right|_{t=0} = k[FeS_2]^{o} \qquad (3.3.6)$$

where $[FeS_2]^o$ is the initial pyrite content. From equation (3.3.4) it is evident that the specific rate of pyrite oxidation (k) is related to the rate of sulphate generation as follows:

$$k = \left.\frac{\frac{1}{2}\,\frac{d\,[SO_4^{2-}]}{dt}}{[FeS_2]^{o}}\right|_{t=0} \qquad (3.3.7)$$

The rate of sulphate formation, in turn, can be related to the flux of sulphate exiting from the unsaturated zone as:

$$\left.\frac{d\,[SO_4^{2-}]}{dt}\right|_{t=0} = \frac{J_s}{\lambda_w} \qquad (3.3.8)$$

where

J_s = sulphate flux ($mol.m^{-2}.yr^{-1}$)

λ_w = thickness of the unsaturated zone (m).

An expression for the sulphate flux in an unsaturated zone has been derived previously (SENES, 1984) as it is related to the oxygen flux into the tailings and the stoichiometry of pyrite oxidation:

$$J_s = \left[\frac{8}{7.5}\,\overline{R}_s\,\rho_T\,[O_2]\,D_{O_2}\left(1 - K'\ln\left(\frac{1+K'}{K'}\right)\right)\right]^{1/2} \qquad (3.3.9)$$

where

$\overline{R}_s$ = sulphate production rate ($mol.g^{-1}_{tailings}.yr^{-1}$)

$[O_2]$ = oxygen concentration on the surface ($mol.m^{-3}$)

D_{O_2} = oxygen diffusivity through tailings ($m^2.yr^{-1}$)

ρ_T = density of tailings ($g.m^{-3}$)

K' = $K_{O_2}/[O_2]$ = ratio of O_2 half saturation constant to the oxygen concentration $[O_2]$.

Substituting equation (3.3.8) into equation (3.3.7) defines k as:

$$k = \frac{J_s}{2\ \lambda_w\ [FeS_2]^o} \qquad (3.3.10)$$

Let us define a time period "Δt". Since pyrite oxidation is assumed to be uniform throughout the unsaturated zone, the moles of remaining pyrite per tailings volume after time t is given by integrating equation (3.3.5) between t-Δt and t:

$$[FeS_2]_t = [FeS_2]_{t-\Delta t}\ e^{-k\Delta t} \qquad (3.3.11)$$

Since such an exponential function can lead to increasingly small values, particularly if kΔt is large, a lower bound on the calculated value of $[FeS_2]$ of 1×10^{-6} $mol.m^{-3}$ was imposed. That is:

if $[FeS_2]_t \leq 1.0 \times 10^{-6}$
then $[FeS_2]_t = 1.0 \times 10^{-6}$

The moles of pyrite/volume oxidized during the time period t-Δt to t is therefore as follows:

$$\Delta[FeS_2]_{t-\Delta t \rightarrow t} = [FeS_2]_{t-\Delta t}\ [1 - e^{-k\Delta t}] \qquad (3.3.12)$$

Assuming, that the net infiltration (I_n in $m.yr^{-1}$) is constant during the time step of choice (Δt), the sulphate concentration in the liquid phase at λ_w resulting from pyrite oxidation is given by :

$$[SO_4^{2-}]_{p,\lambda w} = \frac{2\ \lambda_w [FeS_2]_{t-\Delta t}\ [1 - e^{-k\Delta t}]}{I_n \Delta t} \qquad (3.3.13)$$

where

$[SO_4^{2-}]_{p,\lambda w}$ = sulphate concentration at λ_w resulting from pyrite oxidation ($mol.m^{-3}$).

Note, that equation (3.3.13) defines a time-averaged sulphate concentration for the time period $t-\Delta t$ to t. During this time period, the precipitation rate (P) is held constant, but can vary for the next time period Δt.

Pyrite oxidation acts as the long-term source of sulphates in the system. It can be seen from equation (3.3.13) that this quantity may become very small over time. Thus, we considered it appropriate to include the background sulphate concentration present in the precipitation (P). Equation (3.3.13) can be rewritten to include this background source of sulphate:

$$[SO_4^{2-}]_{p,\lambda w} = \frac{2\ \lambda_w\ [FeS_2]_{t-\Delta t}\ [1-e^{-k\Delta t}]}{I_n \Delta t} + 0.0128 \qquad (3.3.14)$$

where

$0.0128 = [SO_4^{2-}]$ in precipitation ($mol.m^{-3}$).

The term $[SO_4^{2-}]_{p,\lambda w}$ now represents sulphates resulting from pyrite oxidation plus that naturally present in rainwater.

It has been shown previously (SENES, 1985a), that if pyrite oxidation is uniform throughout the oxidizing zone, the sulphate concentration resulting from pyrite oxidation at any distance ($z \leq \lambda_w$) into the tailings is given by:

$$[SO_4^{2-}]_{p,z} = [SO_4^{2-}]_{p,\lambda w} \left(\frac{z}{\lambda_w}\right) \qquad (3.3.15a)$$

This implies that the time-averaged sulphate concentration at "z" from pyrite oxidation is given by:

$$[SO_4^{2-}]_{p,z} = \frac{2z\ [FeS_2]_{t-\Delta t}\ [1 - e^{-k\Delta t}]}{I_n \Delta t} + 0.0128 \qquad (3.3.15b)$$

3.3.2 Gypsum Dissolution and Reprecipitation

In pyritic tailings, it is not uncommon to observe an increase in sulphate concentration with depth. Due to this phenomenon, some of the gypsum which dissolves in the upper portions of the unsaturated zone will reprecipitate (as the $[SO_4^{2-}]$ increases) in the lower portions of the zone. Thus the unsaturated zone can be thought to consist of an upper layer, in which all the gypsum has dissolved and migrated downward with the porewater, and a lower layer in which some of the gypsum has reprecipitated. These are referred to as the gypsum-depleted layer (layer 1) and the gypsum-enriched layer (layer 2) in this discussion. The relative heights of these two layers will change with time; the depleted zone increasing until the entire unsaturated zone is depleted of gypsum. After this time, a number of physical and chemical processes can be ignored and the source term model becomes simpler.

The solubility of gypsum, and hence the concentration of $[Ca^{2+}]$ is dependent on the solubility product as follows:

$$\frac{K^{o}_{s,CaSO_4}}{\left(f_{Ca^{2+}}\right)\left(f_{SO_4^{2-}}\right)} = \left([SO_4^{2-}]\right)\left([Ca^{2+}]\right) \qquad (3.3.16)$$

where

$K^{o}_{s,CaSO_4}$ = solubility equilibrium constant ($mol^2.m^{-6}$)

$f_{Ca^{2+}}$ = activity coefficient (calcium ion)

$f_{SO_4^{2-}}$ = activity coefficient (sulphate ion).

The activity coefficients, assumed to be essentially equal (i.e. f) depend on a number of factors (e.g. ionic strength of solution, temperature, etc.) and are assigned an appropriate distribution in the probabilistic analysis.

It may be assumed that the limestone ($CaCO_3$) content of pyritic tailings is rapidly depleted due to acid generation resulting from pyrite oxidation above the water table. Thus, the dissolution of gypsum is the major source of calcium during the initial years. On the other hand, pyrite oxidation of tailings contributes significantly to the sulphate concentration in the porewater. That is:

$$[\mathrm{Ca}^{2+}] = [\mathrm{Ca}^{2+}]_g \qquad (3.3.17)$$

$$[\mathrm{SO}_4^{2-}] = [\mathrm{SO}_4^{2-}]_g + [\mathrm{SO}_4^{2-}]_p \qquad (3.3.18)$$

where

$[\mathrm{Ca}^{2+}]_g$ = dissolved calcium derived from gypsum ($\mathrm{mol.m}^{-3}$)

$[\mathrm{SO}_4^{2-}]_g$ = dissolved sulphate derived from gypsum ($\mathrm{mol.m}^{-3}$)

$[\mathrm{SO}_4^{2-}]_p$ = dissolved sulphate derived from pyrite oxidation ($\mathrm{mol.m}^{-3}$).

In the relationship expressed above:

$$[\mathrm{Ca}^{2+}]_g = [\mathrm{SO}_4^{2-}]_g$$

Hence, substituting into the equation given previously for the solubility product (equation (3.3.16)) the following expression is obtained:

$$\frac{\overset{o}{K}_{s,\mathrm{CaSO}_4}}{f^2} = ([\mathrm{SO}_4^{2-}]_p + [\mathrm{SO}_4^{2-}]_g)\,[\mathrm{Ca}^{2+}]_g \qquad (3.3.19)$$

or

$$\frac{\overset{o}{K}_{s,\mathrm{CaSO}_4}}{f^2} = [\mathrm{SO}_4^{2-}]_p\,[\mathrm{Ca}^{2+}]_g + \left([\mathrm{Ca}^{2+}]_g\right)^2 \qquad (3.3.20)$$

Solving equation (3.3.20) for $[\mathrm{Ca}^{2+}]$ (or $[\mathrm{Ca}^{2+}]_g$) gives:

$$[\mathrm{Ca}^{2+}] = \sqrt{\frac{\overset{o}{K}_{s,\mathrm{CaSO}_4}}{f^2} + 0.25\,[\mathrm{SO}_4^{2-}]_p^2} - 0.5\,[\mathrm{SO}_4^{2-}]_p \qquad (3.3.21)$$

Thus, determination of the $[Ca^{2+}]$ depends on the concentration of sulphate due to pyrite oxidation. This result is quite significant and forms the basis of much of the following discussion.

Let us assume that at time "t", the gypsum-depleted layer (layer 1) has advanced to a distance "h".

Let $\left(\frac{K_s^o}{f^2}\right)^{\frac{1}{2}} = a$

and note that from equation (3.3.15b):

$$0.25\,[SO_4^{2-}]^2_{p,h} = (0.25)\,\frac{4h^2\,[FeS_2]^2_{t-\Delta t}\,[1 - e^{-k\Delta t}]^2}{(I_n\Delta t)^2}$$

$$= \frac{h^2\,[FeS_2]^2_{t-\Delta t}\,[1 - e^{-k\Delta t}]^2}{(I_n\Delta t)^2} \qquad (3.3.22)$$

Let $[FeS_2]_{t-\Delta t}\,(1 - e^{-k\Delta t}) = \beta$

Thus, $0.25\,[SO_4^{2-}]^2_{p,h} = \frac{\beta^2 h^2}{(I_n\Delta t)^2}$

and $0.5\,[SO_4^{2-}]_{p,h} = \frac{\beta h}{I_n\Delta t}$ (3.3.23)

The term accounting for sulphate concentration in rainwater (0.0128 $mol.m^{-3}$) is not included in the above expression (3.3.22) and in the subsequent derivation. This is done because the rainwater contribution is insignificant relative to the contribution from pyrite oxidation over the several hundred years for which the following equations are used (i.e. until gypsum depletion occurs between 100 and 200 years).

The sulphate concentration in equation (3.3.22), of course, refers to a time-averaged sulphate (from pyrite) concentration for the time period t-Δt to t. Now, let us assume that during this time period, the gypsum-depleted layer (layer 1) advances a distance Δh. It seems appropriate to assume that the sulphate concentration term can be represented by the "midpoint" between h and h + Δh, where the depth of the front at t-Δt is h, i.e.:

$$[SO_4^{2-}]_{p,h\rightarrow h+\Delta h} = \frac{2\,(h+\Delta h/2)\ [FeS_2]_{t-\Delta t}\ [1 - e^{-k\Delta t}]}{I_n\Delta t} \qquad (3.3.24)$$

Thus, the advancement of the gypsum depleted front is given by:

$$g_o\Delta h = I_n\Delta t \left\{ \left[a^2 + \frac{\beta^2(h + \Delta h/2)^2}{(I_n\Delta t)^2}\right]^{1/2} - \frac{\beta\ (h+\Delta h/2)}{I_n\Delta t} \right\} \qquad (3.3.25)$$

where

g_o = initial gypsum concentration in the tailings ($mol.m^{-3}$).

Solving for Δh yields:

$$\Delta h = \left[\frac{\beta^2\ h^2_{t-\Delta t}}{(g_o + \beta)^2} + \frac{(I_n\Delta t)^2\ a^2}{g_o^2 + g_o\beta}\right]^{1/2} - \frac{\beta h_{t-\Delta t}}{g_o + \beta} \qquad (3.3.26)$$

where

$$h_{t-\Delta t} = \sum_{t=0}^{t-\Delta t} \Delta h \qquad (3.3.27)$$

Thus, $h_t = h_{t-\Delta t} + \Delta h$ (3.3.28)

The time-averaged calcium concentration for the time period t-Δt to t at λ_w can be easily derived by substituting equation (3.3.13) into equation (3.3.21) to yield:

$$[Ca^{2+}]_{\lambda w,t-\Delta t\rightarrow t} = \left[a^2 + \frac{\lambda_w^{\ 2}\ \beta^2}{(I_n\Delta t)^2}\right]^{1/2} - \frac{\lambda_w\beta}{I_n\Delta t} \qquad (3.3.29)$$

Thus, the dissolved gypsum (i.e. dissolved calcium/unit area) leaving the unsaturated zone during t-Δt and t is given by:

$$N_{Ca^{2+}} = I_n\Delta t \left\{ \left[a^2 + \frac{\lambda_w{}^2 \beta^2}{(I_n\Delta t)^2} \right]^{1/2} - \frac{\lambda_w \beta}{I_n\Delta t} \right\}$$

or

$$N_{Ca}{}^{2+} = \left[a^2\ (I_n\Delta t)^2 + \lambda_w{}^2\ \beta^2 \right]^{1/2} - \lambda_w\beta \qquad (3.3.30)$$

where

N_{Ca}^{2+} = number of moles of dissolved calcium per unit area (mol.m^{-2}).

The number of moles of gypsum/unit area that has precipitated in zone 2 during t-Δt and t is the difference between the total amount of gypsum dissolved, $g_0\Delta h$ (g_0 times equation (3.3.26)) and the amount of gypsum leaving the unsaturated zone, given by equation (3.3.30), i.e.:

$$\Delta N_{g,t} = g_0 \left\{ \left[\frac{\beta^2 h_{t-\Delta t}}{(g_0 + \beta)^2} + \frac{(I_n\Delta t)^2\ a^2}{g_0{}^2 + g_0\beta} \right]^{1/2} - \frac{\beta h_{t-\Delta t}}{g_0 + \beta} \right\} - \left[a^2\ (I_n\Delta t)^2 + \lambda_w{}^2\ \beta^2 \right]^{1/2} + \lambda_w\beta \qquad (3.3.31)$$

where

$N_{g,t}$ = number of moles of gypsum that has precipitated per unit area at time t (mol.m^{-2}).

note that:

$$N_{g,t-\Delta t} = \sum_{t=0}^{t-\Delta t} \Delta N_g \qquad (3.3.32)$$

and:

$$N_{g,t} = N_{g,t-\Delta t} + \Delta N_g \qquad (3.3.33)$$

The fraction of gypsum remaining in the unsaturated zone at any time t is given by:

$$f_{gypsum} = \frac{(\lambda_w - h_t)\, g_o + N_{g,t}}{\lambda_w\, g_o} \qquad (3.3.34)$$

3.3.3 Calcium and Sulphate Concentrations

Prior to gypsum depletion in the unsaturated zone (layers 1 and 2) the concentrations of Ca^{2+} and SO_4^{2-} are different in the two layers. Following depletion, layers 1 and 2 are assumed to have the same physical and chemical characteristics (including the concentrations of SO_4^{2-} and Ca^{2+}).

Layer 1

Since layer 1 contains, by definition, no gypsum, the concentrations of Ca^{2+} and SO_4^{2-} are easily calculated. We assume that, in the absence of gypsum, the concentration of Ca^{2+} is that found in rainwater:

$$[Ca^{2+}]_1 = 0.008\ mol.m^{-3} \qquad (3.3.35)$$

In the absence of gypsum, the sources of dissolved sulphate are pyrite oxidation and rainwater. The sulphate concentration in layer 1 is taken to be equal to the sulphate concentration at h, the interface between layers 1 and 2 plus the contribution from rainwater, i.e., 0.0128 $mol.m^{-3}$. Hence, from equation (3.3.15):

$$[SO_4^{2-}]_1 = [SO_4^{2-}]_{p,h} = 2h\, \frac{[FeS_2]_{t-\Delta t}[1-e^{-k\Delta t}]}{I_n \Delta t} + 0.0128 \qquad (3.3.36)$$

Layer 2

The calculation of $[Ca^{2+}]$ and $[SO_4^{2-}]$ in layer 2 is somewhat more involved. Estimates of these concentrations, based on equilibrium considerations, can be obtained using equations presented in the previous section (e.g. equation (3.3.21)). However, at the low pH values expected initially in layer 2, the concentration of free sulphate (and hence of calcium) is reduced by the complexation of the sulphate ligand with the ferric ion and the aluminum ion, i.e.:

$$Fe^{3+} + SO_4^{2-} \rightleftharpoons FeSO_4^+$$

$$Al^{3+} + SO_4^{2-} \rightleftharpoons AlSO_4^+$$

These complexation reactions, in turn reduce the concentration of free sulphate somewhat.

The ratio between free (uncomplexed) sulphate and total sulphate can be expressed as:

$$\frac{[SO_4^{2-}]_u}{[SO_4^{2-}]_T} = \frac{1}{d} \qquad (3.3.37)$$

The factor "d" quantifies the amount of sulphates which exist as ferric or aluminum complexes and is given by:

$$d = 1 + f^3\, 10^{8.99-3pH} + f^{3/4}\, 10^{9.7-3pH} \qquad (3.3.38)$$

The calculation of pH in layer 2, as well as further rationale for the above expression, is outlined in Section 3.6.2.

Since $[SO_4^{2-}]_{total} = [Ca^{2+}] + [SO_4^{2-}]_p$

$$[Ca^{2+}]\,[SO_4^{2-}]_u = [Ca^{2+}]\left[\frac{[Ca^{2+}] + [SO_4^{2-}]_p}{d}\right] = \frac{K_s^o}{f^2}$$

$$[Ca^{2+}]_{\lambda w} = \sqrt{\frac{K_s^o d}{f^2} + 0.25\,[SO_4^{2-}]_{p,\lambda w}^2} - 0.5\,[SO_4^{2-}]_{p,\lambda w} \qquad (3.3.39)$$

and

$$[SO_4^{2-}]_{\lambda w} = \sqrt{\frac{K_s^o d}{f^2} + 0.25\,[SO_4^{2-}]_{p,\lambda w}^2} + 0.5\,[SO_4^{2-}]_{p,\lambda w} \qquad (3.3.40)$$

This value ($[SO_4^{2-}]_{\lambda w}$) represents the concentration of total sulphates present.

The concentration of uncomplexed (free) sulphate ($[SO_4^{2-}]_u$) is simply:

$$[SO_4^{2-}]_{u,\lambda w} = \frac{[SO_4^{2-}]_{\lambda w}}{d} \qquad (3.3.41)$$

The previous calculations are applicable prior to gypsum depletion in the unsaturated zone. Once the gypsum is entirely depleted (i.e. layer 2 becomes vanishingly small) the situation is simplified considerably. The appropriate equations for this instance are those presented earlier for layer 1. That is:

$$[Ca^{2+}]_{\lambda w} = 0.008 \qquad (3.3.42)$$

$$[SO_4^{2-}]_{\lambda w} = [SO_4^{2-}]_{p,\lambda w} = \frac{2\lambda_w[FeS_2]_{t-\Delta t}[1-e^{-k\Delta t}]}{I_n\Delta t} + 0.0128 \qquad (3.3.43)$$

3.3.4 Iron Concentration

The total iron concentration in the unsaturated zone (at either h or λ_w) is dependent on the pH and the total sulphate concentration. In these calculations, equilibrium with ferric hydroxide is assumed. As outlined in Section 3.6.1, the most significant dissolved iron (III) complexes include Fe^{3+}, $Fe(OH)^{2+}$, $Fe(OH)_2^+$ and $FeSO_4^+$. Considering these species, the total dissolved iron concentration at λ_w is given by the following expression:

$$[Fe^{3+}]_{\lambda w,} = 10^{5.97-3pH} + 10^{3.78-2pH} + 10^{0.3-pH}$$

$$+ \frac{[SO_4^{2-}]_{\lambda w}}{1000}\left[\frac{f^3\ 10^{8.99-3pH}}{1 + f^{3/4}\ 10^{9.7-3pH} + f^3\ 10^{8.99-3pH}}\right] \qquad (3.3.44)$$

The factor of 1000 is included to convert $[SO_4^{2-}]$ from mol.m^{-3} to mol.L^{-1}. The calculated value ($[Fe^{3+}]_{\lambda w}$) is thus in mol.L^{-1} and must be converted to mol.m^{-3}.

Equation (3.3.44), however, is not applicable under very low pH conditions, i.e. pH <2.5. Under these conditions the dissolved iron (III) is calculated based on stoichiometry:

$$[Fe^{3+}]_{\lambda w} = 0.5\ [SO_4^{2-}]_{\lambda w} \qquad (3.3.45)$$

3.3.5 Modifications for Limestone Addition

The preceeding discussion applies to tailings which have been discharged and allowed to evolve without intervention. This will result in relatively low porewater pH levels for the first 100 or so years, primarily as a result of pyrite oxidation. The models have also been constructed to allow the assessment of another scenario; in which significant quantities of limestone are incorporated into the unsaturated tailings layer. The modifications necessary to model limestone additions are described in this section. Any calculations described in previous sections and not addressed specifically in this section remain unchanged, since they are not affected directly by limestone addition. Furthermore, none of the models for tailings layers below the oxidizing zone differ structurally from those that were developed previously.

Initial Inventory

The initial concentration of limestone ($CaCO_3$; also referred to as calcite), is calculated as a function of the mass fraction of calcite incorporated into the tailings. Namely:

$$[CaCO_3]^o = X_{Lime}\rho_T/100 \qquad (3.3.46)$$

where

$[CaCO_3]^o$ = initial inventory of calcite ($mol.m^{-3}$)

X_{Lime} = initial mass fraction of $CaCO_3$ in tailings

ρ_T = tailings bulk density ($g.m^{-3}$)

100 = molecular weight of $CaCO_3$ ($g.mol^{-1}$).

Pyrite Oxidation

The primary consequence of limestone addition to the tailings is the maintenance of pH values near neutrality in the porewater. It has been shown that elevated pH values reduce the role of bacteria in the oxidation process. Nevertheless, pyrite oxidation would proceed at a reduced rate.

The reaction rate, and hence the sulphate flux resulting from pyrite oxidation, is estimated to be approximately 1/10 of the observed bacteria-assisted rate (flux). It is convenient to express this sulphate generation flux as a fraction of the sulphate flux without calcite addition.

Thus, the sulphate generation flux would become:

$$J_s' = X_{rate} \, J_s \qquad (3.3.47)$$

where

J_s' = sulphate flux with limestone present ($mol.m^{-2}.yr^{-1}$)

J_s = sulphate flux with no limestone present ($mol.m^{-2}.yr^{-1}$)

X_{rate} = fraction of J_s which occurs when limestone is present.

The molar mass balance for the rate of pyrite oxidation in a volume element $\lambda_w A$ must be equal to one half the sulphate export from this volume element:

$$- \lambda_w \frac{d\,[FeS_2]}{dt} = \frac{1}{2} J_s' \qquad (3.3.48)$$

Assuming first order kinetics as previously, the reaction rate at any time "t" is given by:

$$- \frac{d\,[FeS_2]}{dt} = k' \, [FeS_2] \qquad (3.3.49)$$

where

$[FeS_2]$ = pyrite concentration ($mol.m^{-3}$ tailings)

k' = chemical rate constant of pyrite oxidation (yr^{-1}).

Based on initial conditions $[FeS_2]^o$, the first order rate constant for pyrite oxidation in the presence of calcite is as follows:

$$k' = \frac{J_s'}{2\lambda_w[FeS_2]^o} \qquad (3.3.50)$$

As in the calcite-free system, the moles of pyrite oxidized per unit volume between t-Δt and t can be expressed as:

$$\Delta[FeS_2]_{t-\Delta t \rightarrow t} = [FeS_2]_{t-\Delta t}\,(1 - e^{-k'\Delta t}) \qquad (3.3.51)$$

Again a lower limit of 1.0×10^{-6} mol.m^{-3} is imposed on $[FeS_2]_t$.

The sulphate concentration from pyrite oxidation in the porewater at λ_w is equal to:

$$[SO_4^{2-}]_{p,\lambda w} = \frac{2\lambda_w[FeS_2]_{t-\Delta t}\,(1 - e^{-k't})}{I_n\Delta t} + 0.0128 \qquad (3.3.52)$$

Calcium and Sulphate Concentrations

When both gypsum and calcite are present simultaneously, the following two equilibria must be satisfied:

$$CaSO_4 \rightleftharpoons Ca^{2+} + SO_4^{2-} \qquad K_s^o = 10^{-4.6} \qquad (3.3.53)$$

$$CaCO_3(s) + H^+ \rightleftharpoons Ca^{2+} + HCO_3^- \qquad {}^*K_s^o = 10^{2.13} \text{ (at 10°C)} \qquad (3.3.54)$$

Recognizing that $^*K_s^o$ is dependent on the temperature, an annual average temperature of 10°C for the porewater in the unsaturated zone is used herein.

To illustrate the above situation, consider the dissolution of gypsum (g) and calcite (c) in the porewater containing sulphate from both pyrite oxidation (p*) and rainwater (r). Note the ratio of Ca^{+2} to SO_4^{2-} in rainwater = 0.2, hence:

$$[Ca^{2+}] = c + g + 0.2\ r$$

and

$$[SO_4^{2-}] = g + p^* + r$$

A mass balance on the basis of the equilibrium conditions expressed by equations (3.3.53) and (3.3.54) yields the following:

$$(c + g + 0.2\ r)\ (g + p^* + r) = \frac{10^{-4.6}}{f^2} \qquad (3.3.55)$$

$$(c + g + 0.2\ r)\ ([HCO_3^-]) = \frac{10^{2.13}}{f^{5/4}}[H^+] \qquad (3.3.56)$$

where

c = concentration of "dissolved calcite" calcium ($mol.L^{-1}$)

g = concentration of "dissolved gypsum" calcium ($mol.L^{-1}$)

p^* = sulphate concentration resulting from pyrite oxidation ($mol.L^{-1}$)

r = sulphate concentration in rainwater ($10^{-4} mol.L^{-1}$).

In the unsaturated zone, bicarbonate $[HCO_3^-]$ is not conserved, rather, the concentration is an equilibrium value with respect to the partial pressure of CO_2 in the gas phase. In calcite-rich porewaters, the partial pressure of CO_2 (${}^{P}CO_2$) is expected to vary from $10^{-3.5}$ atm at the surface to $2x10^{-2}$ atm at the lower limit of the unsaturated zone (λ_w). It would be reasonable to assume an average value of 10^{-2} atm (Stumm and Morgan, 1981). Using this value of 10^{-2} (at 10°C), the concentration of dissolved CO_2 / carbonic acid in the porewater is:

$$[H_2CO_3] = K_H P_{CO2} = (10^{-1.27})\ (10^{-2}) = 10^{-3.27}\ M \qquad (3.3.57)$$

The dissociation constant for carbonic acid (H_2CO_3) at 10°C is $10^{-6.46}$:

$$H_2CO_3 \rightleftharpoons H^+ + HCO_3 \qquad \log K = -6.46 \qquad (3.3.58)$$

The bicarbonate concentration as a function of pH is, therefore:

$$[HCO_3] = \frac{10^{pH-9.73}}{f^{1/4}} \qquad (3.3.59)$$

Substituting the result of equation (3.3.59) into equation (3.3.56) (calcite equilibrium) we obtain:

$$[Ca^{+2}]_{\lambda w} = 1000\ (c + g + 0.2\ r) = 1000\left(\frac{10^{11.86\ -\ 2pH}}{f}\right) \qquad (3.3.60)$$

and from gypsum equilibrium:

$$[SO_4^{2-}]_{\lambda w} = 1000\ (g + p^* + r) = 1000\left(\frac{10^{2pH\ -\ 16.46}}{f}\right) \qquad (3.3.61)$$

where

$[Ca^{2+}]_{\lambda w}$ = calcium concentration at λ_w ($mol.m^{-3}$)

$[SO_4^{2-}]_{\lambda w}$ = sulphate concentration at λ_w ($mol.m^{-3}$).

From equation (3.3.61), the sulphate concentration resulting from gypsum dissolution is (at λ_w):

$$g_{\lambda w} = \left(\frac{10^{2pH-16.46}}{f}\right) - p^* - r \qquad (3.3.62)$$

$$g_{\lambda w} = \left(\frac{10^{2pH-16.46}}{f}\right) - \left(\frac{2\lambda_w\ [FeS_2]_{t-\Delta t}\ (1 - e^{-k'\Delta t})}{1000\ (I_n \Delta t)}\right) - 10^{-4} \qquad (3.3.63)$$

Similarly, at some distance $h \leq \lambda_w$:

$$g_h = \left(\frac{10^{2pH-16.46}}{f}\right) - \left(\frac{2h\ [FeS_2]_{t-\Delta t}\ (1 - e^{-k'\Delta t})}{1000\ (I_n \Delta t)}\right) - 10^{-4} \qquad (3.3.64)$$

These equations are written with concentrations implicitly expressed in molar quantities (mol.L^{-1}). In keeping with the rest of the model, these may be rewritten with concentrations expressed in mol.m^{-3}. For example, equation (3.3.64) can be written as:

$$g_h = 1000\left(\frac{10^{2pH-16.46}}{f} - 10^{-4}\right) - \left(\frac{2h\ [FeS_2]_{t\Delta t}\ (1 - e^{-k'\Delta t})}{I_n\Delta t}\right) \quad (3.3.65)$$

Since:

$$g_o\Delta h = g_h I_n \Delta t$$

We can calculate Δh:

$$\Delta h = \frac{1}{g_o}\left\{ 1000\left(\frac{10^{2pH-16.46}}{f} - 10^{-4}\right) I_n\Delta t - 2h\ [FeS_2]_{t\Delta t}\ (1 - e^{-k'\Delta t}) \right\} \quad (3.3.66)$$

Gypsum is depleted from the unsaturated layer when:

$$\sum_{t=0}^{t} \Delta h = \lambda_w \quad (3.3.67)$$

From equation (3.3.60), it is evident that the concentration of calcium resulting from calcite dissolution is:

$$c = \frac{10^{11.86-2pH}}{f} - g - 0.2\ r \quad (3.3.68)$$

We have defined g at λ_w by equation (3.3.63). Substituting equation (3.3.63) into equation (3.3.68) yields:

$$c_{\lambda w} = 1000\left(\frac{10^{11.86-2pH}}{f} - \frac{10^{2pH-16.47}}{f} + 0.8\text{x}10^{-4}\right) + \frac{2\lambda_w[FeS_2]_{t-\Delta t}\ (1-e^{-k'\Delta t})}{I_n\Delta t} \quad (3.3.69)$$

Once gypsum is depleted, the gypsum term is removed from the above equation. In this case, calcium resulting from calcite dissolution is expressed as:

$$c_{\lambda w} = 1000\left(\frac{10^{11.86-2pH}}{f} - 0.2\times10^{-4}\right) \qquad (3.3.70)$$

Calcite is thus depleted when:

$$\sum_{t=0}^{t} c_{\lambda w} I_n \Delta t = [CaCO_3]^o \lambda_w \qquad (3.3.71)$$

where

$[CaCO_3]^o$ = initial calcite inventory ($mol.m^{-3}$).

Once calcite is depleted from the unsaturated layer, all of relationships obtained previously (i.e. calcite-free environment) apply. In particular, the pyrite oxidation rate returns to its previous level and the pH equations derived previously apply.

3.4 Ions - Layer 3

3.4.1 Calcium and Sulphate Concentrations Prior to Gypsum Depletion

The volumetric flowrate of water in and out of the mixing zone, the time-averaged flow between t-Δt and t is given by:

$$Q_m = Q_T\ (1 - X_{run}) \qquad (3.4.1)$$

where

X_{run} = fraction of surface runoff from tailings

Q_T = total net precipitation flow ($m^3.yr^{-1}$)

Q_m = flowrate into and out of mixing zone ($m^3.yr^{-1}$).

To model major ion concentrations in the mixing zone, it is most convenient to express the sulphate concentration in the mixing zone resulting from pyrite oxidation in the unsaturated layer by the following differential equation:

$$\epsilon\, \lambda_{mix}\, A_t \frac{d[SO_4^{2-}]_{p,mix}}{dt} = Q_m[SO_4^{2-}]_{p,\lambda w} - Q_m[SO_4^{2-}]_{p,mix} \qquad (3.4.2)$$

where

$[SO_4^{2-}]_{p,\lambda w}$ = sulphate concentration at λ_w resulting from pyrite oxidation in the unsaturated zone ($mol.m^{-3}$)

$[SO_4^{2-}]_{p,mix}$ = sulphate concentration in the mixing zone resulting from pyrite oxidation in the unsaturated zone ($mol.m^{-3}$)

A_t = tailings surface area (m^2)

ϵ = porosity.

We have chosen the above differential equation as the basis for calculations, because it is applicable even when the gypsum is depleted from the mixing zone. Note, that in equation (3.4.2) the term $[SO_4^{2-}]_{p,\lambda w}$ is equal to the sulphate concentration term given by equation (3.3.13), i.e.:

$$[SO_4^{2-}]_{p,\lambda w} = \frac{2\lambda_w [FeS_2]_{t-\Delta t}\,(1-e^{-k\Delta t})}{I_n \Delta t} = \frac{2\lambda_w\,\beta}{I_n \Delta t} \qquad (3.4.3)$$

Substitution of equation (3.4.3) into equation (3.4.2) and integration yields:

$$[SO_4^{2-}]_{p,mix,t} = [SO_4^{2-}]_{p,\lambda w,t} + ([SO_4^{2-}]_{p,mix,t-\Delta t} - [SO_4^{2-}]_{p,\lambda w,t})\ \exp\,(-I_n \Delta t/\epsilon \lambda_{mix}) \qquad (3.4.4)$$

For any time 't' the total sulphate and total calcium concentrations in the mixing zone can be obtained as in Section 3.3.2 to give:

$$[Ca^{2+}]_{mix,t} = \sqrt{\frac{K_s^o}{f^2} + 0.25\,[SO_4^{2-}]^2_{p,mix,t}} - 0.5\,[SO_4^{2-}]_{p,mix,t} \qquad (3.4.5)$$

and

$$[SO_4^{2-}]_{mix,t} = \sqrt{\frac{K_s^o}{f^2} + 0.25\,[SO_4^{2-}]^2_{p,mix,t}} + 0.5\,[SO_4^{2-}]_{p,mix,t} \qquad (3.4.6)$$

3.4.2 Gypsum Depletion

It may be noted that equations (3.4.5) and (3.4.6) are applicable as long as gypsum is present in the mixing zone. Of course, no gypsum from the mixing zone will go into solution as long as the porewater entering (from layer 2) is saturated with gypsum. After the gypsum content of the unsaturated zone is depleted, however, gypsum in the mixing zone will begin to dissolve. The dissolution of gypsum is relatively easy to calculate.

Let t_f equal the time when the gypsum from the unsaturated zone is depleted. At this time, the total sulphate concentration in the mixing zone is given by equation (3.4.6) as some value $[SO_4^{2-}]_{mix,tf}$. If there were no gypsum present in the mixing zone, the sulphate concentration after some time Δt would decline to:

$$[SO_4^{2-}]^*_{mix,t} = [SO_4^{2-}]_{p,\lambda w,t} + ([SO_4^{2-}]^*_{p,mix,t-\Delta t} - [SO_4^{2-}]_{p,\lambda w,t}) \exp\left(-I_n \Delta t / \epsilon \lambda_{mix}\right) \qquad (3.4.7)$$

at $t=t_f$:

$$[SO_4^{2-}]^*_{mix,t} = [SO_4^{2-}]_{mix,tf}$$

This quantity ($[SO_4^{2-}]^*_{mix,t}$) would be the sulphate concentration if there were no gypsum in the mixing zone.

The difference between equation (3.4.6) and (3.4.7) is the concentration of sulphate resulting from gypsum dissolution.

Thus, the amount of gypsum dissolved over a time period Δt is given by:

$$\Delta \text{ gypsum} = \frac{I_n \Delta t}{\lambda_{mix}} \; [\text{eqn } (3.4.6) - \text{eqn } (3.4.7)] \qquad (3.4.8)$$

$$= \frac{I_n \Delta t}{\lambda_{mix}} \left([SO_4^{2-}]_{mix,t} - [SO_4^{2-}]^*_{mix,t} \right) \qquad (3.4.9)$$

where

$\Delta gypsum$ = gypsum dissolved over time Δt ($mol.m^{-3}$).

The total gypsum (per unit volume) dissolved in the mixing zone to any time t is:

$$[gyp]_{diss,t} = \sum_{t=0}^{t} \Delta gypsum \qquad (3.4.10)$$

where

$[gyp]_{diss,t}$ = gypsum dissolved to time 't' ($mol.m^{-3}$).

Thus, gypsum in the mixing zone is depleted when:

$[gyp]_{diss,t} = g_o$

and:

t_{f2} = time at which mixing zone gypsum depletion occurs.

3.4.3 Calcium and Sulphate Concentrations Following Gypsum Depletion

Following gypsum depletion, the calculation of sulphate and calcium concentrations is quite straightforward. The calcium concentration will decrease with time as a result of dilution, according to the following equation:

$$[Ca^{2+}]_{mix,t} = [Ca^{2+}]_{mix,t-\Delta t} \exp\left(-I_n \Delta t/\epsilon \lambda_{mix}\right) \qquad \text{at } t \geq t_{f2} \qquad (3.4.11)$$

The sulphate concentration at any time is given by:

$$[SO_4^{2-}]_{mix,t} = [SO_4^{2-}]_{p,\lambda w,t} + \left([SO_4^{2-}]_{p,mix,t-\Delta t} - [SO_4^{2-}]_{p,\lambda w,t}\right) \exp(-I_n \Delta t/\epsilon \lambda_{mix}) \qquad (3.4.12)$$

3.4.4 Iron Concentration

In the mixing zone, ferric iron is rapidly reduced to the ferrous (Fe^{2+}) state by the following reaction:

$$2\ Fe^{3+} + FeS_2 \longrightarrow 3\ Fe^{2+} + 2S^0 \qquad (3.4.13)$$

Thus, for each mole of ferric iron (Fe^{3+}), 1.5 moles of ferrous iron (Fe^{2+}) is produced. This results in a total ferrous ion flux as given by the following:

$$\text{Flux } Fe^{2+} = 1.5\ I_n\ [Fe^{3+}]_{\lambda w,t} \qquad (3.4.14)$$

where

Flux Fe^{2+} = the total ferrous ion flux ($mol.m^{-2}$).

Also, let us assume, that this flux remains constant for a time period, t-Δt to t. Applying a differential mass balance in the mixing zone gives the following equation:

$$\lambda_{mix}\,\epsilon\,\frac{d\,[Fe^{2+}]_{mix}}{dt} = 1.5I_n\ [Fe^{3+}]_{\lambda w,t} - I_n\ [Fe^{2+}]_{mix,t} \qquad (3.4.15)$$

Integrating between t-Δt and t gives:

$$[Fe^{2+}]_{mix,t} = 1.5\ [Fe^{3+}]_{\lambda w,t} + \left([Fe^{2+}]_{mix,t-\Delta t} - 1.5[Fe^{3+}]_{\lambda w,t}\right)\exp(-\ I_n\Delta t/\epsilon\lambda_{mix}) \qquad (3.4.16)$$

3.5 Ions - Layer 4

The calculation procedure for major ions in layer 4 is similar to that in the mixing zone. The net infiltration into layer 4 is given by the following expression:

$$I_4 = \sum_{j=1}^{5} K_j . I_j . A_{x,j,4}/A_t \quad = \sum_{j=1}^{5} Q_{s,j,4}/A_t \qquad (3.5.1)$$

where

I_4 = net infiltration rate into layer 4 ($m.yr^{-1}$)

K_j = hydraulic conductivity of the jth aquifer ($m.yr^{-1}$)

I_j = hydraulic gradient of the jth groundwater flow path ($m.m^{-1}$)

$A_{x,j,4}$ = cross-sectional area of the jth aquifer discharging from the 4th layer (m^2)

$Q_{s,j,4}$ = volumetric seepage rate through the jth groundwater flow path discharging from layer 4 ($m^3.yr^{-1}$)

A_t = cross-sectional area of the tailings.

If all of the aquifers are discharging from layer 3 then the following nominal infiltration rate is assumed:

$$I_4 = 0.05\ (Q_{s,j,3}/A_t) \qquad (3.5.2)$$

where

$Q_{s,j,3}$ = volumetric seepage rate through the jth groundwater flow path discharging from layer 3 ($m^3.yr^{-1}$).

As in case of the mixing zone, it is advantageous to model the sulphate resulting from pyrite oxidation. The differential equation describing the concentration of sulphate in layer 4 resulting from pyrite oxidation in the unsaturated zone is:

$$\lambda_4\ \epsilon\ \frac{d[SO_4^{2-}]_{p,4}}{dt} = I_4[SO_4^{2-}]_{p,mix,t} - I_4\ [SO_4^{2-}]_{p,4} \qquad (3.5.3)$$

where

$[SO_4^{2-}]_{p,4}$ = concentration of sulphate in zone 4 resulting from pyrite oxidation in the unsaturated layer ($mol.m^{-3}$)

λ_4 = thickness of layer 4 (m)

$[SO_4^{2-}]_{p,mix,t}$ = concentration of sulphate, resulting from pyrite oxidation, in the mixing zone at time "t" ($mol.m^{-3}$).

Equation (3.5.1) can be integrated to yield the following expression:

$$[SO_4^{2-}]_{p,4,t} = [SO_4^{2-}]_{p,mix,t-\Delta t} + ([SO_4^{2-}]_{p,4,t-\Delta t} - [SO_4^{2-}]_{p,mix,t-\Delta t}) \exp(-I_4 \Delta t/\epsilon\lambda_4) \tag{3.5.4}$$

We can calculate the total sulphate and total calcium concentrations by equations analogous to equation (3.4.6):

$$[Ca^{2+}]_{4,t} = \sqrt{\frac{K_S^0}{f^2} + 0.25\,[SO_4^{2-}]_{p,4,t}^2} - 0.5[SO_4^{2-}]_{p,4,t} \tag{3.5.5}$$

and

$$[SO_4^{2-}]_{4,t} = \sqrt{\frac{K_S^0}{f^2} + 0.25\,[SO_4^{2-}]_{p,4,t}^2} + 0.5[SO_4^{2-}]_{p,4,t} \tag{3.5.6}$$

The ferrous ion $[Fe^{2+}]$ concentration can also be calculated in a similar manner. By employing equation (3.4.16) for $[Fe^{2+}]$ in the mixing zone, at time t, $[Fe^{2+}]_{mix,t}$, the concentration in zone (4) is given by:

$$[Fe^{2+}]_{4,t} = [Fe^{2+}]_{mix,t-\Delta t} + \left([Fe^{2+}]_{4,t-\Delta t} - [Fe^{2+}]_{mix,t-\Delta t}\right) \exp\,(-\,I_4\,\Delta t/\epsilon\lambda_4) \tag{3.5.7}$$

It can be shown that the gypsum in layer 4 cannot be depleted for some 4,000 years. Hence, the gypsum in this layer (i.e. layer 4) has been modelled as not being depleted over the 1000 year simulation period.

3.6 pH Calculations

Pyritic uranium ores contain approximately 70% quartz (SiO_2), 23% aluminosilicates (sericite, feldspars, clays) and 6% pyrite (FeS_2). In the highly acidic, oxidative environment of the leaching pachukas (in the milling circuit) a portion of these minerals dissolve and, upon pH adjustment with lime, reprecipitate as secondary minerals including gypsum ($CaSO_4.2H_2O$), gibbsite ($Al_2O_3.3H_2O$), kaolinite ($Al_2Si_2O_5(OH)_4$), aluminite ($Al_4(SO_4)(OH)_{10}$), and iron (III) oxyhydroxides ($Fe(OH)_3$). Since the solubilities of these secondary minerals generally exceed those of the original ore, their dissolved ion products and speciation are expected to be the dominant species in the pH-dependent, ionic equilibrium expression for tailings porewater.

The following sections outline the significant ionic species and their effect on pH in each tailings layer. Since the tailings layers each have different characteristics, as discussed in preceding sections, the pH in each layer is calculated somewhat differently. However, many of the ionic species are common to all 4 layers. Hence, the discussion regarding layer 1 is the most detailed with significant portions applicable to the other layers as such. These general sections are presented in the layer 1 description and are not repeated.

The following sections indicate that the calculation of pH in any layer may require an iterative (trial and error) solution. Information regarding the approach taken to implementing the iterative solutions for the pH equations is presented in Section 3.6.5.

3.6.1 Layer 1

The discussion of pH calculations is divided into two parts. The first section outlines the significant ionic species and their effect on pH. The preceeding section presents the ionic balances for the various scenarios which may occur in layer 1.

Aluminum

To establish the aluminum concentrations in the porewater, the solid phases of significance are taken to be gibbsite ($Al_2O_3.3H_2O$), kaolinite ($Al_2Si_2O_5(OH)_4$), and basaluminite ($Al_4SO_4(OH)_{10}$).

The hydrogen ion (H^+) dependent solution reactions of gibbsite and kaolinite can be expressed as follows (Stumm and Morgan, 1981):

$$0.5\ Al_2O_3.3H_2O(s) + 3H^+ \rightleftharpoons Al^{3+} + 3H_2O \qquad \log K_S^o = 8.5 \quad (3.6.1)$$

$$0.5\ Al_2Si_2O_5(OH)_{4(s)} + 3H^+ \rightleftharpoons Al^{3+} + H_4SiO_4^o + 0.5H_2O \quad \log K_S^o = 3.8 \quad (3.6.2)$$

The dissolved silica (H_4SiO_4) in equation (3.6.2) is expressed as a nonionic species because it is a weak acid and does not protolyze until the pH value in the water exceeds pH 9.4 (Faust and Aly, 1981). It is unlikely, however, that the dissolved silica concentration in acidic porewaters is established by the equilibrium relationship expressed by equation (3.6.2). At pH 5, for example, the dissolved silica concentration would be in the order of 2.5×10^{-6} M H_4SiO_4 (according to equation (3.6.2)) in comparison to observed concentrations of 5×10^{-4} to 6×10^{-3} M H_4SiO_4 in porewaters of igneous soils. In these soils, the dissolved silica concentration is dependent on the dissolution equilibrium of solid silicates ($SiO_2(s)$) as follows:

$$SiO_2(s) + 2H_2O \leftrightharpoons H_4SiO_4^o \qquad K_S^o = 10^{-2.7} \qquad (3.6.3)$$

The equilibrium constant in equation (3.6.3) represents the solution equilibrium of amorphous silicates for their demonstrated presence in tailings solids (Beak, 1985). According to the above equilibrium expression, the dissolved silica concentration in porewaters is independent of pH. Measured silicate concentrations in acidic (pH 2 to pH 5) tailings porewaters ranged from 2.9×10^{-4} M to 2.6×10^{-3} M H_2SiO_4 in the Lacnor Field Study (Golder et al., 1986). The average concentration of 1.71×10^{-3} M is in line with the equilibrium value of 2.0×10^{-3} M predicted by equation (3.6.3).

The combination of equations (3.6.2) and (3.6.3) yields the following expression for the solution equilibrium of kaolinite:

$$0.5\ Al_2Si_2O_5(OH)_{4(s)} + 3H^+ \rightleftharpoons Al^{3+} + SiO_2(s) + 1.5\ H_2O \quad \log K_s^0 = 6.5 \quad (3.6.4)$$

Comparing equation (3.6.1) and equation (3.6.4), it is evident that kaolinite is the more stable solid phase. It has been shown by Stumm and Moryan (1981) that, at dissolved silica concentrations in excess of 2×10^{-5} M (H_4SiO_4), gibbsite dissolves incongruently and reprecipitates as kaolinite. In addition, the kaolinite "reserve" is replenished by the acidic chemical weathering of clay minerals which is likely to take place as a result of acidic conditions brought about by pyrite oxidation. For example, the weathering reaction of muscovite proceeds as follows:

$$\underset{\text{Muscovite}}{2\ KAl_3Si_3O_{10}(OH)_2(s)} + 2H^+ + 3H_2O \rightleftharpoons 2K^+ + \underset{\text{Kaolinite}}{3Al_2Si_2O_5(OH)_4(s)} \quad (3.6.5)$$

The above reaction is thermodynamically favoured (ΔG^o = -13.7 kcal/mol). However, these weathering reactions are likely to be under kinetic rather than equilibrium control.

The third aluminum mineral of significance in tailings is basaluminite ($Al_4SO_4(OH)_{10}(s)$). The solution equilibrium for basaluminite is as follows:

$$Al_4SO_4(OH)_{10}(s) + 10\ H^+ \rightleftharpoons 4\ Al^{3+} + SO_4^{2-} + 10\ H_2O \quad \log K_s^o = 22.7 \quad (3.6.6)$$

It can be shown, that basaluminite is a stable solid phase at pH values below 1.5 with respect to kaolinite and pH values below 5.0 with respect to gibbsite. Since pH levels below 1.5 are not expected to occur in the tailings porewater and observed dissolved silica levels suggest that kaolinite is the most likely stable solid phase, the solution equilibrium of kaolinite (equation (3.6.4)) has been chosen as the basis for long-term modelling of aluminum in the porewater.

In aqueous solutions, dissolved aluminum readily speciates as hydroxo and sulphate complexes:

$$\begin{array}{llll}
Al^{3+} + H_2O \rightleftharpoons Al(OH)^{2+} + H^+ & \log K = -4.97 & \\
Al^{3+} + 2H_2O \rightleftharpoons Al(OH)_2^+ + 2H^+ & \log K = -9.30 & \\
Al^{3+} + 3H_2O \rightleftharpoons Al(OH)_3^0 + 3H^+ & \log K = -15.00 & \\
Al^{3+} + 4H_2O \rightleftharpoons Al(OH)_4^- + 4H^+ & \log K = -23.00 & \\
Al^{3+} + SO_4^{2-} \rightleftharpoons AlSO_4^+ & \log K = 3.20 & (3.6.7)
\end{array}$$

The relative activities of the hydroxo complexes at different pH values are shown in Table 3.1.

Since the non-ionic complex ($Al(OH)_3^0$) is of no importance for the ionic balance, the significant species below pH 7 are Al^{3+}, $Al(OH)^{2+}$, and $Al(OH)_2^+$. The anionic aluminum hydroxo complex ($Al(OH)_4^-$) is significant at pH values above 7.0. The pH of the porewater is not expected to exceed pH 7.0 significantly; and even if this occurs, the concentration of the $Al(OH)_4^-$ would be no more than 10^{-8}M at pH 8, which is insignificant with respect to the other anions (for example sulphate, which is at least 10^{-4} M). The sulphato complex of aluminum, however, is modelled explicitly, since at sulphate concentrations above 6.3×10^{-4} M (61 mg/l), the complexation product ($AlSO_4^+$) is a major dissolved species at acidic pH values. Combining the equilibrium expression (equation (3.6.4)) and the complexation reactions of aluminum (equation (3.6.7)) yields the following "ionic strength corrected" concentrations for the aluminum species in solution:

$$[Al^{3+}] = \frac{10^{6.5-3pH}}{f^{9/4}}$$

$$[Al(OH)^{2+}] = \frac{10^{1.53-2pH}}{f}$$

Table 3.1

RELATIVE ACTIVITIES OF ALUMINUM HYDROXO COMPLEXES

Species	Relative Activity (%)					
	pH-3	pH-4	pH-5	pH-6	pH-7	pH-8
Al^{3+}	98.8	86.3	12.4	0.1	0	0
$Al(OH)^{2+}$	1.2	9.3	13.3	0.7	0	0
$Al(OH)_2^+$	0	4.3	62.0	32.9	4.2	0.2
$Al(OH)_3^0$	0	>0.1	12.4	65.7	83.3	49.9
$Al(OH)_4^-$	0	0	0	0.7	8.3	49.9

$$[Al(OH)_2^+] = \frac{10^{-2.8-pH}}{f^{1/4}}$$

$$[AlSO_4^+] = f^{3/4}\ 10^{9.7-3pH}\ [SO_4^{2}] \qquad (3.6.8)$$

where
[ ] = concentration ($mol.L^{-1}$)
f = activity coefficient of divalent ions.

Iron

It has been shown (Halbert et al., 1983), that the concentration of dissolved iron under oxidizing conditions is controlled by the solution equilibrium and speciation of ferric oxyhydroxides ($Fe(OH)_3(s)$. These hydroxides are originally present in the tailings. In addition, iron (III) compounds are products of pyrite oxidation. It can be shown that pyrite oxidation can give rise to a net precipitation of ferric hydroxide at pH values above pH 4.0, while at pH values below pH 4.0 a net dissolution of precipitated ferric hydroxide is likely to occur. The equilibrium reaction for iron (III) hydroxide dissolution in tailings is as follows (Halbert et al., 1983):

$$Fe(OH)_3(s) + 3H^+ \rightleftharpoons Fe^{3+} + 3H_2O \qquad \log K_s^o = 5.97 \qquad (3.6.9)$$

The dissolved iron (III) readily forms hydroxo and sulphato complexes. The relative activities of the hydroxo complexes, as a function of pH, is shown in Table 3.2.

As shown in Table 3.2, the important hydroxo complexes below pH 7 are Fe^{3+}, $Fe(OH)^{2+}$, and $Fe(OH)_2^+$. The non-ionic complex ($Fe(OH)_3^o$) has no effect on the ionic balance, while anionic species ($Fe(OH)_4^-$, for example) are important at alkaline pH values only. Ferric ion in solution, however, complexes with the sulphate ligand as follows:

$$Fe^{3+} + SO_4^{2-} \rightleftharpoons FeSO_4^{+} \qquad \log K = 3.02 \qquad (3.6.10)$$

The combination of the solubility equilibrium with speciation gives the following expressions for the most significant dissolved iron (III) complexes:

$$\begin{aligned} [Fe^{3+}] &= 10^{5.97-3pH} \\ [Fe(OH)^{2+}] &= 10^{3.78-2pH} \\ [Fe(OH)_2^{+}] &= 10^{0.3-pH} \\ [FeSO_4^{+}] &= f^3 \; 10^{8.99-3pH} \; [SO_4^{2-}] \end{aligned} \qquad (3.6.11)$$

The hydroxo complexes of dissolved iron (III) are not corrected for ionic strength, since they are based on actual concentration (M) units.

Under acidic conditions, at pH values below approximately pH=3.3 for projected ionic strength values in the tailings porewater, solid ferric hydroxide is not stable. Although the incongruent solution of ferric hydroxide and re-precipitation as a jarosite may occur, thermodynamic and solubility data on jarosites are incomplete. For this reason, the iron concentrations under highly acidic conditions were assumed to be controlled by the stoichiometry of pyrite oxidation rather than solubility equilibrium. Thus, the total ferric ion in solution is given by:

$$[Fe]_T = \frac{1}{2} \; [SO_4^{2-}]_T - [Ca^{+2}] \qquad (3.6.12)$$

where

$[Fe]_T$ = total dissolved iron concentration ($mol.m^{-3}$)

$[SO_4^{2-}]_T$ = total sulphate concentration ($mol.m^{-3}$).

Table 3.2

RELATIVE ACTIVITIES OF IRON (III) HYDROXO COMPLEXES

Species	Relative Activity (%)		
	pH-3	pH-5	pH-7
Fe^{3+}	3.8	0	0
$Fe(OH)^{2+}$	88.2	2.8	0
$Fe(OH)_2^+$	8.1	92.8	17.6
$Fe(OH)_3^0$	0	4.4	82.2
$Fe(OH)_4^-$	0	0	0.2

$Fe^{3+} + H_2O \rightleftharpoons Fe(OH)^{2+} + H^+$ log K = -2.19

$Fe^{3+} + 2H_2O \rightleftharpoons Fe(OH)_2^+ + 2H^+$ log K = -5.67

$Fe^{3+} + 3H_2O \rightleftharpoons Fe(OH)_3^0 + 3H^+$ log K = -12.00

$Fe^{3+} + 4H_2O \rightleftharpoons Fe(OH)_4^- + 4H^+$ log K = -21.60

At highly acidic pH values, the ferric state and the sulphato complexes are expected to predominate.

Sulphate

In layer 1 (the gypsum-depleted layer), the sulphate ion concentration is dependent on the pyrite oxidation as expressed by equation (3.3.15) and the rainwater source (10^{-4}M sulphate). Thus, the sulphate concentration is primarily kinetics controlled. The sulphate in solution however, speciates as SO_4^{2-}, $AlSO_4^+$, and $FeSO_4^+$. Collecting the terms for $AlSO_4^+$ (from equation (3.6.8)) and $FeSO_4^+$ (from equation (3.6.11)) gives an expression for the total sulphate concentrations:

$$[SO_4^{2-}]_{T,1} = [SO_4^{2-}]_{U,1} \left(1 + f^{3/4}\ 10^{9.7-3pH} + f^3\ 10^{8.99-3pH}\right) \qquad (3.6.13)$$

where

$[SO_4^{2-}]_{T,1}$ = total sulphate concentration in layer 1 (mol.L^{-1})
= $[SO_4^{2-}]_{p,1}$ (see equation (3.3.15))

$[SO_4^{2-}]_{U,1}$ = concentration of uncomplexed (free) sulphate in layer 1 (mol.L^{-1}).

The concentration of the "free" sulphate and the sulphate complexes are as follows:

$$[SO_4^{2-}]_{U,1} = \frac{1}{1 + f^{3/4}\ 10^{9.7-3pH} + f^3\ 10^{8.99-3pH}} [SO_4\ ]_{T,1}$$

$$[AlSO_4^+] = \frac{f^{3/4}\ 10^{9.7-3pH}}{1 + f^{3/4}\ 10^{9.7-3pH} + f^3\ 10^{8.99-3pH}} [SO_4\ ]_{T,1}$$

$$[FeSO_4^+] = \frac{f^3\ 10^{8.99-3pH}}{1 + f^{3/4}\ 10^{9.7-3pH} + f^3\ 10^{8.99-3pH}} [SO_4\ ]_{T,1} \qquad (3.6.14)$$

Bicarbonate

The dissolved carbon dioxide (H_2CO_3 and CO_2) concentration in the porewater is assumed to be in equilibrium with air. This concentration is related to the partial pressure of CO_2 in air by Henry's Law. To evaluate the concentration, a temperature of 10°C was chosen as a characteristic temperature for the tailings. Using the accepted value of $P_{CO_2} = 10^{-3.5}$ atm, the concentration of dissolved CO_2 (i.e. undissociated) is given by:

$$[H_2CO_3] = K_H \, P_{CO2} \qquad \begin{array}{l} P_{CO2} = 10^{-3.5} \text{ atm} \\ K_H = 10^{-1.27} \text{ (at } 10^\circ\text{C)} \end{array}$$

or

$$[H_2CO_3] = 10^{-3.5} \times 10^{-1.27} = 10^{-4.77} \text{ M} \qquad (3.6.15)$$

Dissolved CO_2 dissociates to form bicarbonate as the principal anion at pH values less than 8.5. The dissociation constant at 10°C (ionic strength = 0) is $K=10^{-6.5}$

i.e.

$$H_2CO_3 \rightleftharpoons HCO_3^- + H^+ \qquad \log K = -6.5 \text{ (at } 10^\circ\text{C)} \qquad (3.6.16)$$

The "ionic strength corrected" concentration of bicarbonate $(HCO^-)_3$ ion is given by:

$$[HCO_3^-] = \frac{10^{pH-6.5}}{f^{1/4}} [H_2CO_3]$$

$$[HCO_3^-] = \frac{10^{pH-11.27}}{f^{1/4}} \qquad (3.6.17)$$

Ionic Balances

There exists three possible scenarios for pH calculation in layer one. The first case is for conditions in which calcite and gypsum are absent, and the effective oxygen diffusivity, D_{O2}, is greater than 1 $m^2.y^{-1}$; i.e. no

Table 3.3

IONIC EQUILIBRIUM FOR ELECTRONEUTRALITY

Equilibrium Reactions in the Unsaturated Zone	Log K
$SiO_2^0(s) + 2H_2O \rightleftharpoons H_4SiO_4^0$	-2.7
$3H^+ + 0.5\ Al_2Si_2O_5(OH)_{4(s)} \rightleftharpoons Al^{3+} + H_4SiO_4 + 0.5H_2O$	3.8
$Al^{3+} + H_2O \rightleftharpoons Al(OH)^{2+} + H^+$	-4.97
$Al^{3+} + 2H_2O \rightleftharpoons Al(OH)_2{}^+ + 2H^+$	-9.30
$Al^{3+} + 3H_2O \rightleftharpoons Al(OH)_3{}^0\ (aq) + 3H^+$	-15.00
$Al^{3+} + SO_4{}^{2-} \rightleftharpoons AlSO_4{}^+$	3.20
$Fe(OH)_3(s) + 3H^+ \rightleftharpoons Fe^{3+} + 3H_2O$	5.97 (K^c)
$Fe(OH)_{3(s)} + 2H^+ \rightleftharpoons Fe(OH)^{2+} + 2H_2O$	3.78 (K^c)
$Fe(OH)_{3(s)} + H^+ \rightleftharpoons Fe(OH)_2^+ + H_2O$	0.30 (K^c)
$Fe^{3+} + SO_4{}^{2-} \rightleftharpoons FeSO_4{}^+(aq)$	3.02
$H_2CO_3^0 \rightleftharpoons H^+ + HCO_3{}^-$	-6.5
	P_{CO2} = -3.5
	K_H = -1.27

restriction to oxygen transport at the tailings surface. Under these conditions it has been assumed that the aluminum hydroxide has been depleted. The overall result of which is acidic conditions, i.e. pH less than 3.5.

In the second case, gypsum and calcite have also been depleted. However, there exists a physical restriction on the mass transfer of oxygen from the atmosphere to the tailings surface, i.e. $D_{O2} < 1.0\ m^2.yr^{-1}$. This restriction can result from the placement of a cover material over the tailings; eg. employing a close-out option of flooding the tailings. Under these conditions it has been assumed that aluminum hydroxide is still present.

The last scenario, case 3, is for conditions in which gypsum is absent but calcite is present.

Case 1.0

As indicated previously, the concentrations of dissolved iron and aluminum are not controlled by solution equilibria at very acidic pH conditions. At pH values below pH=3.3, the ionic balance for electroneutrality becomes:

$$[H^+] + 3[Al^{3+}] + 3[Fe^{3+}] + [Fe(SO_4{}^+] + 2\,[Ca^{2+}] = 2\,[SO^{2-}_4] + [HSO_4{}^-] \qquad (3.6.18)$$

Field observations indicate that the concentrations of aluminum are independent of pH values below 3.3 and can be expressed as the function of the ionic strength:

$$[Al^{3+}] = \frac{3.98 \times 10^{-1}}{f^{\,9/4}}\ (mol.m^{-3}) \qquad (3.6.19)$$

The concentration of iron in solution is controlled by the stoichiometry of iron oxidation. The equation for electroneutrality can be rearranged to give:

$$10^{-pH} + 3[Al^{3+}] + 0.5\,[Ca^{2+}] = 0.5\,[SO_4]_T \left(\frac{1 - \dfrac{10^{1.92-pH}}{f^{3/4}}}{1 + \dfrac{10^{1.92-pH}}{f^{3/4}}} \right) \qquad (3.6.20)$$

The above equation can be solved analytically to give an estimate of the pH value.

Case 2.0

In case 2.0 aluminum hydroxide is present. A summary of the relevant layer 1 equilibrium expressions is given in Table 3.3. The ionic balance for electroneutrality involves the determination of significant species. These are multiplied by the valence number to give the ion concentration in equivalents per litre. The significant cations and anions in layer 1 are:

Cations	Anions
H^+	SO_4^{2-}
Fe^{3+}	HCO_3^-
$FeOH^{2+}$	
$Fe(OH)_2^+$	
$FeSO_4^+$	
Al^{3+}	
$Al(OH)^{2+}$	
$AlSO_4^+$	

The overall ionic balance for electroneutrality in layer 1 becomes:

$$\frac{10^{-pH}}{f^{1/4}} + 3\left(\frac{10^{6.5}}{f^{9/4}} + 10^{5.97}\right)10^{-3pH} + 2\left(\frac{10^{1.53}}{f} + 10^{3.78}\right)10^{-2pH} + 10^{0.3-pH} =$$

$$[SO_4^{2-}]_{T,1}\left(\frac{2 - f^{3/4}\,10^{9.7-3pH} - f^{3}\,10^{8.99-3pH}}{1 + f^{3/4}\,10^{9.7-3pH} + f^{3}\,10^{8.99-3pH}}\right) + \frac{10^{pH-11.27}}{f^{1/4}} \qquad (3.6.21)$$

Note that in equation (3.6.21) the speciation of sulphate as SO_4^{2-}, $AlSO_4^+$ and

$FeSO_4^+$ has been combined to give an overall expression in terms of total sulphate concentration. The negative signs indicate that $AlSO_4^+$ and $FeSO_4^+$ are cationic species. This procedure has been used for expressing the charged sulphate complexes in each zone.

Case 3.0

The previous expressions are only valid for the case where no limestone has been added to the tailings. A further electroneutrality equation must, therefore, be written, for the case where gypsum is absent, but calcite is present. In this case (i.e. for the gypsum-depleted layer) pH is calculated (iteratively) from:

$$2\left(\frac{10^{11.87-2pH}}{f}\right) + 10^{0.3-pH} = 2\left(\frac{[SO_4^{2-}]_{p,h}}{1000}\right) + \left(\frac{10^{pH-9.73}}{f^{1/4}}\right) \qquad (3.6.22)$$

where

pH = pH in the gypsum-depleted layer

$[SO_4^{2-}]_{p,h}$ = concentration of sulphates from pyrite oxidation at h (gypsum-depleted front) ($mol.m^{-3}$).

The factor of 1000 is included to convert $[SO_4^{2-}]$ from $mol.m^{-3}$ to $mol.L^{-1}$.

This equation is also applicable for pH calculations at λ_w once the entire unsaturated zone has been depleted of gypsum. In this case $h = \lambda_w$ and:

$$[SO_4^{2-}]_{p,h} = [SO_4^{2-}]_{p,\lambda w}$$

and the entire unsaturated zone is assumed to be homogeneous with respect to Ca^{2+}, SO_4^{2-} and Fe^{3+} and pH.

3.6.2 Layer 2

Aluminum

same as Layer 1

Iron

same as Layer 1

Calcium

The calcium concentration in layer 2 results from the solution equilibrium of gypsum. The solution equilibrium for gypsum is given by the following reaction:

$$CaSO_4 \leftrightharpoons Ca^{2+} + SO_4^{2-} \qquad \log K_s^o = -4.6 \qquad (3.6.23)$$

Calcium forms a complex with the sulphate ligand in solution:

$$Ca^{2+} + SO_4^{2-} \leftrightharpoons CaSO_4^o \qquad \log K = 2.31 \qquad (3.6.24)$$

The complexation product ($CaSO_4^o$) is nonionic, hence it does not contribute to the net ionic balance. The formation of sulphate complexes with iron and aluminum at acidic pH values enhances the solubility of gypsum. Taking into account the correction for the complexation products and the ionic strength, the molar concentration of calcium is given by (see equation (3.3.39)):

$$[Ca^{2+}]_{\lambda w} = \left(\frac{K^o_{s,CaSO_4} d}{f^2} + 0.25[SO_4^{2-}]^2_{p,\lambda w} \right)^{1/2} - 0.5\,[SO_4^{2-}]_{p,\lambda w} \qquad (3.6.25)$$

where

$d = 1 + f^{3/4}\,10^{9.7-3pH} + f^3\,10^{8.99-3pH}$

Sulphate

The total sulphate concentration is calculated as the sum of sulphate produced by pyrite oxidation (kinetic control), gypsum dissolution (equilibrium control) and contribution from rain water (a constant value). As discussed previously (Section 3.3.3) the total sulphate concentration can be written as:

$$[SO_4^{2-}]_{T,\lambda w} = [Ca^{2+}] + [SO_4^{2-}]_{p,\lambda w} \qquad (3.6.26)$$

The term $[SO_4^{2-}]_{p,\lambda w}$, as calculated in (for example) equation (3.3.14) includes the contribution from rainwater.

The dissolved sulphate speciates as SO_4^{2-}, $CaSO_4^0$, $AlSO_4^+$, $FeSO_4^+$, $BaSO_4^0$, and $PbSO_4^0$. Of these species, SO_4^{2-}, $AlSO_4^+$ and $FeSO_4^+$ are significant for ionic balance calculations.

Bicarbonate

same as Layer 1

Ionic Balance

The important ionic species for calculating the pH in layer 2 are as follows:

Cations	Anions
H^+	SO_4^{2-}
Ca^{2+}	HCO_3^-
Fe^{3+}	
$Fe(OH)^{2+}$	
$Fe(OH)_2^+$	
$FeSO_4^+$	
Al^{3+}	
$Al(OH)^{2+}$	
$AlSO_4^+$	

The pH dependent equation for electroneutrality in layer 2 becomes:

$$3\left(\frac{10^{6.5}}{f^{9/4}} + 10^{5.97}\right) 10^{-3pH} + 2\left(\frac{10^{1.53}}{f} + 10^{3.78}\right) 10^{-2pH}$$

$$+ \left(10^{0.3} + \frac{1}{f^{1/4}}\right) 10^{-pH} + 2\,[Ca^{2+}]_{\lambda w}$$

$$= [SO_4^{2-}]_{T,\lambda w}\left(\frac{2 - f^{3/4}\,10^{9.7-3pH} - f^{3}\,10^{8.99-3pH}}{1 + f^{3/4}\,10^{9.7-3pH} + f^{3}\,10^{8.99-3pH}}\right) + \frac{10^{pH-11.27}}{f^{1/4}} \qquad (3.6.27)$$

Modifications for Limestone Addition

The previous expressions are valid as long as no limestone (calcite) has been added to the tailings. When both gypsum and calcite are present, the pH is expected to be well above 4. In this case, it can be shown that the relative concentrations of Fe^{3+}, Al^{3+}, and their sulphato and hydroxo complexes are negligible. Thus, the electroneutrality equation becomes:

$$2[Ca^{2+}] + [Fe(OH)_2^+] = 2[SO_4{}^{2-}] + [HCO_3^-] \qquad (3.6.28)$$

or:

$$2\left(\frac{10^{11.87-2\,pH}}{f}\right) + 10^{0.3-pH} = 2\left(\frac{10^{2pH-16.47}}{f}\right) + \left(\frac{10^{pH-9.73}}{f^{\,1/4}}\right) \qquad (3.6.29)$$

This equation indicates that the pH stays constant as long as both calcite and gypsum are present. It is thus applicable to the gypsum-enriched layer as long as both solid phases exist.

3.6.3 Layer 3

Aluminum

As in layers 1 and 2, the concentrations of dissolved aluminum species are controlled by the solution equilibrium of aluminum silicates, at dissolved silica concentrations in excess of 2×10^{-5} M:

$$0.5\ Al_2Si_2O_5(OH)_4(s) + 3\ H^+ \rightleftharpoons Al^{3+} + H_4SiO_4^o + 0.5\ H_2O \quad \log K_s^o = 3.8 \quad (3.6.30)$$

The concentration of dissolved Al^{3+} is a function of the pH, the dissolved silica, and the ionic strength as follows:

$$[Al^{3+}] = \frac{10^{3.8-3pH}}{f^{9/4}\,[H_4SiO_4]} \qquad (3.6.31)$$

The dissolved silica, in turn, is dependent on the solution equilibria of amorphous silicate ($SiO_2(am)$) or quartz (SiO_2):

$$SiO_2(am) + 2\ H_2O \rightleftharpoons H_4SiO_4^o \qquad \log K_s = -2.7$$
$$SiO_2(quartz) + 2\ H_2O \rightleftharpoons H_4SiO_4^o \qquad \log K_s = -3.7 \qquad (3.6.32)$$

According to the above equations, the equilibrium concentration of dissolved silica would range from 2×10^{-4}M to 2×10^{-3}M, depending upon either quartz or amorphous silicates as solid phases. It may be argued, that amorphous silicates dissolve initially, hence, the concentration of dissolved silica is time dependent. However, the amorphous silica content of the tailings is not known. In addition, chemical weathering of siliceous minerals contributes to the amorphous SiO_2 pool. The net effect of these weathering reactions cannot be established. Therefore, the dissolved silicate concentration in the mixing zone porewater is assumed to be constant at 10^{-3}M. This H_4SiO_4 concentration gives the following relationships for the important ionic aluminum species in solution:

$$[Al^{3+}] = \frac{10^{6.8-3pH}}{f^{9/4}}$$

$$[Al(OH)^{2+}] = \frac{10^{1.53-2pH}}{f}$$

$$[AlSO_4^+] = f^{3/4}\,10^{9.7-3pH}\,[SO_4^{2-}] \qquad (3.6.33)$$

Iron

Dissolved iron (III) species are not stable under anoxic conditions. Since dissolved oxygen is exhausted above the water table, the ferric ion entering the mixing zone is expected to be reduced to the ferrous state. This reduction occurs most likely as a redox reaction couple involving pyrite as follows:

$$2\ Fe^{3+} + FeS_2 \leftrightharpoons 3\ Fe^{2+} + 2S^0$$

$$14\ Fe^{3+} + FeS_2 + 8\ H_2O \leftrightharpoons 15\ Fe^{2+} + 16\ H^+ + 2\ SO_4^{2-} \qquad (3.6.34)$$

Both of the above reactions are under kinetic control. Thus, the ferrous ion equivalent in the mixing zone can range from 15/14 to 3/2 times the ferric ion concentration entering the mixing zone. Since the formation of elemental sulphur is more rapid than the complete oxidation of pyrite, the iron concentration in the mixing zone is calculated as an iron (III) inflow equivalent to 1.5 times the ferric ion concentration at the zone boundary (i.e. at λ_w). Ferrous ion does not form hydroxo complexes at pH below 9.2. The sulphato complex formation (log K = 2.24) is significant at high sulphate concentrations, however, the sulphato complex is nonionic, thus, it has no effect on the ionic balance. The ferrous ion concentration in this zone is calculated by material balance as indicated in Section 3.4.4. The use of a multiplication factor of 1.07 (15/14) instead of 1.5 to calculate the ferrous ion in this zone has only a marginal effect on the pH.

Calcium

The calcium concentration in the mixing zone depends on gypsum dissolution and depletion in both the unsaturated zone and the mixing zone. The calculation of calcium concentration was outlined in Section 3.4.

Monovalent Cations

Chemical weathering of clay minerals is expected to result in the release of alkali (Na^+, K^+) and alkaline earth (Mg^{2+}, Ca^{2+}) cations in the porewater. Although this weathering occurs in the unsaturated zone (layers 1 and 2), these reactions are most likely to be kinetic controlled (Helgeson et al., 1984; Berner and Holdren, 1979). Since the concentrations of these metal ions is cumulative in the porewater as it seeps through the tailings, concentrations that would have a significant effect on the pH balance would occur in the lower layers (3 and 4). For simplicity, Na feldspar, albite ($NaAlSi_3O_8$), has been chosen as the representative mineral. Albite occupies a mid position in the weathering sequence of silicate minerals.

The equilibrium reaction for albite is given as follows (Stumm and Morgan, 1981):

$$\underset{\text{Albite}}{NaAlSi_3O_8(s)} + H^+ + 4.5H_2O \rightleftharpoons Na^+ + 2\ H_4SiO_4 + 0.5\ \underset{\text{Kaolinite}}{Al_2Si_2O_5(OH)_4(s)} \quad \log K = -1.9$$

$$[Na^+] = \frac{10^{-1.9-pH}}{f^{1/4}\ [H_4SiO_4]^2} \qquad (3.6.35)$$

At dissolved silica concentrations of 10^{-3}M, the concentration of sodium ion in solution would be:

$$[Na^+] = \frac{10^{4.1-pH}}{f^{1/4}} \qquad (3.6.36)$$

However, the weathering of feldspars is unlikely to reach equilibrium. Assuming that the sodium ion concentration is 10% of the equilibrium value (saturation index = -1.0), the concentration (in M) of sodium is given by:

$$[Na^+] = \frac{10^{3.1-pH}}{f^{1/4}} \qquad (3.6.37)$$

For pH modelling, this concentration is used as a characteristic concentration representing cations resulting from weathering reactions.

Sulphate

Dissolved sulphate in the mixing zone (layer 3) speciates as the uncomplexed ion (SO_4^{2-}) and various sulphato complexes ($CaSO_4^0$, $AlSO_4^+$, $FeSO_4$). The complexation products $CaSO_4^0$ and $AlSO_4^+$ are modelled as in layers 1 and 2. Iron (III) sulphate is modelled explicitly in the oxidizing zone. In the mixing zone, the ferric ion is reduced to the ferrous state. The complexation of dissolved iron (II) with sulphate is considerably weaker; the complexation constant being log K = 2.25 with Fe^{2+} in comparison to log K = 3.02 with Fe^{3+} in solution. In addition, the iron (II) complexation product ($FeSO_4^0$) removes equivalent charges of cationic (Fe^{2+}) and anionic (SO_4^{2-}) species in the equation for electroneutrality. For these reasons, the formation of $FeSO_4^0$ need not be modelled explicitly. The total dissolved iron (II), of course, includes both Fe^{2+} and $FeSO_4^0$ species. Hydroxo complexes of ferrous ion ($Fe(OH)^+$, etc.) form only under alkaline conditions (pH>9.0), consequently, they would have no significance in this regard.

Bicarbonate

Due to the presence and the dissolution of calciferous minerals in layer 3, the bicarbonate content in layer 3 is somewhat higher than in layers 1 and 2. The partial pressure of dissolved CO_2 is expected to be $2x10^{-3}$ atm log P_{CO2}= -2.7, which is characteristic of groundwaters unsaturated (saturation index = -1 at pH=7.0) with respect to calcite (Stumm and Morgan, 1981).

The concentration of bicarbonate in equilibrium with this partial pressure of dissolved CO_2 at 10°C is (see equation (3.6.14) and (3.6.15)):

$$[HCO_3^-] = \frac{10^{pH-10.47}}{f^{1/4}} \qquad (3.6.38)$$

Ionic balance

The significant ionic species in the mixing zone include:

Cations	Anions
Na^+	SO_4^{2-}
Ca^{2+}	HCO_3^-
Fe^{2+}	
Al^{3+}	
$Al(OH)^{2+}$	
$Al(SO_4)^+$	

The ionic balance for calculating the pH in the mixing zone is as follows:

$$2[Ca^{2+}]_{mix} + 2[Fe^{2+}]_{mix} + 3\left(\frac{10^{6.8-3pH}}{f^{9/4}}\right) + 2\left(\frac{10^{1.83-2pH}}{f}\right) + \frac{10^{3.1-pH}}{f^{1/4}} =$$

$$= [SO_4^{2-}]_{mix}\left(\frac{2 - f^{3/4}\ 10^{9.7-3pH}}{1 + f^{3/4}\ 10^{9.7-3pH}}\right) + \frac{10^{pH-10.47}}{f^{1/4}} \qquad (3.6.39)$$

3.6.4 Layer 4

The pH in layer 4 is calculated using the same functional relationship derived for calculating pH in layer 3 (the mixing zone). The equation (3.6.39) explicitly includes the concentrations of SO_4^{2-}, Ca^{2+} and Fe^{2+}. Therefore, in calculating pH for layer 4, the appropriate layer 4 concentrations of SO_4^{2-}, Ca^{2+} and Fe^{2+} must be used.

3.6.5 Implementation/Solution of pH Expressions

Due to the nature of the electroneutrality expressions, iterative solutions are required to calculate pH for most cases. The exception being Case 1.0, i.e., a scenario in which gypsum, calcite and aluminum hydroxide are depleted. In this study, a generalized iterative routine (Newton's method) was employed to solve the electroneutrality equations. This method solves the equation $F(x)=0$, and so requires explicit expressions for the function ($F(x)$), its derivative ($F'(x)$), and some initial guess for the value of x. For convergence, the initial guess (x_1) should be "reasonably" close to the root of the function. The method involves calculating ($F(x_1)$, $F'(x_1)$) and then calculating a new guess (x_2) as:

$$x_2 = x_1 - F(x_1)/F'(x_1) \qquad (3.6.40)$$

The new value (x_2) is then used to calculate $F(x_2)$ and $F'(x_2)$. This process continues until the absolute value of the ratio ($F(x_i)/F'(x_i)$) during the "ith" iteration converges to some specified criterion. In this study, all of the iterative solutions involve determining pH. Acceptable convergence has been assumed to be achieved when:

$$F(x_i)/F'(x_i) \quad < 0.01$$

For completeness, the functions F(pH) and derivatives F'(pH) for all of the pH expressions (including those involving limestone addition) are summarized below.

The method requires that the initial guess for the iterative solution be "reasonably" close to the actual root of the equation. For this reason, several empirical relationships were developed to generate these "initial guesses" and alleviate concerns regarding numerical stability. These are also summarized below.

LAYER 1 (GYPSUM DEPLETED)

Case 1: Calcite Absent/No Oxygen Restriction (from equation (3.6.20))

$$pH = -\text{Log}\left(\frac{-b + \ b^2-4ac}{2a}\right) \qquad (3.6.41)$$

where

$a = 10^{1.92} f^{-3/4}$

$$b = 1 + 10^{1.92}\, f^{-3/4}\, d$$

$$c = -0.5\,[SO_4]_t + \frac{1.9 \times 10^{-3}}{f^{9/4}} + 0.5[Ca^{2+}]$$

$$d = 0.5\,[SO_4]_t + \frac{1.9 \times 10^{-3}}{f^{9/4}} + 0.5[Ca^{2+}]$$

Case 2: Calcite Absent/Oxygen Restriction (from equation (3.6.21)

$$F = 3t_2 + 2t_3 + t_4 + t_5 - t_6 - [SO_4^{2-}] \qquad (3.6.42)$$

where

$$[SO_4^{2-}] = [SO_4^{2-}]_{p,h}\left(\frac{2 - t_1}{1 + t_1}\right)$$

$$t_1 = f^{3/4}\, 10^{9.7-3pH} - f^3\, 10^{8.99-3pH}$$

$$t_2 = \left(\frac{10^{6.5}}{f^{9/4}} + 10^{5.97}\right)10^{-3pH}$$

$$t_3 = \left(\frac{10^{1.53}}{f} + 10^{3.78}\right)10^{-2pH}$$

$$t_4 = 10^{0.3-pH}$$

$$t_5 = \frac{10^{-pH}}{f^{1/4}}$$

$$t_6 = \frac{10^{pH-11.27}}{f^{1/4}}$$

and

$$\frac{dF}{dpH} = -9(\ln 10)\, t_2 - 4(\ln 10)t_3 - (\ln 10)t_4 - (\ln 10)t_5$$

$$- (\ln 110)t_6 - [SO_4^{2-}]_{p,h}\, t_7 \qquad (3.6.43)$$

where

$$t_7 = \frac{d}{dpH}\left(\frac{2 - t_1}{1+t_1}\right) = \frac{-dt_1}{dpH}\left[\frac{2 - t_1}{(1+t_1)^2} + \frac{1}{(1+t_1)}\right] = \frac{-dt_1}{dpH}\left[\frac{3}{(1 + t_1)^2}\right]$$

$$\frac{dt_1}{dpH} = -3\,(\ln 10)f^{3/4}\, 10^{9.7-3pH} - 3(\ln 10)f^3\, 10^{8.99 - 3pH}$$

The initial estimate for pH is calculated from the expression:

$$pH_1 = 4.383551 - \frac{2.723818}{\pi} \tan^{-1} (k \log [SO_4^{2-}]_{p,\lambda w} + 4.230414) \tag{3.6.44}$$

where

$$k = 0.7250 + 6.56281 \times 10^{-2} (\log[SO_4^{2-}]_{p,\lambda w} + 3.4)^4$$

This empirical relationship applies (strictly) only for the calcite absent case. It was derived by examining the relationship between the pH in layer 1 and the value of $[SO_4^{2-}]_{p,\lambda w}$.

Case 3: Calcite present (from equation (3.6.22))

$$F = 2\left(\frac{10^{11.87-2pH}}{f}\right) + 10^{0.3-pH} - \frac{2[SO_4^{2-}]_{p,h}}{1000} - \frac{10^{pH-9.73}}{f^{1/4}} \tag{3.6.45}$$

$$\frac{dF}{dpH} = -4(\ln 10)\left(\frac{10^{11.87-2pH}}{f}\right) - (\ln 10)10^{0.3-pH} - (\ln 10)\left(\frac{10^{pH-9.73}}{f^{1/4}}\right) \tag{3.6.46}$$

LAYER 2 (GYPSUM ENRICHED)

Case 1. Calcite present (from equation (3.6.29))

$$F = 2\left(\frac{10^{11.87-2pH}}{f}\right) + 10^{0.3-pH} - 2\left(\frac{10^{2pH-16.47}}{f}\right) - \frac{10^{pH-9.73}}{f^{1/4}} \tag{3.6.46}$$

$$\frac{dF}{dpH} = -4(\ln 10)\left(\frac{10^{11.87-2pH}}{f}\right) - (\ln 10)\, 10^{0.3-pH} - 4(\ln 10)\left(\frac{10^{2pH-16.47}}{f}\right) - (\ln 10)\left(\frac{10^{pH-9.73}}{f^{1/4}}\right) \tag{3.6.47}$$

Case 2: Calcite absent (from equation (3.6.27))

$$F = t_2 + t_3 + t_4 + t_5 + 2\,[Ca^{2+}] - t_6 - [SO_4^{2-}] \qquad (3.6.48)$$

where

$$[Ca^{2+}] = \left(\frac{10^{-4.6}}{f^2}(1+t_1) + 0.25[SO_4^{2-}]_{p,\lambda w}\right)^{1/2} - 0.5\,[SO_4^{2-}]_{p,\lambda w}$$

$$t_1 = f^{3/4}\,10^{9.7-3pH} + f^3\,10^{8.99-3pH}$$

$$[SO_4^{2-}] = ([Ca^{2+}] + [SO_4^{2-}]_{p,\lambda w})\left(\frac{2-t_1}{1+t_1}\right)$$

$$t_2 = 3\left(\frac{10^{6.5}}{f^{9/4}} + 10^{5.97}\right)10^{-3pH}$$

$$t_3 = 2\left(\frac{10^{1.53}}{f} - 10^{3.78}\right)10^{-2pH}$$

$$t_4 = 10^{0.3-pH}$$

$$t_5 = \frac{10^{-pH}}{f^{1/4}}$$

$$t_6 = \frac{10^{pH-11.27}}{f^{1/4}}$$

$$\frac{dF}{dpH} = -3(\ln 10)t_2 - 2(\ln 10)t_3 - (\ln 10)t_4 - (\ln 10)t_5 + 2\,t_8 - (\ln 10)t_6 - t_{10} \qquad (3.6.49)$$

where

$$t_7 = \frac{dt_1}{dpH} = -3(\ln 10)\,f^{3/4}\,10^{9.7-3pH} - 3(\ln 10)\,f^3\,10^{8.97-3pH}$$

$$t_8 = \frac{d[Ca^{2+}]}{dpH} = 1/2\left[\frac{10^{-4.6}}{f^2}(1+t_1) + 0.25\,[SO_4^{2-}]^2_{p,\lambda w}\right]^{-1/2}\frac{10^{4.6}}{f^2}t_7$$

$$t_9 = \frac{d}{dpH}\left(\frac{2-t_1}{1+t_1}\right) = \frac{-dt_1}{dpH}\left(\frac{2-t_1}{(1+t_1)^2} + \frac{1}{(1+t_1)}\right) = -\frac{3\,t_7}{(1+t_1)^2}$$

$$t_{10} = \frac{d[SO_4^{2-}]}{dpH} = [SO_4^{2-}]_{p,\lambda w}\,t_9 + [Ca]t_9 + \frac{(2-t_1)}{(1+t_1)}\,t_8$$

The initial pH estimate is given by an empirical equation derived by observing the relationship between the pH in layer 2 and $[SO_4^{2-}]_{p,\lambda w}$.

$$pH_2 = 4.383551 - \frac{2.723818}{\pi} \tan^{-1} (k \log [SO_4^{2-}]_{p,\lambda w} + 4.230414) \qquad (3.6.50)$$

$$k = 0.7250 + 6.56281 \times 10^{-2} [\log [SO_4^{2-}]_{p,\lambda w} + 3.4]^4$$

LAYER 3 (MIXING ZONE) (from equation (3.6.39))

$$F = 2[Ca^{2+}]_{mix} + 2[Fe^{2+}]_{mix} + t_1 + t_2 + t_3 - \left(\frac{2-t_4}{1+t_4}\right) [SO_4^{2-}]_{mix} - t_5 \qquad (3.6.51)$$

where

$$t_1 = 3\left(\frac{10^{(6.8-3pH)}}{f^{9/4}}\right)$$

$$t_2 = 2\left(\frac{10^{(1.83-2pH)}}{f}\right)$$

$$t_3 = \frac{10^{(3.1-pH)}}{f^{1/4}}$$

$$t_4 = f^{3/4}\, 10^{(9.7-3pH)}$$

$$t_5 = \frac{10^{(pH-10.47)}}{f^{1/4}}$$

$$\frac{dF}{dpH} = -3(\ln 10)t_1 - 2(\ln 10)t_2 - (\ln 10)t_3 - t_6[SO_4^{2-}]_{mix} - (\ln 10)t_5 \qquad (3.6.52)$$

where

$$\frac{dt_4}{dpH} = -3(\ln 10)t_4$$

$$t_6 = \frac{d}{dpH}\left(\frac{2-t_4}{1+t_4}\right) = -\left[\frac{(2-t_4)}{(1+t_4)^2} + \frac{1}{(1+t_4)}\right] \frac{dt_4}{dpH}$$

The initial pH estimate is obtained from a further empirical relationship developed as described previously:

$$pH = 4.91345 - \frac{3.5731}{\pi} \tan^{-1} (k (\log [SO_4^{2-}]_{p,mix} + 2.03)) \qquad (3.6.53)$$

where

$$k = 0.95553 + 1.44448 \left(\log [SO_4^{2-}]_{p,mix} + 1.555\right)^2$$

3.7 Initial Conditions - Radionuclides

As with the initial set of calculations for the ionic species (Section 3.2), the calculations described in this section are performed in the first simulation time step. Again, this first time step actually represents the time step preceding t=0 years. The calculated values are presented as being representative of t=0 years. Thus, the necessary operations include certain initialization steps as well as the calculation of all radionuclide concentrations in the first time step. In some instances, the calculations are not repeated in any other time steps. These are described in detail in this section. However, a number of the calculations appropriate for the first time period are also applicable at all other times. In these cases, no detailed derivations are provided in this section. Rather, reference is made to the appropriate derivation in a subsequent section.

3.7.1 Uranium

The concentrations and activities of uranium in this study refer to total uranium in the tailings. This is a mixture of uranium isotopes often referred to as natural uranium (U-NAT). On an activity basis, several uranium isotopes are significant, however, on a mass (or molar) basis, U-238 is by far the predominant isotope. The initial activity of both U-NAT and U-238 in the ore can be calculated as functions of the (uranium) grade of the ore:

$$a^{o}_{U\text{-}NAT,\ ore} = \frac{m^{o}_{U}}{100} \ \frac{714\text{g U-NAT}}{842\text{g } U_3O_8} \ 2.5 \times 10^{4} \ \frac{\text{Bq U-NAT}}{\text{g U-NAT}} \qquad (3.7.1)$$

and:

$$a^{o}_{U\text{-}238,\ ore} = \frac{m^{o}_{U}}{100} \ \frac{714\text{g U-NAT}}{842\text{g } U_3O_8} \ 1.22 \times 10^{4} \ \frac{\text{Bq U-238}}{\text{g U-NAT}} \qquad (3.7.2)$$

where

$a^o_{U\text{-NAT, ore}}$ = initial activity of U-NAT in the ore ($Bq.g^{-1}$ ore)
$a^o_{U\text{-238,ore}}$ = initial activity of U-238 in the ore ($Bq.g^{-1}$ ore)
m^o_U = mass % of uranium (as U_3O_8) in the ore.

The initial activity of uranium (U-NAT) in the tailings is calculated as a function of the activity of uranium in the ore fed to the mill:

$$a^o_{U\text{-NAT, tails}} = a^o_{U\text{-NAT,ore}} \ (1 - f_U) \qquad (3.7.3)$$

where

$a^o_{U\text{-NAT, tails}}$ = initial activity of U-NAT in the tailings ($Bq.g^{-1}$ tailings)
f_U = mass fraction of uranium recovered in the mill.

The initial concentration of uranium in the solid phase is then easily calculated:

$$[U_s]^o = a^o_{U\text{-NAT,tails}} \ \rho_T \qquad (3.7.4)$$

where

$[U_s]^o$ = initial concentration of uranium in tailings solid phase ($Bq.m^{-3}$)
ρ_T = tailings bulk density ($g.m^{-3}$).

Since a number of subsequent calculations are performed on a mass (molar) basis, rather than on an activity basis, a conversion factor is defined:

$$UCF = 2.5 \times 10^4 \ \frac{Bq}{g} \quad 238 \ \frac{g}{mol}$$

$$= 5.95 \times 10^6 \ Bq.\ mol^{-1} \qquad (3.7.5)$$

where

UCF = uranium conversion factor ($Bq.mol^{-1}$).

It is then assumed that some fraction of the uranium is associated with pyrite. The concentration of this uranium is given by:

$$[U_3O_8]^o_{pyr} = \frac{[U_s]^o \, f_{U/Fe}}{3 \, UCF} \qquad (3.7.6)$$

where

$[U_3O_8]^o_{pyr}$ = initial concentration of U_3O_8 associated with pyrite ($mol.m^{-3}$)
$f_{U/Fe}$ = fraction of U_3O_8 associated with pyrite.

Then:

$$X_{U/Fe} = [U_3O_8]^o_{pyr} \, / \, [FeS_2]^o \qquad (3.7.7)$$

where

$X_{U/Fe}$ = mol fraction of U_3O_8 in pyrite
$[FeS_2]^o$ = initial concentration of pyrite ($mol.m^{-3}$).

The liquid phase concentrations of uranium are determined as a function of pyrite oxidation. This process is described in further detail in Section 3.8. In summary, the initial concentration of uranium in the unsaturated zone is:

$$[U_L]^o_{\lambda w} = \frac{3 \, \lambda_w}{I_n \Delta t} X_{U/Fe} \, [FeS_2]^o \, (1 - \exp(-k\Delta t)) \, UCF \qquad (3.7.8)$$

where

$[U_L]^o_{\lambda w}$ = initial liquid phase concentration of uranium in the unsaturated zone ($Bq.m^{-3}$)
λ_w = thickness of unsaturated zone (m)
I_n = net infiltration rate ($m.yr^{-1}$)
Δt = time step (yr)
k = rate constant for pyrite oxidation (see Section 3.3.1) (yr^{-1}).

Since we assume that no pyrite oxidation occurs in the saturated zone (layers 3 and 4), the only source of dissolved uranium in these layers is that which is transported down from the unsaturated zone. Mass balance equations, accounting for the transport of uranium into layers 3 and 4 and its adsorption there, are developed later (Section 3.8). In summary, the initial concentrations of dissolved uranium in layers 3 and 4 can be calculated as:

$$[U_L]^o_{mix} = [U_L]^o_{\lambda w} - [U_L]^o_{\lambda w} \exp\left(\frac{-I_n \Delta t}{\epsilon \lambda_w (1 + K_{D,U02} \rho_T / \epsilon)}\right) \qquad (3.7.9)$$

$$[U_L]^o_4 = [U_L]^o_{mix} - [U_L]^o_{mix} \exp\left(\frac{-I_4 \Delta t}{\epsilon \lambda_4 (1 + K_{D,U02} \rho_T / \epsilon)}\right) \qquad (3.7.10)$$

where

$[U_L]^o_{mix}$ = initial liquid phase concentration of uranium in layer 3 (the mixing zone) ($Bq.m^{-3}$)

$[U_L]^o_4$ = initial liquid phase concentration of uranium in the bottom layer ($Bq.m^{-3}$)

I_4 = net infiltration rate in layer 4 ($m.yr^{-1}$)

λ_{mix} = thickness of the mixing zone (m)

λ_4 = thickness of the bottom layer (m)
(e.g. 10 - ($\lambda_w + \lambda_{mix}$) assuming 10 m tailings depth)

ρ_T = tailings bulk density ($g.m^{-3}$)

ϵ = tailings porosity

$K_{D,U02}$ = uranium solid-liquid distribution coefficient ($m^3.g^{-1}$).

3.7.2 Thorium

The thorium calculations are complicated by the fact that two thorium isotopes Th-230 and Th-232 must be considered in the calculations. On a mass basis, Th-232 is orders of magnitude more significant than Th-230. However, on an activity basis, both make substantial contributions to the total activity. In the source term calculations, the mass or activity of Th-230 and Th-232 are generally calculated separately and then summed to obtain the mass or activity of total thorium. Again, because some calculations are performed on a mass (molar) basis and others on an activity basis, it is useful to define conversion factors at this stage:

$$\text{T230CF} = \left(7.17 \times 10^{8}\ \frac{\text{Bq}}{\text{g}}\right)\left(230\ \frac{\text{g}}{\text{mol}}\right) \qquad (3.7.11)$$

$$= 1.65 \times 10^{11}\ \text{Bq.mol}^{-1}$$

$$\text{T232CF} = \left(4.033 \times 10^{3}\ \frac{\text{Bq}}{\text{g}}\right)\left(232\ \frac{\text{g}}{\text{mol}}\right) \qquad (3.7.12)$$

$$= 9.35 \times 10^{5}\ \text{Bq. mol}^{-1}$$

where

T230CF = Th-230 conversion factor (Bq.mol^{-1})

T232CF = Th-232 conversion factor (Bq.mol^{-1}).

Assuming that secular equilibrium exists in the ore, the activities of Th-230 and U-238 in the ore would be equal. Further, assuming that no Th-230 is recovered in the mill, the initial activity of Th-230 in the tailings is expected to equal the activity of U-238 in the ore fed to the mill. That is:

$$a^{o}_{\text{Th-230}} = a^{o}_{\text{U-238,ore}} \qquad (3.7.13)$$

where

$a^{o}_{\text{Th-230}}$ = initial activity of Th-230 in the tailings (Bq.g^{-1}).

The initial concentration of Th-230 is then calculated as:

$$[\text{Th-230}_s]^{o} = a^{o}_{\text{Th-230}}\ \rho_T/\text{T230CF} \qquad (3.7.14)$$

where

$[\text{Th-230}_s]^{o}$ = initial solid phase concentration of Th-230 (mol.m^{-3}).

The initial concentration of Th-232 is calculated as a function of the percent of thorium in the ore, as follows:

$$[\text{Th-232}_s]^{o} = \left(\frac{m^{o}_{\text{Th}}}{100}\right)\left(\frac{\rho_T}{264}\right) \qquad (3.7.15)$$

where

$[Th\text{-}232_s]^o$ = initial solid phase concentration of Th-232 ($mol.m^{-3}$)

m^o_{Th} = mass % of thorium (as ThO_2) in the ore

264 = molecular weight of ThO_2 ($g.mol^{-1}$).

The initial activity of Th-232 is easily calculated by multiplying by the conversion factor:

$$a^o_{Th\text{-}232} = [Th\text{-}232_s]^o \; T232CF/\rho_T \qquad (3.7.16)$$

where

$a^o_{Th\text{-}232}$ = initial activity of Th-232 ($Bq.g^{-1}$).

The activity and concentration of total thorium is then obtained by summing the activities or concentrations of Th-230 and Th-232. That is:

$$a^o_{Th} = a^o_{Th\text{-}230} + a^o_{Th\text{-}232} \qquad (3.7.17)$$

$$[Th_s]^o = [Th\text{-}230_s]^o + [Th\text{-}232_s]^o \qquad (3.7.18)$$

where

a^o_{Th} = initial activity of total thorium in the tailings ($Bq.g^{-1}$)

$[Th_s]^o$ = initial concentration of total thorium in the tailings ($mol.m^{-3}$).

Some fraction of the original Th-230 and Th-232 inventories are assumed to be soluble. The soluble and insoluble inventories are calculated as follows:

$$[Th\text{-}230_s]^o_{sol} = f_{Th\text{-}230} \; [Th\text{-}230_s]^o \qquad (3.7.19)$$

$$[Th\text{-}232_s]^o_{sol} = f_{Th\text{-}232} \; [Th\text{-}232_s]^o \qquad (3.7.20)$$

$$[Th\text{-}230_s]^o_{insol} = (1 - f_{Th\text{-}230}) \; [Th\text{-}230_s]^o \qquad (3.7.21)$$

$$[Th\text{-}232_s]^o_{insol} = (1 - f_{Th\text{-}232}) \; [Th\text{-}232_s]^o \qquad (3.7.22)$$

where

$[\text{Th-230}_s]_{sol}$ = initial concentration of soluble Th-230 (mol.m^{-3})
$[\text{Th-232}_s]_{sol}$ = initial concentration of soluble Th-232 (mol.m^{-3})
$[\text{Th-230}_s]_{insol}$ = initial concentration of insoluble Th-230 (mol.m^{-3})
$[\text{Th-232}_s]_{insol}$ = initial concentration of insoluble Th-232 (mol.m^{-3})
$f_{\text{Th-230}}$ = fraction of solid phase Th-230 which is soluble
$f_{\text{Th-232}}$ = fraction of solid phase Th-232 which is soluble.

The concentrations of total soluble and insoluble thorium are then easily determined:

$$[\text{Th}_s]^o_{sol} = [\text{Th-230}_s]^o_{sol} + [\text{Th-232}_s]^o_{sol} \qquad (3.7.23)$$

$$[\text{Th}_s]^o_{insol} = [\text{Th-230}_s]^o_{insol} + [\text{Th-232}_s]^o_{insol} \qquad (3.7.24)$$

where

$[\text{Th}_s]^o_{sol}$ = initial concentration of total soluble thorium (mol.m^{-3})
$[\text{Th}_s]^o_{insol}$ = initial concentration of total insoluble thorium (mol.m^{-3}).

These quantities can also be expressed on an activity basis:

$$a^o_{\text{Th},insol} = [\text{Th-230}]^o_{insol}\ \text{T230CF} + [\text{Th-232}]^o_{insol}\ \text{T232CF} \qquad (3.7.25)$$

$$a^o_{\text{Th},sol} = [\text{Th-230}]^o_{sol}\ \text{T230CF} + [\text{Th-232}]^o_{sol}\ \text{T232CF} \qquad (3.7.26)$$

where

$a^o_{\text{Th},insol}$ = initial activity of total insoluble thorium (Bq.m^{-3})
$a^o_{\text{Th},sol}$ = initial activity of total soluble thorium (Bq.m^{-3}).

Once the initial inventories have been calculated, the mass (or activity) fraction of each isotope can be determined, as follows:

$$X_{\text{Th-230/Th},sol} = [\text{Th-230}_s]^o_{sol} \ / \ [\text{Th}_s]^o_{sol} \qquad (3.7.27)$$

$$X_{\text{Th-232/Th},sol} = [\text{Th-232}_s]^o_{sol} \ / \ [\text{Th}_s]^o_{sol} \qquad (3.7.28)$$

$$XA_{\text{Th-232/Th},sol} = [\text{Th-232}_s]^o_{sol}\ \text{T232CF} \ / \ a^o_{\text{Th},sol} \qquad (3.7.29)$$

$$XA^o_{\text{Th-232/Th},insol} = [\text{Th-232}_s]^o_{insol}\ \text{T232CF} \ / \ a^o_{\text{Th},insol} \qquad (3.7.30)$$

where

$X_{Th\text{-}230/Th,sol}$ = mole fraction of Th-230 in soluble thorium
$X_{Th\text{-}232/Th,sol}$ = mole fraction of Th-232 in soluble thorium
$XA_{Th\text{-}232/Th,sol}$ = activity fraction of Th-232 in the soluble thorium
$XA^{o}_{Th\text{-}232/Th,insol}$ = activity fraction of Th-232 in the insoluble thorium.

The liquid (soluble) phase mole or activity fractions will not change with time. However, the solid (insoluble) phase activity fraction will change with time, as the potentially soluble thorium is leached from the solid phase. As the potentially soluble thorium dissolves, the thorium isotopes will be released in proportion to the mole fraction of each isotope in the soluble thorium. Thus, we can predict the relative concentrations of Th-230 and Th-232 in the liquid phase at any time. Since many of the calculations are performed on a molar basis, it is again useful to define a conversion factor.

In this case:

$$\text{THORCF} = X_{Th\text{-}230/Th,sol}\ \text{T230CF} + (1 - X_{Th\text{-}230/Th,sol})\ \text{T232CF} \qquad (3.7.31)$$

where
THORCF = weighted, liquid phase, thorium conversion factor ($Bq.mol^{-1}$).

The liquid phase concentrations of total thorium are calculated as functions of pH in each of the unsaturated, mixing and bottom layers (layers 2, 3 and 4). Details of this relationship are provided in Section 3.9. In summary, the liquid phase thorium concentration in layer "l" is calculated as:

$$\begin{aligned}[Th_L]_l = \frac{10^{(2.5 - 4\,pH)}}{f^4} \Big\{ & 1 + f^{7/4}\,10^{(pH - 3.2)} + f^3\,10^{(2pH - 6.93)} \\ & + f^{15/4}\,10^{(3pH - 11.7)} + f^4\,10^{(4pH - 15.9)} \\ & + f^4\,10^{5.45}\,[SO_4^{2-}]_{u,l} + f^6\,10^{9.73}\,[SO_4^{-2}]^2_{u,l} \qquad (3.7.32) \\ & + 10^{-(5.0 + 0.32\,pH)} \Big\}\end{aligned}$$

where

$[Th_L]_l$ = liquid phase thorium concentration in layer "l" ($mol.L^{-1}$) (must be converted to $mol.m^{-3}$)

pH = pH in layer "l"

f = activity coefficient for divalent ions

$[SO_4^{2-}]_{u,l}$ = concentration of uncomplexed sulfate ion in layer "l" ($mol.L^{-1}$).

Note that the concentrations in this relationship are in units of $mol.L^{-1}$. They must be converted to and from the $mol.m^{-3}$ units used in the rest of the model. The calculated values of $[Th_L]$ must also be converted to an activity basis, by multiplying by the weighted, liquid phase conversion factor (THORCF).

3.7.3 Radium

Radium dissolved during the milling process is assumed to precipitate with barium sulphate, forming a barium-radium sulphate ($Ba(Ra)SO_4$) coprecipitate. The $Ba(Ra)SO_4$ coprecipitate dissolves in a frontwise manner, resulting in an upper layer depleted of $Ba(Ra)SO_4$ and a lower layer enriched in $Ba(Ra)SO_4$. The solid phase radium inventory is comprised of 2 components; radium associated with barium sulphate and radium associated with the host tailings material. The dissolution of the barium-radium sulphate coprecipitate acts as the source of liquid phase radium.

The initial activity of Ra-226 is calculated by again assuming secular equilibrium in the ore. This indicates that the activities of all the elements of the U-238 decay chain are initially equal. Thus:

$$a^o_{Ra} = a^o_{Th-230} \qquad (3.7.33)$$

where

a^o_{Ra} = initial activity of Ra-226 in the tailings ($Bq.g^{-1}$).

We can, again, calculate a conversion factor, to convert from a molar to an activity basis:

$$\mathrm{RACF} = 3.66 \times 10^{10}\ \frac{\mathrm{Bq}}{\mathrm{g}}\ 226\ \frac{\mathrm{g}}{\mathrm{mol}}$$

$$= 8.26 \times 10^{12}\ \mathrm{Bq.mol^{-1}} \qquad (3.7.34)$$

where
RACF = Ra-226 conversion factor ($\mathrm{Bq.mol^{-1}}$).

Then, the initial concentration of radium can be determined:

$$[Ra_s]^o = a^o_{Ra}\ \rho_T\ /RACF \qquad (3.7.35)$$

where
$[Ra_s]^o$ = initial concentration of solid phase Ra-226 in the tailings ($\mathrm{mol.m^{-3}}$).

We assume that all of the radium dissolved in the mill reprecipitates with $BaSO_4$. Thus, the concentration of radium associated with barium sulphate is expressed as:

$$[Ra_s]^o_{Ba} = f_{Ra}\ [Ra_s]^o \qquad (3.7.36)$$

where
$[Ra_s]^o_{Ba}$ = initial concentration of Ra-226 associated with $BaSO_4$ ($\mathrm{mol.m^{-3}}$)
f_{Ra} = fraction of Ra-226 which is assumed to be soluble.

Similarily, the radium associated with the host tailings is that fraction of radium which was not solubilized in the mill:

$$[Ra_s]^o_m = (1 - f_{Ra})\ [Ra_s]^o \qquad (3.7.37)$$

where
$[Ra_s]^o_m$ = initial concentration of Ra-226 associated with host tailings material ($\mathrm{mol.m^{-3}}$) (Assumed to be not leachable).

The initial concentration of $BaSO_4$ is calculated as a function of the mole fraction of Ra-226 in $BaSO_4$:

$$[BaSO_4]^o = [Ra_s]^o_{Ba}/X^o_{Ra/BaSO_4} \qquad (3.7.38)$$

where

$[BaSO_4]^o$ = initial solid phase concentration of $BaSO_4$ ($mol.m^{-3}$)

$X^o_{Ra/BaSO_4}$ = initial mole fraction of Ra-226 in $BaSO_4$.

The initial inventory of the radium associated with $BaSO_4$ in the unsaturated and mixing zones is calculated as:

$$M^o_{Ra} = X^o_{Ra/BaSO_4}(\lambda_w[BaSO_4]^o + \lambda_{mix}[BaSO_4]^o) \qquad (3.7.39)$$

where

M^o_{Ra} = total radium initially associated with $BaSO_4$ in the unsaturated and mixing zones ($mol.m^{-2}$).

For the purposes of calculating solid phase concentrations, we assume that $BaSO_4$ has been depleted from the upper 1 cm of tailings during the initial time step. Thus:

$$[Ra_s]^o_1 = [Ra_s]^o_m \qquad (3.7.40)$$

and

$$[Ra_s]^o_2 = [Ra_s]^o_m + [Ra_s]^o_{Ba} = [Ra_s]^o_{\lambda w} \qquad (3.7.41)$$

where

$[Ra_s]^o_1$ = initial solid phase radium concentration in the upper (surface) layer ($mol.m^{-3}$)

$[Ra_s]^o_{\lambda w}$ = initial solid phase radium concentration in the remainder of the unsaturated zone ($mol.m^{-3}$).

We further assume that all of the tailings, with the exception of the upper 1 cm are homogeneous with respect to solid phase radium. That is:

$$[Ra_s]^o_{mix} = [Ra_s]^o_4 = [Ra_s]^o_{\lambda w} \qquad (3.7.42)$$

where

$[Ra_s]^o_{mix}$, $[Ra_s]^o_4$ = initial solid phase concentrations of radium in the mixing zone and layer 4 respectively ($mol.m^{-3}$).

All of these concentrations may be converted to an activity basis by multiplying by the conversion factor defined previously (RACF).

The liquid phase concentrations of radium are determined as functions of $BaSO_4$ solubility in the various layers. The details of this process are provided in Section 3.10.2. In summary, the concentration of barium at depth λ_w can be determined as a function of the concentration of uncomplexed sulphate in the same layer. That is:

$$[Ba^{2+}]_{\lambda w} = \frac{K^o_{s,BaSO_4}/f^2}{\sqrt{K^o_{s,BaSO_4}\ /f^2}\ + [SO^{2-}_4]_{u,\lambda w}} \left(1 + f^2\, K_{f,BaSO_4}\, [SO_4^{2-}]_{u,\lambda w}\right) \qquad (3.7.43)$$

where

$[Ba^{2+}]_{\lambda w}$ = liquid phase concentration of Ba^{2+} at depth "λ_w ($mol.m^{-3}$)

$K^o_{s,BaSO_4}$ = solubility equilibrium constant for $BaSO_4$ ($mol^2.m^{-6}$)

f = activity coefficient for divalent ions

$K_{f,BaSO_4}$ = formation constant for $BaSO_4$ ($m^3.mol^{-1}$)

$[SO_4^{2-}]_{u,\lambda w}$ = concentration of uncomplexed sulphate ion at depth "λ_w" ($mol.m^{-3}$).

The concentration of Ra-226 is then given by:

$$[Ra_L]_{\lambda w} = K_{Ra}\, [Ba^{2+}]_{\lambda w}\, X^o{}_{Ra/BaSO_4} \qquad (3.7.44)$$

where

$[Ra_L]_{\lambda w}$ = liquid phase concentration of Ra-226 at depth λ_w ($mol.m^{-3}$)

K_{Ra} = radium distribution coefficient (see Section 3.10.2).

Again, the concentration of radium can be converted to an activity basis by multiplying by the radium conversion factor (RACF).

Similar formulations to equations (3.7.43) and (3.7.44) can be written to calculate the liquid phase barium and radium concentrations in layers 3 and 4. The term for uncomplexed sulphate can be replaced with the total sulphate concentration since the influence of uncomplexed sulphate is negligible in the saturated layer.

3.7.4 Lead

Lead-210 is modelled in a manner very similar to Ra-226. Pb-210 is assumed to dissolve in the mill and to coprecipitate with lead sulphate ($PbSO_4$). The Pb(Pb-210)SO_4 coprecipitate dissolves and reprecipitates in a frontwise manner analogous to Ba(Ra)SO_4. Thus, we can again refer to a $PbSO_4$ depleted zone (layer 1) and a $PbSO_4$ enriched zone (layer 2).

The initial activity of Pb-210 in the tailings is equal to the initial activities of Th-230 and Ra-226 in the tailings. That is:

$$a^o_{Pb} = a^o_{Ra} \qquad (3.7.45)$$

where

a^o_{Pb} = initial activity of Pb-210 in the tailings ($Bq.g^{-1}$).

A conversion factor is defined as:

$$\begin{aligned} PBCF &= \left(3.0 \times 10^{12}\ \frac{Bq}{g}\right)\left(210\ \frac{g}{mol}\right) \qquad (3.7.46) \\ &= 6.3 \times 10^{14}\ Bq.mol^{-1} \end{aligned}$$

where

PBCF = Pb-210 conversion factor ($Bq.mol^{-1}$).

The initial concentration of lead-210 is then calculated as:

$$[Pb\text{-}210_s]^o = a^o_{Pb}\ \rho_T / PBCF \qquad (3.7.47)$$

where

$[Pb\text{-}210_s]^o$ = initial solid phase concentration of Pb-210 ($mol.m^{-3}$).

All of the Pb-210 dissolved in the mill is assumed to be associated with $PbSO_4$. Thus, the concentration of Pb-210 associated with $PbSO_4$ is given by:

$$[Pb\text{-}210_s]^o_{PbSO_4} = f_{Pb}[Pb\text{-}210_s]^o \qquad (3.7.48)$$

where

$[Pb\text{-}210_s]^o_{PbSO_4}$ = initial solid phase concentration of Pb-210 associated with $PbSO_4$ ($mol.m^{-3}$)

f_{Pb} = fraction of Pb-210 assumed to be soluble.

The insoluble Pb-210 remains associated with the host tailings material. In particular:

$$[Pb\text{-}210_s]^o_m = (1 - f_{Pb})\ [Pb\text{-}210_s]^o \qquad (3.7.49)$$

where

$[Pb\text{-}210_s]^o_m$ = initial solid phase concentration of Pb-210 associated with host tailings material ($mol.m^{-3}$) (assumed to be not leachable).

The initial mole fraction of Pb-210 in $PbSO_4$ is calculated as a function of the initial concentration of $PbSO_4$ in the tailings:

$$X^o_{Pb\text{-}210/PbSO_4} = [Pb\text{-}210_s]^o_{PbSO_4}/[PbSO_4]^o \qquad (3.7.50)$$

where

$X^{o}_{Pb\text{-}210/PbSO_4}$ = initial mole fraction of Pb-210 in $PbSO_4$
$[PbSO_4]^{o}$ = initial concentration of $PbSO_4$ in the tailings ($mol.m^{-3}$).

In calculating the solid phase concentrations of Pb-210, we again assume that the upper 1 cm of tailings has been depleted of $PbSO_4$ during the first timestep. The remainder of the tailings are assumed to be homogeneous with respect to $PbSO_4$ in the solid phase. Thus, the solid phase concentrations of Pb-210 are given by:

$$[Pb\text{-}210_s]^{o}_{1} = [Pb\text{-}210_s]^{o}_{m} \qquad (3.7.51)$$

$$[Pb\text{-}210_s]^{o}_{\lambda w} = [Pb\text{-}210_s]^{o}_{mix} = [Pb\text{-}210_s]^{o}_{4} = [Pb\text{-}210_s]^{o} \qquad (3.7.52)$$

where
$[Pb\text{-}210_s]^{o}$ = initial solid phase concentration of Pb-210 in layer "1" ($mol.m^{-3}$).

The liquid phase concentrations are determined as functions of $PbSO_4$ solubility in the various layers. The details of this process, and rationale for the approach used, are provided in Section 3.11. The concentration of Pb-210 is calculated as a function of the total concentration of Pb^{2+} ion, which in turn is a function of sulphate concentration. In summary, the total concentration of Pb^{2+} at λ_w is given by:

$$[Pb^{2+}]_{\lambda w} = \frac{K^{o}_{s,PbSO_4}/f^{2}}{\sqrt{K^{o}_{s,PbSO4}/f^{2}} + [SO_4^{2-}]_{u,\lambda w}} \left(1 + f^{2}\, K_{f,PbSO_4}[SO_4^{2-}]_{u,\lambda w}\right) \qquad (3.7.53)$$

where
$[Pb^{2+}]_{\lambda w}$ = total concentration of Pb^{2+} ion at depth λ_w ($mol.m^{-3}$)
$K^{o}_{s,PbSO_4}$ = solubility equilibrium constant for $PbSO_4$ ($mol^{2}.m^{-6}$)

$K_{F,PbSO_4}$ = formation constant for $PbSO_4$ ($m^{3}.mol^{-1}$)

$[SO_4^{2-}]_{u,\lambda w}$ = concentration of uncomplexed sulphate ion at depth λ_w ($mol.m^{-3}$).

The concentration of Pb-210 is then given by:

$$[Pb\text{-}210]^o_{\lambda_w} = X^o_{Pb\text{-}210/PbSO_4}\ [Pb^{2+}]_{\lambda_w} \qquad (3.7.54)$$

where

$[Pb\text{-}210]^o_{\lambda w}$ = initial liquid phase concentration of Pb-210 at depth λ_w ($mol.m^{-3}$).

Again, all concentrations must be converted from $mol.m^{-3}$ to $Bq.m^{-3}$ using the conversion factor defined previously (PBCF).

Similar formulations to equation (3.7.53) and (3.7.54) can be written to calculate the liquid phase lead and lead-210 concentrations in layers 3 and 4. The term for uncomplexed sulphate can be replaced with the total sulphate concentration as noted for radium in Section 3.7.3.

3.8 Uranium

Most of the uranium present in the ore is dissolved and recovered during the milling process. However, some fraction of the uranium resists solubilization, and hence is present in the tailings. The residual uranium is assumed to be evenly distributed throughout the tailings. Of the uranium in the tailings, it is also assumed that a certain fraction is associated with pyrite, i.e. present as microcrystals of U_3O_8 in pyrite while the remaining fraction is associated with unsoluble monazite. As pyrite oxidizes, the uraninite becomes soluble by either of the following reactions:

$$2\ U_3O_8(s) + 12\ H^+ + O_2 \longrightarrow 6\ UO_2^{2+} + 6\ H_2O$$
$$U_3O_8(s) + 2\ F_e^{3+} + 4\ H^+ \longrightarrow 3\ UO_2^{2+} + 2\ Fe^{2+} + 2\ H_2O$$

We may assume that either of the two reactions are considerably faster than the rate of pyrite oxidation. This means that the rate controlling step is the oxidation of pyrite:

$$\frac{\Delta[FeS_2]}{\Delta t} = \frac{[FeS_2]_{t-\Delta t}\,[1 - \exp(-k\Delta t)]}{\Delta t} \qquad (3.8.1)$$

where

$$\frac{\Delta[FeS_2]}{\Delta t} = \frac{\text{moles of pyrite oxidized}}{m^3\ \text{tailings.year}}$$

If we define $X_{U/Fe}$ as the mole fraction of U_3O_8 in pyrite the mean concentration of UO_2^{2+} in the porewater (at λ_w) is:

$$[UO_2{}^{2+}]_{\lambda w,t} = \frac{3\lambda_w}{I_n\Delta t} X_{U/Fe}\,[FeS_2]_{t-\Delta t}[1 - \exp(-k\Delta t)] \qquad (3.8.2)$$

where

$[UO_2^{2+}]_{\lambda w,t}$ = concentration of UO_2^{2+} in the unsaturated zone (= concentration of U-NAT) ($mol.m^{-3}$)
λ_w = thickness of the unsaturated zone (m)
I_n = net infiltration rate ($m.yr^{-1}$)
$[FeS_2]_{t-\Delta t}$ = concentration of pyrite in the previous timestep ($mol.m^{-3}$)
$X_{U/Fe}$ = mole fraction of U_3O_8 in pyrite
k = rate constant for pyrite oxidation (yr^{-1}).

The solid phase concentration of uranium in the unsaturated layer is determined by subtracting the amount of uranium dissolved during a timestep from the solid phase inventory of uranium at the beginning of the timestep. Specifically:

$$[U_s]_t = [U_s]_{t-\Delta t} - (I_n\Delta t/\lambda_w)\,[UO_2{}^{2+}]_{\lambda w,t} \qquad (3.8.3)$$

where

$[U_s]_t$ = solid phase concentration of uranium in the unsaturated zone at time t ($mol.m^{-3}$)
$[U_s]_{t-\Delta t}$ = solid phase concentration of uranium in the unsaturated zone during the previous timestep ($mol.m^{-3}$).

In the mixing zone, the liquid phase concentration of uranium is dependent on the concentration of uranium entering via the liquid phase from the unsaturated zone. This can be expressed as:

$$[UO_2^{2+}]_{mix,t} = [UO_2^{2+}]_{\lambda w,t} + \Big\{[UO_2^{2+}]_{mix,t-\Delta t} - [UO_2^{2+}]_{\lambda w,t}\Big\}$$

$$\exp\,[-I_n \Delta t/(\epsilon \lambda_{mix}(1 + K_{d,UO2}\ \rho_T/\epsilon))] \qquad (3.8.4)$$

where

$[UO_2^{2+}]_{mix,t}$ = concentration of UO_2^{2+} in the mixing zone at time t ($mol.m^{-3}$)

$[UO_2^{2+}]_{mix,t-\Delta t}$ = concentration of UO_2^{2+} in the mixing zone during the previous timestep ($mol.m^{-3}$)

K_{d,UO_2} = solid-liquid distribution coefficient for UO_2^{2+} ($m^3.g^{-1}$).

Similarily, the uranium concentration in the bottom layer is dependent on the uranium concentration in the mixing zone:

$$[UO_2^{2+}]_{4,t} = [UO_2^{2+}]_{mix,t} + \Big\{[UO_2^{2+}]_{4,t-\Delta t} - [UO_2^{2+}]_{mix,t}\Big\}$$

$$\exp\,[-\ I_4 \Delta t/(\ \epsilon\, \lambda_4\ (1 + K_{d,UO2}\ \ \rho_T/\epsilon))] \qquad (3.8.5)$$

where

$[UO_2^{2+}]_{4,t}$ = concentration of UO_2^{2+} in the bottom layer at time t ($mol.m^{-3}$)

$[UO_2^{2+}]_{4,t-\Delta t}$ = concentration of UO_2^{2+} in the bottom layer during the previous timestep ($mol.m^{-3}$)

I_4 = net infiltration into layer 4 ($m.yr^{-1}$)

λ_4 = thickness of bottom layer (layer 4) (m).

Note that all of the calculated concentrations were expressed in units of $mol.m^{-3}$. These are all converted to units of $Bq.m^{-3}$ by multiplying by the conversion factor defined previously (UCF).

3.9 Thorium

3.9.1 Unsaturated Zone

The solution of thorium hydroxide has been reviewed by Langmuir and Herman (1980). The solution and complexation reactions relevant for pyritic tailings are summarized below:

Reaction	Log K
$Th(OH)_4(s) + 4H^+ \rightleftharpoons Th^{+4} + 4H_2O$	6.30 (amorphous)
	1.78 (crystalline)
$Th^{+4} + H_2O \rightleftharpoons Th(OH)^{3+} + H^+$	-3.20
$Th^{+4} + 2H_2O \rightleftharpoons Th(OH)_2^{2+} + 2H^+$	-6.93
$Th^{+4} + 3H_2O \rightleftharpoons Th(OH)_3^{+} + 3H^+$	-11.70
$Th^{+4} + 4H_2O \rightleftharpoons Th(OH)_4^{0}(aq) + 4H^+$	-15.90
$Th^{+4} + SO_4^{2-} \rightleftharpoons ThSO_4^{2+}$	5.45
$Th^{+4} + 2SO_4^{2-} \rightleftharpoons Th(SO_4)_2^{0}$	9.73

Sulphate and hydroxo complexes of thorium have a significant effect on thorium solubility at acidic pH values. Hence, equilibrium models based on simple complexation reactions are inadequate to describe the total dissolved thorium concentration at near neutral or alkaline pH conditions. Hertz and Tyree (1965) have shown that the hydroxo complexes of thorium tend to form large aggregates. These polymeric forms may contain 140 to 150 thorium atoms per solute particle. These aggregates approach colloidal size (450A) in terms of their light scattering properties, but are an order of magnitude smaller than the pore size of a 0.45μ filter. From the present experimental database it appears that the concentration of these colloidal thorium hydroxides, or possibly other complexes, is slightly pH dependent. The concentration of these colloidal complexes was found to be proportional to $10^{-0.32pH}$ by the best fit of the residual between experimental data and predictions excluding colloidal complexes.

The incorporation of this pH dependent term and a term for sulphate complexation into the aforementioned solubility expression, for total dissolved thorium yields the following equation:

$$[Th_L]_{\lambda w} = \frac{10^{(2.5 - 4pH)}}{f^4} \Big\{ 1 + f^{7/4}\, 10^{(pH-3.2)} + f^3\, 10^{(2pH-6.93)} + f^{15/4}\, 10^{(3pH - 11.7)} + f^4\, 10^{(4pH - 15.9)} + f^4\, 10^{5.45} [SO_4{}^{2-}]_{u,\lambda w} + f^6\, 10^{9.73} [SO_4^{2-}]^2_{u,\lambda w} \Big\} + 10^{-(5.0 + 0.32\, pH)} \qquad (3.9.1)$$

where

$[Th_L]_{\lambda w}$ = liquid phase concentration of total thorium in the unsaturated zone at λ_w ($mol.L^{-1}$)

pH = pH in the unsaturated zone (i.e. at λ_w)

f = activity coefficient for divalent ions

$[SO_4^{2-}]_{u,\lambda w}$ = concentration of uncomplexed sulphate at λ_w ($mol.L^{-1}$).

and

$[SO_4^{2-}]_{u,\lambda w} = [SO_4^{2-}]_{u,\lambda w}/d$

where

d = a correction factor for sulphate complexation (See Section 3.3.3).

The function above (equation (3.9.1)) has the potential to predict unreasonably high total thorium concentrations at low pH values. Since the dissolution of $Th(OH)_4$ may not be equilibrium controlled below about pH 3.5, we have chosen to set an upper limit of $5x10^{-5}$ $mol.L^{-1}$ on the concentration of dissolved thorium. That is:

if $[Th_L]_{\lambda w} > 5x10^{-5}$ $mol.L^{-1}$ (from equation (3.9.1)) then $[Th_L]_{\lambda w} = 5 \times 10^{-5} mol.L^{-1}$ (3.9.2)

This corresponds well to observed field data on total dissolved thorium. Note that the concentrations in this equation are expressed in $mol.L^{-1}$. Conversions to and from $mol.m^{-3}$ must be made to correspond with the remainder of the models. The concentration of total thorium is easily converted to an activity basis, by multiplying by the overall conversion factor defined previously (THORCF).

Solid Thorium Inventory

In examining the solubility dependence of thorium, it becomes evident that the pH is the most important controlling factor. Unlike $Ba(Ra)SO_4$ and $PbSO_4$, dissolved thorium is not expected to reprecipitate in the unsaturated zone. We may assume that the distribution of solid thorium hydroxide in the unsaturated zone is homogeneous initially and remains homogeneous until the potentially soluble solid ($Th(OH)_4(s)$) dissolves. In fact, the solubility of $Th(OH)_4$ increases with depth in the unsaturated zone. One may argue, however, that the solid $Th(OH)_4$ is replenished by the migration of small particles downward in the porewater.

The concentration of total thorium which has dissolved to time t is thus given by:

$$[Th]_{diss,t} = [Th]_{diss,t-\Delta t} + I_n \Delta t/\lambda_w \, [Th_L]_{\lambda w} \qquad (3.9.4)$$

where

$[Th]_{diss,t}$ = concentration of total thorium dissolved in the unsaturated zone to time t ($mol.m^{-3}$)

$[Th]_{diss,t-\Delta t}$ = concentration of total thorium dissolved in the unsaturated zone to time t-Δt ($mol.m^{-3}$).

The total dissolved thorium is comprised of both Th-230 and Th-232. The concentrations of each isotope can be determined by using the fractions calculated initially:

$$[\text{Th-232}]_{diss} = [\text{Th}]_{diss,t}\, X_{\text{Th-232/Th},sol} \tag{3.9.5}$$
$$[\text{Th-230}]_{diss} = [\text{Th}]_{diss,t} - [\text{Th-232}]_{diss} \tag{3.9.6}$$

where

$[\text{Th-230}]_{diss}$, $[\text{Th-232}]_{diss}$ = concentration of dissolved Th-230 and Th-232 to time t in the unsaturated zone ($mol.m^{-3}$).

The concentrations of each isotope remaining in the solid phase can then be calculated. These solid phase concentrations are comprised of the mass of the isotope previously calculated as being insoluble, plus the mass of the isotope potentially soluble but not yet dissolved. That is:

$$[\text{Th-230}_s] = [\text{Th-230}]^o_{insol} + ([\text{Th-230}]^o_{sol} - [\text{Th-230}]_{diss}) \tag{3.9.7}$$
$$[\text{Th-232}_s] = [\text{Th-232}]^o_{insol} + ([\text{Th-232}]^o_{sol} - [\text{Th-232}]_{diss}) \tag{3.9.8}$$

where

$[\text{Th-230}_s]$ = solid phase concentration of Th-230 in unsaturated zone ($mol.m^{-3}$)
$[\text{Th-232}_s]$ = solid phase concentration of Th-232 in unsaturated zone ($mol.m^{-3}$).

The solid phase concentration of total thorium is then easily determined; on either a molar or an activity basis:

$$[\text{Th}_s] = [\text{Th-230}_s]\ \text{T230CF} + [\text{Th-232}_s]\ \text{T232CF} \tag{3.9.10}$$

where

$[\text{Th}_s]$ = solid phase concentration of total thorium in unsaturated zone ($Bq.m^{-3}$).

This is the concentration of thorium in windblown dust dispersed from the tailings surface.

The activity fraction of Th-230 and/or Th-232 in the solid phase can then be calculated:

$$XA_{\text{Th-232/Th},insol} = [\text{Th-232}_s]\ \text{T232CF}/[\text{Th}_s] \tag{3.9.11}$$

where

$XA_{Th\text{-}232/Th,insol}$ = activity fraction of Th-232 in total solid phase thorium.

The entire preceding discussion is applicable only as long as soluble $Th(OH)_4$ is present in the unsaturated zone. Once the soluble thorium is depleted, the calculations are greatly simplified. That is if:

$$[Th]_{diss,t} = [Th]^o_{sol}$$

then:

$$[Th_L]_{\lambda w} = 0.0 \tag{3.9.12}$$

$$[Th_s] = [Th\text{-}230]^o_{insol}T230CF + [Th\text{-}232]^o_{insol}T232CF \tag{3.9.13}$$

$$XA_{Th\text{-}232/Th,insol} = XA^o_{Th\text{-}232/Th,insol} \tag{3.9.14}$$

$$[Th\text{-}230_s] = [Th\text{-}230]^o_{insol} \tag{3.9.15}$$

where

$[Th_L]_{\lambda w}$ = liquid phase concentration of total thorium in the unsaturated zone ($Bq.m^{-3}$)

$[Th_s]$ = solid phase concentration of total thorium in unsaturated zone ($Bq.m^{-3}$)

$[Th\text{-}230_s]$ = solid phase concentration of Th-230 in unsaturated zone ($mol.m^{-3}$).

3.9.2 Layers 3 and 4

The liquid phase concentration of total thorium is again modelled as a function of pH and sulphate concentration. The equation derived for dissolved thorium concentration in the unsaturated zone (equation (3.9.1)) applies equally to the mixing zone and the bottom layer. That is:

$$\begin{aligned}[Th_L]_l = {} & \frac{10^{(2.5 - 4pH)}}{f^4}\Big\{1 + f^{7/4}\,10^{(pH - 3.2)} + f^{3}\,10^{(2pH - 6.93)} \\ & + f^{15/4}\,10^{(3pH - 11.7)} + f^{4}\,10^{(4pH - 15.9)} \\ & + f^{4}\,10^{5.45}\,[SO_4^{2-}]_l + f^{6}\,10^{9.73}\,[SO_4^{2-}]^2{}_l\Big\} \qquad (3.9.16) \\ & + 10^{-(5.0 + 0.32\,pH)}\end{aligned}$$

where

$[Th_L]_l$ = liquid phase concentration of total thorium in layer "l" (where l = 3 or 4) ($mol.L^{-1}$)

pH = pH in layer "l" (where l = 3 or 4)

$[SO_4^{2-}]_l$ = total sulphate concentration in layer "l" (where l = 3 or 4) ($mol.L^{-1}$).

Again, conversion to and from appropriate units must be made. Also, an upper limit of $5x10^{-5}$ $mol.L^{-1}$ is set on the thorium concentration, as discussed previously.

It may also be important to keep track of the thorium inventory in the mixing zone. If the calculated liquid phase thorium concentration in the mixing zone is less than that in the unsaturated zone, then net thorium precipitation is occurring in the mixing zone.

That is, if:

$$[Th_L]_{mix} < [Th_L]_{\lambda w}$$

then:

$$[Th]_{diss,mix,t} = [Th]_{diss,mix,t-\Delta t} - (I_n \Delta t/\lambda_{mix})([Th_L]_{\lambda w} - [Th_L]_{mix}) \quad (3.9.17)$$

otherwise:

$$[Th]_{diss,mix,t} = [Th]_{diss,mix,t-\Delta t} + (I_n \Delta t/\lambda_{mix})\,[Th_L]_{mix} \qquad (3.9.18)$$

where

$[Th]_{diss,mix,t}$ = concentration of total thorium dissolved in the mixing zone at time t ($mol.m^{-3}$)

Note: This may be a negative quantity indicating net precipitation rather than dissolution.

If the potentially soluble thorium in the mixing zone becomes depleted, then the dissolved thorium concentration drops to zero.

Specifically if:

$$[Th]_{diss,mix,t} > [Th_s]_{sol}$$

then

$$[Th_L]_{mix} = 0 \qquad (3.9.19)$$

The bottom layer is assumed to be large enough, and the chemical composition such that thorium depletion is not expected to occur over the 1000 year modelling period.

3.10 Radium

3.10.1 Radioactive Ingrowth and Decay

The radioactive ingrowth and decay of Ra-226 contributes to both its solid and liquid phase concentrations.

The ingrowth of radium from thorium can be estimated from the general laws of radioactive decay. The decay of radium can be represented by:

$$A \xrightarrow{\lambda_A} B \xrightarrow{\lambda_B}$$

where A and B represent the number of atoms of thorium and radium which are present at any time t; and λ_A and λ_B are the decay constants of thorium and radium respectively. If the only source of thorium atoms is the initial supply, $A = A_0$ at t = 0, and if B = 0 at t = 0, then the rate of change in the number of radium atoms is given by (Evans 1955):

$$\frac{dB}{dt} = A_o \lambda_A \exp(-\lambda_A t) - B\lambda_B \quad (3.10.1)$$

The solution of this differential equation is:

$$B(t) = A_o \left(\frac{\lambda_A}{\lambda_B-\lambda_A}\right) [\exp(-\lambda_A t) - \exp(-\lambda_B t)] \quad (3.10.2)$$

which is an expression for the number of radium atoms, $B(t)$, at any time t.

We can also predict the molar concentration of Ra-226 which ingrows from Th-230 during any timestep, Δt, given the molar concentration of Th-230 at the beginning of that time period. That is:

$$[Ra]^{Th} = [Th\text{-}230] \left(\frac{\lambda_{Th-230}}{\lambda_{Ra-226} - \lambda_{Th-230}}\right)[\exp(-\lambda_{Th-230}\Delta t) - \exp(-\lambda_{Ra-226}\Delta t)] \quad (3.10.3)$$

where

$[Ra]^{Th}$ = concentration of Ra resulting from ingrowth from thorium during Δt ($mol.m^{-3}$)

[Th-230] = concentration of Th-230 representative of the beginning of the time period ($mol.m^{-3}$)

λ_{Th-230}, λ_{Ra-226} = radioactive decay constants of Th-230 and Ra-226

Δt = length of timestep (yr).

This result (equation (3.10.3)) is used to determine solid and liquid phase radium concentrations resulting from the ingrowth from Th-230.

3.10.2 Unsaturated Zone

Recent investigations by Beak Consultants Ltd. (1985) indicate that Ra-226 co-precipitates (solid solution) with barite ($BaSO_4(s)$) rather than with gypsum ($CaSO_4(s)$) as modelled previously (SENES, 1985a). Accordingly, the solution of Ra-226 is modelled on the basis of $Ba(Ra)SO_4$ solid solution. The principles underlying the transport of Ra-226, however, remain the same as modelled for $Ca(Ra)SO_4$.

As in the case of gypsum precipitate, Ra-226 is a minor component (mole fraction << 1) of the precipitated barite solid. The solubility of Ra-226, therefore, will depend on the solubility of the host mineral (barite) in the tailings. The relevant equilibrium expressions for barite are as follows:

$$BaSO_4\,(s) \rightleftharpoons Ba^{+2} + SO_4{}^{2-} \qquad K_s^o = 1.07\times10^{-4}\ mol^2.m^{-6}$$
$$Ba^{+2} + SO_4{}^{2-} \rightleftharpoons BaSO_4{}^o\,(aq) \qquad K_f = 5.01\times10^{-1}\ m^3.mol^{-1}$$

We shall assume, that barite (i.e. $Ba(Ra)SO_4$) is occluded as microcystals in the gypsum matrix. Although this assumption is not critical, it aids in visualizing the fate of $BaSO_4$ in the tailings solids. As the gypsum front moves downward in the unsaturated zone, the barite crystals become "exposed" and begin to dissolve in the porewater. Due to the lower solubility of $BaSO_4$, the $BaSO_4$ front will lag the gypsum front. Consequently, the solubility of $BaSO_4$ will depend on the sulphate concentrations resulting from pyrite oxidation only $[SO_4]_p$. The molar concentrations of the barium ion and the sulphate complex $[BaSO_4]^{o}_{aq}$ can be expressed as follows:

$$[Ba]_{T,h_{Ba}} = \frac{K^o_{s,BaSO_4}/f^2}{\sqrt{K^o_{s,BaSO4}/f^2 + [SO_4^{2-}]_{p,h_{Ba}}}} \left(1 + f^2 K_{f,BaSO_4}[SO_4^{2-}]_{p,h_{Ba}}\right) \qquad (3.10.4)$$

where

$[Ba]_{T,h_{Ba}}$ = dissolved concentration of total barium ($mol.m^{-3}$)

$K^o_{s,BaSO4}$ = solubility product of $BaSO_4$ ($mol^2.m^{-6}$)

$K_{f,BaSO4}$ = formation constant of $BaSO^o_{4(aq)}$ ($m^3.mol^{-1}$)

f = activity coefficient for divalent ions

$[SO_4^{2-}]_{p,h_{Ba}}$ = concentration of sulphates at h_{Ba} resulting from pyrite oxidation ($mol.m^{-3}$)

h_{Ba} = the position of the barium sulphate solids front (m).

In analogy to the movement of a gypsum front, we may define a depleted zone for barite in the tailings. If $[BaSO_4]^o$ is the initial molar concentration of barite (moles $BaSO_4/m^3$ tailings), the movement of the barite depleted layer (Δh_{Ba}) is given by:

$$[BaSO_4]^o \, \Delta h_{Ba} = (I_n \Delta t) \left\{ \frac{K^o_{s,BaSO_4}/f^2}{\sqrt{K^o_{s,BaSO_4}/f^2} + (2B/I_n\Delta t)\,(h_{Ba} + \Delta h_{Ba}/2)} \right\}$$

$$\left\{ 1 + (2B\, K_{f,BaSO_4}\, f^2/I_n\Delta t)\,(h_{Ba} + \Delta h_{Ba}/2) \right\} \qquad (3.10.5)$$

where

B = $[FeS_2]_{t-\Delta t}\,(1 - e^{-k\Delta t})$

I_n = net infiltration rate ($m.yr^{-1}$)

$[BaSO_4]^o$ = initial concentration of barite in the tailings ($mol.m^{-3}$)

h_{Ba} = $\sum_{t=0}^{t-\Delta t} \Delta h_{Ba}$

Equation (3.10.5) may be solved for Δh_{Ba}:

$$\Delta h_{Ba} = \left\{ \frac{a^2 (I_n\Delta t)}{[BaSO_4]^o} \left[\frac{I_n\Delta t + 2\, f^2 K_{f,BaSO_4}\, h_{Ba}}{B} \right] + \frac{1}{4} \left[2h_{Ba} + \frac{aI_n\Delta t}{B} - \frac{a^2 f^2 K_{f,BaSO_4}\, I_n\Delta t}{[BaSO_4]^o} \right]^2 \right\}^{1/}$$

$$- \left[h_{Ba} + \frac{aI_n\Delta t}{2B} - \frac{a^2 f^2 K_{f,BaSO_4}\, I_n\Delta t}{2[BaSO_4]^o} \right] \qquad (3.10.6)$$

where

$$a = \sqrt{K^o_{s,BaSO_4}/f^2}$$

The value for h_{Ba} at the end of the current time step is thus:

$$h_{Ba,t} = h_{Ba,t-\Delta t} + \Delta h_{Ba}$$

As the dissolved barium moves downward through the tailings, some of it must precipitate, since the sulphate concentration increases in the unsaturated zone. This increase in sulphate is due to increasing sulphate levels with distance due to pyrite oxidation and, in part, due to gypsum dissolution.

At the limit of the unsaturated zone, i.e. λ_w, we have calculated a time averaged total sulphate concentration $[SO_4^{2-}]_{t,\lambda w}$, equation (3.3.40). We have also estimated a quantity "d", equation (3.3.38), as follows:

$$d = 1 + f^3\, 10^{8.99 - 3pH} + f^{3/4}\, 10^{9.7 - 3pH} \qquad (3.10.7)$$

The concentration of uncomplexed sulphate at λ_w is given by:

$$[SO_4^{2-}]_{u,\lambda w} = \frac{[SO_4^{2-}]_{T,\lambda w}}{1 + f^3\, 10^{8.99 - 3pH} + f^{3/4}\, 10^{9.7 - 3pH}} \qquad (3.10.8)$$

where

$[SO_4^{2-}]_{u,\lambda w}$ = uncomplexed sulphate concentration at λ_w (mol.m^{-3})

$[SO_4^{2-}]_{T,\lambda w}$ = total sulphate concentration at λ_w (mol.m^{-3}).

The total dissolved barium (Ba^{+2} and $BaSO^o$ (aq)) at λ_w can be calculated using an expression analogous to equation (3.10.4), that is:

$$[Ba]_{T,\lambda w} = \frac{K^o_{s,BaSO_4} / f^2}{\sqrt{K^o_{s,BaSO_4} / f^2 + [SO_4^{2-}]_{u,\lambda w}}} \left(1 + f^2 K_{f,BaSO_4}[SO_4^{2-}]_{u,\lambda w}\right) \qquad (3.10.9)$$

We may define the total precipitated barite at any time "t" as $m_{Ba,t}$. The rate of change in reprecipitated barite between t-Δt and t is given by:

$$\frac{m_{Ba,t} - m_{Ba,t-\Delta t}}{\Delta t} = \frac{[BaSO_4]^o\, \Delta h_{Ba}}{\Delta t} - I_n\, [Ba]_{T,\lambda w} \qquad (3.10.10)$$

where

$m_{Ba,t}$ = reprecipitated barite at time t (mol.m^{-2})
$m_{Ba,t-\Delta t}$ = reprecipitated barite at time t-Δt (mol.m^{-2}).

Note that we need not time-average $[Ba]_{T,\lambda w}$ since it is based on the time-averaged sulphate concentration between $t-\Delta t$ and t. Solving equation (3.10.10) for $m_{Ba,t}$ yields:

$$m_{Ba,t} = m_{Ba,t-\Delta t} + [BaSO_4]^o \Delta h_{Ba} - I_n \Delta t \, [Ba]_{T,\lambda w} \qquad (3.10.11)$$

Note that the calculations for Δh_{Ba} and $m_{Ba,t}$ were not performed in the initial timestep, since we felt that the $BaSO_4$ depletion would be minimal over that timestep. It was further assumed that at $t = 0$, the depth of $BaSO_4$ depletion (h_{Ba}) was 1 cm (0.01 m).

To calculate the concentration of dissolved radium-226, a solid solution of $RaSO_4$ in $BaSO_4$ is assumed. We define the mole fraction of radium in the solid phase as:

$$x = \frac{RaSO_4(s)}{RaSO_4(s) + BaSO_4(s)} \qquad (3.10.12)$$

The mole fraction of Ra-226 in the liquid phase is given by:

$$y = \frac{[Ra^{+2}]}{[Ra^{+2}] + [Ba^{+2}]} \qquad (3.10.13)$$

If $BaSO_4$ and $RaSO_4$ form a regular solid solution, the mole fraction in the liquid phase (y) can be related to the mole fraction in the solid phase by the following equality (Gresens, 1981):

$$y = \left[\frac{\dfrac{K^o_{s,RaSO_4}}{f_{Ra}\, f_{SO4}} \, x \exp[\alpha(1 - x)^2]}{\dfrac{K^o_{s,BaSO_4}}{f_{Ba}\, f_{SO4}} \, x \exp[\alpha(1 - x)^2] + K^o_{s,BaSO_4} (1 - x) \exp[\alpha x^2]} \right] \qquad (3.10.14)$$

It has been shown (Beak, 1985) that $BaSO_4$ and $RaSO_4$ form a nearly ideal solid solution ($\alpha = o$). Furthermore, the mole fraction of radium-226 in barite ($BaSO_4$) is very small ($x \ll 1$). In this case, the distribution of radium-226 between the solid and liquid phases is given by:

$$y = \left[\frac{\dfrac{K^o_{s,RaSO_4}}{f_{Ra}\, f_{SO4}}}{\dfrac{K^o_{s,BaSO_4}}{f_{Ba}\, f_{SO4}}} \right] x \qquad (3.10.15)$$

where

$K^o_{s,RaSO_4}$ = solubility product of $RaSO_4$ (s); $K^o_{s,RaSO_4} = 10^{-10.27}$

$K^o_{s,BaSO_4}$ = solubility product of $BaSO_4$ (s); $K^o_{s,BaSO_4} = 10^{-10.27}$

f_{Ra}, f_{Ba}, f_{SO4} = activity coefficients for Ra^{2+}, Ba^{2+} and SO_4^{2-}.

Assuming the activity coefficients of Ra^{+2} and Ba^{+2} are identical, the distribution of radium-226 between the solid and the liquid phases is:

$$y = 0.50\ x \qquad (3.10.16)$$

The coefficient calculated in equation (3.10.16) (i.e. $K_{Ra} = 0.5$) compares with an experimentally determined value of $K_{Ra} = 0.56$ (Stumm and Morgan, 1981). In this analysis, the coefficient (K_{Ra}) is specified as a uniformly distributed input parameter, with a range from 0.50 to 0.56.

To determine a value for the solid phase mole fraction x, we assume equilibrium between reprecipitated barite and dissolved radium. The material balance for radium in the reprecipitated solid phase is given by:

$$[BaSO_4]^o X'_{Ra/BaSO_4}\Delta h_{Ba} + I_n [Ra]^{Th}_{\lambda w}\Delta t = m_{Ba,t}x_t - m_{Ba,t-\Delta t}x_{t-\Delta t} \quad (3.10.17)$$

$$+ I_n\Delta t[Ba]_{T,\lambda w} K_{Ra} (x_t + x_{t-\Delta t})/2$$

or, solving for x_t:

$$x_t = \Big\{ [BaSO_4]^o X'_{Ra/BaSO_4}\Delta h_{Ba} + I_n [Ra]^{Th}_{\lambda w}\Delta t + m_{Ba,t-\Delta t}\, x_{t-\Delta t}$$

$$-I_n\Delta t[Ba]_{T,\lambda w} K_{Ra}x_{t-\Delta t}/2\Big\}$$

$$\div [m_{Ba,t} + I_n\Delta t[Ba]_{T,\lambda w} K_{Ra} /2] \quad (3.10.18)$$

Many of the terms have already been defined. However, a few require further attention. Namely:

$$X'_{Ra/BaSO_4} = X^o_{Ra/BaSO_4} \exp(-\lambda_{Ra-226}t) \quad (3.10.19)$$

where

$X'_{Ra/BaSO_4}$ = mole fraction of Ra-226 in $BaSO_4$; corrected for decay of Ra-226

$X^o_{Ra/BaSO_4}$ = initial mole fraction of Ra-226 in $BaSO_4$.

and:

$$[Ra]^{Th}_{\lambda w} = X_{Th-230/Th,sol}\,[TH_L]_{\lambda w}\left(\frac{\lambda_{Th-230}}{\lambda_{Ra-226} - \lambda_{Th-230}}\right)$$

$$(\exp(-\lambda_{Th-230}\Delta t) - \exp(-\lambda_{Ra-226}\Delta t)) \quad (3.10.20)$$

where

$[Ra]^{Th}_{\lambda w}$ = concentration of Ra-226 resulting from ingrowth from Th-230 during Δt ($mol.m^{-3}$)

$X_{Th-230/Th,sol}$ = mole fraction of Th-230 in soluble thorium

$[Th_L]_{\lambda w}$ = liquid phase concentration of total thorium at λ_w ($mol.m^{-3}$).

The rationale for this last equation was provided previously (Section 3.13.1).

Note that x_t at t = 0 is equal to $X^o_{Ra/BaSO_4}$.

The concentration of radium in solution at λ_w can then be calculated as follows:

$$[Ra_L]_{\lambda w} = K_{Ra}\, [Ba]_{T,\lambda w}\, x_t \qquad (3.10.21)$$

where

$[Ra_L]_{\lambda w}$ = liquid phase concentration of radium at λ_w ($mol.m^{-3}$).

This quantity can be converted to units of $Bq.m^{-3}$ using the conversion factor defined previously (RACF).

The previous discussion applies as long as $BaSO_4$ is present in the unsaturated zone; that is, as long as h_{Ba} is less than λ_w. Once $BaSO_4$ is depleted from the unsaturated zone, radioactive ingrowth from dissolved thorium is the only source of dissolved radium. That is:

$$[Ra_L]_{\lambda w} = [Ra_L]^{Th}_{\lambda w} \qquad \text{for } h \geq \lambda_w \qquad (3.10.22)$$

Unsaturated Zone: Solid Phase

As described earlier, the unsaturated zone can be thought of as consisting of 2 layers for radium; a $BaSO_4$ (and hence radium) depleted layer and a $BaSO_4$ (and hence radium) enriched layer. Since radium acts as the source of radon emanation from the tailings, it is important to characterize the solid phase radium concentrations in both layers.

The solid phase radium resulting from the ingrowth from thorium must be considered in both layers. While we calculate the incremental ingrowth during each time period, we must also keep a cumulative total of the net radium resulting from ingrowth. This is calculated as:

$$[Ra_s]^{Th}_t = [Ra_s]^{Th}_{t-\Delta t} \exp(\lambda_{Ra-226}\ \Delta t)$$

$$+ [Th\text{-}230_s]\left(\frac{\lambda_{Th-230}}{\lambda_{Ra-226} - \lambda_{Th-230}}\right)\left(\exp(-\lambda_{Th-230}\Delta t) - \exp(-\lambda_{Ra-226}\Delta t)\right) \quad (3.10.23)$$

where

$[Ra_s]^{Th}_t$ = cumulative solid phase concentration of Ra-226 resulting from ingrowth to time t ($mol.m^{-3}$)

$[Ra_s]^{Th}_{t-\Delta t}$ = cumulative solid phase concentration of Ra-226 resulting from ingrowth to time $t-\Delta t$ ($mol.m^{-3}$)

$[Th\text{-}230_s]$=solid phase concentration of Th-230 at time t ($mol.m^{-3}$).

In the $BaSO_4$ depleted layer (layer 1) the solid phase radium concentration consists of insoluble radium originally associated with the host tailings material plus radium resulting from ingrowth. Radioactive decay of the insoluble radium inventory must also be considered. Thus, we can write:

$$[Ra_s]_1 = [Ra_s]^o_m \exp(-\lambda_{Ra-226}t) + [Ra_s]_t{}^{Th} \quad (3.10.24)$$

where

$[Ra_s]_1$ = solid phase radium concentration in layer 1 at time t ($mol.m^{-3}$)

$[Ra_s]^o_m$ = initial concentration of radium associated with host tailings material ($mol.m^{-3}$).

In layer 2, the concentration of radium associated with the original $BaSO_4$ and the reprecipitated $BaSO_4$ must also be considered. That is:

$$[Ra_s]_2 = [Ra_s]^{Th}_t + x'_{Ra/BaSO_4}[BaSO_4]^o + x_t\, m_{Ba,t}/(\lambda_w - h_{Ba}) \quad (3.10.25)$$

where

$[Ra_s]_2$ = solid phase radium concentration in layer 2 at time t ($mol.m^{-3}$)

$x'_{Ra/BaSO_4}$ = original mole fraction of Ra in $BaSO_4$; corrected for radioactive decay of radium (see equation (3.10.19)).

According to our concept, the boundary between layer 1 and layer 2 is a dynamic boundary, i.e. it is changing with time. Thus, any position at a fixed depth is in layer 2 until the boundary passes and it becomes part of layer 1. Equation (3.10.25) is a material balance equation of the total (both mobile and immobile) radium fraction. The equation takes into account the accumulation resulting from dissolution/reprecipitation processes. The insoluble radium content is expressed as an initial condition. As the boundary, (i.e. $BaSO_4(s)$ dissolution front) moves by the Ra-226 associated with $BaSO_4(s)$ dissolves and Equation (3.10.24) is applicable for long-term calculations.

Once the unsaturated zone is depleted of $BaSO_4$, the entire unsaturated zone takes on the characteristics of layer 1, and the solid phase radium concentration is give by equation (3.10.24).

3.10.3 Layers 3 and 4

The concentration of dissolved radium in both the mixing zone and the bottom layer depends on a number of conditions. First, the concentration of dissolved radium in each layer resulting from thorium decay depends on the presence or absence of soluble thorium in the layer above. For instance, we assume that as long as thorium is entering the mixing zone from the layer above, no net thorium dissolution is occurring in the mixing zone. Hence, there is no dissolved radium present resulting from thorium dissolution and decay, in that zone. More specifically, we can write:

$$[Ra]^{Th}_{mix} = 0 \quad \text{for} \sum_{t} [Th_L]_{diss,t} < [Th_s]^{o}_{sol} \qquad (3.10.26)$$

(see Section 3.9.1)

otherwise:

$$[Ra]^{Th}_{mix} = X_{Th-230/Th,sol}\,[Th_L]_{mix} \left(\frac{\lambda_{Th-230}}{\lambda_{Ra-226} - \lambda_{Th-230}} \right)$$

$$(\exp(-\lambda_{Th-230}\Delta t) - \exp(-\lambda_{Ra-226}\Delta t)) \qquad (3.10.27)$$

where

$[Ra]_{mix}^{Th}$ = concentration of dissolved radium resulting from the decay of thorium dissolved in the mixing zone at time t ($mol.m^{-3}$)

$[Th_L]_{mix}$ = dissolved total thorium concentration in the mixing zone at time t ($mol.m^{-3}$)

$X_{Th-230/Th,sol}$ = mole fraction of Th-230 in soluble thorium.

$[Th_L]_{diss,t}$ = concentration of dissolved thorium in the unsaturated zone at time t ($mol.m^{-3}$)

$[Th_S]_{sol}^{o}$ = initial concentration of total soluble thorium ($mol.m^{-3}$).

We can write analagous equations for the bottom layer:

$$[Ra]_4^{Th} = 0 \qquad \text{for } \sum_t [Th_L]_{diss,mix,t} < [Th_S]_{sol}^{o} \qquad (3.10.28)$$

otherwise:

$$[Ra]_4^{Th} = X_{Th-230/Th,sol}\,[Th_L]_4 \left(\frac{\lambda_{Th-230}}{\lambda_{Ra-226} - \lambda_{Th-230}}\right) (\exp(-\lambda_{Th-230}\Delta t) - \exp(-\lambda_{Ra-226}\,\Delta t)) \qquad (3.10.29)$$

The differential equation describing the dissolved radium concentration in the mixing zone can be written generally as:

$$\lambda_{mix}\,\epsilon\,(1+\rho_T K_{D,Ra}/\epsilon)\,\frac{d[Ra_L]_{mix}}{dt} = I_n[Ra]_{in} - I_n[Ra_L]_{mix} \qquad (3.10.30)$$

Integrating between t-Δt and t:

$$[Ra_L]_{mix,t} = [Ra]_{in,t} + ([Ra_L]_{mix,t-\Delta t}\exp(-\lambda_{Ra-226}\Delta t) - [Ra]_{in,t}) \exp[-I_n\Delta t/(\epsilon\,\lambda_{mix}(1+K_{D,Ra}\,\rho_T/\epsilon))] \qquad (3.10.31)$$

where

$[Ra_L]_{mix,t}$ = dissolved radium concentration in the mixing zone at time t ($mol.m^{-3}$)

$[Ra_L]_{mix,t-\Delta t}$ = dissolved radium concentration in the mixing zone in the previous time step ($t-\Delta t$) ($mol.m^{-3}$)

$K_{D,Ra}$ = solid-liquid distribution coefficient for radium ($m^3.g^{-1}$)

ϵ = tailings porosity

λ_{mix} = thickness of the mixing zone (m)

ρ_T = tailings bulk density ($g.m^{-3}$)

$[Ra]_{in,t}$ = concentration of radium resulting from inputs at time t ($mol.m^{-3}$) (via infiltration from above and/or ingrowth).

Note that a factor has been incorporated into the above equation to account for the radioactive decay of Ra-226 during each time step. The incorporation of such a "correction factor" is a relatively straightforward, though not fundamentally rigorous, method of including radioactive decay in such an equation. This approach is also used in layer 4 and in the calculations of dissolved Pb-210 concentrations in layers 3 and 4.

The value of $[Ra]_{in}$ depends on whether $BaSO_4$ has been depleted from (a) the unsaturated zone and (b) the mixing zone. Thus several cases can be identified.

Case 1: mixing zone contains $BaSO_4$

(a) unsaturated zone contains $BaSO_4$ (i.e. $h_{Ba} < \lambda_w$)

$$[Ra]_{in} = [Ra_L]_{\lambda w} + [Ra]^{Th}_{mix} \qquad (3.10.32)$$

(b) unsaturated zone depleted of $BaSO_4$ (i.e. $h_{Ba} \geq \lambda_w$)

$$[Ra]_{in} = \left\{ \frac{K^o_{s,BaSO_4}/f^2 \; X'_{Ra/BaSO_4}}{\sqrt{K^o_{s,BaSO_4}/f^2} + [SO_4^{2-}]_{mix}} \left(1 + K_{f,BaSO_4} f^2 [SO_4^{2-}]_{mix}\right) \right\} + [Ra]^{Th}_{mix}$$

In case 1 (b), $BaSO_4$ is dissolving in the mixing zone.

Case 2: mixing zone depleted of $BaSO_4$; unsaturated zone depleted of $BaSO_4$

$$[Ra]_{in} = [Ra]_{mix}^{Th} \qquad (3.10.34)$$

The latter situation (depletion of $BaSO_4$ in the mixing zone) is monitored by summing the radium inputs:

$$\sum_{t=0}^{t} [Ra]_{in} = \sum_{t=0}^{t-\Delta t} [Ra]_{in} + I_n \Delta t \, [Ra]_{in} \qquad (3.10.35)$$

The mixing zone is depleted of $BaSO_4$ when:

$$\sum_{t=0}^{t} [Ra]_{in} = \overset{o}{M}_{Ra} \qquad (3.10.36)$$

where

$\overset{o}{M}_{Ra}$ = total radium initially associated with $BaSO_4$ in the unsaturated and mixing zones ($mol.m^{-2}$).

The bottom layer is treated in a directly analagous fashion. One further simplifying assumption is that the bottom layer will not be depleted of soluble radium over the 1,000 year modelling period. Thus case 2 mentioned above does not have to be considered. The integrated mass balance for this layer is very similar to that for the mixing zone (equation (3.10.31)):

$$[Ra_L]_{4,t} = [Ra]_{in,4,t} + ([Ra_L]_{4,t-\Delta t} \exp(-\lambda_{Ra-226}\Delta t) - [Ra]_{in,4,t})$$
$$\exp\,[-I_4\, \Delta t/(\,\epsilon\, \lambda_4(1 + K_{D,Ra}\rho_T/\,\epsilon\,))] \qquad (3.10.37)$$

where

$[Ra_L]_{4,t}$ = dissolved concentration of radium in layer 4 ($mol.m^{-3}$)

I_4 = net infiltration rate into layer 4 ($m.yr^{-1}$)

$[Ra]_{in,4,t}$ = concentration of radium in porewater infiltrating layer 4 from above at time t ($mol.m^{-3}$).

The value for $[Ra]_{in,4}$ depends on$BaSO_4$ depletion in the mixing zone.

Case 1: mixing zone contains $BaSO_4$

$$[Ra]_{in,4} = [Ra_L]_{mix} + [Ra]_4^h \qquad (3.10.38)$$

Case 2: mixing zone depleted of $BaSO_4$

$$[Ra]_{in,4} = \left(\frac{K^o_{s,BaSO_4}/f^2 \; X'_{Ra/BaSO_4}}{\sqrt{K^o_{s,BaSO_4}/f^2} + [SO_4^{2-}]_4} \; (1+K_{f,BaSO_4} \; f^2[SO_4^{2-}]_4) \right) + [Ra]_4^h \qquad (3.10.39)$$

In case 2, $BaSO_4$ is dissolving in the bottom layer.

Again, all of these concentrations expressed in $mol.m^{-3}$ can be converted to an activity basis by multiplying by the conversion factor (RACF).

3.11 Lead

The solid and liquid phase concentrations of Pb-210 are modelled in a very similar fashion to Ra-226. Lead-210 is assumed to form a solid coprecipitate with lead sulphate ($PbSO_4$). This solid coprecipitate then dissolves in a frontwise manner, analagous to gypsum and barium sulphate. In fact, the solution is even more straightforward for Pb-210 since it forms an ideal solid solution and hence does not concentrate in the nondepleted layer. Because of the similarity in modelling approach, this section is presented in much less detail than the previous section. Many of the detailed derivations are omitted and only the functional relationships required for the simulation are presented.

3.11.1 Unsaturated Zone

As just mentioned, Pb-210 is assumed to coprecipitate with other lead ions in forming lead sulphate ($PbSO_4$). The relevant equilibrium expressions include:

$$PbSO_{4(s)} \rightleftharpoons Pb^{2+} + SO_4^{2-} \quad K^o_{s,PbSO4} = 1.2\times10^{-2}\ mol^2.m^{-6}$$

$$Pb^{2+} + SO_4^{2-} \rightleftharpoons PbSO_4^o\ (aq) \quad K_{f,PbSO4} = 5.01\times10^{-1}\ m^3.mol^{-1}$$

The total dissolved concentration of lead at the bottom of the unsaturated zone can be calculated as:

$$[Pb]_{T,\lambda w} = \frac{K^o_{s,PbSO_4}/f^2}{\sqrt{K^o_{s,PbSO_4}/f^2} + [SO_4^{2-}]_{u,\lambda w}} \left(1+f^2\ K_{f,PbSO_4}[SO_4^{2-}]_{u,\lambda w}\right) \qquad (3.11.1)$$

where

$[Pb]_{T,\lambda w}$ = total dissolved lead concentration at λ_w ($mol.m^{-3}$)

$K^o_{s,PbSO_4}$ = solubility product of $PbSO_4$ ($mol^2.m^{-6}$)

$K_{f,PbSO_4}$ = formation constant of $PbSO_4^o(aq)$ ($m^3.mol^{-1}$)

f = activity coefficient of divalent ions

$[SO_4^{2-}]_{u,\lambda w}$ = concentration of uncomplexed SO_4^{2-} at λ_w ($mol.m^{-3}$).

Having determined the total dissolved lead concentration, we can easily calculate the concentration of dissolved Pb-210. Since all elements form ideal solid solutions with their isotopes, we know that the mole fraction of Pb-210 is the same in the solid and liquid phases. That is, y=x, using the symbols defined previously in the radium discussion.

Having previously calculated the solid phase mole fraction of Pb-210 in $PbSO_4$, we can write:

$$[Pb\text{-}210_L]_{\lambda w} = X'_{Pb\text{-}210/PbSO_4}\ [Pb]_{T,\lambda w} + [Pb\text{-}210_L]^{Ra}_{\lambda w} \qquad (3.11.2)$$

where

$[Pb\text{-}210_L]_{\lambda w}$ = liquid phase concentration of Pb-210 at λ_w ($mol.m^{-3}$)

$X'_{Pb\text{-}210/PbSO_4}$ = mole fraction of Pb-210 in $PbSO_4$; corrected for radioactive decay of Pb-210, i.e.

$= X^o_{Pb\text{-}210/PbSO_4}\ \exp(-\lambda_{Pb\text{-}210}\ t)$

$[\text{Pb-210}_L]^{Ra}_{\lambda w}$ = liquid phase concentration of Pb-210 from Ra-226 decay in the unsaturated zone (mol.m^{-3}).

This last term, representing Pb-210 ingrowth from Ra-226 is calculated using a modified version of (equation (3.10.3):

$$[\text{Pb-210}_L]^{Ra}_{\lambda w} = [\text{Ra}_L]_{\lambda w}\left(\frac{\lambda_{Ra-226}}{\lambda_{Pb-210}-\lambda_{Ra-226}}\right)[\exp(-\lambda_{Ra-226}\Delta t)-\exp(-\lambda_{Pb-210}\Delta t)] \qquad (3.11.3)$$

where

$[\text{Ra}_L]_{\lambda w}$ = liquid phase concentration of Ra-226 at λ_w (mol.m^{-3}).

These expressions for the concentration of Pb-210 are valid as long as $PbSO_4$ is not depleted from the unsaturated zone. To determine this, we track the depth of the $PbSO_4$ depleted front with time. The movement of the $PbSO_4$ depleted layer (Δh_{Pb}) is given by an equation analagous to (equation (3.10.6).

Namely:

$$\Delta h_{Pb} = \left\{\frac{a^2\ (I_n\Delta t)}{[PbSO_4]^o}\left[\frac{I_n\Delta t}{B} + 2f^2K_{f,PbSO_4}h_{Pb}\right] + \frac{1}{4}\left[2h_{Pb} + \frac{a\ (I_n\Delta t)}{B} - \frac{a^2f^2K_{f,PbSO_4}}{[PbSO_4]^o}I_n\Delta t\right]^2\right\}^{1/2}$$

$$-\left[h_{Pb} + \frac{a\ I_n\Delta t}{2\ B} - \frac{a^2f^2K_{f,PbSO_4}\ I_n\Delta t}{2[PbSO_4]^o}\right] \qquad (3.11.4)$$

where

$a = \sqrt{K^o_{s,PbSO_4}/f^2}$

$B = [FeS_2]_{t-\Delta t}\ (1-e^{-k\Delta t})$.

The depth of depletion (h_{Pb}) is then:

$$h_{Pb,t} = h_{Pb,t-\Delta t} + \Delta h_{Pb} \qquad (3.11.5)$$

As in the radium calculations, we arbitrarily assumed that at t=0 the depth of $PbSO_4$ depletion was 1 cm (0.01 m).

Once the depth of depletion reaches the bottom of the unsaturated zone, no further $PbSO_4$ remains as a source of Pb-210. After this point, the dissolved concentration of Pb-210 results only from the decay of Ra-226. That is:

$$[\text{Pb-210}_L]_{\lambda w} = [\text{Pb-210}_L]^{Ra}_{\lambda w} \qquad \text{for } h_{Pb} \geq \lambda_w \qquad (3.11.6)$$

Unsaturated Zone: Solid Phase

We are interested in the solid phase concentration of Pb-210 in the $PbSO_4$ depleted layer only, since this acts as the source of airborne Pb-210. The sources of solid phase Pb-210 are the original insoluble Pb-210 inventory and Pb-210 which ingrows from solid phase Ra-226 in the same layer. The ingrowth can be written as:

$$[\text{Pb-210}_s]^{Ra}_{t} = [\text{Pb-210}_s]^{Ra}_{t-\Delta t} \exp(-\lambda_{\text{Pb-210}}\Delta t)$$
$$+[\text{Ra-226}_s]_1 \left(\frac{\lambda_{\text{Ra-226}}}{\lambda_{\text{Pb-210}}-\lambda_{\text{Ra-226}}}\right)\left(\exp(-\lambda_{\text{Ra-226}}\Delta t) - \exp(-\lambda_{\text{Pb-210}}\Delta t)\right) \qquad (3.11.7)$$

where

$[\text{Pb-210}_s]^{Ra}_{t}$ = cumulative solid phase concentration of Pb-210 resulting from ingrowth to time t ($mol.m^{-3}$)

$[\text{Pb-210}_s]^{Ra}_{t-\Delta t}$ = cumulative solid phase concentration of Pb-210 resulting from ingrowth to time t-Δt ($mol.m^{-3}$)

$[\text{Ra-226}_s]_1$ = solid phase concentration of Ra-226 in the $BaSO_4$ depleted layer at time t ($mol.m^{-3}$).

The total solid phase concentration of Pb-210 can then be calculated:

$$[\text{Pb-210}_s]_1 = [\text{Pb-210}_s]^{o}_{m} \exp(-\lambda_{\text{Pb-210}}t) + [\text{Pb-210}_s]^{Ra}_{t} \qquad (3.11.8)$$

where

$[\text{Pb-210}_s]_1$ = solid phase Pb-210 concentration in the $PbSO_4$ depleted layer (mol.m^{-3})

$[\text{Pb-210}_s]^o_m$ = initial concentration of Pb-210 associated with the host tailings material (mol.m^{-3}).

3.11.2 Layers 3 and 4

As with radium, the concentration of Pb-210 in the mixing zone and bottom layer depends on several factors, including the ingrowth of Pb-210 from dissolved Ra-226 in each layer. Again, we assume that as long as dissolved radium is entering from the layer above, there is no dissolved Pb-210 from radium decay present in the layer. That is:

$$[\text{Pb-210}_L]^{Ra}_{mix} = 0 \qquad \text{for } h_{Ra} < \lambda_w \qquad (3.11.9)$$

otherwise:

$$[\text{Pb-210}_L]^{Ra}_{mix} = [Ra_L]_{mix} \left(\frac{\lambda_{Ra\text{-}226}}{\lambda_{Pb\text{-}210} - \lambda_{Ra\text{-}226}} \right) (\exp(-\lambda_{Ra\text{-}226}\Delta t) - \exp(-\lambda_{Pb\text{-}210}\Delta t)) \qquad (3.11.10)$$

where

$[\text{Pb-210}_L]^{Ra}_{mix}$ = concentration of dissolved Pb-210 resulting from the decay of Ra-226 dissolved in the mixing zone (mol.m^{-3})

$[Ra_L]_{mix}$ = dissolved radium concentration in the mixing zone (mol.m^{-3}).

And analogously for the bottom layer (see Section 3.10.3):

$$[\text{Pb-210}_L]^{Ra}_4 = 0 \qquad \text{for } \sum_{t=0}^{t} [Ra]_{in} < M^o_{Ra} \qquad (3.11.11)$$

otherwise:

$$[\text{Pb-210}_L]^{Ra}_4 = [Ra_L]_4 \left(\frac{\lambda_{Ra\text{-}226}}{\lambda_{Pb\text{-}210} - \lambda_{Ra\text{-}226}} \right) [\exp(-\lambda_{Ra\text{-}226}\Delta t) - \exp(-\lambda_{Pb\text{-}210}\Delta t)] \qquad (3.11.12)$$

The equation describing the dissolved Pb-210 concentration in the mixing zone is similar to (equation (3.10.31)). Namely:

$$[\text{Pb-210}_L]_{mix,t} = [\text{Pb}]_{in,t} + ([\text{Pb-210}]_{mix,t-\Delta t}\exp(-\lambda_{\text{Pb-210}}\Delta t) - [\text{Pb}]_{in,t})$$

$$\exp[-I_n\Delta t/(\epsilon\lambda_{mix}(1+K_{D,Pb}\rho_T/\epsilon))] \qquad (3.11.13)$$

where

$[\text{Pb-210}_L]_{mix,t}$ = dissolved Pb-210 concentration in the mixing zone at time t ($mol.m^{-3}$)

$[\text{Pb-210}_L]_{mix,t-\Delta t}$ = dissolved Pb-210 concentration in the mixing zone in the previous time step ($t-\Delta t$) ($mol.m^{-3}$)

$K_{D,Pb}$ = solid-liquid distribution coefficient for lead ($m^3.g^{-1}$)

ϵ = tailings porosity

λ_{mix} = thickness of the mixing zone (m)

ρ_T = tailings density ($g.m^{-3}$)

$[\text{Pb}]_{in,t}$ = concentration of Pb-210 resulting from inputs (via infiltration from above and/or ingrowth) at time t ($mol.m^{-3}$).

Again, a term has been included in the equation to account for the radioactive decay of Pb-210 over the previous time step.

The value of $[\text{Pb}]_{in}$ depends on whether $PbSO_4$ has been depleted from (a) the unsaturated zone and (b) the mixing zone. Thus several cases can be identified.

Case 1: mixing zone contains $PbSO_4$

(a) unsaturated zone contains $PbSO_4$ (i.e. $h_{Pb}<\lambda_w$)

$$[\text{Pb}]_{in} = [\text{Pb-210}]_{\lambda w} + [\text{Pb-210}_L]^{Ra}_{mix} \qquad (3.11.14)$$

(b) unsaturated zone depleted of $PbSO_4$ (i.e. $h_{Pb} \geq \lambda_w$)

$$[Pb]_{in} = \left\{ \frac{K^{o}_{s,PbSO_4}/f^2 \; X'_{Pb\text{-}210/PbSO_4}}{\sqrt{K^{o}_{s,PbSO_4}/f^2 + [SO_4^{2-}]_{mix}}} \left(1 + K_{f,PbSO_4} f^2 [SO_4^{2-}]_{mix}\right) \right\} + [Pb\text{-}210_L]^{Ra}_{mix} \qquad (3.11.15)$$

In case 1 (b), $PbSO_4$ is dissolving in the mixing zone.

Case 2: mixing zone depleted of $PbSO_4$; unsaturated zone depleted of $PbSO_4$

$$[Pb]_{in} = [Pb\text{-}210_L]^{Ra}_{mix} \qquad (3.11.16)$$

The latter situation (depletion of $PbSO_4$ in the mixing zone) is monitored by summing the Pb-210 inputs:

$$\sum_{t=0}^{t} [Pb]_{in} = \sum_{t=0}^{t-\Delta t} [Pb]_{in} + I_n \Delta t \, [Pb]_{in} \qquad (3.11.17)$$

The mixing zone is depleted of $PbSO_4$ when:

$$\sum_{t=0}^{t} [Pb]_{in} = M^{o}_{Pb} \qquad (3.11.18)$$

where

M^{o}_{Pb} = total lead-210 initially associated with $PbSO_4$ in the unsaturated and mixing zones ($mol.m^{-2}$).

The bottom layer is treated in a directly analogous fashion. One further simplifying assumption is that the bottom layer will not be depleted of soluble lead-210 over the 1,000 year modelling period. Thus case 2 mentioned above does not have to be considered. The integrated mass balance for this layer is very similar to that for the mixing zone (equation 3.11.13):

$$[Pb\text{-}210_L]_{4,t} = [Pb]_{in,4,t} + \left([Pb\text{-}210_L]_{4,t-\Delta t} \exp(-\lambda_{Pb\text{-}210}\Delta t) - [Pb]_{in,4,t}\right) \exp\left[-I_4 \,\Delta t/(\epsilon \, \lambda_4(1 + K_{D,Pb}\rho_T/\epsilon))\right] \qquad (3.11.19)$$

where

$[Pb\text{-}210_L]_{4,t}$ = dissolved concentration of Pb-210 in layer 4 at time t ($mol.m^{-3}$)

I_4 = net infiltration rate into layer 4 ($m.yr^{-1}$)

$[Pb]_{in,4,t}$ = concentration of Pb-210 in porewater infiltrating layer 4 from above at time t ($mol.m^{-3}$).

ϵ = tailings porosity ($m^3 \cdot m^{-3}$).

The value for $[Pb]_{in,4}$ depends on $PbSO_4$ depletion in the mixing zone:

Case 1: mixing zone contains $PbSO_4$

$$[Pb]_{in,4} = [Pb\text{-}210_L]_{mix} + [Pb\text{-}210_L]_4^{Ra} \tag{3.11.20}$$

Case 2: mixing zone depleted of $PbSO_4$

$$[Pb]_{in,4} = \left(\frac{K^o_{s,PbSO4}/f^2 \; X'_{Pb\text{-}210/PbSO4}}{\sqrt{K^o_{s,PbSO4}/f^2} + [SO_4^{2-}]_4} \left(1 + K_{f,PbSO4} \, f^2 [SO_4^{2-}]_4\right) \right) + [Pb\text{-}210_L]_4^{Ra} \tag{3.11.21}$$

In this case, $PbSO_4$ is dissolving in the bottom layer.

Again, all of these concentrations expressed in $mol.m^{-3}$ can be converted to an activity basis by multiplying by the conversion factor (PBCF).

3.12 Input Parameter Values

The input parameters required by the water source model are summarized in Table 3.4. The table provides both the nominal (deterministic) and probabilistic values used in the water source model demonstration (Section 3.13), and in the complete probabilistic analysis described in Phase III, Volume I (SENES, 1986). References are provided for many of the values on Table 3.4. In most cases, these references provide an indication of the expected value of the parameter and its likely range. However, the references do not specify distribution shapes. These have been selected based on our

Table 3.4

WATER SOURCE MODEL INPUT PARAMETERS

Model Symbol	Description	Units	Nominal Value	Probability Distribution	Reference
A	tailings surface area	m^2	5×10^5	Constant 5×10^5	site characteristic
D_{O2}	oxygen diffusivity through tailings	$m^2.yr^{-1}$	45	Triangular min. = 4 mode = 45 max. = 115	See text (Section 3.12.2)
f	activity coefficient for divalent ions	--	0.5	Triangular min. = 0.4 mode = 0.5 max. = 0.6	See text (Section 3.12.3)
$[FeS_2]^o$	initial pyrite content of tailings	$mol.m^{-3}$	700.0	Uniform min. = 600.0 max. = 800.0	SENES, 1983 MacLaren, 1977
f_{Pb}	fraction of Pb-210 assumed to be ultimately soluble	--	0.81	Uniform min. = 0.76 max. = 0.86	See text (Section 3.12.9)
f_{Ra}	fraction of Ra-226 assumed to be ultimately soluble	--	0.60	Triangular min. = 0.25 mode = 0.6 max. = 0.95	See text (Section 3.12.8)
$f_{Th\text{-}230}$	fraction of Th-230 assumed to be ultimately soluble	--	0.80	Triangular min. = 0.65 mode.= 0.80 max. = 0.95	See text (Section 3.12.6)
$f_{Th\text{-}232}$	fraction of Th-232 assumed to be ultimately soluble	--	0.65	Triangular min. = 0.55 mode.= 0.65 max. = 0.75	See text (Section 3.12.7)
f_U	mass fraction of uranium recovered in the mill	--	0.92	Uniform min. = 0.90 max. = 0.94	MacLaren, 1977
$f_{U/Fe}$	fraction of uranium dissolved as a result of pyrite oxidation	--	0.6	Uniform min. = 0.30 max. = 0.90	SENES, 1983
K'	ratio of O_2 half saturation constant (K_{O2}) to $[O_2]$	--	5×10^{-2}	Uniform min.= 1×10^{-2} max.= 1×10^{-1}	Myerson, 1981
$K_{d,Ra}$	radium solid-liquid distribution coefficient	$m^3.g^{-1}$	4.5×10^{-5}	Lognormal Geom. mean = 4.5×10^{-5} Geom. S.D. = 1.5 min. = 1.3×10^{-6} max. = 1.52×10^{-4}	See text (Section 3.12.15)
K_{d,UO_2}	uranium solid-liquid distribution coefficient	$m^3.g^{-1}$	2×10^{-5}	Lognormal Geom. mean = 2×10^{-5} Geom. S.D. = 3.0 min. = 5×10^{-6} max. = 5×10^{-4}	See text (Section 3.12.15)
$K_{d,Pb}$	lead solid-liquid distribution coefficient	$m^3.g^{-1}$	6.0×10^{-5}	Lognormal Geom. mean = 6×10^{-5} Geom. S.D. = 1.5 min. = 2×10^{-5} max. = 1×10^{-4}	See text (Section 3.12.15)
$K_{f,PbSO_4}$	formation constant for $PbSO_4$(aq)	$m^3.mol^{-1}$	5.01×10^{-1}	Constant 5.01×10^{-1}	Sillen and Martell, 1971
$K_{f,BaSO_4}$	formation constant for $BaSO_4$(aq)	$m^3.mol^{-1}$	5.01×10^{-1}	Constant 5.01×10^{-1}	Sillen and Martell, 1971
$K^o_{s,BaSO_4}$	solubility constant for $BaSO_4$	$mol^2.m^{-6}$	1.07×10^{-4}	Constant 1.07×10^{-4}	Sillen and Martell, 1971
$K^o_{s,PbSO_4}$	solubility constant for $PbSO_4$	$mol^2.m^{-6}$	1.2×10^{-2}	Constant 1.2×10^{-2}	Sillen and Martell, 1971

Table 3.4, continued.

Model Symbol	Description	Units	Nominal Value	Probability Distribution	Reference
K_{Ra}	radium distribution between solid and liquid precipitate forms	--	0.53	Uniform min. = 0.5 max. = 0.56	See text (Section 3.10.2)
$K^o_{s,CaSO_4}$	solubility constant for $CaSO_4$	$mol.^2m^{-6}$	50	Constant 50	See text (Section 3.12.5)
m^o_{Th}	mass % of thorium (as ThO_2) in the ore	--	0.03	Uniform min. = 0.02 max. = 0.04	MacLaren, 1977
m^o_u	mass % of uranium (as U_3O_8) in the ore	--	0.1	Constant 0.1	MacLaren, 1977
$[O_2]$	oxygen concentration at the tailings surface	$mol.m^{-3}$	9.04	Constant 9.04	See text (Section 3.12.1)
P	annual net precipitation *	$m.yr^{-1}$	0.4	Normal mean = 0.4 Std. Dev. = 0.1 min. = 0.15 max. = 0.65	See text (Section 3.12.4)
$[PbSO_4]^o$	initial concentration of $PbSO_4$ in tailings	$mol.m^{-3}$	2.0	Triangular min. = 1.0 mode = 2.0 max. = 3.0	See text (Section 3.12.10)
R_s	initial sulphate production rate	$mol.g^{-1}yr^{-1}$	$4.1x10^{-6}$	Triangular min. = $3.0x10^{-6}$ mode.= $4.1x10^{-6}$ max. = $5.3x10^{-6}$	See text (Section 3.12.12)
X_{gyp}	initial mass fraction of gypsum in tailings	--	0.055	Uniform min. = 0.05 max. = 0.06	SENES, 1983 MacLaren, 1977
X_{Lime}	initial mass fraction of $CaCO_3$ in tailings	--		0.0005	site characteristic
$X^o_{Ra/BaSO_4}$	initial mole fraction of Ra-226 in $BaSO_4$	--	$1.2x10^{-5}$	Triangular min. = $6x10^{-6}$ mode = $1.2x10^{-5}$ max. = $1.8x10^{-5}$	See text (Section 3.12.10)
X_{rate}	fraction of R_s which occurs when calcite is present	---	0.10	Constant 0.10	See text (Section 3.12.13)
X_{run}	fraction of net precipitation which is surface runoff	---	0.15	Triangular (0.10,0.15,0.20)	See text (Section 3.12.14)
Λ_w	watershed area	m^2	$5x10^5$		
ρ_T	tailings bulk density	$g.m^{-3}$	$1.4x10^6$	Normal mean = $1.4x10^6$ Std.dev.=$0.1x10^6$ min. = $1.1x10^6$ max. = $1.7x10^6$	MacLaren, 1977
λ_w	thickness of the unsaturated zone	m	1.0	Uniform min. = 0.75 max. = 1.25	site characteristic
λ_{mix}	thickness of the mixing zone	m	1.5	Uniform min. = 1.0 max. = 2.0	site characteristic
λ_4	thickness of layer 4	m	7.5	Uniform min. = 5.0 max. 10.0	site characteristic

Note:

* Time variant parameter

best knowledge of the parameter values.

Other parameters are indicated on the table as "site characteristic". These parameter values (such as tailings area) are specified arbitrarily to represent the characteristics of the reference site. In general, only parameters representing dimension have been specified as site characteristics.

Finally, there are a number of parameters on Table 3.4 for which no reference is provided. These parameter values have been derived in other ways; either from fundamental principles or from a variety of sources. Brief explanations of the derivations of these parameter values are provided below.

3.12.1 $[O_2]$ - Concentration Of O_2 At The Tailings Surface

The O_2 concentration in air is calculated from the ideal gas low:

$$\frac{n}{V} = \frac{P_a}{RT} \tag{3.12.1}$$

where

n = number of moles

V = volume (1 m^3)

P_a = atmospheric pressure (1 atm)

R = gas low constant (82×10^{-6} $m^3.atm.mol^{-1}.K^{-1}$)

T = temperature (10°C = 283 K).

Solving equation (3.12.1) with the values indicated above gives the molar concentration of air at 10°C; namely 43 $mol.m^{-3}$. The oxygen concentration is a fraction (0.21) of the air concentration. Thus, the O_2 concentration at the tailings surface is 9.04 $mol.m^{-3}$.

3.12.2 D_{O2} - O_2 Diffusivity Through The Tailings

An equation for the effective oxygen diffusivity, D_e, through tailings has been developed by Reardon and Moddle (1985).

$$D_e = 630.7 \left(\frac{n_a - 0.05}{0.95} \right)^{1.7} \qquad (3.12.2)$$

where

D_e = effective oxygen diffusivity of the tailings ($m^2.yr^{-1}$)

n_a = air content of the tailings ($m^3_{air}.m^{-3}_{tailings}$)

and

$$n_a = \epsilon - n_w$$

where

ϵ = tailings porosity ($m^3_{void}.m^{-3}_{tailings}$)

n_w = volumetric water content of tailings ($m^3_{water}.m^{-3}_{tailings}$)

and

$$\epsilon = 1 - \rho_T/\rho_S$$

where

ρ_S = the particle density of the tailings; 2.6×10^6 ($kg.m^{-3}$)

ρ_T = soil bulk density ($kg.m^{-3}$).

Employing the nominal value for the soil bulk density, 1.4×10^6 $g.m^{-3}$ in the above equation yields a porosity of 0.46 $m^3.m^{-3}$.

Assuming a water content with a triangular distribution (min. 0.06 $m^3.m^{-3}$, mode 0.21 $m^3.m^{-3}$, and max. of 0.36 $m^3.m^{-3}$) results in an effective diffusivity with a minimum of 4 $m^2.yr^{-1}$, a mode of 45, and a maximum of 115 $m^2.yr^{-1}$.

3.12.3 f - Activity Coefficient For Divalent Ions

Activity coefficients were assigned probabilistic attributes based upon computed ionic strength of typical porewater, using the Debye-Huckel equation, (see SENES and Beak, 1986), and an assumed ±10% standard deviation for their values.

The calculations indicate a minimum of approximately 0.4, an expected value of approximately 0.5 and a maximum of about 0.6. Again, a triangular distribution was selected.

3.12.4 P - Annual Net Precipitation

The distribution derived for annual net precipitation is based on meteorological data from Gore Bay, Ontario, which is located on Manitoulin Island. Annual net precipitation data for the years 1947 to 1983 were analyzed to obtain the parameter distribution. A normal distribution was found to fit the data well.

In the model simulations, annual net precipitation (P) is treated as a "time-varying parameter". That is, a new value for P is sampled for each time step. The distribution indicated in Table 3.4 is appropriate as long as a 1 year time step is used. For longer time steps, the distribution must be adjusted.

In particular, the standard deviation must be corrected to give a "narrower" distribution as outlined in the Phase II study (SENES, 1985a):

$$S.D.' = S.D / (\Delta t)^{0.5} \qquad (3.12.4)$$

where

S.D.' = standard deviation corrected for $\Delta t \neq 1$

S.D = standard deviation for $\Delta t = 1$ year

Δt = simulation time step.

3.12.5 Gypsum Solubility Constant

The published solubility product (K_s^o) for gypsum is 25 $mol^2.m^{-6}$. This value refers to zero ionic strength and does not take into account the complexation reactions of calcium in the liquid phase. The most important of these reactions is the complexation with sulphate. To account for these complexation reactions, a higher apparent solubility product of 50 $mol^2.m^{-6}$ is used. This value was selected as it was found to give better agreement with in situ observations.

3.12.6 f_{Th-230} - Fraction of Th-230 Assumed to be Ultimately Soluble

Isotopes of the uranium-238 decay chain (including Th-230, Ra-226 and Pb-210) are assumed to be present, in the host ore, in the same mineral matrix as the U-238 host ore. These isotopes would dissolve in the highly acidic environment of the leaching pachucas. The extent of the Th-230 dissolution is essentially identical with the uranium species (Melis and SENES, 1986). During the neutralization step, Th-230 would precipitate. Due to its chemistry, however, Th-230 coprecipitates with other thorium isotopes (mainly Th-232), forming a secondary thorium mineral, primarily $Th(OH)_4$. Since thorium solubility declines very rapidly above pH = 3.5, virtually all thorium would precipitate in this manner. The subsequent re-solution of Th-230 is essentially stoichiometric, depending on the mole fraction. However, solubility studies by Melis and SENES (1986) indicate, that on the average 87% of the reprecipitated Th-230 is subject to re-solution in the tailings, resulting in an average ultimately soluble mole fraction of 0.80 (assuming that 92% of the Th-230 in the original ore was dissolved in the mill). The distribution is assumed to be triangular ranging from 0.65 to 0.95. The upper limit implies, that all the Th-230 that dissolved in the mill is ultimately soluble in the tailings.

3.12.7 f_{Th-232} - Fraction of Th-232 Assumed to be Ultimately Soluble

Approximately two-thirds of the Th-232 is dissolved during the milling process. The remainder is associated with very stable minerals such as monazite. All of the Th-232 dissolved in the mill is assumed to be ultimately soluble in the tailings. Taking 65% as a nominal value, a triangular distribution with relatively narrow limits, minimum of 0.55 and maximum of 0.75, was assigned.

3.12.8 f_{Ra} - Fraction of Radium-226 Assumed to be Ultimately Soluble

Since radium-226 is associated with the uranium ore, 92% of the radium is expected to dissolve during the uranium leaching process. Radium dissolution from the host ore is incongruent and most of the dissolved radium coprecipitates with barium as Ba(Ra)SO_4 and possibly other solid solutions. In theory, up to 92% of this radium coprecipitate is subject to redissolving in the tailings. Experimental work however, has shown that only 50% to 75% of the radium-226 is ultimately leachable from the tailings in high salt solutions and substantially less under more natural conditions (Silver and Ritcey, 1980). In view of these observations, the ultimately soluble fraction of radium-226 has been assumed to be 0.6 with a triangular distribution ranging from 0.25 to 0.95.

3.12.9 f_{Pb} - Fraction of Lead-210 Assumed to be Ultimately Soluble

The fate of the lead-210 isotope during uranium processing is similar to thorium. Lead-210 would form a secondary mineral with other lead isotopes as lead sulphates ($PbSO_4$). These isotopes would behave as ideal solid solutions. This implies that the mole fraction of the isotope Pb-210 in the solid and the liquid phases is identical. The nominal ultimately soluble mole fraction is expected to be 0.81. As in the case of other mineral phases, the distribution is assumed to be triangular with lower and upper limits of 0.76 and 0.86 respectively. The solubility of the ultimately soluble lead fraction, hence the Pb-210 isotope, is assumed to be equilibrium controlled.

3.12.10 $X^o_{Ra/BaSO_4}$ - Initial Mole Fraction of Ra-226 in $BaSO_4$

Recent evidence by Beak (1985) suggests that radium-226 coprecipitates as a solid solution of Ba(Ra)SO_4. It may be reasoned that the small Ba(Ra)SO_4 crystals are occluded in gypsum or other secondary minerals in the tailings. Assuming a homogeneous solid solution of Ba(Ra)SO_4, the authors (Beak, 1985) estimated a minimum radium-226 mole fraction of approximately 2.5×10^{-6} and an average of about 3.3×10^{-6} for Ra-226 in Ba(Ra)SO_4. Analysis of the database presented by Skeaff (1977) yields a mole fraction of 4.5×10^{-6} Ra-226 as the upper limit.

Field data, however, indicates the radium-226 mole fraction to be in the range of 1.2×10^{-5} (Beak, 1985). Hence, a triangular distribution with a minimum value of 6×10^{-6}, a mode of 1.2×10^{-5}, and a maximum of 1.8×10^{-5} was assumed.

3.12.11 $[PbSO_4]^o$ - Initial Concentration of $PbSO_4$ In The Tailings

The initial lead sulphate concentration has been calculated from laboratory digestion experiments of tailings solids by Beak (1985). For example, the digestion of 1:3 (solids:liquid) ratio with 3 M HNO_3 as eluent produced an average concentration of 98 mg/L of Pb in the liquid phase. Since $PbSO_4$ is soluble in HNO_3, the corresponding $PbSO_4$ concentration would be:

$$\left(\frac{98 \text{ mg Pb}}{\text{L}}\right) \left(\frac{3 \text{ L}}{1 \text{ kg tailings}}\right) \left(\frac{1 \text{ g}}{1{,}000 \text{ mg}}\right) \left(\frac{1 \text{ mole } PbSO_4}{207.19 \text{ g Pb}}\right) \left(\frac{1{,}400 \text{ kg tailing}}{\text{m}^3 \text{ tailings}}\right)$$

$$= 1.99 \frac{\text{moles } PbSO_4}{\text{m}^3 \text{ tailings}} \qquad (3.12.5)$$

A range of concentrations from 68 to 136 mg/L of Pb in the liquid phase was observed in the study. Based on this information, a triangular distribution was assumed, with a mode of 2 $mol.m^{-3}$; ranging from 1 to 3 $mol.m^{-3}$.

3.12.12 Initial Sulphate Production Rate (FeS_2 Oxidation)

The rate of bacterially-assisted pyrite oxidation, R_s, is a function, f, of several biological and environmental parameters (Hoffman et al., 1981; Halbert et al., 1983; Jaynes et al., 1984; SENES, 1985a; SENES, 1986). It may be stated by:

$$R_s = f(X_p, Y_{x/s}, pH, T, P_{O2}, P_{CO2}, S, [N], [P], E_a, A, [I]) \qquad (3.12.6)$$

where

R_s = rate of sulphate production ($mol.m^{-2}.mth^{-1}$)

X_p = bacterial population density (g biomass per m^2)
$Y_{x/s}$ = growth yield coefficient (g biomass per mol.pyrite)
pH = measure of hydronium concentration
T = soil temperature (°K)
P_{O2} = oxygen partial pressure (atm)
P_{CO2} = carbon dioxide partial pressure (atm)
S = degree of saturation ($m^3_{water} \cdot m^{-3}_{void}$)
[N] = nitrate or ammonia concentration ($mol.m^{-3}$)
[P] = phosphorus concentration ($mol.m^{-3}$)
E_a = biological energy of activation ($cal.mol^{-1}$)
A = surface area of pyrite (m^2)
[I] = inhibitor concentration ($mol.m^{-3}$).

A model which takes into account the aforementioned biological and environmental parameters is the Reactive Acid Tailings Assessment Program, RATAP (SENES and BEAK, 1986). RATAP size and memory requirements make its use in the UTAP code inappropriate for a microcomputer system. Its predictive capability, however, can be used to estimate the sulphate production rate under both the presence or absence of calcite ($CaCO_3$). It is emphasized that the RATAP model was employed in this study to generate a range of "generic" sulphate production rates. Hence, it is not necessary for a user to run RATAP as a prelude to using UTAP.

Three major shifts in the tailings properties that affect the porewater pH and sulphate production rate are distinguishable. During the first stage, the presence of calcite buffers the pH near neutrality, i.e., approximately 6.5, and the rate of sulphate production is chemically controlled. Depending upon the mass fraction of lime initially present, this period may occur within a layer of tailings, i.e. approximately 0.5 m, for a period of one to four years.

In the second stage which begins when the calcite has been depleted, the pH drops to approximately 3.0, and the rate of sulphate production is biologically controlled. Depending upon the mass fraction of aluminum hydroxide present, this period may last from one to three years. It is during this period that high rates of sulphate production have been observed.

In the third stage, both the calcite and aluminum hydroxide have been depleted. In this stage the pH drops to approximately 2.0, and the overall rate of sulphate production is influenced by both chemical and biological processes. Ferric hydroxide or jarosite dissolution may provide some buffering. This period may last for decades.

Table 3.5 presents typical monthly rates of sulphate production for three depths during the three stages of a tailings life in the Elliot Lake area. Detailed discussion of the input parameters and algorithms used to generate these typical rates are given in the SENES and Beak (1986) report. The monthly variation in the rates results from the rate of sulphate oxidation having a strong temperature dependence.

The results indicate that the average sulphate production rates (averaged by month and depth) are approximately $3.96\text{x}10^{-7}$ $\text{mol.g}^{-1}.\text{yr}^{-1}$ for stage 1, 1.84×10^{-6} $\text{mol.g}^{-1}.\text{yr}^{-1}$ for stage 2 and 6.56×10^{-7} $\text{mol.g}^{-1}.\text{yr}^{-1}$ for stage 3.

Employing the stage 1 value, 1.84×10^{-6} $\text{mol.g}^{-1}.\text{yr}^{-1}$, to represent the initial sulphate production rate during conditions in which calcite is absent underestimates the sulphate levels (SENES, 1987; Appendix A). For pyrite levels of 600 mol.m^{-3} to 800 mol.m^{-3}, the corresponding R_s values equal 3.0×10^{-6} $\text{mol.g}^{-1}.\text{yr}^{-1}$ to 5.3×10^{-6} $\text{mol.g}^{-1}.\text{yr}^{-1}$. The probability distribution for the initial rate of sulphate production (R_s) when there is no calcite present has been assumed to be triangular. The mode used was 4.1 x $\text{mol.g}^{-1}.\text{yr}^{-1}$ (representing a pyrite content of 700 mol.m^{-3}) with minimum and maximum values of 3.0×10^{-6} $\text{mol.g}^{-1}.\text{yr}^{-1}$ and 5.3×10^{-6} $\text{mol.g}^{-1}.\text{yr}^{-1}$, respectively.

3.12.13 Rate Fraction

When calcite is present a rate fraction term, X_{rate}, is used to calculate the

Table 3.5

RATES OF SULPHATE PRODUCTION*

Stage	Depth	Rate of Sulphate Production ($mol.g^{-1}.yr^{-1}$)												
		Month												Monthly
	(m)	Jan.	Feb.	Mar.	Apr.	May	June	July	Aug.	Sept.	Oct.	Nov.	Dec.	Avg.
1: calcite	0.2 m	1.2×10^{-7}	6.8×10^{-8}	1.1×10^{-7}	3.5×10^{-7}	6.5×10^{-7}	1.0×10^{-6}	1.2×10^{-6}	1.1×10^{-6}	6.9×10^{-7}	3.5×10^{-7}	1.6×10^{-7}	4.4×10^{-8}	4.9×10^{-7}
controlled	1.0 m	2.3×10^{-7}	9.1×10^{-8}	1.1×10^{-7}	2.4×10^{-7}	3.6×10^{-7}	5.2×10^{-7}	6.8×10^{-7}	7.3×10^{-7}	6.3×10^{-7}	4.6×10^{-7}	2.9×10^{-7}	1.1×10^{-7}	3.7×10^{-7}
	1.6 m	3.4×10^{-7}	1.3×10^{-7}	1.3×10^{-7}	2.2×10^{-7}	2.8×10^{-7}	3.7×10^{-7}	4.7×10^{-7}	5.4×10^{-7}	5.4×10^{-7}	4.7×10^{-7}	3.5×10^{-7}	1.4×10^{-7}	3.3×10^{-7}
														3.96×10^{-7}
2: aluminum	0.2 m	2.1×10^{-8}	2.6×10^{-8}	4.3×10^{-8}	9.7×10^{-7}	2.2×10^{-6}	4.2×10^{-6}	5.4×10^{-6}	1.8×10^{-6}	1.3×10^{-6}	1.1×10^{-6}	7.1×10^{-7}	2.7×10^{-8}	1.5×10^{-6}
hydroxide	1.0 m	3.1×10^{-8}	3.3×10^{-8}	3.7×10^{-8}	9.9×10^{-7}	1.6×110^{-6}	2.7×10^{-6}	3.7×10^{-6}	4.2×10^{-6}	3.7×10^{-6}	2.8×10^{-6}	1.8×10^{-6}	9.7×10^{-7}	1.9×10^{-6}
controlled	1.6 m	1.4×10^{-6}	1.1×10^{-6}	1.1×10^{-6}	1.3×10^{-6}	1.6×10^{-6}	2.2×10^{-6}	3.0×10^{-6}	3.5×10^{-6}	3.6×10^{-6}	3.2×10^{-6}	2.4×10^{-6}	1.5×10^{-6}	2.2×10^{-6}
														1.86×10^{-6}
3: ferric	0.2 m	2.1×10^{-8}	2.4×10^{-8}	4.1×10^{-8}	1.1×10^{-6}	1.4×10^{-6}	1.4×10^{-6}	1.6×10^{-6}	1.7×10^{-6}	1.3×10^{-6}	1.0×10^{-6}	6.6×10^{-7}	3.1×10^{-8}	8.5×10^{-7}
hydroxide	1.0 m	4.0×10^{-8}	3.6×10^{-8}	4.0×10^{-8}	5.0×10^{-7}	7.3×10^{-7}	9.2×10^{-7}	1.0×10^{-6}	1.2×10^{-6}	9.8×10^{-7}	7.3×10^{-7}	4.7×10^{-7}	2.7×10^{-7}	5.7×10^{-7}
controlled	1.6 m	2.7×10^{-7}	2.2×10^{-7}	2.1×10^{-7}	2.8×10^{-7}	4.4×10^{-7}	6.7×10^{-7}	8.3×10^{-7}	9.3×10^{-7}	9.5×10^{-7}	7.8×10^{-7}	6.0×10^{-7}	3.7×10^{-7}	5.5×10^{-7}
														6.56×10^{-7}

Note

* Calculations from RATAP model; SENES and Beak (1986).
Initial conditions are: 6.0% pyrite, 5.0% gypsum, 0.23% basaluminate, 13.6% sericite and 0.05% calcite.

rate of sulphate production:

$$J_s' = X_{rate}\left(\frac{8}{7.5}\ R_s\ .\ \rho_T\ [O_2]\ D_{O2}\ \ 1 - k'\ \ln\left(\frac{1 + k'}{k}\right)\right)^{1/2} \qquad (3.12.7)$$

where

X_{rate} = rate fraction (unitless)
J_s' = sulphate flux when calcite is present ($mol.m^{-2}.yr^{-1}$)
R_s = sulphate production rate ($mol.g^{-1}.yr^{-1}$)
$[O_2]$ = oxygen concentration on the surface ($mol.m^{-3}$)
D_{O2} = oxygen diffusivity through tailings ($m^2.yr^{-1}$)
ρ_T = density of tailings ($g.m^{-3}$)
k' = $K_{O2}/[O_2]$ = ratio of O_2 half saturation constant to the oxygen concentration $[O_2]$.

Employing the rates of sulphate production during stages 1 and 2 to present calcite and no calcite conditions resulted in an X_{rate} value of 0.46. However, analysis of field data, (SENES, 1987, Appendix A), indicated that an X_{rate} value of 0.10 gave the "best fit" between model outputs and measured parameters, i.e. pyrite content and calcite content.

3.12.14 Surface Runoff Fraction

The nominal value of 0.15 for the surface runoff was determined using the Hydrologic Evaluation of Landfill Performance (HELP) model (U.S. Army Corps of Engineers, 1986). A triangular distribution was assumed with a minimum of 0.10, a mode of 0.15 and a maximum of 0.20.

3.12.15 K_d - Solid-Liquid Distribution Coefficient

It is generally observed that radionuclides and other trace cationic constituents speciate between the liquid (porewater) and the solid phases. If the intrinsic properties of a closed system are held constant, this speciation reaches an equilibrium distribution in a relatively short time period, often less than 48 hours. Traditionally, the equilibrium position is evaluated as a ratio of solid phase to liquid phase concentrations. The concentration isotherms are assumed to be linear and are characterized by a distribution coefficient.

This distribution coefficient (K_d value) is recognized to be dependent on numerous intrinsic variables (contaminant, temperature, pH, ionic strength, contaminant concentration, etc.) and should be regarded as an empirical constant specific to the system in question. Being empirical in nature, the distribution coefficient does not explicitly take into account the controlling transport mechanism (adsorption, ion exchange, coprecipitation) between the liquid and the solid phases. Nevertheless, the concept of K_d has been found to be convenient to model the mobility (or retardation) of trace constituents in groundwaters. In the following sections the effect of solid/liquid transport mechanisms of Ra-226, Pb-210 and UO_2^+ on the apparent K_d in the tailings porewater (mixing layer and layer 4) is discussed. (It should be noted that the concentrations of these radionuclides are modelled explicitly in the two unsaturated zones.) The K_d for total thorium is strongly influenced by pH. Section 3.9.1 presents a detailed discussion on thorium solubility at acidic pH thorium values.

i) Radium-226

Recent evidence (Beak, 1985) indicates that the mobility of dissolved Ra-226 is controlled by coprecipitation (i.e. solid solution) of Ra-226 in barite ($BaSO_4$). Their work suggests that low grade, pyritic tailings contain approximately 0.3 mol.m^{-3} (3 x 10^{-4} mol.dm^{-3}) $BaSO_4$ and an initial mole fraction of Ra-226 in the barite of about 3.5 x 10^{-6}.

Barite in tailings is believed to be present as microcrystals occluded in gypsum or other host mineral. It seems reasonable to assume that, at any given time, only a fraction of the solid barite is involved in coprecipitation. We assume a nominal value of 1% (3.0 x 10^{-6} mol.dm^{-3}) $BaSO_4$, recognizing that it may vary with time, first increasing as the host mineral (gypsum) is dissolved (more barite is exposed) then decreasing after 99% of the barite in the mixing zone has gone into solution. Since the coprecipitation mechanism is the most significant when the radium-rich barite is nearly depleted in the unsaturated zone (layer 2), the porewater entering the mixing zone would be saturated with respect to barium. For illustration, this water is assumed to contain 4 x 10^{-10} M (3,350 Bq.L^{-1}) dissolved Ra-226. This concentration can be varied considerably, since the solid/liquid equilibrium distributions, calculated by the coprecipitation mechanism, are relatively insensitive with regard to this initial Ra-226 concentration in the liquid. In any case, the radium-226 input into the pore space (1.6 x 10^{-7} mol.m^{-3} at a porosity of 0.4) represents approximately 15% of the nominal radium-226 reservoir in the unsaturated zone.

The coprecipitation mechanism involves the formation of a solid solution of $RaSO_4$ in barite ($BaSO_4$). The solution of $RaSO_4$ in the $BaSO_4$ lattice is nearly ideal (Stumm and Morgan, 1981) and, at trace $RaSO_4$ mole fractions, the equilibrium ratio between the solid and the liquid phase is given by the distribution constant, D, as follows:

$$D = \left[\frac{\dfrac{[RaSO_4]_S}{[BaSO_4]_S}}{\dfrac{[Ra]_L}{[Ba]_L}}\right] \qquad (3.12.4)$$

where

$[RaSO_4]_S/[BaSO_4]_S$ = the molar ratio of radium-226 in barite

$[Ra]_L/[Ba]_L$ = the ratio of radium-226 to barium concentrations in the liquid phase

D = distribution constant (=1.8 for $RaSO_4$ in $BaSO_4$; the experimentally observed value of D in the present system).

It can be easily shown that, if the mole fraction of radium-226 in the solid phase is small, the molar ratios are numerically equal to the mole fractions. Rearranging equation (3.12.4) yields the moles of radium-226 in the solid solution as follows:

$$[RaSO_4]_s = D \frac{[BaSO_4]_s}{[Ba]_L} [Ra]_L \qquad (3.12.5)$$

Since the activity of barium in the solid phase (Ba_{1-x} Ra_x SO_4; $x = 3.5 \times 10^{-6}$) is essentially unity, the concentration of barium in the saturated solution depends solely on the solubility product of the end member. The formation constants of aqueous barium and radium sulphate species ($BaSO_4$(aq), log K = 2.7 and $RaSO_4$ (aq), log K = 2.74) are virtually identical. Consequently, the molar ratio of radium to barium in the liquid phase does not depend on the sulphate $[SO_4^{2-}]$ concentration. It is therefore sufficient to estimate only the concentration of total dissolved barium in solution.

Assuming a nominal sulphate concentration of 1.5×10^{-2} M and an activity coefficient of 0.4 (nominal value) in the porewater, the following solution and speciation equilibria are relevant:

$$BaSO_{4(s)} \rightleftharpoons Ba^{2+} + SO_4^{2-} \qquad \log K = -9.97$$

$$Ba^{2+} + SO_4^{2-} \rightleftharpoons BaSO_4^0(aq) \qquad \log K = 2.7$$

$$[Ba^{2+}] = 4.46 \times 10^{-8}\ M$$

$$[BaSO_4] = 5.36 \times 10^{-8}\ M \qquad (3.12.6)$$

$$[Ba]_L = 9.82 \times 10^{-8}\ M \text{ (total barium in solution)}$$

Substituting for $[BaSO_4]_s$ and $[Ba]_L$ in equation (3.12.5) yields:

$$[RaSO_4]_s = (1.8) \frac{3 \times 10^{-6}}{9.82 \times 10^{-8}} [Ra]_L = 55\ [Ra]_L \qquad (3.12.7)$$

At this point, the equilibrium concentration of radium-226 in the liquid phase can be calculated by material balance as follows:

$$55\ [Ra]_L + \epsilon\, [Ra]_L = \epsilon\, [Ra]^0 \qquad (3.12.8)$$

Substituting for $[Ra]^{o} = 4 \times 10^{-10}$ M

and

$$\epsilon = 0.4$$

yields $$[Ra]_L = \frac{(0.4)\ (4 \times 10^{-10})}{55 + 0.4} = 2.89 \times 10^{-12} \text{ M Ra-226}$$

Note that equation (3.12.8) is analogous to conventional expressions employing K_d values. In fact, coprecipitation is phenomenologically indistinguishable from adsorption mechanisms if one member of the solid solution (coprecipitate) is present in trace amounts. It can be shown that the characteristic K_d value for the system containing 1.4×10^6 $g.m^{-3}$ solids is given by:

$$K_d = \frac{\dfrac{0.4\ (4 \times 10^{-10} - 2.89 \times 10^{-12})}{1.4 \times 10^6}}{2.89 \times 10^{-12}} = 3.93 \times 10^{-5}\ m^3.g^{-1} \qquad (3.12.9)$$

An upper limit of K_d may be obtained by evaluating the equilibrium expressions at higher barite concentrations. It may be noted, that a higher sulphate concentration (3×10^{-2} M SO_4^{2-}, for example) has only a marginal effect on the coprecipitation equilibrium, since the formation of the sulphate complexes (both $BaSO_4$ and $RaSO_4$) in the liquid phase become predominant. Using $6\times10^{-3}mol.m^{-3}$ $BaSO_{4(s)}$ in equations (3.12.7) and (3.12.8) would yield a liquid phase Ra-226 concentration of 1.45×10^{-12} M and a corresponding K_d value (equation (3.12.9)) of 78.6×10^{-5} $m^3.g^{-1}$. A lower limit value of K_d is established by purely adsorption mechanisms as 5×10^{-6} $m^3.g^{-1}$ (NRC, 1983).

Radium-226 K_d values of 2×10^{-5} $m^3.g^{-1}$ (Veska, 1983) and 7×10^{-5} $m^3.g^{-1}$ (Morin et al., 1982) have been reported for pH conditions of 3.5 to 4.5.

Employing the aforementioned calculated and literature K_d values for radium-226, a lognormal distribution with a nominal value of 4.5×10^{-5} $m^3.g^{-1}$, a standard deviation of 1.5, and a minimum value of 1.3×10^{-6} $m^3.g^{-1}$ and maximum value of 1.5×10^{-4} $m^3.g^{-1}$ was assumed.

ii) Lead-210

The obvious choice for lead-210 coprecipitation is in a solid solution with its stable isotopes. In pyritic uranium tailings, solid lead sulphate ($PbSO_4$) would be the most likely mineral participating in such an event. Lead isotopes tend to form ideal solid solutions with a characteristic distribution constant of unity (D=1). Applying solid solution theory for lead sulphates the distribution between the solid phase and the liquid phase, at equilibrium, is given by:

$$D = \left[\frac{\dfrac{[Pb^{210}SO_4]_S}{[PbSO_4]_S}}{\dfrac{[Pb^{210}]_L}{[Pb]_L}}\right] = 1 \qquad (3.12.10)$$

where

$[Pb^{210}SO_4]_S$ = concentration of Pb-210 in the solid $[PbSO_4]$ phase ($mol.m^{-3}$)

$[PbSO_4]_S$ = total lead sulphate concentration in the solid phase ($mol.m^{-3}$)

$[Pb^{210}]_L$ = concentration of Pb-210 in the liquid phase ($mol.m^{-3}$)

$[Pb]_L$ = concentration of total dissolved lead in the liquid phase ($mol.m^{-3}$).

The nominal concentration of lead sulphate solids in the tailings is estimated to be 2 $mol.m^{-3}$ $PbSO_4$. The liquid phase concentration is dependent on the sulphate concentration $[SO_4^{2-}]$ and the activity coefficients of Pb^{2+} and SO_4^{2-}. As in case of $BaSO_4$ solubility, the solution equilibrium and speciation of lead in the liquid phase involves the following reactions:

$$PbSO_4 \rightleftharpoons Pb^{2+} + SO_4^{2-} \qquad \log K = -7.7$$
$$Pb^{2+} + SO_4^{2-} \rightleftharpoons PbSO^{o}_{4(aq)} \qquad \log K = 2.7 \qquad (3.12.11)$$

Using a nominal sulphate (SO_4^{2-}) concentration of 1.5×10^{-2} M and an activity coefficient of 0.4 for both Pb^{2+} and SO_4^{2-}, the equilibrium expressions (equation (3.12.11)) yield 8.36×10^{-6} M Pb^{2+} and 1.05×10^{-5} M $PbSO^0_{4(aq)}$ as dissolved species (total dissolved lead = 1.83×10^{-5} M).

It is assumed, that approximately 50% of the solid $PbSO_4(s)$ ($1.0\ mol.m^{-3}$) participates in exchange reactions. The remaining solid $PbSO_4$ is assumed to be occluded by gypsum or other secondary precipitates. The distribution of Pb-210 in the solid and liquid phases can be obtained directly (equation (3.12.10) as follows:

$$\frac{[Pb^{210}SO4]s}{[Pb^{210}]_L} = \frac{10^{-3}}{1.83 \times 10^{-5}} = 54.64 \quad 1 \qquad (3.12.12)$$

At a tailings bulk density of $1.4 \times 10^6\ g.m^{-3}$, the apparent K_d value would be:

$$K_d = \frac{54.64}{1.4 \times 10^6} = 3.9 \times 10^{-5}\ m3.g^{-1} \qquad (3.12.13)$$

The driving force for coprecipitation reactions of Pb-210 in $PbSO_4$ is provided by the relatively short half-life of the Pb-210 isotope. Unlike Ra-226, the initial Pb-210 content of the solid phase in the mixing zone is assumed to approach zero prior to $PbSO_4$ depletion from the unsaturated zone. If the Pb-210 in $PbSO_4$ is not zero or the solid $PbSO_4$ content of the mixing zone is partially depleted (solid $PbSO_4$ concentration = $0.5\ mol.m^{-3}$) the apparent K_d value would be $2 \times 10^{-5}\ m^3.g^{-1}$. It has been shown by Veska (1983), that the apparent K_d of Pb-210 in sandy soils at acidic pH values ($pH<5.0$) is $1 \times 10^{-4}\ m^3.g^{-1}$. Consequently, the K_d for Pb-210 is assumed to range from $2 \times 10^{-5}\ m^3.g^{-1}$ to $1 \times 10^{-4}\ m^3.g^{-1}$ with a geometric mean of $6 \times 10^{-5}\ m^3.g^{-1}$ and a geometric standard deviation of 1.5 (lognormal distribution). This particular range takes into account either co-precipitation or adsorption mechanisms.

iii) UO_2^+

Veska (1983) has reported several K_d values at different pH levels using solutions representative of waste-rock-influenced groundwater: pH=3, 7.8×10^{-6} $m^3.g^{-1}$; pH=4, 1.6×10^{-5} $m^3.g^{-1}$; and pH=5, 1.9×10^{-4} $m^3.g^{-1}$. Rancon (1983) reported a K_d range of 1.6×10^{-4} $m^3.g^{-1}$ to 2.7×10^{-4} $m^3.g^{-1}$. The NRC (1983) presented a mean uranium K_d value of 2×10^{-5} $m^3.g^{-1}$ with a range of 5×10^{-5} $m^3.g^{-1}$ to 5×10^{-4} $m^3.g^{-1}$.

Hence, for uranium, a lognormal distribution with a nominal value of 2×10^{-5} $m^3.g^{-1}$, a standard deviation of 3, and minimum and maximum values of 5.0×10^{-5} $m^3.g^{-1}$ and 5×10^{-4} $m^3.g^{-1}$, respectively, was used.

3.12.16 Half-Lives

Table 3.6 presents the half-lives, $t_{1/2}$, of the radionuclides which were used in UTAP to determine the radioactive decay constants, λ, for the respective radionuclides.

3.13 Water Source Model Demonstration

Validation of a large and complex model, such as that described in this chapter, is recognized to be a difficult task. Furthermore, it is impossible to validate model predictions made hundreds of years into the future. In lieu of model validation, a model demonstration exercise was completed to gain confidence in the water source term model before integrating it into the system model. Both deterministic and probabilistic trials were performed during the demonstration. The deterministic demonstration used the nominal values for all input parameters, while the probabilistic demonstration involved 200 random simulation trials. Since the deterministic (nominal) input values are generally very similar to the expected value of an input parameter distribution, the deterministic and probabilistic results may be very similar. The deterministic results provide a basis for comparison with other implementation of the model and may be readily checked by hand

Table 3.6

RADIOACTIVE HALF-LIVES

Radionuclide	Half-life (yr)	Computer Source Symbol
U-238 *	4.51×10^{9}	TH(1)
Th-232 *	1.4×10^{10}	TH(2)
Pb-210	21	TH(3)
Ra-226	1602	TH(4)

Note

* For total thorium and natural uranium it was assumed that the half-lives of Th-232 and U-238 are representative

calculation.

This section includes graphical presentation of deterministic results, using nominal parameter values, and the arithmetic mean values of probabilistic runs, based on 200 random trials, for the concentrations of many ionic species and radionuclides in the different tailings layers. The information is presented in the following figures:

3.3 - sulphate ion concentrations; layers 2, 3 and 4
3.4 - calcium ion concentrations; layers 2, 3 and 4
3.5 - total iron ion concentrations; layers 2, 3 and 4
3.6 - porewater pH; layers 1, 2, 3, 4

3.7 - solid phase radionuclide concentrations in layer 1; uranium, thorium, radium and lead
3.8 - dissolved uranium concentrations; layers 2, 3 and 4
3.9 - dissolved thorium concentrations; layers 2, 3 and 4
3.10 - dissolved radium concentrations; layers 2, 3 and 4
3.11 - dissolved lead concentrations; layers 2, 3 and 4

Deterministic results are presented as part (a) of the figures in all cases, while probabilistic results are presented as part (b) of the figures. The results were generated using the deterministic and probabilistic input parameter values summarized in the previous section. A brief discussion regarding each figure follows.

Sulphate Ion Concentrations

The sulphate concentrations shown on Figure 3.3 are affected by several processes: pyrite oxidation, calcite depletion, gypsum dissolution and the percolation of precipitation. Initially, the sulphate concentrations result primarily from the oxidation of pyrite in the unsaturated zone during conditions of calcite dissolution. Following calcite depletion, the rate of pyrite oxidation increases and hence sulphate production increases. The sulphate concentrations then decrease as the pyrite inventory decreases with time. The layer 4 concentration is assumed initially to be unaffected by sulphates formed via pyrite oxidation. Its concentration therefore increases as high sulphate concentration porewater percolates down from above. As the pyrite inventory and sulphate concentrations decrease in the upper layers, so does the sulphate concentration in layer 4.

Gypsum dissolution also contributes to the sulphate concentration in all layers. As the gypsum inventory is depleted in layers 2 and 3 the sulphate concentration falls to the background level (0.0128 $mol.m^{-3}$). Layer 4 is assumed to be large enough that gypsum depletion does not occur within the simulation time period. Thus the sulphate concentration in layer 4 reaches a steady state value.

Calcium Ion Concentrations

The calcium ion concentrations (shown in Figure 3.4) result from the dissolution of calcite and gypsum. These results thus provide a better illustration of the gypsum depletion phenomena referred to previously. As the sulphate concentrations increase in the first 50 years in layers 2 and 3, the calcium concentration decreases, to satisfy gypsum equilibrium considerations. The calcium concentrations then increase as pyrite oxidation, and hence sulphate levels, decrease. The calcium concentration in layer 4 decreases initially and then rises, as the sulphate concentration in that layer increases then declines.

Gypsum dissolves, maintaining an equilibrium concentration of calcium, until its inventory is depleted. The deterministic results (Figure 3.4(a)) indicate that gypsum is depleted from layer 2 at approximately 150 years and from layer 3 near 350 years. Following gypsum depletion, the concentration of calcium ion drops to 0.008 $mol.m^{-3}$, i.e. the concentration of calcium in rainwater. The steady-state concentration of calcium in layer 4 is essentially equal to that of sulphate, as expected from the stoichiometry of gypsum dissolution.

FIGURE 3.3

SULPHATE ION CONCENTRATIONS

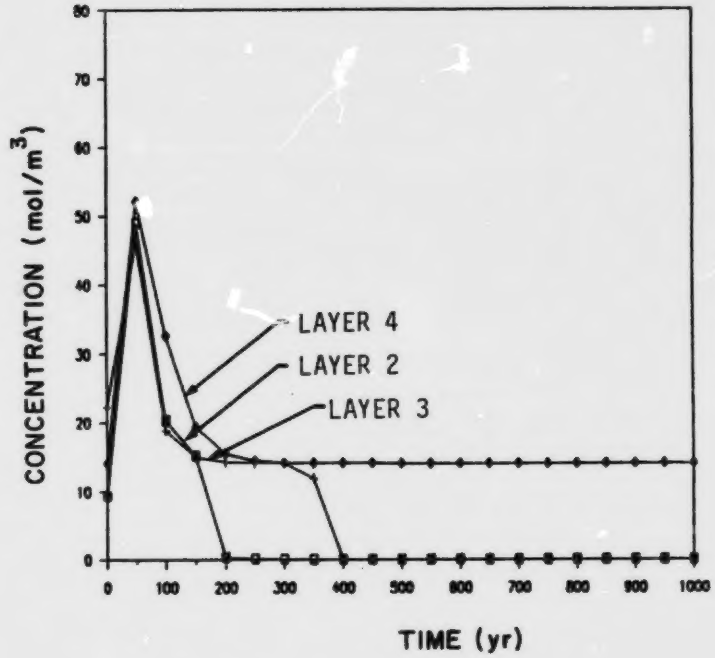

A) DETERMINISTIC RESULTS

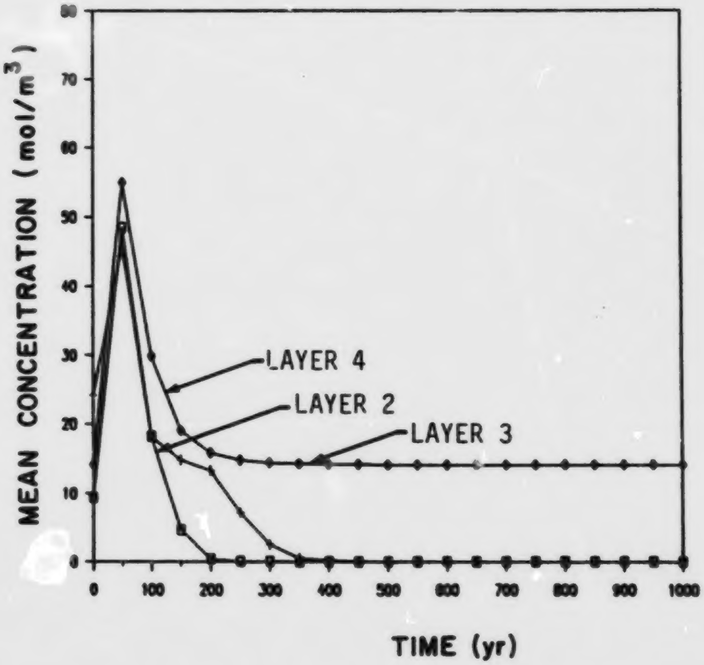

B) PROBABILISTIC RESULTS (100 TRIALS)

FIGURE 3.4

CALCIUM ION CONCENTRATIONS

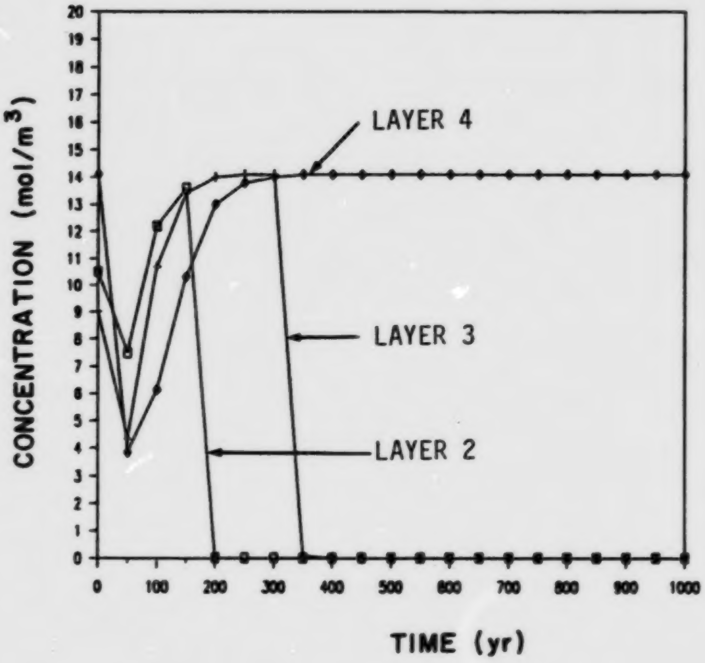

A) DETERMINISTIC RESULTS

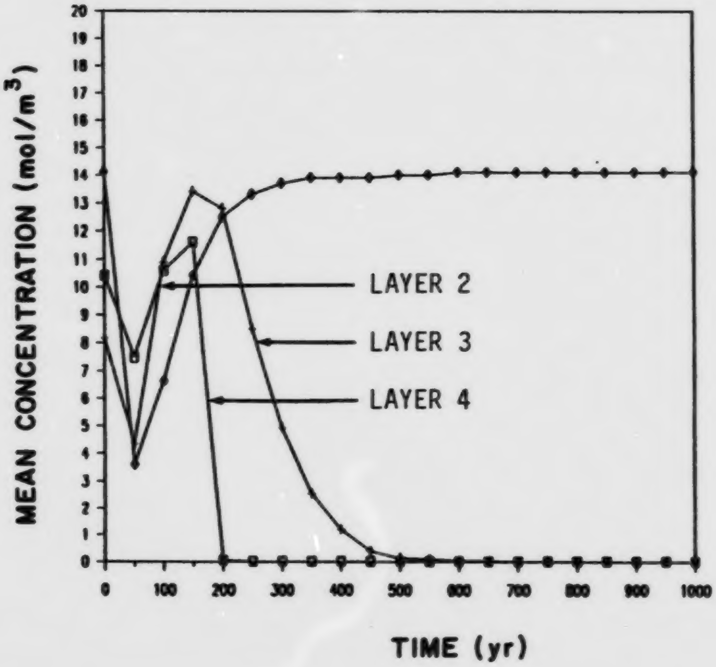

B) PROBABILISTIC RESULTS (100 TRIALS)

The probabilistic results (Figure 3.4(b)) indicate that gypsum depletion in layers 2 and 3 occurs at different times on different trials. This is shown by the gradual, rather than sudden, decrease in calcium concentration. For instance in layer 3, depletion occurs sometime between 180 and 600 years. The mean values of many probabilistic trials show average trends rather than the physically more realistic dynamic behaviour illustrated by a deterministic trial. For this reason, it is often useful to examine both deterministic and probabilistic results.

Iron Ion Concentrations

The concentration of iron in layer 2 is modelled as a function of pH and sulphate concentration. As the sulphate concentration increases/decreases, so does the iron concentration in layer 2 (see Figure 3.5). The concentrations in layers 3 and 4 are functions of the iron inputs from the above layers. Thus, the concentration in layer 4 increases from an initial (assumed) value of zero as iron is transported down from layer 3. Over the long-term, the iron concentration decreases and stabilizes as the sulphate concentration decreases and stabilizes.

Porewater pH

As illustrated in Figure 3.6 (a) and (b), the pH value in layer 2 is initially high as a result of calcite dissolution. After the calcite has been depleted the pH decreases and then increases to a steady-state value. This results from the change in the sulphate concentration with time. After calcite depletion the sulphate concentration is initially high as a result of pyrite oxidation. However, as the sulphate concentration decreases with time, the pH rises. The pH in layer 3 is initially low, approximately 4.8, and gradually rises to a steady-state value. The low pH value results from the discharge of layer 2 sulphates into layer 3, a layer in which there is no calcite to buffer the pH.

As mentioned earlier, layer 4 is initially assumed to be unaffected by sulphates from pyrite oxidation. Hence the pH in layer 4 is initially near neutral, subsequently declines as sulphates are transported in from the layers above and then increases as the sulphate concentration decreases.

Once gypsum is depleted from the unsaturated zone, layers 1 and 2 are indistinguishable, and their pH values are obviously equal. The pH in the unsaturated zone stabilizes near pH 5.2, and is primarily governed by the sulphate and calcium input with the precipitation (i.e. acid rain). On the other hand, the pH in layers 3 and 4 stabilizes near neutrality (pH = 6.7), primarily because of the influence of one or more minerals which are slowly leached from the tailings (e.g. $Al\ (OH)_3$ species, gypsum, calcite).

Solid Phase Radionuclide Concentrations

The radionuclides associated with the solid phase in the tailings surface layer act as a source to the dust and air dispersion models and all subsequent air-related pathways. Some radionuclides (uranium and thorium) are assumed to be uniformly distributed throughout the unsaturated tailings zone. Others (radium and lead) are assumed to dissolve in a frontwise manner, resulting in an upper, depleted layer and a lower, enriched layer. Thus the "surface layer" is of different thicknesses for different radionuclides. For uranium and thorium, it consists of the entire unsaturated zone while for radium and lead it consists of the upper, depleted layer. The distribution of the radionuclides associated with the surface tailings solids is shown on Figure 3.7

Some fraction of the uranium in the tailings is assumed to be associated with pyrite. Thus, as the pyrite oxidizes, this uranium is released from the solid phase. This process accounts for the decrease in solid phase uranium concentration over the first 100 years, or so.

The total thorium concentration consists of Th-230 and Th-232. Thorium solubility is strongly pH dependant, decreasing rapidly as pH rises above approximately 3.5. At the low pH's encountered initially in the unsaturated

FIGURE 3.5

IRON ION CONCENTRATIONS

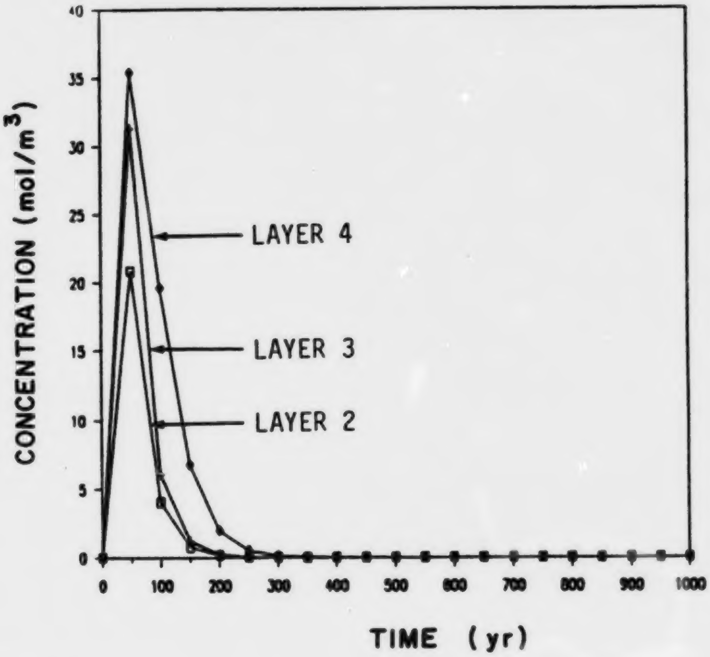

A) DETERMINISTIC RESULTS

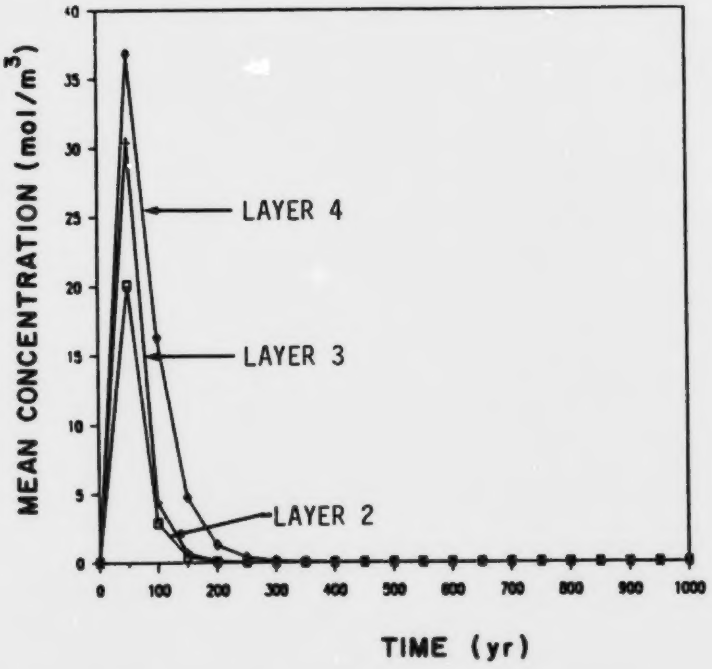

B) PROBABILISTIC RESULTS (100 TRIALS)

FIGURE 3.6

POREWATER pH

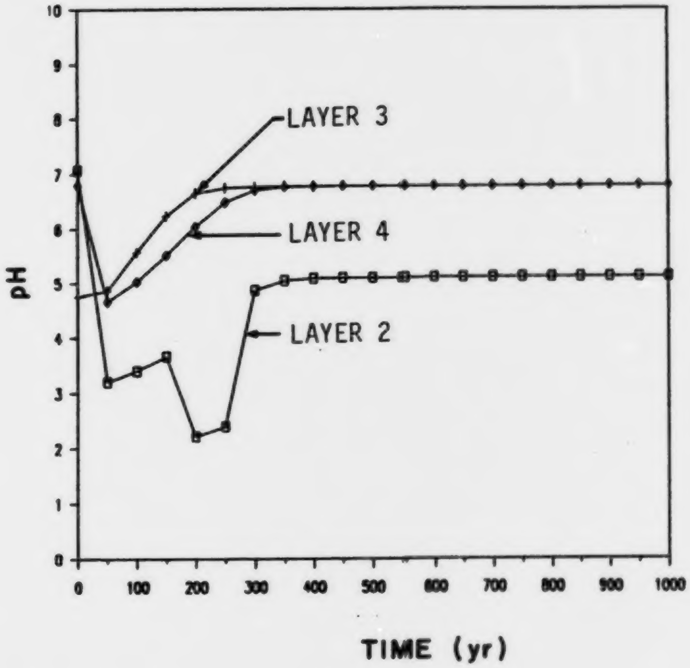

A) DETERMINISTIC RESULTS

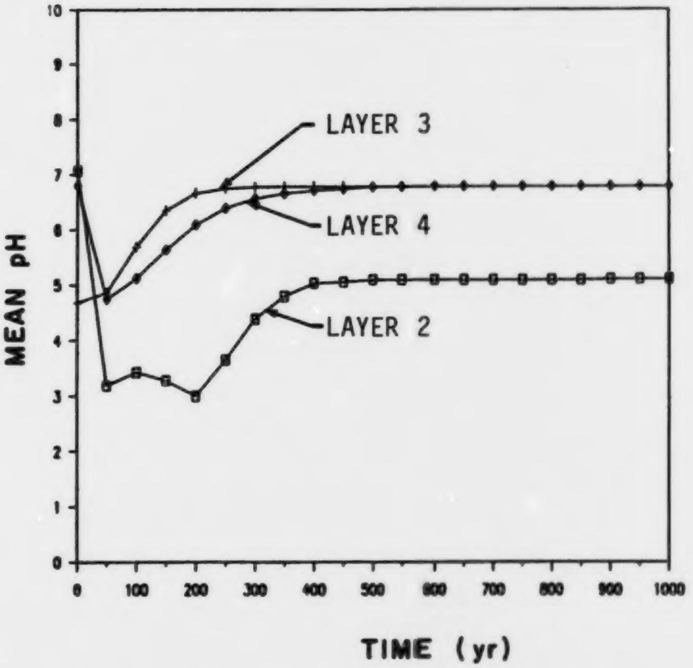

B) PROBABILISTIC RESULTS (100 TRIALS)

FIGURE 3.7

SOLID PHASE RADIONUCLIDE CONCENTRATIONS
IN SURFACE LAYER

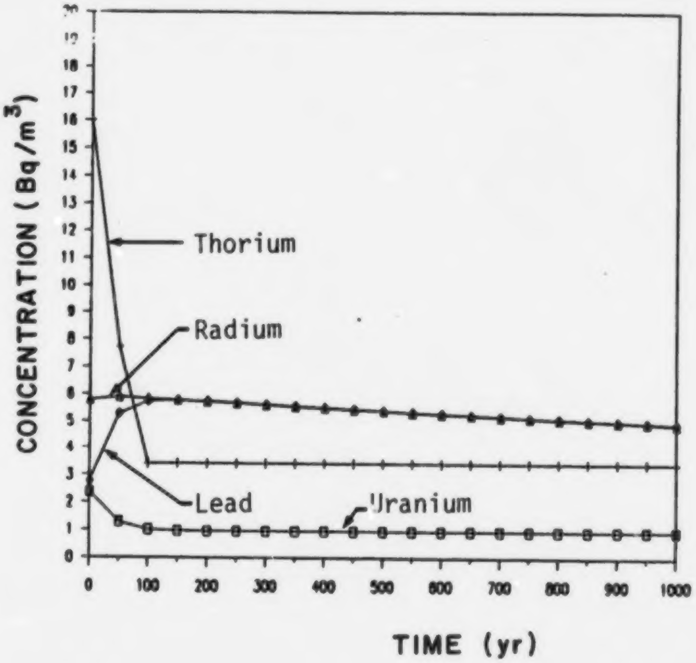

A) DETERMINISTIC RESULTS

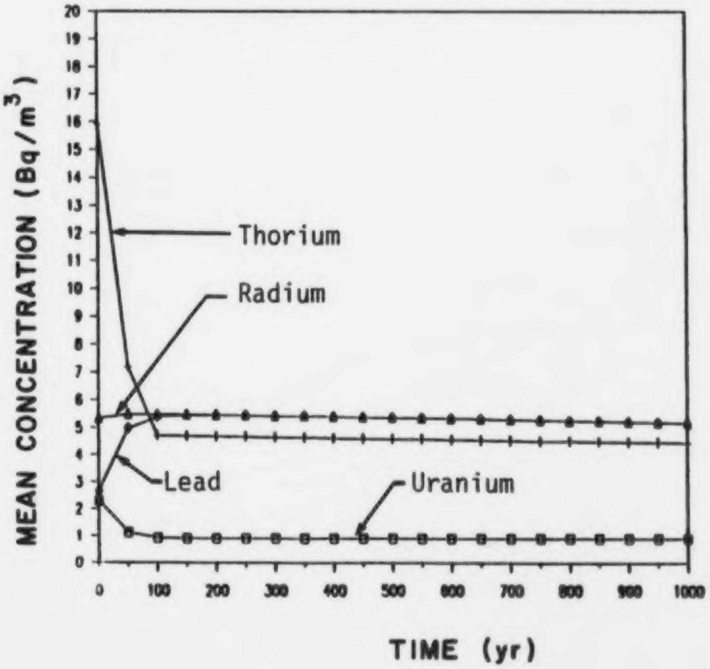

B) PROBABILISTIC RESULTS (100 TRIALS)

zone, a considerable fraction of the thorium dissolves, resulting in the rapid decrease in the solid phase thorium concentration.

The solid phase radium concentrations are those for the radium-depleted layer. The radium in this layer is assumed to be associated with the host tailings material, and hence is insoluble. Thus the decrease in radium concentration with time results from the net radioactive decay of the radium. Ingrowth of radium from thorium decay is significant for only the first 100 years as the thorium is leached from the upper layer in a short time frame.

The solid phase lead concentrations are also those for the lead depleted layer. Again, the lead present is assumed to be insoluble, and associated with the host tailings material. The initial difference in lead and radium concentrations results from the fact that approximately 40% of the radium is assumed to be insoluble while only 5% of the lead is considered insoluble. The lead concentration increases as a result of net radioactive ingrowth from radium and subsequently tracks the radium behaviour exactly as expected.

Dissolved Uranium Concentrations

The dissolved uranium concentration (illustrated in Figure 3.8) in layer 2 reflects the formation of sulphate as a result of pyrite oxidation (see Figure 3.3). Since some (nominally 60%) of the uranium is assumed to be associated with pyrite, the oxidation of pyrite results in the dissolution of uranium, just as it results in the formation of sulphate ions. Thus, the concentration of dissolved uranium increases or decreases as the sulphate flux increases or decreases. The concentrations of uranium in layers 3 and 4 are functions of the concentration of uranium entering from the layer above. Some of the uranium in these layers is adsorbed and subsequently acts as a long-term source of dissolved uranium.

Dissolved Thorium Concentrations

As mentioned previously, the thorium concentration is very strongly pH dependent, falling rapidly as the pH rises above approximately 3.5. Figure 3.9 illustrates the concentration of dissolved thorium in layers 2, 3 and 4. The pH results presented earlier (Figure 3.6) help to explain the dissolved thorium concentrations.

At the 50 year time period, layer 2 has a very low pH (approximately 2.2; Figure 3.6b) and hence thorium solubility and concentration are quite high. In fact, Figure 3.9 (a) and 3.9(b) indicates that all of the soluble thorium in layer 2 is dissolved over the first 100 years. With no further source of soluble thorium, the dissolved thorium concentration falls to zero thereafter.

The layer 3 concentrations show a similar decrease as the pH increases with time. Although not well illustrated on Figure 3.9, the layer 3 thorium inventory is not depleted, and the concentration decreases to a low, but non-zero value.

The initial thorium concentration in layer 4 is several orders of magnitude lower than those in layers 2 and 3. As the pH in layer 4 decreases (between 0 and 100 years) the thorium concentration increases and then decreases again as the pH rises.

Dissolved Radium Concentrations

The dissolved radium concentrations in layers 2, 3 and 4 are illustrated in Figure 3.10 (a) and (b). Soluble radium in the tailings is assumed to be associated with barium sulphate ($BaSO_4$). The barium sulphate (and associated radium) dissolves in a frontwise manner in the unsaturated zone, resulting in a $BaSO_4$ (and radium) depleted layer and a layer (layer 2) which is enriched in $BaSO_4$ (and radium). Because of the chemical properties of radium, it reprecipitates and becomes concentrated in layer 2. Thus, over the initial 150 years or so (see Figure 3.10a) the radium concentration in the porewater is controlled at a comparatively low level. After this time, the concentration of dissolved radium in layer 2 shows a rapid rise as illustrated by the deterministic results in Figure 3.10 (a). This occurs as the thickness

FIGURE 3.8

DISSOLVED URANIUM CONCENTRATIONS

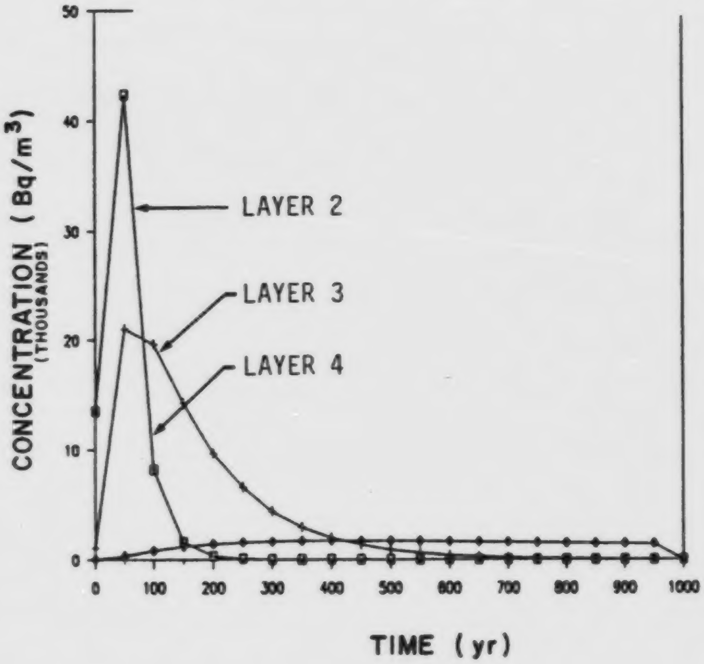

A) DETERMINISTIC RESULTS

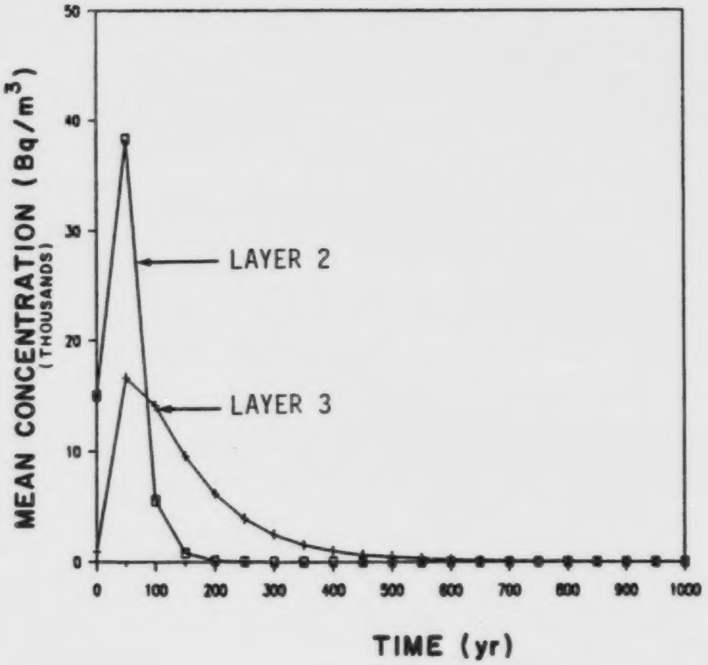

B) PROBABILISTIC RESULTS (100 TRIALS)

FIGURE 3.9

DISSOLVED THORIUM CONCENTRATIONS

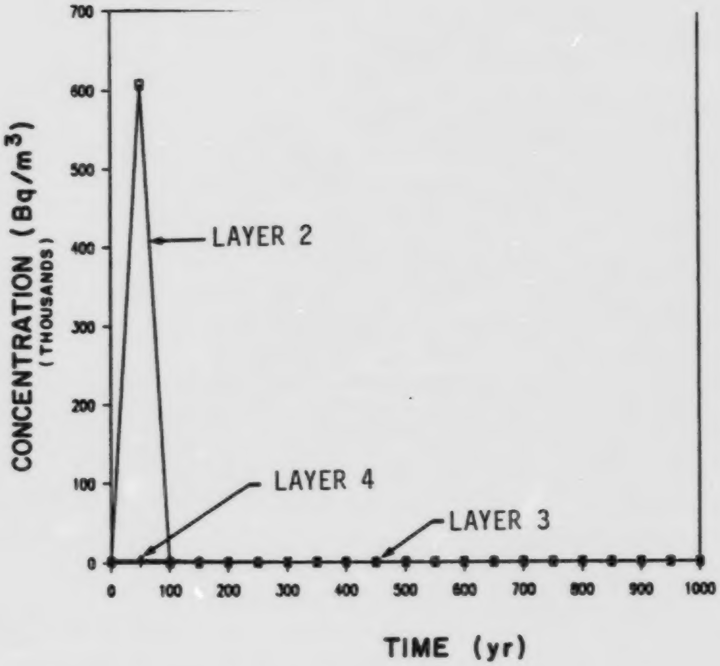

A) DETERMINISTIC RESULTS

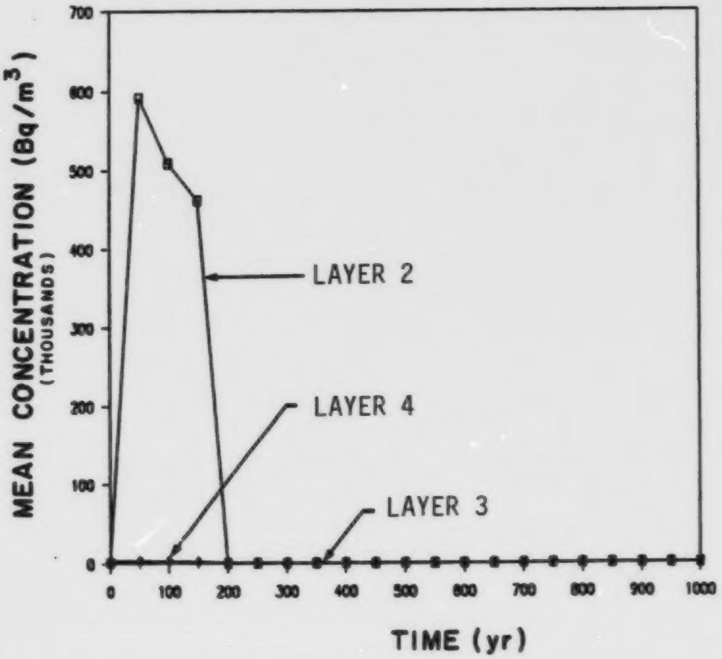

B) PROBABILISTIC RESULTS (100 TRIALS)

FIGURE 3.10

DISSOLVED RADIUM - 226 CONCENTRATIONS

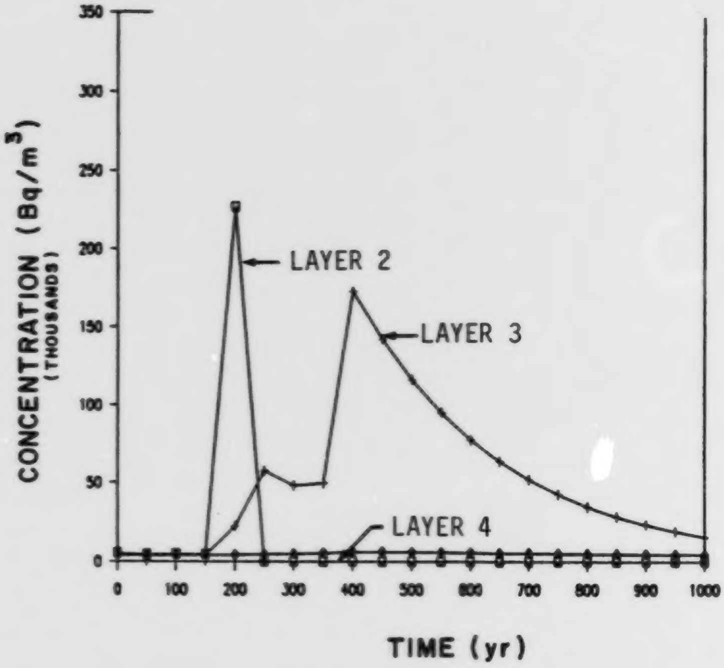

A) DETERMINISTIC RESULTS

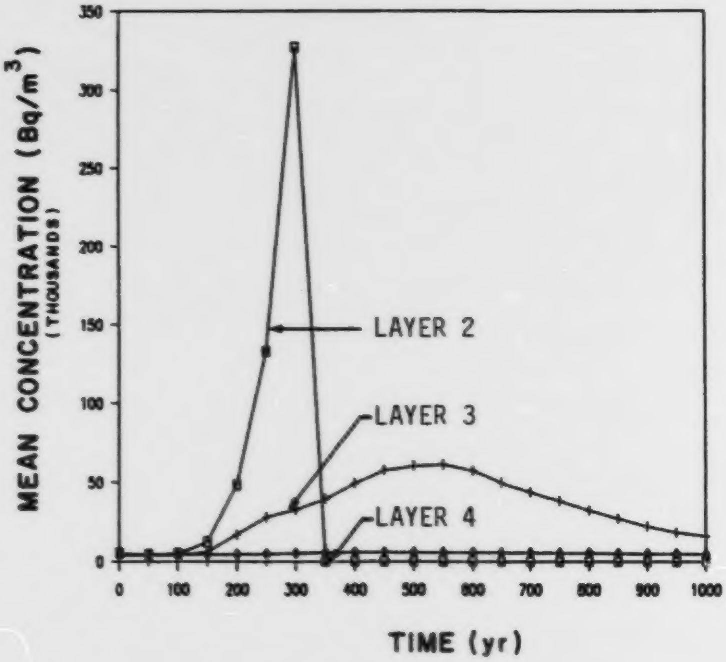

B) PROBABILISTIC RESULTS (100 TRIALS)

of layer 2 (the radium enriched layer) becomes smaller and smaller, and the enriched $BaSO_4$ (with an elevated radium content) starts to dissolve. At some point (250 years in Figure 3.10 (a)) the thickness of layer 2 becomes zero indicating that the unsaturated zone is completely depleted of $BaSO_4$. The concentration of dissolved radium thus falls to zero, since $BaSO_4$ acts as the only source of soluble radium.

The concentration profile for layer 2 is not as pronounced in the probabilistic results shown in Figure 3.10 (b), since the very sharp peak occurs at different times on different trials. The average of a few high concentrations and many lower values at any time is obviously much lower than the few high concentrations of any one time.

The concentration of radium in layer 3 results from both the radium input from layer 2 (as long as $BaSO_4$ is present) and also from $BaSO_4$ dissolution in layer 3. Adsorption mechanisms are also considered in layer 3, which results in a smoothing or spreading of the concentration peaks seen in layer 2.

Because of the large volume of layer 4 and the relatively large solid-liquid distribution coefficient (K_d) for radium, the radium concentration in layer 4 is relatively unaffected by inputs from layer 3. That is, layer 4 has a relatively large sorptive capacity, which serves to dampen out any input fluctuations and maintain a relatively constant radium concentration.

Dissolved Lead Concentrations

Lead-210 is assumed to be associated with lead sulphate ($PbSO_4$), much as radium is associated with $BaSO_4$. The dissolution of $PbSO_4$ is also assumed to occur in a frontwise manner. However, unlike radium, lead-210 does not become increasingly concentrated as it reprecipitates with $PbSO_4$ in layer 2 (a $PbSO_4$ enriched layer). Because of its short radioactive half-life (21 years), much of the behaviour of lead-210 is governed by its radioactive decay and ingrowth from radium-226. Thus, the change in dissolved radium concentration with time (Figure 3.10) can help to explain the lead-210 concentrations in the various tailings layers illustrated in Figure 3.11 (a) and (b).

The initial lead concentrations are governed by the equilibrium dissolution of $PbSO_4$. The decreasing lead concentrations over the initial 50 to 100 years are primarily the result of radioactive decay. Layer 2 and layer 3 both show subsequent concentration increases which correspond to the peaks in dissolved radium concentration illustrated in Figure 3.10.

3.14 Tailings Erosion Model

3.14.1 Introduction

The erosion model detailed in the following section accounts for the physical movement of the tailings surface layer into the river/lake system. This is of particular interest when the surface is bare tailings, since the radioactivity associated with the eroded particles will, to a degree, dissolve in the river/lake system and cause an increase in activity in these waters.

The erosion model accounts for gross soil erosion of the tailings using the Universal Soil Loss Equation. This equation primarily estimates erosion and does not account for deposition. To account for this, the gross erosion is partitioned into bedload and suspended sediment load. The following description, from Haan (1978), distinguishes between the two phenomena: "Sediment is detached as either primary particles (i.e. sands, silts and clays) or as aggregates. Aggregates are simply large numbers of particles bound together by a cementing agent such as organic matter or iron compounds. Soils eroded as aggregates are transported primarily as bedload, that is material that slides along the surface. Soil eroded as primary particles can be transported both as bed material or as suspended load while larger particles are transported as bedload." In the erosion model gross bedload and suspended sediment erosion are calculated and compared to calculated bedload and suspended sediment load capacities and the lesser value in each case is used as the sediment load.

FIGURE 3.11

DISSOLVED LEAD-210 CONCENTRATIONS

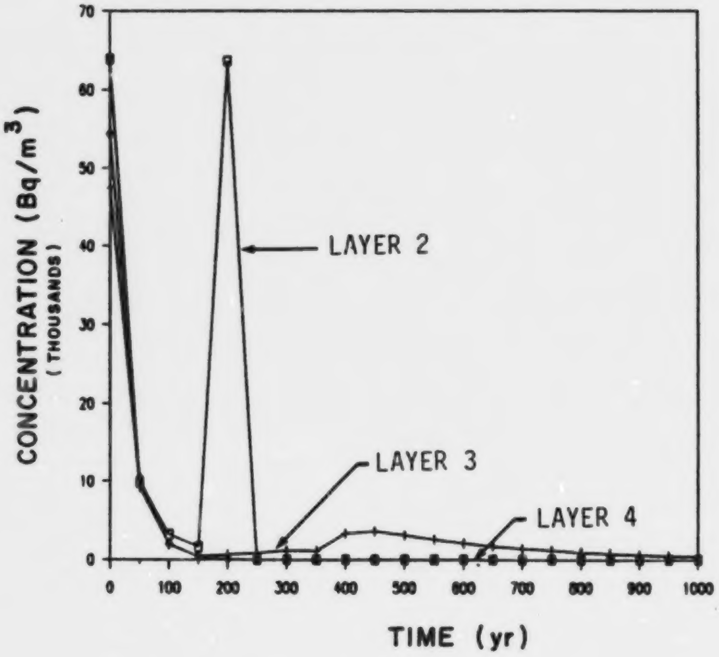

A) DETERMINISTIC RESULTS

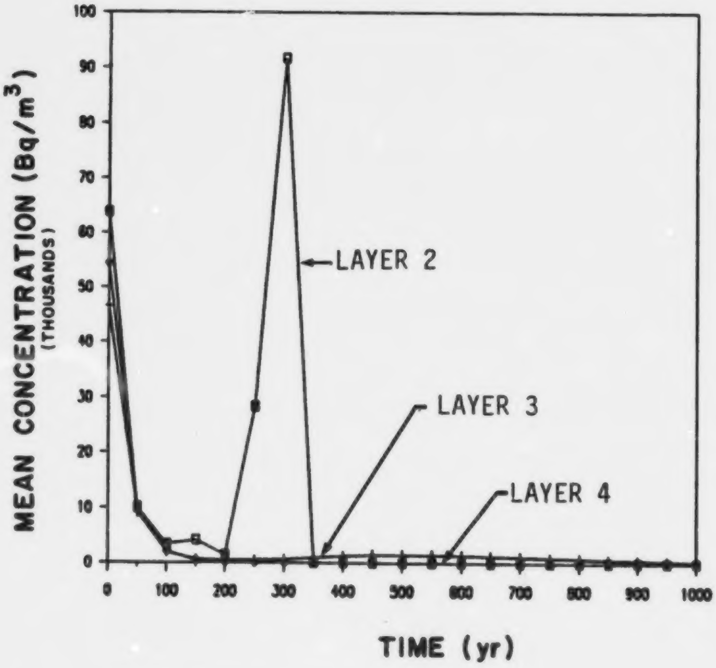

B) PROBABILISTIC RESULTS (100 TRIALS)

Wherever possible, soil and vegetation related variables were treated as functions of more basic variables, to reduce the number of inputs as well as to account for potential dependencies among variables.

A simple exponential tailings vegetation model is also described in this section. This model postulates vegetation as a function of the pH in the surface layer of the tailings.

Finally, the effect of having a pond at the base of the tailings pile can be modelled. A fraction of both the suspended sediment and the bedload leaving the pile is trapped in the pond, with the remaining material then being deposited into the river/lake system.

3.14.2 The Universal Soil Loss Equation

There are two major approaches commonly used to determine erosion rates from disturbed land surfaces. The simplest approach is the use of mathematical models based on regression equations. The Universal Soil Loss Equation is the principal example of this type of model. The other approach involves the use of analytical or physical process models that explicitly account for the physical phenomena involved in soil erosion. While analytical models are desirable from a theoretical point of view, when simulating such complex processes as soil erosion and sediment yield over long periods of time, regression models are preferable.

The Universal Soil Loss Equation (USLE) is the most widely used regression model for predicting soil erosion. It is an empirical formula for predicting soil loss as a result of sheet and rill erosion. The USLE was developed at the National Runoff and Soil Loss Data Center established in 1954 by the Agricultural Research Service in cooperation with Purdue University (Wischmeier and Smith, 1978). Research projects at 49 locations contributed more than 10,000 plot-years of basic runoff and soil loss data for the study. The original equation was developed to predict losses on slopes up to 400 feet long. The basic formulation of the USLE is:

$$A = R\ K\ LS\ C\ P \qquad (3.14.1)$$

where

A = average annual soil loss (tons/acre)

R = annual rainfall erosivity factor (100 (ft.tons/acre) (in.hr))

K = soil erodibility factor (tons/acre per unit of rainfall factor, R)

LS = topographic factor

C = cropping management factor

P = erosion control practice factor.

Imperial units are used in the USLE.

Since a tailings pile has a length considerably greater than 400 feet, a modified version of the USLE has been adopted (Foster and Wischmeier, 1974). The tailings pile has been considered as a series of slope segments of less than 400 feet in length. The following modification of the USLE may then be used to predict the sediment detached in each segment (Haan, 1978):

$$D_j = 0.0459\ R\ K\ CP\ S\ (\lambda_{cj}^{m+1} - \lambda_{cj-1}^{m+1})/72.6^m \qquad (3.14.2)$$

where

D_j = soil detached in slope segment j ($\mathrm{lb.ft^{-1}(width).yr^{-1}}$)

R = annual rainfall erosivity factor

CP = control practice factor

λ_{cj} = length from top of tailings pile to bottom of j^{th} segment

m = exponent dependent upon slope

  m = 0.3 for slopes ≤ 3 percent

  m = 0.4 for slopes of 3 to 5 percent

  m = 0.5 for slopes ≥ 5

K = soil erodibility factor.

S = slope factor.

and

$$S = (0.43 + 0.30\ S_o^2 + 0.043\ S_o^2)/6.613 \qquad (3.14.3)$$

$$100K = 2.1\ M^{1.14}\ (10^{-4})\ (12-a) + 3.25\ (b-2) + 2.5\ (c-3) \qquad (3.14.4)$$

where

S_o = percent slope

M = (% silt) x (100 - % clay) (clay content is assumed to be zero in tailings)

a = percent organic matter (assumed to zero for exposed tailings solids)

b = soil structure code used in soil classification (i.e. 2 for tailings)

c = soil permeability class (i.e. 5 for tailings).

The control practice factor (CP) is, according to Haan (1978), composed of three factors:

$$CP = C_s\ C_r\ C_o \qquad (3.14.5)$$

where

C_s = control factor due to surface stabilizing, protection treatments or vegetation (C_s = 1 for bare, untreated soil)

C_r = control factor due to runoff-reduction practices such as diversion berms, interceptor dikes, benches and terraces, and sectional drawdowns

C_o = control factor due to other practices not included herein.

We will only treat C_s in this development with C_r and C_o being set to 1. This overestimates soil erosion if these other control factors are, in fact, functioning. Haan has presented C_s as a decaying exponential function of mulch rate and has related data for C_s for grass-like plants to the fraction of the surface vegetated (F_v). These data have been fitted to an exponential model, with the following result:

$$C_p = C_s = \exp\left[-0.109 - 0.056\ F_v\right] \qquad (3.14.6)$$

$$C_s = 1 \text{ if } F_v = 0$$

Haan used $C = 0.45$ for $F_v = 0$. This assumption has been replaced in this development with $C = 1$ at $F_v = 0$. This assumption is consistent with the basic definition of control practice factor which is "the ratio of soil loss from land cropped under specified conditions to the corresponding soil loss from clean-tilled, continuous fallow ground" (Walters, 1985). The derivation of a relationship for the fraction of vegetated tailings is discussed in the next section.

3.14.3 Tailings Vegetation

Tailings vegetation is a complex problem. The following discussion of the tailings vegetation growth environment was taken from MacLaren (1978).

> **"Elliot Lake uranium tailings are a most inhospitable medium for growth. The characteristics that make tailings difficult to vegetate are: the presence of acid and metals, deficiency in nutrients, physical characteristics such as their unconsolidated nature and extremes of moisture, and topography (prone to flooding, etc.).**
>
> **The presence of pyrite and the absence of sufficient alkalinity leads to acid generation and heavy metal solubilization. Highly acid soils are generally unacceptable to plants because the acid solutions increase the availability and concentration of metal ions present in the tailings material. In general, a pH range of 5 to 7 is required for good plant growth with the lower limit being about pH 4.**
>
> **Aside from pH, plants also require a balanced intake of macronutrients (nitrogen, phosphorus and potassium) and micronutrients (iron, manganese, copper, magnesium, zinc and others). Tailings deposits are usually devoid of macronutrients.**
>
> **Only minute quantities of micronutrients are required for plant growth; any excess may prove to be toxic. Tailings frequently contain metallic micronutrients in amounts sufficient to inhibit or**

> **kill plant growth....**
>
> **The topography of the tailings areas is also important.... Flat tailings surfaces are frequently subject to ponding and wind erosion. The excessive moisture associated with ponding causes plant mortality, and the windblown fines can cause abrasion sufficient to kill young plants.**
>
> **Tailings are frequently light in colour. As a result, there is excessive reflection of solar rays. This causes young plants and seedlings to dry out and/or be burned, thus adding an additional factor which must be overcome for a successful vegetation programme."**

In spite of these difficulties, both natural and man-assisted vegetation occurs on tailings piles.

In the face of such complexities, it was decided to use a simplified approach to tailings vegetation. When the pH of the tailings surface layer is less than or equal to 4.0, it has been assumed that no natural vegetation would occur. When the pH is greater than 4.0, the following exponential growth relationship has been adopted (SENES, 1985b):

$$F_V = 1 - \exp(-\lambda_T ((T-T_V) - \frac{\Delta T}{2})) \qquad (3.14.7)$$

where

F_V = fraction of tailings pile covered with vegetation

λ_T = ln $2/T_H$

T_H = vegetation half-life

T = time

T_V = time at which pH rises above 4.0

ΔT = time increment used in model.

Equation (3.14.7) is applied with the following qualifications:

$$\text{if } F_v \geq 0.9 \text{ then } F_v = 0.9$$
$$\text{if } T = T_v \text{ then } F_v = 0$$

Once pH in the first layer has risen above 4.0, vegetation will likely take place fairly quickly (i.e. a vegetation half-life from 10 to 20 years). Since the vegetation half-life is short, relative to the time increment, the $\Delta T/2$ term is used to "average" F_v to the middle of the time increment.

To simulate man-assisted vegetation in place at the beginning of the simulation, the minimum (or initial) fraction of ground cover (F_m) is specified. If the tailings can support a higher fraction of cover than this minimum, the fraction is adjusted accordingly. This can be expressed as:

$$\text{If } F_v < F_m \text{ then } F_v = F_m$$

If the user wishes to implement a revegetation strategy, an integral part of this could be a pH increase through lime application. The pH dependence of the vegetation relationship allows for growth to begin as soon as the pH is greater than 4.0. If fertilizing, seeding or other practice methods are to be simulated, then the revegetation half-life can be reduced or the minimum fraction of cover increased.

3.14.4 Tailings Geometry

To simplify the computational process, the following assumptions have been made regarding the tailings geometry. The tailings pile has been assumed to have a constant slope and a rectangular shape. The flow length (L) and the tailings area (A_T) determine the dimensions of the rectangle. The dimensions of the rectangular pile are calculated as follows:

$$L = \frac{L_f}{(0.3048 \text{ m.ft}^{-1})} \qquad (3.14.8)$$

$$W = \frac{A_T}{L_f\ (0.3048\ \mathrm{m.ft^{-1}})} \qquad (3.14.9)$$

where

L = flow length of tailings pile (ft)

L_f = metric flow length (m)

W = width of the tailings pile (ft)

A_T = surface area of the tailings (m^2).

As the maximum slope segment allowable is 400 ft, the tailings pile has been subdivided into the smallest integer number of equal length slope segments (N) possible, of length less than 400 ft.

The length of each segment is calculated as:

$$\lambda_j = \frac{L}{N} \qquad (3.14.10)$$

where

λ_j = length of segment j (ft)

N = number of segments.

and

$$N = \mathrm{INT}\ (L/400\ \mathrm{ft}) + 1 \qquad (3.14.11)$$

3.14.5 Deposition and Transport

As mentioned in the introduction, the USLE only accounts for erosion, and does not account for significant amounts of deposition. Hence the USLE tends to overestimate erosion losses. Two transport mechanisms are developed in the following pages to help account for deposition. These mechanisms are bedload transport capacity and suspended sediment transport capacity. Haan (1978), from work of Neibling and Foster (1977), has proposed to analyze suspended load and bedload separately. These two transport mechanisms are discussed in the following two sections.

Bedload Transport

The bedload model uses the USLE rainfall erosivity factor (R) to predict the bedload transport capacity of a soil using the following equation:

$$T_{cj} = r\ R\ T_s\ \lambda_{cj}^2\ (x)^B\ C_{ro}\ C_T \qquad (3.14.12)$$

where

T_{cj} = bedload transport capacity for segment j (lb/ft(width)yr)

r = proportionality constant which relates the product of runoff volume and peak discharge to rainfall erosivity (ranges from $1\text{x}10^{-8}$ to $1.0\text{x}10^{-7}$ (Haan, 1978)). Units: $(\text{ft}^2/(\text{sec.yr})/\text{"R units"})$

T_s = transportability of the soil particles (lb.sec/ft^5)

λ_{cj} = length from top of the slope to the bottom of the jth segment (ft)

x = sine of slope angle

where $x = \sin(\tan^{-1}(S_0/100))$

S_0 = % slope of pile

B = empirical exponent which is a function of particle size

C_{ro} = runoff reduction factor

C_T = transportability reduction factor (given as a function of the ratio of velocity with respect to that of bare soil)

R = rainfall erosivity factor (100(ft.tons/acre)(in.hr)).

Soil transportability has been graphed as a function of particle diameter by Haan (1978). The following functional relationship has been derived from the graph:

$$T_s = 5.87 \times 10^5\ D_{50}^{0.197} \qquad (3.14.13)$$

where

D_{50} = particle diameter size exceeded by 50% of the tailings (mm).

Figure 3.12 shows a typical grain size distribution for uranium tailings.

FIGURE 3.12

TYPICAL RANGE OF GRAIN SIZE DISTRIBUTION FOR ACID GENERATING TAILINGS

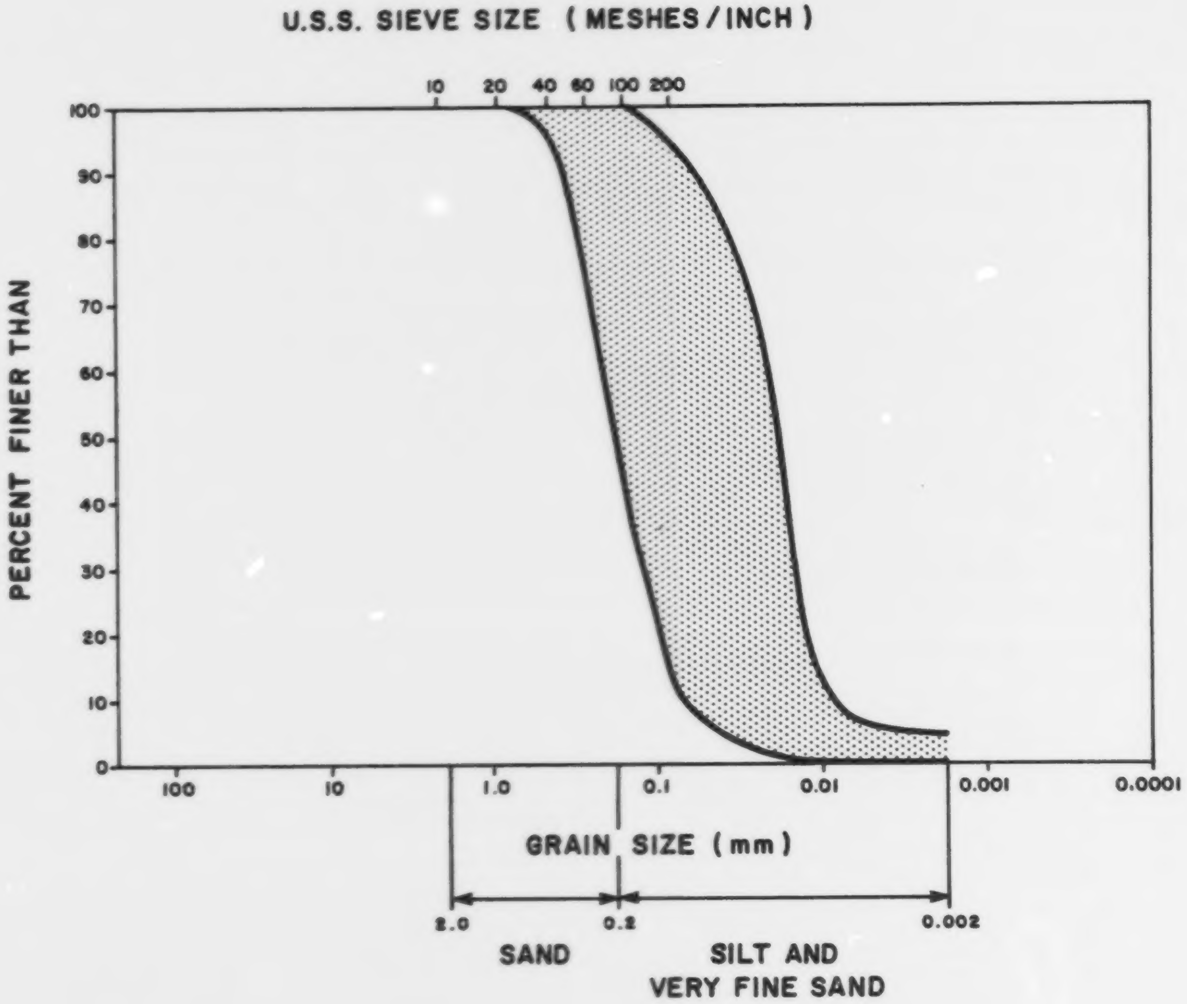

SOURCE: FROM SENES, 1986

From the eleven grain size analyses used to generate Figure 3.12, the following relationship between D_{50} and percent silt has been established:

$$D_{50} = -1.99 \times 10^{-3} \; S_i + 0.215 \qquad (3.14.14)$$

where
S_i = % silt (tailings surface).

The factor B has also been fitted as a function of D_{50}, using graphical information from Haan. These data were fitted over two ranges:

$$\begin{array}{ll} B = 1.83 \, D_{50}{}^{0.049} & 0.016 \le D_{50} < 0.045 \text{ mm} \\ B = -0.714 \, D_{50} + 1.61 & 0.045 \le D_{50} \le 0.215 \text{ mm} \end{array} \qquad (3.14.15)$$

Haan (1978) related the runoff reduction factor C_{ro} to vegetation and tillage practices, with a range of values from 1.4 (untilled packed construction site) to 0.1 (sod, grass, hay). This range has been assumed to be linearly related to percent vegetation with the following relationship:

$$C_{ro} = -1.44 \, F_v + 1.4 \qquad (3.14.16)$$

$$\begin{array}{l} \text{i.e } C_{ro} = 1.4 \text{ at } F_v = 0 \\ \quad C_{ro} = 0.1 \text{ at } F_v = 0.9 \end{array}$$

Haan also presented a series of curves that specified relative transport capacity (C_T) as a function of velocity ratio for several slopes. He related velocity ratio to amount of grass as follows:

Amount of Grass	Velocity Ratio
None	1.0
Poor	0.8
Good	0.5
Very Dense	0.3

The velocity ratio (V_R) was assumed to be linearly related to percent vegetation as follows:

$$V_R = -0.77\ F_v + 1.0 \qquad (3.14.17)$$

$$\text{i.e. } V_R = 1 \text{ at } F_v = 0$$

$$V_R = 0.3 \text{ at } F_v = 0.9$$

The C_T vs V_R relationships from Haan for slopes of 0.5, 1 and 2 percent and medium runoff rates, have been fitted with the following results:

$$\begin{array}{ll} C_T = V_R^{18.53} & S_o \leq 0.75 \\ C_T = V_R^{8.98} & 0.75 < S_o \leq 1.5 \\ C_T = V_R^{6.64} & S_o > 1.5 \end{array} \qquad (3.14.18)$$

where

S_o = percent slope.

Suspended Sediment Transport

According to Haan (1978) the amount of suspended sediment deposited in a vegetated area increases exponentially with distance travelled. The fraction of sediment trapped by simulated vegetation (T_r) has been predicted to be (Haan, 1978):

$$T_r = \exp\left[(-1.05 \times 10^{-3}) \left[\frac{VR_s}{\nu}\right]^{0.82} \left[\frac{\lambda_j V_s}{Vd_f}\right]^{-0.91}\right] \qquad (3.14.19)$$

where

V = the flow velocity through the grass (ft/sec)

d_f = depth of flow (ft)

ν = the kinematic viscosity (1.5×10^{-5} ft^2/sec at 7°C)

R_s = spacing hydraulic radius (ft) given by :

$$R_s = \frac{d_f\ S_s}{2d_f + S_s} \qquad (3.14.20)$$

S_s = average spacing of grass (ft)

λ_j = length of flow path through grassed area of jth segment (ft)
V_s = settling velocity of the silt and/or clay size particles (ft/sec).

The depth of flow (d_f) is calculated as:

$$d_f = S_t L/(V\ (2.633 \times 10^7 \text{ mm d}^{-1}/\text{ft.sec}^{-1}) \qquad (3.14.21)$$

where
S_t = 24 hour rainfall for a 2 year return period (mm.d^{-1})
L = length of the tailings pile (ft).

According to Haan, the settling velocity of silt and clay size particles can be estimated from Stokes' Law as:

$$V_s = \frac{2}{9} \frac{gd^2}{\nu} (SG-1) \qquad (3.14.22)$$

where
g = gravitational constant (32.2 ft/sec^2)
d = particle diameter of silt (ft)
SG = specific gravity (2.65).

and

$$d = d_m/(304.8 \text{ mm.ft}^{-1}) \qquad (3.14.23)$$

where
d_m = median silt particle diameter (mm).

Haan (1978) graphed flow velocity (V) as a function of slope for a variety of roughness factors. The straight line graphical data have been reduced to a linear relationship for nearly bare and untilled soil and short grass pasture. These two relationships are shown below:

$$V = \exp(-0.394 + 0.276S_o) \text{ (nearly bare and untilled soil)} \qquad (3.14.24)$$

$$V = \exp(-0.905 + 0.503S_o) \text{ (short grass pasture)} \qquad (3.14.25)$$

When the tailings are not vegetated (F_v=0) the first equation prevails; when $F_v > 0$, the second equation should be used.

According to Haan (1978) the average spacing of grass ranges from 1.7 cm (sparse) to 0.75 cm (dense). These limits have been assumed to be linearly related to the fraction of vegetated surface (F_v) as follows:

$$S_s = -0.034\ F_v + 0.056 \qquad (3.14.26)$$

where S_s is in feet.

3.14.6 River/Lake System Loading

Haan has suggested the following computational process to determine sediment load from an area. "The slope must be divided into segments and the transport capacity and total sediment available for transport calculated at the end of each segment. The lesser of the two is taken as the sediment exiting the segment. The sediment available for transport at the bottom of any segment is equal to that entering the segment plus that detached in any segment." Gross erosion is partitioned into suspended sediment and bedload by assuming the silt fraction to be suspended and the remainder to be bedload, or:

$$E_{Sj} = E_{Sj-1} + D_j\ (S_i/100)\ (1 - T_r) \qquad (3.14.27)$$

$$E_{Bj} = E_{Bj-1} + D_j - E_{Sj} \qquad (3.14.28)$$

$$\text{If } E_{Bj} \geq T_{Cj} \text{ then } E_{Bj} = T_{Cj}$$

where

E_{Sj} = suspended sediment load leaving segment j ($\text{lb.ft}^{-1}\text{(width).yr}^{-1}$)

E_{Bj} = bedload leaving segment j ($\text{lb.ft}^{-1}\text{(width).yr}^{-1}$)

D_j = soil detached in segment j ($\text{lb.ft}^{-1}\text{(width).yr}^{-1}$)

S_i = % silt
T_r = fraction of suspended sediment trapped.

It is assumed that all of the bedload and suspended sediment load leaving the last segment pass into a pond at the end of the tailings pile. A percentage of this load is then trapped by the pond, which can be expressed as:

$$E_S = (1 - (P_s/100))E_{Sj} \quad \text{for } j=N \qquad (3.14.29)$$

$$E_B = (1 - (P_B/100))E_{Bj} \quad \text{for } j=N \qquad (3.14.30)$$

where
N = number of segments
E_S = suspended load leaving pond (lb.ft^{-1}(width)$.\text{yr}^{-1}$)
E_B = bedload leaving pond (lb.ft^{-1} (width)$.\text{yr}^{-1}$)
P_s = pond trapping efficiency for suspended sediment (%)
P_B = pond trapping efficiency for bedload (%).

The entire process is described in Figure 3.13, adapted from Haan (1978). Note that if there is no tailings pond, the trapping efficiencies are set to zero.

The total sediment mass (T_m) leaving the tailings pond in the simulation time increment Δt is:

$$T_m = \frac{W(E_S + E_B)\Delta t}{(2.2\ \text{lb.kg}^{-1})} \qquad (3.14.31)$$

where
T_m = total sediment mass leaving tailings pond (kg)
W = tailings pile width (ft).

The total sediment leaving the tailings pond has been assumed to be instantaneously deposited in the first segment of the river/lake system at the beginning of the next time increment. A fraction of the activity in the sediment is assumed to instantly dissolve in the river/lake segment. The balance of the activity remains bonded to the sediment, settles, and becomes part of the bottom sediments of the river/lake segment. The radionuclide concentration of the eroded material is that of the surface tailings concentration predicted in the tailings source model.

3.14.7 Review of Input Parameters

The following section outlines the input parameters for the erosion model. Table 3.7 is a summary of their nominal and probabilistic values. Table A.1 includes a listing of the erosion model code.

Rainfall Erosivity Factor

Values for the USLE Rainfall Erosivity Factor (R) have been established for various locations in Canada by Wall *et al*. (1983). For Ontario (north of Superior), annual values (which include the effects of both rainfall and snowmelt erosivity) range from 65 to 97.5 (Imperial units). For a tailings site in the Elliot Lake region, the value of R was taken to be uniformly distributed over this range.

Proportionality Constant for Bedload Transport

In calculating the bedload transport capacity, the proportionality constant (r) relates the product of runoff volume and peak discharge to rainfall erosivity. This constant has been evaluated by Haan (1978) as 10^{-8} for low runoff potential and 10^{-7} for moderate runoff potential. Thus r has been assumed to be uniformly distributed over this range for a tailings surface.

Peak Rainfall

The 24-hour rainfall for a 2-year return period (S_t) is used in calculating the fraction of suspended sediment trapped on the tailings surface. According to the Hydrological Atlas of Canada, the Elliot Lake region lies between S_t isolines of 36 mm and 48 mm. It as assumed that it would be uniformly distributed over this range.

FIGURE 3.13
FLOWSHEET OF COMPUTATIONAL APPROACH

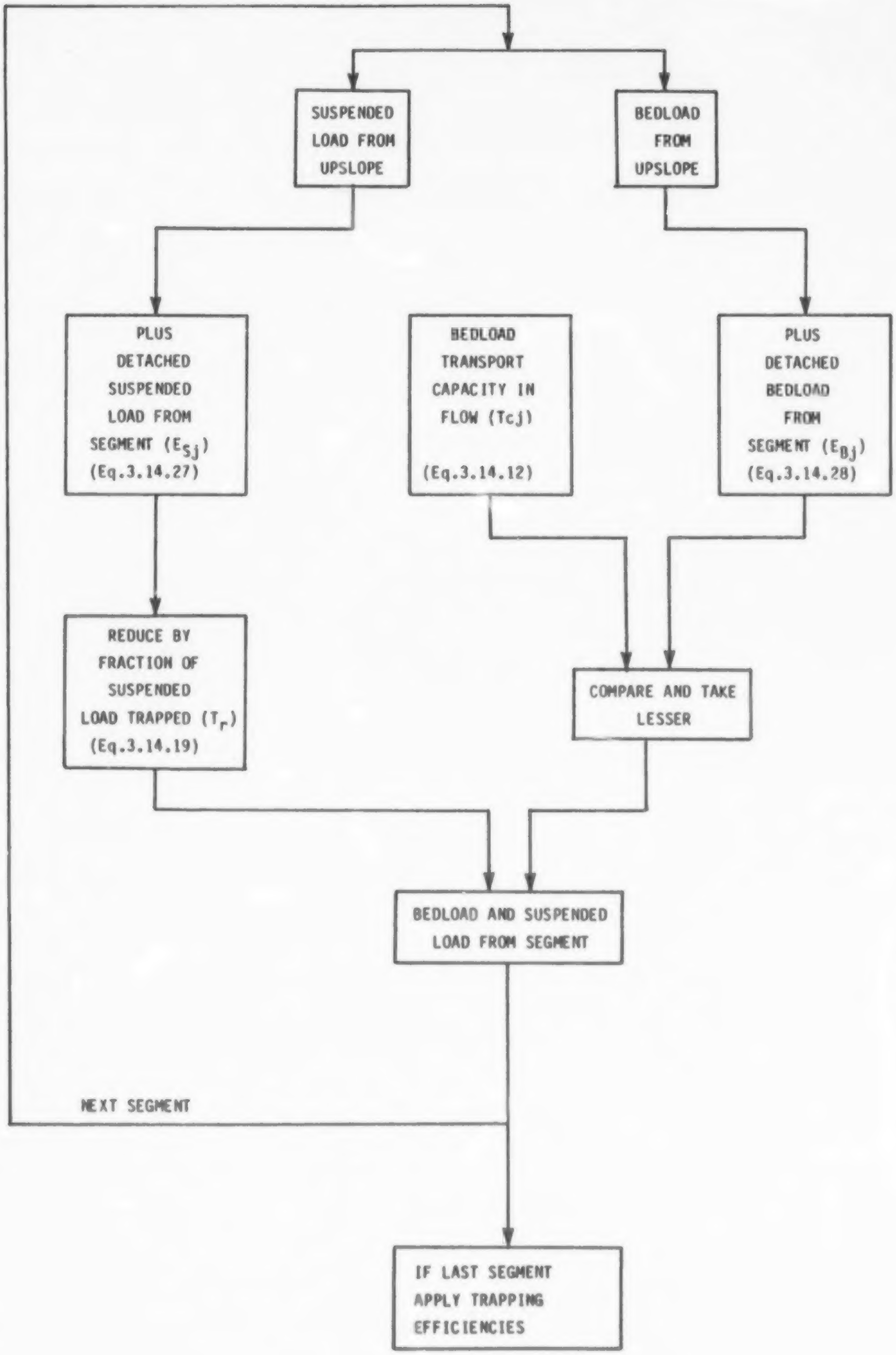
SUSPENDED LOAD FROM UPSLOPE
BEDLOAD FROM UPSLOPE
PLUS DETACHED SUSPENDED LOAD FROM SEGMENT (E_{Sj}) (Eq.3.14.27)
BEDLOAD TRANSPORT CAPACITY IN FLOW (Tcj) (Eq.3.14.12)
PLUS DETACHED BEDLOAD FROM SEGMENT (E_{Bj}) (Eq.3.14.28)
REDUCE BY FRACTION OF SUSPENDED LOAD TRAPPED (T_r) (Eq.3.14.19)
COMPARE AND TAKE LESSER
BEDLOAD AND SUSPENDED LOAD FROM SEGMENT
NEXT SEGMENT
IF LAST SEGMENT APPLY TRAPPING EFFICIENCIES

SOURCE: HAAN, 1978

Table 3.7

EROSION MODEL VARIABLES

Model Symbol	Description	Units	Nominal Value	Probability Distribution*	Computer Origin	Computer Symbol
A_T	surface area of the tailings	m^2	5×10^5	$C(5\times10^5)$	INPUT	ATAIL
E_{Bj}	bedload from segment j	$lb.ft^{-1}(width).yr^{-1}$	calculated	calculated	EROS	BED
E_B	bedload leaving pond	$lb.ft^{-1}(width).yr^{-1}$	calculated	calculated	EROS	BEDPND
P_B	bedload pond trapping efficiency	%	0	C(0)	INPUT	BEDTRP
B	exponent in bedload equation	-	calculated	calculated	EROS	BEXP
b	soil structure code used in soil classification	-	specified in code	specified in code	EROS	BSOIL
C_{ro}	runoff reduction factor	-	calculated	calculated	EROS	CRO
c	soil permeability class	-	specified in code	specified in code	EROS	CSL
CP	control practice factor for USLE	-	calculated	calculated	EROS	CSOIL
C_T	transportability reduction factor in bedload equation	-	calculated	calculated	EROS	CTSOIL
D_{50}	tailings particles size diameter exceeded 50% of time	-	calculated	calculated	EROS	D50
d_f	depth of flow in suspended sediment equation	ft	calculated	calculated	EROS	DF
d	silt particle diameter	ft	calculated	calculated	EROS	DMID
d_m	median silt diameter	mm	0.04	U(0.0015,0.075)	INPUT	DM
T_m	total sediment mass leaving tailings pond	kg	calculated	calculated	EROS	EROTOT
D_j	soil detached in slope segment j	$lb.ft^{-1}(width).yr^{-1}$	calculated	calculated	EROS	ESOIL
L_f	flow length (metric)	m	710	C(710)	INPUT	FLENGT
F_m	minimum fraction of tailings covered with vegetation	m	0	C(0)	INPUT	MINVEG
F_v	fraction of tailings covered with vegetation	-	calculated	calculated	EROS	FVEG

Table 3.7, cont'd.

Model Symbol	Description	Units	Nominal Value	Probability Distribution*	Computer Origin	Computer Symbol
K	soil erodibility factor	tons/acre per unit "R"	calculated	calculated	EROS	KSOIL
L	flow length of tailings pile	ft	calculated	calculated	EROS	LENFT
λ_{cj}	length from top of tailings pile to bottom of jth segment	ft	calculated	calculated	EROS	LENTOT
m	slope exponent for USLE	-	calculated	calculated	EROS	MSLP
M	parameter in soil erodibility equation	-	calculated	calculated	EROS	MSOIL
N	number of slope segments	-	calculated	calculated	EROS	NLEN
a	percent organic matter of tailings	-	specified in code	specified in code	EROS	PEROM
pH	pH of tailings surface layer	-	calculated	calculated	SOURCE	PH(1)
R	annual rainfall erosivity factor	100 (ft.tons/acre)(in.hr)	81.3	U(65,97.5)	INPUT	RRAIN
R_s	spacing hydraulic radius	ft	calculated	calculated	EROS	RS
r	proportionality constant for bedload transport equation	$ft^2.(sec.yr)^{-1}$."R units"	$5.5x10^{-8}$	$U(1x10^{-8},1x10^{-7})$	INPUT	RSOIL
λ_j	length of slope of jth segment	ft	calculated	calculated	EROS	SEGLEN
S_i	percent silt (tailings surface)	-	45	T(30,45,60)	INPUT	SILT
S_o	overall percent slope of tailings pile	%	1.0	C(1.0)	INPUT	SLOPE
S	slope factor	-	calculated	calculated	EROS	SLPFAC
S_s	spacing between grass	ft	calculated	calculated	EROS	SPACE
x	sine of slope angle	-	calculated	calculated	EROS	SPRIME
S_t	24 hour rainfall for 2-year return period	$mm.d^{-1}$	42	U(36,48)	INPUT	STORM
E_{sj}	suspended sediment load from segment j	$lb.ft^{-1}(width).yr^{-1}$	calculated	calculated	EROS	SUS
E_s	suspended sediment load leaving pond	$lb.ft^{-1}(width).yr^{-1}$	calculated	calculated	EROS	SUSPND
P_s	suspended sediment pond trapping efficiency	%	0	C(0)	INPUT	SUSTRP

Table 3.7, cont'd.

Model Symbol	Description	Units	Nominal Value	Probability Distribution*	Computer Origin	Computer Symbol
T_{cj}	bedload transport capacity	$lb.ft^{-1}(width).yr^{-1}$	calculated	calculated	EROS	TCSOIL
T_H	revegetation half-life	yr	15	U(15,25)	INPUT	THALF
T_r	fraction of suspended sediment trapped	-	calculated	calculated	EROS	TRSED
T_s	transportability of soil particles in bedload transport	-	calculated	calculated	EROS	TSOIL
T_v	time at which vegetative growth commences (pH>4)	yr	calculated	calculated	EROS	TVEG
V	flow velocity through grass	$ft.s^{-1}$	calculated	calculated	EROS	VEL
V_R	velocity ratio used in bedload transport equation	-	calculated	calculated	EROS	VELRAT
V_s	settling velocity from Stokes Law	$ft.s^{-1}$	calculated	calculated	EROS	VS
W	width of tailings pile	ft	calculated	calculated	EROS	WIDTH

Note

* Distributions are as described in Table 2.3.

Silt Particle Diameter

The mean diameter (d_m) of the silt particles at the tailings surface was determined using a typical grain size distribution for uranium tailings (SENES, 1986). As shown in Figure 3.12, the maximum silt grain size was 0.075 mm (by definition) and the minimum was 0.0015 mm, with the remaining particles evenly distributed over this range. As a result, the distribution of d_m was modelled as uniform, with a maximum of 0.075 mm and a minimum of 0.0015 mm.

Minimum Fraction of Tailings Covered by Vegetation

Initially, no man-assisted or natural vegetation exists on the reference site, so the minimum fraction of tailings covered by vegetation (F_m) is set to 0.

Vegetation Half-Life

The vegetation half-life (T_H) is the time required for the tailings vegetation coverage to go from 0 % to 50% under natural conditions, given that the surface pH is above 4.0. This half-life was determined based on a study of environmental conditions at the Gunnar uranium tailings site in northern Saskatchewan (Kalin, 1981). The Gunnar site was chosen because of its natural pH and its absence of man assisted vegetation. The study results indicate that, 20 years after the site was abandoned, it was roughly half covered with vegetation. Due to the uncertainty associated with predicting exactly when 50% coverage occurs, the distribution of T_H was modelled as uniform over the range of 15 to 25 years.

Flow Length of Tailings Pile

The length of the tailings pile along the direction of flow (L_f) must be specified. For the reference site, the shape of the pile is assumed to be square. Given that the surface area of the tailings is 5×10^5 m^2, the flow length is caluclated as:

$$L_f = (5 \times 10^5 \ m^2)^{0.5}$$
$$= 7.1 \times 10^2 \ m$$

Pond Trapping Efficiencies

The ability of a pond to trap soil sediment can be determined from the pond area, its outflow rate, and the diameter of the sediment particles (Chen, 1975). Given that bedload consists of all particles greater than 0.075 mm in diameter (and suspended sediment is all particles less than 0.075 mm), Figure 3.14 gives the trapping efficiency for various particle diameters as a function of the ratio of pond area to outflow rate (ft^{-1}).

For the reference site, there is no pond located within the tailings area, and thus the suspended sediment and bedload pond trapping efficiences are both zero.

Slope of the Tailings Piles

For the reference site, the overall slope of the tailings pile is taken to be 1.0%.

3.14.8 Erosion Model Demonstration

A series of tests were performed to check the erosion model for accuracy and reasonableness. Hand calculations were checked against a deterministic run to confirm that the code calculated the equations properly.

Finally, the model was run within the generic framework, with the input parameters set at their nominal values (Table 3.7). The results of this run, over the first 200 years, are shown in Figure 3.15. After an initial drop the surface pH rises above 4 after 80 years. At this point vegetation begins on the tailings surface, which leads to the sharp reduction in sediment mass leaving the pile.

FIGURE 3.14

TRAPPING EFFICIENCY
vs. RATIO OF POND AREA TO OUTFLOW RATE

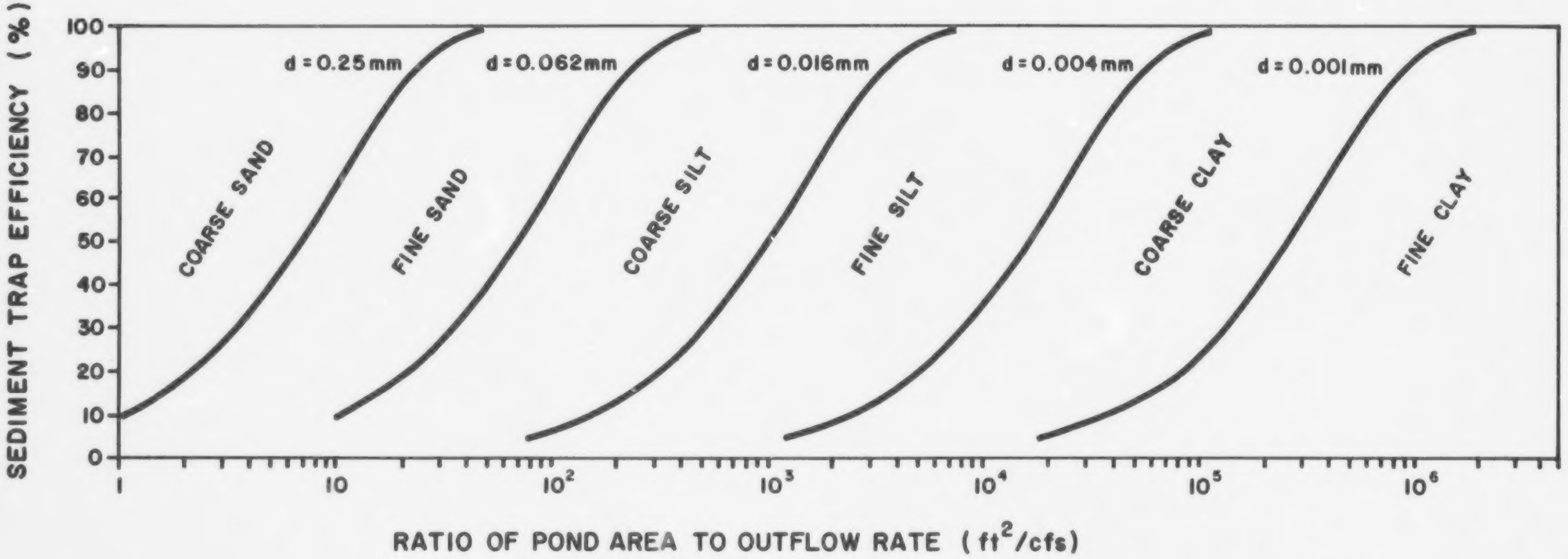

SOURCE: ADAPTED FROM CHEN, 1975

FIGURE 3.15

CUMULATIVE TAILINGS DEPLETION AND pH vs. TIME

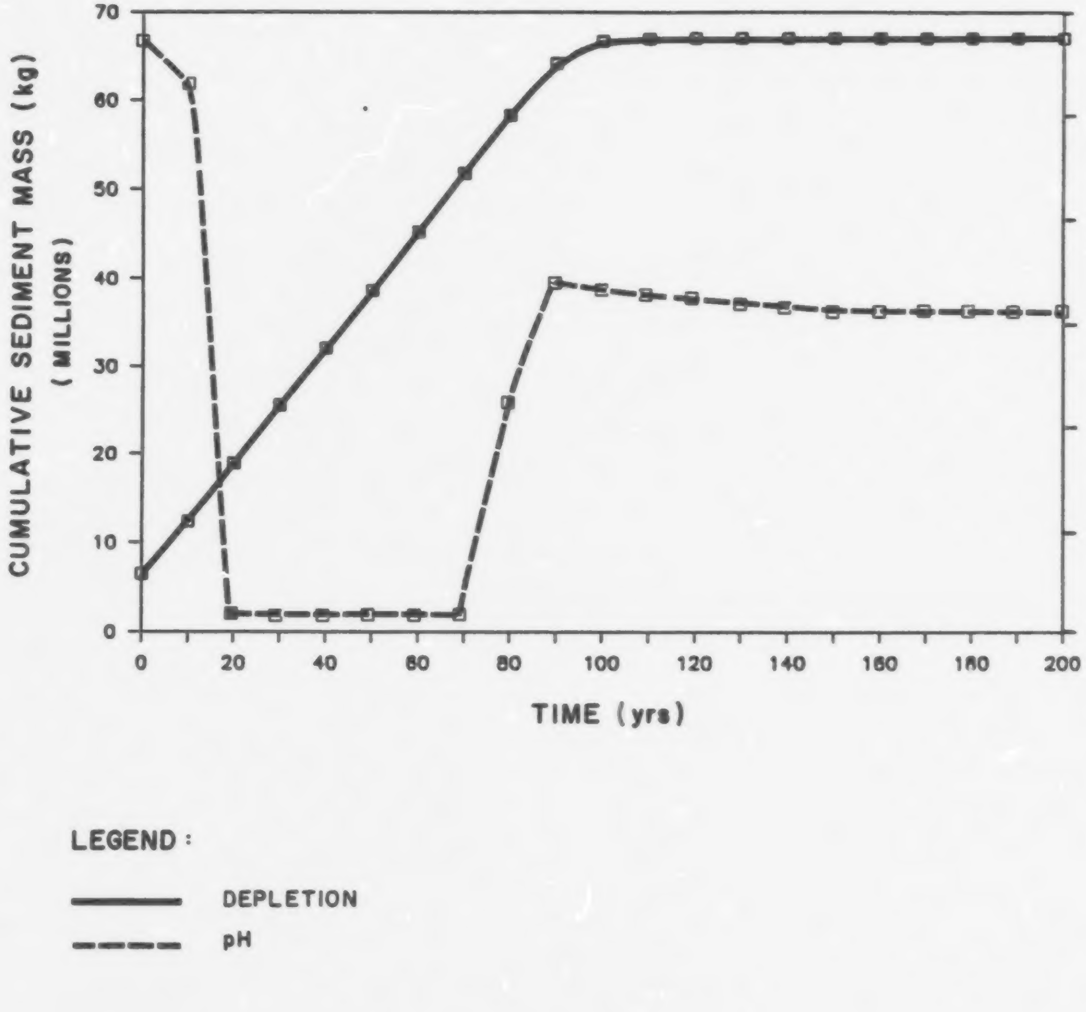

3.15 REFERENCES

Beak Consultants Ltd., 1985. "The Geochemical Mechanism Controlling Ra-226 Dissolution in Uranium Mill Wastes (Tailings)." Research Report prepared for the National Uranium Tailings Program, CANMET, EMR, under Supply and Services Canada Contract No. 15SQ.23241-4-1678.

Berner, R.A., and Holdren, G.R., 1979. "Mechanism of Feldspar Weathering, II, Observation of Feldspars in Soils." Geochim. Cosmochim. Acta. Vol. 43, pp. 1173-1186.

Chen, C.C., 1975. "Design of Sediment Retention Basins." National Symposium on Urban Hydrology and Sediment Control, University of Kentucky, BU109.

Evans, R.D., 1955. "The Atomic Nucleus." McGraw-Hill Book Company Inc.

Faust, S.D., and Aly, O.M., 1981. "Chemistry of Natural Waters." Ann Arbor Science Publishers, Inc., Ann Arbor, Michigan.

Foster, G.R., and Wischmeier, W.H., 1974. "Evaluating Irregular Slopes for Soil Loss Prediction." Trans. Am. Soc. Agr. Eng. 17: 305-309.

Golder Associates, SENES Consultants Limited, Beak Consultants Limited, and Cumming-Cockburn and Associates Limited, 1986. "Lacnor Field Study; The Results of a One Year Field Monitoring Program." Prepared for the National Uranium Tailings Program, CANMET, EMR, under Supply and Services Canada Contract No. 15SQ.23241-4-1680.

Gresens, R.L., 1981. "The Aqueous Solubility Product of Solid Solutions." Chem. Geol., Vol. 32, pp. 73-86.

Haan, Barfield, 1978. "Hydrology and Sedimentology of Surface Mined Lands." Office of Continuing Education and Extension, College of Engineering University of Kentucky, Lexington, Kentucky.

Halbert, B.E., Scharer, J.M., Knapp, J.A., and Gorber, D.M., 1983. "Determiniation of Acid Generation Rates in Pyritic Mine Tailings." Presented at the 56th Annual Conference of the Water Pollution Control Federation, October 2-7, Atlanta, Georgia.

Helgeson, H.C., Murphy, W.M., and Aagaard, P., 1984. "Thermodynamic and Kinetic Constraints on Reaction Rates Among Minerals and Aqueous Solutions, II, Rate Constants, Effective Surface Area, and the Hydrolysis of Feldspar." Geochim. Cosmochim. Acta. Vol. 48, pp. 2405-2432.

Hertz, F.C., Jr., and Tyree, S.Y., Jr., 1965. "A Light-Scattering Investigation of the Hydrolytic Behaviour of Thorium in Aqueous Perchlorate Media". Inorg. Chemi., Vol 4(b), pp. 873-879.

Hoffman, M.R., Faust, B.C., Panda, F.A., Koo, H.H., and Tsuchiya, H.M., 1981. "Kinetics of the Removal of Iron Pyrite from Coal by Microbial Catalysis." Appl. and Env'tl. Microbiol., Vol. 42, pp.259-271.

Jaynes, D.B., Rogouski, A.S., and Pionke, H.B., 1984. "Acid Mine Drainage from Reclaimed Coal Strip Mines; 1. Model Description." Water Resources Research, Vol. 20, No. 2, pp. 233-242, February.

Kalin, M., 1981. "A Preliminary Assessment of the Environmental Conditions of Two Abandoned Uranium Mill Tailings Sites in Saskatchewan." Environment Canada Surveillance Report EPS-5-WNR-81-1.

MacLaren, James. F., Ltd., 1977. "Environmental Assessment of the Proposed Elliot Lake Uranium Mines Expansion. Volume II." Report to Denison Mines Limited and Rio Algom Limited, Elliot Lake, Ontario.

MacLaren, James. F., Ltd., 1978. "Environmental Assessment of the Proposed Elliot Lake Uranium Mines Expansion. Volume 4, Environmental Assessment." Prepared for Denison Mines Limited and Rio Algom Limited, Elliot Lake, Ontario.

Melis Consulting Limited and SENES Consultants Limited, 1986. " Study of the Geochemistry of Thorium in Uranium Mill Tailings". Research Report Prepared for the National Uranium Tailings Assessment Program under Supply on Services Contract No. 15SQ-23317-6-1723.

Morin, K.A., Cherry, J.A., Lim, T.P. and Vivyurka, A.J., 1982. "Contaminant Migration in a Sand Aquifer Near an Inactive Uranium Tailings Impoundment." Elliot Lake, Ontario, Canadian Geotechnology Journal, Vol. 19, pp. 49-62.

Myerson, A.S., 1981. "Oxygen Mass Transfer Requirements During the Growth of Thiobacillus Ferrooxidans on Iron Pyrite." Biotechnology and Bioengineering, Vol. 23, pp. 1413-1416.

National Research Council (NRC), 1983. "Radioactivity in the Canadian Aquatic Environment." Pub. No. NRCC 19250.

Neibling, W.H., and Foster, G.R., 1977. "Estimating Deposition and Sediment Yield from Overland Flow Processes." Proc. Int. Symp. on Urban Hydrology, Hydraulics, and Sediment Control, UK BU 114, College of Engineering, University of Kentucky, Lexington, Kentucky.

Nordstrom, O.K., 1982. "Aqueous Pyrite Oxidation and the Consequent Formation of Secondary Iron Minerals in Acid Sulphate Weathering." Soil Science Society of America, pg. 37-55.

Rancon, D., 1983. "The Behaviour in Underground Environments of Uranium and Thorium Discharged by the Nuclear Industry." In: Environmental Behaviour of Radionuclides Released in the Nuclear Industry, International Atomic Energy Agency Report, IAEA-SM-172/55.

Reardon, E.J., Moddle, P.M., 1985. "Gas Diffusion Coefficient Measurements in Uranium Mill Tailings: Implications to Cover Layer Design". Preprint to Reclamation and Revegetation Research.

SENES Consultants Limited, 1983. "Aid Generation Tests on Pyritic and Depyritized Tailings With and Without Limestone Addition." Research Report prepared for Denison Mines Limited, Elliot Lake, Ontario.

SENES Consultants Limited, 1984. "A Study to Develop and Demonstrate Techniques for the Probabilistic Assessment of the Long-Term Effects of Uranium Mill Tailings in Canada - Phase I." Research Report prepared for the National Uranium Tailings Program, CANMET, EMR, under Supply and Services Canada Contract No. OSQ83-00236.

SENES Consultants Limited, 1985a. "A Study to Develop and Demonstrate Techniques for the Probabilistic Assessment of the Long-Term Effects of Uranium Mill Tailings in Canada - Phase II." Research Report prepared for the National Uranium Tailings Program, CANMET, EMR, under Supply and Services Canada Contract No. OSQ84-00207.

SENES Consultants Limited, 1985b. "The Approaches to Risk Assessment for Canadian Uranium Mill Tailings." Research Report Prepared for the National Uranium Tailings Program under Supply and Services Canada Contract No. 14SQ.23241-4-1695.

SENES Consultants Limited, and BEAK Consultants Limited, 1986. "Estimation of the Limits of Acid Generation by Bacterially Assisted Oxidation in Uranium Mill Tailings." Research Report prepared for the National Uranium Tailings Program under Supply and Services Canada Contract No. OSQ85-00237.

SENES Consultants Limited, 1986. "Probabilistic Model Development for the Assessment of the Long-Term Effects of Uranium Mill Tailings on Canada - Phase III, Volume 3 - Component Models" Research Report prepared for the National Uranium Tailings Assessment Program under Supply and Services Canada Contract No. OSQ85-00182.

SENES Consultants Limited, 1987. "Uranium Tailings Assessment Program (UTAP.3), Application to the Lacnor Tailings Site". Research Report Prepared for the National Uranium Tailings Program, CANMET, under Supply and Services Canada Contract No. 23317-6-17281-SQ.

Sillen, L.G. and Martell, A.E., 1971. "Stability Constants." Special Publication No. 25, The Chemical Society, London, U.K.

Silver, M., and Ritcey, G.M., 1980. "A Simulated Study on the Effects of Bacteria, Organics and Salt Solutions on Uranium Mill Tailings from Elliot Lake, Ontario." Project MRP-4.3.0.6.02, CANMET, Ottawa.

Skeaff, J.M., 1977. "Distribution of Radium-226 in Uranium Tailings." CANMET Report MRP/MSL 77-349 (J), Ottawa.

Stumm, W. and Morgan, J.J., 1981. "Aquatic Chemistry." John Wiley and Sons, New York, NY.

U.S. Army Corps of Engineers, 1986. "Hydrologic Evaluation of Landfill Performance Model (HELP)". Department of the Army, Vicksburg, Mississippi.

Veska, E., 1983. "Origin and Subsurface Migration of Radionuclides from Waste Rock at an Abandoned Uranium Mine Near Bancroft, Ontario." Unpublished Ph.D. Thesis, University of Waterloo.

Wall, G.J., Dickinson, W.T., and Greuel, J., 1983. "Canadian Journal of Soil Science." Vol. 63, pp. 271-280.

Walters, W.H., 1985. "Computational Methods for Estimating Overland Erosion of Uranium Tailings." Nuclear Safety, Vol. 26, No.2 .

Wischmeier, W.H. and Smith, D.D., 1978. "Predicting Rainfall Erosion Losses: A Guide to Conservation Planning. Agri. Handbook Δ537 Science and Education Administration. U.S. DOA.

4.0 AIR SOURCE MODELS

4.1 Introduction

Chapter 3 describes how the concentrations of the radionuclides in the unsaturated layer of the tailings are calculated. This chapter describes how the radon and dust air source rates are calculated.

4.2 Radon Source Model

The model used in the Phase II study (SENES, 1985) to simulate the release of radon from the tailings surface was chosen because of its adaptability to the tailings model derived for the water source term. As described in Chapter 3, the tailings are modelled as a multi-layered system: an upper, unsaturated layer in which the radium concentration is a function of depth, and a lower, saturated layer. The saturated and unsaturated layers are subdivided into various zones in the water source term model.

The saturated layer is not a source of radon that can reach the tailings surface since the water effectively prevents its diffusion; the diffusive transport distance of radon in the water-filled pores of the tailings is orders of magnitude less than the diffusive transport distance in the unsaturated pores. The unsaturated layer can be subdivided into two zones as described in the water source model: an upper, barium sulphate ($BaSO_4$) - depleted zone (with a reduced radium content) and a lower, barium sulphate-enriched zone (with an enriched radium content). The depth of the interface of the two zones depends on the chemistry of the tailings. The depth changes with time (over tens of years) until the entire unsaturated layer is depleted of barium sulphate.

In terms of radon release to the atmosphere, each of these zones in the unsaturated layer can be considered to be homogeneous, with each zone characterized by an average radium concentration, moisture content, porosity, density and radon emanation coefficient. This model for radon release is equivalent to a covered tailings model in which the tailings are of finite thickness and the cover also contains radium i.e. the "cover" is the upper zone and the "tailings" is the lower zone. The theoretical development of such a model has been carried out by Rogers _et al_. (1980). The model accounts for the unique definitions of both the tailings and cover in terms of parameters that affect radon release such as radium concentration and radon diffusion length and thus it can be used to model the total radon release from both zones of the unsaturated layer.

4.2.1 Radon Source Model Development

Denoting the upper zone of the unsaturated layer as zone 1 of thickness $x_{1,t}$, and the lower zone as zone 2 of thickness $x_{2,t}$, the general formula for the radon flux at the surface of the tailings is (following Rogers _et al_., 1980, Chapter 4, Equation 14):

$$J_t = \frac{-D_1 a_1}{\cosh(a_1 x_{1,t})} \left[\frac{[1+Z \coth(a_2 x_{2,t})]([C_o]-s_{1,t}/a_1^2)\exp(a_1 x_{1,t})+(s_{1,t}/a_1^2-s_{2,t}/a_2^2)}{\tanh(a_1 x_{1,t}) + Z \coth(a_2 x_{2,t})} \right]$$

$$+ \quad D_1 a_1 ([C_o] - S_{1,t}/a_1^2) \qquad (4.1)$$

where

J_t = radon flux at time t ($Bq.m^{-2}.s^{-1}$)

D_k = radon diffusion coefficient ($m^2.s^{-1}$)

$[C_o]$ = radon concentration above the tailings surface (considered constant) ($Bq.m^{-3}$)

$a_k = \sqrt{\frac{\lambda \epsilon_k}{D_k}}$ = 1/(radon diffusion length L_k) (m^{-1})

$Z = \frac{D_1 a_1}{D_2 a_2}$

$s_{k,t} = \frac{[Ra]_{k,t} \rho_{k,t} \lambda E_k}{D_k}$

$[Ra]_{k,t}$ = tailings radium concentration at time t ($Bq.g^{-1}$)

ρ_k = tailings density ($g.m^{-3}$)

E_k = emanation coefficient ($0 \leq E \leq 1$, dimensionless)
λ = radon decay constant ($2.1 \times 10^{-6}\ s^{-1}$)
L_k = radon diffusion length in tailings (m)
ϵ_k = porosity (dimensionless)

and where subscript k = 1 or 2 refers to zone 1 or 2, respectively. The product of $[Ra]_{k,t}$ and ρ is sometimes given only by one parameter when $[Ra]_{k,t}$ is measured in units of $Bq.m^{-3}$.

In the limit of no upper zone (i.e. $x_{1,t} = 0$) and negligible atmospheric radon $[C_o] = 0$, which is a good approximation since $[C_o]$ is orders of magnitude less than the radon concentration within the tailings, equation (4.1) becomes:

$$J_t = [Ra]_{2,t}\, E_2\, \rho_2 \sqrt{\frac{\lambda D_2}{\epsilon_2}} \tanh\left[\sqrt{\frac{\lambda\ \epsilon_2}{D_2}}\ x_{2,t}\right] \qquad (4.2a)$$

In situations where the unsaturated layer of tailings is very thick (i.e. $x_{2,t} = \infty$) this further simplifies to:

$$J_t = [Ra]_{2,t}\, E_2\, \rho_2 \sqrt{\frac{\lambda D_2}{\epsilon_2}} \qquad (4.2b)$$

Although somewhat conservative, in the computer model implemented in this study, equation (4.2b) is used when the thickness of the upper zone is less than 1.0×10^{-3} m. Otherwise, equation (4.1) is used.

Equation (4.2b), which is essentially the product of the radon source strength within the tailings ($Bq.m^{-3}.s^{-1}$) and the diffusion length of radon (m), is identical to the equation that is often used to estimate radon release rates from bare, thick tailings (e.g. U.S. NRC, 1980). This equation was used in the Phase I study (SENES, 1984).

The radon diffusion coefficient is highly dependent on tailings moisture content. As noted in the Phase I and Phase II studies, Rogers et al. (1980), suggest an empirical relationship of the form:

$$D = 0.106 \times 10^{-4}\,\epsilon \exp(-0.261\,M) \quad (m^2 \cdot s^{-1}) \tag{4.3}$$

where

M = percent moisture content of (wet) tailings by weight

$$= 100 \times \frac{\text{weight of water in tailings}}{\text{weight of wet tailings}}$$

Since equation (4.3) is used for this study, the radon flux given by equation (4.1) is not explicitly dependent on the porosity ϵ. The flux is implicitly dependent on ϵ because of the empirical constants in equation (4.3). For site-specific evaluations for which more data are available, more recent research suggests that a different form of equation (4.3) can be used (Rogers et al., 1984).

The emanation coefficient E can also depend on the moisture content, especially at low ($\leq 5\%$) moisture levels (Strong and Levins, 1982). However, for the Canadian environment the moisture content is generally greater than 5% and parameterization of the effects of moisture beyond equation (4.3) was not considered necessary for this study.

The generality of equation (4.1) can accommodate completely different characteristics for each zone. For the present modelling exercise, only the thickness and radium concentration of each zone differ. The moisture and porosity, and hence the radon diffusion coefficient, of each zone are assumed to be identical. Under these conditions ($Z=1$, $a_1 = a_2 = a$ and setting $C_0=0$), equation (4.1) reduces to:

$$J_t = -\frac{D}{a\cosh(ax_{1,t})}\left[\frac{-[1+\coth(ax_{2,t})]s_{1,t}\exp(ax_{1,t}) + s_{1,t} - s_{2,t}}{\tanh(ax_{1,t}) + \coth(ax_{2,t})}\right] - \frac{Ds_{1,t}}{a} \tag{4.4}$$

Equation (4.4) can be used to estimate the radon flux from tailings under normal conditions. However, freezing conditions and snow cover greatly attenuate the radon flux because of the much smaller radon diffusion coefficient of ice relative to water. The effect is dependent on the moisture content of the tailings. The ratios of the radon fluxes from unfrozen and frozen tailings samples as measured by Zettwoog et al. (1981) were 3, 100 and 400 for tailings moisture contents of <10%, 30% and saturation, respectively. This effect can be accommodated in the radon source model by using a seasonally-weighted average for radon flux and a winter/summer flux ratio. The annual average flux $J_{avg,t}$ is then given by:

$$J_{avg,t} = J_t(N_wR + (12-N_w))/12 \qquad (4.5)$$

where

N_w = number of winter months (freezing conditions) per year

R = frozen/unfrozen flux ratio (dimensionless)

Since both the radon flux and meteorological conditions are seasonal, a more detailed model could estimate radon concentrations on a seasonal (or even monthly) basis. However, for this study, the approximation engendered by the use of annual averages for both the source term and meteorological conditions is considered acceptable.

$J_{avg,t}$ is the annual average radon flux in units of $Bq.m^{-2}.s^{-1}$. To obtain the total flux $J_{T,t}$ for the tailings area, this must be multiplied by the surface area A_o. In contrast to the dust source model which accommodates the effect of tailings vegetation on dust emissions (Section 4.2), the radon source model assumes that vegetation does not affect radon release rates. No conclusive research data are available to quantify the effects of vegetation on radon releases but measurements on Elliot Lake tailings suggest that vegetation does not significantly affect radon release (DSMA ATCON, 1985). Thus, the surface area is considered a constant A_o for estimating radon release and

$$J_{T,t} = J_{avg,t}A_o \qquad (4.6)$$

Equation (4.6) is used to estimate the average annual radon release rate from a two-layered tailings with a different radium content in each layer. To include the effect of a non-radioactive cover on the tailings, a cover attenuation factor is applied to equation (4.6):

$$J_{T,C,t} = (1-C_{AF})\, J_{avg,t} A_0 \qquad (4.7)$$

where

C_{AF} = cover attenuation factor for radon ($0 \leq C_{AF} \leq 1$, dimensionless).

The cover attenuation factor C_{AF} is intended to be used as an engineering factor, and is set to zero when there is no cover.

Since the barium sulphate zone thicknesses and radium concentrations in the water source model are time-dependent, the average radon flux $J_{avg,t}$ and annual radon release $J_{T,C,t}$ are also time-dependent.

4.2.2 Parameter Values

The variables used to calculate the radon source rate are listed in Table 4.1. All of the input variables, with the exception of the emanation coefficient E, the moisture content M, the number of winter months, N_w, and the winter/summer flux ratio R, are as used in the water source model (Chapter 3).

Emanation Coefficient

The nominal value of 0.2 for the radon emanation coefficient E has often been used to model radon emissions from tailings areas (e.g. U.S. NRC, 1980). The suggested range for E is based on data in Strong and Levins (1982) and U.S. NRC (1980). The triangular distribution for E gives the highest probability to values around 0.2 while accommodating the possibility of some higher values, such as those measured for uranium ores (Austin and Droullard, 1978).

Moisture Content

A nominal value of 15% for the moisture content by weight of (wet) tailings M was selected as our best estimate of the average moisture content of the average tailings. A triangular distribution for M which gives the highest probability to the 15% value, with a value of 25% (which is close to saturation) for the maximum value, and a value of 7% (almost dry tailings) for the minimum value.

Number of Winter Months

The number of winter months (freezing conditions) per year N_w was set constant at 5 months. This value was selected from data gathered at the Gore Bay weather station on Manitoulin Island, Ontario.

Winter/Summer Flux Ratio

The log normal distribution suggested for the winter/summer flux ratio R is based on the measurements of Zettwoog *et al*. (1981). The values are: geometric mean of 0.02, geometric standard deviation of 2.0, minimum of 0.002, and a maximum of 0.2.

Correlations

The radon source model was used to investigate the incorporation of parameter correlations. The results are documented in Appendix I of Volume 2 of this report.

4.2.3 Description of the Computer Model

The radon source model computer code is given in Table 4.2. The computer symbols for the parameters are presented in Table 4.1.

If the thickness of the barium sulphate-enriched zone is less than $1.0\mathrm{x}10^{-3}$ m or the ratio of barium sulphate-depleted zone to the radon diffusion length is greater than 50, then equation (4.2b) is used; otherwise, equation (4.4) is used.

4.3 Dust Source Model

The empirical dust source model used in this assessment was developed by the Colorado Department of Health based on experimental work carried out at mining operations in the western United States (CDOH, 1984). Detailed studies of dust dispersion from tailings in climates similar to those that occur on the Canadian Shield have not been identified. This model will have to be reviewed on a periodic basis and updated in the future to reflect the results of further research in this area.

4.3.1 Dust Source Model Development

The emission rate of the ith radionuclide from the tailings surface at time t can be expressed as:

$$Q_{i,t} = 2.2 \times 10^{-6} \left[\frac{S}{1.5}\right] \left[\frac{365-P_{a,t}}{235}\right] \left[\frac{f_t}{0.15}\right] \left[\frac{[C]_{i,t}}{\rho}\right] A_t \qquad (4.8)$$

where

$Q_{i,t}$ = emission rate of the ith radionuclide at time t ($Bq.s^{-1}$)

S = silt content (%)

$P_{a,t}$ = annual number of days with more than 0.25 mm of precipitation (time variant) (days)

f_t = frequency of the time wind speed at the mean tailings pile height exceeds 5.4 $m.s^{-1}$ (refer to Section 5.3) (time variant)

$[C]_{i,t}$ = concentration of the ith radionuclide at time t in the tailings surface layer (layer 1 as defined in Chapter 3) ($Bq.m^{-3}$)

ρ = tailings bulk density ($g.m^{-3}$)

A_t = the exposed tailings surface area at time t (m^2).

Table 4.1

RADON SOURCE MODEL VARIABLES

Model Symbol	Description	Units	Nominal Value	Probability* Distribution	Computer Origin	Computer Symbol
a	reciprocal of radon diffusion length in tailings	m^{-1}	calculated	calculated	RADON	DIFLEN
D	effective bulk radon diffusion coefficient of tailings	$m^2.s^{-1}$	calculated	calculated	RADON	EBKDFC
E	radon emanation coefficient of tailings	-	0.2	T(0.02, 0.2, 0.9)	INPUT	EMANAT
$J_{T,C,t}$	total radon flux at time t	$Bq.s^{-1}$	calculated	calculated	RADON	EMRATE(5)
R	winter/summer flux ratio	-	0.02	LN(0.02,2.0, 0.002,0.2)	INPUT	WTSFLX
M	moisture content by weight of (wet) tailings	%	15.0	T(5.0,15.0,25.0)	INPUT	MPCH2O
ϵ	porosity of tailings	-	calculated	calculated	SOURCE	POROS
$[Ra]_{k,t}$	radium concentration of zone i = 1 or 2 at time t	$Bq.m^{-3}$	calculated	initialized then calculated	SOURCE	CONC(4,i,3) i=1,2
$X_{1,t}$	thickness of $BaSO_4$ depleted zone at time t	m	calculated	calculated	SOURCE	DBAR(3)
$X_{2,t}$	thickness of $BaSO_4$ enriched zone at time t	m	calculated	calculated	RADON	EBAR(3)
λ	radon decay constant	s^{-1}	2.1×10^{-6}	defined	RADON	LAM(5)
A_0	surface area of the tailings	m^2	5.0×10^5	C (5.0×10^5)	INPUT	ATAIL
N_w	number of winter months (freezing conditions) per year	months	5.0	C (5.0)	INPUT	NSUBW
X_s	thickness of unsaturated layer	m	1.0	U (0.75,1.25)	INPUT	DUNSAT
C_{AF}	cover attenuation factor for radon	-	0.0	C(0.0)	INPUT	CAFR

* Distributions are as described in Table 2.3.

Table 4.2

RADON MODEL CODE LISTING

```
      SUBROUTINE RADON
      INCLUDE 'MODEL.INC'
      INCLUDE 'VAR.INC'
      REAL*4 EBAR(3)
      LAM(5)=2.1E-6
      EBKDFC=0.106E-4*POROS*EXP(-0.261*MPCH2O)
      DIFLEN=SQRT(LAM(5)*POROS/EBKDFC)
      CONST1=LAM(5)*EMANAT/(EBKDFC*DIFLEN*DIFLEN)
      CONST2=EBKDFC*DIFLEN*ATAIL
      CONST3=EMANAT*LAM(5)*ATAIL/DIFLEN
      CONST4=(1.0-CAFR)*(NSUBW*WTSFLX+12.0-NSUBW)/12.0
      EBAR(3)=DUNSAT-DBAR(3)
      IF(EBAR(3).LT.1.0E-3)THEN
         EBAR(3)=0.0
         DBAR(3)=DUNSAT
      ENDIF
      X1=DIFLEN*DBAR(3)
      IF(EBAR(3).EQ.0.0.OR.X1.GT.50.0)THEN
         EMRATE(5)=CONST3*CONST4*TANH(X1)*CONC(4,1,3)
      ELSE
         X2=DIFLEN*EBAR(3)
         XDEN=COSH(X1)*(TANH(X1)+1.0/TANH(X2))
         XNUM=((1.0+1.0/TANH(X2))*CONST1*CONC(4,1,3)*EXP(X1)
     +        -CONST1*(CONC(4,1,3)-CONC(4,2,3)))
         EMRATE(5)=CONST2*CONST4*(XNUM/XDEN-CONST1*CONC(4,1,3))
      ENDIF
C
      IF(CODRAD.EQ.1.0.OR.CODRAD.EQ.2.0.OR.CODRAD.EQ.3.0)THEN
         WRITE(*,100)
      ENDIF
      IF(CODRAD.EQ.3.0)THEN
         WRITE(*,101)POROS,MPCH2O,LAM(5),EMANAT,ATAIL,EBKDFC,DIFLEN,
     +               CAFR,NSUBW,WTSFLX,DUNSAT,DBAR(3),CONC(4,1,3)
         IF(EBAR(3).GT.0.0)THEN
            WRITE(*,102)EBAR(3),CONC(4,2,3)
         ENDIF
      ENDIF
      IF(CODRAD.EQ.2.0.OR.CODRAD.EQ.3.0)THEN
         WRITE(*,103)EMRATE(5)
      ENDIF
C
100   FORMAT(///1X,'RADON SOURCE MODEL')
101   FORMAT(/1X,'POROSITY OF TAILINGS',E12.4/1X,'MOISTURE CONTENT O',
     +       'F TAILINGS',E12.4/1X,'RADON DECAY CONSTANT',E12.4/1X,
     +       'RADON EMANATION CONSTANT',E12.4/1X,'SURFACE AREA OF TA',
     +       'ILINGS',E12.4/1X,'RADON DIFFUSION CONSTANT',E12.4/1X,
     +       'RECIPROCAL OF RADON DIFFUSION LENGTH',E12.4/1X,'COVER ',
     +       'ATTENUATION FACTOR',E12.4/1X,'NUMBER OF WINTER MONTHS ',
     +       'PER YEAR',E12.4/1X,'WINTER/SUMMER FLUX RATIO',E12.4/1X,
     +       'THICKNESS OF UNSATURATED LAYER',E12.4/1X,'THICKNESS OF',
     +       ' BaSO4 DEPLETED ZONE',E12.4/1X,'RADIUM CONCENTRATION I',
```

Table 4.2 continued.

```
     +       'N BaSO4 DEPLETED ZONE',E12.4)
102   FORMAT(1X,'THICKNESS OF BaSO4 ENRICHED ZONE',E12.4/1X,'RADIUM ',
     +       'CONCENTRATION IN BaSO4 ENRICHED ZONE',E12.4)
103   FORMAT(/1X,'EMISSION RATE OF RADON',E12.4)
C
      RETURN
      END
```

The empirical constant in the equation (4.8) (i.e. 2.2×10^{-6} $g.m^{-2}.s^{-1}$) was developed by the Colorado Department of Health as noted above.

As mentioned in Section 4.2.1, the rate of dust generation is proportional to the surface area of the tailings not covered by vegetation. The exposed surface area of the tailings is given by:

$$A_t = (1-F_{v,t})\,A_o \qquad (4.9)$$

where

A_o = surface area of the tailings (m^2)

$F_{v,t}$ = fraction of tailings covered by vegetation at time t (dimensionless).

The originators of this equation rate it as average to below average in its accuracy of prediction; however, higher ratings are only given for models of well-controlled, consistent industrial sources.

During the winter months, frozen ground conditions and snow cover are assumed to reduce dust emissions to zero. This effect has been accommodated in the dust source model by using a seasonally-weighted average for the dust emission rate. The annual average dust emission rate is then given by:

$$Q_{i,avg,t} = Q_{i,t}\,(12 - N_w)/12 \qquad (4.10)$$

where

N_w = number of winter months (freezing conditions) per year.

Equation (4.9) is used to estimate the average annual dust rate from the surface of the tailings. To include the effects of a non-radioactive cover on the tailings, a cover attenuation factor is applied to equation (4.9).

$$Q_{i,C,t} = (1-C_{AF})\,Q_{i,avg,t}$$

where

C_{AF} = cover attenuation factor for dust ($0 \leq C_{AF} \leq 1$, dimensionless)

The cover attenuation factor for dust C_{AF} is intended to be used as an engineering factor and is set to zero when there is no cover.

There are three factors that control the time-varying behaviour of the emission rates of the radionuclides:

- The surficial concentration of the ith radionuclide $[C]_{i,t}$ will vary as the compound is leached from the tailings surface.
- The effective exposed area of the tailings A_t will decrease with the natural or forced revegetation of the exposed surface.
- The intrinsic dust emission rate will decrease as the tailings surface weathers.

The changes in surficial radionuclide concentrations are assumed to be taken care of by the source term model. While a decrease in the intrinsic dust emission rate with time is expected (as might occur for example with the gradual loss of erodible particles), the process is not well understood at present, and is ignored in this study.

4.3.2 Parameter Values

The variables used to calculate the dust source emission rate are listed in Table 4.3. The input variables for the tailings bulk density ρ, the silt content of the tailings S, and the surface area of the tailings A_0 are discussed in the water source model (Chapter 3). The input variable, number of winter months N_w, is discussed in Section 4.2.2.

Number of Days with Precipitation

$P_{a,t}$, a time variant input variable, is the number of days on which there is measurable precipitation. Winter months are excluded from the derivation of

Table 4.3

DUST SOURCE MODEL VARIABLES

Model Symbol	Description	Units	Nominal Value	Probability* Distribution	Computer Origin	Computer Symbol
$Q_{i,C,t}$	emission rate of the ith radionuclide at time t	$Bq.s^{-1}$	calculated	calculated	DUST	EMRATE (i) i=1,4
S	silt content of the tailings (% of particles <75 μm)	%	45.0	T(30.0,45.0,60.0)	INPUT	SILT
$P_{a,t}$	annual number of days with more than 0.25 mm of precipitation (time variant)	days	149.0	N(149.0,17.0,115.0,183.0)	INPUT	FPREC
f_t	frequency of time the wind speed exceeds 5.4 $m.s^{-1}$ at the mean tailings height (time variant)	-	calculated	calculated	WIND	FWINDT
$[C]_{i,t}$	surficial concentration of ith compound at time t	$Bq.m^{-3}$	calculated	calculated	SOURCE	CONC (i,1,3)i=1,4
A_t	exposed surface area of the tailings at time t	m^2	calculated	calculated	DUST	AEXPT
ρ	tailings bulk density (dry)	$g.m^{-3}$	1.4×10^6	$N(1.4 \times 10^6, 0.1 \times 10^6$ $1.1 \times 10^6, 1.7 \times 10^6)$	INPUT	RHOTAL
N_w	number of winter months (freezing conditions) per year	months	5.0	C (5.0)	INPUT	NSUBW
C_{AF}	cover attenuation factor for dust	--	0.0	C (0.0)	INPUT	CAFD
A_0	surface area of the tailings	m^2	5.0×10^5	$C (5.0 \times 10^5)$	INPUT	ATAIL
$F_{v,t}$	fraction of tailings covered by vegetation at time t	--	calculated	calculated	EROS	FVEG

* Distributions are as described in Table 2.3.

this distribution since dust emissions are assumed to be zero in the winter months. The chosen distribution is normal with a mean of 149, standard deviation of 17 and a minimum and maximum of 115 and 183, respectively. These values were obtained from AES precipitation data from the Gore Bay Weather Station, on Manitoulin Island. The net result of these assumptions with regard to meteorological parameters is to spread summer precipitation out over the whole year. Ongoing research in this area may suggest improvements in model formulation or parameter selection.

4.3.3 Description of the Computer Model

The variables used in the dust source term model are summarized in Table 4.3. The computer code listing for this model is provided in Table 4.4.

4.4 Air Source Models Test Program

A series of tests were performed to check the air source models for computational accuracy and reasonableness. Some of these tests are discussed below.

Hand calculations were checked against a deterministic run to confirm that the radon and dust models executed the equations properly. The models were also run probabilistically with the results checked for reasonableness. In another test, the radon model was run probabilistically with the input data being specific to the Lacnor tailings near Elliot Lake, Ontario. The results compared extremely well with radon exhalation field data collected on the Lacnor tailings (Golder et al., 1986).

Figure 4.1 is a plot of the radionuclide air source rate from the unsaturated layer of the tailings versus time, plotted as the log of the geometric mean. The system model was run for 2000 years in 10 year time steps for 100 trials.

4.5 References

Austin, S.R. and Droullard, R.F., 1978. "Radon Emanation from Domestic Uranium Ores Determined by Modifications of the Closed-Can, Gamma-Only Assay Method." U.S. Bureau of Mines, Report of Investigations 8264.

Colorado Department of Health (CDOH), 1984. "Fugitive Particulate Emissions." Internal Memo from T. Tistinic, Colorado Department of Health, July 2, 1984.

DSMA ATCON Limited, 1985. "A Study to Measure and Evaluate the Effect that Vegetation has on the Emanation Rate of Radon from a Uranium Tailings Pile." Research Report prepared for the National Uranium Tailings Program, CANMET, Energy, Mines and Resources Canada, DSS File No. 14SQ.23241-3-1659.

Golder Associates, Beak Consultants Limited, SENES Consultants Limited and Cumming-Cockburn and Associates Limited, 1986. "Lacnor Field Study, Elliot Lake, Ontario - Appendix 1." Prepared for the National Uranium Tailings Program, CANMET, Energy Mines and Resources Canada, under Supply and Services Canada Contract No. 15SQ.23241-4-1680.

Rogers, V.C., Overmyer, R.F., Putzig, K.M., Jensen, C.M., Nielson, K.K., and Sermon, B.W., 1980. "Characterization of Uranium Tailings Cover Materials for Radon Flux Reduction." U.S. Nuclear Regulatory Commission NUREG/CR-1081, March.

Rogers, V.C., Nielson, K.K. and Kalkwarf, D.R., 1984. "Radon Attenuation Handbook for Uranium Mill Tailings Cover Design." U.S. Nuclear Regulatory Commission, NUREG/CR-3533, April.

FIGURE 4.1

PREDICTED RADIONUCLIDE RELEASE RATE TO THE AIR vs TIME

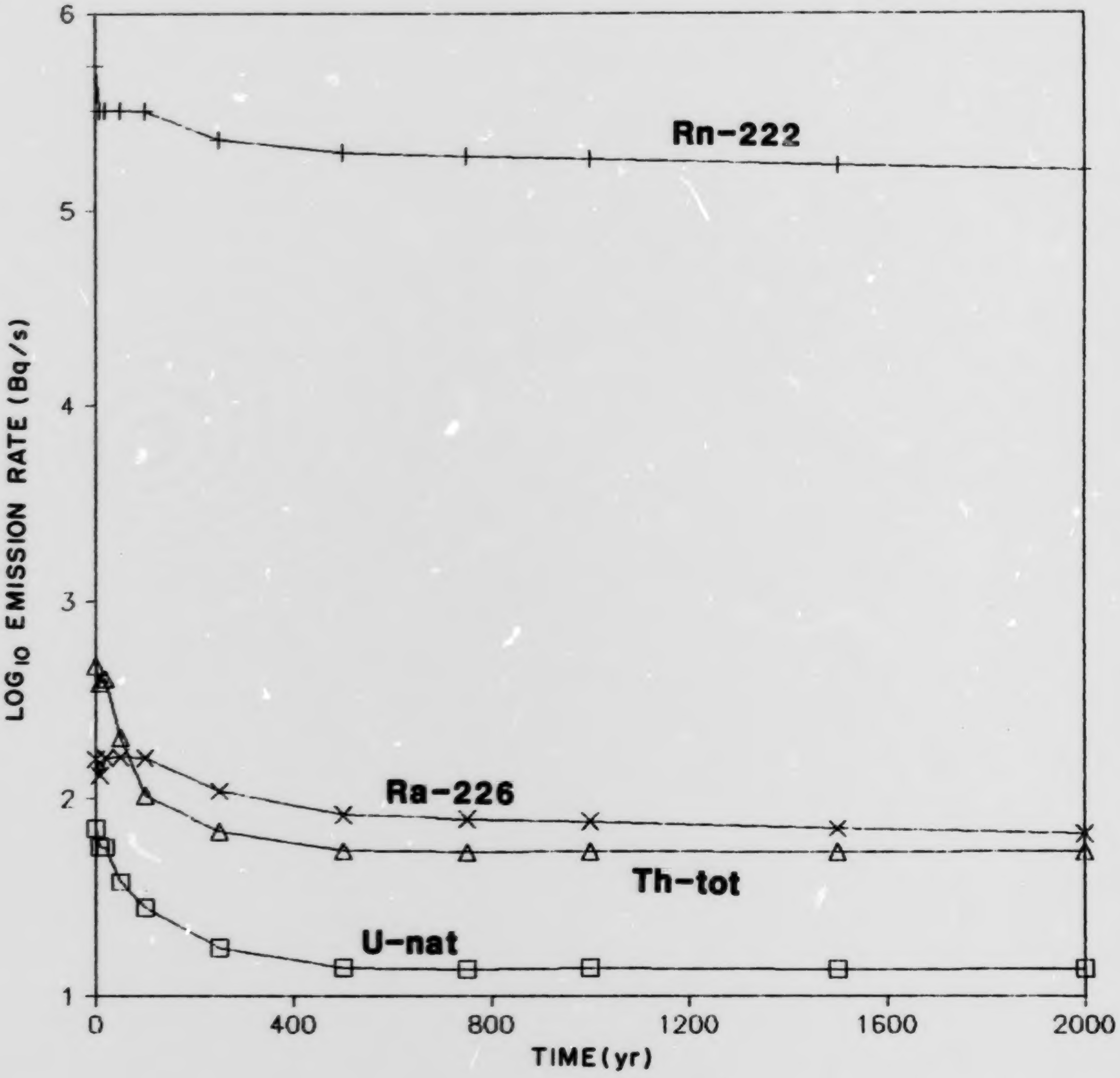

NOTES: 1) The graph shows geometric mean values of 100 trials
2) Pb-210 release rate tracks that predicted for Ra-226

Table 4.4

DUST MODEL CODE LISTING

```
      SUBROUTINE DUST
      INCLUDE 'MODEL.INC'
      INCLUDE 'VAR.INC'
      AEXPT=ATAIL*(1.0-FVEG)
      CONST5=(1.0-CAFD)*(12.0-NSUBW)/12.0*2.2E-6*SILT/1.5*
     +       (365.0-FPREC)/235.0*FWINDT/0.15/RHOTAL*AEXPT
      DO 10 I=1,4
         EMRATE(I)=CONST5*CONC(I,1,3)
10    CONTINUE
C
      IF(CODDUS.EQ.1.0.OR.CODDUS.EQ.2.0.OR.CODDUS.EQ.3.0)THEN
         WRITE(*,100)
      ENDIF
      IF(CODDUS.EQ.3.0)THEN
         WRITE(*,101)FVEG,SILT,FPREC,FWINDT,RHOTAL,AEXPT,CAFD,NSUBW,
     +               CONC(1,1,3)
         DO 11 I=2,4
            WRITE(*,102)CONC(I,1,3)
11       CONTINUE
      ENDIF
      IF(CODDUS.EQ.2.0.OR.CODDUS.EQ.3.0)THEN
         WRITE(*,103)EMRATE(1)
         DO 12 I=2,4
            WRITE(*,104)EMRATE(I)
12       CONTINUE
      ENDIF
C
100   FORMAT(///1X,'DUST SOURCE MODEL')
101   FORMAT(/1X,'FRACTION OF TAILINGS COVERED WITH VEGETATION',E12.4/
     +       1X,'SILT CONTENT',E12.4/1X,'ANNUAL NUMBER OF DAYS WITH ',
     +       'MORE THAN 0.25mm OF PRECIPITATION',E12.4/1X,'TIME WIND',
     +       ' SPEED EXCEEDS 5.4 m/s',E12.4/1X,'TAILINGS BULK DENSIT',
     +       'Y',E12.4/1X,'EXPOSED SURFACE AREA OF TAILINGS',E12.4/1X,
     +       'COVER ATTENUATION FACTOR',E12.4/1X,'NUMBER OF WINTER M',
     +       'ONTHS PER YEAR',E12.4/1X,'RADIONUCLIDES SURFICIAL CONC',
     +       'ENTRATIONS',E12.4)
102   FORMAT(39X,3(E12.4))
103   FORMAT(/1X,'EMISSION RATE OF RADIONUCLIDES',E12.4)
104   FORMAT(31X,3(E12.4))
C
      RETURN
      END
```

SENES Consultants Limited, 1984. "A Study to Develop and Demonstrate Techniques for the Probabilistic Assessment of the Long-Term Effects of Uranium Mill Tailings in Canada - Phase I." Research Report prepared for the National Uranium Tailings Program, CANMET, Energy, Mines and Resources, Canada, under Supply and Services Canada Contract No. OSQ83-00236.

SENES Consultants Limited, 1985. "Probabilistic Model Development for the Assessment of the Long-Term Effects of Uranium Mill Tailings in Canada - Phase II." Research Report prepared for the National Uranium Tailings Program, CANMET, Energy, Mines and Resources, Canada, under Supply and Services Canada Contract No. OSQ84-00207.

Strong, K.P. and Levins, D.M., 1982. "Effect of Moisture Content on Radon Emanation from Uranium Ore and Tailings." Health Physics, Vol. 42, pp. 27-32.

U.S. Nuclear Regulatory Commission (NRC), 1980. "Final Generic Environmental Impact Statement on Uranium Milling." NUREG-0706, September.

Zettwoog, P., Fourcade, N., Campbell, F. and Caplan, H.S., 1981. "The Effect of Freezing on the Emanation of Radon from Uranium Ore and Tailings." Health Physics, Vol 41, pp. 410-411.

5.0 AIR DISPERSION AND WIND MODELS

5.1 Introduction

Chapter 4 describes how the radon and dust air source rates are calculated. This chapter describes how the dispersion of these sources into the atmosphere is modelled.

Data on wind statistics are required to evaluate both the dust source term (Section 4.3) and the atmospheric dispersion model (Section 5.2). The way in which AES wind and stability data are modified for use in these models is also described in this chapter (Section 5.3).

5.2 Air Dispersion Model

In the Phase I and Phase II studies (SENES, 1984; SENES, 1985) the atmospheric dispersion model was predicated on the assumption of a single receptor at a specified location. As discussed in Chapter 2, one of the objectives of subsequent model development was to modify the approach to atmospheric dispersion to accomodate multiple receptors. In addition, the atmospheric dispersion model has been modified to include a simple correction for the finite size (as opposed to a point source) of the tailings source. The essential characteristics of the atmospheric dispersion model used in UTAP.3 studies are outlined below.

5.2.1 Air Dispersion Model Development

The air dispersion equation used in UTAP.3 is a same sector-averaged Gaussian plume model. The formulation of the equation is:

$$[C]_{a,i,t} = \frac{2.032\, f_{K,l,t}\, Q_{i,t}}{\bar{u}_{K,l,t}\, \sigma_{z,x}\, (x+x_0)} \exp\left[\frac{-h^2}{2\,\sigma_{z,x}^2}\right] \qquad (5.1)$$

where

$[C]_{a,i,t}$ = the atmospheric concentration of the ith radionuclide at the receptor at time t ($Bq.m^{-3}$)

$f_{K,1,t}$ = fraction of time the wind blows from the source to the receptor in one of 16 sectors (depends on sector K direction and stability class 1) (time variant)

$Q_{i,t}$ = the emission rate of the ith radionuclide at time t ($Bq.s^{-1}$)

$\bar{u}_{K,1,t}$ = mean wind speed from the source to the receptor (depends on sector K direction and stability class 1) (time variant) ($m.s^{-1}$)

x = downwind distance from the source to the receptor (m)

x_0 = virtual source set back distance (m)

h = height of source (m)

$\sigma_{z,x}$ = vertical dispersion coefficient (m).

An effect sometimes included in air dispersion models, but left out in this case is that of limited vertical mixing. Exclusion of this effect has been shown to have little effect on long-term average concentrations (TCM, 1980).

A commonly used approximation has been used in UTAP.3 to accomodate the fact that a tailings area is actually an area source rather than a point source. The concept is simply to treat the area source as a point source with an initial horizontal spread. In effect, the approach calculates a virtual distance (x_0) that produces the appropriate initial spread of the plume. In this study the virtual source set back distance is calculated by making several assumptions with regard to source geometry. The assumptions are:

- The model is sector averaged (i.e. crosswind concentrations are uniform across a sector).
- It is an "n" sector model (i.e. the compass is divided into n sectors of equal angular width).
- The tailings area is circular (for mathematical convenience).

At the setback distance x_0 the sector angle, θ,(determined from the number of sectors to be $2\pi/n$) subtends an arc of length:

$$L = x_0\theta = \frac{x_0\, 2\pi}{n} \quad (5.2)$$

If we assume that the arc length, L, is equal (or approximately equal) to the diameter, D, of a "circular" tailings area or the diameter of a circle with area equivalent to that of the actual tailings area (any shape), equation (5.2) can be rewritten as:

$$x_0 = \frac{Dn}{2\pi} \quad (5.3)$$

When D is expressed as a function of the tailings' area ($A_0=\pi D^2/4$) then the expression for x_0 becomes:

$$x_0 = \frac{n}{\pi}\sqrt{\frac{A_0}{\pi}} \quad (5.4)$$

which for a 16 sector model reduces to:

$$x_0 = 2.87\sqrt{A_0} \quad (5.5)$$

where

A_0 = the surface area of the tailings (m^2).

The vertical dispersion coefficient, $\sigma_{z,x}$, is calculated as a function of distance. The power law curves proposed are those suggested for use in long-term atmospheric dispersion models, such as the Climatological Dispersion Model (CDM, 1973), and the Texas Climatological Model (TCM, 1980) both of which have been used extensively in the United States and elsewhere for regulatory and assessment purposes (e.g. Hanna, 1982). The general form of the power law equation is:

$$\sigma_{z,x} = ax^b \qquad (5.6)$$

where a and b are power law coefficients which are dependent on stability class, and x is the downwind distance from the source to the receptor. Following the practice of the U.S. EPA (ISC, Vol. 1, 1979), if the calculated value of $\sigma_{z,x}$ exceeds 5000 m, $\sigma_{z,x}$ is set equal to 5000 m. The power law coefficients are shown in Table 5.1.

As is commonly done, the structure of the Phase III air dispersion model assumes that the wind data are resolved into 16 sectors each of angular width 22.5°. In addition, the user can specify up to 5 radial distances (or rings as shown in Figure 2.2) ranging from a minimum distance of 1 km to a maximum of 50 km from the centre of the tailings area. Thus, up to 80 air concentrations are available for use. A receptor located in a particular radial sector (i.e. in a particular 22.5° sector between two rings) is assigned the concentration predicted to occur at the centre of the radial sector, which is assumed to be representative of the entire radial sector.

In addition, two special area-weighted average air concentrations are calculated, one for the entire area, and the other over the watershed area. These area-weighted average concentrations are calculated for use in the soil model and the terrestrial vegetation model. Specifically, the concentration inputs to soil and the terrestrial vegetation models are used to evaluate the radionuclide uptake of caribou (area average) and moose and deer (watershed average) from terrestrial vegetation (see Chapters 6 and 8 respectively).

5.2.2 Parameter Values

The variables used to calculate the air concentration are listed in Table 5.2. The only input variable for this model is the source height h.

Table 5.1

POWER LAW EXPONENTS AND COEFFICIENTS FOR $\sigma_{Z,X}$

Atmospheric Stability Class	Downwind Distance meters $1000 < x \le 5000$		Downwind Distance meters $5000 < x \le 50{,}000$	
	a	b	a	b
A	0.0002539	2.086	0.0002539	2.089
B	0.04936	1.114	0.04936	1.114
C	0.1014	0.9260	0.1154	0.9109
D	0.2591	0.6869	0.7368	0.5642
E and F	0.2017	0.6020	1.5763	0.3606

Notes:

1) $\sigma_{z,x} = ax^b$

2) In this application if $\sigma_{z,x}$ is predicted to be greater than 5000m, $\sigma_{z,x}$ is set equal to 5000m

3) Stability classes E and F are represented by coefficients for class F.

4) Coefficients a and b are from CDM (1973, p. 8).

Table 5.2

AIR DISPERSION MODEL VARIABLES

Model Symbol	Description	Units	Nominal Value	Probability* Distribution	Computer Origin	Compter Symbol
$[C]_{a,i,t}$	atmospheric conc. of ith radionuclide at the receptor	$Bq.m^{-3}$	calculated	calculated	AIRDIS	AIRC (i,j)i=1,5 j ≤ 82
$f_{K,l,t}$	fraction of time wind blows from the source to the receptor (i.e. in sector K) with a particular atmospheric stability (l) (time variant)	-	calculated	calculated	WIND	FWIND2 (K,l)K=1,16 l=1,6
h	source height	m	2.0	U(1.0,3.0)	INPUT	HSRC
$Q_{i,t}$	emission rate from tailings of ith radionuclide at time t	$Bq.s^{-1}$	calculated	calculated	RADON DUST	EMRATE(i) i=1,4
$\bar{u}_{K,l,t}$	mean annual wind speed as a function of direction and stability class (time variant)	$m.s^{-1}$	calculated	calculated	WIND	UWIND(K,l) K=1,16 l=1,6
x	downwind distance to receptor	m	calculated	calculated	C/M	RNGMID(X) X ≤ 5
$\sigma_{z,x}$	vertical dispersion coefficient	m	calculated	calculated (see Table 5.2)	AIRDIS	VDISP(X,l) X ≤ 5 l = 1,6
A_o	surface area of tailings	m^2	5.0×10^5	(5.0×10^5)	INPUT	ATAIL
f_t	frequency of time the wind speed exceeds 5.4 $m.s^{-1}$ (time variant)	-	calculated	calculated	WIND	FWINDT
$f_{K,t}$	frequency of time the wind speed exceeds 5.4 $m.s^{-1}$ as a function of direction (time variant)	-	calculated	calculated	WIND	FWND1(K) K=1,16

Note

* Distributions are as described in Table 2.3.

Source Height

A source height of about 2 m has been assumed on the basis that air turbulence near the surface will result in at least some rapid initial upward mixing.

5.2.3 Description of the Computer Model

The air dispersion model computer code is given in Table 5.3. The computer symbols for the parameters are presented in Table 5.2.

5.3 Wind Model

With only one receptor in the direction of the prevailing wind as in Phase II, only one set of atmospheric input parameters was required. The critical parameters required to make the above formulation work under the more general conditions in UTAP.3 are $f_{K,l}$ (a joint frequency distribution of direction, wind speed and atmospheric stability), the vertical dispersion coefficient σ_z (a function of direction and stability class) and $\bar{u}_{K,l}$ (a function of direction for each stability class).

5.3.1 Wind Model Development

As discussed in Section 5.2.1, in order to calculate the concentration of the radionuclides in the atmosphere after dispersion, relevant wind data is required. Specifically, the fraction of time the wind blows in each of the 16 sectors for each stability category, the mean wind velocity in each sector for each stability category, as well as, the fraction of time the wind velocity exceeds 5.4 $m.s^{-1}$ in each sector, are required. To satisfy these requirements, AES wind and stability data (STAR data) from the Gore Bay weather station on Manitoulin Island, Ontario, for a twenty year period was obtained (refer to Section 3.3. of SENES, 1987).

The subroutine WIND calculates the desired data from the AES STAR data files as follows. The mean wind speed as a function of direction and stability class is calculated assuming the following central wind speed classes.

Wind Speed Class	Speed Interval (knots)	Central Wind Speed ($m.s^{-1}$)
1	0 to 3	1.50
2	4 to 6	2.46
3	7 to 10	4.47
4	11 to 16	6.93
5	17 to 21	9.61
6	> 21	12.52

The lowest wind speed class was arbitrarily taken as 1.5 $m.s^{-1}$. This means that light winds reported in the first wind speed class will be rounded up to this value. Operational wind instruments are designed for durability and also to withstand exposure to strong gusty airflow. For these reasons, most wind sensors have a high starting speed, which can lead to erroneous reporting of light winds as calms (Truppi, 1968). The central wind speed values given above are quite commonly used and are employed in several models including the Texas Climatological Model (TCM, 1980), the Climatological Dispersion Model (CDM, 1973), and the Texas Episodic Model Version 8 (TCM, 1979).

5.3.2 Parameter Values

The fraction of time the wind blows in each of the 16 directions for each stability class, the mean wind velocity in each direction for each stability class, and the fraction of time the wind velocity exceeds 5.4 $m.s^{-1}$ in each direction and overall is caluclated from AES STAR data.

5.3.3 Description of the Computer Model

The wind model computer code is given in Table 5.5. The computer symbols for the parameters are presented in Table 5.4.

Table 5.3

AIR DISPERSION MODEL CODE LISTING

```
      SUBROUTINE AIRDIS
      INCLUDE 'MODEL.INC'
      INCLUDE 'VAR.INC'
      INTEGER*2 STACLS,XDIST,XDIRC
      REAL*4 CONCT(16,5),DIST(5),VDISP(5,6),AIRCON(5,16,5)
      COMMON /AIRDIS/ CONCT,DIST,VDISP
      IF(NT.EQ.0)THEN
         XDISTO=2.87*SQRT(ATAIL)
         DO 10 XDIST=1,NRING
            DIST(XDIST)=RNGMID(XDIST)+XDISTO
            DO 11 STACLS=1,6
               IF(RNGMID(XDIST).LE.5000.0)THEN
                  IF(STACLS.EQ.1)THEN
                     A=0.0002539
                     B=2.089
                  ELSEIF(STACLS.EQ.2)THEN
                     A=0.04936
                     B=1.114
                  ELSEIF(STACLS.EQ.3)THEN
                     A=0.1014
                     B=0.926
                  ELSEIF(STACLS.EQ.4)THEN
                     A=0.2591
                     B=0.6869
                  ELSE
                     A=0.2017
                     B=0.6020
                  ENDIF
               ELSEIF(RNGMID(XDIST).GT.5000.0)THEN
                  IF(STACLS.EQ.1)THEN
                     A=0.0002539
                     B=2.089
                  ELSEIF(STACLS.EQ.2)THEN
                     A=0.04936
                     B=1.114
                  ELSEIF(STACLS.EQ.3)THEN
                     A=0.1154
                     B=0.9109
                  ELSEIF(STACLS.EQ.4)THEN
                     A=0.7368
                     B=0.5642
                  ELSE
                     A=1.5763
                     B=0.3606
                  ENDIF
               ENDIF
               VDISP(XDIST,STACLS)=A*((RNGMID(XDIST))**B)
               IF(VDISP(XDIST,STACLS).GT.5000.0)THEN
                  VDISP(XDIST,STACLS)=5000.0
               ENDIF
11          CONTINUE
```

Table 5.3 continued.

```
10       CONTINUE
      ENDIF
      IF(WINDFG.EQ.'Y'.OR.(NT.EQ.0.AND.NUMTRL.EQ.1))THEN
         DO 12 XDIRC=1,16
            DO 13 XDIST=1,NRING
               CONCT(XDIRC,XDIST)=0.0
               DO 14 STACLS=1,6
                  IF(UWIND(XDIRC,STACLS).LT.0.5)THEN
                     UWIND(XDIRC,STACLS)=0.5
                  ENDIF
                  CONSTC=2.032*FWIND2(XDIRC,STACLS)/UWIND(XDIRC,
     +                   STACLS)/VDISP(XDIST,STACLS)/DIST(XDIST)*EXP
     +                   (-0.5*((HSRC/VDISP(XDIST,STACLS))**2.0))
                  CONCT(XDIRC,XDIST)=CONCT(XDIRC,XDIST)+CONSTC
14             CONTINUE
13          CONTINUE
12       CONTINUE
      ENDIF
      DO 15 XDIRC=1,16
         DO 16 XDIST=1,NRING
            DO 17 I=1,4
               AIRCON(I,XDIRC,XDIST)=FWIND1(XDIRC)/FWINDT*CONCT(XDIRC,
     +                                 XDIST)/6.0*EMRATE(I)
17          CONTINUE
            AIRCON(5,XDIRC,XDIST)=CONCT(XDIRC,XDIST)/6.0*EMRATE(5)
16       CONTINUE
15    CONTINUE
      DO 18 I=1,4
         AIRC(I,NRECEP+1)=0.0
         DO 19 XDIST=1,NRING
            DO 20 XDIRC=1,16
               AIRC(I,NRECEP+1)=AIRC(I,NRECEP+1)+AIRCON(I,XDIRC,XDIST)
     +                            *RAREA(XDIST)
20          CONTINUE
19       CONTINUE
         AIRC(I,NRECEP+1)=AIRC(I,NRECEP+1)/TAREA
         AIRC(I,NRECEP+2)=0.0
         DO 21 K=1,PSNUM
            AIRC(I,NRECEP+2)=AIRC(I,NRECEP+2)+AIRCON(I,PSDIR(K),
     +                       PSRING(K))*RAREA(PSRING(K))
21       CONTINUE
         AIRC(I,NRECEP+2)=AIRC(I,NRECEP+2)/PSAREA
18    CONTINUE
      DO 22 I=1,5
         DO 23 NREC=1,NRECEP
            AIRC(I,NREC)=AIRCON(I,RDIR(NREC),RRING(NREC))
23       CONTINUE
22    CONTINUE
C
      IF(CODAIR.EQ.1.0.OR.CODAIR.EQ.2.0.OR.CODAIR.EQ.3.0)THEN
         WRITE(*,100)
      ENDIF
      IF(CODAIR.EQ.3.0)THEN
```

Table 5.3 continued.

```
         WRITE(*,101)ATAIL,HSRC,XDISTO,RNGMID(1)
         IF(NRING.GT.1)THEN
            DO 24 XDIST=2,NRING
               WRITE(*,102)RNGMID(XDIST)
24          CONTINUE
         ENDIF
         WRITE(*,103)
         DO 25 XDIST=1,NRING
            WRITE(*,104)(VDISP(XDIST,STACLS),STACLS=1,6)
25       CONTINUE
         WRITE(*,105)EMRATE(1)
         DO 26 I=2,5
            WRITE(*,106)EMRATE(I)
26       CONTINUE
         WRITE(*,107)
         DO 27 I=1,4
            DO 28 XDIRC=1,16
               WRITE(*,108)(AIRCON(I,XDIRC,XDIST),XDIST=1,NRING)
28          CONTINUE
            WRITE(*,109)AIRC(I,NRECEP+1),AIRC(I,NRECEP+2)
27       CONTINUE
         DO 29 XDIRC=1,16
            WRITE(*,108)(AIRCON(5,XDIRC,XDIST),XDIST=1,NRING)
29       CONTINUE
      ENDIF
      IF(CODAIR.EQ.2.0)THEN
         WRITE(*,110)
         DO 30 I=1,4
            DO 31 NREC=1,NRECEP
               WRITE(*,111)AIRC(I,NREC)
31          CONTINUE
            WRITE(*,109)AIRC(I,NRECEP+1),AIRC(I,NRECEP+2)
30       CONTINUE
         DO 32 NREC=1,NRECEP
            WRITE(*,111)AIRC(5,NREC)
32       CONTINUE
      ENDIF
C
100   FORMAT(///1X,'AIR DISPERSION MODEL')
101   FORMAT(/1X,'SURFACE AREA OF TAILINGS',E12.4/1X,'HEIGHT OF SOUR',
     +       'CE',E12.4/1X,'VIRTUAL SOURCE SET BACK DISTANCE',E12.4/1X
     +       ,'DOWNWIND DISTANCE FROM SOURCE TO RECEPTOR',E12.4)
102   FORMAT(42X,E12.4)
103   FORMAT(1X,'VERTICAL DISPERSION COEFFICIENT')
104   FORMAT(1X,6(F10.2))
105   FORMAT(1X,'EMISSION RATE OF THE RADIONUCLIDES',E12.4)
106   FORMAT(35X,E12.4)
107   FORMAT(/1X,'ATMOSPHERIC CONCENTRATION OF THE RADIONUCLIDES IN ',
     +       'EACH SECTOR')
108   FORMAT(1X,5(E12.4))
109   FORMAT(1X,'AVERAGE CONCENTRATION',E12.4/1X,'AVERAGE WATERSHED ',
     +       'CONCENTRATION',E12.4)
110   FORMAT(/1X,'ATMOSPHERIC CONCENTRATION OF THE RADIONUCLIDES AT ',
```

Table 5.3 continued.

```
     +       'THE RECEPTORS')
111   FORMAT(1X,E12.4)
C
      RETURN
      END
```

Table 5.4

WIND MODEL VARIABLES

Model Symbol	Description	Units	Nominal Value	Probability* Distribution	Computer Origin	Compter Symbol
YS_t	randon variable for selection of wind data (time variant)	-	1.0	U(1.0,2.09999)	INPUT	WYEAR
SD	AES STAR data	(refer to Table 3.8 of Volume 4)				FWIND(K,l,s,n) K=1,16 l=1,6 s=1,6 n=1,20
$f_{K,l,t}$	fraction of time wind blows from the source to the receptor (i.e. in sector K with a particular atmospheric stability l) (time variant)	-	calculated	calculated	WIND	FWIND2(K,l) K=1,16 l=1,6
$\bar{u}_{K,l,t}$	mean annual wind speed as a function of direction and stability class (time variant)	$m.s^{-1}$	calculated	calculated	WIND	UWIND(K,l) K=1,16 l=1,6
f_t	frequency of time the wind speed exceeds 5.4 $m.s^{-1}$ (time variant)	-	calculated	calculated	WIND	FWINDT
$f_{K,t}$	frequency of time the wind speed exceeds 5.4 $m.s^{-1}$ as a function of direction (time variant)	-	calculated	calculated	WIND	FWND1(K) K=1,16

Note

* Distributions are as described in Table 2.3.

Table 5.5

WIND MODEL CODE LISTING

```
      SUBROUTINE WIND
      INCLUDE 'MODEL.INC'
      INCLUDE 'VAR.INC'
      N=INT(WYEAR)
      IF(WINDFG.NE.'Y')N=1
      DO 10 J=1,6
         DO 11 I=1,16
            FWIND2(I,J)=0.0
            DO 12 K=1,6
               FWIND2(I,J)=FWIND2(I,J)+FWIND(I,J,K,N)
 12         CONTINUE
            UWIND(I,J)=1.50*FWIND(I,J,1,N)+2.46*FWIND(I,J,2,N)+4.47*
     +                 FWIND(I,J,3,N)+6.93*FWIND(I,J,4,N)+9.61*FWIND
     +                 (I,J,5,N)+12.52*FWIND(I,J,6,N)
            SUWIND=FWIND2(I,J)
            IF(SUWIND.EQ.0.0)THEN
               SUWIND=1.0
            ENDIF
            UWIND(I,J)=UWIND(I,J)/SUWIND
 11      CONTINUE
 10   CONTINUE
      FWINDT=0.0
      DO 13 I=1,16
         FWIND1(I)=0.0
         DO 14 J=1,6
            DO 15 K=4,6
               FWIND1(I)=FWIND1(I)+FWIND(I,J,K,N)
 15         CONTINUE
 14      CONTINUE
         FWINDT=FWINDT+FWIND1(I)
 13   CONTINUE
 C
      IF(CODWIN.EQ.1.0.OR.CODWIN.EQ.2.0.OR.CODWIN.EQ.3.0)THEN
         WRITE(*,100)
      ENDIF
      IF(CODWIN.EQ.2.0.OR.CODWIN.EQ.3.0)THEN
         WRITE(*,101)N
         DO 16 L=1,16
            I=L+8
            IF(I.GT.16)I=I-16
            WRITE(*,102)(FWIND2(I,J),J=1,6)
 16      CONTINUE
         WRITE(*,103)
         DO 17 L=1,16
            I=L+8
            IF(I.GT.16)I=I-16
            WRITE(*,104)(UWIND(I,J),J=1,6)
 17      CONTINUE
         WRITE(*,105)
         DO 18 L=1,16
            I=L+8
```

Table 5.5 continued.

```
              IF(I.GT.16)I=I-16
              WRITE(*,106)(FWIND1(I))
18          CONTINUE
            WRITE(*,107)FWINDT
          ENDIF
C
100       FORMAT(///1X,'WIND MODEL')
101       FORMAT(/1X,'WIND DATA SELECTED',I5/1X,'FWIND2')
102       FORMAT(1X,6(E12.4))
103       FORMAT(1X,'UWIND')
104       FORMAT(1X,6(F12.4))
105       FORMAT(1X,'FWIND1')
106       FORMAT(1X,E12.4)
107       FORMAT(1X,'FWINDT'/1X,F8.4)
C
          RETURN
          END
```

5.4 Air Dispersion and Wind Models Test Program

A series of test were performed to check the air dispersion and wind models for computational accuracy and reasonableness. Some of these tests are discussed below.

Hand calculations were checked against a deterministic run to confirm that the air dispersion and wind models executed the equations properly. The models were also run probabilistically with the results checked for reasonableness.

Figure 5.1 is a plot of radionuclide air concentration as a function of distance to the north of the tailings at time 0 years. Figure 5.2 is a plot of the radionuclide air concentration as a function of time at the receptor located 2 km to the north of the tailings area. Both figures are plotted as the log of the geometric mean. The system model was run for 2,000 years in 10 year time steps for 100 trials.

5.5 References

Busse, A.D., Zimmerman, J.R. (CDM), 1973. "User's Guide for the Climatological Dispersion Model." PB227346, December, EPA-R4-73-024.

Bowers, J.F., Bjonklund, J.R., Cheney, C.C. (ISC), 1979. "Industrial Source Complex (ISC) Dispersion Model User's Guide, Volume 1." PB80133044, December, EPA-450/4-79-030.

Hanna, S.R., 1982. "Technical Note No. 177, Review of Atmospheric Duffusion Models for Regulatory Applications." World Meteorological Organization, Geneva, Switzerland.

SENES Consultants Limited, 1984. "A Study to Develop and Demonstrate Techniques for the Probabilistic Assessment of the Long-Term Effects of Uranium Mill Tailings in Canada - Phase I." Research Report prepared for the National Uranium Tailings Program, CANMET, Energy, Mines and Resources Canada.

SENES Consultants Limited, 1985. "Probabilistic Model Development for the Assessment of the Long-Term Effects of Uranium Mill Tailings in Canada - Phase II." Research Report prepared for the National Uranium Tailings Program, CANMET, Energy, Mines and Resources, Canada.

SENES Consultants Limited, 1987. "Uranium Tailings Assessment Program (UTAP.3): User's Manual." Research report prepared for the National Uranium Tailings Program, CANMET, EMR, under Supply and Services Canada Contract No. 23317-6-1728/01-SQ.

Texas Air Control Board (TCM), 1979. "Texas Episodic Model, User's Guide." PB80227572, October, E.P.A./DE-80/0070.

Texas Air Control Board (TCM), 1980. "User's Guide to the Texas Climatological Model." PB164626, August, EPA/DF-81/0016.

Truppi, L.E., 1968. "Bias Introduced by Amemometer Starting Speeds in Climatogical Wind Rose Summaries." Monthly Weather Review, 96(5): 325-327, May.

FIGURE 5.1

PREDICTED RADIONUCLIDE AIR CONCENTRATION vs DISTANCE

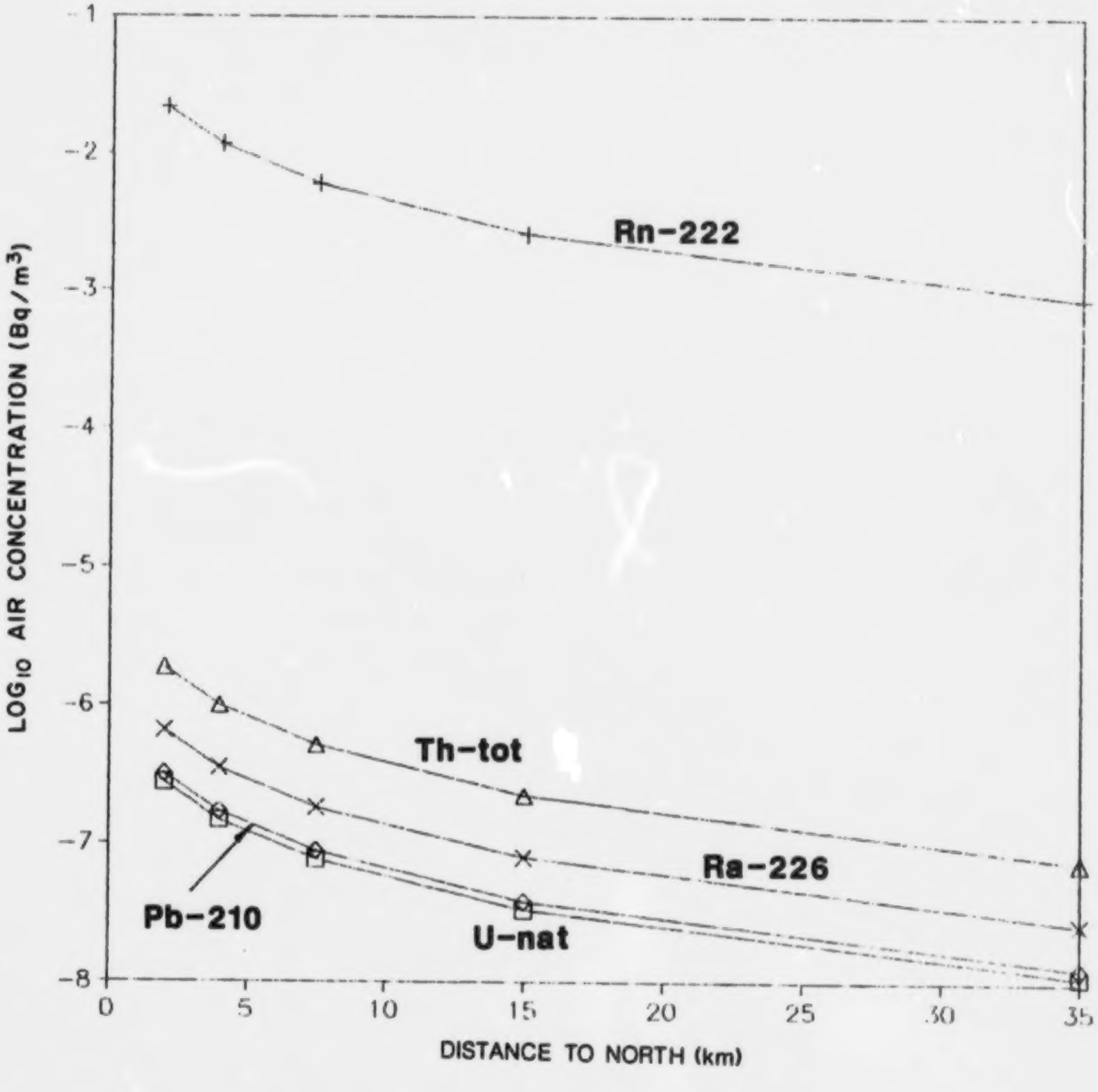

NOTES: 1) The graph shows geometric mean values of 100 trials

2) Air concentration predicted for t=0 years

FIGURE 5.2

PREDICTED RADIONUCLIDE AIR CONCENTRATION vs TIME

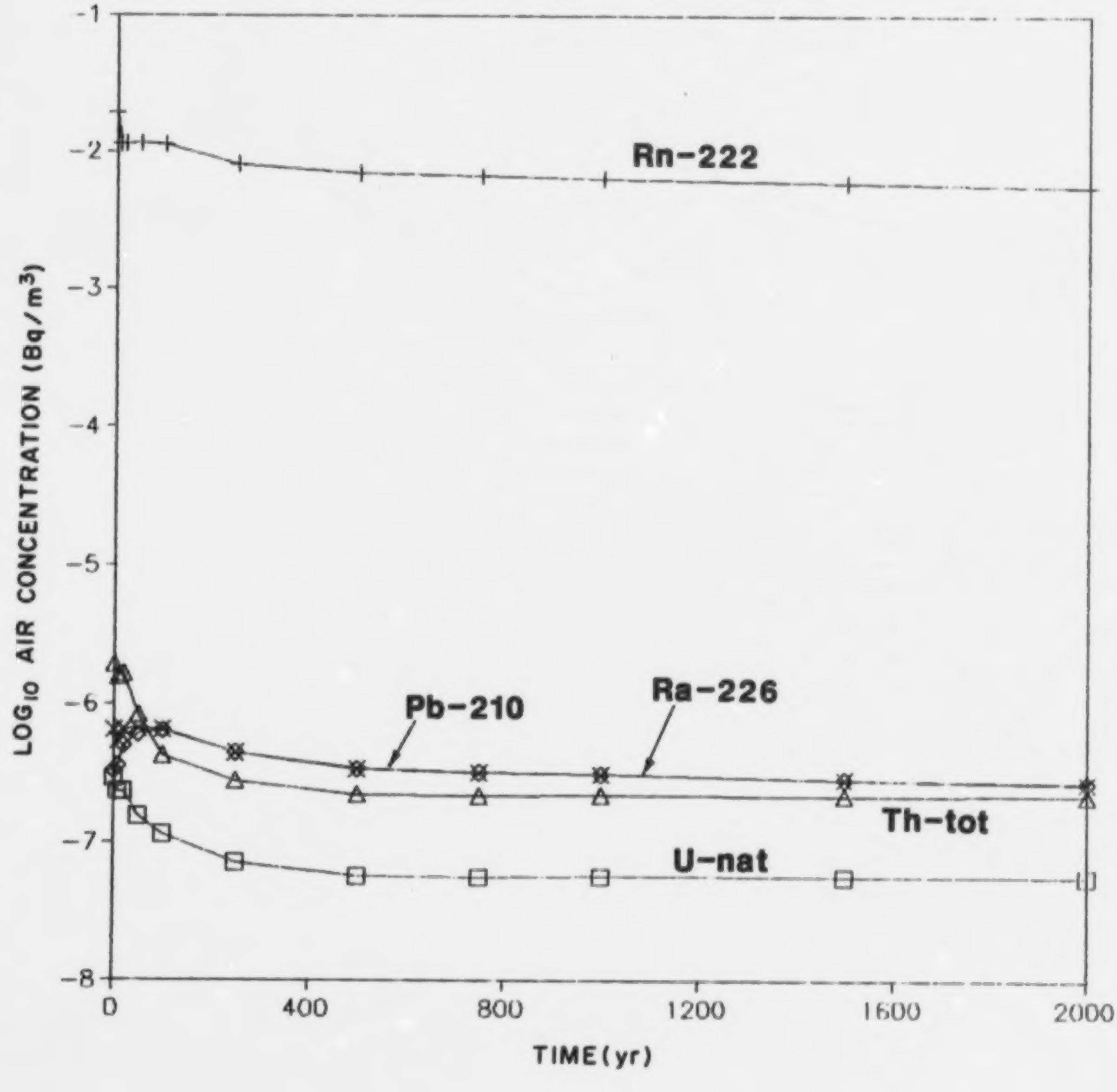

NOTES: 1) The graph shows geometric mean values of 100 trials

2) Receptor located 2km to the north of the tailings area

6.0 SOIL MODEL

6.1 Introduction

This section outlines the development of a two layer soil model that describes the movement of radionuclides in soil that are deposited as particulate matter from the air to the surface of the soil. The model includes atmospheric deposition, runoff and downward transport of radionuclides into the soil profile. It is used to estimate activity in the soil, which is used to compute groundshine dose and dose due to the consumption of vegetation grown in the soil.

6.2 Soil Model Development

Figure 6.1 indicates the major factors at work in balancing radioactivity in the near-surface soil layers. The four factors considered in the development of the soil model are:

1) deposition of incoming airborne radioactivity;
2) radioactivity leaving the soil compartment in solution in the soil water via leaching;
3) radioactivity leaving the surface soil compartment in solution via runoff; and
4) radioactive decay.

To simplify the modelling exercise ingrowth, resuspension, erosion and depletion due to vegetation uptake are not included in the model. Exclusion of resuspension and erosion leads to a conservative overestimate of activity in the soil.

The major assumption used to develop the model is that incoming radioactivity is instantaneously partitioned between the liquid and solid phases according to the distribution coefficient K_d. The activity balance in the surface soil layer (layer 1) receiving radioactivity deposited from the air can be mathematically formulated as:

$$\frac{dZ_{1,i,t}}{dt} = 3.15 \times 10^7 \, V_d[C]_{a,i,t} - P_t[C]_{w,1,i,t} - \lambda_i \, Z_{1,i,t} \qquad (6.1)$$

where

$Z_{1,i,t}$ = the ith radionuclide content per surface area in soil layer 1 at the receptor at time t ($Bq.m^{-2}$)

V_d = the deposition velocity ($m.s^{-1}$)

$[C]_{a,i,t}$ = the atmopsheric concentration of the ith radionuclide at the receptor at time t ($Bq.m^{-3}$)

P_t = total precipitation less evapotranspiration (i.e. annual net precipitation) (time variant) ($m.yr^{-1}$)

$[C]_{w,1,i,t}$ = the ith radionuclide concentrations in the water phase in soil layer 1 at time t ($Bq.m^{-3}$)

λ_i = ith radionuclide decay constant (yr^{-1}).

The first term on the right side of equation (6.1) accounts for the incoming airborne radionuclide. The second term accounts for removal via leaching of the radionuclide in both surface and subsurface flow. The way in which these two mechanisms are accounted for is discussed later. The third term accounts for radioactive decay of U-nat and Th-tot only.

The activity of the kth soil layer at any time is the sum of the activities in the solid, liquid and gaseous phases of the soil space:

$$Z_{k,i,t} = D_k \, V_{w,k}[C]_{w,k,i,t} + D_k \, \rho_{s,k}[C]_{s,k,i,t} + D_k \, V_{a,k}[C]_{g,k,i,t} \qquad (6.2)$$

where

D_k = depth of the kth soil layer (m)

$V_{w,k}$ = volume fraction of water in the kth soil layer (-)

$\rho_{s,k}$ = soil dry bulk density of the kth soil layer ($kg.m^{-3}$)

$[C]_{s,k,i,t}$ = the ith radionuclide concentration in the solid phase in soil layer k at time t ($Bq.kg^{-1}$)

FIGURE 6.1

SCHEMATIC REPRESENTATION OF SOIL DEPOSITION / LEACHING CONCEPTS

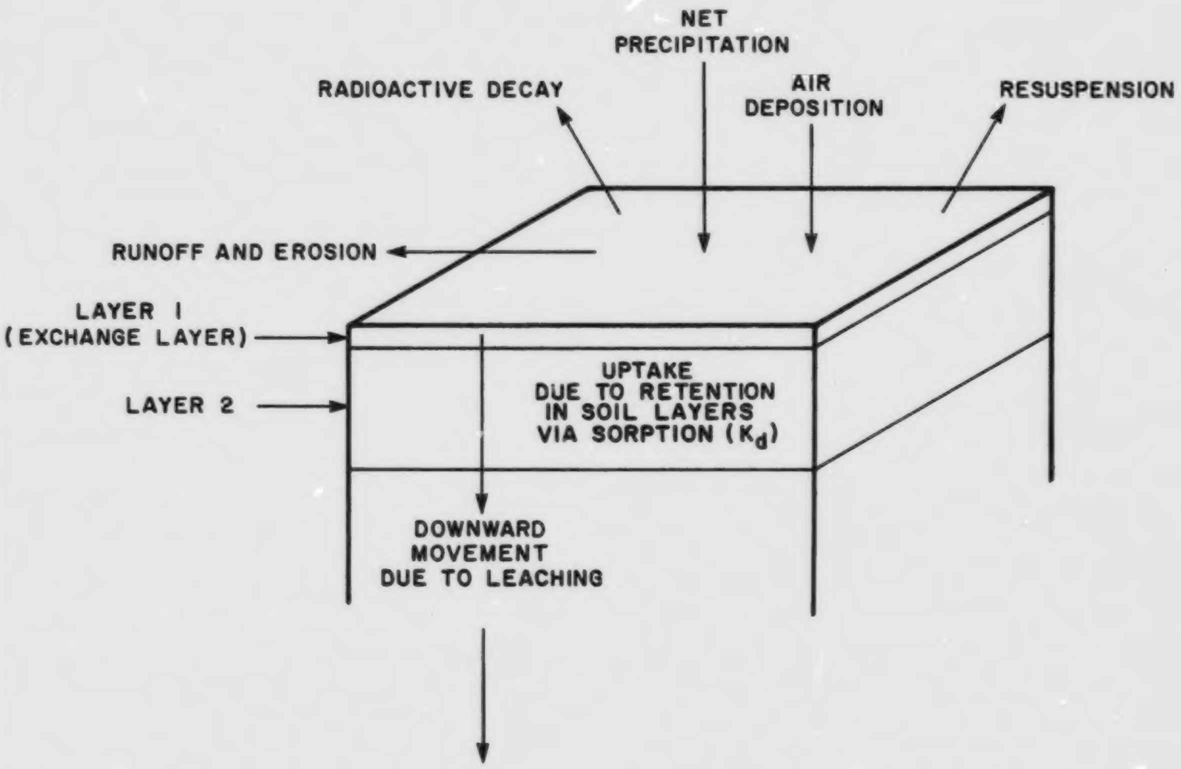

$V_{a,k}$ = volume fraction of air in the kth soil layer (-)

$[C]_{g,k,i,t}$ = the ith radionuclide concentration in the gaseous phase in soil layer k at time t ($Bq.m^{-3}$).

The activity in the gaseous phase for the non-volatile radionculides of concern to this study is assumed to be zero, i.e. $[C]_{g,k,i,t} = 0$.

At all times, the distribution of radionculides between the solid and liquid phases is assumed to be in chemical equilibrium and thus can be characterized by the distribution coefficient $K_{d,k,i}$ ($m^3.kg^{-1}$):

$$K_{d,k,i} = \frac{[C]_{s,k,i,t}}{[C]_{w,k,i,t}} \tag{6.3}$$

The volume function of water in the soil $V_{w,k}$ can be calculated as a function of the water content of the soil W_k (kg water/kg soil (dry)) corrected for the relative densities of the solid and liquid fractions:

$$V_{w,k} = \frac{W_k \rho_{s,k}}{\rho_w} \tag{6.4}$$

where

ρ_w = density of water ($kg.m^{-3}$).

Combining equations 6.2, 6.3 and 6.4, the radionuclide concentration in the water phase gives:

$$[C]_{w,k,i,t} = \frac{Z_{k,i,t}}{\rho_{s,k} D_k (W_k/\rho_w + K_{d,k,i})} \tag{6.5}$$

Substituting equation 6.5 into equation 6.1:

$$\frac{dZ_{1,i,t}}{dt} = 3.15 \times 10^7 V_d[C]_{a,i,t} - \frac{P_t Z_{1,i,t}}{\rho_{s,1} D_1 (W_k/\rho_w + K_{d,1,i})} - \lambda_i Z_{1,i,t} \tag{6.6}$$

or

$$dZ_{1,i,t} = (B_{0,i,t} - B_{1,i,t}Z_{1,i,t} - \lambda_i\, Z_{1,i,t})\, dt \qquad (6.7)$$

where

$$B_{0,i,t} = 3.15 \times 10^7\, V_d[C]_{a,i,t}$$

$$B_{1,i,t} = \frac{P_t}{\rho_{s,1}\, D_1\, (W_1/\rho_w + K_{d,1,i})}$$

Equation 6.7 has the solution:

$$Z_{1,i,t} = \frac{B_{0,i,t}}{B_{1,i,t}+\lambda_i} + \left[Z_{1,i,(t-\Delta t)} - \frac{B_{0,i,t}}{B_{1,i,t}+\lambda_i} \right] \exp[-(B_{1,i,t}+\lambda_i)\Delta t] \qquad (6.8)$$

The term $B_{0,i,t}$ is the input term for ith radionuclide in soil layer 1, the terms $B_{1,i,t}$ and λ_i are the removal terms.

The activity balance in the lower soil layer (layer 2) receiving radioactivity from leaching of the surface layer (layer 1) can be mathematically formulated as:

$$\frac{dZ_{2,i,t}}{dt} = P_t(1-F)\, [C_w]_{1,i,t} - P_t(1-F)\, [C_w]_{2,i,t} - \lambda_i\, Z_{2,i,t} \qquad (6.9)$$

where

F = Fraction of total precipitation which moves as surface runoff (i.e. does not infiltrate the soil profile) (dimensionless)

Substituting equation 6.5 into equation 6.9:

$$\frac{dZ_{2,i,t}}{dt} = \frac{P_t\, (1-F)\, Z_{1,i,t}}{\rho_{s,1}\, D_1\, (W_1/\rho_w + K_{d,1,i})} - \frac{P_t\, (1-F)\, Z_{2,i,t}}{\rho_{s,2}\, D_2\, (W_2/\rho_w + K_{d,2,i})} - \lambda_i\, Z_{2,i,t} \qquad (6.10)$$

or

$$dZ_{2,i,t} = (1-F)\ B_{1,i,t}\ Z_{1,i,t} - (1-F)\ B_{2,i,t}\ Z_{2,i,t} - \lambda_i\ Z_{2,i,t} \qquad (6.11)$$

where

$$B_{2,i,t} = \frac{P_t}{\rho_{s,2}\ D_2\ (W_2/\rho_w + K_{d,2,i})}$$

Substituting equation 6.8 into equation 6.11 gives:

$$\frac{dZ_{2,i,t}}{dt} = \frac{(1-f)B_{1,i,t}B_{0,i,t}}{B_{1,i,t} + \lambda_i} + (1-F)B_{1,i,t}\left[Z_{1,i(t-\Delta t)} - \frac{B_{0,i,t}}{(B_{1,i,t} + \lambda_i)}\right]$$

$$\left[\exp\ [-(B_{1,i,t} + \lambda_i)\ \Delta t]\right] - (1-F)\ B_{2,i,t}Z_{2,i,t} - \lambda_i\ Z_{2,i,t} \qquad (6.12)$$

Solving equation 6.11:

$$Z_{2,i} = \frac{(1-F)B_{1,i,t}}{(B_{1,i,t} - B_{2,i,t})}\left[Z_{1,i,(t-\Delta t)} - \frac{B_{0,i,t}}{(B_{1,i,t} + \lambda_i)}\right]\left[\exp[-(B_{2,i,t} + \lambda_i)\Delta t]\right]$$

$$-\left[\exp\ [-(B_{1,i,t} + \lambda_i)\Delta t]\right] - \frac{(1-F)B_{1,i,t}}{(B_{2,i} + \lambda_i)}\left[\exp[-(B_{2,i,t} + \lambda_i)\Delta t] - 1\right]$$

$$+ (Z_{2,i,(t-\Delta t)})\ \exp\ [-(B_{2,i,t} + \lambda_i)\Delta t] \qquad (6.13)$$

The soil concentration in either layer 1 or layer 2 can be calculated by dividing the radionuclide contents per surface area by the appropriate depth.

$$[S_c]_{k,i,t} = \frac{Z_{k,i,t}}{D_k} \qquad (6.14)$$

Since the vegetation model requires a single soil concentration value, the concentration in the second soil layer (i.e. the root zone is used). Where the entire model area and watershed area average soil concentrations are required for the terrestrial vegetation models, the area-weighted averages are calculated using the area-weighted average air concentrations calculated in the air dispersion model (Section 5.2.1).

Loss mechanisms, such as erosion and resuspension, have been neglected. Thus the activity remaining in the soil column will be overestimated. However, this will partially be compensated for by the neglecting ingrowth.

6.3 Parameter Values

The variables used to calculated the radionuclide concentration in the soil model are listed in Table 6.1. The annual net precipitation P, is discussed in Chapter 3, and the deposition velocity is discussed in Chapter 8. The remaining input variables are discussed below.

Depth of Soil Layers

A two soil layer approach was implemented for the soil model with a 0.05 m organic upper layer and a 0.15 m lower layer possessing the lumped characteristics of sand, silt and clay soils.

Fraction of Net Precipitation in Runoff

According to an analysis of recharge to groundwater on shield watersheds by Wang *et al*. (1978), recharge to groundwater as a percent of annual precipitation ranged from 1 to 24 percent. These values were for total precipitation and would be a larger percent of net precipitation. When adjusted to net precipitation, which is approximately half of total precipitation, the values double. F was assumed to be triangularly distributed.

Soil Dry Bulk Density

The airborne radionuclides are assumed, in the model, to be blown in all

Table 6.1

SOIL MODEL PARAMETERS

Model Symbol	Description	Units	Nominal Value	Probability Distribution*	Computer Origin	Computer Symbol
$[C]_{a,i,t}$	atmospheric concentration of ith radionculide at the receptor at time t	$Bq.m^{-3}$	calculated	calculated	AIRDIS	AIRC(i,j)i=1,4 $j\leq82$
V_d	deposition velocity	$m.s^{-1}$	0.03	U(0.003,0.03)	INPUT	DEPVEL
D_k	depth of soil layer k	m			INPUT	DSOIL(k)k=1,2
	Layer 1		0.05	C(0.05)		
	Layer 2		0.15	C(0.15)		
F	fraction of net precipitation in runoff	-	0.16	T(0.02,0.16, 0.48)	INPUT	FWAT
λ_i	decay constant for ith radionuclide	yr^{-1}				
	Uranium		0.0	DEFINED	SOIL	LAM(1)
	Thorium		0.0	DEFINED	SOIL	LAM(2)
	Lead		3.3×10^{-2}	DEFINED	SOURCE	LAMPB
	Radium		4.33×10^{-4}	DEFINED	SOURCE	LAMRAD
P_t	annual net precipitation (time variant)	$m.yr^{-1}$	0.4	N(0.4,0.1,0.15, 0.65)	INPUT	NPRCP
$\rho_{s,k}$	soil bulk density of kth soil layer	$kg.m^{-3}$			INPUT	RHOS(k)k=1,2
	Layer 1		129	LN(129,1.3,20, 450)		
	Layer 2		1342	LN(1342,1.1, 1000,1800)		
$K_{d,k,i}$	distribution coefficient for kth soil layer and ith radionuclide	$m^3.kg^{-1}$			INPUT	SOILKD(i,k)i=1,4 k=1,2
	Layer 1 Uranium		0.32	LU(1.3×10^{-4},7.9×10^{2})		
	Thorium		0.70	LU(3.29×10^{-3},1.5×10^{2})		
	Lead		3.3	LU(1.8×10^{-1},6.3×10^{1})		
	Radium		2.2	LU(5.1×10^{-3},9.5×10^{2})		
	Layer 2 Uranium		0.32	LU(1.3×10^{-4},7.9×10^{2})		
	Thorium		0.70	LU(3.29×10^{-3},1.5×10^{2})		
	Lead		3.3	LU(1.8×10^{-1},6.3×10^{1})		
	Radium		2.2	LU(5.1×10^{-3},9.5×10^{2})		
W_k	water content of kth soil layer	kg(water) $.kg^{-1}$(dry soil)			INPUT	WC(k)k=1,2
	Layer 1		1.08	U(0.75,1.4)		
	Layer 2		0.13	LN(0.13,1.4, 0.05,0.36)		
$[S_c]_{k,i,t}$	concentration of radionuclide i in soil layer k at the receptor at time t	Bq/m^3	calculated	calculated	SOIL	SOILC(i,j)i=1,4 $j\leq82$ or SOILCN(i,k)i=1,4 k=1,2

Note

* Distributions are as described on Table 2.3.

directions for up to a radius of 50 km from the tailings site. Within this broad area, virtually any soil type can be encountered. In other words, the airborne dust may settle on any type of soil. Hence the full range of soil physical and chemical conditions may be encountered. In UTAP.3 this is the full spectrum of soil types (i.e. sand, silt, clay or organic) were this is represented by widening the distribution of input parameter values. In a site specific (non-generic) type of problem, these ranges of values for soil characteristics could be narrowed.

Shield soils typically have an organic surface layer overlaying a sand, silt or clay layer with organic content decreasing as a function of depth in this second layer (Beals, 1985).

Soil Distribution Coefficient

Data on K_d values for sand, silt, clay and organic soils reported by Sheppard et al. (1984) and Knight and Piesold (1986) were fitted to a variety of distributions. Because the small size of data base limited the number of bins into which the data could be divided, the Chi Square goodness-of-fit statistic could not be used to differentiate the distribution(s) which best characterized the data. From visual inspection, the loguniform distribution seemed to best characterize the data; hence, it was used to characterize K_d for the four radionuclides. The limits of the loguniform distributions correspond to the low and high values for K_d's reported in the above two references. As was indicated above, for the generic problem treated in UTAP.3, a wide range of K_d's was used.

Due to a limited data base, only one set of K_d values was used for the two soil layers.

Water Content of Soil

Due to the very limited data for the water content of organic soils (Beals, 1985) a uniform distribution was selected to encompass the entire data set.

There was slightly more data for the water content of the second layer. Based on data for sandy, silty, and clay soils (Beals, 1985) a lognormal distribution was selected.

6.4 Description of the Computer Model

The variables used in the soil model are summarized in Table 6.1. The computer code listing for this model is provided in Table 6.2.

6.5 Soil Model Test Program

A series of tests were performed to check the soil model for computational accuracy and reasonableness. Some of these tests are discussed below.

Hand calculations were checked against a deterministic run to confirm that the soil model executed the equations properly. The model was also run probabilistically with the results checked for reasonableness.

Figure 6.2 is a plot of the radionuclide concentration in the second soil layer versus time, plotted as the log of the geometric mean. The system model was run for 2,000 years in 10 year time steps for 100 trials.

6.6 References

Beals, D.I., 1985. "Soil and Climate Parameters for Post Closure Biosphere Assessment of Nuclear Fuel Waste Disposal." Atomic Energy of Canada Limited Report TR-285.

Knight and Piesold Ltd., 1986. "Monitoring of Layered Uranium Tailings - Phase I." Research Report prepared for the National Uranium Tailings Program, CANMET, Energy, Mines and Resources Canada, Ottawa.

FIGURE 6.2

PREDICTED RADIONUCLIDE CONCENTRATION IN SOIL LAYER 2 vs TIME

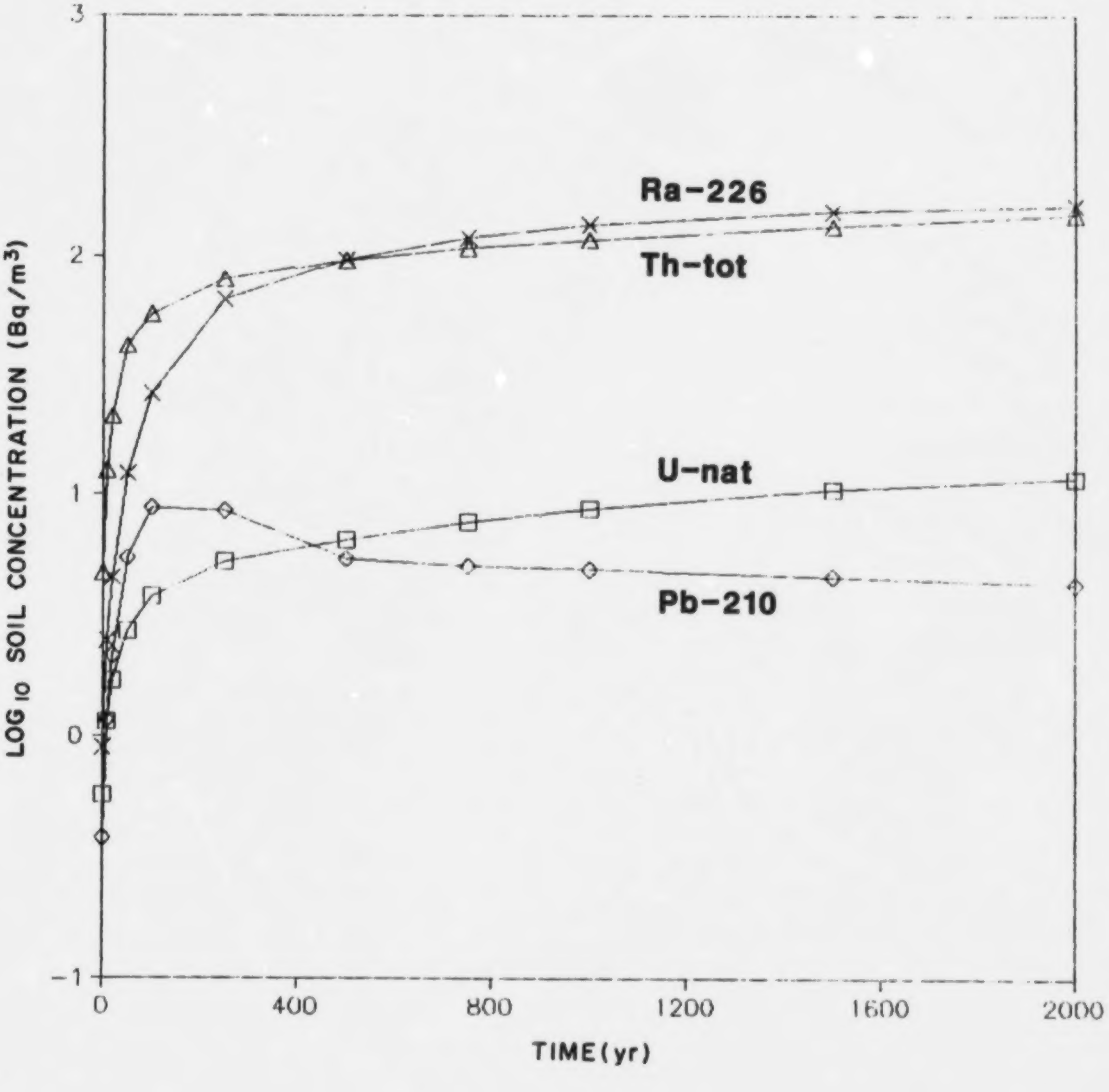

NOTES: 1) The graph shows the geometric mean values of 100 trials
2) Receptor located 2 km to the north of the tailings area

Table 6.2

SOIL MODEL CODE LISTING

```
      SUBROUTINE SOIL
      INCLUDE 'MODEL.INC'
      INCLUDE 'VAR.INC'
      REAL*4 DENOM(4,2),KAPPA1,KAPPA2,ZO(4,82,2)
      COMMON /SOIL/ DENOM,ZO
      IF(NREC.EQ.1)THEN
         IF(NT.EQ.0)THEN
            LAM(1)=0.0
            LAM(2)=0.0
            LAM(3)=LAMPB
            LAM(4)=LAMRAD
         ENDIF
         DO 10 I=1,4
            DO 11 K=1,2
               DENOM(I,K)=RHOS(K)*DSOIL(K)*(WC(K)/998.2+SOILKD(I,K))
11          CONTINUE
10       CONTINUE
      ENDIF
      DO 12 I=1,4
         IF(NT.EQ.0)THEN
            DO 13 K=1,2
               ZO(I,NREC,K)=0.0
13          CONTINUE
         ENDIF
         BETA0=AIRC(I,NREC)*DEPVEL*3.1536E+07
         BETA1=NPRCP/DENOM(I,1)
         GAMMA1=BETA1+LAM(I)
         IF((GAMMA1*DT).GT.50.0)THEN
            ALPHA1=0.0
         ELSE
            ALPHA1=EXP(-GAMMA1*DT)
         ENDIF
         Z1=(ZO(I,NREC,1)-BETA0/GAMMA1)*ALPHA1+BETA0/GAMMA1
         SOILCN(I,1)=Z1/DSOIL(1)
         BETA2=NPRCP*(1-FWAT)/DENOM(I,2)
         GAMMA2=BETA2+LAM(I)
         IF((GAMMA2*DT).GT.50.0)THEN
            ALPHA2=0.0
         ELSE
            ALPHA2=EXP(-GAMMA2*DT)
         ENDIF
         KAPPA1=BETA1*(1-FWAT)*ZO(I,NREC,1)
         KAPPA2=BETA0*BETA1*(1-FWAT)/GAMMA1
         Z2=(KAPPA1-KAPPA2)/(GAMMA2-GAMMA1)*(ALPHA1-ALPHA2)
     +      +KAPPA2/GAMMA2*(1.0-ALPHA2)+ZO(I,NREC,2)*ALPHA2
         SOILCN(I,2)=Z2/DSOIL(2)
         ZO(I,NREC,1)=Z1
         ZO(I,NREC,2)=Z2
         SOILC(I,NREC)=SOILCN(I,2)
         IF(NREC.EQ.NRECEP)THEN
            IF(NT.EQ.0)THEN
```

Table 6.2 continued.

```
               DO 14 K=1,2
                  Z0(I,NRECEP+1,K)=0.0
                  Z0(I,NRECEP+2,K)=0.0
14             CONTINUE
            ENDIF
            BETA0=AIRC(I,NRECEP+1)*DEPVEL*3.1536E+07
            Z1=(Z0(I,NRECEP+1,1)-BETA0/GAMMA1)*ALPHA1+BETA0/GAMMA1
            KAPPA1=BETA1*(1-FWAT)*Z0(I,NRECEP+1,1)
            KAPPA2=BETA0*BETA1*(1-FWAT)/GAMMA1
            Z2=(KAPPA1-KAPPA2)/(GAMMA2-GAMMA1)*(ALPHA1-ALPHA2)
     +         +KAPPA2/GAMMA2*(1.0-ALPHA2)+Z0(I,NRECEP+1,2)*ALPHA2
            Z0(I,NRECEP+1,1)=Z1
            Z0(I,NRECEP+1,2)=Z2
            SOILC(I,NRECEP+1)=Z2/DSOIL(2)
            BETA0=AIRC(I,NRECEP+2)*DEPVEL*3.1536E+07
            Z1=(Z0(I,NRECEP+2,1)-BETA0/GAMMA1)*ALPHA1+BETA0/GAMMA1
            KAPPA1=BETA1*(1-FWAT)*Z0(I,NRECEP+2,1)
            KAPPA2=BETA0*BETA1*(1-FWAT)/GAMMA1
            Z2=(KAPPA1-KAPPA2)/(GAMMA2-GAMMA1)*(ALPHA1-ALPHA2)
     +         +KAPPA2/GAMMA2*(1.0-ALPHA2)+Z0(I,NRECEP+2,2)*ALPHA2
            Z0(I,NRECEP+2,1)=Z1
            Z0(I,NRECEP+2,2)=Z2
            SOILC(I,NRECEP+2)=Z2/DSOIL(2)
         ENDIF
12    CONTINUE
C
      IF(CODSOL.EQ.1.0.OR.CODSOL.EQ.2.0.OR.CODSOL.EQ.3.0)THEN
         WRITE(*,100)
      ENDIF
      IF(CODSOL.EQ.3.0)THEN
         WRITE(*,101)(LAM(I),I=1,4)
         WRITE(*,102)NPRCP,FWAT,DEPVEL
         WRITE(*,103)(RHOS(K),K=1,2)
         WRITE(*,104)(DSOIL(K),K=1,2)
         WRITE(*,105)(WC(K),K=1,2)
         WRITE(*,106)
         DO 15 K=1,2
            WRITE(*,107)(SOILKD(I,K),I=1,4)
15       CONTINUE
         WRITE(*,108)NREC,(AIRC(I,NREC),I=1,4)
         IF(NREC.EQ.NRECEP)THEN
            WRITE(*,109)(AIRC(I,NRECEP+1),I=1,4),
     +                  (AIRC(I,NRECEP+2),I=1,4)
         ENDIF
      ENDIF
      IF(CODSOL.EQ.2.0.OR.CODSOL.EQ.3.0)THEN
         WRITE(*,110)NREC,(SOILCN(I,1),I=1,4),(SOILCN(I,2),I=1,4)
         IF(NREC.EQ.NRECEP)THEN
            WRITE(*,111)(SOILC(I,NRECEP+1),I=1,4),
     +                  (SOILC(I,NRECEP+2),I=1,4)
         ENDIF
      ENDIF
C
```

Table 6.2 continued.

```
100   FORMAT(///1X,'SOIL MODEL')
101   FORMAT(/1X,'RADOINUCLIDE DECAY CONSTANTS'/1X,4(E12.4))
102   FORMAT(1X,'NET PRECIPITATION',E12.4/1X,'FRACTION OF NET PRECIP',
     +       'ITATION IN RUNOFF',E12.4/1X,'DEPOSITION VELOCITY',E12.4)
103   FORMAT(1X,'BULK DENSITY OF SOIL LAYERS',E12.4/28X,E12.4)
104   FORMAT(1X,'DEPTH OF SOIL LAYERS',E12.4/21X,E12.4)
105   FORMAT(1X,'WATER CONTENT OF SOIL LAYERS',E12.4/29X,E12.4)
106   FORMAT(1X,'DISTRIBUTION COEFFICIENT FOR RADIONUCLIDES IN THE S',
     +       'OIL LAYERS')
107   FORMAT(1X,4(E12.4))
108   FORMAT(1X,'RADIONUCLIDE AIR CONCENTATION AT RECEPTOR',I3/1X,
     +       4(E12.4))
109   FORMAT(1X,'AVERAGE RADIONUCLIDE AIR CONCENTATION',/1X,4(E12.4),
     +       1X,'AVERAGE WATERSHED RADIONUCLIDE AIR CONCENTATION',/1X,
     +       4(E12.4))
110   FORMAT(/1X,'RADIONUCLIDE SOIL CONCENTATION AT RECEPTOR',I3,' I',
     +       'N THE SOIL LAYERS',/1X,4(E12.4)/1X,4(E12.4))
111   FORMAT(1X,'AVERAGE RADIONUCLIDE SOIL CONCENTATION',/1X,4(E12.4),
     +       /1X,'AVERAGE WATERSHED RADIONUCLIDE SOIL CONCENTATION',/
     +       1X,4(E12.4))
C
      RETURN
      END
```

Sheppard, M.I., Beals, D.I., Thibault, D.H., and O'Connor, P., 1984. "Soil Nuclide Distribution Coefficients and Their Statistical Distributions." Atomic Energy of Canaa Limited Report 8364.

Wang, K.T., and Chin, V.T., 1978. "Northern Ontario Water Resources Studies - Groundwater Resources." Ontario Ministry of the Environment, Toronto.

7.0 GROUNDSHINE MODEL

7.1 Introduction

The model describing the atmospheric dispersion to the receptor sites of radioactivity resuspended from the tailings piles has been described in Chapter 5. The radionuclide deposition onto and the mixing into the surficial soil layers at each receptor are calculated in the SOIL model described in Chapter 6.

The model developed in this section calculates the surface gamma flux density and receptor (groundshine) dose rate due to the accumulation over time of selected radionuclides in the soil profile. The radionuclides considered in this implementation of the groundshine model include natural uranium (U-238 to U-234), total thorium (Th-232 plus daughters and Th-230), lead-210, radium-226 (plus radon daughters). The model uses the radionuclide concentrations in two soil layers calculated by the soil model described in Chapter 6. The groundshine model accounts approximately for self-shielding by overlying soil layers and the loss of gamma ray flux via radon emanation and subsequent exhalation to the atmosphere.

In the development of the groundshine model a number of assumptions have been introduced to simplify the computations. While the assumptions are discussed as they are introduced into the model development, two assumptions are worth noting here. First, any attenuation which may take place in the medium (air) between the source (i.e. the soil layer) and the receptor is neglected. Second, as discussed in the following section, a simplifying approximation has been made to account for the effect of scattered radiation originating from within the self-absorbing source material (i.e. the soil).

The following sections document the basis for the groundshine model and the parameters required to use it.

7.2. The Basic Model

In the case of a single layer of soil containing one radionuclide distributed uniformly throughout the layer, each volume element within that soil layer will act as a source of gamma rays. When gamma rays pass through matter, in this case soil, they are removed from the beam in an exponential manner described by:

$$\phi = \phi_0 \exp(-\mu b) \qquad (7.1)$$

where ϕ_0 and ϕ are respectively the gamma ray flux densities (gamma rays per square metre per second) before and after passing through a material of thickness b metres. The proportionality constant μ is called the linear attenuation coefficient (units of m^{-1}) and is a function of both the gamma ray energy and the medium. Thus each incremental layer of soil both increases the gamma ray flux density at the soil surface by adding a new source of gamma rays and reduces the gamma ray flux density at the soil surface by attenuating a fraction of the gamma rays originating in lower layers. The combined effect of these phenomena on the gamma ray flux density, ϕ, at the surface of the soil is described mathematically by:

$$\phi = \int_0^b \int_0^{\theta_1} \frac{A}{2} \tan\theta \exp(-\mu x/\cos\theta)\, d\theta\, dx \qquad (7.2a)$$

where

ϕ = gamma photon flux density at receptor (gamma rays.m^{-2}. s^{-1})

μ = linear attenuation coefficient (m^{-1})

$A = \frac{CN}{S_{pa}}$ = gamma ray source strength (gamma rays.m^{-3}.s^{-1})

C = concentration of radionuclide in soil layer (Bq.m^{-3})

N = gamma rays per unit time per unit mass of radionuclide (gamma rays.kg^{-1}.s^{-1})

S_{pa} = activity per unit mass of radionuclide (Bq.kg^{-1})

b = soil layer depth (m).

Equation (7.2) is basically the integration of flux density at a point above the soil surface from a ring-shaped volume element containing radioactivity at depth b within the source. The variables θ and X represent the angle subtended by the ring and the depth of the ring within the source, respectively. As noted previously, the formulation neglects any attenuation of gamma rays in the air between the receptor and the source. In the limit of a very large (semi-infinite) plane source (i.e. $\theta_1 \rightarrow \pi/2$) which is also very thick (i.e. $b \rightarrow \infty$), equation (7.2a) reduces to:

$$\phi = \frac{A}{2\mu} \tag{7.2b}$$

In the case where the semi-infinite plane source has a finite thickness, b, equation (7.2a) must be solved by analytical methods. Using the substitution $x = 1/\cos\theta$, the method of integration by parts and an integration formula from the Chemical Rubber Company handbook (CRC, 1964), the solution of equation (7.2a) is given by:

$$\phi = \frac{A}{2\mu}\left[1 - e^{-\mu b} - \mu b \left(\gamma + \ln(\mu b) - \mu b + \frac{(\mu b)^2}{2.2\,!} - \frac{(\mu b)^3}{3.3\,!} \ldots \right)\right] \tag{7.3}$$

where

γ = a constant having the value 0.5772157.

7.3. Two Soil Layers

Equations (7.2b) and (7.3) give the gamma flux density at the surface of a single soil layer with a constant radionuclide concentration and includes attenuation within the layer. In this study the total gamma ray flux density at the ground surface is taken to be the sum of the gamma ray flux densities from two soil layers taking into account the shielding of the top layer. For the ith radionuclide, this can be expressed as:

$$\phi_{T,i} = \phi_{1,i} + \phi_{2,i} \exp(-\mu_1 b_1) \tag{7.4}$$

where

$\phi_{T,i}$ = the total gamma flux density at the soil surface from radionuclide i (gammas.m^{-2}.s^{-1})

$\phi_{1,i}$ = the gamma flux density at the soil surface from radionuclide i in the top soil layer (gammas.m^{-2}.s^{-1})

$\phi_{2,i}$ = the gamma flux density at the soil surface from radionuclide i in the bottom soil layer if the top layer were not present (gammas.m^{-2}.s^{-1})

μ_1 = the linear attenuation coefficient of the top layer (m^{-1})

b_1 = the thickness of the top layer (m).

7.4 Attenuation Coefficient

Since the attenuation coefficient μ (and hence the flux density) is dependent on the type of scattering medium (in this case, soil) and the gamma energy, equations (7.1), (7.2) and (7.3) must be evaluated for each gamma energy emitted by each radionuclide in the soil. The summation over all energies is discussed later.

Equation (7.2) is based on the assumption that gamma rays scattered by the soil are completely removed from the radiation beam. However, gamma rays which are scattered but not absorbed may also add to the total gamma ray flux density received by someone standing on the soil. The effect of scattered radiation can be taken into account by buildup factors which depend on the nature of the soil, the thickness of the soil, and the type and energy of the radiation. Such calculations are very complex. To make the calculations tractable, an approximation is made to take account of the contribution of scattered radiation to the gamma ray flux at the receptor.

The linear attenuation coefficient (μ) represents the sum of various absorption and scattering processes which affect the energy removed from the primary beam of gamma rays (i.e. $\mu=\mu_a + \mu_{scat}$). In this study, the linear absorption coefficient (μ_a) is substituted for the linear attenuation coefficient μ ($\mu_{scat}=0$), that is, it is assumed that the scattered radiation will always contribute to the resultant energy flux. This assumption appears to be in general agreement with results found using experimentally determined buildup factors (Evans, 1955).

Attenuation coefficients are often tabulated in the form of μ/ρ, where ρ is the density and μ is the linear attenuation coefficient of the medium defined as mass attenuation coefficients which are independent of the physical state (gas, solid, liquid), and density of the medium. As stated above, mass absorption coefficients are used in this analyses (for example, see U.S. DHEW, 1970).

As noted earlier, the attenuation coefficient μ (set equal to the absorption coefficient in this analysis) is a function of the gamma energy and the type of absorbing material. Since the absorption coefficients for soil as a function of energy were not readily available, the mass absorption coefficients of concrete (μ_c/ρ_c), adjusted by the relative density of soil to concrete, were used. This method has been used by Kocher and Sjoreen (1985) to calculate exposure rates from near-surface contamination. The mass absorption coefficients for concrete (μ_c/ρ_c) as a function of energy (Attix and Roesch, 1968) were fitted to a regression model ($r^2 \simeq 0.94$) of the form $y = ax^b$ as follows:

$$\mu_c/\rho_c = 2.7 \times 10^{-3}\ E^{-0.320}\ (m^2.kg^{-1}) \qquad (7.5)$$

The mass absorption coefficients for concrete were adjusted to obtain the linear absorption coefficient for soil (μ_s, where the "s" stands for "soil") as follows:

$$\mu_s = \frac{\mu_c}{\rho_c}\ \rho_c\ \frac{\rho_s}{\rho_c} = \frac{\mu_c}{\rho_c}\ \rho_s \qquad (7.6)$$

Returning to equation (7.4), the total gamma flux density ($gammas.m^{-2}.s^{-1}$) in the jth energy interval at the soil surface for each group of radionuclides (natural uranium, total thorium, lead-210 or radium-226)is then given by :

$$\phi_{T,j} = \phi_{1,j} + \phi_{2,j} \quad \exp\left\{-\mu_{j,1} b_1\right\} \tag{7.7}$$

where the energy-dependent attenuation coefficient μ_j is given by equations (7.5) and (7.6). The energy used to calculate μ_j in equation (7.5) is the average energy of the jth energy interval.

7.5 Radionuclide Groups

The radionuclides of concern in this study have been divided into four groups: natural uranium, total thorium, lead-210 and radium-226. Natural uranium consists of uranium-238 and uranium-234 from one radioactive decay series and uranium-235 from another series. Since the natural abundance of uranium-235 is very low (0.72% on a mass basis), it is not dosimetrically significant and is not considered in these calculations. (One gram of natural uranium contains 1.22×10^4 Bq each of uranium-238 and uranium-234, and 5.8×10^2 Bq of uranium-235.) In this component model, total thorium is taken as the sum of thorium-232 plus thorium-230. The decay chains for the uranium-238 and thorium-232 series are illustrated in Figures 7.1 and 7.2 respectively.

The natural uranium concentrations in each of the two soil layers calculated in the soil model are the sum of the U-238 and U-234 activities. Only the gamma emissions from radionuclides down to uranium-234 (Figure 7.1) need to be considered since the long-lived thorium-230 (8×10^4 yr half-life) effectively limits the ingrowth of the remainder of the decay series during the modelling period (up to 1000 years). It is assumed that secular equilibrium is established for all radionuclides in the chain from U-238 to U-234.

The total thorium concentrations in soil calculated in the soil model are the sum of the Th-232 and Th-230 activities. The fraction of the Th-232 activity in total thorium is also generated in the soil model. Since the longest half-life of any Th-232 daughter is 6.7 years, it is assumed that all members of the chain are in secular equilibrium with the parent Th-232, and all

FIGURE 7.1

URANIUM - 238 DECAY SERIES

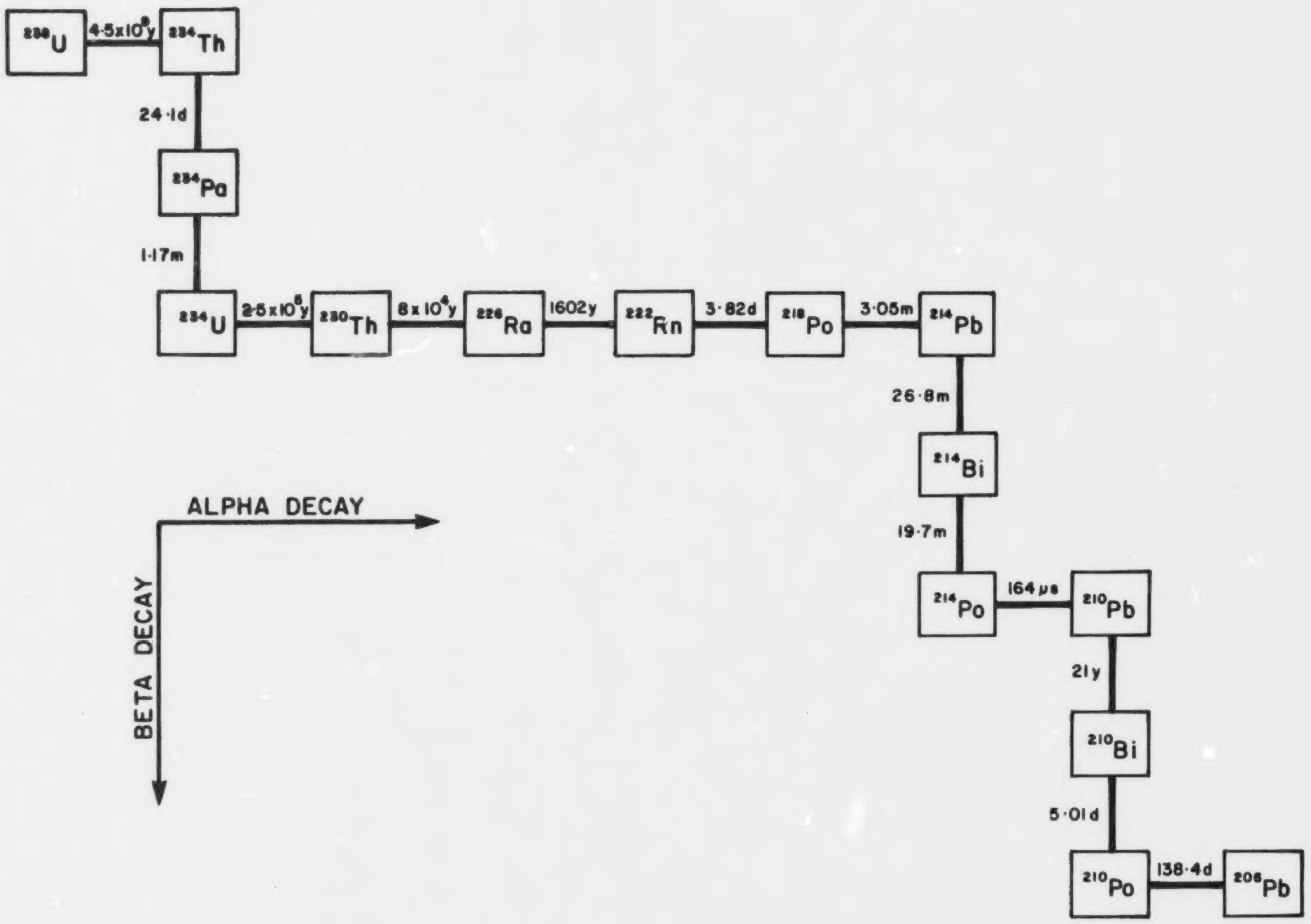

FIGURE 7.2

THORIUM - 232 DECAY SERIES

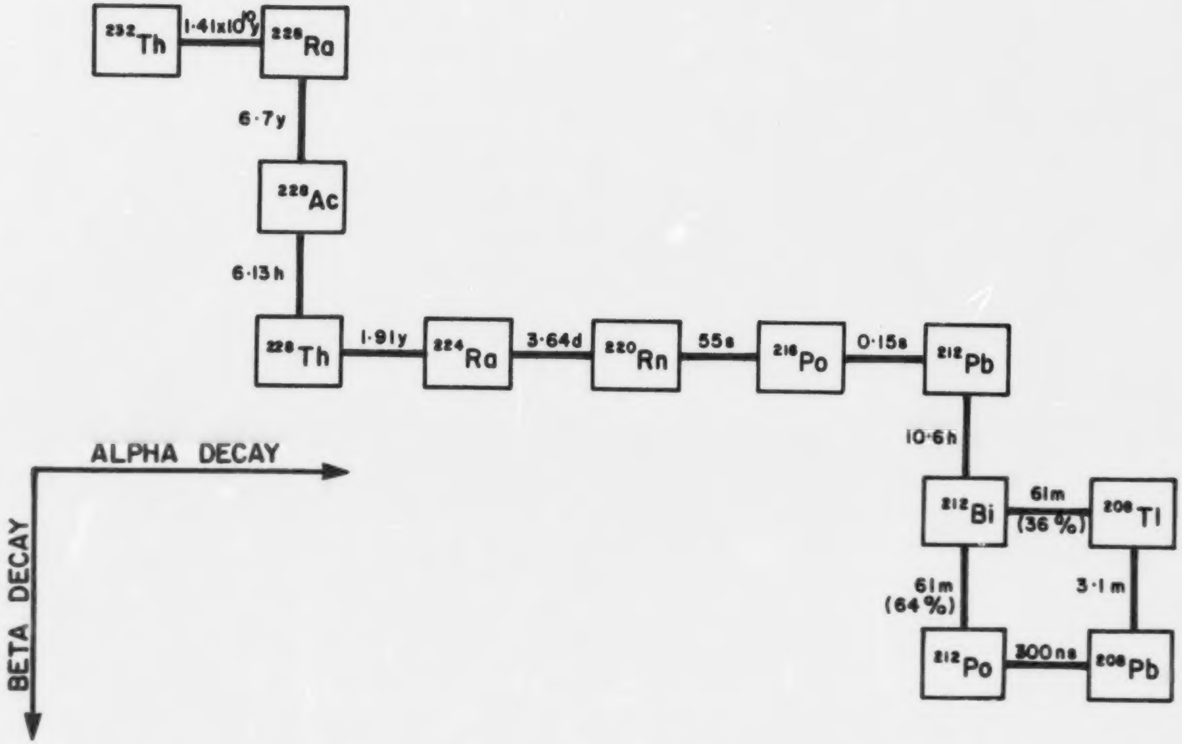

contribute to the gamma dose rate at the soil surface. However, no ingrowth of Ra-226 from Th-230 deposited onto the soil has been credited because of the relatively long half-life ($t_{1/2}$ = 1602 yr) of Ra-226 compared to the modelling period (up to 1000 years).

The concentration of Pb-210 in each soil layer is calculated in the soil model and the surface dose rate from Pb-210 gamma radiation is calculated in the groundshine model. However, contributions to the dose rate from Pb-210 daughters have been ignored because the abundance of gamma rays from Pb-210 daughters is insignificant.

The concentration of Ra-226 in each soil layer is also calculated in the soil model. For the purpose of calculating the gamma dose rate above the soil surface the contribution from radon and its daughters has been included. However, secular equilibrium has not been assumed as there can be significant exhalation of radon gas from the soil. The modelling of radon exhalation is described in Section 7.6

For simplicity, the subscript i denoting radionuclides does not appear in the equations developed below. The reader should consider the subscript i to be implicit in these equations.

As previously noted, the radionuclides being modelled emit gamma rays with a variety of energies. Since the attenuation coefficient is a function of energy, equations (7.3) and (7.4) must account for the different gamma energies. Dealing with each of the large number of gamma rays individually was considered too cumbersome. To decrease the number of calculations, the spectrum of gamma energies for each of the six groups of radionuclides being modelled was divided into five energy intervals (Table 7.1a) (Chambers et al., 1981). The specific gamma ray emission rate was calculated for each radionuclide group and each gamma energy interval.

$$N_{T,j} = S \sum_{l=1}^{n} B_l \sum_{k=1}^{m} N_{j,k} \tag{7.8}$$

where

$N_{T,j}$ = total specific gamma ray emission rate into energy interval j for each radionuclide group (gamma rays.kg^{-1}.s^{-1})

S = specific activity of parent in the radionuclide group (disintegrations.kg^{-1}.s^{-1})

B_l = decay branching ratio of daughter radionuclide l (unitless)

n = number of radionuclides in the group

$N_{j,k}$ = the abundance of gamma rays in energy level k within energy interval j (unitless)

m = number of energy levels within energy interval j.

For each radionuclide group the total energy of the gamma emissions in each energy interval is ($E_{T,j}$):

$$E_{T,j} = \sum_{k=1}^{m} E_{j,k} N_{j,k} \tag{7.9}$$

where

$E_{j,k}$ = energy of kth decay in jth energy interval (MeV).

The average energy in the jth energy interval (E_j) for the radionuclide group of interest is then:

$$E_j = \frac{E_{T,j}}{N_{T,j}} \tag{7.10}$$

An example will help to clarify the above concepts. Consider the thorium-232 decay chain and the lowest energy interval ranging from 0.02 to 0.2 MeV. The two radionuclides in this decay chain (Figure 7.2) which produce gamma

Table 7.1a

AVERAGE RADIONUCLIDE PARAMETERS FOR GROUNDSHINE CALCULATIONS

Gamma Energy Intervals (MeV)	0.02-0.2	0.2-0.43	0.43-0.61	0.61-1.40	1.40-3.0
Specific Emission Rates - (gammas $kg^{-1}.s^{-1}$)					
U238-U234	$9.6x10^5$	0	0	$1.26x10^5$	0
Th232 + daughters	$1.45x10^5$	$2.79x10^6$	$1.58x10^6$	$2.27x10^6$	$1.52x10^6$
Pb210	$1.2x10^{14}$	0	0	0	0
Ra226	$1.46x10^{12}$	0	0	0	0
Rn222 + daughters	$1.46x10^{12}$	$2.01x10^{13}$	$1.72x10^{13}$	$6.23x10^{12}$	$6.22x10^{12}$
Th230	$2.7x10^4$	0	0	0	0
Average Gamma Energy - Mev					
U238-U234	0.097	0	0	0.91	0
Th232 + daughters	0.0596	0.263	0.567	0.90	2.57
Pb210	0.047	0	0	0	0
Ra226	0.186	0	0	0	0
Rn222 + daughters	0.047	0.331	0.609	1.12	1.76
Th230	0.0757	0	0	0	0

radiation within this energy interval are Th-228, which emits a 0.084 MeV gamma on 1.6% of its decays, and Bi-212 which emits a 0.040 MeV gamma on 2% of its decays. Noting that 1 kg of Th-232 has an activity of 4.03 x 10^6 Bq and assuming equilibrium of its daughter products, the total number of decays and the average energy in the lowest energy interval are calculated as follows:

$E_{1,1} = 8.4 \times 10^{-2}$ MeV

$N_{1,1} = 6.45 \times 10^4$ gammas.$kg^{-1}.s^{-1}$ ($4.03 \times 10^6 \times 1.6\%$)

$E_{1,2} = 4.00 \times 10^{-2}$ MeV

$N_{1,2} = 8.07 \times 10^4$ gamma.$kg^{-1}.s^{-1}$ ($4.03 \times 10^6 \times 2\%$)

$N_{T,1} = (6.45 \times 10^4) + (8.07 \times 10^4) = 1.45 \times 10^5$ gammas.$kg^{-1}.s^{-1}$ (equation (7.5))

$E_{T,1} = (8.4 \times 10^{-2} \times 6.45 \times 10^4) + (4.00 \times 10^{-2} \times 8.07 \times 10^4)$

$= 8.65 \times 10^3$ MeV.$kg^{-1}.s^{-1}$ (equation (7.9))

$E_1 = \dfrac{8.65 \times 10^3}{1.45 \times 10^5} = 5.96 \times 10^{-2}$ MeV (equation (7.10))

7.6 Exhalation of Radon

Some of the radon generated by radium in the soil particles can be found in the pore spaces in the soil. The radon, an inert gas, can diffuse through the soil layer into the air above (exhalation) provided it does not undergo radioactive decay to its daughters before reaching the soil surface. Rn-222, the daughter of Ra-226 in the U-238 series, has a sufficiently long half-life (3.8 days) that a significant fraction of the radon produced in the soil can escape. Thoron (radon-220) in the thorium-232 decay series (Figure 7.2) will also diffuse from the soil but its relatively short half-life (55s) precludes any significant exhalation. The thoron diffusion length in normal soils is only 1 to 2 cm. For this model, it is assumed that no thoron is exhaled from the soil.

As a result of Rn-222 exhalation from the surficial soil layers, the radon daughter concentration in the soil will be less than equilibrium. This effect can be modelled by assuming that the radon within the pore space of the soil (the emanation fraction; see Chapter 4) is instantaneously released to the atmosphere. This is a reasonable assumption for the relatively thin (< 0.2 m deep) soil layers being modelled. The emanation of the radon changes the number and average energy of the radon daughter gamma rays emitted from the radionuclides remaining in the soil. The following method was used to adjust the number and average energy of gamma rays emitted in the radium-226 decay chain remaining in the soil after some radon has escaped:

$$N_{T,j,Ra} = N_{Ra,j} + N_{Rn,j}\,(1-E) \qquad (7.11)$$

where

$N_{T,j,Ra}$ = total number of decays in jth energy interval in the entire radium-226 and daughters decay chain (gammas.kg^{-1} (Ra).s^{-1})

$N_{Ra,j}$ = number of decays in the jth energy interval for radium-226 only (see Figure 7.1)(gammas.kg^{-1} (Ra).s^{-1})

$N_{Rn,j}$ = number of decays for radon and daughters in jth energy interval (gammas.kg^{-1} (Ra).s^{-1})

E = emanation fraction of radon.

The average energy of the radiation emitted by radionuclides remaining in the soil ($E'_{j,Ra}$) is:

$$E^{j,Ra} = \frac{E_{Ra,j}N_{Ra,j} + E_{Rn,j}N_{Rn,j}(1-E)}{N^{Ra}_{T,j}} \qquad (7.9)$$

where

$E_{Ra,j}$ = average energy in the jth energy interval (MeV) for radium decay

$E_{Rn,j}$ = average energy in the jth energy interval (MeV) for radon and daughters .

7.7 Energy Flux Density to Dose Rate Conversion

This gamma photon flux density can be converted to an energy flux density and then a dose rate by (Cember, 1969):

$$D_{j,i} = \phi_{T,j,i} \, E_{j,i} \, \frac{\mu_{t,j}}{S_t} \, 5.0 \times 10^{-6} \, (Sv.yr^{-1}) \qquad (7.13)$$

where

$D_{j,i}$ = total dose rate in tissue from radionuclide i in energy interval j ($Sv.yr^{-1}$)

$\mu_{t,j}/\rho_t$ = mass energy absorption coefficient for tissue at energy E_j^n ($m^2.kg^{-1}$)

ρ_t = tissue density ($kg.m^{-3}$).

Since the tissue mass energy absorption coefficient is not highly energy-dependent in the energy range of interest to this study, it is set equal to a constant 3×10^{-3} $m^2.kg^{-1}$ (U.S. DHEW, 1970). The tissue density is taken to be 1×10^3 $kg.m^{-3}$. The constant 5×10^{-6} in equation (7.13) converts $MeV.g^{-1}$ to $Sv.yr^{-1}$ and is based on the conversion factors 1.6×10^{-6} ergs = 1 MeV, 100 $ergs.g^{-1}$ = rad, 1 rad = 1 rem (for gammas), 1 Sv = 100 rem, 10^3 g = 1 kg and 1 yr = 3.15×10^7 seconds.

The total dose rate at the soil surface for the ith radionuclide (D_T^i) is then:

$$D_{T,i} = \sum_{j=1}^{5} D_{j,i}$$

Figure 7.3 is a flowsheet illustrating the concepts involved in computer implementation of the model. Table 7.1b contains a parameter listing and Table 7.2 is a copy of the FORTRAN code for the groundshine model. The series solution of equation (7.2) is treated in subroutine SOL.

7.8 Calibration

It should be noted that although a number of approximations have been used in the development and implementation of the groundshine model, it performs reasonably well. The present model was used to calculate the gamma dose rate at the surface of the soil for a uniform concentration of Th-232 and daughters in a layer one metre (1 m) thick. A similar calculation was made for a uniform concentration of natural uranium, and all its daughters in equilibrium including Th-230, Ra-226 and Ra-222 plus daughters. These predictions were compared to the values provided in NCRP No. 45 (1975) for Th-232 and daughters and U-238 and daughters.

The dose rate from thorium predicted by the UTAP.3 model was less than 3 % greater than the value reported in NCRP No. 45. The model agreement was considered excellent.

The dose rate from the uranium series predicted by the UTAP.3 model was about 63 % of the value reported in NCRP No. 45. Almost 20 % of this difference is attributable to the exhalation of radon gas that was credited at 20 % in the UTAP.3 model. Since the radioisotopes preceeding Ra-226 and radon daughters in the U-238 chain contribute insignificantly to the exposure rate. The agreement was considered acceptable.

The temporal variations of the groundshine dose rate contributions from each of the four radionuclide groups are shown in Figure 7.4. The computer run was based upon the probabilistic parameters given in Table 7.1b.

7.9 References

Cember, H., 1969. "Introduction to Health Physics." Pergamon Press.

Chambers, D.B., Mernagh, J.R., and Torrie, R.T., 1981. "Design for Radiation Protection in The Mining of High Grade Uranium Ore." In Proceedings of: International Conference on Radiation Hazards in Mining-Control, Measurement and Medical Aspects, October 4-9, Golden, Colorado, (M. Gomez, Ed.), Publishers: AIMMPE, New York, NY

FIGURE 7.3

FLOWSHEET FOR GROUNDSHINE MODEL

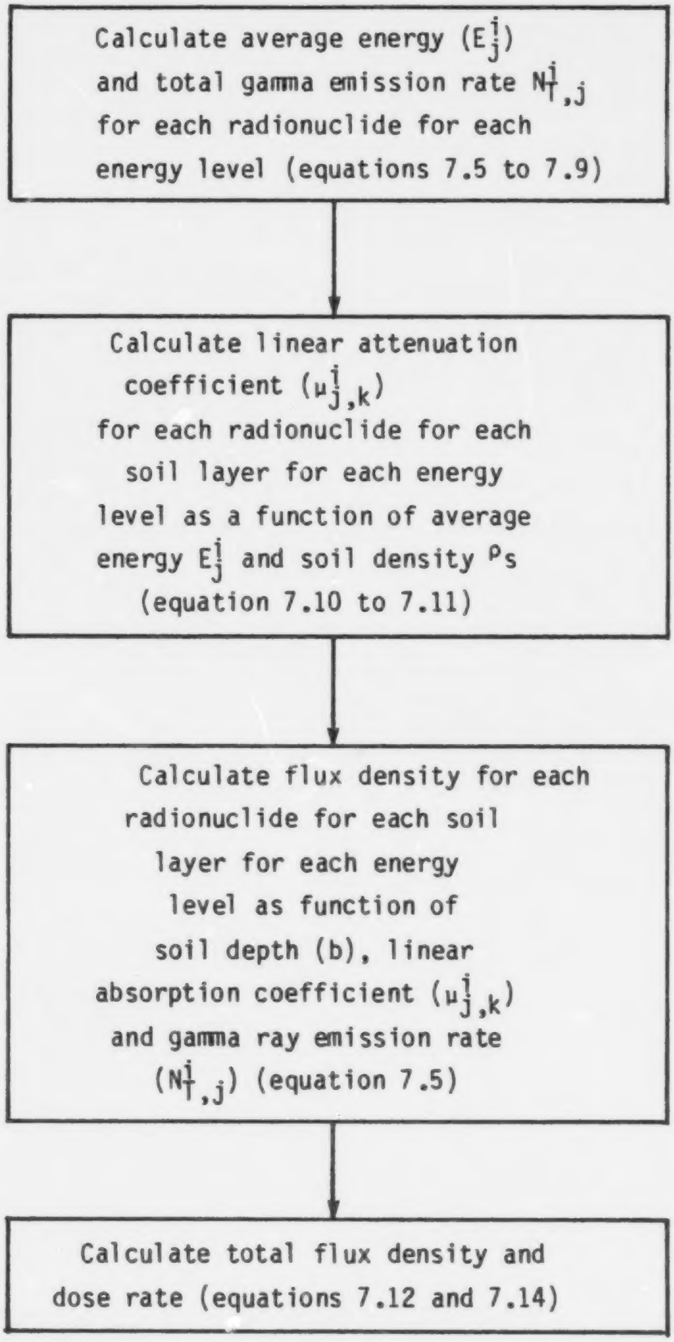

Calculate average energy (E_j^i) and total gamma emission rate $N_{T,j}^i$ for each radionuclide for each energy level (equations 7.5 to 7.9)

Calculate linear attenuation coefficient ($\mu_{j,k}^i$) for each radionuclide for each soil layer for each energy level as a function of average energy E_j^i and soil density ρ_s (equation 7.10 to 7.11)

Calculate flux density for each radionuclide for each soil layer for each energy level as function of soil depth (b), linear absorption coefficient ($\mu_{j,k}^i$) and gamma ray emission rate ($N_{T,j}^i$) (equation 7.5)

Calculate total flux density and dose rate (equations 7.12 and 7.14)

LEGEND:

i = RADIONUCLIDE
j = ENERGY LEVEL
k = SOIL LAYER

FIGURE 7.4

PREDICTED RADIONUCLIDE GROUNDSHINE DOSE RATE vs TIME

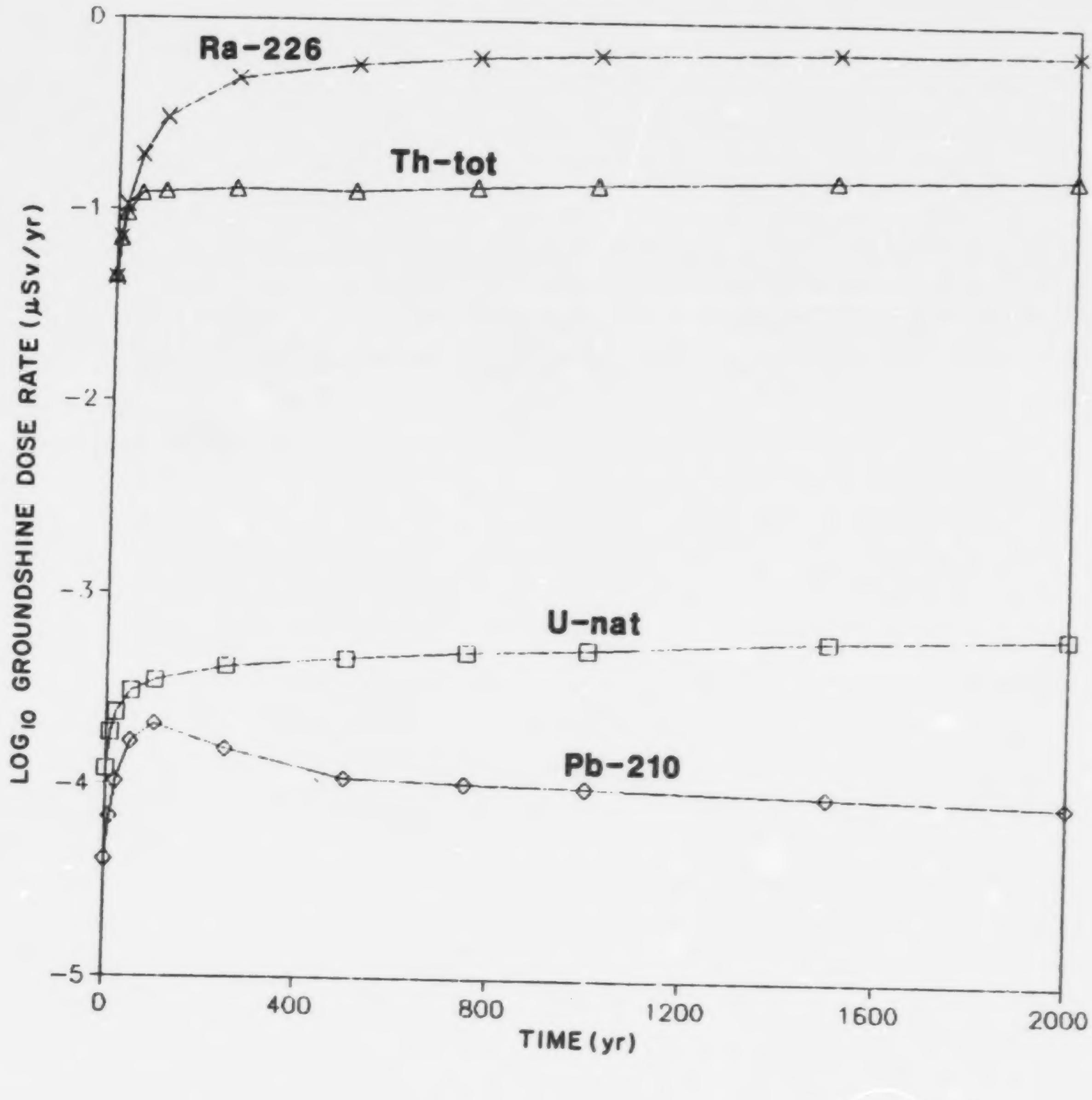

NOTES: 1) The graph shows geometric mean values of 100 trials
2) Receptor located 2km to the north of the tailings area
3) Assumes continuous occupancy

Table 7.1b

GROUNDSHINE MODEL PARAMETERS

Model Symbol	Description	Units	Nominal Value	Probability Distribution*	Computer Origin	Computer Symbol
b_k	depth of kth soil layer	m			INPUT	DSOIL(K)
	Layer 1		0.05	C(0.05)		
	Layer 2		0.15	C(0.15)		
E	fraction of radon exhaled from soil	unitless	0.2	C(0.2)	INPUT	EMFRAC
$E_{j,i}$	average energy in jth energy interval for ith radionuclide	MeV	calculated	calculated	GSHINE	ENERGY(I,J) ENERG(I,J)
$\phi_{T,j,i}$	total flux in jth energy interval for ith radionuclide	gammas $.m^{-2}.s^{-1}$	calculated	calculated	GSHINE	FLUXTOT(I,J)
$D_{j,i}$	tissue dose rate in the jth energy interval for ith radionuclide	$Sv.yr^{-1}$	calculated	calculated	GSHINE	GDSE(I,J)
μ_s	linear absorption coefficient in soil ith radionulcide, kth soil layer and jth energy interval	m^{-1}	calculated	calculated	GSHINE	MU(I,K,J)
$\mu_{t,j}/\rho_t$	mass absorption coefficient in tissue jth energy interval	$m^2.kg^{-1}$	see data statement in code	see data statement in code	GSHINE	MUFLSH(J)
$N_{T,j,i}$	gamma emission rate in jth energy interval for ith radionuclide	gammas $.kg^{-1}.s^{-1}$	see data statement in code	see data statement in code	GSHINE	NDEC(I,J) NNDEC(I,J)
ρ_s	dry soil bulk density of kth layer	$kg.m^{-3}$			INPUT	RHOS(K)
	Layer 1		129	LN(129,1.3,20, 450)		
	Layer 2		1342	LN(1342,1.1, 1000,1800)		
$C_{i,k}$	concentration of ith radionuclide in soil layer k	$Bq.m^{-3}$	calculated	calculated	SOIL	SOILCN(I,K)
$S_{pa,i}$	specific activity for radionuclide i	$Bq.kg^{-1}$	see data statement in code	see data statement in code	GSHINE	SPA(I)
$W_{c,k}$	water content of soil layer k	kg.(water) kg^{-1}.(dry soil)			INPUT	WC(K)
	Layer 1		1.08	U(0.75,1.4)		
	Layer 2		0.13	LN(0.13,1.4,0.05,0.36)		
$N_{T,j,Th-230}$	gamma emission rate in jth energy interval for Th-230	gammas $kg^{-1}.s^{-1}$	see data statement in code	see data statement in code	GSHINE	NTH230(J)
$E_{j,Th-230}$	average energy in jth energy interval for Th-230	MeV	see data statement in code	see data statement in code	GSHINE	ETH230(J)
-	factor to convert total U concentration in soil to U-238 concentration in soil	unitless	1 0.5 2 unity 3 unity 4 unity		GSHINE	FAC(I)
-	print code	unitless	1 print titles 2 print average gamma energy of groups 3 print subroutine SOL parameter values		INPUT	CODGS
-	fraction of total thorium activity that is Th-232	unitless	calculated	calculated	SOIL	X232SA

Notes

* Distributions are as described on Table 2.2.

Table 7.2

GROUNDSHINE MODEL CODE LISTING

```
      SUBROUTINE GSHINE
      INCLUDE 'MODEL.INC'
      INCLUDE 'VAR.INC'
      REAL*4 NNDEC(5,5),NTH230(5),ENERG(5,5),ETH230(5),SPA(4),
     +       MUFLSH(5),FAC(4)

C     INIT'IZE # OF GAMMAS/KG/S IN EACH ENERGY INTERVAL FOR EACH NUCLIDE
      DATA NNDEC /9.6E+5,0.0,0.0,1.26E+5,0.0,
     +            1.45E+5,2.795E+6,1.58E+6,2.27E+6,1.52E+6,
     +            1.2E+14,0.0,0.0,0.0,0.0,
     +            1.46E+12,0.0,0.0,0.0,0.0,
     +            1.46E+12,2.01E+13,1.72E+13,6.23E+12,6.22E+12/
      DATA NTH230 /2.7E+4,0.0,0.0,0.0,0.0/

C     INIT'IZE AV. ENERGY MEV IN EACH ENERGY INTERVAL FOR EACH NUCLIDE
      DATA ENERG /9.7E-2,0.0,0.0,9.10E-1,0.0,
     +            5.96E-2,2.63E-1,5.67E-1,9.0E-1,2.57,
     +            4.7E-2,0.0,0.0,0.0,0.0,
     +            1.86E-1,0.0,0.0,0.0,0.0,
     +            4.7E-02,3.31E-1,6.09E-1,1.12E0,1.76E0/
      DATA ETH230 /7.57E-2,0.0,0.0,0.0,0.0/

C     INITIALIZE SPECIFIC ACTIVITY BQ/KG
      DATA SPA  /1.23E+7,4.03E+6,3.00E+15,3.66E+13/

C     INITIALIZE MASS ABSORPTION COEFF FOR TISSUE M2/KG
      DATA MUFLSH /3.0E-3,3.0E-3,3.0E-3,3.0E-3,3.0E-3/

      DATA FAC /0.5,1.0,1.0,1.0/

      IF(CODGS.GE.1.0)WRITE(*,100)
100   FORMAT(1X,'SUBROUTINE GSHINE')
      IF(CODGS.GE.2.0)WRITE(*,101)
101   FORMAT(1X,'RADIONUCLIDE',1X,'ENERGY BAND',5X,'NDEC',10X,'ENERGY')
C     CALCULATE NUMBER OF DECAYS IN JTH ENERGY BAND FOR RADIUM DECAY
C     CHAIN ACCOUNTING FOR RADON EMANATION
C     REARRANGE ARRAYS INTO PROPER ROW AND COLUMN ORDER
      IF(NT.EQ.0.AND.NREC.EQ.1)THEN
         DO 10 I=1,4
            DO 11 J=1,5
               IF(I.LE.3)THEN
                  IF(I.EQ.2)THEN
                     AAA=NNDEC(J,2)*X232SA
                     BBB=(1.0-X232SA)*NTH230(J)
                     NDEC(2,J)=AAA+BBB
                     IF(NDEC(2,J).EQ.0.0)THEN
                        ENERGY(2,J)=0.0
                     ELSE
                        ENERGY(2,J)=(ENERG(J,2)*AAA+ETH230(J)*BBB)/
     +                              NDEC(2,J)
                     ENDIF
```

Table 7.2 continued.

```
                  ELSE
                     NDEC(I,J)=NNDEC(J,I)
                     ENERGY(I,J)=ENERG(J,I)
                  ENDIF
               ELSE
C     ACCOUNT FOR RADON EMANATION
                  NDEC(4,J)=NNDEC(J,4)+NNDEC(J,5)*(1-EMFRAC)
                  ENERGY(4,J)=((ENERG(J,4)*NNDEC(J,4))+(ENERG(J,5)*
     +                        (NNDEC(J,5)*(1-EMFRAC))))/NDEC(4,J)
               ENDIF
               IF(CODGS.GE.2.0)WRITE(*,102)I,J,NDEC(I,J),ENERGY(I,J)
102            FORMAT(5X,I2,10X,I2,7X,E10.3,5X,E10.3)
               FLXTOT(I,J)=0.0
11          CONTINUE
10       CONTINUE
      ENDIF

C     CALCULATE LINEAR ATTENUATION COEFFICIENT OF SOIL FOR EACH
C     RADIONUCLIDE AS A FUNCTION OF AVERAGE ENERGY LEVEL
      DO 12 I=1,4
         DO 13 K=1,2
            DO 14 J=1,5
               IF(ENERGY(I,J).EQ.0.0)THEN
                  MU(I,K,J)=0.0
               ELSE
                  MU(I,K,J)=(0.0027*ENERGY(I,J)**(-0.320))*RHOS(K)*
     +                      (1.0+WC(K))
               ENDIF
14          CONTINUE
13       CONTINUE
12    CONTINUE

C     CALCULATE FLUX FOR EACH RADIONUCLIDE I FOR EACH
C     FOR EACH SOIL LAYER K AND EACH ENERGY LEVEL J
      DO 15 I=1,4
         DO 16 K=1,2
            DO 17 J=1,5
               IF(NDEC(I,J).EQ.0.0)THEN
                  XMU(I,K,J)=0.0
                  AACT=0.0
                  FLUX(I,K,J)=0.0
               ELSE
                  XMU(I,K,J)=DSOIL(K)*MU(I,K,J)
                  AACT=(SOILCN(I,K)*NDEC(I,J)*FAC(I))/SPA(I)
                  IF(CODGS.EQ.3.0)WRITE(*,103)I,K,J,MU(I,K,J),
     +                                            XMU(I,K,J),AACT,
     +                                            SOILCN(I,K)
103               FORMAT(1X,'I=',I2,1X,'K=',I2,1X,'J=',I2,1X,'MU=',
     +                   E10.3,1X,'XMU=',E10.3,1X,'A=',E10.3,1X,
     +                   'SOILC='E10.3)
                  IF(AACT.EQ.0.0)THEN
                     FLUX(I,K,J)=0.0
                  ELSE
```

Table 7.2 continued.

```
                     FLUX(I,K,J)=SOL(MU(I,K,J),XMU(I,K,J),AACT,DSOIL(K))
                  ENDIF
               ENDIF
17          CONTINUE
16       CONTINUE
15    CONTINUE

      IF (CODGS.GE.2.0)THEN
         DO 18 K=1,2
            WRITE(*,104)K,DSOIL(K),RHOS(K)*(1.0+WC(K))
104         FORMAT(1X,'SOIL LAYER=',I2,1X,'DSOIL=',E10.3,1X,'RHOS=',
     +             E10.3)
18       CONTINUE
      ENDIF
      IF(CODGS.GE.2.0)WRITE(*,105)
105   FORMAT(1X,'RADIONUCLIDE',1X,'ENERGY LEVEL',1X,'LAYER',5X,
     +       'FLUXTOT',5X,'XMU',5X,'XMUTOT',5X,'FLUX')
C
C     CALCULATE FLUX FOR EACH RADIONUCLIDE FOR EACH LAYER
      SHINE(5,NREC)=0.0
      DO 19 I=1,4
         SHINE(I,NREC)=0.0
         DO 20 J=1,5
            XMUTOT=0.0
            DO 21 K=1,2
               IF(K.EQ.1)THEN
                  FLXTOT(I,J)=FLUX(I,1,J)
               ELSE
                  XMUTOT=XMUTOT+XMU(I,1,J)
                  FLXTOT(I,J)=FLXTOT(I,J)+FLUX(I,2,J)*EXP(-1.0*XMUTOT)
               ENDIF
               IF(CODGS.GE.2.0)WRITE(*,106)I,J,K,FLXTOT(I,J),
     &         XMU(I,K,J),XMUTOT,FLUX(I,K,J)
106            FORMAT(6X,I2,8X,I2,10X,I2,5X,E10.3,1X,E10.3,1X,E10.3,
     &         1X,E10.3)
21          CONTINUE
            GDSE=FLXTOT(I,J)*ENERGY(I,J)*MUFLSH(J)*5.0
            SHINE(I,NREC)=SHINE(I,NREC)+GDSE
20       CONTINUE
C        CALCULATE TOTAL DOSE RATE
         SHINE(5,NREC)=SHINE(5,NREC)+SHINE(I,NREC)
         IF(CODGS.GE.2.0)WRITE(*,107)I,NREC,SHINE(I,NREC)
107      FORMAT(1X,'I=',I2,1X,'NREC=',I2,1X,'SHINE=',E10.3)
19    CONTINUE
      IF(CODGS.GE.2.0)WRITE(*,108)NREC,SHINE(I,NREC)
108   FORMAT(1X,'NREC=',I3,'TOTAL DOSE=',E10.3)
      RETURN
      END

      FUNCTION SOL(MUF,XMU1,AF,B)
C     THE FOLLOWING FUNCTION SUBROUTINE CALCULATES FLUX USING A SERIES
C     SOLUTION
      INCLUDE 'MODEL.INC'
```

Table 7.2 continued.

```
      INCLUDE 'VAR.INC'
      REAL*4 MUF,XMU1,SIGN,XN
      REAL*8 PROD,SUM1
C     INITIALIZE NON-ITERATIVE SEGMENT OF SOLUTION
      IF(CODGS.GE.1.0)WRITE(*,300)
300   FORMAT(1X,'SUBFUNCTION SOL')
      SUM1=0.5*(((-1.0/MUF)*EXP(-XMU1))+(1.0/MUF)-(B*(0.5772157+
     +     LOG(XMU1)-XMU1)))
      SOL2=SUM1*AF
      SIGN=1.0
      PROD=1.0
      XN=1.0
C     LOOP TO ADD NEXT PRODUCT ONTO SUM,CALCULATE FLUX AND COMPARE
C     PREVIOUS ITERATION WITH CURRENT ONE
30    CONTINUE
         XN=XN+1.0
         PROD=PROD*XN
         SIGN=SIGN*(-1.0)
         PART=(0.5*B*((XMU1**XN*SIGN)/(XN*PROD)))
         SUM1=SUM1+PART
C     CALCULATE FLUX
         SOL1=SUM1*AF
         IF(CODGS.EQ.3.0)WRITE(*,301)XN,SOL2,SOL1,SUM1,PART,B
301      FORMAT(1X,'XN=',I2,1X,'SOL2=',E10.3,1X,'SOL1='E10.3,1X,
     +          'SUM1=',E10.3,1X,'PART=',E10.3,1X,'B=',E10.3)
C     COMPARE FLUXES
         IF(SOL1.GE.SOL2)THEN
            RATIO=SOL2/SOL1
         ELSE
            RATIO=SOL1/SOL2
         ENDIF
         IF(RATIO.GE.0.99)THEN
            IF(CODGS.EQ.3.0)WRITE(*,302)
302         FORMAT(1X,'RETURN TO SUBROUTINE GSHINE')
            SOL=SOL1
         ELSE
            SOL2=SOL1
         GO TO 30
      ENDIF
      RETURN
      END
```

Chemical Rubber Company (CRC), 1964. "Standard Mathematical Tables." Fourteenth Edition. S.M. Selby and B. Girling (Eds.), CRC Press, Cleveland, Ohio.

Evans, R.D., 1955. "The Atomic Nucleus." McGraw Hill Book Company Inc.

Kocher, D.C. and Sjoreen, A.L., 1985. "Dose-Rate Conversion Factors for External Exposure to Photon Emitters in Soil." Health Physics, Vol. 48, No. 2, pp. 193-205.

National Council on Radiation Protection (NCRP), 1975. "Natural Background Radiation in the United States." Report No. 45.

SENES Consultants Limited, 1985. "Evaluation of Current Predictive Models for Radiation Exposures in Uranium Mines." Prepared for the Saskatchewan Mine Development Corporation, March.

U.S. Department of Health, Education and Welfare (U.S. DHEW), 1970. "Radiological Health Handbook." Revised edition, January.

8.0 TERRESTRIAL VEGETATION MODEL

8.1 Introduction

Chapters 4 and 5 describe how the concentration of a radionuclide in the air is calculated (source and dispersion models respectively). Chapter 6 describes how the concentration of a radionuclide in the soil rooting zone is calculated. This chapter shows how these air and soil concentrations are used in the model which calculates the concentration of a radionuclide in five classes of terrestrial vegetation: above-ground vegetables (AVEGC); below-ground vegetables (BVEGC); summer forage (SUFOC); browse (BRWSC); and lichens (LICHC).

Terrestrial vegetation calculations include direct deposition of radionuclide-bearing dust particles and root uptake. Four radionuclides are considered (U-nat, Th-tot, Ra-226, and Pb-210) for each time step. However, not all calculated concentrations vary with location: as explained below, the summer forage, browse, and lichen concentrations are calculated on an area basis, not for each receptor location, and as such are only calculated for specified areas for each radionuclide at each time interval. Vegetable concentrations are, however, calculated at each location j specified as a receptor location (critical or average) for each radionuclide i at each time t.

One basic model is used for all types of terrestrial vegetation. This model is described below. The remaining sections describe how the model is adapted for each type of vegetation.

In this chapter the following subscripts are used to simplify parameter symbols: i is used to identify those parameters that vary with the radionuclide being modelled; t and j indicate that a parameter may vary with time and location respectively; and various environmental media are abbreviated as follows:

v = vegetation

a = air

g = soil (root zone)

Airborne materials can be transferred to the edible portions of vegetables consumed by man or to forage consumed by animals either by direct foliar retention or root uptake.

The following equation was used to calculate the average annual concentration of radionuclide i in vegetation type v at location j and time t (U.S. NRC, 1982):

$$[C]_{v,i,j,t} = [C]_{a,i,j,t}\, V_d\, F_{r,v}\, E_v\, \frac{(1 - \exp(-\lambda_{w,v}\, t_v))}{Y_v\ \lambda_{w,v}} + B_{v,i}\, \frac{[C]_{g,i,j,t}}{P_g} \qquad (8.1)$$

where

$[C]_{v,i,j,t}$ = the resulting concentration of radionuclide i in vegetation v at time t at location j ($Bq.g^{-1}$ (wet weight))

$[C]_{a,i,j,t}$ = the average concentration of radionuclide i in the air at location j at time t ($Bq.m^{-3}$)

V_d = the deposition velocity ($m.s^{-1}$)

$F_{r,v}$ = the fraction of the total deposition retained on the plant surface of vegetation type v (0 to 1)

E_v = the fraction of the foliar deposition retained on edible portions of vegetation type v (0 to 1)

$\lambda_{w,v}$ = a decay constant accounting for weathering losses from vegetation type v (s^{-1}) and if significant, radioactive decay

t_v = the duration of the plant exposure to atmospheric deposition for vegetation type v (s)

Y_v = the yield density for vegetation type v (g(wet weight).m^{-2})

$B_{v,i}$ = the soil-to-plant transfer coefficient for radionuclide i and vegetation type v ($Bq.g^{-1}$ (wet weight) plant per $Bq.g^{-1}$ (dry weight) soil)

$[C]_{g,i,j,t}$ = the average concentration of radionuclide i in the root zone of the soil at location j at time t ($Bq.m^{-3}$)

P_g = density of soil ($g(dry\ wt).m^{-3}$)

The first term on the right-hand side of equation (8.1) represents direct foliar retention; the second term represents root uptake. Irrigation is not included in this model.

Note that time dependence is due only to the time dependence of the air and soil concentrations.

The model assumes that the system is in equilibrium. For the foliar deposition model this means that the weathering half-life is sufficiently less than the period of deposition and radioactive half-life so that the concentration of the radionuclide reaches a steady state level. For annual vegetation this is a valid assumption. However, this may not be entirely appropriate for lichens (see Section 8.6 for further details), although it is a reasonable approximation. The reader is referred to Cassaday et al. (1985) for more information on what this model and its parameters represent and their limitations.

The deposition velocity (V_d) is common in all models, as it relates to characteristics of the windborne tailings dust particles. In this report V_d is intended to capture the combined effect of the various dry and wet deposition processes which effectively transfer dust particles from the air either to the ground or to vegetation. Literature values of dry deposition velocities vary widely, however, a nominal value of about $1x10^{-2}$ $m.s^{-1}$ is sometimes used in the absence of specific data (Sehmel, 1980). Similarly, literature values for particle wet deposition velocities also vary widely. For present purposes and largely based on data reported by McMahon and Denison (1979) a nominal wet deposition velocity of 1×10^{-2} $m.s^{-1}$ has been assumed. Thus a nominal all inclusive deposition velocity of 0.02 $m.s^{-1}$ has been assumed. Based on the experience of study team members (SENES, 1983) the deposition velocity was assumed to range uniformly over the interval from

0.003 to 0.03 $m.s^{-1}$.

Probabilistic analysis requires that appropriate probability distributions be ascribed to the model input parameters. The distributions of transfer factors reported are generally skewed in shape with a peak concentration at some relatively low level and a long tail towards the high end of the scale. Several studies have found radionuclide concentrations to be lognormally distributed (Tracy et al., 1983; Sheppard and Thibault, 1983). Cassaday et al. (1985) examined the data base available for characterizing the soil-to-plant transfer coefficients for root uptake of a specific radionuclide and vegetation type as included in the model of terrestrial transport of radionuclides. Appropriate probability distributions were derived for the soil-to-plant transfer coefficients from this data base. The data available was best characterized by lognormal distributions. Beta and Weibull distributions also characterized the data fairly well. Where data for a specific radionuclide and vegetation type was not available, U.S. NRC (1982) values were used for the geometric mean with the geometric standard deviation assigned from evaluation of the derived transfer coefficient distributions.

Other parameters were also assigned distributions. The extent of this variation was based on the collective opinion of the study group as to how certain they were about the nominal value of particular parameters. Such parameters were typically allowed to vary 10 to 50% about the nominal values and were given a triangular or uniform distribution. The vegetation model parameters are summarized in Tables 8.1 to 8.5. A computer code listing for the terrestrial vegetation models is provided in Table 8.6.

The component model aspects of the UTAP.3 studies have largely focussed on the implementation of environmental and dose models. Comparatively little effort has been expended on issues of fundamental environmental science or on the development of parameter distributions. Both aspects would need to be reviewed on a case by case basis with models being modified or upgraded if required and site/species-specific parameters being input to the models insofar as practicable.

8.2 Above-Ground and Below-Ground Vegetables (AVEGC and BVEGC)

The concentrations in above- and below-ground vegetables are both calculated using equation (8.1) at each specified receptor location j, for each radionuclide i, at each time t. The model and parameter values do not vary with receptor type.

Tables 8.1 and 8.2 summarize the parameter values and distributions used for above-ground and below-ground vegetables respectively. The values for $F_{r,v}$, E_v, Y_v and $\lambda_{w,v}$ were allowed to vary uniformly around the nominal value recommended by the U.S. NRC (1982), whereas t_v, because it was felt to be better known, was assigned a triangular distribution around the nominal value recommended by the U.S. NRC (1982).

Values for $B_{v,i}$ are from the brief literature review conducted as part of Phase II studies (see the introduction for further details).

The modelling approach adopted is very general in that all types of above-ground vegetation are grouped together, as are all types of below-ground vegetation. In some instances the user may wish to incorporate parameters for a single crop. Potatoes in particular are often specifically modelled. This may be done by varying parameter values as appropriate.

8.3 Summer Forage (SUFOC)

The average concentration of radionuclide i in summer forage is used as an input to the calculation of the concentration of radionuclide i in caribou flesh. Caribou are migratory animals, and, as such, any caribou that do feed in the model area were assumed to range over the entire model area. Thus, for caribou, the value of the concentration of radionuclide i in summer forage is modelled at each time t using a model area average air concentration (see Section 5.2.1) and an average soil concentration calculated using the same model area average air concentration (see Chapter 6).

Deer also feed on summer forage. However, deer range over a much smaller area than caribou (Blouch, 1984). For the purposes of this model, the deer was assumed to range over the watershed. Therefore, an area average air concentration of radionuclide i was also calculated for the watershed (see Section 5.2.1) and an average soil concentration was calculated using this average air concentration. These two values were then used to calculate the average concentration of radionuclide i in summer forage in the watershed.

Summer forage is assumed to consist largely of grass. Table 8.3 summarizes the parameter values and distributions used. The values for E_v, t_v, Y_v and $\lambda_{w,v}$ were allowed to vary uniformly around the nominal value recommended by the U.S. NRC (1982). $F_{r,v}$ was taken from the discussion paper by Hoffman et al. (1985), presented in Volume 2 of Phase II. Values for $B_{v,i}$ are from Cassaday et al. (1985), which was included in Volume 2 of Phase II (see also the introduction to this chapter).

8.4 Browse (BRWSC)

Browse is meant to represent the average concentration of radionuclide i in that portion of a moose's diet which comes from terrestrial vegetation. This covers a wide range - from grasses and foliage of small shrubs in the summer to twigs in the winter. Aquatic vegetation eaten by moose is described in Section 11.3.3. Browse is also used to characterize the winter forage of a deer.

Data which would permit direct estimation of the transfer of radionuclides from air and soil to browse were not found in the literature. Hence the parameter values for summer forage shown in Table 8.4 were used to evaluate this pathway. Some small comfort is provided however for the pathway of deposition from air to vegetation since studies reported by Bondietti et al. (1984) indicate that normalized deposition velocities ($m^3.kg^{-1}.s^{-1}$) for submicron particles do not vary greatly among different deciduous and coniferous species.

Table 8.1

ABOVE-GROUND VEGETABLES MODEL VARIABLES

Model Symbol	Description	Units	Nominal Value	Probability Distribution[1]	Computer Origin	Computer Symbol
$[C]_{a,i,j,t}$	air concentration of radionuclide i at the receptor at time t	$Bq.m^{-3}$	calculated	calculated	AIRDIS	AIRC(i,j) $i=1,4$ $j\leq 80$
$[C]_{u,i,j,t}$	concentration of radionuclide i in above ground vegetables at the receptor at time t	$Bq.g^{-1}$ (wet)	calculated	calculated	VEGCON	AVEGC(i,j) $i=1,4$ $j\leq 80$
$F_{r,u}$	fraction of total deposition retained on surface of above ground vegetables	-	0.2	U(0.1,0.3)	INPUT	FDEPSF(1)
E_u	fraction of plant deposition retained on edible portions of above ground vegetables	-	1.0	U(0.8,1.0)	INPUT	FDEPED(1)
t_u	duration of exposure to deposition for above ground vegetables	s	5.184×10^6	T(2.6×10^6, 5.2×10^6, 7.8×10^6)	INPUT	DUREXP(1)
V_d	deposition velocity	$m.s^{-1}$	0.02	U(0.003, 0.03)	INPUT	DEPVEL
Y_u	yield density for above ground vegetables	$g(wet).m^{-2}$	2.0×10^3	U(1.0×10^3,3.0×10^3)	INPUT	YDEN(1)
$\lambda_{w,u}$	decay constant accounting for weathering loss for above ground vegetables	s^{-1}	5.73×10^{-7}	U(2.9×10^{-7},1.2×10^{-6})	INPUT	VEGLAM(1)
$B_{u,i}$	soil-to-plant transfer coefficient for above ground vegetables for:	$\frac{Bq.g^{-1}\ (wet)}{Bq.g^{-1}\ (dry)}$			INPUT	SPTCAV(i) $i=1,4$
	U-nat		6.08×10^{-4}	LN(6.08×10^{-4},8.90,7.67×10^{-6},7.00×10^{-3})		
	Th-tot		4.20×10^{-3}	LN(4.20×10^{-3},9.00,5.19×10^{-5},3.40×10^{-1})		
	Pb-210		4.00×10^{-3}	LN(4.00×10^{-3},9.00,4.94×10^{-5},3.24×10^{-1})		
	Ra-226		8.47×10^{-3}	LN(8.47×10^{-3},10.3,8.03×10^{-5},8.93×10^{-1})		
P_g	soil density	$g(dry).m^{-3}$	calculated	calculated	VEGCON	DRYRHO
$[C]_{g,i,j,t}$	concentration of radionuclide i in the root zone of the soil at the receptor at time t	$Bq.m^{-3}$	calculated	calculated	SOIL	SOILC(i,j) $i=1,4$ $j\leq 80$

Notes

1 Distributions are as described in Table 2.3

2 AVEGC is available as AVEGCA (air pathway) and AVEGCS (soil pathway) which may be specified as additional outputs (see Users Manual, Section 6.4 (SENES, 1987)).

Table 8.2

BELOW-GROUND VEGETABLES MODEL VARIABLES

Model Symbol	Description	Units	Nominal Value	Probability Distribution[1]	Computer Source	Computer Symbol
$[C]_{a,i,j,t}$	air concentration of radionuclide i at the receptor at time t	$Bq.m^{-3}$	calculated	calculated	AIRDIS	AIRC(i,j) i=1,4 $j \leq 80$
$[C]_{d,i,j,t}$	concentration of radionuclide i in below ground vegetables at the receptor at time t	$Bq.g^{-1}$ (wet)	calculated	calculated	VEGCOW	BVEGC(i,j) i=1,4 $j \leq 80$
$F_{r,d}$	fraction of total deposition retained on surface of below ground vegetables:	-	0.2	U(0.1,0.3)	INPUT	FDEPSF(2)
E_d	fraction of plant deposition retained on edible portions of below ground vegetables	-	0.1	U(0.05, 0.15)	INPUT	FDEPED(2)
t_d	duration of exposure to deposition for below ground vegetables	s	5.184×10^6	$T(2.6 \times 10^6, 5.2 \times 10^6, 7.8 \times 10^6)$	INPUT	DUREXP (2)
V_d	deposition velocity	$m.s^{-1}$	0.02	U(0.003, 0.03)	INPUT	DEPVEL
Y_d	yield density for below ground vegetables	$g(wet).m^{-2}$	2.0×10^3	$U(1.0 \times 10^3, 3.0 \times 10^3)$	INPUT	YDEN(2)
$\lambda_{w,d}$	decay constant accounting for weathering loss for below ground vegetables	s^{-1}	5.73×10^{-7}	$U(2.9 \times 10^{-7}, 1.2 \times 10^{-6})$	INPUT	VEGLAM (2)
$B_{d,i}$	soil-to-plant transfer coefficient for below ground vegetables for:	$\frac{Bq.g^{-1} \text{ (wet)}}{Bq.g^{-1} \text{ (dry)}}$			INPUT	SPTCBV(i) i=1,4
	U-nat		3.17×10^{-4}	$LN(3.17 \times 10^{-4}, 3.93, 2.06 \times 10^{-5}, 4.89 \times 10^{-3})$		
	Th-tot		4.20×10^{-3}	$LN(4.20 \times 10^{-3}, 4.00, 2.62 \times 10^{-4}, 6.72 \times 10^{-2})$		
	Pb-210		4.00×10^{-3}	$LN(4.00 \times 10^{-3}, 4.00, 2.50 \times 10^{-4}, 6.40 \times 10^{-2})$		
	Ra-226		2.65×10^{-3}	$LN(2.65 \times 10^{-3}, 4.52, 1.29 \times 10^{-4}, 6.60 \times 10^{-2})$		
P_g	soil density	$g(dry).m^{-3}$	calculated	calculated	VEGCON	DRYRHO
$[C]_{g,i,j,t}$	concentration of radionuclide i in the root zone of the soil at the receptor at time t	$Bq.m^{-3}$	calculated	calculated	SOIL	SOILC(i,j) i=1,4 $j \leq 80$

Notes

1 Distributions are as described in Table 2.3.
2 BVEGC is available as BVEGCA (air pathway) and BVEGCS (soil pathway) which may be specified as additional outputs (see Users Manual, Section 6.4 (SENES, 1987)).

Table 8.3

SUMMER FORAGE MODEL VARIABLES

Model Symbol	Description	Units	Nominal Value	Probability Distribution[1]	Computer Origin	Computer Symbol
$[C]_{a,i,t}$	average air concentration of radionuclide i over the whole airshed (n locations) at time t	$Bq.m^{-3}$	calculated	calculated	AIRDIS	AIRC(i,n+1)i=1,4 n = total number of receptor locations
$[C]_{a,i,t}$	average air concentration of radionuclide i over the watershed at time t	$Bq.m^{-3}$	calculated	calculated	AIRDIS	AIRC(i,n+2)i=1,4 n = total number of receptor locations
$[C]_{s,i,t}$	concentration of radionuclide i in summer forage over the whole airshed at time t	$Bq.g^{-1}$ (wet)	calculated	calculated	VEGCON	SUFOC(i,1)i=1,4
$[C]_{s,i}$	concentration of radionuclide i in summer forage over the watershed at time t	$Bq.g^{-1}$ (wet)	calculated	calculated	VEGCON	SUFOC(i,2)i=1,4
$F_{r,s}$	fraction of total deposition retained on surface of summer forage	-	0.2	N(0.47,0.3,0.01,1.0)	INPUT	FDEPSF(3)
E_s	fraction of plant deposition retained on edible portions of summer forage	-	1.0	U(0.8,1.0)	INPUT	FDEPED(3)
t_s	duration of exposure to deposition for summer forage	s	2.592×10^6	$U(1.3 \times 10^6, 3.9 \times 10^6)$	INPUT	DUREXP (3)
V_d	deposition velocity	$m.s^{-1}$	0.02	U(0.003, 0.03)	INPUT	DEPVEL
Y_s	yield density for summer forage	$g(wet).m^{-2}$	7.5×10^2	$U(5.0 \times 10^2, 1.0 \times 10^3)$	INPUT	YDEN(3)
$\lambda_{w,s}$	decay constant accounting for weathering loss for summer forage	s^{-1}	5.73×10^{-7}	$U(2.9 \times 10^{-7}, 1.2 \times 10^{-6})$	INPUT	VEGLAM (3)
$B_{s,i}$	soil-to-plant transfer coefficient for summer forage for:	$\frac{Bq.g^{-1}\ (wet)}{Bq.g^{-1}\ (dry)}$			INPUT	SPTCSF(i) i=1,4
	U-nat		6.60×10^{-3}	$LN(6.60 \times 10^{-3}, 8.91, 8.31 \times 10^{-5}, 5.24 \times 10^{-1})$		
	Th-tot		2.23×10^{-2}	$LN(2.23 \times 10^{-2}, 9.50, 2.47 \times 10^{-4}, 2.01 \times 10^{0})$		
	Pb-210		2.16×10^{-2}	$LN(2.16 \times 10^{-2}, 3.55, 1.71 \times 10^{-3}, 2.71 \times 10^{-1})$		
	Ra-226		2.11×10^{-1}	$LN(2.11 \times 10^{-1}, 3.63, 1.87 \times 10^{-3}, 2.39 \times 10^{-1})$		
ρ_g	soil density	$g(dry).m^{-3}$	calculated	calculated	VEGCON	DRYRHO
$[C]_{g,i,t}$	concentration of radionuclide i in the root zone of the soil over the whole airshed at time t	$Bq.m^{-3}$	calculated	calculated	SOIL	SOILC(i,n+1) i=1,4 n = total number of receptor locations
$[C]_{g,i,t}$	concentration of radionuclide i in the root zone of the soil over the watershed at time t	$Bq.m^{-3}$	calculated	calculated	SOIL	SOILC(i,n+2) i=1,4 n = total number of receptor locations

Note

1 Distributions are as described in Table 2.3.
2 SUFOC is available as SUFOCA (air pathway) and SUFOCS (soil pathway) which may be specified as additional outputs (see Users Manual, Section 6.4 (SENES, 1987)).

Table 8.4

BROWSE MODEL VARIABLES

Model Symbol	Description	Units	Nominal Value	Probability Distribution[1]	Computer Origin	Computer Symbol
$[C]_{a,i,t}$	average air concentration of radionuclide i over the watershed (n+2 locations) at time t	$Bq.m^{-3}$	calculated	calculated	AIRDIS	AIRC(i,n+2) i=1,4 n = total number of receptor locations
$[C]_{b,i,t}$	concentration of radionuclide i in browse at time t	$Bq.g^{-1}$ (wet)	calculated	calculated	VEGCON	BRWSC(i)i=1,4
$F_{r,b}$	fraction of total deposition retained on surface of browse	-	0.2	N(0.47,0.3,0.01,1.0)	INPUT	FDEPSF(4)
E_b	fraction of plant deposition retained on edible portions of browse	-	1.0	U(0.8,1.0)	INPUT	FDEPED(4)
t_b	duration of exposure to deposition for browse	s	2.592×10^6	$U(1.3 \times 10^6, 3.9 \times 10^6)$	INPUT	DUREXP (4)
V_d	deposition velocity	$m.s^{-1}$	0.02	U(0.003, 0.03)	INPUT	DEPVEL
Y_b	yield density for browse	$g(wet).m^{-2}$	7.5×10^2	$U(5.0 \times 10^2, 1.0 \times 10^3)$	INPUT	YDEN(4)
$\lambda_{w,b}$	decay constant accounting for weathering loss for browse	s^{-1}	5.73×10^{-7}	$U(2.9 \times 10^{-7}, 1.2 \times 10^{-6})$	INPUT	VEGLAM (4)
$B_{b,i}$	soil-to-plant transfer coefficient for browse for:	$\frac{Bq.g^{-1} \text{ (wet)}}{Bq.g^{-1} \text{ (dry)}}$			INPUT	SPTCB(i) i=1,4
	U-nat		6.60×10^{-3}	$LN(6.60 \times 10^{-3}, 8.91, 8.31 \times 10^{-5}, 5.24 \times 10^{-1})$		
	Th-tot		2.23×10^{-2}	$LN(2.23 \times 10^{-2}, 9.50, 2.47 \times 10^{-4}, 2.01 \times 10^{0})$		
	Pb-210		2.16×10^{-2}	$LN(2.16 \times 10^{-2}, 3.55, 1.71 \times 10^{-3}, 2.71 \times 10^{-1})$		
	Ra-226		2.11×10^{-1}	$LN(2.11 \times 10^{-1}, 3.63, 1.87 \times 10^{-3}, 2.39 \times 10^{-1})$		
ρ_g	soil density	$g(dry).m^{-3}$	calculated	calculated	VEGCON	DRYRHO
$[C]_{g,i,t}$	concentration of radionuclide i in the root zone of the soil at time t	$Bq.m^{-3}$	calculated	calculated	SOIL	SOILC(i,n+2) i=1,4 n = total number of receptor locations

Notes

1 Distributions are as described in Table 2.3.
2 BRWSC is available as BRWSCA (air pathway) and BRWSCS (soil pathway) which may be specified as additional outputs (see Users Manual, Section 6.4 (SENES, 1987)).

Although individuals may roam over very large areas, in general moose and deer are not migratory and tend to have much smaller home ranges than caribou (Lynch, 1976; Taylor and Ballard, 1979; Saunders and Williamson, 1972; Blouch, 1984). For this reason, the moose and deer were assumed to range over the watershed. An area average air concentration of radionuclide i was calculated for the watershed (see Section 5.2.1) and an average soil concentration was calculated using this area average air concentration. These two values were then used to calculate the concentration of radionuclide i in browse in the watershed.

8.5 Lichens (LICHC)

The average concentration of radionuclide i in lichens is used as an input to the calculation of the concentration of radionuclide i in caribou flesh. Caribou are migratory animals, and as such any caribou that do feed in the model area were assumed to range over the entire area. Thus, only one value of the concentration of radionuclide i in lichens is modelled at each time t using an area average air concentration (see Section 5.2.1).

The description of the lichen model presented here is much more detailed than that given for the other types of vegetation, as lichens are substantially different in that they have no root system and have a very long life span. The following is largely excerpted from SENES (1983).

Since lichens have no root system, only the accumulation of radionuclides via direct deposition from the air was considered, i.e. using equation (8.1) with $B_{v,i} = 0$ for all radionuclides. Nominal values for the other parameters in equation (3.1) that are specific to the lichen were chosen as discussed below and summarized in Table 8.5. Distributions were assigned as discussed in the introduction to this chapter.

Studies of cesium-137 deposition from fallout in northern Sweden indicate that up to 95% of that deposited on the lichen may be retained (Garner, 1972). For this study, a value of $F_{r,v} = 0.95$ was assumed for all radionuclides. Because the entire plant may be eaten by the grazing caribou, the fraction E_v of the deposited radionuclides reaching edible portions of the plant was assumed to equal 1.0. The yield density Y_v of the lichens was assumed to have a nominal value of 500 $g.m^{-2}$ (Garner, 1972).

Accumulation of deposited material occurs over long periods because of the relatively long lifetimes of lichens (tens of years). For this study, the deposition period t_v in equation (8.1) was assumed to be sufficiently long so that an equilibrium concentration of radionuclides in the lichens was reached, that is, $\exp(-\lambda_{w,v}t_v) = 0$.

The value of the "weathering" decay constant $\lambda_{w,v}$ required special consideration because of the unique nature of lichens. The decay constant accounts for all mechanisms by which the deposited radioactivity is removed from the plant.

Most studies on the accumulation of radionuclides by lichen refer to radionuclides in fallout. The effective half-life of cesium-137 has been estimated variously as 17 years and 6 to 10 years (Garner, 1972); the weathering half-life excluding radioactive decay may thus be as long as 30 years although many studies point to shorter half-lives. Miettinen (1967) estimated the overall effective half-life in lichens in Finland to be about 5 years. A number of other studies indicate effective half-lives of less than 10 years for cesium-137 (Tuominen and Jaakkola, 1973) or less than 15 years if only processes other than radioactive decay are considered. It has also been noted that the effective half-life of strontium-90, which is chemically similar to radium, is much shorter than that of cesium-137 (Tuominen and Jaakkola, 1973). Niebvoer _et_ _al_. (1978) report "mean turnover times" of calcium (which is also chemically similar to radium) of 1.7 years or an effective half-life of about 2.5 years. The effective half-life of lead-210 in the lichen carpet has been estimated to be 7 ± 2 years (Garner, 1972).

Based on the above considerations a conservative effective half-life in lichens of 10 years was assumed for all radionuclides considered in this

Table 8.5

LICHEN MODEL VARIABLES

Model Symbol	Description	Units	Nominal Value	Probability Distribution[1]	Computer Origin	Computer Symbol
$[C]_{a,i,t}$	average air concentration of radionuclide i over the whole airshed (n+1 locations) at time t	$Bq.m^{-3}$	calculated	calculated	AIRDIS	AIRC(i,n+1) i=1,4 n = total number of receptor locations
$[C]_{l,i,t}$	concentration of radionuclide i in lichen at time t	$Bq.g^{-1}$ (wet)	calculated	calculated	VEGCON	LICHC (i)i=1,4
$F_{r,l}$	fraction of total deposition retained on surface of lichen:	-	0.95	U(0.8,1.0)	INPUT	FDEPSF(5)
E_l	fraction of plant deposition retained on edible portions of lichen	-	1.0	U(0.8,1.0)	INPUT	FDEPED(5)
t_l	duration of exposure to deposition for lichen	s	$1x10^{10}$	$C(1x10^{10})$	INPUT	DUREXP (5)
V_d	deposition velocity	$m.s^{-1}$	0.02	U(0.003, 0.03)	INPUT	DEPVEL
Y_l	yield density for lichens	$g(wet).m^{-2}$	$5.0x10^2$	$U(4.0x10^2,6.0x10^2)$	INPUT	YDEN(5)
$\lambda_{w,l}$	decay constant accounting for weathering loss for lichens	s^{-1}	$2.19x10^{-9}$	$U(1.5x10^{-9},4.4x10^{-9})$	INPUT	VEGLAM (5)
$B_{l,i}$	soil-to-plant transfer coefficient for lichens for:	$\frac{Bq.g^{-1}\ (wet)}{Bq.g^{-1}\ (dry)}$			INPUT	SPTCL(i) i=1,4
	U-nat		0.0	C(0.0)		
	Th-tot		0.0	C(0.0)		
	Pb-210		0.0	C(0.0)		
	Ra-226		0.0	C(0.0)		
P_g	soil density	$g(dry).m^{-3}$	calculated	calculated	VEGCON	DRYRHO
$[C]_{g,i,t}$	concentration of radionuclide i in the root zone of the soil at time t	$Bq.m^{-3}$	calculated	calculated	SOIL	SOILC(i,n+1) i=1,4 n = total number of receptor locations

Notes

1 Distributions are as described in Table 2.3.
2 LICHC is available as LICHCA (air pathway) and LICHCS (soil pathway) which may be specified as additional outputs (see Users Manual, Section 6.4 (SENES, 1987)).

study. It is recognized that this is an approximation but until better information is available on the weathering half-life, including the radioactive half-life explicitly in the calculation is not worthwhile.

8.6 Description of Computer Model

The variables used in the terrestrial vegetation model are summarized in Tables 8.1 to 8.5. The computer code listing for this model is provided in Table 8.6.

8.7 Terrestrial Vegetation Model Test Program

A series of tests were performed to check the terrestrial vegetation model for computational accuracy and reasonableness. Some of these tests are discussed below.

Hand calculations were checked against a deterministic run to confirm that the terrestrial vegetation model executed the equations properly. The model was also run probabilistically with the results checked for reasonableness.

Figures 8.1 and 8.2 are some example plots of the radionuclide concentrations in selected vegetation types, plotted as the log of the geometric mean. The system model was run for 2,000 years in 10 year time steps for 100 trials.

8.8 References

Blouch, R.I., 1984. "Chapter 20. Northern Great Lakes States and Ontario Forests." in "White-Tailed Deer - Ecology and Management." Edited by L.K. Halls, Stackpole Books, Harrisburg, PA.

Bondietti, E.A., Hoffman, F.O., and Larsen, I.L., 1984. "Air-to-Vegetation Transfer Rates of Natural Submicron Aerosols." J. Environmental Radioactivity, Vol. 1, pp. 5-27.

Cassaday, V.J., Halbert, B.E. and Stone, D., 1985. "The Data Base Available to Develop Distributions for Use in Modelling the Transfer of Airborne Radioactivity to Terrestrial Vegetation". Presented in a Report Entitled - Probabilistic Model Development for the Assessment of the Long-Term Effects of Uranium Mill Tailings in Canada: Phase II, Vol. 2. Prepared by SENES Consultants Limited for the National Uranium Tailings Program, Canada Centre for Mineral and Water Technology, Energy, Mines and Resources Canada, Ottawa, Ontario.

Garner, R.J., 1972. "Transfer of Radioactive Materials from the Terrestrial Environment to Animals and Man." CRC Press, Cleveland.

Hoffman, F.O., Gardner, R.H. and Blaylock, B.G., 1985. "The Transfer of Radium from the Atmosphere to Pasture Vegetation." Presented in a Report Entitled - Probabilistic Model Development for the Assessment of the Long-Term Effects of Uranium Mill Tailings in Canada: Phase II, Vol. 2. Prepared by SENES Consultants Limited for the National Uranium Tailings Program, Canada Centre for Mineral and Water Technology, Energy, Mines and Resources Canada, Ottawa, Ontario.

Lynch, G.M., 1976. "Some Long Range Movements of Radio-Tagged Moose in Alberta." Proceedings of the 12th North American Moose Conference and Workshop, St. John's, Nfld., March, pp. 220-235.

McMahon, T.A., and Denison, P.J., 1979. "Empirical Atmospheric Deposition Parameters - A Survey." Atmos. Env., Vol. 13, pp. 571-585.

Miettinen, J.K., 1967. "Concentration of Cs-137 and Fe-55 Through Food Chains in Arctic and Subarctic Regions." Proceedings of an International Symposium held in Stockholm, 1966.

Niebvoer, E., Richardson, D.H.S., and Tomassini, F.D., 1978. "Mineral Uptake and Release by Lichens: An Overview." The Bryologist, Vol. 82, No.2, pp. 226-246.

FIGURE 8.1

PREDICTED RADIONUCLIDE CONCENTRATION IN ABOVE AND BELOW-GROUND VEGETATION vs TIME

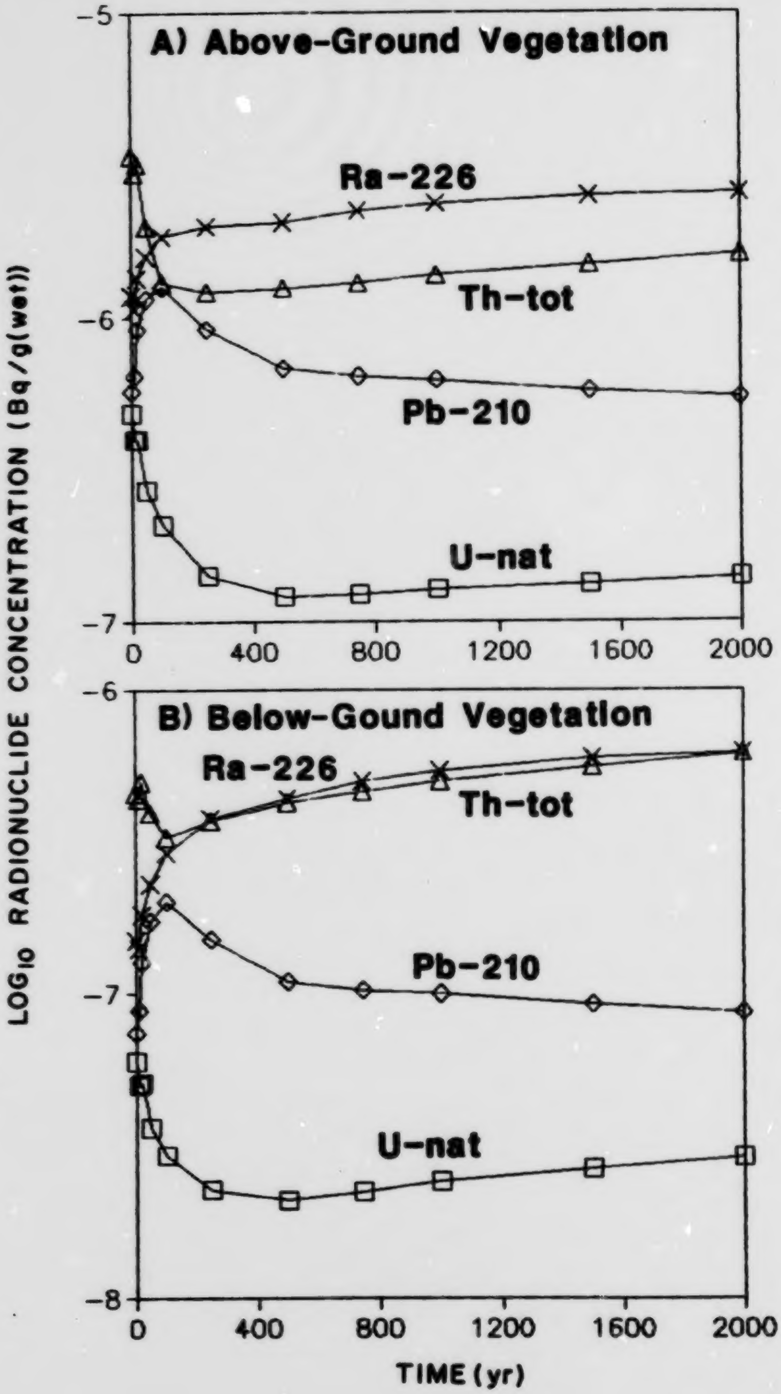

NOTES: 1) The graph shows geometric mean values of 100 trials

2) Receptor located 2km to the north of the tailings area

FIGURE 8.2

PREDICTED RADIONUCLIDE CONCENTRATION IN LICHEN AND SUMMER FORAGE vs TIME

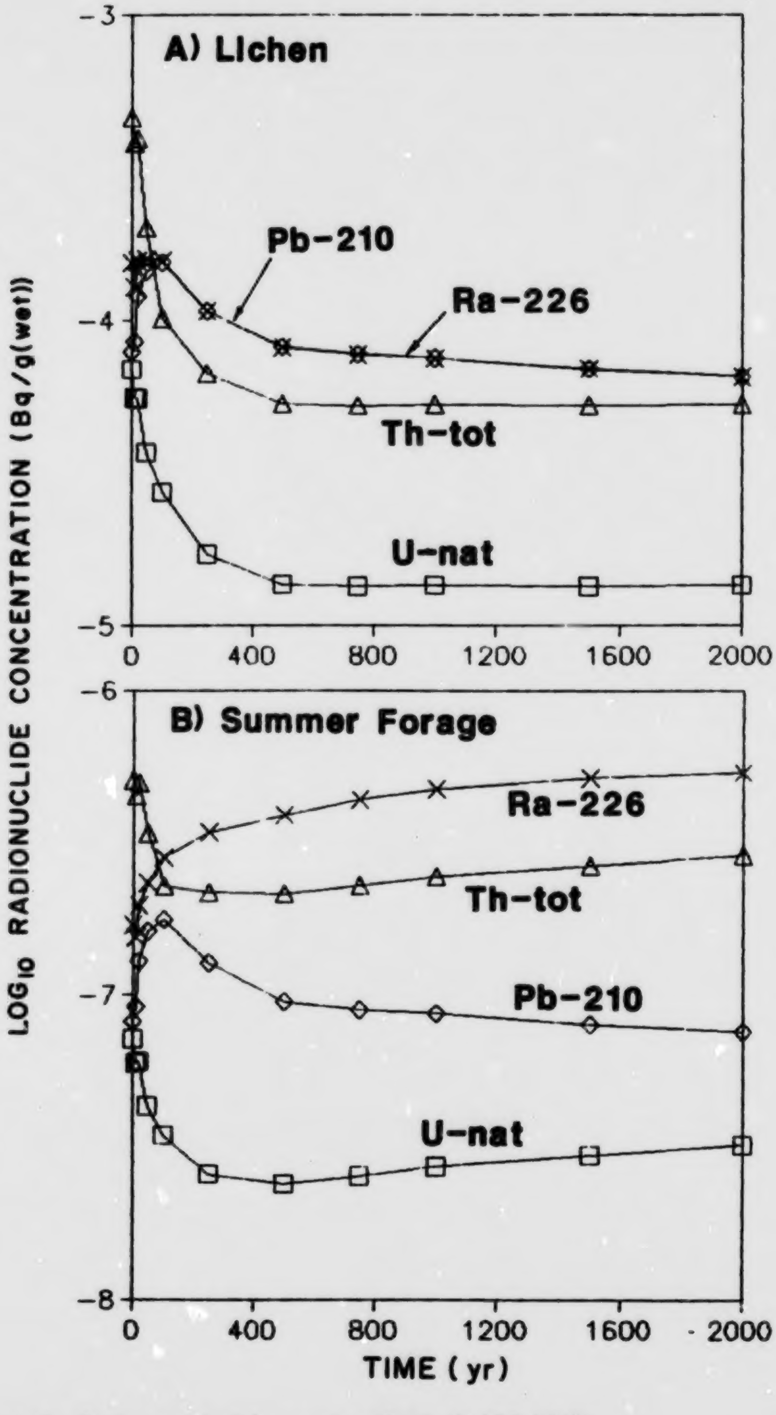

NOTES: 1) The graph shows geometric mean values of 100 trials

2) Vegetation concentrations are based on an average air concentration in the overall study area

Table 8.6

TERRESTRIAL VEGETATION MODEL CODE LISTING

```
      SUBROUTINE VEGCON
      INCLUDE 'MODEL.INC'
      INCLUDE 'VAR.INC'
      REAL*4 CONST(5),AVEGCA(4,80),AVEGCS(4,80),BVEGCA(4,80),
     +       BVEGCS(4,80),SUFOCA(4,2),SUFOCS(4,2),BRWSCA(4),
     +       BRWSCS(4),LICHCA(4),LICHCS(4)
      COMMON /VEGCON/ CONST,DRYRHO
      IF(NREC.EQ.1)THEN
         DO 10 N=1,5
            IF((VEGLAM(N)*DUREXP(N)).GT.75.0)THEN
               REMOV=0.0
            ELSE
               REMOV=EXP(-VEGLAM(N)*DUREXP(N))
            ENDIF
            CONST(N)=DEPVEL*FDEPSF(N)*FDEPED(N)*(1.0-REMOV)/
     +               (YDEN(N)*VEGLAM(N))
10       CONTINUE
         DRYRHO=1000.0*RHOS(2)
      ENDIF
      DO 11 I=1,4
         AVEGCA(I,NREC)=CONST(1)*AIRC(I,NREC)
         AVEGCS(I,NREC)=SPTCAV(I)*SOILC(I,NREC)/DRYRHO
         AVEGC(I,NREC)=AVEGCA(I,NREC)+AVEGCS(I,NREC)
         BVEGCA(I,NREC)=CONST(2)*AIRC(I,NREC)
         BVEGCS(I,NREC)=SPTCBV(I)*SOILC(I,NREC)/DRYRHO
         BVEGC(I,NREC)=BVEGCA(I,NREC)+BVEGCS(I,NREC)
         IF(NREC.EQ.NRECEP)THEN
            SUFOCA(I,1)=CONST(3)*AIRC(I,NRECEP+1)
            SUFOCS(I,1)=SPTCSF(I)*SOILC(I,NRECEP+1)/DRYRHO
            SUFOC(I,1)=SUFOCA(I,1)+SUFOCS(I,1)
            SUFOCA(I,2)=CONST(3)*AIRC(I,NRECEP+2)
            SUFOCS(I,2)=SPTCSF(I)*SOILC(I,NRECEP+2)/DRYRHO
            SUFOC(I,2)=SUFOCA(I,2)+SUFOCS(I,2)
            BRWSCA(I)=CONST(4)*AIRC(I,NRECEP+2)
            BRWSCS(I)=SPTCB(I)*SOILC(I,NRECEP+2)/DRYRHO
            BRWSC(I)=BRWSCA(I)+BRWSCS(I)
            LICHCA(I)=CONST(5)*AIRC(I,NRECEP+1)
            LICHCS(I)=SPTCL(I)*SOILC(I,NRECEP+1)/DRYRHO
            LICHC(I)=LICHCA(I)+LICHCS(I)
         ENDIF
11    CONTINUE
C
      IF(CODVEG.EQ.1.0.OR.CODVEG.EQ.2.0.OR.CODVEG.EQ.3.0)THEN
         WRITE(*,100)
      ENDIF
      IF(CODVEG.EQ.3.0)THEN
         WRITE(*,101)DRYRHO,DEPVEL,FDEPSF(1)
         DO 12 N=2,5
            WRITE(*,102)FDEPSF(N)
12       CONTINUE
         WRITE(*,103)FDEPED(1)
```

Table 8.6 continued.

```
         DO 13 N=2,5
            WRITE(*,104)FDEPED(N)
13       CONTINUE
            WRITE(*,105)VEGLAM(1)
         DO 14 N=2,5
            WRITE(*,106)VEGLAM(N)
14       CONTINUE
            WRITE(*,107)DUREXP(1)
         DO 15 N=2,5
            WRITE(*,108)DUREXP(N)
15       CONTINUE
            WRITE(*,109)YDEN(1)
         DO 16 N=2,5
            WRITE(*,110)YDEN(N)
16       CONTINUE
         WRITE(*,111)(SPTCAV(I),I=1,4)
         WRITE(*,112)(SPTCBV(I),I=1,4)
         WRITE(*,113)(SPTCSF(I),I=1,4)
         WRITE(*,114)(SPTCB(I),I=1,4)
         WRITE(*,115)(SPTCL(I),I=1,4)
         WRITE(*,116)NREC,(AIRC(I,NREC),I=1,4)
         WRITE(*,117)NREC,(AVEGCA(I,NREC),I=1,4)
         WRITE(*,118)NREC,(BVEGCA(I,NREC),I=1,4)
         WRITE(*,119)NREC,(SOILC(I,NREC),I=1,4)
         WRITE(*,120)NREC,(AVEGCS(I,NREC),I=1,4)
         WRITE(*,121)NREC,(BVEGCS(I,NREC),I=1,4)
         IF(NREC.EQ.NRECEP)THEN
            WRITE(*,122)(AIRC(I,NRECEP+1),I=1,4),
     +                  (AIRC(I,NRECEP+2),I=1,4)
            WRITE(*,123)(SUFOCA(I,1),I=1,4),
     +                  (SUFOCA(I,2),I=1,4)
            WRITE(*,124)(BRWSCA(I),I=1,4)
            WRITE(*,125)(LICHCA(I),I=1,4)
            WRITE(*,126)(SOILC(I,NRECEP+1),I=1,4),
     +                  (SOILC(I,NRECEP+2),I=1,4)
            WRITE(*,127)(SUFOCS(I,1),I=1,4),
     +                  (SUFOCS(I,2),I=1,4)
            WRITE(*,128)(BRWSCS(I),I=1,4)
            WRITE(*,129)(LICHCS(I),I=1,4)
         ENDIF
      ENDIF
      IF(CODVEG.EQ.2.0.OR.CODVEG.EQ.3.0)THEN
         WRITE(*,130)NREC,(AVEGC(I,NREC),I=1,4)
         WRITE(*,131)NREC,(BVEGC(I,NREC),I=1,4)
         IF(NREC.EQ.NRECEP)THEN
            WRITE(*,132)(SUFOC(I,1),I=1,4)
            WRITE(*,133)(SUFOC(I,2),I=1,4)
            WRITE(*,134)(BRWSC(I),I=1,4)
            WRITE(*,135)(LICHC(I),I=1,4)
         ENDIF
      ENDIF
C
100   FORMAT(///1X,'VEGETATION MODEL')
```

Table 8.6 continued.

```
101   FORMAT(/1X,'DRY SOIL DENSITY',E12.4/1X,'DEPOSITION VELOCITY',
  +         E12.4/1X,'FRACTION OF DEPOSITION RETAINED ON SURFACE OF',
  +         ' PLANT',E12.4)
102   FORMAT(52X,E12.4)
103   FORMAT(1X,'FRACTION OF DEPOSITION RETAINED ON EDIBLE PORTION O',
  +         'F PLANT',E12.4)
104   FORMAT(59X,E12.4)
105   FORMAT(1X,'DECAY CONSTANT ACCOUNTING FOR WEATHERING LOSS',E12.4)
106   FORMAT(46X,E12.4)
107   FORMAT(1X,'DURATION OF EXPOSURE TO DEPOSITION',E12.4)
108   FORMAT(35X,E12.4)
109   FORMAT(1X,'YIELD DENSITY',E12.4)
110   FORMAT(14X,E12.4)
111   FORMAT(1X,'SOIL-TO-PLANT TRANSFER COEFFICIENT FOR ABOVE GROUND',
  +         ' VEGETATION'/1X,4(E12.4))
112   FORMAT(1X,'SOIL-TO-PLANT TRANSFER COEFFICIENT FOR BELOW GROUND',
  +         ' VEGETATION'/1X,4(E12.4))
113   FORMAT(1X,'SOIL-TO-PLANT TRANSFER COEFFICIENT FOR SUMMER FORAG',
  +         'E VEGETATION'/1X,4(E12.4))
114   FORMAT(1X,'SOIL-TO-PLANT TRANSFER COEFFICIENT FOR BROWSE VEGET',
  +         'ATION'/1X,4(E12.4))
115   FORMAT(1X,'SOIL-TO-PLANT TRANSFER COEFFICIENT FOR LICHEN VEGET',
  +         'ATION'/1X,4(E12.4))
116   FORMAT(1X,'RADIONUCLIDE AIR CONCENTRATION AT RECEPTOR',I3/1X,
  +        4(E12.4))
117   FORMAT(1X,'RADIONUCLIDE CONCENTRATION IN ABOVE GROUND VEGETAT',
  +         'ABLES (AIR PATHWAY) AT RECEPTOR',I3/1X,4(E12.4))
118   FORMAT(1X,'RADIONUCLIDE CONCENTRATION IN BELOW GROUND VEGETAT',
  +         'ABLES (AIR PATHWAY) AT RECEPTOR',I3/1X,4(E12.4))
119   FORMAT(1X,'RADIONUCLIDE SOIL CONCENTRATION AT RECEPTOR',I3/1X,
  +        4(E12.4))
120   FORMAT(1X,'RADIONUCLIDE CONCENTRATION IN ABOVE GROUND VEGETAT',
  +         'ABLES (SOIL PATHWAY) AT RECEPTOR',I3/1X,4(E12.4))
121   FORMAT(1X,'RADIONUCLIDE CONCENTRATION IN BELOW GROUND VEGETAT',
  +         'ABLES (SOIL PATHWAY) AT RECEPTOR',I3/1X,4(E12.4))
122   FORMAT(1X,'AVERAGE RADIONUCLIDE AIR CONCENTRATION'/1X,4(E12.4)/
  +        1X,'AVERAGE WATERSHED RADIONUCLIDE AIR CONCENTRATION'/1X,
  +        4(E12.4))
123   FORMAT(1X,'AVERAGE RADIONUCLIDE CONCENTRATION IN SUMMER FORAGE',
  +         ' (AIR PATHWAY)'/1X,4(E12.4)/1X,'AVERAGE WATERSHED RADI',
  +         'ONUCLIDE CONCENTRATION IN SUMMER FORAGE (AIR PATHWAY)',/
  +         1X,4(E12.4))
124   FORMAT(1X,'AVERAGE WATERSHED RADIONUCLIDE CONCENTRATION IN BRO',
  +         'WSE (AIR PATHWAY)'/1X,4(E12.4))
125   FORMAT(1X,'AVERAGE RADIONUCLIDE CONCENTRATION IN LICHEN (AIR P',
  +         'ATHWAY)'/1X,4(E12.4))
126   FORMAT(1X,'AVERAGE RADIONUCLIDE SOIL CONCENTRATION'/1X,4(E12.4)/
  +         1X,'AVERAGE WATERSHED RADIONUCLIDE SOIL CONCENTRATION'/
  +         1X,4(E12.4))
127   FORMAT(1X,'AVERAGE RADIONUCLIDE CONCENTRATION IN SUMMER FORAGE',
  +         ' (SOIL PATHWAY)'/1X,4(E12.4)/1X,'AVERAGE WATERSHED RAD',
  +         'IONUCLIDE CONCENTRATION IN SUMMER FORAGE (SOIL PATHWAY',
  +         ')'/1X,4(E12.4))
```

Table 8.6 continued.

```
128   FORMAT(1X,'AVERAGE WATERSHED RADIONUCLIDE CONCENTRATION IN BRO',
     +       'WSE (SOIL PATHWAY)'/1X,4(E12.4))
129   FORMAT(1X,'AVERAGE RADIONUCLIDE CONCENTRATION IN LICHEN (SOIL ',
     +       'PATHWAY)'/1X,4(E12.4))
130   FORMAT(/1X,'RADIONUCLIDE CONCENTRATION IN ABOVE GROUND VEGETAT',
     +       'ABLES AT RECEPTOR',I3/1X,4(E12.4))
131   FORMAT(1X,'RADIONUCLIDE CONCENTRATION IN BELOW GROUND VEGETATA',
     +       'BLES AT RECEPTOR',I3/1X,4(E12.4))
132   FORMAT(1X,'AVERAGE RADIONUCLIDE CONCENTRATION IN SUMMER FORAGE',
     +       /1X,4(E12.4))
133   FORMAT(1X,'AVERAGE WATERSHED RADIONUCLIDE CONCENTRATION IN SUM',
     +       'MER FORAGE',/1X,4(E12.4))
134   FORMAT(1X,'AVERAGE WATERSHED RADIONUCLIDE CONCENTRATION IN BRO',
     +       'WSE',/1X,4(E12.4))
135   FORMAT(1X,'AVERAGE RADIONUCLIDE CONCENTRATION IN LICHEN'/1X,
     +       4(E12.4))
C
      RETURN
      END
```

Saunders, B.P. and Williamson, J.C., 1972. "Moose Movements from Ear-Tag Returns." Proceedings of the 8th North American Moose Conference and Workshop. Thunder Bay, Ontario, Feb., pp. 177-184.

Sehmel, G.A., 1980. "Particle Resuspension: A Review." Environment International, Vol. 4, pp. 107-127.

SENES Consultants Limited, 1983. "Decommissioning of the Beaverlodge Mine/Mill Operations and the Reclamation of the Site. Radiological and Environmental Assessment of Close-out Options." Prepared for Eldorado Resources Limited, Ottawa.

SENES Consultants Limited, 1987. "Uranium Tailings Assessment Program (UTAP.3): Users' Manual." Research report prepared for the National Uranium Tailings Program, CANMET, EMR, under Supply and Services Canada Contract No. 23317-6-1728/01-SQ.

Sheppard, M.I., and Thibault, D.H., 1983. "Natural Uranium Concentration Factor Distributions for Ten Plant Species Indigenous to the Precambrian Shield." Atomic Energy of Canada Limited, Technical Record TR-220, Pinawa.

Taylor, K.P. and Ballard, W.B., 1979. "Moose Movements and Habitat Use Along the Susitna River near Devil's Canyon." Proceedings of the 15th North American Moose Conference and Workshop, Soldotna-Kenai, Alaska. pp. 169 - 185.

Tracy, B.L., Pranti, F.A., and Quinn, J.M., 1983. "Transfer of Ra-226, Pb-210 and Uranium from Soil and Garden Produce; Assessment of Risk." Health Physics, Vol. 44, pp. 469-477.

Tuominen, Y., and Jaakkola, T., 1973. "Absorption and Accumulation of Elements." Chapter 6 in "The Lichens" edited by V. Ahmadjian and M.E. Hale, Academic Press, New York.

United States Nuclear Regulatory Commission (U.S. NRC), 1982. "Calculational Models for Estimating Radiation Doses to Man from Airborne Radioactive Material Resulting from Uranium Milling Operations." Reg. Guide 3.51, March.

9.0 SUBSURFACE CONTAMINANT TRANSPORT MODEL

9.1 Introduction

In the subsurface transport model the movement of contaminants carried by tailings porewater emerging from the bottom of the tailings pile is traced along several groundwater flowpaths (i.e. subsurface flow systems). A maximum of five groundwater flowpaths can be modelled during a particular trial. The model takes into consideration contaminant retardation in calculating the concentration as a function of time at any selected point(s) along a particular flowpath. In this study contaminant profiles were calculated for each point where the groundwater discharges from an aquifer and becomes surface water. Contaminants modelled include lead-210, radium-226, total thorium, natural uranium, sulphate and calcium.

The structure of the subsurface transport model is presented in Figure 9.1. For each trial the model requires a set of discrete data points comprised of the source concentration for each modelled constituent at a particular time, (i.e. $C_{s,i}(t)$), as input. This set of data points is provided by the tailings source model. In addition, the probabilistic inputs which are all independent of time, (e.g. radionuclide distribution coefficients) are provided by the random sampling routine in the control module, which is implemented in subprogram CHOOSE.

The modelling of the radionuclides is based on a solution of the advection-dispersion equation which has been modified to include the effects of geochemical retardation and radioactive decay. In order to maintain a reasonable computation time, steady-state, one-dimensional flow conditions have been assumed. The governing partial differential equation is solved using an analytical solution to determine the concentration of radionuclides at each discharge point at various specified times.

The aqueous phase sulphate and calcium concentrations are also derived for the groundwater discharge points. It is assumed, however, that the buffering capacity of the aquifer has been exhausted. Hence, the sulphate and calcium concentrations in the groundwater discharge are set equal to the tailings source concentrations.

The calculated contaminant fluxes at each discharge point are subsequently utilized as input to the surface water (river/lake system) model.

The following sections describe: the characteristics of the aquifer for the reference site; the theoretical basis and approach chosen to model the various processes; the overall contaminant mass balance and assumptions used in the mass balance calculations; the analytical solution of the mass balance for steady-state flow conditions; and the values selected for the model parameters.

9.2 Aquifer Characteristics

Groundwater Flowpath

At the reference tailings site there exists two groundwater flowpaths. These flowpaths pass through glaciofluvial sandy aquifers underlying the dam structures at the outlet valleys. Figure 9.2 presents a conceptual view of the subsurface flow at one of the dams. The cross-sectional area below the dam through which the groundwater flow passes is referred to on the figure as the "window".

Conceptually it was assumed that all of the subsurface seepage from layer 4 of the tailings enters the aquifers and emerges some distance downstream of the dams, the distance being dependent on the hydrogeological characteristics of the particular aquifer. The distance between a tailings dam and point "X" is called the discharge distance. For the reference tailings site, "X" can be anywhere between the toe of the dam and the river located some 200 m from the tailings dam. It is a randomly selected input parameter with a triangular probability distribution. The probability distribution indirectly reflects the distribution of the groundwater discharge downstream of the dam.

FIGURE 9.1

STRUCTURE OF SUBSURFACE TRANSPORT MODEL

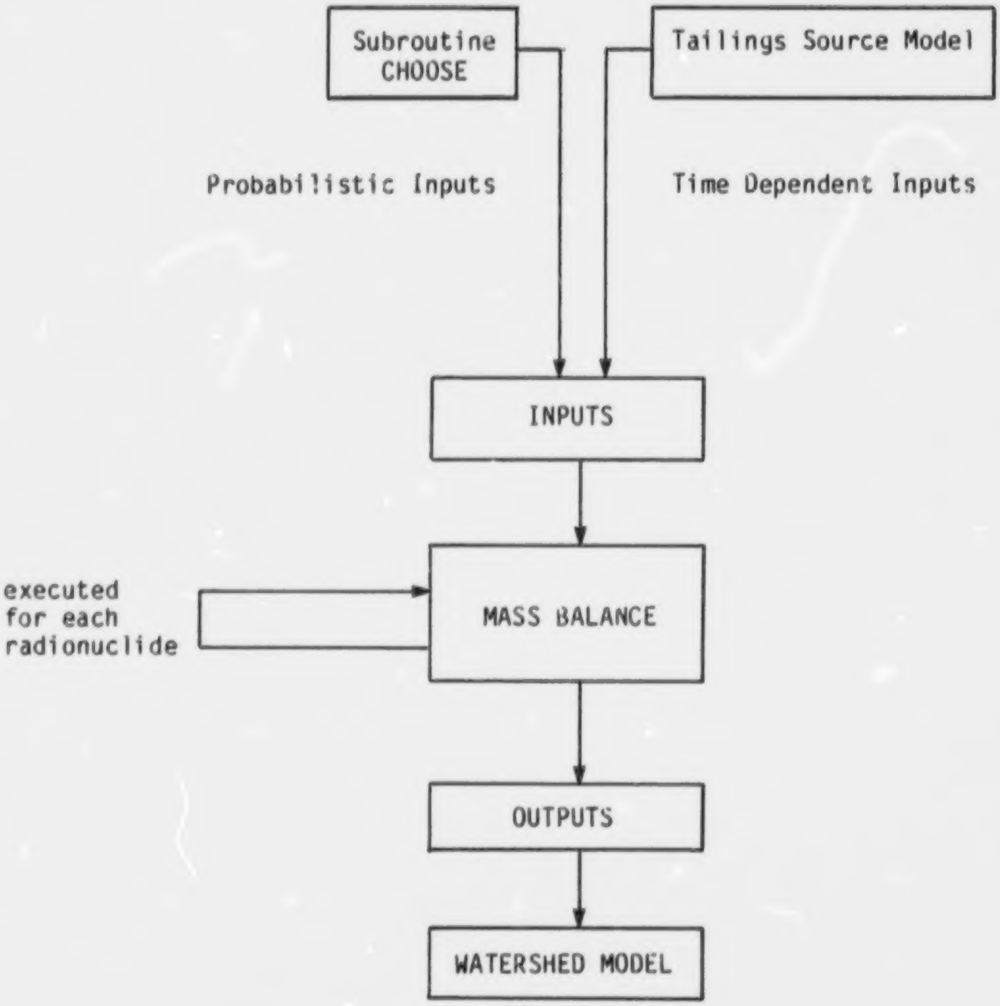

FIGURE 9.2

CONCEPT OF GROUNDWATER FLOWPATH
AT EACH DAM ON THE REFERENCE TAILINGS SITE

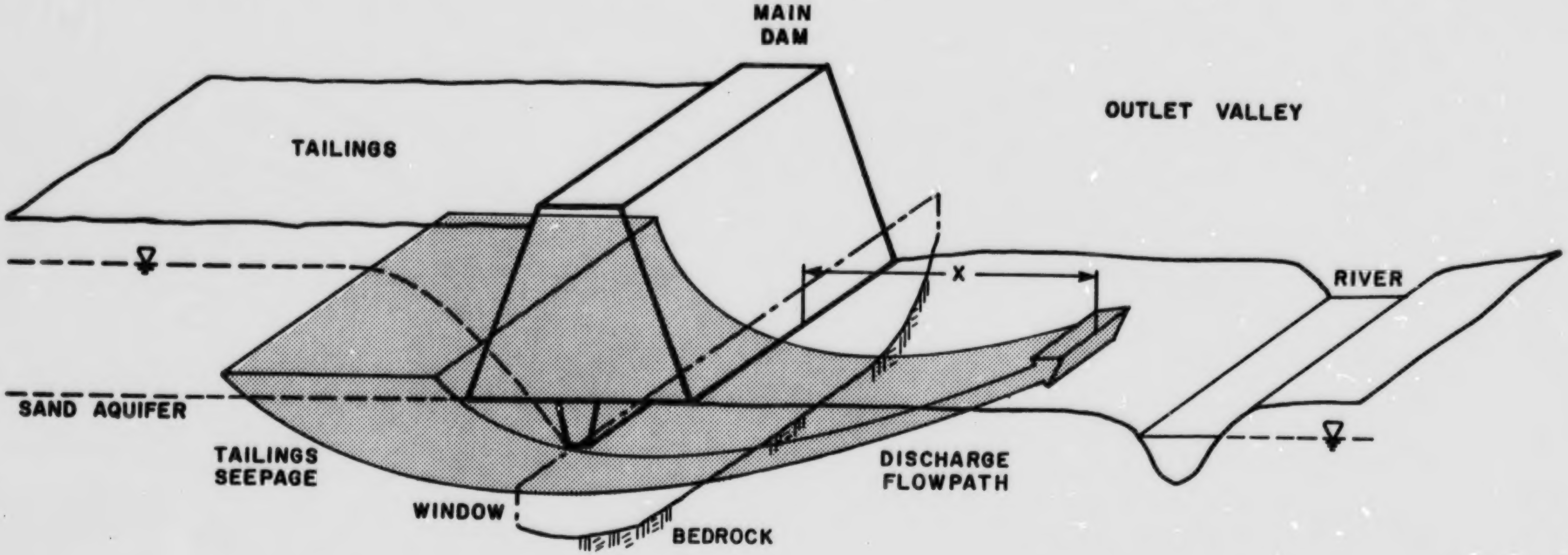

Contaminant Plume

Several studies have been conducted on the migration of groundwater-borne contaminants in the sandy aquifer underlying the Nordic uranium tailings area in Elliot Lake (Blair, 1980; Blair et al., 1980; Cherry et al., 1980a; Cherry et al., 1980b; Morin et al., 1982; Feenstra et al., 1981; Cherry et al., 1984). The contaminant plume emanating from the tailings has been characterized in these investigations as consisting of two distinct segments, referred to as the inner core and the outer zone. The inner core of contaminated groundwater extends a short distance, approximately 15 m at the Nordic site (Morin et al., 1982), from the tailings impoundment, has a pH in the range of 3.0 to 5.0 and an elevated radionuclide content in the porewater. The outer zone, which extends a few hundred metres downgradient from the dam, has a higher pH (greater than 5.7) and a low dissolved radionuclide content.

Retardation of the movement of the acid porewater relative to the groundwater flow in the inner core has been attributed to the neutralization of the acidic water as a result of dissolution of calcium carbonate in the sand (Morin et al., 1982). The retardation of radionuclide movement possibly involves several mechanisms including coprecipitation with major chemical species, adsorption or absorption on solid particles and ion exchange.

The movement of radionuclides in the groundwater regime is retarded in the groundwater model by applying appropriate distribution (or partitioning) coefficients. The distribution coefficient concept is widely used as a surrogate for the various mechanisms which may act to retard chemical species movement through soils (U.S. EPA, 1978).

The model includes decay terms for the activity of the radionuclides. It also includes a term to approximate the ingrowth of lead-210 at the discharge point. With the inclusion of an ingrowth term, the model predicts that lead-210 will be present when radium-226 breaks through. Without this term lead-210 would not be present in the groundwater discharge, as it is strongly retarded and has a relatively short half-life.

9.3 Theoretical Approach

9.3.1 Auxiliary Equations

Several basic processes are included in the subsurface transport model: advection, mechanical dispersion, retardation, radioactive decay and ingrowth.

Advection is a process by which the radionuclides are transported by the bulk motion of the flowing groundwater. To calculate the effect of advection on contaminant concentration, the Darcy velocity must be determined:

$$q_j = K_j \, I_j \tag{9.1}$$

where

q_j = Darcy velocity of the jth groundwater flowpath ($m.yr^{-1}$)

K_j = the hydraulic conductivity of the jth groundwater flowpath ($m.yr^{-1}$)

I_j = the hydraulic gradient of the jth groundwater flowpath ($m.m^{-1}$)

The flow through the aquifer can be estimated from :

$$Q_{s,j} = q_j \, A_{x,j} \tag{9.2}$$

where

$Q_{s,j}$ = volumetric seepage rate through the jth groundwater flowpath ($m^3.yr^{-1}$)

$A_{x,j}$ = cross-sectional area of the jth aquifer window (m^2).

Once the volumetric seepage rates have been calculated their sum is compared against the mean net precipitation and runoff rates:

$$\sum_j Q_{s,j} = Q_T - Q_r - Q_{sr} \tag{9.3}$$

where

Q_r = unsaturated zone runoff rate ($m^3.yr^{-1}$)

Q_T = net precipitation rate which accounts for evapotranspiration ($m^3.yr^{-1}$)
Q_{sr} = surface runoff rate ($m^3.yr^{-1}$)

and:

$Q_T = P_a A_T$
P_a = mean net annual precipitation ($m.yr^{-1}$)
A_T = surface area of watershed (m^2)

and:

$Q_{sr} = Q_T X_{run}$
X_{run} = fraction of net precipitation which is surface runoff.

If the left hand side of equation 9.3, the sum of the volumetric seepage rates, exceeds the right hand side, the revised volumetric seepage rates, $Q'_{s,j}$, for the individual flowpaths are calculated from:

$$Q'_{s,j} = \frac{Q_T (1 - X_{run}) \cdot Q_{s,j}}{\sum_j Q_{s,j}} \qquad (9.4)$$

In the above equation it has been assumed that the unsaturated zone runoff is zero.

This condition results when the aquifer(s) are quite pervious, hence limiting the horizontal movement of the unsaturated zone runoff.

Mechanical dispersion is a spreading phenomenon caused entirely by the motion of the fluid. Mechanical dispersion may occur in the direction parallel to the bulk fluid flow (longitudinal dispersion) or in the direction perpendicular to the flow (transverse dispersion). Since longitudinal dispersion is normally much stronger than transverse dispersion, the latter is often neglected (Freeze and Cherry, 1979). In order to account for the longitudinal dispersion process, a dispersion coefficient is required:

$$D_{\ell,j} = \frac{\alpha_j \, q_j}{n_j} \qquad (9.5)$$

where

$D_{\ell,j}$ = the longitudinal dispersion coefficient of the jth groundwater flowpath ($m^2.yr^{-1}$)

α_j = the dispersivity of the jth groundwater flowpath (m)

n_j = the porosity of the jth groundwater flowpath ($m^3.m^{-3}$)

Dispersivity (α) is used as a measure of the medium's capability to cause mechanical dispersion. Unfortunately, unique values of dispersivity are not easily defined for a porous medium because dispersivity is scale dependent, increasing with distance as the transported mass encounters larger scale heterogeneity in the solid phase medium. This scale dependency is one of the problems in applying the classical advection-dispersion equation for predictive purposes.

Anderson (1979) has presented values of regional dispersivities which range in values from 12 to 200 m for alluvial sediments.

In the subsurface flow model, the dispersivity is estimated from the relationship:

$$\alpha_j = 0.12.X_j \qquad (9.6)$$

where

α_j = longitudinal dispersivity along the jth aquifer (m)

X_j = discharge distance (m).

The dispersivity is considered to be a quasi-constant for the particular discharge distance under study.

To account for the complex geochemical processes (dissolution, adsorption and coprecipitation) which tend to retard the rate of radionuclide migration relative to the rate of groundwater flow, a "bulk" retardation factor is used:

$$R_{i,j} = 1 + \frac{\rho_{b,j}}{n_j} K_{d,i} \qquad (9.7)$$

where

$R_{i,j}$ = the retardation factor for the ith radionuclide in the jth groundwater flowpath

$\rho_{b,j}$ = the bulk density of the jth groundwater flowpath ($kg.m^{-3}$)

$K_{d,i}$ = the distribution coefficient for the ith radionuclide ($m^3.kg^{-1}$).

The bulk density is determined from:

$$\rho_{b,j} = \rho_{s,j} (1-n_j) \qquad (9.8)$$

where

$\rho_{s,j}$ = the soil density of the jth groundwater flowpath ($kg.m^{-3}$).

The radioactive decay constant of each radionuclide is determined from the following equation:

$$\lambda_i = \ln(2)/t_{0.5,i} \qquad (9.9)$$

where

λ_i = the radioactive decay constant of the ith radionuclide (yr^{-1})

$t_{0.5,i}$ = the ith radionuclide radioactive half-life (yr).

The ingrowth of lead-210, a daughter product of radium-226, may be expressed as:

$$A_{Pb} = A_{Ra} (1 - e^{-\lambda_{Pb} t}) \qquad (9.10)$$

where

A_{Pb} = lead-210 activity (Bq)

A_{Ra} = radium-226 activity (Bq)

λ_{Pb} = the radioactive decay constant for lead-210 (yr^{-1})
t = time period (yr).

In the above expression it has been assumed that radium-226 decays directly to lead-210. This assumption is based upon the intermediate daughters having very short half-lives compared to lead-210.

The ingrowth of lead-210 was approximated at the discharge point by dividing equation (9.10) by the soil volume and then multiplying this expression by the ratio of retardation factors. The retardation factors were included in the ingrowth term to account for the much stronger sorption of lead-210 as compared to radium-226:

$$C_{Pb} = C_{Ra} \; I_g \qquad (9.11a)$$

and:

$$I_g = (1-e^{-\lambda_{Pb} \, t}) \; \frac{R_{Ra}}{R_{Pb}} \qquad (9.11b)$$

where

C_{Pb} = the concentration of lead-210 per unit soil volume in the subsurface flow ($Bq.m^{-3}$)
C_{Ra} = the concentration of radium-226 per unit soil volume in the subsurface flow ($Bq.m^{-3}$)
I_g = the ingrowth factor
R_{Pb} = the bulk retardation factor for lead-210
R_{Ra} = the bulk retardation factor for radium-226

and:

$$C_{Pb} = A_{Pb}/V_s \qquad (9.11c)$$

$$C_{Ra} = A_{Ra}/V_s \qquad (9.11d)$$

where

V_s = soil volume (m^3).

The ingrowth of radium-226 from thorium-230 decay is not included in the model since its retardation is approximately seven times less than that of thorium-230 and hence will break through first.

Models do exist which incorporate radioactive ingrowth during the transport of radionuclides through an aquifer (Birchall, 1986; Petrie et al., 1983; Rogers, 1978). The addition of an ingrowth term, however, significantly increases the complexity and computer run time of the model. This degree of complexity was not considered to be warranted for the purposes of this assessment level model.

9.3.2 Mass Balance

The one-dimensional movement of a nonreactive radionuclide in a saturated, homogeneous, isotropic, semi-infinite column undergoing continuous radioactive decay can be described by the following partial differential equation given by Bear (1979):

$$\frac{\partial C_{i,j}}{\partial t} = D_{\ell,j}\frac{\partial^2 C_{i,j}}{\partial X_j^2} - \frac{q_j}{n_j}\frac{\partial C_{i,j}}{\partial X_j} - \lambda_i C_{i,j} \qquad (9.12)$$

where

X_j = the distance from the tailings impoundment for the jth groundwater flowpath (m)

t = the time (yr)

$C_{i,j}$ = the volumetric concentration activity of the ith radionuclide in the jth groundwater flowpath ($Bq.m^{-3}$).

The terms on the right hand side of equation (9.12) account respectively for longitudinal dispersion, advection and radioactive decay.

Modifying equation (9.12) to include the retardation term previously described by the bulk retardation factor results in (Bear, 1979):

$$\frac{\partial C_{i,j}}{\partial t} = \frac{D_{\ell,j}}{R_{i,j}} \frac{\partial^2 C_{i,j}}{\partial X_j^2} - \frac{q_j}{n_j R_{i,j}} \frac{\partial C_{i,j}}{\partial X_j} - \lambda_i C_{i,j} \qquad (9.13)$$

This mass balance equation was employed in the model.

The contaminant flux to the surface water at a distance (X_j) from the tailings along the jth groundwater flowpath was calculated by:

$$J_{i,j,t} = \frac{C_{i,j,x,t} \; Q_{s,i}}{A_{x,i}} \qquad (9.14)$$

where

$J_{i,j,t}$ = the contaminant flux ($Bq.m^{-2}yr^{-1}$)

$Q_{s,j}$ = the aquifer's volumetric seepage rate ($m^3.yr^{-1}$)

$A_{x,j}$ = cross-sectional area of the aquifer window (m^2)

$C_{i,j,x,t}$ = the concentration of contaminant i along groundwater flowpath j at distance X_j and time t ($Bq.m^{-3}$)

The aqueous phase sulphate and calcium concentrations at the groundwater discharge points are calculated from:

$$[SO_4^{2-}]_{g,j} = [SO_4^{2-}]_{\ell,j} \qquad (9.15)$$

$$[CA^{2+}]_{g,j} = [Ca^{2+}]_{\ell,j} \qquad (9.16)$$

where

$[SO_4^{2-}]_{g,j}$ = sulphate concentration in the jth aquifer ($mol.m^{-3}$)

$[Ca^{2+}]_{g,j}$ = calcium concentration in the jth aquifer ($mol.m^{-3}$)

$[SO_4^{2-}]_{\ell}$ = sulphate concentration in layer ℓ of the tailings discharging to the jth aquifer ($mol.m^{-3}$)

$[Ca^{2+}]_{\ell}$ = calcium concentration in layer ℓ of the tailings discharging to the jth aquifer ($mol.m^{-3}$).

In the above expressions layer ℓ can be either 3 or 4.

9.3.3 Assumptions

Several assumptions were employed in the development of equation (9.13). A list of these assumptions is presented in Table 9.1. The first assumption implies that the seepage from the bottom of the tailings pile will fluctuate much less than the annual variations in net precipitation infiltrating the tailings pile due to the dampening effect of the tailings. Hence, the seepage rate to the aquifer is assumed to be constant for each trial. This assumption greatly simplifies the mass balance calculations. Its effect on the contaminant flux, however, should be minimal.

The second assumption states that the hydraulic conductivity is homogeneous (independent of position) and isotropic (equal in all directions). It is anticipated that the inherent nonuniformity or heterogeneity of porous media which is generally believed to exist (Freeze and Cherry, 1979), will be partially accounted for in the model via the probabilistic method of parameter input.

The third assumption is that a bulk retardation factor provides an estimate of the many reactions involved. The geochemical reactions which will occur in the aquifer and affect the radionuclide movement include acid neutralization (dissolution of carbonate minerals), adsorption, coprecipitation and ion exchange. The use of sorption partition coefficients, K_d's, in the calculation of the bulk retardation factors is a valid representation because the partitioning for the most part is fast and reversible and exhibits a linear isotherm. This assumption may tend to underestimate the radionuclide flux when the source concentration is high, or after a long period of time since the aquifer's exchange capacity may be exceeded (i.e. all the available adsorption sites are filled).

In the fourth assumption, the volumetric rate of groundwater discharge to the surface water system in the zone influenced by the tailings impoundment is assumed to be equal to the volumetric rate of porewater seepage from the tailings into the subsurface flow system. This assumption will lead to an overestimation of the radionuclide concentrations in the aquifer, but will have little effect on the value of the contaminant flux to the surface water system.

Molecular diffusion has not been included, the fifth assumption, as its effects should be negligible for the advection - dominated environment considered for this study. A typical diffusion coefficient is in the order of 1×10^{-9} $m^2.yr^{-1}$ (Jury et al., 1983). In contrast, a calculated dispersion coefficient using the data presented in Section 9.5 is approximately 2×10^{-4} $m^2.yr^{-1}$. Transverse dispersion has been neglected since it is normally weaker than longitudinal dispersion (Freeze and Cherry, 1979).

Employing the sixth assumption greatly reduces the complexity of the model. For the short-lived radionuclides, radium-226 and lead-210, this assumption results in a small error in their concentrations within the aquifer. Since the lead-210, in particular, is strongly retarded, ingrowth within the aquifer will have a negligible effect on the discharge concentration of lead-210. However, because radium-226 is less strongly retarded and will be present in the groundwater discharge, some lead-210 can also be expected to be formed at the discharge point. As discussed previously the concentration of lead-210 in the groundwater discharge resulting from ingrowth is approximated by using the discharge radium-226 concentration and a ratio of the bulk retardation factors in the expression presented in equation (9.10b).

In assumption seven the buffering capacity of the aquifer has been neglected since the aquifer is usually void of gypsum and/or calcite. If gypsum and/or calcite were present it would be depleted relatively quickly in relation to the duration of the simulation, i.e. 2000 years.

At the Nordic tailings the buffering capacity of the aquifer has resulted from calcite dissolution, gypsum and an iron compound, probably siderite precipitate. As a result the migration of the acidified inner core has been restricted to 2-5 $m.yr^{-1}$.

Table 9.1

ASSUMPTIONS EMPLOYED IN SUBSURFACE TRANSPORT MODEL

1. The volumetric flow rate through an aquifer is constant for each trial.

2. The flowpath is isotropic and homogeneous.

3. Bulk retardation factors are used which assume equilibrium isotherms and instantaneous and reversible geochemical reactions.

4. The volumetric rate of groundwater discharge to the surface water system is equal to volumetric rate of groundwater flowing under the tailings dam.

5. Molecular diffusion and transverse dispersion are considered to be negligible.

6. The ingrowth of radionuclides within the aquifer is considered to be unimportant with regards to the concentration at the discharge point.

7. Buffering capacity of the aquifer has been depleted.

Based upon the aforementioned migration velocity of the acidified plume and the aquifers discharge distance, approximately 150 m, the buffering capacity of the aquifer will be depleted in approximately 50 years.

9.4 Solution to Mass Balance

9.4.1 Constant Source

For a constant source and assuming steady-state flow conditions, an analytical solution to equation (9.12) has been provided by Bear (1979):

$$C_{i,j,x,t} = \frac{C_{s,i}}{2} \exp\left[\frac{q_j X_j}{2 n_j D_{\ell,j}}\right] \cdot \left\{ \exp(-X_j B).\operatorname{erfc}\left(\frac{X_j - [(q_j/(n_j R_{i,j}))^2 + (4\lambda_i D_{\ell,j}/R_{i,j})]^{0.5} t}{2(D_{\ell,j} t/R_{i,j})^{0.5}}\right) + \exp(BX_j).\operatorname{erfc}\left(\frac{X_j + [(q_i/(n_j R_{i,j}))^2 + (4\lambda_i D_{\ell,j}/R_{i,j})]^{0.5} t}{2(D_{\ell,j} t/R_{i,j})^{0.5}}\right) \right\} \qquad (9.17)$$

where

B^2 = $[q_j/(2n_j D_{\ell,j})]^2 + \frac{\lambda_i R_{i,j}}{D_{\ell,j}}$

$C_{s,i}$ = the radionuclide activity of the ith source input to the groundwater region at t=0 ($Bq.m^{-3}$)

$C_{i,j,x,t}$ = the concentration of the ith radionuclide along groundwater flowpath j at distance X_j from the source at time t ($Bq.m^{-3}$).

The above equation can be rewritten as:

$$C_{i,j,x,t} = C_{s,i} \cdot G_{i,j,x,t} \qquad (9.18)$$

where $G_{i,j,x,t}$ is a Green's Function and represents the elementary solution for a stationary unit source.

9.4.2 Time-Variant Source

Contaminant transfer is described by a linear continuous partial differential equation. An increase in source concentration by some factor will cause a change in the contaminant concentration at any distance following an appropriate time lag. If a contaminant source can be represented as the sum of two (or more) sources, the resulting response can be represented as a sum of responses to each source. This is a consequence of the linearity of the contaminant transport equation and can be applied by using the principle of superposition.

A nonstationary (i.e. time-variant) source, as in Figure 9.3a, can be approximated as a sum of elementary stationary sources originating at discrete time intervals. The numerical approximation of a time-variant source function is illustrated in Figure 9.3b and is summarized below for the total source concentration at time t_k:

$$\begin{aligned} C_{s,i}(t_k) = {} & C_{s,i}(t_0) + [C_{s,i}(t_1) - C_{s,i}(t_0)] \\ & + [C_{s,i}(t_2) - C_{s,i}(t_1)] + [C_{s,i}(t_3) - C_{s,i}(t_2)] \\ & + \dots + [C_{s,i}(t_k) - C_{s,i}(t_{k-1})] \end{aligned} \qquad (9.19)$$

where $C_{s,i}(t)$ = source activity of radionuclide i at time t ($Bq.m^{-3}$).

For any time t, this type of approximation increases in accuracy as the incremental time step decreases. The series of concentration changes can be thought of as elemental step functions which are equivalent to several time-constant sources of different concentrations.

Employing the principle of superposition allows for the tracking of the unit impulse of source values for each time period:

FIGURE 9.3

TIME - VARIANT SOURCE

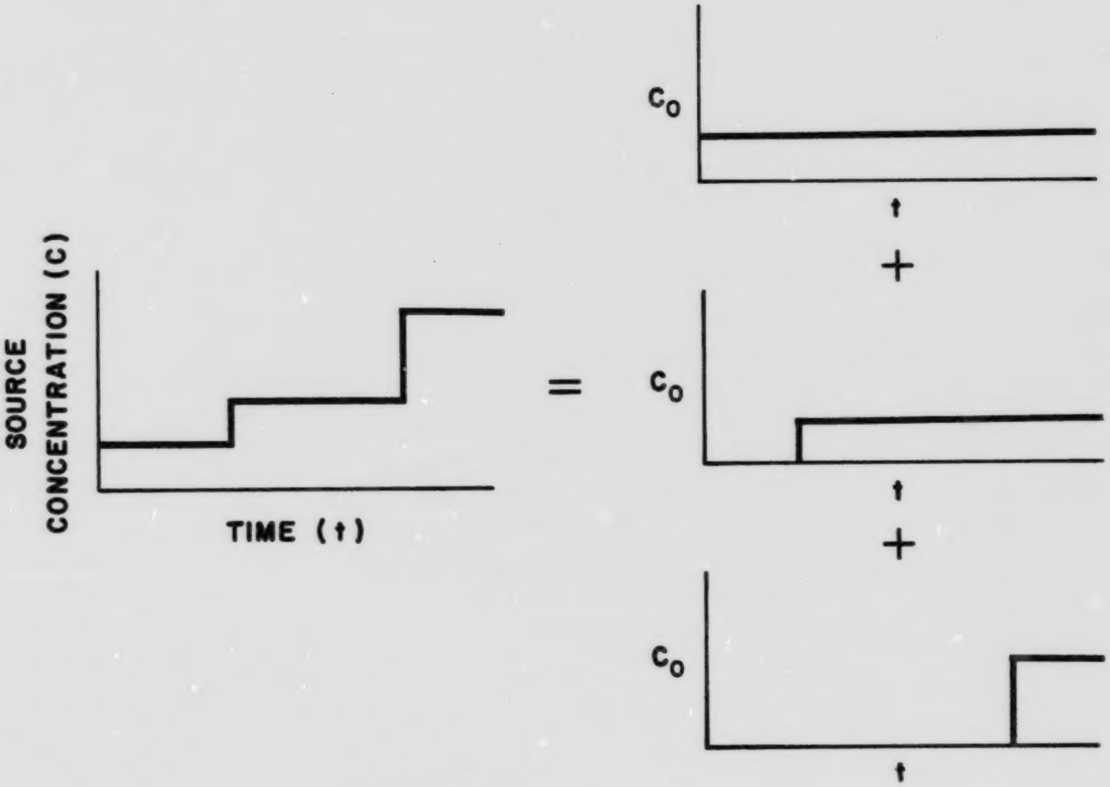

A) PRINCIPLE OF SUPERPOSITION

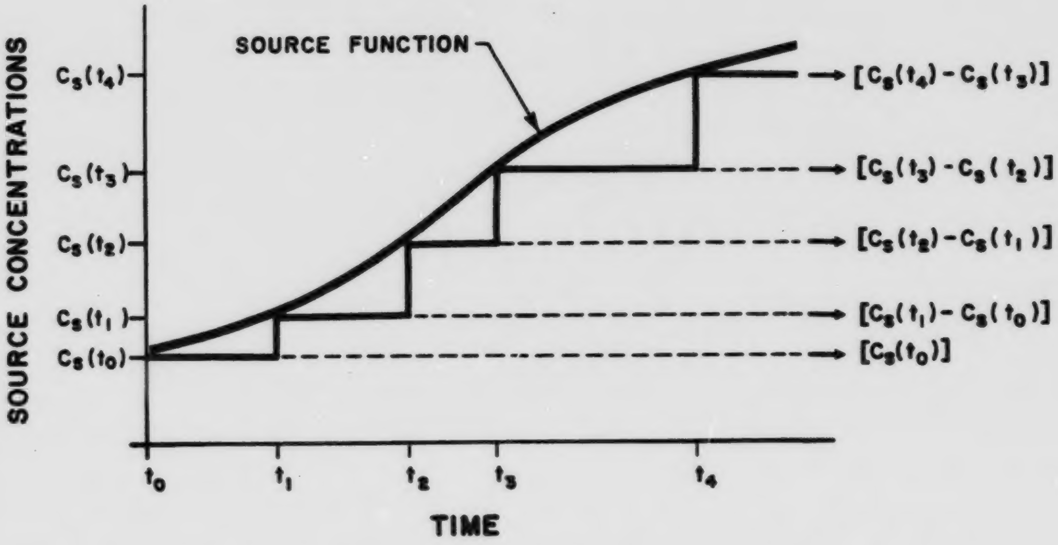

B) APPROXIMATION OF TIME - VARIANT SOURCE

$$\begin{aligned} C_{i,j}(X,t_k) = {} & C_{s,i}(t_0).G_{i,j}(X,t_k) + (C_{s,i}(t_1)-C_{s,i}(t_0)).G_{i,j}(X,t_k-t_1) \\ & + (C_{s,i}(t_2)-C_{s,i}(t_1)).G_{i,j}(X,t_k-t_2) + \ldots. \\ & + (C_{s,i}(t_{k-1})-C_{s,i}(t_{k-2})).G_{i,j}(X,t_k-t_{k-1}) \\ & + (C_{s,i}(t_k)-C_{s,i}(t_{k-1})).G_{i,j}(X,t_k-t_{k-1})/2.0 \end{aligned} \qquad (9.20)$$

The last term approximates the changing source strength during the last time increment.

9.5 Review of Parameters and Constants

The hydrogeological and geochemical parameters employed in the subsurface contaminant transport model are listed in Table 9.2. The generic site is assumed to have two dams. Also listed in the table are the probability distribution types and descriptors and computer source symbols assigned to the parameters.

The probability distributions reflect the uncertainties in the parameter values due to inhomogeneities in the geological formation and variability in the measurement techniques. The majority of the parameters are reviewed below in the context of a reference site located in a drainage basin on the Canadian Precambrian Shield. The radionuclide distribution coefficients, however, are generic in nature and may have a wider distribution than would be expected for a specific location.

9.5.1 Discharge Distance

The discharge distance (X) is the distance between a tailings dam and the point where the subsurface flow becomes surface flow (see Figure 9.2). This distance is a function of local conditions; examples of which are the hydraulic conductivity of the aquifer, the depth to the water table in the tailings and the hydraulic conductivity of the dam.

For the reference site, subsurface flow occurs below the impermeable cutoff walls which extend into the aquifer below the dams. Given this restriction to the flowpaths, it is conceptually appropriate to define the discharge points as occurring a considerable distance downstream of the dams. The groundwater discharge distance is assumed to have a triangular distribution. The minimum distance represents the closest distance at which water will emerge from the tailings dam as a result of the dam's subsurface cutoff wall. The maximum distance coincides with the location of the river.

Dam 1 has a minimum discharge distance of 25 m and a mode of 35 m. Dam 2 has a mimimum discharge distance of 50 m and a mode of 70 m. Both dams have maximum discharge distances of 200 m.

9.5.2 Porosity

The porosity (n) of a porous medium is the ratio of void volume to total unit volume. Porosity of unconsolidated deposits are dependent on the texture and grain size distribution of the material. The range of porosity for unconsolidated deposits is 0.25 to 0.70 $m^3.m^{-3}$, with coarse rounded materials having lower porosities than platey clayey materials (Freeze and Cherry, 1979).

Sandy aquifers commonly have porosities ranging between 0.30 $m^3.m^{-3}$ and 0.36 $m^3.m^{-3}$. Given this narrow range, the probability distribution for porosity for both aquifers was assumed to be uniform with a mean value of 0.33 $m^3.m^{-3}$. These parameter values may be considered as generic for sandy aquifers.

9.5.3 Hydraulic Conductivity

Hydraulic conductivity (K) is a function of not only the porous media but also the fluid permeating the media:

$$K = \frac{Cd^2\rho g}{\mu} \qquad (9.21)$$

where

K = the hydraulic conductivity ($m.yr^{-1}$)

Table 9.2

SUBSURFACE TRANSPORT MODEL PARAMETERS

Model Symbol	Description	Units	Nominal Value	Probability Distribution*	Computer Origin	Computer Symbol
A_T	cross-sectional area of tailings	m^2	$5x10^5$	$C(5x10^5)$	Input	ATAIL
$A_{x,j}$	cross-sectional area of the jth aquifer window	m^2	Dam 1-2000 Dam 2-1000	Dam 1 C(2000) Dam 2 C(1000)	Input	AXGWAT(j)
$[CA^{2+}]_{g,j}$	calcium concentration in the jth aquifer	$mol.m^{-3}$	calculated	calculated	GWATER	GWAT(8,t)
$C_{i,j,x,t}$	discharge concentration of ith radionuclide from jth groundwater seepage path at distance X_j and time t	$Bq.m^{-3}$	calculated	calculated	GWATER	GWATC(i,t)
$C_{s,i,t}$	source concentration leaving tailings area to groundwater for the ith radionuclide at time t	$Bq.m^{-3}$	calculated	calculated	SOURCE	CO(i,t)
$D_{\ell,j}$	longitudinal dispersion coefficient	$m^2.yr^{-1}$	calculated	calculated	GWATER	LDC(j)
I_g	the ingrowth factor	unit less	calculated	calculated	GWATER	F
I_j	hydraulic gradient	$m.m^{-1}$	Dam 1-0.05 Dam 2-0.03	Dam 1 N(0.05,0.01,0.03,0.07) Dam 2 N(0.03,0.01,0.01,0.05)	Input	HGGWAT(j)
$J_{i,j}$	contaminant flux	$Bq.m^{-2}.yr^{-1}$	calculated	calculated	GWATER	GFLUX(i,j,t)
$K_{d,i}$	distribution coefficients of ith radionuclide	$m^3.kg^{-1}$				
	uranium		0.02	$LN[0.02,2.5,5x10^{-3},0.5]$	Input	DCGWAT(1)
	thorium		0.5	LN[0.5,2.15,0.05,5]	Input	DCGWAT(2)
	lead		0.67	LN[0.67,1.73,0.13,3.5]	Input	DCGWAT(3)
	radium		0.07	LN[0.07,1.9,0.01,0.5]	Input	DCGWAT(4)
K_j	hydraulic conductivity	$m.yr^{-1}$	Dam 1-420 Dam 2-300	Dam 1 LN(420,1.95,60,3100) Dam 2 LN(300,1.95,40,2200)	Input	HCGWAT(j)
n_j	porosity	$m^3.m^{-3}$	Dam 1-0.33 Dam 2-0.33	Dam 1 U[0.30,0.36] Dam 2 U[0.30,0.36]	Input	POGWAT(j)
P_a	mean net annual precipitation	$m.yr^{-1}$	0.4	C(0.4)	Input	AVPRCP
q_j	Darcy velocity	$m.yr^{-1}$	calculated	calculated	GWATER	DV(j)
$Q_{s,j}$	volumetric seepage	$m^3.yr^{-1}$	calculated	calculated	GWATER	VSRGW(j)
$R_{i,j}$	retardation factor	unitless	calculated	calculated	GWATER	RGW(j)
$[SO_4^{2-}]_{g,j}$	sulphate concentration in the jth aquifer	$mol.m^{-3}$	calculated	calculated	GWATER	GWAT(7,t)
X_j	discharge distance	m	Dam 1-35 Dam 2-70	Dam 1 T(25,35,200) Dam 2 T(50,70,200)	Input	XRGWAT(j)
X_{run}	fraction of net precipitation which is surface runoff	unitless	0.15	T(0.10,0.15,0.20)	Input	XRUNOF
$\rho_{s,j}$	soil density	$kg.m^{-3}$	Dam 1-2650 Dam 2-2650	Dam 1 N[2650,110,2320,2980] Dam 2 N[2650,110,2320,2980]	Input	SDGWAT(j)
λ_i	radioactive decay constant of the ith radionuclide	yr^{-1}	calculated	calculated	Source	XLAMDA(i)
$\lambda_{d,j}$	layer at which tailings discharge enters aquifer	unitless	Dam 1-4 Dam 2-4	Dam 1 C(4) Dam 2 C(4)	Input	LAYER(j)

Notes

i = ith radionuclide
j = jth subsurface flowpath

* Distributions are as described in Table 2.3.

ρ = the fluid density $(kg.m^{-3})$
μ = the fluid viscosity $(kg.m^{-1}.yr^{-1})$
g = gravitational constant $(m.yr^{-2})$
d = the mean grain diameter (m)
C = a proportionality constant.

Hydraulic conductivity values representative of sandy soils are typically in the range of 113 $m.yr^{-1}$ (3.6×10^{-6} $m.s^{-1}$) to 438 $m.yr^{-1}$ (1.4×10^{-5} $m.s^{-1}$) (Beals, 1985). For the glaciofluvial sandy aquifers often found in the Elliot Lake area, estimated and measured hydraulic conductivities are reported to be in the range of 315 $m.yr^{-1}$ (10^{-5} $m.s^{-1}$) to 3150 $m.yr^{-1}$ ($10^{-4}$$m.s^{-1}$) (Blair et al., 1980; Morin et al., 1982). There is a large body of direct and indirect evidence supporting a lognormal probability distribution for hydraulic conductivity (Freeze, 1975). This has been observed in a variety of materials from unconsolidated soils to rock cores. It is also well known that grain size distributions are lognormal and that hydraulic conductivity is related to the intrinsic permeability of the porous media and hence, the grain size.

Freeze (1975) has tabulated frequency distributions for thousands of hydraulic conductivity values and has observed an average geometric standard deviation of 1.95 for sands and gravels.

The probability distribution for hydraulic conductivity is assumed to be a lognormal distribution. For dam 1, the hydraulic conductivity has a geometric mean of 420 $m.yr^{-1}$, a geometric standard deviation of 1.95 and lower and upper limits of 60 and 3100 $m.yr^{-1}$. At dam 2, the hydraulic conductivity has a geometric mean of 300 $m.yr^{-1}$, a standard deviation of 1.95 and lower and upper limits of 40 and 2200 $m.yr^{-1}$. The lower and upper limits represent three standard deviations from the mean.

9.5.4 Hydraulic Gradient

The hydraulic gradient (I) in sandy aquifers is generally considered to be in the range of 0.005 m.m^{-1} to 0.01 m.m^{-1}. A high gradient of 0.05 m.m^{-1} has been reported by Morin et al., (1982) for the sandy/gravelly aquifer at Nordic. This value represents a hydraulic gradient that exists between the tailings water table and the water table in the outlet valley.

Due to inhomogeneities, hydraulic gradients vary not only from site to site on a macroscale level but also within a site at the microscale level. Uncertainty in hydraulic gradient data is often due to measurement or extrapolation errors between data points. Such errors can be considered to be normally distributed.

The hydraulic gradient for dam 1 was assumed have a mean of 0.05 m.m^{-1}, a standard deviation of 0.01, and lower and upper limits of 0.03 and 0.07 m.m^{-1}. For dam 2, the mean was assumed to be 0.03 m.m^{-1} with a standard deviation of 0.01, and lower and upper limits of 0.01 and 0.05 m.m^{-1}.

9.5.5 Soil Density

The soil density (ρ_s) is the ratio of a particle's mass to the volume it occupies. The soil density of sands is generally reported to be approximately 2,650 kg.m^{-3} (2.65 g.cm^{-3}). Morin et al. (1982) have reported that the sandy aquifer near the Nordic tailings area has a significantly higher soil density, 2,980 kg.m^{-3} (2.98 g.cm^{-3}), for the solid phase minerals.

For this investigation, the soil density for both aquifers was assumed to be normally distributed with a mean of 2,650 kg.m^{-3} and a standard deviation of 110.

9.5.6 Distribution Coefficient

The distribution coefficient, K_d, is the ratio of the mass of contaminant adsorbed on a unit mass of solid material (e.g. sand) to the mass of contaminant in a unit volume of solution (e.g. groundwater). The coefficient is very much dependent on the contaminant, soil type and groundwater pH;

generally the K_d value is found to decrease as the pH decreases. It is also dependent on the contaminant concentration in the liquid phase; at high concentrations saturation of available exchange sites can occur (Rancon, 1973). In most cases the K_d values are found to be lognormally distributed (Sheppard et al., 1984).

The modelling approach described in this study is based on conditions considered to be representative of an acidified plume on a glaciofluvial sandy aquifer. The movement of the radionuclide fronts through the aquifer are assumed to lag behind the acid plume front such that K_d values representing low pH conditions (i.e. pH of 3.0 to 5.0) are considered to apply. This assumption is consistent with the observations reported by Morin et al., (1982) at the Nordic tailings area.

The information available on K_d values and their distributions is limited. The K_d values listed on Table 9.2 for the reference site are generic in nature. When using the model for a particular site, site-specific K_d values should be employed, especially if local chemistry causes the pH to deviate outside the range of 3.0 to 5.0.

Site-specific data may also allow narrower bounds to be placed on the K_d values.

Uranium

The summary of uranium geochemistry presented by Johnston and Gillham (1980) indicates that:

- the important oxidation states of uranium with respect to groundwater environments are U(VI) and U(IV).
- in an oxidizing environment, U(VI) compounds are stable and can precipitate, whereas U(IV) is stable in a reducing environment and would precipitate as UO_2, thus implying that the oxidation-reduction status is important.

- soluble uranium U(VI) can be adsorbed or reduced by organic matter; if U(VI) is reduced to U(IV), precipitation can occur.
- UO_2^{2+} can be adsorbed by clay minerals by cation exchange, but may also form complexes with anions such as carbonate or phosphate.

Wide variations in literature values for uranium K_d in sandy soils have been reported. Rancon (1973) determined that uranium K_d values were in the range of 0.016 to 0.27 $m^3.kg^{-1}$ for a variety of soil types: river sediment, organic peat, low organic sediment and altered schist. The low organic sediment had the lowest K_d value.

Batch K_d experiments were conducted by Veska (1983) using solutions representative of waste-rock-influenced groundwater. Table 9.3 presents the results of this study for tetravalent (IV) and hexavalent (VI) U-238. The average K_d value for solutions of pH 4.0, which corresponded to groundwater at the acid front for the field under study, was 0.015 $m^3.kg^{-1}$.

Typical literature values range from 0.005 $m^3.kg^{-1}$ to 0.50 $m^3.kg^{-1}$ with a mean value of 0.02 $m^3.kg^{-1}$ (NRC, 1983). Hence, a geometric mean K_d value of 0.02 $m^3.kg^{-1}$ and a geometric standard deviation of 2.5 were selected to be representative of the acid plume in this investigation.

Thorium

Johnston and Gillham (1980) summarized the information relevant to thorium K_d values as follows:

- the primary thorium adsorption mechanism is ion exchange.
- in noncalcareous soils, thorium adsorption is extremely sensitive to initial thorium solution concentrations. In organic materials, increased pH causes increased humic acid solubility and thorium complexation, resulting in lower K_d values. In calcareous soils, K_d values are high (≥ 1 $m^3.kg^{-1}$) regardless of pH or thorium concentration, because of the buffering capacity of the soil and precipitation of thorium hydroxide

Table 9.3

COMPARISON OF K_d VALUES FOR U-238(IV) AND U-238(VI)

AS A FUNCTION OF pH

pH	K_d U-238(IV) ($m^3.kg^{-1}$)		K_d U-238(VI) ($m^3.kg^{-1}$)	
	A	B	C	D
3	$7\pm2 \times10^{-3}$	$7\pm2 \times10^{-3}$	$8\pm1 \times10^{-3}$	$9\pm2 \times10^{-3}$
4	$1.2\pm.2 \times10^{-2}$	$1.3\pm.2 \times10^{-2}$	$1.7\pm.2 \times10^{-2}$	$2.0\pm.3 \times10^{-2}$
5	$2.14\pm.20 \times10^{-1}$	$2.56\pm.38 \times10^{-1}$	$1.37\pm.24 \times10^{-1}$	$1.49\pm.26 \times10^{-1}$
5.5	$3.52\pm.44 \times10^{-1}$	$3.84\pm.61 \times10^{-1}$	$1.62\pm.28 \times10^{-1}$	$1.73\pm.42 \times10^{-1}$
6	$3.33\pm.53 \times10^{-1}$	$3.55\pm.36 \times10^{-1}$	$1.68\pm.40 \times10^{-1}$	$1.94\pm.43 \times10^{-1}$
7	$9.1\pm1.0 \times10^{-2}$	$1.19\pm.16 \times10^{-2}$	$3.9\pm.4 \times10^{-2}$	$4.9\pm.6 \times10^{-2}$
8	$1.7\pm.3 \times10^{-2}$	$1.9\pm.3 \times10^{-2}$	$6\pm1 \times10^{-3}$	$8\pm2 \times10^{-3}$

Reference

Veska, 1983

Note

Letters A,B,C and D indicate experiment number.

$(Th(OH)_4)$.

- K_d values are generally high, ≥ 1 $m^3.kg^{-1}$, in dilute solutions, indicating limited thorium migration.

Our review suggested that there is a dearth of data on thorium K_d values in sandy soils. Allard et al., (1977) reported K_d ranges from 0.04 $m^3.kg^{-1}$ to 0.32 $m^3.kg^{-1}$ and 0.50 $m^3.kg^{-1}$ to 1.26 $m^3.kg^{-1}$ for clay, mud and granite, respectively. Vandergraaf (1982) recommended a K_d value for thorium of 0.85 $m^3.kg^{-1}$ for granite. Veska (1983) reported average K_d values, for Th-232 onto sand, at pH's of 3.5, 5.5 and 7.0, of 0.086, 0.570 and 1.75 $m^3.kg^{-1}$, respectively.

Typical K_d values cited in this literature for thorium range from 0.05 to 5 $m^3.kg^{-1}$ (NRC, 1983). A geometric mean value of 0.50 $m^3.kg^{-1}$ and a geometric standard deviation of 2.15 are suggested.

Lead

As with the previously described elements there is only limited information on lead-210 K_d values. Veska (1983) determined the average K_d values of Pb-210 in sand at pH's 3.5, 5.5 and 7.0 to be 0.102, 1.239 and 0.215 $m^3.kg^{-1}$, respectively. Gerritse et al. (1982) have reported K_d values ranging from 0.28 to 3.5 $m^3.kg^{-1}$ for a sandy soil.

For this study, the K_d value for Pb-210 was described as being lognormally distributed with a geometric mean value of 0.67 and a geometric standard deviation of 1.73.

Radium

Johnston and Gillham (1980) summarized the information relevant to radium-226 K_d values as follows:

- radium is present as Ra^{2+} in the pH range 4 to 8, and does not readily form complex species.
- radium can be expected to coprecipitate with barium sulphate, carbonates and ferric hydroxides.
- cation exchange is an important adsorption mechanism, since K_d values have been correlated to cation exchange capacity.

In high sulphate waters (greater than 10^{-2} mol.m^{-3}), however, $RaSO_4$ complexes may dominate Ra^{2+}.

In a study by Ames and Rai (1978), K_d values of 0.21 $m^3.kg^{-1}$ to 0.47 $m^3.kg^{-1}$ were reported for Utah soils using simulated river water. Veska (1983) reported average K_d values, for radium on sand, at pH's 3.5, 5.5 and 7.0, of 0.02, 0.088, and 1.53 $m^3.kg^{-1}$, respectively. The K_d values for radium are generally accepted to be in the range of 5×10^{-3} $m^3.kg^{-1}$ to 0.5 $m^3.kg^{-1}$ (NRC, 1983).

A geometric mean K_d value of 0.07 $m^3.kg^{-1}$ was selected based on observations from a contaminant plume in the Elliot Lake area (Morin et al., 1982). This value is close to the mean literature value of 0.05 $m^3.kg^{-1}$ suggested by NRC (1983) and agrees well with the value of about 0.08 $m^3.kg^{-1}$ calculated from an equilibrium constant by Lester et al. (1975). A geometric standard deviation of 1.9 was estimated to cover the wide range of possible values for this parameter.

9.5.7 Mean Net Annual Precipitation

The mean net annual precipitation (P_a) is used to calculate the net preciptation rate, equation (9.3). The net precipitation rate is considered to be the upper limit of the sum of the volumetric seepage rates. It is set constant since the solution to the mass balance, equation (9.13), is only applicable for a constant seepage flow rate. A value of 0.4 $m.yr^{-1}$ is employed in this model for the mean net precipitation.

In other models (e.g. the SOURCE model) a different parameter called net precipitation (P) is employed which is sampled each time-step and has an associated probability distribution. The mean value of P is the parameter Pa.

9.5.8 Cross-Sectional Area

The cross-sectional area (A_x) referred to is that of the window through which the recharge flow passes. It is given by:

$$A_{x,j} = L_j \; W_j \qquad (9.22)$$

where

$A_{x,j}$ = cross-sectional area of jth flow-path (m^2)
L_j = total length of jth dam (m)
W_j = thickness of jth aquifer below the dam (m).

For the reference site it was assumed that all of the subsurface flow was through two dams. The rest of the perimeter is assumed to be impermeable. The total length of dam 1 and 2 are assumed to be 200 and 100 m, respectively. The thickness of underlying aquifers are both assumed to be 10 m. Hence, the cross-sectional areas are 2000 m^2 and 1000 m^2 for dam 1 and dam 2.

9.5.9 Discharge Layer

The discharge layer, λ_d, is the layer of the tailings from which contaminated seepage enters the aquifer. At the generic site the aquifers are beneath the dam structures and as such receive discharge from layer 4 (the bottom layer) of the tailings.

9.6 Model Demonstration

In this section the performance of the subsurface transport model is demonstrated for both constant and time-variant source scenarios. For both scenarios, probabilistic runs were performed; each run consisting of 200 trials with each trial simulating a 1000 year period. The input parameters used are those presented in Table 9.2.

In Figure 9.4 the tailings source discharge concentration, assumed to be the same (10 $Bq.m^{-3}$) for all four radionuclides, is presented for the constant source scenario. In Figures 9.5 to 9.8 the groundwater concentrations of the radionuclides at the toe of dam 1, resulting from the aforementioned source discharge, are presented in terms of arithmetic means, and lower and upper 95% confidence limits on the point estimates. Uranium, Ra-226 and Pb-210 approach steady-state at the end of the 1000 year simulation period. Almost all of the lead present is a result of ingrowth. The total thorium mean concentration at 1000 years is approximately 15% of its steady-state value, a consequence of thorium's high distribution coefficient.

To verify the aforementioned observations one can compare times to steady-state for radionuclides by comparing their retardation factors. For example, the comparison for radionuclides uranium and radium is given by:

$$\frac{t_U}{t_{Ra}} = \frac{R_U}{R_{Ra}} \qquad (9.23)$$

where

t_U, t_{Ra} = steady-state breakthrough times of uranium and radium, respectively
R_U, R_{Ra} = retardation factors of uranium and radium, respectively.

The retardation factor for compounds which are strongly absorbed, can be expressed as:

$$R_i \propto \frac{\rho_b}{n} K_{d,i} \qquad (9.24)$$

where

R_i = retardation factor of ith radionuclide = $\overline{V}/V_i$

SOURCE 9.4

CONSTANT SOURCE CONCENTRATION OF EACH RADIONUCLIDE (MODEL DEMONSTRATION)

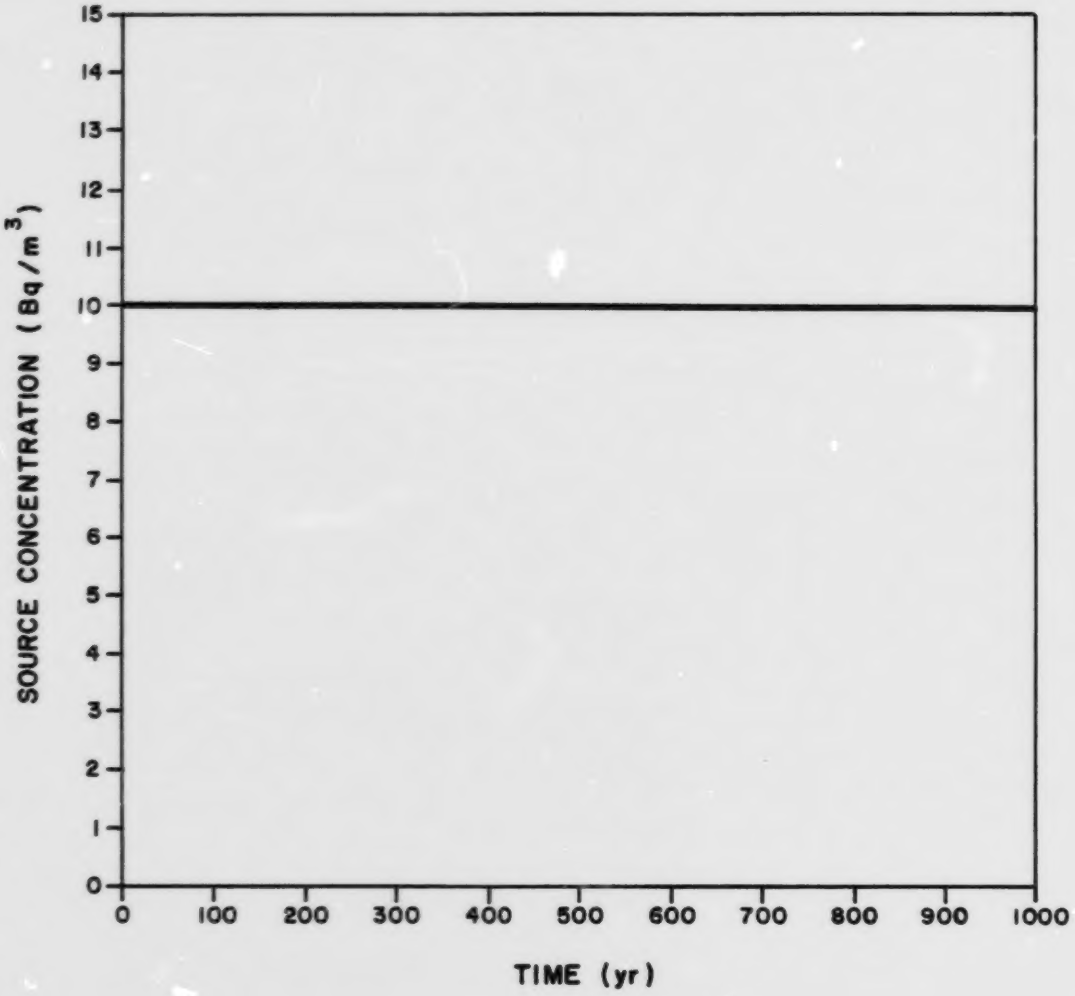

FIGURE 9.5

GROUNDWATER CONCENTRATION OF URANIUM (CONSTANT SOURCE, DAM I)

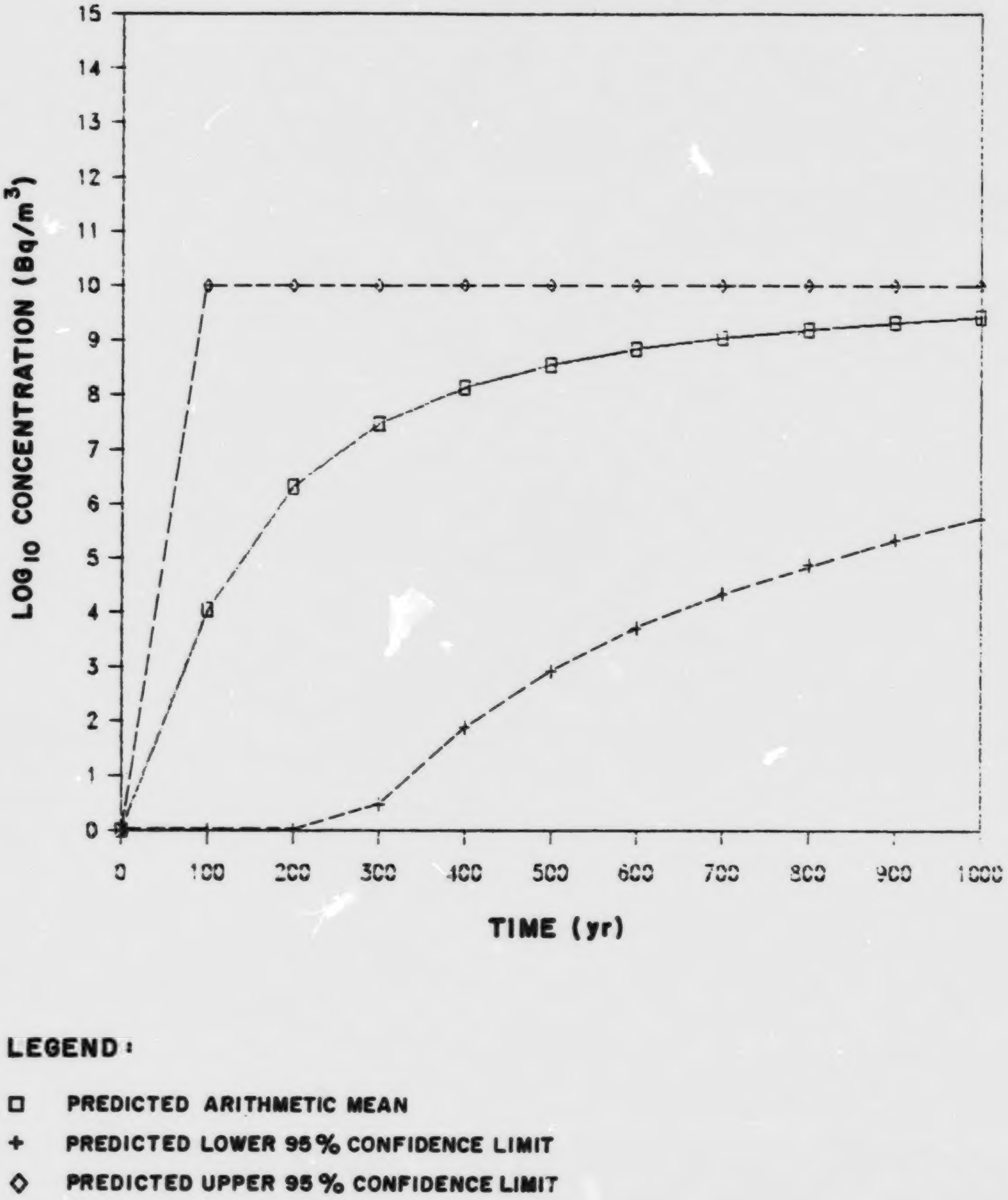

FIGURE 9.6

GROUNDWATER CONCENTRATION OF TOTAL THORIUM
(CONSTANT SOURCE, DAM I)

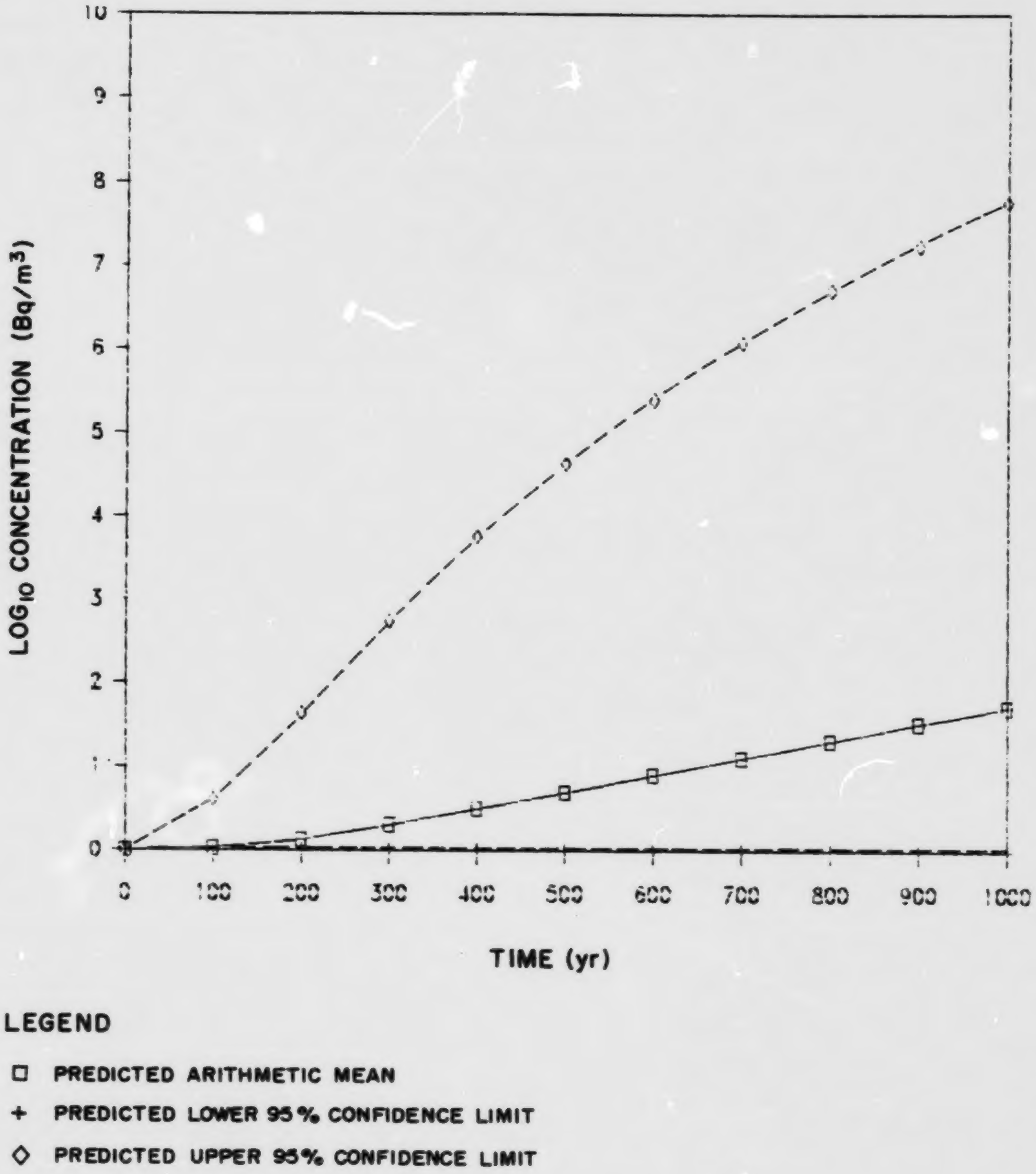

FIGURE 9.7

GROUNDWATER CONCENTRATION FOR LEAD - 210
(CONSTANT SOURCE, DAM I)

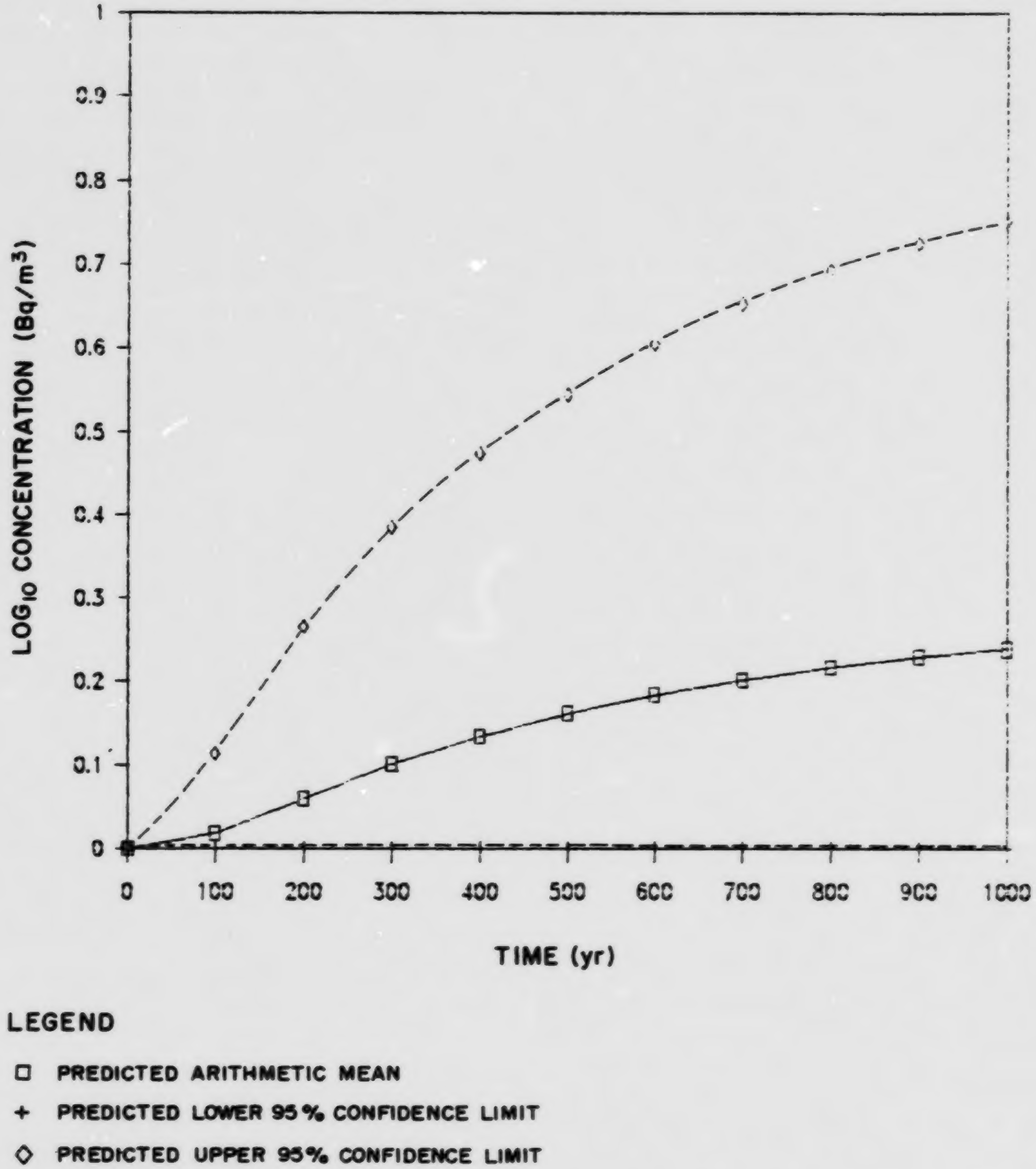

FIGURE 9.8

GROUNDWATER CONCENTRATION FOR RADIUM-226
(CONSTANT SOURCE, DAM I)

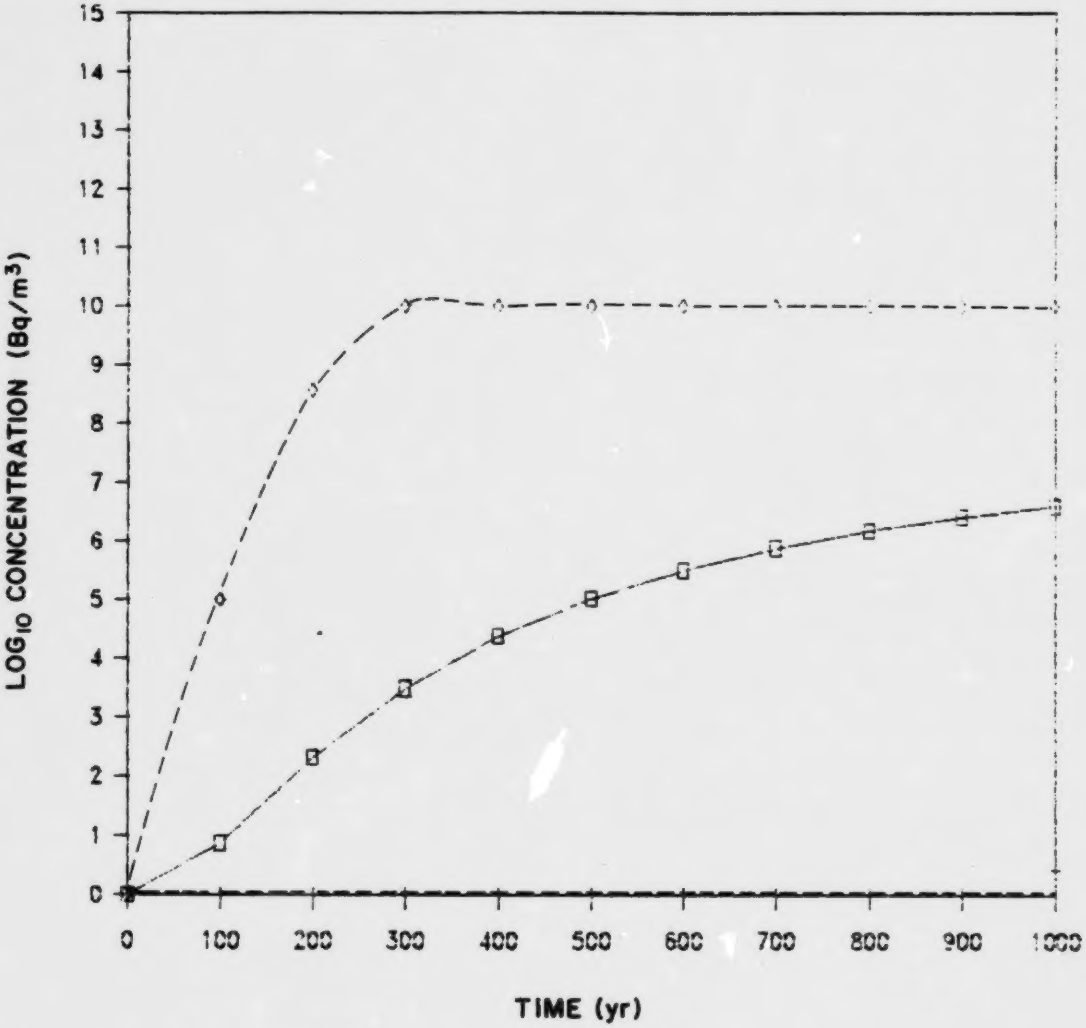

LEGEND

- □ PREDICTED ARITHMETIC MEAN
- + PREDICTED LOWER 95% CONFIDENCE LIMIT
- ◇ PREDICTED UPPER 95% CONFIDENCE LIMIT

ρ_b = soil density
n = porosity
$K_{d,i}$ = distribution coefficient of ith radionuclide
$\overline{V}$ = average linear groundwater velocity
V_i = velocity of ith radionuclide in the aquifer.

Hence, the ratio of breakthrough times for uranium and radium can be approximated by:

$$\frac{T_U}{T_{Ra}} \simeq \frac{K_{d,U}}{K_{d,Ra}} = \frac{0.02}{0.07} = \frac{1}{3.5} \tag{9.25}$$

Using these ratios it is predicted that radium will reach 5 $Bq.m^{-3}$, the concentration of uranium at approximately year 145 (Figure 9.6), by year 508. The model results for radium, presented in Figure 9.9, are in very good agreement with the aforementioned predictions.

In Figure 9.9 the assumed time-variant concentration of the four radionuclides in the tailings source discharge is presented. In Figures 9.10 to 9.13 the corresponding variation in the concentrations of the radionuclides in the groundwater discharge at the toe of dam 1 are presented. The concentrations are expressed in terms of arithmetic means, and lower and upper 95% confidence limits on the point estimates. The time lags, in terms of response to changes in the source concentrations, vary for each radionuclide. The approximate time lags, as calculated by equation (9.25), are: 100 years for uranium; 500 years for total thorium; 400 years for Pb-210; and 300 years for Ra-226.

9.7 Description of the Computer Model

The algorithms used in the subsurface transport model are given in the source code listing, Table 9.4. The computer source symbols for the parameters are presented in Table 9.2. The computer source symbol of FNG(i,t) represents the Green's function, G(X,t), shown in equation (9.18).

9.8 References

AES, not dated. "Precipitation Data from AES Computer Centre." AES Computer Centre Downsview.

Allard, B., Kipatsi, H. and Rydberg, J., 1977. "Sorption of Long-Lived Radionuclides in Clay and Rock. Part 1. Determination of Distribution Coefficient." KBS Technical Report 55.

Ames, L.L., and Rai, D., 1978. "Radionuclide Interactions with Soil and Rock Media, Volume 1." U.S. Environmental Protection Agency Report, U.S. EPA 520/6-78-007.

Anderson, M.P., 1979. "Using Models to Simulate the Movement of Contaminants Through Groundwater Flow Systems." CRC Critical Reviews in Environmental Controls, Vol. 9, pp. 97-156.

Beals, D.I., 1985. "Soil and Climate Parameters for Post-Closure Biosphere Assessment." Atomic Energy of Canada Limited, Technical Record TR-285.

Bear, J., 1979. "Hydraulics of Groundwater." McGraw-Hill, Israel.

Birchall, A., 1986. "A Microcomputer Alogorithm for Solving Compartmental Models Involving Radionuclide Transformations." Health Physics, Vol. 50, No. 3.

Blair, R.D., 1980. "Hydrogeochemistry of an Active Pyritic Uranium Tailings Basin, Nordic Mine, Elliot Lake, Ontario." M.Sc. thesis, Dept. of Earth Sciences, University of Waterloo, Waterloo. pp. 125.

FIGURE 9.9

TIME VARIANT SOURCE CONCENTRATION OF EACH RADIONUCLIDE (MODEL DEMONSTRATION)

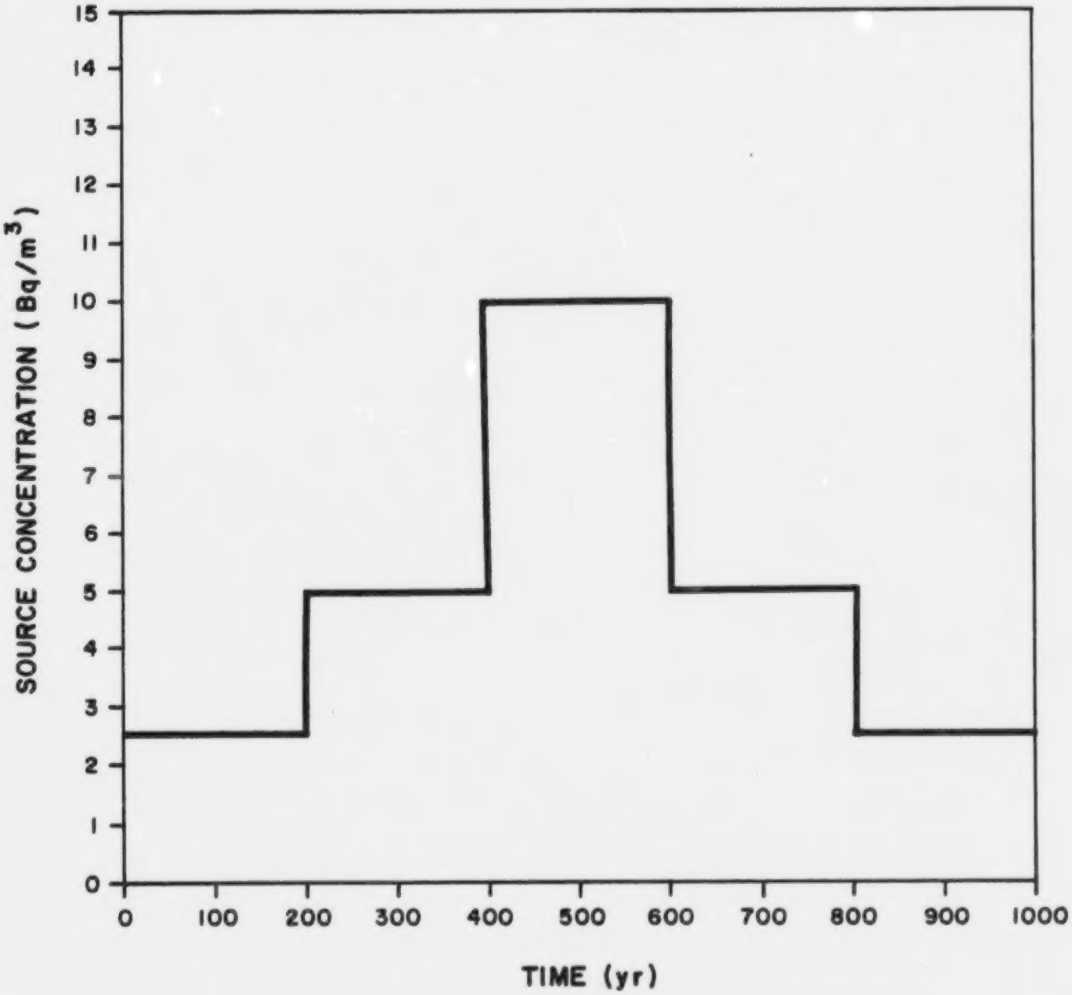

FIGURE 9.10

GROUNDWATER CONCENTRATION FOR URANIUM
(VARIANT SOURCE – TIME)

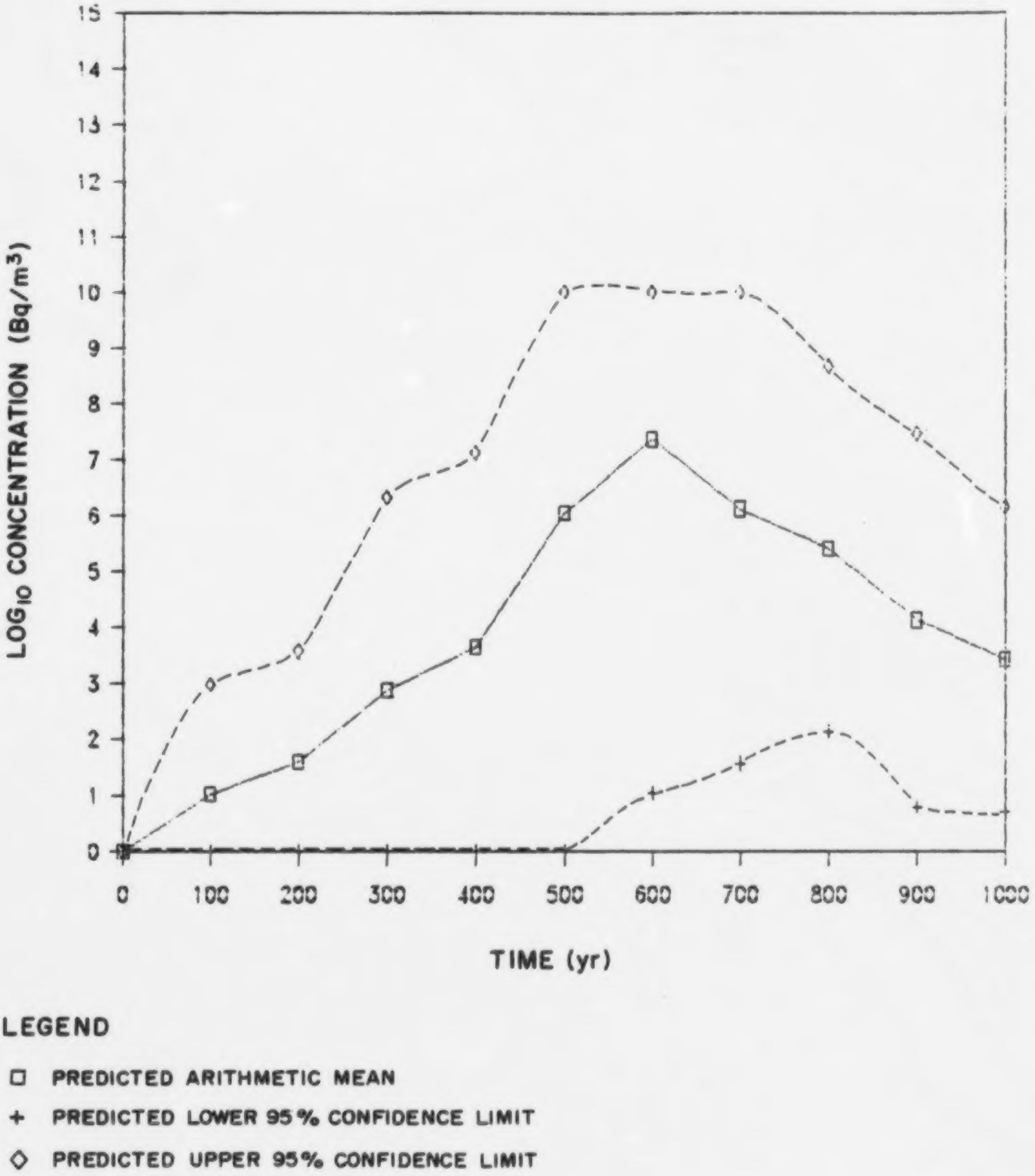

FIGURE 9.11

GROUNDWATER CONCENTRATION OF TOTAL THORIUM
(VARIANT SOURCE - TIME)

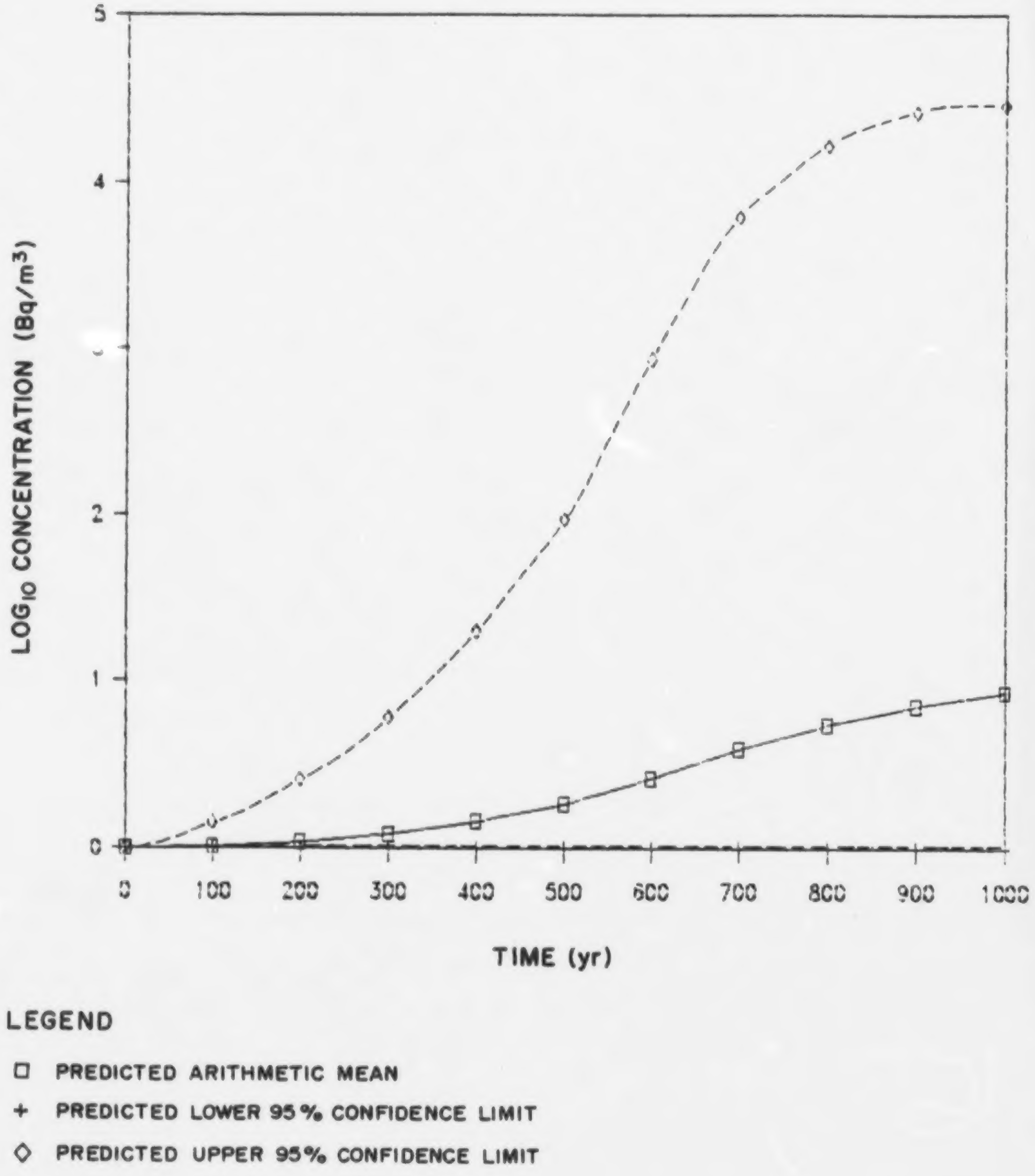

FIGURE 9.12

GROUNDWATER CONCENTRATION FOR LEAD - 210 (VARIANT SOURCE - TIME)

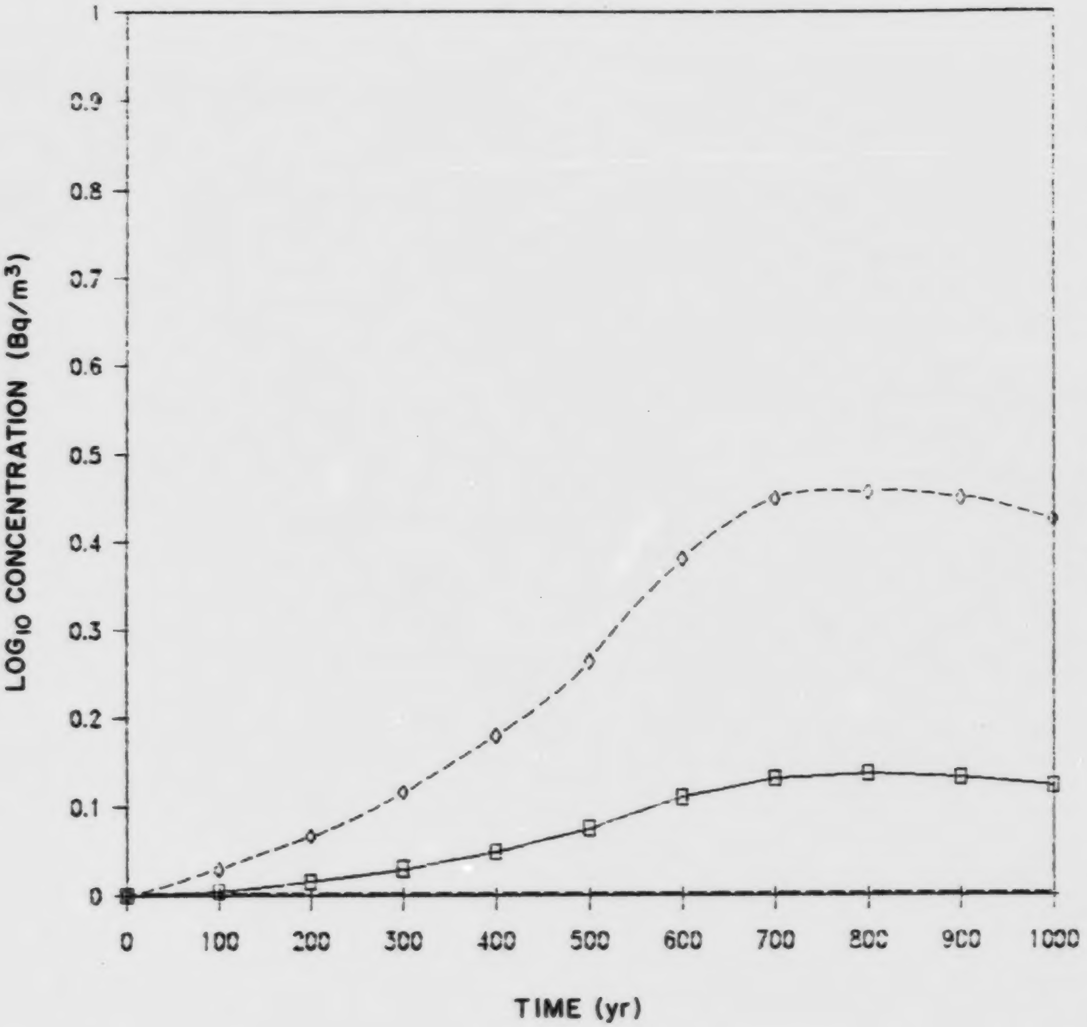

LEGEND

- □ PREDICTED ARITHMETIC MEAN
- + PREDICTED LOWER 95% CONFIDENCE LIMIT
- ◇ PREDICTED UPPER 95% CONFIDENCE LIMIT

FIGURE 9.13

GROUNDWATER CONCENTRATION FOR RADIUM - 226
(VARIANT SOURCE - TIME)

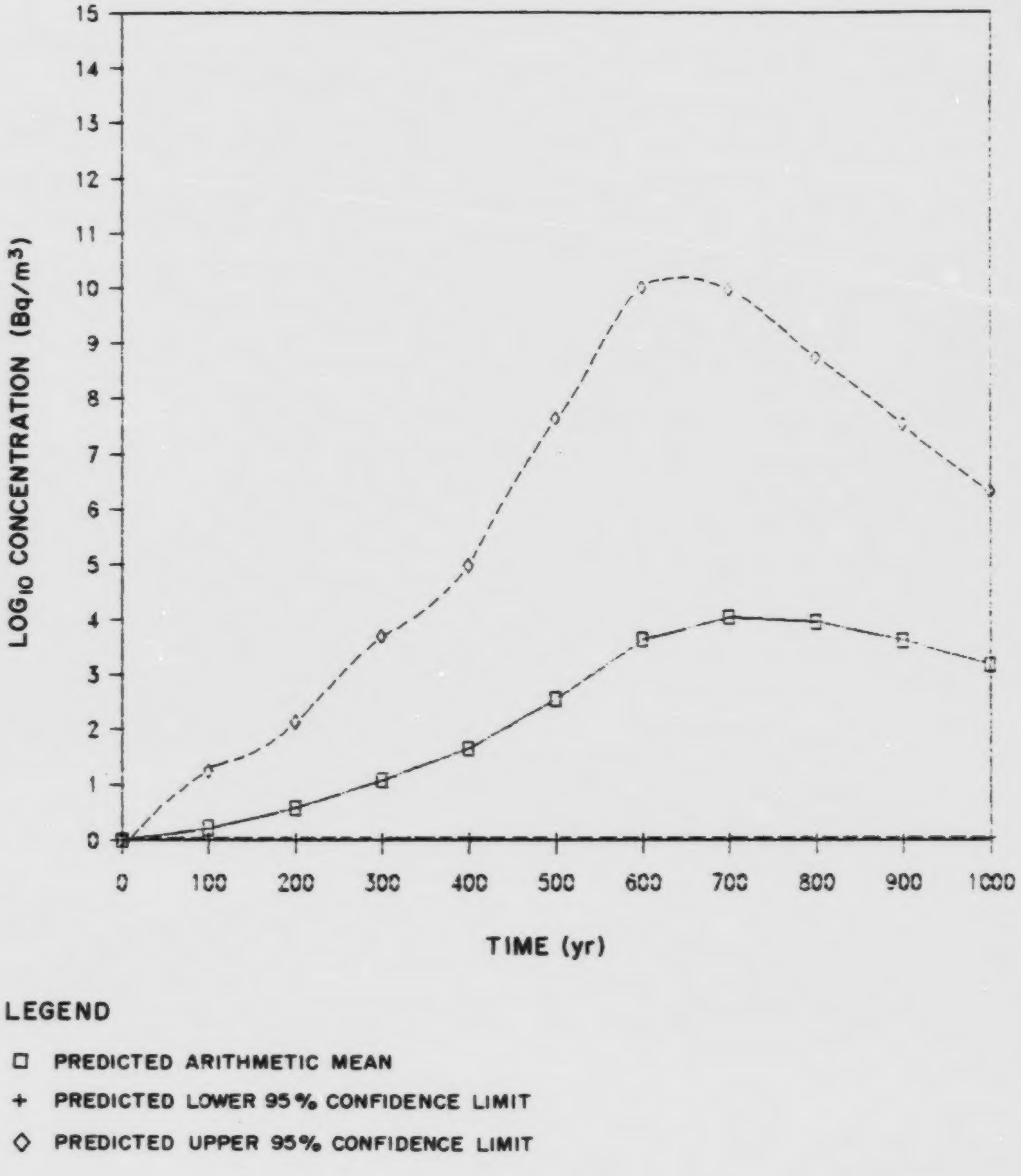

Table 9.4

SUBSURFACE CONTAMINANT TRANSPORT MODEL CODE LISTING

```
      SUBROUTINE GWATER
C       27 FEB 1987
C       (PORE WATER AND CONTAMINANT MOVEMENT IN THE SATURATED ZONE
C        THROUGH MULTIPLE FLOWPATHS)
C
      INCLUDE 'MODEL.INC'
      INCLUDE 'VAR.INC'
C
      REAL*4 FNERF(2),ZZ(2),GWAT(5,5,502),X(5),LD(5),BD(5),F,D,Z,
     &       TG
      REAL*8 E1,E2,E3,E4
      INTEGER*2 K,ID,LL,I,J,KK,TT,TTT
C
C
      IF (CODGW .GE. 1.) THEN
        WRITE(*,10)
10      FORMAT(1X,'SUBROUTINE GWATER')
      END IF
C
      IF(T.EQ.0.0)THEN
C
C        CALCULATION OF TIME-INVARIANT PROCESS VARIABLES WHEN T=-DT
C
         VSRTOT=0
         DO 150 ID=1,DAM
C
C            CALCULATE VARS. FOR EACH DAM
             DV(ID)=HCGWAT(ID)*HGGWAT(ID)
             VSRGW(ID)=DV(ID)*AXGWAT(ID)
             VSRTOT=VSRTOT+VSRGW(ID)
C
             LD(ID) = 0.12*XRGWAT(ID)
             LDC(ID)= LD(ID)*DV(ID)/POGWAT(ID)
             BD(ID)= SDGWAT(ID)*(1-POGWAT(ID))
C
             DO 100  I=1,4
               RGW(I,ID)=1+BD(ID)*DCGWAT(I)/POGWAT(ID)
C
               AGW(I,ID)=DV(ID)/(POGWAT(ID)*RGW(I,ID))
               BGW(I,ID)=((DV(ID)/(2*POGWAT(ID)*LDC(ID)))**2
     &         +LAM(I)*RGW(I,ID)/LDC(ID))**0.5
               CGW(I,ID)=4*LAM(I)*LDC(ID)/RGW(I,ID)
C
C              ALSO SET CONCENTRATION AT T=-DT (K=1)
C              SOURCE CONC. IS TAKEN FROM DAM'S SPECIFIED LAYER
               CO(ID,I,1)=WCONC(I,GWLAYR(ID),3)
100          CONTINUE
150      CONTINUE
C
C        MASS BALANCE CHECK OF THE VOLUMETRIC FLOW
C        VSR IS CALCULATED IN WATER SOURCE
```

Table 9.4 continued.

```
C
         IF (VSRTOT.GT. VSR ) THEN
                 DO 180 LL=1,DAM
                     VSRGW(LL)= VSR*VSRGW(LL)/VSRTOT
180              CONTINUE
         END IF
C
C        AT T=-DT (K=1) THE CONCENTRATIONS IN THE AQUIFER ARE ZERO
         DO 495 ID=1,DAM
             DO 485 I=1,5
               GWAT(I,ID,1) = 0
               FNG(I,ID,1) = 0
485          CONTINUE
495      CONTINUE
C
      END IF
C
C
C        CALCULATE VARIABLES FOR THIS TIME INTERVAL AND FOR EACH DAM
C
         DO 465 ID=1,DAM
             X(ID)=XRGWAT(ID)
C            K IS THE TIME INTERVAL BEING CALCULATED
C            NOTE THAT AT T=0 , K=2  (I.E. K=1 AT T=-DT)
             TG= T+DT
             K = INT(TG/DT) + 1
C
C            CALCULATION OF PROCESS
C
             DO 400 I=1,4
C             THE ORDER OF RADIONUCLIDES USED IN THIS SUBROUTINE IS
C             URANIUM, THORIUM, LEAD AND RADIUM
C             CO IS THE SOURCE CONCENTRATION (FROM THE SOURCE MODEL)
C
C             SOURCE CONC. IS TAKEN FROM DAM'S SPECIFIED LAYER
               CO(ID,I,K) = WCONC(I,GWLAYR(ID),3)
C
               D=LDC(ID)*TG/RGW(I,ID)
C
C              GREEN FUNCTION, FNG, AND ERROR FUNCTION, FNERF
               ZZ(1)=(X(ID)-(AGW(I,ID)**2+CGW(I,ID))**0.5*TG)/(2*D**0.5)
               ZZ(2)=(X(ID)+(AGW(I,ID)**2+CGW(I,ID))**0.5*TG)/(2*D**0.5)
                 DO 250 J=1,2
                    Z=ZZ(J)
                    FNERF(J)=FN(Z)
250              CONTINUE
C
C
                 E1 = EXP(-X(ID)*BGW(I,ID))
                 E2 = EXP( X(ID)*BGW(I,ID))
                 E3 = E1*FNERF(1)
                 E4 = E2*FNERF(2)
                 FNG(I,ID,K) =  0.5*EXP(DV(ID)*X(ID)
```

Table 9.4 continued.

```
   &     /(2*POGWAT(ID)*LDC(ID)))*(E3+E4)
C
         IF ( FNG(I,ID,K) .LT. 1E-20) THEN
           FNG(I,ID,K) = 0.
         END IF
C
C
C    MASS BALANCE CALCULATION  ********************************
C
C       MASS BALANCE OF THE INITIAL SLUG
        GWAT(I,ID,1)= CO(ID,I,1)*FNG(I,ID,K)
C
        IF (CODGW .GE. 3 ) THEN
         WRITE(*,260) I,K,GWAT(I,ID,1),CO(ID,I,1),FNG(I,ID,K)
260      FORMAT(' ',"INITIAL,I,K,GWAT-1,CO-1,FNG-K",2I2,3E10.3)
        END IF
C
C       MASS BALANCE FOR THE INTERMEDIATE CONTAMINANT SLUGS
        KK = K-1
        IF (KK .GE. 2) THEN
         GWAT(I,ID,KK) = 0
         DO 300 TT=2,KK
          TTT=TT-1
          GWAT(I,ID,KK)=GWAT(I,ID,KK)+(CO(ID,I,TT)-
   &      CO(ID,I,TTT))*FNG(I,ID,K-TT+1)
C         THE "+1" TERM IN FNG IS REQUIRED SINCE THE
C         MINIMUM ARRAY MEMBER IS FNG(I,ID,1)
C
          IF (CODGW .GE. 3.) THEN
           WRITE(*,275) K,GWAT(I,ID,KK),CO(ID,I,TT),
   &       CO(ID,I,TTT),FNG(I,ID,K-TT+1)
275        FORMAT(' ',"K,GWAT-KK,CO-TT,TTT,FNG-TT",I2,4E13.5)
          END IF
C
300      CONTINUE
        END IF
C
C       MASS BALANCE FOR THE LAST CONTAMINANT SLUG
        GWAT(I,ID,K) = (CO(ID,I,K)-CO(ID,I,KK))*0.5*FNG(I,ID,2)
C
        IF (CODGW .GE. 3) THEN
      WRITE(*,350) GWAT(I,ID,K),CO(ID,I,K),CO(ID,I,KK),FNG(I,ID,2)
350      FORMAT(' ',"GWAT-K,CO-K,CO-KK,FNG-2",4E10.3)
        END IF
C
C        TOTAL MASS OF INITIAL, INTERMEDIATE & FINAL SLUGS
        IF (KK .GE. 2) THEN
         GWAT(I,ID,K) = GWAT(I,ID,1) + GWAT(I,ID,KK)
   &     + GWAT(I,ID,K)
        ELSE
         GWAT(I,ID,K) = GWAT(I,ID,1) + GWAT(I,ID,K)
        END IF
C
```

Table 9.4 continued.

```
                IF (GWAT(I,ID,K) .LT. 0.) THEN
                  GWAT(I,ID,K) = 0.
                END IF
C
C          END OF THE MASS BALANCE ***********************************
C
C               INCLUDING THE IN-GROWTH OF LEAD "GWAT(5,ID,K)"
                IF (I .EQ. 4) THEN
                  F = (1-EXP(-LAM(3)*DT))*RGW(4,ID)/RGW(3,ID)
                  GWAT(5,ID,K) = GWAT(4,ID,K)*F
                  GWAT(3,ID,K) = GWAT(5,ID,K) + GWAT(3,ID,K)
                END IF
C
C               THE FOLLOWING IS THE FLUX OF CONTAMINANT (BQ/(YEAR M2))
                GFLUX(I,ID) = GWAT(I,ID,K)*VSRGW(ID)/AXGWAT(ID)
C
C               END OF LOOP FOR EACH RADIONUCLIDE
400          CONTINUE
C
C            SETTING OUTPUT CONCENTRATIONS FOR OTHER MODULES
             GWATC(1,ID) = GWAT(1,ID,K)
             GWATC(2,ID) = GWAT(2,ID,K)
             GWATC(3,ID) = GWAT(3,ID,K)
             GWATC(4,ID) = GWAT(4,ID,K)
C
C            ALSO CALCULATE OUTPUT CONC. AND FLUX FOR TOTAL SULPHATE
C            AND TOTAL CALCIUM
             GWATC(7,ID)=WCONC(7,GWLAYR(ID),3)
             GWATC(8,ID)=WCONC(8,GWLAYR(ID),3)
             GFLUX(7,ID)=GWATC(7,ID)*VSRGW(ID)/AXGWAT(ID)
             GFLUX(8,ID)=GWATC(8,ID)*VSRGW(ID)/AXGWAT(ID)
C
C
             IF (CODGW .GE. 2.) THEN
               WRITE(*,450) T,CO(ID,1,K),GWAT(1,ID,K),
     &         GWAT(2,ID,K),GWAT(3,ID,K),GWAT(4,ID,K),GWAT(5,ID,K)
450            FORMAT(3X,I6,6E10.3)
             END IF
C
C            END OF LOOP FOR EACH DAM
465      CONTINUE
C
      RETURN
      END
C
      REAL  FUNCTION FN(Z)
C
C
      IF (Z .LT. 0.0) THEN
         SGN =-1.
      ELSE IF (Z .EQ. 0.0) THEN
         SGN =0.
      ELSE
```

Table 9.4 continued.

```
           SGN = 1.
        END IF
C
        C1=0.1441106
        C2=0.6105416
        C3=0.6077388
        C4=0.8530848
        C5=0.381965
C
        IF (Z .GT. 8.) THEN
          FN= 0.0
        ELSE
          IF (Z .LT. -8.) THEN
            Z=-8.0
          ENDIF
          D1= EXP(-Z*Z)
          D2= C1/(1+C5*ABS(Z))
          D3= C2/(1+C5*ABS(Z))**2
          D4= C3/(1+C5*ABS(Z))**3
          D5= C4/(1+C5*ABS(Z))**4
          FN = 1-SGN + SGN*D1*(D2+D3-D4+D5)
        END IF
C
        RETURN
        END
```

Blair, R.D., Cherry, J.A., Lim, T.P. and Vivyurka, A.J., 1980. "Groundwater Monitoring and Contaminant Occurrence at an Abandoned Tailings Area, Elliot Lake, Ontario." Proceedings, 1st International Conference on Uranium Mine Waste Disposal, Vancouver. Society of Mining Engineers, New York, pp. 411-444.

Cherry, J.A., Blackport, R.A., Dubrovsky, N., Gillham, R.W., Lim, T.P., Murray, D., Reardon, E.J. and Smyth, D.J.A., 1980a. "Subsurface Hydrology and Geochemical Evolution of Inactive Pyritic Tailings in the Elliot Lake Uranium District, Canada." Proceedings, 3rd Symposium on Uranium Tailings Management, Colorado State University, Fort Collins.

Cherry, J.A., Gillham, R.W., Anderson, F.G., and Johnson, P.E., 1980b. "Hydrogeological Studies of a Sandy Aquifer at an Abandoned Landfill: Part 2, Monitoring Devices." In CFB Borden Landfill Study, Vol. I. Waterloo Research Institute, Waterloo, Ont.

Cherry, J.A., Morin, K.A., and Dubrovsky, N.M., 1984. "Modelling of Contaminant Migration in Acidic Groundwater Plumes at Uranium Tailings Inpoundments: ADNEUT3." Prepared for National Uranium Tailings Program, Energy Mines and Resources, Contract No. OST83-00284, Dept. of Earth Sciences, University of Waterloo.

Feenstra, S., Blair, R.D., Cherry, J.A., Chakravatti, J.L., and LaRocque, E., 1981. "Hydrogeochemical Investigations of Two Inactive Tailings Areas in the Elliot Lake Uranium District Ontario, Canada." Uranium Mill Tailings Management, Proceedings of the Fourth Symposium, November, Geotechnical Engineering Program, Civil Engineering Department, Colorado State University.

Freeze, R.A., 1975. "A Stochastic-Conceptual Analysis of One-Dimensional Groundwater Flow in Nonuniform Homogeneous Media." Water Res. Research, Vol. 11, No. 5, pp. 725-741.

Freeze, R.A., and Cherry, J.A., 1979. "Groundwater." Prentice Hall Inc., New Jersey.

Gerritse, R.W., Vriesema, R., Dalenberg, J.W, and De Roos, H.P. 1982. "Effect of Sewage Sludge on Trace Element Mobility in Soils." J. Environ. Qual., Vol. II, pp. 359-364.

Johnston, H.M. and Gillham, R.W., 1980. "A Review of Selected Radionuclide Distribution Coefficients of Geologic Material." Atomic Energy of Canada Limited Technical Record, TR-90.

Jury, W., Spencer, W., and Farmer, W., 1983. "Use of Models for Assessing Relative Volatility, Mobility and Persistence of Pesticides and Other Trace Organics in Soil Systems." Hazard Assessment of Chemicals, Vol. 2, Academic Press.

Lester, D.H., Janson, G., and Burkholder, H.C., 1975. "Migration of Radionuclide Chains Through an Adsorbing Medium." American Institute of Chemical Engineers Symposium Series, No. 152, Vol. 71.

Morin, K.A., 1986. Personal Communication, Government of Saskatchewan, March.

Morin, K.A., Cherry, J.A., Lim, T.P. and Vivyurka, A.J., 1982. "Contaminant Migration in a Sand Aquifer Near an Inactive Uranium Tailings Impoundment, Elliot Lake, Ontario, Can. Geotech. Jour. Vol. 19, pp. 49-62.

National Research Council (NRC), 1983. "A Study of the Isolation System for Geologic Disposal of Radioactive Wastes." Waste Isolation Systems Panel, Board on Radioactive Waste Management, Commission on Physical Sciences, Mathematics and Resources, Washington.

Petrie, G., Sneider, S., Napier, B., and Barnard, J., 1983. "Simplified Codes for Performance Evaluation (Scope) of Radionuclide Transport: Version 1.0." Prepared for the U.S. Department of Energy, Under Contract No. DE-AC06-76RLO 1830, Pacific Northwest Laboratory, Richland, Washington.

Rancon, D., 1973. "The Behaviour in Underground Environments of Uranium and Thorium Discharged by the Nuclear Industry." In: Environmental Behaviour of Radionuclides Released in the Nuclear Industry, International Atomic Energy Agency Report, IAEA-SM-172/55.

Rogers, V.C., 1978. "Migration of Radionuclide Chains in Groundwater." Nuclear Technology, Vol. 40, October.

Sheppard, M.I., Beals, D.I., Thibault, D.H., and O'Connor, P., 1984. "Soil Nuclide Distribution Coefficients and Their Statistical Distributions." Atomic Energy of Canada Limited, Whiteshell Nuclear Research Establishment, December.

U.S. Department of Health, Education and Welfare, 1970. "Radiological Health Handbook." Public Health Service, January.

U.S. EPA, 1978. "Radionuclide Interaction with Soil and Rock Media, Volume 1: Processes Influencing Radionuclides Mobility and Retention, Element Chemistry and Geochemistry, Conclusion and Evaluation." United States Environmental Protection Agency, EPA 520/6-78-007-A.

Vandergraaf, T.T., 1982. "Compilation of Sorption Coefficients for Radionuclides on Granites and Granite Rocks." Atomic Energy of Canada Limited, Technical Record TR-120.

Veska, E., 1983. "Origin and Subsurface Migration of Radionuclides from Waste Rock at an Abandoned Uranium Mine Near Bancroft, Ontario". Unpublished Ph.d. Thesis, University of Waterloo.

10.0 SURFACE WATER DISPERSION MODELS

10.1 Approach to Watershed Modelling

One objective of this study was to develop the capability to model watersheds with variable characteristics. A typical watershed involves a series of lakes linked by rivers. Such a watershed is specified in this study as comprising a series of nodes, with each node representing the outflow from a watershed sub-basin. The distances between the nodes are known as "segments". Two types of watershed segments have been defined: rivers and lakes.

Selected physical and chemical characteristics for each segment must be specified as model inputs, for example, drainage area size, river reach length, lake depth, lake area. The behaviour of various ionic species and radionuclides is modelled for each segment. Dilution is the only mechanism accounted for by the river model. The lake model, on the other hand, accounts for transfer to and from lake sediment as well as dilution. Radioactive ingrowth and decay is taken into account for the short-lived radionuclides.

10.2 The Reference Watershed

In the Phase I and Phase II probabilistic assessment studies, the dose to a reference receptor was calculated for six key pathways including two related to surface water: consumption of contaminated drinking water and fish (SENES, 1984 and 1985). The receptor was situated on the edge of a lake approximately 2 km downstream of the tailings area. The hypothetical reference site was chosen to reflect the major environmental features of a Precambrian Shield setting. Contaminated surface and groundwater flows from the tailings area were intercepted in a major river which discharged into an oligotrophic lake (i.e. a low productivity lake) with a surface area of 160 ha and mean depth of 10 m. The drainage basin at the outflow of the lake equalled 2000 ha (20 km^2) as compared to the tailings area which covered 50 ha (0.5 km^2). The waters of the drainage basin had a naturally low buffering capacity, low nutrient content and low total dissolved solids level.

These basic concepts of the reference site were retained in their entirety in Phase III (SENES, 1986) and UTAP.3. The scope of the drainage basin however, was expanded to include a whole reference watershed having a total drainage area of approximately 40,000 ha (400 km^2) and a river reach of about 60 km. A schematic representation of the watershed is portrayed on Figure 10.1.

The reference tailings area was featured as being located in the headwaters of the watershed. The watershed contained three lakes of substantially different size and was divided into eight sub-basins to permit computation of flow and water quality at several points in the surface water system. These points are indicated on the figure as node numbers (i.e. Node 1,2....8). Details of the characteristics of the watershed sub-basins, lakes and river reaches are summarized on Table 10.1.

The upstream end of the watershed within the 3 km ring of the tailings area comprises that part of the watershed modelled in Phases I and II. The radium-226 levels computed at Node 2 on the outlet of the first lake of the system were used in the previous phases for computing the dose to the reference receptor.

The approach adopted in Phase III and continued in UTAP.3 permits dose to be calculated for receptors located in any or all of 80 windrose locations. Details of the windrose structure are presented in Section 5.0. The contribution to the total dose from the consumption of contaminated drinking water is achieved by linking receptors to appropriate nodes on the watershed. Not all receptors however need to be linked to watershed nodes as some receptors may be situated in windrose locations far removed from the reference watershed and receive their drinking water supply from uncontaminated sources.

10.3 The Hydrologic Component

Flow at each node in the reference watershed is calculated using the simple model:

FIGURE 10.1

REFERENCE WATERSHED SCHEMATIC

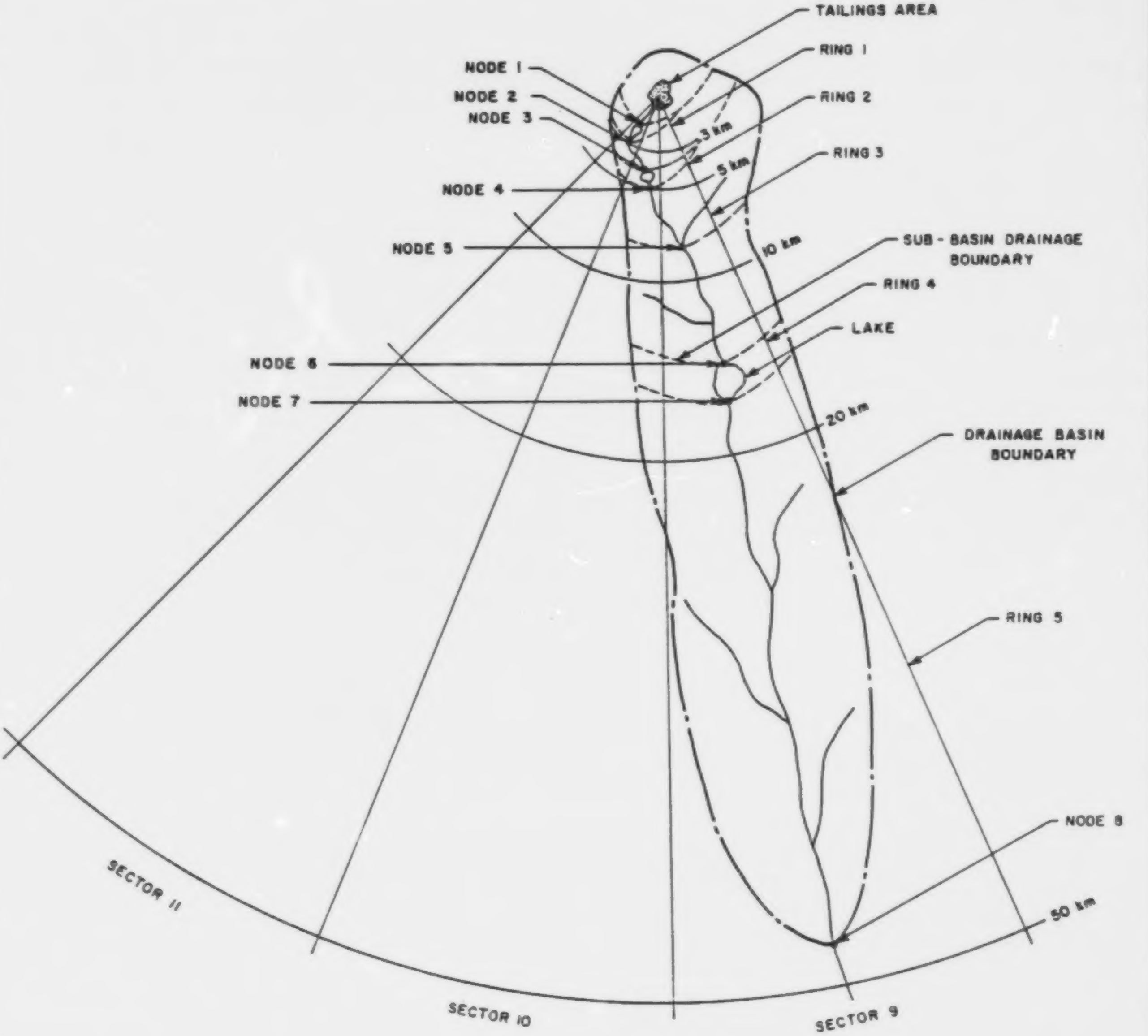

SENES

Table 10.1

CHARACTERISTICS OF THE REFERENCE WATERSHED

	Segment Details				Watershed Area			
End Node No.	Segment Type	River Reach Length (m)	Lake Mean Depth (m)	Lake Surface Area (m**2)	Sub-basin Area (km**2)	Cumulative Area (km**2)	End Node Windrose Location Direction	End Node Windrose Location Sector
1	River	3.0E3		-	15	15	11	1
2	Lake	-	10	5.0E5	5	20	11	1
3	River	3.5E3		-	12	32	10	2
4	Lake	-	4	2.5E5	6	38	10	2
5	River	7.0E3		-	32	70	9	3
6	River	1.3E4		-	50	120	9	4
7	Lake	-	5	4.0E6	20	140	9	4
8	River	3.0E4		-	260	400	9	5

$$Q_{n,t} = \sum_{n} P_t A_n + \sum_{s} Q_{s,t} \qquad (10.1)$$

where

$Q_{n,t}$ = volumetric surface water flow at node 'n' at time 't' ($m^3.yr^{-1}$)

$Q_{s,t}$ = volumetric discharge rate of tailings source term 's' (surface and subsurface flows) from the reference tailings area at time 't' ($m^3.yr^{-1}$)

P_t = mean annual net precipitation at time 't', which occurs as surface runoff (i.e. after evapotranspiration losses) ($m.yr^{-1}$)

A_n = area of the nth sub-basin in the watershed (m^2)

n = the node number for the nth segment in the watershed numbered consecutively commencing in the upper reaches of the watershed.

In using net precipitation in the model, it is implicitly assumed that the same runoff factor applies to all sub-basins irrespective of size. This assumption is reasonable for the size of the reference watershed which increases in sub-basin area from 15 to 400 km^2. A statistical comparison of monthly flow data from four stations on the Serpent River Basin in northern Ontario with drainage areas ranging in size from 157 to 1349 km^2 showed that the area pro-rating basis provided the best correlation with historical data (SENES and Golder, 1981). In other words, it was found that monthly flow in the Serpent River could be adequately predicted as the product of a uniform runoff factor and the size of the drainage basin. Application of this approach to predict annual surface flows is equally valid.

Of the parameters in equation (10.1), the net precipitation (P_t) is a time-variant input parameter. Hence, it must be sampled from the appropriate distribution of values each time step (Δt) over the duration of each trial. Since the size of the time step may vary from 1 to 10 years (a predetermined decision in developing the system code), the probability distribution of annual precipitation must be adjusted accordingly.

The areas of the watershed sub-basins (A_n) are treated as input constants since they are specific to each application. The sub-basin areas for the reference site are listed on Table 10.1. The calculation of flow at each node in the watershed is determined as the summation of the flows to all upstream nodes. This requires that the nodes be ordered in the correct sequence starting from the upper end of the watershed. The tailings source is linked to node 1 on the watershed (see Figure 10.1).

10.4 Major Ions Component

10.4.1 Baseline Levels

The concentration of the major water quality constituents, including calcium and sulphate, were modelled as conservative substances as in the Phase I and II studies. The natural background levels assumed for several of the major constituents were:

calcium - 10^{-4} $mol.L^{-1}$ (10^{-1} $mol.m^{-3}$)
sulphate - $10^{-4.15}$ $mol.L^{-1}$ ($10^{-1.15}$ $mol.m^{-3}$)
sodium - $10^{-4.1}$ $mol.L^{-1}$ ($10^{-1.1}$ $mol.m^{-3}$)
potassium - $10^{-4.8}$ $mol.L^{-1}$ ($10^{-1.8}$ $mol.m^{-3}$)
magnesium - $10^{-4.5}$ $mol.L^{-1}$ ($10^{-1.5}$ $mol.m^{-3}$)
chloride - $10^{-4.7}$ $mol.L^{-1}$ ($10^{-1.7}$ $mol.m^{-3}$)

The concentrations for calcium, sulphate, magnesium and chloride in Precambrian Shield water were obtained from water quality data summary reports prepared by the Ontario Ministry of the Environment (1972 to 1980). Since comparable data were not available for sodium and potassium, typical concentrations for these constituents were taken from Stumm and Morgan (1981).

10.4.2 River Segments

The major ionic constituents affected by the tailings source are calcium and sulphate. Calculation of the concentrations of these constituents at the river node locations is based on mass balance principles for these conservative substances:

$$[Ca]_{n,t} = \frac{Q_{n-1,t}[Ca]_{n-1,t} + Q_{s,t}[Ca]_{s,t} + (Q_{n,t}-Q_{n-1,t})[Ca]_B}{Q_{n,t}} \quad (10.2)$$

and

$$[SO_4]_{n,t} = \frac{Q_{n-1,t}[SO_4]_{n-1,t} + Q_{s,t}[SO_4]_{s,t} + (Q_{n,t}-Q_{n-1,t})[SO_4]_B}{Q_{n,t}} \quad (10.3)$$

where

$[Ca]_{n-1,t}$ = calcium concentration in the flow at node 'n-1' at time 't' ($mol.m^{-3}$)

$[Ca]_{n,t}$ = calcium concentration in the flow at node 'n' at time 't' ($mol.m^{-3}$)

$[Ca]_B$ = natural background level of calcium in the freshwater flow in the watershed ($mol.m^{-3}$)

$[Ca]_{s,t}$ = calcium concentration in the tailings source term discharge 's' from the tailings area at time 't' ($mol.m^{-3}$)

$Q_{n-1,t}$ = volume of the surface water flow at node 'n-1' at time 't' ($m^3.yr^{-1}$)

$Q_{n,t}$ = volume of the surface water flow at node 'n' at time 't' ($m^3.yr^{-1}$)

$Q_{s,t}$ = volume of the tailings source term discharge 's' from the tailings area at time 't' ($m^3.yr^{-1}$)

$[SO_4]_{n-1,t}$= sulphate concentration in the flow at node 'n-1' at time 't' ($mol.m^{-3}$)

$[SO_4]_{n,t}$ = sulphate concentration in the flow at node 'n' at time 't' ($mol.m^{-3}$)

$[SO_4]_B$ = natural background level of sulphate in the freshwater flow in the watershed ($mol.m^{-3}$)

$[SO_4]_{s,t}$ = sulphate concentration in the tailings source term discharge 's' from the tailings area at time 't' ($mol.m^{-3}$).

These expressions provide estimates of the average annual calcium and sulphate concentrations at the river nodes. They are used in a subsequent section to determine pH in the river system.

10.4.3 Lake Segments

The estimation of calcium and sulphate levels in the lakes of the watershed takes into consideration not only dilution but also the history of the levels of the ions in the lake water column in the previous time step. The concentrations of the major constituents are represented by a simple differential equation of the form:

$$V \frac{dC}{dt} = Q_{in} C_{in} - Q_{out} C \qquad (10.4)$$

where

V = volume of the lake (m^3)

Q_{in} = summation of all input flows to the lake ($m^3.yr^{-1}$)

Q_{out} = outflow from the lake ($m^3.yr^{-1}$)

C_{in} = constituent concentration in the inflow waters ($mol.m^{-3}$)

C = constituent concentration in the lake ($mol.m^{-3}$)

Integration of equation (10.4) yields the basic equation used to predict the behaviour of the major ions in the lakes:

$$C_{n,t} = \left(\frac{Q_{n-1,t} C_{n-1,t} + (Q_{n,t} - Q_{n-1,t}) C_B}{Q_{n,t}} \right) + \left\{ C_{n,t-\Delta t} - \left(\frac{Q_{n-1,t} C_{n-1,t} + (Q_{n,t} - Q_{n-1,t}) C_B}{Q_{n,t}} \right) \right\} \exp \left(\frac{-Q_{n,t} \Delta t}{V_n} \right) \qquad (10.5)$$

where

$C_{n-1,t}$ = ion concentration in the inlet flow to the lake, designated node 'n-1', at time't' ($mol.m^{-3}$)

$C_{n,t}$ = ion concentration in the lake designated node 'n' at time 't' ($mol.m^{-3}$)

$C_{n,t-\Delta t}$ = ion concentration in the lake designated node 'n' at the previous time step denoted by 't-Δt' ($mol.m^{-3}$)
C_B = baseline or natural background ion concentration ($mol.m^{-3}$)
$Q_{n-1,t}$ = river flow at the inlet to the lake, designated node 'n-1', at time 't' ($m^3.yr^{-1}$)
$Q_{n,t}$ = flow out of the lake, designated by node 'n', at time 't' ($m^3.yr^{-1}$)
V_n = volume of the lake designated by node 'n' (m^3)
Δt = size of the time step (yr).

The volumes of the lakes (V_n) are calculated as a function of the surface areas (L_n) and mean depths (h_n) of the lakes which are specified as input parameters.

10.5 pH Component

To calculate the pH in the surface water system, it is assumed that the concentrations of iron and aluminum are in equilibrium with solid phases of ferric hydroxide ($Fe(OH)_3(s)$) and gibbsite ($Al(OH)_3(s)$). The concentrations of calcium and sulphate are modelled as described in the previous section. The concentrations of sodium, potassium, magnesium and chloride are essentially unaffected by the tailings area drainage and are characterized by the assumed natural background levels. The waters are considered to be slightly super-saturated (Saturation Index = 0.3) with respect to dissolved carbonate in equilibrium with carbon dioxide (CO_2) in the air. The latter is very common in oligotrophic lakes on the Canadian Shield. The concentration of all ions is expressed on a $mol.L^{-1}$ basis internally in the pH model. The equilibrium reactions are as follows:

Equilibrium Reactions in Lake Water

	Log K
$Al(OH)_3(s) + 3H^+ \rightleftharpoons Al^{3+} + 3H_2O$	8.5
$Al^{3+} + H_2O \rightleftharpoons Al(OH)^{2+} + H^+$	-4.97
$Al^{3+} + 2H_2O \rightleftharpoons Al(OH)_2^+ + 2H^+$	-9.30

$Al^{3+} + 3H_2O \rightleftharpoons Al(OH)_3(aq) + 3H^+$	-15.00
$Al^{3+} + SO_4^{2-} \rightleftharpoons AlSO_4^+$	3.2
$Fe(OH)_3(s) + 3H^+ \rightleftharpoons Fe^{3+} + 3H_2O$	5.97 (K^c)
$Fe(OH)_3(s) + 2H^+ \rightleftharpoons FeOH^{2+} + 2H_2O$	3.78 (K^c)
$Fe(OH)_3(s) + H^+ \rightleftharpoons Fe(OH)_2^+ + H_2O$	0.30 (K^c)
$H_2CO_3 \rightleftharpoons H^+ + HCO_3^-$	-6.5
	$pCO_2 = -3.2$
	$K_H = -1.27$

The ionic charge balance at any point in the watershed is given by:

$$\begin{aligned} 2[Ca^{2+}]_{n,t} &+ 2[Mg^{2+}] + [Na^+] + [K^+] + 3[Fe^{3+}] + 2[FeOH^{2+}] \\ &+ [Fe(OH)_2^+] + [FeSO_4^+] + 3[Al^{3+}] + 2[AlOH^{2+}] + [Al(OH)_2^+] \\ &+ [AlSO_4^+] = 2[SO_4^{2-}]_{n,t} + [Cl^-] + [HCO_3^-] \end{aligned} \qquad (10.6)$$

Note that for the reference watershed:

$$[HCO_3^-] = \frac{10^{pH-11.0}}{f^{1/4}}$$

where

$f^{1/4}$ = activity coefficient of monovalent ions

The contribution of the remaining components of equation (10.6) to the pH equation are discussed below.

Trivalent Cations Al^{3+} and Fe^{3+}

The predicted concentration of Fe^{3+} is several orders of magnitude less than the concentration of Al^{3+} for any pH value:

$$[Fe^{3+}] = 10^{5.97-3pH}$$

$$[Al^{3+}] = \frac{10^{8.5-3pH}}{f^{9/4}}$$

In fact, the sum of the trivalent cations ($[Al^{3+}]+[Fe^{3+}]$) is equal to:

$$\frac{10^{5.97}}{10^{3pH}} + \frac{10^{8.5}}{f^{9/4}10^{3pH}} = \frac{10^{8.501}}{f^{9/4}10^{3pH}} \qquad \text{for } 0.6 \leq f \leq 0.9$$

Divalent Hydroxo Complexes $Al(OH)^{2+}$ and $Fe(OH)^{2+}$

The concentration of $Fe(OH)^{2+}$ is given on the basis of solubility data from tailings oxidation tests:

$$[Fe(OH)^{2+}] = 10^{3.78-2pH}$$

Since the average activity coefficient for divalent cations is estimated to be 0.8; the activity of $Fe(OH)^{2+}$ is equal to:

$$\{Fe(OH)^{2+}\} = 0.8(10^{3.78-2pH}) = 10^{3.683-2pH}$$

In the pH equation, the activities of $Al(OH)^{2+}$ and $Fe(OH)^{2+}$ can be readily combined (since both involve the same power with respect to pH) to give:

$$\{Al(OH)^{2+}\} + \{Fe(OH)^{2+}\} = \frac{10^{3.683}}{10^{2pH}} + \frac{10^{3.53}}{10^{2pH}} = \frac{10^{3.91}}{10^{2pH}}$$

It follows that the sum of concentrations of $Al(OH)^{2+}$ and $Fe(OH)^{2+}$ is given by:

$$[Al(OH)^{2+}] + [Fe(OH)^{2+}] = \frac{10^{3.91}}{f\ 10^{2pH}} = \frac{10^{3.91-2pH}}{f}$$

Monovalent Hydroxo Complexes $Fe(OH)_2^+$ and $Al(OH)_2^+$

The activity coefficients of monovalent ions ($f^{1/4}$) in the surface runoff is always close to unity:

$$f^{1/4} = 0.88 \text{ if } f = 0.6$$
$$f^{1/4} = 0.97 \text{ if } f = 0.9$$

Thus the sum of $Fe(OH)_2^+$ and $Al(OH)_2^+$ equals:

$$[Fe(OH)_2^+] + [Al(OH)_2^+] = \frac{10^{0.3}}{10^{pH}} + \frac{10^{-0.8}}{10^{pH}} = \frac{10^{0.33}}{10^{pH}}$$

which may be restated as:

$$[Fe(OH)_2^+] + [Al(OH)_2^+] = 10^{0.33-pH}$$

Term for the Sulphate Concentration

The term given in equation (10.6) for sulphate is given by the sum of free sulphate and sulphato complexes:

$$[SO_4^{2-}]_{n,t} = [SO_4^{2-}] + [FeSO_4^+] + [AlSO_4^+] \qquad (10.7)$$

A simple comparison of the complexation reactions reveals that the concentration of $FeSO_4^+$ is negligible in comparison to either $AlSO_4^+$ or SO_4^{2-}. The formation of the $AlSO_4^+$ complex can be expressed from the following two equilibrium expressions:

$$Al(OH)_3(s) + 3H^+ \rightleftharpoons Al^{3+} + 3H_2O \qquad \log K = 8.5$$
$$Al^{3+} + SO_4^{2-} \rightleftharpoons AlSO_4^+ \qquad \log K = 3.2$$

Therefore:

$$Al(OH)_3(s) + 3H^+ + SO_4^{2-} \rightleftharpoons AlSO_4^+ + 3H_2O$$

The concentration of $AlSO_4^+$ is given (including the activity coefficients) as:

$$[AlSO_4^+] = \frac{f}{f^{1/4}} \; 10^{(8.5+3.2)} \; 10^{-3pH} \; [SO_4^{2-}]$$

$$= f^{3/4} \; 10^{11.7-3pH} \; [SO_4^{2-}]$$

The total concentration of sulphate includes the free sulphate and the sulphato complex:

$$[SO_4^{2-}]_{n,t} = [SO_4^{2-}] + [AlSO_4^+] = [SO_4^{2-}] \;\; 1 + f^{3/4} \; 10^{11.7-3pH}$$

Therefore:

$$[SO_4^{2-}] = \left[\frac{[SO_4^{2-}]_{n,t}}{1 + f^{3/4} \; 10^{11.7-3pH}}\right]$$

and

$$[AlSO_4{}^+] = [SO_4^{2-}]_{n,t} - [SO_4^{2-}] = \left[\frac{f^{3/4} 10^{11.7-3pH}}{1 + f^{3/4} 10^{11.7-3pH}}\right] \; [SO_4^{2-}]_{n,t}$$

Note that in the ionic balance the $[AlSO_4^+]$ (a cation) and the $[SO_4^{2-}]$ (an anion) appear on the left and the right side of the equation.

$$\ldots + [AlSO_4^+] = 2[SO_4^{2-}] + \ldots$$

$$\ldots + \left[\frac{f^{3/4} \; 10^{11.7-3pH}}{1 + f^{3/4} \; 10^{11.7-3pH}}\right] [SO_4^{2-}]_{n,t} = 2 \left[\frac{1}{1 + f^{3/4} \; 10^{11.7-3pH}}\right] [SO_4^{2-}]_{n,t} \;\; + \ldots$$

Since both terms have a common denominator, they may be combined to yield:

$$\ldots = \left[\frac{2 - f^{3/4} \; 10^{11.7-3pH}}{1 + f^{3/4} \; 10^{11.7-3pH}}\right] [SO_4^{2-}]_{n,t} \; \ldots$$

pH Model

From the above, the equation for calculating pH at any point in the watershed becomes:

$$3\left[\frac{10^{8.5-3pH_{n,t}}}{f^{9/4}}\right]+2\left[\frac{10^{3.91-2pH_{n,t}}}{f}\right]+\left[10^{0.3-pH_{n,t}}\right]+\left[10^{-3.86}\right]+2[Ca^{2+}]_{n,t}+$$

$$2[Mg^{2+}]+[Na^{+}]+[K^{+}]=[SO_4^{2-}]_{n,t}\left[\frac{2-f^{3/4}\,10^{11.7-3pH_{n,t}}}{1+f^{3/4}\,10^{11.7-3pH_{n,t}}}\right]+\left[\frac{10^{pH_{n,t}-11.0}}{f^{1/4}}\right]$$

$$+[Cl^{-}]$$

where

f = the activity coefficient; for the reference watershed environment f would be expected to fall between 0.6 an 0.9 with a probable value of 0.8.

$pH_{n,t}$ = the pH level of the surface water in the watershed at node 'n' at time 't'.

The above pH equation requires an iterative solution.

10.6 Radionuclide Component

A wide variety of mathematical models have been developed for assessing the hydrologic transport of radionuclides. The models range from simple algebraic models to sophisticated multi-dimensional models based on numerical solutions to advection-diffusion and hydrodynamic equations. The selection of any particular model requires careful consideration of its applicability to the specific situation.

The movement of radionuclides through the aquatic pathways depends on numerous physical, biological and chemical processes which affect the resulting concentrations in water, sediment and aquatic biota. Since exposure to man may result from consumption of contaminated water or biota (eg. fish flesh), estimation of the radionuclide concentrations in these media is of particular interest in radiological assessments, especially in Canada where the aquatic pathways have generally been found to be the largest contributors to dose. Typically, the concentrations in water have been estimated taking into account only the effects of dilution, and removal to bottom sediments in the case of lake water. The concentration in fish flesh has usually been calculated using the aggregate, one-parameter transfer factor model (see Volume 2 of SENES (1985)).

The transport of radionuclides in the surface water system involves both dilution with fresh water flow and transfer to mineral and biological solids. The transfer to solid matter is often a reversible process, hence, the radionuclides may return to the aqueous phase as conditions change. These mechanisms were included in the model developed in Phase III for modelling the behaviour of all radionuclides in the lakes of the watershed (SENES, 1986).

Ingrowth and decay of radionuclides held in the waters and sediments of the watershed were assessed to be important only for the relatively short-lived radionuclides: radium-226 and lead-210. Since water is flushed from the lakes and rivers in a comparatively short time (i.e. a matter of years) and sedimenting solids also are buried in the deep lake sediments in a short time (i.e. in tens of years), the change in inventory due to radioactive decay in the water column or exchangeable sediment for the long-lived radionuclides, such as uranium and thorium, is inconsequential. The approach taken to modelling the ingrowth and decay of the radioactive species, therefore, was to disregard these processes for the long-lived species (i.e. uranium and thorium) but to take them into account for the relatively short-lived radionuclides considered in this study (i.e. radium-226 and lead-210). Furthermore, the processes of radioactive ingrowth and decay were accounted for in a simplified fashion by adjusting the inventories at the start of each time-step for the elapsed time since the end of the last step rather than incorporating the processes directly into the differential equations for calculating mass balance. This simplification reduced the complexity of the equation and is believed to introduce minimal error. The approach is also consistent with the approach taken in this study to developing assessment level models. Details of the approach used to incorporate radioactive ingrowth and decay are presented at the end of Section 10.6.

10.6.1 River Segments

A simple approach was chosen to model radionuclide behaviour in the river segments of the watershed. The algorithm for the river reaches considers only dilution. Transfer to bottom sediment is ignored. The rationale for this simplification is as follows:

- While sediment will deposit on the bottom of the river segments during low flow conditions, sediment will also be resuspended from the river bed during high flow periods and be transported downstream. Over the time scale of the assessment, the net result would be that most, if not all, of the sediment is transported to the nearest downstream lake.
- Watersheds on the Canadian Precambrian Shield typically contain several lakes. The quiescent conditions in the lakes present a natural sink for the sediment-bound radionuclides.

The simple mass balance equation used to calculate radionuclide levels at river nodes is as follows:

$$[R_i]_{n,t} = \frac{Q_{n-1,t}[R_i]_{n-1,t} + Q_{s,t}\,[R_i]_{s,t}}{Q_{n,t}} \qquad (10.9)$$

where

$Q_{n-1,t}$ = volume of surface water flow at node 'n-1' at time 't' ($m^3.yr^{-1}$)

$Q_{n,t}$ = volume of surface water flow at node 'n' at time 't' ($m^3.yr^{-1}$)

$Q_{s,t}$ = volume of the tailings source term discharge 's' from the tailings area at time 't' ($m^3.yr^{-1}$)

$[R_i]_{n-1,t}$ = concentration of radionuclide 'i' in the surface water flow at node 'n-1' at time 't' ($Bq.m^{-3}$)

$[R_i]_{n,t}$ = concentration of radionuclide 'i' in the surface water flow at node 'n' at time 't' ($Bq.m^{-3}$)

$[R_i]_{s,t}$ = concentration of radionuclide 'i' in the tailings source term discharge 's' from the tailings area at time 't' ($Bq.m^{-3}$).

The above formulation excludes the natural background activity of the radionuclides which is consistent with the methodology employed for calculating incremental dose to reference man. The radionuclide content in the tailings source term discharges includes dissolved species in the surface and subsurface flows originating from the tailings area and sediment-bound species associated with the solids eroded from the tailings surface. Equation (10.9) does not distinguish between the dissolved and solid fraction of the radionuclides. Removal of radionuclides with sedimenting solids is accounted for in the lake model.

10.6.2 Lake Segments

Modelling Approach

Radionuclides are introduced into the lakes of the reference watershed with the inflow from the upstream watershed. Removal of radionuclides from the aqueous phase occurs through transfer to suspended solids including inorganic solids and organic matter (e.g. aquatic biota) and direct transfer to bottom sediment. Ultimately that portion of the radionuclides which transfer to the suspended solids enters the lake sediments as the solids settle out of the water column. As a result of the oxidation of organic matter at the lake bottom, however, a portion of the radionuclides are released from the sediment solids to the sediment interstitial water from which they may diffuse back to the lake water column. The remaining fraction of the solid-bound radionuclides eventually become buried in the sediment and thus are unavailable for exchange with the water column.

A conceptual schematic of the lake sediment model is shown in Figure 10.2 and comprises two active compartments, the water column and the exchangeable sediment. The basic parameters defined for the assessment of radionuclide transfer between the water column and sediment are given as follows:

h_n = mean depth of water column of the lake designated node 'n' (m)
λ = thickness of the sediment exchange zone (m)
$[R_i]_{n,t}$ = activity concentration of radionuclide 'i' in the water column of lake 'n' at time 't' ($Bq.m^{-3}$)
$[R_i]_{1,t}$ = average activity concentration of radionuclide 'i' in the interstitial water of the exchanging sediment of lake 'n' at time 't' ($Bq.m^{-3}$)
$[R_i]_{\lambda,t}$ = activity concentration of radionuclide 'i' at depth 'λ' in the sediment interstitial water of lake 'n' at time 't' ($Bq.m^{-3}$)
u = current velocity in lakes of the watershed ($m.yr^{-1}$).

The accumulation of radionuclides (as a flux term) in the exchangeable sediment (thickness = λ) is given by:

$$\frac{\lambda d[R_i]_{1,t}}{dt} = \underbrace{[\sigma_{s,n}k_{d,i}[R_i]_{n,t}]}_{\substack{\text{deposition flux}\\ \text{of radionuclide 'i' in}\\ \text{fresh sedimenting}\\ \text{matter}}} - \underbrace{[k_{L,n}([R_i]_{\lambda,t}-[R_i]_{n,t})]}_{\substack{\text{flux of radionuclide}\\ \text{'i' from sediment}\\ \text{into the water}\\ \text{column}}} - \underbrace{[\sigma_{D,n}k_{d,i}[R_i]_{\lambda,t}]}_{\substack{\text{flux of radionuclide 'i'}\\ \text{out of the exchange}\\ \text{zone due to continuous}\\ \text{deposition of sediment}\\ \text{(i.e. loss due to burial)}}} \qquad (10.10)$$

where

$\sigma_{s,n}$ = rate of sedimenting material removal from the lake water column ($g.m^{-2}.yr^{-1}$)
$k_{d,i}$ = distribution coefficient for radionuclide 'i' between sedimenting material (both organic and inorganic fractions) and lake water ($m^3.g^{-1}$)
$k_{L,n}$ = mass transfer coefficient of the radionuclides into the lake water column from the sediment in lake 'n' ($m.yr^{-1}$)

FIGURE 10.2

CONCEPTUAL SCHEMATIC
OF REFERENCE LAKE

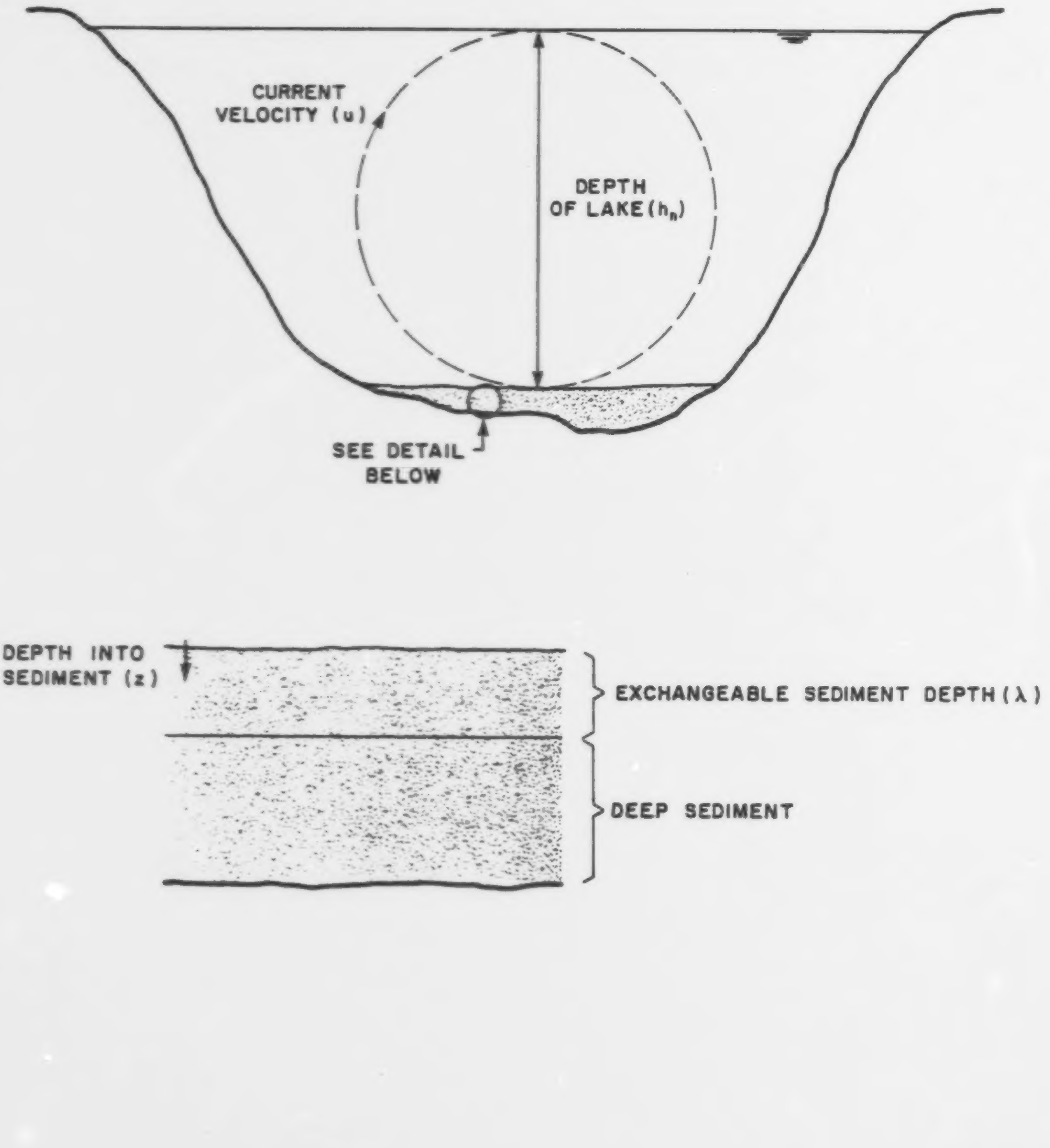

$\sigma_{D,n}$ = rate of sediment burial (or removal from the active exchange layer) ($g.m^{-2}.yr^{-1}$).

Collecting the lake water column concentration terms ($[R_i]_{n,t}$) in equation (10.10) yields:

$$\lambda \frac{d[R_i]_{1,t}}{dt} = \underbrace{[(\sigma_{s,n}k_{d,i}+k_{L,n})[R_i]_{n,t}]}_{\substack{\text{apparent net deposition} \\ \text{(settling and diffusion)}}} - [k_{L,n}[R_i]_{\lambda,t}] - [\sigma_{D,n}k_{d,i}\,[R_i]_{\lambda,t}] \qquad (10.11)$$

Sediment Characteristics

The lakes of the reference watershed are assumed to be oligotrophic, hence the sedimentation rate is characteristic of a low productivity lake environment. For a net primary biomass production on a dry weight solids basis of 100 $g.m^{-2}.yr^{-1}$ (range 40 to 200 $g.m^{-2}.yr^{-1}$) (Wetzel, 1975) and an organic content of 55% in the sedimenting solids, the total biomass sedimentation flux equals 180 $g.m^{-2}.yr^{-1}$.

The sedimenting material comprises not only that resulting from biomass production but also the suspended solids load carried in surface runoff from the watershed. The contribution of the inflow surface runoff to the sedimentation flux is dependent on the size of the sub-basin drainage areas and the suspended solids content of the surface runoff. Runoff from undisturbed Canadian Shield watersheds typically has a low suspended solids content of about 3 $g.m^{-3}$ (range 1 to 15 $g.m^{-3}$) comprised of both organic and inorganic fractions.

The sedimentation flux to each of the lakes in the reference watershed for a mean annual runoff of 0.4 $m.yr^{-1}$ was assessed given the above data on sedimenting material and the lake surface and drainage basin areas reported previously in Table 10.1. The calculated flux values are reported on Table 10.2 The nominal sedimentation fluxes of 210 to 260 $g.m^{-2}.yr^{-1}$ equate to sedimentation rates of 0.0020 to 0.0024 $m.yr^{-1}$ (0.20 to 0.24 $cm.yr^{-1}$) assuming an average solids density of $1.84x10^6$ $g.m^{-3}$ and a porosity of 94 percent. Similarly the minimum and maximum values of 85 and 765 $g.m^{-2}.yr^{-1}$ equate to sedimentation rates of 0.0008 and 0.0069 $m.yr^{-1}$ (0.08 to 0.69 $cm.yr^{-1}$). These rates are comparable to net sediment deposition velocities reported in the literature for Canadian Shield lakes of 0.0007 to 0.0080 $m.yr^{-1}$ (0.07 to 0.8 $cm.yr^{-1}$) (Kipphut, 1978). The sedimentation fluxes of total solids are specified as triangular distributions in the model using the nominal, minimum and maximum values given in Table 10.2 for each lake.

In addition to the above, the solids eroded from the reference tailings area are added to the solids loading on the upstream receiving lake (i.e. node 2). The solids loading (T_m), calculated in the source term component (see Section 3.14), is converted into a sediment flux in the lake model component and added to the flux values reported in Table 10.2.

On deposition on the lake bottom, the organic content of sedimented material undergoes continuous decomposition thus reducing the organic fraction. Typically, stabilized lake sediment in Canadian Shield Lakes contains between 20 and 50 percent organic matter. Sediments collected in the Elliot Lake and Wollaston Lake areas (Swanson 1985) had an average organic content of about 25%. This is a sharp reduction from the 55% organic fraction characteristic of fresh sedimenting material. The reduction is reflected in the flux of stable sediment out of the exchange zone into the deep sediment. For an average 55% organic content in the settling solids and 25% in the stabilized solids, the rate of sediment burial ($\sigma_{D,n}$) equals about 60% of the rate of sedimenting material ($\sigma_{s,n}$). On a more general level, the rate of sediment burial may be expressed as a function of the rate of sediment removed from the water column as follows:

$$\sigma_{D,n} = f_s \sigma_{s,n} \qquad (10.12)$$

Table 10.2

LAKE SEDIMENTATION FLUX VALUES

Lake Node Number	Lake Surface Area (m^2)	Contributing Drainage Area (m^2)	Sedimentation Flux ($g.m^{-2}.yr^{-1}$) Runoff Solids	Biomass Solids	Total Solids Values Nominal	Minimum	Maximum
2	5.0E5	2.0E7	50	180	230	95	615
4	2.5E5	1.8E7	80	180	260	105	765
7	4.0E6	1.02E8	30	180	210	85	515

where

f_s = the fraction of sedimenting material ultimately removed to the deep sediment.

This relationship has been incorporated into the lake model component. The fraction of sedimenting material entering the deep sediment (f_s) was estimated to range from 0.5 to 0.7 for the reference lakes. As previously reported, a nominal value of 0.6 was used.

The densities of the individual components of stable sediment were assumed to be:

$$\rho_{inorganic} = 2.45 \text{ g.cm}^{-3} \text{ or } 2.45 \times 10^6 \text{ g.m}^{-3}$$

$$\rho_{organic} = 1.05 \text{ g.cm}^{-3} \text{ or } 1.05 \times 10^6 \text{ g.m}^{-3}$$

On the basis of 1 g sediment having an organic content of 25%, the true density of stabilized sediment solids was determined as follows:

$$\rho_s = \left[\frac{1 \text{ g}}{\frac{0.25 \text{ g}}{1.05 \text{ g.cm}^{-3}} + \frac{0.75 \text{ g}}{2.45 \text{ g.cm}^{-3}}} \right] = 1.84 \text{ g.cm}^{-3} \text{ or } 1.84 \times 10^6 \text{ g.m}^{-3}$$

To calculate the volume fraction of solids (ϵ_s), a moisture content of 89% by weight was used based on the results of the field studies reported by Swanson (1985). For a moisture density of 1.0 g.cm^{-3} and a solids density of 1.84 g.cm^{-3}, the volume fraction occupied by the solids equals:

$$\epsilon_s = \left[\frac{\frac{0.11 \text{ g solid}}{1.84 \text{ g.cm}^{-3}}}{\frac{0.11 \text{ g solid}}{1.84 \text{ g.cm}^{-3}} + \frac{0.89 \text{ g } H_2O}{1.00 \text{ g.cm}^{-3}}} \right] = 0.06 \text{ cm}^3.\text{cm}^{-3}$$

Thus the porosity, volume fraction of liquid , equals:

$$\begin{aligned}\epsilon &= 1-0.06\\ &= 0.94\ \mathrm{cm}^3.\mathrm{cm}^{-3}\end{aligned}$$

The bulk density of sediment therefore may be calculated as follows:

$$\begin{aligned}\rho &= (1.84)\ (0.06) + 1.00\ (0.94)\\ &= 1.05\ \mathrm{g.cm}^{-3}\end{aligned}$$

These calculated porosity and bulk density values compare favourably with literature data for Canadian Shield lakes which have a reported bulk density of 1.02 to 1.10 g.cm^{-3} and a porosity of 0.83 to 0.97 cm^3.cm^{-3} (Beak, 1982).

Distribution Coefficients

Radionuclides entering freshwater environments may be removed by one or more mechanisms on organic and inorganic matter. The removal mechanisms usually cited include ion exchange, adsorption and precipitation. Because the magnitude of these processes can seldom be quantified separately, however, the overall removal process is usually expressed in terms of a distribution coefficient, k_d. The concept of k_d was developed from ion-exchange theory to represent the equilibrium distribution of a trace constituent between the solid exchange media and the solution. In the broader sense as it is applied to environmental and waste management studies, it is defined as:

$$k_d = \frac{\text{amount of radionuclide sorbed on solid phase}}{\text{amount of radionuclide left in solution}}$$

Values of k_d reported in the literature vary widely for all radionuclides. The variability is dependent on many factors including the nature of the solid material. The radionuclide k_d values reported for river and lake sediments are generally much higher than what is normally cited for geological materials. The difference may be due to the fine nature of the solids and the fact that they contain a significant organic content.

The sediment/water data base reviewed in establishing $k_{d,i}$ values for the radionuclides for use in the watershed model was derived mainly from the work by Swanson (1984, 1985). The $k_{d,i}$ values for all radionuclides were assumed to be lognormally distributed, an assumption which is consistent with other reported work on this subject. The attributes of the distributions given in Table 10.3 for uranium, radium-226 and lead-210 were used in the model.

Thorium is believed to be removed mainly as a precipitate. As such, its removal is pH dependent. The formulation used in the surface water model to calculate thorium removal as a function of pH is as follows:

$$k_{d,Th} = 2.0 \times 10^{-3} + k'_{d,Th} (pH_{n,t} - 4.0) \qquad \text{for pH} \geq 4.0 \qquad (10.13)$$
$$k_{d,Th} = 2.0 \times 10^{-3} \qquad \text{for pH} < 4.0$$

where

$k'_{d,Th}$ = the slope of the linear function relating the distribution coefficient ($k_{d,Th}$) to pH ($m^3.g^{-1}$). The distribution attributes of $k'_{d,Th}$, assuming a lognormal distribution, were assessed as follows:
geometric mean = 2.0×10^{-2}
geometric standard deviation = 2.5
minimum = 2.0×10^{-3}
maximum = 3.0×10^{-1}

$pH_{n,t}$ = the pH of the lake designated by node 'n' at time 't'

$k_{d,Th}$ = the distribution coefficient for thorium removal on sedimenting matter ($m^3.g^{-1}$)

Mass Transfer Coefficient

To estimate the range of the mass transfer coefficient ($k_{L,n}$ in equation (10.10)), it was assumed that the organic content decays rapidly at the sediment surface before significant burial by fresh sedimenting material occurs. In this case, mass transfer is controlled by a laminar-flow film next to the sediment boundary. The estimation of the mass transfer coefficient requires the application of Fick's law for unsteady state diffusion:

$$\frac{\delta [R_i]_{1,t}}{\delta t} = - D\left(\frac{\delta^2 [R_i]_{1,t}}{\delta z^2}\right) \qquad (10.14)$$

where

D = diffusivity coefficient ($m^2.yr^{-1}$)

z = the depth of penetration into the sediment (m).

Equation (10.14) has been solved by Higbie (1935) by applying his penetration theory for diffusion into a "semi-infinite" medium represented by the water column above a flat (sediment) surface as follows:

$$k_{L,n} = \sqrt{\frac{D}{\tau}} \qquad (10.15)$$

where

τ = the surface renewal time (yr).

This requires an evaluation of the surface renewal time. An approximate value for surface renewal may be taken as a function of the mean depth "h_n" (or depth of the hypolimnion during stratification) and mean current velocity "u":

$$\tau = \frac{\pi h_n}{u} \qquad (10.16)$$

In relation to the schematic shown on Figure 10.2, the diffusion out of the sediment exchange layer may be equated as:

$$\left(\begin{array}{c}\text{rate of diffusion}\\ \text{through sediment}\end{array}\right) = \left(\begin{array}{c}\text{rate of transport}\\ \text{from surface of}\\ \text{sediment}\end{array}\right)$$

which translates to:

$$D\left(\frac{d^2[R_i]_{1,t}}{dz^2}\right) = \left(\frac{u}{\pi h_n}\right)[R_i]_{n,t} \qquad (10.17)$$

Table 10.3

SEDIMENT TO WATER k_d VALUES ($m^3.g^{-1}$)
(dry weight basis)

Radionuclide	Geo. Mean	Geo. Std. Dev.	Minimum	Maximum
Uranium	4.5×10^{-3}	2.2	0.4×10^{-3}	4.8×10^{-2}
Radium-226	6.5×10^{-3}	2.5	0.4×10^{-3}	1.0×10^{-1}
Lead-210	15.0×10^{-3}	2.5	1.0×10^{-3}	2.3×10^{-1}

The approximate solution to equation (10.17) is given by:

$$\left.\frac{d[R_i]_{1,t}}{dz}\right|_{z=0} = \left(\frac{u}{\pi D h_n}\right)^{1/2} ([R_i]_{\lambda,t} - [R_i]_{n,t}) \qquad (10.18)$$

or

$$\text{Flux} = D \left.\frac{d[R_i]_{1,t}}{dz}\right|_{z=0} = \left(\frac{uD}{\pi h_n}\right)^{1/2} ([R_i]_{\lambda,t} - [R_i]_{n,t})$$

$$= k_{L,n} ([R_i]_{\lambda,t} - [R_i]_{n,t})$$

where $k_{L,n} = \left(\frac{uD}{\pi h_n}\right)^{1/2}$

Equation (10.18), known as the Dobbins-O'Connor relationship, has been used successfully to describe mass transfer in lakes and rivers (Bailey and Ollis, 1977). Typical values for the parameters in equation (10.18) are:

$D = 6.36 \times 10^{-6}$ cm^2.s^{-1} = 0.02 m^2.yr^{-1}
$u = 0.1$ to 1.0 cm.s^{-1} = 3.15×10^4 to 3.15×10^5 m.yr^{-1}

To assess the effect of lake depth (h_n) on the mass transfer coefficient ($k_{L,n}$), the mean depths of 4, 5 and 10 m for the lakes of the reference watershed were selected. Using extreme values for the current velocity, $k_{L,n}$ values were calculated as given on Table 10.4. The $k_{L,n}$ values presented in the table are seen to range from about 4.5 to 22.4 m.yr^{-1}.

Derivation of Rate Constants

The rate of change of the total activity of the radionuclides in the water column and sediments can be expressed as follows:

$$\frac{d\{R_i\}_{n,t}}{dt} = k_{2,i}\{R_i\}_{1,t} - k_{1,i}\{R_i\}_{n,t} \qquad (10.19)$$

and

$$\frac{d\{R_i\}_{1,t}}{dt} = k_{1,i}\{R_i\}_{n,t} - k_{2,i}\{R_i\}_{1,t} - k_{3,i}\{R_i\}_{1,t} \qquad (10.20)$$

where

$\{R_i\}_{n,t}$ = the activity of radionuclide 'i' in the water column at time 't' (Bq)

$\{R_i\}_{1,t}$ = the average activity of radionuclide 'i' in the sediment exchange zone at time 't' (Bq)

$k_{1,i}$ = the rate of radionuclide 'i' removal from the water column to the sediment (yr^{-1})

$k_{2,i}$ = the rate of radionuclide 'i' introduction back to the water column from the sediment (yr^{-1})

$k_{3,i}$ = the rate of loss of radionuclide 'i' to deep sediment, i.e. the rate of burial (yr^{-1})

By definition, the activity of radionuclide 'i' in the sediment is given by:

$$\{R_i\}_{1,t} = L_n\lambda\,[k_{d,i}\,\rho_s\,(1-\epsilon) + \epsilon]\,[R_i]_{1,t} \qquad (10.21)$$

where

L_n = surface area of lake 'n' (m^2)

ρ_s = density of stabilized solids ($g.m^{-3}$)

ϵ = sediment porosity ($m^3.m^{-3}$)

$\lambda, K_{d,i}$ and $[R_i]_{1,t}$ are as defined previously.

In the water column, the activity of radionuclide 'i' equals:

$$\{R_i\}_{n,t} = L_n h_n [R_i]_{n,t} \qquad (10.22)$$

In equation (10.21), $[R_i]_{1,t}$ is unknown, but our best estimate is:

$$[R_i]_{1,t} = \frac{[R_i]_{n,t} + [R_i]_{\lambda,t}}{2} = \left[\frac{\dfrac{[R_i]_{\lambda,t}}{1.1} + [R_i]_{\lambda,t}}{2}\right] \qquad (10.23)$$

$$= 0.95\,[R_i]_{\lambda,t}$$

Table 10.4

ASSESSED MASS TRANSFER COEFFICIENT VALUES

Mean Lake Depth (m)	Diffusivity Coefficient ($m.yr^{-1}$)	Mean Lake Current Velocity ($m.yr^{-1}$)	Mass Transfer Coefficient ($m.yr^{-1}$)
4	0.02	3.15×10^4	7.1
4	0.02	3.15×10^5	22.4
5	0.02	3.15×10^4	6.3
5	0.02	3.15×10^5	20.0
10	0.02	3.15×10^4	4.5
10	0.02	3.15×10^5	14.2

where

$[R_i]_{n,t} = [R_i]_{\lambda,t} \div 1.1$ represents the average expected concentration differential at steady state.

Rearranging equation (10.23) we get:

$$[R_i]_{\lambda,t} = \frac{[R_i]_{1,t}}{0.95} = 1.05\,[R_i]_{1,t}$$

Substitution into equation (10.10) yields:

$$\lambda \frac{d[R_i]_{1,t}}{dt} = [\sigma_{s,n}\, k_{d,i}[R_i]_{n,t}] - [k_{L,n}\,(1.05[R_i]_{1,t} - [R_i]_{n,t})] - [\sigma_{D,n}k_{d,i}\; 1.05[R_i]_{,1,t}] \qquad (10.24)$$

Multiplying equation (10.24) by the area L_n and re-ordering we get:

$$\frac{\lambda L_n d[R_i]_{1,t}}{dt} = [(\sigma_{s,n}k_{d,i} + k_{L,n})L_n[R_i]_{n,t}] - [\,1.05k_{L,n}\, L_n[R_i]_{1,t}] - [1.05\sigma_{D,n}k_{d,i}L_n[R_i]_{1,t}] \qquad (10.25)$$

Comparing equation (10.25) to equation (10.20), it is seen that:

$$\lambda L_n \frac{d[R_i]_{1,t}}{dt} = \frac{d\{R_i\}_{1,t}}{dt}$$

Thus collecting the terms for $\{R_i\}_{n,t}$ and $\{R_i\}_{1,t}$ yields:

$$k_{1,i} = \frac{\sigma_{s,n}k_{d,i} + k_{L,n}}{h_n} \qquad (10.26)$$

$$k_{2,i} = \frac{1.05\; k_{L,n}}{\lambda[k_{d,i}\; \rho_s\; (1-\epsilon\,) + \epsilon\,]} \qquad (10.27)$$

$$k_{3,i} = \frac{1.05\,\sigma_{D,n}\,k_{d,i}}{\lambda[k_{d,i}\,\rho_s(1-\epsilon)+\epsilon]} \tag{10.28}$$

The rates of radionuclide exchange between the water column and the sediment (given by $k_{1,i}$ and $k_{2,i}$) and the rate of permanent loss to the deep sediment (given by $k_{3,i}$) can be determined by substitution of appropriate values for the independent parameters in equations (10.26), (10.27) and (10.28).

Model Implemented

As previously noted, the behaviour of the uranium series radionuclides in the lakes is modelled on a activity basis to permit removal from the water column and feedback from the sediment to be followed with time. The accumulation of radionuclides in the lake water column may be represented by the following expression:

$$\frac{d\{R_i\}_{n,t}}{dt} = Q_{n-1,t}[R_i]_{n-1,t} - \left(k_{1,i} + \frac{1}{d_{n,t}}\right)\{R_i\}_{n,t} + k_{2,i}\{R_i\}_{1,t} \tag{10.29}$$

where

$[R_i]_{n-1,t}$ = activity concentration of radionuclide 'i' in the inflow to the lake at node 'n-1' at time 't' ($Bq.m^{-3}$)

$\{R_i\}_{n,t}$ = activity of radionuclide 'i' in the water column of lake 'n' at time 't' (Bq)

$\{R_i\}_{1,t}$ = activity of radionuclide 'i' in the exchange zone of the lake sediment at time 't' (Bq)

$k_{1,i}$ = rate of radionuclide 'i' removal from the lake water column to the lake sediment (yr^{-1})

$k_{2,i}$ = rate of radionuclide 'i' release from the lake sediment to the lake water column (yr^{-1})

$d_{n,t} = \frac{V_n}{Q_{n,t}}$ = retention time (or travel time) in the lake designated by node 'n' at time 't' (yr)

$Q_{n-1,t}$ = volumetric surface water flow at node 'n-1' at time 't' ($m^3.yr^{-1}$)

$Q_{n,t}$ = volumetric surface water flow at node 'n', the lake outflow, at time 't' ($m^3.yr^{-1}$)

$V_n = L_n h_n$ = volume of the lake designated by node 'n' at time 't' (m^3)

L_n = surface area of lake 'n' (m^2)

h_n = mean depth of lake 'n' (m).

Similarly, the changing inventory of radionuclides in the lake sediment is given by equation (10.20), restated as:

$$\frac{d\{R_i\}_{1,t}}{dt} = k_{1,i}\{R_i\}_{n,t} - (k_{2,i} + k_{3,i})\{R_i\}_{1,t} \qquad (10.30)$$

where

$\{R_i\}_{1,t}$ = average activity of radionuclide 'i' in the exchange zone of the lake sediment at time 't' (Bq)

$k_{3,i}$ = rate of radionuclide 'i' removal (burial) to deep lake sediment (yr^{-1}).

At time t=0, the initial radionuclide content of the lake water column and sediment is:

$$\{R_i\}_{n,t=0} = 0$$
$$\{R_i\}_{1,t=0} = 0$$

The term of interest is the activity concentration of radionuclide 'i' in the lake.

Once the activity $\{R_i\}_{n,t}$ is obtained, the concentration is given by:

$$[R_i]_{n,t} = \frac{\{R_i\}_{n,t}}{V_n} \qquad (10.31)$$

The two differential equations given above may be restated in matrix notation:

$$\begin{array}{l} \frac{d\{R_i\}_{n,t}}{dt} = \\ \\ \frac{d\{R_i\}_{1,t}}{dt} = \end{array} \begin{bmatrix} a_{11} & -a_{12} & +a_{13} \\ & & \\ a_{21} & a_{22} & -a_{23} \end{bmatrix} \begin{bmatrix} 1 \\ R_{i\ n,t} \\ R_{i\ 1,t} \end{bmatrix}$$

where

$a_{11} = Q_{n-1,t}\,[R_i]_{n-1,t}$ $\qquad a_{21} = 0$

$a_{12} = k_{1,i} + \frac{1}{d_{n,t}}$ $\qquad a_{22} = k_{1,i}$

$a_{13} = k_{2,i}$ $\qquad a_{23} = k_{2,i} + k_{3,i}$

The general solution is:

$$\{R_i\}_{n,t} = K_{n,i} + D_i \exp(Z_{1,i}\,\Delta t) + (X_{i,t} - D_i) \exp(Z_{2,i}\,\Delta t) \qquad (10.32)$$

$$\{R_i\}_{1,t} = K_{1,i} + B_i \exp(Z_{1,i}\,\Delta t) + (Y_{i,t} - B_i) \exp(Z_{2,i}\,\Delta t) \qquad (10.33)$$

where

$$K_{n,i} = \frac{a_{11}a_{23}}{a_{12}a_{23} - a_{22}a_{13}}$$

$$K_{1,i} = \frac{a_{11}a_{22}}{a_{12}a_{23} - a_{13}a_{22}}$$

$$Z_{1,i} = -\frac{(a_{12} + a_{23}) + \sqrt{(a_{12} + a_{23})^2 + 4(a_{13}a_{22} - a_{12}a_{23})}}{2}$$

$Z_{2,i} = -(a_{12} + a_{23} + Z_{i,1})$

$X_{i,t} = \{R_i\}_{n,t-\Delta t} - K_{n,i}$

$Y_{i,t} = \{R_i\}_{1,t-\Delta t} - K_{1,i}$

$$D_i = \left[\frac{a_{13} + a_{23} + Z_{1,i}}{(a_{12}+a_{22}) - (a_{13}+a_{23})}\right]\left[\frac{(a_{12}+a_{22}+Z_{2,i})\, X_{i,t} - (a_{13}+a_{23}+ Z_{2,i})Y_{i,t}}{\sqrt{(a_{12}+a_{23})^2 + 4(a_{13}a_{22}-a_{12}a_{23})}}\right]$$

and

$$B_i = \left[\frac{a_{12} + a_{22} + Z_{1,i}}{a_{13} + a_{23} + Z_{1,i}}\right] D_i$$

Radioactive Ingrowth and Decay

The approach adopted in the source term component model (see Chapter 3) to account for radioactive ingrowth and decay has been employed directly in the surface water dispersion model. Briefly, radioactive decay and ingrowth of natural uranium and thorium are not modelled as the effects on the activity inventories are inconsequential when one considers the long half-lives of these radionuclides and the magnitudes of the competing processes that affect their retention in the watershed. For radium-226 and lead-210, radioactive ingrowth and decay are potentially more important and are accounted for in the activity inventories retained within the lake water columns and sediments. These processes are not accounted for in the river segments.

The radioactive decay processes are included by correcting the activity inventories of radium-226 and lead-210 calculated from equations (10.32) and (10.33) each time-step. Specifically, the correction is made by adjusting the values of $X_{i,t}$ and $Y_{i,t}$ (since these terms include the radionuclide activities from the previous timestep) in the equations as follows:

$$X_{i,t} = \}R_i\{^{*}_{n,t-\Delta t} - K_{n,i}$$

and

$$Y_{i,t} = \}R_i\{^{*}_{1,t-\Delta t} - K_{1,i}$$

where, for lead-210:

$$\}R_{Pb-210}\{^{*}_{n,t-\Delta t} = \left[\}R_{Pb-210}\{_{n,t-\Delta t} \exp(-\lambda_{Pb-210} d_{n,t-\Delta t})\right] + \left[\}R_{Ra-226}\{_{n,t-\Delta t} \left(\frac{\lambda_{Pb-210}}{\lambda_{Pb-210} - \lambda_{Ra-226}}\right) (\exp(-\lambda_{Ra-226} d_{n,t-\Delta t}) - \exp(-\lambda_{Pb-210} d_{n,t-\Delta t}))\right]$$

$$\}R_{Pb-210}\{^{*}_{1,t-\Delta t} = \left[\}R_{Pb-210}\{_{1,t-\Delta t} \exp(-\lambda_{Pb-210} \Delta t)\right] + \left[\}R_{Ra-226}\{_{1,t-\Delta t} \left(\frac{\lambda_{Pb-210}}{\lambda_{Pb-210} - \lambda_{Ra-226}}\right) (\exp(-\lambda_{Ra-226} \Delta t) - \exp(-\lambda_{Pb-210} \Delta t))\right]$$

and for Ra-226:

$$\}R_{Ra-226}\{^{*}_{n,t-\Delta t} = \left[\}R_{Ra-226}\{_{n,t-\Delta t} \exp(-\lambda_{Ra-226} d_{n,t-\Delta t})\right] + \left[(XA_{Th-230/Th,sol})\}R_{Th}\{_{n,t-\Delta t} \left(\frac{\lambda_{Ra-226}}{\lambda_{Ra-226} - \lambda_{Th-230}}\right) (\exp(-\lambda_{Th-230} d_{n,t-\Delta t}) - \exp(-\lambda_{Ra-226} d_{n,t-\Delta t}))\right]$$

$$\}R_{Ra-226}\{^{*}_{\ell,t-\Delta t} = \left[\}R_{Ra-226}\{_{\ell,t-\Delta t} \exp(-\lambda_{Ra-226} \Delta t)\right] + \left[(XA_{Th-230/Th}) \}R_{Th}\{_{\ell,t-\Delta t} \left(\frac{\lambda_{Ra-226}}{\lambda_{Ra-226} - \lambda_{Th-230}}\right) (\exp(-\lambda_{Th-230} \Delta t) - \exp(-\lambda_{Ra-226} \Delta t))\right]$$

where

$XA_{Th-230/Th,sol}$ = the activity fraction of Th-230 in soluble thorium.

The first term on the right hand side of the above expressions accounts for radioactive decay of lead-210 and radium-226 respectively. The second term on the right hand side accounts for the net ingrowth of lead-210 from radium-226 and of radium-226 from thorium-230 respectively. The incorporation of these corrections is a relatively straight-forward method of including radioactive decay and ingrowth though not fundamentally rigorous. The approach is consistent with the concept of assessment level models.

10.7 Parameter Values and Code Listing

A summary of all parameters included in the surface water dispersion models is provided in Table 10.5. Parameter values and their distributions are specified for the input parameters on the table. The basis for the specified values are discussed in the appropriate sections in the text of Chapter 10.

A copy of the code for calculating pH, major ion and radionuclide levels in the surface water system is included in Table 10.6 for the interested reviewer. Certain features of the code (e.g. calculation of the circumference of lakes) are included for use in the aquatic transfer models discussed in Chapter 11.

10.8 Surface Water Dispersion Models Test Program

A series of tests were performed to check the surface water dispersion models for computational accuracy and reasonableness. The tests were made on both deterministic and probabilistic output results. The tests included hand calculations to confirm that the river and lake models executed the equations properly. The models were also run probabilistically with the results checked for reasonableness.

10.9 References

Baily, J.E., and Ollis, D.F., 1977. "Biochemical Engineering Fundamentals." McGraw Hill Book Company, Toronto.

Beak Consultants Limited, 1982. "An Approach to Long Term Aquatic Modelling of a Generic Uranium Tailings Site." Draft Report to the Atomic Energy Control Board, Ottawa.

Higbie, R. 1935. Transactions of AIChE, Vol. 35, pp. 365-372.

Kipphut, G.W., 1978. "An Investigation of Sedimenting Processes in Lakes." Ph.D. Thesis, Columbia University.

Ontario Ministry of the Environment, 1972 to 1980. "Water Quality Data, Ontario Lakes and Streams." Annual Reports Prepared by the Water Resources Branch, Toronto.

SENES Consultants Limited and Golder Associates Limited, 1981. "Quirke Lake Tailings Disposal Study, Stage 1 Background Information." Draft Report to Rio Algom Limited and Denison Mines Limited.

SENES Consultants Limited and Saskatchewan Research Council (SRC), 1984. "A Study of the Distribution of Naturally Occurring Radionuclides in Freshwater Benthos and Their Environment - Phase I." Research Report to the National Uranium Tailings Program, CANMET, EMR, Ottawa. Under Supply and Services Canada Contract Number 0SQ83-00241.

SENES Consultants Limited, 1984. "A Study to Develop and Demonstrate Techniques for the Probabilistic Assessment of the Long-Term Effects of Uranium Mill Tailings in Canada - Phase I." Research Report prepared for the National Uranium Tailings Program, CANMET, EMR, under Supply and Services Canada Contract No. 0SQ83-00236.

Table 10.5

WATERSHED MODEL VARIABLES

Model Symbol	Description	Units	Nominal Value	Probability Distribution*	Computer Origin	Computer Symbol
$\sum_{1}^{n} A_n$	cumulative drainage area over the n sub-basins in the watershed	m^2	Site specific: see Table 10.1		INPUT	SHEDAR(n)
n	node number for the nth segment in the watershed (maximum of 10)	-	-	-	INPUT	WTSEG
P_t	mean annual net precipitation at time t	$m.yr^1$	0.4	N(0.4,0.1,0.1,0.65)	INPUT	NPRCP
$Q_{n-1,t}$	volume of surface water flow at node n-1 at time t	$m^3.yr^{-1}$	calculated	calculated	WATEX	FLOWQ(n-1)
$Q_{n,t}$	volume of surface water flow at node n at time t	$m^3.yr^{-1}$	calculated	calculated	WATEX	FLOWQ(n)
$Q_{s,t}$	volume of source term discharge s from reference tailings area at time t	$m^3.yr^{-1}$	calculated	calculated	SEXEC	SFLOW
$[Ca]_{n-1,t}$	calcium concentration in the flow at node n-1 at time t	$mol.m^{-3}$	calculated	calculated	WATEX	WATC(8,n-1)
$[Ca]_{n,t}$	calcium concentration in the flow at node n at time t	$mol.m^{-3}$	calculated	calculated	WATEX	WATC(8,n)
$[Ca]_B$	natural background calcium level in freshwater flow	$mol.m^{-3}$	0.1	C(0.1)	INPUT	WATCAB
$[Ca]_{s,t}$	calcium concentration in the source team discharge s from reference tailings at time t	$mol.m^{-3}$	calculated	calculated	SEXEC	WCONC(8,3,3)
$[SO_4]_{n-1,t}$	sulphate concentration in the flow at node n-1 at time t	$mol.m^{-3}$	calculated	calculated	WATEX	WATC(7,n-1)

Table 10.5 cont'd

Model Symbol	Description	Units	Nominal Value	Probability Distribution*	Computer Origin	Computer Symbol
$[SO_4]_{n,t}$	sulphate concentration in the flow at node n at time t	$mol.m^{-3}$	calculated	calculated	WATEX	WATC(7,n)
$[SO_4]_B$	natural background sulphate level in freshwater flow	$mol.m^{-3}$	0.071	C(0.071)	INPUT	WTSO4B
$[SO_4]_{s,t}$	sulphate concentration in the source term discharge s from reference tailings at time t	$mol.m^{-3}$	calculated	calculated	SEXEC	WCONC(7,3,3)
V_n	volume of the lake designated by node n	m^3	calculated	calculated	WATEX	LAKVOL(n)
L_n	surface area of lake designated by node n	m^2	Site specific: See Table 10.1		INPUT	LAREA(n)
h_n	mean depth of lake designated by node n	m	Site specific: See Table 10.1		INPUT	SDEPTH(n)
Δt	size of the time step specified for any run (values limited to 1 or 10)	yr	-	-	INPUT	DT
f	activity coefficients for watershed pH calculations	-	0.8	T(0.6,0.8,0.9)	INPUT	ACTCO
pH_n	pH of the surface water at node n in the watershed at time t	-	calculated	calculated	WATEX	WATPH(n)
$[R_i]_{n-1,t}$	activity concentration of radionuclide i in the surface water at node n-1 at time t	$Bq.m^{-3}$	calculated	calculated	WATEX	WATC(i,n-1)
$[R_i]_{n,t}$	activity concentration of radionuclide i in the surface water at node n at time t	$Bq.m^{-3}$	calculated	calculated	WATEX	WATC(i,n)
$[R_i]_{s,t}$	activity concentration of radionuclide i in the source term discharge s from the reference tailings area at time t	$Bq.m^{-3}$	calculated	calculated	SEXEC	WCONC(i,3,3)

Table 10.5 cont'd

Model Symbol	Description	Units	Nominal Value	Probability Distribution*	Computer Origin	Computer Symbol
$[R_i]_{I,t}$	average activity concentration of radionuclide i in the interstitial water of the sediment of lake n at time t	$Bq.m^{-3}$	calculated	calculated	WATEX	not used
$[R_i]_{\lambda,t}$	activity concentration of radionuclide i at depth λ in the sediment of lake n at time t	$Bq.m^{-3}$	calculated	calculated	WATEX	not used
u	current velocity in the lakes of the watershed	$m.yr^{1}$	1.7×10^{5}	$U(3.15\times10^{4},3.15\times10^{5})$	INPUT	CURRNT
λ	thickness of the sediment exchange zone in the lakes of the watershed	m	0.05	C(0.05)	INPUT	WTMIXD
s,n	rate of sedimenting material removal from the water column of the lake designated node n	$g.m^{-2}.yr^{-1}$	Lake specific: See Table 10.2		INPUT	WSIGS(k) where k is counter of lakes
D,n	rate of sediment burial or removal from the active exchange zone	$g.m^{-2}.yr^{-1}$	calculated	calculated	WATEX	WSIGD(k)
f_s	fraction of sedimenting material removed to the deep sediment	-	0.6	U(0.5,0.7)	INPUT	BURYF
$k_{d,i}$	radionuclide distribution coefficient from water to lake sediment for:	$m^3.g^{-1}$				
	uranium		4.5×10^{-3}	$LN(4.5\times10^{-3},2.2,0.4\times10^{-3},4.8\times10^{-2})$	INPUT	WKDU
	thorium		calculated	calculated	WATEX	WKDTH
	lead-210		1.5×10^{-2}	$LN(1.5\times10^{-2},2.5,1.0\times10^{-3},2.3\times10^{-1})$	INPUT	WKDPB
	radium-226		6.5×10^{-3}	$LN(6.5\times10^{-3},2.5,0.4\times10^{-3},1.0\times10^{-1})$	INPUT	WKDRA

Table 10.5 cont'd

Model Symbol	Description	Units	Nominal Value	Probability Distribution*	Computer Origin	Computer Symbol
$k'_{d,Th}$	slope of the linear function relating the thorium distribution coefficient to $pH_{n,t}$	$m^3.g^{-1}$	2.0×10^{-2}	$LN(2.0\times10^{-2},2.5,2.0\times10^{-3},3.0\times10^{-1})$		KDPRIM
$k_{L,n}$	mass transfer coefficient of the radionuclides into the water column of lake n from the sediments	$m.yr^{-1}$	calculated	calculated	WATEX	WATKL
ρ_s	density of stabilized sediment solids	$g.m^{-3}$	1.84×10^6	$C(1.84\times10^6)$	INPUT	WTRHOS
	sediment porosity, volume fraction of liquid	$m^3.m^{-3}$	0.94	T(0.83,0.94,0.97)	INPUT	WATEPS
D	diffusivity coefficient	$m^2.yr^{-1}$	0.02	C(0.02)	INPUT	DIFFC
$R_{i\ n,t}$	activity of radionuclide i in the water column of lake n at time t	Bq	calculated	calculated	WATEX	WATRW(i,n)
$R_{i\ n,t-\Delta t}$	activity of radionuclide i in lake sediment exchange zone at time t	Bq	calculated	calculated	WATEX	WATRW(i,n) calculated in previous time step
$R_{i\ 1,t}$	activity of radionuclide i in lake sediment exchange zone at time t	Bq	calculated	calculated	WATEX	WATRS(i,n)
$R_{i\ 1,t-\Delta t}$	activity of radionuclide i in lake sediment exchange zone at time t-Δt	Bq	calculated	calculated	WATEX	WATRS(i,n) calculated in previous time step
$k_{1,i}$	rate of radionuclide i removal from the lake water column	yr^{-1}	calculated	calculated	WATEX	K1

Table 10.5 cont'd

Model Symbol	Description	Units	Nominal Value	Probability Distribution*	Computer Origin	Computer Symbol
$k_{2,i}$	rate of radionuclide i release from exchangeable sediment back to the lake water column	yr^{-1}	calculated	calculated	WATEX	K2
$k_{3,i}$	rate of radionuclide loss to deep lake sediment	yr^{-1}	calculated	calculated	WATEX	K3
$d_{n,t}$	retention time (or travel time) in lake n at time t	yr	calculated	calculated	WATEX	DETIME
a_{11}	matrix parameters	-	calculated	calculated	WATEX	A11
a_{12}	matrix parameters	-	calculated	calculated	WATEX	A12
a_{13}	matrix parameters	-	calculated	calculated	WATEX	A13
a_{21}	matrix parameters	-	calculated	calculated	WATEX	A21
a_{22}	matrix parameters	-	calculated	calculated	WATEX	A22
a_{23}	matrix parameters	-	calculated	calculated	WATEX	A23
$K_{n,i}$	radionuclide i specific computed parameter	-	calculated	calculated	WATEX	KW
$K_{1,i}$	radionuclide i specific computed parameter	-	calculated	calculated	WATEX	KS
$X_{i,t}$	radionuclide i specific computed parameter	-	calculated	calculated	WATEX	X
$Y_{i,t}$	radionuclide i specific computed parameter	-	calculated	calculated	WATEX	Y
$Z_{1,i}$	radionuclide i specific computed parameter	-	calculated	calculated	WATEX	V1
$Z_{2,i}$	radionuclide i specific computed parameter	-	calculated	calculated	WATEX	V2

Table 10.5 cont'd

Model Symbol	Description	Units	Nominal Value	Probability Distribution*	Computer Origin	Computer Symbol
B_i	radionuclide i specific computed parameter	-	calculated	calculated	WATEX	BB
D_i	radionuclide i specific computed parameter	-	calculated	calculated	WATEX	AA
λ_{Th-230}	radioactive decay constant for Th-230	yr^{-1}	$8.66x10^{-6}$	$C(8.66x10^{-6})$	SOURCE (SUBROUTINE INCONN)	LAM230
λ_{Ra-226}	radioactive decay constant for Ra-226	yr^{-1}	$4.33x10^{-4}$	$C(4.33x10^{-4})$	SOURCE (SUBROUTINE INCONN)	LAMRAD
λ_{Pb-210}	radioactive decay constant for Pb-210	yr^{-1}	$3.3x10^{-2}$	$C(3.3x10^{-2})$	SOURCE (SUBROUTINE INCONN)	LAMPB
$XA_{Th-230/Th}$	activity fraction of Th-230 in soluble thorium	-	calculated	calculated	SOURCE	X230LA

Note

* Distributions are as described in Table 2.3.

Table 10.6

WATERSHED MODEL CODE LISTING

```
      SUBROUTINE WATEX
C
C     SUBROUTINE CALCULATES RIVER LENGTHS, LAKE CIRCUMFERENCES, FLOW
C     RATES IN LAKES AND RIVERS, AND CALLS APPROPRIATE SUBROUTINE
C
      INCLUDE 'MODEL.INC'
      INCLUDE 'VAR.INC'
      REAL*4 PI
      DATA PI /3.1415927/
      IF (CODWAT.GE.1.0) WRITE (*,*) ' ***** SUBROUTINE WATEX *****'
      IF (NT.EQ.0.AND.NUMTRL.EQ.1) THEN
C
C     CALCULATE RIVER LENGTHS & LAKE CIRCUMFERENCES
C
         LTOT=0.
         DO 20 WTSEG=1,NSEG
            IF (STYPE(WTSEG).EQ.'R') THEN
               WTLNG(WTSEG)=LAREA(WTSEG)
            ELSE
               WTLNG(WTSEG)=2.*SQRT(LAREA(WTSEG)*PI)
            ENDIF
            LTOT=LTOT+WTLNG(WTSEG)
            IF (CODWAT.EQ.4) WRITE (*,100) 'WTLNG',WTLNG(WTSEG)
20       CONTINUE
         IF (CODWAT.EQ.4) WRITE (*,100) 'TOTAL',LTOT
      ENDIF
C
C     LOOP THROUGH WATERSHED SEGMENTS
C
      LAKCNT=0
      DO 10 WTSEG=1,NSEG
C
C        CALCULATE FLOW
C
         FLOWQ(WTSEG)=NPRCP*SHEDAR(WTSEG)+SFLOW+RFLOW
         DO 30 I=1,DAM
            IF (WTSEG.GE.GSEG(I)) FLOWQ(WTSEG)=FLOWQ(WTSEG)+VSRGW(I)
30       CONTINUE
         IF (CODWAT.GE.2.0) WRITE (*,200) WTSEG,FLOWQ(WTSEG)
         IF (STYPE(WTSEG).EQ.'R') THEN
            CALL RIVER
         ELSE
            CALL LAKE
         ENDIF
         CALL FISH
10    CONTINUE
      RETURN
100   FORMAT (1X,A6,1X,E9.3)
200   FORMAT (' FLOWQ(',I2,') ',E9.3)
      END
C
```

Table 10.6 continued.

```
C
C
      SUBROUTINE RIVER
C
C     SUBROUTINE CALCULATES RADIONUCLIDE, CALCIUM, AND SULPHATE
C     CONCENTRATIONS AND pH IN RIVERS
C
      INCLUDE 'MODEL.INC'
      INCLUDE 'VAR.INC'
      EXTERNAL PHW
      IF (CODWAT.GE.1.0) WRITE (*,*) ' ***** SUBROUTINE RIVER *****'
      ISUB=1
10    CONTINUE
C
C        CALCULATE CONCENTRATION
C
         WATC(ISUB,WTSEG)=RMASSB(ISUB)
         IF (CODWAT.EQ.2.0.OR.CODWAT.EQ.6.0) WRITE (*,100) ISUB,WTSEG,
     &      WATC(ISUB,WTSEG)
         IF (ISUB.LT.5) THEN
C
C           UPDATE AVERAGE WATERSHED CONCENTRATION
C
            IF (WTSEG.EQ.1) WATAVG(ISUB)=0.0
            WATAVG(ISUB)=WATAVG(ISUB)+WATC(ISUB,WTSEG)*WTLNG(WTSEG)/
     &         LTOT
            IF (CODWAT.EQ.4.0) WRITE (*,200) 'WATAVG',WATAVG(ISUB)
         ENDIF
         ISUB=ISUB+1
         IF (ISUB.EQ.5) ISUB=7
      IF (ISUB.LT.9) GOTO 10
C
C     GUESS pH LEVEL
C
      PMIN=1.
      PMAX=14.
      IF (NT.EQ.0) THEN
         GUESS=4.
      ELSE
         GUESS=WATPH(WTSEG)
      ENDIF
      POLD=GUESS
      IF (CODWAT.EQ.3.0) WRITE (*,120) ' GUESS',GUESS
C
C     CALL MODULE FOR ITERATIVE SOLUTION OF pH EQUATION
C
      CALL NEWTON (7,GUESS,WATPH(WTSEG),PHW)
      IF (CODWAT.EQ.3.0.OR.CODWAT.EQ.6.0) WRITE (*,300) WTSEG,
     &   WATPH(WTSEG)
      RETURN
100   FORMAT (' WATC(',I2,',',I3,') ',E9.3)
120   FORMAT (2(2X,A6,1X,E9.3))
200   FORMAT (1X,A6,1X,E9.3)
```

Table 10.6 continued.

```
300   FORMAT (' WATPH(',I3,') ',E9.3)
      END
C
C
C
      FUNCTION RMASSB (ISUB)
C
C     FUNCTION CALCULATES RADIONUCLIDE, CALCIUM, AND SULPHATE
C     CONCENTRATIONS IN RIVERS AND FACTOR IN LAKE EQUATION FOR
C     CALCIUM AND SULPHATE CONCENTRATIONS
C
      INCLUDE 'MODEL.INC'
      INCLUDE 'VAR.INC'
      IF (CODWAT.EQ.2.0) WRITE (*,*) ' FUNCTION RMASSB'
C
C     CALCULATE SOURCE LOADING
C
      IF (WTSEG.EQ.1) THEN
         US=0.
         SMASS=SFLOW*WCONC(ISUB,3,3)
         A=SMASS
C
C        CALCULATE LOADING FROM EROSION OF TAILINGS
C
         IF(ISUB.LT.5)THEN
            EMASS=EROTOT*1000.*CONC(ISUB,1,3)*FCONC(ISUB)/DT/RHOTAL
            A=A+EMASS
         ENDIF
C
C     CALCULATE UPSTREAM LOADING
C
      ELSE
         SMASS=0.0
         EMASS=0.0
         US=FLOWQ(WTSEG-1)
         A=US*WATC(ISUB,WTSEG-1)
      ENDIF
C
C     CALCULATE LOADING FROM GROUNDWATER
C
      DO 10 I=1,DAM
         IF (WTSEG.EQ.GSEG(I)) THEN
            GMASS=GFLUX(ISUB,I)*AXGWAT(I)
            A=A+GMASS
         ELSE
            GMASS=0.0
         ENDIF
10    CONTINUE
C
C     CALCULATE LOADING FROM BACKGROUND CONCENTRATION
C
      IF (ISUB.LT.5) THEN
         B=0.
```

Table 10.6 continued.

```
      ELSE
         B=FLOWQ(WTSEG)-US
         IF (ISUB.EQ.7) THEN
            B=B*WTSO4B
         ELSE
            B=B*WATCAB
         ENDIF
      ENDIF
C
C     CALCULATE TOTAL CONCENTRATION
C
      RMASSB=(A+B)/FLOWQ(WTSEG)
      IF (CODWAT.EQ.2.0) WRITE (*,100) 'WCON',WCONC(ISUB,3,3),'US',US,
     &   'A',A,'B',B,'RMAS',RMASSB,'SMASS',SMASS,'EMASS',EMASS,'GMASS',
     &   GMASS
      RETURN
100   FORMAT (8(2X,A5,1X,E9.3))
      END
C
C
C
      SUBROUTINE LAKE
C
C     SUBROUTINE CALCULATES CONCENTRATIONS OF RADIONUCLIDES, CALCIUM,
C     AND SULPHATE AND pH IN LAKES
C
      EXTERNAL PHW
      INCLUDE 'MODEL.INC'
      INCLUDE 'VAR.INC'
      REAL*4 KW,KS,K1,K2,K3,WATKD(4),PI
      DATA PI /3.1415927/
      IF (CODWAT.GE.1.0) WRITE (*,*) ' ***** SUBROUTINE LAKE *****'
      LAKCNT=LAKCNT+1
      DETIME=LAKVOL(WTSEG)/FLOWQ(WTSEG)
C
C     INITIALIZE CALCIUM AND SULPHATE FOR PREVIOUS TIME STEP AS
C     EQUALLING BACKGROUND LEVELS
C
      IF (NT.EQ.0) THEN
         WATC(7,WTSEG)=WTSO4B
         WATC(8,WTSEG)=WATCAB
C
C        CALCULATE CONSTANT DECAY TERMS
C
         IF(NUMTRL.EQ.1)THEN
            LAK1=EXP(-LAMRAD*DT)
            LAK2=LAM230/(LAMRAD-LAM230)*(EXP(-LAM230*DT)-LAK1)
            LAK3=EXP(-LAMPB*DT)
            LAK4=LAMRAD/(LAMPB-LAMRAD)*(LAK1-LAK3)
            LAK5=EXP(-LAMRAD*DETIME)
            LAK6=LAM230/(LAMRAD-LAM230)*(EXP(-LAM230*DETIME)-LAK5)
            LAK7=EXP(-LAMPB*DETIME)
            LAK8=LAMRAD/(LAMPB-LAMRAD)*(LAK5-LAK7)
```

Table 10.6 continued.

```
            IF(CODWAT.EQ.6.0)WRITE(*,*)' LAMRAD',LAMRAD,' LAM230',LAM230
     &         ,' LAMPB',LAMPB,
     &         ' LAK1',LAK1,' LAK2',LAK2,' LAK3',LAK3,' LAK4',LAK4,
     &         ' LAK5',LAK5,' LAK6',LAK6,' LAK7',LAK7,' LAK8',LAK8
         ENDIF
C
C        GUESS pH LEVEL
C
         GUESS=4.
      ELSE
         GUESS=WATPH(WTSEG)
      ENDIF
      PMIN=1.
      PMAX=14.
      POLD=GUESS
C
C     SET UP LOOP FOR CALCIUM AND SULPHATE
C
      DO 20 ISUB=7,8
         F=RMASSB(ISUB)
C
C        CHECK IF 1/DETENTION TIME APPROACHES 0
C
         CK=-DT/DETIME
         IF (CK.LT.-85.) THEN
            ECK=0.
         ELSE
            ECK=EXP(CK)
         ENDIF
         WATC(ISUB,WTSEG)=F+(WATC(ISUB,WTSEG)-F)*ECK
         IF (CODWAT.GE.2.0) WRITE (*,100) ISUB,WTSEG,WATC(ISUB,WTSEG)
20    CONTINUE
      IF (CODWAT.EQ.3.0) WRITE (*,120) ' GUESS',GUESS
C
C     CALL MODULE FOR ITERATIVE SOLUTION OF pH EQUATION
C
      CALL NEWTON (8,GUESS,WATPH(WTSEG),PHW)
      IF (CODWAT.EQ.3.0.OR.CODWAT.EQ.6.0) WRITE (*,200) WTSEG,
     &   WATPH(WTSEG)
C
C     CALCULATE CONCENTRATIONS OF RADIONUCLIDES
C
      IF(WATPH(WTSEG).GE.4)THEN
         WKDTH=2.0E-2+KDPRIM*(WATPH(WTSEG)-4.0)
      ELSE
         WKDTH=2.0E-2
      ENDIF
      WATKL=(CURRNT*DIFFC/PI/SDEPTH(WTSEG))**0.5
      WATKD(1)=WKDU
      WATKD(2)=WKDTH
      WATKD(3)=WKDPB
      WATKD(4)=WKDRA
      IF(LAKCNT.EQ.1)THEN
```

Table 10.6 continued.

```
         WSIGD=BURYF*(WSIGS(1)+EROTOT*1000./DT/LAREA(WTSEG))
      ELSE
         WSIGD=BURYF*WSIGS(LAKCNT)
      ENDIF
      IF (CODWAT.EQ.6.0) THEN
         WRITE(*,*)' KDPRIM',KDPRIM,'  WATKL',WATKL,'  WATKD',WATKD,
     &      '  WSIGS',WSIGS(LAKCNT),'  BURYF',BURYF,'  WSIGD',WSIGD,
     &      '  WTMIXD',WTMIXD,'  WTRHOS',WTRHOS,'WATEPS',WATEPS
      ENDIF
      DO 10 ISUB=1,4
         IF (NT.EQ.0) THEN
C
C           SET INITIAL MASSES IN WATER COLUMN AND SEDIMENT
C
            RWADJ(ISUB,WTSEG)=0.0
            RSADJ(ISUB,WTSEG)=0.0
         ENDIF
C
C        CALCULATE RATE CONSTANTS FOR LAKE SETTLING
C
         K1=(WSIGS(LAKCNT)*WATKD(ISUB)+WATKL)/SDEPTH(WTSEG)
         A=1.05/WTMIXD/(WATKD(ISUB)*WTRHOS*(1.-WATEPS)+WATEPS)
         K2=A*WATKL
         K3=A*WSIGD*WATKD(ISUB)
C
C        COMPUTE RADIONUCLIDE CONCENTRATIONS
C
         A11=FLOWQ(WTSEG-1)*WATC(ISUB,WTSEG-1)
         A12=K1+1/DETIME
         A13=K2
         A21=0.0
         A22=K1
         A23=K2+K3
         IF(CODWAT.EQ.6.0)WRITE(*,110)'ISUB',ISUB,' K1',K1,'K2',K2,
     &      ' K3',K3
         B=A12*A23-A22*A13
         C=A13+A23
         D=A12+A22
         E=A12+A23
         KW=(A13*A21+A11*A23)/B
         KS=(A12*A21+A11*A22)/B
         V1=(-E+SQRT(E*E-4.*B))/2.
         V2=-E-V1
         X=RWADJ(ISUB,WTSEG)-KW
         Y=RSADJ(ISUB,WTSEG)-KS
         AA=(C+V1)/(D-C)*((D+V2)*X-(C+V2)*Y)/SQRT(E*E-4.*B)
         BB=(D+V1)/(C+V1)*AA
         CK1=V1*DT
         CK2=V2*DT
C
C        CHECK IF EXPONENTIAL TERMS APPROACH 0
C
         IF (CK1.LT.-50.) THEN
```

Table 10.6 continued.

```
            ECK1=0.
         ELSE
            ECK1=EXP(CK1)
         ENDIF
         IF (CK2.LT.-50.) THEN
            ECK2=0.
         ELSE
            ECK2=EXP(CK2)
         ENDIF
         WATRW(ISUB,WTSEG)=KW+AA*ECK1+(X-AA)*ECK2
         WATRS(ISUB,WTSEG)=KS+BB*ECK1+(Y-BB)*ECK2
         IF (CODWAT.EQ.6.0) WRITE (*,110) ' KW',KW,'KS',KS,'AA',AA,'BB',
     &      BB,' WATRW',WATRW(ISUB,WTSEG),' WATRS',WATRS(ISUB,WTSEG),
     &      ' WATC(i,n-1)',WATC(ISUB,WTSEG-1),' V1',V1,' V2',V2,' X',X,
     &      ' Y',Y
         WATC(ISUB,WTSEG)=WATRW(ISUB,WTSEG)/LAKVOL(WTSEG)
         IF (CODWAT.EQ.6.0) WRITE (*,100) ISUB,WTSEG,WATC(ISUB,WTSEG)
C
C        UPDATE AVERAGE WATERSHED CONCENTRATION
C
         WATAVG(ISUB)=WATAVG(ISUB)+WATC(ISUB,WTSEG)*WTLNG(WTSEG)/LTOT
         IF (CODWAT.EQ.4) WRITE (*,120) 'WATAVG',WATAVG(ISUB)
10    CONTINUE
C
C     ADJUST FOR DECAY
C
      DO 15 ISUB=1,2
         RWADJ(ISUB,WTSEG)=WATRW(ISUB,WTSEG)
         RSADJ(ISUB,WTSEG)=WATRS(ISUB,WTSEG)
15    CONTINUE
      RWADJ(3,WTSEG)=WATRW(3,WTSEG)*LAK7+WATRW(4,WTSEG)*LAK8
      RSADJ(3,WTSEG)=WATRS(3,WTSEG)*LAK3+WATRS(4,WTSEG)*LAK4
      RWADJ(4,WTSEG)=WATRW(4,WTSEG)*LAK5+WATRW(2,WTSEG)*LAK6*X230LA
      RSADJ(4,WTSEG)=WATRS(4,WTSEG)*LAK1+WATRS(2,WTSEG)*LAK2*X230LA
      IF(CODWAT.EQ.6.0)THEN
         WRITE(*,*) ' RWADJ(1=>4,WTSEG)',(RWADJ(ISUB,WTSEG),ISUB=1,4),
     &      ' RSADJ(1=>4,WTSEG)',(RSADJ(ISUB,WTSEG),ISUB=1,4),
     &      ' X230LM',X230LM
      ENDIF
      RETURN
100   FORMAT (' WATC(',I2,',',I3,') ',E9.3)
110   FCRMAT (4(2X,A4,1X,E9.3),2(2X,A6,1X,E9.3),/,A12,1X,E9.3,
     &   4(2X,A4,1X,E9.3))
120   FORMAT (2(2X,A6,1X,E9.3))
200   FORMAT (' WATPH(',I3,') ',E9.3)
      END
C
C
C
      SUBROUTINE PHW (FUNC,FPRIME,P)
C
C     SUBROUTINE CALCULATES pH EQUATION AND DERIVATIVE FOR GUESS, P
C
```

Table 10.6 continued.

```
      INCLUDE 'MODEL.INC'
      INCLUDE 'VAR.INC'
      IF (CODWAT.EQ.3.0) THEN
         WRITE (*,*) ' SUBROUTINE PHW'
         WRITE (*,100) 'P IN',P
      ENDIF
C
C     CHECK IF pH GUESS TOO EXTREME AND RESET TO MORE REASONABLE VALUE
C
      IF(P.LT.PMIN)THEN
         P=PMIN
         IF(POLD.EQ.PMAX)P=P+0.1
      ELSEIF(P.GT.PMAX)THEN
         P=PMAX
         IF(POLD.EQ.PMIN)P=P-0.1
      ELSEIF(P.GT.POLD)THEN
         PMIN=POLD
      ELSEIF(P.LT.POLD)THEN
         PMAX=POLD
      ENDIF
      POLD=P
C
C     CALCULATE pH EQUATION
C
      T1=3.*10.**(8.5-3.*P)/ACTCO**2.25
      T2=2.*10.**(3.91-2.*P)/ACTCO
      T3=10.**(.3-P)
      T4=2.*WATC(8,WTSEG)/1000.
      B=ACTCO**0.75*10.**(11.7-3.*P)
      T5=-WATC(7,WTSEG)/1000.*(2.-B)/(1.+B)
      T6=-(10.**(P-11.))/(ACTCO**0.25)
      T7=(2*WATMGB+WATNAB+WATKB-WATCLB)/1000.
      FUNC=T1+T2+T3+T4+T5+T6+T7
C
C     CALCULATE DERIVATIVE OF EQUATION
C
      A=ALOG(10.)
      DT1=-3.*T1*A
      DT2=-2.*T2*A
      DT3=-T3*A
      DT5=-WATC(7,WTSEG)/1000.*9.*A*B/(1.+B)**2.
      DT6=A*T6
      FPRIME=DT1+DT2+DT3+DT5+DT6
      IF (CODWAT.EQ.3.0)
     &   WRITE (*,100) 'P',P,
     &   'ACTCO',ACTCO,'T1',T1,'T2',T2,
     &   'T3',T3,'T4',T4,'B',B,'T5',T5,'T6',T6,'T7',T7,
     &   'A',A,'DT1',DT1,'DT2',DT2,'DT3',DT3,'DT5',DT5,
     &      'DT6',DT6,
     &   'FUNC',FUNC,'FPRIME',FPRIME
      RETURN
100   FORMAT (2(5(1X,A5,E10.3),/),2(4(1X,A6,E10.3),/))
      END
```

SENES Consultants Limited, 1985. "A Study to Develop and Demonstrate Techniques for the Probabilistic Assessment of the Long-Term Effects of Uranium Mill Tailings in Canada - Phase II." Research Report prepared for the National Uranium Tailings Program, CANMET, EMR, under Supply and Services Canada Contract No. OSQ84-00207.

SENES Consultants Limited, 1986. "Probabilistic Model Development for the Assessment of the Long-Term Effects of Uranium Mill Tailings in Canada - Phase III." Research Report prepared for the National Uranium Tailings Program, CANMET, EMR, under Supply and Services Canada Contract No. OSQ85-00182.

Stumm, W., and Morgan, J.J., 1981. "Aquatic Chemistry: An Introduction Emphasizing Chemical Equilibria in Natural Waters." A. Wiley - Interscience Publication, John Wiley and Sons, Inc.

Swanson, S.M., 1984. "Food Chain Transfer of Uranium - Series Radionuclides in a Northern Saskatchewan Aquatic System." Saskatchewan Research Council Report #E-901-7-A-84.

Swanson, S.M., 1985. "A Study of the Distribution of Naturally Occurring Radionuclides in Freshwater Benthos and Their Environment - Phase II." Prepared by SENES Consultants Limited and Saskatchewan Research Council For the National Uranium Tailings Program, CANMET, EMR, Ottawa. Under Supply and Services Canada Contract Number OSQ83-00241.

Wetzel, R.G., 1975. "Limnology." Saunders College Publishing, Philadelphia.

11.0 AQUATIC MODELS

11.1 Components Considered

Exposure, via aquatic pathways, of receptors living within the boundaries of the reference site can occur by consumption of river or lake water and consumption of fish taken from the lakes or rivers in the reference watershed. In addition, receptor exposure can occur indirectly through consumption of caribou, moose or deer which have ingested water or, in the case of moose, ingested aquatic vegetation from the river reaches or lake shorelines in the reference watershed.

The component models for predicting the chemical and radiological quality of the surface waters in the reference watershed have been discussed in Section 10. In this section, the effects of chemical changes in surface water quality on the viability of fish are reviewed. In particular, the literature was examined to derive a basic relationship between pH and fish viability for use in assessing the availability of game fish for consumption by the receptors. In addition, the literature was searched to obtain data for use in estimating transfer coefficients (or bioaccumulation factors) which relate the movement of radionuclides from water to game fish flesh. Similarly, the data base relating radionuclide levels in aquatic vegetation to those in water was consulted to establish appropriate transfer factor values. The results of these investigations are discussed in the following sections.

11.2 Effect of pH on Fish Populations

While it is recognized that an alteration in pH invokes many dramatic physical, chemical, and consequent biotic changes in lakes and streams, emphasis in the following discussion is placed solely on its effects on the sport fish that would likely be encountered in Canadian Shield waters and subsequently eaten by a receptor. Most of the available field data is limited to declining pH, so the discussion is centered on the effects of acidification on fish populations. However, the resultant effects at a particular pH are assumed to be valid whether the pH is decreasing or increasing. In the case of sport fish, the expected population at a pH of 5, for example, is considered to be the same regardless of the pH trend at that time. It is further assumed that when the aquatic environment is recovering from acidification and conditions again become favourable for viable fish populations, there is sufficient access to the lake and river segments for migrating fish.

No attempt has been made to explain mechanisms by which pH affects fish; rather, background information is provided as a rationale for choosing certain pH values as critical for sport fish catches and local fish consumption.

All trophic levels are affected by declining pH, but perhaps the most visible effect is the loss of entire fish populations. Loss of fish populations in acid-stressed waters has been documented in Scandinavia (Jensen and Snekvik, 1972; Schofield, 1976) and in North America (Beamish and Harvey, 1972; Beamish et al., 1975; Rahel and Magnuson, 1983; Schindler et al., 1985).

The distribution of fish species among acid-stressed and non-acidic lakes suggests major interspecies differences in acid tolerance (Rahel and Magnuson, 1983; Beamish and Harvey, 1972). These differences are in part genetically inherent to the species and relate to fundamental differences in metabolism and physiology. However, within the strictly freshwater species, the apparent differences in acid tolerance, as determined from either field or laboratory studies, do not reveal any consistent taxonomic or ecological pattern (Schofield, 1976). Field data for lake trout, whitefish and walleye show that these fish populations are affected within similar ranges of pH, and so are considered as one population unit in the aquatic model.

Size is an important factor and small fish appear to be most sensitive to low pH. Small fish have greater body and gill surface area per unit weight than larger fish, which means that detrimental ion fluxes proceed more rapidly with the greater exchange area of small fish in contact with water (Schofield, 1976). Fish of interest to the aquatic model are the larger game fish, so size _per se_ is not an important consideration.

Much of the published data on the effects of acid water on aquatic organisms are difficult to interpret because reductions in pH also cause changes in other water characteristics such as free CO_2, alkalinity, and the solubility of some metals (Menendez, 1976). The toxicity of many metals increases as pH declines. Fish mortality in various lakes has been attributed to increased uptake of aluminum, copper, or zinc. For aquatic biota that can tolerate pH levels between 6 and 5, such as the sport fish of concern in this study, pH-metal interactions may be of practical importance (Neville, 1985). However, for the purposes of this component model, metal concentrations are assumed to be in equilibrium and the effects of declining pH on fish populations are considered to be a result of a change in hydrogen ion concentration only.

Although fish can die from acidification, more commonly they fail to reproduce and recruitment ceases. Adult fish are more resistant than any other life stage to changes in pH, and the phenomenon of reduced and missing age classes has been observed frequently in fish populations of acid-stressed lakes. Larval fish may be the most pH-susceptible stage of the life history, but recruitment failure can also result from the vulnerability of eggs to low pH, the inhibition of spawning, and the disruption of egg production (Schofield, 1976; NRCC, 1981). There are large species differences in pH tolerance during early life history, but data for sport fish such as walleye and lake trout indicate that reproductive failures occur at a pH of approximately 5.2 to 5.8 (Rahel and Magnuson, 1983).

If recruitment fails, the population density decreases, more food becomes available per individual, and in the short-term there is an increase in growth, size and quality of large fish (Jensen and Snekvik, 1972). Schindler _et al_. (1985) point out that a decrease in food supply and loss of younger year classes may make it easier for anglers to catch more and larger sport fish at the early stages of acidification. However, if there is continuous failure of recruitment for a number of years, and the food web is severely disrupted, the species will eventually disappear from the lake. At sub-lethal pH, the condition of the fish declines and growth is impaired. Depending on the rate of acidification this increase in availability of adult sport fish may last from approximately one to five years. In the time frame of the study modelling period (several hundred years), however, this relatively short-lived increase is insignificant.

There are insufficient data to quantify accurately the declines in fish population with decreasing pH, but sufficient information is available to allow some general conclusions to be made concerning the range of acidity that is acceptable for fish. Beamish and Harvey (1972) summarize these conclusions as follows:

> "After reviewing the literature, the EIFAC Working Party on Water Quality (1969) concluded a pH range of 5 to 9 was not directly lethal for fishes. Doudoroff and Katz (1950) concluded that most freshwater fishes could live in waters above pH 5.0, but questioned the suitability of waters close to 5.0 for successful reproduction of the more sensitive species. The National Technical Advisory Committee (1968) set the minimum desirable pH at 6.0 for aquatic organisms. McKee and Wolf (1963) stated that the optimum pH of water for fish culture was in the range of 6.7 to 8.6, with a practical extreme lower limit of 6.3. They reviewed some of the literature on acid tolerance and recorded fish surviving in water of pH 3.3; however, tolerable lower limits for most fish were close to 5.0."

Other assessments (Menendez, 1976) have suggested that although fish have been found at pH 4 to 10, the safe range is 5 to 9, and for maximum productivity, the pH value should be 6.5 to 8.5.

Both field and laboratory studies on the sport fish which would be expected from Canadian Shield waters (lake trout, whitefish, walleye) suggest that normal productivity occurs at a pH greater than 6.0 to 6.5 and that a pH of less than 5.5 initiates significant reproductive failure as well as some stress to the adult population (Beamish et al, 1975; Schindler et al., 1985). At pH levels between 4 and 5, disturbance of normal ion and acid-base balance is a likely cause of adult mortality and a rapid decline in population is to be expected. For example, in a 5 year study of the fish population in George Lake, Ontario, Beamish et al. (1975) estimated that the adult population of white suckers decreased in number by 75 percent and in biomass by 90 percent as the pH dropped from an average of 5.0 to an average of 4.5. Those individuals that can survive a pH of 4.0 to 4.5 would experience very reduced growth and would be in poor condition.

Based on this qualitative data, the expected availability (expressed as a percentage) of the adult population of fish, such as walleye, lake trout, brook trout and whitefish, is modelled as a function of pH. The key pH values for these sport fish can be summarized as follows:

pH > 6.0	- normal populations; expect normal catches
pH 6.0 to 5.0	- some decline in population due to recruitment failure; some adults stressed; expect 75 to 90% catch
pH 5.0 to 4.5	- a rapid decline in adult population; condition of the fish poor; expect limited catches of perhaps 25%
pH 4.5 to 3.5	- adult population heavily stressed; population likely to become extinct; expect no catches below pH = 3.5

Based on the above, the model proposed for calculating the availability of game fish from the lakes and rivers in the reference watershed for consumption by receptors took the following form:

$$\begin{array}{ll} \text{for } pH_{n,t} > 6.0 & F_a = 1.0 \\ \text{for } 5.0 < pH_{n,t} \leq 6.0 & F_a = 0.75 + 0.25\,(pH_{n,t} - 5.0) \\ \text{for } 4.5 < pH_{n,t} \leq 5.0 & F_a = 0.25 + 1.0\,(pH_{n,t} - 4.5) \\ \text{for } 3.5 < pH_{n,t} \leq 4.5 & F_a = 0.25\,(pH_{n,t} - 3.5) \\ \text{for } pH_{n,t} \leq 3.5 & F_a = 0.0 \end{array} \qquad (11.1)$$

where

F_a = availability factor of game fish for consumption expressed as a function of pH

$pH_{n,t}$ = pH level of surface water at the nth node in the reference watershed at time t.

This model formulation is used in the calculation of dose from fish consumption (see Chapter 13).

11.3 Radionuclide Transfer to Aquatic Biota

11.3.1 Modelling Approach

Modelling the uptake of radionuclides by aquatic biota can be quite involved and require consideration of several interactions; for example, direct uptake from water by aquatic vegetation, sedimentation and deposition of aquatic vegetation in lake sediment, decomposition and release of contaminants from lake sediments to the water phase, harvesting of aquatic vegetation by invertebrates, predation of large fish on small fish, etc. In a separate investigation in Phase II, a multi-component model was developed for predicting the dynamics of radium-226 transfer between six key components in a hypothetical, oligotrophic lake (Gardner et al., 1985). The model considered twenty-three (23) pathways of radium-226 transfer between the six components (i.e. the water column, sediment, aquatic vegetation, invertebrates, forage fish and game fish flesh). The analysis was extended in Phase III to examine the transfer of uranium for the same reference system considered in Phase II. The results of the Phase III investigation are included in Appendix B of Volume 3, (SENES, 1986).

The primary objective in these investigations was to compare the multi-component dynamic model concept with the mathematically simple bioaccumulation factor (or concentration factor) approach generally applied in assessment level models. In applying the bioaccumulation factor approach it is assumed that the concentrations in the system components are in equilibrium and that all pathways and mechanisms of radionuclide uptake and elimination are included in the factor.

The results of the investigations of the transfer of radium-226 and uranium to game fish flesh showed that, at equilibrium, the concentrations predicted by the multi-component dynamic model were not appreciably different from those obtained from the simple, water-to-game fish flesh bioaccumulation factor model. More specifically, the authors concluded that:

1. time-dependent concentrations of radium-226 and uranium in the flesh of game fish were most sensitive to changes in the rate constants describing the direct transfer of radium-226 and uranium from water to game fish flesh;

2. equilibrium values of the water-to-game fish flesh concentration factors may give biased results when the aquatic system is not in equilibrium; and,

3. a simpler model involving three components can adequately predict the dynamic behaviour of radium-226 and uranium in game fish.

These conclusions support the use of the aggregate model approach taken in Phase II and again in Phase III for predicting radionuclide transfer to game fish flesh. Because radium-226 and uranium are more mobile in the environment than lead-210 or thorium, the simple bioaccumulation factor approach is equally applicable to the latter radionuclides.

The components and pathways considered in the aggregate model are shown on Figure 11.1. The aquatic model, which was described in part in the previous chapter, considers seven pathways of radionuclide transfer between four components; namely, the water column and sediment components, which hold most of the radionuclide inventories, and sedimenting solids and game fish components. Game fish flesh rather than whole fish is considered as it is this tissue which is consumed by humans. The sedimenting solids consist of inorganic solids and organic solids (primarily phytoplankton). Together these act as the primary mechanism of radionuclide removal from the water column to the sediment. In addition to the above aquatic macrophytes (rooted aquatic plants) are also modelled. They represent a significant pathway of radionuclide ingestion by moose, and are modelled on an average basis, over the entire watershed.

11.3.2 Bioaccumulation in Fish

The concentration in game fish flesh is calculated as a function of the concentration in the water phase from the relationship:

$$[F_i]_{n,t} = B_{f,i}\,[R_i]_{n,t} \qquad (11.2)$$

where

$B_{f,i}$ = the water-to-game fish flesh bioaccumulation factor, for radionuclide "i" ($Bq.g^{-1}$ (wet wt).$Bq^{-1}.m^3$)

$[F_i]_{n,t}$ = concentration of radionuclide "i" in game fish flesh at node "n" in the watershed at time "t" ($Bq.m^{-3}$)

$[R_i]_{n,t}$ = concentration of radionuclide "i" at node "n" in the watershed at time "t" ($Bq.m^{-3}$).

The bioaccumulation factor used in the model is an aggregate representation of numerous pathways and mechanisms of radionuclide transfer through the aquatic environment.

As numerous investigators have reported, the accumulation of radionuclides in aquatic biota is a complex phenomenon which is influenced by many possible

FIGURE II.1

AGGREGATE AQUATIC TRANSFER MODEL

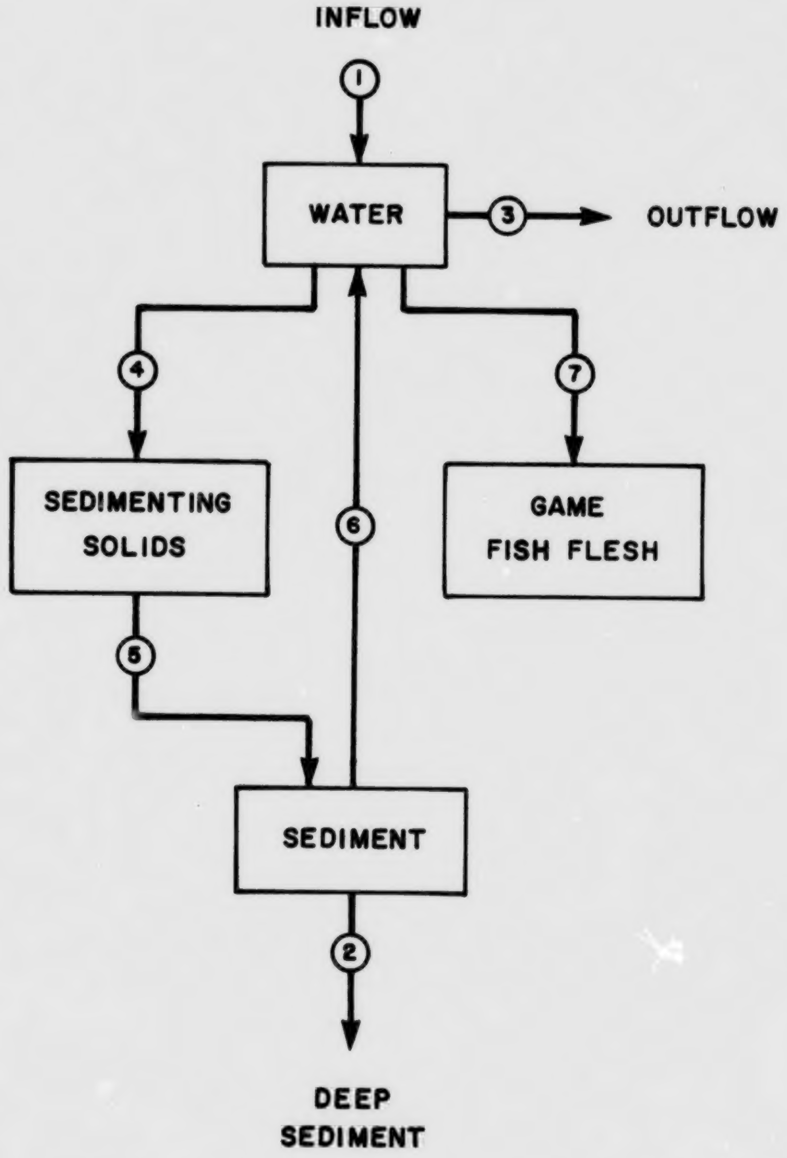

factors. Examples of the factors cited in the literature include: the chemical state of the radionuclides; the chemical composition of the water; the characteristics of the aquatic biota; and the affinity of the radionuclides for different tissues. The method used to calculate bioaccumulation factors can also have a significant influence. The different methods use either wet weight (fresh weight), dry weight, or ash weight of the biota and either filtered or unfiltered water sample measurements in the calculations. The issue is complicated further by the fact that the method used to calculate bioaccumulation factors is often not reported. Considering the number of variables that can influence the levels measured in aquatic biota, it is not unexpected that bioaccumulation factors reported in the literature vary over several orders of magnitude.

To minimize the influence of some of these variables, the literature was searched for data on radionuclide levels in game fish flesh specific to northern Canadian waters. The literature consulted included: published articles; environmental baseline studies; environmental impact assessments; and, routine mine monitoring reports. The data presented below is representative of low alkalinity, low hardness waters.

The data compiled from the literature on radionuclide levels in game fish flesh and water are presented in Tables 11.1 to 11.4 for natural uranium, total thorium, radium-226 and lead-210 respectively. All fish flesh values are reported on a wet (fresh) weight basis while the water data are total (unfiltered) levels. The calculated bioaccumulation factors (BF's) are reported on a $L.kg^{-1}$ (or $mL.g^{-1}$) basis as usually found in the literature. These BF values were converted to a $m^3.g^{-1}$ basis for input to the aquatic model.

The calculated BF's vary over a fairly wide range for all radionuclides as expected. Frequency histogram plots of the data (see Figures 11.2 to 11.5) show that the BF's for all radionuclides are skewed to the right, typical of a lognormal distribution. Several distribution curves were fitted to the frequency histograms using commercially available statistical software. Of the distributions fitted to the data, the lognormal distribution was found to be the best overall. The chi-squared goodness of fit statistic indicated that the fit was good for the total thorium and radium-226 data. The test indicated a poorer fit for the total uranium and lead-210 data. However, since the lognormal distribution was found to be the most representative overall, it was selected to characterize the bioaccumulation factors for all four radionuclides.

11.3.3 Bioaccumulation in Aquatic Macrophytes

Calculation of the radionuclide levels in aquatic macrophytes was included in the Phase III model as macrophytes are a source of food for moose. The radionuclide levels in the aquatic macrophytes are calculated from the aggregate model:

$$[C_{q,i}] = B_{q,i} \ [R_i]_t \tag{11.3}$$

where

$[C_{q,i}]_t$ = concentration of radionuclide "i" in aquatic vegetation at time "t" ($Bq.g^{-1}$)

$B_{q,i}$ = the water-to-aquatic vegetation transfer coefficient ($Bq.g^{-1}$ (wet)$.Bq^{-1}.m^3$)

$[R_i]_t$ = average concentration of radionuclide "i" in the waters over the entire reach of the watershed ($Bq.m^{-3}$).

The model calculates an average radionuclide content in the vegetation which is applicable to the entire length of the watershed. This approach was taken to permit moose consumption of both water and aquatic vegetation to be treated independent of location in the watershed. The average radionuclide content in surface water, and hence average radionuclide content in aquatic vegetation, is calculated based on the length of river reach and circumference of the

FIGURE II.2

FREQUENCY HISTOGRAM OF URANIUM BIOACCUMULATION FACTOR VALUES

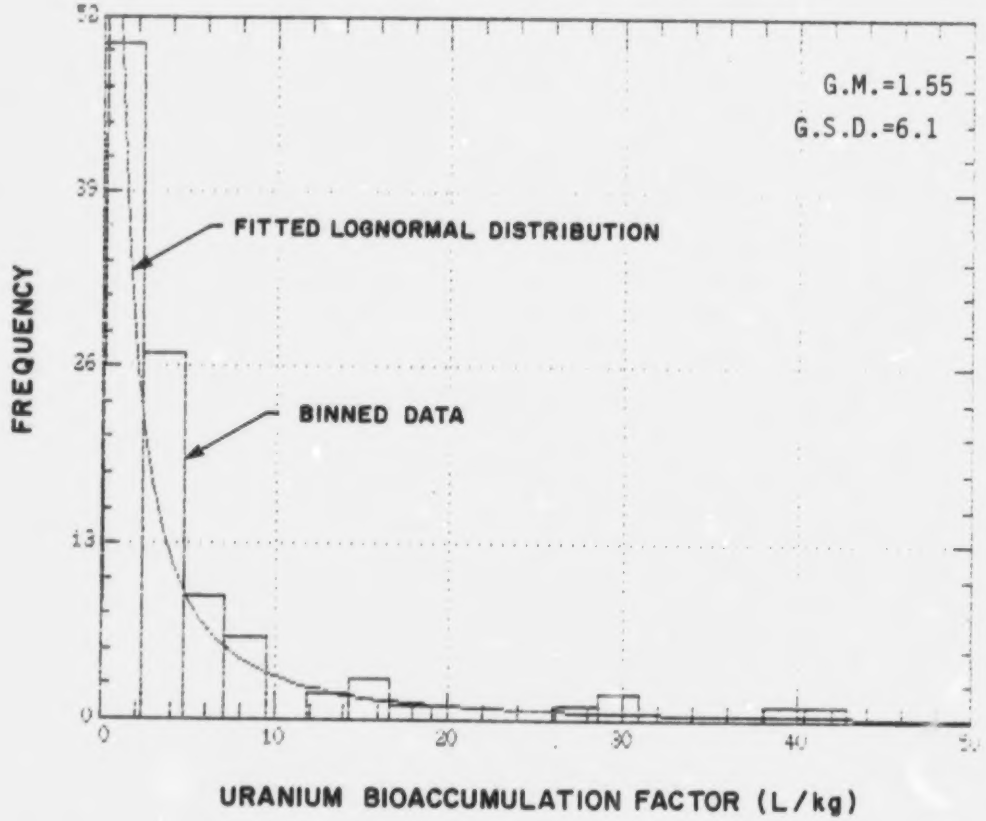

FIGURE 11.3

FREQUENCY HISTOGRAM
OF THORIUM BIOACCUMULATION FACTOR VALUES

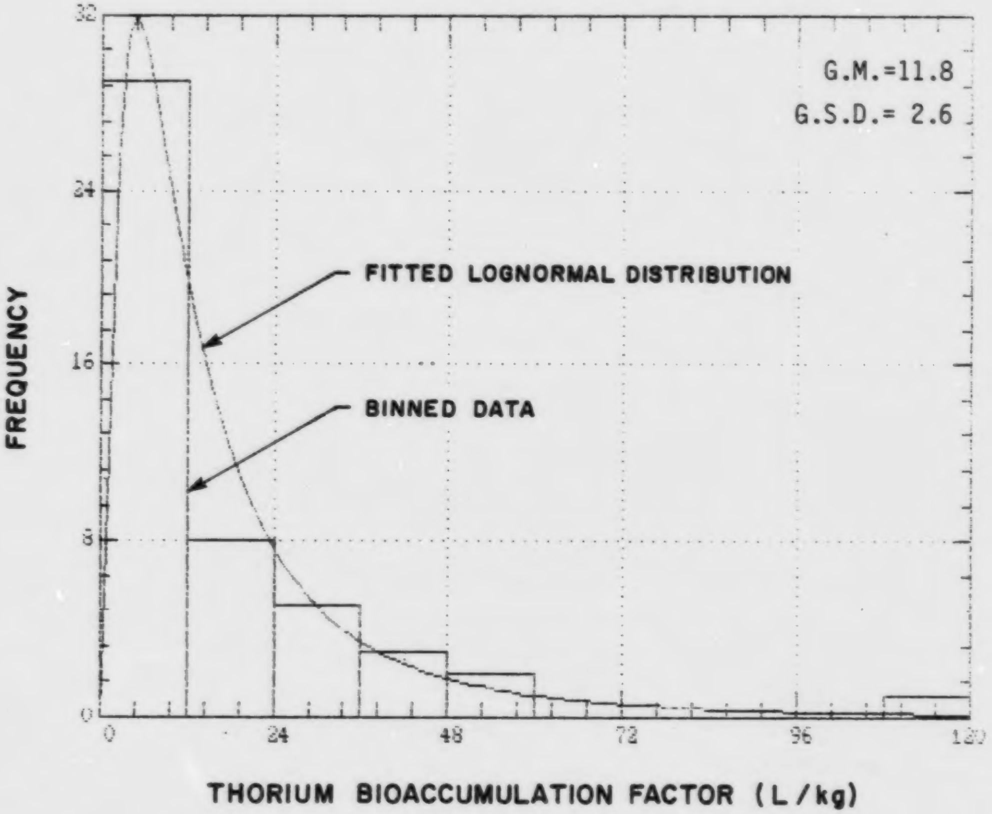

FIGURE II.4

FREQUENCY HISTOGRAM
OF RADIUM - 226 BIOACCUMULATION FACTOR VALUES

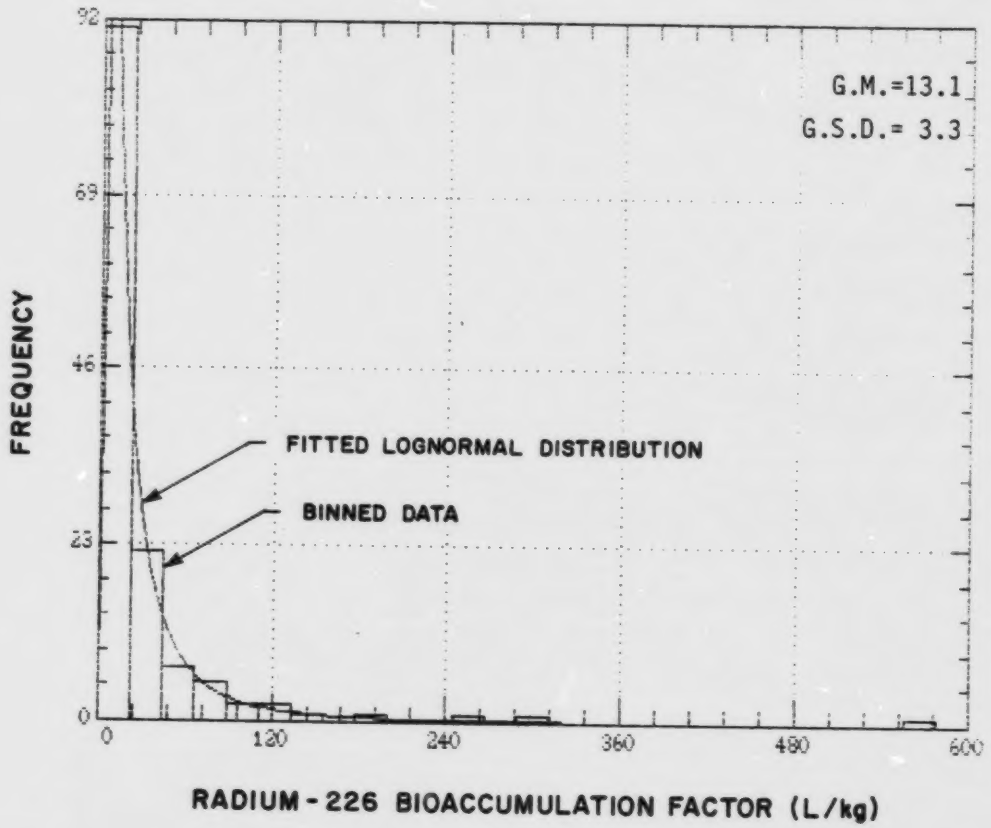

FIGURE 11.5

FREQUENCY HISTOGRAM OF LEAD-210 BIOACCUMULATION FACTOR VALUES

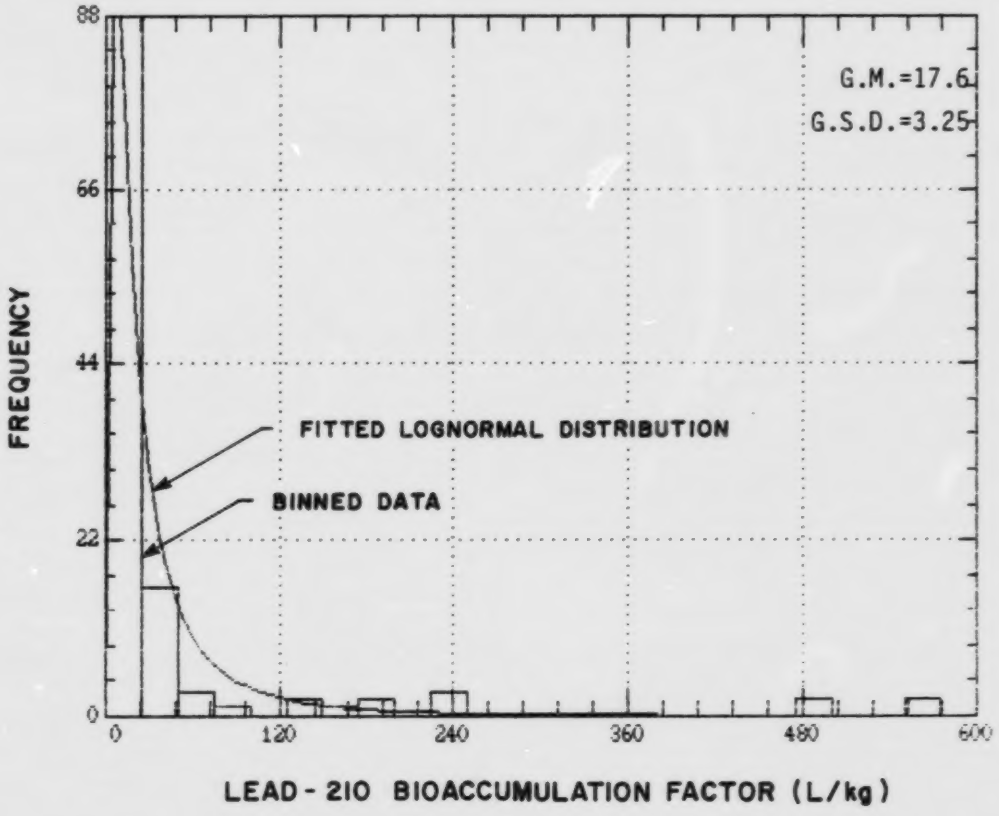

Table 11.1

LARGE (GAME) FISH FLESH URANIUM BIOACCUMULATION FACTORS (BF's)

Location	Species	No. Fish Samples	Fish Flesh Concentration (ug/kg fresh)	Water Level (ug/L)	Uranium BF (L/kg)	Reference
Trapper Lake, B.C.	Rainbow Trout	13	5	0.335	14.9	Norcen 1980
McClean Lake, Sask.	Walleye	5	7.69	0.5	15.4	Canadian Occidental 1981
" "	Lake Whitefish	5	7.18	0.5	14.4	"
Kewen Lake, Sask.	Walleye	5	6.87	0.82	8.4	Canadian Occidental 1981
" "	Lake Whitefish	5	5.23	0.82	6.4	"
McDonald Lake, Sask.	Northern Pike	5			2	I.E.S. Inc. 1983
" "	Lake Whitefish	5			30	"
Delta Lake, Sask.	Northern Pike	5			1	"
" "	Lake Whitefish	5			5	"
Russell Lake, Sask.	Northern Pike	5			4	"
" "	Lake Whitefish	5			3	"
Beaverlodge Lake, Sask.	Lake Trout	5			0.3	Swanson 1983
" "	Lake Whitefish	5			0.2	"
Dubyna Lake, Sask.	Northern Pike	5	3.69	22	.2	Eldorado 1978
" "	Lake Trout ('77)	2	78	22	3.5	"
" "	Lake Trout ('78)	5	17	22	.8	"
Schmoo Lake, Sask.	Lake Trout	5	6.8	19.7	.3	"
Wollaston Lake, Sask						
- Pow Bay	Lake Trout	5	≤38	17.8	2.1	ELDOR (Gulf Minerals) 1982
- Pow Bay	Northern Pike	5	18	17.8	1.0	"
- Hidden Bay	Northern Pike	5	8	25.9	.3	"
Russell Lake, Sask.	Walleye	1	14.1	<0.5	28.2	Key Lake 1979
" "	"	1	20.1	"	40.2	"
" "	"	1	8.4	"	16.8	"
" "	"	1	6.9	"	13.8	"
" "	"	1	<2.1	"	4.2	"
" "	"	1	<1.7	"	3.4	"
" "	"	1	<2.3	"	4.6	"
" "	"	1	20.7	"	41.4	"
" "	"	1	1.3	"	2.6	"
" "	"	1	<2.3	"	4.6	"

Table 11.1 continued

Location	Species	No. Fish Samples	Fish Flesh Concentration (ug/kg fresh)	Water Level (ug/L)	Uranium BF (L/kg)	Reference
Russell Lake, Sask.	Lake Whitefish	1	4.4	<0.5	8.9	Key Lake 1979
" "	"	1	<2.2	"	<4.5	"
" "	"	1	<2.3	"	<4.7	"
" "	"	1	<2.3	"	<4.7	"
" "	"	1	<2.5	"	<5.0	"
" "	"	1	<2.0	"	<4.0	"
" "	"	1	<2.1	"	<4.2	"
" "	"	1	<2.1	"	<4.2	"
" "	"	1	<2.3	"	<4.6	"
" "	"	1	<2.0	"	<4.0	"
Beaverlodge Lake, Sask.	Lake Whitefish	1	2.0	338	0.01	Swanson 1982
" "	"	1	577.8	"	1.71	" "
" "	"	1	32.4	"	0.10	" "
" "	"	1	18.8	"	0.06	" "
" "	"	1	102.2	"	0.30	" "
" "	"	1	68.5	"	0.20	" "
" "	"	1	163.6	"	0.48	" "
" "	"	1	254.2	"	0.75	" "
" "	"	1	49.9	"	0.15	" "
" "	"	1	65.3	"	0.19	" "
" "	"	1	37.5	"	0.11	" "
" "	"	1	24.3	"	0.07	" "
" "	"	1	59.1	"	0.18	" "
" "	"	1	81.7	"	0.24	" "
" "	"	1	19.3	"	0.06	" "
" "	"	1	38.7	"	0.12	" "
" "	"	1	55.4	"	0.16	" "
" "	"	1	16.1	"	0.05	" "
" "	"	1	47.1	"	0.14	" "
" "	"	1	42.3	"	0.13	" "
" "	"	1	31.1	"	0.09	" "
" "	"	1	39.0	"	0.12	" "
Milliken Lake, Sask.	Lake Whitefish	1	35.1	1.2	29.25	Swanson 1982
" "	"	1	<2.0	"	1.67	" "
" "	"	1	2.1	"	1.75	" "
" "	"	1	5.5	"	4.58	" "
" "	"	1	6.1	"	5.08	" "
" "	"	1	7.8	"	6.50	" "
" "	"	1	11.3	"	9.42	" "
" "	"	1	6.1	"	5.08	" "
" "	"	1	2.1	"	1.75	" "
" "	"	1	3.8	"	3.17	" "
" "	"	1	3.3	"	2.75	" "
" "	"	1	10.4	"	8.67	" "

Table 11.1 continued

Location	Species	No. Fish Samples	Fish Flesh Concentration (ug/kg fresh)	Water Level (ug/L)	Uranium BF (L/kg)	Reference
Milliken Lake, Sask.	Lake Whitefish	1	5.1	1.2	4.25	Swanson 1982
" "	"	1	6.0	"	5.00	" "
" "	"	1	3.6	"	3.00	" "
" "	"	1	4.7	"	3.92	" "
" "	"	1	<1.8	"	1.50	" "
" "	"	1	<1.9	"	1.58	" "
" "	"	1	3.1	"	2.58	" "
" "	"	1	4.8	"	4.00	" "
Fredette Lake, Sask.	Lake Whitefish	1	46.8	3.3	14.18	Swanson 1982
" "	"	1	12.6	"	3.82	" "
" "	"	1	4.6	"	1.39	" "
" "	"	1	<0.2	"	<0.06	" "
" "	"	1	<0.2	"	<0.06	" "
" "	"	1	4.6	"	1.39	" "
" "	"	1	10.2	"	3.09	" "
" "	"	1	2.9	"	0.88	" "
" "	"	1	<2.0	"	0.61	" "
" "	"	1	10.2	"	3.09	" "
" "	"	1	17.6	"	5.33	" "
" "	"	1	7.4	"	2.24	" "
" "	"	1	1.7	"	0.52	" "
" "	"	1	25.5	"	7.73	" "
" "	"	1	29.4	"	8.91	" "
" "	"	1	3.7	"	1.12	" "
" "	"	1	>0.2	"	<0.06	" "
" "	"	1	19.1	"	5.79	" "
" "	"	1	6.9	"	2.09	" "
" "	"	1	5.0	"	1.52	" "
" "	"	1	4.7	"	1.42	" "

Summary Statistics	
Number of Data Points	103
Geometric Mean	1.55
Geometric Std. Deviation	6.1
Range of Values	0.01 to 41.4

Table 11.2

LARGE (GAME) FISH FLESH THORIUM BIOACCUMULATION FACTORS (BF's)

Location	Species	No. Fish Samples	Fish Flesh Concentration (ug/kg fresh)	Water Level (ug/L)	Thorium BF (L/kg)	Reference
McDonald Lake, Sask.	Northern Pike	5			30	I.E.S. Inc. 1983
" "	Lake Whitefish	5			110	"
Russell Lake, Sask.	Nortnern Pike	5			20	I.E.S. Inc. 1983
" "	Lake Whitefish	5			20	"
Dubyna Lake, Sask.	Northern Pike	5	5.3	0.7	7.6	Eldorado 1978
" "	Lake Trout	5	14.3	0.7	20.4	"
Schmoo Lake, Sask.	Lake Trout	5	15.0	0.5	30.0	"
Donaldson Lake, Sask.	Lake Trout	5	27.9	0.5	55.8	"
Russell Lake, Sask.	Walleye	1	4.7	0.84	5.6	Key Lake 1979
" "	"	1	1.3	"	1.5	"
" "	"	1	19.8	"	23.6	"
" "	"	1	4.9	"	5.8	"
" "	"	1	30.0	"	35.7	"
" "	"	1	0.9	"	1.1	"
" "	"	1	23.2	"	27.6	"
" "	"	1	1.0	"	1.2	"
" "	"	1	7.9	"	9.4	"
" "	"	1	4.7	"	5.6	"
Russell Lake, Sask.	Lake Whitefish	1	4.0	0.84	4.8	Key Lake 1979
" "	"	1	19.9	"	23.7	"
" "	"	1	2.2	"	2.6	"
" "	"	1	19.4	"	23.1	"
" "	"	1	44.5	"	52.9	"
" "	"	1	6.2	"	7.3	"
" "	"	1	39.8	"	47.4	"
" "	"	1	12.6	"	15.0	"
" "	"	1	7.9	"	9.4	"
" "	"	1	6.1	"	7.3	"
Kewen Lake, Sask.	Walleye	1	<4.2	0.38	<11.0	Canadian Occidental 1981
" "	"	1	13.8	"	36.3	" "
" "	"	1	<4.2	"	<11.0	" "
" "	"	1	<4.3	"	<11.3	" "
" "	"	1	10.5	"	27.6	" "
Kewen Lake, Sask.	Lake Whitefish	1	<4.6	0.38	<12.1	Canadian Occidental 1981
" "	"	1	<4.5	"	<11.8	" "
" "	"	1	<4.1	"	<10.8	" "
" "	"	1	16.5	"	43.4	" "
" "	"	1	<3.9	"	<10.3	" "

Table 11.2 continued

Location	Species	No. Fish Samples	Fish Flesh Concentration (ug/kg fresh)	Water Level (ug/L)	Thorium BF (L/kg)	Reference
McLean Lake, Sask.	Walleye	1	<4.9	0.63	<7.8	Canadian Occidental 1981
" "	"	1	<5.0	"	<7.9	" "
" "	"	1	<4.9	"	<7.8	" "
" "	"	1	<5.3	"	<8.4	" "
" "	"	1	<3.3	"	<5.3	" "
McClean Lake, Sask.	Lake Whitefish	1	<5.5	0.63	<8.7	Canadian Occidental 1981
" "	"	1	<6.5	"	<10.3	" "
" "	"	1	<5.3	"	<8.4	" "
" "	"	1	<5.0	"	<7.9	" "
" "	"	1	<5.0	"	<7.9	" "

Summary Statistics	
Number of Data Points	48
Geometric Mean	11.8
Geometric Std. Deviation	2.6
Range of Values	1.1 to 110

Table 11.3

LARGE (GAME) FISH FLESH RADIUM-226 BIOACCUMULATION FACTORS (BF'S)

Location	Species	No. Fish Samples	Fish Flesh Concentration Bq/kg (fresh)	Water Level Bq/L	Ra-226 BF (L/kg)	Reference
Sandrift Lake Δ2, BC	Rainbow Trout	5	0.26	0.007	37.1	Norcen 1980
Beaverdell Creek, BC	Rainbow Trout	14	0.11	0.007	15.9	" "
Kewen Lake, Sask.	Walleye	1	0.15	0.004	37.5	Canadian Occidental, 1981
" "	"	1	0.51	"	127.5	" "
" "	"	1	0.31	"	77.5	" "
" "	"	1	0.26	"	40.0	" "
" "	"	1	2.23	"	557.5	" "
Kewen Lake, Sask.	Lake Whitefish	1	0.07	0.004	17.5	Canadian Occidental 1981
" "	"	1	0.33	"	82.5	" "
" "	"	1	0.22	"	55.0	" "
" "	"	1	0.07	"	17.5	" "
" "	"	1	0.14	"	35.0	" "
McClean Lake, Sask.	Walleye	1	0.09	0.004	22.5	Canadian Occidental 1981
" "	"	1	1.00	"	250.0	" "
" "	"	1	0.09	"	22.5	" "
" "	"	1	0.49	"	122.5	" "
" "	"	1	0.55	"	137.5	" "
McClean Lake, Sask.	Lake Whitefish	1	0.20	0.004	50.0	" "
" "	"	1	0.12	"	30.0	" "
" "	"	1	0.10	"	25.0	" "
" "	"	1	0.09	"	22.5	" "
" "	"	1	0.19	"	47.5	" "
McDonald Lake, Sask.	Northern Pike	5	-	-	10	I.E.S. Inc. 1983
" "	Lake Whitefish	5	-	-	10	" "
Delta Lake, Sask	Northern Pike	5	-	-	10	" "
" "	Lake Whitefish	5	-	-	30	" "
Russell Lake, Sask.	Northern Pike	5	-	-	5	
" "	Lake Whitefish	5	-	-	60	" "
Dubyna Lake, Sask.	Lake Trout	1	0.13	0.02	6.5	Eldorado 1978
" "	" "	1	0.13	"	6.5	"
" "	" "	1	0.13	"	6.5	"
" "	" "	1	0.25	"	12.5	"
Dubyna Lake, Sask.	Northern Pike	1	0.49	0.02	24.5	Eldorado 1978
" "	" "	1	0.49	"	24.5	"
" "	" "	1	0.79	"	39.5	"
" "	" "	1	0.49	"	24.5	"
" "	" "	1	0.49	"	24.5	"

Table 11.3 continued

Location	Species	No. Fish Samples	Fish Flesh Concentration Bq/kg (fresh)	Water Level Bq/L	Ra-226 BF (L/kg)	Reference
Donaldson Lake, Sask.	Lake Trout	1	0.13	0.03	4.3	Eldorado 1978
" "	" "	1	0.13	"	4.3	"
" "	" "	1	0.13	"	4.3	"
" "	" "	1	0.25	"	8.3	"
Schmoo Lake, Sask.	Lake Trout	1	0.25	0.02	12.5	Eldorado 1978
" "	" "	1	0.13	"	6.5	"
" "	" "	1	0.25	"	12.5	"
" "	" "	1	0.13	"	6.5	"
" "	" "	1	0.13	"	6.5	"
Wollaston Lake, Sask.						
- Pow Bay	Lake Trout	5	0.3	0.008	37.5	ELDOR (Gulf Minerals) 1982
" "	Northern Pike	5	0.2	0.008	25.0	" "
- Hidden Bay	Northern Pike	5	0.2	0.014	14.2	" "
Russell Lake, Sask.	Walleye	1	0.03	0.006	5.0	Key Lake 1979
" "	"	1	0.04	"	6.7	"
" "	"	1	0.07	"	11.7	"
" "	"	1	0.03	"	5.0	"
" "	"	1	0.04	"	6.7	"
" "	"	1	0.04	"	6.7	"
" "	"	1	0.04	"	<6.7	"
" "	"	1	0.04	"	<6.7	"
" "	"	1	0.05	"	8.3	"
" "	"	1	0.04	"	6.7	"
Russell Lake, Sask.	Lake Whitefish	1	0.04	0.006	6.7	Key Lake 1979
" "	"	1	0.04	"	6.7	"
" "	"	1	0.04	"	6.7	"
" "	"	1	0.04	"	6.7	"
" "	"	1	0.04	"	6.7	"
" "	"	1	0.04	"	6.7	"
" "	"	1	0.04	"	6.7	"
" "	"	1	0.04	"	6.7	"
" "	"	1	0.04	"	6.7	"
" "	"	1	0.04	"	6.7	"
Beaverlodge Lake, Sask.	Lake Whitefish	1	>0.1	0.06	>1.7	Swanson 1982
" "	"	1	0.1	"	1.7	" "
" "	"	1	0.5	"	8.3	" "
" "	"	1	0.1	"	1.7	" "
" "	"	1	0.2	"	3.3	" "
" "	"	1	<0.1	"	<1.7	" "
" "	"	1	0.3	"	5.0	" "
" "	"	1	0.9	"	15.0	" "
" "	"	1	0.5	"	8.3	" "

Table 11.3 continued

Location	Species	No. Fish Samples	Fish Flesh Concentration Bq/kg (fresh)	Water Level Bq/L	Ra-226 BF (L/kg)	Reference
Beaverlodge Lake, Sask.	Lake Whitefish	1	0.2	0.06	3.3	Swanson 1982
" "	"	1	0.1	"	1.7	" "
" "	"	1	0.1	"	1.7	" "
" "	"	1	0.1	"	1.7	" "
" "	"	1	0.1	"	1.7	" "
" "	"	1	<0.1	"	<1.7	" "
" "	"	1	0.1	"	1.7	" "
" "	"	1	6.1	"	1.7	" "
" "	"	1	1.0	"	16.7	" "
Milliken Lake, Sask.	Lake Whitefish	1	<0.1	0.01	<10.0	Swanson 1982
" "	"	1	<0.1	"	<10.0	" "
" "	"	1	0.1	"	10.0	" "
" "	"	1	0.6	"	60.0	" "
" "	"	1	<0.1	"	<10.0	" "
" "	"	1	0.2	"	20.0	" "
" "	"	1	0.9	"	90.0	" "
" "	"	1	0.3	"	30.0	" "
" "	"	1	0.6	"	60.0	" "
" "	"	1	0.2	"	20.0	" "
" "	"	1	<1.1	"	<110.0	" "
" "	"	1	<0.1	"	<10.0	" "
" "	"	1	0.3	"	30.0	" "
" "	"	1	<0.1	"	<10.0	" "
" "	"	1	0.1	"	10.0	" "
" "	"	1	0.1	"	10.0	" "
" "	"	1	<0.1	"	<10.0	" "
Fredette Lake, Sask.	Lake Whitefish	1	0.1	0.02	5.0	Swanson 1982
" "	"	1	>0.6	"	30.0	" "
" "	"	1	<0.1	"	<5.0	" "
" "	"	1	0.7	"	35.0	" "
" "	"	1	0.2	"	10.0	" "
" "	"	1	<0.1	"	<5.0	" "
" "	"	1	0.1	"	5.0	" "
" "	"	1	0.1	"	5.0	" "
" "	"	1	<0.1	"	<5.0	" "
" "	"	1	4.0	"	200.0	" "
" "	"	1	<0.1	"	<5.0	" "
" "	"	1	<0.1	"	<5.0	" "
" "	"	1	<0.1	"	<5.0	" "
" "	"	1	<0.1	"	<5.0	" "
" "	"	1	<0.1	"	<5.0	" "
Wollaston Lake, Sask. - Hidden Bay	Northern Pike	1	1.54	<0.005	308.0	John 1985
" "	"	1	0.06	"	11.2	"
" "	"	1	0.06	"	11.2	"
" "	"	1	<0.06	"	<11.2	"

Table 11.3 continued

Location	Species	No. Fish Samples	Fish Flesh Concentration Bq/kg (fresh)	Water Level Bq/L	Ra-226 BF (L/kg)	Reference
Wollaston Lake, Sask. - Hidden Bay	Walleye	1	0.10	<0.005	20.0	John 1985
" "	"	1	0.25	"	50.0	"
" "	Lake Whitefish	1	0.41	<0.005	82.0	"
" "	"	1	0.04	"	80.0	"
" "	"	1	0.11	"	22.0	"
" "	Lake Trout	1	<0.11	<0.005	<22.0	"
- Collins Bay	Northern Pike	1	0.06	<0.005	12.0	"
" "	"	1	<0.05	"	<10.0	"
" "	Walleye	1	0.35	<0.005	70.0	"
" "	"	1	0.11	"	22.0	"
" "	Lake Whitefish	1	0.20	<0.005	40.0	"

Summary Statistics	
Number of Data Points	134
Geometric Mean	13.1
Geometric Std. Deviation	3.3
Range of Values	1.7 to 603

Table 11.4

LARGE (GAME) FISH FLESH LEAD-210 BIOACCUMULATION FACTORS (BF's)

Location	Species	No. Fish Samples	Fish Flesh Concentration (Bq/kg fresh)	Water Level (Bq/L)	Pb-210 BF (L/kg)	Reference
Okanagan Highlands, BC	Trout	17			<40	Mahon 1982
McDonald Lake, Sask.	Northern Pike	5			250	I.E.S. Inc. 1983
" "	Lake Whitefish	5			250	"
Delta Lake, Sask.	Northern Pike	5			570	"
" "	Lake Whitefish	5			570	"
Russell Lake, Sask.	Northern Pike	5			490	"
" "	Lake Whitefish	5			490	"
Beaverlodge Lake, Sask.	Lake Trout	5			18.0	Swanson 1983
" "	Lake Whitefish	5			18.0	"
Dubyna Lake, Sask.	Northern Pike	5			58	Eldorado 1978
" "	Lake Trout	5			180	"
Schmoo Lake, Sask.	Lake Trout	5			193	"
Donaldson Lake, Sask.	" "	5			153	"
Wollaston Lake, Sask - Pow Bay	Lake Trout ('82)	5	<0.07	0.015	<4.7	ELDOR (Gulf Minerals) 1982
" "	Northern Pike('82)	5	<0.07	0.015	<4.7	"
" "	Lake Trout ('81)	5	<0.22	<0.002	<11.0	"
" "	Northern Pike('81)	5	<0.22	<0.002	<11.0	"
Russell Lake, Sask.	Walleye	1	0.3	0.04	7.5	Key Lake 1979
" "	"	1	2.0	"	50.0	"
" "	"	1	0.2	"	5.0	"
" "	"	1	0.2	"	5.0	"
" "	"	1	1.6	"	40.0	"
" "	"	1	0.3	"	7.5	"
" "	"	1	0.3	"	7.5	"
" "	"	1	0.3	"	7.5	"
" "	"	1	0.5	"	12.5	"
" "	"	1	0.2	"	5.0	"
Russell Lake, Sask.	Lake Whitefish	1	0.5	0.04	12.5	Key Lake 1979
" "	"	1	0.3	"	7.5	"
" "	"	1	0.5	"	12.5	"
" "	"	1	0.3	"	7.5	"
" "	"	1	0.2	"	5.0	"
" "	"	1	0.4	"	10.0	"
" "	"	1	0.4	"	10.0	"

Table 11.4 continued

Location	Species	No. Fish Samples	Fish Flesh Concentration (Bq/kg fresh)	Water Level (Bq/L)	Pb-210 BF (L/kg)	Reference
Russell Lake, Sask.	Lake Whitefish	1	0.2	0.04	5.0	Key Lake 1979
" "	"	1	0.2	"	5.0	"
" "	"	1	0.3	"	7.5	"
Keevan Lake, Sask.	Walleye	1	0.4	<0.02	20.0	Canadian Occidental 1981
" "	"	1	0.8	"	40.0	" "
" "	"	1	0.4	"	20.0	" "
" "	"	1	0.4	"	20.0	" "
" "	"	1	0.6	"	30.0	" "
Keevan Lake, Sask.	Lake Whitefish	1	0.4	<0.02	20.0	Canadian Occidental 1981
" "	"	1	0.4	"	20.0	" "
" "	"	1	0.6	"	30.0	" "
" "	"	1	0.4	"	20.0	" "
" "	"	1	0.4	"	20.0	" "
McClean Lake, Sask.	Walleye	1	0.5	<0.02	25.0	Canadian Occidental 1981
" "	"	1	0.8	"	40.0	" "
" "	"	1	0.5	"	25.0	" "
" "	"	1	2.0	"	100.0	" "
" "	"	1	0.3	"	15.0	" "
McClean Lake, Sask.	Lake Whitefish	1	0.5	<0.02	25.0	Canadian Occidental 1981
" "	"	1	0.6	"	30.0	" "
" "	"	1	0.5	"	25.0	" "
" "	"	1	0.5	"	25.0	" "
" "	"	1	0.5	"	25.0	" "
Beaverlodge Lake, Sask.	Lake Whitefish	1	<0.4	0.03	13.3	Swanson 1982
" "	"	1	0.2	"	6.7	" "
" "	"	1	0.6	"	20.0	" "
" "	"	1	<0.2	"	6.7	" "
" "	"	1	0.4	"	13.3	" "
" "	"	1	0.7	"	23.3	" "
" "	"	1	1.8	"	60.0	" "
" "	"	1	1.3	"	43.3	" "
" "	"	1	0.6	"	20.0	" "
" "	"	1	4.0	"	133.3	" "
" "	"	1	0.3	"	10.0	" "
" "	"	1	<0.2	"	6.7	" "
" "	"	1	0.3	"	10.0	" "
" "	"	1	<0.2	"	6.7	" "
" "	"	1	<0.2	"	6.7	" "
" "	"	1	0.3	"	10.0	" "
" "	"	1	0.3	"	10.0	" "
" "	"	1	7.5	"	250.0	" "
" "	"	1	0.4	"	13.3	" "
" "	"	1	1.2	"	40.0	" "
" "	"	1	0.4	"	13.3	" "
" "	"	1	1.3	"	43.3	" "

Table 11.4 continued

Location	Species	No. Fish Samples	Fish Flesh Concentration (Bq/kg fresh)	Water Level (Bq/L)	Pb-210 BF (L/kg)	Reference
Milliken Lake, Sask.	Lake Whitefish	1	<0.2	0.04	5.0	Swanson 1982
" "	"	1	<0.2	"	5.0	" "
" "	"	1	<0.2	"	5.0	" "
" "	"	1	0.4	"	10.0	" "
" "	"	1	0.3	"	7.5	" "
" "	"	1	<0.3	"	7.5	" "
" "	"	1	1.7	"	42.5	" "
" "	"	1	1.2	"	30.0	" "
" "	"	1	0.7	"	17.5	" "
" "	"	1	<0.2	"	5.0	" "
" "	"	1	0.1	"	2.5	" "
" "	"	1	<0.4	"	10.0	" "
" "	"	1	0.5	"	12.5	" "
" "	"	1	0.6	"	15.0	" "
" "	"	1	0.3	"	7.5	" "
" "	"	1	<0.2	"	5.0	" "
" "	"	1	<0.2	"	5.0	" "
" "	"	1	<0.2	"	5.0	" "
" "	"	1	<0.2	"	5.0	" "
" "	"	1	<0.2	"	5.0	" "
" "	"	1	0.4	"	10.0	" "
" "	"	1	<0.2	"	5.0	" "
Fredette Lake, Sask.	Lake Whitefish	1	<0.2	0.02	10.0	Swanson 1982
" "	"	1	>0.6	"	30.0	" "
" "	"	1	0.5	"	25.0	" "
" "	"	1	0.2	"	10.0	" "
" "	"	1	0.8	"	40.0	" "
" "	"	1	0.3	"	15.0	" "
" "	"	1	2.9	"	145.0	" "
" "	"	1	<1.4	"	70.0	" "
" "	"	1	0.1	"	5.0	" "
" "	"	1	<0.2	"	10.0	" "
" "	"	1	0.2	"	10.0	" "
" "	"	1	<0.2	"	10.0	" "
" "	"	1	0.4	"	20.0	" "
" "	"	1	0.2	"	10.0	" "
" "	"	1	0.2	"	10.0	" "
" "	"	1	<0.2	"	10.0	" "
" "	"	1	<0.2	"	10.0	" "
" "	"	1	0.7	"	35.0	" "
" "	"	1	<0.2	"	10.0	" "

Summary Statistics	
Number of Data Points	120
Geometric Mean	17.6
Geometric Std. Deviation	3.25
Range of Values	2.5 to 570

lakes from the relationship:

$$[\overline{R_i}]_t = \frac{\Sigma S_n\ [R_i]_{n,t} + \Sigma(4\pi L_n)^{0.5}[R_i]_{n,t}}{\Sigma S_n + \Sigma(4\pi L_n)^{0.5}} \qquad (11.4)$$

where

S_n = the length of the reach of river segment "n" (m)

$[R_i]_{n,t}$ = concentration of radionuclide "i" in the surface water at node "n" at time "t" ($Bq.m^{-3}$)

L_n = surface area of the lake designated node "n" (m^2).

The averaging was done on a length rather than a volume basis, since it was felt that this provided a more relevant quantity. Moose might be expected to drink and graze from lakes and rivers in a watershed in proportion to river lengths and lake circumferences, rather than in proportion to the volume of flow at any point in the system.

The literature search for data on radionuclide levels in aquatic macrophytes produced only limited data which was directly usable in calculating bioaccumulation factors. Several sources of data were found to be of little value because the results were reported on either a dry or ash weight basis rather than a wet weight basis. The most useful data was reported by Integrated Environmental Sciences Inc. (1983) for northern Saskatchewan. A review of BF values reported for each radionuclide on twelve samples showed the data to be skewed to the right. Therefore, the data were treated as being lognormally distributed. The calculated statistics for these data are summarized as follows:

Radionuclide	Bioaccumulation Factor ($L.kg^{-1}$) Geometric Mean Value	Bioaccumulation Factor ($L.kg^{-1}$) Geometric Standard Deviation
Uranium	15.5	5.5
Thorium	11.3	6.8
Radium-226	45	2.9
Lead-210	127	2.0

The high geometric standard deviations reported for uranium and thorium reflect the high variability of the data. The mean values suggest that thorium and uranium accumulate much less than either radium-226 or lead-210. The mean value for lead-210, on the other hand, is three times greater than the mean value calculated for radium-226.

11.4 Parameter Values and Code Listing

A summary of the parameters included in the aquatic models is provided in Table 11.5. Parameter values and their distributions are specified for the input parameters on the table. The basis for the specified values are discussed in the appropriate sections in the text of this chapter.

A copy of the codes for calculating radionuclide levels in game fish flesh and aquatic macrophytes are included in Tables 11.6 and 11.7 for the interested reader. Certain features of the codes (e.g. calculation of the radionuclide levels in the surface waters of the drainage basin) are contained in the code for the surface water models discussed in Chapter 10.

11.5 Aquatic Biota Models Test Program

A series of tests were performed to check the aquatic biota models for computational accuracy and reasonableness. Some of these tests are discussed below.

Table 11.5

AQUATIC MODEL VARIABLES

Model Symbol	Description	Units	Nominal Value	Probability Distribution*	Computer Origin	Computer Symbol
$B_{f,i}$	water-to-game fish flesh transfer coefficient:	$Bq.g^{-1}$ (wet wt) $Bq^{-1}.m^3$				
	U-nat		$1.55x10^{-6}$	$LN(1.55x10^{-6},6.1, 1.0x10^{-8},5.8x10^{-5})$	INPUT	BIOACF(1)
	Th-tot		$1.18x10^{-5}$	$LN(1.18x10^{-5},2.6, 1.1x10^{-6},1.1x10^{-4})$	INPUT	BIOACF(2)
	Ra-226		$1.31x10^{-5}$	$LN(1.31x10^{-5},3.3, 1.2x10^{-6},6.0x10^{-4})$	INPUT	BIOACF(4)
	Pb-210		$1.74x10^{-5}$	$LN(1.74x10^{-5},3.25, 1.7x10^{-6},5.7x10^{-4})$	INPUT	BIOACF(3)
$[F_i]_{n,t}$	concentration of radionuclide i in fish flesh at node n	$Bq.g^{-1}$	calculated	calculated	FISH	FISHC(i,n)
$[R_i]_{n,t}$	concentration of radionuclide i in water at node n	$Bq.m^{-3}$	calculated	calculated	LAKE	WATC(i,n)
$B_{q,i}$	water-to-aquatic vegetation transfer coefficient:	$Bq.g^{-1}$ (wet wt) $Bq^{-1}.m^3$				
	U-nat		$1.5x10^{-5}$	$LN(1.5x10^{-5},5.5, 1.0x10^{-6},7.0x10^{-4})$	INPUT	WATVTC(1)
	Th-tot		$1.1x10^{-5}$	$LN(1.1x10^{-5},6.8\ 1x10^{-6},1.6x10^{-4})$	INPUT	WATVTC(2)
	Ra-226		$4.5x10^{-5}$	$LN(4.5x10^{-5},2.9, 1x10^{-5}, 3.3x10^{-4})$	INPUT	WATVTC(4)
	Pb-210		$1.3x10^{-4}$	$LN(1.3x10^{-4},2.0, 4.0x10^{-5},4.3x10^{-4})$	INPUT	WATVTC(3)
$[C_{q,i}]_t$	concentration of radionuclide i in aquatic vegetation	$Bq.g^{-1}$	calculated	calculated	WATVEG	AQVEGC(i)
$[R_i]_t$	average concentration of radionuclide i in water over the watershed	$Bq.m^{-3}$	calculated	calculated	LAKE, RIVER	WATAVG(i)
L_n	surface area of the lake designated node n	m^2	site specific: see Table 10.1		INPUT	LAREA(n)
S_n	length of river segment n	m	site specific: see Table 10.1		INPUT	LAREA(n)

Note

* Distributions are as described in Table 2.3.

Table 11.6

FISH MODEL CODE LISTING

```
      SUBROUTINE FISH
C
C     SUBROUTINE CALCULATES CONCENTRATIONS OF RADIONUCLIDES IN FISH
C
      INCLUDE 'VAR.INC'
      INCLUDE 'MODEL.INC'
      IF (CODFIS.GE.1) WRITE (*,*) ' SUBROUTINE FISH'
C
C     CALCULATE MASS OF RADIONUCLIDES IN FISH
C
      DO 10 ISUB=1,4
         FISHC(ISUB,WTSEG)=BIOACF(ISUB)*WATC(ISUB,WTSEG)
         IF (CODFIS.EQ.2) WRITE (*,100) ISUB,WTSEG,FISHC(ISUB,WTSEG),
     &      BIOACF(ISUB),WATC(ISUB,WTSEG)
10    CONTINUE
C
C     CALCULATE FISH AVAILABILITY
C
      IF(WATPH(WTSEG).GT.6.)THEN
         FISHA(WTSEG)=1.0
      ELSEIF(WATPH(WTSEG).GT.5.)THEN
         FISHA(WTSEG)=0.75+0.25*(WATPH(WTSEG)-5.)
      ELSEIF(WATPH(WTSEG).GT.4.5)THEN
         FISHA(WTSEG)=0.25+WATPH(WTSEG)-4.5
      ELSEIF(WATPH(WTSEG).GT.3.5)THEN
         FISHA(WTSEG)=0.25*(WATPH(WTSEG)-3.5)
      ELSE
         FISHA(WTSEG)=0.0
      ENDIF
      IF(CODFIS.EQ.2.)WRITE(*,200)WATPH(WTSEG),FISHA(WTSEG)
      RETURN
100   FORMAT (' FISHC(',I1,',',I2,') ',E10.3,'  BIOACF',E10.3,'  WATC',
     &   E10.3)
200   FORMAT (' WATPH = ',E10.3,'   FISHA = ',E10.3)
      END
```

Table 11.7

AQUATIC MACROPHYTE MODEL CODE LISTING

```
      SUBROUTINE WATVEG
C
C     SUBROUTINE CALCULATES AVERAGE RADIONUCLIDE CONCENTRATION
C     FOR AQUATIC VEGETATION IN WATERSHED.  AVERAGE BASED ON
C     AVERAGE WATER CONCENTRATION; NAMELY, AVERAGE OVER LENGTH
C     OF RIVERS AND CIRCUMFERENCE OF LENGTHS.
C
      INCLUDE 'VAR.INC'
      INCLUDE 'MODEL.INC'
      IF (CODWVG.GE.1) WRITE (*,*) ' SUBROUTINE WATVEG'
      DO 10 ISUB=1,4
         AQVEGC(ISUB)=WATVTC(ISUB)*WATAVG(ISUB)
         IF (CODWVG.EQ.2) WRITE (*,100) ISUB,AQVEGC(ISUB)
10    CONTINUE
      RETURN
100   FORMAT (' AQVEGC(',I1,') ',E10.3)
      END
```

Hand calculations were checked against a deterministic run to confirm that the models executed the equations properly. The models were also run probabilistically with the results checked for reasonableness.

11.6 References

Beamish, R.J., and Harvey, H.H., 1972. "Acidification of the La Cloche Mountain Lakes, Ontario, and Resulting Fish Mortalities." J. Fish. Res. Bd. Canada, Vol. 29, pp. 1131-1143.

Beamish, R.J., Lockhart, W., Van Loon, J., and Harvey, H.H., 1975. "Long-Term Acidification of a Lake and Resulting Effects on Fishes." Ambio, Vol. 4, pp. 98-102.

Canadian Occidental Inc., 1981. "Environmental Baseline Studies for Project Wolly, McClean Lake Area." Interim Report No. 3.

ELDOR/Gulf Minerals Canada Limited, 1982. "Rabbit Lake Environmental Monitoring Report."

Eldorado Nuclear Limited, 1978. "Dubyna Lake Environmental Assessment." Prepared by Saskatchewan Research Council, Saskatoon.

Gardner, R.H., Hoffman, F.O. and Blaylock, B.G., 1985. "A Dynamic Model of Radium-226 Behaviour in an Oligotrophic Lake." Presented in a Research Report Entitled - Probabilistic Model Development for the Assessment of the Long-term Effects of Uranium Mill Tailings. Prepared by SENES Consultants Limited for the National Uranium Tailings Program, CANMET, Energy, Mines and Resources Canada, Ottawa.

Integrated Environmental Sciences Inc., 1983. "Baseline Studies of Aquatic Sediments and Macrophytes, Fish, Soil and Terrestrial Vegetation at Key Lake, Saskatchewan." Prepared for Key Lake Mining Corporation, Saskatoon.

Jensen, K.W., and Snekvik, E., 1972. "Low pH Levels Wipe out Salmon and Trout Populations in Southernmost Norway." Ambio, Vol. 1(6), pp. 223-225.

John, R.D., 1985. "Fish Study for the National Uranium Tailings Program (NUTP)." A Research Report Prepared for the NUTP, CANMET, Energy, Mines and Resources Canada, Ottawa.

Key Lake Mining Corporation, 1979. "Key Lake Project Environmental Impact Assessment." Volume II.

Mahon, D.C., 1982. "Uptake and Translocation of Naturally-Occurring Radionuclides of the Uranium Series." Bull.Environment.Contam. Toxicol., Vol. 29, pp. 697-703.

Menendez, R., 1976. "Chronic Effects of Reduced pH on Brook Trout (Salvelinus fontinalis)." J. Fish. Res. Bd. Canada, Vol. 33, pp. 118-123.

National Research Council of Canada (NRCC), 1981. "Acidification in the Canadian Aquatic Environment: Scientific Criteria for Assessing the Effects of Acidic Deposition on Squatic Ecosystems." Publication No. NRCC 18475.

Neville, C.M., 1985. "Physiological Response of Juvenile Rainbow Trout, Salmo gairdneri, to Acid and Aluminum - Prediction of Field Responses from Laboratory Data." Can. J. Fish. Aquat. Sci., Vol. 42, pp. 2004-2019.

Norcen Energy Resources Limited, 1980. "Blizzard Uranium Project Phase 6 Report - Environment."

Rahel, F.J., and Magnuson, J.J., 1983. "Low pH and the Absence of Fish Species in Naturally Acidic Wisconsin Lakes: Inferences for Cultural Acidification." Can. J. Fish. Aquat. Sci., Vol. 40, pp. 3-9.

Schindler, D.W., Mills, K.H., Malley, D.F., Findlay, D.L., Shearer, J.A., Davies, I.J., Turner, M.A., Linsey, G.A., and Cruikshank, D.R., 1985. "Long-Term Ecosystem Stress: The Effects of Years of Experimental Acidification on a Small Lake." Science, Vol. 228, pp. 1395-1401.

Schofield, C.L., 1976. "Acid Precipitation: Effects on Fish." Ambio, Vol. 5 (5-6), pp. 228-230.

SENES Consultants Limited, 1986. "Probabilistic Model Development for the Assessment of the Long-Term Effects of Uranium Mill Tailings in Canada - Phase III." Research Report prepared for the National Uranium Tailings Program, CANMET, EMR, under Supply and Services Canada Contract No. 0SQ85-00182.

Swanson, S.M., 1982. "Levels and Effects of Radionuclides in Aquatic Fauna of the Beaverlodge Area (Saskatchewan)." Saskatchewan Research Council Publication No. C-806-5-E-82.

Swanson, S.M., 1983. "Levels of Ra-226, Pb-210 and U-total in Fish Near a Saskatchewan Uranium Mine and Mill." Health Physics, Vol. 45, pp. 67-80.

12.0 ANIMAL PRODUCE MODEL

12.1 Introduction

Chapter 10 described how the concentration of a radionuclide in surface water is calculated and Chapter 11 detailed how this concentration is used to model aquatic vegetation. Chapter 5 presents how air concentrations are calculated and Chapter 8 documents the model used to calculate the concentration in summer forage (airshed and watershed averages), lichens and browse (watershed average) air-related pathways. This chapter documents how these various environmental concentrations are used to calculate the concentration of radionuclide i in the flesh of caribou, moose and deer.

In UTAP.3, the model has been expanded to include the summer forage/browse/water-to-deer flesh pathways. The caribou model includes the lichen/summer forage/water-to-caribou flesh pathways. The calculation of the concentration of radionuclide i in moose flesh is a new addition, and includes the browse/water/aquatic vegetation-to-moose flesh pathways. Four radionuclide concentrations in animal flesh are calculated (U-nat, Th-tot, Ra-226 and Pb-210) for each time step. Only one value, representing an average annual concentration of radionuclide i for the entire area modelled, is calculated for each of deer, moose and caribou flesh for each time step. Thus the concentration of radionuclide i in deer, caribou or moose flesh used in subsequent dose calculations (see Chapter 13) does not vary with the location or type of receptor, but varies with time.

In this chapter, the following subscripts are used to simplify parameter symbols: i is used to identify those parameters that vary with the radionuclide being modelled; and t indicates that a parameter may vary with time. Various environmental media are abbreviated as follows:

v = vegetation
c = caribou
d = deer
w = average water over all nodes
m = moose
q = aquatic vegetation
a = air

Each animal produce model has been divided into two components: air-pathway-related intakes and water-pathway-related intakes. This is because the relative ratios of Th-232:Th-230 are different for these two pathways. Thus the pathway-related intakes must be kept separate so that appropriate dose conversion factors may be used in the calculation of dose due to the ingestion of animal produce as described in Chapter 13.

Details on the caribou- moose- and deer-flesh models and parameter selection are provided below. Where considered appropriate, parameters were assigned distributions. The extent of this variation was based on the collective opinion of the study group as to how certain they were about the nominal value of particular parameters. Such parameters were typically allowed to vary 10 to 50% about the nominal values and were given a triangular or uniform distribution.

The component model aspects of the UTAP studies have largely focussed on the implementation of environmental and dose models. Comparatively little effort has been expended on issues of fundamental environmental science or on the development of parameter distributions. Both aspects would need to be reviewed on a case-by-case basis with models being modified or upgraded if required and site/species-specific parameters being input to the models insofar as practicable. The computer code for the animal produce models is presented in Table 12.4.

12.2 Radionuclides in Caribou Flesh

A number of factors were considered in designing the caribou flesh models: migration; grazing habits; and the time of year the animal is harvested by the receptor in question.

Caribou are migratory animals, and as such range over very wide areas. It is therefore very unlikely that any one caribou would spend the entire year in the study area or that it would stay in one small portion of the study area. Instead, it is much more likely to pass through the area in a more or less random fashion at one or more times during the year. Thus, for the time spent in the area, caribou were assumed to roam freely and equally over the entire model area.

The grazing habits of the caribou are also very important determinants in the concentration of radionuclides in their flesh. During the summer months, caribou eat mainly fresh green vegetation. During the winter months, they eat mainly lichens. Lichens tend to have much higher concentrations of radionuclides than annual plants. It has been estimated that the daily intake of a radionuclide from lichens would be 5-10 times greater than that from plants whose edible foliage is replaced annually (Garner, 1972). It is for this reason that the levels of radionuclides in caribou flesh show considerable seasonal changes (Garner, 1972). Thus the time of year that the animal is likely to be slaughtered and consumed must also be taken into consideration in any one application of this model.

The models presented below were designed to offer maximum flexibility to the user, based on the above considerations.

12.2.1 Air Pathway to Caribou Flesh (ACARC)

Radionuclides in winter (lichen) and summer (grass) forage may be eaten by caribou which in turn may be eaten by man. The transfer of radionuclide i from vegetation to meat was modelled as follows (U.S. NRC, 1982):

$$[C(air)]_{c,i,t} = Q_c F_{c,i} \sum_{v} F_{c,v} [C]_{v,i,t} \qquad (12.1)$$

where

$[C(air)]_{c,i,t}$ = the annual average concentration of radionuclide i in caribou flesh at time t ($Bq.g^{-1}$ (wet weight)) due to the air pathway

Q_c = the average daily feed intake rate of the caribou (g (wet weight).d^{-1})

$F_{c,i}$ = the feed-to-meat transfer coefficient for caribou ($Bq.g^{-1}$ (wet weight).Bq^{-1}.d)

$F_{c,v}$ = the fraction of the caribou's annual feed intake that is local vegetation type v (lichens and summer forage in this case)

$[C]_{v,i,t}$ = the average concentration of radionuclide i in vegetation type v (lichens and summer forage in this case) at time t, where the average is taken over the entire area being modelled (see Sections 8.5 and 8.3) ($Bq.g^{-1}$ (wet weight)).

The time dependence in this case is only due to the time dependence in the vegetation concentrations.

Table 12.1 summarizes these variables and their distributions. Very little information is available in the literature on which to base these distributions. The information and assumptions used are summarized below.

The average daily feed intake of the caribou is based on McDowell-Boyer et al., (1979). The values for $F_{c,i}$ are based on SENES (1983) as follows:

Uranium, Thorium

Values used were for cattle in the absence of available information on caribou (U.S. NRC, 1982).

Table 12.1

CARIBOU FLESH MODEL VARIABLES

Model Symbol	Description	Units	Nominal Value	Probability Distribution[1]	Computer Origin	Computer Symbol
$[C(air)]_{c,i,t}$	concentration of radionuclide i in caribou flesh due to the air pathway at time t	$Bq.g^{-1}$ (wet wt)	calculated	calculated	ANIMAL	ACARC(i) i=1,4
$[C]_{v,i,t}$	concentration of radionuclide i in vegetation type v	$Bq.g^{-1}$ (wet wt)				
	lichen		calculated	calculated	VEGCON	LICHC(i) i=1,4
	summer forage		calculated	calculated	VEGCON	SUFOC(i) i=1,4
	at time t					
$F_{c,i}$	feed-to-caribou meat transfer coefficient for radionuclide i:	$Bq.g^{-1}$ (wet wt). $Bq.^{-1}d$			INPUT	FMTCC(i) i=1,4
	U-nat		$3.4x10^{-7}$	$T(1.1x10^{-7},3.4x10^{-7},1.0x10^{-6})$		
	Th-tot		$2.0x10^{-7}$	$T(0.7x10^{-7},2.0x10^{-7},6.0x10^{-7})$		
	Pb-210		$4.0x10^{-7}$	$T(1.3x10^{-7},4.0x10^{-7},1.2x10^{-6})$		
	Ra-226		$5.1x10^{-7}$	$T(1.7x10^{-7},5.1x10^{-7},1.5x10^{-6})$		
$F_{c,v}$	fraction of annual intake that is local vegetation type v:	-				
	lichen		0.4	T(0.05,0.2,0.5)	INPUT	FAILC
	summer forage		0.4	T(0.05,0.2,0.5)	INPUT	FAISFC
Q_c	feed ingestion rate for caribou	$g(wet\ wt).d^{-1}$	$7.0x10^3$	$T(5.0x10^3,7.0x10^3,9.0x10^3)$	INPUT	FIRC
$[C(water)]_{c,i,t}$	concentration of radionuclide i in caribou flesh due to the water pathway at time t	$Bq.g^{-1}$ (wet wt)	calculated	calculated	ANIMAL	WCARC(i) i=1,4
W_c	water ingestion rate for caribou	$m^3.d^{-1}$	$11.5x10^{-3}$	$T(7.7x10^{-3},11.5x10^{-3},15.3x10^{-3})$	INPUT	WIRC
$[C]_{w,i,t}$	concentration of radionuclide i in water at time t	$Bq.m^{-3}$	calculated	calculated	WATEX	WATAVG(i) i=1,4
f	adjustment factor for fraction of time spent in watershed	-	calculated	calculated	ANIMAL	FT
$[C(total)]_{c,i,t}$	concentration of radionuclide i in caribou flesh at time t	$Bq.g^{-1}$ (wet.wt)	calculated	calculated	ANIMAL	CARC(i)i=1,4

Note

1 Distributions are as described on Table 2.3

2 ACARC is available as ACARCF (summer forage pathway) and ACARCL (lichen pathway) which may be specified as additional outputs (see Users Manual Section 6.4 (SENES, 1987)).

Radium

Although some information was available on background radium levels in caribou and lichens, it was considered too limited to derive a $F_{c,Ra}$. Thus the number used is for cattle (U.S. NRC, 1982).

Lead

A value for $F_{c,Pb}$ was derived from a review of available data on the concentrations in lichens and caribou. (McDowell-Boyer et al., 1979; Holtzman, 1966a and 1966b; Kauranen and Miettinen, 1969; UNSCEAR, 1977; Blanchard, 1966; Blanchard and Moore, 1970).

The fractions of the annual intake of the caribou that were local (ie. in the model area) lichen and summer forage ($F_{c,v}$) were allowed to vary independently between 0.05 and 0.5. Thus the total local annual feed intake will seldom add up to 100 per cent. This was included to try to reflect the migratory nature of caribou, as it was considered too conservative to assume 100 per cent consumption of local feed. Note that the user may change this model to account for any other caribou grazing and/or migratory pattern or human consumption pattern by careful adjustment of this factor.

12.2.2 Water Pathway to Caribou Flesh (WCARC)

Surface water containing radionuclides may be drunk by caribou which in turn may be eaten by man. The transfer of radionuclide i from water to meat was modelled as follows:

$$[C(water)]_{c,i,t} = F_{c,i} \, W_c \, [C]_{w,i,t} \, f\left(\sum_{v} F_{c,v}\right) \qquad (12.2)$$

where

$[C(water)]_{c,i,t}$ = the annual average concentration of radionuclide i in caribou flesh at time t due to the water pathway ($Bq.g^{-1}$ (wet weight))

$F_{c,i}$ = the water-to-meat transfer coefficient for caribou ($Bq.g^{-1}$ (wet weight)$.Bq^{-1}.d$) (taken to be the same as feed-to-meat transfer coefficient in section 12.2.1)

W_c = the average daily water intake of the caribou ($m^3.d^{-1}$)

$[C]_{w,i,t}$ = the average annual concentration of radionuclide i in the surface waters of the watershed at time t ($Bq.m^{-3}$)(see Section 11.3.3)

f = an adjustment factor to reflect that the watershed is a fraction of the total area being modelled

$F_{c,v}$ = the fraction of the annual water intake that is local (taken to be the same as the fraction of annual feed that is local).

Table 12.1 summarizes these variables and their distributions.

No estimate of the daily water intake of caribou was found in the literature. Therefore, an estimate for W_c was derived by scaling the daily water intake of a 450 kg beef cow (30 to 60 L, midpoint 45 L) (Comar, 1966) by a typical caribou body weight of 115 kg (Palmer, 1934, as cited by Miller, not dated).

No literature was found to indicate that $F_{c,i}$ would change for the ingestion of water versus vegetation.

The two factors, f and $F_{c,v}$, are included to account for the migratory and grazing habits of caribou referred to earlier. The factor $F_{c,v}$ for summer forage is used as a surrogate for the amount of time the caribou spends in the modelled area during summer, while $F_{c,v}$ for lichen is a surrogate for the amount of time spent in the area during the winter. Thus, $\sum_v F_{c,v}$ represents the fraction of the entire year a caribou would spend in the area modelled in this study. While the caribou is present in the study area, it is assumed to roam equally over the entire area. Since the watershed affected by the tailings is only a small fraction of the total study area, the caribou is assumed to be present, and drink water there, for only a small fraction of the time. The factor f is used to account for the difference between the entire study area and the watershed area, or equivalently the difference between the caribou's total water intake and its contaminated water intake. The factor f is calculated as the ratio of area of the watershed divided by the total study area.

12.3 Radionuclides in Moose Flesh

Two main factors were considered in designing the moose flesh model: ranging and grazing habits.

Although the individual animals may roam over very large areas, in general moose are not migratory and tend to have much smaller home ranges than caribou (Lynch, 1976; Taylor and Ballard, 1979; Saunders and Williamson, 1972). For this reason, the moose was assumed to range over the watershed. Any moose not harvested in the watershed were assumed to have no radionuclide content due to the tailings area. This is not strictly correct, as there may still be some elevated concentrations in other moose in the model area due to the air pathway. However moose flesh was not considered to play a major role in population dose estimates, and it was felt that the added complexity of calculating browse and then moose flesh concentrations for each receptor location was not warranted at this time. Therefore only the "watershed" moose as described above was considered.

In contrast to the caribou, there is no literature to indicate that the radionuclide content of moose flesh may vary widely over the course of the year (indeed very little information of any sort on the concentration of U, Th, Ra and Pb in moose flesh was identified during the project). However, the moose does have a different diet in the winter versus summer months.

As noted by Krefting (1974), "...The moose is a browsing species, especially during the winter months. Its food habits are quite different in eastern and western North America where significant differences exist in the availability of browse species. Most investigators agree that willows are the main source of winter browse in the west (Murce, 1944). And in the east, balsam fir, aspen, and paper birch are the major species (Pimlott, 1961)." In the warm months, many moose supplement their woody diet (twigs and leaves) with aquatic vegetation, tending to prefer smaller submerged species of aquatic plants, usually in shallow waters (Fraser et al., 1984).

Thus, a moose consuming strictly browse in the winter, and a mixture of browse and aquatic vegetation in the summer was modelled. These intakes were averaged over the year to derive average daily intakes of aquatic vegetation and browse for use in the models described below. This results in the calculation of an average annual concentration of radionuclide i in moose flesh. The user may calculate the concentration in the moose flesh on a seasonal basis (if the animal is only slaughtered in one season) by adjusting these intakes accordingly.

12.3.1 Air Pathway to Moose Flesh (AMOSC)

Radionuclides in browse may be eaten by moose which may in turn be eaten by man. This transfer was modelled as follows:

$$[C(air)]_{m,i,t} = F_{m,i}\ Q_m\ F_{m,b}\ [C]_{b,i,t} \qquad (12.3)$$

where

$[C(air)]_{m,i,t}$ = the annual average concentration of radionuclide i in moose flesh at time t ($Bq.g^{-1}$ (wet weight))

$F_{m,i}$ = the feed-to-moose meat transfer coefficient for radionuclide i ($Bq.g^{-1}$(wet weight)$.Bq^{-1}.d$)

Q_m = the average daily feed intake of the moose (g (wet weight)$.d^{-1}$)

$F_{m,b}$ = the fraction of the moose annual feed intake that is browse

$[C]_{b,i,t}$ = the average concentration of radionuclide i in browse at time t, where the average is taken over the watershed ($Bq.g^{-1}$(wet weight)) (see Section 8.4)

The time dependence in this case is only due to the time dependence in the browse concentration.

The values selected for the variables in the moose flesh model outlined above are presented in Table 12.2. The values of Q_m and $F_{m,b}$ are based on a study by Belovsky et al. (1973). Moose were found to have an average feed intake of 27 kg (wet weight) per day. In the summer months (assumed to be May to September inclusive), moose consumed an average of 21 kg of browse, the remaining 6 kg being aquatic macrophytes (see Section 12.3.2). During the winter months (the remaining 7 months of the year), moose were assumed to consume 27 kg per day of browse. Hence, the nominal value of $F_{m,b}$ can be determined as:

$$(21/27)\ (5/12) + (27/27)\ (7/12) = 0.90$$

A triangular distribution about this nominal value was assigned to $F_{m,b}$.

Values for $F_{m,i}$ are the same as those used for caribou (see Section 12.2) in the absence of sufficient moose-specific data to derive more suitable transfer coefficients.

12.3.2 Water Pathway to Moose Flesh (WMOSC)

Surface water and aquatic macrophytes containing radionuclides may be ingested by moose which in turn may be eaten by man. This transfer was modelled as follows:

$$[C(water)]_{m,i,t} = F_{m,i}\ (Q_m\ F_{m,q}\ [C]_{q,i,t} + W_m\ [C]_{w,i,t}) \qquad (12.4)$$

where

$[C(water)]_{m,i,t}$ = the annual average concentration of radionuclide i in moose flesh at time t ($Bq.g^{-1}$(wet weight))

$F_{m,i}$ = the feed-to-moose meat transfer coefficent for radionuclide i ($Bq.g^{-1}$(wet weight). $Bq^{-1}.d$) (see Section 12.3.1)

Q_m = the average daily intake of aquatic macrophytes the moose (g(wet weight).d^{-1})

$F_{m,q}$ = the fraction of the moose annual feed intake that is aquatic macrophytes (= 1 - F_{mb})

$[C]_{q,i,t}$ = the average concentration of radionuclide i in aquatic macrophytes (Bq.g^{-1}(wet weight)) at time t, where the average is taken over the watershed (see Section 11.3.3)

W_m = the average daily water intake of the moose ($m^3.d^{-1}$)

$[C]_{w,i,t}$ = the average concentration of radionuclide i in the water at time t, where the average is taken over the watershed (Bq.m^{-3} (see Section 11.3.3)).

Table 12.2 summarizes the parameter values used in the moose flesh model. W_m was derived by scaling the daily water intake of a 450 kg beef cow (30 to 60 L) (Comar, 1966) by a typical moose body weight of 360 kg (Belovsky et al., 1973).

12.4 Radionuclides in Deer Flesh

Ranging and grazing habits were the two main considerations in designing the deer flesh model.

Like the moose, deer (specifically white-tailed deer) are in general not migratory and tend to have much smaller home ranges than caribou. In the winter in Eastern Canada, deer usually stay in "yards". These yards are small and typically are well sheltered conifer areas. In the summer they range over somewhat larger areas, typically from 60 to 520 hectares. The deer tend to maintain these ranges year after year in the southern portion of the Great Lakes Region and Eastern Canada. However, in more northern areas, as in much of Ontario and in Western Canada, the home range is hard to define (Blouch, 1984; Huot et al., 1984; Wishart, 1984). For the purposes of this model the deer was assumed to range over the watershed year round. Any deer not harvested in the watershed were assumed to have no radionuclide content due to the tailings area. This is not strictly correct, as there may still be some

Table 12.2

MOOSE FLESH MODEL VARIABLES

Model Symbol	Description	Units	Nominal Value	Probability Distribution[1]	Computer Origin	Computer Symbol
$[C(air)]_{m,i,t}$	concentration of radionuclide i in moose flesh due to the air pathway at time t	$Bq.g^{-1}$ (wet wt)	calculated	calculated	ANIMAL	AMOSC(i) i=1,4
$[C]_{b,i,t}$	concentration of radionuclide i in browse at time t	$Bq.g^{-1}$ (wet wt)	calculated	calculated	VEGCON	BRWSC(i) i=1,4
$F_{m,i}$	feed-to-moose meat transfer coefficient for radionuclide i:	$Bq.g^{-1}$ (wet wt) $Bq^{-1}.d$			INPUT	FMTCM(i) i=1,4
	U-nat		$3.4x10^{-7}$	$T(1.1x10^{-7},3.4x10^{-7},1.0x10^{-6})$		
	Th-tot		$2.0x10^{-7}$	$T(0.7x10^{-7},2.0x10^{-7},6.0x10^{-7})$		
	Pb-210		$4.0x10^{-7}$	$T(1.3x10^{-7},4.0x10^{-7},1.2x10^{-5})$		
	Ra-226		$5.1x10^{-7}$	$T(1.7x10^{-7},5.1x10^{-7},1.5x10^{-6})$		
Q_m	feed ingestion rate for moose	$g(wet\ wt).d^{-1}$	$27.0x10^3$	$C(27.0x10^3)$	INPUT	FIRM
$F_{m,b}$	fraction of moose intake that is browse	---	0.9	T(0.8,0.9,0.95)	INPUT	FAIBM
$F_{m,q}$	fraction of moose intake that is aquatic macrophyte	---	calculated	calculated	ANIMAL	FAIAM
$[C]_{q,i,t}$	concentration of radionuclide i in aquatic macrophytes at time t	$Bq.g^{-1}$ (wet wt)	calculated	calculated	WATVEG	AQVEGC(i) i=1,4
W_m	water ingestion rate for moose	$m^3.d^{-1}$	.036	T(.024,0.036,0.048)	INPUT	WIRM
$[C]_{w,i,t}$	concentration of radionuclide i in water at time t	$Bq.m^{-3}$	calculated	calculated	WATEX	WATAVG(i) i=1,4
$[C(water)]_{m,i,t}$	concentration of radionuclide i in moose flesh due to the water pathway at time t	$Bq.g^{-1}$ (wet wt)	calculated	calculated	ANIMAL	WMOSC(i) i=1,4
$[C(total)]_{m,i,t}$	concentration of radionuclide i in moose flesh at time t	$Bq.g^{-1}$ (wet wt)	calculated	calculated	ANIMAL	MOSC(i) i=1,4

Notes

1 Distributions are as described on Table 2.3.
2 WMOSC is available as WMOSCA (aquatic macrophytes pathway) and WMOSCW (water pathway) which may be specified as additional outputs (see Users Manual Section 6.4 (SENES, 1987)).

elevated concentrations in other deer in the model area due to the air pathway. However it was felt that the added complexity of calculating summer forage and browse concentrations for each receptor location was not warranted at this time. Therefore only the "watershed" deer as described above was modelled. It should be noted that through careful selection of parameter values the user could manipulate the caribou model to calculate an average deer flesh concentration for the model area. This would involve changing the parameters for lichens to those for browse (thereby creating a "model area" browse vs. the watershed browse) and the parameters for caribou to those for deer (thereby creating a "model area" deer vs. a "watershed" deer).

As for the moose, there was no literature indicating that the radionuclide content of deer flesh may vary widely over the year. However, the deer does have a different diet in the winter versus summer months. Browse is the primary source of food for deer during the winter months. The type of browse depends on what is available regionally - for instance in Ontario northern white cedar, red maple, hemlock, American mountain ash and alternate leaf dogwood are preferred. From spring to fall, herbaceous vegetation is preferred, and if available deer will graze on grasses, sedges and new tree growths (Blouch, 1984). The deer modelled in UTAP was thus assumed to eat browse from the watershed in the winter and summer forage from the watershed in the summer. These intakes were averaged over the year to derive average daily intakes of browse and summer forage for use in the models described below. This results in the calculation of an average annual concentration of radionuclide i in deer flesh. As for the caribou and moose, the user may calculate the concentration in deer flesh on a seasonal basis (if the animal is only slaughtered in one season) by adjusting these intakes accordingly.

12.4.1 Air Pathway to Deer Flesh (ADERC)

Radionuclides in summer forage and browse may be eaten by deer which may in turn be eaten by man. The transfer from vegetation to deer flesh was modelled as follows:

$$[C(air)]_{d,i,t} = F_{d,i}\, Q_d \sum_{v} F_{d,v}\, [C]_{v,i,t} \qquad (12.5)$$

where

$[C(air)]_{d,i,t}$ = the annual average concentration of radionuclide i in deer flesh at time t ($Bq.g^{-1}$ (wet weight)) due to the air pathway

$F_{d,i}$ = the feed-to-meat transfer coefficient for deer for radionuclide i ($Bq.g^{-1}$ (wet weight)$.Bq^{-1}.d$)

Q_d = the average daily feed intake of the deer (g (wet weight)$.d^{-1}$)

$F_{d,v}$ = the fraction of the deer's annual feed intake that is local vegetation type v (browse and summer forage in this case)

$[C]_{v,i,t}$ = the average concentration of radionuclide i in vegetation type v (browse and summer forage in this case) at time t, where the average is taken over the watershed (see Sections 8.3 and 8.4) ($Bq.g^{-1}$ (wet weight)).

The time dependence in $[C(air)]_{d,i,t}$ is only due to the time dependence in $[C]_{v,i,t}$.

Table 12.3 summarizes these variables and their distributions.

Q_d was based on Verme and Ullrey (1984), assuming a moisture content of 50 to 80%. $F_{d,sf}$ is based on the assumption that summer forage is available 3 to 5 months of the year, with a nominal value of 5 months. $F_{d,b}$ is calculated after $F_{d,sf}$ is selected ($F_{d,b}=1-F_{d,sf}$).

$F_{d,i}$ values are the same as those used for caribou (see Section 12.2) in the absence of sufficient deer-specific data to derive more suitable transfer coefficients.

12.4.2 Water Pathway to Deer Flesh (WDERC)

Radionuclides in surface water may be transferred to man through the water-deer flesh-man pathway. The transfer of radionuclide i from water to deer

Table 12.3

DEER FLESH MODEL VARIABLES

Model Symbol	Description	Units	Nominal Value	Probability Distribution[1]	Computer Origin	Computer Symbol
$[C(air)]_{d,i,t}$	concentration of radionuclide i in deer flesh due to the air pathway at time t	$Bq.g^{-1}$ (wet wt)	calculated	calculated	ANIMAL	ADERC(i) i=1,4
$[C]_{v,i,t}$	concentration of radionuclide i in vegetation type v	$Bq.g^{-1}$ (wet wt)				
	browse		calculated	calculated	VEGCON	BRWSC(i) i=1,4
	summer forage		calculated	calculated	VEGCON	SUFOC(i,2) i=1,4
	at time t					
$F_{d,i}$	feed-to-deer meat transfer coefficient for radionuclide i:	$Bq.g^{-1}$ (wet wt). $Bq.^{-1}d$			INPUT	FMTCD(i) i=1,4
	U-nat		$3.4x10^{-7}$	$T(1.1x10^{-7},3.4x10^{-7},1.0x10^{-6})$		
	Th-tot		$2.0x10^{-7}$	$T(0.7x10^{-7},2.0x10^{-7},6.0x10^{-7})$		
	Pb-210		$4.0x10^{-7}$	$T(1.3x10^{-7},4.0x10^{-7},1.2x10^{-6})$		
	Ra-226		$5.1x10^{-7}$	$T(1.7x10^{-7},5.1x10^{-7},1.5x10^{-6})$		
$F_{d,v}$	fraction of annual intake that is local vegetation type v:	---				
	browse		calculated	calculated	INPUT	FAIBD
	summer forage		0.4	T(0.25,.33,.40)	INPUT	FAISFD
Q_d	feed ingestion rate for deer	$g(wet\ wt).d^{-1}$	$7.5x10^3$	$U(4.5x10^3,1.0x10^4)$	INPUT	FIRD
$[C(water)]_{d,i,t}$	concentration of radionuclide i in deer flesh due to the water pathway at time t	$Bq.g^{-1}$ (wet wt)	calculated	calculated	ANIMAL	WDERC(i) i=1,4
W_d	water ingestion rate for deer	$m^3.d^{-1}$	$1.0x10^{-3}$	$U(0.7x10^{-3},1.4x10^{-3})$	INPUT	WIRD
$[C]_{w,i,t}$	concentration of radionuclide i in water at time t	$Bq.m^{-3}$	calculated	calculated	WATEX	WATAVG(i) i=1,4
$[C(total)]_{d,i,t}$	concentration of radionuclide i in deer flesh at time t	$Bq.g^{-1}$ (wet.wt)	calculated	calculated	ANIMAL	DERC(i) i=1,4)

Notes

1 Distributions are as described on Table 2.3

2 ADERC is available as ADERCF (summer forage pathway) and ADERCB (browse pathway) which may be specified as additional outputs (see Users Manual Section 6.4 (SENES, 1987))

flesh was modelled as follows:

$$[C(water)]_{d,i,t} = F_{d,i}\ W_d\ [C]_{w,i,t} \qquad (12.6)$$

where

$[C(water)]_{d,i,t}$ = the annual average concentration of radionuclide i in deer flesh at time t due to the water pathway ($Bq.g^{-1}$ (wet weight))

$F_{d,i}$ = the water-to-meat transfer coefficient for deer ($Bq.g^{-1}$ (wet weight).$Bq^{-1}.d$) (taken to be the same as $F_{d,i}$ in Section 12.4.1)

W_d = the average daily water intake of the deer ($m^3.d^{-1}$)

$[C]_{w,i,t}$ = the average annual concentration of radionuclide i in the surface waters of the watershed at time t ($Bq.m^{-3}$) (see Section 11.3.3).

Table 12.3 lists these parameters and their distributions. The time dependence of $[C(water)]_{d,i,t}$ is strictly due to the time variance of $[C]_{w,i,t}$.

The water intake of deer is quite variable, depending on the climate and type of food being consumed. W_d is based on Marchinton and Hirth (1984).

12.5 Description of Computer Model

The variables used in the animal produce model are summarized in Tables 12.1 to 12.3. The computer code listing for this model is provided in Table 12.4.

12.6 Animal Produce Model Test Program

A series of tests were performed to check the animal produce model for computational accuracy and reasonableness. Some of these tests are discussed below.

Hand calculations were checked against a deterministic run to confirm that the animal produce model executed the equations properly. The model was also run probabilistically with the results checked for reasonableness.

Figures 12.1, 12.2 and 12.3 are some example plots of the radionuclide concentrations in caribou, moose and deer flesh respectively, plotted as the log of the geometric mean. The system model was run for 2,000 years in 10 year time steps for 100 trials.

12.7 References

Belovsky, G.E., Jordan, P.A., and Botkin, D.B., 1973. "Summer Browsing by Moose in Relation to Preference, and Animal Density: A New Quantitative Approach." Proceedings of the 9th North American Moose Conference and Workshop, Quebec City, March. pp. 101-122.

Blanchard, R.L., 1966. "Relationship Between Po-210 and Pb-210 in Man and His Environment." Article in Radioecological Concentration Processes: Proceedings of an International Symposium held in Stockholm, 1966.

Blanchard, R.L., and Moore, J.B., 1970. "Pb-210 and Po-210 in Tissues of Some Alaskan Residents as Related to Consumption of Caribou or Reindeer Meat." Health Physics, Vol. 18, pp. 127-134.

Blouch, R.I., 1984. "Chapter 20. Northern Great Lakes States and Ontario Forests." In "White-tailed Deer - Ecology and Management." Edited by L.K. Halls. Stackpole Books, Harrisburg, Pa.

Comar, C.L., 1966. "Radioactive Materials in Animals - Entry and Metabolism." Chapter 7 in "Radioactivity and Human Diet." Edited by R. Scott Russell. Pergamon Press, Oxford.

FIGURE 12.1

PREDICTED RADIONUCLIDE CONCENTRATION IN CARIBOU FLESH vs TIME

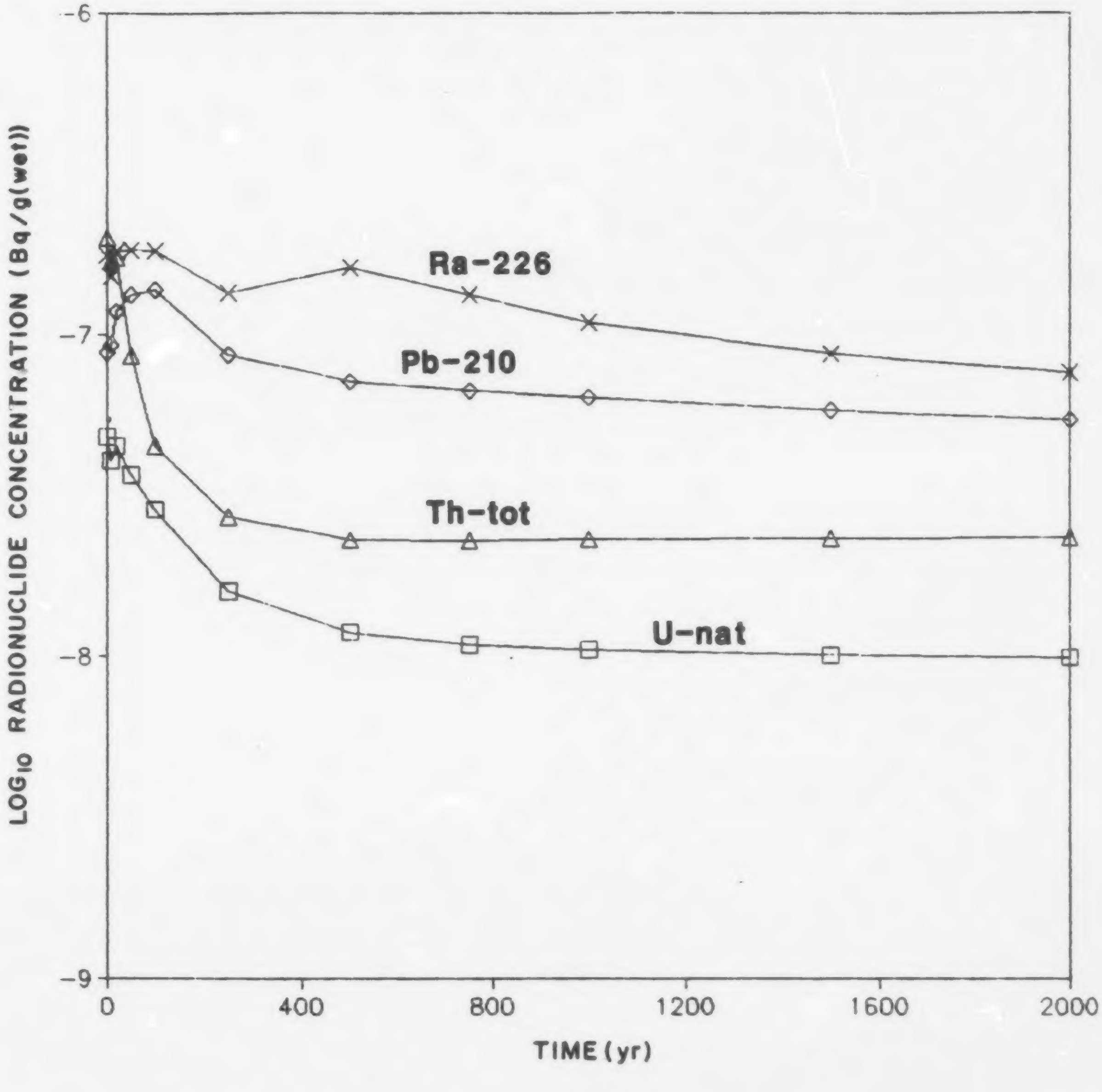

NOTES: 1) The graph shows geometric mean values of 100 trials
2) Assumes the Caribou consumes area average lichen, summer forage and water (see Figure 8.2)

FIGURE 12.2

PREDICTED RADIONUCLIDE CONCENTRATION IN MOOSE FLESH vs TIME

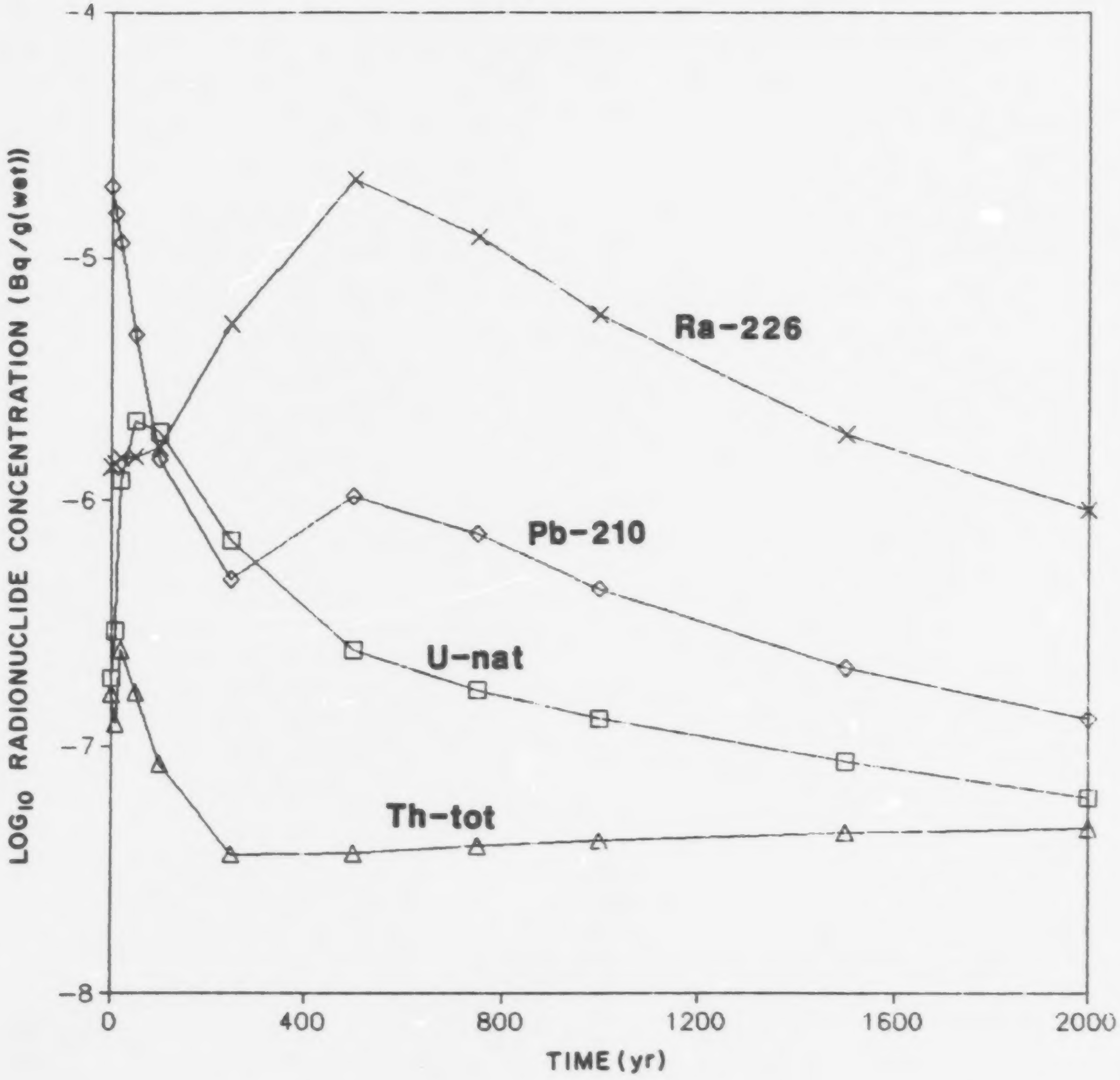

NOTES: 1) The graph shows geometric mean values of 100 trials
2) Assumes the moose consumes watershed average browse, aquatic macrophytes and water

FIGURE 12.3

PREDICTED RADIONUCLIDE CONCENTRATION IN DEER FLESH vs TIME

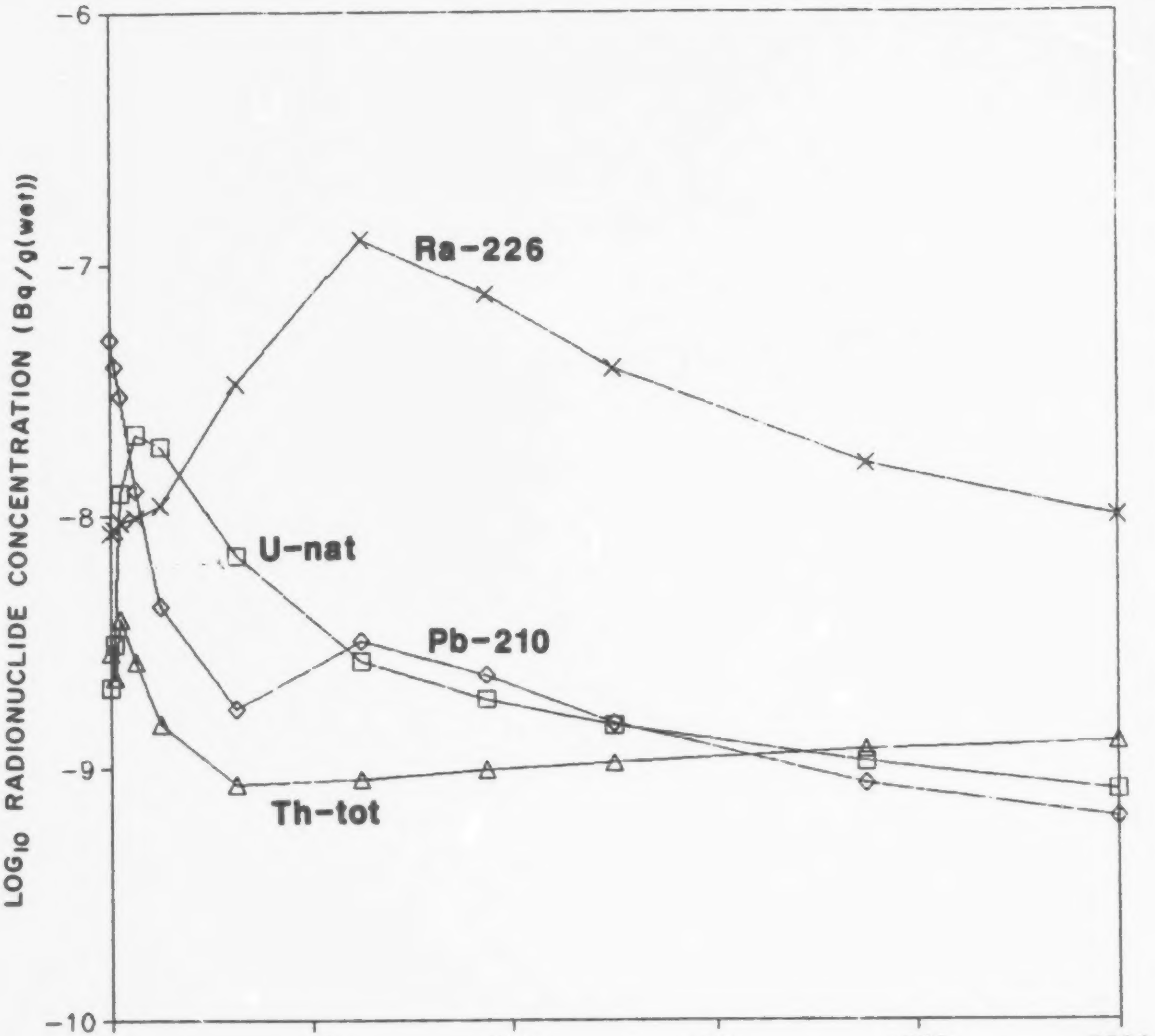

NOTES: 1) The graph shows geometric mean values of 100 trials
2) Assumes the deer consumes watershed average summer forage, browse and water

Table 12.4

ANIMAL PRODUCE MODEL CODE LISTING

```
      SUBROUTINE ANIMAL
      INCLUDE 'MODEL.INC'
      INCLUDE 'VAR.INC'
      REAL*4 ACARCF(4),ACARCL(4),WMOSCA(4),WMOSCW(4),ADERCF(4),
     +       ADERCB(4),CARC(4),MOSC(4),DERC(4)
      FT=PSAREA/TAREA
      FAIAM=1.0-FAIBM
      FAIBD=1.0-FAISFD
      DO 10 I=1,4
         ACARCF(I)=FMTCC(I)*FIRC*FAISFC*SUFOC(I,1)
         ACARCL(I)=FMTCC(I)*FIRC*FAILC*LICHC(I)
         ACARC(I)=ACARCF(I)+ACARCL(I)
         WCARC(I)=FMTCC(I)*WIRC*FT*(FAISFC+FAILC)*WATAVG(I)
         CARC(I)=ACARC(I)+WCARC(I)
         AMOSC(I)=FMTCM(I)*FIRM*FAIBM*BRWSC(I)
         WMOSCA(I)=FMTCM(I)*FIRM*FAIAM*AQVEGC(I)
         WMOSCW(I)=FMTCM(I)*WIRM*WATAVG(I)
         WMOSC(I)=WMOSCA(I)+WMOSCW(I)
         MOSC(I)=AMOSC(I)+WMOSC(I)
         ADERCF(I)=FMTCD(I)*FIRD*FAISFD*SUFOC(I,2)
         ADERCB(I)=FMTCD(I)*FIRD*FAIBD*BRWSC(I)
         ADERC(I)=ADERCF(I)+ADERCB(I)
         WDERC(I)=FMTCD(I)*WIRD*WATAVG(I)
         DERC(I)=ADERC(I)+WDERC(I)
10    CONTINUE
C
      IF(CODANI.EQ.1.0.OR.CODANI.EQ.2.0.OR.CODANI.EQ.3.0)THEN
         WRITE(*,100)
      ENDIF
      IF(CODANI.EQ.3.0)THEN
         WRITE(*,101)FT,FIRC,WIRC,FAISFC,FAILC
         WRITE(*,102)(FMTCC(I),I=1,4)
         WRITE(*,103)FIRM,WIRM,FAIBM,FAIAM
         WRITE(*,104)(FMTCM(I),I=1,4)
         WRITE(*,105)FIRD,WIRD,FAISFD,FAIBM
         WRITE(*,106)(FMTCD(I),I=1,4)
         WRITE(*,107)(SUFOC(I,1),I=1,4)
         WRITE(*,108)(SUFOC(I,2),I=1,4)
         WRITE(*,109)(LICHC(I),I=1,4)
         WRITE(*,110)(BRWSC(I),I=1,4)
         WRITE(*,111)(AQVEGC(I),I=1,4)
         WRITE(*,112)(WATAVG(I),I=1,4)
         WRITE(*,113)(ACARCF(I),I=1,4)
         WRITE(*,114)(ACARCL(I),I=1,4)
         WRITE(*,115)(WCARC(I),I=1,4)
         WRITE(*,116)(AMOSC(I),I=1,4)
         WRITE(*,117)(WMOSCA(I),I=1,4)
         WRITE(*,118)(WMOSCW(I),I=1,4)
         WRITE(*,119)(ADERCF(I),I=1,4)
         WRITE(*,120)(ADERCB(I),I=1,4)
         WRITE(*,121)(WDERC(I),I=1,4)
```

Table 12.4 continued.

```
      ENDIF
      IF(CODANI.EQ.2.0.OR.CODANI.EQ.3.0)THEN
        WRITE(*,122)(ACARC(I),I=1,4)
        WRITE(*,123)(WCARC(I),I=1,4)
        WRITE(*,124)(CARC(I),I=1,4)
        WRITE(*,125)(AMOSC(I),I=1,4)
        WRITE(*,126)(WMOSC(I),I=1,4)
        WRITE(*,127)(MOSC(I),I=1,4)
        WRITE(*,128)(ADERC(I),I=1,4)
        WRITE(*,129)(WDERC(I),I=1,4)
        WRITE(*,130)(DERC(I),I=1,4)
      ENDIF
C
100   FORMAT(///1X,'ANIMAL MODEL')
101   FORMAT(/1X,'FRACTION OF TIME CARIBOU SPEND IN WATERSHED',E12.4/
     +       1X,'AVERAGE DAILY FEED INTAKE FOR CARIBOU',E12.4/1X,'AV',
     +       'ERAGE DAILY WATER INTAKE FOR CARIBOU',E12.4/1X,'FRACTI',
     +       'ON OF CARIBOU INTAKE THAT IS LOCAL SUMMER FORAGE'E12.4/
     +       1X,'FRACTION OF CARIBOU INTAKE THAT IS LOCAL LICHEN'
     +       E12.4)
102   FORMAT(1X,'FEED-TO-MEAT TRANSFER COEFFICIENT FOR CARIBOU'/1X,
     +       4(E12.4))
103   FORMAT(1X,'AVERAGE DAILY FEED INTAKE FOR MOOSE',E12.4/1X,'AVER',
     +       'AGE DAILY WATER INTAKE FOR MOOSE',E12.4/1X,'FRACTION O',
     +       'F MOOSE INTAKE THAT IS BROWSE'E12.4/1X,'FRACTION OF MO',
     +       'OSE INTAKE THAT IS AQUATIC MACROPHYTES'E12.4)
104   FORMAT(1X,'FEED-TO-MEAT TRANSFER COEFFICIENT FOR MOOSE'/1X,
     +       4(E12.4))
105   FORMAT(1X,'AVERAGE DAILY FEED INTAKE FOR DEER',E12.4/1X,'AVERA',
     +       'GE DAILY WATER INTAKE FOR DEER',E12.4/1X,'FRACTION OF ',
     +       'DEER INTAKE THAT IS SUMMER FORAGE'E12.4/1X,'FRACTION O',
     +       'F DEER INTAKE THAT IS BROWSE'E12.4)
106   FORMAT(1X,'FEED-TO-MEAT TRANSFER COEFFICIENT FOR DEER'/1X,
     +       4(E12.4))
107   FORMAT(1X,'AVERAGE RADIONUCLIDE CONCENTRATION IN SUMMER FORAGE'
     +       /1X,4(E12.4))
108   FORMAT(1X,'AVERAGE WATERSHED RADIONUCLIDE CONCENTRATION IN SU',
     +       'MMER FORAGE'/1X,4(E12.4))
109   FORMAT(1X,'AVERAGE RADIONUCLIDE CONCENTRATION IN LICHEN'/1X,
     +       4(E12.4))
110   FORMAT(1X,'AVERAGE WATERSHED RADIONUCLIDE CONCENTRATION IN BR',
     +       'OWSE'/1X,4(E12.4))
111   FORMAT(1X,'AVERAGE RADIONUCLIDE CONCENTRATION IN AQUATIC MACRO',
     +       'PHYTES'/1X,4(E12.4))
112   FORMAT(1X,'AVERAGE RADIONUCLIDE CONCENTRATION IN THE WATER'/1X,
     +       4(E12.4))
113   FORMAT(/1X,'AVERAGE RADIONUCLIDE CONCENTRATION IN CARIBOU FLES',
     +       'H (INGESTION OF SUMMER FORAGE)'/1X,4(E12.4))
114   FORMAT(1X,'AVERAGE RADIONUCLIDE CONCENTRATION IN CARIBOU FLESH',
     +       ' (INGESTION OF LICHEN)'/1X,4(E12.4))
115   FORMAT(1X,'AVERAGE RADIONUCLIDE CONCENTRATION IN CARIBOU FLESH',
     +       ' (INGESTION OF WATER)'/1X,4(E12.4))
116   FORMAT(1X,'AVERAGE RADIONUCLIDE CONCENTRATION IN MOOSE FLESH ',
```

Table 12.4 continued.

```
     +       '(INGESTION OF BROWSE)'/1X,4(E12.4))
117   FORMAT(1X,'AVERAGE RADIONUCLIDE CONCENTRATION IN MOOSE FLESH ',
     +       '(INGESTION OF AQUATIC MACROPHYTES)'/1X,4(E12.4))
118   FORMAT(1X,'AVERAGE RADIONUCLIDE CONCENTRATION IN MOOSE FLESH ',
     +       '(INGESTION OF WATER)'/1X,4(E12.4))
119   FORMAT(1X,'AVERAGE RADIONUCLIDE CONCENTRATION IN DEER FLESH ',
     +       '(INGESTION OF SUMMER FORAGE)'/1X,4(E12.4))
120   FORMAT(1X,'AVERAGE RADIONUCLIDE CONCENTRATION IN DEER FLESH ',
     +       '(INGESTION OF BROWSE)'/1X,4(E12.4))
121   FORMAT(1X,'AVERAGE RADIONUCLIDE CONCENTRATION IN DEER FLESH ',
     +       '(INGESTION OF WATER)'/1X,4(E12.4))
122   FORMAT(/1X,'AVERAGE RADIONUCLIDE CONCENTRATION IN CARIBOU FLES',
     +       'H (AIR PATHWAY)'/1X,4(E12.4))
123   FORMAT(1X,'AVERAGE RADIONUCLIDE CONCENTRATION IN CARIBOU FLESH',
     +       ' (WATER PATHWAY)'/1X,4(E12.4))
124   FORMAT(1X,'AVERAGE RADIONUCLIDE CONCENTRATION IN CARIBOU FLESH',
     +       /1X,4(E12.4))
125   FORMAT(1X,'AVERAGE RADIONUCLIDE CONCENTRATION IN MOOSE FLESH ',
     +       '(AIR PATHWAY)'/1X,4(E12.4))
126   FORMAT(1X,'AVERAGE RADIONUCLIDE CONCENTRATION IN MOOSE FLESH ',
     +       '(WATER PATHWAY)'/1X,4(E12.4))
127   FORMAT(1X,'AVERAGE RADIONUCLIDE CONCENTRATION IN MOOSE FLESH ',
     +       /1X,4(E12.4))
128   FORMAT(1X,'AVERAGE RADIONUCLIDE CONCENTRATION IN DEER FLESH ',
     +       '(AIR PATHWAY)'/1X,4(E12.4))
129   FORMAT(1X,'AVERAGE RADIONUCLIDE CONCENTRATION IN DEER FLESH ',
     +       '(WATER PATHWAY)'/1X,4(E12.4))
130   FORMAT(1X,'AVERAGE RADIONUCLIDE CONCENTRATION IN DEER FLESH ',
     +       /1X,4(E12.4))
C
      RETURN
      END
```

Fraser, D., Chavez, E.R., and Paloheimo, J.E., 1984. "Aquatic Feeding by Moose: Selection of Plant Species and Feeding Areas in Relation to Plant Chemical Composition and Characteristics of Lakes." Can. J. Zool., Vol. 62, pp. 80-87.

Garner, R.J., 1972. "Transfer of Radioactive Materials from the Terrestrial Environment to Animals and Man." CRC Press, Cleveland.

Holtzman, R.B., 1966a. "Natural Levels of Lead-210, Polonium-210 and Radium-226 in Humans and Biota of the Arctic." Nature, Vol. 210, pp. 1094-1097.

Holtzman, R.B., 1966b. "Ra-226 and the Natural Airborne Nuclides Pb-210 and Po-210 in Arctic Biota." Proceedings of the First International Congress of Radiation Protection, Stockholm.

Huot, J., Potvin, F. and Belanger, M., 1984. "Chapter 13. Southeastern Canada." In "White-tailed Deer - Ecology and Management." Edited by L.K. Halls. Stackpole Books, Harrisburg, Pa.

Kauranen, P., and Miettinen, J.K., 1969. "Po-210 and Pb-210 in the Arctic Food Chain and the Natural Radiation Exposure to Lapps." Health Physics, Vol. 16, pp. 287-295.

Krefting, L.W., 1974. "The Ecology of the Isle Royale Moose with Special Reference to the Habitat." Technical Bulletin 297, Forestry Series 15, Agricultural Experiment Station, University of Minnesota.

Lynch, G.M., 1976. "Some Long Range Movements of Radio-Tagged Moose in Alberta." Proceedings of the 12th North American Moose Conference and Workshop, St. John's Nfld., March 1976. pp.220-235.

Marchinton, R.L. and Hirth, D., 1984. "Chapter 6. Behaviour." In "White-tailed Deer - Ecology and Management." Edited by L.K. Halls. Stackpole Books, Harrisburg, Pa.

McDowell-Boyer, L.M., Watson, A.P., and Travis, C.C., 1979. "Review and Recommendations of Dose Conversion Factors and Environmental Transport Parameters for Pb-210 and Ra-226." Report PB 294-242. Oak Ridge National Laboratories, March 1979.

Miller, O.R., no date. "Biology of the Kaminuriak Population of Barren-Ground Caribou. Part 3." Canadian Wildlife Service. Report Services Number 36.

Saunders, B.P., and Williamson, J.C., 1972. "Moose Movements from Ear-Tag Returns." Proceedings of the 8th North American Moose Conference and Workshop, Thunder Bay, Ontario, Feb. 1972. pp. 177-184.

SENES Consultants Limited, 1983. "Decommissioning of the Beaverlodge Mine/Mill Operations and the Reclamation of the Site. Radiological and Environmental Assessment of Close-Out Options." Prepared for Eldorado Resources Limited.

SENES Consultants Limited, 1987. "Uranium Tailings Assessment Program (UTAP.3): Users' Manual." Research report prepared for the National Uranium Tailings Program, CANMET, EMR, under Supply and Services Canada Contract No. 23317-6-1728/01-SQ.

Taylor, K.P., and Ballard, W.B., 1979. "Moose Movements and Habitat Use Along the Susitna River near Devil's Canyon." Proceedings of the 15th North American Moose Conference and Workshop, Soldotna-Kenai, Alaska. pp. 169-186.

United Nations Scientific Committee on the Effects of Atomic Radiation (UNSCEAR), 1977. "Sources and Effects of Ionizing Radiation." Report to the General Assembly, United Nations, New York.

United States Nuclear Regulatory Commission (U.S. NRC), 1982. "Calculational Models for Estimating Radiation Doses to Man from Airborne Radioactive Material Resulting from Uranium Milling Operations." Reg. Guide 3.51, March.

Verme, L.J. and Ullrey, D.E., 1984. "Chapter 4. Physiology and Nutrition." In "White-tailed Deer - Ecology and Management." Edited by L.K. Halls. Stackpole Books, Harrisburg, Pa.

Wishart, W.D., 1984. "Chapter 26. Western Canada." In "White-tailed Deer - Ecology and Management.: Edited by L.K. Halls. Stackpole Books, Harrisburg, Pa.

13.0 DOSE MODEL

13.1 Introduction

13.1.1 Background

In UTAP.3, the annual average committed effective dose equivalent (herein called annual average dose, or simply dose) for each receptor is calculated. Two types of receptors may be specified: an average receptor and a critical receptor, located in one or more of the 80 possible sectors. Up to 80 receptors (sum of critical and average) may be specified. Both receptor types are assumed to live and raise vegetables in their sector, and eat caribou, moose and/or deer representative of the study area. However, their water and fish come from a user-specified river or lake.

For the purposes of dose calculations, and aside from the above choices made by the user, the average and critical receptors differ only in the parameter specifications: the dose models themselves are identical.

There are three main types of dose models presented in this chapter: ingestion, inhalation, and external. These models are grouped into one subroutine called DOSEIN. The external dose-rate model, for groundshine, is documented in Chapter 7.

The inhalation and ingestion models all involve two main aspects: calculation of the receptor's intake and multiplication of that intake by a dose conversion factor (DCF). Because the DCF's are common to all models they are discussed in Section 13.1.2 of this introduction. Details of the ingestion, inhalation and external exposure models are then presented in Sections 13.2, 13.3 and 13.4 respectively. The description of each model is structured as follows: discussion of parameters common to all receptor types; discussion of the receptor-specific parameters chosen for critical receptors; and finally discussion of receptor-specific parameters chosen for average receptors. All parameters are listed in Tables 13.3 and 13.4. The computer code listing for these models is presented in Table 13.5.

Note that once all of the parameters are chosen, the characteristics of any one critical or average receptor have been specified. However, the location and source of vegetables, water and fish must still be specified for each of the up to 80 receptors previously mentioned. Section 13.5 gives details on this aspect. Finally, Section 13.6 describes how the model may be used to calculate population dose.

In this chapter the subscript "i" is used to indicate that a parameter will vary with the radionuclide; "t" and "j" indicate that a parameter varies with time and location; "r" indicates that the parameter is receptor type specific (average vs. critical); and the following abbreviations are also used as subscripts:

a = air
w = water
v = vegetables
c = caribou
m = moose
d = deer
f = fish.

13.1.2 Dose Conversion Factors

The calculation of the dose to a specific receptor resulting from the inhalation and ingestion of various radionuclides involves the multiplication of the receptor's estimated annual intakes of the radionuclides by the appropriate dose conversion factors (DCF). DCF's for the special case of radon and its daughters are given in Section 13.3.2. The remaining radionuclides being modelled in this study, namely, natural uranium, total thorium, radium-226 and lead-210, are discussed below.

DCF's for reference man (i.e. an adult male) for individual radionuclides are given in Table 13.1. These are taken from ICRP-30 (1979) and Johnson (1986) and are based on the methodology described in ICRP-26 (1977); that is, the 50-year committed effective dose resulting from the intake of a radionuclide is assigned to the year of intake. For example, the intake by inhalation of 1 Bq of thorium-230 in one year would result in a committed effective dose equivalent of 70 μSv that is assumed to occur in the year of intake. This methodology is accepted by the Atomic Energy Control Board of Canada (AECB) for both occupational and environmental dose assessments. Doses to individual body organs, which must be below 0.5 $Sv.yr^{-1}$ to limit the possibility of non-stochastic effects, are not considered here since it is extremely unlikely that potential environmental doses would ever reach this limiting value.

The DCFs for inhalation given in Table 13.1 correspond to the least soluble form of the radionuclides described by the ICRP-30 solubility classifications (D, W or Y) since it is assumed that the radionuclides that remain on the surface of the tailings for several years (the source of the inhaled radioactivity) are relatively insoluble. The DCFs for ingestion given in Table 13.1 are for the most soluble forms of the radionuclides listed in ICRP-30 since much of the intake by ingestion is from water, meat and vegetation which contain the soluble form of the radionuclides. Only deposited dust that remains on surface vegetation would be in a relatively insoluble form.

The ICRP DCFs given in Table 13.1 agree to within 25% with the DCFs calculated by Johnson and Dunford (1983) if the same assumptions on the solubility in the stomach of ingested radionuclides are used. However, Johnson and Dunford (1983) suggest that the ICRP solubility value for thorium is too small by a factor of 150 for thorium that is incorporated in environmental matrices. Consequently, they calculate DCFs for ingested thorium radionuclides that are 150 times larger than the corresponding ICRP estimates. More recent investigations by Johnson (1986) suggest that the original difference between the ICRP value and that used by Johnson and Dunford was too large by about a factor of 6, resulting in a continuing difference of about a factor of 25. The most recent DCFs by Johnson (1986) have been incorporated into the current model. Whether or not further investigation of factors such as the chemical form of the thorium (e.g. organic or inorganic) may help to further reduce these differences is unclear. This aspect should continue to be monitored and updated dose conversion factors should be used as they become available.

The use of the DCFs for radium-226 and lead-210 is relatively straightforward since they are modelled as individual, specific radionuclides. However, natural uranium and total thorium, which are being modelled in this study, are a mixture of isotopes of these radionuclides and their resultant DCFs must be based on the proper mixture of the DCFs of the individual uranium and thorium isotopes.

One gram of natural uranium contains 1.22×10^4 Bq each of uranium-238 and uranium-234, and 5.8×10^2 Bq of uranium-235, for a total of 2.50×10^4 Bq. Using the values given in Table 13.1 for these radionuclides, the DCF for ingestion of natural uranium is then 1.7×10^3 $\mu Sv.g^{-1}$ or 6.7×10^{-2} $\mu Sv.Bq^{-1}$ (essentially the average of the DCFs for uranium-238 and uranium-234). Similarly, the DCF for inhalation of natural uranium is 3.4×10^1 $\mu Sv.Bq^{-1}$. These values are shown in Table 13.2.

For the purpose of the present discussion, total thorium is assumed to consist of the thorium isotopes Th-230, from the uranium-238 decay chain, and Th-232 and Th-228, from the thorium-232 decay chain. Natural thorium is assumed to consist of the Th-232 and Th-228 isotopes from the thorium decay chain noted above. Since the dosimetric implications of all three isotopes are different, the calculations of DCFs for total thorium modelled in this study are somewhat complicated. Natural thorium is essentially 100% thorium-232 by mass. Natural thorium also contains an equal activity (but very little mass) of thorium-228 since it is a short-lived daughter product of thorium-232. For the inhalation pathway, other radionuclides in the thorium-232 decay chain do not occur in natural thorium in concentrations that are dosimetrically significant (Hannibal, 1982). For the ingestion pathway, radium-228 and radium-224 would increase the DCF for ingestion of natural thorium by about 60%, but since they are chemically different, it is assumed that they do not follow the thorium isotopes through the ingestion pathways (e.g. plant uptake). The DCFs for

Table 13.1

DOSE CONVERSION FACTORS**

Radionuclide	Ingestion	Inhalation
Uranium-238	6.3×10^{-2}	3.2×10^{1}
Uranium-235	6.8×10^{-2}	3.3×10^{1}
Uranium-234	7.1×10^{-2}	3.6×10^{1}
Radium-226	3.1×10^{-1}	2.1
Lead-210	1.4	3.4
Thorium-232	$1.9 \times 10^{+1}$*	3.1×10^{2}
Thorium-230	3.5*	7.0×10^{1}
Thorium-228	2.5*	8.3×10^{1}

Note:

* DCFs are given in μSv.Bq^{-1} and are taken from Johnson (1986). See text for discussion.

** The DCFs are given in units of μSv.Bq^{-1} where the dose (μSv) is the committed effective dose equivalent derived according to ICRP methodology (ICRP 30, 1979) unless noted otherwise.

Table 13.2

DOSE CONVERSION FACTORS FOR THIS STUDY

	Ingestion[4]	Inhalation[5]
Natural uranium (μSv.Bq^{-1})[1]	6.7×10^{-2}	3.4×10^{1}
Radium-226 (μSv.Bq^{-1})	3.1×10^{-1}	2.1
Lead-210 (μSv.Bq^{-1})	1.4	3.4
Natural thorium (μSv.Bq^{-1})[2]	$2.15 \times 10^{+1}$	3.9×10^{2}
Total thorium (μSv.Bq^{-1})[3]		
- air pathway	$3.5 + 18 (X_a)$	$(7.0\times10^{1}) + X_a(3.2\times10^{2})$
- water pathway	$3.5 + 18 (X_w)$	-----

1. The uranium activity of 1 g of natural uranium is 2.50×10^{4} Bq.

2. The Th-232 activity of 1 g of natural thorium (thorium-232) is 4.05×10^{3} Bq.

3. X_a (X_w) = activity fraction of natural thorium in total thorium in the air (water) pathway.

4. For U-nat, Ra-226 and Pb-210 $DCF_{a,i}$(ing) = $DCF_{w,i}$(ing). However, as explained in the text $DCF_{a,Th}$(ing) $\neq$ $DCF_{w,Th}$(ing), where Th refers to total thorium as above.

5. Referred to in the text as $DCF_{a,i}$(inh). See Section 13.3.2 for the dose conversion factor for the inhalation of radon and its daughters.

natural thorium are therefore the sum of the DCFs for thorium-232 and thorium-228, or 21.5 $\mu Sv.Bq^{-1}$ for ingestion and 3.9 x 10^2 $\mu Sv.Bq^{-1}$ for inhalation. The DCFs for natural thorium are shown in Table 13.2. (It should be noted when converting from a mass to a radioactivity basis that chemical modelling calculations, which are sensitive to mass rather than radioactivity, conventionally assume that natural thorium is 100% thorium-232 or 4.03×10^3 $Bq.g^{-1}$; see for example Section 3.7.2. Thus, ingesting for example 1 g of natural thorium would result in a dose of 21.5 $\mu Sv.Bq^{-1}$ x 4.03×10^3 Bq or 8.66×10^4 μSv.)

As previously noted, total thorium also contains thorium-230. As discussed in Chapter 3, the natural thorium to thorium-230 ratio is relatively constant in water whereas this ratio changes with time in the near-surface tailings. The DCFs for total thorium are a function of this ratio since the DCFs for thorium-230 are different than the DCFs for natural thorium. In addition, there must be two DCFs for ingestion of total thorium since ingested thorium can originate both from the water pathway (e.g. drinking water) and the air pathway (e.g. eating vegetation contaminated with deposited dust).

If X_a is the activity fraction of natural thorium in total thorium in the near-surface tailings (the source of dust), the DCF for inhalation of total thorium is:

$$X_a \times \text{DCF(natural thorium)} + (1 - X_a) \times \text{DCF(thorium-230)}$$

Using the DCFs for natural thorium (3.9×10^2) and thorium-230 (7.0×10^1) the DCF for inhalation of total thorium is then:

$$\begin{aligned} &X_a(3.9 \times 10^2) + (1-X_a)\,(7.0 \times 10^1) \\ &= (7.0 \times 10^1) + X_a(3.2 \times 10^2)\ \mu Sv.Bq^{-1} \text{ total thorium} \end{aligned}$$

The DCF for ingestion of total thorium that originates in the air pathway is:

$$X_a(21.5) + (1-X_a)\ (3.5)$$
$$= (3.5) + X_a(18)\ \mu Sv.Bq^{-1} \text{ total thorium}$$

Similarily, the DCF for ingestion of total thorium that originates in the water pathway is (3.5) + X_w(18) μSv.Bq $^{-1}$ where X_w is the activity fraction of natural thorium in total thorium in water. All DCFs are summarized in Table 13.2.

13.2 Ingestion Dose

13.2.1 Annual Dose Due to the Ingestion of Vegetables

The annual average dose received by an individual due to the ingestion of above- and below-ground vegetables was calculated as follows:

$$d_{v,i,r,j,t}(ing) = DCF_{a,i}(ing) \sum_{v} U_{v,r} [C]_{v,i,j,t} R_v \ L_{v,r} \qquad (13.1)$$

where

$d_{v,i,r,j,t}(ing)$ = the average annual dose due to the ingestion of radionuclide i in vegetables v (in this case above- and below- ground vegetables) at time t for receptor type r at location j (μSv.yr^{-1})

$DCF_{a,i}(ing)$ = the whole body dose conversion factor for the ingestion of radionuclide i for the air pathway (μSv.Bq^{-1}) (see Section 13.1.2)

$U_{v,r}$ = the average annual intake of vegetable type v (in this case above- and below-ground vegetables) (g (wet wt).yr^{-1}) (receptor specific)

$[C]_{v,i,j,t}$ = the calculated average annual concentration of radionuclide i in vegetation type v at time t (Bq.g^{-1} (wet weight)) (location specific)

R_v = the fraction of activity in vegetable type v remaining after food preparation (0 to 1)

$L_{v,r}$ = the fraction of the vegetable type v that is grown locally (0 to 1) (receptor specific).

Note that the time dependence in $d_{v,i,r,j,t}(ing)$ is due only to the time dependence of $[C]_{v,i,j,t}$.

The parameter R_v, was chosen to be uniformly distributed from 0.5 to 1.0. The lower value is that recommended by the U.S. NRC (1982). The large upper value was chosen in recognition of the uncertainty of this number.

Chapter 8.0 details how $[C]_{v,i,j,t}$ is calculated. The receptors are assumed to consume vegetables grown in the sector in which they live (see Section 13.5).

Critical Receptor

The annual intakes of above- and below-ground vegetables used in this model are for an average adult male, age 20-39, as derived from Nutrition Canada (not dated). Food consumption patterns do vary widely from one region to another. Therefore a range was taken from the data for the Ontario, Prairies and National average, and a uniform distribution was assumed. The user is encouraged to adjust these intakes to reflect regional data. Also, the user may wish to change the age and/or sex of the critical receptor for any particular application. As discussed in Section 13.1.2, the dose conversion factors are for an adult male and would need to be adjusted in parallel with any changes to the age or sex of the receptor. The data for above-ground vegetables does not include any fruit or fruit products.

The parameter $L_{v,r}$, was assigned a triangular distribution from 0.1 to 0.6, with a peak at 0.3. The range, although somewhat arbitrary, was chosen in recognition of the fact that even for a critical receptor it would be very unlikely that someone could or would grow a large percentage of their vegetables in the area being modelled (i.e. the Canadian Shield).

Average Receptor

The annual intake of above- and below-ground vegetables used in this model are identical to those for the critical receptor.

The parameter $L_{v,r}$, was assigned a triangular distribution of 0.0 to 0.2, with a peak at 0.1. This range is again somewhat arbitrary. It was based on two assumptions: the average person grows very little if any of his/her own vegetables, and in the area being modelled (the Canadian Shield) there are not likely to be a large number of market gardens.

13.2.2 Annual Dose Due to the Ingestion of Caribou

The model used for calculating the average annual dose received by an individual due to the ingestion of caribou meat is (U.S. NRC, 1982):

$$d_{c,i,r,j,t}(ing) = U_{c,r}\, L_{c,r}\, (DCF_{a,i}(ing)\, [C(air)]_{c,i,t} + DCF_{w,i}(ing)\, [C(water)]_{c,i,t}) \qquad (13.2)$$

where

$d_{c,i,r,j,t}(ing)$ = the average annual dose due to the ingestion of radionuclide i in caribou meat at time t for receptor type r at location j (μSv.yr^{-1})

$U_{c,r}$ = the average annual intake of caribou meat (g.yr^{-1} wet wt) (receptor specific)

$L_{c,r}$ = the fraction of the annual intake that is local caribou meat (0 to 1) (receptor specific)

$DCF_{a,i}(ing)$ = the dose conversion factor for the ingestion of radionuclide i for the air pathway ($\mu Sv.Bq^{-1}$) (see Section 13.1.2)

$[C(air)]_{c,i,t}$ = the calculated average annual concentration of radionuclide i in caribou meat at time t, taken over the whole model area, due to the air pathway ($Bq.g^{-1}$ wet wt) (see Section 12.2)

$DCF_{w,i}(ing)$ = the dose conversion factor for the ingestion of radionuclide i for the water pathway ($\mu Sv.Bq^{-1}$) (see Section 13.1.2)

$[C(water)]_{c,i,t}$ = is the calculated average annual concentration of radionuclide i in caribou meat at time t, taken over the whole model area due to the water pathway ($Bq.g^{-1}$ wet wt) (see Section 12.2).

The time dependence in $d_{c,i,r,j}(ing)$ is due to the time dependence of $[C(air)]_{c,i,t}$ and $[C(water)]_{c,i,t}$. This model is not dependent on the location of the receptor, only the type of receptor. This is because only one value of radionuclide concentration in caribou meat is calculated for each of the air and water pathways (see Section 12.2).

Critical Receptor

For the critical receptor, all of an adult (Ontario and Prairie regions, age 20-39) male's meat was assumed to come from moose, deer and caribou (79 kg a year) (Nutrition Canada, not dated). Of this, it was assumed that one third is caribou.

The fraction of the annual intake that is local ($L_{c,r}$) (i.e. from a caribou killed in the immediate area) was allowed to range uniformly from 0 to 100% as this would vary greatly from year to year.

Average Receptor

For the average receptor, it was assumed that wild game was eaten once per week. Of this, one third was assumed to be caribou.

The parameter $L_{c,r}$ was allowed to vary uniformly over the range from 0 to 100% as for the critical receptor.

13.2.3 Annual Dose Due to the Ingestion of Moose

The average annual dose received by an individual due to the ingestion of moose meat was calculated as follows (U.S. NRC, 1982):

$$d_{m,i,r,j,t}(ing) = U_{m,r} L_{m,r} (DCF_{a,i}(ing) [C(air)]_{m,i,t} + DCF_{w,i}(ing) [C(water)]_{m,i,t}) \tag{13.3}$$

where

$d_{m,i,r,j,t}(ing)$ = the average annual dose due to the ingestion of radionuclide i in moose meat at time t for receptor type r at location j ($\mu Sv.yr^{-1}$)

$U_{m,r}$ = the average annual intake of moose meat ($g.yr^{-1}$ wet wt) (receptor specific)

$L_{m,r}$ = the fraction of the annual intake that is moose meat from the watershed (0 to 1) (receptor specific)

$DCF_{a,i}(ing)$ = the dose conversion factor for the ingestion of radionuclide i for the air pathway (see Section 13.1.2) ($\mu Sv.Bq^{-1}$)

$[C(air)]_{m,i,t}$ = the calculated average annual concentration of radionuclide i in moose meat at time t, due to the air pathway, in the watershed area ($Bq.g^{-1}$ wet wt) (see Section 12.3)

$DCF_{w,i}(ing)$ = the dose conversion factor for the ingestion of radionuclide i for the water pathway ($\mu Sv.Bq^{-1}$) (see Section 13.1.2)

$[C(water)]_{m,i,t}$ = the calculated average annual concentration of radionuclide i in moose meat at time t, due to the water pathway, in the watershed area ($Bq.g^{-1}$ wet wt) (see Section 12.3).

Note that the time dependence of $d_{m,i,r,j,t}(ing)$ is due to the time dependence of $[C(air)]_{m,i,t}$ and $[C(water)]_{m,i,t}$. As for caribou, this model is not dependent on the location of the receptor, only the type of receptor (see Section 12.3).

Critical Receptor

As previously mentioned, all of the critical receptor's meat was assumed to come from moose, deer and caribou (79 kg a year) (Nutrition Canada, not dated). Of this it was assumed that one third is moose meat.

The fraction of the annual intake that is from the watershed was in this case assumed to be one. This might not be appropriate for critical receptors outside the watershed, but it was not considered possible to allow for all situations.

Average Receptor

The average receptor's intake of moose meat was assumed to be the same as caribou and deer.

As discussed in Section 12.3, only a moose living in the watershed containing the tailings is modelled. Other moose, not in that watershed, but still in the modelling area could have elevated levels of radionuclides due to air emissions from the tailings area. However, it was beyond the scope of model development to calculate both an area and a watershed moose meat concentration. Thus it is only possible to model a situation where the average receptor would eat meat from moose in the watershed. However, this raises a problem when the average receptor is used in a population dose calculation: only so many moose can be harvested annually from the watershed. For large populations, it would be inappropriate to assume a total intake that exceeds the available supply. It is for this reason that $L_{m,r}$ must be carefully selected. In this case it was decided not to include watershed moose meat consumption in the population dose estimates, as the watershed is a small fraction of the total area. Thus, in this study $L_{m,r}$ was set to zero for an average receptor.

13.2.4 Annual Dose Due to the Ingestion of Deer

The average annual dose received by an individual due to the ingestion of deer was modelled as follows (U.S. NRC, 1982):

$$d_{d,i,r,j,t}\,(ing) = U_{d,r}\,L_{d,r}\,(DCF_{a,i}(ing)\,[C(air)]_{d,i,t} + DCF_{w,i}(ing)\,[C(water)]_{d,i,t}) \qquad (13.4)$$

where

$d_{d,i,r,j,t}(ing)$ = the average dose due to the ingestion of radionuclide i in deer meat at time t for receptor type r at location j ($\mu Sv.yr^{-1}$)

$U_{d,r}$ = the average annual intake of deer meat ($g.yr^{-1}$ wet wt) (receptor specific)

$L_{d,r}$ = the fraction of the annual intake that is deer meat from the watershed (0 to 1) (receptor specific)

$DCF_{a,i}(ing)$ = the dose conversion factor for the ingestion of radionuclide i for the air pathway (see Section 13.1.2) ($\mu Sv.Bq^{-1}$)

$[C(air)]_{d,i,t}$ = the calculated average annual concentration of radionuclide i in deer meat at time t, due to the air pathway, in the watershed area ($Bq.g^{-1}$ wet wt) (see Section 12.4)

$DCF_{w,i}(ing)$ = the dose conversion factor for the ingestion of radionuclide i for the water pathway ($\mu Sv.Bq^{-1}$) (see Section 13.1.2)

$[C(water)]_{d,i,t}$ = the calculated average annual concentration of radionuclide i in deer meat at time t, due to the water pathway, in the watershed area ($Bq.g^{-1}$ wet wt) (see Section 12.4).

Note that the time dependence of $d_{d,i,r,j,t}(ing)$ is due to the time dependence of $[C(air)]_{d,a,i,t}$ and $[C(water)]_{d,w,i,t}$. As for caribou and moose, this model is not dependent on the location of the receptor, only the type of receptor (see Section 12.4).

Critical Receptor

One-third of the critical receptor's total annual intake of meat (79 kg, Nutrition Canada, not dated) is assumed to be deer meat.

The fraction of the annual intake that is from the watershed, $L_{d,r}$, was assumed to be one.

Average Receptor

The average receptor was assumed to eat wild game once a week. One-third of this was assumed to be deer meat.

$L_{d,r}$ was set to zero for an average receptor for the same reasons that $L_{m,r}$ for the average receptor was set to zero (see Section 13.2.3).

13.2.5 Annual Dose Due to the Ingestion of Drinking Water

The average annual dose received by an individual as a result of drinking water was modelled as (U.S. NRC, 1982):

$$d_{w,i,r,j,t}(\mathrm{ing}) = DCF_{w,i}(\mathrm{ing})\ U_{w,r}\ [C]_{w,i,j,t}\ OF_r \qquad (13.5)$$

where

$d_{w,i,r,j,t}(\mathrm{ing})$ = the average annual dose due to the ingestion of radionuclide i in drinking water at time t for receptor type r at location j ($\mu Sv.yr^{-1}$)

$DCF_{w,i}(\mathrm{ing})$ = the dose conversion factor for the ingestion of radionuclide i for the water pathway ($\mu Sv.Bq^{-1}$)(see Section 13.1.2)

$U_{w,r}$ = the average annual intake of drinking water ($m^3.yr^{-1}$) (receptor specific)

$[C]_{w,i,j,t}$ = the calculated average annual concentration of radionuclide i in the water (node n) specified for receptor r at location j at time t ($Bq.m^{-3}$) (see Section 11.3.3)

OF_r = the fraction of the year that is spent at that location (0 to 1) (receptor specific).

The time dependence of $d_{w,i,j}(\mathrm{ing})$ is due to the time dependence of $[C]_{w,i,j,t}$. Note that j in this case still means the sector in which the receptor is located, but that the water source is specified by the user (see Section 13.5).

Critical Receptor

The annual water intake of 600 L chosen is for Reference Man (ICRP, 1975).

The fraction of the year that the critical receptor stays at the site (see Section 13.3.1) was used as a surrogate for the fraction of the annual water consumption that is from the specified source.

Average Receptor

The annual water consumption rate is assumed to be the same for the average and critical receptors (600 L). As for the critical receptor, the fraction of the year that the average receptor stays at the site was used as a surrogate for the fraction of the annual water consumption that is from the specified source (see Section 13.3.1).

13.2.6 Annual Dose Due to the Ingestion of Fish

The average annual dose received by an individual as a result of eating fish was modelled as follows (U.S. NRC, 1982):

$$d_{f,i,r,j,t}(ing) = DCF_{w,i}(ing)\ U_{f,r}\ [C]_{f,i,j,t}\ L_{f,r}\ F_a \qquad (13.6)$$

where

$d_{f,i,r,j,t}(ing)$ = the average annual dose due to the ingestion of radionuclide i in fish at time t for receptor type r at location j ($\mu Sv.yr^{-1}$)

$DCF_{w,i}(ing)$ = the dose conversion factor for the ingestion of radionuclide i due to the water pathway ($\mu Sv.Bq^{-1}$) (see Section 13.1.2)

$U_{f,r}$ = the average annual intake of fish ($g.yr^{-1}$ wet wt) (receptor specific)

$[C]_{f,i,j,t}$ = the calculated average annual concentration of radionuclide i in fish in the water (node n) specified for receptor r at location j at time t ($Bq.g^{-1}$wet wt) (see Section 11.3.2)

$L_{f,r}$ = the fraction of the annual intake that is local fish (0 to 1) (receptor specific)

F_a = availability factor of game fish (for the water (node n) specified for receptor r) for consumption expressed as a function of pH (see Section 11.2).

Note that the time dependence of $d_{f,i,r,j,t}(ing)$ is due to the time dependence of $[C]_{f,i,j,t}$. As in Section 13.2.5, j still means the sector in which the receptor is located, but the fish source is specified by the user (see Section 13.5).

Critical Receptor

The average annual intake of 8 kg of fish is for an average Ontario and Prairie Male (age 20 to 39) (Nutrition Canada, not dated). It was assumed that all of his yearly intake of fish is from the lake from which he takes his drinking water (user specified). Note that $L_{f,r}$ is adjusted by Fa if the lake becomes too acidic to support a normal fishery (see Section 11.2).

Average Receptor

The average annual intake of 8 kg of fish is the same as for the critical receptor (Nutrition Canada, not dated). It is also adjusted by Fa. It was assumed that from 0 to 10 percent of this was local (uniformly distributed). As discussed for moose and deer (see Sections 13.2.3 and 13.2.4), if the average receptor is used to estimate population dose and the population is very large, it is possible that the fish population would not support this consumption rate.

13.3 Inhalation Dose

13.3.1 Annual Dose Due to the Inhalation of Suspended Particulates

The average annual dose received by an individual due to inhalation (excluding radon) was calculated as follows:

$$d_{i,r,j,t}(inh) = DCF_{a,i}(inh)\ U_{a,r}\ [C]_{a,i,j,t}\ OF_r \qquad (13.7)$$

where

$d_{i,r,j,t}(inh)$ = the average annual dose due to the inhalation of radionuclide i at time t for receptor r at location j ($\mu Sv.yr^{-1}$)

$DCF_{a,i}(inh)$ = the dose conversion factor for the inhalation of radionuclide i ($\mu Sv.Bq^{-1}$) (see Section 13.1.2)

$U_{a,r}$ = the average annual inhalation rate of the individual ($m^3.yr^{-1}$) (receptor specific)

$[C]_{a,i,j,t}$ = the calculated average air concentration of radionuclide i at location j at time t ($Bq.m^{-3}$) (see Section 5.2)

OF_r = the fraction of the year that is spent at that location (receptor specific).

The time dependence of $d_{i,r,j,t}(inh)$ is due to the time dependence of $[C]_{a,i,j,t}$.

Critical Receptor

The annual inhalation rate of 8400 m^3 was taken for Reference Man (ICRP, 1975). The occupancy factor of 0.9 is based on 11 months at home per year. This was allowed to vary, with a triangular distribution, from 0.8 to 1.0.

Average Receptor

The annual inhalation rate of 8400 m^3 was also assumed for the average receptor (ICRP, 1975). The occupancy factor of 0.9 is based on 11 months at home per year. This was allowed to vary between 0.8 and 1.0.

13.3.2 Annual Dose Due to the Inhalation of Radon and Its Daughters

The radon source and air dispersion models result in an estimation of the radon-in-air concentration at the receptor of interest. This concentration must be converted to a dose (actually a dose rate measured in units of $\mu Sv.yr^{-1}$) so that it can be added to the doses from the other exposure pathways being evaluated.

Since it is the radon daughters rather than the radon that produces the dose to the receptor, the radon-in-air concentration must be converted to an appropriate radon daughter concentration. This conversion requires an estimation of the equilibrium factor, F, between radon and its daughters. Theoretically, F can range from 0.0 (no radon daughters) to 1.0 (complete radon daughter ingrowth). The value of F outdoors at the receptor depends only on the transit time between the radon source and the receptor if it is assumed that there are no radon daughter removal mechanisms other than radioactive decay. Since in reality the daughters are removed by several other mechanisms that are difficult to quantify (e.g. attachment to dust that falls to the ground) and since the major exposure occurs indoors where F is dependent on several additional factors (such as the building ventilation rate), it has been customary to select, rather than calculate, an F factor that is representative of annual average indoor conditions. The radon concentration at the receptor is converted to a radon daughter concentration using this F factor. For this study, the assumed F value is selected from an input distribution, triangular in shape, with a range of 0.2 to 0.8 and a mode of 0.5. This distribution is based on a large number of indoor F values reported by Case et al. (1983).

The neglect of outdoor radon daughter exposure in the calculation of the receptor's exposure produces only a small error. First, the typical receptor spends only about 25% of the time outdoors. Second, the ingrowth of radon daughters from the radon released from the tailings area is dependent on the source-receptor transit time. The ingrowth, assuming no physical removal mechanisms, is small ($F<0.2$) for receptors who spend their time outdoors within about 4 km of the tailings area (based on an average windspeed of 5 $m.s^{-1}$). Third, as noted above, radon daughters are removed from the air by various mechanisms so that outdoor F values are seldom greater than 0.6 (U.S. EPA, 1985). All of these factors suggest that the outdoor radon daughter exposure would be a maximum of 20 to 25% of the total radon daughter exposure at a specific site.

The value of F is used to calculate the receptor's annual radon daughter exposure in WLM. In the Phase II study, a factor of 0.05 Sv per 4.8 WLM (ICRP, 1981) was used to convert the radon daughter exposure to dose. It was noted that this factor is considered debatable by some (e.g. see Stewart, 1984). This factor was derived for occupational exposures. A study by a group of experts of the Nuclear Energy Agency (NEA, 1983) suggests a lower factor of 5×10^{-3} $Sv.WLM^{-1}$ for non-occupational exposures due mainly to the lower breathing rates of the public compared to workers. This latter conversion factor is used for this study.

Based on this factor, the fraction of the time spent indoors when at the site of interest ($INOCC_r$), and the definitions of working level (WL, the concentration of radon daughters in equilibrium with 100 $pCi.L^{-1}$ of radon), working level month (WLM, exposure to 1 WL for 170 h), and occupancy factor (OF_r, the fraction of time at the receptor site, an input variable), the conversion between exposure to 1 $Bq.m^{-3}$ of radon and annual dose is given by:

$$\begin{aligned}\text{Dose } (\mu Sv.yr^{-1}) &= \text{Radon } (Bq.m^{-3}) \times OF_r \times INOCC_r \times 10^{-3}\ m^3.L^{-1} \times 27\ pCi.Bq^{-1} \\ &\quad \times F \times WL/(100\ pCi.L^{-1}) \times 8760\ h.yr^{-1} \times WLM/(WL \times 170\ h) \\ &\quad \times 5 \times 10^3\ \mu Sv.WLM^{-1} \\ &= \text{Radon } (Bq.m^{-3}) \times OF_r \times INOCC_r \times F \times 69.6\ (\mu Sv.Bq^{-1}.m^3.yr^{-1})\end{aligned}$$

Thus, the model used to calculate the annual dose due to exposure to radon is:

$$d_{Rn,r,j}(inh) = [C]_{a,Rn,j,t}\ OF_r\ INOCC_r\ F\ 69.6 \qquad (13.8)$$

where

$d_{Rn,r,j,t}(inh)$ = the average annual dose due to the inhalation of radon and its daughters at time t for receptor r at location j ($\mu Sv.yr^{-1}$)

$[C]_{a,Rn,j,t}$ = the average air concentration of radon at location j at time t ($Bq.m^{-3}$) (see Chapter 5).

OF_r = the fraction of the year that is spent at that location (receptor specific) (see Section 13.3.1).

$INOCC_r$ = the fraction of time spent indoors when at the site of interest (receptor specific) (see below)

F = the equilibrium factor between radon and its daughters (see above).

$INOCC_r$ and OF_r are the only parameters in this model that might possibly be used to differentiate between an average and a critical receptor. There is however, no logical reason to assume that an individual who is a critical receptor would spend more or less time indoors than an average receptor. For this reason, $INOCC_r$, was chosen to be the same for both the critical and average receptors. Report No. 76 of the U.S. NCRP (1984) suggests that it is probably reasonable to assume that the distribution for $INOCC_r$ ranges from 0.7 to 0.95, with only a small percentage of the population spending on average 100% of their time indoors, or less than 70% of their time indoors. UNSCEAR (1982, p. 63) gives a value of 0.9 for $INOCC_r$ for people in the United States and suggests that the value would be lower in warmer or less urbanized countries - Canada is neither. A probable range for $INOCC_r$ for Canadian residents is 0.6 to 1.0. Based on these considerations, $INOCC_r$ was assumed to have a triangular distribution with a mode of 0.9 and a range from 0.6 to 1.0.

13.4 External Dose

Only the external dose due to groundshine is calculated in UTAP.3.

The annual average dose received by an individual due to groundshine was calculated as follows:

$$d_{i,r,j,t}(ext) = D_{i,j,t}\ OF_r\ \left((1 - INOCC_r) + INOCC_r\ SHLD\right) \qquad (13.9)$$

where

$d_{i,r,j,t}(ext)$ = the average annual dose due to groundshine of radionuclide i at time t for receptor r at location j ($\mu Sv.yr^{-1}$)

$D_{i,j,t}$ = the average groundshine dose rate due to radionuclide i at location j at time t ($\mu Sv.yr^{-1}$) (see Chapter 7)

OF_r = the fraction of the year that is spent at that location (receptor specific) (see Section 13.3.1)

$INOCC_r$ = the fraction of time spent indoors when at that location (receptor specific) (see Section 13.3.2)

SHLD = the effective reduction factor for structural shielding for indoor exposure periods.

When indoors, protection afforded by buildings from external gamma radiation varies considerably. According to the U.S NCRP (1984), reported reduction factors (ratio of the exposure rate in the structure to the exposure rate in open air) for radionuclides deposited on the ground range from an average of about 0.27 for single story wooden houses to 0.06 for reinforced concrete and brick homes. Basements provide more protection than other areas of the house and average reduction factors range from 0.003 to 0.08. UNSCEAR (1982, p. 62) derives a world wide average reduction factor of 0.2 based on reduction factors of 0.05, 0.2 and 0.4 for offices, masonry homes and wooden homes respectively. Based on the above considerations, a reduction factor of 0.2 from external gamma exposure when indoors was selected for this analysis.

13.5 Receptor Specification

In UTAP.3, up to 80 possible receptors may be specified. This section summarizes what options may be selected to characterize each of these receptors.

13.5.1 Receptor Identification Number

This is simply a number from 1 to 80 (referred to in this chapter).

13.5.2 Sector Number

This is a number from 1 to 16 which indicates the sector in which the receptor is located (see Figure 2.2 and Section 13.5.3).

13.5.3 Ring Number

This is a number from 1 to NRING (number of rings) which specifies the ring in which the receptor is located (see Figure 2.3). This number, in combination with the sector number, specifies where the receptor lives (and therefore receives his inhalation and groundshine exposures) and grows his vegetables.

This does not affect the source of caribou and moose meat, as only one average value is calculated for each radionuclide for the entire area.

13.5.4 Water Source Segment Number

This number assigns where the receptor obtains his drinking water. Chapter 10 gives details on the nodes that may be selected, what they represent and how they are numbered.

13.5.5 Fish Source Segment Number

This number assigns where the receptor obtains his fish. Chapter 10 gives details on the nodes that may be selected, what they represent and how they are numbered.

13.5.6 Receptor Type

Two types of receptors may be selected: critical or average. Each of these may be specified by the user as described in previous sections. However, in any given run, one critical receptor only differs from another critical receptor in terms of his location and sources of water and fish (see above). All other parameters are common to all critical receptors. Similarly all average receptors are the same except for their location and source of water and fish.

13.5.7 Population

This specifies how many people of this type of receptor are to be included in the population dose estimate (see Section 13.6).

If the receptor is not to be used in the population dose calculation, the user simply enters a 0 in this space.

13.6 Population Dose

The dose to a population is:

$$D_P = \sum_n D_n P_n \qquad (13.10)$$

where

D_p = population average annual dose ($\mu Sv.yr^{-1}$)

P_n = population of receptor n (see Section 13.5.6)

D_n = average annual dose to receptor n ($\mu Sv.yr^{-1}$)

When the user is calculating a population dose, care should be taken to ensure that the caribou, moose and fish intakes that would be consumed by the specified population could be harvested from the area being modelled.

13.7 Description of Computer Model

The variables used in the dose model are summarized in Tables 13.3 and 13.4. The computer code listing for this model is provided in Table 13.5.

13.8 Dose Model Test Program

A series of tests were performed to check the dose model for computational accuracy and reasonableness. Some of these tests are discussed below.

Hand calculations were checked against a deterministic run to confirm that the dose model executed the equations properly. The model was also run probabilistically with the results checked for reasonableness.

Figure 13.1 is an example plot of the dose received by the receptor by the different pathways, plotted as the log of the geometric mean. Figures 13.2 and 13.3 are frequency histograms of the total dose received by the receptor at 0 and 500 year respectively. The system model was run for 2,000 years in 10 year time steps for 100 trials.

13.9 References

Case, G.G., Chambers, D.B., and Lowe,L.M., 1983. "Calculation of Radiation Exposures in a Case Control Study of Lung Cancers in Port Hope, Ontario." Presented at the Fourth Annual Conference of the Canadian Radiation Protection Association, May 3-5, 1983, Toronto, Ontario.

FIGURE 13.1

PREDICTED DOSE vs TIME BY PATHWAY

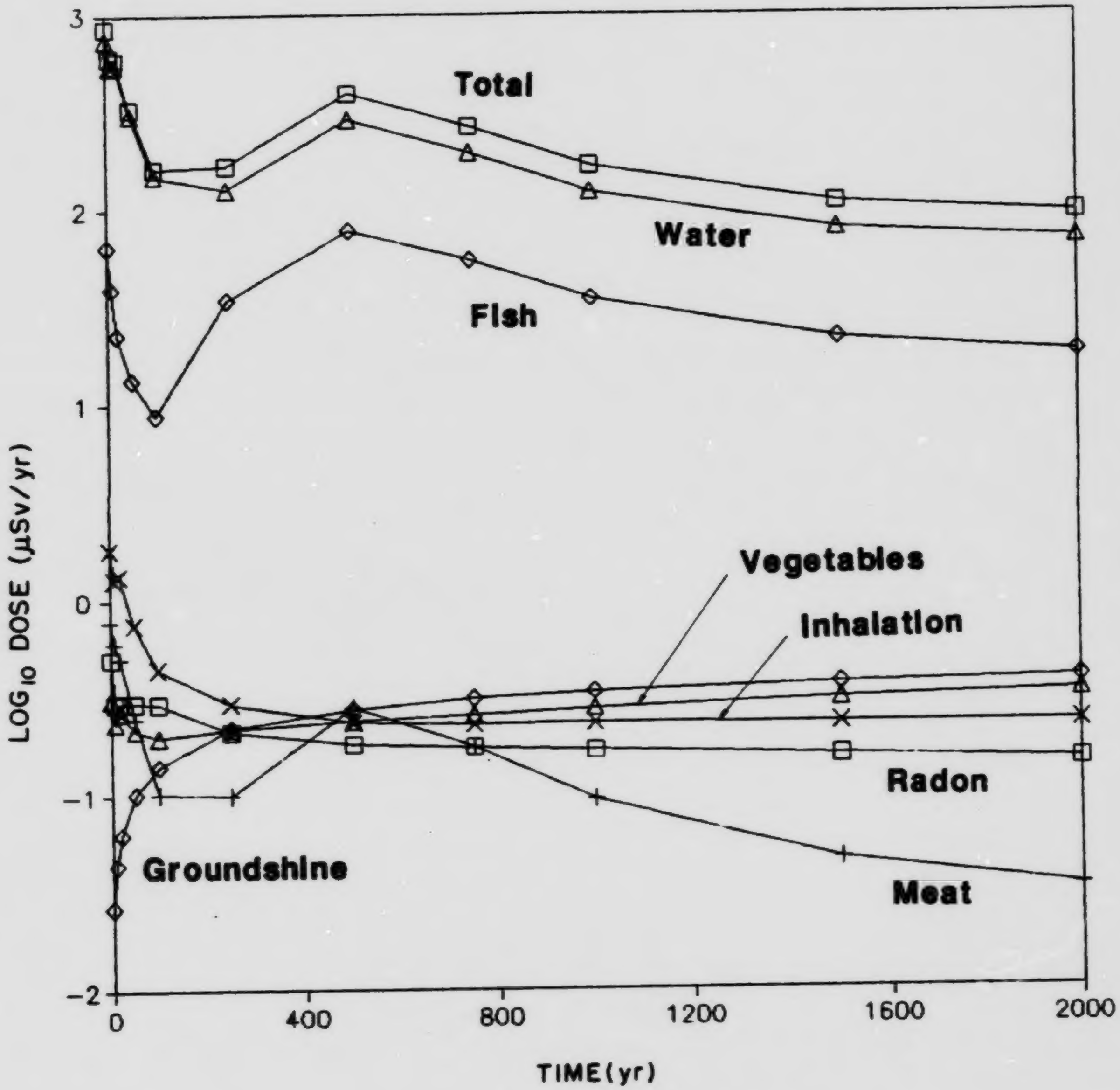

NOTES: 1) The graph shows geometric mean values of 100 trials
2) Receptor located 2km to the north of the tailings area

FIGURE 13.2

FREQUENCY HISTOGRAM OF TOTAL DOSE AT t=0 YEARS

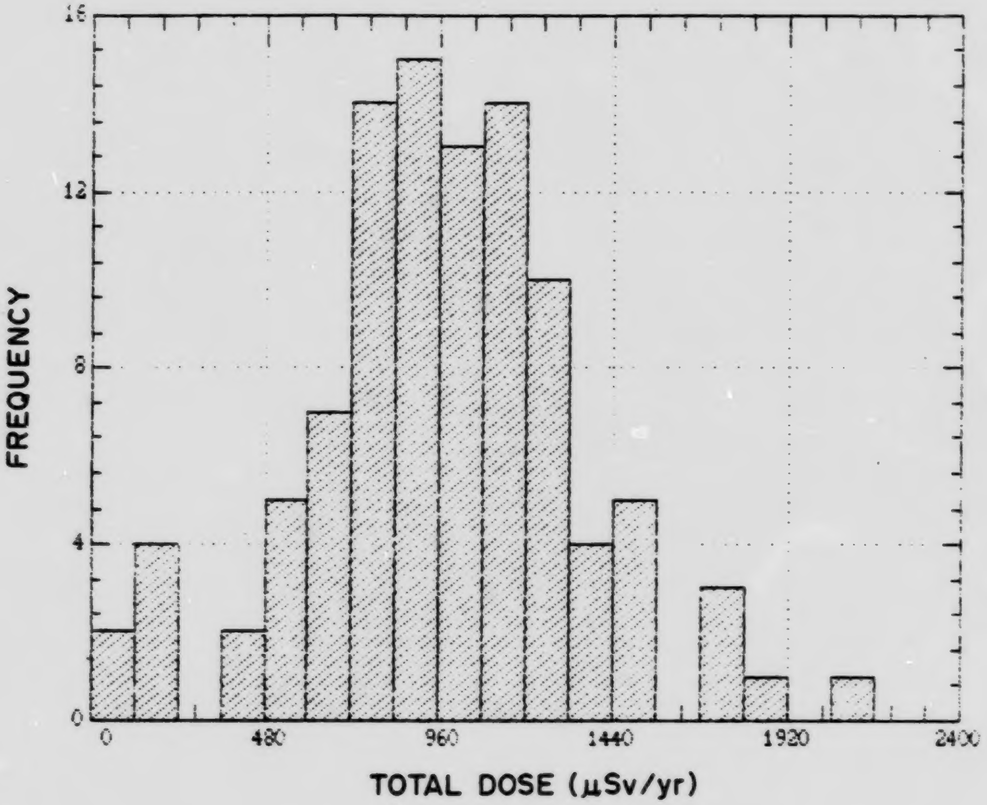

NOTES: 1 100 trials

FIGURE 13.3

FREQUENCY HISTOGRAM OF TOTAL DOSE AT t=500 YEARS

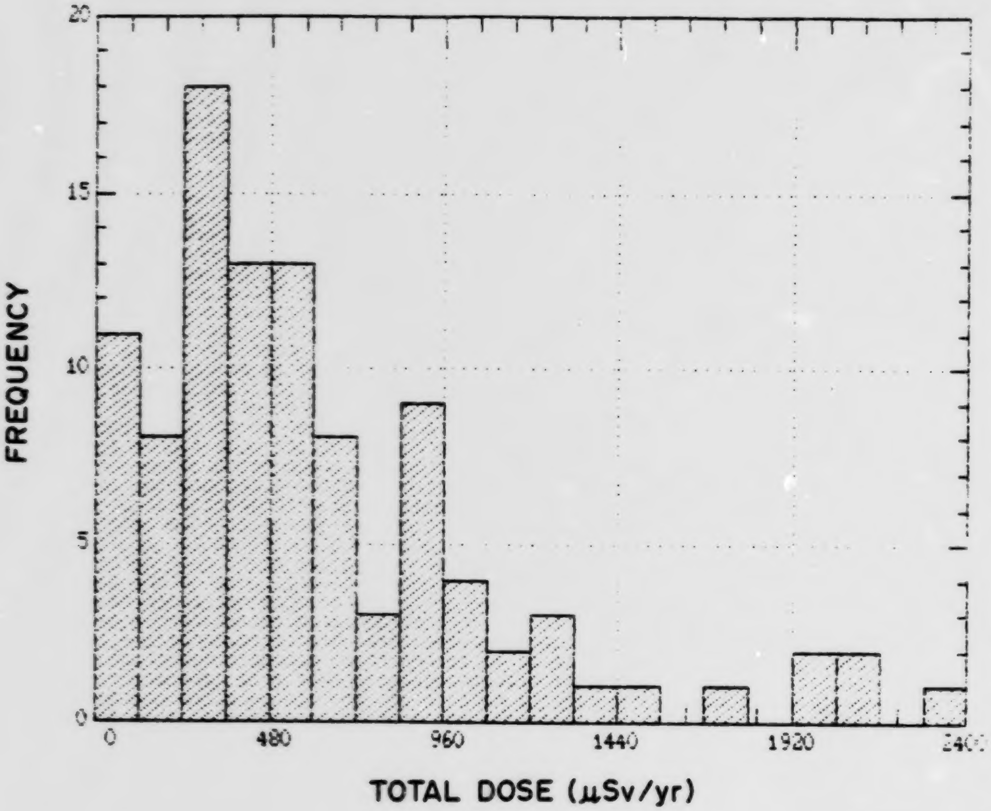

NOTES: 9 100 trials

Table 13.3

VARIABLES USED IN THE CALCULATION OF ANNUAL DOSE TO THE CRITICAL RECEPTOR

Model Symbol	Description	Units	Nominal Value	Probability Distribution	Computer Origin	Computer Symbol
Vegetation Model						
$d_{v,i,r,j,t}$(ing)	annual dose due to ingestion of radionuclide i in vegetables at time t	$\mu Sv \cdot yr^{-1}$	calculated	calculated	DOSEIN	VEGD(i,j) i=1,4 $j \leq 80$
$DCF_{a,i}$(ing)	whole body DCF for ingestion of radionuclide i (air pathway):	$\mu Sv \cdot Bq^{-1}$			DOSEIN	DCFGA(i) i=1,4
	U-nat		6.7×10^{-2}	$C(6.7 \times 10^{-2})$		
	Th-tot		calculated	calculated		
	Pb-210		1.4	C(1.4)		
	Ra-226		3.1×10^{-1}	$C(3.1 \times 10^{-1})$		
$U_{v,r}$	average annual intake of vegetable type v:	$g(wet\ wt).yr^{-1}$			INPUT	
	above ground veg.		4.81×10^4	$U\ (4.53 \times 10^4, 5.08 \times 10^4)$		AVEGIN(2)
	below ground veg.		7.81×10^4	$U\ (7.38 \times 10^4, 8.24 \times 10^4)$		BVEGIN(2)
$[C]_{v,i,j,t}$	concentration of radionuclide i in vegetation type v:	$Bq \cdot g^{-1}$			VEGCON	
	above ground veg.		calculated	calculated		AVEGC(i,j) i=1,4 $j \leq 80$
	below ground veg.		calculated	calculated		BVEGC(i,j) i=1,4 $j \leq 80$
	at time t					
$R_{v,r}$	fraction of activity in vegetable type v after food preparation:	-			INPUT	
	above ground veg.		0.75	U(0.5, 1.0)		AFACT
	below ground veg.		0.75	U(0.5, 1.0)		BFACT
$L_{v,r}$	fraction of vegetable type v grown locally:	-			INPUT	
	above ground veg.		0.5	T(0.1,0.3,0.6)		AFLOC(2)
	below ground veg.		0.5	T(0.1,0.3,0.6)		BFLOC(2)
Caribou Ingestion Model						
$d_{c,i,r,j,t}$(ing)	annual dose due to ingestion of radionuclide i in caribou meat at time t	$\mu Sv \cdot yr^{-1}$	calculated	calculated	DOSEIN	CARDOS(i,j) i=1,4 $j \leq 80$
$DCF_{a,i}$(ing)	whole body DCF for ingestion of radionuclide i (air pathway):	$\mu Sv \cdot Bq^{-1}$			DOSEIN	DCFGA(i) i=1,4
	U-nat		6.7×10^{-2}	$C(6.7 \times 10^{-2})$		
	Th-tot		calculated	calculated		
	Pb-210		1.4	C(1.4)		
	Ra-226		3.1×10^{-1}	$C(3.1 \times 10^{-1})$		
$DCF_{w,i}$(ing)	whole body DCF for ingestion of radionuclide i (water pathway):	$\mu Sv \cdot Bq^{-1}$			DOSEIN	DCFGW(i) i=1,4
	U-nat		6.7×10^{-2}	$C(6.7 \times 10^{-2})$		
	Th-tot		calculated	calculated		
	Pb-210		1.4	C(1.4)		
	Ra-226		3.1×10^{-1}	$C(3.1 \times 10^{-1})$		
$U_{c,r}$	annual intake of caribou meat	$g \cdot yr^{-1}$	2.6×10^4	$C(2.6 \times 10^4)$	INPUT	CARMIN(2)
$[C(air)]_{c,i,t}$	annual concentration of radionuclide i in caribou meat at time t (air pathway)	$Bq \cdot g^{-1}$	calculated	calculated	ANIMAL	ACARC(i) i=1,4
$L_{c,r}$	fraction of annual caribou meat intake that is local	-	0.5	U(0.0, 1.0)	INPUT	CFLOC(2)
$[C(water)]_{c,i,t}$	annual concentration of radionuclide i in caribou meat at time t (water pathway)	$Bq \cdot g^{-1}$	calculated	calculated	ANIMAL	WCARC(i) i=1,4

Table 13.3 continued

Model Symbol	Description	Units	Nominal Value	Probability Distribution	Computer Origin	Computer Symbol
Moose Ingestion Model						
$d_{m,i,r,j,t}(ing)$	annual dose due to ingestion of radionuclide i in moose meat at time t	$\mu Sv \cdot yr^{-1}$	calculated	calculated	DOSEIN	MOSDOS(i,j) i=1,4 $j \leq 80$
$DCF_{a,i}(ing)$	whole body DCF for ingestion of radionuclide i (air pathway): U-nat Th-tot Pb-210 Ra-226	$\mu Sv \cdot Bq^{-1}$	 6.7×10^{-2} calculated 1.4 3.1×10^{-1}	 $C(6.7 \times 10^{-2})$ calculated C(1.4) $C(3.1 \times 10^{-1})$	DOSEIN	DCFGA(i) i=1,4
$DCF_{w,i}(ing)$	whole body DCF for ingestion of radionuclide i: U-nat Th-tot Pb-210 Ra-226	$\mu Sv \cdot Bq^{-1}$	 6.7×10^{-2} calculated 1.4 3.1×10^{-1}	 $C(6.7 \times 10^{-2})$ calculated C(1.4) $C(3.1 \times 10^{-1})$	DOSEIN	DCFGW(i) i=1,4
$U_{m,r}$	annual intake of moose meat	$g \cdot yr^{-1}$	2.6×10^4	$C(2.6 \times 10^4)$	INPUT	MOSMIN(2)
$[C(air)]_{m,i,t}$	annual concentration of radionuclide i in moose meat at time t (air pathway)	$Bq \cdot g^{-1}$	calculated	calculated	ANIMAL	AMOSC(i) i=1,4
$L_{m,r}$	fraction of annual moose meat intake that is local	-	1.0	C(1.0)	INPUT	MFLOC(2)
$[C(water)]_{m,i,t}$	annual concentration of radionuclide i in moose meat at time t (water pathway)	$Bq \cdot g^{-1}$	calculated	calculated	ANIMAL	WMOSC(i) i=1,4
Deer Ingestion Model						
$d_{d,i,r,j,t}(ing)$	annual dose due to ingestion of radionuclide i in deer meat at time t	$\mu Sv \cdot yr^{-1}$	calculated	calculated	DOSEIN	DERDOS(i,j) i=1,4 $j \leq 80$
$DCF_{a,i}(ing)$	whole body DCF for ingestion of radionuclide i (air pathway); U-nat Th-tot Pb-210 Ra-225	$\mu Sv \cdot Bq^{-1}$	 6.7×10^{-2} calculated 1.4 3.1×10^{-1}	 $C(6.7 \times 10^{-2})$ calculated C(1.4) $C(3.1 \times 10^{-1})$	DOSEIN	DCFGA(i) i=1,4
$DCF_{w,i}(ing)$	whole body DCF for ingestion of radionuclide i: U-nat Th-tot Pb-210 Ra-225	$\mu Sv \cdot Bq^{-1}$	 6.7×10^{-2} calculated 1.4 3.1×10^{-1}	 $C(6.7 \times 10^{-2})$ calculated C(1.4) $C(3.1 \times 10^{-1})$	DOSEIN	DCFGW(i) i=1,4
$U_{d,r}$	annual intake of of deer meat	$g \cdot yr^{-1}$	2.6×10^4	$C(2.6 \times 10^4)$	INPUT	DERMIN(2)
$[C(air)]_{d,i,t}$	annual concentration of radionuclide i in deer meat at time t (air pathway)	$Bq \cdot g^{-1}$	calculated	calculated	ANIMAL	ADERC(i) i=1,4
$L_{d,r}$	fraction of annual deer meat intake that is local	-	1.0	C(1.0)	INPUT	DFLOC(2)
$[C(water)]_{d,i,t}$	annual concentration of radionuclide i in deer meat at time t (water pathway)	$Bq \cdot g^{-1}$	calculated	calculated	ANIMAL	WDERC(i) i=1,4

Table 13.3 continued

Model Symbol	Description	Units	Nominal Value	Probability Distribution	Computer Origin	Computer Symbol
Drinking Water Model						
$d_{w,i,r,j,t}(ing)$	annual dose due to ingestion of radionuclide i in drinking water at time t	$\mu Sv \cdot yr^{-1}$	calculated	calculated	DOSEIN	WATD(i,j) i=1,4 $j \leq 80$
$DCF_{w,i}(ing)$	whole body DCF for ingestion of radionuclide i (water pathway):	$\mu Sv \cdot Bq^{-1}$			DOSEIN	DCFGW(i) i=1,4
	U-nat		6.7×10^{-2}	$C(6.7 \times 10^{-2})$		
	Th-tot		calculated	calculated		
	Pb-210		1.4	C(1.4)		
	Ra-226		3.1×10^{-1}	$C(3.1 \times 10^{-1})$		
$U_{w,r}$	average annual intake of water	$m^3 \cdot yr^{-1}$	0.6	C (0.6)	INPUT	WATIN(2)
$[C]_{w,i,j,t}$	annual concentration of radionuclide i in drinking water at time t	$Bq.m^{-3}$	calculated	calculated	LAKE	WATC(i,n) i=4 $n \leq 10$
OF_r	fraction of year at that location	-	0.9	T(0.8,0.9,1.0)	INPUT	OF(2)
Fish Ingestion Model						
$d_{f,i,r,j,t}(ing)$	annual dose due to ingestion of radionuclide i in fish at time t	$\mu Sv.yr^{-1}$	calculated	calculated	DOSEIN	FISHD(i,j) i=1,4 $j \leq 80$
$DCF_{w,i}(ing)$	whole body DCF for ingestion of radionuclide i:	$\mu Sv \cdot Bq^{-1}$			DOSEIN	DCFGW(i) i=1,4
	U-nat		6.7×10^{-2}	$C(6.7 \times 10^{-2})$		
	Th-tot		calculated	calculated		
	Pb-210		1.4	C(1.4)		
	Ra-226		3.1×10^{-1}	$C(3.1 \times 10^{-1})$		
$U_{f,r}$	average annual intake of fish	$g.yr^{-1}$	8.0×10^3	$C(8.0 \times 10^3)$	INPUT	FISHIN(2)
$[C]_{f,i,j,t}$	concentration of radionuclide in i fish at time t	$Bq.g^{-1}$	calculated	calculated	FISH	FISHC(i,n) i=1,4 $n \leq 10$
$L_{f,r}$	fraction of annual intake that is local fish	-	1.0	C(1.0)	INPUT	FFLOC(2)
F_a	fish availability factor	-	calculated	calculated	FISH	FISHA(n) $n \leq 10$
Inhalation Model (Particulates)						
$d_{i,r,j,t}(inh)$	annual dose due to inhalation of radionuclide i at time t	$\mu Sv.yr^{-1}$	calculated	calculated	DOSEIN	INHD(i,j) i=1,4 $j \leq 80$
$DCF_{a,i}(inh)$	whole body DCF due to inhalation of radionuclide i (air pathway):	$Sv.Bq^{-1}$			DOSEIN	DCFHA(i) i=1,4
	U-nat		3.4×10^1	$C(3.4 \times 10^1)$		
	Th-tot		calculated	calculated		
	Pb-210		3.4	C(3.4)		
	Ra-226		2.1	C(2.1)		
$U_{a,r}$	average annual inhalation rate	$m^3.yr^{-1}$	8.4×10^3	$C(8.4 \times 10^3)$	INPUT	AIRIN(2)
$[C]_{a,i,j,t}$	concentration of radionuclide i in air at time t	$Bq.m^{-3}$	calculated	calculated	AIRDIS	AIRC(i,j) i=1,4 $j \leq 80$
OF_r	fraction of year in location	-	0.9	T (0.8,0.9,1.0)	INPUT	OF(2)

Table 13.3 continued

Model Symbol	Description	Units	Nominal Value	Probability Distribution	Computer Origin	Computer Symbol
Inhalation Model (Radon)						
$d_{Rn,r,j,t}(inh)$	annual dose due to inhalation of radon plus daughters at time t	$\mu Sv.yr^{-1}$	calculated	calculated	DOSEIN	RADD(j) $j \le 80$
F	equilibrium factor for radon daughters to radon	-	0.5	T (0.2,0.5,0.8)	INPUT	EFR
OF_r	fraction of year in location	-	0.9	T (0.8,0.9,1.0)	INPUT	OF(2)
$INOCC_r$	fraction of time spent indoors	-	0.9	T (0.6, 0.9,1.0)	INPUT	INOCC(2)
$[C]_{a,Rn,j,t}$	concentration of radon in air at time t	$Bq \cdot m^{-3}$	calculated	calculated	AIRDIS	AIRC(5,j) $j \le 80$
External Dose Model						
$d_{i,r,j,t}(ext)$	annual dose due to groundshine and radionuclide i at time t	$\mu Sv.yr^{-1}$	calculated	calculated	DOSEIN	SHINED(i,j) i=1,4 $j \le 80$
$D_{i,j,t}$	average groundshine dose rate due to radionuclide i at time t	$\mu Sv.yr^{-1}$	calculated	calculated	GSHINE	SHINE(i,j) i=1,4 $j \le 80$
OF_r	fraction of year in location	-	0.9	T (0.8,0.9,1.0)	INPUT	OF(2)
$INOCC_r$	fraction of time spent indoors	-	0.9	T (0.6,0.9,1.0)	INPUT	INOCC(2)
SHLD	shielding factor	-	0.2	T (0.05,0.2,0.4)	INPUT	SHLD

Table 13.4

VARIABLES USED IN THE CALCULATION OF ANNUAL DOSE TO THE AVERAGE RECEPTOR

Model Symbol	Description	Units	Nominal Value	Probability Distribution	Computer Origin	Computer Symbol
Vegetation Model						
$d_{v,i,r,j,t}$(ing)	annual dose due to ingestion of radionuclide i in vegetables at time t	$\mu Sv \cdot yr^{-1}$	calculated	calculated	DOSEIN	VEGD(i,j) i=1,4 $j \leq 80$
$DCF_{a,i}$(ing)	whole body DCF for ingestion of radionuclide i (air pathway):	$\mu Sv \cdot Bq^{-1}$			DOSEIN	DCFGA(i) i=1,4
	U-nat		6.7×10^{-2}	$C(6.7 \times 10^{-2})$		
	Th-tot		calculated	calculated		
	Pb-210		1.4	C(1.4)		
	Ra-226		3.1×10^{-1}	$C(3.1 \times 10^{-1})$		
$U_{v,r}$	average annual intake of vegetable type v:	g(wet wt).yr^{-1}			INPUT	
	above ground veg.		4.81×10^4	$U(4.53 \times 10^4, 5.08 \times 10^4)$		AVEGIN(1)
	below ground veg.		7.81×10^4	$U(7.38 \times 10^4, 8.24 \times 10^4)$		BVEGIN(1)
$[C]_{v,i,j,t}$	concentration of radionuclide i in vegetation type v:	$Bq \cdot g^{-1}$			VEGCON	
	above ground veg.		calculated	calculated		AVEGC(i,j) i=1,4 $j \leq 80$
	below ground veg.		calculated	calculated		BVEGC(i,j) i=1,4 $j \leq 80$
	at time t					
$R_{v,r}$	fraction of activity in vegetable type v after food preparation:	-			INPUT	
	above ground veg.		0.75	U(0.5, 1.0)		AFACT
	below ground veg.		0.75	U(0.5, 1.0)		BFACT
$L_{v,r}$	fraction of vegetable type v grown locally:	-			INPUT	
	above ground veg.		0.1	T(0.0,0.1,0.2)		AFLOC(1)
	below ground veg.		0.1	T(0.0,0.1,0.2)		BFLOC(1)
Caribou Ingestion Model						
$d_{c,i,r,j,t}$(ing)	annual dose due to ingestion of radionuclide i in caribou meat at time t	$\mu Sv \cdot yr^{-1}$	calculated	calculated	DOSEIN	CARDOS(i,j) i=1,4 $j \leq 80$
$DCF_{a,i}$(ing)	whole body DCF for ingestion of radionuclide i (air pathway):	$\mu Sv \cdot Bq^{-1}$			DOSEIN	DCFGA(i) i=1,4
	U-nat		6.7×10^{-2}	$C(6.7 \times 10^{-2})$		
	Th-tot		calculated	calculated		
	Pb-210		1.4	C(1.4)		
	Ra-226		3.1×10^{-1}	$C(3.1 \times 10^{-1})$		
$DCF_{w,i}$(ing)	whole body DCF for ingestion of radionuclide i (water pathway):	$\mu Sv \cdot Bq^{-1}$			DOSEIN	DCFGW(i) i=1,4
	U-nat		6.7×10^{-2}	$C(6.7 \times 10^{-2})$		
	Th-tot		calculated	calculated		
	Pb-210		1.4	C(1.4)		
	Ra-226		3.1×10^{-1}	$C(3.1 \times 10^{-1})$		
$U_{c,r}$	annual intake of caribou meat	$g \cdot yr^{-1}$	3.8×10^3	$C(3.8 \times 10^3)$	INPUT	CARMIN(1)
$[C(air)]_{c,i,t}$	annual concentration of radionuclide i in caribou meat at time t (air pathway)	$Bq \cdot g^{-1}$	calculated	calculated	ANIMAL	ACARC(i) i=1,4
$L_{c,r}$	fraction of annual caribou meat intake that is local	-	0.5	U(0.0, 1.0)	INPUT	CFLOC(1)
$[C(water)]_{c,i,t}$	annual concentration of radionuclide i in Caribou meat at time t (water pathway)	$Bq \cdot g^{-1}$	calculated	calculated	ANIMAL	WCARC(i) i=1,4

Table 13.4 continued

Model Symbol	Description	Units	Nominal Value	Probability Distribution	Computer Origin	Computer Symbol
Moose Ingestion Model						
$d_{m,i,r,j,t}(ing)$	annual dose due to ingestion of radionuclide i in moose meat at time t	$\mu Sv \cdot yr^{-1}$	calculated	calculated	DOSEIN	MOSDOS(i,j) i=1,4 j≤80
$DCF_{a,i}(ing)$	whole body DCF for ingestion of radionuclide i (air pathway):	$\mu Sv \cdot Bq^{-1}$			DOSEIN	DCFGA(i) i=1,4
	U-nat		6.7×10^{-2}	$C(6.7 \times 10^{-2})$		
	Th-tot		calculated	calculated		
	Pb-210		1.4	C(1.4)		
	Ra-226		3.1×10^{-1}	$C(3.1 \times 10^{-1})$		
$DCF_{w,i}(ing)$	whole body DCF for ingestion of radionuclide i:	$\mu Sv \cdot Bq^{-1}$			DOSEIN	DCFGW(i) i=1,4
	U-nat		6.7×10^{-2}	$C(6.7 \times 10^{-2})$		
	Th-tot		calculated	calculated		
	Pb-210		1.4	C(1.4)		
	Ra-226		3.1×10^{-1}	$C(3.1 \times 10^{-1})$		
$U_{m,r}$	annual intake of moose meat	$g \cdot yr^{-1}$	3.8×10^3	$C(3.8 \times 10^3)$	INPUT	MOSMIN(1)
$[C(air)]_{m,i,t}$	annual concentration of radionuclide i in moose meat at time t (air pathway)	$Bq \cdot g^{-1}$	calculated	calculated	ANIMAL	AMOSC(i) i=1,4
$L_{m,r}$	fraction of annual moose meat intake that is local	-	0.0	C(0.0)	INPUT	MFLOC(1)
$[C(water)]_{m,i,t}$	annual concentration of radionuclide i in moose meat at time t (water pathway)	$Bq \cdot g^{-1}$	calculated	calculated	ANIMAL	WMOSC(i) i=1,4
Deer Ingestion Model						
$d_{d,i,r,j,r}(ing)$	annual dose due to ingestion of radionuclide i in deer meat at time t	$\mu Sv \cdot yr^{-1}$	calculated	calculated	DOSEIN	DERDOS(i,j) i=1,4 j≤80
$DCF_{a,i}(ing)$	whole body DCF for ingestion of radionuclide i (air pathway):	$\mu Sv \cdot Bq^{-1}$			DOSEIN	DCFGA(i) i=1,4
	U-nat		6.7×10^{-2}	$C(6.7 \times 10^{-2})$		
	Th-tot		calculated	calculated		
	Pb-210		1.4	C(1.4)		
	Ra-226		3.1×10^{-1}	$C(3.1 \times 10^{-1})$		
$DCF_{w,i}(ing)$	whole body DCF for ingestion of radionuclide i:	$\mu Sv \cdot Bq^{-1}$			DOSEIN	DCFGW(i) i=1,4
	U-nat		6.7×10^{-2}	$C(6.7 \times 10^{-2})$		
	Th-tot		calculated	calculated		
	Pb-210		1.4	C(1.4)		
	Ra-226		3.1×10^{-1}	$C(3.1 \times 10^{-1})$		
$U_{d,r}$	annual intake of deer meat	$g \cdot yr^{-1}$	3.8×10^3	$C(3.8 \times 10^3)$	INPUT	DERMIN(1)
$[C(air)]_{d,i,t}$	annual concentration of radionuclide i in deer meat at time t (air pathway)	$Bq \cdot g^{-1}$	calculated	calculated	ANIMAL	ADERC(i) i=1,4
$L_{d,r}$	fraction of annual deer meat intake that is local	-	0.0	C(0.0)	INPUT	DFLOC(1)
$[C(water)]_{d,i,t}$	annual concentration of radionuclide i in deer meat at time t (water pathway)	$Bq \cdot g^{-1}$	calculated	calculated	ANIMAL	WDERC(i) i=1,4

Table 13.4 continued

Model Symbol	Description	Units	Nominal Value	Probability Distribution	Computer Origin	Computer Symbol
Drinking Water Model						
$d_{w,i,r,j,t}(ing)$	annual dose due to ingestion of radionuclide i in drinking water at time t	$\mu Sv \cdot yr^{-1}$	calculated	calculated	DOSEIN	WATD(i,j) i=1,4 j≤80
$DCF_{w,i}(ing)$	whole body DCF for ingestion of radionuclide i (water pathway): U-nat Th-tot Pb-210 Ra-226	$\mu Sv \cdot Bq^{-1}$	 6.7×10^{-2} calculated 1.4 3.1×10^{-1}	 $C(6.7 \times 10^{-2})$ calculated C(1.4) $C(3.1 \times 10^{-1})$	DOSEIN	DCFGW(i) i=1,4
$U_{w,r}$	average annual intake of water	$m^3 \cdot yr^{-1}$	0.6	C (0.6)	INPUT	WATIN(1)
$[C]_{w,i,j,t}$	annual concentration of radionuclide i in drinking water at time t	$Bq.m^{-3}$	calculated	calculated	LAKE	WATC(i,n) i=4 n≤10
OF_r	fraction of year at that location	-	0.9	T(0.8,0.9,1.0)	INPUT	OF(1)
Fish Ingestion Model						
$d_{f,i,r,j,t}(ing)$	annual dose due to ingestion of radionuclide i in fish at time t	$\mu Sv.yr^{-1}$	calculated	calculated	DOSEIN	FISHD(i,j) i=1,4 j≤80
$DCF_{w,i}(ing)$	whole body DCF for ingestion of radionuclide i: U-nat Th-tot Pb-210 Ra-226	$\mu Sv \cdot Bq^{-1}$	 6.7×10^{-2} calculated 1.4 3.1×10^{-1}	 $C(6.7 \times 10^{-2})$ calculated C(1.4) $C(3.1 \times 10^{-1})$	DOSEIN	DCFGW(i) i=1,4
$U_{f,r}$	average annual intake of fish	$g.yr^{-1}$	8.0×10^3	$C(8.0 \times 10^3)$	INPUT	FISHIN(1)
$[C]_{f,i,j,t}$	concentration of radionuclide in i fish at time t	$Bq.g^{-1}$	calculated	calculated	FISH	FISHC(i,n) i=1,4 n≤10
$L_{f,r}$	fraction of annual intake that is local fish	-	0.05	U(0.0,0.1)	INPUT	FFLOC(1)
F_a	fish availability factor	-	calculated	calculated	FISH	FISHA(n) n≤10
Inhalation Model (Particulates)						
$d_{i,r,j,t}(inh)$	annual dose due to inhalation of radionuclide i at time t	$\mu Sv.yr^{-1}$	calculated	calculated	DOSEIN	INHD(i,j) i=1,4 j≤80
$DCF_{a,i}(inh)$	whole body DCF due to inhalation of radionuclide i (air pathway): U-nat Th-tot Pb-210 Ra-226	$Sv.Bq^{-1}$	 3.4×10^1 calculated 3.4 2.1	 $C3.4 \times 10^1)$ calculated C(3.4) C(2.1)	DOSEIN	DCFHA(i) i=1,4
$U_{a,r}$	average annual inhalation rate	$m^3.yr^{-1}$	8.4×10^3	$C(8.4 \times 10^3)$	INPUT	AIRIN(1)
$[C]_{a,i,j,t}$	concentration of radionuclide i in air at time t	$Bq.m^{-3}$	calculated	calculated	AIRDIS	AIRC(i,j) i=1,4 j≤80
OF_r	fraction of year in location	-	0.9	T (0.8,0.9,1.0)	INPUT	OF(1)

Table 13.4 continued

Model Symbol	Description	Units	Nominal Value	Probability Distribution	Computer Origin	Computer Symbol
Inhalation Model (Radon)						
$d_{Rn,r,j,t}^{(inh)}$	annual dose due to inhalation of radon plus daughters at time t	$\mu Sv.yr^{-1}$	calculated	calculated	DOSEIN	RADD(J) $J \le 80$
F	equilibrium factor for radon daughters to radon	-	0.5	T (0.2,0.5,0.8)	INPUT	EFR
OF_r	fraction of year in location	-	0.9	T (0.8,0.9,1.0)	INPUT	OF(1)
$INOCC_r$	fraction of time spent indoors	-	0.9	T (0.6, 0.9, 1.0)	INPUT	INOCC(1)
$[C]_{a,Rn,j,t}$	concentration of radon in air at time t	$Bq \cdot m^{-3}$	calculated	calculated	AIRDIS	AIRC(5,J) $J \le 80$
External Dose Model						
$d_{i,r,j,t}^{(ext)}$	annual dose due to groundshine and radionuclide i at time t	$\mu Sv.yr^{-1}$	calculated	calculated	DOSEIN	SHINED(i,J) $i=1,4$ $J \le 80$
$D_{i,j,t}$	average groundshine dose rate due to radionuclide i at time t	$\mu Sv.yr^{-1}$	calculated	calculated	GSHINE	SHINE(i,J) $i=1,4$ $J \le 80$
OF_r	fraction of year in location	-	0.9	T (0.8,0.9,1.0)	INPUT	OF(1)
$INOCC_r$	fraction of time spent indoors	-	0.9	T (0.6,0.9,1.0)	INPUT	INOCC(1)
SHLD	shielding factor	-	0.2	T (0.05,0.2,0.4)	INPUT	SHLD

Table 13.5

DOSE MODEL CODE LISTING

```
      SUBROUTINE DOSEIN
      INCLUDE 'MODEL.INC'
      INCLUDE 'VAR.INC'
      REAL*4 DCFGA(4),DCFGW(4),DCFHA(4),CARDOS(4,80),MOSDOS(4,80),
     +       DERDOS(4,80)
      COMMON /DOSEIN/ DCFGA,DCFGW,DCFHA
      IF(NREC.EQ.1)THEN
         DCFGA(1)=6.7E-2
         DCFGA(2)=3.5+18.0*X232SA
         DCFGA(3)=1.4
         DCFGA(4)=3.1E-1
         DCFGW(1)=6.7E-2
         DCFGW(2)=3.5+18.0*X232LA
         DCFGW(3)=1.4
         DCFGW(4)=3.1E-1
         DCFHA(1)=3.4E+1
         DCFHA(2)=7.0E+1+3.2E+2*X232SA
         DCFHA(3)=3.4
         DCFHA(4)=2.1
         POPDT=0.0
      ENDIF
      SHINED(5,NREC)=0.0
      INHD(5,NREC)=0.0
      VEGD(5,NREC)=0.0
      MEATD(5,NREC)=0.0
      WATD(5,NREC)=0.0
      FISHD(5,NREC)=0.0
      N=1
      IF(RTYPE(NREC).EQ.'C')N=2
      RADD(NREC)=69.6*INOCC(N)*OF(N)*EFR*AIRC(5,NREC)
      DOSE(5,NREC)=RADD(NREC)
      DO 10 I=1,4
         SHINED(I,NREC)=(1.0-INOCC(N)+SHLD*INOCC(N))*OF(N)*
     +                  SHINE(I,NREC)
         SHINED(5,NREC)=SHINED(5,NREC)+SHINED(I,NREC)
         INHD(I,NREC)=DCFHA(I)*AIRIN(N)*OF(N)*AIRC(I,NREC)
         INHD(5,NREC)=INHD(5,NREC)+INHD(I,NREC)
         VEGD(I,NREC)=DCFGA(I)*(AFACT*AVEGIN(N)*AFLOC(N)*AVEGC(I,NREC)
     +                +BFACT*BVEGIN(N)*BFLOC(N)*BVEGC(I,NREC))
         VEGD(5,NREC)=VEGD(5,NREC)+VEGD(I,NREC)
         CARDOS(I,NREC)=CARMIN(N)*CFLOC(N)*(DCFGA(I)*ACARC(I)+DCFGW(I)
     +                  *WCARC(I))
         MOSDOS(I,NREC)=MOSMIN(N)*MFLOC(N)*(DCFGA(I)*AMOSC(I)+DCFGW(I)
     +                  *WMOSC(I))
         DERDOS(I,NREC)=DERMIN(N)*DFLOC(N)*(DCFGA(I)*ADERC(I)+DCFGW(I)
     +                  *WDERC(I))
         MEATD(I,NREC)=CARDOS(I,NREC)+MOSDOS(I,NREC)+DERDOS(I,NREC)
         MEATD(5,NREC)=MEATD(5,NREC)+MEATD(I,NREC)
         IF(RWSSEG(NREC).EQ.0)THEN
            WATD(I,NREC)=0.0
         ELSE
```

Table 13.5 continued.

```
            WATD(I,NREC)=DCFGW(I)*WATIN(N)*OF(N)*WATC(I,RWSSEG(NREC))
         ENDIF
         WATD(5,NREC)=WATD(5,NREC)+WATD(I,NREC)
         IF(RFSEG(NREC).EQ.0)THEN
            FISHD(I,NREC)=0.0
         ELSE
            FISHD(I,NREC)=DCFGW(I)*FISHIN(N)*FFLOC(N)*FISHA(RFSEG
     +                    (NREC))*FISHC(I,RFSEG(NREC))
         ENDIF
         FISHD(5,NREC)=FISHD(5,NREC)+FISHD(I,NREC)
         DOSE(I,NREC)=INHD(I,NREC)+VEGD(I,NREC)+MEATD(I,NREC)+WATD(I,
     +                NREC)+FISHD(I,NREC)
         DOSE(5,NREC)=DOSE(5,NREC)+DOSE(I,NREC)
10    CONTINUE
      POPDT=POPDT+RPOP(NREC)*DOSE(5,NREC)
C
      IF(CODDOS.EQ.1.0.OR.CODDOS.EQ.2.0.OR.CODDOS.EQ.3.0)THEN
         WRITE(*,100)
      ENDIF
      IF(CODDOS.EQ.3.0)THEN
         WRITE(*,101)X232SA,X232LA
         WRITE(*,102)(DCFGA(I),DCFGW(I),DCFHA(I),I=1,4)
         IF(RTYPE(NREC).EQ.'C')THEN
            WRITE(*,103)NREC
         ELSE
            WRITE(*,104)NREC
         ENDIF
         WRITE(*,105)EFR,OF(N),INOCC(N),(AIRC(I,NREC),I=1,5)
         WRITE(*,106)AFACT,AVEGIN(N),AFLOC(N),(AVEGC(I,NREC),I=1,4)
         WRITE(*,107)BFACT,BVEGIN(N),BFLOC(N),(BVEGC(I,NREC),I=1,4)
         WRITE(*,108)CARMIN(N),CFLOC(N),(ACARC(I),I=1,4),
     +              (WCARC(I),I=1,4)
         WRITE(*,109)MOSMIN(N),MFLOC(N),(AMOSC(I),I=1,4),
     +              (WMOSC(I),I=1,4)
         WRITE(*,110)DERMIN(N),DFLOC(N),(AMOSC(I),I=1,4),
     +              (WDERC(I),I=1,4)
         IF(RWSSEG(NREC).EQ.0)THEN
            WRITE(*,111)
         ELSE
            WRITE(*,112)WATIN(N),(WATC(I,RWSSEG(NREC)),I=1,4)
         ENDIF
         IF(RFSEG(NREC).EQ.0)THEN
            WRITE(*,113)
         ELSE
            WRITE(*,114)FISHIN(N),FFLOC(N),FISHA(RFSEG(NREC)),
     +                  (FISHC(I,RFSEG(NREC)),I=1,4)
         ENDIF
         IF(RTYPE(NREC).EQ.'C')THEN
            WRITE(*,115)RPOP(NREC)
         ELSE
            WRITE(*,116)RPOP(NREC)
         ENDIF
         WRITE(*,117)(SHINE(I,NREC),I=1,4)
```

Table 13.5 continued.

```
         WRITE(*,118)(CARDOS(I,NREC),I=1,4)
         WRITE(*,119)(MOSDOS(I,NREC),I=1,4)
         WRITE(*,120)(DERDOS(I,NREC),I=1,4)
      ENDIF
      IF(CODDOS.EQ.2.0.OR.CODDOS.EQ.3.0)THEN
         WRITE(*,121)RADD(NREC)
         WRITE(*,122)(SHINED(I,NREC),I=1,5)
         WRITE(*,123)(INHD(I,NREC),I=1,5)
         WRITE(*,124)(VEGD(I,NREC),I=1,5)
         WRITE(*,125)(MEATD(I,NREC),I=1,5)
         WRITE(*,126)(WATD(I,NREC),I=1,5)
         WRITE(*,127)(FISHD(I,NREC),I=1,5)
         WRITE(*,128)(DOSE(I,NREC),I=1,5)
         IF(NREC.EQ.NRECEP)THEN
            WRITE(*,129)POPDT
         ENDIF
      ENDIF
C
100   FORMAT(///1X,'DOSE MODEL')
101   FORMAT(/1X,'ACTIVITY OF Th-nat IN Th-tot IN THE AIR PATHWAY',
     +       E12.4/1X,'ACTIVITY OF Th-nat IN Th-tot IN THE WATER PAT',
     +       'HWAY',E12.4)
102   FORMAT(1X,'DOSE CONVERSION FACTORS'/5X,'INGESTION (AIR PATHWAY',
     +       ')',4(E12.4)/5X,'INGESTION (WATER PATHWAY)',4(E12.4)/5X,
     +       'INHALATION (AIR PATHWAY)',4(E12.4))
103   FORMAT(1X,'RECEPTOR',I3,': CRITICAL')
104   FORMAT(1X,'RECEPTOR',I3,': AVERAGE')
105   FORMAT(1X,'EQUILIBRIUM FACTOR BETWEEN RADON AND ITS DAUGHTERS',
     +       E12.4/1X,'FRACTION OF TIME SPENT AT LOCATION',E12.4/1X,
     +       'FRACTION OF TIME SPENT INDOORS',E12.4/1X,'RADIONUCLIDE',
     +       'AIR CONCENTRATION'/1X,5(E12.4))
106   FORMAT(1X,'FRACTION OF ACTIVITY REMAINING IN ABOVE GROUND VEGE',
     +       'TABLES AFTER'/5X,'FOOD PREPARATION',E12.4/1X,'AVERAGE ',
     +       'ANNUAL INTAKE OF ABOVE GROUND VEGETABLES',E12.4/1X,'FR',
     +       'ACTION OF ABOVE GROUND VEGETABLES GROWN LOCALLY',E12.4/
     +       1X,'RADIONUCLIDE CONCENTRATION IN ABOVE GROUND VEGETABL',
     +       'ES'/1X,4(E12.4))
107   FORMAT(1X,'FRACTION OF ACTIVITY REMAINING IN BELOW GROUND VEGE',
     +       'TABLES AFTER'/5X,'FOOD PREPARATION',E12.4/1X,'AVERAGE ',
     +       'ANNUAL INTAKE OF BELOW GROUND VEGETABLES',E12.4/1X,'FR',
     +       'ACTION OF BELOW GROUND VEGETABLES GROWN LOCALLY',E12.4/
     +       1X,'RADIONUCLIDE CONCENTRATION IN BELOW GROUND VEGETABL',
     +       'ES'/1X,4(E12.4))
108   FORMAT(1X,'AVERAGE ANNUAL INTAKE OF CARIBOU MEAT',E12.4/1X,'FR',
     +       'ACTION OF ANNUAL INTAKE THAT IS LOCAL CARIBOU MEAT',
     +       E12.4/1X,'RADIONUCLIDE CONCENTRATION IN CARIBOU MEAT (A',
     +       'IR PATHWAY)'/1X,4(E12.4),'RADIONUCLIDE CONCENTRATION I',
     +       'N CARIBOU MEAT (WATER PATHWAY)'/1X,4(E12.4))
109   FORMAT(1X,'AVERAGE ANNUAL INTAKE OF MOOSE MEAT',E12.4/1X,'FRAC',
     +       'TION OF ANNUAL INTAKE THAT IS LOCAL MOOSE MEAT',E12.4/
     +       1X,'RADIONUCLIDE CONCENTRATION IN MOOSE MEAT (AIR PATHW',
     +       'AY)'/1X,4(E12.4),'RADIONUCLIDE CONCENTRATION IN MOOSE ',
     +       ' MEAT (WATER PATHWAY)'/1X,4(E12.4))
```

Table 13.5 continued.

```
110   FORMAT(1X,'AVERAGE ANNUAL INTAKE OF DEER MEAT',E12.4/1X,'FRACT',
    +       'ION OF ANNUAL INTAKE THAT IS LOCAL MOOSE MEAT',E12.4/1X,
    +       'RADIONUCLIDE CONCENTRATION IN DEER MEAT (AIR PATHWAY)',/
    +       1X,4(E12.4),'RADIONUCLIDE CONCENTRATION IN DEER MEAT (W',
    +       'ATER PATHWAY)'/1X,4(E12.4))
111   FORMAT(1X,'NO RADIONUCLIDE CONCENTRATION IN DRINKING WATER'/5X,
    +       'WATER SUPPLY FROM OUTSIDE AREA')
112   FORMAT(1X,'AVERAGE ANNUAL INTAKE OF DRINKING WATER',E12.4/1X,
    +       'RADIONUCLIDE WATER CONCENTRATION'/1X,4(E12.4))
113   FORMAT(1X,'NO RADIONUCLIDE CONCENTRATION IN FISH'/5X,'FISH SUP',
    +       'PLY FROM OUTSIDE AREA')
114   FORMAT(1X,'AVERAGE ANNUAL INTAKE OF FISH',E12.4/1X,'FRACTION O',
    +       'F ANNUAL INTAKE THAT IS LOCAL FISH',E12.4/1X,'FISH AVA',
    +       'ILABILITY FACTOR',E12.4/1X,'RADIONUCLIDE CONCENTRATION',
    +       ' IN FISH'/1X,4(E12.4))
115   FORMAT(1X,'CRITICAL RECEPTOR POPULATION',I7)
116   FORMAT(1X,'AVERAGE RECEPTOR POPULATION',I7)
117   FORMAT(1X,'TOTAL GROUNDSHINE'/1X,4(E12.4))
118   FORMAT(1X,'DOSE FROM INGESTION OF CARIBOU MEAT'/1X,4(E12.4))
119   FORMAT(1X,'DOSE FROM INGESTION OF MOOSE MEAT'/1X,4(E12.4))
120   FORMAT(1X,'DOSE FROM INGESTION OF DEER MEAT'/1X,4(E12.4))
121   FORMAT(/1X,'DOSE FROM RADON INHALATION'/1X,E12.4)
122   FORMAT(1X,'DOSE FROM GROUNDSHINE'/1X,5(E12.4))
123   FORMAT(1X,'DOSE FROM PARTICULATE INHALATION'/1X,5(E12.4))
124   FORMAT(1X,'DOSE FROM INGESTION OF VEGETABLES'/1X,5(E12.4))
125   FORMAT(1X,'DOSE FROM INGESTION OF MEAT'/1X,5(E12.4))
126   FORMAT(1X,'DOSE FROM INGESTION OF DRINKING WATER'/1X,5(E12.4))
127   FORMAT(1X,'DOSE FROM INGESTION OF FISH'/1X,5(E12.4))
128   FORMAT(1X,'TOTAL DOSE'/1X,5(E12.4))
129   FORMAT(1X,'POPULATION DOSEL'/1X,E12.4)
C
      RETURN
      END
```

Hannibal, L., 1982. "On the Radiological Significance of Inhaled Uranium and Thorium Ore Dust." Health Physics, Vol. 42, No. 3, pp. 367-371.

International Commission on Radiological Protections, (ICRP), 1975. "Report of the Task Group on Reference Man." ICRP Publication 23, Pergamon Press, Oxford.

International Commission on Radiological Protection (ICRP), 1977. "Recommendations of the International Commission on Radiological Protection." ICRP Publication 26, Pergamon Press, Oxford.

International Commission on Radiological Protection (ICRP), 1979. "Limits for Intakes of Radionuclides by Workers." ICRP Publication 30, Part 1 and Supplement, Pergamon Press, Oxford.

International Commission on Radiological Protection (ICRP), 1981. "Limits for Inhalation of Radon Daughters by Workers." ICRP Publication 32, Annals of the ICRP, Vol. 6, No.1.

Johnson, J.R. and Dunford, D.W., 1983. "Dose Conversion Factors For Intakes of Selected Radionuclides by Infants and Adults." Atomic Energy of Canada Limited, AECL-7919.

Johnson, J.R., 1986. "A Literature Review of Thorium Uptake, Retention and Excretion." Prepared for Eldorado Resources, November.

Nuclear Energy Agency (NEA) Group of Experts, 1983. "Dosimetry Aspects of Exposure to Radon and Thoron Daughter Products." Nuclear Energy Agency, Organization for Economic Co-operation and Development, Paris, France.

Nutrition Canada, not dated. "Food Consumption Patterns Report." Prepared by the Department of National Health and Welfare.

Stewart, C.G., 1984. "Comments Upon 'Basis of Intake Limits for Radon and Thoron Daughters' Proposed by the Atomic Energy Control Board of Canada in Consultative Document C-78 Entitled 'Limitation of Exposure to Ionizing Radiation' Issued for Comment 14 November 1983." Prepared in Association with SENES Consultants Limited for the Canadian Nuclear Association.

United Nations Scientific Committee on the Effects of Atomic Radiation (UNSCEAR), 1982. "Ionizing Radiation Sources and Biological Effects." United Nations Publication.

United States Environmental Protection Agency (U.S.EPA), 1985. "Background Information Document - Standard for Radon-222 Emissions from Underground Uranium Mines." EPA 520/1-85-010.

United States National Council on Radiation Protection and Measurements (NCRP), 1984. "Radiological Assessment: Predicting the Transport Bioaccumulation and Uptake by Man of Radionuclides Related to the Environment." NCRP Report No. 76, 15 March.

United States Nuclear Regulatory Commission (U.S. NRC), 1982. "Calculational Models for Estimating Radiation Doses to Man from Airborne Radioactive Materials Resulting from Uranium Milling Operations." Reg. Guide, 3.51, March.

APPENDIX A

WATER SOURCE MODELS: CODE LISTING AND VARIABLE DICTIONARY

Since the water source models are by far the lengthiest component models in UTAP, they are listed here (as Table A.1) rather than in Chapter 3. Following the code listing is a variable dictionary for these models, which acts as a bridge between the model derivation and description in Chapter 3 and the computer implementation in Table A.1

The variable dictionary presented in Table A.3 is meant to be exhaustive as far as the model descriptions (Chapter 3) are concerned. That is, any variable in any equation in Chapter 3 which is used in the computer model is included in the variable dictionary. There will be some variables used in the computer implementation, (primarily those used in intermediate calculations) which will not appear in the variable dictionary.

Many of the calculated concentrations of radionuclides and ions are stored in two arrays in the computer program. These arrays appear many times in Table A.3. A summary of the information stored in them is provided in Table A.2. There may be some confusion regarding the units for radionuclide concentrations used in Tables A.2 and A.3 and those used in Chapter 3. Virtually all of the calculations within the water source model are performed on a mass basis ($mol.m^{-3}$). However, to meet system specifications, all radionuclide concentrations being passed between environmental compartments (i.e. leaving the water source model) must be expressed on an activity basis ($Bq.m^{-3}$). Thus in the derivations and descriptions in Chapter 3, mass or molar units are widely used. Indications are provided throughout Chapter 3 where calculated values must be converted from a molar to an activity basis. All calculated radionuclide concentrations which are used outside of the water source model are expressed on an activity basis. That is, following the source model calculations, all radionuclide concentrations in the arrays CONC or WCONC (see Table A.2) are in units of $Bq.m^{-3}$.

Table A.1

SOURCE MODEL CODE LISTING

```
      SUBROUTINE SEXEC
      INCLUDE 'MODEL.INC'
      INCLUDE 'VAR.INC'
C
C     THIS ROUTINE ACCESSES THE SOURCE MODEL ROUTINES IN
C     THE APPROPRIATE ORDER.
C
      IF (T.EQ.0.) THEN
         CALL INCONI
         CALL INCONN
         CALL EROS
         CALL RADON
         CALL DUST
      ELSE
         IF (XLIME.NE.0.0) THEN
            CALL IONS1L
         ELSE
            CALL IONS1
         ENDIF
         CALL IONS3
         CALL IONS4
         CALL URANUM
         CALL THORUM
         CALL RADIUM
         CALL LEAD
         CALL EROS
         CALL RADON
         CALL DUST
      ENDIF
C
      RETURN
      END
C
C
C
C
      SUBROUTINE NEWTON(IND,X1,X,FCNF)
      INCLUDE 'VAR.INC'
      REAL*4 X1,X
C
C     ROUTINE TO CALCULATE THE ROOT OF AN EQUATION; USING NEWTON'S
C     METHOD.SEE GERALD,C.F. (1980) 'APPLIED NUMERICAL ANALYSIS' P16.
C
      EPS = 0.01
      IMAX = 50
      NPHIT = 0
      DO 20 I=1,IMAX
         CALL FCNF(FCN,FPRIME,X1)
         DELTA = -1.*FCN/FPRIME
         NPHIT = NPHIT+1
         X1 = X1+DELTA
```

```
          IF (ABS(DELTA).LE.EPS) GO TO 30
          IF (I.EQ.IMAX) THEN
             WRITE(*,900) IND
             STOP
900          FORMAT(1X,'CONVERGENCE FAILED IN FUNCTION',I1)
          ENDIF
20     CONTINUE
30     CONTINUE
       X = X1
       RETURN
       END
```

```
      SUBROUTINE INCONI
      EXTERNAL PH1,PH2,PH3,PH4,PH1L,PH2GL
      INCLUDE 'MODEL.INC'
      INCLUDE 'VAR.INC'
      REAL*4 PHIN
C
C     THIS ROUTINE CALCULATES INITIAL INVENTORIES FOR SEVERAL IONIC
C     SPECIES AND pH. THESE CALCULATIONS ARE PERFORMED AT T=0 AND
C     REPRESENT THE INITIAL CONDITION OF THE TAILINGS.
C
C     FIRST SEVERAL VARIABLES ARE ASSIGNED INITIAL VALUES.
C
      INFILT= (NPRCP*(1.-XRUNOF))*WSTAIL/ATAIL
      TFLOW  = NPRCP*WSTAIL
      RFLOW = XRUNOF*TFLOW
C
      VSR = 0.
      DO 50  J = 1,5
         VSR = HCGWAT(J)*HGGWAT(J)*AXGWAT(J) + VSR
50    CONTINUE
C
      SFLOW = TFLOW - VSR - RFLOW
C
C     CHECKING TO SEE IF INFILTRATION IS LARGER THAN AVAILABLE
C     PRECIPITATION
C
      IF (SFLOW .LT. 0.) THEN
         VSR = TFLOW - RFLOW
         SFLOW = 0.
      ENDIF
C
      PYRITE(1) = PYRITI
      PYRITE(3) = PYRITE(1)
      DGYP(1) = 0.0
      DGYP(3) = DGYP(1)
      REPGYP = 0.0
      GYPMIX = 0.0
      GYPI = RHOTAL*FRACGP/136.0
      LIMEIN = DUNSAT*XLIME*RHOTAL/100.
      CALDEP = 0.0
      CHECKU = 'GYPSUM'
      CHECKM = 'GYPSUM'
      CHECKL = 'LIME'
C
C     SOIL PROPERTIES
      SG= 2.6E6
      POROS = 1.0-RHOTAL/SG
C
C     CONSTANTS
         T1 = 1.0-(KPRIME*ALOG((1.0+KPRIME)/KPRIME))
         KCONST = 1.067*RHOTAL*O2CONC*O2DIFF*T1
C
C     INITIAL CALCULATIONS FOR LAYERS 1 AND 2.
```

```
C     SOME PARAMETERS ARE CALCULATED DIFFERENTLY IF LIME HAS BEEN
C     INCORPORATED INTO THE UNSATURATED TAILINGS LAYER.
C
      IF (XLIME.GT.0.0) THEN
C
C     SULPHATE FLUX FROM PYRITE OXIDATION.
C
         SFLUX = XRATE*((1.067*SULPRD*RHOTAL*O2CONC*O2DIFF*T1)**0.5)
         KRATE = 0.5*SFLUX/(DUNSAT*PYRITE(1))
         EQUIL = (KSUBSO/FACTCO**2.)**0.5
C
C     INITIAL PH CALCULATIONS.
C
         IND = 6
         PHIN = 6.5
         CALL NEWTON(IND,PHIN,PH2LIM,PH2GL)
         PH(1) = PH2LIM
         PH(2) = PH2LIM
C
C     INITIAL SULPHATE AND CALCIUM CONCENTRATIONS.
C
         TEMP = KRATE*DT
         IF ( TEMP .GT. 30.) THEN
            WCONC(6,2,1) = (2.0*DUNSAT*PYRITI)/(INFILT*DT)
         ELSE
            WCONC(6,2,1) = (2.0*DUNSAT*PYRITI*(1.0-EXP(-1.*TEMP)))/
     &                    (INFILT*DT)
         ENDIF
         WCONC(6,2,3) = WCONC(6,2,1)
         T1 = EXP((-1.0*INFILT*DT)/(POROS*DMIX))
         WCONC(6,3,3) = WCONC(6,2,3)-WCONC(6,2,3)*T1
         WCONC(6,4,3) = 0.0
         WCONC(7,2,3) = 1000.*(10.**(2.*PH(2)-16.47))/FACTCO
         WCONC(8,2;3) = 1000.*(10.**(11.86-2.*PH(2)))/FACTCO
      ELSE
C
C     OTHERWISE, THE FOLLOWING CALCULATIONS APPLY.
C     STEADY STATE SULPHATE FLUX FROM PYRITE OXIDATION IS CALCULATED.
C
         SFLUX = (1.067*SULPRD*RHOTAL*O2CONC*O2DIFF*T1)**0.5
         KRATE = SFLUX/(2.0*DUNSAT*PYRITE(1))
         EQUIL = (KSUBSO/(FACTCO**2.0))**0.5
C
C     THE CONCENTRATION OF SULPHATE FROM PYRITE OXIDATION.
C
         TEMP = KRATE*DT
         IF (TEMP .GT. 30.) THEN
           WCONC(6,2,1) = (2.0*DUNSAT*PYRITI)/(INFILT*DT)
         ELSE
           WCONC(6,2,1) = (2.0*DUNSAT*PYRITI*(1.0-EXP(-1.*KRATE*DT)))/
     &                    (INFILT*DT)
         ENDIF
         WCONC(6,2,3) = WCONC(6,2,1)
         T1 = EXP((-1.0*INFILT*DT)/(POROS*DMIX))
         WCONC(6,3,3) = WCONC(6,2,3)-WCONC(6,2,3)*T1
         WCONC(6,4,3) = 0.0
C
C     LAYER 1 AND 2 PH CALCULATIONS. PH IS CALCULATED ITERATIVELY,
C     USING SUBROUTINES 'NEWTON' AND 'PH2'.
C
         IND = 2
         PHIN = 3.2
         CALL NEWTON (IND,PHIN,PH(2),PH2)
         PH(1) = PH(2)
C
C     CALCIUM AND SULPHATE CONCENTRATIONS IN THE UNSATURATED ZONE.
C
         WCONC(7,1,3) = 0.0
         WCONC(8,1,3) = 0.0
         T7 = (FACTCO**3.)*(10.**(8.99-3.*PH(2)))
         T8 = (FACTCO**(3./4.))*10.**(9.7-3.*PH(2))
         DELT = 1.0+T7+T8
         T9 = (KSUBSO*DELT/(FACTCO**2.)+(0.25*(WCONC(6,2,3)**2.)))**0.5
         WCONC(8,2,3) = T9-0.5*WCONC(6,2,3)
         WCONC(7,2,3) = T9+0.5*WCONC(6,2,3)
      ENDIF
C
C     CONCENTRATION OF FE3 IS DEPENDENT ON PH AND SULPHATE.
C
      T2 = 10.0**(5.97-3.0*PH(2))+10.0**(3.78-2.0*PH(2))
     &     +10.0**(0.3-PH(2))
      T3 = (FACTCO**3.0)*10.0**(8.99-3.0*PH(2))
      T4 = 1.0+(FACTCO**(3.0/4.0)*10.0**(9.7-3.0*PH(2)))
      WCONC(9,2,1) = T2+(WCONC(7,2,3)/1000.)*T3/(T4+T3)
      WCONC(9,2,1) = WCONC(9,2,1)*1000.
      WCONC(9,2,3) = WCONC(9,2,1)
C
C     LAYER 3 (MIXING ZONE) INITIAL CONDITIONS.
C     IONIC CONCENTRATIONS ARE CALCULATED FIRST.
C
      T1 = ((KSUBSO/FACTCO**2.)+0.25*WCONC(6,3,3)**2.)**0.5
      WCONC(7,3,3) = T1+0.5*WCONC(6,3,3)
      WCONC(8,3,3) = T1-0.5*WCONC(6,3,3)
      WCONC(10,3,3) = 1.5*WCONC(9,2,3)
C
C     PH IS CALCULATED ITERATIVELY USING SUBROUTINES 'NEWTON' AND 'PH3'
C
      IND = 3
      PHIN = 4.0
      CALL NEWTON(IND,PHIN,PH(3),PH3)
C
C     VOLUMETRIC FLOW FROM THE MIXING ZONE INTO LAYER 4 IS CALCULATED
C     AS A FUNCTION OF LONG-TERM MEAN ANNUAL PRECIPITATION.
C
      VSR4 = 0.
      DO 10  J=1,5
```

```
         IF ( GWLAYR(J) .EQ. 4 ) THEN
              VSR4 = HCGWAT(J)*HGGWAT(J)*AXGWAT(J) + VSR4
         ENDIF
10    CONTINUE
C
C     CHECKING TO ENSURE MINIMUM FLOW
      IF ( VSR4  .EQ. 0. ) THEN
          WVEL = 0.05*VSR/ATAIL
       ELSE
C        CHECKING TO ENSURE VSR4 IS NOT GREATER THAT TOTAL VSR
         IF ( VSR4 .GT. VSR ) THEN
             VSR4 =  VSR
             WVEL = VSR4/ATAIL
         ELSE
             WVEL = VSR4/ATAIL
         ENDIF
      ENDIF
C
C     LAYER 4 INITIAL CONDITIONS
C
      WCONC(7,4,3) = EQUIL
      WCONC(8,4,3) = EQUIL
      WCONC(10,4,1) = 0.0
      WCONC(10,4,3) = WCONC(10,4,1)
      IND = 4
      PHIN = 6.7
      CALL NEWTON(IND,PHIN,PH(4),PH4)
C
C     PRINT DETAILED RESULTS IF SPECIFIED.
C
      IF (CODION.EQ.1.) THEN
      WRITE(*,900)
      WRITE(*,910) GYPI,PYRITI,SFLUX,KRATE
      WRITE(*,920) EQUIL,PH(1),PH(2),PH(3),PH(4),LIMEIN
      WRITE(*,930) WCONC(7,2,3),WCONC(8,2,3),WCONC(9,2,3)
      WRITE(*,940) WCONC(7,3,3),WCONC(8,3,3),WCONC(10,3,3)
      WRITE(*,950) WCONC(7,4,3),WCONC(8,4,3),WCONC(10,4,3)
900   FORMAT(1X,'   INITIAL CONDITIONS')
910   FORMAT(1X,'[GYP]I=',E10.4,' PYRITE=',E10.4,' SFLUX=',E10.4,
     &       ' KRATE=',E10.4)
920   FORMAT(1X,'EQUIL=',E10.4,' PH1=',F5.2,' PH2=',F5.2,' PH3=',F5.2,
     &       ' PH4=',F5.2,' LIME=',E10.4)
930   FORMAT(1X,'[SO4]T2=',E10.4,' [CA2]T2=',E10.4,' [FE3]T2=',E10.4)
940   FORMAT(1X,'[SO4]T3=',E10.4,' [CA2]T3=',E10.4,' [FE3]T3=',E10.4)
950   FORMAT(1X,'[SO4]T4=',E10.4,' [CA2]T4=',E10.4,' [FE3]T4=',E10.4)
      ENDIF

      RETURN
      END
      SUBROUTINE INCONN
      INCLUDE 'MODEL.INC'
      INCLUDE 'VAR.INC'
C
C     THIS ROUTINE INITIALIZES VARIABLES USED IN THE CALCULATION
C     OF RADIONUCLIDE CONCENTRATIONS; AS WELL AS PERFORMING THE
C     NECESSARY CALCULATIONS IN THE FIRST TIME STEP.
C
C     URANIUM: INITIAL CONDITIONS AND CALCULATIONS.
C
      UCF = 5.95E6
      AUNATO = (PCURAN/100.)*(714./842.)*2.5E4
      AU2380 = (PCURAN/100.)*(714./842.)*1.22E4
      AUNATT = AUNATO*(1.0-FURAN)
      MUNATT = PCURAN*(238./842.)*(1.0-FURAN)
      CONC(1,1,1) = AUNATT*RHOTAL
      UPYRI = (CONC(1,1,1)*FRACU)/(3.0*UCF)
      IF(PYRITI.EQ.0.0)THEN
         XURANI = 0.0
      ELSE
         XURANI = UPYRI/PYRITI
      ENDIF
      CONC(1,1,3) = CONC(1,1,1)
      TEMP = KRATE*DT
      IF (TEMP .GT. 30.) THEN
        WCONC(1,2,3) = ((3.0*DUNSAT)/(INFILT*DT))*XURANI*PYRITI
      ELSE
        WCONC(1,2,3) = ((3.0*DUNSAT)/(INFILT*DT))*XURANI*PYRITI
     &               *(1.0-EXP(-1.0*KRATE*DT))
      ENDIF
      T1A = INFILT*DT/(POROS*DMIX*(1.0+(KDUO2*RHOTAL/POROS)))
      IF ( T1A .GT. 30.) THEN
          T1 = 0.
      ELSE
          T1 = EXP(-1.0*T1A)
      ENDIF
      WCONC(1,3,3) = WCONC(1,2,3)-WCONC(1,2,3)*T1
C
      T2A = WVEL*DT/(POROS*DBOT*(1.0+(KDUO2*RHOTAL/POROS)))
      IF ( T2A .GT. 30.) THEN
        T2 = 0.0
      ELSE
        T2 = EXP(-1.0*T2A)
      ENDIF
      WCONC(1,4,3) = WCONC(1,3,3)-WCONC(1,3,3)*T2
      WCONC(1,2,3) = WCONC(1,2,3)*UCF
      WCONC(1,3,3) = WCONC(1,3,3)*UCF
      WCONC(1,4,3) = WCONC(1,4,3)*UCF
C
C     PRINT SELECTED RESULTS IF SPECIFIED.
C
C      IF (CODNUC.EQ.1.0) THEN
C      ENDIF
```

```
C
C     THORIUM: INITIAL CONDITIONS AND CALCULATIONS.
C     SOLID PHASE CONDITIONS FIRST.
C
      T230CF = 1.65E11
      T232CF = 9.35E5
      LAM230 = 8.66E-6
      THDISS = 0.0
      THDISM = 0.0
      CHKTHU = 'ENRICHED'
      CHKTHS = 'ENRICHED'

      AT230I = AU2380
      CT230I = AT230I*RHOTAL*(1.0/T230CF)
      CT232I = (PCTHOR/100.)*RHOTAL*(1.0/264.)
      AT232I = CT232I*T232CF/RHOTAL
      ATHORI = AT232I+AT230I
      CTHORI = CT230I+CT232I
      CONC(2,1,1) = ATHORI*RHOTAL
      CONC(2,1,3) = CONC(2,1,1)
C
C     CALCULATION OF INITIAL SOLUBLE AND INSOLUBLE THORIUM FRACTIONS.
C
      T232IS = (1.0-FT232)*CT232I
      T230IS = (1.0-FT230)*CT230I
      T232SO = FT232*CT232I
      T230SO = FT230*CT230I
      THSOL = T232SO+T230SO
      TINSOL = T232IS+T230IS
      THSOLA = T230SO*T230CF+T232SO*T232CF
      TINSLA = T232IS*T232CF+T230IS*T230CF
      X232LM = T232SO/THSOL
      X230LM = T230SO/THSOL
      X230LA = (T230SO*T230CF)/THSOLA
      X232LA = (T232SO*T232CF)/THSOLA
      X232A = T232IS*T232CF/TINSLA
      X232SA = X232A
C
C     INITIAL THORIUM LIQUID PHASE CONCENTRATIONS.
C
      THORCF = X230LM*T230CF+(1.0-X230LM)*T232CF
C
C     THE SAME PROCEDURE IS USED TO CALCULATE CONCENTRATIONS
C     IN EACH LAYER.
C
      DELTA = 1.0+(FACTCO**3.*10.**(8.99-3.*PH(2)))+
     &            (FACTCO**0.75*10.**(9.7-3.*PH(2)))
      DO 100 I=2,4
         IF (I.EQ.2) THEN
            SO4 = WCONC(7,2,3)/(DELTA*1000.)
         ELSE
            SO4 = WCONC(7,I,3)/1000.
         ENDIF
         P = PH(I)
         F = FACTCO
         T1 = (10.**(2.5-4.*P))/F**4.
         T2 = F**(7./4.)*10.**(P-3.2)+F**3.*10.**(2.*P-6.93)
         T3 = F**(15./4.)*10.**(3.*P-11.7)+F**4.*10.**(4.*P-15.9)
         T4 = F**4.*10.**5.45*SO4+F**6.*10.**8.73*SO4**2.
         T5 = 10**(-1.*(5.0+0.32*P) )
         WCONC(2,I,3) = ( T1*(1.0+T2+T3+T4) +T5)*1000.
         IF (WCONC(2,I,3).GT.0.05) WCONC(2,I,3)=0.05
         WCONC(2,I,3) = WCONC(2,I,3)*THORCF
100   CONTINUE
C
C     PRINT SELECTED RESULTS IF SPECIFIED.
C
C      IF (CODNUC.EQ.1.0) THEN
C      ENDIF
C
C     RADIUM: INITIAL CONDITIONS AND CALCULATIONS.
C     SOLID PHASE CONDITIONS ARE DETERMINED FIRST.
C
      RACF = 8.26E12
      LAMRAD = 4.33E-4
      RADEC = EXP(-1.0*LAMRAD*DT)
      TDECAY = (LAM230/(LAMRAD-LAM230))*(EXP(-1.0*LAM230*DT)
     &         -RADEC)
      CRATHS = 0.0
      CHKBAS = 'ENRICHED'
      CHKBAU = 'ENRICHED'
      SUMBAR = 0.0
      DBAR(1) = 0.01
      DBAR(3) = DBAR(1)
      MBAR(1) = 0.0
      MBAR(3) = MBAR(1)
      XBAR(1) = XRADI
      XBAR(3) = XBAR(1)

      ARADI = AT230I
      CRADI = ARADI*RHOTAL*(1.0/RACF)
      CRADBA = FRAD*CRADI
      CRADTI = (1.0-FRAD)*CRADI
      CBARI = CRADBA/XRADI
      BASATI = XRADI*(DUNSAT*CBARI+DMIX*CBARI)

      CONC(4,1,3) = CRADTI*RACF
      CONC(4,2,3) = CRADI*RACF
      CONC(4,3,3) = CONC(4,2,3)
      CONC(4,4,3) = CONC(4,3,3)
C
C     RADIUM LIQUID PHASE CONCENTRATIONS ARE THEN DETERMINED.
C
      DELTA = 1.0+(FACTCO**3.*10.**(8.99-3.*PH(2)))+
     &            (FACTCO**0.75*10.**(9.7-3.*PH(2)))
      SO4 = WCONC(7,2,3)/DELTA
      EQBAR = (KSBAR/FACTCO**2.)**0.5
      CBAR = ((EQBAR**2.)/(EQBAR+SO4))*(1.0+FACTCO**2.*KFBAR*SO4)
      WCONC(4,2,3) = XRADI*CBAR*KRAD*RACF
      SO4 = WCONC(7,3,3)
      CBAR = ((EQBAR**2.)/(EQBAR+SO4))*(1.0+FACTCO**2.*KFBAR*SO4)
      WCONC(4,3,3) = XRADI*CBAR*KRAD*RACF
      SO4 = WCONC(7,4,3)
      CBAR = ((EQBAR**2.)/(EQBAR+SO4))*(1.0+FACTCO**2.*KFBAR*SO4)
      WCONC(4,4,3) = XRADI*CBAR*KRAD*RACF
C
C     PRINT SELECTED RESULTS IF SPECIFIED.
C
C      IF (CODNUC.EQ.1.0) THEN
C      ENDIF
C
C     LEAD: INITIAL CONDITIONS AND CALCULATIONS.
C     SOLID PHASE CONDITIONS ARE DETERMINED FIRST.
C
      PBCF = 6.3E14
      LAMPB = 3.3E-2
      PBDEC = EXP(-1.0*LAMPB*DT)
      RDECAY = (LAMRAD/(LAMPB-LAMRAD))*(EXP(-1.0*LAMRAD*DT)
     &         -PBDEC)
      CPBRAS = 0.0
      CHKPBU = 'ENRICHED'
      CHKPBS = 'ENRICHED'
      SUMPB = 0.0
      DLEAD(1) = 0.01
      DLEAD(3) = DLEAD(1)

      APBI = ARADI
      CPBI = APBI*RHOTAL*(1.0/PBCF)
      CPBPB = FLEAD*CPBI
      CPBTI = (1.0-FLEAD)*CPBI
      XPBI = CPBPB/CLEADI
      PBSATI = XPBI*(DUNSAT*CLEADI+DMIX*CLEADI)
      CONC(3,1,3) = CPBTI*PBCF
      CONC(3,2,3) = CPBI*PBCF
      CONC(3,3,3) = CONC(3,2,3)
      CONC(3,4,3) = CONC(3,3,3)
C
C     LEAD CONCENTRATIONS IN THE LIQUID PHASE ARE THEN DETERMINED.
C
      SO4 = WCONC(7,2,3)/DELTA
      EQLEAD = (KSLEAD/FACTCO**2)**0.5
      CLEAD = ((EQLEAD**2.)/(EQLEAD+SO4))*(1.0+FACTCO**2.*KFLEAD*SO4)
      WCONC(3,2,3) = XPBI*CLEAD*PBCF
      SO4 = WCONC(7,3,3)
      CLEAD = ((EQLEAD**2.)/(EQLEAD+SO4))*(1.0+FACTCO**2.*KFLEAD*SO4)
      WCONC(3,3,3) = XPBI*CLEAD*PBCF
      SO4 = WCONC(7,4,3)
      CLEAD = ((EQLEAD**2.)/(EQLEAD+SO4))*(1.0+FACTCO**2.*KFLEAD*SO4)
      WCONC(3,4,3) = XPBI*CLEAD*PBCF
```

```
C
C     PRINT SELECTED RESULTS IF SPECIFIED.
C
C      IF (CODNUC.EQ.1.0) THEN
C      ENDIF
C
C     PRINT SUMMARY RESULTS IF SPECIFIED.
C
      IF (CODNUC.EQ.1.0) THEN
         WRITE(*,900) T
         WRITE(*,910) CONC(1,1,3),WCONC(1,2,3),WCONC(1,3,3),
     &                WCONC(1,4,3)
         WRITE(*,920) CONC(2,1,3),WCONC(2,2,3),WCONC(2,3,3),
     &                WCONC(2,4,3),X232SA
         WRITE(*,930) CONC(4,1,3),WCONC(4,2,3),WCONC(4,3,3),
     &                WCONC(4,4,3),CONC(4,2,3)
         WRITE(*,940) CONC(3,1,3),WCONC(3,2,3),WCONC(3,3,3),
     &                WCONC(3,4,3)
         WRITE(*,950) THSOL,TINSOL,BASATI,PBSATI
      ENDIF
900   FORMAT(1X,'T=',F5.0,4X,'SOLID1',5X,'LIQUID2',5X,'LIQUID3',5X,
     &       'LIQUID4',7X,'OTHER')
910   FORMAT(1X,'URANIUM',2X,E10.4,3(2X,E10.4))
920   FORMAT(1X,'THORIUM',2X,E10.4,4(2X,E10.4))
930   FORMAT(1X,'RADIUM',3X,E10.4,4(2X,E10.4))
940   FORMAT(1X,'LEAD',5X,E10.4,3(2X,E10.4))
950   FORMAT(1X,'[TH]SOL=',E10.4,' [TH]INSOL=',E10.4,' [RA]BA1=',E10.4
     &         ,' [PB]PB1=',E10.4)

      RETURN
      END
      SUBROUTINE IONS1
      EXTERNAL PH2,PH1,PH1B
      INCLUDE 'MODEL.INC'
      INCLUDE 'VAR.INC'
      REAL*4 K
C
C     THIS ROUTINE PERFORMS CALCULATIONS RELEVANT TO GYPSUM DISSOLUTION
C     IONIC CONCENTRATIONS AND PH IN LAYERS 1 AND 2.
C
C     FIRST SEVERAL CURRENT AND PREVIOUS VARIABLE VALUES ARE RESET.
C
      PYRITE(2) = PYRITE(3)
      DGYP(2) = DGYP(3)
      WCONC(9,2,2) = WCONC(9,2,3)
      WCONC(6,2,2) = WCONC(6,2,3)
C
C     CALCULATE SO4 PRODUCTION VIA PYRITE OXIDATION.
C
      PYRITE(3) = PYRITE(2)*EXP(-1.0*KRATE*DT)
      IF (PYRITE(3).LE.1.E-6) PYRITE(3) = 1.0E-6
      BETA = PYRITE(2)*(1.0-EXP(-1.0*KRATE*DT))
      WCONC(6,2,3) = (2.0*DUNSAT*BETA)/(INFILT*DT)+0.0128
C
C     CHECK FOR GYPSUM DEPLETION.
C
      IF (CHECKU.NE.'DEPLETED') THEN
C
C     CALCULATE CHANGE IN DEPTH OF DEPLETED ZONE OVER DT.
C
C
         T1  = ( (BETA**2.0)*(DGYP(2)**2.0))/((GYPI+BETA)**2.0)
         T2 = (((INFILT*DT)**2.)*(EQUIL**2.))/((GYPI**2.)+GYPI*BETA)
C
         T3  = ( BETA*DGYP(2))/(GYPI+BETA)
         DELTAH = ((T1+T2)**0.5)-T3
         DGYP(3) = DGYP(2)+DELTAH
C     CHECK NEW DEPTH OF DEPLETED ZONE.
C
         IF (DGYP(3).GE.DUNSAT) THEN
C
C     RESET INDICATOR VARIABLES.
C
            DGYP(3) = DUNSAT
            FGYP = 0.0
            TFINAL = T
            CHECKU = 'DEPLETED'
            WCONC(8,2,3) = 0.008
         ENDIF
      ENDIF
C
C     CHECK ONCE AGAIN FOR GYPSUM DEPLETION.
C
      IF (CHECKU.NE.'DEPLETED') THEN
```

```
C
C     CALCULATE GYPSUM REPRECIPITATION, IONIC CONCENTRATIONS AND PH.
C
        T4 = ((EQUIL**2.*(INFILT*DT)**2.)+(DUNSAT**2.*BETA**2.))**0.5
        DELTAR = (GYPI*DELTAH)-T4+(DUNSAT*BETA)
        REPGYP = REPGYP+DELTAR
        FGYP = ((DUNSAT-DGYP(3))*GYPI+REPGYP)/(DUNSAT*GYPI)
        WCONC(6,1,3) = WCONC(6,2,3)*(DGYP(3)/DUNSAT)
        WCONC(7,1,3) = WCONC(6,1,3)
        WCONC(8,1,3) = 0.008
        WCONC(9,1,3) = 0.5*WCONC(6,1,3)
C
C     GENERATE INITIAL GUESS FOR ITERATIVE PH CALCULATION.
C
         IF (WCONC(6,2,3).EQ.0.0) WCONC(6,2,3) = 1.0E-20
         T5 = (ALOG10(WCONC(6,2,3)/1000.)+3.4)**4.
         K = 0.725+(6.56281E-2*T5)
         T6 = (K*(ALOG10(WCONC(6,2,3)/1000.)+4.230414))
         PHIN = 4.383551-((2.723818/(22./7.))*ATAN(T6))
         IND1 = 1
         IND2 = 2
         PHIN1 = PHIN
         PHIN2 = PHIN
C
C
C     FOR LAYER ONE IT IS ASSUMED THAT AL(OH)3 DEPLETION OCCURS
C     SIMULTANEOUSLY WITH THE GYPSUM DEPLETION WHEN THERE IS NO
C     LIME PRESENT  AND O2DIFF    > 1.0
C
         IF (O2DIFF .GT. 1.0 .AND. PYRITE(3) .GT. 0.1 ) THEN
              CALL PH1B( PH(1) )
C             THE 50 INDICATES NON CONVERGENCE USING PH1B
C             AND HENCE NON ACIDIC CONDITIONS
              IF ( PH(1) .EQ. 50.) THEN
                 CALL NEWTON(IND1,PHIN1,PH(1),PH1)
              ENDIF
         ELSE
              CALL NEWTON(IND1,PHIN1,PH(1),PH1)
         ENDIF
C
C     PH IS CALCULATED ITERATIVELY USING SUBROUTINES 'NEWTON',
C     'PH2' (LAYER 2).
         CALL NEWTON(IND2,PHIN2,PH(2),PH2)
C
C
C
C     CA AND SO4 CONCENTRATIONS IN LAYER 2 ARE FUNCTIONS OF PH.
C
         T7 = (FACTCO**3.)*(10.**(8.99-3.*PH(2)))
         T8 = (FACTCO**(3./4.))*10.**(9.7-3.*PH(2))
         DELT = 1.0+T7+T8
         T9 = (KSUBSO*DELT/(FACTCO**2.)+(0.25*(WCONC(6,2,3)**2.)))**0.5
         WCONC(8,2,3) = T9-0.5*WCONC(6,2,3)
```

```
           WCONC(7,2,3) = T9+0.5*WCONC(6,2,3)

          ELSE
C
C      CALCULATE IONIC CONCENTRATIONS AND PH AFTER UNSATURATED ZONE
C      IS DEPLETED OF GYPSUM.
C      FIRST, GENERATE INITIAL GUESS FOR PH CALCULATION.
C
           WCONC(7,2,3) = WCONC(6,2,3)
           WCONC(6,1,3) = WCONC(6,2,3)
           WCONC(7,1,3) = WCONC(7,2,3)
           WCONC(8,1,3) = 0.008
           WCONC(9,1,3) = 0.5*WCONC(6,1,3)
           IF (WCONC(6,2,3).EQ.0.0) WCONC(6,2,3) = 1.0E-20
            T5 = (ALOG10(WCONC(6,2,3)/1000.)+3.4)**4.
            K = 0.725+(6.56281E-2*T5)
            T6 = (K*(ALOG10(WCONC(6,2,3)/1000.)+4.230414))
            PHIN1 = 4.383551-((2.723818/(22./7.))*ATAN(T6))
            IND1 = 1
C
C
C      FOR LAYER 1 IT IS ASSUMED THAT AL(OH)3 WITH BE DEPLETED
C      SIMULTANEOUSLY WITH GYPSUM WHEN THERE IS NO LIME PRESENT
C      AND O2DIFF > 1.0
C
            IF ( O2DIFF .GT. 1.0 .AND. PYRITE(3)  .GT. 0.1) THEN
              CALL PH1B( PH(1) )
C             THE 50 INDICATES THAT NON CONVERGENCE HAS OCCURRED
C             HENCE, NON ACIDIC CONDITIONS EXIST
              IF ( PH(1) .EQ. 50) THEN
                 CALL NEWTON(IND1,PHIN1,PH(1),PH1)
              ENDIF
            ELSE
              CALL NEWTON(IND1,PHIN1,PH(1),PH1)
            ENDIF
C
            PH(2) = PH(1)
C
       ENDIF
C
C      FE3 CONCENTRATION AS A FUNCTION OF SULPHATE FROM PYRITE
C      OXIDATION
C
       WCONC(9,2,3) = 0.5*WCONC(6,2,3)
C
C
C
C      PRINT DETAILED RESULTS IF SPECIFIED
C
       IF (CODION.EQ.1.) THEN
       WRITE(*,900) T,DGYP(3),REPGYP,PH(1),PH(2),PYRITE(3)
       WRITE(*,910) WCONC(6,1,3),WCONC(6,2,3),WCONC(9,2,3)
       WRITE(*,920) WCONC(7,1,3),WCONC(7,2,3),WCONC(8,2,3)
```

```
900   FORMAT(1X,'LAYERS 1&2 T=',F6.1,' DEPTH=',F6.3,' REPGYP= ',E10.4,
     &        ' PH1=',F5.2,' PH2=',F5.2,' PYRITE =',F6.3)
910   FORMAT(1X,'[SO4]P1=',E10.4,' [SO4]P2=',E10.4,' [FE3]T2=',E10.4)
920   FORMAT(1X,'[SO4]T1=',E10.4,' [SO4]T2=',E10.4,' [CA2]T2=',E10.4)
      ENDIF

      RETURN
      END
C
C
C
      SUBROUTINE PH1(F,FPRIME,P)
      INCLUDE 'MODEL.INC'
      INCLUDE 'VAR.INC'
C
C     THIS ROUTINE IS INVOLVED IN THE ITERATIVE CALCULATION OF PH IN
C     THE UNSATURATED ZONE; FOR THE  GYPSUM DEPLETED CASE.
C
C
C     FIRST THE FUNCTION (F) IS EVALUATED.
C
        F1 = FACTCO
        CS = WCONC(6,1,3)/1000.
        T1 = (F1**(3./4.)*10.**(9.7-3.*P))+(F1**3.*10.**(8.97-3*P))
        SO4 = CS*(2.-T1)/(1.+T1)
        T2 = 10.**(-3.*P)*(((10.**6.5)/F1**(9./4.))+10**5.97)
        T3 = 10.**(-2.*P)*(((10.**1.53)/F1)+10.**3.78)
        T4 = 10.**(0.3-P)
        T5 = (10.**(-1.*P))/F1**(1./4.)
        T6 = (10.**(P-11.27))/F1**(1./4.)
        F = 3.*T2+2.*T3+T4+T5-SO4-T6
C
C     THEN THE DERIVATIVE OF THE FUNCTION (FPRIME) IS EVALUATED.
C
        XL = ALOG(10)
        DT1 = (-3.*XL*F1**(3./4.)*10.**(9.7-3.*P))-3.*XL*F1**3.
     &     *10.**(8.97-3.*P)
        T7 = -1.0*DT1*((2.-T1)/((1.+T1)**2.)+1./(1.+T1))
        FPRIME = -9.*XL*T2-4.*XL*T3-XL*T4-XL*T5-CS*T7-XL*T6
C
C     PRINT DETAILED RESULTS IF SPECIFIED.
C
      IF (CODPH.EQ.1) THEN
      WRITE(*,900) T,P,F,FPRIME
900   FORMAT(1X,'PH1: T=',F6.1,' PH=',F5.2,' F=',E10.4,' FPRIME=',E10.4)
      ENDIF
C
      RETURN
      END
C
C
C
      SUBROUTINE PH1B(P)
```

```
C
      INCLUDE 'MODEL.INC'
      INCLUDE 'VAR.INC'
C
C     PH1-B SUBROUTINE FOR ACIDIC CONDITIONS
        F1 = FACTCO
        CA2 = WCONC(8,1,3)
        SO4TOT = WCONC(7,1,3)
        ZETA = -0.5*(SO4TOT) + 1.19E-3/(F1**(9./4.)) + 0.5*CA2
        ZETA2 = 0.5*(SO4TOT) + 1.19E-3/(F1**(9./4.)) + 0.5*CA2
        AA = 10.**1.92/(F1**(3./4.))
        BB =  1.+10**1.92*ZETA2/(F1**(3./4.))
        CC = ZETA
C       THE XX1 AND XX2 REPRESENT THE TWO ROOTS FOR THE "H+" CONC.
        XX1 = ( -BB + (BB**2-4.*AA*CC)**0.5 )/(2.*AA)
        XX2 = ( -BB - (BB**2-4.*AA*CC)**0.5 )/(2.*AA)
C
C
        IF ( XX1 .GT. 0.) THEN
           P = -ALOG10(XX1)
        ELSE
C          GO BACK TO ORIGINAL PH EQUATIONS
C          THE 50 INDICATES NON CONVERGENCE AND
C          HENCE NON ACID CONDITIONS
               P = 50.
        ENDIF
C
      IF (CODPH.EQ.1) THEN
        WRITE(*,75) WCONC(7,1,3),WCONC(8,1,3),FACTCO,XX1,XX2,BB,AA,CC,P
75      FORMAT(' ',"PH1B- SO4T,CA,F1,XX1,XX2,BB,AA,CC,P =",9(E10.3,1X))
      ENDIF
C
      RETURN
      END
C
C
C
      SUBROUTINE PH2(F,FPRIME,P)
      INCLUDE 'MODEL.INC'
      INCLUDE 'VAR.INC'
C
C     THIS ROUTINE IS INVOLVED IN THE ITERATIVE CALCULATION OF PH IN
C     THE UNSATURATED ZONE; FOR THE  GYPSUM ENRICHED CASE.
C
C     FIRST THE FUNCTION (F) IS EVALUATED.
C
        F1 = FACTCO
        CS = WCONC(6,2,3)/1000.
        T1 = (F1**(3./4.)*10.**(9.7-3.*P))+(F1**3.*10.**(8.97-3*P))
        CA2 = (((10**(-4.6)*(1.+T1))/F1**2.)+.25*CS**2.)**0.5-0.5*CS
        SO4 = (CA2+CS)*(2.-T1)/(1.+T1)
        T2 = 3.*10.**(-3.*P)*(((10.**6.5)/F1**(9./4.))+10**5.97)
        T3 = 2.*10.**(-2.*P)*(((10.**1.53)/F1)+10.**3.78)
```

Table A.1 continued.

```
        T4 = 10.**(0.3-P)
        T5 = (10.**(-1.*P))/F1**(1./4.)
        T6 = (10.**(P-11.27))/F1**(1./4.)
        F = 2.*CA2+T2+T3+T4+T5-SO4-T6
C
C     THEN THE DERIVATIVE OF THE FUNCTION (FPRIME) IS EVALUATED.
C
        XL = ALOG(10)
        T7 = (-3.*XL*F1**(3./4.)*10.**(9.7-3.*P))-3.*XL*F1**3.
     &     *10.**(8.97-3.*P)
        T8 = 0.5*T7*((10.**(-4.6))/F1**2.)*(((10.**(-4.6)*T1)/F1**2.)+
     &     .25*CS**2.)**(-0.5)
        T9 = -1.0*T7*((2.-T1)/((1.+T1)**2.)+1./(1.+T1))
        T10 = CS*T9+CA2*T9+((2.-T1)/(1.+T1))*T8
        FPRIME = 2.*T8-3.*XL*T2-2.*XL*T3-XL*T4-XL*T5-XL*T6-T10
C
C     PRINT DETAILED RESULTS IF SELECTED
C
      IF (CODPH.EQ.1) THEN
      WRITE(*,900) T,P,F,FPRIME
900   FORMAT(1X,'PH2: T=',F6.1,' PH=',F5.2,' F=',E10.4,' FPRIME=',E10.4)
      ENDIF
C
      RETURN
      END
      SUBROUTINE IONS1L
      EXTERNAL PH1,PH1B,PH2,PH1L
      INCLUDE 'MODEL.INC'
      INCLUDE 'VAR.INC'
C
C     THIS ROUTINE PERFORMS CALCULATIONS RELEVANT TO GYPSUM DISSOLUTION
C     IONIC CONCENTRATIONS AND PH IN LAYERS 1 AND 2; FOR THE CASE WHERE
C     LIME HAS BEEN INCORPORATED INTO THE UNSATURATED TAILINGS LAYER.
C
C     FIRST SEVERAL CURRENT AND PREVIOUS VARIABLE VALUES ARE RESET.
C
      PYRITE(2) = PYRITE(3)
      DGYP(2) = DGYP(3)
      WCONC(9,2,2) = WCONC(9,2,3)
      WCONC(6,2,2) = WCONC(6,2,3)
C
C
      IF ( CHECKL .EQ. 'DEPLETED') THEN
C         LIME IS DEPLETED
          T1 = 1.0-(KPRIME*ALOG((1.0+KPRIME)/KPRIME))
          SFLUX = (1.067*SULPRD*RHOTAL*O2CONC*O2DIFF*T1)**0.5
          KRATE = SFLUX/(2.0*DUNSAT*PYRITE(1))
      ENDIF
C
C     CALCULATE SO4 PRODUCTION VIA PYRITE OXIDATION.
C
      IF(KRATE.LE.30.0/DT)THEN
         PYRITE(3) = PYRITE(2)*EXP(-1.0*KRATE*DT)
      ELSE
         PYRITE(3)=1.0E-6
      ENDIF
      IF (PYRITE(3).LE.1.E-6) PYRITE(3)=1.0E-6
      IF(KRATE.LE.30.0/DT)THEN
        BETA = PYRITE(2)*(1.0-EXP(-1.0*KRATE*DT))
      ELSE
        BETA = PYRITE(2)
      ENDIF
      WCONC(6,2,3) = (2.0*DUNSAT*BETA)/(INFILT*DT)+0.0128
C
C     THE PH AT THE BOTTOM OF THE UNSATURATED LAYER IS CALCULATED,
C     USING DIFFERENT EQUATIONS FOR THE DIFFERENT CASES WHICH EXIST.
C
      PHIN = PH(2)
      IF (CHECKU.EQ.'DEPLETED') THEN
         IF (CHECKL.EQ.'DEPLETED') THEN
C           GYPSUM DEPLETED; LIME DEPLETED
            WCONC(6,1,3) = WCONC(6,2,3)
            WCONC(9,1,3) = 0.5*WCONC(6,1,3)
            PHIN1= 3.5
            IND = 1
C
C           USING NEW PH ALGORITHM (PH1B) IF O2DIFF > 1.0
C           AND IF THE PYRITE IS PRESENT
```

```
            IF (O2DIFF .GT. 1.0 .AND. PYRITE(3) .GT. 0.1 ) THEN
               CALL PH1B( PH(1) )
C              THE 50 INDICATES NON CONVERGENCE USING PH1B
C              AND HENCE NON ACIDIC CONDITIONS
               IF ( PH(1) .EQ. 50.) THEN
                  CALL NEWTON(IND1,PHIN1,PH(1),PH1)
               ENDIF
            ELSE
               CALL NEWTON(IND1,PHIN1,PH(1),PH1)
            ENDIF
C
C
         ELSE
C           GYPSUM DEPLETED; LIME PRESENT
            WCONC(6,1,3) = WCONC(6,2,3)
            WCONC(9,1,3) = 0.5*WCONC(6,1,3)
            IND = 5
C
C           ELEVATED PH LEVELS SINCE LIME PRESENT
            CALL NEWTON(IND,PHIN,PH(2),PH1L)
         ENDIF
C
      ELSE
C
         IF (CHECKL.EQ.'DEPLETED') THEN
C           GYPSUM PRESENT; LIME DEPLETED
            IND = 2
            PHIN = 3.5
            CALL NEWTON(IND,PHIN,PH(2),PH2)
C
         ELSE
C           GYPSUM PRESENT; LIME PRESENT
            PH(2) = PH2LIM
         ENDIF
      ENDIF
C
C     CHECK FOR GYPSUM DEPLETION.
C
      IF (CHECKU.NE.'DEPLETED') THEN
C
C     CALCULATE CHANGE IN DEPTH OF DEPLETED ZONE OVER DT.
C
         IF (CHECKL.EQ.'DEPLETED') THEN
            T1 = (4.0*(BETA**2.0)*(DGYP(2)**2.0))/((GYPI+BETA)**2.0)
            T2 = (((INFILT*DT)**2.)*(EQUIL**2.))/((GYPI**2.)+GYPI*BETA)
            T3 = (2.0*BETA*DGYP(2))/(GYPI+BETA)
            DELTAH = ((T1+T2)**0.5)-T3
         ELSE
            T1 = (10.**(2.*PH(2)-16.47))/FACTCO-10.**(-4.0)
            DELTAH = (T1*1000.*INFILT*DT-2.*DGYP(2)*BETA)/GYPI
         ENDIF
         DGYP(3) = DGYP(2)+DELTAH
C
```

```
C      CHECK NEW DEPTH OF DEPLETED ZONE.
C
          IF (DGYP(3).GE.DUNSAT) THEN
C
C      RESET INDICATOR VARIABLES.
C
             DGYP(3) = DUNSAT
             FGYP = 0.0
             TFINAL = T
             CHECKU = 'DEPLETED'
          ENDIF
       ENDIF
C
C      CHECK ONCE AGAIN FOR GYPSUM DEPLETION.
C
       IF (CHECKU.NE.'DEPLETED') THEN
C
          WCONC(6,1,3) = WCONC(6,2,3)*(DGYP(3)/DUNSAT)
          WCONC(7,1,3) = WCONC(6,1,3)
          WCONC(8,1,3) = 0.008
          WCONC(9,1,3) = 0.5*WCONC(6,1,3)
C
C         CALCULATE CALCIUM AND SULPHATE CONCENTRATIONS,AND PH IN LAYER
C         1. FIRST FOR THE CASE WHERE LIME IS PRESENT AND DISSOLVING.
C
          IF (CHECKL.NE.'DEPLETED') THEN
             WCONC(7,2,3) = 1000.*(10.**(2.*PH(2)-16.47))/FACTCO
             WCONC(8,2,3) = 1000.*(10.**(11.86-2.*PH(2)))/FACTCO
             PHIN = PH(1)
             IND = 5
C
C         CALC. PH FOR LAYER 1 WITH LIME PRESENT
             CALL NEWTON(IND,PHIN,PH(1),PH1L)
C
C            CALCULATE LIME DEPLETION OVER DT.
C
             CALIME = WCONC(8,2,3)-WCONC(7,2,3)+(2.*DUNSAT*BETA)/
     &               (INFILT*DT)+0.08
             CALDEP = CALDEP+CALIME*INFILT*DT
             IF (CALDEP.GE.LIMEIN) THEN
                CHECKL = 'DEPLETED'
             ENDIF
          ELSE
C            LIME DEPLETED CASE.
             T7 = (FACTCO**3.)*(10.**(8.99-3.*PH(2)))
             T8 = (FACTCO**(3./4.))*10.**(9.7-3.*PH(2))
             DELT = 1.0+T7+T8
             T9 = KSUBSO*DELT/(FACTCO**2.)+(0.25*(WCONC(6,2,3)**2.))
             T10 = SQRT(T9)
             WCONC(8,2,3) = T10-0.5*WCONC(6,2,3)
             WCONC(7,2,3) = T10+0.5*WCONC(6,2,3)
             PHIN1= 3.5
             IND = 1
```

```
C
C        FOR LAYER 1 HAVE ASSUMED THAT AL(OH)3 DEPLETIONS OCCURS
C        SIMULTANEOUSLY WITH GYPSUM DEPLETION WHEN THERE IS NO LIME
C        AND O2DIFF > 1.0 AND PYRITE IS PRESENT
C
            IF (O2DIFF .GT. 1.0 .AND. PYRITE(3) .GT. 0.1 ) THEN
               CALL PH1B( PH(1) )
C              THE 50 INDICATES NON CONVERGENCE USING PH1B
C              AND HENCE NON ACIDIC CONDITIONS
               IF ( PH(1) .EQ. 50.) THEN
                  CALL NEWTON(IND1,PHIN1,PH(1),PH1)
               ENDIF
            ELSE
               CALL NEWTON(IND1,PHIN1,PH(1),PH1)
            ENDIF
C
          ENDIF
        ELSE
C
C       CALCULATE IONIC CONCENTRATIONS AND PH AFTER UNSATURATED ZONE
C       IS DEPLETED OF GYPSUM.
C
          WCONC(7,2,3) = WCONC(6,2,3)
          WCONC(6,1,3) = WCONC(6,2,3)
          WCONC(9,1,3) = 0.5*WCONC(6,1,3)
          WCONC(7,1,3) = WCONC(7,2,3)
          WCONC(8,1,3) = 0.008
          PH(1) = PH(2)
C
C       CALCIUM CONCENTRATION IS CALCULATED DIFFERENTLY DEPENDING ON THE
C       PRESENCE OR ABSENCE OF LIME.
C       LIME DEPLETED CASE FIRST.
C
          IF (CHECKL.EQ.'DEPLETED') THEN
             WCONC(8,2,3) = 0.008
          ELSE
C            LIME PRESENT CASE.
C
              T1 =  (10.**(11.86-2.*PH(2)))/FACTCO
              CALIME = T1*1000. - 0.02
C
C
             WCONC(8,2,3) = CALIME
             CALDEP = CALDEP+CALIME*INFILT*DT
             IF (CALDEP.GE.LIMEIN) THEN
                CHECKL = 'DEPLETED'
             ENDIF
          ENDIF
        ENDIF
C
C
C       FE3 CONCENTRATION AS A FUNCTION OF SULPHATE FROM PYRITE
C       OXIDATION
```

```
C
      WCONC(9,2,3) = 0.5*WCONC(6,2,3)
C
C
C
C     PRINT DETAILED RESULTS IF SPECIFIED
C
      IF (CODION.EQ.1.) THEN
      WRITE(*,900) T,DGYP(3),PH(1),PH(2),PYRITE(3)
      WRITE(*,910) WCONC(6,1,3),WCONC(6,2,3),WCONC(9,2,3),CALDEP
      WRITE(*,920) WCONC(7,1,3),WCONC(7,2,3),WCONC(8,2,3)
900   FORMAT(1X,'LAYERS 1&2 T=',F6.1,' DEPTH=',F6.3,
     &       ' PH1=',F5.2,' PH2=',F5.2,' PYRITE =',F6.3)
910   FORMAT(1X,'[S04]P1=',E10.4,' [S04]P2=',E10.4,' [FE3]T2=',E10.4,
     &       ' CALDEP=',E10.4)
920   FORMAT(1X,'[S04]T1=',E10.4,' [S04]T2=',E10.4,' [CA2]T2=',E10.4)
      ENDIF

      RETURN
      END
C
C
C
C
      SUBROUTINE PH1L(F,FPRIME,P)
      INCLUDE 'MODEL.INC'
      INCLUDE 'VAR.INC'
C
C     THIS ROUTINE IS INVOLVED IN THE ITERATIVE CALCULATION OF PH IN
C     THE UNSATURATED ZONE; FOR THE GYPSUM DEPLETED,LIME PRESENT CASE.
C
C     FIRST THE FUNCTION (F) IS EVALUATED.
C
      F1 = FACTCO
      S04 = WCONC(6,1,3)/1000.
      T1 = 2.*(10.**(11.87-2.*P))/F1+10.**(0.3-P)
      T2 = (10.**(P-9.73))/(F1**0.25)
      F = T1-2.*S04-T2
C
C     THEN THE DERIVATIVE OF THE FUNCTION (FPRIME) IS EVALUATED.
C
      XL = ALOG(10)
      DT1 = -4.*XL*(10.**(11.87-2.*P))/F1-XL*10.**(0.3-P)
      FPRIME = DT1-XL*T2
C
C     PRINT DETAILED RESULTS IF SPECIFIED.
C
      IF (CODPH.EQ.1) THEN
      WRITE(*,900) T,P,F,FPRIME
900   FORMAT(1X,'PH1L: T=',F6.1,' PH=',F5.2,'F=',E10.4,'FPRIME=',E10.4)
      ENDIF

      RETURN
      END
C
C
C
C
      SUBROUTINE PH2GL(F,FPRIME,P)
      INCLUDE 'MODEL.INC'
      INCLUDE 'VAR.INC'
C
C     THIS ROUTINE IS INVOLVED IN THE ITERATIVE CALCULATION OF PH IN
C     THE UNSATURATED ZONE; FOR THE GYPSUM AND LIME PRESENT CASE.
C
C     FIRST THE FUNCTION (F) IS EVALUATED.
C
      F1 = FACTCO
      T1 = (2.*10.**(11.87-2.*P))/F1+10.**(0.3-P)
      T2 = (2.*10.**(2.*P-16.47))/F1+(10.**(P-9.73))/F1**0.25
      F = T1-T2
C
C     DO NOT HAVE TO INCLUDE FEMAX TERM SINCE PH ALWAYS > 3.1
C
C
C     THEN THE DERIVATIVE OF THE FUNCTION (FPRIME) IS EVALUATED.
C
      XL = ALOG(10)
      DT1 = -4.*XL*(10.**(11.87-2.*P))/F1-XL*10.**(0.3-P)
      DT2 = 4.0*XL*(10.**(2.*P-16.47))/F1+XL*(10.**(P-9.73))/F1**0.25
      FPRIME = DT1-DT2
C
C     PRINT DETAILED RESULTS IF SELECTED
C
      IF (CODPH.EQ.1) THEN
      WRITE(*,900) T,P,F,FPRIME
900   FORMAT(1X,'PH2GL:T=',F6.1,'PH=',F5.2,'F=',E10.4,'FPRIME=',E10.4)
      ENDIF

      RETURN
      END
      SUBROUTINE IONS3
      EXTERNAL PH3
      INCLUDE 'MODEL.INC'
      INCLUDE 'VAR.INC'
      REAL*4 K
C
C     THIS ROUTINE CALCULATES IONIC CONCENTRATIONS IN LAYER 3
C     (THE MIXING ZONE)
C
C     FIRST, SEVERAL VALUES FROM THE PREVIOUS TIME STEP ARE RESET.
C
      WCONC(6,3,2) = WCONC(6,3,3)
      WCONC(7,3,2) = WCONC(7,3,3)
      WCONC(8,3,2) = WCONC(8,3,3)
      WCONC(10,3,2) = WCONC(10,3,3)
C
C     FE2 IS CALCULATED AS A FUNCTION OF FE3 IN LAYER 2.
C
      T1A = (INFILT*DT)/(POROS*DMIX)
      IF ( T1A .GT. 30.) THEN
          T1  = 0.
      ELSE
          T1 = EXP(-1.0*T1A)
      ENDIF
      WCONC(10,3,3) = 1.5*WCONC(9,2,3)+(WCONC(10,3,2)-1.5*
     &               WCONC(9,2,3))*T1
C
C     CALCULATE SULPHATES IN LAYER 3 RESULTING FROM PYRITE OXIDATION
C     IN UPPER LAYERS.
C
         WCONC(6,3,3) = WCONC(6,2,3)+(WCONC(6,3,2)-WCONC(6,2,3))*T1
C
C     CHECK FOR DEPLETION OF GYPSUM.
C
      IF (CHECKM.NE.'DEPLETED') THEN
C
C     CA AND SO4 CONCENTRATIONS ARE FUNCTIONS OF PYRITE OXIDATION
C     IN LAYERS 1 AND 2.
C
         T2 = ((KSUBSO/FACTCO**2.)+0.25*WCONC(6,3,3)**2.)**0.5
         WCONC(7,3,3) = T2 + 0.5*WCONC(6,3,3)+ 0.0128
         WCONC(8,3,3) = T2 - 0.5*WCONC(6,3,3)+ 0.008
C
C     IF THE UNSATURATED ZONE IS DEPLETED OF GYPSUM; GYPSUM IS
C     DISSOLVING IN THE MIXING ZONE.
C
         IF (CHECKU.EQ.'DEPLETED') THEN
            IF (T.EQ.TFINAL) THEN
               SSTAR = WCONC(7,3,3)
               ELSE
               SSTARI = SSTAR
               SSTAR = WCONC(6,2,3)+(SSTARI-WCONC(6,2,3))*T1
            ENDIF
            DELTAG = (INFILT*DT/DMIX)*(WCONC(7,3,3)-SSTAR)
            GYPMIX = GYPMIX+DELTAG
C
C     CHECK FOR GYPSUM DEPLETION IN MIXING ZONE.
C
            IF (GYPMIX.GE.GYPI) THEN
               CHECKM = 'DEPLETED'
               DELTAG = 0.0
               GYPMIX = GYPI
            ENDIF
         ENDIF
      ENDIF
C
C     IF GYPSUM IS DEPLETED IN MIXING ZONE IONIC CONCENTRATIONS
C     ARE CALCULATED DIFERENTLY.
C
      IF (CHECKM.EQ.'DEPLETED') THEN
       WCONC(7,3,3) = WCONC(6,2,3)+(WCONC(7,3,2)-WCONC(6,2,3))*T1+.0128
         WCONC(8,3,3) = WCONC(8,3,2)*T1 + 0.008
      ENDIF
C
C     CALCULATE INITIAL GUESS FOR PH CALCULATION.
C
      T3 = (ALOG10(WCONC(7,3,3)/1000.)+1.555)**2.
      K = 0.95553+1.44448*T3
      T4 = (K*(ALOG10(WCONC(7,3,3)/1000.)+2.03))
      PHIN = 4.91345-((3.5731/(22./7.))*ATAN(T4))
C
C     PH IS CALCULATED ITERATIVELY USING SUBROUTINES 'NEWTON' AND 'PH3'
C
      IND = 3
      CALL NEWTON(IND,PHIN,PH(3),PH3)
C
C     PRINT DETAILED RESULTS IF SPECIFIED.
C
      IF (CODION.EQ.1.) THEN
         WRITE(*,900) T,WCONC(6,3,3),WCONC(7,3,3),WCONC(8,3,3)
         WRITE(*,910) GYPMIX,WCONC(10,3,3),PH(3)
900   FORMAT(1X,'LAYER 3 T=',F6.1,' [SO4]P3=',E10.4,' [SO4]T3=',E10.4,
     &       ' [CA2]T3=',E10.4)
910   FORMAT(1X,'GYPMIX=',E10.4,' [FE2]T3=',E10.4,' PH3=',F5.2)
      ENDIF

      RETURN
      END
C
C
C
C
      SUBROUTINE PH3(F,FPRIME,P)
      INCLUDE 'MODEL.INC'
      INCLUDE 'VAR.INC'
C
```

Table A.1 continued.

```
C     THIS ROUTINE IS INVOLVED IN THE ITERATIVE CALCULATION OF PH
C     IN THE MIXING ZONE.
C
C     FIRST THE FUNCTION (F) IS EVALUATED.
C
      F1 = FACTCO
      S04 = WCONC(7,3,3)/1000.
      CA2 = WCONC(8,3,3)/1000.
      FE2 = WCONC(10,3,3)/1000.
      T1 = 3.*((10.**(6.8-3.*P))/F1**(9./4.))
      T2 = 2.*((10.**(1.83-2.*P))/F1)
      T3 = (10.**(3.1-P))/F1**(1./4.)
      T4 = F1**(3./4.)*10.**(9.7-3*P)
      T5 = (10.**(P-10.47))/F1**(1./4.)
      F = 2*CA2+2*FE2+T1+T2+T3-((2.-T4)/(1.+T4))*S04-T5
C
C     THEN THE DERIVATIVE OF THE FUNCTION (FPRIME) IS CALCULATED.
C
      XL = ALOG(10.)
      DT4 = -3.*XL*T4
      T6 = -1.*DT4*(((2.-T4)/((1.+T4)**2.))+(1./(1.+T4)))
      FPRIME = -3.*XL*T1-2.*XL*T2-1.*XL*T3-T6*S04-1.*XL*T5
C
C     PRINT DETAILED RESULTS IF SELECTED
C
      IF (CODPH.EQ.1) THEN
      WRITE(*,900) T,P,F,FPRIME
900   FORMAT(1X,'PH3: T=',F6.1,' PH=',F5.2,' F=',E10.4,' FPRIME=',E10.4)
      ENDIF

      RETURN
      END
      SUBROUTINE IONS4
      EXTERNAL PH4
      INCLUDE 'MODEL.INC'
      INCLUDE 'VAR.INC'
      REAL*4 K
C
C     THIS ROUTINE CALCULATES IONIC CONCENTRATIONS IN LAYER 4.
C
C     FIRST, SEVERAL VALUES FROM THE PREVIOUS TIME STEP ARE RESET.
C
      WCONC(6,4,2) = WCONC(6,4,3)
      WCONC(10,4,2) = WCONC(10,4,3)
C
C     CALCULATION OF [SO4] IN LAYER 4 RESULTING FROM PYRITE
C     OXIDATION IN LAYERS 1 AND 2.
C
      T1A  =  WVEL*DT/(POROS*DBOT)
      IF ( T1A .GT. 30.) THEN
          T1  = 0.0
      ELSE
          T1 = EXP(-1.0*T1A)
      ENDIF
C
C
      WCONC(6,4,3) = WCONC(6,3,2)+(WCONC(6,4,2)-WCONC(6,3,2))*T1
C
C     CALCULATION OF TOTAL SO4,CA2 AND FE2.
C
      T2 = ((KSUBSO/FACTCO**2)+0.25*WCONC(6,4,3)**2.)**0.5
      WCONC(7,4,3) = T2+0.5*WCONC(6,4,3)+ 0.0128
      WCONC(8,4,3) = T2-0.5*WCONC(6,4,3)+ 0.008
      WCONC(10,4,3) = WCONC(10,3,2)+(WCONC(10,4,2)-WCONC(10,3,2))*T1
C
C     THE PH IN LAYER 4 IS CALCULATED USING THE SAME EQUATIONS
C     AS LAYER 3. THESE ARE FOUND IN SUBROUTINE 'PH4'.
C
C     CALCULATE INITIAL GUESS FOR PH CALCULATION.
C
          IF (WCONC(7,4,3).EQ.0.0) WCONC(7,4,3)=1.0E-20
          T3 = (ALOG10(WCONC(7,4,3)/1000.)+1.555)**2.
          K = 0.95553+1.44448*T3
          T4 = (K*(ALOG10(WCONC(7,4,3)/1000.)+2.03))
          PHIN = 4.91345-((3.5731/(22./7.))*ATAN(T4))
C
C     PH IS CALCULATED ITERATIVELY USING SUBROUTINES 'NEWTON' AND 'PH4'
C
          IND = 4
          CALL NEWTON(IND,PHIN,PH(4),PH4)
C
C     PRINT DETAILED RESULTS IF SPECIFIED.
C
      IF (CODION.EQ.1.) THEN
      WRITE(*,900) T,WCONC(6,4,3),WCONC(7,4,3),WCONC(8,4,3)
      WRITE(*,910) WCONC(10,4,3),PH(4)
900   FORMAT(1X,'LAYER 4 T=',F6.1,' [SO4]P4=',E10.4,' [SO4]T4=',E10.4,
     & ' [CA2]T4=',E10.4)
910   FORMAT(1X,'[FE2]T4=',E10.4,' PH4=',F5.2)
      ENDIF

      RETURN
      END
C
C
C
C
      SUBROUTINE PH4(F,FPRIME,P)
      INCLUDE 'MODEL.INC'
      INCLUDE 'VAR.INC'
C
C     THIS ROUTINE IS INVOLVED IN THE ITERATIVE CALCULATION OF PH
C     IN LAYER 4
C
C     FIRST THE FUNCTION (F) IS EVALUATED.
C
      F1 = FACTCO
      SO4 = WCONC(7,4,3)/1000.
      CA2 = WCONC(8,4,3)/1000.
      FE2 = WCONC(10,4,3)/1000.
      T1 = 3.*((10.**(6.8-3.*P))/F1**(9./4.))
      T2 = 2.*((10.**(1.83-2.*P))/F1)
      T3 = (10.**(3.1-P))/F1**(1./4.)
      T4 = F1**(3./4.)*10.**(9.7-3*P)
      T5 = (10.**(P-10.47))/F1**(1./4.)
      F = 2*CA2+2*FE2+T1+T2+T3-((2.-T4)/(1.+T4))*SO4-T5
C
C     THEN THE DERIVATIVE OF THE FUNCTION (FPRIME) IS CALCULATED.
C
      XL = ALOG(10.)
      DT4 = -3.*XL*T4
      T6 = -1.*DT4*(((2.-T4)/((1.+T4)**2.))+(1./(1.+T4)))
      FPRIME = -3.*XL*T1-2.*XL*T2-1.*XL*T3-T6*SO4-1.*XL*T5
C
C     PRINT DETAILED RESULTS IF SELECTED
C
      IF (CODPH.EQ.1) THEN
      WRITE(*,900) T,P,F,FPRIME
900   FORMAT(1X,'PH4: T=',F6.1,' PH=',F5.2,' F=',E10.4,' FPRIME=',E10.4)
      ENDIF

      RETURN
      END
```

Table A.1 continued.

```
      SUBROUTINE URANUM
      INCLUDE 'MODEL.INC'
      INCLUDE 'VAR.INC'
C
C     THIS ROUTINE CALCULATES SOLID AND LIQUID PHASE URANIUM
C     CONCENTRATIONS.
C     FIRST, VALUES FROM THE PREVIOUS TIME STEP ARE SAVED.
C
      WCONC(1,3,2) = WCONC(1,3,3)/UCF
      WCONC(1,4,2) = WCONC(1,4,3)/UCF
      CONC(1,1,2) = CONC(1,1,3)/UCF
C
C     LIQUID PHASE CONCENTRATIONS ARE THEN CALCULATED.
C
      TEMP = KRATE*DT
      IF ( TEMP  .GT. 30. ) THEN
         WCONC(1,2,3)=((3.0*DUNSAT)/(INFILT*DT))*XURANI*PYRITE(2)
      ELSE
         WCONC(1,2,3)=((3.0*DUNSAT)/(INFILT*DT))*XURANI*PYRITE(2)
     &                *(1.0-EXP(-1.0*TEMP))
      ENDIF
      T1 = 1.0+(KDUO2*RHOTAL)/POROS
      T2 = (-1.0*INFILT*DT)/(POROS*DMIX*T1)
      T3 = (-1.0*WVEL*DT)/(POROS*DBOT*T1)
      IF (T2 .GT.-34.0)THEN
         WCONC(1,3,3)=WCONC(1,2,3)+(WCONC(1,3,2)-WCONC(1,2,3))*EXP(T2)
      ELSE
         WCONC(1,3,3)=WCONC(1,2,3)
      ENDIF
      IF(T3.GT.-34.0)THEN
         WCONC(1,4,3)=WCONC(1,3,3)+(WCONC(1,4,2)-WCONC(1,3,3))*EXP(T3)
      ELSE
         WCONC(1,4,3)=WCONC(1,3,3)
      ENDIF
C
C     SOLID PHASE CONCENTRATION IN THE FIRST LAYER.
C
      CONC(1,1,3) = CONC(1,1,2)-((INFILT*DT)/DUNSAT)*WCONC(1,2,3)
C
C     THE CONCENTRATIONS ARE THEN CONVERTED FROM A MOLAR BASIS TO
C     AN ACTIVITY BASIS.
C
      CONC(1,1,3) = CONC(1,1,3)*UCF
      WCONC(1,2,3) = WCONC(1,2,3)*UCF
      WCONC(1,3,3) = WCONC(1,3,3)*UCF
      WCONC(1,4,3) = WCONC(1,4,3)*UCF
C
C     PRINT SUMMARY RESULTS IF SPECIFIED.
C
      IF (CODNUC.EQ.1.0) THEN
         WRITE(*,900) T
         WRITE(*,910) CONC(1,1,3),WCONC(1,2,3),WCONC(1,3,3),
     &                WCONC(1,4,3)
```

```
      ENDIF
900   FORMAT(1X,'T=',F5.0,4X,'SOLID1',5X,'LIQUID2',5X,'LIQUID3',5X,
     &       'LIQUID4')
910   FORMAT(1X,'URANIUM',2X,E10.4,3(2X,E10.4))

      RETURN
      END
      SUBROUTINE THORUM
      INCLUDE 'MODEL.INC'
      INCLUDE 'VAR.INC'
C
C     THIS ROUTINE CALCULATES SOLID AND LIQUID PHASE THORIUM
C     CONCENTRATIONS.
C     CONCENTRATIONS IN THE UNSATURATED ZONE ARE DETERMINED FIRST.
C
      IF (CHKTHU.EQ.'DEPLETED') THEN
C
C     IF THORIUM IS DEPLETED IN THE UNSATURATED ZONE THE CALCULATIONS
C     ARE QUITE SIMPLE.
C
         T230S = T230IS
         CONC(2,1,3) = TINSLA
         X232SA = X232A
         WCONC(2,2,3) = 0.0
      ELSE
C
C     LIQUID PHASE CONCENTRATION.
C
          IF ( PH(2) .GT. 3.0 ) THEN
              DELTA = 1.0+FACTCO**3.*10.**(8.99-3.*PH(2))
     &                   +FACTCO**0.75*10.**(9.7-3.*PH(2))
              S04 = WCONC(7,2,3)/DELTA
          ELSE
              AA= FACTCO**2.*8.317+FACTCO**2.25*10**(1.99-PH(2))*8.317
              BB= 1. + WCONC(7,2,3)*FACTCO**2.*8.317 +
     &              FACTCO**0.25*10**(1.99-PH(2) )
              CC = -WCONC(7,2,3)
              S04 = ( -BB+ (BB**2.-4.*AA*CC)**0.5  )/(2*AA)
              IF ( S04 .LT. 0.) THEN
                S04 = ( -BB- (BB**2.-4.*AA*CC)**0.5  )/(2*AA)
              ENDIF
         ENDIF
C
         P = PH(2)
         F = FACTCO
         T1 = (10.**(2.5-4.*P))/F**4.
         T2 = F**(7./4.)*10.**(P-3.2)+F**3.*10.**(2.*P-6.93)
         T3 = F**(15./4.)*10.**(3.*P-11.7)+F**4.*10.**(4.*P-15.9)
         T4 = F**4.*10.**5.45*S04+F**6.*10.**8.73*S04**2.
         T5 = 10**(-1.*(5.0+0.32*P))
         WCONC(2,2,3) = ( T1*(1.0+T2+T3+T4) +T5)*1000.
         IF (WCONC(2,2,3).GT.0.05) WCONC(2,2,3) = 0.05
C
C     SOLID PHASE INVENTORY AND CONCENTRATION.
C
         THDISS = THDISS+((INFILT*DT)/DUNSAT)*WCONC(2,2,3)
         T232D = X232LM*THDISS
         T230D = THDISS-T232D
         T232S = T232IS+(T232SO-T232D)
         T230S = T230IS+(T230SO-T230D)
         CONC(2,1,3) = T232S*T232CF+T230S*T230CF
         X232SA = (T232S*T232CF)/CONC(2,1,3)
C
C     RECHECK AMOUNT OF THORIUM DISSOLVED AND CORRECT IF NECESSARY.
C
         IF (THDISS.GE.THSOL) THEN
            CHKTHU = 'DEPLETED'
            WCONC(2,2,3) = 0.0
            CONC(2,1,3) = T232IS*T232CF+T230IS*T230CF
            T230S = T230IS
            X232SA = T232IS*T232CF/CONC(2,1,3)
         ENDIF
      ENDIF
C
C     LIQUID PHASE CONCENTRATION IN THE MIXING LAYER.
C     THE CONCENTRATION IS 0 IF THORIUM IS DEPLETED FROM THIS LAYER.
C
      IF (CHKTHS.EQ.'DEPLETED') THEN
         WCONC(2,3,3) = 0.0
      ELSE
C
C     OTHERWISE THE CALCULATIONS ARE SIMILAR TO THOSE IN THE
C     UNSATURATED LAYER.
C
         S04 = WCONC(7,3,3)/1000.
         P = PH(3)
         F = FACTCO
         T1 = (10.**(2.5-4.*P))/F**4.
         T2 = F**(7./4.)*10.**(P-3.2)+F**3.*10.**(2.*P-6.93)
         T3 = F**(15./4.)*10.**(3.*P-11.7)+F**4.*10.**(4.*P-15.9)
         T4 = F**4.*10.**5.45*S04+F**6.*10.**8.73*S04**2.
         T5 = 10**(-1.*(5.0+0.32*P))
         WCONC(2,3,3) = ( T1*(1.0+T2+T3+T4) +T5)*1000.
         IF (WCONC(2,3,3).GT.0.05) WCONC(2,3,3) = 0.05
C
C     IF THE CALCULATED CONCENTRATION IN THIS LAYER IS LESS THAN IN
C     THE UNSATURATED LAYER THEN THORIUM IS PRECIPITATING IN THIS LAYER
C
         IF (WCONC(2,3,3).LT.WCONC(2,2,3)) THEN
            DELTH = WCONC(2,2,3)-WCONC(2,3,3)
            THDISM = THDISM-(INFILT*DT/DMIX)*DELTH
         ELSE
            THDISM = THDISM+(INFILT*DT/DMIX)*WCONC(2,3,3)
         ENDIF
C
C     RECHECK AMOUNT OF THORIUM DISSOLVED IN MIXING ZONE AND CORRECT
C     IF NECESSARY.
C
         IF (THDISM.GE.THSOL) THEN
            CHKTHS = 'DEPLETED'
            WCONC(2,3,3) = 0.0
         ENDIF
      ENDIF
```

```
C
C     LIQUID PHASE CONCENTRATION IN THE BOTTOM LAYER.
C
      SO4 = WCONC(7,4,3)/1000.
      P = PH(4)
      F = FACTCO
      T1 = (10.**(2.5-4.*P))/F**4.
      T2 = F**(7./4.)*10.**(P-3.2)+F**3.*10.**(2.*P-6.93)
      T3 = F**(15./4.)*10.**(3.*P-11.7)+F**4.*10.**(4.*P-15.9)
      T4 = F**4.*10.**5.45*SO4+F**6.*10.**8.73*SO4**2.
      T5 = 10**(-1.*(5.0+0.32*P) )
      WCONC(2,4,3) = ( T1*(1.0+T2+T3+T4) +T5)*1000.
      IF (WCONC(2,4,3).GT.0.05) WCONC(2,4,3) = 0.05
C
C     LIQUID PHASE CONCENTRATIONS ARE CONVERTED FROM A MOLAR BASIS
C     TO AN ACTIVITY BASIS.
C
      WCONC(2,2,3) = WCONC(2,2,3)*THORCF
      WCONC(2,3,3) = WCONC(2,3,3)*THORCF
      WCONC(2,4,3) = WCONC(2,4,3)*THORCF
C
C     PRINT SUMMARY RESULTS IF SPECIFIED.
C
      IF (CODNUC.EQ.1.0) THEN
         WRITE(*,900) T
         WRITE(*,910) CONC(2,1,3),X232SA,WCONC(2,2,3),WCONC(2,3,3),
     &                WCONC(2,4,3)
         WRITE(*,920) T230S,THDISS,THDISM
      ENDIF
900   FORMAT(1X,'T=',F5.0,4X,'SOLID1',5X,'THRATIO',5X,'LIQUID2',5X,
     &      'LIQUID3',5X, 'LIQUID4')
910   FORMAT(1X,'THORIUM',2X,E10.4,4(2X,E10.4))
920   FORMAT(1X,'[TH230]S=',E10.4,' [TH]DISS=',E10.4,' [TH]DISM=',E10.4)

      RETURN
      END
      SUBROUTINE LEAD
      INCLUDE 'MODEL.INC'
      INCLUDE 'VAR.INC'
C
C     THIS ROUTINE CALCULATES LIQUID AND SOLID PHASE CONCENTRATIONS
C     OF LEAD-210.
C     FIRST,SEVERAL VARIABLES ARE RESET.
C
      DLEAD(2) = DLEAD(3)
      WCONC(3,3,2) = WCONC(3,3,3)/PBCF
      WCONC(3,4,2) = WCONC(3,4,3)/PBCF
C
C     SOLID PHASE LEAD CONCENTRATION IS THEN DETERMINED.
C
      CPBRAS = CPBRAS*PBDEC+(CONC(4,1,3)/RACF)*RDECAY
      CPBRL2 = (WCONC(4,2,3)/RACF)*RDECAY
      IF(LAMPB*T.LT. 34.)THEN
         CLEADT = CPBTI*EXP(-1.0*LAMPB*T)
         XLEAD = XPBI*EXP(-1.0*LAMPB*T)
      ELSE
         CLEADT=0.0
         XLEAD=0.0
      ENDIF
      CONC(3,1,3) = CLEADT+CPBRAS
C
C     LIQUID PHASE CALCULATIONS FOR THE UNSATURATED ZONE.
C     IF THE UNSATURATED ZONE IS DEPLETED OF PBSO4, THE CALCULATIONS
C     ARE VERY SIMPLE.
C
      IF (CHKPBU.EQ.'DEPLETED') THEN
         WCONC(3,2,3) = CPBRL2
C
C     OTHERWISE THE CONC'N DEPENDS ON THE DISSOLUTION AND REPRECIP-
C     ITATION OF PBSO4. THE DEPTH OF DEPLETION IS DETERMINED FIRST.
C
      ELSE
         T1 = (EQLEAD**2.*INFILT*DT)/CLEADI
         IF ( BETA .GT. 0.) THEN
           T2 = (INFILT*DT)/BETA+2.0*FACTCO**2.*KFLEAD*DLEAD(2)
           T3 = 2.0*DLEAD(2)+(EQLEAD*INFILT*DT)/BETA
           T4 = (EQLEAD**2.*FACTCO**2.*KFLEAD*INFILT*DT)/CLEADI
           T5 = DLEAD(2)+(EQLEAD*INFILT*DT)/(2.0*BETA)-T4/2.0
         ELSE
           T2 =                 2.0*FACTCO**2.*KFLEAD*DLEAD(2)
           T3 = 2.0*DLEAD(2)
           T4 = (EQLEAD**2.*FACTCO**2.*KFLEAD*INFILT*DT)/CLEADI
           T5 = DLEAD(2)                                 -T4/2.0
         ENDIF
         DHLEAD = (T1*T2+0.25*(T3-T4)**2.)**0.5-T5
         DLEAD(3) = DLEAD(2)+DHLEAD
C
         IF (DLEAD(3).GE.DUNSAT) THEN
            DLEAD(3) = DUNSAT
            CHKPBU = 'DEPLETED'
            WCONC(3,2,3) = CPBRL2
         ELSE
C
            IF ( PH(2) .GT. 3.0 ) THEN
              DELTA = 1.0+FACTCO**3.*10.**(8.99-3.*PH(2))
     &                         +FACTCO**0.75*10.**(9.7-3.*PH(2))
              SO4 = WCONC(7,2,3)/DELTA
            ELSE
              AA= FACTCO**2.*8.317+FACTCO**2.25*10**(1.99-PH(2))*8.317
              BB= 1. + WCONC(7,2,3)*FACTCO**2.*8.317 +
     &                    FACTCO**0.25*10**(1.99-PH(2) )
              CC = -WCONC(7,2,3)
              SO4 = ( -BB+ (BB**2.-4.*AA*CC)**0.5  )/(2*AA)
              IF ( SO4 .LT. 0.) THEN
                SO4 = ( -BB- (BB**2.-4.*AA*CC)**0.5  )/(2*AA)
              ENDIF
           ENDIF
C
            CLEAD=(EQLEAD**2.)/(EQLEAD+SO4)*(1.+FACTCO**2.*KFLEAD*SO4)
            WCONC(3,2,3) = XLEAD*CLEAD+CPBRL2
         ENDIF

      ENDIF
C
C     LIQUID PHASE CONCENTRATION OF LEAD IN THE MIXING ZONE.
C
      IF (CHKBAU.EQ.'DEPLETED') THEN
         CPBRL3 = (WCONC(4,3,3)/RACF)*RDECAY
      ELSE
         CPBRL3 = 0.0
      ENDIF

      IF (CHKPBS.EQ.'DEPLETED') THEN
         CPBIN = CPBRL3
      ELSE

         IF (CHKPBU.EQ.'ENRICHED') THEN
            CPBIN = WCONC(3,2,3)+CPBRL3
         ELSE
            T1 = (EQLEAD**2.*XLEAD)/(EQLEAD+WCONC(7,3,3))
            CPBIN = T1*(1.0+KFLEAD*FACTCO**2.*WCONC(7,3,3))+CPBRL3
         ENDIF

         SUMPB = SUMPB+INFILT*DT*CPBIN

         IF (SUMPB.GE.PBSATI) THEN
            CHKPBS = 'DEPLETED'
            CPBIN = CPBRL3
         ENDIF

      ENDIF
      T1 = (INFILT*DT)/(POROS*DMIX*(1.0+KDLEAD*RHOTAL/POROS))
      IF (T1 .LT. 30. ) THEN
         WCONC(3,3,3) = CPBIN+(WCONC(3,3,2)*PBDEC-CPBIN)*EXP(-1.0*T1)
      ELSE
         WCONC(3,3,3) = CPBIN
      ENDIF
C
C     LIQUID PHASE LEAD CONCENTRATION IN THE BOTTOM LAYER.
C
      IF (CHKBAS.EQ.'DEPLETED') THEN
         CPBRL4 = (WCONC(4,4,3)/RACF)*RDECAY
      ELSE
         CPBRL4 = 0.0
      ENDIF

      IF (CHKPBS.EQ.'ENRICHED') THEN
         CPBIN = WCONC(3,3,3)+CPBRL4
      ELSE
         T1 = (EQLEAD**2.*XLEAD)/(EQLEAD+WCONC(7,4,3))
         CPBIN = T1*(1.0+KFLEAD*FACTCO**2.*WCONC(7,3,3))+CPBRL4
      ENDIF
C
      T1 = (WVEL*DT)/(POROS*DBOT*(1.0+KDLEAD*RHOTAL/POROS))
      IF (T1 .LT. 30. ) THEN
         WCONC(3,4,3) = CPBIN+(WCONC(3,4,2)*PBDEC-CPBIN)*EXP(-1.0*T1)
      ELSE
         WCONC(3,4,3) = CPBIN
      ENDIF
C
C     THE CONCENTRATIONS ARE THEN CONVERTED FROM A MOLAR BASIS
C     TO AN ACTIVITY BASIS.
C
      IF (WCONC(3,2,3) .LT. 0.) THEN
          WCONC(3,2,3) = 0.
      ENDIF
C
      CONC(3,1,3) = CONC(3,1,3)*PBCF
      WCONC(3,2,3) = WCONC(3,2,3)*PBCF
      WCONC(3,3,3) = WCONC(3,3,3)*PBCF
      WCONC(3,4,3) = WCONC(3,4,3)*PBCF
C
C     PRINT SUMMARY RESULTS IF SPECIFIED.
C
      IF (CODNUC.EQ.1.0) THEN
         WRITE(*,900) T
         WRITE(*,910) CONC(3,1,3),WCONC(3,2,3),WCONC(3,3,3),
     &                WCONC(3,4,3)
         WRITE(*,920) RDECAY,DLEAD(3),SUMPB
         WRITE(*,930) CPBRL2,CPBRL3,CPBRL4
      ENDIF
900   FORMAT(1X,'T=',F5.0,4X,'SOLID1',5X,'LIQUID2',5X,'LIQUID3',5X,
     &       'LIQUID4')
910   FORMAT(1X,'LEAD',5X,E10.4,3(2X,E10.4))
```

```
920    FORMAT(1X,'RDECAY=',E10.4,' DLEAD=',E10.4,' [PB]DEP=',E10.4)
930    FORMAT(1X,'[PB]RA2=',E10.4,'[PB]RA3=',E10.4,' [PB]RA4=',E10.4)

       RETURN
       END
```

```
      SUBROUTINE RADIUM
      INCLUDE 'MODEL.INC'
      INCLUDE 'VAR.INC'
C
C     THIS ROUTINE CALCULATES SOLID AND LIQUID PHASE RADIUM CONCEN-
C     TRATIONS. FIRST, SEVERAL VARIABLES ARE RESET.
C
      DBAR(2) = DBAR(3)
      MBAR(2) = MBAR(3)
      XBAR(2) = XBAR(3)
      WCONC(4,3,2) = WCONC(4,3,3)/RACF
      WCONC(4,4,2) = WCONC(4,4,3)/RACF
C
C     VALUES IN THE UNSATURATED ZONE ARE DETERMINED.
C     LAYER 1 SOLID PHASE FIRST.
C
      CRATHS = CRATHS*RADEC+T230S*TDECAY
      CRATL2 = X230LM*(WCONC(2,2,3)/THORCF)*TDECAY
      TEMP = LAMRAD*T
      IF ( TEMP .GT. 30.) THEN
          CRADT = 0.0
          XRAD = 0.0
      ELSE
          CRADT = CRADTI*EXP(-1.0*LAMRAD*T)
          XRAD = XRADI*EXP(-1.0*LAMRAD*T)
      ENDIF
      CONC(4,1,3) = CRADT+CRATHS
C
C     IF THE UNSATURATED ZONE IS DEPLETED OF BASO4, THE CALCULATIONS
C     ARE VERY SIMPLE.
C
      IF (CHKBAU.EQ.'DEPLETED') THEN
         CONC(4,2,3) = CONC(4,1,3)
         WCONC(4,2,3) = CRATL2
C
C     OTHERWISE, THE CONCENTRATIONS DEPEND ON THE DISSOLUTION AND
C     REPRECIPITATION OF BASO4. FIRST THE DEPTH OF THE BASO4 DEPLETED
C     ZONE IS CALCULATED.
C
      ELSE
         IF(CBARI.EQ.0.0)THEN
            T1=0.0
         ELSE
            T1 = (EQBAR**2.*INFILT*DT)/CBARI
         ENDIF
         IF ( BETA .GT. 0.) THEN
            T2 = (INFILT*DT)/BETA+2.0*FACTCO**2.*KFBAR*DBAR(2)
            T3 = 2.0*DBAR(2)+(EQBAR*INFILT*DT)/BETA
            T4 = (EQBAR**2.*FACTCO**2.*KFBAR*INFILT*DT)/CBARI
            T5 = DBAR(2)+(EQBAR*INFILT*DT)/(2.0*BETA)-T4/2.0
         ELSE
            T2 = 2.0*FACTCO**2.*KFBAR*DBAR(2)
            T3 = 2.0*DBAR(2)
            IF(CBARI.EQ.0.0)THEN
              T1=0.0
            ELSE
              T4 = (EQBAR**2.*FACTCO**2.*KFBAR*INFILT*DT)/CBARI
            ENDIF
            T5 = DBAR(2)-T4/2.0
         ENDIF
         DHBAR = (T1*T2+0.25*(T3-T4)**2.)**0.5-T5
         DBAR(3) = DBAR(2)+DHBAR
C
C     IF THE DEPTH OF DEPLETION IS LESS THAN THE DEPTH OF THE
C     UNSATURATED ZONE, THE AMOUNT OF REPRECIPITATED BASO4 AND THE
C     MOL FRACTION OF RA IN THAT BASO4 IS CALCULATED.
C
         IF (DBAR(3).LT.DUNSAT) THEN
C
            IF ( PH(2) .GT. 3.0 ) THEN
              DELTA = 1.0+FACTCO**3.*10.**(8.99-3.*PH(2))
     &                   +FACTCO**0.75*10.**(9.7-3.*PH(2))
              S04 = WCONC(7,2,3)/DELTA
            ELSE
              AA= FACTCO**2.*8.317+FACTCO**2.25*10**(1.99-PH(2))*8.317
              BB= 1. + WCONC(7,2,3)*FACTCO**2.*8.317 +
     &              FACTCO**0.25*10**(1.99-PH(2) )
              CC = -WCONC(7,2,3)
              S04 = ( -BB+ (BB**2.-4.*AA*CC)**0.5  )/(2*AA)
              IF ( S04 .LT. 0.) THEN
                S04 = ( -BB- (BB**2.-4.*AA*CC)**0.5  )/(2*AA)
              ENDIF
           ENDIF
C
            CBAR = (EQBAR**2.)/(EQBAR+S04)*(1.0+FACTCO**2.*KFBAR*S04)
            MBAR(3) = MBAR(2)+CBARI*DHBAR-INFILT*DT*CBAR
C
            IF (MBAR(3) .LT. 0.) THEN
                MBAR(3) = 0.
            ENDIF
C
            T1 = CBARI*XRAD*DHBAR+INFILT*CRATL2*DT
            T2 = MBAR(2)*XBAR(2)-0.5*DT*INFILT*CBAR*XBAR(2)*KRAD
            XBAR(3) = (T1+T2)/(MBAR(3)+0.5*DT*INFILT*CBAR*KRAD)
            WCONC(4,2,3) = KRAD*CBAR*XBAR(3)
            CONC(4,2,3) = CRATHS+XRAD*CBARI+((XBAR(3)*MBAR(3))/
     &                    (DUNSAT-DBAR(3)))
C
C     OTHERWISE, SEVERAL VARIABLES ARE RESET.
C
         ELSE
            DBAR(3) = DUNSAT
            CHKBAU = 'DEPLETED'
            CBAR = 0.0
            MBAR(3) = 0.0
            WCONC(4,2,3) = CRATL2
```

```
          CONC(4,2,3) = CONC(4,1,3)
        ENDIF
      ENDIF
C
C     NEXT, THE LIQUID PHASE RADIUM CONCENTRATION IN THE MIXING ZONE
C     IS DETERMINED.
C
      IF (CHKTHU.EQ.'DEPLETED') THEN
        CRATL3 = X230LM*(WCONC(2,3,3)/THORCF)*TDECAY
      ELSE
        CRATL3 = 0.0
      ENDIF

      IF (CHKBAS.EQ.'DEPLETED') THEN
        CRADIN = CRATL3
      ELSE

        IF (CHKBAU.EQ.'ENRICHED') THEN
          CRADIN = WCONC(4,2,3)+CRATL3
        ELSE
          T1 = (EQBAR**2.*XRAD)/(EQBAR+WCONC(7,3,3))
          CRADIN = T1*(1.0+KFBAR*FACTCO**2.*WCONC(7,3,3))+CRATL3
        ENDIF

        SUMBAR = SUMBAR+INFILT*DT*CRADIN

        IF (SUMBAR.GE.BASATI) THEN
          CHKBAS = 'DEPLETED'
          CRADIN = CRATL3
        ENDIF

      ENDIF

      T1 = (INFILT*DT)/(POROS*DMIX*(1.0+KDRAD*RHOTAL/POROS))
      IF ( T1 .GT. 30.0 ) THEN
        WCONC(4,3,3) = CRADIN
      ELSE
        WCONC(4,3,3) = CRADIN+(WCONC(4,3,2)*RADEC-CRADIN)*EXP(-1.*T1)
      ENDIF
C
C     THE LIQUID PHASE RADIUM CONCENTRATION IN THE BOTTOM LAYER
C     IS THEN DETERMINED.
C
      IF (CHKTHS.EQ.'DEPLETED') THEN
        CRATL4 = X230LM*(WCONC(2,4,3)/THORCF)*TDECAY
      ELSE
        CRATL4 = 0.0
      ENDIF

      IF (CHKBAS.EQ.'ENRICHED') THEN
        CRADIN = WCONC(4,3,3)+CRATL4
      ELSE
        T1 = (EQBAR**2.*XRAD)/(EQBAR+WCONC(7,4,3))
```

```
         CRADIN = T1*(1.0+KFBAR*FACTCO**2.*WCONC(7,3,3))+CRATL4
      ENDIF
C
      T1 = (WVEL*DT)/(POROS*DBOT*(1.0+KDRAD*RHOTAL/POROS))
      IF ( T1 .GT. 30.) THEN
          WCONC(4,4,3) = CRADIN
      ELSE
          WCONC(4,4,3) = CRADIN+(WCONC(4,4,2)*RADEC-CRADIN)*EXP(-1.*T1)
      ENDIF
C
C     FINALLY,ALL RADIUM CONCENTRATIONS ARE CONVERTED FROM A MOLAR
C     BASIS TO AN ACTIVITY BASIS.
C
      IF (WCONC(4,2,3)  .LT. 0.) THEN
          WCONC(4,2,3) = 0.
      ENDIF
C
      CONC(4,1,3) = CONC(4,1,3)*RACF
      CONC(4,2,3) = CONC(4,2,3)*RACF
      WCONC(4,2,3) = WCONC(4,2,3)*RACF
      WCONC(4,3,3) = WCONC(4,3,3)*RACF
      WCONC(4,4,3) = WCONC(4,4,3)*RACF
C
C     PRINT SUMMARY RESULTS IF SPECIFIED.
C
      IF (CODNUC.EQ.1.0) THEN
         WRITE(*,900) T
         WRITE(*,910) CONC(4,1,3),CONC(4,2,3),WCONC(4,2,3),WCONC(4,3,3)
     &                ,WCONC(4,4,3)
         WRITE(*,920) TDECAY,DBAR(3),SUMBAR,BETA
         WRITE(*,930) CRATL2,CRATL3,CRATL4
      ENDIF
900   FORMAT(1X,'T=',F5.0,4X,'SOLID1',5X,'SOLID2',6X,'LIQUID2',5X,
     &       'LIQUID3',5X, 'LIQUID4')
910   FORMAT(1X,'RADIUM',3X,E10.4,4(2X,E10.4))
920   FORMAT(1X,'TDECAY=',E10.4,' DBAR=',E10.4,' [BAR]DEP=',E10.4,
     &       ' BETA=',E10.4)
930   FORMAT(1X,'[RA]TH2=',E10.4,' [RA]TH3=',E10.4,' [RA]TH4=',E10.4)

      RETURN
      END
```

Table A.1 continued.

```
C
C     EROSION MODEL - VERSION FOR PHASE 4 (18 MAR 1987)
C
      SUBROUTINE EROS
      INCLUDE 'MODEL.INC'
      INCLUDE 'VAR.INC'
      IF(CODERO.GE.1.0)THEN
         WRITE(*,1008)
1008     FORMAT(1X,'SUBROUTINE EROS')
      ENDIF
C
      REAL*4 CSOIL,VELRAT,CTSOIL,LENTOT,BED,ESOIL,TCSOIL
     &,BEDTEM,SUS,MSOIL,TRSED,SPACE,VS,RS,P1,P2,CRO,DF,BEDPND,SUSPND
C
C  INITIALIZE PARAMETERS THAT STAY CONSTANT FOR A GIVEN TRIAL
      IF (T.EQ.0.0)THEN
C
C     CALCULATE WIDTH, SEGMENT LENGTH AND NUMBER OF SEGMENTS
         LENFT=FLENGT/0.3048
         WIDTH=ATAIL/(FLENGT*0.3048)
         NLEN=INT(LENFT/400.0)+1
         SEGLEN=LENFT/FLOAT(NLEN)
C
C     CALCULATE SLOPE FACTOR AND SINE OF SLOPE ANGLE
         SPRIME=SIN(ATAN(SLOPE/100.0))
         SLPFAC=(0.43+(0.3*SLOPE)+(0.043*SPRIME**2))/6.613
C
C     CALCULATE SLOPE LENGTH EXPONENT
         IF(SLOPE.LE.3.0)THEN
            MSLP=0.3
         ELSEIF(SLOPE.LT.5.0)THEN
            MSLP=0.4
         ELSE
            MSLP=0.5
         ENDIF
C
C     INITIALIZE EQUATIONS FOR SOIL ERODIBILITY EQUATION
         CSL=5.0
         PEROM=0.0
         BSOIL=2.0
C
         IF(CODERO.EQ.2.0)THEN
            WRITE(*,1000)LENFT,NLEN,SEGLEN,SLOPE,ATAIL,MSLP
1000        FORMAT(1X,'LENFT=',E10.3,1X,'NLEN=',E10.3,1X,
     &      'SEGLEN=',E10.3,1X,'SLOPE=',E10.3,1X,'ATAIL=',E10.3,
     &      1X,'MSLP=',E10.3)
            WRITE(*,1004)SLPFAC,SPRIME
1004        FORMAT(1X,'SLPFAC=',E10.3,1X,'SPRIME=',E10.3)
         ENDIF
C
C    SOLVE FOR SOIL ERODIBILITY(K)
         MSOIL=SILT*100.0
         KSOIL=((2.1*(MSOIL**1.14)*1E-4*(12.0-PEROM))+
     &   ((3.25*(BSOIL-2.0))+(2.5*(CSL-3.0)))))/100.0
C
C    SOLVE FOR D50 AND PARAMETERS FUNCTIONALLY RELATED TO D50
         D50=-1.99E-3*SILT+0.215
         TSOIL=5.87E5*D50**0.197
         IF(D50.LT.0.045)THEN
            BEXP=1.83*D50**0.049
         ELSE
            BEXP=-0.714*D50+1.61
         ENDIF
C   FLAG TVEG AT T=0
         TVEG=-1.0
C
         IF(CODERO.EQ.2.0)THEN
            WRITE(*,1002)KSOIL,D50,TSOIL,BEXP,SILT,RSOIL,THALF
1002        FORMAT(1X,'KSOIL=',E10.3,1X,'D50=',E10.3,1X,'TSOIL=',
     &      E10.3,1X,'BEXP='E10.3,1X,'SILT',E10.3,1X,'RSOIL=',
     &      E10.3,1X,'THALF=',E10.3)
         ENDIF
C
      ENDIF
C
C    SOLVE FOR FRACTION OF TAILINGS THAT ARE VEGETATED
      IF(PH(1).LE.4.0)THEN
         FVEG=0.0
         TVEG=-1.0
      ELSE
         IF(TVEG.EQ.-1.0) THEN
             TVEG=T
             FVEG=0.0
         ELSE
             FVEG=1-EXP(((-.693)*((T-TVEG)-(DT/2.0)))/THALF)
         ENDIF
      ENDIF
C
C     CHECK USER-SET MIN. VEGETATION
      IF (FVEG.LE.MINVEG)FVEG=MINVEG
C
C     FRACTION VEGETATED CANNOT EXCEED 0.9
      IF(FVEG.GE.0.9)FVEG=0.9
C
C     CALCULATE CONTROL PRACTICE FACTOR
      IF (FVEG.EQ.0.0) THEN
         CSOIL=1.0
      ELSE
         CSOIL=EXP(-0.109-(0.056*FVEG))
      ENDIF
C
C     SOLVE FOR VELOCITY RATIO
      VELRAT=-.77*FVEG+1.0
C
C     SOLVE FOR TRANSPORTABILITY REDUCTION FACTOR FOR THREE SLOPE RANGES
      IF(SLOPE.LE.0.75)THEN
```

Table A.1 continued.

```
         CTSOIL=VELRAT**18.53
      ELSEIF(SLOPE.GT.0.75.AND.SLOPE.LE.1.5)THEN
         CTSOIL=VELRAT**8.98
      ELSE
         CTSOIL=VELRAT**6.64
      ENDIF
C
C     SOLVE FOR RUNOFF REDUCTION FACTOR
      CRO=-1.44*FVEG+1.4
C
      IF(CODERO.EQ.2.0)THEN
         WRITE(*,1003)FVEG,CSOIL,VELRAT,CTSOIL,CRO,RRAIN,PH(1)
1003     FORMAT(1X,'FVEG='E10.3,1X,'CSOIL=',E10.3,1X,'VELRAT=',E10.3,
     &    1X,'CTSOIL='E10.3,1X,'CRO='E10.3,1X,'RRAIN='E10.3,1X,
     &   'PH(1)',E10.3)
      ENDIF
C
C  SOLVE FOR SUSPENDED SEDIMENT TRANSPORT CAPABILITY
      IF(FVEG.EQ.0.0)THEN
C     SOLVE FOR BARE SOIL VELOCITY
         VEL=EXP(-0.394+0.276*SLOPE)
      ELSE
C     SOLVE FOR VEGETATED SOIL VELOCITY
         VEL=EXP(-0.905+0.503*SLOPE)
      ENDIF
C
C     SOLVE FOR DEPTH OF FLOW
      DF=(STORM*LENFT)/(VEL*2.633E7)
C     CONVERT SILT DIAMETER FROM MM TO FT
      DMID=DM/304.8
C
C     SOLVE FOR SPACING BETWEEN GRASS AS A FUNCTION OF FVEG
      SPACE=(-.034)*FVEG+0.056
C
C     SOLVE FOR SETTLING VELOCITY USING STOKES LAW
      VS=2*((32.2*(DMID**2)*1.65)/(9*1.5E-5))
C
C     SOLVE FOR SPACING HYDRAULIC RADIUS
      RS=(DF*SPACE)/((2*DF)+SPACE)
C
      P1=(VEL*RS)/1.5E-5
      P2=(SEGLEN*VS)/(VEL*DF)
C
C     SOLVE FOR FRACTION OF SUSPENDED SEDIMENT TRAPPED
      TRSED=EXP((-1.05E-3)*(P1**.82)*(P2**(-.91)))
C
      IF(CODERO.EQ.2.0)THEN
         WRITE(*,1005)SPACE,VS,RS,P1,P2,STORM,VEL,DMID
1005     FORMAT(1X,'SPACE=',E10.3,1X,'VS='
     &   ,E10.3,1X,'RS=',E10.3,1X,'P1=',E10.3,1X,'P2=',
     &   E10.3,1X,'STORM=',E10.3,1X,'VEL=',E10.3,'DMID=',E10.3)
      ENDIF
C
```

```
      IF(CODERO.EQ.2.0)THEN
         WRITE(*,1006)TRSED
1006     FORMAT(1X,'TRSED=',E10.3)
      ENDIF
C
C   INITIALIZE PARAMETERS
      LENTOT=0.0
      BED=0.0
      SUS=0.0
C
C   CALCULATE EROSION AND TRANSPORT FOR EACH SEGMENT
      DO 10 I=1,NLEN
         LENTOT=LENTOT+SEGLEN
C     CALCULATE GROSS EROSION
         ESOIL=(0.0459*RRAIN*KSOIL*CSOIL*SLPFAC*((LENTOT**(MSLP+1.0))
     &   -((LENTOT-SEGLEN)**(MSLP+1.0)))/(72.6**MSLP))
C
C     CALCULATE BEDLOAD FROM GROSS EROSION
         BEDTEM=ESOIL-(ESOIL*(SILT/100.0))
C
C     ESTIMATE TOTAL BEDLOAD
         BED=BED+BEDTEM
C
C     CALCULATE SUSPENDED SEDIMENT LOAD
         SUS=(1-TRSED)*(SUS+(ESOIL*SILT/100.0))
C
C     SOLVE FOR BEDLOAD TRANSPORT CAPABILITY
         TCSOIL=RSOIL*RRAIN*TSOIL*(LENTOT**2.0)*(SPRIME**BEXP)*CRO
     &   *CTSOIL
C     CHECK IF ESTIMATED BEDLOAD EXCEEDS BEDLOAD TRANSPORT CAPACITY
         IF(BED.GE.TCSOIL) BED=TCSOIL
C
         IF(CODERO.EQ.2.0)THEN
            WRITE(*,1001)TCSOIL,ESOIL,BEDTEM,BED,SUS
1001        FORMAT(1X,'TCSOIL=',E10.3,'ESOIL=',E10.3,'BEDTEM=',E10.3
     &      ,1X,'BED=',E10.3,1X,'SUS='E10.3)
         ENDIF
10    CONTINUE
C
C   APPLY POND TRAPPING EFFICIENCY
      BEDPND=(1-(BEDTRP/100.0))*BED
      SUSPND=(1-(SUSTRP/100.0))*SUS
C
C   CALCULATE TOTAL SEDIMENT TRANSPORT IN KG
      EROTOT=(((BEDPND+SUSPND)*WIDTH)*DT)/2.2
C
      IF(CODERO.EQ.2.0)THEN
         WRITE(*,1007)EROTOT
1007     FORMAT(1X,'TOTAL EROSION=',E10.3)
      ENDIF
      RETURN
      END
```

Table A.2

STORAGE ARRAYS FOR CALCULATED CONCENTRATIONS

WCONC (substance, location, time)
- stores liquid phase (porewater) concentrations

CONC (substance, location, time)
- stores solid phase concentrations

Substances 1 = Natural Uranium ($Bq.m^{-3}$)
2 = Total Thorium (Th-230 + Th-232) ($Bq.m^{-3}$)
3 = Lead-210 ($Bq.m^{-3}$)
4 = Radium-226 ($Bq.m^{-3}$)
5 = Radon-222 ($Bq.m^{-3}$)
6 = $[SO_4^{2-}]$ from pyrite oxidation ($mol.m^{-3}$)
7 = $[SO_4^{2-}]$ total sulphate ion ($mol.m^{-3}$)
8 = $[Ca^{2+}]$ total calcium ion ($mol.m^{-3}$)
9 = $[Fe^{III}]$ ferric ion ($mol.m^{-3}$)
10 = $[Fe^{II}]$ ferrous ion ($mol.m^{-3}$)

Locations 1 = tailings layer 1; surface layer of varying thickness
2 = tailings layer 2; at the bottom of the unsaturated zone
3 = tailings layer 3; the mixing zone
4 = tailings layer 4; the bottom layer

Times 1 = initial time (representative of t=o years)
2 = previous time step ($t-\Delta t$)
3 = current time (t)

Table A.3

WATER SOURCE MODEL VARIABLE DICTIONARY

Model Symbol	Description	Units	Nominal Value	Probability Distribution	Computer Origin	Computer Symbol
a	equilibrium expression for $CaSO_4$	$mol.m^{-3}$	calculated	calculated	SOURCE (INCONI)	EQUIL
A	tailings surface area	m^2	5×10^5	$C(5\times10^5)$	INPUT	ATAIL
a^0_{Pb}	initial activity of Pb-210 in the tailings	$Bq.g^{-1}$	calculated	calculated	SOURCE (INCONN)	APBI
a^0_{Ra}	initial activity of Ra-226 in tailings	$Bq.g^{-1}$	calculated	calculated	SOURCE (INCONN)	ARADI
a^0_{Th-230}	initial activity of Th-230 in the tailings	$Bq.g^{-1}$	calculated	calculated	SOURCE (INCONN)	AT230I
a^0_{Th-232}	initial activity of Th-232 in the tailings	$Bq.g^{-1}$	calculated	calculated	SOURCE (INCONN)	AT232I
a^0_{Th}	initial activity of total thorium in the tailings	$Bq.g^{-1}$	calculated	calculated	SOURCE (INCONN)	ATHORI
$a^0_{Th,sol}$	initial activity of total soluble thorium	$Bq.m^{-3}$	calculated	calculated	SOURCE (INCONN)	THSOLA
$a^0_{Th,insol}$	initial activity of total insoluble thorium	$Bq.m^{-3}$	calculated	calculated	SOURCE (INCONN)	TINSLA
$a^0_{U-nat,ore}$	initial activity of U-nat in the ore	$Bq.g^{-1}$	calculated	calculated	SOURCE (INCONN)	AUNATO
$a^0_{U-238,ore}$	initial activity of U-238 in the ore	$Bq.g^{-1}$	calculated	calculated	SOURCE (INCONN)	AU238O
$a^0_{U-nat,tails}$	initial activity of U-nat in tailings	$Bq.g^{-1}$	calculated	calculated	SOURCE (INCONN)	AUNATT
β	pyrite oxidation factor	-	calculated	calculated	SOURCE (IONS1)	BETA
$[Ba]_{T,\lambda w}$	concentration of total barium at λ_w	$mol.m^{-3}$	calculated	calculated	SOURCE (RADIUM)	CBAR
$[Ba^{2+}]_\ell$	concentration of Ba^{2+} in layer ℓ (ℓ=2,3,4)	$mol.m^{-3}$	calculated	calculated	SOURCE (INCONN)	CBAR
$[BaSO_4]^0$	initial solid phase concentration of $BaSO_4$	$mol.m^{-3}$	calculated	calculated	SOURCE (INCONN)	CBARI

Table A.3 continued.

Model Symbol	Description	Units	Nominal Value	Probability Distribution	Computer Origin	Computer Symbol
c	concentration of Ca^{2+} from calcite dissolution	mol.m^{-3}	calculated	calculated	SOURCE (IONSIL)	CALIME
$[Ca^{2+}]_{4,t}$	Ca^{2+} concentration in layer 4	mol.m^{-3}	calculated	calculated	SOURCE (IONS4)	WCONC(8,4,3)
$[Ca^{2+}]_{\lambda w}$	concentration of Ca^{2+} at bottom of unsaturated zone	mol.$^{-3}$	calculated	calculated	SOURCE (IONS1)	WCONC(8,2,3)
$[Ca^{2+}]_{mix,t}$	Ca^{2+} concentration in mixing zone	mol.m^{-3}	calculated	calculated	SOURCE (IONS3)	WCONC(8,3,3)
$[Ca^{2+}]_1$	concentration of Ca^{2+} in gypsum depleted layer	mol.m^{-3}	calculated	calculated	SOURCE (IONS1)	WCONC(8,1,3)
$CaCO_3^0$	initial inventory of calcite ($CaCO_3$)	mol.m^{-3}	calculated	calculated	SOURCE (INCONI)	LIMEIN
d	correction factor for sulphate complexation	-	calculated	calculated	SOURCE (IONS1)	DELT
D_{O2}	oxygen concentration at the surface	m^2.yr^{-1}	45	T(4,45,115)	INPUT	O2DIFF
f	activity coefficient (for divalent ions)	-	0.5	T(0.4,0.5,0.6)	INPUT	FACTCO
$[Fe^{2+}]_{4,t}$	Fe^{2+} concentration in layer 4	mol.m^{-3}	calculated	calculated	SOURCE (IONS4)	WCONC(10,4,3)
$[Fe^{2+}]_{mix,t}$	concentration of Fe^{2+}	mol.m^{-3}	calculated	calculated	SOURCE	WCONC(10,3,3)
$[Fe^{3+}]_{\lambda w}$	concentration of Fe^{3+} at bottom of unsaturated zone	mol.m^{-3}	calculated	calculated	SOURCE (IONS1)	WCONC(9,2,3)
$[FeS_2]o$	initial concentration of pyrite in tailings	mol.m^{-3}	700	U(600,800)	INPUT	PYRITI PYRITE(1)
$[FeS_2]_t$	concentration of pyrite at time t	mol.m^{-3}	calculated	calculated	SOURCE (IONS1)	PYRITE(3)
$[FeS_2]_{t-\Delta t}$	as above, at t-Δt	mol.m^{-3}	calculated	calculated	SOURCE (IONS1)	PYRITE(2)
f_{gypsum}	fraction of initial gypsum remaining in unsaturated zone at any time t	-	calculated	calculated	SOURCE (IONS1)	FGYP
f_{Pb}	fraction of Pb-210 assumed to be soluble	-	0.81	U(0.76,0.86)	INPUT	FLEAD

Model Symbol	Description	Units	Nominal Value	Probability Distribution	Computer Origin	Computer Symbol
f_{Ra}	fraction of Ra-226 which is assumed to be soluble	-	0.60	T(0.25,0.6,0.95)	INPUT	FRAD
f_{Th-230}	fraction of Th-230 which is soluble	-	0.80	T(0.65,0.80,0.95)	INPUT	FT230
f_{Th-232}	fraction of Th-232 which is soluble	-	0.65	T(0.55,0.65,0.75)	INPUT	FT232
$f_{U/Fe}$	fraction of uranium associated with pyrite	-	0.6	U(0.3,0.9)	INPUT	FRACU
f_u	mass fraction of uranium recovered in the mill	-	0.95	U(0.92.0.98)	INPUT	FURAN
$[gyp]_{diss,t}$	gypsum dissolved to time t	$mol.m^{-3}$	calculated	calculated	SOURCE (IONS3)	GYPMIX
h^o_{Ba}	initial thickness of barite depleted layer	m	0.01	C(0.01)	SOURCE (INCONN)	DBAR(1) DBAR(3)
h_{Ba}	thickness of barite depleted layer at time, t	m	calculated	calculated	SOURCE (RADIUM)	DBAR(3)
h^o_{Pb}	initial thickness of $PbSO_4$ depleted layer	m	0.01	C(0.01)	SOURCE (INCONN)	DLEAD(1) DLEAD(3)
h_{Pb}	thickness of $PbSO_4$ depleted layer at time t	m	calculated	calculated	SOURCE (LEAD)	DLEAD(3)
h_t	thickness of gypsum depleted front at t	m	calculated	calculated	SOURCE (IONS1)	DGYP(3)
$h_{t-\Delta t}$	thickness of gypsum depleted front at t-Δt	m	calculated	calculated	SOURCE (IONS1)	DGYP(2)
J_s	net sulphate flux	$mol.m^{-2}.yr^{-1}$	calculated	calculated	SOURCE (INCONI)	SFLUX
J_s'	net sulphate flux with calcite present	$mol.m^{-2}yr^{-1}$	calculated	calculated	SOURCE (IONSIL)	SFLUX
K'	ratio of O_2 half saturation constant (KO_2) to $[O_2]$	-	$5x10^{-2}$	$U(1x10^{-2},1x10^{-1})$	INPUT	KPRIME
k	rate constant for pyrite oxidation	yr^{-1}	calculated	calculated	SOURCE (INCONI)	KRATE